

4th Edition

# Digital Signal Processing

Using MATLAB®

A Problem Solving Companion

Vinay K. Ingle • John G. Proakis



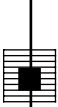
# **Digital Signal Processing**

## **Using MATLAB<sup>®</sup>**

### **A PROBLEM SOLVING COMPANION**

#### **Fourth Edition**





# **Digital Signal Processing**

## **Using MATLAB<sup>®</sup>**

### **A PROBLEM SOLVING COMPANION**

### **Fourth Edition**

**Vinay K. Ingle  
John G. Proakis  
Northeastern University**



---

Australia • Brazil • Mexico • Singapore • United Kingdom • United States

This is an electronic version of the print textbook. Due to electronic rights restrictions, some third party content may be suppressed. Editorial review has deemed that any suppressed content does not materially affect the overall learning experience. The publisher reserves the right to remove content from this title at any time if subsequent rights restrictions require it. For valuable information on pricing, previous editions, changes to current editions, and alternate formats, please visit [www.cengage.com/highered](http://www.cengage.com/highered) to search by ISBN#, author, title, or keyword for materials in your areas of interest.

Important Notice: Media content referenced within the product description or the product text may not be available in the eBook version.



**Digital Signal Processing Using MATLAB®:  
A Problem Solving Companion, Fourth Edition**  
Vinay K. Ingle and John G. Proakis

Product Director, Global Engineering:  
Timothy L. Anderson

Media Assistant: Ashley Kaupert

Product Assistant: Teresa Versaggi

Marketing Manager: Kristin Stine

Director, Content and Media Production:  
Sharon L. Smith

Senior Content Project Manager: Jennifer Risden

Production Service: MPS Limited

Copyeditor: Richard Camp

Proofreader: Jennifer Grubba

Indexer: Larry Sweazy

Compositor: MPS Limited

Senior Art Director: Michelle Kunkler

Internal Designer: Carmela Periera

Cover Designer: Jennifer Wahi

Cover Image: Zeljko Radojko/Shutterstock.com

#### Intellectual Property

Analyst: Christine Myaskovsky

Project Manager: Sarah Shainwald

Text and Image Permissions Researcher:  
Kristiina Paul

Manufacturing Planner: Doug Wilke

© 2017, 2012 Cengage Learning®

WCN: 02-200-203

ALL RIGHTS RESERVED. No part of this work covered by the copyright herein may be reproduced, transmitted, stored, or used in any form or by any means graphic, electronic, or mechanical, including but not limited to photocopying, recording, scanning, digitizing, taping, Web distribution, information networks, or information storage and retrieval systems, except as permitted under Section 107 or 108 of the 1976 United States Copyright Act, without the prior written permission of the publisher.

For product information and technology assistance, contact us at  
**Cengage Learning Customer & Sales Support, 1-800-354-9706.**

For permission to use material from this text or product,  
submit all requests online at [www.cengage.com/permissions](http://www.cengage.com/permissions).

Further permissions questions can be emailed to  
[permissionrequest@cengage.com](mailto:permissionrequest@cengage.com).

Library of Congress Control Number: 2015944167

ISBN: 978-1-305-63512-8

#### Cengage Learning

20 Channel Center Street  
Boston, MA 02210  
USA

Cengage Learning is a leading provider of customized learning solutions with employees residing in nearly 40 different countries and sales in more than 125 countries around the world. Find your local representative at [www.cengage.com](http://www.cengage.com).

Cengage Learning products are represented in Canada by Nelson Education Ltd.

To learn more about Cengage Learning Solutions, visit  
[www.cengage.com/engineering](http://www.cengage.com/engineering).

Purchase any of our products at your local college store or at our preferred online store [www.cengagebrain.com](http://www.cengagebrain.com).

MATLAB is a registered trademark of The MathWorks,  
3 Apple Hill Drive, Natick, MA.

Printed in the United States of America  
Print Number: 01 Print Year: 2015

# Contents

---

PREFACE xi

## 1 INTRODUCTION 1

---

- 1.1 Overview of Digital Signal Processing 2
- 1.2 A Brief Introduction to MATLAB 5
- 1.3 Applications of Digital Signal Processing 18
- 1.4 Brief Overview of the Book 20

## 2 DISCRETE-TIME SIGNALS AND SYSTEMS 22

---

- 2.1 Discrete-Time Signals 22
- 2.2 Discrete Systems 36
- 2.3 Convolution 40
- 2.4 Difference Equations 47
- 2.5 Problems 53

### 3 THE DISCRETE-TIME FOURIER ANALYSIS 59

---

- 3.1 The Discrete-Time Fourier Transform (DTFT) 59
- 3.2 The Properties of the DTFT 67
- 3.3 The Frequency Domain Representation of LTI Systems 74
- 3.4 Sampling and Reconstruction of Analog Signals 80
- 3.5 Problems 97

### 4 THE $z$ -TRANSFORM 103

---

- 4.1 The Bilateral  $z$ -Transform 103
- 4.2 Important Properties of the  $z$ -Transform 107
- 4.3 Inversion of the  $z$ -Transform 112
- 4.4 System Representation in the  $z$ -Domain 118
- 4.5 Solutions of the Difference Equations 128
- 4.6 Problems 134

### 5 THE DISCRETE FOURIER TRANSFORM 141

---

- 5.1 The Discrete Fourier Series 142
- 5.2 Sampling and Reconstruction in the  $z$ -Domain 149
- 5.3 The Discrete Fourier Transform 154
- 5.4 Properties of the Discrete Fourier Transform 165
- 5.5 Linear Convolution Using the DFT 180
- 5.6 The Fast Fourier Transform 187
- 5.7 Problems 200

---

## 6 IMPLEMENTATION OF DISCRETE-TIME FILTERS 212

---

- 6.1 Basic Elements 213
- 6.2 IIR Filter Structures 214
- 6.3 FIR Filter Structures 228
- 6.4 Overview of Finite-Precision Numerical Effects 239
- 6.5 Representation of Numbers 240
- 6.6 The Process of Quantization and Error Characterizations 255
- 6.7 Quantization of Filter Coefficients 262
- 6.8 Problems 277

---

## 7 FIR FILTER DESIGN 291

---

- 7.1 Preliminaries 292
- 7.2 Properties of Linear-Phase FIR Filters 295
- 7.3 Window Design Technique 309
- 7.4 Frequency-Sampling Design Technique 330
- 7.5 Optimal Equiripple Design Technique 344
- 7.6 Problems 360

---

## 8 IIR FILTER DESIGN 370

---

- 8.1 Some Preliminaries 371
- 8.2 Some Special Filter Types 374
- 8.3 Characteristics of Prototype Analog Filters 385
- 8.4 Analog-to-Digital Filter Transformations 407

8.5 Lowpass Filter Design Using MATLAB 427

8.6 Frequency-Band Transformations 432

8.7 Problems 445

## 9 SAMPLING RATE CONVERSION 458

---

9.1 Introduction 459

9.2 Decimation by a Factor  $D$  461

9.3 Interpolation by a Factor  $I$  470

9.4 Sampling Rate Conversion by a Rational Factor  $I/D$  477

9.5 FIR Filter Designs for Sampling Rate Conversion 482

9.6 FIR Filter Structures for Sampling Rate Conversion 500

9.7 Problems 510

## 10 ROUND-OFF EFFECTS IN DIGITAL FILTERS 518

---

10.1 Analysis of A/D Quantization Noise 518

10.2 Round-Off Effects in IIR Digital Filters 530

10.3 Round-Off Effects in FIR Digital Filters 557

10.4 Problems 569

## 11 APPLICATIONS IN ADAPTIVE FILTERING 573

---

11.1 LMS Algorithm for Coefficient Adjustment 575

11.2 System Identification or System Modeling 578

11.3 Suppression of Narrowband Interference in  
a Wideband Signal 579

11.4 Adaptive Line Enhancement 582

11.5 Adaptive Channel Equalization 582

---

**12 APPLICATIONS IN COMMUNICATIONS 586**

- 
- 12.1 Pulse-Code Modulation 586**
  - 12.2 Differential PCM (DPCM) 590**
  - 12.3 Adaptive PCM and DPCM (ADPCM) 593**
  - 12.4 Delta Modulation (DM) 597**
  - 12.5 Linear Predictive Coding (LPC) of Speech 601**
  - 12.6 Dual-Tone Multifrequency (DTMF) Signals 605**
  - 12.7 Binary Digital Communications 609**
  - 12.8 Spread-Spectrum Communications 611**

---

**13 RANDOM PROCESSES\* 614**

- 
- 13.1 Random Variable 615**
  - 13.2 A Pair of Random Variables 628**
  - 13.3 Random Signals 642**
  - 13.4 Power Spectral Density 650**
  - 13.5 Stationary Random Processes through LTI Systems 658**
  - 13.6 Useful Random Processes 668**
  - 13.7 Summary and References 684**

---

**14 LINEAR PREDICTION AND OPTIMUM LINEAR FILTERS\* 686**

- 
- 14.1 Innovations Representation of a Stationary Random Process 687**

\*Chapters 13–15 are available for download from the Instructor's Companion Website at [www.cengage.com/login](http://www.cengage.com/login).

<b>14.2 Forward and Backward Linear Prediction</b>	<b>701</b>
<b>14.3 Solution of the Normal Equations</b>	<b>717</b>
<b>14.4 Properties of the Linear Prediction-Error Filters</b>	<b>730</b>
<b>14.5 AR Lattice and ARMA Lattice-Ladder Filters</b>	<b>734</b>
<b>14.6 Wiener Filters for Filtering and Prediction</b>	<b>743</b>
<b>14.7 Summary and References</b>	<b>766</b>

## **15 ADAPTIVE FILTERS\*** 769

---

<b>15.1 Applications of Adaptive Filters</b>	<b>769</b>
<b>15.2 Adaptive Direct-Form FIR Filters</b>	<b>815</b>
<b>15.3 Summary and References</b>	<b>849</b>

**BIBLIOGRAPHY** B-1

**INDEX** I-1

\*Chapters 13–15 are available for download from the Instructor's Companion Website at [www.cengage.com/login](http://www.cengage.com/login).

# Preface

---

Since the beginning of the 1980s, we have witnessed a revolution in computer technology and an explosion in user-friendly applications. This revolution is still continuing today, with low-cost laptop systems that rival the performance of expensive workstations. This technological prowess should be brought to bear on the educational process and, in particular, on effective teaching that can result in enhanced learning. This problem-solving companion book on digital signal processing (DSP) makes a contribution toward reaching that goal. The fourth edition continues our innovative approach of blending MATLAB®-based learning with traditional teaching to advanced DSP topics such as optimal and adaptive filters.

The teaching methods in signal processing have changed over the years from the simple “lecture-only” format to a more integrated “lecture-laboratory” environment in which practical hands-on issues are taught using DSP hardware. However, for effective teaching of DSP, the lecture component must also make extensive use of computer-based explanations, examples, and exercises. For the past three decades, the MATLAB software developed by *The MathWorks, Inc.* has established itself as the de facto standard for numerical computation in the signal-processing community and as a platform of choice for algorithm development. There are several reasons for this development, but the most important reason is that MATLAB is available on practically all computing platforms. In this book, we have made an attempt at integrating MATLAB with traditional topics in DSP so that it can be used to explore difficult topics and solve problems to gain insight. Many problems or design algorithms in DSP require considerable amount of computation. It is for these that MATLAB provides a convenient tool so that multiple scenarios can be tried with ease. Such an approach can enhance the learning process.

## SCOPE OF THE BOOK

---

This book is primarily intended for use as a problem-solving companion book in senior-level undergraduate or first-year graduate courses on DSP. Although we assume that the student (or user) is familiar with the fundamentals of MATLAB, we have provided a brief introduction to MATLAB in Chapter 1. This book is not written as a textbook in DSP, because of the ready availability of excellent textbooks. What we have tried to do is to provide enough depth to the material augmented by MATLAB functions and examples so that the presentation is consistent, logical, and enjoyable. Therefore, this book can also be used as a self-study guide by anyone interested in DSP.

## WHAT IS NEW IN THE FOURTH EDITION

---

- A new Chapter 13 provides a review on random variables and random processes, including bandpass processes. Extensive use of MATLAB examples makes these topics easier to understand.
- A new Chapter 14 discusses linear prediction and optimal (or Wiener) filters, preparing students for graduate studies.
- A new Chapter 15 deals with theory and applications of adaptive filters. This chapter contains easy-to-understand LMS and RLS algorithms with an extensive set of practical applications, including system identification, echo and noise cancellation, and adaptive arrays. All algorithms and applications are explained and analyzed using MATLAB.
- The coverage of lattice/ladder filters has moved from Chapter 6 to Chapter 14 for a more logical presentation of information.
- All MATLAB functions and scripts have been tested and updated so that they can execute on MATLAB-2014b version and later. Similarly, all MATLAB plots have been recreated with superior graphic elements.
- We have trimmed many included MATLAB scripts from their plotting commands to streamline their appearance and to reduce unnecessary printing. However, all scripts and functions will be made available in their entirety on the book website.

## ORGANIZATION OF THE BOOK

---

The first ten chapters of this book discuss traditional material typically covered in an introductory course on DSP. The next two chapters are

presented as applications in DSP, with emphasis on MATLAB-based projects. The last three chapters deal with advanced material in DSP and are intended for graduate studies. In order to keep the size and the cost of the book down, we have provided these last three chapters through our book's instructor website. Information on how to obtain these chapters is provided in the next section. The following is a list of chapters and a brief description of their contents.

*Chapter 1, Introduction:* This chapter introduces readers to the discipline of signal processing and presents several applications of digital signal processing, including musical sound processing, echo generation, echo removal, and digital reverberation. A brief introduction to MATLAB is also provided.

*Chapter 2, Discrete-Time Signals and Systems:* This chapter provides a brief review of discrete-time signals and systems in the time domain. Appropriate use of MATLAB functions is demonstrated.

*Chapter 3, The Discrete-Time Fourier Analysis:* This chapter discusses discrete-time signal and system representation in the frequency domain. Sampling and reconstruction of analog signals are also presented.

*Chapter 4, The z-Transform:* This chapter provides signal and system description in the complex frequency domain. MATLAB techniques are introduced to analyze  $z$ -transforms and to compute inverse  $z$ -transforms. Solutions of difference equations using the  $z$ -transform and MATLAB are provided.

*Chapter 5, The Discrete Fourier Transform:* This chapter is devoted to the computation of the Fourier transform and its efficient implementation. The discrete Fourier series is used to introduce the discrete Fourier transform, and several of its properties are demonstrated using MATLAB. Topics such as fast convolution and fast Fourier transform are thoroughly discussed.

*Chapter 6, Implementation of Discrete-Time Filters:* This chapter discusses several structures for the implementation of digital filters. Several useful MATLAB functions are developed for the determination and implementation of these structures. In addition to considering various filter structures, we also treat quantization effects when finite-precision arithmetic is used in the implementation of IIR and FIR filters.

*Chapter 7, FIR Filter Design:* This chapter and the next introduce the important topic of digital filter design. Three important design techniques for FIR filters—namely, window design, frequency sampling design, and the equiripple filter design—are discussed. Several design examples are provided using MATLAB.

*Chapter 8, IIR Filter Design:* Included in this chapter are techniques used in IIR filter design. The chapter begins with the treatment of some

basic filter types—namely, digital resonators, notch filters, comb filters, allpass filters, and digital sinusoidal oscillators. This is followed by a brief description of the characteristics of three widely used analog filters. Transformations are described for converting these prototype analog filters into different frequency-selective digital filters. The chapter concludes with several IIR filter designs using MATLAB.

*Chapter 9, Sampling Rate Conversion:* This chapter treats the important problem of sampling rate conversion in digital signal processing. Topics treated include decimation and interpolation by integer factors, sampling rate conversion by a rational factor, and polyphase filter structures for sampling rate conversion.

*Chapter 10, Round-Off Effects in Digital Filters:* The focus of this chapter is on the effects of finite-precision arithmetic to the filtering aspects in signal processing. Quantization noise introduced in analog-to-digital conversion is characterized statistically, and the quantization effects in finite-precision multiplication and additions are also modeled statistically. The effects of these errors in the filter output are characterized as correlated errors, called limit cycles, and as uncorrelated errors, called round-off noise.

*Chapter 11, Applications in Adaptive Filtering:* This chapter is the first of two chapters on projects using MATLAB. Included is an introduction to the theory and implementation of adaptive FIR filters with projects in system identification, interference suppression, narrowband frequency enhancement, and adaptive equalization.

*Chapter 12, Applications in Communications:* This chapter focuses on several projects dealing with waveform representation and coding and with digital communications. Included is a description of pulse-code modulation (PCM), differential PCM (DPCM) and adaptive DPCM (ADPCM), delta modulation (DM) and adaptive DM (ADM), linear predictive coding (LPC), generation and detection of dual-tone multifrequency (DTMF) signals, and a description of signal detection applications in binary communications and spread-spectrum communications.

*Chapter 13, Random Processes:* This is the first of the last three chapters that are available online through the website for the book. In this chapter, we provide a brief review of analytical concepts in random signals that model waveform variations and provide sound techniques to calculate the response of linear filters to random signals. We begin by defining probability functions and statistical averages, and continue with pairs of random variables. These concepts are extended to random signals, in terms of second-order statistics, and then delve into stationary and ergodic processes, correlation functions, and power spectra. We apply this theory to processing of random signals through LTI systems

using both the time and frequency domains. Finally, we discuss a few representative random processes, including Gaussian, Markov, white noise, and filtered noise processes.

*Chapter 14, Linear Prediction and Optimum Linear Filters:* In this chapter, we treat the problem of optimum filter design from a statistical viewpoint. The filters are constrained to be linear, and the optimization criterion is based on the minimization of the mean square error. We discuss the design of optimum filters for linear prediction, which has applications in speech signal processing, image processing, and noise suppression in communication systems. This design technique requires the solution of a set of linear equations with special symmetry. We describe two algorithms, Levinson–Durbin and Schur, which provide the solution to the equations through computationally efficient procedures that exploit the symmetry properties. The last section of this chapter treats an important class of optimum filters called Wiener filters, which are widely used in many applications involving the estimation of signals corrupted with additive noise.

*Chapter 15, Adaptive Filters:* The focus of this chapter is on *adaptive filters*, which have adjustable coefficients for use in applications in which the filter coefficients cannot be designed a priori due to unknown or changing statistics. We begin with several practical applications in which adaptive filters have been successfully used in the estimation of signals corrupted by noise and other interference. Adaptive filters incorporate algorithms that allow the filter coefficients to adapt to changes in the signal statistics. We describe two basic algorithms: the least-mean-square (LMS) algorithm, which is based on gradient optimization for determining the coefficients, and the class of recursive least-squares (RLS) algorithms.

## ABOUT THE ONLINE RESOURCES

---

This book is an outgrowth of our teaching of a MATLAB-based undergraduate DSP course over several years. Most of the MATLAB functions discussed in this book were developed for this course. These functions are collected in the book toolbox called `DSPUM_v4` and are available online on the book's companion website. Many examples in the book contain MATLAB scripts. Similarly, many figure plots were created using MATLAB scripts. All these scripts are made available at the companion website for the benefit of students and instructors. Students should study these scripts to gain insight into MATLAB procedures. We will appreciate any comments, corrections, or compact coding of these functions.

and scripts. Solutions to problems and the associated script files will be made available to instructors adopting the book through the companion website.

To access the book's companion website and all additional course materials, please visit [www.cengage.com/login](http://www.cengage.com/login). After signing in, search for the ISBN of your title (from the back cover of your book) using the search box at the top of the page. This will take you to the companion site where these resources can be found.

Further information about MATLAB and related publications may be obtained from:

The MathWorks, Inc.  
Natick, MA 01760  
Phone: (508) 647-7000 Fax: (508) 647-7001  
E-mail: [info@mathworks.com](mailto:info@mathworks.com)  
WWW: <http://www.mathworks.com>

## ACKNOWLEDGMENTS

---

We are indebted to numerous students in our undergraduate DSP course at Northeastern University who provided us a forum to test teaching ideas using MATLAB and who endured our constant emphasis on MATLAB. Many efficient MATLAB functions used in this book were developed by some of these students. We are also indebted to reviewers of the original edition, whose constructive criticism resulted in a better presentation of the material: Abeer A. H. Alwan, University of California, Los Angeles; Steven Chin, Catholic University; Prof. Huaichen, Xidian University, P. R. China; and Joel Trussel, North Carolina State University. The following reviewers provided additional encouragement, numerous refinements, and useful comments for the second edition: Jyotsna Bapat, Fairleigh Dickinson University; David Clark, California State Polytechnic University; Artyom Grigoryan, University of Texas, San Antonio; Tao Li, University of Florida; and Zixiang Xiong, Texas A & M University. Based on their use of the second edition, the following reviewers provided several suggestions, changes, and modifications that led to the third edition: Kalyan Mondal, Fairleigh Dickinson University; Artyom M. Grigoryan, University of Texas at San Antonio; A. David Salvia, Pennsylvania State University; Matthew Valenti, West Virginia University; and Christopher J. James, University of Southampton, UK. Finally, the fourth edition was motivated by the constructive feedback and comments provided by Wasfy B. Mikhael, University of Central Florida; Hongbin Li, Stevens

Institute of Technology; Robert Paz, New Mexico State University; and Ramakrishnan Sundaram, Gannon University. We sincerely thank all of them.

We would also like to take this opportunity to acknowledge several people at Cengage Learning without whom this project would not have been possible. We thank the Product Director, Timothy Anderson, who oversees the Global Engineering publishing program at Cengage, for encouraging the fourth edition. Media Assistant Ashley Kaupert worked on the revisions and helped see the fourth edition through development to production. This project could not have been completed within time limits without their constant push. Senior Content Project Manager Jennifer Risden oversaw the book's production process. We thank them all for their professional help. Finally, we express our sincere gratitude to Richard Camp for his diligent copy editing and everyone at Cengage Learning who aided in the development of this edition.

*Vinay K. Ingle  
John G. Proakis  
Boston, Massachusetts*



# CHAPTER 1

---

## Introduction

---

During the past several decades, the field of digital signal processing (DSP) has grown to be important, both theoretically and technologically. A major reason for its success in industry is the development and use of low-cost software and hardware. New technologies and applications in various fields are now taking advantage of DSP algorithms. This will lead to a greater demand for electrical and computer engineers with a background in DSP. Therefore, it is necessary to make DSP an integral part of any electrical engineering curriculum.

Three decades ago an introductory course on DSP was given mainly at the graduate level. It was supplemented by computer exercises on filter design, spectrum estimation, and related topics using mainframe (or mini) computers. However, considerable advances in personal computers and software during the past three decades have made it necessary to introduce a DSP course to undergraduates. Since DSP applications are primarily algorithms that are implemented either on a DSP processor [36] or in software, a fair amount of programming is required. Using interactive software, such as MATLAB, it is now possible to place more emphasis on learning new and difficult concepts than on programming algorithms. Interesting practical examples can be discussed, and useful problems can be explored.

With this philosophy in mind, we have developed this book as a *companion book* (to traditional textbooks like [71, 79]) in which MATLAB is an integral part in the discussion of topics and concepts. We have chosen MATLAB as the programming tool primarily because of its wide availability on computing platforms in many universities across the world. Furthermore, a low-cost student version of MATLAB has been available for several years, placing it among the least expensive software products

for educational purposes. We have treated MATLAB as a computational and programming toolbox containing several tools (sort of a super calculator with several keys) that can be used to explore and solve problems and, thereby, enhance the learning process.

This book is written at an introductory level in order to introduce undergraduate students to the exciting and practical field of DSP. We emphasize that this is not a textbook in the traditional sense but a companion book in which more attention is given to problem solving and hands-on experience with MATLAB. Similarly, it is not a tutorial book in MATLAB. We assume that the student is familiar with MATLAB and is currently taking a course in DSP. The book provides basic analytical tools needed to process real-world signals (a.k.a. analog signals) using digital techniques. We deal mostly with discrete-time signals and systems, which are analyzed in both the time and the frequency domains. The analysis and design of processing structures called *filters* and *spectrum analyzers* are among some of the most important aspects of DSP and are treated in great detail in this book. Similarly, the topics of finite word-length effects on filter performance as well as on filter output and the sampling-rate conversion between two DSP systems are of practical significance. These are also treated extensively in this book. To further our philosophy of MATLAB-based learning to advanced topics taught in graduate courses, we have also included some material from statistical and adaptive signal processing areas such as random signals, linear prediction, optimal filters, and adaptive filters.

In this chapter, we provide a brief overview of DSP and an introduction to MATLAB.

## 1.1 OVERVIEW OF DIGITAL SIGNAL PROCESSING

---

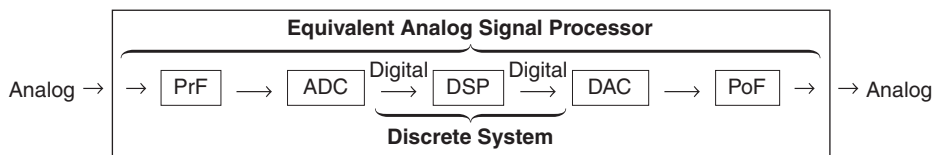
In this modern world, we are surrounded by all kinds of signals in various forms. Some of the signals are natural, but most of the signals are man-made. Some signals are necessary (speech), some are pleasant (music), while many are unwanted or unnecessary in a given situation. In an engineering context, signals are carriers of information, both useful and unwanted. Therefore, extracting or enhancing the useful information from a mix of conflicting information is the simplest form of signal processing. More generally, signal processing is an operation designed for extracting, enhancing, storing, and transmitting useful information. The distinction between useful and unwanted information is often subjective as well as objective. Hence signal processing tends to be application dependent.

### 1.1.1 HOW ARE SIGNALS PROCESSED?

The signals that we encounter in practice are mostly analog signals. These signals, which vary continuously in time and amplitude, are processed using electrical networks containing active and passive circuit elements. This approach is known as analog signal processing (ASP)—for example, radio and television receivers.



They can also be processed using digital hardware containing adders, multipliers, and logic elements or using special-purpose microprocessors. However, one needs to convert analog signals into a form suitable for digital hardware. This form of the signal is called a digital signal. It takes one of the finite number of values at specific instances in time, and hence it can be represented by binary numbers, or bits. The processing of digital signals is called DSP; in block diagram form it is represented by



The various block elements are discussed as follows.

**PrF:** This is a prefilter or an antialiasing filter, which conditions the analog signal to prevent aliasing.

**ADC:** This is an analog-to-digital converter, which produces a stream of binary numbers from analog signals.

**Digital Signal Processor:** This is the heart of DSP and can represent a general-purpose computer or a special-purpose processor, or digital hardware, and so on.

**DAC:** This is the inverse operation to the ADC, called a digital-to-analog converter, which produces a staircase waveform from a sequence of binary numbers, a first step toward producing an analog signal.

**PoF:** This is a postfilter to smooth out staircase waveform into the desired analog signal.

It appears from the above two approaches to signal processing, analog and digital, that the DSP approach is the more complicated, containing more components than the “simpler looking” ASP. Therefore, one might ask, Why process signals digitally? The answer lies in the many advantages offered by DSP.

### 1.1.2 ADVANTAGES OF DSP OVER ASP

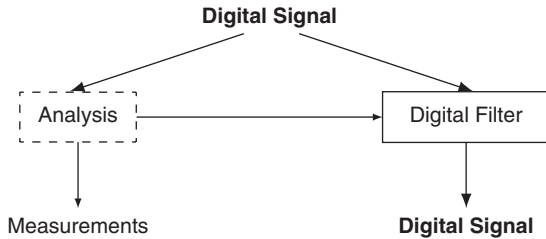
A major drawback of ASP is its limited scope for performing complicated signal-processing applications. This translates into nonflexibility in processing and complexity in system designs. All of these generally lead to expensive products. On the other hand, using a DSP approach, it is possible to convert an inexpensive personal computer into a powerful signal processor. Some important advantages of DSP are these:

1. Systems using the DSP approach can be developed using software running on a general-purpose computer. Therefore, DSP is relatively convenient to develop and test, and the software is portable.
2. DSP operations are based solely on additions and multiplications, leading to extremely stable processing capability—for example, stability independent of temperature.
3. DSP operations can easily be modified in real time, often by simple programming changes or by reloading of registers.
4. DSP has lower cost due to VLSI technology, which reduces costs of memories, gates, microprocessors, and so forth.

The principal disadvantage of DSP is the limited speed of operations due to the DSP hardware, especially at very high frequencies. Primarily because of its advantages, DSP is now becoming a first choice in many technologies and applications, such as consumer electronics, communications, wireless telephones, and medical imaging.

### 1.1.3 TWO IMPORTANT CATEGORIES OF DSP

Most DSP operations can be categorized as being either signal *analysis* tasks or signal *filtering* tasks:



**Signal analysis** This task deals with the measurement of signal properties. It is generally a frequency-domain operation. Some of its applications are

- spectrum (frequency and/or phase) analysis,
- speech recognition,
- speaker verification, and
- target detection.

**Signal filtering** This task is characterized by the signal-in signal-out situation. The systems that perform this task are generally called *filters*. It is usually (but not always) a time-domain operation. Some of the applications are

- removal of unwanted background noise,
- removal of interference,
- separation of frequency bands, and
- shaping of the signal spectrum.

In some applications, such as voice synthesis, a signal is first analyzed to study its characteristics, which are then used in digital filtering to generate a synthetic voice.

## 1.2 A BRIEF INTRODUCTION TO MATLAB

---

MATLAB is an interactive, matrix-based system for scientific and engineering numeric computation and visualization. Its strength lies in the fact that complex numerical problems can be solved easily and in a fraction of the time required by a programming language such as Fortran or C. It is also powerful in the sense that, with its relatively simple programming capability, MATLAB can be easily extended to create new commands and functions.

MATLAB is available in a number of computing environments: PCs running all flavors of Windows, Apple Macs running OS-X, UNIX/Linux workstations, and parallel computers. The basic MATLAB program is further enhanced by the availability of numerous toolboxes (collections of specialized functions in specific topics) over the years. The information in this book generally applies to all these environments. In addition to the basic MATLAB product, the Signal Processing toolbox (SP toolbox) is required for this book. The original development of the book was done using the professional version 3.5 running under DOS. The MATLAB scripts and functions described in the book were later extended and made compatible with the present version of MATLAB. Furthermore, through the services of [www.cengagebrain.com](http://www.cengagebrain.com), every effort will be made to preserve this compatibility under future versions of MATLAB.

In this section, we will undertake a brief review of MATLAB. The scope and power of MATLAB go far beyond the few topics discussed in this section. For more detailed tutorial-based discussion, students and readers new to MATLAB should also consult several excellent reference books available in the literature, including [29], [35], and [76]. The information given in all these references, along with the online MATLAB's `help` facility, usually is sufficient to enable readers to use this book.

The best approach to become familiar with MATLAB is to open a MATLAB session and experiment with various operators, functions, and commands until their use and capabilities are understood. Then one can progress to writing simple MATLAB scripts and functions to execute a sequence of instructions to accomplish an analytical goal.

### 1.2.1 GETTING STARTED

The interaction with MATLAB is through the command window of its graphical user interface (GUI). In the command window, the user types MATLAB instructions, which are executed instantaneously, and the results are displayed in the window. In the MATLAB command window, the characters “>>” indicate the prompt that is waiting for the user to type a command to be executed. For example,

```
>> command;
```

means an instruction `command` has been issued at the MATLAB prompt. If a semicolon (;) is placed at the end of a command, then all output from that command is suppressed. Multiple commands can be placed on the same line, separated by semicolons. Comments are marked by the percent sign (%), in which case MATLAB ignores anything to the right of the sign. The comments allow the reader to follow code more easily. The integrated help manual provides help for every command through the fragment

```
>> help command;
```

which will provide information on the inputs, outputs, usage, and functionality of the command. A complete listing of commands sorted by functionality can be obtained by typing `help` at the prompt.

There are three basic elements in MATLAB: numbers, variables, and operators. In addition, punctuation marks (,, :, :, etc.) have special meanings.

**Numbers** MATLAB is a high-precision numerical engine and can handle all types of numbers—that is, integers, real numbers, complex numbers, among others—with relative ease. For example, the real number 1.23 is represented as simply 1.23, while the real number  $4.56 \times 10^7$  can be written as `4.56e7`. The imaginary number  $\sqrt{-1}$  is denoted either by `1i` or `1j`, although in this book we will use the symbol `1j`. Hence the complex number whose real part is 5 and whose imaginary part is 3 will be written as `5+1j*3`. Other constants preassigned by MATLAB are `pi` for  $\pi$ , `inf` for  $\infty$ , and `NaN` for not a number (e.g.,  $0/0$ ). These preassigned constants are very important and, to avoid confusion, should not be redefined by users.

**Variables** In MATLAB, which stands for MATrix LABoratory, the basic variable is a matrix, or an array. Hence, when MATLAB operates on this variable, it operates on all its elements. This is what makes it a powerful and an efficient engine. MATLAB now supports multidimensional arrays; we will discuss only up to two-dimensional arrays of numbers.

1. **Matrix:** A matrix is a two-dimensional set of numbers arranged in rows and columns. Numbers can be real- or complex-valued.
2. **Array:** This is another name for matrix. However, operations on arrays are treated differently from those on matrices. This difference is very important in implementation.

The following are four types of matrices (or arrays).

- **Scalar:** This is a  $1 \times 1$  matrix or a single number that is denoted by the *variable* symbol, that is, lowercase italic typeface like

$$a = a_{11}$$

- **Column vector:** This is an  $(N \times 1)$  matrix or a vertical arrangement of numbers. It is denoted by the *vector* symbol, that is, lowercase bold typeface like

$$\mathbf{x} = [x_{i1}]_{i:1,\dots,N} = \begin{bmatrix} x_{11} \\ x_{21} \\ \vdots \\ x_{N1} \end{bmatrix}$$

A typical vector in linear algebra is denoted by the column vector.

- **Row vector:** This is a  $(1 \times M)$  matrix or a horizontal arrangement of numbers. It is also denoted by the vector symbol, that is,

$$\mathbf{y} = [y_{1j}]_{j=1,\dots,M} = [y_{11} \ y_{12} \ \cdots \ y_{1M}]$$

A one-dimensional discrete-time signal is typically represented by an array as a row vector.

- **General matrix:** This is the most general case of an  $(N \times M)$  matrix and is denoted by the matrix symbol, that is, uppercase bold typeface like

$$\mathbf{A} = [a_{ij}]_{i=1,\dots,N;j=1,\dots,m} = \begin{bmatrix} a_{11} & a_{12} & \cdots & a_{1M} \\ a_{21} & a_{22} & \cdots & a_{2M} \\ \vdots & \vdots & \ddots & \vdots \\ a_{N1} & a_{N2} & \cdots & a_{NM} \end{bmatrix}$$

This arrangement is typically used for two-dimensional discrete-time signals or images.

MATLAB does not distinguish between an array and a matrix except for operations. The following assignments denote indicated matrix types in MATLAB:

$a = [3]$  is a scalar,  
 $x = [1, 2, 3]$  is a row vector,  
 $y = [1; 2; 3]$  is a column vector, and  
 $A = [1, 2, 3; 4, 5, 6]$  is a matrix.

MATLAB provides many useful functions to create special matrices. These include `zeros(M,N)` for creating a matrix of all zeros, `ones(M,N)` for creating matrix of all ones, `eye(N)` for creating an  $N \times N$  identity matrix, and so on. Consult MATLAB's help manual for a complete list.

**Operators** MATLAB provides several arithmetic and logical operators, some of which follow. For a complete list, MATLAB's help manual should be consulted.

= assignment	== equality
+ addition	- subtraction or minus
* multiplication	.* array multiplication
^ power	.^ array power
/ division	./ array division
<> relational operators	& logical AND
logical OR	~ logical NOT
' transpose	.' array transpose

We now provide a more detailed explanation on some of these operators.

### 1.2.2 MATRIX OPERATIONS

Following are the most useful and important operations on matrices.

- **Matrix addition and subtraction:** These are straightforward operations that are also used for array addition and subtraction. Care must be taken that the two matrix operands be *exactly* the same size.
- **Matrix conjugation:** This operation is meaningful only for complex-valued matrices. It produces a matrix in which all imaginary parts are negated. It is denoted by  $\mathbf{A}^*$  in analysis and by `conj(A)` in MATLAB.
- **Matrix transposition:** This is an operation in which every row (column) is turned into column (row). Let  $\mathbf{X}$  be an  $(N \times M)$  matrix. Then

$$\mathbf{X}' = [x_{ji}] ; \quad j = 1, \dots, M, \quad i = 1, \dots, N$$

is an  $(M \times N)$  matrix. In MATLAB, this operation has one additional feature. If the matrix is real-valued, then the operation produces the

usual transposition. However, if the matrix is complex-valued, then the operation produces a complex-conjugate transposition. To obtain just the transposition, we use the array operation of conjugation, that is,  $\mathbf{A}.'$  will do just the transposition.

- **Multiplication by a scalar:** This is a simple straightforward operation in which each element of a matrix is scaled by a constant, that is,

$$ab \Rightarrow \mathbf{a} * \mathbf{b} \text{ (scalar)}$$

$$a\mathbf{x} \Rightarrow \mathbf{a} * \mathbf{x} \text{ (vector or array)}$$

$$a\mathbf{X} \Rightarrow \mathbf{a} * \mathbf{X} \text{ (matrix)}$$

This operation is also valid for an array scaling by a constant.

- **Vector-vector multiplication:** In this operation, one has to be careful about matrix dimensions to avoid invalid results. The operation produces either a scalar or a matrix. Let  $\mathbf{x}$  be an  $(N \times 1)$  vector and  $\mathbf{y}$  be a  $(1 \times M)$  vector. Then

$$\mathbf{x} * \mathbf{y} \Rightarrow \mathbf{xy} = \begin{bmatrix} x_1 \\ \vdots \\ x_N \end{bmatrix} [y_1 \ \cdots \ y_M] = \begin{bmatrix} x_1 y_1 & \cdots & x_1 y_M \\ \vdots & \ddots & \vdots \\ x_N y_1 & \cdots & x_N y_M \end{bmatrix}$$

produces a matrix. If  $M = N$ , then

$$\mathbf{y} * \mathbf{x} \Rightarrow \mathbf{yx} = [y_1 \ \cdots \ y_M] \begin{bmatrix} x_1 \\ \vdots \\ x_M \end{bmatrix} = x_1 y_1 + \cdots + x_M y_M$$

- **Matrix-vector multiplication:** If the matrix and the vector are compatible (i.e., the number of matrix-columns is equal to the vector-rows), then this operation produces a column vector:

$$\mathbf{y} = \mathbf{A} * \mathbf{x} \Rightarrow \mathbf{y} = \mathbf{Ax} = \begin{bmatrix} a_{11} & \cdots & a_{1M} \\ \vdots & \ddots & \vdots \\ a_{N1} & \cdots & a_{NM} \end{bmatrix} \begin{bmatrix} x_1 \\ \vdots \\ x_M \end{bmatrix} = \begin{bmatrix} y_1 \\ \vdots \\ y_N \end{bmatrix}$$

- **Matrix-matrix multiplication:** Finally, if two matrices are compatible, then their product is well defined. The result is also a matrix with the number of rows equal to that of the first matrix and the number of columns equal to that of the second matrix. Note that the order in matrix multiplication is very important.

**Array Operations** These operations treat matrices as arrays. They are also known as *dot operations* because the arithmetic operators are prefixed by a dot (.), that is, .\*, ./, or .^.

- **Array multiplication:** This is an element by element multiplication operation. For it to be a valid operation, both arrays must be the same size. Thus we have

$$\mathbf{x}.\ast\mathbf{y} \rightarrow \text{1D array}$$

$$\mathbf{X}.\ast\mathbf{Y} \rightarrow \text{2D array}$$

- **Array exponentiation:** In this operation, a scalar (real- or complex-valued) is raised to the power equal to every element in an array, that is,

$$\mathbf{a}.\hat{\wedge}\mathbf{x} \equiv \begin{bmatrix} a^{x_1} \\ a^{x_2} \\ \vdots \\ a^{x_N} \end{bmatrix}$$

is an  $(N \times 1)$  array, whereas

$$\mathbf{a}.\hat{\wedge}\mathbf{X} \equiv \begin{bmatrix} a^{x_{11}} & a^{x_{12}} & \cdots & a^{x_{1M}} \\ a^{x_{21}} & a^{x_{22}} & \cdots & a^{x_{2M}} \\ \vdots & \vdots & \ddots & \vdots \\ a^{x_{N1}} & a^{x_{N2}} & \cdots & a^{x_{NM}} \end{bmatrix}$$

is an  $(N \times M)$  array.

- **Array transposition:** As explained, the operation  $\mathbf{A}.'$  produces transposition of real- or complex-valued array  $\mathbf{A}$ .

**Indexing Operations** MATLAB provides very useful and powerful array-indexing operations using operator `:`. It can be used to generate sequences of numbers as well as to access certain row/column elements of a matrix. Using the fragment  $\mathbf{x} = [\mathbf{a}:\mathbf{b}:\mathbf{c}]$ , we can generate numbers from  $\mathbf{a}$  to  $\mathbf{c}$  in  $\mathbf{b}$  increments. If  $\mathbf{b}$  is positive (negative), then we get increasing (decreasing) values in the sequence  $\mathbf{x}$ .

The fragment  $\mathbf{x}(\mathbf{a}:\mathbf{b}:\mathbf{c})$  accesses elements of  $\mathbf{x}$  beginning with index  $\mathbf{a}$  in steps of  $\mathbf{b}$  and ending at  $\mathbf{c}$ . Care must be taken to use integer values for indexing elements. Similarly, the `:` operator can be used to extract a submatrix from a matrix. For example,  $\mathbf{B} = \mathbf{A}(2:4,3:6)$  extracts a  $3 \times 4$  submatrix starting at row 2 and column 3.

Another use of the `:` operator is in forming column vectors from row vectors or matrices. When used on the right-hand side of the equality (`=`) operator, the fragment  $\mathbf{x}=\mathbf{A}(:)$  forms a long column vector  $\mathbf{x}$  of elements

of  $A$  by concatenating its columns. Similarly,  $x=A(:,3)$  forms a vector  $x$  from the third column of  $A$ . However, when used on the right-hand side of the  $=$  operator, the fragment  $A(:)=x$  reformats elements in  $x$  into a predefined size of  $A$ .

**Control-Flow** MATLAB provides a variety of commands that allow us to control the flow of commands in a program. The most common construct is the **if-elseif-else** structure. With these commands, we can allow different blocks of code to be executed depending on some condition. The format of this construct is

```
if condition1
    command1
elseif condition2
    command2
else
    command3
end
```

which executes statements in `command1` if `condition-1` is satisfied; otherwise, it executes statements in `command2` if `condition-2` is satisfied, or, finally, statements in `command3`.

Another common control flow construct is the **for..end** loop. It is simply an iteration loop that tells the computer to repeat some task a given number of times. The format of a **for..end** loop is

```
for index = values
    program statements
    :
end
```

Although **for..end** loops are useful for processing data inside of arrays by using the iteration variable as an index into the array, whenever possible the user should try to use MATLAB's whole array mathematics. This will result in shorter programs and more efficient code. In some situations, the use of the **for..end** loop is unavoidable. The following example illustrates these concepts.

- **EXAMPLE 1.1** Consider the following sum of sinusoidal functions:

$$x(t) = \sin(2\pi t) + \frac{1}{3} \sin(6\pi t) + \frac{1}{5} \sin(10\pi t) = \sum_{k=1,3,5} \frac{1}{k} \sin(2\pi kt), \quad 0 \leq t \leq 1$$

Using MATLAB, we want to generate samples of  $x(t)$  at time instances  $0:0.01:1$ . We will discuss three approaches.

**Approach 1**

Here we will consider a typical C or Fortran approach, that is, we will use two `for..end` loops, one each on `t` and `k`. This is the most inefficient approach in MATLAB, but possible.

```
>> t = 0:0.01:1; N = length(t); xt = zeros(1,N);
>> for n = 1:N
>>     temp = 0;
>>     for k = 1:2:5
>>         temp = temp + (1/k)*sin(2*pi*k*t(n));
>>     end
>>     xt(n) = temp;
>> end
```

**Approach 2**

In this approach, we will compute each sinusoidal component in one step as a vector, using the time vector `t = 0:0.01:1`, and then add all components using one `for..end` loop.

```
>> t = 0:0.01:1; xt = zeros(1,length(t));
>> for k = 1:2:5
>>     xt = xt + (1/k)*sin(2*pi*k*t);
>> end
```

Clearly, this is a better approach with fewer lines of code than the first one.

**Approach 3**

In this approach, we will use matrix-vector multiplication, in which MATLAB is very efficient. For the purpose of demonstration, consider only four values for  $t = [t_1, t_2, t_3, t_4]$ . Then

$$x(t_1) = \sin(2\pi t_1) + \frac{1}{3} \sin(2\pi 3t_1) + \frac{1}{5} \sin(2\pi 5t_1)$$

$$x(t_2) = \sin(2\pi t_2) + \frac{1}{3} \sin(2\pi 3t_2) + \frac{1}{5} \sin(2\pi 5t_2)$$

$$x(t_3) = \sin(2\pi t_3) + \frac{1}{3} \sin(2\pi 3t_3) + \frac{1}{5} \sin(2\pi 5t_3)$$

$$x(t_4) = \sin(2\pi t_4) + \frac{1}{3} \sin(2\pi 3t_4) + \frac{1}{5} \sin(2\pi 5t_4)$$

which can be written in matrix form as

$$\begin{bmatrix} x(t_1) \\ x(t_2) \\ x(t_3) \\ x(t_4) \end{bmatrix} = \begin{bmatrix} \sin(2\pi t_1) & \sin(2\pi 3t_1) & \sin(2\pi 5t_1) \\ \sin(2\pi t_2) & \sin(2\pi 3t_2) & \sin(2\pi 5t_2) \\ \sin(2\pi t_3) & \sin(2\pi 3t_3) & \sin(2\pi 5t_3) \\ \sin(2\pi t_4) & \sin(2\pi 3t_4) & \sin(2\pi 5t_4) \end{bmatrix} \begin{bmatrix} 1 \\ \frac{1}{3} \\ \frac{1}{5} \end{bmatrix}$$

$$= \sin \left( 2\pi \begin{bmatrix} t_1 \\ t_2 \\ t_3 \\ t_4 \end{bmatrix} \begin{bmatrix} 1 & 3 & 5 \end{bmatrix} \right) \begin{bmatrix} 1 \\ \frac{1}{3} \\ \frac{1}{5} \end{bmatrix}$$

or, after taking transposition,

$$[x(t_1) \quad x(t_2) \quad x(t_3) \quad x(t_4)] = [1 \quad \frac{1}{3} \quad \frac{1}{5}] \sin\left(2\pi \begin{bmatrix} 1 \\ 3 \\ 5 \end{bmatrix} [t_1 \quad t_2 \quad t_3 \quad t_4]\right)$$

Thus the MATLAB code is

```
>> t = 0:0.01:1; k = 1:2:5;
>> xt = (1./k)*sin(2*pi*k'*t);
```

Note the use of the array division ( $1./k$ ) to generate a row vector and matrix multiplications to implement all other operations. This is the most compact code and the most efficient execution in MATLAB, especially when the number of sinusoidal terms is very large.

### 1.2.3 SCRIPTS AND FUNCTIONS

MATLAB is convenient in the interactive command mode if we want to execute few lines of code. But it is not efficient if we want to write code of several lines that we want to run repeatedly or if we want to use the code in several programs with different variable values. MATLAB provides two constructs for this purpose.

**Scripts** The first construct can be accomplished by using the so-called block mode of operation. In MATLAB, this mode is implemented using a *script* file called an m-file (with an extension `.m`), which is only a text file that contains each line of the file as though you typed them at the command prompt. These scripts are created using MATLAB's built-in editor, which also provides for context-sensitive colors and indents for making fewer mistakes and for easy reading. The script is executed by typing the name of the script at the command prompt. The script file must be in the current directory or in the directory of the **path** environment. As an example, consider the sinusoidal function in Example 1.1. A general form of this function is

$$x(t) = \sum_{k=1}^K c_k \sin(2\pi kt) \quad (1.1)$$

If we want to experiment with different values of the coefficients  $c_k$  and/or the number of terms  $K$ , then we should create a script file. To implement the third approach in Example 1.1, we can write a script file

```
% Script file to implement (1.1)
t = 0:0.01:1; k = 1:2:5; ck = 1./k;
xt = ck * sin(2*pi*k'*t);
```

Now we can experiment with different values.

**Functions** The second construct of creating a block of code is through subroutines. These are called *functions*, which also allow us to extend the capabilities of MATLAB. In fact, a major portion of MATLAB is assembled using function files in several categories and using special collections called *toolboxes*. Functions are also m-files (with extension .m). A major difference between script and function files is that the first executable line in a function file begins with the keyword **function** followed by an output-input variable declaration. As an example, consider the computation of the  $x(t)$  function in Example 1.1 with an arbitrary number of sinusoidal terms, which we will implement as a function stored as m-file **sinsum.m**.

```
function xt = sinsum(t,ck)
% Computes sum of sinusoidal terms of the form in (1.1)
% x = sinsum(t,ck)
%
K = length(ck); k = 1:K;
ck = ck(:)'; t = t(:)';
xt = ck * sin(2*pi*k'*t);
```

The vectors **t** and **ck** should be assigned prior to using the **sinsum** function. Note that **ck(:)'** and **t(:)'** use indexing and transposition operations to force them to be row vectors. Also note the comments immediately following the **function** declaration, which are used by the **help sinsum** command. Sufficient information should be given there for the user to understand what the function is supposed to do.

#### 1.2.4 PLOTTING

One of the most powerful features of MATLAB for signal and data analysis is its graphical data plotting. MATLAB provides several types of plots, starting with simple two-dimensional (2D) graphs and progressing to complex, higher-dimensional full-color plots. We will examine only the 2D plotting, which is the plotting of one array versus another in a 2D coordinate system. The basic plotting command is the **plot(t,x)** command, which generates a plot of **x** values versus **t** values in a separate figure window. The arrays **t** and **x** should be the same length and orientation. Optionally, some additional formatting keywords can also be provided in the **plot** function. The commands **xlabel** and **ylabel** are used to add text to the axes, and the command **title** is used to provide a title on the top of the graph. When plotting data, one should get into the habit of always labeling the axes and providing a title. Almost all aspects of a plot (style, size, color, etc.) can be changed by appropriate commands embedded in the program or directly through the GUI.

The following set of commands creates a list of sample points, evaluates the sine function at those points, and then generates a plot of a simple sinusoidal wave, putting axis labels and title on the plot.

```
>> t = 0:0.01:2; % sample points from 0 to 2 in steps of 0.01
>> xt = sin(2*pi*t); % Evaluate sin(2 pi t)
>> plot(t,xt,'b'); % Create plot with blue line
>> xlabel('t in sec'); ylabel('x(t)'); % Label axis
>> title('Plot of sin(2\pi t)'); % Title plot
```

The resulting plot is shown in Figure 1.1.

For plotting a set of discrete numbers (or discrete-time signals), we will use the `stem` command, which displays data values as a stem, that is, a small circle at the end of a line connecting it to the horizontal axis. The circle can be open (default) or filled (using the option '`'filled'`'). Using Handle Graphics (MATLAB's extensive manipulation of graphics primitives), we can resize circle markers. The following set of commands displays a discrete-time sine function using these constructs.

```
>> n = 0:1:40; % sample index from 0 to 40
>> xn = sin(0.1*pi*n); % Evaluate sin(0.1 pi n)
>> stem(n,xn,'b','filled','marker size',4); % Stem-plot
>> xlabel('n'); ylabel('x(n)'); % Label axis
>> title('Stem Plot of sin(0.1\pi n)'); % Title plot
```

The resulting plot is shown in Figure 1.2.

MATLAB provides an ability to display more than one graph in the same figure window. By means of the `hold on` command, several graphs

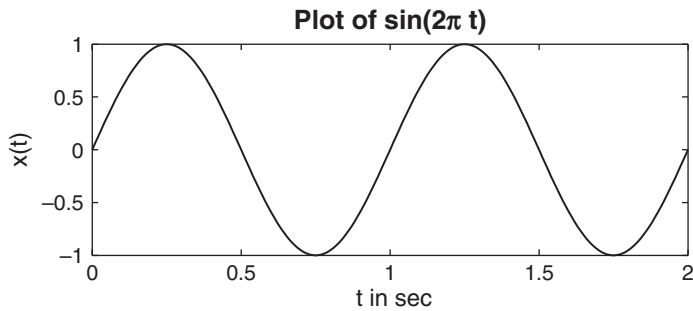


**FIGURE 1.1** Plot of the  $\sin(2\pi t)$  function

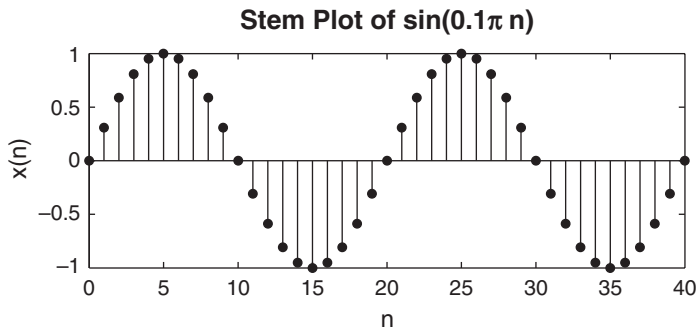


**FIGURE 1.2** Plot of the  $\sin(0.1\pi n)$  sequence

can be plotted on the same set of axes. The `hold off` command stops the simultaneous plotting. The following MATLAB fragment (Figure 1.3) displays graphs in Figures 1.1 and 1.2 as one plot, depicting a “sampling” operation that we will study later.

```
>> plot(t,xt,'b'); hold on; % Create plot with blue line
>> Hs = stem(n*0.05,xn,'b','filled'); % Stem-plot with handle Hs
>> set(Hs,'markersize',4); hold off; % Change circle size
```

Another approach is to use the `subplot` command, which displays several graphs in each individual set of axes arranged in a grid, using the parameters in the `subplot` command. The following fragment (Figure 1.4) displays graphs in Figure 1.1 and 1.2 as two separate plots in two rows.

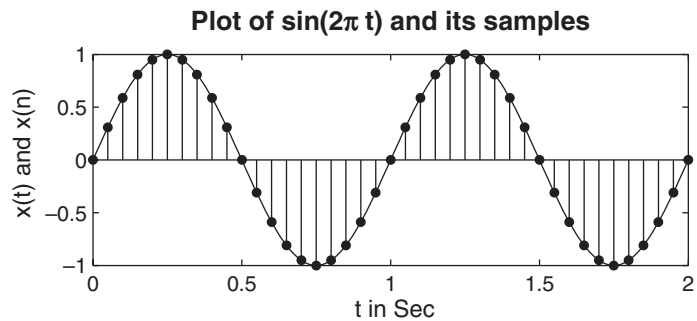


**FIGURE 1.3** Simultaneous plots of  $x(t)$  and  $x(n)$

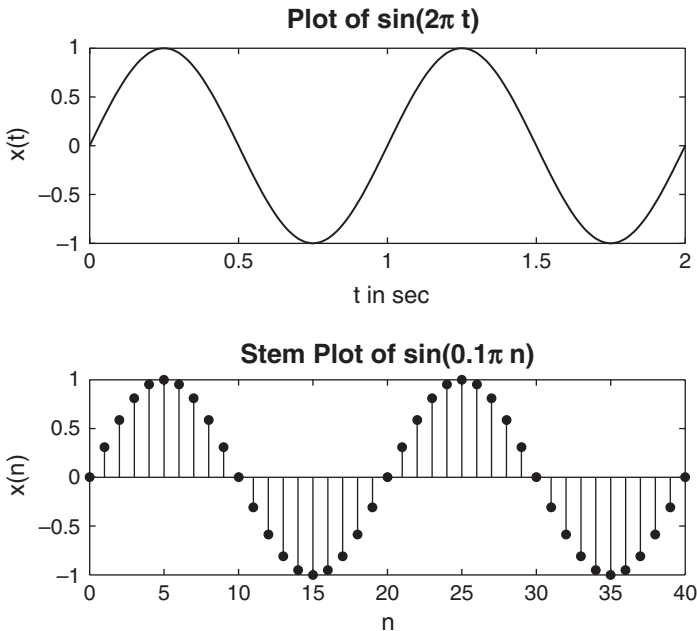


**FIGURE 1.4** Plots of  $x(t)$  and  $x(n)$  in two rows

```

. . .
>> subplot(2,1,1); % Two rows, one column, first plot
>> plot(t,xt,'b'); % Create plot with blue line
. . .
>> subplot(2,1,2); % Two rows, one column, second plot
>> Hs = stem(n,xn,'b','filled','marker size',4); % Stem-plot
. . .

```

The plotting environment provided by MATLAB is very rich in its complexity and usefulness. It is made even richer using the Handle Graphics constructs. Therefore, readers are strongly recommended to consult MATLAB's manuals on plotting. Many of these constructs will be used throughout this book.

In this brief review, we have barely made a dent in the enormous capabilities and functionalities in MATLAB. Using its basic integrated help system, detailed help browser, and tutorials, it is possible to acquire sufficient skills in MATLAB in a reasonable amount of time.

## 1.3 APPLICATIONS OF DIGITAL SIGNAL PROCESSING

The field of DSP has matured considerably over the last several decades and now is at the core of many diverse applications and products. These include

- speech/audio (speech recognition/synthesis, digital audio, equalization, etc.),
- image/video (enhancement, coding for storage and transmission, robotic vision, animation, etc.),
- military/space (radar processing, secure communication, missile guidance, sonar processing, etc.),
- biomedical/health care (scanners, ECG analysis, X-ray analysis, EEG brain mappers, etc.), and
- consumer electronics (cellular/mobile phones, digital television, digital camera, Internet voice/music/video, interactive entertainment systems, etc.).

These applications and products require many interconnected complex steps, such as collection, processing, transmission, analysis, audio/display of real-world information in near real time. DSP technology has made it possible to incorporate these steps into devices that are innovative, affordable, and of high quality (e.g., the iPhone from Apple). A typical application to music is now considered as a motivation for the study of DSP.

**Musical sound processing** In the music industry, almost all musical products (songs, albums, etc.) are produced in basically two stages. First, the sound from an individual instrument or performer is recorded in an acoustically inert studio on a single track of a multitrack recording device. Then, stored signals from each track are digitally processed by the sound engineer by adding special effects and combined into a stereo recording, which is then made available either on a CD or as an audio file.

The audio effects are artificially generated using various signal-processing techniques. These effects include echo generation, reverberation (concert hall effect), flanging (in which audio playback is slowed down by placing the DJ's thumb on the *flange* of the feed reel), chorus effect (when several musicians play the same instrument with small changes in amplitudes and delays), and phasing (a.k.a. phase shifting, in which an audio effect takes advantage of how sound waves interact with each other when they are out of phase). We now discuss a few of these sound effects in some detail.

**Echo Generation** The most basic of all audio effects is that of *time delay*, or echoes. It is used as the building block of more complicated effects such as reverb or flanging. In a listening space such as a room, sound waves arriving at our ears consist of *direct* sound from the source as well as *reflected* off the walls, arriving with different amounts of attenuation and delays.

Echoes are delayed signals, and as such they are generated using delay units. For example, the combination of the direct sound represented by discrete signal  $y[n]$  and a single echo appearing  $D$  samples later (which is related to delay in seconds) can be generated by an equation (called a difference equation) of the form

$$x[n] = y[n] + \alpha y[n - D], \quad |\alpha| < 1 \quad (1.2)$$

where  $x[n]$  is the resulting signal and  $\alpha$  models attenuation of the direct sound. Difference equations are implemented in MATLAB using the `filter` function. Available in MATLAB is a short snippet of Handel's "Hallelujah Chorus," which is a digital sound about 9 seconds long, sampled at 8192 sam/sec. To experience the sound with echo in (1.2), execute the following fragment at the command window. The echo is delayed by  $D = 4196$  samples, which amount to 0.5 sec of delay.

```
load handel; % The signal is in y and sampling freq in Fs
sound(y,Fs); pause(10); % Play the original sound
alpha = 0.9; D = 4196; % Echo parameters
b = [1,zeros(1,D),alpha]; % Filter parameters
x = filter(b,1,y); % Generate sound plus its echo
sound(x,Fs); % Play sound with echo
```

You should be able to hear the distinct echo of the chorus in about a half second.

**Echo Removal** After executing this simulation, you may experience that the echo is an objectionable interference while listening. Again DSP can be used effectively to reduce (almost eliminate) echoes. Such an echo-removal system is given by the difference equation

$$w[n] + \alpha w[n - D] = x[n] \quad (1.3)$$

where  $x[n]$  is the echo-corrupted sound signal and  $w[n]$  is the output sound signal, which has the echo (hopefully) removed. Note again that

this system is very simple to implement in software or hardware. Now try the following MATLAB script on the signal  $x[n]$ .

```
w = filter(1,b,x);
sound(w,Fs)
```

The echo should no longer be audible.

**Digital Reverberation** Multiple close-spaced echoes eventually lead to reverberation, which can be created digitally using a somewhat more involved difference equation

$$x[n] = \sum_{k=0}^{N-1} \alpha^k y[n - kD] \quad (1.4)$$

which generates multiple echoes spaced  $D$  samples apart with exponentially decaying amplitudes. Another natural-sounding reverberation is given by

$$x[n] = \alpha y[n] + y[n - D] + \alpha x[n - D], \quad |\alpha| < 1 \quad (1.5)$$

which simulates a higher echo density.

These simple applications are examples of DSP. Using techniques, concepts, and MATLAB functions learned in this book, you should be able to simulate these and other interesting sound effects.

## 1.4 BRIEF OVERVIEW OF THE BOOK

---

The book is organized roughly in four parts. The first three parts are included in the printed copy, as was done in the previous editions of the book, while the last part on advanced topics is available only through the book's website (see the Preface for instructions on accessing the book's website).

The first part of this book, which comprises Chapters 2 through 5, deals with the signal-analysis aspect of DSP. Chapter 2 begins with basic descriptions of discrete-time signals and systems. These signals and systems are analyzed in the frequency domain in Chapter 3. A generalization of the frequency-domain description, called the  $z$ -transform, is introduced in Chapter 4. The practical algorithms for computing the Fourier transform are discussed in Chapter 5 in the form of the discrete Fourier transform and the fast Fourier transform.

Chapters 6 through 8 constitute the second part of this book, which is devoted to the signal-filtering aspect of DSP. Chapter 6 describes various

implementations and structures of digital filters. It also introduces finite-precision number representation and filter coefficient quantization and their effect on filter performance. Chapter 7 introduces design techniques and algorithms for designing one type of digital filter called *finite-duration impulse response (FIR) filters*, and Chapter 8 provides a similar treatment for another type of filter called *infinite-duration impulse response (IIR) filters*. In both chapters, only the simpler but practically useful techniques of filter design are discussed. More advanced techniques are not covered.

The third part, which consists of Chapters 9 through 12, provides important topics and applications in DSP. Chapter 9 deals with the useful topic of sampling-rate conversion and applies FIR filter designs from Chapter 7 to implement practical sample-rate converters. Chapter 10 extends the treatment of finite-precision numerical representation to signal quantization and the effect of finite-precision arithmetic on filter performance. The last two chapters provide some practical applications in the form of projects that can be done using material presented in the first 10 chapters. In Chapter 11, concepts in adaptive filtering are introduced, and simple projects in system identification, interference suppression, adaptive line enhancement, and so forth, are discussed. In Chapter 12, a brief introduction to digital communications is presented, with projects involving such topics as PCM, DPCM, and LPC being outlined.

Finally, Chapters 13 through 15 round out the last part of the book and it is intended as topics in advanced undergraduate or graduate courses. In Chapter 13, we treat signals as stochastic entities, called *random processes* (or *signals*), and provide their probabilistic as well as statistical descriptions through the concept of random variables. We also discuss a few representative random processes. In Chapter 14, we develop theory for *optimum filters* for processing random signals. For this treatment, we consider filters for linear prediction and Wiener filters for estimating signals corrupted by additive noise. In Chapter 15, we present *adaptive filters*, which are stochastic systems for applications in which statistics is not known a priori. We provide descriptions of LMS and RLS, two basic yet important adaptive algorithms.

In all these chapters, the central theme is the generous use and adequate demonstration of MATLAB, which can be used as an effective teaching as well as learning tool. Most of the existing MATLAB functions for DSP are described in detail, and their correct use is demonstrated in many examples. Furthermore, many new MATLAB functions are developed to provide insights into the working of many algorithms. The authors believe that this hand-holding approach enables students to dispel fears about DSP and provides an enriching learning experience.

# CHAPTER 2

---

## Discrete-Time Signals and Systems

---

We begin with the concepts of signals and systems in discrete time. A number of important types of signals and their operations are introduced. Linear and shift-invariant systems are discussed mostly because they are easier to analyze and implement. The convolution and the difference equation representations are given special attention because of their importance in digital signal processing and in MATLAB. The emphasis in this chapter is on the representations and implementation of signals and systems using MATLAB.

### 2.1 DISCRETE-TIME SIGNALS

---

Signals are broadly classified into analog and discrete signals. An analog signal will be denoted by  $x_a(t)$ , in which the variable  $t$  can represent any physical quantity but we will assume that it represents time in seconds. A discrete signal will be denoted by  $x(n)$ , in which the variable  $n$  is integer-valued and represents discrete instances in time. Therefore, it is also called a discrete-time signal, which is a *number sequence* and will be denoted by one of the following notations:

$$x(n) = \{x(n)\} = \{\dots, x(-1), x(0), \underset{\uparrow}{x(1)}, \dots\}$$

where the *up-arrow* indicates the sample at  $n = 0$ .

In MATLAB, we can represent a *finite-duration* sequence by a *row vector* of appropriate values. However, such a vector does not have any information about sample position  $n$ . Therefore, a correct representation of  $x(n)$  would require two vectors, one each for  $x$  and  $n$ . For example, a sequence  $x(n) = \{2, 1, -1, 0, 1, 4, 3, 7\}$  can be represented in MATLAB by

```
>> n=[-3,-2,-1,0,1,2,3,4]; x=[2,1,-1,0,1,4,3,7];
```

Generally, we will use the  $\mathbf{x}$ -vector representation alone when the sample position information is not required or when such information is trivial (e.g., when the sequence begins at  $n = 0$ ). An arbitrary *infinite-duration* sequence cannot be represented in MATLAB, due to the finite memory limitations.

### 2.1.1 TYPES OF SEQUENCES

We use several elementary sequences in digital signal processing for analysis purposes. Their definitions and MATLAB representations follow.

#### 1. Unit sample sequence:

$$\delta(n) = \begin{cases} 1, & n = 0 \\ 0, & n \neq 0 \end{cases} = \left\{ \dots, 0, 0, \underset{\uparrow}{1}, 0, 0, \dots \right\}$$

In MATLAB, the function `zeros(1,N)` generates a row vector of  $N$  zeros, which can be used to implement  $\delta(n)$  over a finite interval. However, the logical relation `n==0` is an elegant way of implementing  $\delta(n)$ . For example, to implement

$$\delta(n - n_0) = \begin{cases} 1, & n = n_0 \\ 0, & n \neq n_0 \end{cases}$$

over the  $n_1 \leq n_0 \leq n_2$  interval, we will use the following MATLAB function.

```
function [x,n] = impseq(n0,n1,n2)
% Generates x(n) = delta(n-n0); n1 <= n <= n2
%
% [x,n] = impseq(n0,n1,n2)
%
n = [n1:n2]; x = [(n-n0) == 0];
```

#### 2. Unit step sequence:

$$u(n) = \begin{cases} 1, & n \geq 0 \\ 0, & n < 0 \end{cases} = \{ \dots, 0, 0, \underset{\uparrow}{1}, 1, 1, \dots \}$$

In MATLAB, the function `ones(1,N)` generates a row vector of  $N$  ones. It can be used to generate  $u(n)$  over a finite interval. Once again, an elegant approach is to use the logical relation `n>=0`. To implement

$$u(n - n_0) = \begin{cases} 1, & n \geq n_0 \\ 0, & n < n_0 \end{cases}$$

over the  $n_1 \leq n_0 \leq n_2$  interval, we will use the following MATLAB function.

```
function [x,n] = stepseq(n0,n1,n2)
% Generates x(n) = u(n-n0); n1 <= n <= n2
%
% -----
% [x,n] = stepseq(n0,n1,n2)
%
n = [n1:n2]; x = [(n-n0) >= 0];
```

### 3. Real-valued exponential sequence:

$$x(n) = a^n, \forall n; a \in \mathbb{R}$$

In MATLAB, an array operator “.<sup>n</sup>” is required to implement a real exponential sequence. For example, to generate  $x(n) = (0.9)^n$ ,  $0 \leq n \leq 10$ , we will need the following MATLAB script.

```
>> n = [0:10]; x = (0.9).^n;
```

### 4. Complex-valued exponential sequence:

$$x(n) = e^{(\sigma+j\omega_0)n}, \forall n$$

where  $\sigma$  produces an attenuation (if  $<0$ ) or amplification (if  $>0$ ) and  $\omega_0$  is the frequency in radians. A MATLAB function `exp` is used to generate exponential sequences. For example, to generate  $x(n) = \exp[(2 + j3)n]$ ,  $0 \leq n \leq 10$ , we will need the following MATLAB script.

```
>> n = [0:10]; x = exp((2+3j)*n);
```

### 5. Sinusoidal sequence:

$$x(n) = A \cos(\omega_0 n + \theta_0), \forall n$$

where  $A$  is an amplitude and  $\theta_0$  is the phase in radians. A MATLAB function `cos` (or `sin`) is used to generate sinusoidal sequences.

For example, to generate  $x(n) = 3\cos(0.1\pi n + \pi/3) + 2\sin(0.5\pi n)$ ,  $0 \leq n \leq 10$ , we will need the following MATLAB script.

```
>> n = [0:10]; x = 3*cos(0.1*pi*n+pi/3) + 2*sin(0.5*pi*n);
```

6. **Random sequences:** Many practical sequences cannot be described by mathematical expressions like those above. These sequences are called random (or stochastic) sequences and are characterized by parameters of the associated probability density functions. In MATLAB, two types of (pseudo-) random sequences are available. The `rand(1,N)` generates a length  $N$  random sequence whose elements are uniformly distributed between  $[0, 1]$ . The `randn(1,N)` generates a length  $N$  Gaussian random sequence with mean 0 and variance 1. Other random sequences can be generated using transformations of the above functions.
7. **Periodic sequence:** A sequence  $x(n)$  is periodic if  $x(n) = x(n + N)$ ,  $\forall n$ . The smallest integer  $N$  that satisfies this relation is called the *fundamental period*. We will use  $\tilde{x}(n)$  to denote a periodic sequence. To generate  $P$  periods of  $\tilde{x}(n)$  from one period  $\{x(n), 0 \leq n \leq N-1\}$ , we can copy  $x(n)$   $P$  times:

```
>> xtilde = [x,x,...,x];
```

But an elegant approach is to use MATLAB's powerful indexing capabilities. First we generate a matrix containing  $P$  rows of  $x(n)$  values. Then we can concatenate  $P$  rows into a long row vector using the construct `(:)`. However, this construct works only on columns. Hence we will have to use the matrix transposition operator `'` to provide the same effect on rows.

```
>> xtilde = x' * ones(1,P); % P columns of x; x is a row vector
>> xtilde = xtilde(:); % Long column vector
>> xtilde = xtilde'; % Long row vector
```

Note that the last two lines can be combined into one for compact coding. This is shown in Example 2.1.

### 2.1.2 OPERATIONS ON SEQUENCES

Here we briefly describe basic sequence operations and their MATLAB equivalents.

1. **Signal addition:** This is a sample-by-sample addition given by

$$\{x_1(n)\} + \{x_2(n)\} = \{x_1(n) + x_2(n)\}$$

It is implemented in MATLAB by the arithmetic operator “+”. However, the lengths of  $x_1(n)$  and  $x_2(n)$  must be the same. If sequences are of unequal lengths, or if the sample positions are different for equal-length sequences, then we cannot directly use the operator +. We have to first augment  $x_1(n)$  and  $x_2(n)$  so that they have the same position vector  $n$  (and hence the same length). This requires careful attention to MATLAB’s indexing operations. In particular, logical operation of intersection “&”, relational operations like “ $<=$ ” and “ $=$ ”, and the **find** function are required to make  $x_1(n)$  and  $x_2(n)$  of equal length. The following function, called the **sigadd** function, demonstrates these operations.

```
function [y,n] = sigadd(x1,n1,x2,n2)
% Implements y(n) = x1(n)+x2(n)
%
% -----
% [y,n] = sigadd(x1,n1,x2,n2)
%   y = sum sequence over n, which includes n1 and n2
%   x1 = first sequence over n1
%   x2 = second sequence over n2 (n2 can be different from n1)
%
n = min(min(n1),min(n2)):max(max(n1),max(n2)); % Duration of y(n)
y1 = zeros(1,length(n)); y2 = y1; % Initialization
y1(find((n>=min(n1))&(n<=max(n1))==1))=x1; % x1 with duration of y
y2(find((n>=min(n2))&(n<=max(n2))==1))=x2; % x2 with duration of y
y = y1+y2; % Sequence addition
```

Its use is illustrated in Example 2.2.

2. **Signal multiplication:** This is a sample-by-sample (or “dot”) multiplication given by

$$\{x_1(n)\} \cdot \{x_2(n)\} = \{x_1(n)x_2(n)\}$$

It is implemented in MATLAB by the array operator **.\***. Once again, the similar restrictions apply for the **.\*** operator as for the **+** operator. Therefore, we have developed the **sigmult** function, which is similar to the **sigadd** function.

```
function [y,n] = sigmult(x1,n1,x2,n2)
% Implements y(n) = x1(n)*x2(n)
%
% -----
% [y,n] = sigmult(x1,n1,x2,n2)
%   y = product sequence over n, which includes n1 and n2
%   x1 = first sequence over n1
%   x2 = second sequence over n2 (n2 can be different from n1)
%
```

```

n = min(min(n1),min(n2)):max(max(n1),max(n2)); % Duration of y(n)
y1 = zeros(1,length(n)); y2 = y1; % 
y1(find((n>=min(n1))&(n<=max(n1))==1))=x1; % x1 with duration of y
y2(find((n>=min(n2))&(n<=max(n2))==1))=x2; % x2 with duration of y
y = y1 .* y2; % Sequence multiplication

```

Its use is also given in Example 2.2.

3. **Scaling:** In this operation, each sample is multiplied by a scalar  $\alpha$ .

$$\alpha \{x(n)\} = \{\alpha x(n)\}$$

An arithmetic operator (\*) is used to implement the scaling operation in MATLAB.

4. **Shifting:** In this operation, each sample of  $x(n)$  is shifted by an amount  $k$  to obtain a shifted sequence  $y(n)$ .

$$y(n) = \{x(n - k)\}$$

If we let  $m = n - k$ , then  $n = m + k$  and the above operation is given by

$$y(m + k) = \{x(m)\}$$

Hence this operation has no effect on the vector  $x$ , but the vector  $n$  is changed by adding  $k$  to each element. This is shown in the function **sigshift**.

```

function [y,n] = sigshift(x,m,k)
% Implements y(n) = x(n-k)
%
% [y,n] = sigshift(x,m,k)
%
n = m+k; y = x;

```

Its use is given in Example 2.2.

5. **Folding:** In this operation, each sample of  $x(n)$  is flipped around  $n = 0$  to obtain a folded sequence  $y(n)$ .

$$y(n) = \{x(-n)\}$$

In MATLAB, this operation is implemented by **fliplr(x)** function for sample values and by **-fliplr(n)** function for sample positions, as shown in the **sigfold** function.

```

function [y,n] = sigfold(x,n)
% Implements y(n) = x(-n)
%
% [y,n] = sigfold(x,n)
%
y = fliplr(x); n = -fliplr(n);

```

6. **Sample summation:** This operation differs from the signal addition operation. It adds all sample values of  $x(n)$  between  $n_1$  and  $n_2$ .

$$\sum_{n=n_1}^{n_2} x(n) = x(n_1) + \cdots + x(n_2)$$

It is implemented by the `sum(x(n1:n2))` function.

7. **Sample products:** This operation also differs from the signal multiplication operation. It multiplies all sample values of  $x(n)$  between  $n_1$  and  $n_2$ .

$$\prod_{n_1}^{n_2} x(n) = x(n_1) \times \cdots \times x(n_2)$$

It is implemented by the `prod(x(n1:n2))` function.

8. **Signal energy:** The energy of a sequence  $x(n)$  is given by

$$\mathcal{E}_x = \sum_{-\infty}^{\infty} x(n)x^*(n) = \sum_{-\infty}^{\infty} |x(n)|^2$$

where superscript \* denotes the operation of complex conjugation.<sup>1</sup> The energy of a finite-duration sequence  $x(n)$  can be computed in MATLAB using

```
>> Ex = sum(x .* conj(x)); % One approach
>> Ex = sum(abs(x) .^ 2); % Another approach
```

9. **Signal power:** The average power of a periodic sequence  $\tilde{x}(n)$  with fundamental period  $N$  is given by

$$\mathcal{P}_x = \frac{1}{N} \sum_0^{N-1} |\tilde{x}(n)|^2$$

- **EXAMPLE 2.1** Generate and plot each of the following sequences over the indicated interval.

- a.  $x(n) = 2\delta(n+2) - \delta(n-4)$ ,  $-5 \leq n \leq 5$ .
- b.  $x(n) = n[u(n) - u(n-10)] + 10e^{-0.3(n-10)}[u(n-10) - u(n-20)]$ ,  $0 \leq n \leq 20$ .
- c.  $x(n) = \cos(0.04\pi n) + 0.2w(n)$ ,  $0 \leq n \leq 50$ , where  $w(n)$  is a Gaussian random sequence with zero mean and unit variance.
- d.  $\tilde{x}(n) = \{..., 5, 4, 3, 2, 1, 5, 4, 3, 2, 1, 5, 4, 3, 2, 1, ...\}$ ;  $-10 \leq n \leq 9$ .  
↑

<sup>1</sup>The symbol \* denotes many operations in digital signal processing. Its font (roman or computer) and its position (normal or superscript) will distinguish each operation.

**Solution**

$$\text{a. } x(n) = 2\delta(n+2) - \delta(n-4), \quad -5 \leq n \leq 5.$$

```
>> n = [-5:5];
>> x = 2*impseq(-2,-5,5) - impseq(4,-5,5);
>> stem(n,x); title('Sequence in Problem 2.1a')
>> xlabel('n'); ylabel('x(n)');
```

The plot of the sequence is shown in Figure 2.1.

$$\text{b. } x(n) = n[u(n) - u(n-10)] + 10e^{-0.3(n-10)}[u(n-10) - u(n-20)], \quad 0 \leq n \leq 20.$$

```
>> n = [0:20]; x1 = n.* (stepseq(0,0,20)-stepseq(10,0,20));
>> x2 = 10*exp(-0.3*(n-10)).*(stepseq(10,0,20)-stepseq(20,0,20));
>> x = x1+x2;
>> subplot(2,2,3); stem(n,x); title('Sequence in Problem 2.1b')
>> xlabel('n'); ylabel('x(n)');
```

The plot of the sequence is shown in Figure 2.1.

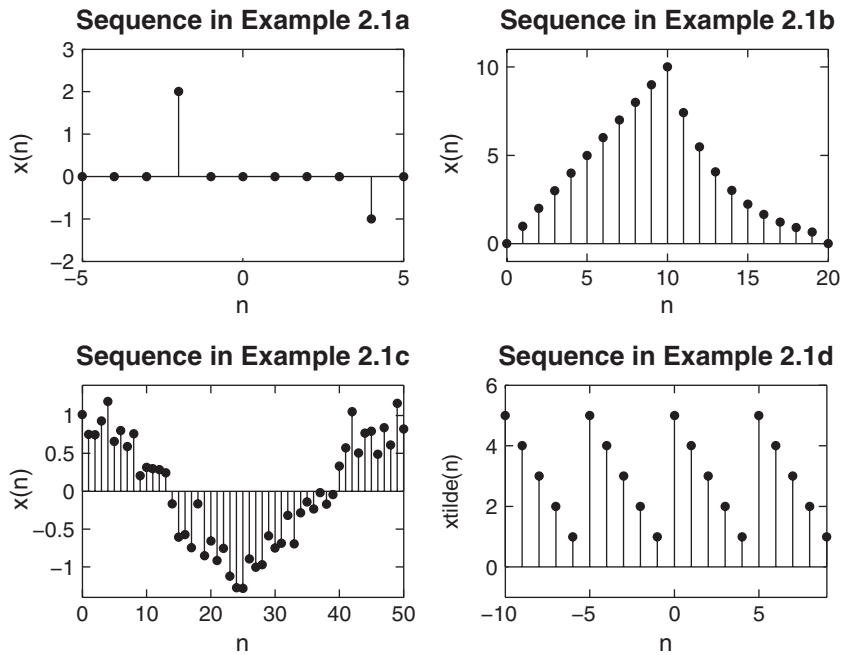


**FIGURE 2.1** Sequences in Example 2.1

c.  $x(n) = \cos(0.04\pi n) + 0.2w(n)$ ,  $0 \leq n \leq 50$ .

```
>> n = [0:50]; x = cos(0.04*pi*n)+0.2*randn(size(n));
>> subplot(2,2,2); stem(n,x); title('Sequence in Problem 2.1c')
>> xlabel('n'); ylabel('x(n)');
```

The plot of the sequence is shown in Figure 2.1.

d.  $\tilde{x}(n) = \{..., 5, 4, 3, 2, 1, 5, 4, 3, 2, 1, 5, 4, 3, 2, 1, ... \}$ ;  $-10 \leq n \leq 9$ .

↑

Note that over the given interval, the sequence  $\tilde{x}(n)$  has four periods.

```
>> n = [-10:9]; x = [5,4,3,2,1];
>> xtilde = x' * ones(1,4); xtilde = (xtilde(:))';
>> subplot(2,2,4); stem(n,xtilde); title('Sequence in Problem 2.1d')
>> xlabel('n'); ylabel('xtilde(n)');
```

The plot of the sequence is shown in Figure 2.1.  $\square$

□ **EXAMPLE 2.2** Let  $x(n) = \{1, 2, 3, 4, 5, \underset{\uparrow}{6}, 7, 6, 5, 4, 3, 2, 1\}$ . Determine and plot the following sequences.

- a.  $x_1(n) = 2x(n - 5) - 3x(n + 4)$
- b.  $x_2(n) = x(3 - n) + x(n)x(n - 2)$

### Solution

The sequence  $x(n)$  is nonzero over  $-2 \leq n \leq 10$ . Hence

```
>> n = -2:10; x = [1:7,6:-1:1];
```

will generate  $x(n)$ .

a.  $x_1(n) = 2x(n - 5) - 3x(n + 4)$ .

The first part is obtained by shifting  $x(n)$  by 5, and the second part by shifting  $x(n)$  by -4. This shifting and the addition can be easily done using the **sigshift** and the **sigadd** functions.

```
>> [x11,n11] = sigshift(x,n,5); [x12,n12] = sigshift(x,n,-4);
>> [x1,n1] = sigadd(2*x11,n11,-3*x12,n12);
>> subplot(2,1,1); stem(n1,x1); title('Sequence in Example 2.2a')
>> xlabel('n'); ylabel('x1(n)');
```

The plot of  $x_1(n)$  is shown in Figure 2.2.

b.  $x_2(n) = x(3 - n) + x(n)x(n - 2)$ .

The first term can be written as  $x(-(n - 3))$ . Hence it is obtained by first folding  $x(n)$  and then shifting the result by 3. The second part is a multiplication of  $x(n)$  and  $x(n - 2)$ , both of which have the same length but different

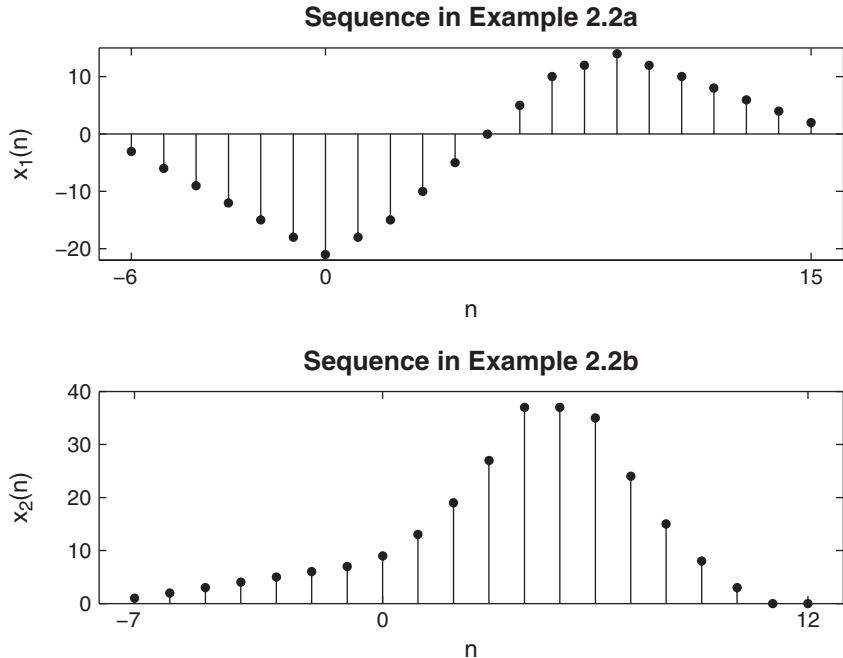


**FIGURE 2.2** Sequences in Example 2.2

support (or sample positions). These operations can be easily done using the **sigfold** and the **sigmult** functions.

```
>> [x21,n21] = sigfold(x,n); [x21,n21] = sigshift(x21,n21,3);
>> [x22,n22] = sigshift(x,n,2); [x22,n22] = sigmult(x,n,x22,n22);
>> [x2,n2] = sigadd(x21,n21,x22,n22);
>> subplot(2,1,2); stem(n2,x2); title('Sequence in Example 2.2b')
>> xlabel('n'); ylabel('x2(n)');
```

The plot of  $x_2(n)$  is shown in Figure 2.2. □

Example 2.2 shows that the four **sig\*** functions developed in this section provide a convenient approach for sequence manipulations.

□ **EXAMPLE 2.3** Generate the complex-valued signal

$$x(n) = e^{(-0.1+j0.3)n}, \quad -10 \leq n \leq 10$$

and plot its magnitude, its phase, its real part, and its imaginary part in four separate subplots.

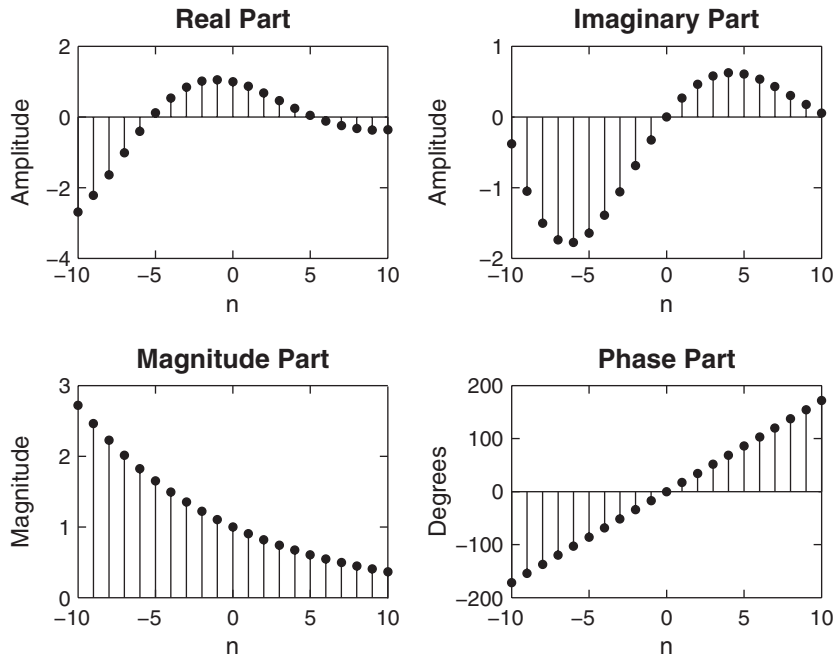


**FIGURE 2.3** Complex-valued sequence plots in Example 2.3

**Solution**

MATLAB script:

```
>> n = [-10:1:10]; alpha = -0.1+0.3j;
>> x = exp(alpha*n);
>> subplot(2,2,1); stem(n,real(x));title('Real Part'); xlabel('n')
>> subplot(2,2,2); stem(n,imag(x));title('Imaginary Part'); xlabel('n')
>> subplot(2,2,3); stem(n,abs(x));title('Magnitude Part'); xlabel('n')
>> subplot(2,2,4); stem(n,(180/pi)*angle(x));title('Phase Part'); xlabel('n')
```

The plot of the sequence is shown in Figure 2.3. □

### 2.1.3 DISCRETE-TIME SINUSOIDS

In the last section, we introduced the discrete-time sinusoidal sequence  $x(n) = A \cos(\omega_0 n + \theta_0)$ , for all  $n$ , as one of the basic signals. This signal is very important in signal theory as a basis for Fourier transform and in system theory as a basis for steady-state analysis. It can be conveniently related to the continuous-time sinusoid  $x_a(t) = A \cos(\Omega_0 t + \theta_0)$  using an operation called *sampling* (Chapter 3), in which continuous-time sinusoidal values at equally spaced points  $t = nT_s$  are assigned to  $x(n)$ .

The quantity  $T_s$  is called the sampling interval, and  $\Omega_0 = \omega_0/T_s$  is called the analog frequency, measured in radians per second.

The fact that  $n$  is a discrete variable, whereas  $t$  is a continuous variable, leads to some important differences between discrete-time and continuous-time sinusoidal signals.

**Periodicity in time** From our definition of periodicity, the sinusoidal sequence is periodic if

$$x[n+N] = A \cos(\omega_0 n + \omega_0 N + \theta) = A \cos(\omega_0 n + \theta_0) = x[n] \quad (2.1)$$

This is possible if and only if  $\omega_0 N = 2\pi k$ , where  $k$  is an integer. This leads to the following important result (see Problem P2.5):

The sequence  $x(n) = A \cos(\omega_0 n + \theta_0)$  is periodic if and only if  $f_0 \triangleq \omega_0/2\pi = k/N$ , that is,  $f_0$  is a rational number. If  $k$  and  $N$  are a pair of prime numbers, then  $N$  is the fundamental period of  $x(n)$  and  $k$  represents an integer number of periods  $kT_s$  of the corresponding continuous-time sinusoid.

**Periodicity in frequency** From the definition of the discrete-time sinusoid, we can easily see that

$$\begin{aligned} A \cos[(\omega_0 + k2\pi)n + \theta_0] &= A \cos(\omega_0 n + kn2\pi + \theta_0) \\ &= A \cos(\omega_0 n + \theta_0) \end{aligned}$$

since  $(kn)2\pi$  is always an integer multiple of  $2\pi$ . Therefore, we have the following property:

The sequence  $x(n) = A \cos(\omega_0 n + \theta)$  is periodic in  $\omega_0$  with fundamental period  $2\pi$  and periodic in  $f_0$  with fundamental period 1.

This property has a number of very important implications:

1. Sinusoidal sequences with radian frequencies separated by integer multiples of  $2\pi$  are identical.
2. All distinct sinusoidal sequences have frequencies within an interval of  $2\pi$  radians. We shall use the so-called *fundamental* frequency ranges

$$-\pi < \omega \leq \pi \quad \text{or} \quad 0 \leq \omega < 2\pi \quad (2.2)$$

Therefore, if  $0 \leq \omega_0 < 2\pi$ , the frequencies  $\omega_0$  and  $\omega_0 + m2\pi$  are indistinguishable from the observation of the corresponding sequences.

3. Since  $A \cos[\omega_0(n + n_0) + \theta] = A \cos[\omega_0 n + (\omega_0 n_0 + \theta)]$ , a time shift is equivalent to a phase change.
4. The rate of oscillation of a discrete-time sinusoid increases as  $\omega_0$  increases from  $\omega_0 = 0$  to  $\omega_0 = \pi$ . However, as  $\omega_0$  increases from  $\omega_0 = \pi$  to  $\omega_0 = 2\pi$ , the oscillations become slower. Therefore, low frequencies (slow oscillations) are at the vicinity of  $\omega_0 = k2\pi$ , and high frequencies (rapid oscillations) are at the vicinity of  $\omega_0 = \pi + k2\pi$ .

### 2.1.4 SOME USEFUL RESULTS

There are several important results in discrete-time signal theory. We will discuss some that are useful in digital signal processing.

**Unit sample synthesis** Any arbitrary sequence  $x(n)$  can be synthesized as a weighted sum of delayed and scaled unit sample sequences, such as

$$x(n) = \sum_{k=-\infty}^{\infty} x(k)\delta(n-k) \quad (2.3)$$

We will use this result in the next section.

**Even and odd synthesis** A real-valued sequence  $x_e(n)$  is called even (symmetric) if

$$x_e(-n) = x_e(n)$$

Similarly, a real-valued sequence  $x_o(n)$  is called odd (antisymmetric) if

$$x_o(-n) = -x_o(n)$$

Then any arbitrary real-valued sequence  $x(n)$  can be decomposed into its even and odd components

$$x(n) = x_e(n) + x_o(n) \quad (2.4)$$

where the even and odd parts are given by

$$x_e(n) = \frac{1}{2} [x(n) + x(-n)] \quad \text{and} \quad x_o(n) = \frac{1}{2} [x(n) - x(-n)] \quad (2.5)$$

respectively. We will use this decomposition in studying properties of the Fourier transform. Therefore, it is a good exercise to develop a simple MATLAB function to decompose a given sequence into its even and odd components. Using MATLAB operations discussed so far, we can obtain the following `evenodd` function.

```
function [xe, xo, m] = evenodd(x,n)
% Real signal decomposition into even and odd parts
%
% [xe, xo, m] = evenodd(x,n)
%
if any(imag(x) ~= 0)
    error('x is not a real sequence')
end
m = -fliplr(n);
m1 = min([m,n]); m2 = max([m,n]); m = m1:m2;
nm = n(1)-m(1); n1 = 1:length(n);
x1 = zeros(1,length(m)); x1(n1+nm) = x; x = x1;
xe = 0.5*(x + fliplr(x)); xo = 0.5*(x - fliplr(x));
```

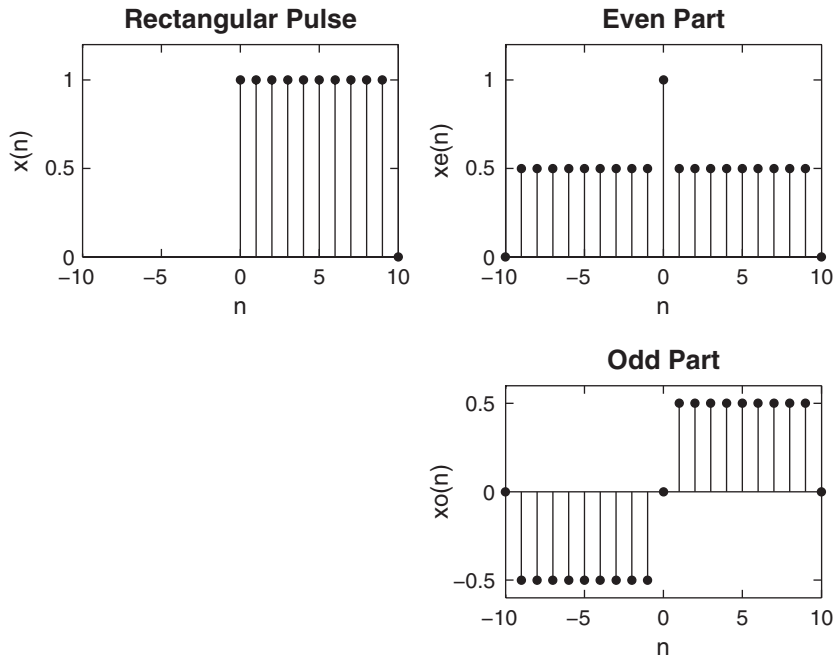


**FIGURE 2.4** Even-odd decomposition in Example 2.4

The sequence and its support are supplied in  $x$  and  $n$  arrays, respectively. It first checks if the given sequence is real and determines the support of the even and odd components in  $m$  array. It then implements (2.5) with special attention to the MATLAB indexing operation. The resulting components are stored in  $xe$  and  $xo$  arrays.

□ **EXAMPLE 2.4** Let  $x(n) = u(n) - u(n - 10)$ . Decompose  $x(n)$  into even and odd components.

#### Solution

The sequence  $x(n)$ , which is nonzero over  $0 \leq n \leq 9$ , is called a *rectangular pulse*. We will use MATLAB to determine and plot its even and odd parts.

```
>> n = [0:10]; x = stepseq(0,0,10)-stepseq(10,0,10);
>> [xe,xo,m] = evenodd(x,n);
>> subplot(2,2,1); stem(n,x); title('Rectangular Pulse')
>> xlabel('n'); ylabel('x(n)'); axis([-10,10,0,1.2])
>> subplot(2,2,2); stem(m,xe); title('Even Part')
>> xlabel('n'); ylabel('xe(n)'); axis([-10,10,0,1.2])
>> subplot(2,2,4); stem(m,xo); title('Odd Part')
>> xlabel('n'); ylabel('xo(n)'); axis([-10,10,-0.6,0.6])
```

The plots shown in Figure 2.4 clearly demonstrate the decomposition. □

A similar decomposition for complex-valued sequences is explored in Problem P2.5.

**The geometric series** A one-sided exponential sequence of the form  $\{\alpha^n, n \geq 0\}$ , where  $\alpha$  is an arbitrary constant, is called a geometric series. In digital signal processing, the convergence and expression for the sum of this series are used in many applications. The series converges for  $|\alpha| < 1$ , while the sum of its components converges to

$$\sum_{n=0}^{\infty} \alpha^n \rightarrow \frac{1}{1-\alpha}, \quad \text{for } |\alpha| < 1 \quad (2.6)$$

We will also need an expression for the sum of any finite number of terms of the series given by

$$\sum_{n=0}^{N-1} \alpha^n = \frac{1 - \alpha^N}{1 - \alpha}, \forall \alpha \quad (2.7)$$

These two results will be used throughout this book.

**Correlations of sequences** Correlation is an operation used in many applications in digital signal processing. It is a measure of the degree to which two sequences are similar. Given two real-valued sequences  $x(n)$  and  $y(n)$  of finite energy, the *cross-correlation* of  $x(n)$  and  $y(n)$  is a sequence  $r_{xy}(\ell)$  defined as

$$r_{xy}(\ell) = \sum_{n=-\infty}^{\infty} x(n)y(n-\ell) \quad (2.8)$$

The index  $\ell$  is called the shift or lag parameter. The special case of (2.8) when  $y(n) = x(n)$  is called *autocorrelation* and is defined by

$$r_{xx}(\ell) = \sum_{n=-\infty}^{\infty} x(n)x(n-\ell) \quad (2.9)$$

It provides a measure of self-similarity between different alignments of the sequence. MATLAB functions to compute auto- and cross-correlations are discussed later in the chapter.

## 2.2 DISCRETE SYSTEMS

---

Mathematically, a discrete-time system (or *discrete system* for short) is described as an operator  $T[\cdot]$  that takes a sequence  $x(n)$  (called *excitation*) and transforms it into another sequence  $y(n)$  (called *response*). That is,

$$y(n) = T[x(n)]$$

In DSP, we will say that the system processes an *input* signal into an *output* signal. Discrete systems are broadly classified into *linear* and *nonlinear* systems. We will deal mostly with linear systems.

### 2.2.1 LINEAR SYSTEMS

A discrete system  $T[\cdot]$  is a linear operator  $L[\cdot]$  if and only if  $L[\cdot]$  satisfies the principle of superposition, namely,

$$L[a_1x_1(n) + a_2x_2(n)] = a_1L[x_1(n)] + a_2L[x_2(n)], \forall a_1, a_2, x_1(n), x_2(n) \quad (2.10)$$

Using (2.3) and (2.10), the output  $y(n)$  of a linear system to an arbitrary input  $x(n)$  is given by

$$y(n) = L[x(n)] = L\left[\sum_{n=-\infty}^{\infty} x(k) \delta(n-k)\right] = \sum_{n=-\infty}^{\infty} x(k)L[\delta(n-k)]$$

The response  $L[\delta(n-k)]$  can be interpreted as the response of a linear system at time  $n$  due to a unit sample (a well-known sequence) at time  $k$ . It is called an *impulse response* and is denoted by  $h(n, k)$ . The output then is given by the *superposition summation*

$$y(n) = \sum_{n=-\infty}^{\infty} x(k)h(n, k) \quad (2.11)$$

The computation of (2.11) requires the *time-varying* impulse response  $h(n, k)$ , which in practice is not very convenient. Therefore, time-invariant systems are widely used in DSP.

**EXAMPLE 2.5** Determine whether the following systems are linear.

1.  $y(n) = T[x(n)] = 3x^2(n)$
2.  $y(n) = 2x(n-2) + 5$
3.  $y(n) = x(n+1) - x(n-1)$

**Solution**

Let  $y_1(n) = T[x_1(n)]$  and  $y_2(n) = T[x_2(n)]$ . We will determine the response of each system to the linear combination  $a_1x_1(n) + a_2x_2(n)$  and check whether it is equal to the linear combination  $a_1y_1(n) + a_2y_2(n)$  where  $a_1$  and  $a_2$  are arbitrary constants.

1.  $y(n) = T[x(n)] = 3x^2(n)$ : Consider

$$\begin{aligned} T[a_1x_1(n) + a_2x_2(n)] &= 3[a_1x_1(n) + a_2x_2(n)]^2 \\ &= 3a_1^2x_1^2(n) + 3a_2^2x_2^2(n) + 6a_1a_2x_1(n)x_2(n) \end{aligned}$$

which is not equal to

$$a_1y_1(n) + a_2y_2(n) = 3a_1^2x_1^2(n) + 3a_2^2x_2^2(n)$$

Hence the given system is nonlinear.

2.  $y(n) = 2x(n - 2) + 5$ : Consider

$$\begin{aligned} T[a_1x_1(n) + a_2x_2(n)] &= 2[a_1x_1(n - 2) + a_2x_2(n - 2)] + 5 \\ &= a_1y_1(n) + a_2y_2(n) - 5 \end{aligned}$$

Clearly, the given system is nonlinear even though the input-output relation is a straight-line function.

3.  $y(n) = x(n + 1) - x(1 - n)$ : Consider

$$\begin{aligned} T[a_1x_1(n) + a_2x_2(n)] &= a_1x_1(n + 1) + a_2x_2(n + 1) + a_1x_1(1 - n) \\ &\quad + a_2x_2(1 - n) \\ &= a_1[x_1(n + 1) - x_1(1 - n)] \\ &\quad + a_2[x_2(n + 1) - x_2(1 - n)] \\ &= a_1y_1(n) + a_2y_2(n) \end{aligned}$$

Hence the given system is linear. □

**Linear time-invariant (LTI) system** A linear system in which an input-output pair,  $x(n)$  and  $y(n)$ , is invariant to a shift  $k$  in time is called a linear time-invariant system, that is,

$$y(n) = L[x(n)] \Rightarrow L[x(n - k)] = y(n - k) \quad (2.12)$$

For an LTI system, the  $L[\cdot]$  and the shifting operators are reversible as shown here.

$$x(n) \longrightarrow \boxed{L[\cdot]} \longrightarrow y(n) \longrightarrow \boxed{\text{Shift by } k} \longrightarrow y(n - k)$$

$$x(n) \longrightarrow \boxed{\text{Shift by } k} \longrightarrow x(n - k) \longrightarrow \boxed{L[\cdot]} \longrightarrow y(n - k)$$

□ **EXAMPLE 2.6** Determine whether the following linear systems are time-invariant.

1.  $y(n) = L[x(n)] = 10 \sin(0.1\pi n)x(n)$
2.  $y(n) = L[x(n)] = x(n + 1) - x(1 - n)$
3.  $y(n) = L[x(n)] = \frac{1}{4}x(n) + \frac{1}{2}x(n - 1) + \frac{1}{4}x(n - 2)$

**Solution**

First we will compute the response  $y_k(n) \triangleq L[x(n - k)]$  to the shifted input sequence. This is obtained by subtracting  $k$  from the arguments of

every input sequence term on the right-hand side of the linear transformation. To determine time-invariance, we will then compare it to the shifted output sequence  $y(n - k)$ , obtained after replacing every  $n$  by  $(n - k)$  on the right-hand side of the linear transformation.

1.  $y(n) = L[x(n)] = 10 \sin(0.1\pi n)x(n)$ : The response due to shifted input is

$$y_k(n) = L[x(n - k)] = 10 \sin(0.1\pi n)x(n - k)$$

while the shifted output is

$$y(n - k) = 10 \sin[0.1\pi(n - k)]x(n - k) \neq y_k(n)$$

Hence the given system is not time-invariant.

2.  $y(n) = L[x(n)] = x(n + 1) - x(1 - n)$ : The response due to shifted input is

$$y_k(n) = L[x(n - k)] = x(n - k + 1) - x(1 - n - k)$$

while the shifted output is

$$y(n - k) = x(n - k) - x(1 - [n - k]) = x(n - k + 1) - x(1 - n + k) \neq y_k(n).$$

Hence the given system is not time-invariant.

3.  $y(n) = L[x(n)] = \frac{1}{4}x(n) + \frac{1}{2}x(n - 1) + \frac{1}{4}x(n - 2)$ : The response due to shifted input is

$$y_k(n) = L[x(n - k)] = \frac{1}{4}x(n - k) + \frac{1}{2}x(n - 1 - k) + \frac{1}{4}x(n - 2 - k)$$

while the shifted output is

$$y(n - k) = \frac{1}{4}x(n - k) + \frac{1}{2}x(n - k - 1) + \frac{1}{4}x(n - k - 2) = y_k(n)$$

Hence the given system is time-invariant.  $\square$

We will denote an LTI system by the operator  $LTI[\cdot]$ . Let  $x(n)$  and  $y(n)$  be the input-output pair of an LTI system. Then the time-varying function  $h(n, k)$  becomes a time-invariant function  $h(n - k)$ , and the output from (2.11) is given by

$$y(n) = LTI[x(n)] = \sum_{k=-\infty}^{\infty} x(k)h(n - k) \quad (2.13)$$

The impulse response of an LTI system is given by  $h(n)$ . The mathematical operation in (2.13) is called a *linear convolution sum* and is denoted by

$$y(n) \triangleq x(n) * h(n) \quad (2.14)$$

Hence an LTI system is completely characterized in the time domain by the impulse response  $h(n)$ .

$$x(n) \longrightarrow \boxed{h(n)} \longrightarrow y(n) = x(n) * h(n)$$

We will explore several properties of the convolution in Problem P2.14.

**Stability** This is a very important concept in linear system theory. The primary reason for considering stability is to avoid building harmful systems or to avoid burnout or saturation in the system operation. A system is said to be *bounded-input bounded-output (BIBO) stable* if every bounded input produces a bounded output.

$$|x(n)| < \infty \Rightarrow |y(n)| < \infty, \forall x, y$$

An LTI system is BIBO stable if and only if its impulse response is *absolutely summable*.

$$\text{BIBO Stability} \iff \sum_{-\infty}^{\infty} |h(n)| < \infty \quad (2.15)$$

**Causality** This important concept is necessary to make sure that systems can be built. A system is said to be causal if the output at index  $n_0$  depends only on the input up to and including the index  $n_0$ ; that is, the output does not depend on the future values of the input. An LTI system is causal if and only if the impulse response

$$h(n) = 0, \quad n < 0 \quad (2.16)$$

Such a sequence is termed a *causal sequence*. In signal processing, unless otherwise stated, we will always assume that the system is causal.

## 2.3 CONVOLUTION

---

We introduced the convolution operation (2.14) to describe the response of an LTI system. In DSP, it is an important operation and has many other uses that we will see throughout this book. Convolution can be evaluated in many different ways. If the sequences are mathematical functions (of finite or infinite duration), then we can analytically evaluate (2.14) for all  $n$  to obtain a functional form of  $y(n)$ .

- **EXAMPLE 2.7** Let the rectangular pulse  $x(n) = u(n) - u(n - 10)$  of Example 2.4 be an input to an LTI system with impulse response

$$h(n) = (0.9)^n u(n)$$

Determine the output  $y(n)$ .

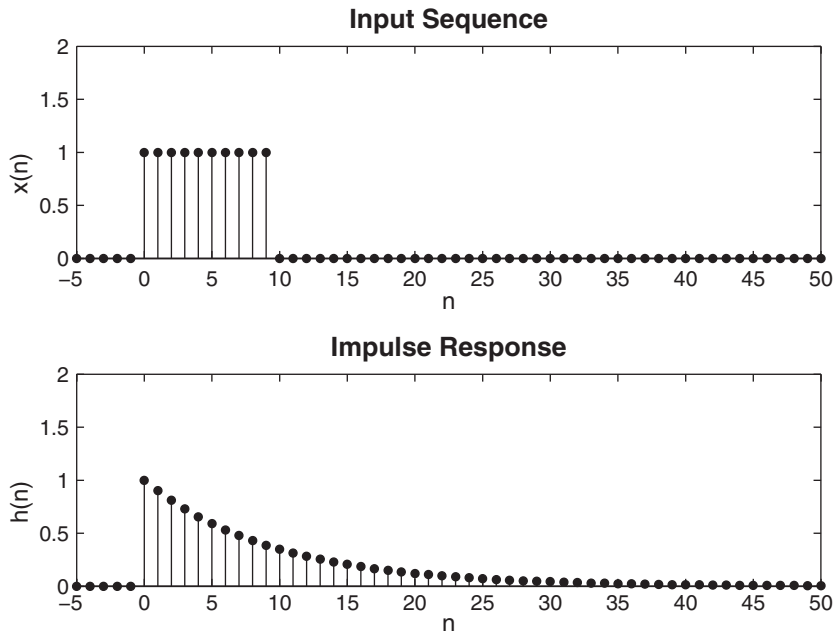


**FIGURE 2.5** The input sequence and the impulse response in Example 2.7

### Solution

The input  $x(n)$  and the impulse response  $h(n)$  are shown in Figure 2.5. From (2.14),

$$y(n) = \sum_{k=0}^9 (1)(0.9)^{(n-k)} u(n-k) = (0.9)^n \sum_{k=0}^9 (0.9)^{-k} u(n-k) \quad (2.17)$$

The sum in (2.17) is almost a geometric series sum except that the term  $u(n-k)$  takes different values depending on  $n$  and  $k$ . There are three possible conditions under which  $u(n-k)$  can be evaluated.

**CASE i**  $n < 0$ : Then  $u(n-k) = 0$ ,  $0 \leq k \leq 9$ . Hence, from (2.17),

$$y(n) = 0 \quad (2.18)$$

In this case, the nonzero values of  $x(n)$  and  $h(n)$  do not overlap.

**CASE ii**  $0 \leq n < 9$ : Then  $u(n-k) = 1$ ,  $0 \leq k \leq n$ . Hence, from (2.17),

$$\begin{aligned} y(n) &= (0.9)^n \sum_{k=0}^n (0.9)^{-k} = (0.9)^n \sum_{k=0}^n [(0.9)^{-1}]^k \\ &= (0.9)^n \frac{1 - (0.9)^{-(n+1)}}{1 - (0.9)^{-1}} = 10[1 - (0.9)^{n+1}], \quad 0 \leq n < 9 \end{aligned} \quad (2.19)$$

In this case, the impulse response  $h(n)$  partially overlaps the input  $x(n)$ .

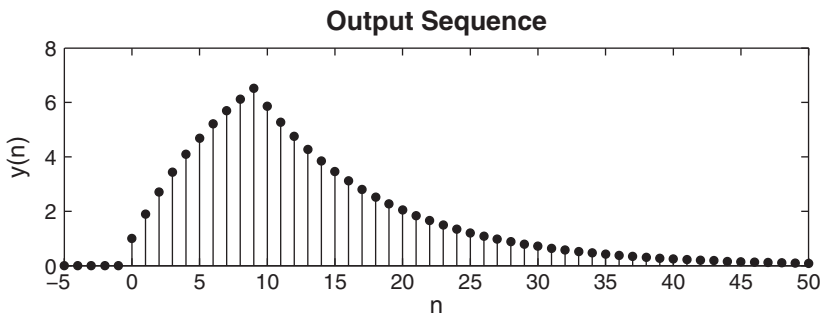


FIGURE 2.6 The output sequence in Example 2.7

**CASE iii**  $n \geq 9$ : Then  $u(n-k) = 1$ ,  $0 \leq k \leq 9$ , and from (2.17),

$$\begin{aligned} y(n) &= (0.9)^n \sum_{k=0}^9 (0.9)^{-k} \\ &= (0.9)^n \frac{1 - (0.9)^{-10}}{1 - (0.9)^{-1}} = 10(0.9)^{n-9}[1 - (0.9)^{10}], \quad n \geq 9 \end{aligned} \quad (2.20)$$

In this last case,  $h(n)$  completely overlaps  $x(n)$ .

The complete response is given by (2.18), (2.19), and (2.20). It is shown in Figure 2.6, which depicts the distortion of the input pulse.  $\square$

This example can also be done using a method called graphical convolution, in which (2.14) is given a graphical interpretation. In this method,  $h(n-k)$  is interpreted as a *folded-and-shifted* version of  $h(k)$ . The output  $y(n)$  is obtained as a sample sum under the overlap of  $x(k)$  and  $h(n-k)$ . We use an example to illustrate this.

$\square$  **EXAMPLE 2.8** Given the two sequences

$$x(n) = [3, 11, 7, 0, -1, 4, 2], \quad -3 \leq n \leq 3; \quad h(n) = [2, 3, 0, -5, 2, 1], \quad -1 \leq n \leq 4$$

determine the convolution  $y(n) = x(n) * h(n)$ .

### Solution

In Figure 2.7, we show four plots. The top-left plot shows  $x(k)$  and  $h(k)$ , the original sequences. The top-right plot shows  $x(k)$  and  $h(-k)$ , the folded version of  $h(k)$ . The bottom-left plot shows  $x(k)$  and  $h(-1-k)$ , the “folded and shifted by  $-1$ ” version of  $h(k)$ . Then

$$\sum_k x(k)h(-1-k) = 3 \times (-5) + 11 \times 0 + 7 \times 3 + 0 \times 2 = 6 = y(-1)$$

The bottom-right plot shows  $x(k)$  and  $h(2-k)$ , the “folded and shifted by  $2$ ” version of  $h(k)$ , which gives

$$\sum_k x(k)h(2-k) = 11 \times 1 + 7 \times 2 + 0 \times (-5) + (-1) \times 0 + 4 \times 3 + 2 \times 2 = 41 = y(2)$$

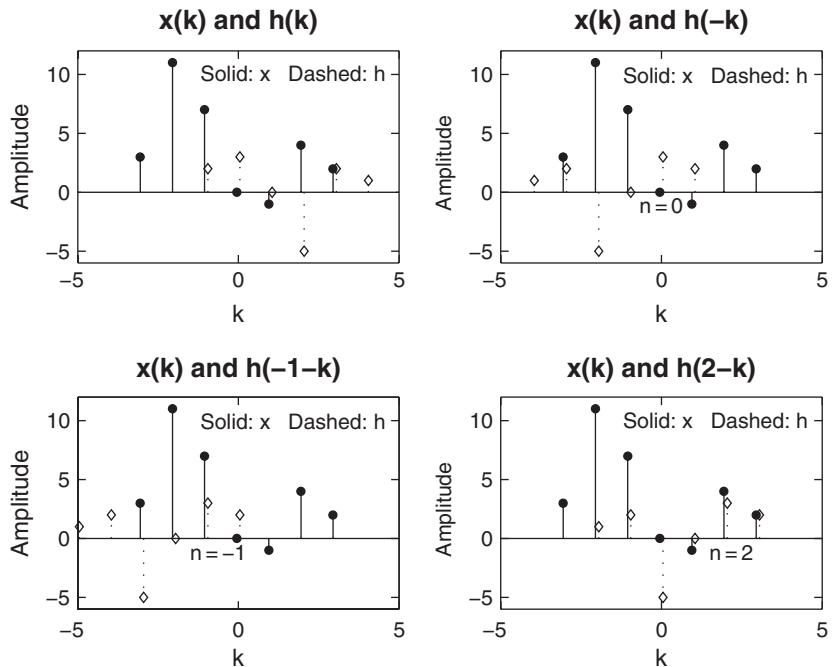


**FIGURE 2.7** Graphical convolution in Example 2.8

Thus we have obtained two values of  $y(n)$ . Similar graphical calculations can be done for other remaining values of  $y(n)$ . Note that the beginning point (first nonzero sample) of  $y(n)$  is given by  $n = -3 + (-1) = -4$ , while the end point (the last nonzero sample) is given by  $n = 3 + 4 = 7$ . The complete output is given by

$$y(n) = \{6, 31, 47, 6, -51, -5, 41, 18, -22, -3, 8, 2\}$$

Students are strongly encouraged to verify the above result. Note that the resulting sequence  $y(n)$  has a *longer length* than both the  $x(n)$  and  $h(n)$  sequences.  $\square$

### 2.3.1 MATLAB IMPLEMENTATION

If arbitrary sequences are of infinite duration, then MATLAB cannot be used *directly* to compute the convolution. MATLAB does provide a built-in function called `conv` that computes the convolution between two finite-duration sequences. The `conv` function assumes that the two sequences begin at  $n = 0$  and is invoked by

```
>> y = conv(x,h);
```

For example, to do the convolution in Example 2.7, we could use

```
>> x = [3, 11, 7, 0, -1, 4, 2]; h = [2, 3, 0, -5, 2, 1];
>> y = conv(x, h)
y =
    6     31     47     6    -51    -5     41     18    -22    -3     8     2
```

to obtain the correct  $y(n)$  values. However, the `conv` function neither provides nor accepts any timing information if the sequences have arbitrary support. What is needed is a beginning point and an end point of  $y(n)$ . Given finite duration  $x(n)$  and  $h(n)$ , it is easy to determine these points. Let

$$\{x(n); n_{xb} \leq n \leq n_{xe}\} \quad \text{and} \quad \{h(n); n_{hb} \leq n \leq n_{he}\}$$

be two finite-duration sequences. Then referring to Example 2.8, we observe that the beginning and end points of  $y(n)$  are

$$n_{yb} = n_{xb} + n_{hb} \quad \text{and} \quad n_{ye} = n_{xe} + n_{he}$$

respectively. A simple modification of the `conv` function, called `conv_m`, which performs the convolution of arbitrary support sequences, can now be designed.

```
function [y,ny] = conv_m(x,nx,h,nh)
% Modified convolution routine for signal processing
%
% [y,ny] = conv_m(x,nx,h,nh)
% [y,ny] = convolution result
% [x,nx] = first signal
% [h,nh] = second signal
%
nyb = nx(1)+nh(1); nye = nx(length(x)) + nh(length(h));
ny = [nyb:nye]; y = conv(x,h);
```

- **EXAMPLE 2.9** Perform the convolution in Example 2.8 using the `conv_m` function.

**Solution** MATLAB script:

```
>> x = [3, 11, 7, 0, -1, 4, 2]; nx = [-3:3];
>> h = [2, 3, 0, -5, 2, 1]; nh = [-1:4];
```

```
>> [y,ny] = conv_m(x,nx,h,nh)
y =
    6     31     47     6    -51    -5     41     18    -22    -3     8     2
ny =
   -4     -3     -2     -1      0      1      2      3      4      5      6      7
```

Hence

$$y(n) = \{6, 31, 47, 6, -51, -5, 41, 18, -22, -3, 8, 2\}$$

as in Example 2.8. □

An alternate method in MATLAB can be used to perform the convolution. This method uses a matrix-vector multiplication approach, which we will explore in Problem P2.17.

### 2.3.2 SEQUENCE CORRELATIONS REVISITED

If we compare the convolution operation (2.14) with that of the cross-correlation of two sequences defined in (2.8), we observe a close resemblance. The cross-correlation  $r_{yx}(\ell)$  can be put in the form

$$r_{yx}(\ell) = y(\ell) * x(-\ell)$$

with the autocorrelation  $r_{xx}(\ell)$  in the form

$$r_{xx}(\ell) = x(\ell) * x(-\ell)$$

Therefore, these correlations can be computed using the `conv_m` function if sequences are of finite duration.

- **EXAMPLE 2.10** In this example, we will demonstrate one application of the cross-correlation sequence. Let

$$x(n) = [3, 11, 7, 0, -1, 4, 2]$$

be a prototype sequence, and let  $y(n)$  be its noise-corrupted-and-shifted version

$$y(n) = x(n - 2) + w(n)$$

where  $w(n)$  is a Gaussian sequence with mean 0 and variance 1. Compute the cross-correlation between  $y(n)$  and  $x(n)$ .

#### Solution

From the construction of  $y(n)$ , it follows that  $y(n)$  is “similar” to  $x(n - 2)$  and hence their cross-correlation would show the strongest similarity at  $\ell = 2$ . To test this out using MATLAB, let us compute the cross-correlation using two different noise sequences.

```
% Noise sequence 1
>> x = [3, 11, 7, 0, -1, 4, 2]; nx=[-3:3]; % Given signal x(n)
>> [y,ny] = sigshift(x,nx,2); % Obtain x(n-2)
>> w = randn(1,length(y)); nw = ny; % Generate w(n)
>> [y,ny] = sigadd(y,ny,w,nw); % Obtain y(n) = x(n-2) + w(n)
>> [x,nx] = sigfold(x,nx); % Obtain x(-n)
```

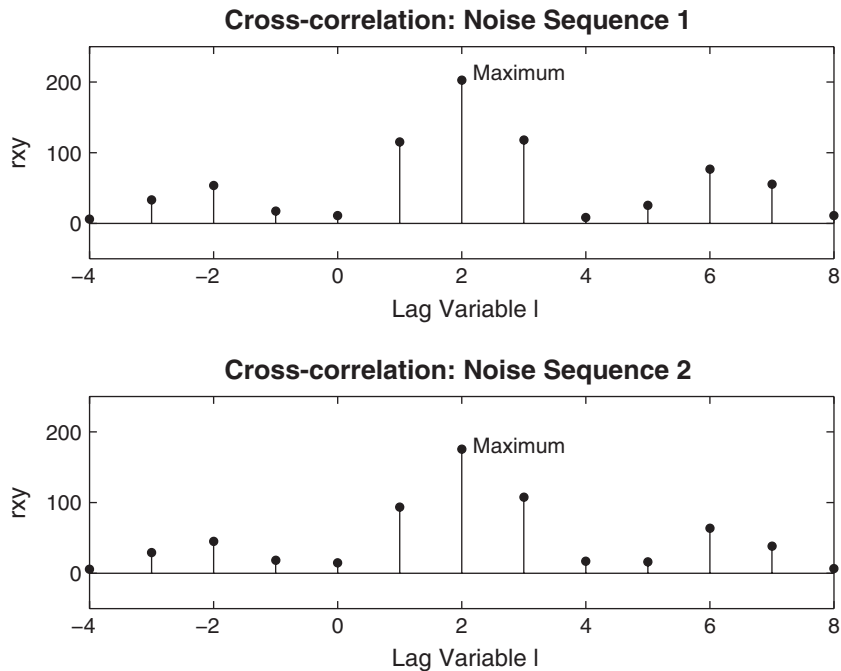


**FIGURE 2.8** Cross-correlation sequence with two different noise realizations

```

>> [rxy,nrxy] = conv_m(y,ny,x,nx); % Cross-correlation
>> subplot(1,1,1), subplot(2,1,1);stem(nrxy,rxy)
>> axis([-5,10,-50,250]); xlabel('Lag Variable 1')
>> ylabel('rxy'); title('Cross-correlation: Noise Sequence 1')
%
% Noise sequence 2
>> x = [3, 11, 7, 0, -1, 4, 2]; nx=[-3:3]; % Given signal x(n)
>> [y,ny] = sigshift(x,nx,2); % Obtain x(n-2)
>> w = randn(1,length(y)); nw = ny; % Generate w(n)
>> [y,ny] = sigadd(y,ny,w,nw); % Obtain y(n) = x(n-2) + w(n)
>> [x,nx] = sigfold(x,nx); % Obtain x(-n)
>> [rxy,nrxy] = conv_m(y,ny,x,nx); % Cross-correlation
>> subplot(2,1,2);stem(nrxy,rxy)
>> axis([-5,10,-50,250]); xlabel('Lag Variable 1')
>> ylabel('rxy'); title('Cross-correlation: Noise sequence 2')

```

From Figure 2.8, we observe that the cross-correlation indeed peaks at  $\ell = 2$ , which implies that  $y(n)$  is similar to  $x(n)$  shifted by 2. This approach can be used in applications like radar signal processing in identifying and localizing targets.  $\square$

Note that the signal-processing toolbox in MATLAB also provides a function called **xcorr** for sequence correlation computations. In its simplest form,

```
>> xcorr(x,y)
```

computes the cross-correlation between vectors **x** and **y**, while

```
>> xcorr(x)
```

computes the autocorrelation of vector **x**. It generates results that are identical to the one obtained from the proper use of the **conv\_m** function. However, the **xcorr** function cannot provide the timing (or lag) information (as done by the **conv\_m** function), which then must be obtained by some other means.

## 2.4 DIFFERENCE EQUATIONS

---

An LTI discrete system can also be described by a linear constant coefficient difference equation of the form

$$\sum_{k=0}^N a_k y(n-k) = \sum_{m=0}^M b_m x(n-m), \quad \forall n \quad (2.21)$$

If  $a_N \neq 0$ , then the difference equation is of order  $N$ . This equation describes a recursive approach for computing the current output, given the input values and previously computed output values. In practice, this equation is computed forward in time, from  $n = -\infty$  to  $n = \infty$ . Therefore, another form of this equation is

$$y(n) = \sum_{m=0}^M b_m x(n-m) - \sum_{k=1}^N a_k y(n-k) \quad (2.22)$$

A solution to this equation can be obtained in the form

$$y(n) = y_H(n) + y_P(n)$$

The *homogeneous part* of the solution,  $y_H(n)$ , is given by

$$y_H(n) = \sum_{k=1}^N c_k z_k^n$$

where  $z_k, k = 1, \dots, N$  are  $N$  roots (also called *natural frequencies*) of the characteristic equation

$$\sum_0^N a_k z^{N-k} = 0$$

This characteristic equation is important in determining the stability of systems. If the roots  $z_k$  satisfy the condition

$$|z_k| < 1, k = 1, \dots, N \quad (2.23)$$

then a causal system described by (2.22) is stable. The *particular part* of the solution,  $y_P(n)$ , is determined from the right-hand side of (2.21). In Chapter 4, we will discuss the analytical approach of solving difference equations using the  $z$ -transform.

#### 2.4.1 MATLAB IMPLEMENTATION

A function called `filter` is available to solve difference equations numerically, given the input and the difference equation coefficients. In its simplest form, this function is invoked by

```
y = filter(b,a,x)
```

where

```
b = [b0, b1, ..., bM]; a = [a0, a1, ..., aN];
```

are the coefficient arrays from the equation given in (2.21) and  $x$  is the input sequence array. The output  $y$  has the same length as input  $x$ . One must ensure that the coefficient  $a_0$  not be zero.

To compute and plot impulse response, MATLAB provides the function `impz`. When invoked by

```
h = impz(b,a,n);
```

it computes samples of the impulse response of the filter at the sample indices given in  $n$  with numerator coefficients in  $b$  and denominator coefficients in  $a$ . When no output arguments are given, the `impz` function plots the response in the current figure window using the `stem` function. We will illustrate the use of these functions in the following example.

- **EXAMPLE 2.11** Consider the following difference equation:

$$y(n) - y(n - 1) + 0.9y(n - 2) = x(n); \quad \forall n$$

- a. Calculate and plot the impulse response  $h(n)$  at  $n = -20, \dots, 100$ .
- b. Calculate and plot the unit step response  $s(n)$  at  $n = -20, \dots, 100$ .
- c. Is the system specified by  $h(n)$  stable?

**Solution**

From the given difference equation, the coefficient arrays are

```
b = [1]; a=[1, -1, 0.9];
```

**a. MATLAB script:**

```
>> b = [1]; a = [1, -1, 0.9]; n = [-20:120];
>> h = impz(b,a,n);
>> subplot(2,1,1); stem(n,h);
>> title('Impulse Response'); xlabel('n'); ylabel('h(n)')
```

The plot of the impulse response is shown in Figure 2.9.

**b. MATLAB script:**

```
>> x = stepseq(0,-20,120); s = filter(b,a,x);
>> subplot(2,1,2); stem(n,s)
>> title('Step Response'); xlabel('n'); ylabel('s(n)')
```

The plot of the unit step response is shown in Figure 2.9.

- c.** To determine the stability of the system, we have to determine  $h(n)$  for all  $n$ . Although we have not described a method to solve the difference equation,

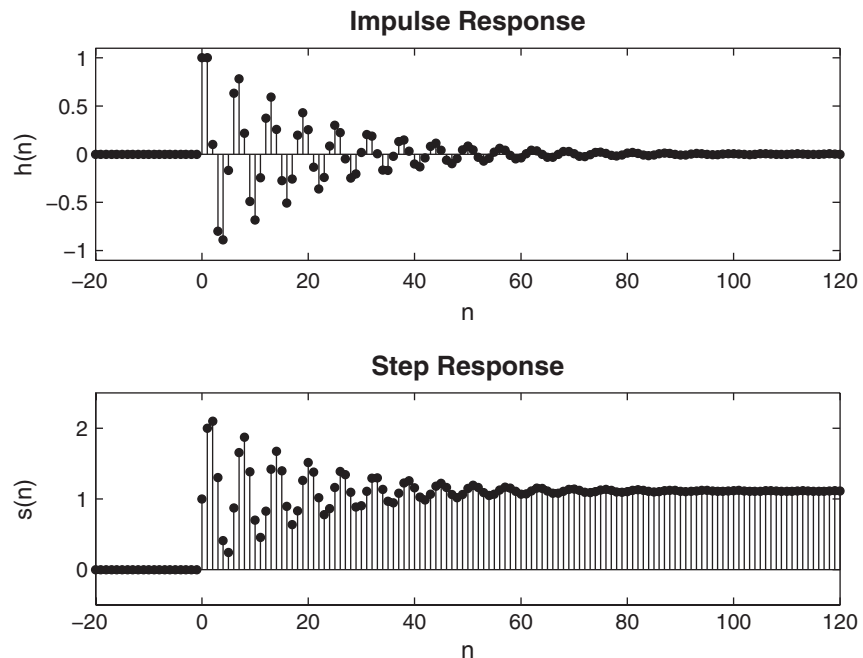


**FIGURE 2.9** Impulse response and step response plots in Example 2.11

we can use the plot of the impulse response to observe that  $h(n)$  is practically zero for  $n > 120$ . Hence the sum  $\sum |h(n)|$  can be determined from MATLAB using

```
>> sum(abs(h))
ans = 14.8785
```

which implies that the system is stable. An alternate approach is to use the stability condition (2.23) using MATLAB's **roots** function.

```
>>z = roots(a); magz = abs(z)
magz =
    0.9487
    0.9487
```

Since the magnitudes of both roots are less than 1, the system is stable.

□

In the previous section, we noted that if one or both sequences in the convolution are of infinite length, then the **conv** function cannot be used. If one of the sequences is of infinite length, then it is possible to use MATLAB for numerical evaluation of the convolution. This is done using the **filter** function, as we will see in the following example.

- **EXAMPLE 2.12** Let us consider the convolution given in Example 2.7. The input sequence is of finite duration

$$x(n) = u(n) - u(n - 10)$$

while the impulse response is of infinite duration

$$h(n) = (0.9)^n u(n)$$

Determine  $y(n) = x(n) * h(n)$ .

### Solution

If the LTI system, given by the impulse response  $h(n)$ , can be described by a difference equation, then  $y(n)$  can be obtained from the **filter** function. From the  $h(n)$  expression,

$$(0.9) h(n - 1) = (0.9) (0.9)^{n-1} u(n - 1) = (0.9)^n u(n - 1)$$

or

$$\begin{aligned} h(n) - (0.9) h(n - 1) &= (0.9)^n u(n) - (0.9)^n u(n - 1) \\ &= (0.9)^n [u(n) - u(n - 1)] = (0.9)^n \delta(n) \\ &= \delta(n) \end{aligned}$$

The last step follows from the fact that  $\delta(n)$  is nonzero only at  $n = 0$ . By definition,  $h(n)$  is the output of an LTI system when the input is  $\delta(n)$ . Hence substituting  $x(n)$  for  $\delta(n)$  and  $y(n)$  for  $h(n)$ , the difference equation is

$$y(n) - 0.9y(n - 1) = x(n)$$

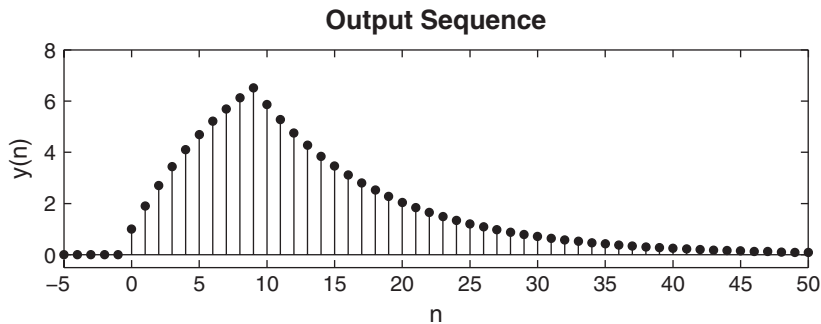


**FIGURE 2.10** Output sequence in Example 2.12

Now MATLAB's `filter` function can be used to compute the convolution indirectly.

```
>> b = [1]; a = [1, -0.9];
>> n = -5:50; x = stepseq(0,-5,50) - stepseq(10,-5,50);
>> y = filter(b,a,x);
>> subplot(2,1,2); stem(n,y); title('Output Sequence')
>> xlabel('n'); ylabel('y(n)'); axis([-5,50,-0.5,8])
```

The plot of the output is shown in Figure 2.10, which is exactly the same as that in Figure 2.6.  $\square$

In Example 2.12, the impulse response was a one-sided exponential sequence for which we could determine a difference equation representation. This means that not all infinite-length impulse responses can be converted into difference equations. The above analysis, however, can be extended to a linear combination of one-sided exponential sequences, which results in higher-order difference equations. We will discuss this topic of conversion from one representation to another one in Chapter 4.

#### 2.4.2 ZERO-INPUT AND ZERO-STATE RESPONSES

In DSP, the difference equation is generally solved forward in time from  $n = 0$ . Therefore, initial conditions on  $x(n)$  and  $y(n)$  are necessary to determine the output for  $n \geq 0$ . The difference equation is then given by

$$y(n) = \sum_{m=0}^M b_m x(n-m) - \sum_{k=1}^N a_k y(n-k); \quad n \geq 0 \quad (2.24)$$

subject to the initial conditions

$$\{y(n); -N \leq n \leq -1\} \quad \text{and} \quad \{x(n); -M \leq n \leq -1\}$$

A solution to (2.24) can be obtained in the form

$$y(n) = y_{ZI}(n) + y_{ZS}(n)$$

where  $y_{ZI}(n)$  is called the *zero-input* solution, which is a solution due to the initial conditions alone (assuming they exist), while the *zero-state* solution,  $y_{ZS}(n)$ , is a solution due to input  $x(n)$  alone (or assuming that the initial conditions are zero). In MATLAB, another form of the function `filter` can be used to solve for the difference equation, given its initial conditions. We will illustrate the use of this form in Chapter 4.

#### 2.4.3 DIGITAL FILTERS

*Filter* is a generic name that means a linear time-invariant system designed for a specific job of frequency selection or frequency discrimination. Hence discrete-time LTI systems are also called digital filters. There are two types of digital filters.

**FIR filter** If the unit impulse response of an LTI system is of finite duration, then the system is called a *finite-duration impulse response* (or FIR) filter. Hence, for an FIR filter,  $h(n) = 0$  for  $n < n_1$  and for  $n > n_2$ . The following part of the difference equation (2.21) describes a *causal* FIR filter:

$$y(n) = \sum_{m=0}^M b_m x(n-m) \quad (2.25)$$

Furthermore,  $h(0) = b_0$ ,  $h(1) = b_1, \dots, h(M) = b_M$ , while all other  $h(n)$ 's are 0. FIR filters are also called *nonrecursive* or *moving average* (MA) filters. In MATLAB, FIR filters are represented either as impulse response values  $\{h(n)\}$  or as difference equation coefficients  $\{b_m\}$  and  $\{a_0 = 1\}$ . Therefore, to implement FIR filters, we can use either the `conv(x,h)` function (and its modification that we discussed) or the `filter(b,1,x)` function. There is a difference in the outputs of these two implementations that should be noted. The output sequence from the `conv(x,h)` function has a *longer length* than both the  $x(n)$  and  $h(n)$  sequences. On the other hand, the output sequence from the `filter(b,1,x)` function has exactly the *same length* as the input  $x(n)$  sequence. In practice (and especially for processing signals), the use of the `filter` function is encouraged.

**IIR filter** If the impulse response of an LTI system is of infinite duration, then the system is called an *infinite-duration impulse response* (or IIR) filter. The part of difference equation (2.21)

$$\sum_{k=0}^N a_k y(n-k) = x(n) \quad (2.26)$$

describes a *recursive* filter in which the output  $y(n)$  is recursively computed from its previously computed values and is called an *autoregressive* (AR) filter. The impulse response of such a filter is of infinite duration, and hence it represents an IIR filter. The general equation (2.21) also describes an IIR filter. It has two parts: an AR part and an MA part. Such an IIR filter is called an *autoregressive moving average*, or an ARMA, filter. In MATLAB, IIR filters are described by the difference equation coefficients  $\{b_m\}$  and  $\{a_k\}$  and are implemented by the `filter(b,a,x)` function.

## 2.5 PROBLEMS

---

**P2.1** Generate the following sequences using the basic MATLAB signal functions and the basic MATLAB signal operations discussed in this chapter. Plot signal samples using the `stem` function.

1.  $x_1(n) = 3\delta(n+2) + 2\delta(n) - \delta(n-3) + 5\delta(n-7)$ ,  $-5 \leq n \leq 15$ .
2.  $x_2(n) = \sum_{k=-5}^5 e^{-|k|}\delta(n-2k)$ ,  $-10 \leq n \leq 10$ .
3.  $x_3(n) = 10u(n) - 5u(n-5) - 10u(n-10) + 5u(n-15)$ .
4.  $x_4(n) = e^{0.1n}[u(n+20) - u(n-10)]$ .
5.  $x_5(n) = 5[\cos(0.49\pi n) + \cos(0.51\pi n)]$ ,  $-200 \leq n \leq 200$ . Comment on the waveform shape.
6.  $x_6(n) = 2\sin(0.01\pi n)\cos(0.5\pi n)$ ,  $-200 \leq n \leq 200$ . Comment on the waveform shape.
7.  $x_7(n) = e^{-0.05n}\sin(0.1\pi n + \pi/3)$ ,  $0 \leq n \leq 100$ . Comment on the waveform shape.
8.  $x_8(n) = e^{0.01n}\sin(0.1\pi n)$ ,  $0 \leq n \leq 100$ . Comment on the waveform shape.

**P2.2** Generate the following random sequences and obtain their histogram using the `hist` function with 100 bins. Use the `bar` function to plot each histogram.

1.  $x_1(n)$  is a random sequence whose samples are independent and uniformly distributed over  $[0, 2]$  interval. Generate 100,000 samples.
2.  $x_2(n)$  is a Gaussian random sequence whose samples are independent with mean 10 and variance 10. Generate 10,000 samples.
3.  $x_3(n) = x_1(n) + x_1(n-1)$  where  $x_1(n)$  is the random sequence given in part 1 above. Comment on the shape of this histogram and explain the shape.
4.  $x_4(n) = \sum_{k=1}^4 y_k(n)$  where each random sequence  $y_k(n)$  is independent of others with samples uniformly distributed over  $[-0.5, 0.5]$ . Comment on the shape of this histogram.

**P2.3** Generate the following periodic sequences and plot their samples (using the `stem` function) over the indicated number of periods.

1.  $\tilde{x}_1(n) = \{\dots, -2, -1, 0, 1, 2, \dots\}_{\text{periodic}}$ . Plot five periods.  
↑
2.  $\tilde{x}_2(n) = e^{0.1n}[u(n) - u(n - 20)]_{\text{periodic}}$ . Plot three periods.
3.  $\tilde{x}_3(n) = \sin(0.1\pi n)[u(n) - u(n - 10)]$ . Plot four periods.
4.  $\tilde{x}_4(n) = \{\dots, 1, 2, 3, \dots\}_{\text{periodic}} + \{\dots, 1, 2, 3, 4, \dots\}_{\text{periodic}}, 0 \leq n \leq 24$ . What is the period of  $\tilde{x}_4(n)$ ?  
↑

**P2.4** Let  $x(n) = \{2, 4, -3, 1, -5, 4, 7\}$ . Generate and plot the samples (use the `stem` function) of the following sequences.

1.  $x_1(n) = 2x(n - 3) + 3x(n + 4) - x(n)$
2.  $x_2(n) = 4x(4 + n) + 5x(n + 5) + 2x(n)$
3.  $x_3(n) = x(n + 3)x(n - 2) + x(1 - n)x(n + 1)$
4.  $x_4(n) = 2e^{0.5n}x(n) + \cos(0.1\pi n)x(n + 2), -10 \leq n \leq 10$

**P2.5** The complex exponential sequence  $e^{j\omega_0 n}$  or the sinusoidal sequence  $\cos(\omega_0 n)$  are periodic if the normalized frequency  $f_0 \triangleq \frac{\omega_0}{2\pi}$  is a rational number; that is,  $f_0 = \frac{K}{N}$ , where  $K$  and  $N$  are integers.

1. Prove the above result.
2. Generate  $\exp(j0.1\pi n), -100 \leq n \leq 100$ . Plot its real and imaginary parts using the `stem` function. Is this sequence periodic? If it is, what is its fundamental period? From the examination of the plot, what interpretation can you give to the integers  $K$  and  $N$  above?
3. Generate and plot  $\cos(0.1n), -20 \leq n \leq 20$ . Is this sequence periodic? What do you conclude from the plot? If necessary, examine the values of the sequence in MATLAB to arrive at your answer.

**P2.6** Using the `evenodd` function, decompose the following sequences into their even and odd components. Plot these components using the `stem` function.

1.  $x_1(n) = \{0, 1, 2, 3, 4, 5, 6, 7, 8, 9\}$   
↑
2.  $x_2(n) = e^{0.1n}[u(n + 5) - u(n - 10)]$
3.  $x_3(n) = \cos(0.2\pi n + \pi/4), -20 \leq n \leq 20$
4.  $x_4(n) = e^{-0.05n} \sin(0.1\pi n + \pi/3), 0 \leq n \leq 100$

**P2.7** A complex-valued sequence  $x_e(n)$  is called *conjugate-symmetric* if  $x_e(n) = x_e^*(-n)$ , and a complex-valued sequence  $x_o(n)$  is called *conjugate-antisymmetric* if  $x_o(n) = -x_o^*(-n)$ . Then any arbitrary complex-valued sequence  $x(n)$  can be decomposed into  $x(n) = x_e(n) + x_o(n)$ , where  $x_e(n)$  and  $x_o(n)$  are given by

$$x_e(n) = \frac{1}{2} [x(n) + x^*(-n)] \quad \text{and} \quad x_o(n) = \frac{1}{2} [x(n) - x^*(-n)] \quad (2.27)$$

respectively.

1. Modify the **evenodd** function discussed in the text so that it accepts an arbitrary sequence and decomposes it into its conjugate-symmetric and conjugate-antisymmetric components by implementing (2.27).
2. Decompose the sequence

$$x(n) = 10 \exp([-0.1 + j0.2\pi]n), \quad 0 \leq n \leq 10$$

into its conjugate-symmetric and conjugate-antisymmetric components. Plot their real and imaginary parts to verify the decomposition. (Use the **subplot** function.)

- P2.8** The operation of *signal dilation* (or *decimation* or *down-sampling*) is defined by

$$y(n) = x(nM)$$

in which the sequence  $x(n)$  is down-sampled by an integer factor  $M$ . For example, if

$$x(n) = \{\dots, -2, 4, 3, -6, 5, -1, 8, \dots\}$$

↑

then the down-sampled sequences by a factor 2 are given by

$$y(n) = \{\dots, -2, 3, 5, 8, \dots\}$$

↑

1. Develop a MATLAB function **dnsample** that has the form

```
function [y,m] = dnsample(x,n,M)
% Downsample sequence x(n) by a factor M to obtain y(m)
```

- to implement the above operation. Use the indexing mechanism of MATLAB with careful attention to the origin of the time axis  $n = 0$ .
2. Generate  $x(n) = \sin(0.125\pi n)$ ,  $-50 \leq n \leq 50$ . Decimate  $x(n)$  by a factor of 4 to generate  $y(n)$ . Plot both  $x(n)$  and  $y(n)$  using **subplot**, and comment on the results.
  3. Repeat the above using  $x(n) = \sin(0.5\pi n)$ ,  $-50 \leq n \leq 50$ . Qualitatively discuss the effect of down-sampling on signals.

- P2.9** Using the **conv\_m** function, determine the autocorrelation sequence  $r_{xx}(\ell)$  and the cross-correlation sequence  $r_{xy}(\ell)$  for the following sequences:

$$x(n) = (0.9)^n, \quad 0 \leq n \leq 20; \quad y(n) = (0.8)^{-n}, \quad -20 \leq n \leq 0$$

Describe your observations of these results.

- P2.10** In a certain concert hall, echoes of the original audio signal  $x(n)$  are generated due to the reflections at the walls and ceiling. The audio signal experienced by the listener  $y(n)$  is a combination of  $x(n)$  and its echoes. Let

$$y(n) = x(n) + \alpha x(n - k)$$

where  $k$  is the amount of delay in samples and  $\alpha$  is its relative strength. We want to estimate the delay using the correlation analysis.

- Determine analytically the cross-correlation  $r_{yx}(\ell)$  in terms of the autocorrelation  $r_{xx}(\ell)$ .
- Let  $x(n) = \cos(0.2\pi n) + 0.5 \cos(0.6\pi n)$ ,  $\alpha = 0.1$ , and  $k = 50$ . Generate 200 samples of  $y(n)$  and determine its cross-correlation. Can you obtain  $\alpha$  and  $k$  by observing  $r_{yx}(\ell)$ ?

**P2.11** Consider the following discrete-time systems:

$$\begin{array}{ll} T_1[x(n)] = x(n)u(n) & T_2[x(n)] = x(n) + n x(n+1) \\ T_3[x(n)] = x(n) + \frac{1}{2}x(n-2) - \frac{1}{3}x(n-3)x(2n) & T_4[x(n)] = \sum_{k=-\infty}^{n+5} 2x(k) \\ T_5[x(n)] = x(2n) & T_6[x(n)] = \text{round}[x(n)] \end{array}$$

where  $\text{round}[\cdot]$  denotes rounding to the nearest integer.

- Use (2.10) to determine analytically whether these systems are linear.
- Let  $x_1(n)$  be a uniformly distributed random sequence between  $[0, 1]$  over  $0 \leq n \leq 100$ , and let  $x_2(n)$  be a Gaussian random sequence with mean 0 and variance 10 over  $0 \leq n \leq 100$ . Using these sequences, verify the linearity of these systems. Choose any values for constants  $a_1$  and  $a_2$  in (2.10). You should use several realizations of the above sequences to arrive at your answers.

**P2.12** Consider the discrete-time systems given in Problem P2.11.

- Use (2.12) to determine analytically whether these systems are time-invariant.
- Let  $x(n)$  be a Gaussian random sequence with mean 0 and variance 10 over  $0 \leq n \leq 100$ . Using this sequence, verify the time invariance of the above systems. Choose any values for sample shift  $k$  in (2.12). You should use several realizations of the above sequence to arrive at your answers.

**P2.13** For the systems given in Problem P2.11, determine analytically their stability and causality.

**P2.14** The linear convolution defined in (2.14) has several properties:

$$\begin{aligned} x_1(n) * x_2(n) &= x_1(n) * x_2(n) && : \text{Commutation} \\ [x_1(n) * x_2(n)] * x_3(n) &= x_1(n) * [x_2(n) * x_3(n)] && : \text{Association} \\ x_1(n) * [x_2(n) + x_3(n)] &= x_1(n) * x_2(n) + x_1(n) * x_3(n) && : \text{Distribution} \\ x(n) * \delta(n - n_0) &= x(n - n_0) && : \text{Identity} \end{aligned} \tag{2.28}$$

- Analytically prove these properties.
- Using the following three sequences, verify the above properties:

$$\begin{aligned} x_1(n) &= \cos(\pi n/4)[u(n+5) - u(n-25)] \\ x_2(n) &= (0.9)^{-n}[u(n) - u(n-20)] \\ x_3(n) &= \text{round}[5w(n)], -10 \leq n \leq 10, \text{ where } w(n) \text{ is uniform over } [-1, 1] \end{aligned}$$

Use the `conv_m` function.

**P2.15** Determine analytically the convolution  $y(n) = x(n) * h(n)$  of the following sequences, and verify your answers using the `conv_m` function.

- $x(n) = \{2, -4, 5, 3, -1, -2, 6\}$ ,  $h(n) = \{1, -1, 1, -1, 1\}$

2.  $x(n) = \{1, 1, 0, 1, 1\}$ ,  $h(n) = \{1, -2, -3, 4\}$
3.  $x(n) = (1/4)^{-n}[u(n+1) - u(n-4)]$ ,  $h(n) = u(n) - u(n-5)$
4.  $x(n) = n/4[u(n) - u(n-6)]$ ,  $h(n) = 2[u(n+2) - u(n-3)]$

**P2.16** Let  $x(n) = (0.8)^n u(n)$ ,  $h(n) = (-0.9)^n u(n)$ , and  $y(n) = h(n) * x(n)$ . Use three columns and one row of subplots for the following parts.

1. Determine  $y(n)$  analytically. Plot first 51 samples of  $y(n)$  using the `stem` function.
2. Truncate  $x(n)$  and  $h(n)$  to 26 samples. Use `conv` function to compute  $y(n)$ . Plot  $y(n)$  using the `stem` function. Compare your results with those of part 1.
3. Using the `filter` function, determine the first 51 samples of  $x(n) * h(n)$ . Plot  $y(n)$  using the `stem` function. Compare your results with those of parts 1 and 2.

**P2.17** When the sequences  $x(n)$  and  $h(n)$  are of finite duration  $N_x$  and  $N_h$ , respectively, then their linear convolution (2.13) can also be implemented using *matrix-vector multiplication*. If elements of  $y(n)$  and  $x(n)$  are arranged in column vectors  $\mathbf{x}$  and  $\mathbf{y}$ , respectively, then from (2.13) we obtain

$$\mathbf{y} = \mathbf{H}\mathbf{x}$$

where linear shifts in  $h(n-k)$  for  $n = 0, \dots, N_h - 1$  are arranged as rows in the matrix  $\mathbf{H}$ . This matrix has an interesting structure and is called a *Toeplitz* matrix. To investigate this matrix, consider the sequences

$$x(n) = \begin{matrix} \{1, 2, 3, 4, 5\} \\ \uparrow \end{matrix} \quad \text{and} \quad h(n) = \begin{matrix} \{6, 7, 8, 9\} \\ \uparrow \end{matrix}$$

1. Determine the linear convolution  $y(n) = h(n) * x(n)$ .
2. Express  $x(n)$  as a  $5 \times 1$  column vector  $\mathbf{x}$  and  $y(n)$  as a  $8 \times 1$  column vector  $\mathbf{y}$ . Now determine the  $8 \times 5$  matrix  $\mathbf{H}$  so that  $\mathbf{y} = \mathbf{H}\mathbf{x}$ .
3. Characterize the matrix  $\mathbf{H}$ . From this characterization, can you give a definition of a Toeplitz matrix? How does this definition compare with that of time invariance?
4. What can you say about the first column and the first row of  $\mathbf{H}$ ?

**P2.18** MATLAB provides a function called `toeplitz` to generate a Toeplitz matrix, given the first row and the first column.

1. Using this function and your answer to Problem P2.17, part 4, develop another MATLAB function to implement linear convolution. The format of the function should be

```
function [y,H]=conv_tp(h,x)
% Linear Convolution using Toeplitz Matrix
%
% [y,H] = conv_tp(h,x)
% y = output sequence in column vector form
% H = Toeplitz matrix corresponding to sequence h so that y = Hx
% h = Impulse response sequence in column vector form
% x = input sequence in column vector form
```

2. Verify your function on the sequences given in Problem P2.17.

**P2.19** A linear and time-invariant system is described by the difference equation

$$y(n) - 0.5y(n-1) + 0.25y(n-2) = x(n) + 2x(n-1) + x(n-3)$$

1. Using the `filter` function, compute and plot the impulse response of the system over  $0 \leq n \leq 100$ .
2. Determine the stability of the system from this impulse response.
3. If the input to this system is  $x(n) = [5 + 3 \cos(0.2\pi n) + 4 \sin(0.6\pi n)] u(n)$ , determine the response  $y(n)$  over  $0 \leq n \leq 200$  using the `filter` function.

**P2.20** A “simple” *digital differentiator* is given by

$$y(n) = x(n) - x(n-1)$$

which computes a backward first-order difference of the input sequence. Implement this differentiator on the following sequences, and plot the results. Comment on the appropriateness of this simple differentiator.

1.  $x(n) = 5[u(n) - u(n-20)]$ : a rectangular pulse
2.  $x(n) = n[u(n) - u(n-10)] + (20-n)[u(n-10) - u(n-20)]$ : a triangular pulse
3.  $x(n) = \sin\left(\frac{\pi n}{25}\right)[u(n) - u(n-100)]$ : a sinusoidal pulse

# CHAPTER 3

## The Discrete-Time Fourier Analysis

We have seen how a linear and time-invariant system can be represented using its response to the unit sample sequence. This response, called the *unit impulse response*  $h(n)$ , allows us to compute the system response to any arbitrary input  $x(n)$  using the linear convolution

$$x(n) \longrightarrow [h(n)] \longrightarrow y(n) = h(n) * x(n)$$

This convolution representation is based on the fact that any signal can be represented by a linear combination of scaled and delayed unit samples. Similarly, we can also represent any arbitrary discrete signal as a linear combination of basis signals introduced in Chapter 2. Each basis signal set provides a new signal representation. Each representation has some advantages and some disadvantages depending upon the type of system under consideration. However, when the system is linear and time-invariant, only one representation stands out as the most useful. It is based on the complex exponential signal set  $\{e^{j\omega n}\}$  and is called the *discrete-time Fourier transform*.

### 3.1 THE DISCRETE-TIME FOURIER TRANSFORM (DTFT)

If  $x(n)$  is absolutely summable, that is,  $\sum_{-\infty}^{\infty} |x(n)| < \infty$ , then its discrete-time Fourier transform is given by

$$X(e^{j\omega}) \triangleq \mathcal{F}[x(n)] = \sum_{n=-\infty}^{\infty} x(n)e^{-j\omega n} \quad (3.1)$$

The inverse discrete-time Fourier transform (IDTFT) of  $X(e^{j\omega})$  is given by

$$x(n) \triangleq \mathcal{F}^{-1}[X(e^{j\omega})] = \frac{1}{2\pi} \int_{-\pi}^{\pi} X(e^{j\omega}) e^{j\omega n} d\omega \quad (3.2)$$

The operator  $\mathcal{F}[\cdot]$  transforms a discrete signal  $x(n)$  into a complex-valued continuous function  $X(e^{j\omega})$  of real variable  $\omega$ , called a digital frequency, which is measured in radians/sample.

- **EXAMPLE 3.1** Determine the discrete-time Fourier transform of  $x(n) = (0.5)^n u(n)$ .

**Solution**

The sequence  $x(n)$  is absolutely summable; therefore, its discrete-time Fourier transform exists.

$$\begin{aligned} X(e^{j\omega}) &= \sum_{-\infty}^{\infty} x(n) e^{-j\omega n} = \sum_{0}^{\infty} (0.5)^n e^{-j\omega n} \\ &= \sum_{0}^{\infty} (0.5e^{-j\omega})^n = \frac{1}{1 - 0.5e^{-j\omega}} = \frac{e^{j\omega}}{e^{j\omega} - 0.5} \end{aligned}$$

□

- **EXAMPLE 3.2** Determine the discrete-time Fourier transform of the following finite-duration sequence:

$$x(n) = \begin{cases} 1, 2, 3, 4, 5 \\ \uparrow \end{cases}$$

**Solution**

Using definition (3.1),

$$X(e^{j\omega}) = \sum_{-\infty}^{\infty} x(n) e^{-j\omega n} = e^{j\omega} + 2 + 3e^{-j\omega} + 4e^{-j2\omega} + 5e^{-j3\omega}$$

□

Since  $X(e^{j\omega})$  is a complex-valued function, we will have to plot its magnitude and its angle (or the real part and the imaginary part) with respect to  $\omega$  separately to visually describe  $X(e^{j\omega})$ . Now  $\omega$  is a real variable between  $-\infty$  and  $\infty$ , which would mean that we can plot only a part of the  $X(e^{j\omega})$  function using MATLAB. Using two important properties of the discrete-time Fourier transform, we can reduce this domain to the  $[0, \pi]$  interval for real-valued sequences. We will discuss other useful properties of  $X(e^{j\omega})$  in the next section.

### 3.1.1 TWO IMPORTANT PROPERTIES

We will state the following two properties without proof.

1. **Periodicity:** The discrete-time Fourier transform  $X(e^{j\omega})$  is periodic in  $\omega$  with period  $2\pi$ .

$$X(e^{j\omega}) = X(e^{j[\omega+2\pi]})$$

**Implication:** We need only one period of  $X(e^{j\omega})$  (i.e.,  $\omega \in [0, 2\pi]$ , or  $[-\pi, \pi]$ , etc.) for analysis and not the whole domain  $-\infty < \omega < \infty$ .

2. **Symmetry:** For real-valued  $x(n)$ ,  $X(e^{j\omega})$  is conjugate symmetric.

$$X(e^{-j\omega}) = X^*(e^{j\omega})$$

or

$$\operatorname{Re}[X(e^{-j\omega})] = \operatorname{Re}[X(e^{j\omega})] \quad (\text{even symmetry})$$

$$\operatorname{Im}[X(e^{-j\omega})] = -\operatorname{Im}[X(e^{j\omega})] \quad (\text{odd symmetry})$$

$$|X(e^{-j\omega})| = |X(e^{j\omega})| \quad (\text{even symmetry})$$

$$\angle X(e^{-j\omega}) = -\angle X(e^{j\omega}) \quad (\text{odd symmetry})$$

**Implication:** To plot  $X(e^{j\omega})$ , we now need to consider only a half-period of  $X(e^{j\omega})$ . Generally, in practice this period is chosen to be  $\omega \in [0, \pi]$ .

### 3.1.2 MATLAB IMPLEMENTATION

If  $x(n)$  is of infinite duration, then MATLAB cannot be used directly to compute  $X(e^{j\omega})$  from  $x(n)$ . However, we can use it to evaluate the expression  $X(e^{j\omega})$  over  $[0, \pi]$  frequencies and then plot its magnitude and angle (or real and imaginary parts).

- **EXAMPLE 3.3** Evaluate  $X(e^{j\omega})$  in Example 3.1 at 501 equispaced points between  $[0, \pi]$  and plot its magnitude, angle, real part, and imaginary part.

**Solution**

MATLAB script:

```
>> w = [0:1:500]*pi/500; % [0, pi] axis divided into 501 points.
>> X = exp(j*w) ./ (exp(j*w) - 0.5*ones(1,501));
>> magX = abs(X); angX = angle(X); realX = real(X); imagX = imag(X);
>> subplot(2,2,1); plot(w/pi,magX); grid
>> title('Magnitude Part'); ylabel('Magnitude')
>> subplot(2,2,3); plot(w/pi,angX); grid
>> xlabel('frequency in pi units'); title('Angle Part'); ylabel('Radians')
>> subplot(2,2,2); plot(w/pi,realX); grid
>> title('Real Part'); ylabel('Real')
>> subplot(2,2,4); plot(w/pi,imagX); grid
>> xlabel('frequency in pi units'); title('Imaginary Part'); ylabel('Imaginary')
```

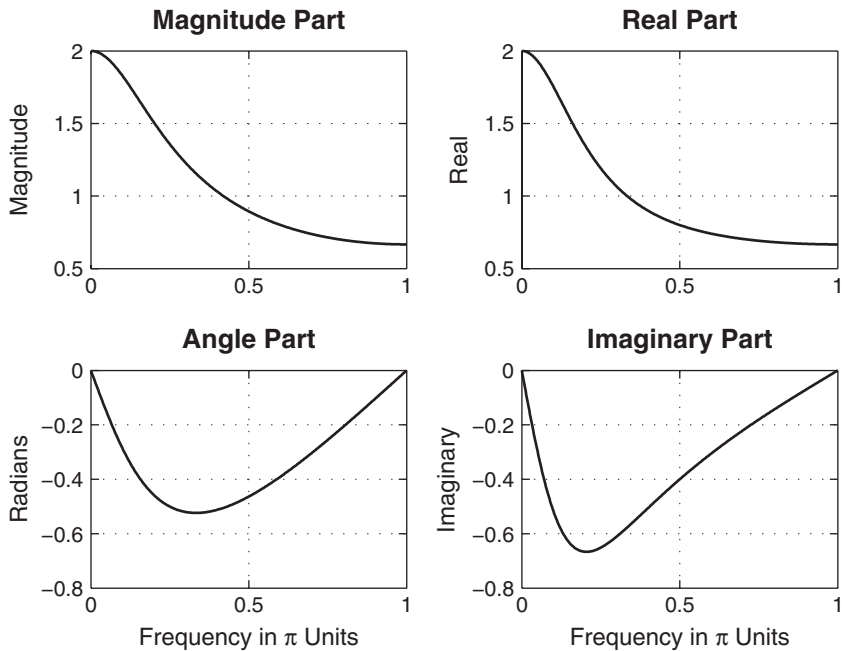


**FIGURE 3.1** Plots in Example 3.3

The resulting plots are shown in Figure 3.1. Note that we divided the  $\omega$  array by  $\pi$  before plotting so that the frequency axes are in the units of  $\pi$  and therefore easier to read. *This practice is strongly recommended.*  $\square$

If  $x(n)$  is of finite duration, then MATLAB can be used to compute  $X(e^{j\omega})$  numerically at any frequency  $\omega$ . The approach is to implement (3.1) directly. If, in addition, we evaluate  $X(e^{j\omega})$  at equispaced frequencies between  $[0, \pi]$ , then (3.1) can be implemented as a *matrix-vector multiplication* operation. To understand this, let us assume that the sequence  $x(n)$  has  $N$  samples between  $n_1 \leq n \leq n_N$  (i.e., not necessarily between  $[0, N - 1]$ ) and that we want to evaluate  $X(e^{j\omega})$  at

$$\omega_k \triangleq \frac{\pi}{M} k, \quad k = 0, 1, \dots, M$$

which are  $(M + 1)$  equispaced frequencies between  $[0, \pi]$ . Then (3.1) can be written as

$$X(e^{j\omega_k}) = \sum_{\ell=1}^N e^{-j(\pi/M)k n_\ell} x(n_\ell), \quad k = 0, 1, \dots, M$$

When  $\{x(n_\ell)\}$  and  $\{X(e^{j\omega_k})\}$  are arranged as *column* vectors  $\mathbf{x}$  and  $\mathbf{X}$ , respectively, we have

$$\mathbf{X} = \mathbf{W}\mathbf{x} \quad (3.3)$$

where  $\mathbf{W}$  is an  $(M + 1) \times N$  matrix given by

$$\mathbf{W} \triangleq \left\{ e^{-j(\pi/M)kn_\ell}; n_1 \leq n \leq n_N, \quad k = 0, 1, \dots, M \right\}$$

In addition, if we arrange  $\{k\}$  and  $\{n_\ell\}$  as *row* vectors  $\mathbf{k}$  and  $\mathbf{n}$ , respectively, then

$$\mathbf{W} = \left[ \exp \left( -j \frac{\pi}{M} \mathbf{k}^T \mathbf{n} \right) \right]$$

In MATLAB, we represent sequences and indices as row vectors; therefore, taking the transpose of (3.3), we obtain

$$\mathbf{X}^T = \mathbf{x}^T \left[ \exp \left( -j \frac{\pi}{M} \mathbf{n}^T \mathbf{k} \right) \right] \quad (3.4)$$

Note that  $\mathbf{n}^T \mathbf{k}$  is an  $N \times (M + 1)$  matrix. Now (3.4) can be implemented in MATLAB as follows.

```
>> k = [0:M]; n = [n1:n2];
>> X = x * (exp(-j*pi/M)) .^ (n'*k);
```

- EXAMPLE 3.4** Numerically compute the discrete-time Fourier transform of the sequence  $x(n)$  given in Example 3.2 at 501 equispaced frequencies between  $[0, \pi]$ .

### Solution

MATLAB script:

```
>> n = -1:3; x = 1:5; k = 0:500; w = (pi/500)*k;
>> X = x * (exp(-j*pi/500)) .^ (n'*k);
>> magX = abs(X); angX = angle(X);
>> realX = real(X); imagX = imag(X);
>> subplot(2,2,1); plot(k/500,magX);grid
>> title('Magnitude Part')
>> subplot(2,2,3); plot(k/500,angX/pi);grid
>> xlabel('Frequency in \pi Units'); title('Angle Part')
>> subplot(2,2,2); plot(k/500,realX);grid
>> title('Real Part')
>> subplot(2,2,4); plot(k/500,imagX);grid
>> xlabel('Frequency in \pi Units'); title('Imaginary Part')
```

The frequency-domain plots are shown in Figure 3.2. Note that the angle plot is depicted as a discontinuous function between  $-\pi$  and  $\pi$ . This is because the `angle` function in MATLAB computes the principal angle.  $\square$

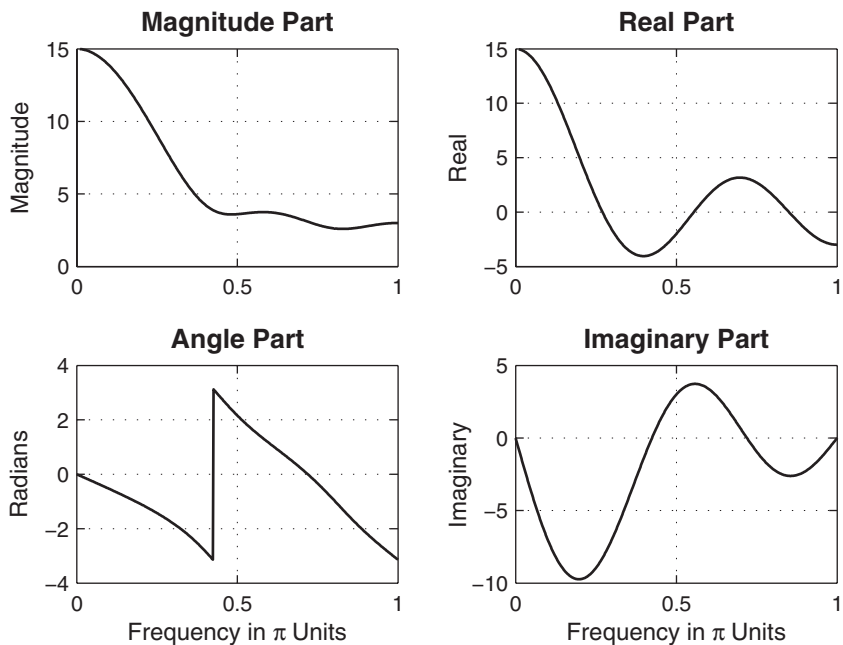


FIGURE 3.2 Plots in Example 3.4

The procedure of Example 3.4 can be compiled into a MATLAB function—say, a `dtft` function—for ease of implementation. This is explored in Problem P3.1. This numerical computation is based on definition (3.1). It is not the most elegant way of numerically computing the discrete-time Fourier transform of a finite-duration sequence. In Chapter 5, we will discuss in detail the topic of a computable transform called the discrete Fourier transform (DFT) and its efficient computation, called the fast Fourier transform (FFT). Also, there is an alternate approach based on the  $z$ -transform using the MATLAB function `freqz`, which we will discuss in Chapter 4. In this chapter, we will continue to use the approaches discussed so far for calculation as well as for investigation purposes.

In the next two examples, we investigate the periodicity and symmetry properties using complex-valued and real-valued sequences.

- **EXAMPLE 3.5** Let  $x(n) = (0.9 \exp(j\pi/3))^n$ ,  $0 \leq n \leq 10$ . Determine  $X(e^{j\omega})$  and investigate its periodicity.

#### Solution

Since  $x(n)$  is complex-valued,  $X(e^{j\omega})$  satisfies only the periodicity property. Therefore, it is uniquely defined over one period of  $2\pi$ . However, we will evaluate and plot it at 401 frequencies over two periods between  $[-2\pi, 2\pi]$  to observe its periodicity.

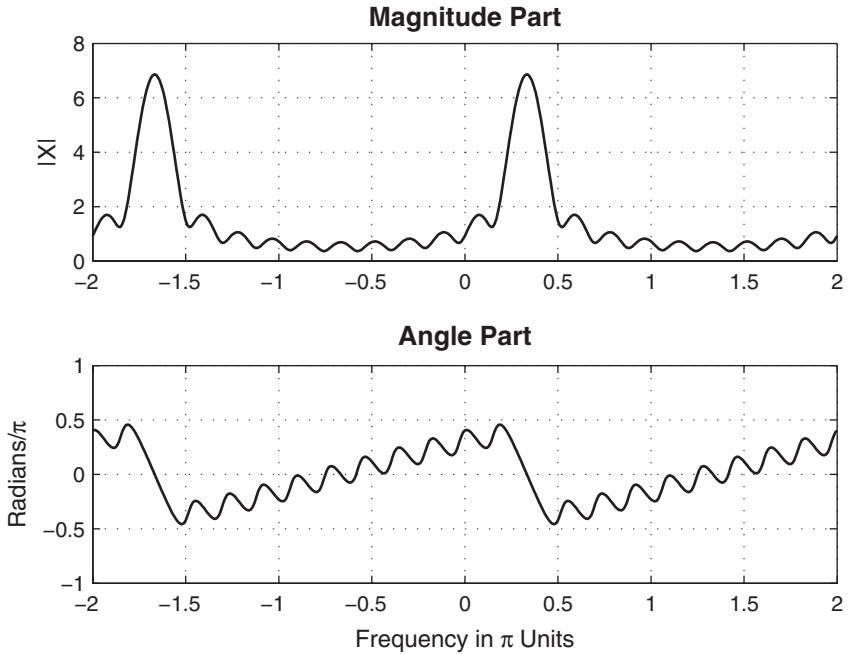


**FIGURE 3.3** Plots in Example 3.5

MATLAB script:

```

>> n = 0:10; x = (0.9*exp(j*pi/3)).^n;
>> k = -200:200; w = (pi/100)*k;
>> X = x * (exp(-j*pi/100)) .^ (n*k);
>> magX = abs(X); angX = angle(X);
>> subplot(2,1,1); plot(w/pi,magX);grid
>> ylabel('|X|')
>> title('Magnitude Part')
>> subplot(2,1,2); plot(w/pi,angX/pi);grid
>> xlabel('Frequency in \pi Units'); ylabel('Radians/\pi')
>> title('Angle Part')

```

From the plots in Figure 3.3, we observe that  $X(e^{j\omega})$  is periodic in  $\omega$  but is not conjugate-symmetric.  $\square$

- EXAMPLE 3.6** Let  $x(n) = (-0.9)^n$ ,  $-5 \leq n \leq 5$ . Investigate the conjugate-symmetry property of its discrete-time Fourier transform.

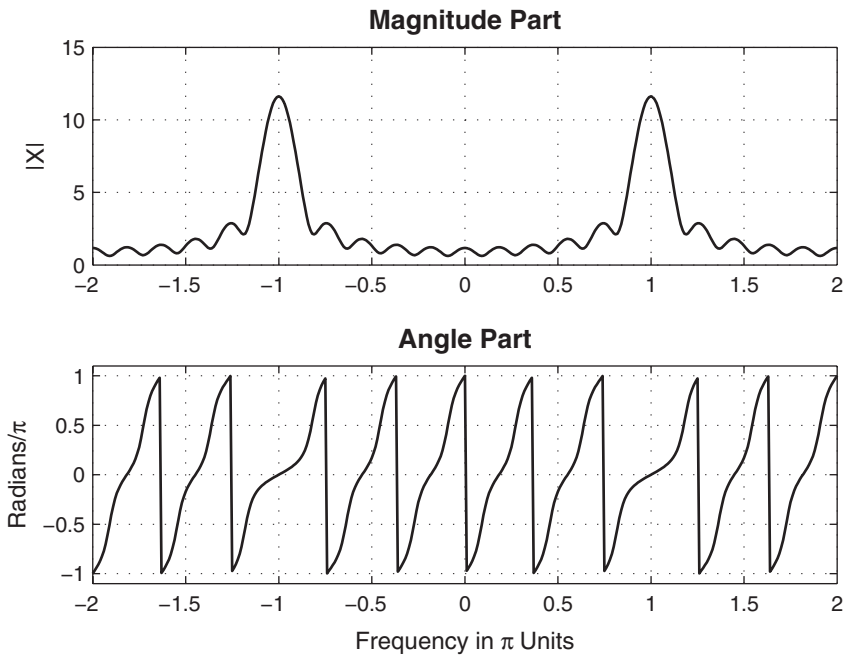


**FIGURE 3.4** Plots in Example 3.6

### Solution

Once again, we will compute and plot  $X(e^{j\omega})$  over two periods to study its symmetry property.

MATLAB script:

```
>> n = -5:5; x = (-0.9).^n;
>> k = -200:200; w = (pi/100)*k; X = x * (exp(-j*pi/100)) .^ (n.*k);
>> magX = abs(X); angX = angle(X);
>> subplot(2,1,1); plot(w/pi,magX);grid; axis([-2,2,0,15])
>> ylabel('|X|')
>> title('Magnitude Part')
>> subplot(2,1,2); plot(w/pi,angX/pi);grid; axis([-2,2,-1,1])
>> xlabel('Frequency in \pi Units'); ylabel('Radians/\pi')
>> title('Angle Part')
```

From the plots in Figure 3.4, we observe that  $X(e^{j\omega})$  is not only periodic in  $\omega$  but is also conjugate-symmetric. Therefore, for real sequences we will plot their Fourier transform magnitude and angle graphs from 0 to  $\pi$ .  $\square$

### 3.1.3 SOME COMMON DTFT PAIRS

The discrete-time Fourier transforms of the basic sequences discussed in Chapter 2 are very useful. The discrete-time Fourier transforms of some

**TABLE 3.1** Some common DTFT pairs

Signal Type	Sequence $x(n)$	DTFT $X(e^{j\omega})$ , $-\pi \leq \omega \leq \pi$
Unit impulse	$\delta(n)$	1
Constant	1	$2\pi\delta(\omega)$
Unit step	$u(n)$	$\frac{1}{1 - e^{-j\omega}} + \pi\delta(\omega)$
Causal exponential	$\alpha^n u(n)$	$\frac{1}{1 - \alpha e^{-j\omega}}$
Complex exponential	$e^{j\omega_0 n}$	$2\pi\delta(\omega - \omega_0)$
Cosine	$\cos(\omega_0 n)$	$\pi[\delta(\omega - \omega_0) + \delta(\omega + \omega_0)]$
Sine	$\sin(\omega_0 n)$	$j\pi[\delta(\omega + \omega_0) - \delta(\omega - \omega_0)]$
Double exponential	$\alpha^{ n }$	$\frac{1 - \alpha^2}{1 - 2\alpha \cos(\omega) + \alpha^2}$

Note: Since  $X(e^{j\omega})$  is periodic with period  $2\pi$ , expressions over only the primary period of  $-\pi \leq \omega \leq \pi$  are given.

of these sequences can be easily obtained using the basic definitions (3.1) and (3.2). These transform pairs and those of few other pairs are given in Table 3.1. Note that, even if sequences like unit step  $u(n)$  are not absolutely summable, their discrete-time Fourier transforms exist in the limiting sense if we allow impulses in the Fourier transform. Such sequences are said to have finite power, that is,  $\sum_n |x(n)|^2 < \infty$ . Using this table and the properties of the Fourier transform (discussed in Section 3.2), it is possible to obtain discrete-time Fourier transform of many more sequences.

## 3.2 THE PROPERTIES OF THE DTFT

---

In the previous section, we discussed two important properties that we needed for plotting purposes. We now discuss the remaining useful properties, which are given below without proof. Let  $X(e^{j\omega})$  be the discrete-time Fourier transform of  $x(n)$ .

1. **Linearity:** The discrete-time Fourier transform is a linear transformation; that is,

$$\mathcal{F}[\alpha x_1(n) + \beta x_2(n)] = \alpha \mathcal{F}[x_1(n)] + \beta \mathcal{F}[x_2(n)] \quad (3.5)$$

for every  $\alpha, \beta$ ,  $x_1(n)$ , and  $x_2(n)$ .

2. **Time shifting:** A shift in the time domain corresponds to the phase shifting.

$$\mathcal{F}[x(n-k)] = X(e^{j\omega})e^{-j\omega k} \quad (3.6)$$

3. **Frequency shifting:** Multiplication by a complex exponential corresponds to a shift in the frequency domain.

$$\mathcal{F}[x(n)e^{j\omega_0 n}] = X(e^{j(\omega-\omega_0)}) \quad (3.7)$$

4. **Conjugation:** Conjugation in the time domain corresponds to the folding and conjugation in the frequency domain.

$$\mathcal{F}[x^*(n)] = X^*(e^{-j\omega}) \quad (3.8)$$

5. **Folding:** Folding in the time domain corresponds to the folding in the frequency domain.

$$\mathcal{F}[x(-n)] = X(e^{-j\omega}) \quad (3.9)$$

6. **Symmetries in real sequences:** We have already studied the conjugate symmetry of real sequences. These real sequences can be decomposed into their even and odd parts, as discussed in Chapter 2.

$$x(n) = x_e(n) + x_o(n)$$

Then

$$\begin{aligned}\mathcal{F}[x_e(n)] &= \operatorname{Re}[X(e^{j\omega})] \\ \mathcal{F}[x_o(n)] &= j \operatorname{Im}[X(e^{j\omega})]\end{aligned} \quad (3.10)$$

**Implication:** If the sequence  $x(n)$  is real and even, then  $X(e^{j\omega})$  is also real and even. Hence only one plot over  $[0, \pi]$  is necessary for its complete representation.

A similar property for complex-valued sequences is explored in Problem P3.7.

7. **Convolution:** This is one of the most useful properties that makes system analysis convenient in the frequency domain.

$$\mathcal{F}[x_1(n) * x_2(n)] = \mathcal{F}[x_1(n)] \mathcal{F}[x_2(n)] = X_1(e^{j\omega})X_2(e^{j\omega}) \quad (3.11)$$

8. **Multiplication:** This is a dual of the convolution property.

$$\mathcal{F}[x_1(n) \cdot x_2(n)] = \mathcal{F}[x_1(n)] \odot \mathcal{F}[x_2(n)] \triangleq \frac{1}{2\pi} \int_{-\pi}^{\pi} X_1(e^{j\theta}) X_2(e^{j(\omega-\theta)}) d\theta \quad (3.12)$$

This convolution-like operation is called a *periodic convolution* and hence denoted by  $\odot$ . It is discussed (in its discrete form) in Chapter 5.

9. **Energy:** The energy of the sequence  $x(n)$  can be written as

$$\begin{aligned} \mathcal{E}_x &= \sum_{-\infty}^{\infty} |x(n)|^2 = \frac{1}{2\pi} \int_{-\pi}^{\pi} |X(e^{j\omega})|^2 d\omega \\ &= \int_0^{\pi} \frac{|X(e^{j\omega})|^2}{\pi} d\omega \quad (\text{for real sequences using even symmetry}) \end{aligned} \quad (3.13)$$

This is also known as Parseval's theorem. From (3.13), the *energy density spectrum* of  $x(n)$  is defined as

$$\Phi_x(\omega) \triangleq \frac{|X(e^{j\omega})|^2}{\pi} \quad (3.14)$$

Then the energy of  $x(n)$  in the  $[\omega_1, \omega_2]$  band is given by

$$\int_{\omega_1}^{\omega_2} \Phi_x(\omega) d\omega, \quad 0 \leq \omega_1 < \omega_2 \leq \pi$$

In the next several examples, we will verify some of these properties using finite-duration sequences. We will follow our numerical procedure to compute discrete-time Fourier transforms in each case. Although this does not analytically prove the validity of each property, it provides us with an experimental tool in practice.

- EXAMPLE 3.7** In this example, we will verify the linearity property (3.5) using real-valued finite-duration sequences. Let  $x_1(n)$  and  $x_2(n)$  be two random sequences uniformly distributed between  $[0, 1]$  over  $0 \leq n \leq 10$ . Then we can use our numerical discrete-time Fourier transform procedure as follows.

MATLAB script:

```
>> x1 = rand(1,11); x2 = rand(1,11); n = 0:10;
>> alpha = 2; beta = 3; k = 0:500; w = (pi/500)*k;
>> X1 = x1 * (exp(-j*pi/500)).^(n'*k); % DTFT of x1
>> X2 = x2 * (exp(-j*pi/500)).^(n'*k); % DTFT of x2
>> x = alpha*x1 + beta*x2; % Linear combination of x1 & x2
```

```

>> X = x * (exp(-j*pi/500)).^(n'*k);      % DTFT of x
>> % Verification
>> X_check = alpha*X1 + beta*X2;           % Linear combination of X1 & X2
>> error = max(abs(X-X_check))            % Difference
error =
    7.1054e-015

```

Since the maximum absolute error between the two Fourier transform arrays is less than  $10^{-14}$ , the two arrays are identical within the limited numerical precision of MATLAB.  $\square$

- $\square$  **EXAMPLE 3.8** Let  $x(n)$  be a random sequence uniformly distributed between  $[0, 1]$  over  $0 \leq n \leq 10$ , and let  $y(n) = x(n - 2)$ . Then we can verify the sample shift property (3.6) as follows.

```

>> x = rand(1,11); n = 0:10;
>> k = 0:500; w = (pi/500)*k;
>> X = x * (exp(-j*pi/500)).^(n'*k);      % DTFT of x
>> % Signal shifted by two samples
>> y = x; m = n+2;
>> Y = y * (exp(-j*pi/500)).^(m'*k);      % DTFT of y
>> % verification
>> Y_check = (exp(-j*2).^w).*X;           % Multiplication by exp(-j2w)
>> error = max(angle(Y-Y_check))          % Difference
error =
    1.2204e-015

```

$\square$

- $\square$  **EXAMPLE 3.9** To verify the frequency shift property (3.7), we will use the graphical approach. Let

$$x(n) = \cos(\pi n/2), \quad 0 \leq n \leq 100 \quad \text{and} \quad y(n) = e^{j\pi n/4}x(n)$$

Then using MATLAB,

```

>> n = 0:100; x = cos(pi*n/2);
>> k = -100:100; w = (pi/100)*k;           % Frequency between -pi and +pi
>> X = x * (exp(-j*pi/100)).^(n'*k);      % DTFT of x
>> y = exp(j*pi*n/4).*x;                   % Signal multiplied by exp(j*pi*n/4)
>> Y = y * (exp(-j*pi/100)).^(n'*k);      % DTFT of y
% Graphical verification
>> subplot(2,2,1); plot(w/pi,abs(X)); grid; axis([-1,1,0,60])
>> title('Magnitude of X'); ylabel('|X|')
>> subplot(2,2,2); plot(w/pi,angle(X)/pi); grid; axis([-1,1,-1,1])
>> title('Angle of X'); ylabel('radians/\pi')
>> subplot(2,2,3); plot(w/pi,abs(Y)); grid; axis([-1,1,0,60])

```

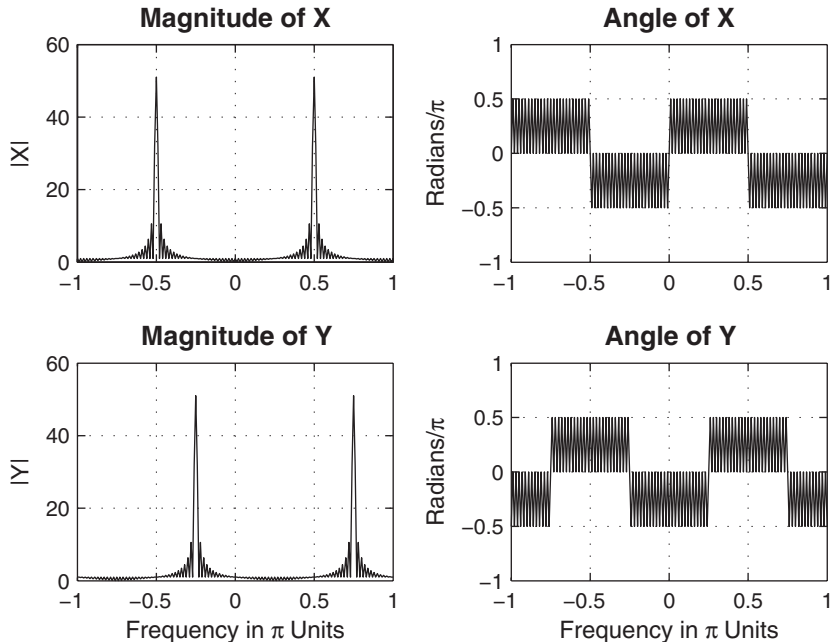


**FIGURE 3.5** Plots in Example 3.9

```
>> xlabel('Frequency in \pi Units'); ylabel('|Y|')
>> title('Magnitude of Y')
>> subplot(2,2,4); plot(w/pi,angle(Y)/pi); grid; axis([-1,1,-1,1])
>> xlabel('Frequency in \pi Units'); ylabel('radians/\pi')
>> title('Angle of Y')
```

From the plots in Figure 3.5, we observe that  $X(e^{j\omega})$  is indeed shifted by  $\pi/4$  in both magnitude and angle.  $\square$

- **EXAMPLE 3.10** To verify the conjugation property (3.8), let  $x(n)$  be a complex-valued random sequence over  $-5 \leq n \leq 10$  with real and imaginary parts uniformly distributed between  $[0, 1]$ . The MATLAB verification is as follows.

```
>> n = -5:10; x = rand(1,length(n)) + j*rand(1,length(n));
>> k = -100:100; w = (pi/100)*k; % Frequency between -pi and +pi
>> X = x * (exp(-j*pi/100)).^(n'*k); % DTFT of x
% Conjugation property
>> y = conj(x); % Signal conjugation
>> Y = y * (exp(-j*pi/100)).^(n'*k); % DTFT of y
% Verification
```

```
>> Y_check = conj(fliplr(X));           % conj(X(-w))
>> error = max(abs(Y-Y_check))        % Difference
error =
0
```

□

- **EXAMPLE 3.11** To verify the folding property (3.9), let  $x(n)$  be a random sequence over  $-5 \leq n \leq 10$  uniformly distributed between  $[0, 1]$ . The MATLAB verification is as follows.

```
>> n = -5:10; x = rand(1,length(n));
>> k = -100:100; w = (pi/100)*k;          % Frequency between -pi and +pi
>> X = x * (exp(-j*pi/100)).^(n'*k);    % DTFT of x
% Folding property
>> y = fliplr(x); m = -fliplr(n);       % Signal folding
>> Y = y * (exp(-j*pi/100)).^(m'*k);    % DTFT of y
% Verification
>> Y_check = fliplr(X);                  % X(-w)
>> error = max(abs(Y-Y_check))           % Difference
error =
0
```

□

- **EXAMPLE 3.12** In this problem, we verify the symmetry property (3.10) of real signals. Let

$$x(n) = \sin(\pi n/2), \quad -5 \leq n \leq 10$$

Then, using the **evenodd** function developed in Chapter 2, we can compute the even and odd parts of  $x(n)$  and then evaluate their discrete-time Fourier transforms. We will provide the numerical as well as graphical verification.

MATLAB script:

```
>> n = -5:10; x = sin(pi*n/2);
>> k = -100:100; w = (pi/100)*k;          % Frequency between -pi and +pi
>> X = x * (exp(-j*pi/100)).^(n'*k);    % DTFT of x
% Signal decomposition
>> [xe,xo,m] = evenodd(x,n);            % Even and odd parts
>> XE = xe * (exp(-j*pi/100)).^(m'*k);  % DTFT of xe
>> XO = xo * (exp(-j*pi/100)).^(m'*k);  % DTFT of xo
% Verification
>> XR = real(X);                      % Real part of X
>> error1 = max(abs(XE-XR))           % Difference
error1 =
1.8974e-019
>> XI = imag(X);                     % Imag part of X
```

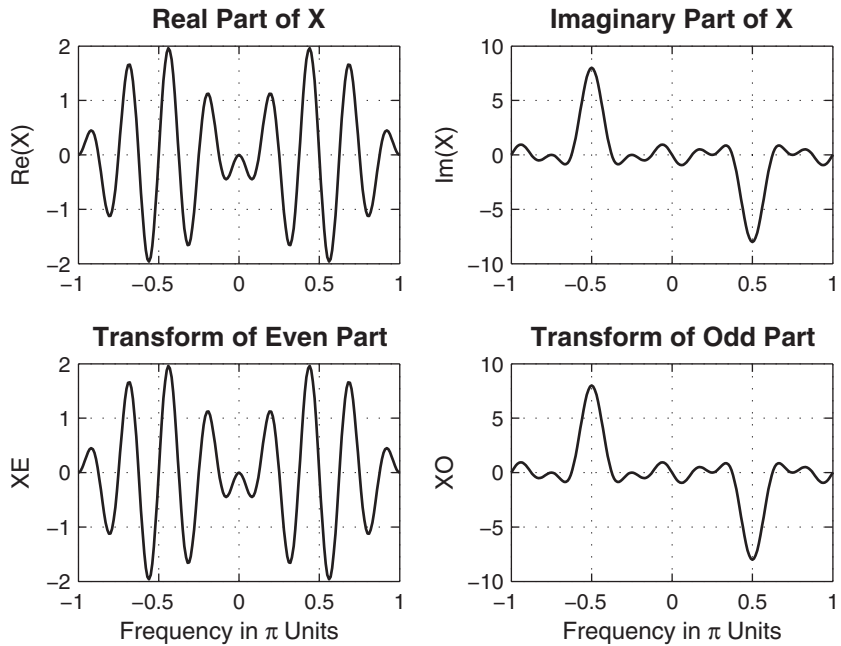


**FIGURE 3.6** Plots in Example 3.12

```

>> error2 = max(abs(X0-j*X1)) % Difference
error2 =
    1.8033e-019
% Graphical verification
>> subplot(2,2,1); plot(w/pi,XR); grid; axis([-1,1,-2,2])
>> title('Real Part of X'); ylabel('Re(X)');
>> subplot(2,2,2); plot(w/pi,XI); grid; axis([-1,1,-10,10])
>> title('Imaginary Part of X'); ylabel('Im(X)');
>> subplot(2,2,3); plot(w/pi,real(XE)); grid; axis([-1,1,-2,2])
>> xlabel('Frequency in \pi Units'); ylabel('XE');
>> title('Transform of Even Part')
>> subplot(2,2,4); plot(w/pi,imag(XO)); grid; axis([-1,1,-10,10])
>> xlabel('Frequency in \pi Units'); ylabel('XO');
>> title('Transform of Odd Part')

```

From the plots in Figure 3.6, we observe that the real part of  $X(e^{j\omega})$  [or the imaginary part of  $X(e^{j\omega})$ ] is equal to the discrete-time Fourier transform of  $x_e(n)$  [or  $x_o(n)$ ].  $\square$

### 3.3 THE FREQUENCY DOMAIN REPRESENTATION OF LTI SYSTEMS

---

We earlier stated that the Fourier transform representation is the most useful signal representation for LTI systems. This is due to the following result.

#### 3.3.1 RESPONSE TO A COMPLEX EXPONENTIAL $e^{j\omega_0 n}$

Let  $x(n) = e^{j\omega_0 n}$  be the input to an LTI system represented by the impulse response  $h(n)$ .

$$e^{j\omega_0 n} \longrightarrow [h(n)] \longrightarrow h(n) * e^{j\omega_0 n}$$

Then

$$\begin{aligned} y(n) &= h(n) * e^{j\omega_0 n} = \sum_{-\infty}^{\infty} h(k)e^{j\omega_0(n-k)} \\ &= \left[ \sum_{-\infty}^{\infty} h(k)e^{-j\omega_0 k} \right] e^{j\omega_0 n} \quad (3.15) \\ &= [\mathcal{F}[h(n)]|_{\omega=\omega_0}] e^{j\omega_0 n} \end{aligned}$$

■ **DEFINITION 1 Frequency Response**

The discrete-time Fourier transform of an impulse response is called the frequency response (or transfer function) of an LTI system and is denoted by

$$H(e^{j\omega}) \triangleq \sum_{n=-\infty}^{\infty} h(n)e^{-j\omega n} \quad (3.16)$$

Then from (3.15) we can represent the system by

$$x(n) = e^{j\omega_0 n} \longrightarrow [H(e^{j\omega})] \longrightarrow y(n) = H(e^{j\omega_0}) \times e^{j\omega_0 n} \quad (3.17)$$

Hence the output sequence is the input exponential sequence modified by the response of the system at frequency  $\omega_0$ . This justifies the definition of  $H(e^{j\omega})$  as a frequency response because it is what the complex exponential is multiplied by to obtain the output  $y(n)$ . This powerful result can be extended to a linear combination of complex exponentials using the linearity of LTI systems:

$$\sum_k A_k e^{j\omega_k n} \longrightarrow [h(n)] \longrightarrow \sum_k A_k H(e^{j\omega_k}) e^{j\omega_k n}$$

In general, the frequency response  $H(e^{j\omega})$  is a complex function of  $\omega$ . The magnitude  $|H(e^{j\omega})|$  of  $H(e^{j\omega})$  is called the *magnitude (or gain) response* function, and the angle  $\angle H(e^{j\omega})$  is called the *phase response* function, as we shall see below.

### 3.3.2 RESPONSE TO SINUSOIDAL SEQUENCES

Let  $x(n) = A \cos(\omega_0 n + \theta_0)$  be an input to an LTI system  $h(n)$ . Then from (3.17) we can show that the response  $y(n)$  is another sinusoid of the same frequency  $\omega_0$ , with amplitude *gained* by  $|H(e^{j\omega_0})|$  and phase *shifted* by  $\angle H(e^{j\omega_0})$ , that is,

$$y(n) = A|H(e^{j\omega_0})| \cos(\omega_0 n + \theta_0 + \angle H(e^{j\omega_0})) \quad (3.18)$$

This response is called the *steady-state response*, denoted by  $y_{ss}(n)$ . It can be extended to a linear combination of sinusoidal sequences.

$$\sum_k A_k \cos(\omega_k n + \theta_k) \longrightarrow [H(e^{j\omega})] \longrightarrow \sum_k A_k |H(e^{j\omega_k})| \cos(\omega_k n + \theta_k + \angle H(e^{j\omega_k}))$$

### 3.3.3 RESPONSE TO ARBITRARY SEQUENCES

Finally, (3.17) can be generalized to arbitrary *absolutely summable* sequences. Let  $X(e^{j\omega}) = \mathcal{F}[x(n)]$ , and let  $Y(e^{j\omega}) = \mathcal{F}[y(n)]$ ; then, using the convolution property (3.11), we have

$$Y(e^{j\omega}) = H(e^{j\omega}) X(e^{j\omega}) \quad (3.19)$$

Therefore, an LTI system can be represented in the frequency domain by

$$X(e^{j\omega}) \longrightarrow [H(e^{j\omega})] \longrightarrow Y(e^{j\omega}) = H(e^{j\omega}) X(e^{j\omega})$$

The output  $y(n)$  is then computed from  $Y(e^{j\omega})$  using the inverse discrete-time Fourier transform (3.2). This requires an integral operation, which is not a convenient operation in MATLAB. As we shall see in Chapter 4, there is an alternate approach to the computation of output to arbitrary inputs using the  $z$ -transform and partial fraction expansion. In this chapter, we will concentrate on computing the steady-state response.

- EXAMPLE 3.13** Determine the frequency response  $H(e^{j\omega})$  of a system characterized by  $h(n) = (0.9)^n u(n)$ . Plot the magnitude and the phase responses.

**Solution**

Using (3.16),

$$\begin{aligned} H(e^{j\omega}) &= \sum_{-\infty}^{\infty} h(n) e^{-j\omega n} = \sum_{0}^{\infty} (0.9)^n e^{-j\omega n} \\ &= \sum_{0}^{\infty} (0.9e^{-j\omega})^n = \frac{1}{1 - 0.9e^{-j\omega}} \end{aligned}$$

Hence

$$|H(e^{j\omega})| = \sqrt{\frac{1}{(1 - 0.9 \cos \omega)^2 + (0.9 \sin \omega)^2}} = \frac{1}{\sqrt{1.81 - 1.8 \cos \omega}}$$

and

$$\angle H(e^{j\omega}) = -\arctan \left[ \frac{0.9 \sin \omega}{1 - 0.9 \cos \omega} \right]$$

To plot these responses, we can either implement the  $|H(e^{j\omega})|$  and  $\angle H(e^{j\omega})$  functions or the frequency response  $H(e^{j\omega})$  and then compute its magnitude and phase. The latter approach is more useful from a practical viewpoint [as shown in (3.18)].

```
>> w = [0:1:500]*pi/500; % [0, pi] axis divided into 501 points.
>> H = exp(j*w) ./ (exp(j*w) - 0.9*ones(1,501));
>> magH = abs(H); angH = angle(H);
>> subplot(2,1,1); plot(w/pi,magH); grid;
>> title('Magnitude Response'); ylabel('|H|');
>> subplot(2,1,2); plot(w/pi,angH/pi); grid
>> xlabel('Frequency in \pi Units'); ylabel('Phase in \pi Radians');
>> title('Phase Response');
```

The plots are shown in Figure 3.7. □

- **EXAMPLE 3.14** Let an input to the system in Example 3.13 be  $0.1u(n)$ . Determine the steady-state response  $y_{ss}(n)$ .

#### Solution

Since the input is not absolutely summable, the discrete-time Fourier transform is not particularly useful in computing the complete response. However, it can be used to compute the steady-state response. In the steady state (i.e.,  $n \rightarrow \infty$ ), the input is a constant sequence (or a sinusoid with  $\omega_0 = \theta_0 = 0$ ). Then the output is

$$y_{ss}(n) = 0.1 \times H(e^{j0}) = 0.1 \times 10 = 1$$

where the gain of the system at  $\omega = 0$  (also called the DC gain) is  $H(e^{j0}) = 10$ , which is obtained from Figure 3.7. □

### 3.3.4 FREQUENCY RESPONSE FUNCTION FROM DIFFERENCE EQUATIONS

When an LTI system is represented by the difference equation

$$y(n) + \sum_{\ell=1}^N a_\ell y(n-\ell) = \sum_{m=0}^M b_m x(n-m) \quad (3.20)$$

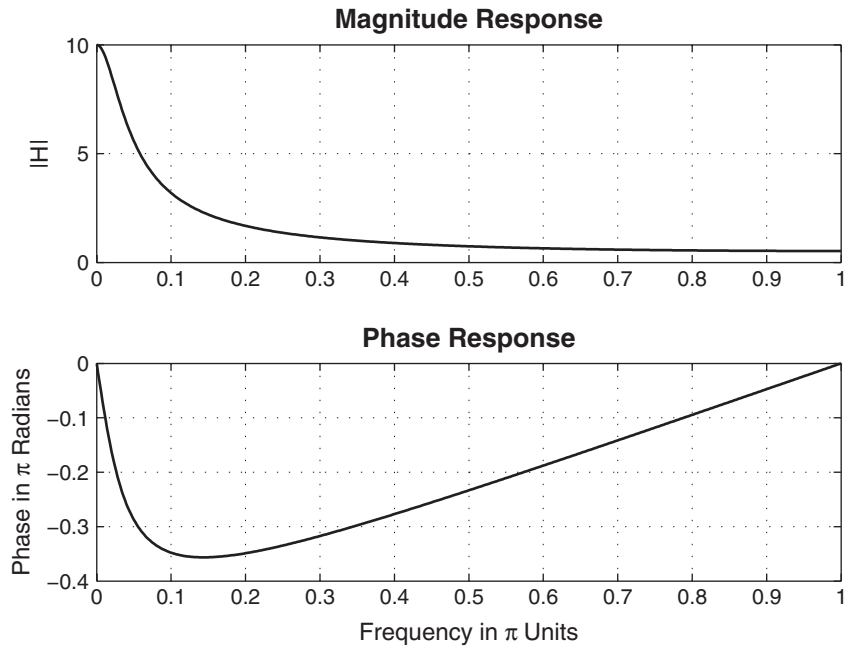


**FIGURE 3.7** Frequency response plots in Example 3.13

then to evaluate its frequency response from (3.16), we would need the impulse response  $h(n)$ . However, using (3.17), we can easily obtain  $H(e^{j\omega})$ . We know that when  $x(n) = e^{j\omega n}$ , then  $y(n)$  must be  $H(e^{j\omega})e^{j\omega n}$ . Substituting in (3.20), we have

$$H(e^{j\omega})e^{j\omega n} + \sum_{\ell=1}^N a_\ell H(e^{j\omega})e^{j\omega(n-\ell)} = \sum_{m=0}^M b_m e^{j\omega(n-m)}$$

or

$$H(e^{j\omega}) = \frac{\sum_{m=0}^M b_m e^{-j\omega m}}{1 + \sum_{\ell=1}^N a_\ell e^{-j\omega\ell}} \quad (3.21)$$

after canceling the common factor  $e^{j\omega n}$  term and rearranging. This equation can easily be implemented in MATLAB, given the difference equation parameters.

- **EXAMPLE 3.15** An LTI system is specified by the difference equation

$$y(n) = 0.8y(n-1) + x(n)$$

- a. Determine  $H(e^{j\omega})$ .
- b. Calculate and plot the steady-state response  $y_{ss}(n)$  to

$$x(n) = \cos(0.05\pi n)u(n)$$

**Solution**

Rewrite the difference equation as  $y(n) - 0.8y(n-1) = x(n)$ .

a. Using (3.21), we obtain

$$H(e^{j\omega}) = \frac{1}{1 - 0.8e^{-j\omega}} \quad (3.22)$$

b. In the steady state, the input is  $x(n) = \cos(0.05\pi n)$  with frequency  $\omega_0 = 0.05\pi$  and  $\theta_0 = 0^\circ$ . The response of the system is

$$H(e^{j0.05\pi}) = \frac{1}{1 - 0.8e^{-j0.05\pi}} = 4.0928e^{-j0.5377}$$

Therefore,

$$y_{ss}(n) = 4.0928 \cos(0.05\pi n - 0.5377) = 4.0928 \cos[0.05\pi(n - 3.42)]$$

This means that at the output the sinusoid is scaled by 4.0928 and shifted by 3.42 sampling intervals. This can be verified using MATLAB.

```
>> subplot(1,1,1)
>> b = 1; a = [1,-0.8];
>> n=[0:100];x = cos(0.05*pi*n);
>> y = filter(b,a,x);
>> subplot(2,1,1); stem(n,x);
>> ylabel('x(n)'); title('Input Sequence')
>> subplot(2,1,2); stem(n,y);
>> xlabel('n'); ylabel('y(n)'); title('Output Sequence')
```

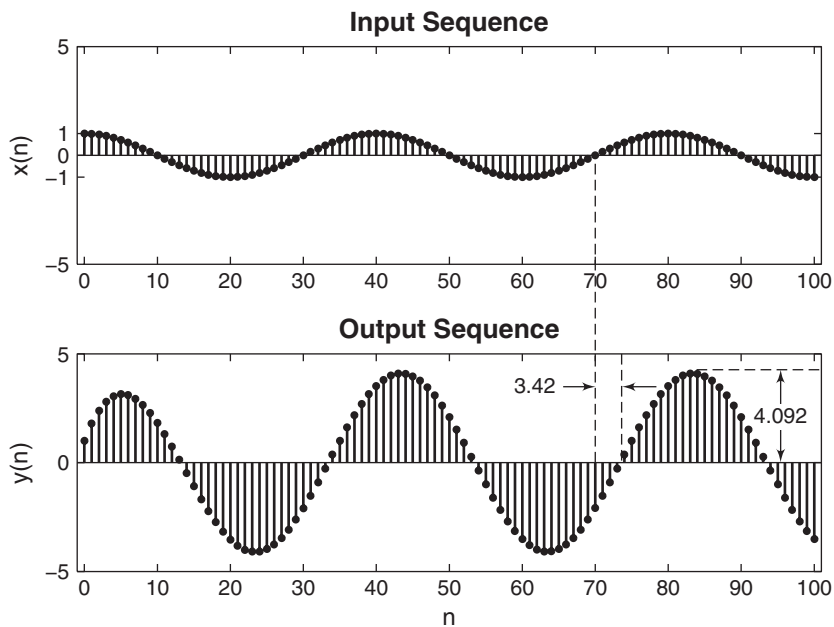
From the plots in Figure 3.8, we note that the amplitude of  $y_{ss}(n)$  is approximately 4. To determine the shift in the output sinusoid, we can compare zero crossings of the input and the output. This is shown in Figure 3.8, from which the shift is approximately 3.4 samples.  $\square$

In Example 3.15, the system was characterized by a first-order difference equation. It is fairly straightforward to implement (3.22) in MATLAB, as we did in Example 3.13. In practice, the difference equations are of large order, and hence we need a compact procedure to implement the general expression (3.21). This can be done using a simple matrix-vector multiplication. If we evaluate  $H(e^{j\omega})$  at  $k = 0, 1, \dots, K$  equispaced frequencies over  $[0, \pi]$ , then

$$H(e^{j\omega_k}) = \frac{\sum_{m=0}^M b_m e^{-j\omega_k m}}{1 + \sum_{\ell=1}^N a_\ell e^{-j\omega_k \ell}}, \quad k = 0, 1, \dots, K \quad (3.23)$$

If we let  $\{b_m\}$ ,  $\{a_\ell\}$  (with  $a_0 = 1$ ),  $\{m = 0, \dots, M\}$ ,  $\{\ell = 0, \dots, N\}$ , and  $\{\omega_k\}$  be arrays (or row vectors), then the numerator and the denominator of (3.23) become

$$\underline{b} \exp(-jm^T \underline{\omega}); \quad \underline{a} \exp(-j\underline{\ell}^T \underline{\omega})$$

**FIGURE 3.8** Plots in Example 3.15

respectively. Now the array  $H(e^{j\omega_k})$  in (3.23) can be computed using a  $\text{./}$  operation. This procedure can be implemented in a MATLAB function to determine the frequency response function, given  $\{b_m\}$  and  $\{a_\ell\}$  arrays. We will explore this in Example 3.16 and in Problem P3.16.

- EXAMPLE 3.16** A 3rd-order lowpass filter is described by the difference equation

$$\begin{aligned}y(n) = & 0.0181x(n) + 0.0543x(n-1) + 0.0543x(n-2) + 0.0181x(n-3) \\& + 1.76y(n-1) - 1.1829y(n-2) + 0.2781y(n-3)\end{aligned}$$

Plot the magnitude and the phase response of this filter, and verify that it is a lowpass filter.

**Solution**

We will implement this procedure in MATLAB and then plot the filter responses.

```
>> b = [0.0181, 0.0543, 0.0543, 0.0181]; % Filter coefficient array b
>> a = [1.0000, -1.7600, 1.1829, -0.2781]; % Filter coefficient array a
>> m = 0:length(b)-1; l = 0:length(a)-1; % Index arrays m and l
>> K = 500; k = 0:1:K; % Index array k for frequencies
>> w = pi*k/K; % [0, pi] axis divided into 501 points.
>> num = b * exp(-j*m'*w); % Numerator calculations
>> den = a * exp(-j*l'*w); % Denominator calculations
>> H = num ./ den; % Frequency response
>> magH = abs(H); angH = angle(H); % Mag and phase responses
```

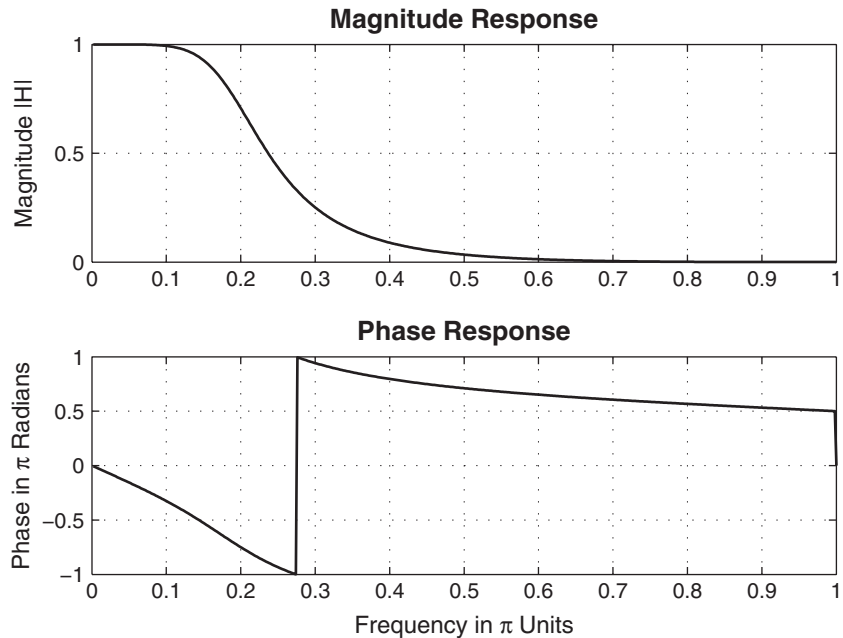


**FIGURE 3.9** Plots for Example 3.16

```
>> subplot(2,1,1); plot(w/pi,magH); grid; axis([0,1,0,1])
>> ylabel('Magnitude |H|');
>> title('Magnitude Response');
>> subplot(2,1,2); plot(w/pi,angH/pi); grid
>> xlabel('Frequency in \pi Units'); ylabel('Phase in \pi Radians');
>> title('Phase Response');
```

From the plots in Figure 3.9, we see that the filter is indeed a lowpass filter. □

## 3.4 SAMPLING AND RECONSTRUCTION OF ANALOG SIGNALS

---

In many applications—for example, in digital communications—real-world analog signals are converted into discrete signals using sampling and quantization operations (collectively called analog-to-digital conversion, or ADC). These discrete signals are processed by digital signal processors, and the processed signals are converted into analog signals using a reconstruction operation (called digital-to-analog conversion, or

DAC). Using Fourier analysis, we can describe the sampling operation from the frequency-domain viewpoint, analyze its effects, and then address the reconstruction operation. We will also assume that the number of quantization levels is sufficiently large that the effect of quantization on discrete signals is negligible. We will study the effects of quantization in Chapter 10.

### 3.4.1 SAMPLING

Let  $x_a(t)$  be an analog (absolutely integrable) signal. Its continuous-time Fourier transform (CTFT) is given by

$$X_a(j\Omega) \triangleq \int_{-\infty}^{\infty} x_a(t)e^{-j\Omega t} dt \quad (3.24)$$

where  $\Omega$  is an analog frequency in radians/sec. The inverse continuous-time Fourier transform is given by

$$x_a(t) = \frac{1}{2\pi} \int_{-\infty}^{\infty} X_a(j\Omega)e^{j\Omega t} d\Omega \quad (3.25)$$

We now sample  $x_a(t)$  at *sampling interval*  $T_s$  seconds apart to obtain the discrete-time signal  $x(n)$ :

$$x(n) \triangleq x_a(nT_s)$$

Let  $X(e^{j\omega})$  be the discrete-time Fourier transform of  $x(n)$ . Then it can be shown [79] that  $X(e^{j\omega})$  is a countable sum of amplitude-scaled, frequency-scaled, and translated versions of the Fourier transform  $X_a(j\Omega)$ .

$$X(e^{j\omega}) = \frac{1}{T_s} \sum_{\ell=-\infty}^{\infty} X_a \left[ j \left( \frac{\omega}{T_s} - \frac{2\pi}{T_s} \ell \right) \right] \quad (3.26)$$

This relation is known as the *aliasing formula*. The analog and digital frequencies are related through  $T_s$ ,

$$\omega = \Omega T_s \quad (3.27)$$

while the sampling frequency  $F_s$  is given by

$$F_s \triangleq \frac{1}{T_s}, \quad \text{sam/sec} \quad (3.28)$$

The graphical illustration of (3.26) is shown in Figure 3.10, from which we observe that, in general, the discrete signal is an *aliased version* of the corresponding analog signal because higher frequencies are aliased into lower frequencies if there is an overlap. However, it is possible to recover the Fourier transform  $X_a(j\Omega)$  from  $X(e^{j\omega})$  [or equivalently, the analog

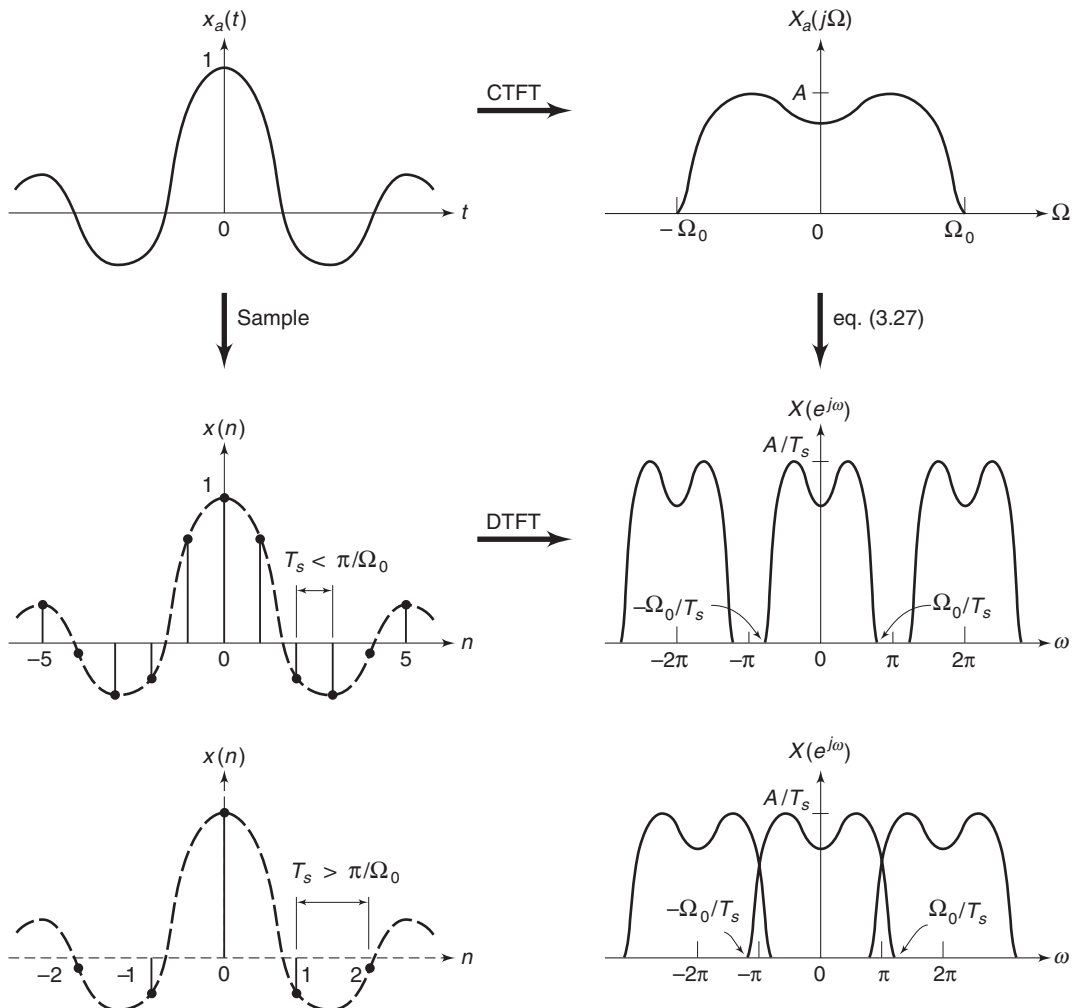


**FIGURE 3.10** Sampling operation in the time and frequency domains

signal  $x_a(t)$  from its samples  $x(n)$ ] if the infinite “replicas” of  $X_a(j\Omega)$  do not overlap with each other to form  $X(e^{j\omega})$ . This is true for band-limited analog signals.

■ **DEFINITION 2 Band-Limited Signal**

A signal is band-limited if there exists a finite radian frequency  $\Omega_0$  such that  $X_a(j\Omega)$  is zero for  $|\Omega| > \Omega_0$ . The frequency  $F_0 = \Omega_0/2\pi$  is called the signal bandwidth in Hz.

Referring to Figure 3.10, if  $\pi > \Omega_0 T_s$ —or equivalently,  $F_s/2 > F_0$ —then

$$X(e^{j\omega}) = \frac{1}{T_s} X\left(j\frac{\omega}{T_s}\right); \quad -\frac{\pi}{T_s} < \frac{\omega}{T_s} \leq \frac{\pi}{T_s} \quad (3.29)$$

which leads to the sampling theorem for band-limited signals.

■ **THEOREM 3 Sampling Principle**

A band-limited signal  $x_a(t)$  with bandwidth  $F_0$  can be reconstructed from its sample values  $x(n) = x_a(nT_s)$  if the sampling frequency  $F_s = 1/T_s$  is greater than twice the bandwidth  $F_0$  of  $x_a(t)$ .

$$F_s > 2F_0$$

Otherwise, aliasing would result in  $x(n)$ . The sampling rate of  $2F_0$  for an analog band-limited signal is called the Nyquist rate.

*Note:* After  $x_a(t)$  is sampled, the highest analog frequency that  $x(n)$  represents is  $F_s/2$  Hz (or  $\omega = \pi$ ). This agrees with the implication stated in property 2 of the discrete-time Fourier transform in Section 3.1. Before we delve into MATLAB implementation of sampling, we first consider sampling of sinusoidal signals and the resulting Fourier transform in the following example.

- **EXAMPLE 3.17** The analog signal  $x_a(t) = 4 + 2 \cos(150\pi t + \pi/3) + 4 \sin(350\pi t)$  is sampled at  $F_s = 200$  sam/sec to obtain the discrete-time signal  $x(n)$ . Determine  $x(n)$  and its corresponding DTFT  $X(e^{j\omega})$ .

**Solution**

The highest frequency in the given  $x_a(t)$  is  $F_0 = 175$  Hz. Since  $F_s = 200$ , which is less than  $2F_0$ , there will be aliasing in  $x(n)$  after sampling. The sampling interval is  $T_s = 1/F_s = 0.005$  sec. Hence we have

$$\begin{aligned} x(n) &= x_a(nT_s) = x_a(0.005n) \\ &= 4 + 2 \cos\left(0.75\pi n + \frac{\pi}{3}\right) + 4 \sin(1.75\pi n) \end{aligned} \quad (3.30)$$

Note that the digital frequency,  $1.75\pi$ , of the third term in (3.30) is outside the primary interval of  $-\pi \leq \omega \leq \pi$ , signifying that aliasing has occurred. From the periodicity property of digital sinusoidal sequences in Chapter 2, we know that the period of the digital sinusoid is  $2\pi$ . Hence we can determine the alias of the frequency  $1.75\pi$ . From (3.30), we have

$$\begin{aligned} x(n) &= 4 + 2 \cos(0.75\pi n + \frac{\pi}{3}) + 4 \sin(1.75\pi n - 2\pi n) \\ &= 4 + 2 \cos(0.75\pi n + \frac{\pi}{3}) - 4 \sin(0.25\pi n) \end{aligned} \quad (3.31)$$

Using Euler's identity, we can express  $x(n)$  as

$$x(n) = 4 + e^{j\pi/3}e^{j0.75\pi n} + e^{-j\pi/3}e^{-j0.75\pi n} + 2je^{j0.25\pi n} - 2je^{j0.25\pi n} \quad (3.32)$$

From Table 3.1 and the DTFT properties, the DTFT of  $x(n)$  is given by

$$\begin{aligned} X(e^{j\omega}) &= 8\pi\delta(\omega) + 2\pi e^{j\pi/3}\delta(\omega - 0.75\pi) + 2\pi e^{-j\pi/3}\delta(\omega + 0.75\pi) \\ &\quad + j4\pi\delta(\omega - 0.25\pi) - j4\pi\delta(\omega + 0.25\pi), \quad -\pi \leq \omega \leq \pi \end{aligned} \quad (3.33)$$

The plot of  $X(e^{j\omega})$  is shown in Figure 3.15. □

### 3.4.2 MATLAB IMPLEMENTATION

In a strict sense, it is not possible to analyze analog signals using MATLAB unless we use the Symbolic toolbox. However, if we sample  $x_a(t)$  on a fine grid that has a sufficiently small time increment to yield a smooth plot and a large enough maximum time to show all the modes, then we can approximate its analysis. Let  $\Delta t$  be the grid interval such that  $\Delta t \ll T_s$ . Then

$$x_G(m) \triangleq x_a(m\Delta t) \quad (3.34)$$

can be used as an array to simulate an analog signal. The sampling interval  $T_s$  should not be confused with the grid interval  $\Delta t$ , which is used strictly to represent an analog signal in MATLAB. Similarly, the Fourier transform relation (3.24) should also be approximated in light of (3.34) as follows:

$$X_a(j\Omega) \approx \sum_m x_G(m)e^{-j\Omega m \Delta t} \Delta t = \Delta t \sum_m x_G(m)e^{-j\Omega m \Delta t} \quad (3.35)$$

Now if  $x_a(t)$  [and hence  $x_G(m)$ ] is of finite duration, then (3.35) is similar to the discrete-time Fourier transform relation (3.3) and hence can be implemented in MATLAB in a similar fashion to analyze the sampling phenomenon.

□ **EXAMPLE 3.18** Let  $x_a(t) = e^{-1000|t|}$ . Determine and plot its Fourier transform.

**Solution**

From (3.24),

$$\begin{aligned} X_a(j\Omega) &= \int_{-\infty}^{\infty} x_a(t)e^{-j\Omega t} dt = \int_{-\infty}^0 e^{1000t}e^{-j\Omega t} dt + \int_0^{\infty} e^{-1000t}e^{-j\Omega t} dt \\ &= \frac{0.002}{1 + (\frac{\Omega}{1000})^2} \end{aligned} \quad (3.36)$$

which is a real-valued function since  $x_a(t)$  is a real and even signal. To evaluate  $X_a(j\Omega)$  numerically, we have to first approximate  $x_a(t)$  by a finite-duration grid sequence  $x_G(m)$ . Using the approximation  $e^{-5} \approx 0$ , we note that  $x_a(t)$  can be approximated by a finite-duration signal over  $-0.005 \leq t \leq 0.005$  (or equivalently, over  $[-5, 5]$  msec). Similarly from (3.36),  $X_a(j\Omega) \approx 0$  for  $\Omega \geq 2\pi/(2000)$ . Hence choosing

$$\Delta t = 5 \times 10^{-5} \ll \frac{1}{2(2000)} = 25 \times 10^{-5}$$

we can obtain  $x_G(m)$  and then implement (3.35) in MATLAB.

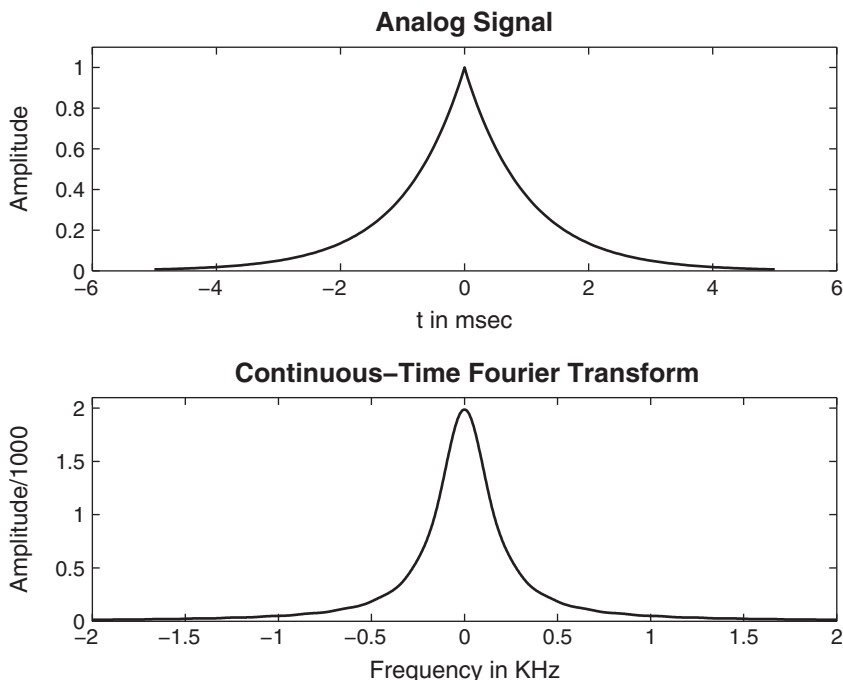
```
% Analog signal
>> Dt = 0.00005; t = -0.005:Dt:0.005; xa = exp(-1000*abs(t));
% Continuous-time Fourier transform
>>Wmax = 2*pi*2000; K = 500; k = 0:1:K; W = k*Wmax/K;
>>Xa = xa * exp(-j*t'*W) * Dt; Xa = real(Xa);
>>W = [-fliplr(W), W(2:501)]; % Omega from -Wmax to Wmax
>>Xa = [fliplr(Xa), Xa(2:501)]; % Xa over -Wmax to Wmax interval
>>subplot(2,1,1);plot(t*1000,xa);
>>xlabel('t in msec'); ylabel('Amplitude')
>>title('Analog Signal')
>>subplot(2,1,2);plot(W/(2*pi*1000),Xa*1000);
>>xlabel('Frequency in KHz'); ylabel('Amplitude/1000')
>>title('Continuous-Time Fourier Transform')
```

Figure 3.11 shows the plots of  $x_a(t)$  and  $X_a(j\Omega)$ . Note that to reduce the number of computations, we computed  $X_a(j\Omega)$  over  $[0, 4000\pi]$  rad/sec (or equivalently, over  $[0, 2]$  KHz) and then duplicated it over  $[-4000\pi, 0]$  for plotting purposes. The displayed plot of  $X_a(j\Omega)$  agrees with (3.36).  $\square$

- EXAMPLE 3.19** To study the effect of sampling on the frequency-domain quantities, we will sample  $x_a(t)$  in Example 3.18 at two different sampling frequencies.
- Sample  $x_a(t)$  at  $F_s = 5000$  sam/sec to obtain  $x_1(n)$ . Determine and plot  $X_1(e^{j\omega})$ .
  - Sample  $x_a(t)$  at  $F_s = 1000$  sam/sec to obtain  $x_2(n)$ . Determine and plot  $X_2(e^{j\omega})$ .

### Solution

- Since the bandwidth of  $x_a(t)$  is 2KHz, the Nyquist rate is 4000 sam/sec, which is less than the given  $F_s$ . Therefore, aliasing will be (almost) nonexistent.



**FIGURE 3.11** Plots in Example 3.18

MATLAB script:

```
% Analog signal
>> Dt = 0.00005; t = -0.005:Dt:0.005; xa = exp(-1000*abs(t));
% Discrete-time signal
>> Ts = 0.0002; n = -25:1:25; x = exp(-1000*abs(n*Ts));
% Discrete-time Fourier transform
>> K = 500; k = 0:1:K; w = pi*k/K;
>> X = x * exp(-j*n'*w); X = real(X);
>> w = [-fliplr(w), w(2:K+1)]; X = [fliplr(X), X(2:K+1)];
>> subplot(2,1,1);plot(t*1000,xa);
>> xlabel('t in msec'); ylabel('Amplitude')
>> title('Discrete Signal'); hold on
>> stem(n*Ts*1000,x); gtext('Ts=0.2 msec'); hold off
>> subplot(2,1,2);plot(w/pi,X);
>> xlabel('Frequency in \pi Units'); ylabel('Amplitude')
>> title('Discrete-Time Fourier Transform')
```

In the top plot in Figure 3.12, we have superimposed the discrete signal  $x_1(n)$  over  $x_a(t)$  to emphasize the sampling. The plot of  $X_2(e^{j\omega})$  shows that it is a scaled version (scaled by  $F_s = 5000$ ) of  $X_a(j\Omega)$ . Clearly there is no aliasing.

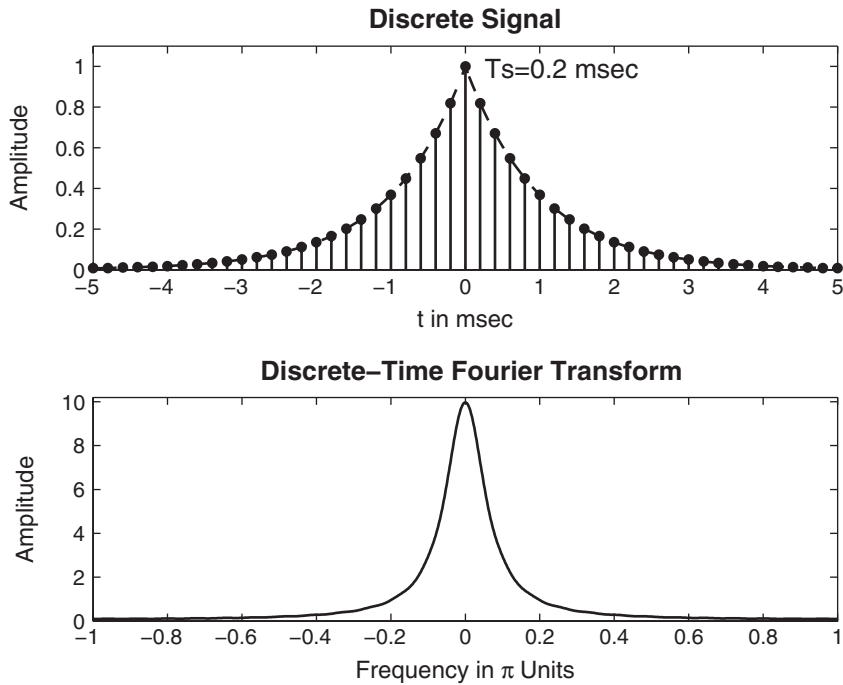


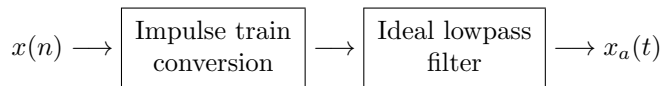
**FIGURE 3.12** Plots in Example 3.19a

- b. Here  $F_s = 1000 < 4000$ . Hence there will be a considerable amount of aliasing. This is evident from Figure 3.13, in which the shape of  $X(e^{j\omega})$  is different from that of  $X_a(j\Omega)$  and can be seen to be a result of adding overlapping replicas of  $X_a(j\Omega)$ .  $\square$

### 3.4.3 RECONSTRUCTION

From the sampling theorem and the preceding examples, it is clear that if we sample band-limited  $x_a(t)$  above its Nyquist rate, then we can reconstruct  $x_a(t)$  from its samples  $x(n)$ . This reconstruction can be thought of as a two-step process:

- First, the samples are converted into a weighted impulse train:
- $$\sum_{n=-\infty}^{\infty} x(n)\delta(t-nT_s) = \cdots + x(-1)\delta(n+T_s) + x(0)\delta(t) + x(1)\delta(n-T_s) + \cdots$$
- Then, the impulse train is filtered through an ideal analog lowpass filter band-limited to the  $[-F_s/2, F_s/2]$  band:



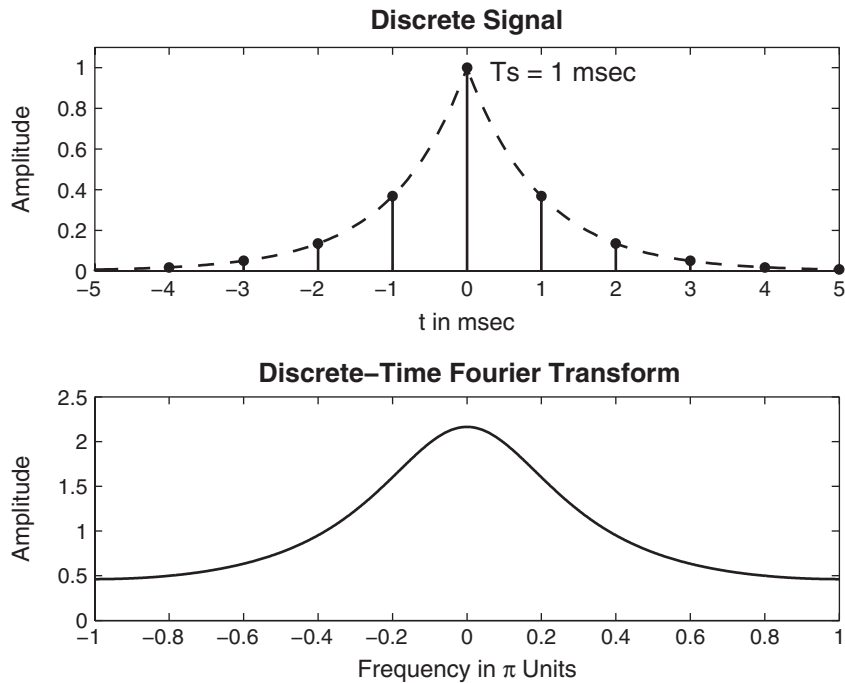


**FIGURE 3.13** Plots in Example 3.19b

This two-step procedure can be described mathematically using an interpolating formula [79],

$$x_a(t) = \sum_{n=-\infty}^{\infty} x(n) \operatorname{sinc}[F_s(t - nT_s)] \quad (3.37)$$

where  $\operatorname{sinc}(x) = \frac{\sin \pi x}{\pi x}$  is an interpolating function. The physical interpretation of the above reconstruction (3.37) is given in Figure 3.14, from which we observe that this *ideal* interpolation is not practically feasible, because the entire system is noncausal and hence not realizable.

- **EXAMPLE 3.20** Consider the sampled signal  $x(n)$  from Example 3.17. It is applied as an input to an ideal D/A converter (i.e., an ideal interpolator) to obtain the analog signal  $y_a(t)$ . The ideal D/A converter is also operating at  $F_s = 200$  sam/sec. Obtain the reconstructed signal  $y_a(t)$ , and determine whether the sampling/reconstruction operation resulted in any aliasing. Also, plot the Fourier transforms  $X_a(j\Omega)$ ,  $X(e^{j\omega})$ , and  $Y_a(j\Omega)$ .

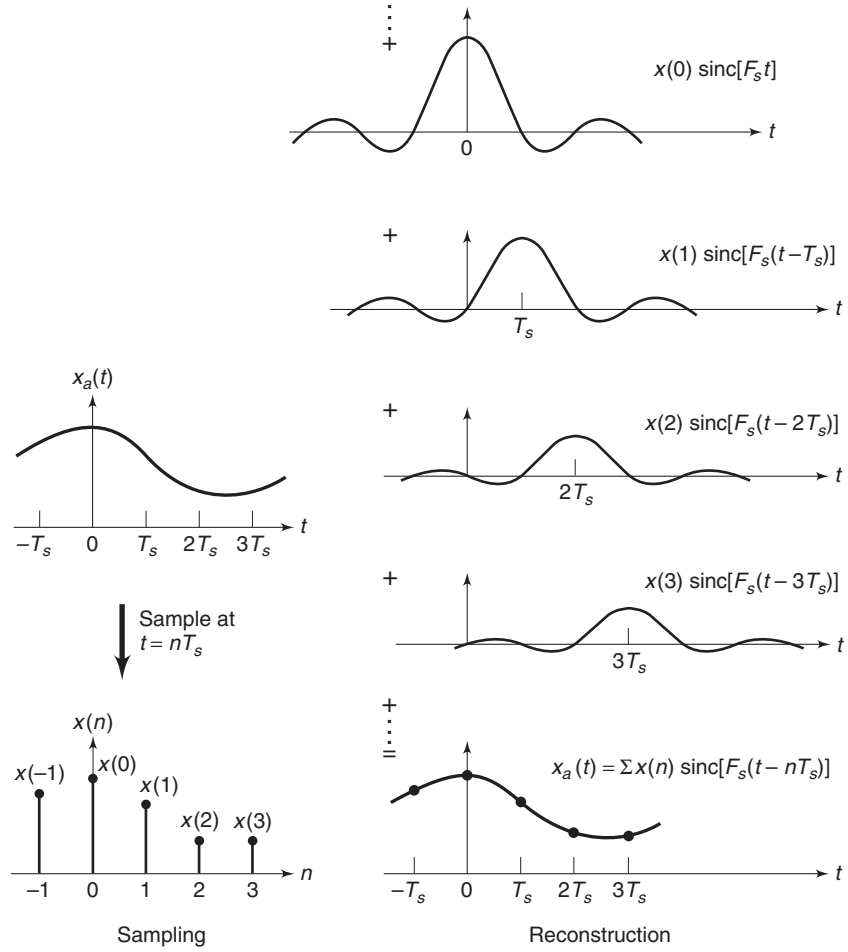


**FIGURE 3.14** Reconstruction of band-limited signal from its samples

### Solution

We can determine  $y_a(t)$  using (3.31). However, since all frequencies in the sinusoidal sequence  $x(n)$  are between the primary period of  $-\pi \leq \omega \leq \pi$ , we can equivalently obtain  $y_a(t)$  by substituting  $n$  by  $tF_s$ . Thus from (3.31), we have

$$\begin{aligned}
 y_a(t) &= x(n)|_{n=tF_s} = x(n)|_{n=200t} \\
 &= 4 + 2 \cos\left(0.75\pi 200t + \frac{\pi}{3}\right) - 4 \sin(0.25\pi 200t) \\
 &= 4 + 2 \cos\left(150\pi t + \frac{\pi}{3}\right) - 4 \sin(50\pi t)
 \end{aligned} \tag{3.38}$$

As expected, the 175 Hz component in  $x_a(t)$  is aliased into the 25 Hz component in  $y_a(t)$ .

Using Euler's identity on the given  $x_a(t)$  and the CTFT properties, the CTFT  $X_a(j\Omega)$  is given by

$$\begin{aligned} X_a(j\Omega) = & 8\pi\delta(\Omega) + 2\pi e^{j\pi/3}\delta(\Omega - 150\pi) + 2\pi e^{-j\pi/3}\delta(\Omega + 150\pi) \\ & + 4j\pi\delta(\Omega - 350\pi) - 4j\pi\delta(\Omega + 350\pi) \end{aligned} \quad (3.39)$$

It is informative to plot the CTFT  $X_a(j\Omega)$  as a function of the cyclic frequency  $F$  in Hz using  $\Omega = 2\pi F$ . Thus the quantity  $X_a(j2\pi F)$  from (3.39) is given by

$$\begin{aligned} X_a(j2\pi F) = & 4\delta(F) + e^{j\pi/3}\delta(F - 75) + e^{-j\pi/3}\delta(F + 75) \\ & + 2j\delta(F - 175) - 2j\delta(F + 175) \end{aligned} \quad (3.40)$$

where we have used the identity  $\delta(\Omega) = \delta(2\pi F) = \frac{1}{2\pi}\delta(F)$ . Similarly, the CTFT  $Y_a(j2\pi F)$  is given by

$$\begin{aligned} Y_a(j2\pi F) = & 4\delta(F) + e^{j\pi/3}\delta(F - 75) + e^{-j\pi/3}\delta(F + 75) \\ & + 2j\delta(F - 25) - 2j\delta(F + 25) \end{aligned} \quad (3.41)$$

Figure 3.15a shows the CTFT of the original signal  $x_a(t)$  as a function of  $F$ . The DTFT  $X(e^{j\omega})$  of the sampled sequence  $x(n)$  is shown as a function of  $\omega$  in Figure 3.15b, in which the impulses due to shifted replicas are shown in gray shade for clarity. The ideal D/A converter response is also shown in gray shade. The CTFT of the reconstructed signal  $y_a(t)$  is shown in Figure 3.15c, which clearly shows the aliasing effect.  $\square$

**Practical D/A converters** In practice, we need a different approach than (3.37). The two-step procedure is still feasible, but now we replace the ideal lowpass filter by a practical analog lowpass filter. Another interpretation of (3.37) is that it is an infinite-order interpolation. We want finite-order (and in fact low-order) interpolations. There are several approaches to do this.

- **Zero-order-hold (ZOH) interpolation:** In this interpolation, a given sample value is held for the sample interval until the next sample is received,

$$\hat{x}_a(t) = x(n), \quad nT_s \leq t < (n+1)T_s$$

which can be obtained by filtering the impulse train through an interpolating filter of the form

$$h_0(t) = \begin{cases} 1, & 0 \leq t \leq T_s \\ 0, & \text{otherwise} \end{cases}$$

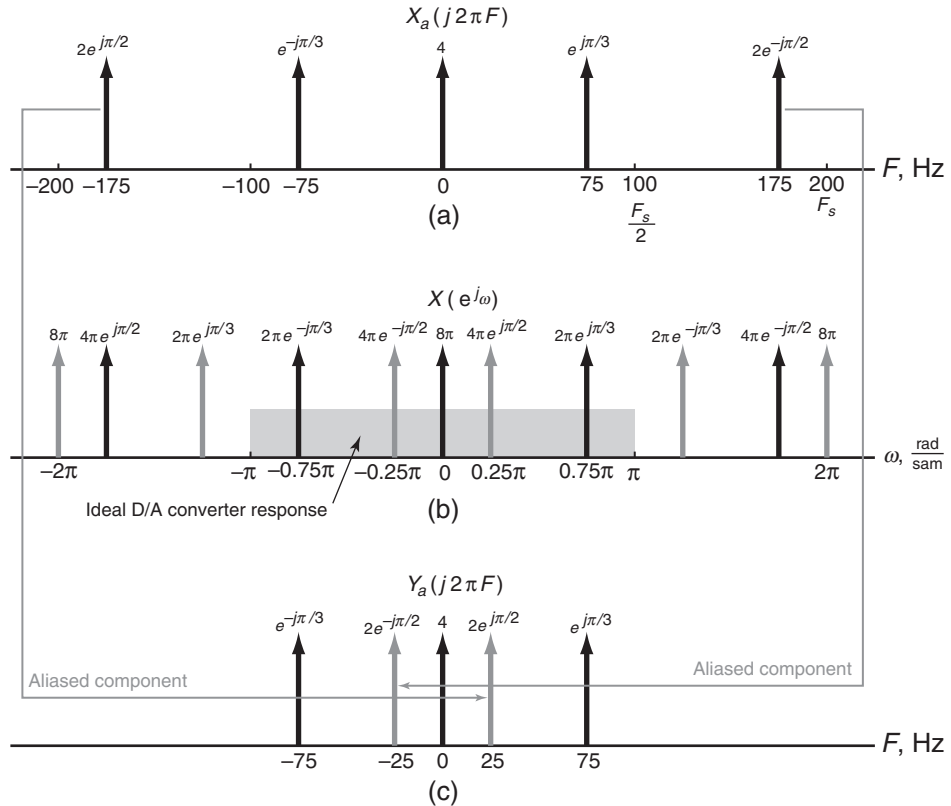


**FIGURE 3.15** Fourier transforms of the sinusoidal signals  $x_a(t)$ ,  $x(n)$ , and  $y_a(t)$

which is a rectangular pulse. The resulting signal is a piecewise-constant (staircase) waveform that requires an appropriately designed analog postfilter for accurate waveform reconstruction.

$$x(n) \rightarrow \boxed{\text{ZOH}} \rightarrow \hat{x}_a(t) \rightarrow \boxed{\text{Postfilter}} \rightarrow x_a(t)$$

- **First-order-hold (FOH) interpolation:** In this case, the adjacent samples are joined by straight lines. This can be obtained by filtering the impulse train through

$$h_1(t) = \begin{cases} 1 + \frac{t}{T_s}, & 0 \leq t \leq T_s \\ 1 - \frac{t}{T_s}, & T_s \leq t \leq 2T_s \\ 0, & \text{otherwise} \end{cases}$$

Once again, an appropriately designed analog postfilter is required for accurate reconstruction. These interpolations can be extended to higher

orders. One particularly useful interpolation employed by MATLAB is the following.

- **Cubic spline interpolation:** This approach uses spline interpolants for a smoother, but not necessarily more accurate, estimate of the analog signals between samples. Hence this interpolation does not require an analog postfilter. The smoother reconstruction is obtained by using a set of piecewise continuous third-order polynomials called *cubic splines*, given by

$$\begin{aligned} x_a(t) = & \alpha_0(n) + \alpha_1(n)(t - nT_s) + \alpha_2(n)(t - nT_s)^2 \\ & + \alpha_3(n)(t - nT_s)^3, \quad nT_s \leq n < (n+1)T_s \end{aligned} \quad (3.42)$$

where  $\{\alpha_i(n), 0 \leq i \leq 3\}$  are the polynomial coefficients, which are determined by using least-squares analysis on the sample values [10]. (Strictly speaking, this is not a causal operation but is a convenient one in MATLAB.)

#### 3.4.4 MATLAB IMPLEMENTATION

For interpolation between samples, MATLAB provides several approaches. The function `sinc(x)`, which generates the  $(\sin \pi x)/\pi x$  function, can be used to implement (3.37), given a finite number of samples. If  $\{x(n), n_1 \leq n \leq n_2\}$  is given, and if we want to interpolate  $x_a(t)$  on a very fine grid with the grid interval  $\Delta t$ , then, from (3.37),

$$x_a(m\Delta t) \approx \sum_{n=n_1}^{n_2} x(n) \operatorname{sinc}[F_s(m\Delta t - nT_s)], \quad t_1 \leq m\Delta t \leq t_2 \quad (3.43)$$

which can be implemented as a matrix-vector multiplication operation as shown below.

```
>> n = n1:n2; t = t1:t2; Fs = 1/Ts; nTs = n*Ts; % Ts is the sampling interval
>> xa = x * sinc(Fs*(ones(length(n),1)*t-nTs'*ones(1,length(t))));
```

Note that it is not possible to obtain an *exact* analog  $x_a(t)$  in light of the fact that we have assumed a finite number of samples. We now demonstrate the use of the `sinc` function in the following two examples and also study the aliasing problem in the time domain.

- EXAMPLE 3.21** From the samples  $x_1(n)$  in Example 3.19a, reconstruct  $x_a(t)$  and comment on the results.

**Solution**

Note that  $x_1(n)$  was obtained by sampling  $x_a(t)$  at  $T_s = 1/F_s = 0.0002$  sec. We will use the grid spacing of 0.00005 sec over  $-0.005 \leq t \leq 0.005$ , which gives  $x(n)$  over  $-25 \leq n \leq 25$ .

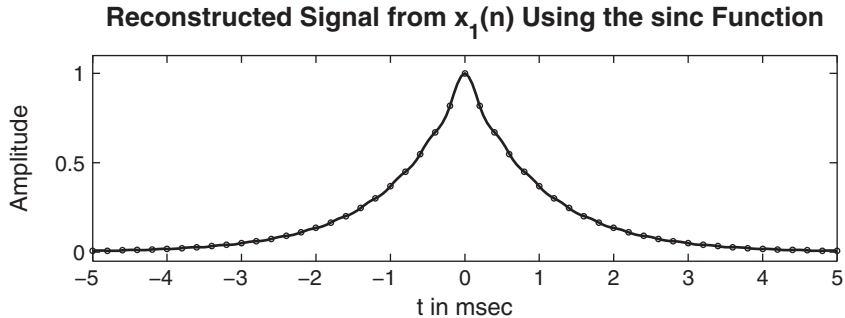


**FIGURE 3.16** Reconstructed signal in Example 3.21

MATLAB script:

```
% Discrete-time signal x1(n)
>> Ts = 0.0002; n = -25:1:25; nTs = n*Ts; x = exp(-1000*abs(nTs));
% Analog signal reconstruction
>> Dt = 0.00005; t = -0.005:Dt:0.005;
>> xa = x * sinc(Fs*(ones(length(n),1)*t-nTs'*ones(1,length(t))));
% Check
>> error = max(abs(xa - exp(-1000*abs(t))))
error =
0.0363
```

The maximum error between the reconstructed and the actual analog signal is 0.0363, which is due to the fact that  $x_a(t)$  is not strictly band-limited (and also we have a finite number of samples). From Figure 3.16, we note that visually the reconstruction is excellent.  $\square$

- **EXAMPLE 3.22** From the samples  $x_2(n)$  in Example 3.17b, reconstruct  $x_a(t)$  and comment on the results.

**Solution**

In this case,  $x_2(n)$  was obtained by sampling  $x_a(t)$  at  $T_s = 1/F_s = 0.001$  sec. We will again use the grid spacing of 0.00005 sec over  $-0.005 \leq t \leq 0.005$ , which gives  $x(n)$  over  $-5 \leq n \leq 5$ .

```
% Discrete-time signal x2(n)
>> Ts = 0.001; n = -5:1:5; nTs = n*Ts; x = exp(-1000*abs(nTs));
% Analog signal reconstruction
>> Dt = 0.00005; t = -0.005:Dt:0.005;
>> xa = x * sinc(Fs*(ones(length(n),1)*t-nTs'*ones(1,length(t))));
% Check
>> error = max(abs(xa - exp(-1000*abs(t))))
error =
0.1852
```

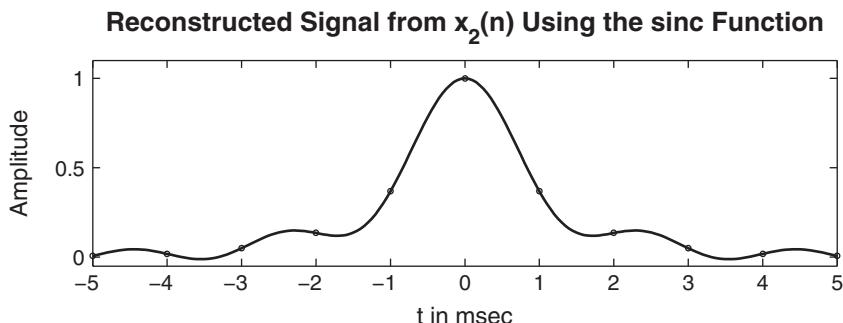


**FIGURE 3.17** Reconstructed signal in Example 3.22

The maximum error between the reconstructed and the actual analog signals is 0.1852, which is significant and cannot be attributed to the nonband-limitedness of  $x_a(t)$  alone. From Figure 3.17, observe that the reconstructed signal differs from the actual one in many places over the interpolated regions. This is the visual demonstration of aliasing in the time domain.  $\square$

The second MATLAB approach for signal reconstruction is a plotting approach. The `stairs` function plots a staircase (ZOH) rendition of the analog signal, given its samples, while the `plot` function depicts a linear (FOH) interpolation between samples.

- $\square$  **EXAMPLE 3.23** Plot the reconstructed signal from the samples  $x_1(n)$  in Example 3.19 using the ZOH and the FOH interpolations. Comment on the plots.

**Solution**

Note that in this reconstruction, we do not compute  $x_a(t)$  but merely plot it using its samples.

```
% Discrete-time signal x1(n) : Ts = 0.0002
>> Ts = 0.0002; n = -25:1:25; nTs = n*Ts; x = exp(-1000*abs(nTs));
% Plots
>> subplot(2,1,1); stairs(nTs*1000,x);
>> xlabel('t in msec'); ylabel('Amplitude')
>> title('Reconstructed Signal from x_1(n) Using ZOH'); hold on
>> stem(n*Ts*1000,x); hold off
%
% Discrete-time signal x1(n) : Ts = 0.001
>> Ts = 0.001; n = -5:1:5; nTs = n*Ts; x = exp(-1000*abs(nTs));
% Plots
>> subplot(2,1,2); plot(nTs*1000,x);
>> xlabel('t in msec'); ylabel('Amplitude')
>> title('Reconstructed Signal from x_1(n) Using FOH'); hold on
>> stem(n*Ts*1000,x); hold off
```

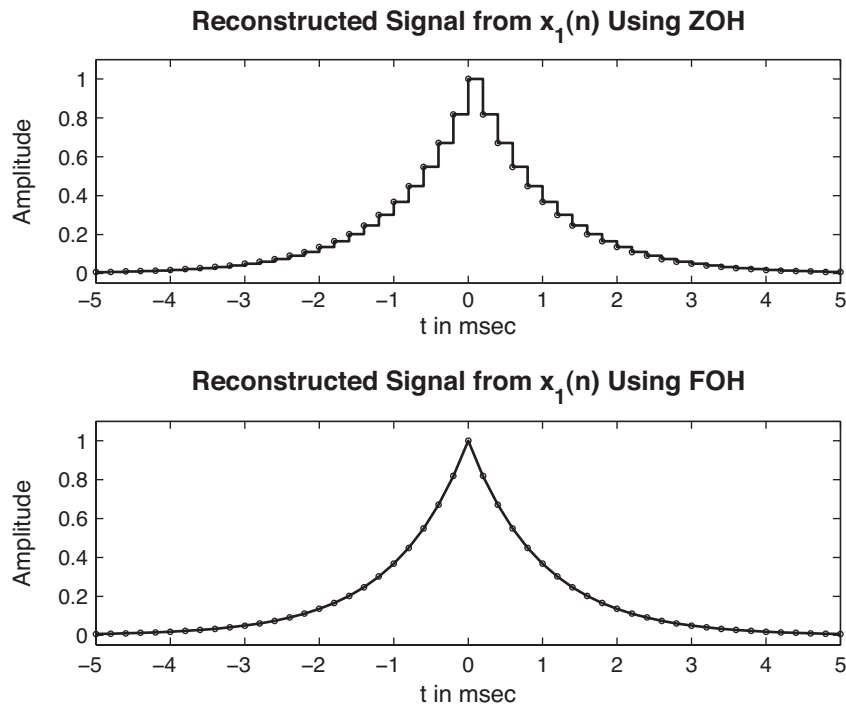


**FIGURE 3.18** Signal reconstruction in Example 3.23

The plots are shown in Figure 3.18, from which we observe that the ZOH reconstruction is a crude one and that the further processing of analog signal is necessary. The FOH reconstruction appears to be a good one, but a careful observation near  $t = 0$  reveals that the peak of the signal is not correctly reproduced. In general, if the sampling frequency is much higher than the Nyquist rate, then the FOH interpolation provides an acceptable reconstruction.  $\square$

The third approach of reconstruction in MATLAB involves the use of cubic spline functions. The `spline` function implements interpolation between sample points. It is invoked by `xa = spline(nTs, x, t)`, in which `x` and `nTs` are arrays containing samples  $x(n)$  at  $nT_s$  instances, respectively, and `t` array contains a fine grid at which  $x_a(t)$  values are desired. Note once again that it is not possible to obtain an *exact* analog  $x_a(t)$ .

- EXAMPLE 3.24** From the samples  $x_1(n)$  and  $x_2(n)$  in Example 3.19, reconstruct  $x_a(t)$  using the `spline` function. Comment on the results.

#### Solution

This example is similar to Examples 3.21 and 3.22. Hence sampling parameters are the same as before.

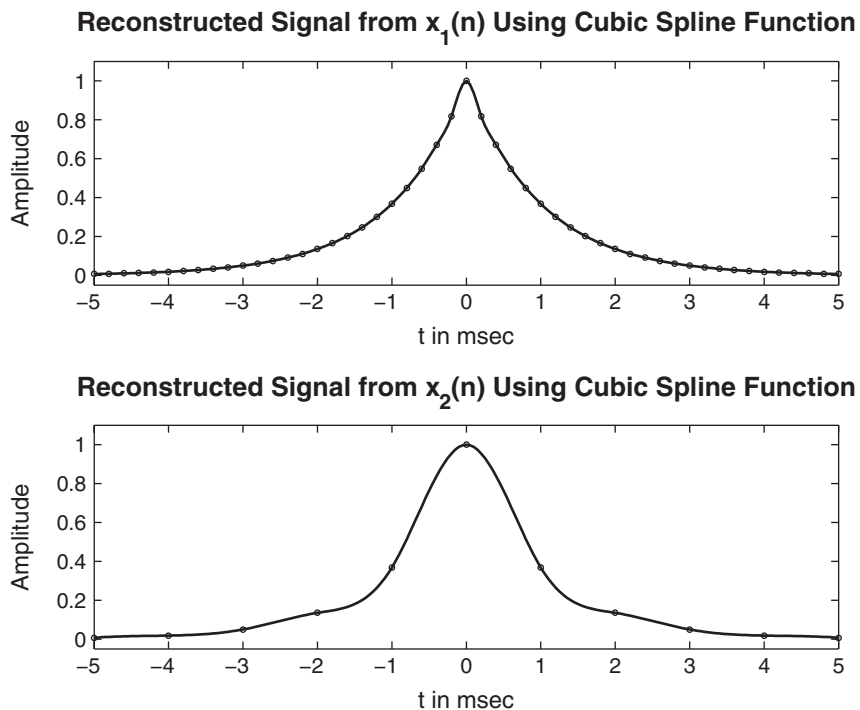


**FIGURE 3.19** Reconstructed signal in Example 3.24

MATLAB script:

```
% a) Discrete-time signal x1(n): Ts = 0.0002
>> Ts = 0.0002; n = -25:1:25; nTs = n*Ts; x = exp(-1000*abs(nTs));
% Analog signal reconstruction
>> Dt = 0.00005; t = -0.005:Dt:0.005; xa = spline(nTs,x,t);
% Check
>> error = max(abs(xa - exp(-1000*abs(t))))
error = 0.0317
```

The maximum error between the reconstructed and the actual analog signal is 0.0317, which is due to the nonideal interpolation and the fact that  $x_a(t)$  is nonband-limited. Comparing this error with that from the sinc (or ideal) interpolation, we note that this error is lower. The ideal interpolation generally suffers more from time-limitedness (or from a finite number of samples). From the top plot in Figure 3.19, we observe that visually the reconstruction is excellent.

MATLAB script:

```
% Discrete-time signal x2(n): Ts = 0.001
>> Ts = 0.001; n = -5:1:5; nTs = n*Ts; x = exp(-1000*abs(nTs));
% Analog signal reconstruction
>> Dt = 0.00005; t = -0.005:Dt:0.005; xa = spline(nTs,x,t);
```

```
% Check
>> error = max(abs(xa - exp(-1000*abs(t))))
error = 0.1679
```

The maximum error in this case is 0.1679, which is significant and cannot be attributed to the nonideal interpolation or nonband-limitedness of  $x_a(t)$ . From the bottom plot in Figure 3.19, observe that the reconstructed signal again differs from the actual one in many places over the interpolated regions.  $\square$

From these examples, it is clear that for practical purposes the **spline** interpolation provides the best results.

## 3.5 PROBLEMS

---

- P3.1** Using the matrix-vector multiplication approach discussed in this chapter, write a MATLAB function to compute the DTFT of a finite-duration sequence. The format of the function should be

```
function [X] = dtft(x,n,w)
% Computes discrete-time Fourier transform
% [X] = dtft(x,n,w)
% X = DTFT values computed at w frequencies
% x = finite duration sequence over n
% n = sample position vector
% w = frequency location vector
```

Use this function to compute the DTFT  $X(e^{j\omega})$  of the following finite-duration sequences over  $-\pi \leq \omega \leq \pi$ . Plot DTFT magnitude and angle graphs in one figure window.

1.  $x(n) = (0.6)^{|n|} [u(n+10) - u(n-11)]$ . Comment on the angle plot.
2.  $x(n) = n(0.9)^n [u(n) - u(n-21)]$ .
3.  $x(n) = [\cos(0.5\pi n) + j \sin(0.5\pi n)][u(n) - u(n-51)]$ . Comment on the magnitude plot.
4.  $x(n) = \{4, 3, 2, 1, 1, 2, 3, 4\}$ . Comment on the angle plot.
5.  $x(n) = \overset{\uparrow}{\{4, 3, 2, 1, -1, -2, -3, -4\}}$ . Comment on the angle plot.

- P3.2** Let  $x_1(n) = \begin{cases} 1, & n=0 \\ 2, & n=1 \\ 2, & n=2 \\ 1, & n=3 \end{cases}$ . A new sequence  $x_2(n)$  is formed using

$$x_2(n) = \begin{cases} x_1(n), & 0 \leq n \leq 3 \\ x_1(n-4), & 4 \leq n \leq 7 \\ 0, & \text{otherwise} \end{cases} \quad (3.44)$$

1. Express  $X_2(e^{j\omega})$  in terms of  $X_1(e^{j\omega})$  without explicitly computing  $X_1(e^{j\omega})$ .
2. Verify your result using MATLAB by computing and plotting magnitudes of the respective DTFTs.

- P3.3** Determine analytically the DTFT of each of the following sequences. Plot the magnitude and angle of  $X(e^{j\omega})$  over  $0 \leq \omega \leq \pi$ .

1.  $x(n) = 2(0.5)^n u(n+2)$
2.  $x(n) = (0.6)^{|n|} [u(n+10) - u(n-11)]$
3.  $x(n) = n(0.9)^n u(n+3)$
4.  $x(n) = (n+3)(0.8)^{n-1} u(n-2)$
5.  $x(n) = 4(-0.7)^n \cos(0.25\pi n)u(n)$

- P3.4** The following finite-duration sequences are called *windows* and are very useful in DSP:

$$\begin{aligned}\text{Rectangular: } \mathcal{R}_M(n) &= \begin{cases} 1, & 0 \leq n < M \\ 0, & \text{otherwise} \end{cases} \\ \text{Hanning: } \mathcal{C}_M(n) &= 0.5 \left[ 1 - \cos \frac{2\pi n}{M-1} \right] \mathcal{R}_M(n) \\ \text{Triangular: } \mathcal{T}_M(n) &= \left[ 1 - \frac{|M-1-2n|}{M-1} \right] \mathcal{R}_M(n) \\ \text{Hamming: } \mathcal{H}_M(n) &= \left[ 0.54 - 0.46 \cos \frac{2\pi n}{M-1} \right] \mathcal{R}_M(n)\end{aligned}$$

For each of these windows, determine their DTFTs for  $M = 10, 25, 50, 101$ . Scale transform values so that the maximum value is equal to 1. Plot the magnitude of the normalized DTFT over  $-\pi \leq \omega \leq \pi$ . Study these plots and comment on their behavior as a function of  $M$ .

- P3.5** Using the definition of the DTFT in (3.1), determine the sequences corresponding to the following DTFTs.

1.  $X(e^{j\omega}) = 3 + 2\cos(\omega) + 4\cos(2\omega)$
2.  $X(e^{j\omega}) = [1 - 6\cos(3\omega) + 8\cos(5\omega)] e^{-j3\omega}$
3.  $X(e^{j\omega}) = 2 + j4\sin(2\omega) - 5\cos(4\omega)$
4.  $X(e^{j\omega}) = [1 + 2\cos(\omega) + 3\cos(2\omega)] \cos(\omega/2)e^{-j5\omega/2}$
5.  $X(e^{j\omega}) = j[3 + 2\cos(\omega) + 4\cos(2\omega)] \sin(\omega)e^{-j3\omega}$

- P3.6** Using the definition of the inverse DTFT in (3.2), determine the sequences corresponding to the following DTFTs.

1.  $X(e^{j\omega}) = \begin{cases} 1, & 0 \leq |\omega| \leq \pi/3 \\ 0, & \pi/3 < |\omega| \leq \pi \end{cases}$
2.  $X(e^{j\omega}) = \begin{cases} 0, & 0 \leq |\omega| \leq 3\pi/4 \\ 1, & 3\pi/4 < |\omega| \leq \pi \end{cases}$
3.  $X(e^{j\omega}) = \begin{cases} 2, & 0 \leq |\omega| \leq \pi/8 \\ 1, & \pi/8 < |\omega| \leq 3\pi/4 \\ 0, & 3\pi/4 < |\omega| \leq \pi \end{cases}$
4.  $X(e^{j\omega}) = \begin{cases} 0, & -\pi \leq |\omega| < \pi/4 \\ 1, & \pi/4 \leq |\omega| \leq 3\pi/4 \\ 0, & 3\pi/4 < |\omega| \leq \pi \end{cases}$
5.  $X(e^{j\omega}) = \omega e^{j(\pi/2 - 10\omega)}$

Remember that the above transforms are periodic in  $\omega$  with period equal to  $2\pi$ . Hence functions are given only over the primary period of  $-\pi \leq \omega \leq \pi$ .

- P3.7** A complex-valued sequence  $x(n)$  can be decomposed into a conjugate symmetric part  $x_e(n)$  and a conjugate antisymmetric part  $x_o(n)$  as discussed in Chapter 2. Show that

$$\mathcal{F}[x_e(n)] = X_R(e^{j\omega}) \quad \text{and} \quad \mathcal{F}[x_o(n)] = jX_I(e^{j\omega})$$

where  $X_R(e^{j\omega})$  and  $X_I(e^{j\omega})$  are the real and imaginary parts of the DTFT  $X(e^{j\omega})$ , respectively. Verify this property on

$$x(n) = 2(0.9)^{-n} [\cos(0.1\pi n) + j \sin(0.9\pi n)] [u(n) - u(n - 10)]$$

using the MATLAB functions developed in Chapter 2.

- P3.8** A complex-valued DTFT  $X(e^{j\omega})$  can also be decomposed into its conjugate symmetric part  $X_e(e^{j\omega})$  and conjugate antisymmetric part  $X_o(e^{j\omega})$ , that is,

$$X(e^{j\omega}) = X_e(e^{j\omega}) + X_o(e^{j\omega})$$

where

$$X_e(e^{j\omega}) = \frac{1}{2}[X(e^{j\omega}) + X^*(e^{-j\omega})] \quad \text{and} \quad X_o(e^{j\omega}) = \frac{1}{2}[X(e^{j\omega}) - X^*(e^{-j\omega})]$$

Show that

$$\mathcal{F}^{-1}[X_e(e^{j\omega})] = x_R(n) \quad \text{and} \quad \mathcal{F}^{-1}[X_o(e^{j\omega})] = jx_I(n)$$

where  $x_R(n)$  and  $x_I(n)$  are the real and imaginary parts of  $x(n)$ . Verify this property on

$$x(n) = e^{j0.1\pi n} [u(n) - u(n - 20)]$$

using the MATLAB functions developed in Chapter 2.

- P3.9** Using the frequency-shifting property of the DTFT, show that the real part of  $X(e^{j\omega})$  of a sinusoidal pulse

$$x(n) = (\cos \omega_0 n) \mathcal{R}_M(n)$$

where  $\mathcal{R}_M(n)$  is the rectangular pulse given in Problem P3.4 is given by

$$\begin{aligned} X_R(e^{j\omega}) &= \frac{1}{2} \cos \left\{ \frac{(\omega - \omega_0)(M - 1)}{2} \right\} \frac{\sin \{(\omega - \omega_0) M/2\}}{\sin \{(\omega - \omega_0)/2\}} \\ &\quad + \frac{1}{2} \cos \left\{ \frac{(\omega + \omega_0)(M - 1)}{2} \right\} \frac{\sin \{[\omega - (2\pi - \omega_0)] M/2\}}{\sin \{[\omega - (2\pi - \omega_0)]/2\}} \end{aligned}$$

Compute and plot  $X_R(e^{j\omega})$  for  $\omega_0 = \pi/2$  and  $M = 5, 15, 25, 100$ . Use the plotting interval  $[-\pi, \pi]$ . Comment on your results.

- P3.10** Let  $x(n) = \mathcal{T}_{10}(n)$  be a triangular pulse given in Problem P3.4. Using properties of the DTFT, determine and plot the DTFT of the following sequences.

1.  $x(n) = \mathcal{T}_{10}(-n)$
2.  $x(n) = \mathcal{T}_{10}(n) - \mathcal{T}_{10}(n - 10)$
3.  $x(n) = \mathcal{T}_{10}(n) * \mathcal{T}_{10}(-n)$
4.  $x(n) = \mathcal{T}_{10}(n)e^{j\pi n}$
5.  $x(n) = \cos(0.1\pi n)\mathcal{T}_{10}(n)$

- P3.11** For each of the linear, shift-invariant systems described by the impulse response, determine the frequency response function  $H(e^{j\omega})$ . Plot the magnitude response  $|H(e^{j\omega})|$  and the phase response  $\angle H(e^{j\omega})$  over the interval  $[-\pi, \pi]$ .

1.  $h(n) = (0.9)^{|n|}$
2.  $h(n) = \text{sinc}(0.2n)[u(n+20) - u(n-20)]$ , where  $\text{sinc}(0) = 1$
3.  $h(n) = \text{sinc}(0.2n)[u(n) - u(n-40)]$
4.  $h(n) = [(0.5)^n + (0.4)^n]u(n)$
5.  $h(n) = (0.5)^{|n|} \cos(0.1\pi n)$

- P3.12** Let  $x(n) = A \cos(\omega_0 n + \theta_0)$  be an input sequence to an LTI system described by the impulse response  $h(n)$ . Show that the output sequence  $y(n)$  is given by

$$y(n) = A|H(e^{j\omega_0})| \cos[\omega_0 n + \theta_0 + \angle H(e^{j\omega_0})]$$

- P3.13** Let  $x(n) = 3 \cos(0.5\pi n + 60^\circ) + 2 \sin(0.3\pi n)$  be the input to each of the systems described in Problem P3.11. In each case, determine the output sequence  $y(n)$ .

- P3.14** An ideal lowpass filter is described in the frequency domain by

$$H_d(e^{j\omega}) = \begin{cases} 1 \cdot e^{-j\alpha\omega}, & |\omega| \leq \omega_c \\ 0, & \omega_c < |\omega| \leq \pi \end{cases}$$

where  $\omega_c$  is called the cutoff frequency and  $\alpha$  is called the phase delay.

1. Determine the ideal impulse response  $h_d(n)$  using the IDTFT relation (3.2).
2. Determine and plot the truncated impulse response

$$h(n) = \begin{cases} h_d(n), & 0 \leq n \leq N-1 \\ 0, & \text{otherwise} \end{cases}$$

for  $N = 41$ ,  $\alpha = 20$ , and  $\omega_c = 0.5\pi$ .

3. Determine and plot the frequency response function  $H(e^{j\omega})$ , and compare it with the ideal lowpass filter response  $H_d(e^{j\omega})$ . Comment on your observations.

- P3.15** An ideal highpass filter is described in the frequency-domain by

$$H_d(e^{j\omega}) = \begin{cases} 1 \cdot e^{-j\alpha\omega}, & \omega_c < |\omega| \leq \pi \\ 0, & |\omega| \leq \omega_c \end{cases}$$

where  $\omega_c$  is called the cutoff frequency and  $\alpha$  is called the phase delay.

1. Determine the ideal impulse response  $h_d(n)$  using the IDTFT relation (3.2).
2. Determine and plot the truncated impulse response

$$h(n) = \begin{cases} h_d(n), & 0 \leq n \leq N-1 \\ 0, & \text{otherwise} \end{cases}$$

for  $N = 31$ ,  $\alpha = 15$ , and  $\omega_c = 0.5\pi$ .

3. Determine and plot the frequency response function  $H(e^{j\omega})$ , and compare it with the ideal highpass filter response  $H_d(e^{j\omega})$ . Comment on your observations.

- P3.16** For a linear, shift-invariant system described by the difference equation

$$y(n) = \sum_{m=0}^M b_m x(n-m) - \sum_{\ell=1}^N a_\ell y(n-\ell)$$

the frequency-response function is given by

$$H(e^{j\omega}) = \frac{\sum_{m=0}^M b_m e^{-j\omega m}}{1 + \sum_{\ell=1}^N a_\ell e^{-j\omega \ell}}$$

Write a MATLAB function `freqresp` to implement this relation. The format of this function should be

```
function [H] = freqresp(b,a,w)
% Frequency response function from difference equation
% [H] = freqresp(b,a,w)
% H = frequency response array evaluated at w frequencies
% b = numerator coefficient array
% a = denominator coefficient array (a(1)=1)
% w = frequency location array
```

- P3.17** Determine  $H(e^{j\omega})$ , and plot its magnitude and phase for each of the following systems.

1.  $y(n) = \frac{1}{5} \sum_{m=0}^4 x(n-m)$
2.  $y(n) = x(n) - x(n-2) + 0.95y(n-1) - 0.9025y(n-2)$
3.  $y(n) = x(n) - x(n-1) + x(n-2) + 0.95y(n-1) - 0.9025y(n-2)$
4.  $y(n) = x(n) - 1.7678x(n-1) + 1.5625x(n-2) + 1.1314y(n-1) - 0.64y(n-2)$
5.  $y(n) = x(n) - \sum_{\ell=1}^5 (0.5)^\ell y(n-\ell)$

- P3.18** A linear, shift-invariant system is described by the difference equation

$$y(n) = \sum_{m=0}^3 x(n-2m) - \sum_{\ell=1}^3 (0.81)^\ell y(n-2\ell)$$

Determine the steady-state response of the system to the following inputs.

1.  $x(n) = 5 + 10(-1)^n$
2.  $x(n) = 1 + \cos(0.5\pi n + \pi/2)$
3.  $x(n) = 2 \sin(\pi n/4) + 3 \cos(3\pi n/4)$
4.  $x(n) = \sum_{k=0}^5 (k+1) \cos(\pi kn/4)$
5.  $x(n) = \cos(\pi n)$

In each case, generate  $x(n)$ ,  $0 \leq n \leq 200$ , and process it through the `filter` function to obtain  $y(n)$ . Compare your  $y(n)$  with the steady-state responses in each case.

- P3.19** An analog signal  $x_a(t) = \sin(1000\pi t)$  is sampled using the following sampling intervals. In each case, plot the spectrum of the resulting discrete-time signal.

1.  $T_s = 0.1$  msec
2.  $T_s = 1$  msec
3.  $T_s = 0.01$  sec

**P3.20** We implement the following analog filter using a discrete filter:

$$x_a(t) \longrightarrow \boxed{\text{A/D}} \xrightarrow{x(n)} \boxed{h(n)} \xrightarrow{y(n)} \boxed{\text{D/A}} \longrightarrow y_a(t)$$

The sampling rate in the A/D and D/A is 8000 sam/sec, and the impulse response is  $h(n) = (-0.9)^n u(n)$ .

1. What is the digital frequency in  $x(n)$  if  $x_a(t) = 10 \cos(10,000\pi t)$ ?
  2. Determine the steady-state output  $y_a(t)$  if  $x_a(t) = 10 \cos(10,000\pi t)$ .
  3. Determine the steady-state output  $y_a(t)$  if  $x_a(t) = 5 \sin(8,000\pi t)$ .
  4. Find two other analog signals  $x_a(t)$ , with different analog frequencies, that will give the same steady-state output  $y_a(t)$  when  $x_a(t) = 10 \cos(10,000\pi t)$  is applied.
  5. To prevent aliasing, a prefilter would be required to process  $x_a(t)$  before it passes to the A/D converter. What type of filter should be used, and what should be the largest cutoff frequency that would work for the given configuration?
- P3.21** Consider an analog signal  $x_a(t) = \cos(20\pi t)$ ,  $0 \leq t \leq 1$ . It is sampled at  $T_s = 0.01$ ,  $0.05$ , and  $0.1$  sec intervals to obtain  $x(n)$ .
1. For each  $T_s$ , plot  $x(n)$ .
  2. Reconstruct the analog signal  $y_a(t)$  from the samples  $x(n)$  using the sinc interpolation (use  $\Delta t = 0.001$ ) and determine the frequency in  $y_a(t)$  from your plot. (Ignore the end effects.)
  3. Reconstruct the analog signal  $y_a(t)$  from the samples  $x(n)$  using the cubic spline interpolation, and determine the frequency in  $y_a(t)$  from your plot. (Again, ignore the end effects.)
  4. Comment on your results.
- P3.22** Consider the analog signal  $x_a(t) = \cos(20\pi t + \theta)$ ,  $0 \leq t \leq 1$ . It is sampled at  $T_s = 0.05$  sec intervals to obtain  $x(n)$ . Let  $\theta = 0, \pi/6, \pi/4, \pi/3, \pi/2$ . For each of these  $\theta$  values, perform the following.
1. Plot  $x_a(t)$  and superimpose  $x(n)$  on it using the `plot(n,x,'o')` function.
  2. Reconstruct the analog signal  $y_a(t)$  from the samples  $x(n)$  using the sinc interpolation (Use  $\Delta t = 0.001$ ) and superimpose  $x(n)$  on it.
  3. Reconstruct the analog signal  $y_a(t)$  from the samples  $x(n)$  using the cubic spline interpolation and superimpose  $x(n)$  on it.
  4. You should observe that the resultant reconstruction in each case has the correct frequency but a different amplitude. Explain this observation. Comment on the role of phase of  $x_a(t)$  on the sampling and reconstruction of signals.

# CHAPTER 4

---

## The $z$ -Transform

---

In Chapter 3, we studied the discrete-time Fourier transform approach for representing discrete signals using complex exponential sequences. This representation clearly has advantages for LTI systems because it describes systems in the frequency domain using the frequency response function  $H(e^{j\omega})$ . The computation of the sinusoidal steady-state response is greatly facilitated by the use of  $H(e^{j\omega})$ . Furthermore, response to any arbitrary absolutely summable sequence  $x(n)$  can easily be computed in the frequency domain by multiplying the transform  $X(e^{j\omega})$  and the frequency response  $H(e^{j\omega})$ . However, there are two shortcomings to the Fourier transform approach. First, there are many useful signals in practice—such as  $u(n)$  and  $nu(n)$ —for which the discrete-time Fourier transform does not exist. Second, the transient response of a system due to initial conditions or due to changing inputs cannot be computed using the discrete-time Fourier transform approach.

Therefore, we now consider an extension of the discrete-time Fourier transform to address these two problems. This extension is called the *z-transform*. Its bilateral (or two-sided) version provides another domain in which a larger class of sequences and systems can be analyzed, and its unilateral (or one-sided) version can be used to obtain system responses with initial conditions or changing inputs.

### 4.1 THE BILATERAL $z$ -TRANSFORM

---

The  $z$ -transform of a sequence  $x(n)$  is given by

$$X(z) \triangleq \mathcal{Z}[x(n)] = \sum_{n=-\infty}^{\infty} x(n)z^{-n} \quad (4.1)$$

where  $z$  is a complex variable. The set of  $z$  values for which  $X(z)$  exists is called the *region of convergence (ROC)* and is given by

$$R_{x-} < |z| < R_{x+} \quad (4.2)$$

for some nonnegative numbers  $R_{x-}$  and  $R_{x+}$ .

The inverse  $z$ -transform of a complex function  $X(z)$  is given by

$$x(n) \triangleq \mathcal{Z}^{-1}[X(z)] = \frac{1}{2\pi j} \oint_C X(z) z^{n-1} dz \quad (4.3)$$

where  $C$  is a **counterclockwise contour** encircling the origin and lying in the ROC.

*Comments:*

1. The complex variable  $z$  is called the *complex frequency* given by  $z = |z|e^{j\omega}$ , where  $|z|$  is the magnitude and  $\omega$  is the real frequency.
2. Since the ROC (4.2) is defined in terms of the magnitude  $|z|$ , the shape of the ROC is an open ring, as shown in Figure 4.1. Note that  $R_{x-}$  may be equal to zero and/or  $R_{x+}$  could possibly be  $\infty$ .
3. If  $R_{x+} < R_{x-}$ , then the ROC is a *null space* and the  $z$ -transform *does not exist*.
4. The function  $|z| = 1$  (or  $z = e^{j\omega}$ ) is a circle of unit radius in the  $z$ -plane and is called the *unit circle*. If the ROC contains the unit circle, then we can evaluate  $X(z)$  on the unit circle:

$$X(z)|_{z=e^{j\omega}} = X(e^{j\omega}) = \sum_{n=-\infty}^{\infty} x(n)e^{-j\omega n} = \mathcal{F}[x(n)]$$

Therefore, the discrete-time Fourier transform  $X(e^{j\omega})$  may be viewed as a special case of the  $z$ -transform  $X(z)$ .

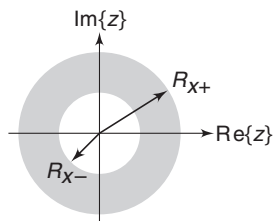


**FIGURE 4.1** A general region of convergence

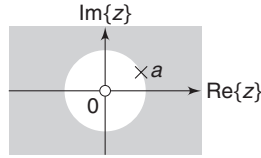


**FIGURE 4.2** The ROC in Example 4.1

- **EXAMPLE 4.1** Let  $x_1(n) = a^n u(n)$ ,  $0 < |a| < \infty$ . (This sequence is called a *positive-time sequence*.) Then

$$\begin{aligned} X_1(z) &= \sum_0^{\infty} a^n z^{-n} = \sum_0^{\infty} \left(\frac{a}{z}\right)^n = \frac{1}{1 - az^{-1}}; \quad \text{if } \left|\frac{a}{z}\right| < 1 \\ &= \frac{z}{z - a}, \quad |z| > |a| \Rightarrow \text{ROC}_1: \underbrace{|a|}_{R_{x-}} < |z| < \underbrace{\infty}_{R_{x+}} \end{aligned}$$

Note:  $X_1(z)$  in this example is a rational function; that is,

$$X_1(z) \triangleq \frac{B(z)}{A(z)} = \frac{z}{z - a}$$

where  $B(z) = z$  is the *numerator polynomial* and  $A(z) = z - a$  is the *denominator polynomial*. The roots of  $B(z)$  are called the *zeros* of  $X(z)$ , whereas the roots of  $A(z)$  are called the *poles* of  $X(z)$ . In this example,  $X_1(z)$  has a zero at the origin  $z = 0$  and a pole at  $z = a$ . Hence  $x_1(n)$  can also be represented by a *pole-zero diagram* in the  $z$ -plane in which zeros are denoted by  $\circ$  and poles by  $\times$ , as shown in Figure 4.2. □

- **EXAMPLE 4.2** Let  $x_2(n) = -b^n u(-n-1)$ ,  $0 < |b| < \infty$ . (This sequence is called a *negative-time sequence*.) Then

$$\begin{aligned} X_2(z) &= -\sum_{-\infty}^{-1} b^n z^{-n} = -\sum_{-\infty}^{-1} \left(\frac{b}{z}\right)^n = -\sum_1^{\infty} \left(\frac{z}{b}\right)^n = 1 - \sum_0^{\infty} \left(\frac{z}{b}\right)^n \\ &= 1 - \frac{1}{1 - z/b} = \frac{z}{z - b}, \quad \text{ROC}_2: \underbrace{0}_{R_{x-}} < |z| < \underbrace{|b|}_{R_{x+}} \end{aligned}$$

The  $\text{ROC}_2$  and the pole-zero plot for this  $x_2(n)$  are shown in Figure 4.3.

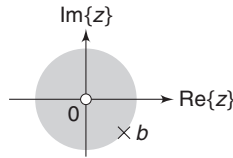


**FIGURE 4.3** The ROC in Example 4.2

*Note:* If  $b = a$  in this example, then  $X_2(z) = X_1(z)$  except for their respective ROCs; that is,  $\text{ROC}_1 \neq \text{ROC}_2$ . This implies that the ROC is a distinguishing feature that guarantees the uniqueness of the  $z$ -transform. Hence it plays a very important role in system analysis.  $\square$

- **EXAMPLE 4.3** Let  $x_3(n) = x_1(n) + x_2(n) = a^n u(n) - b^n u(-n-1)$  (This sequence is called a *two-sided sequence*.) Then, using the preceding two examples,

$$\begin{aligned} X_3(z) &= \sum_{n=0}^{\infty} a^n z^{-n} - \sum_{-\infty}^{-1} b^n z^{-n} \\ &= \left\{ \frac{z}{z-a}, \text{ROC}_1: |z| > |a| \right\} + \left\{ \frac{z}{z-b}, \text{ROC}_2: |z| < |b| \right\} \\ &= \frac{z}{z-a} + \frac{z}{z-b}; \quad \text{ROC}_3: \text{ROC}_1 \cap \text{ROC}_2 \end{aligned}$$

If  $|b| < |a|$ , then  $\text{ROC}_3$  is a null space, and  $X_3(z)$  does not exist. If  $|a| < |b|$ , then the  $\text{ROC}_3$  is  $|a| < |z| < |b|$ , and  $X_3(z)$  exists in this region as shown in Figure 4.4.  $\square$

#### 4.1.1 PROPERTIES OF THE ROC

From the observation of the ROCs in the preceding three examples, we state the following properties.

1. The ROC is **always bounded by a circle** since the convergence condition is on the magnitude  $|z|$ .
2. The sequence  $x_1(n) = a^n u(n)$  in Example 4.1 is a special case of a *right-sided sequence*, defined as a sequence  $x(n)$  that is zero for some  $n < n_0$ . From Example 4.1, the ROC for right-sided sequences is **always outside of a circle of radius  $R_{x-}$** . If  $n_0 \geq 0$ , then the right-sided sequence is also called a *causal* sequence.
3. The sequence  $x_2(n) = -b^n u(-n-1)$  in Example 4.2 is a special case of a *left-sided sequence*, defined as a sequence  $x(n)$  that is zero for some  $n > n_0$ . If  $n_0 \leq 0$ , the resulting sequence is called an *anticausal* sequence. From Example 4.2, the ROC for left-sided sequences is **always inside of a circle of radius  $R_{x+}$** .

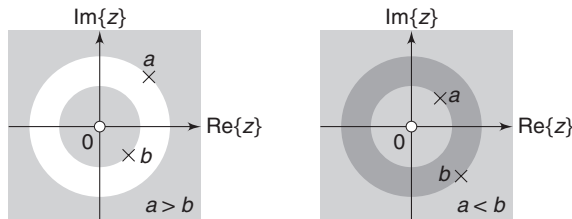


**FIGURE 4.4** The ROC in Example 4.3

4. The sequence  $x_3(n)$  in Example 4.3 is a two-sided sequence. The ROC for two-sided sequences is **always an open ring**  $R_{x-} < |z| < R_{x+}$ , if it exists.
5. The sequences that are zero for  $n < n_1$  and  $n > n_2$  are called *finite-duration sequences*. The ROC for such sequences is **the entire  $z$ -plane**. If  $n_1 < 0$ , then  $z = \infty$  is not in the ROC. If  $n_2 > 0$ , then  $z = 0$  is not in the ROC.
6. The ROC cannot include a pole, since  $X(z)$  converges uniformly in there.
7. There is at least one pole on the boundary of a ROC of a rational  $X(z)$ .
8. The ROC is one contiguous region; that is, the ROC does not come in pieces.

In digital signal processing, signals are assumed to be causal since almost every digital data is acquired in real time. Therefore, the only ROC of interest to us is the one given in statement 2.

## 4.2 IMPORTANT PROPERTIES OF THE $z$ -TRANSFORM

---

The properties of the  $z$ -transform are generalizations of the properties of the discrete-time Fourier transform that we studied in Chapter 3. We state the following important properties of the  $z$ -transform without proof.

### 1. Linearity:

$$\mathcal{Z}[a_1x_1(n) + a_2x_2(n)] = a_1X_1(z) + a_2X_2(z); \quad \text{ROC: } \text{ROC}_{x_1} \cap \text{ROC}_{x_2} \quad (4.4)$$

### 2. Sample shifting:

$$\mathcal{Z}[x(n - n_0)] = z^{-n_0}X(z); \quad \text{ROC: } \text{ROC}_x \quad (4.5)$$

### 3. Frequency shifting:

$$\mathcal{Z}[a^n x(n)] = X\left(\frac{z}{a}\right); \quad \text{ROC: } \text{ROC}_x \text{ scaled by } |a| \quad (4.6)$$

### 4. Folding:

$$\mathcal{Z}[x(-n)] = X(1/z); \quad \text{ROC: Inverted ROC}_x \quad (4.7)$$

### 5. Complex conjugation:

$$\mathcal{Z}[x^*(n)] = X^*(z^*); \quad \text{ROC: } \text{ROC}_x \quad (4.8)$$

**6. Differentiation in the  $z$ -domain:**

$$\mathcal{Z}[nx(n)] = -z \frac{dX(z)}{dz}; \quad \text{ROC: } \text{ROC}_x \quad (4.9)$$

This property is also called the *multiplication-by-a-ramp property*.

**7. Multiplication:**

$$\mathcal{Z}[x_1(n)x_2(n)] = \frac{1}{2\pi j} \oint_C X_1(\nu)X_2(z/\nu) \nu^{-1} d\nu; \quad (4.10)$$

ROC:  $\text{ROC}_{x_1} \cap \text{Inverted ROC}_{x_2}$

where  $C$  is a closed contour that encloses the origin and lies in the common ROC.

**8. Convolution:**

$$\mathcal{Z}[x_1(n) * x_2(n)] = X_1(z)X_2(z); \quad \text{ROC: } \text{ROC}_{x_1} \cap \text{ROC}_{x_2} \quad (4.11)$$

This last property transforms the time-domain convolution operation into a multiplication between two functions. It is a significant property in many ways. First, if  $X_1(z)$  and  $X_2(z)$  are two polynomials, then their product can be implemented using the `conv` function in MATLAB.

- **EXAMPLE 4.4** Let  $X_1(z) = 2 + 3z^{-1} + 4z^{-2}$ , and let  $X_2(z) = 3 + 4z^{-1} + 5z^{-2} + 6z^{-3}$ . Determine  $X_3(z) = X_1(z)X_2(z)$ .

**Solution**

From the definition of the  $z$ -transform, we observe that

$$x_1(n) = \begin{matrix} \{2, 3, 4\} \\ \uparrow \end{matrix} \quad \text{and} \quad x_2(n) = \begin{matrix} \{3, 4, 5, 6\} \\ \uparrow \end{matrix}$$

Then the convolution of these two sequences will give the coefficients of the required polynomial product.

MATLAB script:

```
>> x1 = [2,3,4]; x2 = [3,4,5,6]; x3 = conv(x1,x2)
x3 =
       6      17      34      43      38      24
```

Hence

$$X_3(z) = 6 + 17z^{-1} + 34z^{-2} + 43z^{-3} + 38z^{-4} + 24z^{-5}$$

Using the `conv.m` function developed in Chapter 2, we can also multiply two  $z$ -domain polynomials corresponding to noncausal sequences. □

- **EXAMPLE 4.5** Let  $X_1(z) = z + 2 + 3z^{-1}$ , and let  $X_2(z) = 2z^2 + 4z + 3 + 5z^{-1}$ . Determine  $X_3(z) = X_1(z)X_2(z)$ .

**Solution**

Note that

$$x_1(n) = \{1, 2, 3\} \quad \text{and} \quad x_2(n) = \{2, 4, 3, 5\}$$

Using the MATLAB script

```
>> x1 = [1,2,3]; n1 = [-1:1]; x2 = [2,4,3,5]; n2 = [-2:1];
>> [x3,n3] = conv_m(x1,n1,x2,n2)
x3 =
      2      8     17     23     19     15
n3 =
     -3     -2     -1      0      1      2
```

we have

$$X_3(z) = 2z^3 + 8z^2 + 17z + 23 + 19z^{-1} + 15z^{-2}$$

□

In passing, we note that to divide one polynomial by another one, we would require an inverse operation called *deconvolution* [79, Chapter 6]. In MATLAB, `[p,r] = deconv(b,a)` computes the result of dividing `b` by `a` in a polynomial part `p` and a remainder `r`. For example, if we divide the polynomial  $X_3(z)$  in Example 4.4 by  $X_1(z)$ , as follows,

```
>> x3 = [6,17,34,43,38,24]; x1 = [2,3,4]; [x2,r] = deconv(x3,x1)
x2 =
      3      4      5      6
r =
      0      0      0      0      0      0
```

then we obtain the coefficients of the polynomial  $X_2(z)$  as expected. To obtain the sample index, we will have to modify the `deconv` function as we did in the `conv_m` function. This is explored in Problem P4.10. This operation is useful in obtaining a *proper* rational part from an *improper* rational function.

The second important use of the convolution property is in system output computations, as we shall see in a later section. This interpretation is particularly useful for verifying the  $z$ -transform expression  $X(z)$  of a causal sequence using MATLAB. Note that since MATLAB is a numerical processor (unless the Symbolic toolbox is used), it cannot be used for symbolic  $z$ -transform calculations. We will now elaborate on this. Let  $x(n)$  be a sequence with a rational transform

$$X(z) = \frac{B(z)}{A(z)}$$

where  $B(z)$  and  $A(z)$  are polynomials in  $z^{-1}$ . If we use the coefficients of  $B(z)$  and  $A(z)$  as the `b` and `a` arrays in the `filter` routine and excite this

filter by the impulse sequence  $\delta(n)$ , then from (4.11) and using  $\mathcal{Z}[\delta(n)] = 1$ , the output of the filter will be  $x(n)$ . (This is a numerical approach of computing the inverse  $z$ -transform; we will discuss the analytical approach in the next section.) We can compare this output with the given  $x(n)$  to verify that  $X(z)$  is indeed the transform of  $x(n)$ . This is illustrated in Example 4.6. An equivalent approach is to use the `impz` function discussed in Chapter 2.

#### 4.2.1 SOME COMMON $z$ -TRANSFORM PAIRS

Using the definition of  $z$ -transform and its properties, one can determine  $z$ -transforms of common sequences. A list of some of these sequences is given in Table 4.1.

**TABLE 4.1** Some common  $z$ -transform pairs

Sequence	Transform	ROC
$\delta(n)$	1	$\forall z$
$u(n)$	$\frac{1}{1 - z^{-1}}$	$ z  > 1$
$-u(-n - 1)$	$\frac{1}{1 - z^{-1}}$	$ z  < 1$
$a^n u(n)$	$\frac{1}{1 - az^{-1}}$	$ z  >  a $
$-b^n u(-n - 1)$	$\frac{1}{1 - bz^{-1}}$	$ z  <  b $
$[a^n \sin \omega_0 n] u(n)$	$\frac{(a \sin \omega_0) z^{-1}}{1 - (2a \cos \omega_0) z^{-1} + a^2 z^{-2}}$	$ z  >  a $
$[a^n \cos \omega_0 n] u(n)$	$\frac{1 - (a \cos \omega_0) z^{-1}}{1 - (2a \cos \omega_0) z^{-1} + a^2 z^{-2}}$	$ z  >  a $
$na^n u(n)$	$\frac{az^{-1}}{(1 - az^{-1})^2}$	$ z  >  a $
$-nb^n u(-n - 1)$	$\frac{bz^{-1}}{(1 - bz^{-1})^2}$	$ z  <  b $

- **EXAMPLE 4.6** Using  $z$ -transform properties and the  $z$ -transform table, determine the  $z$ -transform of

$$x(n) = (n - 2)(0.5)^{(n-2)} \cos\left[\frac{\pi}{3}(n - 2)\right] u(n - 2)$$

**Solution**

Applying the sample-shift property,

$$X(z) = \mathcal{Z}[x(n)] = z^{-2} \mathcal{Z}\left[n(0.5)^n \cos\left(\frac{\pi n}{3}\right) u(n)\right]$$

with no change in the ROC. Applying the multiplication by a ramp property,

$$X(z) = z^{-2} \left\{ -z \frac{d\mathcal{Z}[(0.5)^n \cos(\frac{\pi}{3}n)u(n)]}{dz} \right\}$$

with no change in the ROC. Now the  $z$ -transform of  $(0.5)^n \cos(\frac{\pi}{3}n)u(n)$  from Table 4.1 is

$$\begin{aligned} \mathcal{Z}\left[(0.5)^n \cos\left(\frac{\pi n}{3}\right) u(n)\right] &= \frac{1 - (0.5 \cos \frac{\pi}{3})z^{-1}}{1 - 2(0.5 \cos \frac{\pi}{3})z^{-1} + 0.25z^{-2}}; \quad |z| > 0.5 \\ &= \frac{1 - 0.25z^{-1}}{1 - 0.5z^{-1} + 0.25z^{-2}}; \quad |z| > 0.5 \end{aligned}$$

Hence

$$\begin{aligned} X(z) &= -z^{-1} \frac{d}{dz} \left\{ \frac{1 - 0.25z^{-1}}{1 - 0.5z^{-1} + 0.25z^{-2}} \right\}, \quad |z| > 0.5 \\ &= -z^{-1} \left\{ \frac{-0.25z^{-2} + 0.5z^{-3} - 0.0625z^{-4}}{1 - z^{-1} + 0.75z^{-2} - 0.25z^{-3} + 0.0625z^{-4}} \right\}, \quad |z| > 0.5 \\ &= \frac{0.25z^{-3} - 0.5z^{-4} + 0.0625z^{-5}}{1 - z^{-1} + 0.75z^{-2} - 0.25z^{-3} + 0.0625z^{-4}}, \quad |z| > 0.5 \end{aligned}$$

MATLAB verification: To check that this  $X(z)$  is indeed the correct expression, let us compute the first eight samples of the sequence  $x(n)$  corresponding to  $X(z)$ , as discussed before.

```
>> b = [0,0,0,0.25,-0.5,0.0625]; a = [1,-1,0.75,-0.25,0.0625];
>> [delta,n]=impseq(0,0,7)
delta =
    1     0     0     0     0     0     0     0
n =
    0     1     2     3     4     5     6     7
>> x = filter(b,a,delta) % check sequence
x =
    Columns 1 through 4
            0                  0                  0  0.2500000000000000
    Columns 5 through 8
   -0.2500000000000000  -0.3750000000000000  -0.1250000000000000  0.0781250000000000
>> x = [(n-2).*(1/2).^(n-2).*cos(pi*(n-2)/3)].*stepseq(2,0,7) % original sequence
x =
    Columns 1 through 4
            0                  0                  0  0.2500000000000000
    Columns 5 through 8
   -0.2500000000000000  -0.3750000000000000  -0.1250000000000000  0.0781250000000000
```

This approach can be used to verify the  $z$ -transform computations. □

## 4.3 INVERSION OF THE $z$ -TRANSFORM

From equation (4.3), the inverse  $z$ -transform computation requires an evaluation of a complex contour integral that, in general, is a complicated procedure. The most practical approach is to use the partial fraction expansion method. It makes use of the  $z$ -transform Table 4.1 (or similar tables available in many textbooks). The  $z$ -transform, however, must be a rational function. This requirement is generally satisfied in digital signal processing.

*Central Idea* When  $X(z)$  is a rational function of  $z^{-1}$ , it can be expressed as a sum of simple factors using the partial fraction expansion. The individual sequences corresponding to these factors can then be written down using the  $z$ -transform table.

The inverse  $z$ -transform procedure can be summarized using the following steps:

1. Consider the rational function

$$X(z) = \frac{b_0 + b_1 z^{-1} + \cdots + b_M z^{-M}}{1 + a_1 z^{-1} + \cdots + a_N z^{-N}}, R_{x-} < |z| < R_{x+} \quad (4.12)$$

2. Express (4.12) as

$$X(z) = \underbrace{\frac{\tilde{b}_0 + \tilde{b}_1 z^{-1} + \cdots + \tilde{b}_{N-1} z^{-(N-1)}}{1 + a_1 z^{-1} + \cdots + a_N z^{-N}}}_{\text{Proper rational part}} + \underbrace{\sum_{k=0}^{M-N} C_k z^{-k}}_{\text{Polynomial part if } M \geq N}$$

where the first term on the right-hand side is the proper rational part and the second term is the polynomial (finite-length) part. This can be obtained by performing polynomial division if  $M \geq N$  using the `deconv` function.

3. Perform a partial fraction expansion on the proper rational part of  $X(z)$  to obtain

$$X(z) = \sum_{k=1}^N \frac{R_k}{1 - p_k z^{-1}} + \underbrace{\sum_{k=0}^{M-N} C_k z^{-k}}_{M \geq N} \quad (4.13)$$

where  $p_k$  is the  $k$ th pole of  $X(z)$  and  $R_k$  is the residue at  $p_k$ . It is assumed that the poles are distinct, for which the residues are given by

$$R_k = \left. \frac{\tilde{b}_0 + \tilde{b}_1 z^{-1} + \cdots + \tilde{b}_{N-1} z^{-(N-1)}}{1 + a_1 z^{-1} + \cdots + a_N z^{-N}} (1 - p_k z^{-1}) \right|_{z=p_k}$$

For repeated poles, the expansion (4.13) has a more general form. If a pole  $p_k$  has multiplicity  $r$ , then its expansion is given by

$$\sum_{\ell=1}^r \frac{R_{k,\ell} z^{-(\ell-1)}}{(1-p_k z^{-1})^\ell} = \frac{R_{k,1}}{1-p_k z^{-1}} + \frac{R_{k,2} z^{-1}}{(1-p_k z^{-1})^2} + \cdots + \frac{R_{k,r} z^{-(r-1)}}{(1-p_k z^{-1})^r} \quad (4.14)$$

where the residues  $R_{k,\ell}$  are computed using a more general formula, which is available in reference [79].

4. Assuming distinct poles as in (4.13), write  $x(n)$  as

$$x(n) = \sum_{k=1}^N R_k \mathcal{Z}^{-1} \left[ \frac{1}{1-p_k z^{-1}} \right] + \underbrace{\sum_{k=0}^{M-N} C_k \delta(n-k)}_{M \geq N}$$

5. Finally, use the relation from Table 4.1

$$\mathcal{Z}^{-1} \left[ \frac{1}{1-p_k z^{-1}} \right] = \begin{cases} p_k^n u(n) & |z_k| \leq R_{x-} \\ -p_k^n u(-n-1) & |z_k| \geq R_{x+} \end{cases} \quad (4.15)$$

to complete  $x(n)$ .

A similar procedure is used for repeated poles.

- EXAMPLE 4.7** Find the inverse  $z$ -transform of  $x(z) = \frac{z}{3z^2 - 4z + 1}$ .

**Solution**

Write

$$\begin{aligned} X(z) &= \frac{z}{3(z^2 - \frac{4}{3}z + \frac{1}{3})} = \frac{\frac{1}{3}z^{-1}}{1 - \frac{4}{3}z^{-1} + \frac{1}{3}z^{-2}} \\ &= \frac{\frac{1}{3}z^{-1}}{(1-z^{-1})(1-\frac{1}{3}z^{-1})} = \frac{\frac{1}{2}}{1-z^{-1}} - \frac{\frac{1}{2}}{1-\frac{1}{3}z^{-1}} \end{aligned}$$

or

$$X(z) = \frac{1}{2} \left( \frac{1}{1-z^{-1}} \right) - \frac{1}{2} \left( \frac{1}{1-\frac{1}{3}z^{-1}} \right)$$

Now,  $X(z)$  has two poles:  $z_1 = 1$  and  $z_2 = \frac{1}{3}$ , and since the ROC is not specified, there are *three* possible ROCs, as shown in Figure 4.5.

- a.  $\text{ROC}_1: 1 < |z| < \infty$ . Here both poles are on the interior side of the  $\text{ROC}_1$ ; that is,  $|z_1| \leq R_{x-} = 1$  and  $|z_2| \leq 1$ . Hence from (4.15),

$$x_1(n) = \frac{1}{2} u(n) - \frac{1}{2} \left( \frac{1}{3} \right)^n u(n)$$

which is a right-sided sequence.

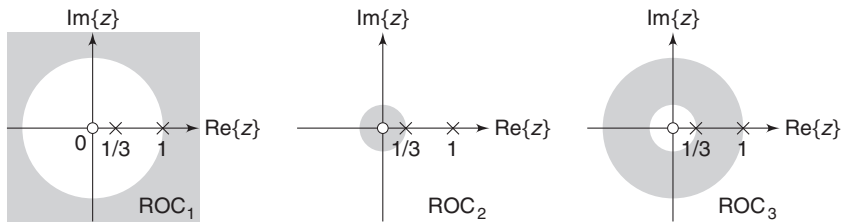


**FIGURE 4.5** The ROCs in Example 4.7

- b.  $\text{ROC}_2: 0 < |z| < \frac{1}{3}$ . Here both poles are on the exterior side of the  $\text{ROC}_2$ ; that is,  $|z_1| \geq R_{x+} = \frac{1}{3}$  and  $|z_2| \geq \frac{1}{3}$ . Hence from (4.15),

$$\begin{aligned} x_2(n) &= \frac{1}{2} \{-u(-n-1)\} - \frac{1}{2} \left\{ -\left(\frac{1}{3}\right)^n u(-n-1) \right\} \\ &= \frac{1}{2} \left(\frac{1}{3}\right)^n u(-n-1) - \frac{1}{2} u(-n-1) \end{aligned}$$

which is a left-sided sequence.

- c.  $\text{ROC}_3: \frac{1}{3} < |z| < 1$ . Here pole  $z_1$  is on the exterior side of the  $\text{ROC}_3$ , that is,  $|z_1| \geq R_{x+} = 1$  and pole  $z_2$  is on the interior side, that is,  $|z_2| \leq \frac{1}{3}$ . Hence from (4.15),

$$x_3(n) = -\frac{1}{2} u(-n-1) - \frac{1}{2} \left(\frac{1}{3}\right)^n u(n)$$

which is a two-sided sequence.  $\square$

#### 4.3.1 MATLAB IMPLEMENTATION

A MATLAB function `residuez` is available to compute the residue part and the direct (or polynomial) terms of a rational function in  $z^{-1}$ . Let

$$\begin{aligned} X(z) &= \frac{b_0 + b_1 z^{-1} + \cdots + b_M z^{-M}}{a_0 + a_1 z^{-1} + \cdots + a_N z^{-N}} = \frac{B(z)}{A(z)} \\ &= \sum_{k=1}^N \frac{R_k}{1 - p_k z^{-1}} + \underbrace{\sum_{k=0}^{M-N} C_k z^{-k}}_{M \geq N} \end{aligned}$$

be a rational function in which the numerator and the denominator polynomials are in *ascending* powers of  $z^{-1}$ . Then `[R,p,C]=residuez(b,a)` computes the residues, poles, and direct terms of  $X(z)$  in which two polynomials  $B(z)$  and  $A(z)$  are given in two vectors `b` and `a`, respectively. The returned column vector `R` contains the residues, column vector `p` contains the pole locations, and row vector `C` contains the direct terms.

If  $p(k)=\dots=p(k+r-1)$  is a pole of multiplicity  $r$ , then the expansion includes the term of the form

$$\frac{R_k}{1-p_k z^{-1}} + \frac{R_{k+1}}{(1-p_k z^{-1})^2} + \dots + \frac{R_{k+r-1}}{(1-p_k z^{-1})^r} \quad (4.16)$$

which is different from (4.14).

Similarly,  $[b, a] = \text{residuez}(R, p, C)$ , with three input arguments and two output arguments, converts the partial fraction expansion back to polynomials with coefficients in row vectors  $b$  and  $a$ .

- **EXAMPLE 4.8** To verify our residue calculations, let us consider the rational function

$$X(z) = \frac{z}{3z^2 - 4z + 1}$$

given in Example 4.7.

**Solution** First, rearrange  $X(z)$  so that it is a function in ascending powers of  $z^{-1}$ :

$$X(z) = \frac{z^{-1}}{3 - 4z^{-1} + z^{-2}} = \frac{0 + z^{-1}}{3 - 4z^{-1} + z^{-2}}$$

Now, using the MATLAB script

```
>> b = [0,1]; a = [3,-4,1]; [R,p,C] = residuez(b,a)
R =
    0.5000
   -0.5000
p =
    1.0000
    0.3333
c =
    []
```

we obtain

$$X(z) = \frac{\frac{1}{2}}{1 - z^{-1}} - \frac{\frac{1}{2}}{1 - \frac{1}{3}z^{-1}}$$

as before. Similarly, to convert back to the rational function form,

```
>> [b,a] = residuez(R,p,C)
b =
    0.0000
    0.3333
```

```
a =
1.0000
-1.3333
0.3333
```

so that

$$X(z) = \frac{0 + \frac{1}{3}z^{-1}}{1 - \frac{4}{3}z^{-1} + \frac{1}{3}z^{-2}} = \frac{z^{-1}}{3 - 4z^{-1} + z^{-2}} = \frac{z}{3z^2 - 4z + 1}$$

as before.  $\square$

$\square$  **EXAMPLE 4.9** Compute the inverse  $z$ -transform of

$$X(z) = \frac{1}{(1 - 0.9z^{-1})^2 (1 + 0.9z^{-1})}, \quad |z| > 0.9$$

### Solution

We will evaluate the denominator polynomial as well as the residues using the following MATLAB script:

```
>> b = 1; a = poly([0.9,0.9,-0.9])
a =
    1.0000    -0.9000    -0.8100     0.7290
>> [R,p,C]=residuez(b,a)
R =
    0.2500
    0.5000
    0.2500
p =
    0.9000
    0.9000
   -0.9000
c =
[]
```

Note that the denominator polynomial is computed using MATLAB's polynomial function **poly**, which computes the polynomial coefficients, given its roots. We could have used the **conv** function, but the use of the **poly** function is more convenient for this purpose. From the residue calculations and using the order of residues given in (4.16), we have

$$\begin{aligned} X(z) &= \frac{0.25}{1 - 0.9z^{-1}} + \frac{0.5}{(1 - 0.9z^{-1})^2} + \frac{0.25}{1 + 0.9z^{-1}}, \quad |z| > 0.9 \\ &= \frac{0.25}{1 - 0.9z^{-1}} + \frac{0.5z}{0.9} \frac{(0.9z^{-1})}{(1 - 0.9z^{-1})^2} + \frac{0.25}{1 + 0.9z^{-1}}, \quad |z| > 0.9 \end{aligned}$$

Hence from Table 4.1 and using the  $z$ -transform property of time-shift,

$$x(n) = 0.25(0.9)^n u(n) + \frac{5}{9}(n+1)(0.9)^{n+1} u(n+1) + 0.25(-0.9)^n u(n)$$

which, upon simplification, becomes

$$x(n) = 0.75(0.9)^n u(n) + 0.5n(0.9)^n u(n) + 0.25(-0.9)^n u(n)$$

MATLAB verification:

```
>> [delta,n] = impseq(0,0,7); x = filter(b,a,delta) % Check sequence
x =
    Columns 1 through 4
    1.0000000000000000  0.9000000000000000  1.6200000000000000  1.4580000000000000
    Columns 5 through 8
    1.9683000000000000  1.7714700000000000  2.1257640000000000  1.9131876000000000
>> x = (0.75)*(0.9).^n + (0.5)*n.* (0.9).^n + (0.25)*(-0.9).^n % answer sequence
x =
    Columns 1 through 4
    1.0000000000000000  0.9000000000000000  1.6200000000000000  1.4580000000000000
    Columns 5 through 8
    1.9683000000000000  1.7714700000000000  2.1257640000000000  1.9131876000000000
```

□

- **EXAMPLE 4.10** Determine the inverse  $z$ -transform of

$$X(z) = \frac{1 + 0.4\sqrt{2}z^{-1}}{1 - 0.8\sqrt{2}z^{-1} + 0.64z^{-2}}$$

so that the resulting sequence is causal and contains no complex numbers.

### Solution

We will have to find the poles of  $X(z)$  in the polar form to determine the ROC of the causal sequence.

MATLAB script:

```
>> b = [1,0.4*sqrt(2)]; a=[1,-0.8*sqrt(2),0.64];
>> [R,p,C] = residue(b,a)
R =
    0.5000 - 1.0000i
    0.5000 + 1.0000i
p =
    0.5657 + 0.5657i
    0.5657 - 0.5657i
C =
    []
>> Mp=(abs(p))' % Pole magnitudes
Mp =
    0.8000    0.8000
>> Ap=(angle(p))'/pi % Pole angles in pi units
Ap =
    0.2500   -0.2500
```

From these calculations,

$$X(z) = \frac{0.5 - j}{1 - 0.8e^{+j\frac{\pi}{4}}z^{-1}} + \frac{0.5 + j}{1 - 0.8e^{-j\frac{\pi}{4}}z^{-1}}, \quad |z| > 0.8$$

and from Table 4.1, we have

$$\begin{aligned} x(n) &= (0.5 - j)0.8^n e^{+j\frac{\pi}{4}n} u(n) + (0.5 + j)0.8^n e^{-j\frac{\pi}{4}n} u(n) \\ &= 0.8^n [0.5\{e^{+j\frac{\pi}{4}n} + e^{-j\frac{\pi}{4}n}\} - j\{e^{+j\frac{\pi}{4}n} - e^{-j\frac{\pi}{4}n}\}] u(n) \\ &= 0.8^n \left[ \cos\left(\frac{\pi n}{4}\right) + 2 \sin\left(\frac{\pi n}{4}\right) \right] u(n) \end{aligned}$$

MATLAB verification:

```
>> [delta, n] = impseq(0,0,6);
x = filter(b,a,delta) % Check sequence
x =
Columns 1 through 4
1.00000000000000 1.69705627484771 1.28000000000000 0.36203867196751
Columns 5 through 8
-0.40960000000000 -0.69511425017762 -0.52428800000000 -0.14829104003789
>> x = ((0.8).^n).*(cos(pi*n/4)+2*sin(pi*n/4))
x =
Columns 1 through 4
1.00000000000000 1.69705627484771 1.28000000000000 0.36203867196751
Columns 5 through 8
-0.40960000000000 -0.69511425017762 -0.52428800000000 -0.14829104003789
```

□

## 4.4 SYSTEM REPRESENTATION IN THE $z$ -DOMAIN

Similar to the frequency response function  $H(e^{j\omega})$ , we can define the  $z$ -domain function,  $H(z)$ , called the *system function*. However, unlike  $H(e^{j\omega})$ ,  $H(z)$  exists for systems that may not be BIBO stable.

■ **DEFINITION 1** *The System Function*

*The system function  $H(z)$  is given by*

$$H(z) \triangleq \mathcal{Z}[h(n)] = \sum_{-\infty}^{\infty} h(n)z^{-n}; \quad R_{h-} < |z| < R_{h+} \quad (4.17)$$

Using the convolution property (4.11) of the  $z$ -transform, the output transform  $Y(z)$  is given by

$$Y(z) = H(z) X(z) : \text{ROC}_y = \text{ROC}_h \cap \text{ROC}_x \quad (4.18)$$

provided  $\text{ROC}_x$  overlaps with  $\text{ROC}_h$ . Therefore, a linear and time-invariant system can be represented in the  $z$ -domain by

$$X(z) \longrightarrow [H(z)] \longrightarrow Y(z) = H(z) X(z)$$

#### 4.4.1 SYSTEM FUNCTION FROM THE DIFFERENCE EQUATION REPRESENTATION

When LTI systems are described by a difference equation

$$y(n) + \sum_{k=1}^N a_k y(n-k) = \sum_{\ell=0}^M b_\ell x(n-\ell) \quad (4.19)$$

the system function  $H(z)$  can easily be computed. Taking the  $z$ -transform of both sides, and using properties of the  $z$ -transform,

$$Y(z) + \sum_{k=1}^N a_k z^{-k} Y(z) = \sum_{\ell=0}^M b_\ell z^{-\ell} X(z)$$

or

$$\begin{aligned} H(z) &\stackrel{\triangle}{=} \frac{Y(z)}{X(z)} = \frac{\sum_{\ell=0}^M b_\ell z^{-\ell}}{1 + \sum_{k=1}^N a_k z^{-k}} = \frac{B(z)}{A(z)} \\ &= \frac{b_0 z^{-M} \left( z^M + \dots + \frac{b_M}{b_0} \right)}{z^{-N} (z^N + \dots + a_N)} \end{aligned} \quad (4.20)$$

After factorization, we obtain

$$H(z) = b_0 z^{N-M} \frac{\prod_{\ell=1}^N (z - z_\ell)}{\prod_{k=1}^N (z - p_k)} \quad (4.21)$$

where  $z_\ell$ 's are the system zeros and  $p_k$ 's are the system poles. Thus  $H(z)$  (and hence an LTI system) can also be represented in the  $z$ -domain using a pole-zero plot. This fact is useful in designing simple filters by proper placement of poles and zeros.

To determine zeros and poles of a rational  $H(z)$ , we can use the MATLAB function `roots` on both the numerator and the denominator polynomials. (Its inverse function `poly` determines polynomial coefficients from its roots, as discussed in the previous section.) It is also possible to use MATLAB to plot these roots for a visual display of a pole-zero plot. The function `zplane(b,a)` plots poles and zeros, given the numerator *row* vector **b** and the denominator *row* vector **a**. As before, the symbol **o** represents a zero and the symbol **x** represents a pole. The plot includes the unit circle for reference. Similarly, `zplane(z,p)` plots the zeros in *column* vector **z** and the poles in *column* vector **p**. Note very carefully the form of the input arguments for the proper use of this function.

#### 4.4.2 TRANSFER FUNCTION REPRESENTATION

If the ROC of  $H(z)$  includes a unit circle ( $z = e^{j\omega}$ ), then we can evaluate  $H(z)$  on the unit circle, resulting in a frequency response function or transfer function  $H(e^{j\omega})$ . Then from (4.21),

$$H(e^{j\omega}) = b_0 e^{j(N-M)\omega} \frac{\prod_1^M (e^{j\omega} - z_\ell)}{\prod_1^N (e^{j\omega} - p_k)} \quad (4.22)$$

The factor  $(e^{j\omega} - z_\ell)$  can be interpreted as a *vector* in the complex  $z$ -plane from a zero  $z_\ell$  to the unit circle at  $z = e^{j\omega}$ , while the factor  $(e^{j\omega} - p_k)$  can be interpreted as a vector from a pole  $p_k$  to the unit circle at  $z = e^{j\omega}$ . This is shown in Figure 4.6. Hence the magnitude response function

$$|H(e^{j\omega})| = |b_0| \frac{|e^{j\omega} - z_1| \cdots |e^{j\omega} - z_M|}{|e^{j\omega} - p_1| \cdots |e^{j\omega} - p_N|} \quad (4.23)$$

can be interpreted as a product of the lengths of vectors from the zeros to the unit circle *divided* by the lengths of vectors from the poles to the unit circle and *scaled* by  $|b_0|$ . Similarly, the phase response function

$$\angle H(e^{j\omega}) = \underbrace{[0 \text{ or } \pi]}_{\text{Constant}} + \underbrace{[(N-M)\omega]}_{\text{Linear}} + \underbrace{\sum_1^M \angle(e^{j\omega} - z_k) - \sum_1^N \angle(e^{j\omega} - p_k)}_{\text{Nonlinear}} \quad (4.24)$$

can be interpreted as a sum of a constant factor, a linear-phase factor, and a nonlinear-phase factor (angles from the “zero vectors” *minus* the sum of angles from the “pole vectors”).

#### 4.4.3 MATLAB IMPLEMENTATION

In Chapter 3, we plotted magnitude and phase responses in MATLAB by directly implementing their functional forms. MATLAB also provides

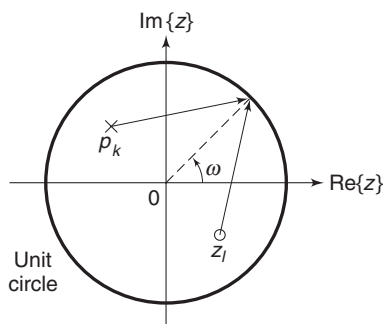


**FIGURE 4.6** Pole and zero vectors

a function called **freqz** for this computation, which uses the preceding interpretation. In its simplest form, this function is invoked by

```
[H,w] = freqz(b,a,N)
```

which returns the  $N$ -point frequency vector  $w$  and the  $N$ -point complex frequency response vector  $H$  of the system, given its numerator and denominator coefficients in vectors  $b$  and  $a$ . The frequency response is evaluated at  $N$  points equally spaced around the upper half of the unit circle. Note that the  $b$  and  $a$  vectors are the same vectors we use in the **filter** function or derived from the difference equation representation (4.19).

The second form

```
[H,w] = freqz(b,a,N,'whole')
```

uses  $N$  points around the whole unit circle for computation.

In yet another form,

```
H = freqz(b,a,w)
```

it returns the frequency response at frequencies designated in vector  $w$ , normally between 0 and  $\pi$ . It should be noted that the **freqz** function can also be used for numerical computation of the DTFT of a *finite-duration, causal* sequence  $x(n)$ . In this approach,  $b = x$  and  $a = 1$ .

**EXAMPLE 4.11** Consider a causal system

$$y(n) = 0.9y(n-1) + x(n)$$

- a. Determine  $H(z)$  and sketch its pole-zero plot.
- b. Plot  $|H(e^{j\omega})|$  and  $\angle H(e^{j\omega})$ .
- c. Determine the impulse response  $h(n)$ .

**Solution**

The difference equation can be put in the form

$$y(n) - 0.9y(n-1) = x(n)$$

- a. From (4.21),

$$H(z) = \frac{1}{1 - 0.9z^{-1}}; \quad |z| > 0.9$$

since the system is causal. There is one pole at 0.9 and one zero at the origin. We will use MATLAB to illustrate the use of the **zplane** function.

```
>> b = [1, 0]; a = [1, -0.9]; zplane(b,a)
```

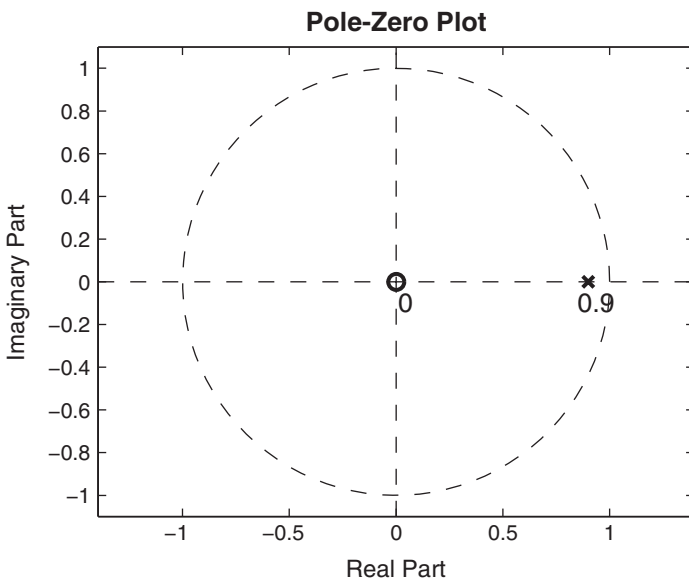


**FIGURE 4.7** Pole-zero plot of Example 4.11a

Note that we specified  $b=[1,0]$  instead of  $b=1$  because the `zplane` function assumes that scalars are zeros or poles. The resulting pole-zero plot is shown in Figure 4.7.

- b.** Using (4.23) and (4.24), we can determine the magnitude and phase of  $H(e^{j\omega})$ . Once again, we will use MATLAB to illustrate the use of the `freqz` function. Using its first form, we will take 100 points along the upper half of the unit circle.

MATLAB script:

```
>> [H,w] = freqz(b,a,100); magH = abs(H); phaH = angle(H);
>> subplot(2,1,1);plot(w/pi,magH);grid
>> title('Magnitude Response'); ylabel('Magnitude');
>> subplot(2,1,2);plot(w/pi,phaH/pi);grid
>> xlabel('Frequency in \pi Units'); ylabel('Phase in \pi Units');
>> title('Phase Response')
```

The response plots are shown in Figure 4.8. If you study these plots carefully, you will observe that the plots are computed between  $0 \leq \omega \leq 0.99\pi$  and fall short at  $\omega = \pi$ . This is due to the fact that in MATLAB the lower half

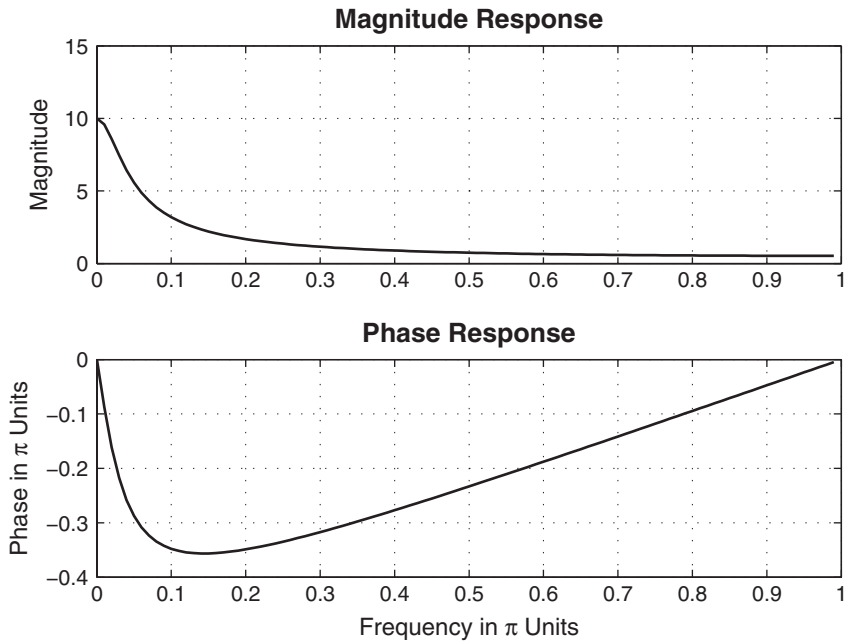


**FIGURE 4.8** Frequency response plots in Example 4.11

of the unit circle begins at  $\omega = \pi$ . To overcome this problem, we will use the second form of the `freqz` function as follows.

```
>> [H,w] = freqz(b,a,200,'whole');
>> magH = abs(H(1:101)); phaH = angle(H(1:101));
```

Now the 101st element of the array  $H$  will correspond to  $\omega = \pi$ . A similar result can be obtained using the third form of the `freqz` function.

```
>> w = [0:1:100]*pi/100; H = freqz(b,a,w);
>> magH = abs(H); phaH = angle(H);
```

In the future, we will use any one of these forms, depending on our convenience. Also note that in the plots we divided the  $w$  and  $phaH$  arrays by  $\pi$  so that the plot axes are in the units of  $\pi$  and easier to read. *This practice is strongly recommended.*

- c. From the  $z$ -transform in Table 4.1,

$$h(n) = \mathcal{Z}^{-1} \left[ \frac{1}{1 - 0.9z^{-1}}, |z| > 0.9 \right] = (0.9)^n u(n)$$

□

□ **EXAMPLE 4.12** Given that

$$H(z) = \frac{z+1}{z^2 - 0.9z + 0.81}$$

is a causal system, find

- a. its transfer function representation,
- b. its difference equation representation, and
- c. its impulse response representation.

**Solution**

The poles of the system function are at  $z = 0.9 \angle \pm \pi/3$ . Hence the ROC of this causal system is  $|z| > 0.9$ . Therefore, the unit circle is in the ROC, and the discrete-time Fourier transform  $H(e^{j\omega})$  exists.

- a. Substituting  $z = e^{j\omega}$  in  $H(z)$ ,

$$H(e^{j\omega}) = \frac{e^{j\omega} + 1}{e^{j2\omega} - 0.9e^{j\omega} + 0.81} = \frac{e^{j\omega} + 1}{(e^{j\omega} - 0.9e^{j\pi/3})(e^{j\omega} - 0.9e^{-j\pi/3})}$$

- b. Using  $H(z) = Y(z)/X(z)$ ,

$$\frac{Y(z)}{X(z)} = \frac{z+1}{z^2 - 0.9z + 0.81} \left( \frac{z^{-2}}{z^{-2}} \right) = \frac{z^{-1} + z^{-2}}{1 - 0.9z^{-1} + 0.81z^{-2}}$$

Cross multiplying,

$$Y(z) - 0.9z^{-1}Y(z) + 0.81z^{-2}Y(z) = z^{-1}X(z) + z^{-2}X(z)$$

Now taking the inverse  $z$ -transform,

$$y(n) - 0.9y(n-1) + 0.81y(n-2) = x(n-1) + x(n-2)$$

or

$$y(n) = 0.9y(n-1) - 0.81y(n-2) + x(n-1) + x(n-2)$$

- c. Using the MATLAB script

```
>> b = [0,1,1]; a = [1,-0.9,0.81]; [R,p,C] = residue(b,a)
R =
-0.6173 - 0.9979i
-0.6173 + 0.9979i
p =
0.4500 + 0.7794i
0.4500 - 0.7794i
C =
1.2346
>> Mp = (abs(p))'
Mp =
0.9000    0.9000
>> Ap = (angle(p))/pi
Ap =
0.3333   -0.3333
```

we have

$$H(z) = 1.2346 + \frac{-0.6173 + j0.9979}{1 - 0.9e^{-j\pi/3}z^{-1}} + \frac{-0.6173 - j0.9979}{1 - 0.9e^{j\pi/3}z^{-1}}, \quad |z| > 0.9$$

Hence from Table 4.1,

$$\begin{aligned} h(n) &= 1.2346\delta(n) + [(-0.6173 + j0.9979)0.9^n e^{-j\pi n/3} \\ &\quad + (-0.6173 - j0.9979)0.9^n e^{j\pi n/3}]u(n) \\ &= 1.2346\delta(n) + 0.9^n [-1.2346 \cos(\pi n/3) + 1.9958 \sin(\pi n/3)]u(n) \\ &= 0.9^n [-1.2346 \cos(\pi n/3) + 1.9958 \sin(\pi n/3)]u(n-1) \end{aligned}$$

The last step results from the fact that  $h(0) = 0$ .  $\square$

#### 4.4.4 RELATIONSHIPS BETWEEN SYSTEM REPRESENTATIONS

In this and the previous two chapters, we developed several system representations. Figure 4.9 depicts the relationships among these representations in a graphical form.

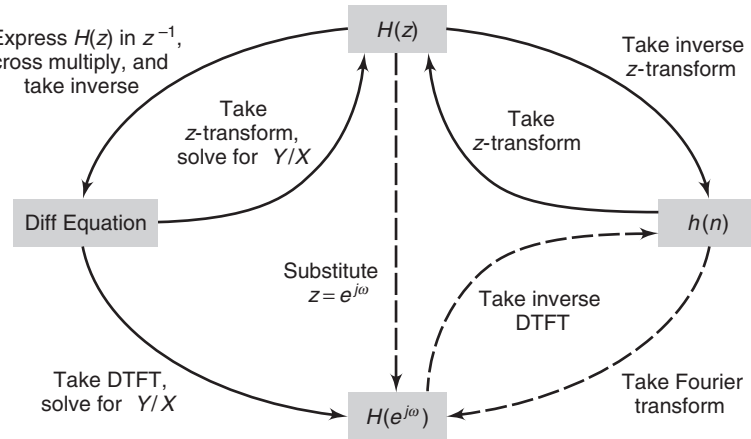


**FIGURE 4.9** System representations in pictorial form

#### 4.4.5 STABILITY AND CAUSALITY

For LTI systems, the BIBO stability is equivalent to  $\sum_{-\infty}^{\infty} |h(k)| < \infty$ . From the existence of the discrete-time Fourier transform, this stability implies that  $H(e^{j\omega})$  exists, which further implies that the unit circle  $|z|=1$  must be in the ROC of  $H(z)$ . This result is called the *z-domain stability theorem*; therefore, the dashed paths in Figure 4.9 exist only if the system is stable.

■ **THEOREM 2  $z$ -Domain LTI Stability**

An LTI system is stable if and only if the unit circle is in the ROC of  $H(z)$ .

For LTI causality, we require that  $h(n) = 0$ , for  $n < 0$  (i.e., a right-sided sequence). This implies that the ROC of  $H(z)$  must be outside some circle of radius  $R_{h-}$ . This is not a sufficient condition, since any right-sided sequence has a similar ROC. However, when the system is stable, then its causality is easy to check.

■ **THEOREM 3  $z$ -Domain Causal LTI Stability**

A causal LTI system is stable if and only if the system function  $H(z)$  has all its poles inside the unit circle.

- **EXAMPLE 4.13** A causal LTI system is described by the following difference equation:

$$y(n) = 0.81y(n-2) + x(n) - x(n-2)$$

Determine

- the system function  $H(z)$ ,
- the unit impulse response  $h(n)$ ,
- the unit step response  $v(n)$ , that is, the response to the unit step  $u(n)$ , and
- the frequency response function  $H(e^{j\omega})$ , and plot its magnitude and phase over  $0 \leq \omega \leq \pi$ .

**Solution**

Since the system is causal, the ROC will be outside a circle with radius equal to the largest pole magnitude.

- Taking the  $z$ -transform of both sides of the difference equation and then solving for  $Y(z)/X(z)$  or using (4.20), we obtain

$$H(z) = \frac{1 - z^{-2}}{1 - 0.81z^{-2}} = \frac{1 - z^{-2}}{(1 + 0.9z^{-1})(1 - 0.9z^{-1})}, \quad |z| > 0.9$$

- Using the MATLAB script for the partial fraction expansion,

```
>> b = [1,0,-1]; a = [1,0,-0.81]; [R,p,C] = residue(b,a);
R =
-0.1173
-0.1173
p =
-0.9000
0.9000
C =
1.2346
```

we have

$$H(z) = 1.2346 - 0.1173 \frac{1}{1 + 0.9z^{-1}} - 0.1173 \frac{1}{1 - 0.9z^{-1}}, |z| > 0.9$$

or from Table 4.1,

$$h(n) = 1.2346\delta(n) - 0.1173 \{1 + (-1)^n\} (0.9)^n u(n)$$

- c. From Table 4.1,  $\mathcal{Z}[u(n)] = U(z) = \frac{1}{1 - z^{-1}}$ ,  $|z| > 1$ . Hence

$$\begin{aligned} V(z) &= H(z)U(z) \\ &= \left[ \frac{(1+z^{-1})(1-z^{-1})}{(1+0.9z^{-1})(1-0.9z^{-1})} \right] \left[ \frac{1}{1-z^{-1}} \right], \quad |z| > 0.9 \cap |z| > 1 \\ &= \frac{1+z^{-1}}{(1+0.9z^{-1})(1-0.9z^{-1})}, \quad |z| > 0.9 \end{aligned}$$

or

$$V(z) = 1.0556 \frac{1}{1-0.9z^{-1}} - 0.0556 \frac{1}{1+0.9z^{-1}}, \quad |z| > 0.9$$

Finally,

$$v(n) = [1.0556(0.9)^n - 0.0556(-0.9)^n] u(n)$$

Note that in the calculation of  $V(z)$  there is a pole-zero cancellation at  $z = 1$ . This has two implications. First, the ROC of  $V(z)$  is still  $\{|z| > 0.9\}$  and not  $\{|z| > 0.9 \cap |z| > 1 = |z| > 1\}$ . Second, the step response  $v(n)$  contains no steady-state term  $u(n)$ .

- d. Substituting  $z = e^{j\omega}$  in  $H(z)$ ,

$$H(e^{j\omega}) = \frac{1 - e^{-j2\omega}}{1 - 0.81e^{-j2\omega}}$$

We will use the MATLAB script to compute and plot responses.

```
>> w = [0:1:500]*pi/500; H = freqz(b,a,w);
>> magH = abs(H); phaH = angle(H);
>> subplot(2,1,1); plot(w/pi,magH); grid
>> title('Magnitude Response'); ylabel('Magnitude')
>> subplot(2,1,2); plot(w/pi,phaH/pi); grid
>> xlabel('Frequency in \pi Units'); ylabel('Phase in \pi Units')
>> title('Phase Response')
```

The frequency response plots are shown in Figure 4.10. □

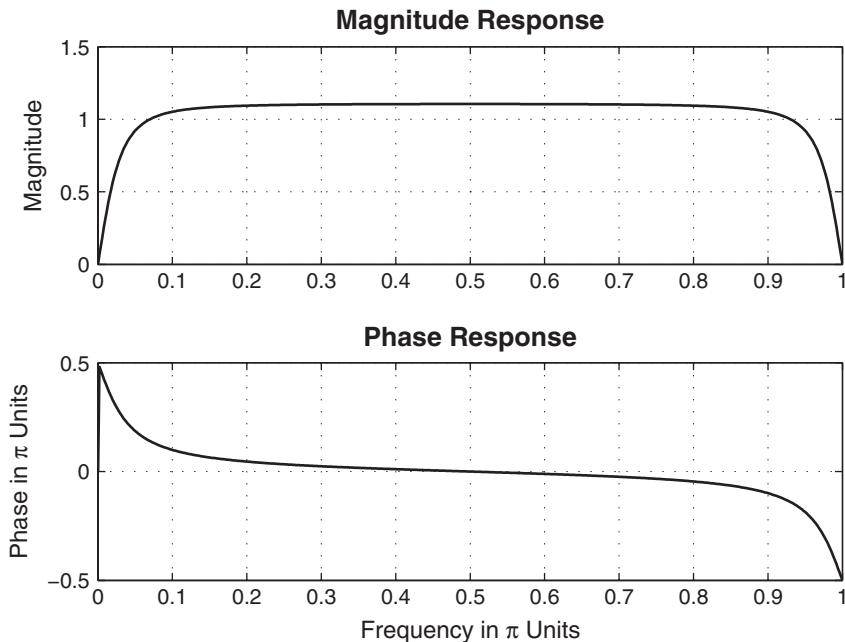


**FIGURE 4.10** Frequency response plots for Example 4.13

## 4.5 SOLUTIONS OF THE DIFFERENCE EQUATIONS

---

In Chapter 2, we mentioned two forms for the solution of linear constant coefficient difference equations. One form involved finding the particular and the homogeneous solutions, while the other form involved finding the zero-input (initial condition) and the zero-state responses. Using  $z$ -transforms, we now provide a method for obtaining these forms. In addition, we will also discuss the *transient* and the *steady-state* responses. In digital signal processing, difference equations generally evolve in the positive  $n$  direction. Therefore, our time frame for these solutions will be  $n \geq 0$ . For this purpose, we define a version of the bilateral  $z$ -transform called the *one-sided  $z$ -transform*.

■ **DEFINITION 4** *The One-Sided  $z$ -Transform*

*The one-sided  $z$ -transform of a sequence  $x(n)$  is given by*

$$\mathcal{Z}^+[x(n)] \triangleq \mathcal{Z}[x(n)u(n)] \triangleq X^+(z) = \sum_{n=0}^{\infty} x(n)z^{-n} \quad (4.25)$$

Then the sample shifting property is given by

$$\begin{aligned}\mathcal{Z}^+ [x(n - k)] &= \mathcal{Z} [x(n - k)u(n)] \\&= \sum_{n=0}^{\infty} x(n - k)z^{-n} = \sum_{m=-k}^{\infty} x(m)z^{-(m+k)} \\&= \sum_{m=-k}^{-1} x(m)z^{-(m+k)} + \left[ \sum_{m=0}^{\infty} x(m)z^{-m} \right] z^{-k}\end{aligned}$$

or

$$\mathcal{Z}^+ [x(n - k)] = x(-1)z^{1-k} + x(-2)z^{2-k} + \cdots + x(-k) + z^{-k}X^+(z) \quad (4.26)$$

This result can now be used to solve difference equations with nonzero initial conditions or with changing inputs. We want to solve the difference equation

$$y(n) + \sum_{k=1}^N a_k y(n - k) = \sum_{m=0}^M b_m x(n - m), \quad n \geq 0$$

subject to these initial conditions:

$$\{y(i), i = -1, \dots, -N\} \quad \text{and} \quad \{x(i), i = -1, \dots, -M\}$$

We now demonstrate its solution using an example.

**EXAMPLE 4.14** Solve

$$y(n) - \frac{3}{2}y(n - 1) + \frac{1}{2}y(n - 2) = x(n), \quad n \geq 0$$

where

$$x(n) = \left(\frac{1}{4}\right)^n u(n)$$

subject to  $y(-1) = 4$  and  $y(-2) = 10$ .

### Solution

Taking the one-sided  $z$ -transform of both sides of the difference equation, we obtain

$$Y^+(z) - \frac{3}{2}[y(-1) + z^{-1}Y^+(z)] + \frac{1}{2}[y(-2) + z^{-1}y(-1) + z^{-2}Y^+(z)] = \frac{1}{1 - \frac{1}{4}z^{-1}}$$

Substituting the initial conditions and rearranging,

$$Y^+(z) \left[ 1 - \frac{3}{2}z^{-1} + \frac{1}{2}z^{-2} \right] = \frac{1}{1 - \frac{1}{4}z^{-1}} + (1 - 2z^{-1})$$

or

$$Y^+(z) = \frac{1}{1 - \frac{1}{4}z^{-1}} + \frac{1 - 2z^{-1}}{1 - \frac{3}{2}z^{-1} + \frac{1}{2}z^{-2}} \quad (4.27)$$

Finally,

$$Y^+(z) = \frac{2 - \frac{9}{4}z^{-1} + \frac{1}{2}z^{-2}}{(1 - \frac{1}{2}z^{-1})(1 - z^{-1})(1 - \frac{1}{4}z^{-1})}$$

Using the partial fraction expansion, we obtain

$$Y^+(z) = \frac{1}{1 - \frac{1}{2}z^{-1}} + \frac{\frac{2}{3}}{1 - z^{-1}} + \frac{\frac{1}{3}}{1 - \frac{1}{4}z^{-1}} \quad (4.28)$$

After inverse transformation, the solution is

$$y(n) = \left[ \left( \frac{1}{2} \right)^n + \frac{2}{3} + \frac{1}{3} \left( \frac{1}{4} \right)^n \right] u(n) \quad (4.29)$$

□

**Forms of the solutions** The preceding solution is the *complete response* of the difference equation. It can be expressed in several forms.

- Homogeneous and particular parts:

$$y(n) = \underbrace{\left[ \left( \frac{1}{2} \right)^n + \frac{2}{3} \right] u(n)}_{\text{Homogeneous part}} + \underbrace{\frac{1}{3} \left( \frac{1}{4} \right)^n u(n)}_{\text{Particular part}}$$

The homogeneous part is due to the *system poles*, and the particular part is due to the *input poles*.

- Transient and steady-state responses:

$$y(n) = \underbrace{\left[ \frac{1}{3} \left( \frac{1}{4} \right)^n + \left( \frac{1}{2} \right)^n \right] u(n)}_{\text{Transient response}} + \underbrace{\frac{2}{3} u(n)}_{\text{Steady-state response}}$$

The transient response is due to poles that are *inside* the unit circle, whereas the steady-state response is due to poles that are *on* the unit circle. Note that when the poles are *outside* the unit circle, the response is termed an *unbounded* response.

- Zero-input (or initial condition) and zero-state responses:

In equation (4.27),  $Y^+(z)$  has two parts. The first part can be interpreted as

$$Y_{\text{ZS}}(z) = H(z)X(z)$$

while the second part as

$$Y_{ZI}(z) = H(z)X_{IC}(z)$$

where  $X_{IC}(z)$  can be thought of as an equivalent *initial-condition input* that generates the same output  $Y_{ZI}(z)$  as generated by the initial conditions. In this example,  $x_{IC}(n)$  is

$$x_{IC}(n) = \begin{matrix} \{1, -2\} \\ \uparrow \end{matrix}$$

Now taking the inverse  $z$ -transform of each part of (4.27), we write the complete response as

$$y(n) = \underbrace{\left[ \frac{1}{3} \left( \frac{1}{4} \right)^n - 2 \left( \frac{1}{2} \right)^n + \frac{8}{3} \right] u(n)}_{\text{Zero-state response}} + \underbrace{\left[ 3 \left( \frac{1}{2} \right)^n - 2 \right] u(n)}_{\text{Zero-input response}}$$

From this example, it is clear that each part of the complete solution is, in general, a different function and emphasizes a different aspect of system analysis.

#### 4.5.1 MATLAB IMPLEMENTATION

In Chapter 2, we used the `filter` function to solve the difference equation, given its coefficients and an input. This function can also be used to find the complete response when initial conditions are given. In this form, the `filter` function is invoked by

```
y = filter(b,a,x,xic)
```

where `xic` is an equivalent initial-condition input array. To find the complete response in Example 4.14, we will use the MATLAB script

```
>> n = [0:7]; x = (1/4).^n; xic = [1, -2];
>> format long; y1 = filter(b,a,x,xic)
y1 =
    Columns 1 through 4
    2.00000000000000    1.25000000000000    0.93750000000000    0.79687500000000
    Columns 5 through 8
    0.73046875000000    0.69824218750000    0.68237304687500    0.67449951171875
>> y2 = (1/3)*(1/4).^n+(1/2).^n+(2/3)*ones(1,8) % MATLAB check
y2 =
    Columns 1 through 4
    2.00000000000000    1.25000000000000    0.93750000000000    0.79687500000000
    Columns 5 through 8
    0.73046875000000    0.69824218750000    0.68237304687500    0.67449951171875
```

which agrees with the response given in (4.29). In Example 4.14, we computed  $x_{IC}(n)$  analytically. However, in practice, and especially for large-order difference equations, it is tedious to determine  $x_{IC}(n)$  analytically. MATLAB provides a function called **filtic**, which is available only in the Signal Processing toolbox. It is invoked by

```
xic = filtic(b,a,Y,X)
```

in which **b** and **a** are the filter coefficient arrays and **Y** and **X** are the initial-condition arrays from the initial conditions on  $y(n)$  and  $x(n)$ , respectively, in the form

$$\begin{aligned} Y &= [y(-1), y(-2), \dots, y(-N)] \\ X &= [x(-1), x(-2), \dots, x(-M)] \end{aligned}$$

If  $x(n) = 0$ ,  $n \leq -1$ , then **X** need not be specified in the **filtic** function. In Example 4.14, we could have used

```
>> Y = [4, 10]; xic = filtic(b,a,Y)
xic =
1 -2
```

to determine  $x_{IC}(n)$ .

□ **EXAMPLE 4.15** Solve the difference equation

$$y(n) = \frac{1}{3}[x(n) + x(n-1) + x(n-2)] + 0.95y(n-1) - 0.9025y(n-2), \quad n \geq 0$$

where  $x(n) = \cos(\pi n/3)u(n)$  and

$$y(-1) = -2, \quad y(-2) = -3; \quad x(-1) = 1, \quad x(-2) = 1$$

First determine the solution analytically and then by using MATLAB.

**Solution**

Taking a one-sided  $z$ -transform of the difference equation

$$\begin{aligned} Y^+(z) &= \frac{1}{3}[X^+(z) + x(-1) + z^{-1}X^+(z) + x(-2) + z^{-1}x(-1) + z^{-2}X^+(z)] \\ &\quad + 0.95[y(-1) + z^{-1}Y^+(z)] - 0.9025[y(-2) + z^{-1}y(-1) + z^{-2}Y^+(z)] \end{aligned}$$

and substituting the initial conditions, we obtain

$$Y^+(z) = \frac{\frac{1}{3} + \frac{1}{3}z^{-1} + \frac{1}{3}z^{-2}}{1 - 0.95z^{-1} + 0.9025z^{-2}}X^+(z) + \frac{1.4742 + 2.1383z^{-1}}{1 - 0.95z^{-1} + 0.9025z^{-2}}$$

Clearly,  $x_{IC}(n) = [1.4742, 2.1383]$ . Now substituting  $X^+(z) = \frac{1 - 0.5z^{-1}}{1 - z^{-1} + z^{-2}}$  and simplifying, we will obtain  $Y^+(z)$  as a rational function. This simplification and further partial fraction expansion can be done using MATLAB.

MATLAB script:

```

>> b = [1,1,1]/3; a = [1,-0.95,0.9025];
>> Y = [-2,-3]; X = [1,1]; xic=filtic(b,a,Y,X)
xic =
    1.4742    2.1383
>> bxplus = [1,-0.5]; axplus = [1,-1,1]; % X(z) transform coeff.
>> ayplus = conv(a,axplus) % Denominator of Yplus(z)
ayplus =
    1.0000   -1.9500    2.8525   -1.8525    0.9025
>> byplus = conv(b,bxplus)+conv(xic,axplus) % Numerator of Yplus(z)
byplus =
    1.8075    0.8308   -0.4975    1.9717
>> [R,p,C] = residuez(byplus,ayplus)
R =
    0.0584 + 3.9468i   0.0584 - 3.9468i   0.8453 + 2.0311i   0.8453 - 2.0311i
p =
    0.5000 - 0.8660i   0.5000 + 0.8660i   0.4750 + 0.8227i   0.4750 - 0.8227i
C =
    []
>> Mp = abs(p), Ap = angle(p)/pi % Polar form
Mp =
    1.0000    1.0000    0.9500    0.9500
Ap =
    -0.3333    0.3333    0.3333   -0.3333

```

Hence

$$\begin{aligned}
 Y^+(z) &= \frac{1.8075 + 0.8308z^{-1} - 0.4975z^{-2} + 1.9717z^{-3}}{1 - 1.95z^{-1} + 2.8525z^{-2} - 1.8525z^{-3} + 0.9025z^{-4}} \\
 &= \frac{0.0584 + j3.9468}{1 - e^{-j\pi/3}z^{-1}} + \frac{0.0584 - j3.9468}{1 - e^{j\pi/3}z^{-1}} \\
 &\quad + \frac{0.8453 + j2.0311}{1 - 0.95e^{j\pi/3}z^{-1}} + \frac{0.8453 - j2.0311}{1 - 0.95e^{-j\pi/3}z^{-1}}
 \end{aligned}$$

Now from Table 4.1,

$$\begin{aligned}
 y(n) &= (0.0584 + j3.9468)e^{-j\pi n/3} + (0.0584 - j3.9468)e^{j\pi n/3} \\
 &\quad + (0.8453 + j2.031)(0.95)^n e^{j\pi n/3} + (0.8453 - j2.031)(0.95)^n e^{-j\pi n/3} \\
 &= 0.1169 \cos(\pi n/3) + 7.8937 \sin(\pi n/3) \\
 &\quad + (0.95)^n [1.6906 \cos(\pi n/3) - 4.0623 \sin(\pi n/3)], \quad n \geq 0
 \end{aligned}$$

The first two terms of  $y(n)$  correspond to the steady-state response, as well as to the particular response, while the last two terms are the transient response (and homogeneous response) terms.

To solve this example using MATLAB, we will need the **filtic** function, which we have already used to determine the  $x_{IC}(n)$  sequence. The solution will be a numerical one. Let us determine the first eight samples of  $y(n)$ .

MATLAB script:

```
>> n = [0:7]; x = cos(pi*n/3); y = filter(b,a,x,xic)
y =
    Columns 1 through 4
    1.80750000000000  4.35545833333333  2.83975000000000  -1.56637197916667
    Columns 5 through 8
    -4.71759442187500  -3.40139732291667  1.35963484230469  5.02808085078841
% MATLAB verification
>> A=real(2*R(1)); B=imag(2*R(1)); C=real(2*R(3)); D=imag(2*R(4));
>> y=A*cos(pi*n/3)+B*sin(pi*n/3)+((0.95).^n).*(C*cos(pi*n/3)+D*sin(pi*n/3))
y =
    Columns 1 through 4
    1.80750000000048  4.35545833333359  2.83974999999978  -1.56637197916714
    Columns 5 through 8
    -4.71759442187528  -3.40139732291648  1.35963484230515  5.02808085078871
```

□

## 4.6 PROBLEMS

---

- P4.1** Determine the  $z$ -transform of the following sequences using the definition (4.1). Indicate the region of convergence for each sequence and verify the  $z$ -transform expression using MATLAB.

1.  $x(n) = \{3, 2, 1, -2, -3\}$ .
2.  $x(n) = (0.8)^n u(n-2)$ . Verify the  $z$ -transform expression using MATLAB.
3.  $x(n) = [(0.5)^n + (-0.8)^n]u(n)$ . Verify the  $z$ -transform expression using MATLAB.
4.  $x(n) = 2^n \cos(0.4\pi n)u(-n)$ .
5.  $x(n) = (n+1)(3)^n u(n)$ . Verify the  $z$ -transform expression using MATLAB.

- P4.2** Consider the sequence  $x(n) = (0.9)^n \cos(\pi n/4)u(n)$ . Let

$$y(n) = \begin{cases} x(n/2), & n = 0, \pm 2, \pm 4, \dots \\ 0, & \text{otherwise} \end{cases}$$

1. Show that the  $z$ -transform  $Y(z)$  of  $y(n)$  can be expressed in terms of the  $z$ -transform  $X(z)$  of  $x(n)$  as  $Y(z) = X(z^2)$ .
2. Determine  $Y(z)$ .
3. Using MATLAB, verify that the sequence  $y(n)$  has the  $z$ -transform  $Y(z)$ .

- P4.3** Determine the  $z$ -transform of the following sequences using the  $z$ -transform table and the  $z$ -transform properties. Express  $X(z)$  as a rational function in  $z^{-1}$ . Verify your results using MATLAB. Indicate the region of convergence in each case, and provide a pole-zero plot.

1.  $x(n) = 2\delta(n-2) + 3u(n-3)$
2.  $x(n) = 3(0.75)^n \cos(0.3\pi n)u(n) + 4(0.75)^n \sin(0.3\pi n)u(n)$
3.  $x(n) = n \sin(\frac{\pi n}{3})u(n) + (0.9)^n u(n-2)$

4.  $x(n) = n^2(2/3)^{n-2}u(n-1)$
5.  $x(n) = (n-3)(\frac{1}{4})^{n-2} \cos\{\frac{\pi}{2}(n-1)\}u(n)$

**P4.4** Let  $x(n)$  be a complex-valued sequence with the real part  $x_R(n)$  and the imaginary part  $x_I(n)$ .

1. Prove the following  $z$ -transform relations:

$$X_R(z) \triangleq \mathcal{Z}[x_R(n)] = \frac{X(z) + X^*(z^*)}{2} \quad \text{and} \quad X_I(z) \triangleq \mathcal{Z}[x_I(n)] = \frac{X(z) - X^*(z^*)}{2}$$

2. Verify these relations for  $x(n) = \exp\{(-1 + j0.2\pi)n\} u(n)$ .

**P4.5** The  $z$ -transform of  $x(n)$  is  $X(z) = 1/(1 + 0.5z^{-1})$ ,  $|z| > 0.5$ . Determine the  $z$ -transforms of the following sequences and indicate their region of convergence.

1.  $x_1(n) = x(3-n) + x(n-3)$
2.  $x_2(n) = (1+n+n^2)x(n)$
3.  $x_3(n) = (\frac{1}{2})^n x(n-2)$
4.  $x_4(n) = x(n+2) * x(n-2)$
5.  $x_5(n) = \cos(\pi n/2)x^*(n)$

**P4.6** Repeat Problem P4.5 if

$$X(z) = \frac{1+z^{-1}}{1+\frac{5}{6}z^{-1}+\frac{1}{6}z^{-2}}; |z| > \frac{1}{2}$$

**P4.7** The inverse  $z$ -transform of  $X(z)$  is  $x(n) = (1/2)^n u(n)$ . Using the  $z$ -transform properties, determine the sequences in each of the following cases.

1.  $X_1(z) = \frac{z-1}{z} X(z)$
2.  $X_2(z) = zX(z^{-1})$
3.  $X_3(z) = 2X(3z) + 3X(z/3)$
4.  $X_4(z) = X(z)X(z^{-1})$
5.  $X_5(z) = z^2 \frac{dX(z)}{dz}$

**P4.8** If sequences  $x_1(n)$ ,  $x_2(n)$ , and  $x_3(n)$  are related by  $x_3(n) = x_1(n) * x_2(n)$ , then

$$\sum_{n=-\infty}^{\infty} x_3(n) = \left( \sum_{n=-\infty}^{\infty} x_1(n) \right) \left( \sum_{n=-\infty}^{\infty} x_2(n) \right)$$

1. Prove this result by substituting the definition of convolution in the left-hand side.
2. Prove this result using the convolution property.
3. Verify this result using MATLAB and choosing any two random sequences  $x_1(n)$  and  $x_2(n)$ .

**P4.9** Determine the results of the following polynomial operations using MATLAB.

1.  $X_1(z) = (1 - 2z^{-1} + 3z^{-2} - 4z^{-3})(4 + 3z^{-1} - 2z^{-2} + z^{-3})$
2.  $X_2(z) = (z^2 - 2z + 3 + 2z^{-1} + z^{-2})(z^3 - z^{-3})$
3.  $X_3(z) = (1 + z^{-1} + z^{-2})^3$
4.  $X_4(z) = X_1(z)X_2(z) + X_3(z)$
5.  $X_5(z) = (z^{-1} - 3z^{-3} + 2z^{-5} + 5z^{-7} - z^{-9})(z + 3z^2 + 2z^3 + 4z^4)$

- P4.10** The `deconv` function is useful in dividing two causal sequences. Write a MATLAB function `deconv_m` to divide two noncausal sequences (similar to the `conv` function). The format of this function should be

```
function [p,np,r,nr] = deconv_m(b,nb,a,na)
% Modified deconvolution routine for noncausal sequences
% function [p,np,r,nr] = deconv_m(b,nb,a,na)
%
% p = polynomial part of support np1 <= n <= np2
% np = [np1, np2]
% r = remainder part of support nr1 <= n <= nr2
% nr = [nr1, nr2]
% b = numerator polynomial of support nb1 <= n <= nb2
% nb = [nb1, nb2]
% a = denominator polynomial of support na1 <= n <= na2
% na = [na1, na2]
%
```

Check your function on the following operation:

$$\frac{z^2 + z + 1 + z^{-1} + z^{-2} + z^{-3}}{z + 2 + z^{-1}} = (z - 1 + 2z^{-1} - 2z^{-2}) + \frac{3z^{-2} + 3z^{-3}}{z + 2 + z^{-1}}$$

- P4.11** Determine the following inverse  $z$ -transforms using the partial fraction expansion method.

1.  $X_1(z) = (1 - z^{-1} - 4z^{-2} + 4z^{-3}) / (1 - \frac{11}{4}z^{-1} + \frac{13}{8}z^{-2} - \frac{1}{4}z^{-3})$ . The sequence is right-sided.
2.  $X_2(z) = (1 + z^{-1} - 4z^{-2} + 4z^{-3}) / (1 - \frac{11}{4}z^{-1} + \frac{13}{8}z^{-2} - \frac{1}{4}z^{-3})$ . The sequence is absolutely summable.
3.  $X_3(z) = (z^3 - 3z^2 + 4z + 1) / (z^3 - 4z^2 + z - 0.16)$ . The sequence is left-sided.
4.  $X_4(z) = z / (z^3 + 2z^2 + 1.25z + 0.25)$ ,  $|z| > 1$ .
5.  $X_5(z) = z / (z^2 - 0.25)^2$ ,  $|z| < 0.5$ .

- P4.12** Consider the sequence

$$x(n) = A_c(r)^n \cos(\pi v_0 n) u(n) + A_s(r)^n \sin(\pi v_0 n) u(n) \quad (4.30)$$

The  $z$ -transform of this sequence is a second-order (proper) rational function that contains a complex-conjugate pole pair. The objective of this problem is to develop a MATLAB function that can be used to obtain the inverse  $z$ -transform of such a rational function so that the inverse does not contain any complex numbers.

1. Show that the  $z$ -transform of  $x(n)$  in (4.30) is given by

$$X(z) = \frac{b_0 + b_1 z^{-1}}{1 + a_1 z^{-1} + a_2 z^{-2}}; \quad |z| > |r| \quad (4.31)$$

where

$$b_0 = A_c; \quad b_1 = r[A_s \sin(\pi v_0) - A_c \cos(\pi v_0)]; \quad a_1 = -2r \cos(\pi v_0); \quad a_2 = r^2 \quad (4.32)$$

2. Using (4.32), determine the signal parameters  $A_c$ ,  $A_s$ ,  $r$ , and  $v_0$  in terms of the rational function parameters  $b_0$ ,  $b_1$ ,  $a_1$ , and  $a_2$ .
3. Using your results in part b above, design a MATLAB function, `invCCPP`, that computes signal parameters using the rational function parameters. The format of this function should be

```
function [As,Ac,r,v0] = invCCPP(b0,b1,a1,a2)
```

**P4.13** Suppose  $X(z)$  is given as follows:

$$X(z) = \frac{2 + 3z^{-1}}{1 - z^{-1} + 0.81z^{-2}}, |z| > 0.9$$

1. Using the MATLAB function `invCCPP` given in Problem P4.12, determine  $x(n)$  in a form that contains no complex numbers.
2. Using MATLAB, compute the first 20 samples of  $x(n)$ , and compare them with your answer in the above part.

**P4.14** The  $z$ -transform of a causal sequence is given as

$$X(z) = \frac{-2 + 5.65z^{-1} - 2.88z^{-2}}{1 - 0.1z^{-1} + 0.09z^{-2} + 0.648z^{-3}} \quad (4.33)$$

which contains a complex-conjugate pole pair as well as a real-valued pole.

1. Using the `residuez` function, express (4.33) as

$$X(z) = \frac{(\ ) + (\ )z^{-1}}{1 + (\ )z^{-1} + (\ )z^{-2}} + \frac{(\ )}{1 + (\ )z^{-1}} \quad (4.34)$$

Note that you will have to use the `residuez` function in both directions.

2. Now using your function `invCCPP` and the inverse of the real-valued pole factor, determine the causal sequence  $x(n)$  from the  $X(z)$  in (4.34) so that it contains no complex numbers.

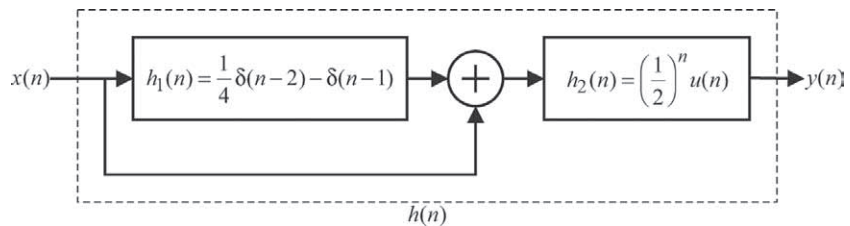
**P4.15** For the linear and time-invariant systems described by the following impulse responses, determine (i) the system function representation, (ii) the difference equation representation, (iii) the pole-zero plot, and (iv) the output  $y(n)$  if the input is  $x(n) = \left(\frac{1}{4}\right)^n u(n)$ .

1.  $h(n) = 5(1/4)^n u(n)$
2.  $h(n) = n(1/3)^n u(n) + (-1/4)^n u(n)$
3.  $h(n) = 3(0.9)^n \cos(\pi n/4 + \pi/3)u(n+1)$
4.  $h(n) = \frac{(0.5)^n \sin[(n+1)\pi/3]}{\sin(\pi/3)} u(n)$
5.  $h(n) = [2 - \sin(\pi n)]u(n)$

**P4.16** Consider the system shown in Figure P4.1.

1. Using the  $z$ -transform approach, show that the impulse response,  $h(n)$ , of the overall system is given by

$$h(n) = \delta(n) - \frac{1}{2}\delta(n-1)$$

**FIGURE P4.1** System for Problem 4.16

2. Determine the difference equation representation of the overall system that relates the output  $y(n)$  to the input  $x(n)$ .
3. Is this system causal? BIBO stable? Explain clearly to receive full credit.
4. Determine the frequency response  $H(e^{j\omega})$  of the overall system.
5. Using MATLAB, provide a plot of this frequency response over  $0 \leq \omega \leq \pi$ .

**P4.17** For the linear and time-invariant systems described by the following system functions, determine (i) the impulse response representation, (ii) the difference equation representation, (iii) the pole-zero plot, and (iv) the output  $y(n)$  if the input is  $x(n) = 3 \cos(\pi n/3)u(n)$ .

1.  $H(z) = (z + 1)/(z - 0.5)$ , causal system
2.  $H(z) = (1 + z^{-1} + z^{-2})/(1 + 0.5z^{-1} - 0.25z^{-2})$ , stable system
3.  $H(z) = (z^2 - 1)/(z - 3)^2$ , anticausal system
4.  $H(z) = \frac{z}{z - 0.25} + \frac{1 - 0.5z^{-1}}{1 + 2z^{-1}}$ , stable system
5.  $H(z) = (1 + z^{-1} + z^{-2})^2$

**P4.18** For the linear, causal, and time-invariant systems described by the following difference equations, determine (i) the impulse response representation, (ii) the system function representation, (iii) the pole-zero plot, and (iv) the output  $y(n)$  if the input is  $x(n) = 2(0.9)^n u(n)$ .

1.  $y(n) = [x(n) + 2x(n - 1) + x(n - 3)]/4$
2.  $y(n) = x(n) + 0.5x(n - 1) - 0.5y(n - 1) + 0.25y(n - 2)$
3.  $y(n) = 2x(n) + 0.9y(n - 1)$
4.  $y(n) = -0.45x(n) - 0.4x(n - 1) + x(n - 2) + 0.4y(n - 1) + 0.45y(n - 2)$
5.  $y(n) = \sum_{m=0}^4 (0.8)^m x(n - m) - \sum_{\ell=1}^4 (0.9)^\ell y(n - \ell)$

**P4.19** The output sequence  $y(n)$  in Problem P4.18 is the total response. For each of the systems given in Problem P4.18, separate  $y(n)$  into (i) the homogeneous part, (ii) the particular part, (iii) the transient response, and (iv) the steady-state response.

**P4.20** A stable system has four zeros and four poles as given below.

$$\text{zeros: } \pm 1, \pm j1 \quad \text{Poles: } \pm 0.9, \pm j0.9$$

It is also known that the frequency response function  $H(e^{j\omega})$  evaluated at  $\omega = \pi/4$  is equal to 1, that is,

$$H(e^{j\pi/4}) = 1$$

1. Determine the system function  $H(z)$ , and indicate its region of convergence.
2. Determine the difference equation representation.
3. Determine the steady-state response  $y_{ss}(n)$  if the input is  $x(n) = \cos(\pi n/4)u(n)$ .
4. Determine the transient response  $y_{tr}(n)$  if the input is  $x(n) = \cos(\pi n/4)u(n)$ .

**P4.21** A digital filter is described by the frequency response function

$$H(e^{j\omega}) = [1 + 2\cos(\omega) + 3\cos(2\omega)] \cos\left(\frac{\omega}{2}\right) e^{-j5\omega/2}$$

1. Determine the difference equation representation.
2. Using the **freqz** function, plot the magnitude and phase of the frequency response of the filter. Note the magnitude and phase at  $\omega = \pi/2$  and at  $\omega = \pi$ .
3. Generate 200 samples of the signal  $x(n) = \sin(\pi n/2) + 5\cos(\pi n)$ , and process through the filter to obtain  $y(n)$ . Compare the steady-state portion of  $y(n)$  to  $x(n)$ . How are the amplitudes and phases of two sinusoids affected by the filter?

**P4.22** Repeat Problem 4.21 for the following filter:

$$H(e^{j\omega}) = \frac{1 + e^{-j4\omega}}{1 - 0.8145e^{-j4\omega}}$$

**P4.23** Solve the following difference equation for  $y(n)$  using the one-sided  $z$ -transform approach:

$$\begin{aligned} y(n) &= 0.81y(n-2) + x(n) - x(n-1), \quad n \geq 0; \quad y(-1) = 2, \quad y(-2) = 2 \\ x(n) &= (0.7)^n u(n+1) \end{aligned}$$

Generate the first 20 samples of  $y(n)$  using MATLAB, and compare them with your answer.

**P4.24** Solve the difference equation for  $y(n)$ ,  $n \geq 0$ ,

$$y(n) - 0.4y(n-1) - 0.45y(n-2) = 0.45x(n) + 0.4x(n-1) - x(n-2)$$

driven by the input  $x(n) = \left[2 + \left(\frac{1}{2}\right)^n\right] u(n)$  and subject to

$$y(-1) = 0, \quad y(-2) = 3; \quad x(-1) = x(-2) = 2$$

Decompose the solution  $y(n)$  into (i) transient response, (ii) steady-state response, (iii) zero-input response, and (iv) zero-state response.

**P4.25** A stable, linear, and time-invariant system is given by the system function

$$H(z) = \frac{4z^2 - 2\sqrt{2}z + 1}{z^2 - 2\sqrt{2}z + 4}$$

1. Determine the difference equation representation for this system.
2. Plot the poles and zeros of  $H(z)$ , and indicate the ROC.
3. Determine the unit sample response  $h(n)$  of this system.
4. Is this system causal? If the answer is yes, justify it. If the answer is no, find a causal unit sample response that satisfies the system function.

**P4.26** Determine the zero-input, zero-state, and steady-state responses of the system

$$y(n) = 0.9801y(n-2) + x(n) + 2x(n-1) + x(n-2), \quad n \geq 0; \quad y(-2) = 1, \quad y(-1) = 0$$

to the input  $x(n) = 5(-1)^n u(n)$ .

# CHAPTER

---

# 5

## The Discrete Fourier Transform

---

In Chapters 3 and 4, we studied transform-domain representations of discrete signals. The discrete-time Fourier transform provided the frequency-domain ( $\omega$ ) representation for absolutely summable sequences. The  $z$ -transform provided a generalized frequency-domain ( $z$ ) representation for arbitrary sequences. These transforms have two features in common. First, the transforms are defined for infinite-length sequences. Second, and the most important, they are functions of continuous variables ( $\omega$  or  $z$ ). From the numerical computation viewpoint (or from MATLAB's viewpoint), these two features are troublesome because one has to evaluate *infinite sums* at *uncountably infinite* frequencies. To use MATLAB, we have to truncate sequences and then evaluate the expressions at finitely many points. This is what we did in many examples in the two previous chapters. The evaluations were obviously approximations to the exact calculations. In other words, the discrete-time Fourier transform and the  $z$ -transform are not *numerically computable* transforms.

Therefore, we turn our attention to a numerically computable transform. It is obtained by sampling the discrete-time Fourier transform in the frequency domain (or the  $z$ -transform on the unit circle). We develop this transform by first analyzing periodic sequences. From Fourier analysis, we know that a periodic function (or sequence) can always be represented by a linear combination of harmonically related complex exponentials (which is a form of sampling). This gives us the *discrete Fourier series* (DFS) representation. Since the sampling is in the frequency domain, we study the effects of sampling in the time domain and the issue of reconstruction in

the  $z$ -domain. We then extend the DFS to *finite-duration sequences*, which leads to a new transform, called the *discrete Fourier transform* (DFT). The DFT avoids the two problems mentioned and is a numerically computable transform that is suitable for computer implementation. We study its properties and its use in system analysis in detail. The numerical computation of the DFT for long sequences is prohibitively time-consuming. Therefore, several algorithms have been developed to efficiently compute the DFT. These are collectively called fast Fourier transform (or FFT) algorithms. We will study two such algorithms in detail.

## 5.1 THE DISCRETE FOURIER SERIES

---

In Chapter 2, we defined the periodic sequence by  $\tilde{x}(n)$ , satisfying the condition

$$\tilde{x}(n) = \tilde{x}(n + kN), \quad \forall n, k \quad (5.1)$$

where  $N$  is the fundamental period of the sequence. From Fourier analysis, we know that the periodic functions can be synthesized as a linear combination of complex exponentials whose frequencies are multiples (or harmonics) of the fundamental frequency (which in our case is  $2\pi/N$ ). From the frequency-domain periodicity of the discrete-time Fourier transform, we conclude that there are a finite number of harmonics; the frequencies are  $\{\frac{2\pi}{N}k, \quad k = 0, 1, \dots, N - 1\}$ . Therefore, a periodic sequence  $\tilde{x}(n)$  can be expressed as

$$\tilde{x}(n) = \frac{1}{N} \sum_{k=0}^{N-1} \tilde{X}(k) e^{j \frac{2\pi}{N} kn}, \quad n = 0, \pm 1, \dots \quad (5.2)$$

where  $\{\tilde{X}(k), \quad k = 0, \pm 1, \dots, N-1\}$  are called the discrete Fourier series coefficients, which are given by

$$\tilde{X}(k) = \sum_{n=0}^{N-1} \tilde{x}(n) e^{-j \frac{2\pi}{N} nk}, \quad k = 0, \pm 1, \dots \quad (5.3)$$

Note that  $\tilde{X}(k)$  is itself a (complex-valued) periodic sequence with fundamental period equal to  $N$ , that is,

$$\tilde{X}(k + N) = \tilde{X}(k) \quad (5.4)$$

The pair of equations (5.3) and (5.2), taken together, is called the *discrete Fourier series* representation of periodic sequences. Using  $W_N \stackrel{\triangle}{=} e^{-j \frac{2\pi}{N}}$  to

denote the complex exponential term, we express (5.3) and (5.2) as

$$\begin{aligned}\tilde{X}(k) &\stackrel{\Delta}{=} \text{DFS}[\tilde{x}(n)] = \sum_{n=0}^{N-1} \tilde{x}(n) W_N^{nk} && \text{Analysis or a DFS equation} \\ \tilde{x}(n) &\stackrel{\Delta}{=} \text{IDFS}[\tilde{X}(k)] = \frac{1}{N} \sum_{k=0}^{N-1} \tilde{X}(k) W_N^{-nk} && \text{Synthesis or an inverse DFS equation}\end{aligned}\tag{5.5}$$

**EXAMPLE 5.1** Find the DFS representation of the periodic sequence

$$\tilde{x}(n) = \{\dots, 0, 1, 2, 3, 0, 1, 2, 3, 0, 1, 2, 3, \dots\}$$

**Solution** The fundamental period of this sequence is  $N = 4$ . Hence  $W_4 = e^{-j\frac{2\pi}{4}} = -j$ . Now

$$\tilde{X}(k) = \sum_{n=0}^3 \tilde{x}(n) W_4^{nk}, \quad k = 0, \pm 1, \pm 2, \dots$$

Hence

$$\tilde{X}(0) = \sum_0^3 \tilde{x}(n) W_4^{0 \cdot n} = \sum_0^3 \tilde{x}(n) = \tilde{x}(0) + \tilde{x}(1) + \tilde{x}(2) + \tilde{x}(3) = 6$$

Similarly,

$$\tilde{X}(1) = \sum_0^3 \tilde{x}(n) W_4^n = \sum_0^3 \tilde{x}(n)(-j)^n = (-2 + 2j)$$

$$\tilde{X}(2) = \sum_0^3 \tilde{x}(n) W_4^{2n} = \sum_0^3 \tilde{x}(n)(-j)^{2n} = -2$$

$$\tilde{X}(3) = \sum_0^3 \tilde{x}(n) W_4^{3n} = \sum_0^3 \tilde{x}(n)(-j)^{3n} = (-2 - 2j)$$

□

### 5.1.1 MATLAB IMPLEMENTATION

A careful look at (5.5) reveals that the DFS is a numerically computable representation. It can be implemented in many ways. To compute each sample  $\tilde{X}(k)$ , we can implement the summation as a `for...end` loop. To compute all DFS coefficients would require another `for...end` loop. This will result in a two nested `for...end` loop implementation. This is clearly inefficient in MATLAB. An efficient implementation in MATLAB

would be to use a matrix-vector multiplication for each of the relations in (5.5). We have used this approach earlier in implementing a numerical approximation to the discrete-time Fourier transform. Let  $\tilde{\mathbf{x}}$  and  $\tilde{\mathbf{X}}$  denote column vectors corresponding to the primary periods of sequences  $\tilde{x}(n)$  and  $\tilde{X}(k)$ , respectively. Then (5.5) is given by

$$\begin{aligned}\tilde{\mathbf{X}} &= \mathbf{W}_N \tilde{\mathbf{x}} \\ \tilde{\mathbf{x}} &= \frac{1}{N} \mathbf{W}_N^* \tilde{\mathbf{X}}\end{aligned}\quad (5.6)$$

where the matrix  $\mathbf{W}_N$  is given by

$$\mathbf{W}_N \triangleq \left[ W_N^{kn} \right]_{0 \leq k, n \leq N-1} = k \begin{bmatrix} 1 & 1 & \cdots & 1 \\ 1 & W_N^1 & \cdots & W_N^{(N-1)} \\ \vdots & \vdots & \ddots & \vdots \\ 1 & W_N^{(N-1)} & \cdots & W_N^{(N-1)^2} \end{bmatrix} \quad (5.7)$$

The matrix  $\mathbf{W}_N$  is a square matrix and is called a *DFS matrix*. The following MATLAB function `dfs` implements this procedure.

```
function [Xk] = dfs(xn,N)
% Computes discrete Fourier series coefficients
%
% [Xk] = dfs(xn,N)
% Xk = DFS coeff. array over 0 <= k <= N-1
% xn = One period of periodic signal over 0 <= n <= N-1
% N = Fundamental period of xn
%
n = [0:1:N-1]; % Row vector for n
k = [0:1:N-1]; % Row vector for k
WN = exp(-j*2*pi/N); % Wn factor
nk = n'*k; % Creates an N by N matrix of nk values
WNnk = WN .^ nk; % DFS matrix
Xk = xn * WNnk; % Row vector for DFS coefficients
```

The DFS in Example 5.1 can be computed using MATLAB as

```
>> xn = [0,1,2,3]; N = 4; Xk = dfs(xn,N)
Xk =
    6.0000      -2.0000 + 2.0000i   -2.0000 - 0.0000i   -2.0000 - 2.0000i
```

The following `idfs` function implements the synthesis equation.

```
function [xn] = idfs(Xk,N)
% Computes inverse discrete Fourier series
%
% [xn] = idfs(Xk,N)
% xn = one period of periodic signal over 0 <= n <= N-1
% Xk = DFS coeff. array over 0 <= k <= N-1
% N = fundamental period of Xk
%
n = [0:1:N-1]; % Row vector for n
k = [0:1:N-1]; % Row vector for k
WN = exp(-j*2*pi/N); % Wn factor
nk = n'*k; % Creates an N by N matrix of nk values
WNnk = WN .^ (-nk); % IDFS matrix
xn = (Xk * WNnk)/N; % Row vector for IDFS values
```

*Caution:* These functions are efficient approaches of implementing (5.5) in MATLAB. They are not computationally efficient, especially for large  $N$ . We will deal with this problem later in this chapter.

- **EXAMPLE 5.2** A periodic “square wave” sequence is given by

$$\tilde{x}(n) = \begin{cases} 1, & mN \leq n \leq mN + L - 1 \\ 0, & mN + L \leq n \leq (m+1)N - 1 \end{cases}; \quad m = 0, \pm 1, \pm 2, \dots$$

where  $N$  is the fundamental period and  $L/N$  is the duty cycle.

- Determine an expression for  $|\tilde{X}(k)|$  in terms of  $L$  and  $N$ .
- Plot the magnitude  $|\tilde{X}(k)|$  for  $L = 5$ ,  $N = 20$ ;  $L = 5$ ,  $N = 40$ ;  $L = 5$ ,  $N = 60$ ; and  $L = 7$ ,  $N = 60$ .
- Comment on the results.

### Solution

A plot of this sequence for  $L = 5$  and  $N = 20$  is shown in Figure 5.1.

- By applying the analysis equation (5.3),

$$\begin{aligned} \tilde{X}(k) &= \sum_{n=0}^{N-1} \tilde{x}(n) e^{-j\frac{2\pi}{N}nk} = \sum_{n=0}^{L-1} e^{-j\frac{2\pi}{N}nk} = \sum_{n=0}^{L-1} \left( e^{-j\frac{2\pi}{N}k} \right)^n \\ &= \begin{cases} L, & k = 0, \pm N, \pm 2N, \dots \\ \frac{1 - e^{-j2\pi Lk/N}}{1 - e^{-j2\pi k/N}}, & \text{otherwise} \end{cases} \end{aligned}$$

The last step follows from the sum of the geometric terms formula (2.7) in Chapter 2. The last expression can be simplified to

$$\begin{aligned} \frac{1 - e^{-j2\pi Lk/N}}{1 - e^{-j2\pi k/N}} &= \frac{e^{-j\pi Lk/N}}{e^{-j\pi k/N}} \frac{e^{j\pi Lk/N} - e^{-j\pi Lk/N}}{e^{j\pi k/N} - e^{-j\pi k/N}} \\ &= e^{-j\pi(L-1)k/N} \frac{\sin(\pi k L / N)}{\sin(\pi k / N)} \end{aligned}$$

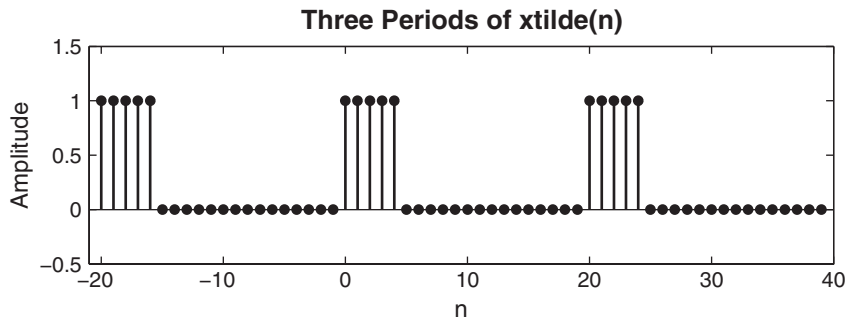


**FIGURE 5.1** Periodic square wave sequence

or the magnitude of  $\tilde{X}(k)$  is given by

$$|\tilde{X}(k)| = \begin{cases} L, & k = 0, \pm N, \pm 2N, \dots \\ \left| \frac{\sin(\pi k L/N)}{\sin(\pi k/N)} \right|, & \text{otherwise} \end{cases}$$

b. The MATLAB script for  $L = 5$  and  $N = 20$ :

```
>> L = 5; N = 20; k = [-N/2:N/2]; % Sq wave parameters
>> xn = [ones(1,L), zeros(1,N-L)]; % Sq wave x(n)
>> Xk = dfs(xn,N); % DFS
>> magXk = abs([Xk(N/2+1:N) Xk(1:N/2+1)]); % DFS magnitude
>> subplot(2,2,1); stem(k,magXk); axis([-N/2,N/2,-0.5,5.5])
>> xlabel('k'); ylabel('Amplitude')
>> title('DFS of SQ. Wave: L=5, N=20')
```

The plots for this and all other cases are shown in Figure 5.2. Note that since  $\tilde{X}(k)$  is periodic, the plots are shown from  $-N/2$  to  $N/2$ .

c. Several interesting observations can be made from plots in Figure 5.2. The envelopes of the DFS coefficients of square waves look like “sinc” functions. The amplitude at  $k = 0$  is equal to  $L$ , while the zeros of the functions are at multiples of  $N/L$ , which is the reciprocal of the duty cycle. We will study these functions later in this chapter.  $\square$

### 5.1.2 RELATION TO THE $z$ -TRANSFORM

Let  $x(n)$  be a finite-duration sequence of duration  $N$  such that

$$x(n) = \begin{cases} \text{Nonzero}, & 0 \leq n \leq N-1 \\ 0, & \text{elsewhere} \end{cases} \quad (5.8)$$

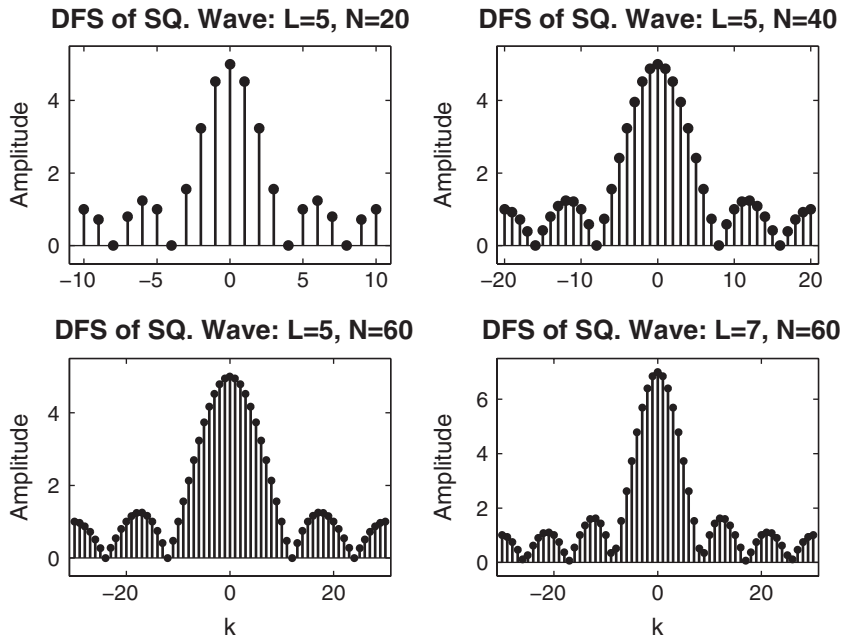


**FIGURE 5.2** The DFS plots of a periodic square wave for various  $L$  and  $N$

Then we can compute its  $z$ -transform:

$$X(z) = \sum_{n=0}^{N-1} x(n)z^{-n} \quad (5.9)$$

Now we construct a periodic sequence  $\tilde{x}(n)$  by periodically repeating  $x(n)$  with period  $N$ , that is,

$$x(n) = \begin{cases} \tilde{x}(n), & 0 \leq n \leq N-1 \\ 0, & \text{elsewhere} \end{cases} \quad (5.10)$$

The DFS of  $\tilde{x}(n)$  is given by

$$\tilde{X}(k) = \sum_{n=0}^{N-1} \tilde{x}(n)e^{-j\frac{2\pi}{N}nk} = \sum_{n=0}^{N-1} x(n) \left[ e^{-j\frac{2\pi}{N}k} \right]^{-n} \quad (5.11)$$

Comparing it with (5.9), we have

$$\tilde{X}(k) = X(z)|_{z=e^{j\frac{2\pi}{N}k}} \quad (5.12)$$

which means that the DFS  $\tilde{X}(k)$  represents  $N$  evenly spaced samples of the  $z$ -transform  $X(z)$  around the unit circle.

### 5.1.3 RELATION TO THE DTFT

Since  $x(n)$  in (5.8) is of finite duration of length  $N$ , it is also absolutely summable. Hence its DTFT exists and is given by

$$X(e^{j\omega}) = \sum_{n=0}^{N-1} x(n)e^{-j\omega n} = \sum_{n=0}^{N-1} \tilde{x}(n)e^{-j\omega n} \quad (5.13)$$

Comparing (5.13) with (5.11), we have

$$\tilde{X}(k) = X(e^{j\omega})|_{\omega=\frac{2\pi}{N}k} \quad (5.14)$$

Let

$$\omega_1 \triangleq \frac{2\pi}{N} \quad \text{and} \quad \omega_k \triangleq \frac{2\pi}{N}k = k\omega_1$$

Then the DFS  $X(k) = X(e^{jk\omega_k}) = X(e^{jk\omega_1})$ , which means that the DFS is obtained by *evenly sampling* the DTFT at  $\omega_1 = \frac{2\pi}{N}$  intervals. From (5.12) and (5.14), we observe that the DFS representation gives us a sampling mechanism in the frequency domain that, in principle, is similar to sampling in the time domain. The interval  $\omega_1 = \frac{2\pi}{N}$  is the *sampling interval* in the frequency domain. It is also called the *frequency resolution* because it tells us how close the frequency samples (or measurements) are.

□ **EXAMPLE 5.3** Let  $x(n) = \begin{cases} 0, & n < 0 \\ 1, & n = 0 \\ 2, & n = 1 \\ 3, & n = 2 \\ 0, & n > 2 \end{cases}$ .

- a. Compute its discrete-time Fourier transform  $X(e^{j\omega})$ .
- b. Sample  $X(e^{j\omega})$  at  $k\omega_1 = \frac{2\pi}{4}k$ ,  $k = 0, 1, 2, 3$  and show that it is equal to  $\tilde{X}(k)$  in Example 5.1.

#### Solution

The sequence  $x(n)$  is not periodic but is of finite duration.

- a. The discrete-time Fourier transform is given by

$$X(e^{j\omega}) = \sum_{n=-\infty}^{\infty} x(n)e^{-j\omega n} = e^{-j\omega} + 2e^{-j2\omega} + 3e^{-j3\omega}$$

- b. Sampling at  $k\omega_1 = \frac{2\pi}{4}k$ ,  $k = 0, 1, 2, 3$ , we obtain

$$X(e^{j0}) = 1 + 2 + 3 = 6 = \tilde{X}(0)$$

$$X(e^{j2\pi/4}) = e^{-j2\pi/4} + 2e^{-j4\pi/4} + 3e^{-j6\pi/4} = -2 + 2j = \tilde{X}(1)$$

$$X(e^{j4\pi/4}) = e^{-j4\pi/4} + 2e^{-j8\pi/4} + 3e^{-j12\pi/4} = 2 = \tilde{X}(2)$$

$$X(e^{j6\pi/4}) = e^{-j6\pi/4} + 2e^{-j12\pi/4} + 3e^{-j18\pi/4} = -2 - 2j = \tilde{X}(3)$$

as expected. □

## 5.2 SAMPLING AND RECONSTRUCTION IN THE $z$ -DOMAIN

---

Let  $x(n)$  be an arbitrary absolutely summable sequence, which may be of infinite duration. Its  $z$ -transform is given by

$$X(z) = \sum_{m=-\infty}^{\infty} x(m)z^{-m}$$

and we assume that the ROC of  $X(z)$  includes the unit circle. We sample  $X(z)$  on the unit circle at equispaced points separated in angle by  $\omega_1 = 2\pi/N$  and call it a DFS sequence,

$$\begin{aligned}\tilde{X}(k) &\triangleq X(z)|_{z=e^{j\frac{2\pi}{N}k}}, \quad k = 0, \pm 1, \pm 2, \dots \\ &= \sum_{m=-\infty}^{\infty} x(m)e^{-j\frac{2\pi}{N}km} = \sum_{m=-\infty}^{\infty} x(m)W_N^{km}\end{aligned}\quad (5.15)$$

which is periodic with period  $N$ . Finally, we compute the IDFS of  $\tilde{X}(k)$ ,

$$\tilde{x}(n) = \text{IDFS}[\tilde{X}(k)]$$

which is also periodic with period  $N$ . Clearly, there must be a relationship between the arbitrary  $x(n)$  and the periodic  $\tilde{x}(n)$ . This is an important issue. In order to compute the inverse DTFT or the inverse  $z$ -transform numerically, we must deal with a finite number of samples of  $X(z)$  around the unit circle. Therefore, we must know the effect of such sampling on the time-domain sequence. This relationship is easy to obtain.

$$\begin{aligned}\tilde{x}(n) &= \frac{1}{N} \sum_{k=0}^{N-1} \tilde{X}(k) W_N^{-kn} \quad [\text{from (5.2)}] \\ &= \frac{1}{N} \sum_{k=0}^{N-1} \left\{ \sum_{m=-\infty}^{\infty} x(m) W_N^{km} \right\} W_N^{-kn} \quad [\text{from (5.15)}]\end{aligned}$$

or

$$\begin{aligned}\tilde{x}(n) &= \sum_{m=-\infty}^{\infty} x(m) \underbrace{\frac{1}{N} \sum_{k=0}^{N-1} W_N^{-k(n-m)}}_{\begin{cases} 1, & n-m = rN \\ 0, & \text{elsewhere} \end{cases}} = \sum_{m=-\infty}^{\infty} x(m) \sum_{r=-\infty}^{\infty} \delta(n-m-rN) \\ &= \sum_{r=-\infty}^{\infty} \sum_{m=-\infty}^{\infty} x(m) \delta(n-m-rN)\end{aligned}$$

or

$$\tilde{x}(n) = \sum_{r=-\infty}^{\infty} x(n-rN) = \cdots + x(n+N) + x(n) + x(n-N) + \cdots \quad (5.16)$$

which means that when we sample  $X(z)$  on the unit circle, we obtain a periodic sequence in the time domain. This sequence is a linear combination of the original  $x(n)$  and its infinite replicas, each shifted by multiples of  $\pm N$ . This is illustrated in Example 5.5. From (5.16), we observe that if  $x(n) = 0$  for  $n < 0$  and  $n \geq N$ , then there will be no overlap or aliasing in the time domain. Hence we should be able to recognize and recover  $x(n)$  from  $\tilde{x}(n)$ , that is,

$$x(n) = \tilde{x}(n) \text{ for } 0 \leq n \leq (N-1)$$

or

$$x(n) = \tilde{x}(n)\mathcal{R}_N(n) = \begin{cases} \tilde{x}(n), & 0 \leq n \leq N-1 \\ 0, & \text{elsewhere} \end{cases}$$

where  $\mathcal{R}_N(n)$  is called a *rectangular window* of length  $N$ . Therefore, we have the following theorem.

■ **THEOREM 1 Frequency Sampling**

If  $x(n)$  is time-limited (i.e., of finite duration) to  $[0, N-1]$ , then  $N$  samples of  $X(z)$  on the unit circle determine  $X(z)$  for all  $z$ .

- **EXAMPLE 5.4** Let  $x_1(n) = \{6, 5, 4, 3, 2, 1\}$ . Its DTFT  $X_1(e^{j\omega})$  is sampled at

$$\omega_k = \frac{2\pi k}{4}, \quad k = 0, \pm 1, \pm 2, \pm 3, \dots$$

to obtain a DFS sequence  $\tilde{X}_2(k)$ . Determine the sequence  $\tilde{x}_2(n)$ , which is the inverse DFS of  $\tilde{X}_2(k)$ .

**Solution**

Without computing the DTFT, the DFS, or the inverse DFS, we can evaluate  $\tilde{x}_2(n)$  by using the aliasing formula (5.16).

$$\tilde{x}_2(n) = \sum_{r=-\infty}^{\infty} x_1(n-4r)$$

Thus  $x(4)$  is aliased into  $x(0)$ , and  $x(5)$  is aliased into  $x(1)$ . Hence

$$\tilde{x}_2(n) = \{\dots, 8, 6, 4, 3, 8, 6, 4, 3, 8, 6, 4, 3, \dots\}$$

□

- EXAMPLE 5.5** Let  $x(n) = (0.7)^n u(n)$ . Sample its  $z$ -transform on the unit circle with  $N = 5, 10, 20, 50$  and study its effect in the time domain.

**Solution**

From Table 4.1, the  $z$ -transform of  $x(n)$  is

$$X(z) = \frac{1}{1 - 0.7z^{-1}} = \frac{z}{z - 0.7}, \quad |z| > 0.7$$

We can now use MATLAB to implement the sampling operation

$$\hat{X}(k) = X(z)|_{z=e^{j2\pi k/N}}, \quad k = 0, \pm 1, \pm 2, \dots$$

and the inverse DFS computation to determine the corresponding time-domain sequence. The MATLAB script for  $N = 5$  is as follows.

```
>> N = 5; k = 0:1:N-1; % Sample index
>> wk = 2*pi*k/N; zk = exp(j*wk); % Samples of z
>> Xk = (zk)./(zk-0.7); % DFS as samples of X(z)
>> xn = real(idfs(Xk,N)); % IDFS
>> xtilde = xn'* ones(1,8); xtilde = (xtilde(:))'; % Periodic sequence
>> subplot(2,2,1); stem(0:39,xtilde); axis([0,40,-0.1,1.5])
>> ylabel('Amplitude'); title('N=5')
```

The plots in Figure 5.3 clearly demonstrate the aliasing in the time domain, especially for  $N = 5$  and  $N = 10$ . For large values of  $N$ , the tail end of  $x(n)$

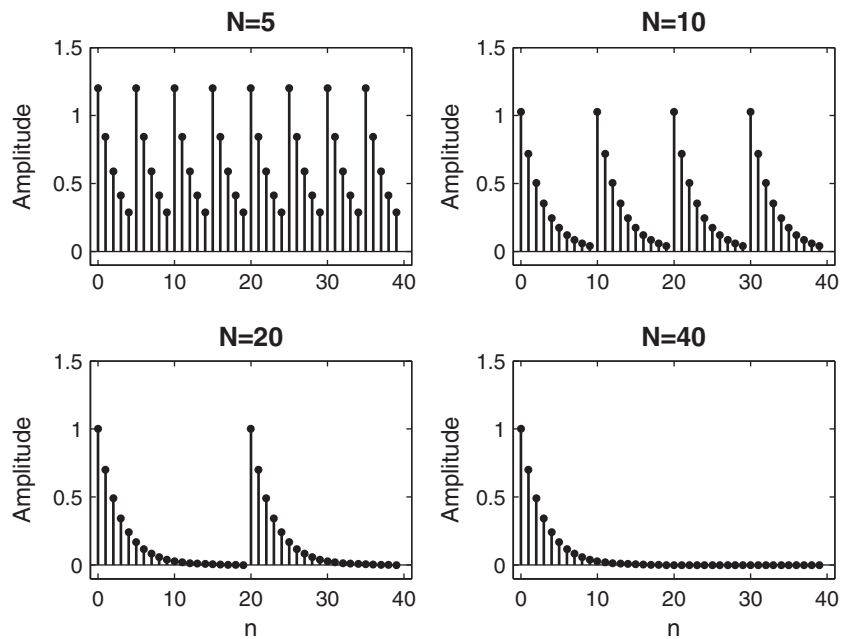


**FIGURE 5.3** Plots in Example 5.5

is sufficiently small to result in any appreciable amount of aliasing in practice. Such information is useful in effectively truncating an infinite-duration sequence prior to taking its transform.  $\square$

### 5.2.1 THE $z$ -TRANSFORM RECONSTRUCTION FORMULA

Let  $x(n)$  be time-limited to  $[0, N - 1]$ . Then from Theorem 1 we should be able to recover the  $z$ -transform  $X(z)$  using its samples  $\tilde{X}(k)$ . This is given by

$$\begin{aligned} X(z) &= \mathcal{Z}[x(n)] = \mathcal{Z}[\tilde{x}(n)\mathcal{R}_N(n)] \\ &= \mathcal{Z}[\text{IDFS}\{\underbrace{\tilde{X}(k)}_{\text{Samples of } X(z)}\}\mathcal{R}_N(n)] \end{aligned}$$

This approach results in the  $z$ -domain reconstruction formula:

$$\begin{aligned} X(z) &= \sum_0^{N-1} x(n)z^{-n} = \sum_0^{N-1} \tilde{x}(n)z^{-n} \\ &= \sum_0^{N-1} \left\{ \frac{1}{N} \sum_0^{N-1} \tilde{X}(k) W_N^{-kn} \right\} z^{-n} \\ &= \frac{1}{N} \sum_{k=0}^{N-1} \tilde{X}(k) \left\{ \sum_0^{N-1} W_N^{-kn} z^{-n} \right\} \\ &= \frac{1}{N} \sum_{k=0}^{N-1} \tilde{X}(k) \left\{ \sum_0^{N-1} (W_N^{-k} z^{-1})^n \right\} \\ &= \frac{1}{N} \sum_{k=0}^{N-1} \tilde{X}(k) \left\{ \frac{1 - W_N^{-kN} z^{-N}}{1 - W_N^{-k} z^{-1}} \right\} \end{aligned}$$

Since  $W_N^{-kN} = 1$ , we have

$$X(z) = \frac{1 - z^{-N}}{N} \sum_{k=0}^{N-1} \frac{\tilde{X}(k)}{1 - W_N^{-k} z^{-1}} \quad (5.17)$$

### 5.2.2 THE DTFT INTERPOLATION FORMULA

The reconstruction formula (5.17) can be specialized for the discrete-time Fourier transform by evaluating it on the unit circle  $z = e^{j\omega}$ . Then

$$\begin{aligned} X(e^{j\omega}) &= \frac{1 - e^{-j\omega N}}{N} \sum_{k=0}^{N-1} \frac{\tilde{X}(k)}{1 - e^{j2\pi k/N} e^{-j\omega}} \\ &= \sum_{k=0}^{N-1} \tilde{X}(k) \frac{1 - e^{-j\omega N}}{N \{1 - e^{j2\pi k/N} e^{-j\omega}\}} \end{aligned}$$

Consider

$$\begin{aligned}\frac{1 - e^{-j\omega N}}{N \{1 - e^{j2\pi k/N}e^{-j\omega}\}} &= \frac{1 - e^{-j(\omega - \frac{2\pi k}{N})N}}{N \left\{1 - e^{-j(\omega - \frac{2\pi k}{N})}\right\}} \\ &= \frac{e^{-j\frac{N}{2}(\omega - \frac{2\pi k}{N})}}{e^{-\frac{1}{2}j(\omega - \frac{2\pi k}{N})}} \left\{ \frac{\sin \left[ (\omega - \frac{2\pi k}{N}) \frac{N}{2} \right]}{N \sin \left[ (\omega - \frac{2\pi k}{N}) \frac{1}{2} \right]} \right\}\end{aligned}$$

Let

$$\Phi(\omega) \triangleq \frac{\sin(\frac{\omega N}{2})}{N \sin(\frac{\omega}{2})} e^{-j\omega(\frac{N-1}{2})} : \text{an interpolating function} \quad (5.18)$$

Then

$$X(e^{j\omega}) = \sum_{k=0}^{N-1} \tilde{X}(k) \Phi \left( \omega - \frac{2\pi k}{N} \right) \quad (5.19)$$

This is the DTFT interpolation formula to reconstruct  $X(e^{j\omega})$  from its samples  $\tilde{X}(k)$ . Since  $\Phi(0) = 1$ , we have that  $X(e^{j2\pi k/N}) = \tilde{X}(k)$ , which means that the interpolation is exact at sampling points. Recall the time-domain interpolation formula (3.33) for analog signals:

$$x_a(t) = \sum_{n=-\infty}^{\infty} x(n) \operatorname{sinc}[F_s(t - nT_s)] \quad (5.20)$$

The DTFT interpolating formula (5.19) looks similar.

However, there are some differences. First, the time-domain formula (5.20) reconstructs an arbitrary *nonperiodic* analog signal, while the frequency-domain formula (5.19) gives us a periodic waveform. Second, in (5.19) we use a  $\frac{\sin(Nx)}{N \sin x}$  interpolation function instead of our more familiar  $\frac{\sin x}{x}$  (sinc) function. The  $\Phi(\omega)$  function is a periodic function and hence is known as a *periodic-sinc* function. It is also known as the Dirichlet function. This is the function we observed in Example 5.2.

### 5.2.3 MATLAB IMPLEMENTATION

The interpolation formula (5.19) suffers the same fate as that of (5.20) while trying to implement it in practice. One has to generate several interpolating functions (5.18) and perform their linear combinations to obtain the discrete-time Fourier transform  $X(e^{j\omega})$  from its computed samples  $\tilde{X}(k)$ . Furthermore, in MATLAB we have to evaluate (5.19) on a finer grid over  $0 \leq \omega \leq 2\pi$ . This is clearly an inefficient approach. Another approach is to use the cubic spline interpolation function as an efficient approximation to (5.19). This is what we did to implement the time-domain interpolation formula for analog signals in Chapter 3. However, there is an alternate and efficient approach based on the DFT, which we will study in the next section.

## 5.3 THE DISCRETE FOURIER TRANSFORM

---

The discrete Fourier series provides a mechanism for numerically computing the discrete-time Fourier transform. It also alerts us to a potential problem of aliasing in the time domain. Mathematics dictates that the sampling of the discrete-time Fourier transform result in a periodic sequence  $\tilde{x}(n)$ . But most of the signals in practice are not periodic. They are likely to be of finite duration. How can we develop a numerically computable Fourier representation for such signals? Theoretically, we can take care of this problem by defining a periodic signal whose primary shape is that of the finite-duration signal and then using the DFS on this periodic signal. Practically, we define a new transform called the *discrete Fourier transform* (DFT), which is the primary period of the DFS. This DFT is the ultimate numerically computable Fourier transform for arbitrary finite-duration sequences.

First we define a finite-duration sequence  $x(n)$  that has  $N$  samples over  $0 \leq n \leq N - 1$  as an  *$N$ -point sequence*. Let  $\tilde{x}(n)$  be a periodic signal of period  $N$ , created using the  $N$ -point sequence  $x(n)$ ; that is, from (5.19),

$$\tilde{x}(n) = \sum_{r=-\infty}^{\infty} x(n - rN)$$

This is a somewhat cumbersome representation. Using the modulo- $N$  operation on the argument, we can simplify it to

$$\tilde{x}(n) = x(n \bmod N) \quad (5.21)$$

A simple way to interpret this operation is the following: if the argument  $n$  is between 0 and  $N - 1$ , then leave it as it is; otherwise add or subtract multiples of  $N$  from  $n$  until the result is between 0 and  $N - 1$ . Note carefully that (5.21) is valid only if the length of  $x(n)$  is  $N$  or less. Furthermore, we use the following convenient notation to denote the modulo- $N$  operation:

$$x((n))_N \triangleq x(n \bmod N) \quad (5.22)$$

Then the compact relationships between  $x(n)$  and  $\tilde{x}(n)$  are

$$\begin{aligned} \tilde{x}(n) &= x((n))_N && \text{(Periodic extension)} \\ x(n) &= \tilde{x}(n)\mathcal{R}_N(n) && \text{(Window operation)} \end{aligned} \quad (5.23)$$

The `rem(n,N)` function in MATLAB determines the remainder after dividing  $n$  by  $N$ . This function can be used to implement our modulo- $N$

operation when  $n \geq 0$ . When  $n < 0$ , we need to modify the result to obtain correct values. This is shown below in the `m=mod(n,N)` function.

```
function m = mod(n,N)
% Computes m = (n mod N) index
%
% m = mod(n,N)
m = rem(n,N); m = m+N; m = rem(m,N);
```

In this function, `n` can be any integer array, and the array `m` contains the corresponding modulo- $N$  values.

From the frequency sampling theorem, we conclude that  $N$  equispaced samples of the discrete-time Fourier transform  $X(e^{j\omega})$  of the  $N$ -point sequence  $x(n)$  can uniquely reconstruct  $X(e^{j\omega})$ . These  $N$  samples around the unit circle are called the discrete Fourier transform coefficients. Let  $\tilde{X}(k) = \text{DFS } \tilde{x}(n)$ , which is a periodic sequence (and hence of infinite duration). Its primary interval then is the discrete Fourier transform, which is of finite duration. These notions are made clear in the following definitions. The discrete Fourier transform of an  $N$ -point sequence is given by

$$X(k) \triangleq \text{DFT}[x(n)] = \begin{cases} \tilde{X}(k), & 0 \leq k \leq N-1 \\ 0, & \text{elsewhere} \end{cases} = \tilde{X}(k)\mathcal{R}_N(k)$$

or

$$X(k) = \sum_{n=0}^{N-1} x(n)W_N^{nk}, \quad 0 \leq k \leq N-1 \quad (5.24)$$

Note that the DFT  $X(k)$  is also an  $N$ -point sequence; that is, it is not defined outside of  $0 \leq k \leq N-1$ . From (5.23),  $\tilde{X}(k) = X((k))_N$ ; that is, outside the  $0 \leq k \leq N-1$  interval only the DFS  $\tilde{X}(k)$  is defined, which of course is the periodic extension of  $X(k)$ . Finally,  $X(k) = \tilde{X}(k)\mathcal{R}_N(k)$  means that the DFT  $X(k)$  is the primary interval of  $\tilde{X}(k)$ .

The inverse discrete Fourier transform of an  $N$ -point DFT  $X(k)$  is given by

$$x(n) \triangleq \text{IDFT}[X(k)] = \tilde{x}(n)\mathcal{R}_N(n)$$

or

$$x(n) = \frac{1}{N} \sum_{k=0}^{N-1} X(k)W_N^{-kn}, \quad 0 \leq n \leq N-1 \quad (5.25)$$

Once again,  $x(n)$  is not defined outside  $0 \leq n \leq N-1$ . The extension of  $x(n)$  outside this range is  $\tilde{x}(n)$ .

### 5.3.1 MATLAB IMPLEMENTATION

It is clear from the discussions at the top of this section that the DFS is practically equivalent to the DFT when  $0 \leq n \leq N - 1$ . Therefore, the implementation of the DFT can be done in a similar fashion. If  $x(n)$  and  $X(k)$  are arranged as column vectors  $\mathbf{x}$  and  $\mathbf{X}$ , respectively, then from (5.24) and (5.25) we have

$$\begin{aligned}\mathbf{X} &= \mathbf{W}_N \mathbf{x} \\ \mathbf{x} &= \frac{1}{N} \mathbf{W}_N^* \mathbf{X}\end{aligned}\tag{5.26}$$

where  $\mathbf{W}_N$  is the matrix defined in (5.7) and will now be called a *DFT matrix*. Hence the earlier `dfs` and `idfs` MATLAB functions can be renamed as the `dft` and `idft` functions to implement the discrete Fourier transform computations.

```
function [Xk] = dft(xn,N)
% Computes discrete Fourier transform
%
% [Xk] = dft(xn,N)
% Xk = DFT coeff. array over 0 <= k <= N-1
% xn = N-point finite-duration sequence
% N = Length of DFT
%
n = [0:1:N-1]; % Row vector for n
k = [0:1:N-1]; % Row vector for k
WN = exp(-j*2*pi/N); % Wn factor
nk = n'*k; % Creates an N by N matrix of nk values
WNnk = WN .^ nk; % DFT matrix
Xk = xn * WNnk; % Row vector for DFT coefficients

function [xn] = idft(Xk,N)
% Computes inverse discrete transform
%
% [xn] = idft(Xk,N)
% xn = N-point sequence over 0 <= n <= N-1
% Xk = DFT coeff. array over 0 <= k <= N-1
% N = length of DFT
%
n = [0:1:N-1]; % Row vector for n
k = [0:1:N-1]; % Row vector for k
WN = exp(-j*2*pi/N); % Wn factor
nk = n'*k; % Creates an N by N matrix of nk values
WNnk = WN .^ (-nk); % IDFT matrix
xn = (Xk * WNnk)/N; % Row vector for IDFT values
```

- EXAMPLE 5.6** Let  $x(n)$  be a four-point sequence:

$$x(n) = \begin{cases} 1, & 0 \leq n \leq 3 \\ 0, & \text{otherwise} \end{cases}$$

- a. Compute the discrete-time Fourier transform  $X(e^{j\omega})$  and plot its magnitude and phase.
- b. Compute the four-point DFT of  $x(n)$ .

**Solution**

- a. The discrete-time Fourier transform is given by

$$\begin{aligned} X(e^{j\omega}) &= \sum_0^3 x(n)e^{-j\omega n} = 1 + e^{-j\omega} + e^{-j2\omega} + e^{-j3\omega} \\ &= \frac{1 - e^{-j4\omega}}{1 - e^{-j\omega}} = \frac{\sin(2\omega)}{\sin(\omega/2)} e^{-j3\omega/2} \end{aligned}$$

Hence

$$|X(e^{j\omega})| = \left| \frac{\sin(2\omega)}{\sin(\omega/2)} \right|$$

and

$$\angle X(e^{j\omega}) = \begin{cases} -\frac{3\omega}{2}, & \text{when } \frac{\sin(2\omega)}{\sin(\omega/2)} > 0 \\ -\frac{3\omega}{2} \pm \pi, & \text{when } \frac{\sin(2\omega)}{\sin(\omega/2)} < 0 \end{cases}$$

The plots are shown in Figure 5.4.

- b. Let us denote the four-point DFT by  $X_4(k)$ . Then

$$X_4(k) = \sum_{n=0}^3 x(n)W_4^{nk}; \quad k = 0, 1, 2, 3; \quad W_4 = e^{-j2\pi/4} = -j$$

These calculations are similar to those in Example 5.1. We can also use MATLAB to compute this DFT.

```
>> x = [1,1,1,1]; N = 4; X = dft(x,N);
>> magX = abs(X), phaX = angle(X)*180/pi
magX =
    4.0000    0.0000    0.0000    0.0000
phaX =
    0  -134.9810  -90.0000  -44.9979
```

Hence

$$X_4(k) = \{4, 0, 0, 0\}$$

Note that when the magnitude sample is zero, the corresponding angle is not zero. This is due to a particular algorithm used by MATLAB to compute the

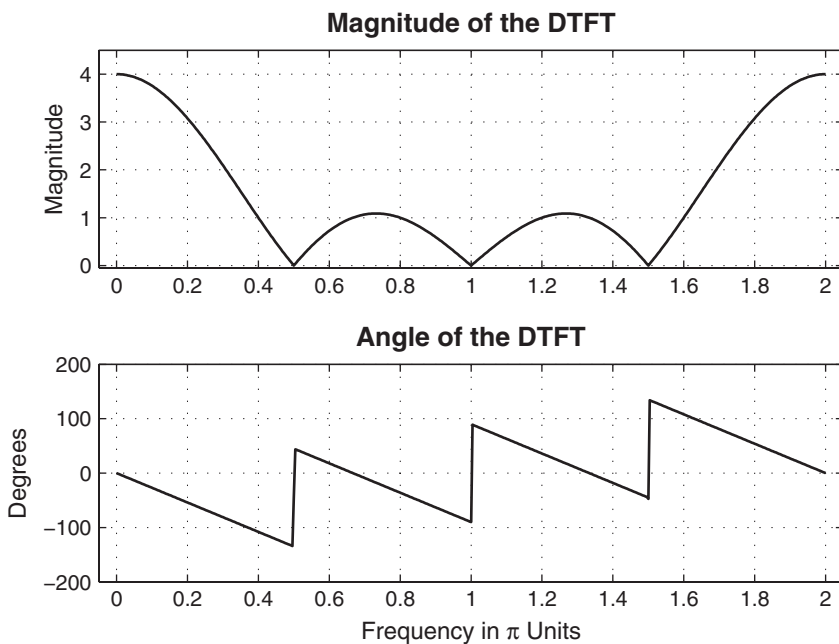


**FIGURE 5.4** The DTFT plots in Example 5.6

angle part. Generally, these angles should be ignored. The plot of DFT values is shown in Figure 5.5. The plot of  $X(e^{j\omega})$  is also shown as a dashed line for comparison. From the plot in Figure 5.5, we observe that  $X_4$  correctly gives four samples of  $X(e^{j\omega})$ , but it has only one nonzero sample. Is this surprising? By looking at the four-point  $x(n)$ , which contains all 1's, one must conclude that its periodic extension is

$$\tilde{x}(n) = 1, \forall n$$

which is a constant (or a DC) signal. This is what is predicted by the DFT  $X_4(k)$ , which has a nonzero sample at  $k = 0$  (or  $\omega = 0$ ) and has no values at other frequencies.  $\square$

- **EXAMPLE 5.7** How can we obtain other samples of the DTFT  $X(e^{j\omega})$ ?

**Solution**

It is clear that we should sample at dense (or finer) frequencies; that is, we should increase  $N$ . Suppose we take twice the number of points, or  $N = 8$  instead of  $N = 4$ . This we can achieve by treating  $x(n)$  as an eight-point sequence by appending four zeros.

$$x(n) = \{1, 1, 1, 1, 0, 0, 0, 0\}$$

↑

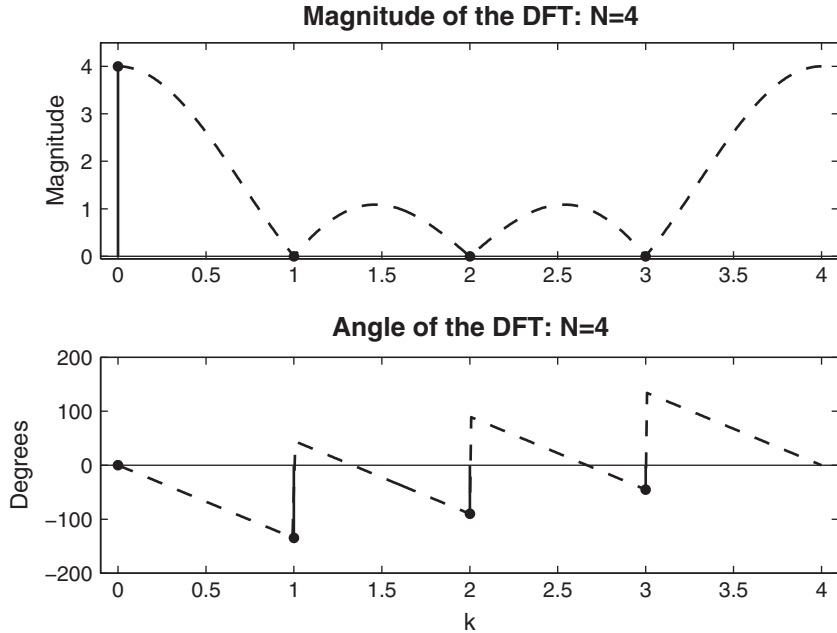


**FIGURE 5.5** The DFT plots of Example 5.6

This is a very important operation called a *zero-padding operation*. This operation is necessary in practice to obtain a *dense spectrum* of signals, as we shall see. Let  $X_8(k)$  be an eight-point DFT, then

$$X_8(k) = \sum_{n=0}^7 x(n)W_8^{nk}; \quad k = 0, 1, \dots, 7; \quad W_8 = e^{-j\pi/4}$$

In this case, the frequency resolution is  $\omega_1 = 2\pi/8 = \pi/4$ .

MATLAB script:

```
>> x = [1,1,1,1, zeros(1,4)]; N = 8; X = dft(x,N);
>> magX = abs(X), phaX = angle(X)*180/pi
magX =
    4.0000    2.6131    0.0000    1.0824    0.0000    1.0824    0.0000    2.6131
phaX =
     0   -67.5000  -134.9810   -22.5000   -90.0000   22.5000   -44.9979   67.5000
```

Hence

$$X_8(k) = \{4, 2.6131e^{-j67.5^\circ}, 0, 1.0824e^{-j22.5^\circ}, 0, 1.0824e^{j22.5^\circ}, \\ \uparrow \\ 0, 2.6131e^{j67.5^\circ}\}$$

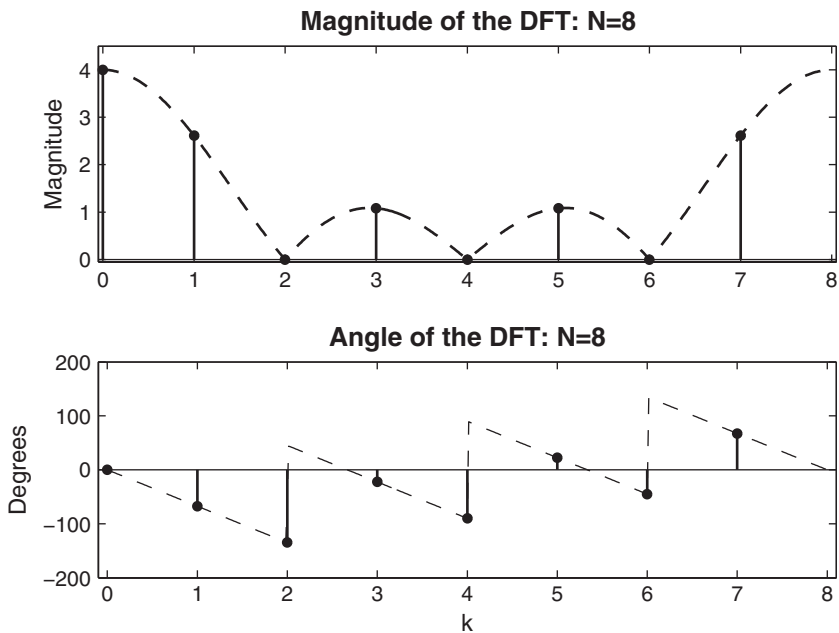


**FIGURE 5.6** The DFT plots of Example 5.7:  $N = 8$

which is shown in Figure 5.6. Continuing further, if we treat  $x(n)$  as a 16-point sequence by padding 12 zeros, such that

$$x(n) = \{1, 1, 1, 1, 0, \underset{\uparrow}{0}, 0, 0, 0, 0, 0, 0, 0, 0, 0, 0\}$$

then the frequency resolution is  $\omega_1 = 2\pi/16 = \pi/8$  and  $W_{16} = e^{-j\pi/8}$ . Therefore, we get a more dense spectrum with spectral samples separated by  $\pi/8$ . The sketch of  $X_{16}(k)$  is shown in Figure 5.7.

It should be clear then that if we obtain many more spectral samples by choosing a large  $N$  value, then the resulting DFT samples will be very close to each other and we will obtain plot values similar to those in Figure 5.4. However, the displayed stem-plots will be dense. In this situation, a better approach to display samples is to either show them using dots or join the sample values using the `plot` command (i.e., using the FOH studied in Chapter 3). Figure 5.8 shows the magnitude and phase of the 128-point DFT  $x_{128}(k)$  obtained by padding 120 zeros. The DFT magnitude plot overlaps the DTFT magnitude plot shown as dotted-line, while the phase plot shows discrepancy at discontinuities due to finite  $N$  value, which should be expected.  $\square$

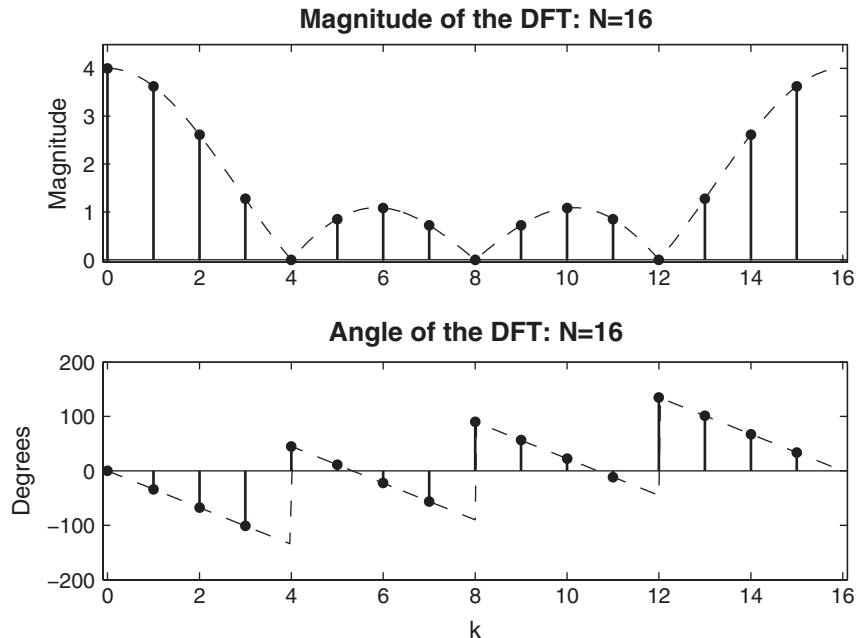


**FIGURE 5.7** The DFT plots of Example 5.7:  $N = 16$

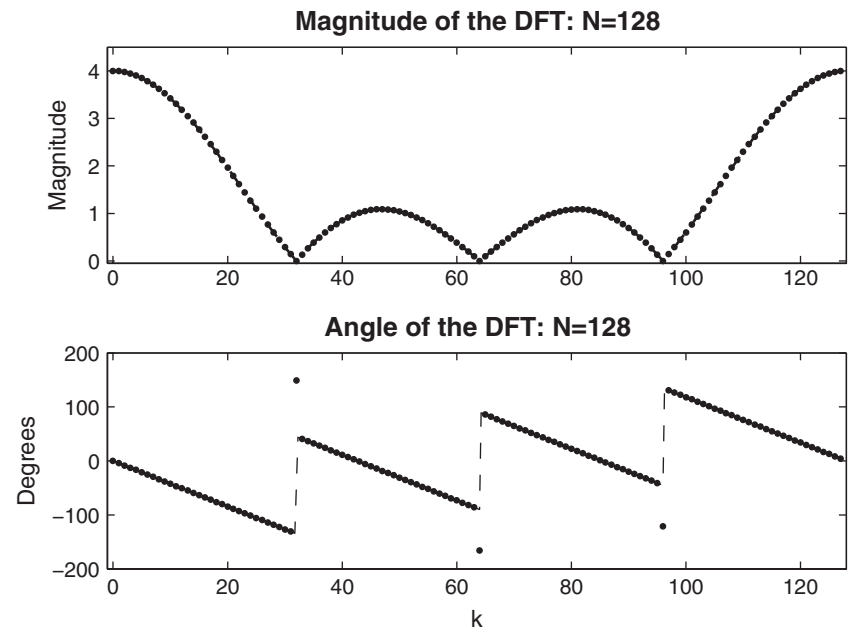


**FIGURE 5.8** The DFT plots of Example 5.7 for  $N = 128$  are shown as line plots

*Comments:* Based on the last two examples, there are several comments that we can make.

1. Zero-padding is an operation in which more zeros are appended to the original sequence. The resulting longer DFT provides closely spaced samples of the discrete-time Fourier transform of the original sequence. In MATLAB, zero-padding is implemented using the `zeros` function.
2. In Example 5.6, all we needed to accurately plot the discrete-time Fourier transform  $X(e^{j\omega})$  of  $x(n)$  was  $X_4(k)$ , the four-point DFT. This is because  $x(n)$  had only four nonzero samples, so we could have used the interpolation formula (5.19) on  $X_4(k)$  to obtain  $X(e^{j\omega})$ . However, in practice, it is easier to obtain  $X_8(k)$  and  $X_{16}(k)$ , and so on, to *fill in* the values of  $X(e^{j\omega})$  rather than using the interpolation formula. This approach can be made even more efficient using fast Fourier transform algorithms to compute the DFT.
3. The zero-padding gives us a *high-density spectrum* and provides a better displayed version for plotting. But it does not give us a *high-resolution spectrum*, because no new information is added to the signal; only additional zeros are added in the data.
4. To get a high-resolution spectrum, one has to obtain more data from the experiment or observations (see Example 5.8, below). There are also other advanced methods that use additional side information or nonlinear techniques.

- **EXAMPLE 5.8** To illustrate the difference between the high-density spectrum and the high-resolution spectrum, consider the sequence

$$x(n) = \cos(0.48\pi n) + \cos(0.52\pi n)$$

We want to determine its spectrum based on the finite number of samples.

- a. Determine and plot the discrete-time Fourier transform of  $x(n)$ ,  $0 \leq n \leq 10$ .
- b. Determine and plot the discrete-time Fourier transform of  $x(n)$ ,  $0 \leq n \leq 100$ .

### Solution

We could determine analytically the discrete-time Fourier transform in each case, but MATLAB is a good vehicle to study these problems.

- a. We can first determine the 10-point DFT of  $x(n)$  to obtain an estimate of its discrete-time Fourier transform.  
MATLAB script:

```
>> n = [0:1:99]; x = cos(0.48*pi*n)+cos(0.52*pi*n);
>> n1 = [0:1:9] ;y1 = x(1:1:10);
>> subplot(2,1,1) ;stem(n1,y1); title('signal x(n), 0 <= n <= 9'); xlabel('n')
```

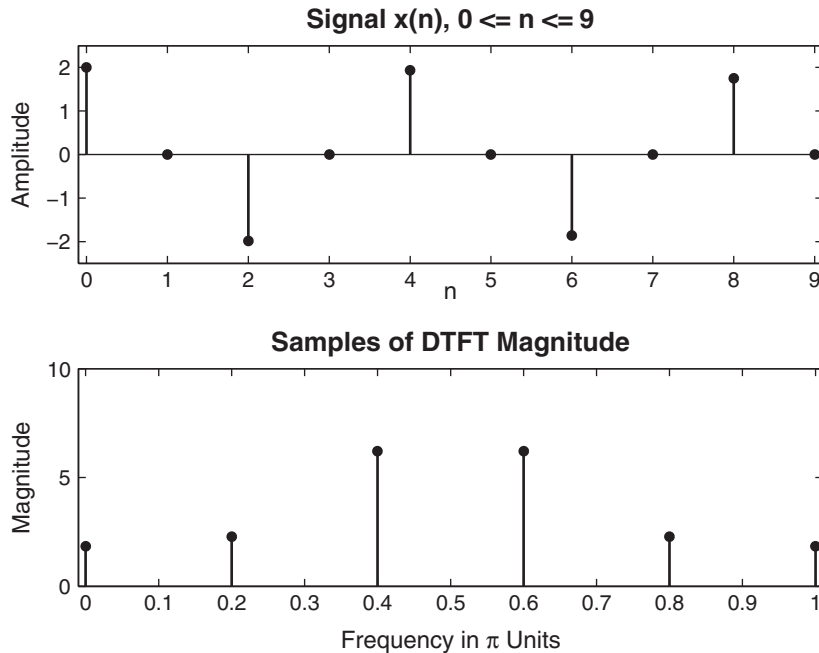


**FIGURE 5.9** Signal and its spectrum in Example 5.8a:  $N = 10$

```
>> Y1 = dft(y1,10); magY1 = abs(Y1(1:1:6));
>> k1 = 0:1:5 ;w1 = 2*pi/10*k1;
>> subplot(2,1,2);stem(w1/pi,magY1);title('Samples of DTFT Magnitude');
>> xlabel('Frequency in \pi Units')
```

The plots in Figure 5.9 show there aren't enough samples to draw any conclusions. Therefore, we will pad 90 zeros to obtain a dense spectrum. As explained in Example 5.7, this spectrum is plotted using the `plot` command.

MATLAB script:

```
>> n2 = [0:1:99]; y2 = [x(1:1:10) zeros(1,90)];
>> subplot(2,1,1) ;stem(n2,y2) ;title('signal x(n), 0 <= n <= 9 + 90 zeros');
>> xlabel('n')
>> Y2 =dft(y2,100); magY2 = abs(Y2(1:1:51));
>> k2 = 0:1:50; w2 = 2*pi/100*k2;
>> subplot(2,1,2); plot(w2/pi,magY2); title('DTFT Magnitude');
>> xlabel('Frequency in \pi Units')
```

Now the plot shows that the sequence has a dominant frequency at  $\omega = 0.5\pi$  (Figure 5.10). This fact is not supported by the original sequence, which has two

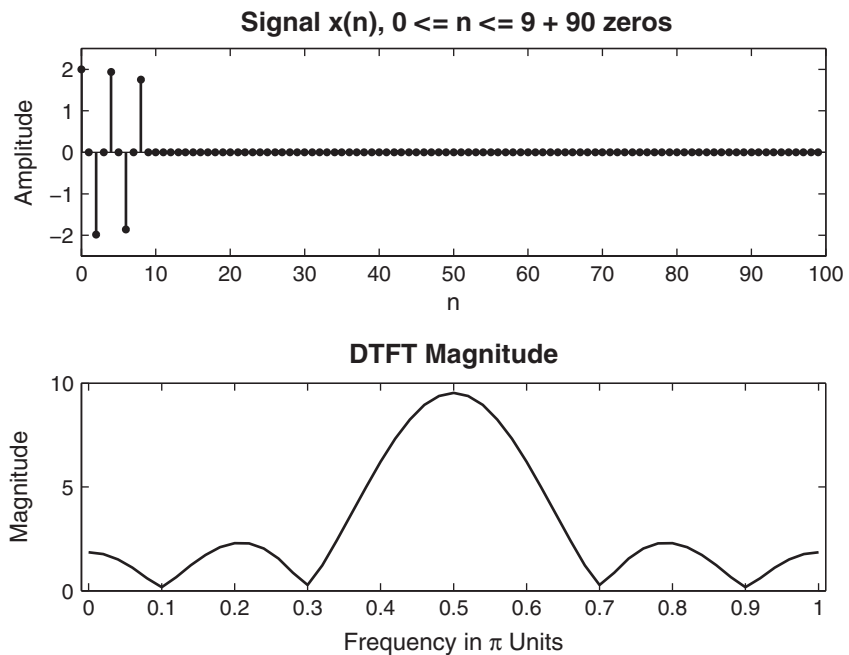


**FIGURE 5.10** Signal and its spectrum in Example 5.8a:  $N = 100$

frequencies. The zero-padding provided a smoother version of the spectrum in Figure 5.9.

- b. To get better spectral information, we will take the first 100 samples of  $x(n)$  and determine its discrete-time Fourier transform.

MATLAB script:

```
>> subplot(2,1,1); stem(n,x);
>> title('signal x(n), 0 <= n <= 99'); xlabel('n')
>> X = dft(x,100); magX = abs(X(1:1:51));
>> k = 0:1:50; w = 2*pi/100*k;
>> subplot(2,1,2); plot(w/pi,magX); title('DTFT Magnitude');
>> xlabel('Frequency in \pi Units')
```

Now the discrete-time Fourier transform plot clearly shows two frequencies, which are very close to each other (Figure 5.11). This is the high-resolution spectrum of  $x(n)$ . Note that padding more zeros to the 100-point sequence will result in a smoother rendition of the spectrum in Figure 5.11 but will not reveal any new information. Readers are encouraged to verify this.  $\square$

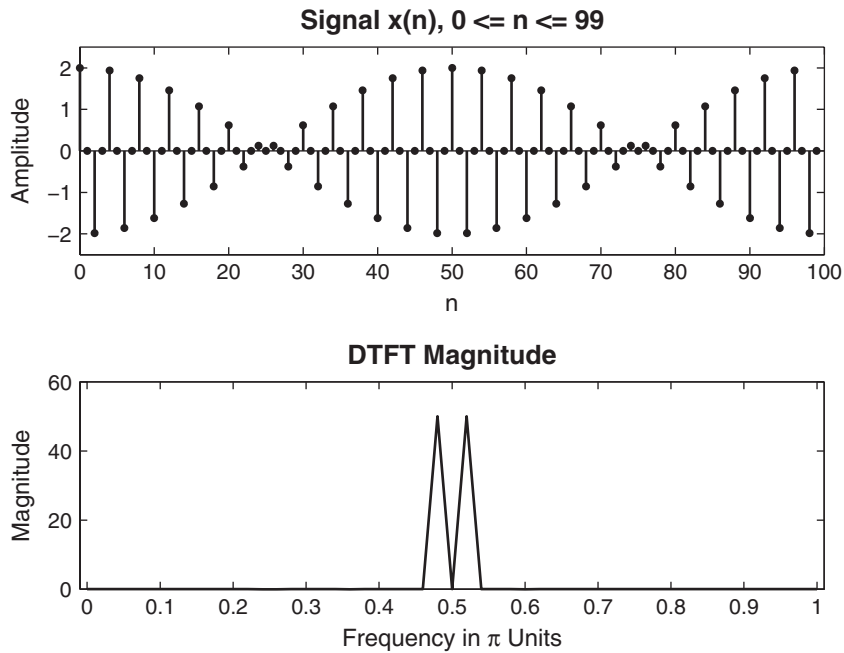


**FIGURE 5.11** Signal and its spectrum in Example 5.8b:  $N = 100$

## 5.4 PROPERTIES OF THE DISCRETE FOURIER TRANSFORM

The DFT properties are derived from those of the DFS because mathematically DFS is the valid representation. We discuss several useful properties, which are given without proof. These properties also apply to the DFS with necessary changes. Let  $X(k)$  be an  $N$ -point DFT of the sequence  $x(n)$ . Unless otherwise stated, the  $N$ -point DFTs will be used in these properties.

1. **Linearity:** The DFT is a linear transform

$$\text{DFT}[ax_1(n) + bx_2(n)] = a \text{DFT}[x_1(n)] + b \text{DFT}[x_2(n)] \quad (5.27)$$

*Note:* If  $x_1(n)$  and  $x_2(n)$  have different durations—that is, they are  $N_1$ -point and  $N_2$ -point sequences, respectively—then choose  $N_3 = \max(N_1, N_2)$  and proceed by taking  $N_3$ -point DFTs.

2. **Circular folding:** If an  $N$ -point sequence is folded, then the result  $x(-n)$  would not be an  $N$ -point sequence, and it would not be possible

to compute its DFT. Therefore, we use the modulo- $N$  operation on the argument  $(-n)$  and define folding by

$$x((-n))_N = \begin{cases} x(0), & n = 0 \\ x(N - n), & 1 \leq n \leq N - 1 \end{cases} \quad (5.28)$$

This is called a *circular folding*. To visualize it, imagine that the sequence  $x(n)$  is wrapped around a circle in the counterclockwise direction so that indices  $n = 0$  and  $n = N$  overlap. Then  $x((-n))_N$  can be viewed as a clockwise wrapping of  $x(n)$  around the circle; hence the name circular folding. In MATLAB, the circular folding can be achieved by  $x=x(\text{mod}(-n,N)+1)$ . Note that the arguments in MATLAB begin with 1. The DFT of a circular folding is given by

$$\text{DFT}[x((-n))_N] = X((-k))_N = \begin{cases} X(0), & k = 0 \\ X(N - k), & 1 \leq k \leq N - 1 \end{cases} \quad (5.29)$$

□ **EXAMPLE 5.9** Let  $x(n) = 10(0.8)^n$ ,  $0 \leq n \leq 10$ .

- Determine and plot  $x((-n))_{11}$ .
- Verify the circular folding property.

#### Solution

- MATLAB script:

```
>> n = 0:10; x = 10*(0.8).^n; y = x(mod(-n,11)+1);
>> subplot(2,1,1); stem(n,x); title('Original Sequence')
>> xlabel('n'); ylabel('Amplitude');
>> subplot(2,1,2); stem(n,y);
>> title('Circularly Folded Sequence x((-n))_{11}');
>> xlabel('n'); ylabel('Amplitude');
```

The plots in Figure 5.12 show the effect of circular folding.

- MATLAB script:

```
>> X = dft(x,11); Y = dft(y,11);
>> subplot(2,2,1); stem(n,real(X));
>> title('Real(DFT[x(n)])'); xlabel('k');
>> subplot(2,2,2); stem(n,imag(X));
>> title('Imag(DFT[x(n)])'); xlabel('k');
>> subplot(2,2,3); stem(n,real(Y));
>> title('Real(DFT[x((-n))_{11}])'); xlabel('k');
>> subplot(2,2,4); stem(n,imag(Y));
>> title('Imag(DFT[x((-n))_{11}])'); xlabel('k');
```

The plots in Figure 5.13 verify the property. □

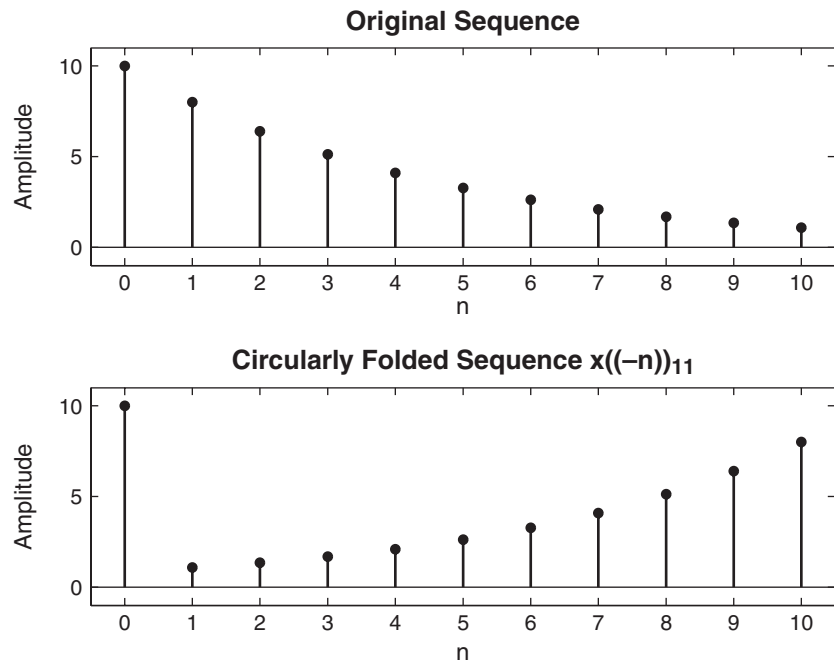


FIGURE 5.12 Circular folding in Example 5.9a

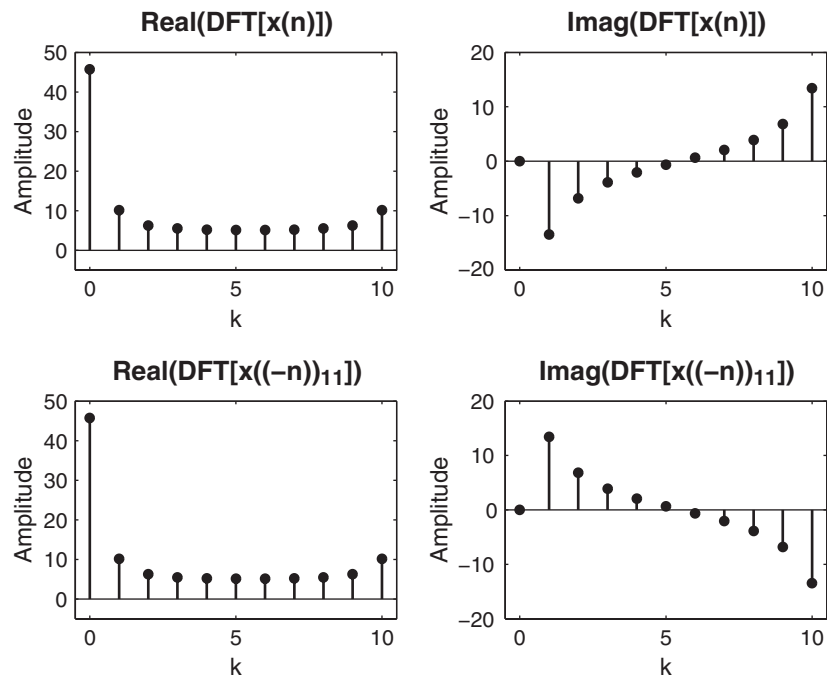


FIGURE 5.13 Circular folding property in Example 5.9b

3. **Conjugation:** Similar to the above property, we have to introduce the circular folding in the frequency domain:

$$\text{DFT}[x^*(n)] = X^*((-k))_N \quad (5.30)$$

4. **Symmetry properties for real sequences:** Let  $x(n)$  be a real-valued  $N$ -point sequence. Then  $x(n) = x^*(n)$ . Using (5.30),

$$X(k) = X^*((-k))_N \quad (5.31)$$

This symmetry is called a *circular conjugate symmetry*. It further implies that

$$\begin{aligned} \text{Re}[X(k)] &= \text{Re}[X((-k))_N] &&\Rightarrow \text{Circular-even sequence} \\ \text{Im}[X(k)] &= -\text{Im}[X((N-k))_N] &&\Rightarrow \text{Circular-odd sequence} \\ |X(k)| &= |X((-k))_N| &&\Rightarrow \text{Circular-even sequence} \\ \angle X(k) &= -\angle X((-k))_N &&\Rightarrow \text{Circular-odd sequence} \end{aligned} \quad (5.32)$$

*Comments:*

- Observe the magnitudes and angles of the various DFTs in Examples 5.6 and 5.7. They do satisfy the above circular symmetries. These symmetries are different than the usual even and odd symmetries. To visualize this, imagine that the DFT samples are arranged around a circle so that the indices  $k = 0$  and  $k = N$  overlap; then the samples will be symmetric with respect to  $k = 0$ , which justifies the name circular symmetry.
- The corresponding symmetry for the DFS coefficients is called the *periodic conjugate symmetry*.
- Since these DFTs have symmetry, one needs to compute  $X(k)$  only for

$$k = 0, 1, \dots, \frac{N}{2}; \quad N \text{ even}$$

or for

$$k = 0, 1, \dots, \frac{N-1}{2}; \quad N \text{ odd}$$

This results in about 50 percent savings in computation as well as in storage.

- From (5.30)

$$X(0) = X^*((-0))_N = X^*(0)$$

which means that the DFT coefficient at  $k = 0$  must be a real number. But  $k = 0$  means that the frequency  $\omega_k = k\omega_1 = 0$ , which is the DC frequency. Hence the DC coefficient for a real-valued  $x(n)$  must be a

real number. In addition, if  $N$  is even, then  $N/2$  is also an integer. Then from (5.32),

$$X(N/2) = X^*((-N/2))_N = X^*(N/2)$$

which means that even the  $k = N/2$  component is also real-valued. This component is called the *Nyquist component* since  $k = N/2$  means that the frequency  $\omega_{N/2} = (N/2)(2\pi/N) = \pi$ , which is the digital Nyquist frequency.

The real-valued signals can also be decomposed into their even and odd components,  $x_e(n)$  and  $x_o(n)$ , respectively, as discussed in Chapter 2. However, these components are not  $N$ -point sequences, and therefore we cannot take their  $N$ -point DFTs. Hence we define a new set of components using the circular folding discussed above. These are called *circular-even* and *circular-odd* components defined by

$$\begin{aligned} x_{ec}(n) &\triangleq \frac{1}{2}[x(n) + x((-n))_N] = \begin{cases} x(0), & n = 0 \\ \frac{1}{2}[x(n) + x(N-n)], & 1 \leq n \leq N-1 \end{cases} \\ x_{oc}(n) &\triangleq \frac{1}{2}[x(n) - x((-n))_N] = \begin{cases} 0, & n = 0 \\ \frac{1}{2}[x(n) - x(N-n)], & 1 \leq n \leq N-1 \end{cases} \end{aligned} \quad (5.33)$$

Then

$$\begin{aligned} \text{DFT}[x_{ec}(n)] &= \text{Re}[X(k)] = \text{Re}[X((-k))_N] \\ \text{DFT}[x_{oc}(n)] &= \text{Im}[X(k)] = \text{Im}[X((-k))_N] \end{aligned} \quad (5.34)$$

*Implication:* If  $x(n)$  is real and circular-even, then its DFT is also real and circular-even. Hence only the first  $0 \leq n \leq N/2$  coefficients are necessary for complete representation.

Using (5.33), it is easy to develop a function to decompose an  $N$ -point sequence into its circular-even and circular-odd components. The following `circevod` function uses the `mod` function given earlier to implement the modulo- $N$  operation.

```
function [xec, xoc] = circevod(x)
% Signal decomposition into circular-even and circular-odd parts
%
% [xec, xoc] = circevod(x)
%
if any(imag(x) ~= 0)
    error('x is not a real sequence')
```

```

end
N = length(x); n = 0:(N-1);
xec = 0.5*(x + x(mod(-n,N)+1)); xoc = 0.5*(x - x(mod(-n,N)+1));

```

- **EXAMPLE 5.10** Let  $x(n) = 10(0.8)^n$ ,  $0 \leq n \leq 10$  as in Example 5.9.

- Decompose and plot the  $x_{ec}(n)$  and  $x_{oc}(n)$  components of  $x(n)$ .
- Verify the property in (5.34).

**Solution**

- MATLAB script:

```

>> n = 0:10; x = 10*(0.8) .^ n;
>> [xec,xoc] = circevod(x);
>> subplot(2,1,1); stem(n,xec); title('Circular-Even Component')
>> xlabel('n'); ylabel('Amplitude'); axis([-0.5,10.5,-1,11])
>> subplot(2,1,2); stem(n,xoc); title('Circular-Odd Component')
>> xlabel('n'); ylabel('Amplitude'); axis([-0.5,10.5,-4,4])

```

The plots in Figure 5.14 show the circularly symmetric components of  $x(n)$ .

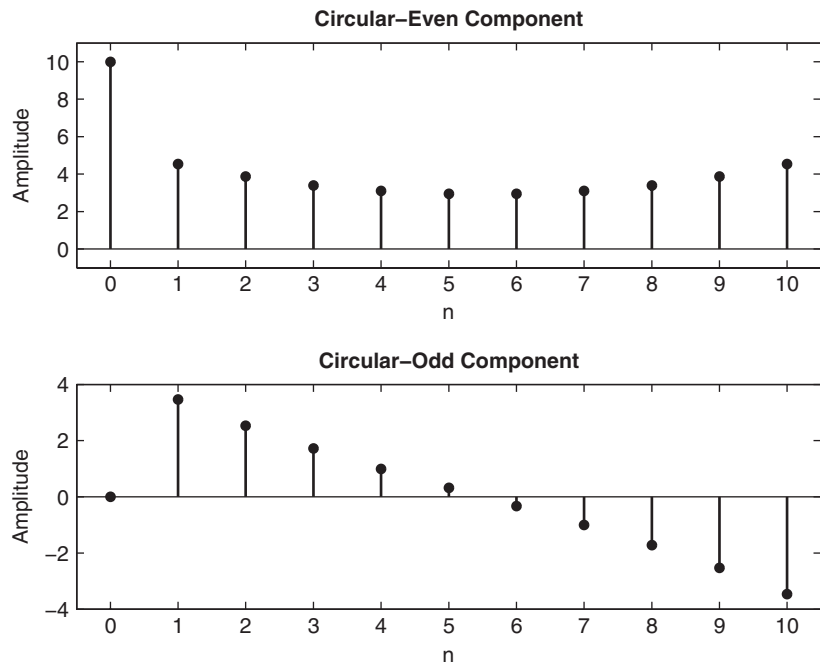


**FIGURE 5.14** Circular-even and circular-odd components of the sequence in Example 5.10a

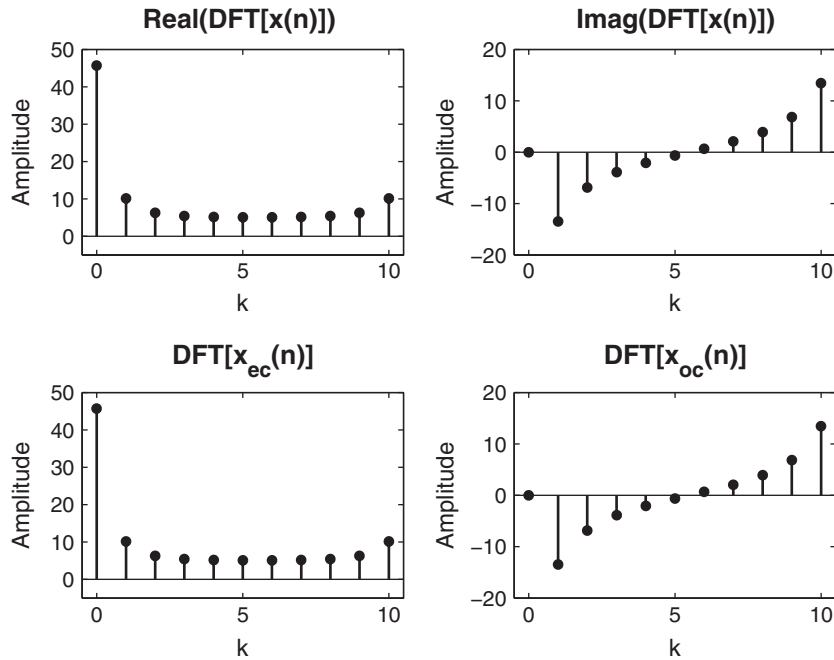


**FIGURE 5.15** Plots of DFT symmetry properties in Example 5.10b

b. MATLAB script:

```
>> X = dft(x,11); Xec = dft(xec,11); Xoc = dft(xoc,11);
>> subplot(2,2,1); stem(n,real(X)); axis([-0.5,10.5,-5,50])
>> title('Real(DFT[x(n)])'); xlabel('k');
>> subplot(2,2,2); stem(n,imag(X)); axis([-0.5,10.5,-20,20])
>> title('Imag(DFT[x(n)])'); xlabel('k');
>> subplot(2,2,3); stem(n,real(Xec)); axis([-0.5,10.5,-5,50])
>> title('DFT[xec(n)]'); xlabel('k');
>> subplot(2,2,4); stem(n,imag(Xoc)); axis([-0.5,10.5,-20,20])
>> title('DFT[xoc(n)]'); xlabel('k');
```

From the plots in Figure 5.15, we observe that the DFT of  $x_{ec}(n)$  is the same as the real part of  $X(k)$  and that the DFT of  $x_{oc}(n)$  is the same as the imaginary part of  $X(k)$ .  $\square$

A similar property for complex-valued sequences is explored in Problem P5.18.

5. **Circular shift of a sequence:** If an  $N$ -point sequence is shifted in either direction, then the result is no longer between  $0 \leq n \leq N - 1$ .

Therefore, we first convert  $x(n)$  into its periodic extension  $\tilde{x}(n)$ , and then shift it by  $m$  samples to obtain

$$\tilde{x}(n - m) = x((n - m))_N \quad (5.35)$$

This is called a *periodic shift* of  $\tilde{x}(n)$ . The periodic shift is then converted into an  $N$ -point sequence. The resulting sequence

$$\tilde{x}(n - m)\mathcal{R}_N(n) = x((n - m))_N \mathcal{R}_N(n) \quad (5.36)$$

is called the *circular shift* of  $x(n)$ . Once again, to visualize this, imagine that the sequence  $x(n)$  is wrapped around a circle. Now rotate the circle by  $k$  samples and unwrap the sequence from  $0 \leq n \leq N - 1$ . Its DFT is given by

$$\text{DFT}[x((n - m))_N \mathcal{R}_N(n)] = W_N^{km} X(k) \quad (5.37)$$

□ **EXAMPLE 5.11** Let  $x(n) = 10(0.8)^n$ ,  $0 \leq n \leq 10$  be an 11-point sequence.

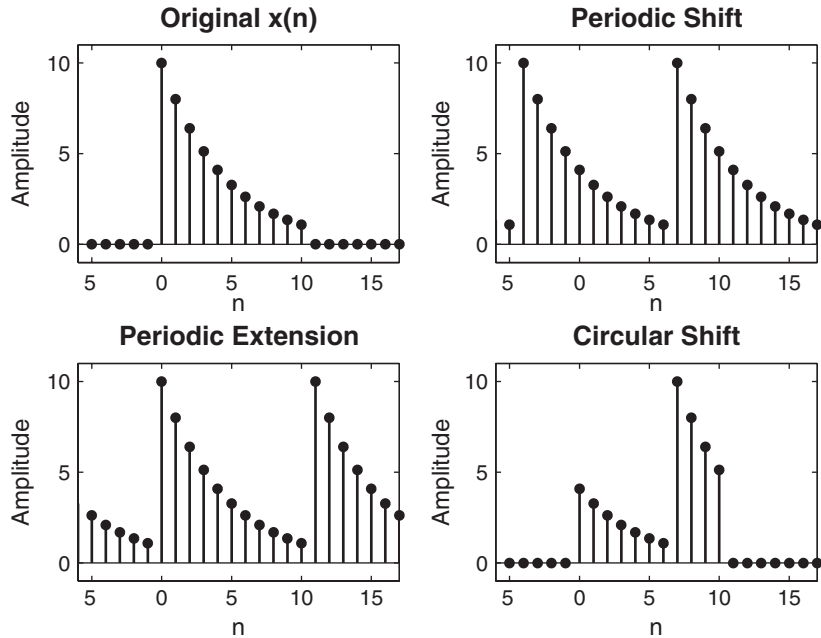
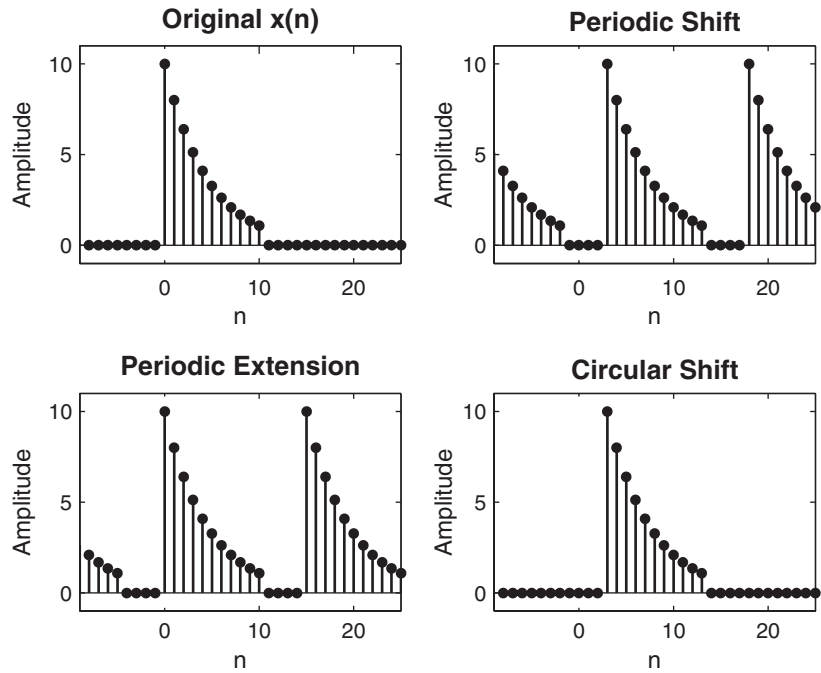
- a. Sketch  $x((n + 4))_{11} R_{11}(n)$ , that is, a circular shift by four samples toward the left.
- b. Sketch  $x((n - 3))_{15} R_{15}(n)$ , that is, a circular shift by three samples toward the right, where  $x(n)$  is assumed to be a 15-point sequence.

### Solution

We will use a step-by-step graphical approach to illustrate the circular shifting operation. This approach shows the periodic extension  $\tilde{x}(n) = x((n))_N$  of  $x(n)$ , followed by a linear shift in  $\tilde{x}(n)$  to obtain  $\tilde{x}(n - m) = x((n - m))_N$ , and finally truncating  $\tilde{x}(n - m)$  to obtain the circular shift.

- a. Figure 5.16 shows four sequences. The top-left shows  $x(n)$ , the bottom-left shows  $\tilde{x}(n)$ , the top-right shows  $\tilde{x}(n + 4)$ , and, finally, the bottom-right shows  $x((n + 4))_{11} R_{11}(n)$ . Note carefully that as samples move out of the  $[0, N - 1]$  window in one direction, they reappear from the opposite direction. This is the meaning of the circular shift, and it is different from the linear shift.
- b. In this case, the sequence  $x(n)$  is treated as a 15-point sequence by padding four zeros. Now the circular shift will be different than when  $N = 11$ . This is shown in Figure 5.17. In fact, the circular shift  $x((n - 3))_{15}$  looks like a linear shift  $x(n - 3)$ . □

To implement a circular shift, we do not have to go through the periodic shift as shown in Example 5.11. It can be implemented directly in two ways. In the first approach, the modulo- $N$  operation can be used on the argument  $(n - m)$  in the time domain. This is shown below in the `cirshftt` function.

**FIGURE 5.16** Graphical interpretation of circular shift,  $N = 11$ **FIGURE 5.17** Graphical interpretation of circular shift,  $N = 15$

```

function y = cirshftt(x,m,N)
% Circular shift of m samples wrt size N in sequence x: (time domain)
%
% [y] = cirshftt(x,m,N)
% y = output sequence containing the circular shift
% x = input sequence of length <= N
% m = sample shift
% N = size of circular buffer
% Method: y(n) = x((n-m) mod N)
% Check for length of x
if length(x) > N
    error('N must be >= the length of x')
end
x = [x zeros(1,N-length(x))];
n = [0:1:N-1]; n = mod(n-m,N); y = x(n+1);

```

In the second approach, the property (5.37) can be used in the frequency domain. This is explored in Problem P5.20.

- **EXAMPLE 5.12** Given an 11-point sequence  $x(n) = 10(0.8)^n$ ,  $0 \leq n \leq 10$ , determine and plot  $x((n - 6))_{15}$ .

**Solution**

MATLAB script:

```

>> n = 0:10; x = 10*(0.8) .^ n; y = cirshftt(x,6,15);
>> n = 0:14; x = [x, zeros(1,4)];
>> subplot(2,1,1); stem(n,x); title('Original Sequence x(n)')
>> xlabel('n'); ylabel('Amplitude');
>> subplot(2,1,2); stem(n,y);
>> title('Circularly Shifted Sequence x((n-6))_{15}')
>> xlabel('n'); ylabel('Amplitude');

```

The results are shown in Figure 5.18. □

6. **Circular shift in the frequency domain:** This property is a dual of the preceding property given by

$$\text{DFT} [W_N^{-\ell n} x(n)] = X((k - \ell))_N R_N(k) \quad (5.38)$$

7. **Circular convolution:** A linear convolution between two  $N$ -point sequences will result in a longer sequence. Once again, we have to restrict our interval to  $0 \leq n \leq N - 1$ . Therefore, instead of linear shift, we should consider the circular shift. A convolution operation

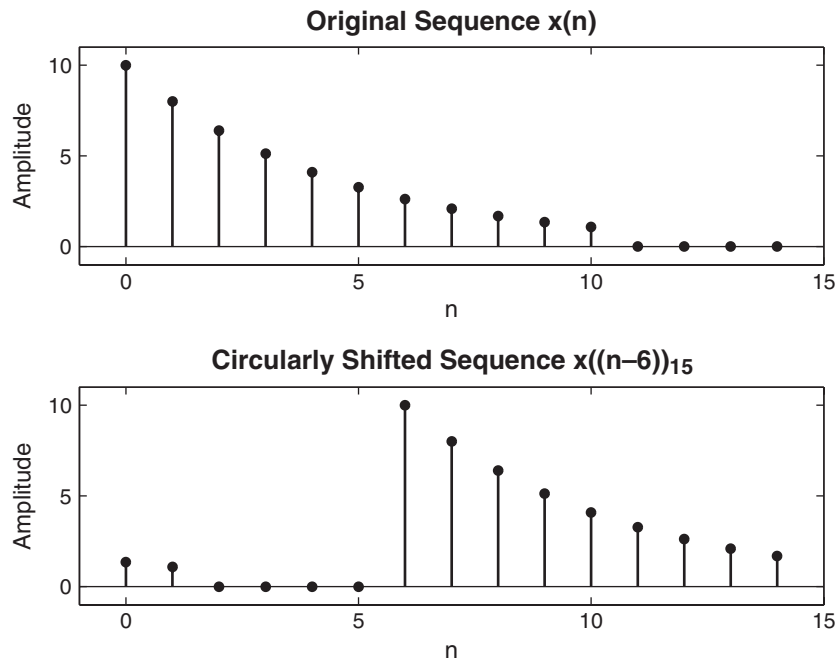


**FIGURE 5.18** Circularly shifted sequence in Example 5.12

that contains a circular shift is called the *circular convolution* and is given by

$$x_1(n) \textcircled{N} x_2(n) = \sum_{m=0}^{N-1} x_1(m)x_2((n-m))_N, \quad 0 \leq n \leq N-1 \quad (5.39)$$

Note that the circular convolution is also an  $N$ -point sequence. It has a structure similar to that of a linear convolution. The differences are in the summation limits and in the  $N$ -point circular shift. Hence it depends on  $N$  and is also called an  $N$ -point circular convolution. Therefore, the use of the notation  $\textcircled{N}$  is appropriate. The DFT property for the circular convolution is

$$\text{DFT} [x_1(n) \textcircled{N} x_2(n)] = X_1(k) \cdot X_2(k) \quad (5.40)$$

An alternate interpretation of this property is that when we multiply two  $N$ -point DFTs in the frequency domain, we get the circular convolution (and not the usual linear convolution) in the time domain.

- **EXAMPLE 5.13** Let  $x_1(n) = \{1, 2, 2\}$  and  $x_2(n) = \{1, 2, 3, 4\}$ . Compute the four-point circular convolution  $x_1(n) \textcircled{4} x_2(n)$ .

**Solution**

Note that  $x_1(n)$  is a three-point sequence, and hence we will have to pad one zero to make it a four-point sequence before we perform the circular convolution. We will compute this convolution in the time domain as well as in the frequency domain. In the time domain, we will use the mechanism of circular convolution; in the frequency domain, we will use the DFTs.

- *Time-domain approach:* The four-point circular convolution is given by

$$x_1(n) \textcircled{4} x_2(n) = \sum_{m=0}^3 x_1(m) x_2((n-m))_4$$

Thus we have to create a circularly folded and shifted sequence  $x_2((n-m))_N$  for each value of  $n$ , multiply it sample by sample with  $x_1(m)$ , add the samples to obtain the circular convolution value for that  $n$ , and then repeat the procedure for  $0 \leq n \leq 3$ . Consider

$$x_1(m) = \{1, 2, 2, 0\} \quad \text{and} \quad x_2(m) = \{1, 2, 3, 4\}$$

for  $n = 0$

$$\begin{aligned} \sum_{m=0}^3 x_1(m) \cdot x_2((0-m))_5 &= \sum_{m=0}^3 [\{1, 2, 2, 0\} \cdot \{1, 4, 3, 2\}] \\ &= \sum_{m=0}^3 \{1, 8, 6, 0\} = 15 \end{aligned}$$

for  $n = 1$

$$\begin{aligned} \sum_{m=0}^3 x_1(m) \cdot x_2((1-m))_5 &= \sum_{m=0}^3 [\{1, 2, 2, 0\} \cdot \{2, 1, 4, 3\}] \\ &= \sum_{m=0}^3 \{2, 2, 8, 0\} = 12 \end{aligned}$$

for  $n = 2$

$$\begin{aligned} \sum_{m=0}^3 x_1(m) \cdot x_2((2-m))_5 &= \sum_{m=0}^3 [\{1, 2, 2, 0\} \cdot \{3, 2, 1, 4\}] \\ &= \sum_{m=0}^3 \{3, 4, 2, 0\} = 9 \end{aligned}$$

for  $n = 3$

$$\begin{aligned} \sum_{m=0}^3 x_1(m) \cdot x_2((3-m))_5 &= \sum_{m=0}^3 [\{1, 2, 2, 0\} \cdot \{4, 3, 2, 1\}] \\ &= \sum_{m=0}^3 \{4, 6, 4, 0\} = 14 \end{aligned}$$

Hence

$$x_1(n) \circledast x_2(n) = \{15, 12, 9, 14\}$$

- *Frequency-domain approach:* In this approach, we first compute four-point DFTs of  $x_1(n)$  and  $x_2(n)$ , multiply them sample by sample, and then take the inverse DFT of the result to obtain the circular convolution.

DFT of  $x_1(n)$

$$x_1(n) = \{1, 2, 2, 0\} \implies X_1(k) = \{5, -1 - j2, 1, -1 + j2\}$$

DFT of  $x_2(n)$

$$x_2(n) = \{1, 2, 3, 4\} \implies X_2(k) = \{10, -2 + j2, -2, -2 - j2\}$$

Now

$$X_1(k) \cdot X_2(k) = \{50, 6 + j2, -2, 6 - j2\}$$

Finally, after IDFT,

$$x_1(n) \circledast x_2(n) = \{15, 12, 9, 14\}$$

which is the same as before.  $\square$

Similar to the circular shift implementation, we can implement the circular convolution in a number of different ways. The simplest approach would be to implement (5.39) literally by using the `cirshftt` function and requiring two nested `for...end` loops. Obviously, this is not efficient. Another approach is to generate a sequence  $x((n - m))_N$  for each  $n$  in  $[0, N - 1]$  as rows of a matrix and then implement (5.39) as a matrix-vector multiplication similar to our `dft` function. This would require one `for...end` loop. The following `circonvt` function incorporates these steps.

```
function y = circonvt(x1,x2,N)
% N-point circular convolution between x1 and x2: (time-domain)
%
% [y] = circonvt(x1,x2,N)
%   y = output sequence containing the circular convolution
%   x1 = input sequence of length N1 <= N
%   x2 = input sequence of length N2 <= N
%   N = size of circular buffer
%   Method: y(n) = sum (x1(m)*x2((n-m) mod N))
%   Check for length of x1
if length(x1) > N
    error('N must be >= the length of x1')
end
```

```
% Check for length of x2
if length(x2) > N
    error('N must be >= the length of x2')
end
x1=[x1 zeros(1,N-length(x1))];
x2=[x2 zeros(1,N-length(x2))];
m = [0:1:N-1]; x2 = x2(mod(-m,N)+1); H = zeros(N,N);
for n = 1:N
H(n,:) = cirshftt(x2,n-1,N);
end
y = x1*conj(H');
```

Problems P5.24 and P5.25 explore an approach to eliminate the `for...end` loop in the `circonvt` function. The third approach would be to implement the frequency-domain operation (5.40) using the `dft` function. This is explored in Problem P5.26.

- **EXAMPLE 5.14** Let us use MATLAB to perform the circular convolution in Example 5.13.

**Solution**

The sequences are  $x_1(n) = \{1, 2, 2\}$  and  $x_2(n) = \{1, 2, 3, 4\}$ .

MATLAB script:

```
>> x1 = [1,2,2]; x2 = [1,2,3,4]; y = circonvt(x1, x2, 4)
y =
    15     12      9     14
```

Hence

$$x_1(n) \circledcirc_4 x_2(n) = \{15, 12, 9, 14\}$$

as before. □

- **EXAMPLE 5.15** In this example, we will study the effect of  $N$  on the circular convolution. Obviously,  $N \geq 4$ ; otherwise, there will be a time-domain aliasing for  $x_2(n)$ . We will use the same two sequences from Example 5.13.

- a. Compute  $x_1(n) \circledcirc_5 x_2(n)$ .
- b. Compute  $x_1(n) \circledcirc_6 x_2(n)$ .
- c. Comment on the results.

**Solution**

The sequences are  $x_1(n) = \{1, 2, 2\}$  and  $x_2(n) = \{1, 2, 3, 4\}$ . Even though the sequences are the same as in Example 5.14, we should expect different results for different values of  $N$ . This is not the case with the linear convolution, which is unique, given two sequences.

- a. MATLAB script for five-point circular convolution:

```
>> x1 = [1,2,2]; x2 = [1,2,3,4]; y = circonvt(x1, x2, 5)
y =
    9     4     9    14    14
```

Hence

$$x_1(n) \circledcirc_5 x_2(n) = \{9, 4, 9, 14, 14\}$$

- b. MATLAB script for six-point circular convolution:

```
>> x1 = [1,2,2]; x2 = [1,2,3,4]; y = circonvt(x1, x2, 6)
y =
    1     4     9    14    14     8
```

Hence

$$x_1(n) \circledcirc_6 x_2(n) = \{1, 4, 9, 14, 14, 8\}$$

- c. A careful observation of four-, five-, and six-point circular convolutions from this and the previous example indicates some unique features. Clearly, an  $N$ -point circular convolution is an  $N$ -point sequence. However, some samples in these convolutions have the same values, while other values can be obtained as a sum of samples in other convolutions. For example, the first sample in the five-point convolution is a sum of the first and the last samples of the six-point convolution. The linear convolution between  $x_1(n)$  and  $x_2(n)$  is given by

$$x_1(n) * x_2(n) = \{1, 4, 9, 14, 14, 8\}$$

which is equivalent to the six-point circular convolution. These and other issues are explored in the next section.  $\square$

8. **Multiplication:** This is the dual of the circular convolution property. It is given by

$$\text{DFT} [x_1(n) \cdot x_2(n)] = \frac{1}{N} X_1(k) \circledast N X_2(k) \quad (5.41)$$

in which the circular convolution is performed in the frequency domain. The MATLAB functions developed for circular convolution can also be used here since  $X_1(k)$  and  $X_2(k)$  are also  $N$ -point sequences.

9. **Parseval's relation:** This relation computes the energy in the frequency domain.

$$E_x = \sum_{n=0}^{N-1} |x(n)|^2 = \frac{1}{N} \sum_{k=0}^{N-1} |X(k)|^2 \quad (5.42)$$

The quantity  $\frac{|X(k)|^2}{N}$  is called the *energy spectrum* of finite-duration sequences. Similarly, for periodic sequences, the quantity  $|\frac{\tilde{X}(k)}{N}|^2$  is called the *power spectrum*.

## 5.5 LINEAR CONVOLUTION USING THE DFT

---

One of the most important operations in linear systems is the linear convolution. In fact, FIR filters are generally implemented in practice using this linear convolution. On the other hand, the DFT is a practical approach for implementing linear system operations in the frequency domain. As we shall see later, it is also an efficient operation in terms of computations. However, there is one problem. The DFT operations result in a circular convolution (something that we do not desire), not in a linear convolution that we want. Now we shall see how to use the DFT to perform a linear convolution (or equivalently, how to make a circular convolution identical to the linear convolution). We alluded to this problem in Example 5.15.

Let  $x_1(n)$  be an  $N_1$ -point sequence, and let  $x_2(n)$  be an  $N_2$ -point sequence. Define the linear convolution of  $x_1(n)$  and  $x_2(n)$  by  $x_3(n)$ , that is,

$$\begin{aligned} x_3(n) &= x_1(n) * x_2(n) \\ &= \sum_{k=-\infty}^{\infty} x_1(k)x_2(n-k) = \sum_0^{N_1-1} x_1(k)x_2(n-k) \end{aligned} \quad (5.43)$$

Then  $x_3(n)$  is an  $(N_1 + N_2 - 1)$ -point sequence. If we choose  $N = \max(N_1, N_2)$  and compute an  $N$ -point circular convolution  $x_1(n) \textcircled{N} x_2(n)$ , then we get an  $N$ -point sequence, which obviously is different from  $x_3(n)$ . This observation also gives us a clue. Why not choose  $N = N_1 + N_2 - 1$  and perform an  $(N_1 + N_2 - 1)$ -point circular convolution? Then at least both of these convolutions will have an equal number of samples.

Therefore, let  $N = N_1 + N_2 - 1$ , and let us treat  $x_1(n)$  and  $x_2(n)$  as  $N$ -point sequences. Define the  $N$ -point circular convolution by  $x_4(n)$ .

$$\begin{aligned} x_4(n) &= x_1(n) \textcircled{N} x_2(n) \\ &= \left[ \sum_{m=0}^{N-1} x_1(m)x_2((n-m)_N) \right] \mathcal{R}_N(n) \\ &= \left[ \sum_{m=0}^{N-1} x_1(m) \sum_{r=-\infty}^{\infty} x_2(n-m-rN) \right] \mathcal{R}_N(n) \end{aligned} \quad (5.44)$$

$$\begin{aligned}
 &= \left[ \sum_{r=-\infty}^{\infty} \underbrace{\sum_{m=0}^{N_1-1} x_1(m)x_2(n-m-rN)}_{x_3(n-rN)} \right] \mathcal{R}_N(n) \\
 &= \left[ \sum_{r=-\infty}^{\infty} x_3(n-rN) \right] \mathcal{R}_N(n) \quad \text{using (5.43)}
 \end{aligned}$$

This analysis shows that, in general, the circular convolution is an aliased version of the linear convolution. We observed this fact in Example 5.15. Now since  $x_3(n)$  is an  $N = (N_1 + N_2 - 1)$ -point sequence, we have

$$x_4(n) = x_3(n); \quad 0 \leq n \leq (N-1)$$

which means that there is no aliasing in the time domain.

*Conclusion:* If we make both  $x_1(n)$  and  $x_2(n)$   $N = (N_1 + N_2 - 1)$ -point sequences by padding an appropriate number of zeros, then the circular convolution is identical to the linear convolution.

□ **EXAMPLE 5.16** Let  $x_1(n)$  and  $x_2(n)$  be the following two four-point sequences:

$$x_1(n) = \{1, 2, 2, 1\}, \quad x_2(n) = \{1, -1, -1, 1\}$$

- a. Determine their linear convolution  $x_3(n)$ .
- b. Compute the circular convolution  $x_4(n)$  so that it is equal to  $x_3(n)$ .

### Solution

We will use MATLAB to do this problem.

- a. MATLAB script:

```
>> x1 = [1,2,2,1]; x2 = [1,-1,-1,1]; x3 = conv(x1,x2)
x3 =      1       1      -1      -2      -1       1       1
```

Hence the linear convolution  $x_3(n)$  is a seven-point sequence given by

$$x_3(n) = \{1, 1, -1, -2, -1, 1, 1\}$$

- b. We will have to use  $N \geq 7$ . Choosing  $N = 7$ , we have

```
>> x4 = circonvt(x1,x2,7)
x4 =      1       1      -1      -2      -1       1       1
```

Hence

$$x_4 = \{1, 1, -1, -2, -1, 1, 1\} = x_3(n)$$

□

### 5.5.1 ERROR ANALYSIS

To use the DFT for linear convolution, we must choose  $N$  properly. However, in practice it may not be possible to do so, especially when  $N$  is very large and there is a limit on memory. Then an error will be introduced when  $N$  is chosen less than the required value to perform the circular convolution. We want to compute this error, which is useful in practice. Obviously,  $N \geq \max(N_1, N_2)$ . Therefore, let

$$\max(N_1, N_2) \leq N < (N_1 + N_2 - 1)$$

Then, from our previous analysis (5.44),

$$x_4(n) = \left[ \sum_{r=-\infty}^{\infty} x_3(n - rN) \right] \mathcal{R}_N(n)$$

Let an error  $e(n)$  be given by

$$\begin{aligned} e(n) &\triangleq x_4(n) - x_3(n) \\ &= \left[ \sum_{r \neq 0} x_3(n - rN) \right] \mathcal{R}_N(n) \end{aligned}$$

Since  $N \geq \max(N_1, N_2)$ , only two terms corresponding to  $r = \pm 1$  remain in the above summation. Hence

$$e(n) = [x_3(n - N) + x_3(n + N)] \mathcal{R}_N(n)$$

Generally,  $x_1(n)$  and  $x_2(n)$  are causal sequences. Then  $x_3(n)$  is also causal, which means that

$$x_3(n - N) = 0; \quad 0 \leq n \leq N - 1$$

Therefore,

$$e(n) = x_3(n + N), \quad 0 \leq n \leq N - 1 \quad (5.45)$$

This is a simple yet important relation. It implies that when  $\max(N_1, N_2) \leq N < (N_1 + N_2 - 1)$  the error value at  $n$  is the same as the linear convolution value computed  $N$  samples away. Now the linear convolution will be zero after  $(N_1 + N_2 - 1)$  samples. This means that the first few samples of the circular convolution are in error, while the remaining ones are the correct linear convolution values.

- **EXAMPLE 5.17** Consider the sequences  $x_1(n)$  and  $x_2(n)$  from the previous example. Evaluate circular convolutions for  $N = 6, 5$ , and  $4$ . Verify the error relations in each case.

**Solution**

Clearly, the linear convolution  $x_3(n)$  is still the same.

$$x_3(n) = \{1, 1, -1, -2, -1, 1, 1\}$$

When  $N = 6$ , we obtain a six-point sequence:

$$x_4(n) = x_1(n) \odot x_2(n) = \{2, 1, -1, -2, -1, 1\} \quad (6)$$

Therefore,

$$\begin{aligned} e(n) &= \{2, 1, -1, -2, -1, 1\} - \{1, 1, -1, -2, -1, 1\}, \quad 0 \leq n \leq 5 \\ &= \{1, 0, 0, 0, 0, 0\} \\ &= x_3(n+6) \end{aligned}$$

as expected. When  $N = 5$ , we obtain a five-point sequence,

$$x_4(n) = x_1(n) \odot x_2(n) = \{2, 2, -1, -2, -1\} \quad (5)$$

and

$$\begin{aligned} e(n) &= \{2, 2, -1, -2, -1\} - \{1, 1, -1, -2, -1\}, \quad 0 \leq n \leq 4 \\ &= \{1, 1, 0, 0, 0\} \\ &= x_3(n+5) \end{aligned}$$

Finally, when  $N = 4$ , we obtain a four-point sequence,

$$x_4(n) = x_1(n) \odot x_2(n) = \{0, 2, 0, -2\} \quad (4)$$

and

$$\begin{aligned} e(n) &= \{0, 2, 0, -2\} - \{1, 1, -1, -2\}, \quad 0 \leq n \leq 3 \\ &= \{-1, 1, 1, 0\} \\ &= x_3(n+4) \end{aligned}$$

The last case of  $N = 4$  also provides the following useful observation.

*Observation:* When  $N = \max(N_1, N_2)$  is chosen for circular convolution, then the first  $(M - 1)$  samples are in error (i.e., different from the linear convolution), where  $M = \min(N_1, N_2)$ . This result is useful in implementing long convolutions in the form of block processing.  $\square$

### 5.5.2 BLOCK CONVOLUTIONS

When we want to filter an input sequence that is being received continuously, such as a speech signal from a microphone, then for practical purposes we can think of this sequence as an infinite-length sequence. If we want to implement this filtering operation as an FIR filter in which the linear convolution is computed using the DFT, then we experience some practical problems. We will have to compute a large DFT, which is generally impractical. Furthermore, output samples are not available until all input samples are processed. This introduces an unacceptably large

amount of delay. Therefore, we have to segment the infinite-length input sequence into smaller sections (or blocks), process each section using the DFT, and finally assemble the output sequence from the outputs of each section. This procedure is called a *block convolution* (or block processing) operation.

Let us assume that the sequence  $x(n)$  is sectioned into  $N$ -point sequences and that the impulse response of the filter is an  $M$ -point sequence, where  $M < N$ . Then from the observation in Example 5.17, we note that the  $N$ -point circular convolution between the input block and the impulse response will yield a block output sequence in which the first  $(M - 1)$  samples are not the correct output values. If we simply partition  $x(n)$  into nonoverlapping sections, then the resulting output sequence will have intervals of incorrect samples. To correct this problem, we can partition  $x(n)$  into sections, each overlapping with the previous one by exactly  $(M - 1)$  samples, save the last  $(N - M + 1)$  output samples, and finally concatenate these outputs into a sequence. To correct for the first  $(M - 1)$  samples in the first output block, we set the first  $(M - 1)$  samples in the first input block to zero. This procedure is called an *overlap-save* method of block convolutions. Clearly, when  $N \gg M$ , this method is more efficient. We illustrate it using a simple example.

- **EXAMPLE 5.18** Let  $x(n) = (n + 1)$ ,  $0 \leq n \leq 9$  and  $h(n) = \{1, 0, -1\}$ . Implement the overlap-save method using  $N = 6$  to compute  $y(n) = x(n) * h(n)$ .

### Solution

Since  $M = 3$ , we will have to overlap each section with the previous one by two samples. Now  $x(n)$  is a 10-point sequence, and we will need  $(M - 1) = 2$  zeros in the beginning. Since  $N = 6$ , we will need three sections. Let the sections be

$$x_1(n) = \{0, 0, 1, 2, 3, 4\}$$

$$x_2(n) = \{3, 4, 5, 6, 7, 8\}$$

$$x_3(n) = \{7, 8, 9, 10, 0, 0\}$$

Note that we have to pad  $x_3(n)$  by two zeros since  $x(n)$  runs out of values at  $n = 9$ . Now we will compute the six-point circular convolution of each section with  $h(n)$ .

$$y_1 = x_1(n) \textcircled{6} h(n) = \{-3, -4, 1, 2, 2, 2\}$$

$$y_2 = x_2(n) \textcircled{6} h(n) = \{-4, -4, 2, 2, 2, 2\}$$

$$y_3 = x_3(n) \textcircled{6} h(n) = \{7, 8, 2, 2, -9, -10\}$$

Noting that the first two samples in each section are to be discarded, we assemble the output  $y(n)$  as

$$y(n) = \{1, \underset{\uparrow}{2}, 2, 2, 2, 2, 2, 2, 2, 2, -9, -10\}$$

The linear convolution is given by

$$x(n) * h(n) = \{1, \underset{\uparrow}{2}, 2, 2, 2, 2, 2, 2, 2, 2, -9, -10\}$$

which agrees with the overlap-save method.  $\square$

### 5.5.3 MATLAB IMPLEMENTATION

Using this example as a guide, we can develop a MATLAB function to implement the overlap-save method for a very long input sequence  $x(n)$ . The key step in this function is to obtain a proper indexing for the segmentation. Given  $x(n)$  for  $n \geq 0$ , we have to set the first  $(M - 1)$  samples to zero to begin the block processing. Let this augmented sequence be

$$\hat{x}(n) \stackrel{\triangle}{=} \underbrace{\{0, 0, \dots, 0\}}_{(M-1) \text{ zeros}}, \quad n \geq 0, \quad x(n), \quad n \geq 0$$

and let  $L = N - M + 1$ ; then the  $k$ th block  $x_k(n)$ ,  $0 \leq n \leq N - 1$ , is given by

$$x_k(n) = \hat{x}(m); \quad kL \leq m \leq kL + N - 1, \quad k \geq 0, \quad 0 \leq n \leq N - 1$$

The total number of blocks is given by

$$K = \left\lfloor \frac{N_x + M - 2}{L} \right\rfloor + 1$$

where  $N_x$  is the length of  $x(n)$  and  $\lfloor \cdot \rfloor$  is the truncation operation. Now each block can be circularly convolved with  $h(n)$  using the **circonv** function developed earlier to obtain

$$y_k(n) = x_k(n) \circledast h(n)$$

Finally, discarding the first  $(M - 1)$  samples from each  $y_k(n)$  and concatenating the remaining samples, we obtain the linear convolution  $y(n)$ . This procedure is incorporated in the following **ovrlpsav** function.

```

function [y] = ovrlpsav(x,h,N)
% Overlap-Save method of block convolution
%
% [y] = ovrlpsav(x,h,N)
% y = output sequence
% x = input sequence
% h = impulse response
% N = block length
%

Lenx = length(x); M = length(h); M1 = M-1; L = N-M1;
h = [h zeros(1,N-M)];
%
x = [zeros(1,M1), x, zeros(1,N-1)]; % Preappend (M-1) zeros
K = floor((Lenx+M1-1)/(L)); % # of blocks
Y = zeros(K+1,N);
% Convolution with successive blocks
for k=0:K
    xk = x(k*L+1:k*L+N);
    Y(k+1,:) = circonv(xk,h,N);
end
Y = Y(:,M:N); % Discard the first (M-1) samples
y = (Y(:))'; % Assemble output

```

*Note:* The `ovrlpsav` function as developed here is not the most efficient approach. We will come back to this issue when we discuss the fast Fourier transform.

- **EXAMPLE 5.19** To verify the operation of the `ovrlpsav` function, let us consider the sequences given in Example 5.18.

**Solution** MATLAB script:

```

>> n = 0:9; x = n+1; h = [1,0,-1]; N = 6; y = ovrlpsav(x,h,N)
y =
    1     2     2     2     2     2     2     2     2     -9    -10

```

This is the correct linear convolution as expected. □

There is an alternate method called an *overlap-add* method of block convolutions. In this method, the input sequence  $x(n)$  is partitioned into nonoverlapping blocks and convolved with the impulse response. The resulting output blocks are overlapped with the subsequent sections and added to form the overall output. This is explored in Problem P5.32.

## 5.6 THE FAST FOURIER TRANSFORM

---

The DFT (5.24) introduced earlier is the only transform that is discrete in both the time and the frequency domains and is defined for finite-duration sequences. Although it is a computable transform, the straightforward implementation of (5.24) is very inefficient, especially when the sequence length  $N$  is large. In 1965, Cooley and Tukey [8] showed a procedure to substantially reduce the amount of computations involved in the DFT. This led to the explosion of applications of the DFT, including in the digital signal processing area. Furthermore, it also led to the development of other efficient algorithms. All these efficient algorithms are collectively known as fast Fourier transform (FFT) algorithms.

Consider an  $N$ -point sequence  $x(n)$ . Its  $N$ -point DFT is given by (5.24) and reproduced here,

$$X(k) = \sum_{n=0}^{N-1} x(n)W_N^{nk}, \quad 0 \leq k \leq N-1 \quad (5.46)$$

where  $W_N = e^{-j2\pi/N}$ . To obtain one sample of  $X(k)$ , we need  $N$  complex multiplications and  $(N-1)$  complex additions. Hence to obtain a complete set of DFT coefficients, we need  $N^2$  complex multiplications and  $N(N-1) \simeq N^2$  complex additions. Also, one has to store  $N^2$  complex coefficients  $\{W_N^{nk}\}$  (or generate internally at an extra cost). Clearly, the number of DFT computations for an  $N$ -point sequence depends quadratically on  $N$ , which will be denoted by the notation

$$C_N = o(N^2)$$

For large  $N$ ,  $o(N^2)$  is unacceptable in practice. Generally, the processing time for one addition is much less than that for one multiplication. Hence from now on we will concentrate on the number of complex multiplications, which itself requires four real multiplications and two real additions.

### 5.6.1 GOAL OF AN EFFICIENT COMPUTATION

In an efficiently designed algorithm, the number of computations should be constant per data sample, and therefore the total number of computations should be linear with respect to  $N$ .

The quadratic dependence on  $N$  can be reduced by realizing that most of the computations (which are done again and again) can be eliminated using the periodicity property

$$W_N^{kn} = W_N^{k(n+N)} = W_N^{(k+N)n}$$

and the symmetry property

$$W_N^{kn+N/2} = -W_N^{kn}$$

of the factor  $\{W_N^{nk}\}$ .

One algorithm that considers only the periodicity of  $W_N^{nk}$  is the Goertzel algorithm. This algorithm still requires  $C_N = o(N^2)$  multiplications, but it has certain advantages. This algorithm is described in Chapter 12. We first begin with an example to illustrate the advantages of the symmetry and periodicity properties in reducing the number of computations. We then describe and analyze two specific FFT algorithms that require  $C_N = o(N \log N)$  operations. They are the *decimation-in-time* (DIT-FFT) and *decimation-in-frequency* (DIF-FFT) algorithms.

- **EXAMPLE 5.20** Let us discuss the computations of a four-point DFT and develop an efficient algorithm for its computation.

$$X(k) = \sum_{n=0}^3 x(n)W_4^{nk}, \quad 0 \leq k \leq 3; \quad W_4 = e^{-j2\pi/4} = -j$$

### Solution

These computations can be done in the matrix form

$$\begin{bmatrix} X(0) \\ X(1) \\ X(2) \\ X(3) \end{bmatrix} = \begin{bmatrix} W_4^0 & W_4^0 & W_4^0 & W_4^0 \\ W_4^0 & W_4^1 & W_4^2 & W_4^3 \\ W_4^0 & W_4^2 & W_4^4 & W_4^6 \\ W_4^0 & W_4^3 & W_4^6 & W_4^9 \end{bmatrix} \begin{bmatrix} x(0) \\ x(1) \\ x(2) \\ x(3) \end{bmatrix}$$

which requires 16 complex multiplications.

*Efficient Approach* Using periodicity,

$$\begin{aligned} W_4^0 &= W_4^4 = 1 & ; \quad W_4^1 &= W_4^9 = -j \\ W_4^2 &= W_4^6 = -1 & ; \quad W_4^3 &= j \end{aligned}$$

and substituting in the above matrix form, we get

$$\begin{bmatrix} X(0) \\ X(1) \\ X(2) \\ X(3) \end{bmatrix} = \begin{bmatrix} 1 & 1 & 1 & 1 \\ 1 & -j & -1 & j \\ 1 & -1 & 1 & -1 \\ 1 & j & -1 & -j \end{bmatrix} \begin{bmatrix} x(0) \\ x(1) \\ x(2) \\ x(3) \end{bmatrix}$$

Using symmetry, we obtain

$$X(0) = x(0) + x(1) + x(2) + x(3) = \underbrace{[x(0) + x(2)]}_{g_1} + \underbrace{[x(1) + x(3)]}_{g_2}$$

$$X(1) = x(0) - jx(1) - x(2) + jx(3) = \underbrace{[x(0) - x(2)]}_{h_1} - j\underbrace{[x(1) - x(3)]}_{h_2}$$

$$X(2) = x(0) - x(1) + x(2) - x(3) = \underbrace{[x(0) + x(2)]}_{g_1} - \underbrace{[x(1) + x(3)]}_{g_2}$$

$$X(3) = x(0) + jx(1) - x(2) - jx(3) = \underbrace{[x(0) - x(2)]}_{h_1} + j\underbrace{[x(1) - x(3)]}_{h_2}$$

Hence an efficient algorithm is

$$\begin{array}{ll} \text{Step 1} & \text{Step 2} \\ g_1 = x(0) + x(2) & X(0) = g_1 + g_2 \\ g_2 = x(1) + x(3) & X(1) = h_1 - jh_2 \\ h_1 = x(0) - x(2) & X(2) = g_1 - g_2 \\ h_2 = x(1) - x(3) & X(3) = h_1 + jh_2 \end{array} \quad (5.47)$$

which requires only two complex multiplications, which is a considerably smaller number, even for this simple example. A signal flowgraph structure for this algorithm is given in Figure 5.19.

*An Interpretation* This efficient algorithm (5.47) can be interpreted differently. First, a four-point sequence  $x(n)$  is divided into two two-point sequences, which are arranged into column vectors as shown here:

$$\left[ \begin{bmatrix} x(0) \\ x(2) \end{bmatrix}, \begin{bmatrix} x(1) \\ x(3) \end{bmatrix} \right] = \begin{bmatrix} x(0) & x(1) \\ x(2) & x(3) \end{bmatrix}$$

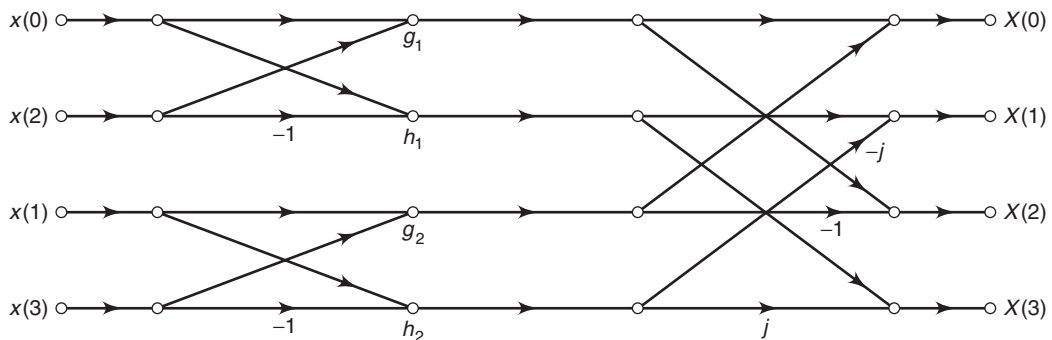


FIGURE 5.19 Signal flowgraph in Example 5.20

Second, a smaller two-point DFT of each column is taken.

$$\begin{aligned}\mathbf{W}_2 \begin{bmatrix} x(0) & x(1) \\ x(2) & x(3) \end{bmatrix} &= \begin{bmatrix} 1 & 1 \\ 1 & -1 \end{bmatrix} \begin{bmatrix} x(0) & x(1) \\ x(2) & x(3) \end{bmatrix} \\ &= \begin{bmatrix} x(0) + x(2) & x(1) + x(3) \\ x(0) - x(2) & x(1) - x(3) \end{bmatrix} = \begin{bmatrix} g_1 & g_2 \\ h_1 & h_2 \end{bmatrix}\end{aligned}$$

Then each element of the resultant matrix is multiplied by  $\{W_4^{pq}\}$ , where  $p$  is the row index and  $q$  is the column index; that is, the following *dot-product* is performed:

$$\begin{bmatrix} 1 & 1 \\ 1 & -j \end{bmatrix} \cdot * \begin{bmatrix} g_1 & g_2 \\ h_1 & h_2 \end{bmatrix} = \begin{bmatrix} g_1 & g_2 \\ h_1 & -jh_2 \end{bmatrix}$$

Finally, two more smaller two-point DFTs are taken of *row vectors*.

$$\begin{aligned}\begin{bmatrix} g_1 & g_2 \\ h_1 & -jh_2 \end{bmatrix} \mathbf{W}_2 &= \begin{bmatrix} g_1 & g_2 \\ h_1 & -jh_2 \end{bmatrix} \begin{bmatrix} 1 & 1 \\ 1 & -1 \end{bmatrix} = \begin{bmatrix} g_1 + g_2 & g_1 - g_2 \\ h_1 - jh_2 & h_1 + jh_2 \end{bmatrix} \\ &= \begin{bmatrix} X(0) & X(2) \\ X(1) & X(3) \end{bmatrix}\end{aligned}$$

Although this interpretation seems to have more multiplications than the efficient algorithm, it does suggest a systematic approach of computing a larger DFT based on smaller DFTs.  $\square$

### 5.6.2 DIVIDE-AND-COMBINE APPROACH

To reduce the DFT computation's quadratic dependence on  $N$ , one must choose a composite number  $N = LM$  since

$$L^2 + M^2 \ll N^2 \quad \text{for large } N$$

Now divide the sequence into  $M$  smaller sequences of length  $L$ , compute  $M$  smaller  $L$ -point DFTs, and then combine these into a larger DFT using  $L$  smaller  $M$ -point DFTs. This is the essence of the divide-and-combine approach. Let  $N = LM$ ; then the indices  $n$  and  $k$  in (5.46) can be written as

$$\begin{aligned}n &= \ell + Lm, \quad 0 \leq \ell \leq L-1, \quad 0 \leq m \leq M-1 \\ k &= q + Mp, \quad 0 \leq p \leq L-1, \quad 0 \leq q \leq M-1\end{aligned}\tag{5.48}$$

and write sequences  $x(n)$  and  $X(k)$  as arrays  $x(\ell, m)$  and  $X(p, q)$ , respectively. Then (5.46) can be written as

$$\begin{aligned}
 X(p, q) &= \sum_{\ell=0}^{L-1} \sum_{m=0}^{M-1} x(\ell, m) W_N^{(\ell+Lm)(q+Mp)} \\
 &= \sum_{\ell=0}^{L-1} \left\{ W_N^{\ell q} \left[ \sum_{m=0}^{M-1} x(\ell, m) W_N^{Lmq} \right] \right\} W_N^{M\ell p} \\
 &= \underbrace{\sum_{\ell=0}^{L-1} \left\{ W_N^{\ell q} \underbrace{\left[ \sum_{m=0}^{M-1} x(\ell, m) W_M^{mq} \right]}_{M\text{-point DFT}} \right\}}_{L\text{-point DFT}} W_L^{\ell p} \quad (5.49)
 \end{aligned}$$

Hence (5.49) can be implemented as a three-step procedure:

1. First, we compute the  $M$ -point DFT array

$$F(\ell, q) \triangleq \sum_{m=0}^{M-1} x(\ell, m) W_M^{mq}; \quad 0 \leq q \leq M-1 \quad (5.50)$$

for each of the rows  $\ell = 0, \dots, L-1$ .

2. Second, we modify  $F(\ell, q)$  to obtain another array.

$$G(\ell, q) = W_N^{\ell q} F(\ell, q), \quad \begin{matrix} 0 \leq \ell \leq L-1 \\ 0 \leq q \leq M-1 \end{matrix} \quad (5.51)$$

The factor  $W_N^{\ell q}$  is called a *twiddle* factor.

3. Finally, we compute the  $L$ -point DFTs

$$X(p, q) = \sum_{\ell=0}^{L-1} G(\ell, q) W_L^{\ell p} \quad 0 \leq p \leq L-1 \quad (5.52)$$

for each of the columns  $q = 0, \dots, M-1$ .

The total number of complex multiplications for this approach can now be given by

$$C_N = LM^2 + N + ML^2 < O(N^2) \quad (5.53)$$

We illustrate this approach in the following example.

- EXAMPLE 5.21** Develop the divide-and-combine FFT algorithm for  $N = 15$ .

**Solution**

Let  $L = 3$  and  $M = 5$ . Then from (5.48), we have

$$\begin{aligned} n &= \ell + 3M, \quad 0 \leq \ell \leq 2, \quad 0 \leq m \leq 4 \\ k &= q + 5p, \quad 0 \leq p \leq 2, \quad 0 \leq q \leq 4 \end{aligned} \quad (5.54)$$

Hence (5.49) becomes

$$X(p, q) = \sum_{\ell=0}^2 \left\{ W_{15}^{\ell q} \left[ \sum_{m=0}^4 x(\ell, m) W_5^{mq} \right] \right\} W_3^{\ell p} \quad (5.55)$$

To implement (5.55), we arrange the given sequence  $x(n)$  in the form of an array  $\{x(\ell, m)\}$  using a column-wise ordering as

$$\begin{array}{ccccc} x(0) & x(3) & x(6) & x(9) & x(12) \\ x(1) & x(4) & x(7) & x(10) & x(13) \\ x(2) & x(5) & x(8) & x(11) & x(14) \end{array} \quad (5.56)$$

The first step is to compute five-point DFTs  $F(\ell, q)$  for each of the three rows and arrange them back in the same array formation

$$\begin{array}{ccccc} F(0, 0) & F(0, 1) & F(0, 2) & F(0, 3) & F(0, 4) \\ F(1, 0) & F(1, 1) & F(1, 2) & F(1, 3) & F(1, 4) \\ F(2, 0) & F(2, 1) & F(2, 2) & F(2, 3) & F(2, 4) \end{array} \quad (5.57)$$

which requires a total of  $3 \times 5^2 = 75$  complex operations. The second step is to modify  $F(\ell, q)$  to obtain the array  $G(\ell, q)$  using the twiddle factors  $W_{15}^{\ell q}$

$$\begin{array}{ccccc} G(0, 0) & G(0, 1) & G(0, 2) & G(0, 3) & G(0, 4) \\ G(1, 0) & G(1, 1) & G(1, 2) & G(1, 3) & G(1, 4) \\ G(2, 0) & G(2, 1) & G(2, 2) & G(2, 3) & G(2, 4) \end{array} \quad (5.58)$$

which requires 15 complex operations. The last step is to perform three-point DFTs  $X(p, q)$  for each of the five columns to obtain

$$\begin{array}{ccccc} X(0, 0) & X(0, 1) & X(0, 2) & X(0, 3) & X(0, 4) \\ X(1, 0) & X(1, 1) & X(1, 2) & X(1, 3) & X(1, 4) \\ X(2, 0) & X(2, 1) & X(2, 2) & X(2, 3) & X(2, 4) \end{array} \quad (5.59)$$

using a total of  $5 \times 3^2 = 45$  complex operations. According to (5.54), the array in (5.59) is a rearrangement of  $X(k)$  as

$$\begin{array}{ccccc} X(0) & X(1) & X(2) & X(3) & X(4) \\ X(5) & X(6) & X(7) & X(8) & X(9) \\ X(10) & X(11) & X(12) & X(13) & X(14) \end{array} \quad (5.60)$$

Finally, after “unwinding” this array in the row-wise fashion, we obtain the required 15-point DFT  $X(k)$ . The total number of complex operations required for this divide-and-combine approach is 135, whereas the direct approach for the 15-point DFT requires 225 complex operations. Thus the divide-and-combine approach is clearly efficient.  $\square$

The divide-and-combine procedure can be further repeated if  $M$  or  $L$  are composite numbers. Clearly, the most efficient algorithm is obtained when  $N$  is a highly composite number, that is,  $N = R^\nu$ . Such algorithms are called *radix-R* FFT algorithms. When  $N = R_1^{\nu_1} R_2^{\nu_2} \dots$ , then such decompositions are called *mixed-radix* FFT algorithms. The one most popular and easily programmable algorithm is the radix-2 FFT algorithm.

### 5.6.3 RADIX-2 FFT ALGORITHM

Let  $N = 2^\nu$ ; then we choose  $L = 2$  and  $M = N/2$  and divide  $x(n)$  into two  $N/2$ -point sequences according to (5.48) as

$$\begin{aligned} g_1(n) &= x(2n) \\ g_2(n) &= x(2n+1); \quad 0 \leq n \leq \frac{N}{2} - 1 \end{aligned}$$

The sequence  $g_1(n)$  contains even-ordered samples of  $x(n)$ , while  $g_2(n)$  contains odd-ordered samples of  $x(n)$ . Let  $G_1(k)$  and  $G_2(k)$  be  $N/2$ -point DFTs of  $g_1(n)$  and  $g_2(n)$ , respectively. Then (5.49) reduces to

$$X(k) = G_1(k) + W_N^k G_2(k), \quad 0 \leq k \leq N - 1 \quad (5.61)$$

This is called a *merging formula*, which combines two  $N/2$ -point DFTs into one  $N$ -point DFT. The total number of complex multiplications and additions reduces to

$$C_N = \frac{N^2}{2} + N = O(N^2/2)$$

This procedure can be repeated again and again. At each stage, the sequences are decimated and the smaller DFTs combined. This decimation ends after  $\nu$  stages when we have  $N$  one-point sequences, which are also one-point DFTs. The resulting procedure is called the *decimation-in-time* FFT (DIT-FFT) algorithm, for which the total number of complex multiplications is

$$C_N = N\nu = N \log_2 N$$

Clearly, if  $N$  is large, then  $C_N$  is approximately linear in  $N$ , which was the goal of our efficient algorithm. Using additional symmetries,  $C_N$  can be reduced to  $\frac{N}{2} \log_2 N$ . The signal flowgraph for this algorithm is shown in Figure 5.20 for  $N = 8$ .

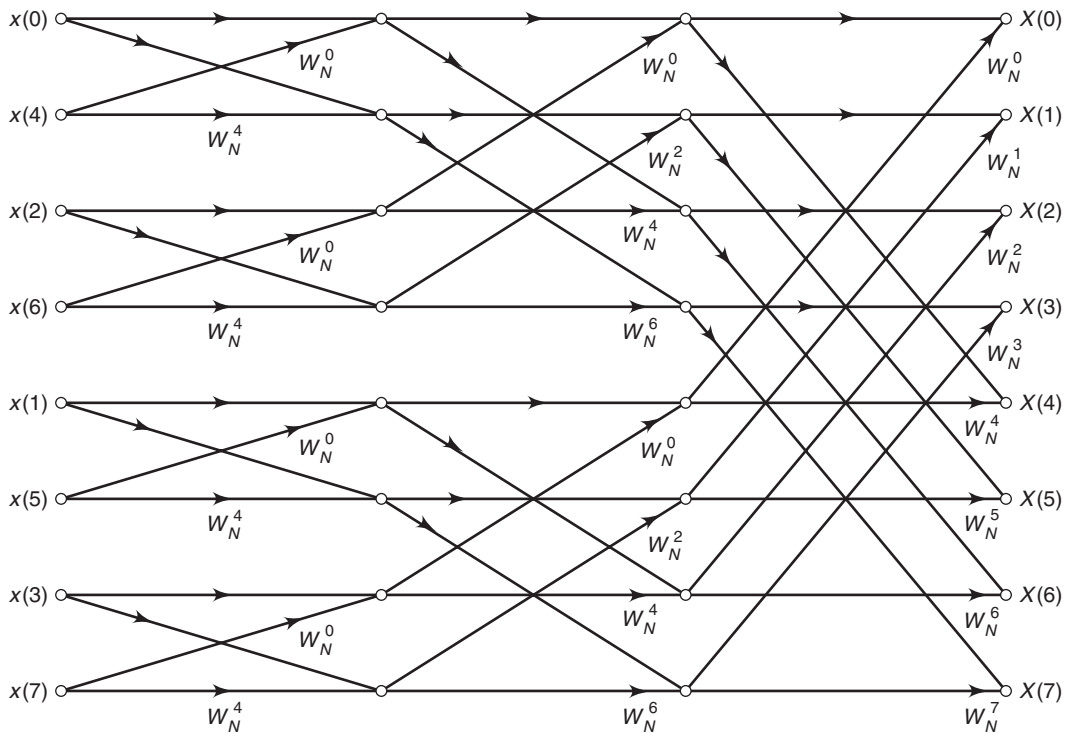


**FIGURE 5.20** Decimation-in-time FFT structure for  $N = 8$

In an alternate approach, we choose  $M = 2$ ,  $L = N/2$  and follow the steps in (5.49). Note that the initial DFTs are two-point DFTs, which contain no complex multiplications. From (5.50),

$$\begin{aligned} F(0, m) &= x(0, m) + x(1, m)W_2^0 \\ &= x(n) + x(n + N/2), \quad 0 \leq n \leq N/2 \\ F(1, m) &= x(0, m) + x(1, m)W_2^1 \\ &= x(n) - x(n + N/2), \quad 0 \leq n \leq N/2 \end{aligned}$$

and from (5.51),

$$\begin{aligned} G(0, m) &= F(0, m)W_N^0 \\ &= x(n) + x(n + N/2), \quad 0 \leq n \leq N/2 \\ G(1, m) &= F(1, m)W_N^m \\ &= [x(n) - x(n + N/2)]W_N^n, \quad 0 \leq n \leq N/2 \end{aligned} \tag{5.62}$$

Let  $G(0, m) = d_1(n)$  and  $G(1, m) = d_2(n)$  for  $0 \leq n \leq N/2 - 1$  (since they can be considered as time-domain sequences); then from (5.52) we have

$$\begin{aligned} X(0, q) &= X(2q) &= D_1(q) \\ X(1, q) &= X(2q + 1) = D_2(q) \end{aligned} \quad (5.63)$$

This implies that the DFT values  $X(k)$  are computed in a decimated fashion. Therefore, this approach is called a *decimation-in-frequency* FFT (DIF-FFT) algorithm. Its signal flowgraph is a transposed structure of the DIT-FFT structure, and its computational complexity is also equal to  $\frac{N}{2} \log_2 N$ .

#### 5.6.4 MATLAB IMPLEMENTATION

MATLAB provides a function called `fft` to compute the DFT of a vector `x`. It is invoked by `X = fft(x, N)`, which computes the  $N$ -point DFT. If the length of `x` is less than `N`, then `x` is padded with zeros. If the argument `N` is omitted, then the length of the DFT is the length of `x`. If `x` is a matrix, then `fft(x, N)` computes the  $N$ -point DFT of each column of `x`.

This `fft` function is written in machine language and not using MATLAB commands (i.e., it is not available as a `.m` file). Therefore, it executes very fast. It is written as a mixed-radix algorithm. If  $N$  is a power of two, then a high-speed radix-2 FFT algorithm is employed. If  $N$  is not a power of two, then  $N$  is decomposed into prime factors and a slower mixed-radix FFT algorithm is used. Finally, if  $N$  is a prime number, then the `fft` function is reduced to the raw DFT algorithm.

The inverse DFT is computed using the `ifft` function, which has the same characteristics as `fft`.

- EXAMPLE 5.22** In this example, we will study the execution time of the `fft` function for  $1 \leq N \leq 2048$ . This will reveal the divide-and-combine strategy for various values of  $N$ . One note of caution. The results obtained in this example are valid only for MATLAB Versions 5 and earlier. Beginning in Version 6, MATLAB is using a new numerical computing core called LAPACK. It is optimized for memory references and cache usage and not for individual floating-point operations. Therefore, results for Version 6 and later are difficult to interpret. Also, the execution times given here are for a specific computer and may vary on different computers.

#### Solution

To determine the execution time, MATLAB provides two functions. The `clock` function provides the instantaneous clock reading, while the `etime(t1, t2)` function computes the elapsed time between two time marks `t1` and `t2`. To determine the execution time, we will generate random vectors from length 1 through 2048,

compute their FFTs, and save the computation time in an array. Finally, we will plot this execution time versus  $N$ .

MATLAB script:

```
>> Nmax = 2048; fft_time=zeros(1,Nmax);
>> for n=1:1:Nmax
>>     x=rand(1,n);
>>     t=clock;fft(x);fft_time(n)=etime(clock,t);
>> end
>> n=[1:1:Nmax]; plot(n,fft_time,'.')
>> xlabel('N');ylabel('Time in Sec'); title('FFT Execution Times')
```

The plot of the execution times is shown in Figure 5.21. This plot is very informative. The points in the plot do not show one clear function but appear to group themselves into various trends. The uppermost group depicts a  $\Theta(N^2)$  dependence on  $N$ , which means that these values must be prime numbers between 1 and 2048 for which the FFT algorithm defaults to the DFT algorithm. Similarly, there are groups corresponding to the  $\Theta(N^2/2)$ ,  $\Theta(N^2/3)$ ,  $\Theta(N^2/4)$ , and so on, dependencies for which the number  $N$  has fewer decompositions. The last group shows the (almost linear)  $\Theta(N \log N)$  dependence, which is for

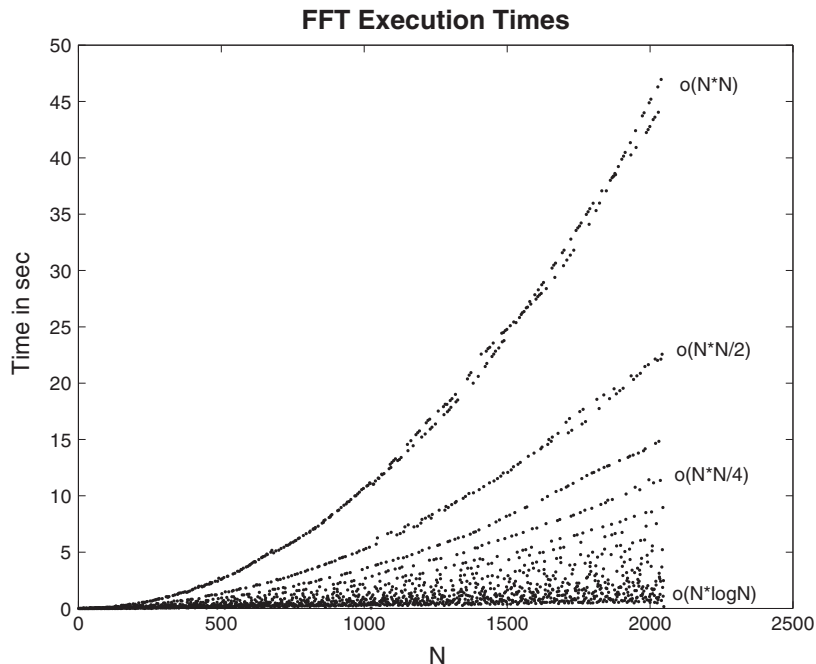


**FIGURE 5.21** FFT execution times for  $1 \leq N \leq 2048$

$N = 2^\nu$ ,  $0 \leq \nu \leq 11$ . For these values of  $N$ , the radix-2 FFT algorithm is used. For all other values, a mixed-radix FFT algorithm is employed. This shows that the divide-and-combine strategy is very effective when  $N$  is highly composite. For example, the execution time is 0.16 sec for  $N = 2048$ , 2.48 sec for  $N = 2047$ , and 46.96 sec for  $N = 2039$ .  $\square$

The MATLAB functions developed previously in this chapter should now be modified by substituting the `fft` function in place of the `dft` function. From the preceding example, care must be taken to use a highly composite  $N$ . A good practice is to choose  $N = 2^\nu$  unless a specific situation demands otherwise.

### 5.6.5 FAST CONVOLUTIONS

The `conv` function in MATLAB is implemented using the `filter` function (which is written in C) and is very efficient for smaller values of  $N$  ( $< 50$ ). For larger values of  $N$ , it is possible to speed up the convolution using the FFT algorithm. This approach uses the circular convolution to implement the linear convolution, and the FFT to implement the circular convolution. The resulting algorithm is called a *fast convolution* algorithm. In addition, if we choose  $N = 2^\nu$  and implement the radix-2 FFT, then the algorithm is called a *high-speed convolution*. Let  $x_1(n)$  be an  $N_1$ -point sequence, and let  $x_2(n)$  be an  $N_2$ -point sequence; then for high-speed convolution  $N$  is chosen to be

$$N = 2^{\lceil \log_2(N_1+N_2-1) \rceil} \quad (5.64)$$

where  $\lceil x \rceil$  is the smallest integer greater than  $x$  (also called a *ceiling* function). The linear convolution  $x_1(n) * x_2(n)$  can now be implemented by two  $N$ -point FFTs, one  $N$ -point IFFT, and one  $N$ -point dot-product.

$$x_1(n) * x_2(n) = \text{IFFT}[\text{FFT}[x_1(n)] \cdot \text{FFT}[x_2(n)]] \quad (5.65)$$

For large values of  $N$ , (5.65) is faster than the time-domain convolution, as we see in the following example.

- $\square$  **EXAMPLE 5.23** To demonstrate the effectiveness of the high-speed convolution, let us compare the execution times of two approaches. Let  $x_1(n)$  be an  $L$ -point uniformly distributed random number between  $[0, 1]$ , and let  $x_2(n)$  be an  $L$ -point Gaussian random sequence with mean 0 and variance 1. We will determine the average execution times for  $1 \leq L \leq 150$ , in which the average is computed over the 100 realizations of random sequences. (Please see the cautionary note given in Example 5.22.)

**Solution**

MATLAB script:

```

conv_time = zeros(1,150); fft_time = zeros(1,150);
%
for L = 1:150
    tc = 0; tf=0;
    N = 2*L-1; nu = ceil(log10(N)/log10(2)); N = 2^nu;
    for I=1:100
        h = randn(1,L); x = rand(1,L);
        t0 = clock; y1 = conv(h,x); t1=etime(clock,t0); tc = tc+t1;
        t0 = clock; y2 = ifft(fft(h,N).*fft(x,N)); t2=etime(clock,t0);
        tf = tf+t2;
    end
    %
    conv_time(L)=tc/100; fft_time(L)=tf/100;
end
%
n = 1:150; subplot(1,1,1);
plot(n(25:150),conv_time(25:150),n(25:150),fft_time(25:150))

```

Figure 5.22 shows the linear convolution and the high-speed convolution times for  $25 \leq L \leq 150$ . It should be noted that these times are affected by the

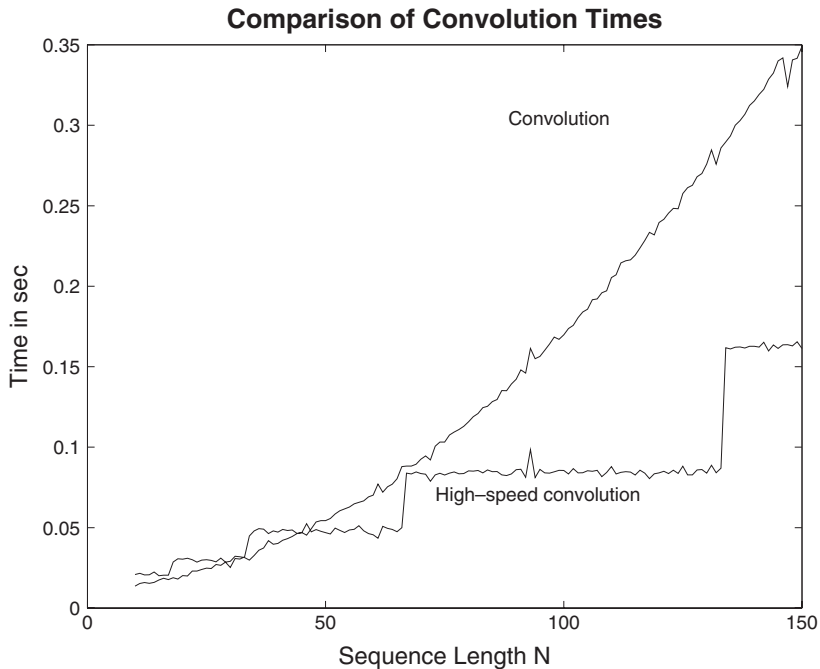


**FIGURE 5.22** Comparison of linear and high-speed convolution times

computing platform used to execute the MATLAB script. The plot in Figure 5.22 was obtained on a 33 MHz 486 computer. It shows that for low values of  $L$ , the linear convolution is faster. The crossover point appears to be  $L = 50$ , beyond which the linear convolution time increases exponentially, while the high-speed convolution time increases fairly linearly. Note that since  $N = 2^\nu$ , the high-speed convolution time is constant over a range on  $L$ .  $\square$

### 5.6.6 HIGH-SPEED BLOCK CONVOLUTIONS

Earlier we discussed a block convolution algorithm called the overlap-and-save method (and its companion the overlap-and-add method), which is used to convolve a very large sequence with a relatively smaller sequence. The MATLAB function `ovrlpsav` developed in that section uses the DFT to implement the linear convolution. We can now replace the DFT by the radix-2 FFT algorithm to obtain a *high-speed* overlap-and-save algorithm. To further reduce the computations, the FFT of the shorter (fixed) sequence can be computed only once. The following `hsolpsav` function shows this algorithm.

```
function [y] = hsolpsav(x,h,N)
% High-speed Overlap-Save method of block convolutions using FFT
%
% [y] = hsolpsav(x,h,N)
% y = output sequence
% x = input sequence
% h = impulse response
% N = block length (must be a power of two)
%
N = 2^(ceil(log10(N)/log10(2)));
Lenx = length(x); M = length(h);
M1 = M-1; L = N-M1; h = fft(h,N);
%
x = [zeros(1,M1), x, zeros(1,N-1)];
K = floor((Lenx+M1-1)/(L)); % # of blocks
Y = zeros(K+1,N);
for k=0:K
    xk = fft(x(k*L+1:k*L+N));
    Y(k+1,:) = real(ifft(xk.*h));
end
Y = Y(:,M:N)'; y = (Y(:))';
```

A similar modification can be done to the overlap-and-add algorithm. MATLAB also provides the function `fftfilt` to implement the overlap-and-add algorithm.

## 5.7 PROBLEMS

---

**P5.1** Compute the DFS coefficients of the following periodic sequences using the DFS definition, and then verify your answers using MATLAB.

1.  $\tilde{x}_1(n) = \{4, 1, -1, 1\}, N = 4$
2.  $\tilde{x}_2(n) = \{2, 0, 0, 0, -1, 0, 0, 0\}, N = 8$
3.  $\tilde{x}_3(n) = \{1, 0, -1, -1, 0\}, N = 5$
4.  $\tilde{x}_4(n) = \{0, 0, 2j, 0, 2j, 0\}, N = 6$
5.  $\tilde{x}_5(n) = \{3, 2, 1\}, N = 3$

**P5.2** Determine the periodic sequences given the following periodic DFS coefficients. First use the IDFS definition, and then verify your answers using MATLAB.

1.  $\tilde{X}_1(k) = \{4, 3j, -3j\}, N = 3$
2.  $\tilde{X}_2(k) = \{j, 2j, 3j, 4j\}, N = 4$
3.  $\tilde{X}_3(k) = \{1, 2 + 3j, 4, 2 - 3j\}, N = 4$
4.  $\tilde{X}_4(k) = \{0, 0, 2, 0, 0\}, N = 5$
5.  $\tilde{X}_5(k) = \{3, 0, 0, 0, -3, 0, 0, 0\}, N = 8$

**P5.3** Let  $\tilde{x}_1(n)$  be periodic with fundamental period  $N = 40$ , where one period is given by

$$\tilde{x}_1(n) = \begin{cases} 5 \sin(0.1\pi n), & 0 \leq n \leq 19 \\ 0, & 20 \leq n \leq 39 \end{cases}$$

and let  $\tilde{x}_2(n)$  be periodic with fundamental period  $N = 80$ , where one period is given by

$$\tilde{x}_2(n) = \begin{cases} 5 \sin(0.1\pi n), & 0 \leq n \leq 19 \\ 0, & 20 \leq n \leq 79 \end{cases}$$

These two periodic sequences differ in their periodicity but otherwise have the same nonzero samples.

1. Compute the DFS  $\tilde{X}_1(k)$  of  $\tilde{x}_1(n)$ , and plot samples (using the `stem` function) of its magnitude and angle versus  $k$ .
2. Compute the DFS  $\tilde{X}_2(k)$  of  $\tilde{x}_2(n)$ , and plot samples of its magnitude and angle versus  $k$ .
3. What is the difference between the two preceding DFS plots?

**P5.4** Consider the periodic sequence  $\tilde{x}_1(n)$  given in Problem P5.3. Let  $\tilde{x}_2(n)$  be periodic with fundamental period  $N = 40$ , where one period is given by

$$\tilde{x}_2(n) = \begin{cases} \tilde{x}_1(n), & 0 \leq n \leq 19 \\ -\tilde{x}_1(n - 20), & 20 \leq n \leq 39 \end{cases}$$

1. Determine analytically the DFS  $\tilde{X}_2(k)$  in terms of  $\tilde{X}_1(k)$ .
2. Compute the DFS  $\tilde{X}_2(k)$  of  $\tilde{x}_2(n)$ , and plot samples of its magnitude and angle versus  $k$ .
3. Verify your answer in part 1 using the plots of  $\tilde{X}_1(k)$  and  $\tilde{X}_2(k)$ ?

**P5.5** Consider the periodic sequence  $\tilde{x}_1(n)$  given in Problem P5.3. Let  $\tilde{x}_3(n)$  be periodic with period 80, obtained by concatenating two periods of  $\tilde{x}_1(n)$ , that is,

$$\tilde{x}_3(n) = [\tilde{x}_1(n), \tilde{x}_1(n)]_{\text{PERIODIC}}$$

Clearly,  $\tilde{x}_3(n)$  is different from  $\tilde{x}_2(n)$  of Problem P5.3 even though both of them are periodic with period 80.

1. Compute the DFS  $\tilde{X}_3(k)$  of  $\tilde{x}_3(n)$ , and plot samples of its magnitude and angle versus  $k$ .
2. What effect does the periodicity doubling have on the DFS?
3. Generalize this result to  $M$ -fold periodicity. In particular, show that if

$$\tilde{x}_M(n) = \left[ \underbrace{\tilde{x}_1(n), \tilde{x}_1(n), \dots, \tilde{x}_1(n)}_{M \text{ times}} \right]_{\text{PERIODIC}}$$

then

$$\begin{aligned} \tilde{X}_M(Mk) &= M\tilde{X}_1(k), \quad k = 0, 1, \dots, N-1 \\ \tilde{X}_M(k) &= 0, \quad \quad \quad k \neq 0, M, \dots, MN \end{aligned}$$

**P5.6** Let  $X(e^{j\omega})$  be the DTFT of a finite-length sequence

$$x(n) = \begin{cases} n+1, & 0 \leq n \leq 49 \\ 100-n, & 50 \leq n \leq 99 \\ 0, & \text{otherwise} \end{cases}$$

1. Let

$$y_1(n) = \overset{10\text{-point}}{\text{IDFS}} \left[ X(e^{j0}), X(e^{j2\pi/10}), X(e^{j4\pi/10}), \dots, X(e^{j18\pi/10}) \right]$$

Determine  $y_1(n)$  using the frequency sampling theorem. Verify your answer using MATLAB.

2. Let

$$y_2(n) = \overset{200\text{-point}}{\text{IDFS}} \left[ X(e^{j0}), X(e^{j2\pi/200}), X(e^{j4\pi/200}), \dots, X(e^{j398\pi/200}) \right]$$

Determine  $y_2(n)$  using the frequency sampling theorem. Verify your answer using MATLAB.

3. Comment on your results in parts (a) and (b).

**P5.7** Let  $\tilde{x}(n)$  be a periodic sequence with period  $N$ , and let

$$\tilde{y}(n) \stackrel{\Delta}{=} \tilde{x}(-n) = \tilde{x}(N-n)$$

that is,  $\tilde{y}(n)$  is a periodically folded version of  $\tilde{x}(n)$ . Let  $\tilde{X}(k)$  and  $\tilde{Y}(k)$  be the DFS sequences.

1. Show that

$$\tilde{Y}(k) = \tilde{X}(-k) = \tilde{X}(N-k)$$

that is,  $\tilde{Y}(k)$  is also a periodically folded version of  $\tilde{X}(k)$ .

2. Let  $\tilde{x}(n) = \{2, 4, 6, 1, 3, 5\}_{\text{PERIODIC}}$  with  $N = 6$ .

- (a) Sketch  $\tilde{y}(n)$  for  $0 \leq n \leq 5$ .
- (b) Compute  $\tilde{X}(k)$  for  $0 \leq k \leq 5$ .
- (c) Compute  $\tilde{Y}(k)$  for  $0 \leq k \leq 5$ .
- (d) Verify the relation in part 1.

**P5.8** Consider the following finite-length sequence:

$$x(n) = \begin{cases} \text{sinc}^2\{(n - 50)/2\}, & 0 \leq n \leq 100 \\ 0, & \text{else} \end{cases}$$

1. Determine the DFT  $X(k)$  of  $x(n)$ . Plot (using the `stem` function) its magnitude and phase.
2. Plot the magnitude and phase of the DTFT  $X(e^{j\omega})$  of  $x(n)$  using MATLAB.
3. Verify that the above DFT is the sampled version of  $X(e^{j\omega})$ . It might be helpful to combine the above two plots in one graph using the `hold` function.
4. Is it possible to reconstruct the DTFT  $X(e^{j\omega})$  from the DFT  $X(k)$ ? If possible, give the necessary interpolation formula for reconstruction. If not possible, state why this reconstruction cannot be done.

**P5.9** Let a finite-length sequence be given by

$$x(n) = \begin{cases} 2e^{-0.9|n|}, & -5 \leq n \leq 5 \\ 0, & \text{otherwise} \end{cases}$$

Plot the DTFT  $X(e^{j\omega})$  of the above sequence using DFT as a computation tool. Choose the length  $N$  of the DFT so that this plot appears to be a smooth graph.

**P5.10** Plot the DTFT magnitude and angle of each of the following sequences using the DFT as a computation tool. Make an educated guess about the length  $N$  so that your plots are meaningful.

1.  $x(n) = (0.6)^{|n|} [u(n + 10) - u(n - 11)]$
2.  $x(n) = n(0.9)^n [u(n) - u(n - 21)]$
3.  $x(n) = [\cos(0.5\pi n) + j \sin(0.5\pi n)][u(n) - u(n - 51)]$
4.  $x(n) = \{1, 2, 3, 4, 3, 2, 1\}$   
↑
5.  $x(n) = \{-1, -2, -3, 0, 3, 2, 1\}$   
↑

**P5.11** Let  $H(e^{j\omega})$  be the frequency response of a real, causal discrete-time LSI system.

1. If

$$\operatorname{Re} \left\{ H \left( e^{j\omega} \right) \right\} = \sum_{k=0}^5 (0.9)^k \cos(k\omega)$$

determine the impulse response  $h(n)$  analytically. Verify your answer using DFT as a computation tool. Choose the length  $N$  appropriately.

2. If

$$\operatorname{Im} \left\{ H \left( e^{j\omega} \right) \right\} = \sum_{\ell=0}^5 2\ell \sin(\ell\omega), \quad \text{and} \quad \int_{-\pi}^{\pi} H(e^{j\omega}) d\omega = 0$$

determine the impulse response  $h(n)$  analytically. Verify your answer using DFT as a computation tool. Again choose the length  $N$  appropriately.

**P5.12** Let  $X(k)$  denote the  $N$ -point DFT of an  $N$ -point sequence  $x(n)$ . The DFT  $X(k)$  itself is an  $N$ -point sequence.

1. If the DFT of  $X(k)$  is computed to obtain another  $N$ -point sequence  $x_1(n)$ , show that

$$x_1(n) = Nx((-n))_N, \quad 0 \leq n \leq N - 1$$

2. Using this property, design a MATLAB function to implement an  $N$ -point circular folding operation  $x_2(n) = x_1((-n))_N$ . The format should be

```
x2 = circfold(x1,N)
% Circular folding using DFT
% x2 = circfold(x1,N)
% x2 = circularly folded output sequence
% x1 = input sequence of length <= N
% N = circular buffer length
```

3. Determine the circular folding of the following sequence:

$$x_1(n) = \{1, 3, 5, 7, 9, -7, -5, -3, -1\}$$

**P5.13** Let  $X(k)$  be an  $N$ -point DFT of an  $N$ -point sequence  $x(n)$ . Let  $N$  be an even integer.

1. If  $x(n) = x(n + N/2)$  for all  $n$ , then show that  $X(k) = 0$  for  $k$  odd (i.e., nonzero for  $k$  even). Verify this result for  $x(n) = \{1, 2, -3, 4, 5, 1, 2, -3, 4, 5\}$ .
2. If  $x(n) = -x(n + N/2)$  for all  $n$ , then show that  $X(k) = 0$  for  $k$  even (i.e., nonzero for  $k$  odd). Verify this result for  $x(n) = \{1, 2, -3, 4, 5, -1, -2, 3, -4, -5\}$ .

**P5.14** Let  $X(k)$  be an  $N$ -point DFT of an  $N$ -point sequence  $x(n)$ . Let  $N = 4\nu$  where  $\nu$  is an integer.

1. If  $x(n) = x(n + \nu)$  for all  $n$ , then show that  $X(k)$  is nonzero for  $k = 4\ell$  for  $0 \leq \ell \leq \nu - 1$ . Verify this result for  $x(n) = \{1, 2, 3, 1, 2, 3, 1, 2, 3, 1, 2, 3\}$ .
2. If  $x(n) = -x(n + \nu)$  for all  $n$ , then show that  $X(k)$  is nonzero for  $k = 4\ell + 2$  for  $0 \leq \ell \leq \nu - 1$ . Verify this result for  $x(n) = \{1, 2, 3, -1, -2, -3, 1, 2, 3, -1, -2, -3\}$ .

**P5.15** Let  $X(k)$  be an  $N$ -point DFT of an  $N$ -point sequence  $x(n)$ . Let  $N = 2\mu\nu$  where  $\mu$  and  $\nu$  are integers.

1. If  $x(n) = x(n + \nu)$  for all  $n$ , then show that  $X(k)$  is nonzero for  $k = 2(\mu\ell)$  for  $0 \leq \ell \leq \nu - 1$ . Verify this result for  $x(n) = \{1, -2, 3, 1, -2, 3, 1, -2, 3, 1, -2, 3, 1, -2, 3\}$ .
2. If  $x(n) = -x(n + \nu)$  for all  $n$ , then show that  $X(k)$  is nonzero for  $k = 2(\mu\ell + 1)$  for  $0 \leq \ell \leq \nu - 1$ . Verify this result for  $x(n) = \{1, -2, 3, -1, 2, -3, 1, -2, 3, -1, 2, -3, 1, -2, 3, -1, 2, -3\}$ .

**P5.16** Let  $X(k)$  and  $Y(k)$  be 10-point DFTs of two 10-point sequences  $x(n)$  and  $y(n)$ , respectively. If

$$X(k) = \exp(j0.2\pi k), \quad 0 \leq k \leq 9$$

determine  $Y(k)$  in each of the following cases without computing the DFT.

1.  $y(n) = x((n - 5))_{10}$
2.  $y(n) = x((n + 4))_{10}$
3.  $y(n) = x((3 - n))_{10}$
4.  $y(n) = x(n)e^{j3\pi n/5}$
5.  $y(n) = x(n) \textcircled{10} x((-n))_{10}$

Verify your answers using MATLAB.

**P5.17** The first six values of the 10-point DFT of a real-valued sequence  $x(n)$  are given by

$$\{10, -2 + j3, 3 + j4, 2 - j3, 4 + j5, 12\}$$

Determine the DFT of each of the following sequences using DFT properties.

1.  $x_1(n) = x((2 - n))_{10}$
2.  $x_2(n) = x((n + 5))_{10}$
3.  $x_3(n) = x(n)x((-n))_{10}$
4.  $x_4(n) = x(n) \textcircled{10} x((-n))_{10}$
5.  $x_5(n) = x(n)e^{-j4\pi n/5}$

**P5.18** Complex-valued  $N$ -point sequence  $x(n)$  can be decomposed into  $N$ -point circular-conjugate-symmetric and circular-conjugate-antisymmetric sequences using the following relations:

$$x_{\text{ccs}}(n) \triangleq \frac{1}{2} [x(n) + x^*((-n))_N]$$

$$x_{\text{cca}}(n) \triangleq \frac{1}{2} [x(n) - x^*((-n))_N]$$

If  $X_R(k)$  and  $X_I(k)$  are the real and imaginary parts of the  $N$ -point DFT of  $x(n)$ , then

$$\text{DFT}[x_{\text{ccs}}(n)] = X_R(k) \quad \text{and} \quad \text{DFT}[x_{\text{cca}}(n)] = jX_I(k)$$

1. Prove these relations property analytically.
2. Modify the `circevod` function developed in the chapter so that it can be used for complex-valued sequences.
3. Let  $X(k) = [3 \cos(0.2\pi k) + j4 \sin(0.1\pi k)][u(k) - u(k - 20)]$  be a 20-point DFT. Verify this symmetry property using your `circevod` function.

**P5.19** If  $X(k)$  is the  $N$ -point DFT of an  $N$ -point complex-valued sequence

$$x(n) = x_R(n) + jx_I(n)$$

where  $x_R(n)$  and  $x_I(n)$  are the real and imaginary parts of  $x(n)$ , then

$$\text{DFT}[x_R(n)] = X_{\text{ccs}}(k) \quad \text{and} \quad \text{DFT}[jx_I(n)] = X_{\text{cca}}(k)$$

where  $X_{\text{ccs}}(k)$  and  $X_{\text{cca}}(k)$  are the circular-even and circular-odd components of  $X(k)$  as defined in Problem P5.18.

1. Prove this property analytically.
2. This property can be used to compute the DFTs of two real-valued  $N$ -point sequences using one  $N$ -point DFT operation. Specifically, let  $x_1(n)$  and  $x_2(n)$  be two  $N$ -point sequences. Then we can form a complex-valued sequence

$$x(n) = x_1(n) + jx_2(n)$$

and use this property. Develop a MATLAB function to implement this approach with the following format.

```
function [X1,X2] = real2dft(x1,x2,N)
% DFTs of two real sequences
% [X1,X2] = real2dft(x1,x2,N)
% X1 = n-point DFT of x1
% X2 = n-point DFT of x2
% x1 = sequence of length <= N
% x2 = sequence of length <= N
% N = length of DFT
```

3. Compute and plot the DFTs of the following two sequences using this function:

$$x_1(n) = \cos(0.1\pi n), x_2(n) = \sin(0.2\pi n); \quad 0 \leq n \leq 39$$

- P5.20** Using the frequency domain approach, devise a MATLAB function to determine a circular shift  $x((n-m))_N$ , given an  $N_1$ -point sequence  $x(n)$  where  $N_1 \leq N$ . Your function should have the following format.

```
function y = cirshftf(x,m,N)
% Circular shift of m samples wrt size N in sequence x: (freq domain)
%
% -----
% y = cirshftf(x,m,N)
%     y : output sequence containing the circular shift
%     x : input sequence of length <= N
%     m : sample shift
%     N : size of circular buffer
% Method: y(n) = idft(dft(x(n))*WN^(mk))
%
% If m is a scalar then y is a sequence (row vector)
% If m is a vector then y is a matrix, each row is a circular shift
%     in x corresponding to entries in vector m
% M and x should not be matrices
```

Verify your function on the following sequence:

$$x(n) = \{5, 4, 3, 2, 1, 0, 0, 1, 2, 3, 4\}, \quad 0 \leq n \leq 10$$

with (a)  $m = -5$ ,  $N = 12$  and (b)  $m = 8$ ,  $N = 15$ .

- P5.21** Using the analysis and synthesis equations of the DFT, show that the energy of a sequence satisfies

$$\mathcal{E}_X \triangleq \sum_{n=0}^{N-1} |x(n)|^2 = \frac{1}{N} \sum_{k=0}^{N-1} |X(k)|^2$$

This is commonly referred to as a *Parseval's relation for the DFT*. Verify this relation using MATLAB on the sequence in Problem P5.20.

**P5.22** A 512-point DFT  $X(k)$  of a real-valued sequence  $x(n)$  has the DFT values

$$\begin{aligned} X(0) &= 20 + j\alpha; & X(5) &= 20 + j30; & X(k_1) &= -10 + j15; & X(152) &= 17 + j23; \\ X(k_2) &= 20 - j30; & X(k_3) &= 17 - j23; & X(480) &= -10 - j15; & X(256) &= 30 + j\beta \end{aligned}$$

and all other values are known to be zero.

1. Determine the real-valued coefficients  $\alpha$  and  $\beta$ .
2. Determine the values of the integers  $k_1$ ,  $k_2$ , and  $k_3$ .
3. Determine the energy of the signal  $x(n)$ .
4. Express the sequence  $x(n)$  in a closed form.

**P5.23** Let  $x(n)$  be a finite length sequence given by

$$x(n) = \left\{ \dots, 0, 0, 0, \underset{\uparrow}{1}, 2, -3, 4, -5, 0, \dots \right\}$$

Determine and sketch the sequence  $x((-8 - n))_7 \mathcal{R}_7(n)$  where

$$\mathcal{R}_7(n) = \begin{cases} 1, & 0 \leq n \leq 6 \\ 0, & \text{elsewhere} \end{cases}$$

**P5.24** The `circonv` function developed in this chapter implements the circular convolution as a matrix-vector multiplication. The matrix corresponding to the circular shifts  $\{x((n - m))_N; 0 \leq n \leq N - 1\}$  has an interesting structure. This matrix is called a *circulant* matrix, which is a special case of Toeplitz matrix introduced in Chapter 2.

1. Consider the sequences given in Example 5.13. Express  $x_1(n)$  as a column vector  $\mathbf{x}_1$  and  $x_2((n - m))_N$  as a circulant matrix  $\mathbf{X}_2$  with rows corresponding to  $n = 0, 1, 2, 3$ . Characterize this matrix  $\mathbf{X}_2$ . Can it completely be described by its first row (or column)?
2. Determine the circular convolution as  $\mathbf{X}_2 \mathbf{x}_1$  and verify your calculations.

**P5.25** Develop a MATLAB function to construct a circulant matrix  $\mathbf{C}$  given an  $N$ -point sequence  $x(n)$ . Use the `toeplitz` function to implement matrix  $\mathbf{C}$ . Your subroutine function should have the following format.

```
function [C] = circulant(x,N)
% Circulant Matrix from an N-point sequence
% [C] = circulant(x,N)
% C = circulant matrix of size NxN
% x = sequence of length <= N
% N = size of circulant matrix
```

Using this function, modify the circular convolution function `circonv` discussed in the chapter so that the `for...end` loop is eliminated. Verify your functions on the sequences in Problem P5.24.

**P5.26** Using the frequency domain approach, devise a MATLAB function to implement the circular convolution operation between two sequences. The format of the sequence should be

```

function x3 = circonvf(x1,x2,N)
% Circular convolution in the frequency domain
% x3 = circonvf(x1,x2,N)
% x3 = convolution result of length N
% x1 = sequence of length <= N
% x2 = sequence of length <= N
% N = length of circular buffer

```

Using your function, compute the circular convolution  $\{4, 3, 2, 1\} \odot \{1, 2, 3, 4\}$ .

**P5.27** The following four sequences are given:

$$x_1(n) = \begin{cases} 1, 3, 2, -1 \\ \uparrow \end{cases}; x_2(n) = \begin{cases} 2, 1, 0, -1 \\ \uparrow \end{cases}; x_3(n) = x_1(n) * x_2(n); x_4(n) = x_1(n) \odot x_2(n)$$

1. Determine and sketch  $x_3(n)$ .
2. Using  $x_3(n)$  alone, determine and sketch  $x_4(n)$ . Do not directly compute  $x_4(n)$ .

**P5.28** Compute the  $N$ -point circular convolution for the following sequences. Plot their samples.

1.  $x_1(n) = \sin(\pi n/3)\mathcal{R}_6(n), x_2(n) = \cos(\pi n/4)\mathcal{R}_8(n); N = 10$
2.  $x_1(n) = \cos(2\pi n/N)\mathcal{R}_N(n), x_2(n) = \sin(2\pi n/N)\mathcal{R}_N(n); N = 32$
3.  $x_1(n) = (0.8)^n \mathcal{R}_N(n), x_2(n) = (-0.8)^n \mathcal{R}_N(n); N = 20$
4.  $x_1(n) = n\mathcal{R}_N(n), x_2(n) = (N-n)\mathcal{R}_N(n); N = 10$
5.  $x_1(n) = (0.8)^n R_{20}, x_2(n) = u(n) - u(n-40); N = 50$

**P5.29** Let  $x_1(n)$  and  $x_2(n)$  be two  $N$ -point sequences.

1. If  $y(n) = x_1(n) \odot x_2(n)$  show that

$$\sum_{n=0}^{N-1} y(n) = \left( \sum_{n=0}^{N-1} x_1(n) \right) \left( \sum_{n=0}^{N-1} x_2(n) \right)$$

2. Verify this result for the following sequences:

$$x_1(n) = \{9, 4, -1, 4, -4, -1, 8, 3\}; x_2(n) = \{-5, 6, 2, -7, -5, 2, 2, -2\}$$

**P5.30** Let  $X(k)$  be the eight-point DFT of a three-point sequence  $x(n) = \{5, -4, 3\}$ . Let  $Y(k)$  be the eight-point DFT of a sequence  $y(n)$ . Determine  $y(n)$  when  $Y(k) = W_8^{5k} X(-k)_8$ .

**P5.31** For the following sequences, compute (i) the  $N$ -point circular convolution  $x_3(n) = x_1(n) \odot x_2(n)$ , (ii) the linear convolution  $x_4(n) = x_1(n) * x_2(n)$ , and (iii) the error sequence  $e(n) = x_3(n) - x_4(n)$ .

1.  $x_1(n) = \{1, 1, 1, 1\}, x_2(n) = \cos(\pi n/4)\mathcal{R}_6(n); N = 8$
2.  $x_1(n) = \cos(2\pi n/N)\mathcal{R}_{16}(n), x_2(n) = \sin(2\pi n/N)\mathcal{R}_{16}(n); N = 32$
3.  $x_1(n) = (0.8)^n \mathcal{R}_{10}(n), x_2(n) = (-0.8)^n \mathcal{R}_{10}(n); N = 15$
4.  $x_1(n) = n\mathcal{R}_{10}(n), x_2(n) = (N-n)\mathcal{R}_{10}(n); N = 10$
5.  $x_1(n) = \{1, -1, 1, -1\}, x_2(n) = \{1, 0, -1, 0\}; N = 5$

In each case, verify that  $e(n) = x_4(n + N)$ .

- P5.32** The overlap-add method of block convolution is an alternative to the overlap-save method. Let  $x(n)$  be a long sequence of length  $ML$  where  $M, L \gg 1$ . Divide  $x(n)$  into  $M$  segments  $\{x_m(n), m = 1, \dots, M\}$  each of length  $L$

$$x_m(n) = \begin{cases} x(n), & mL \leq n \leq (m+1)L-1 \\ 0, & \text{elsewhere} \end{cases} \quad \text{so that} \quad x(n) = \sum_{m=0}^{M-1} x_m(n)$$

Let  $h(n)$  be an  $L$ -point impulse response. Then

$$y(n) = x(n) * h(n) = \sum_{m=0}^{M-1} x_m(n) * h(n) = \sum_{m=0}^{M-1} y_m(n); \quad y_m(n) \triangleq x_m(n) * h(n)$$

Clearly,  $y_m(n)$  is a  $(2L - 1)$ -point sequence. In this method, we have to save the intermediate convolution results and then properly overlap these before adding to form the final result  $y(n)$ . To use DFT for this operation, we have to choose  $N \geq (2L - 1)$ .

1. Develop a MATLAB function to implement the overlap-add method using the circular convolution operation. The format should be

```
function [y] = ovlpadd(x,h,N)
% Overlap-Add method of block convolution
% [y] = ovlpadd(x,h,N)
%
% y = output sequence
% x = input sequence
% h = impulse response
% N = block length >= 2*length(h)-1
```

2. Incorporate the radix-2 FFT implementation in this function to obtain a high-speed overlap-add block convolution routine. Remember to choose  $N = 2^\nu$ .
3. Verify your functions on the following two sequences:

$$x(n) = \cos(\pi n/500) \mathcal{R}_{4000}(n), \quad h(n) = \{1, -1, 1, -1\}$$

- P5.33** Given the following sequences  $x_1(n)$  and  $x_2(n)$ :

$$x_1(n) = \{2, 1, 1, 2\}, \quad x_2(n) = \{1, -1, -1, 1\}$$

1. Compute the circular convolution  $x_1(n) \odot x_2(n)$  for  $N = 4, 7$ , and  $8$ .
2. Compute the linear convolution  $x_1(n) * x_2(n)$ .
3. Using results of calculations, determine the minimum value of  $N$  necessary so that linear and circular convolutions are the same on the  $N$ -point interval.
4. Without performing the actual convolutions, explain how you could have obtained the result of P5.33.3.

- P5.34** Let

$$x(n) = \begin{cases} A \cos(2\pi\ell n/N), & 0 \leq n \leq N-1 \\ 0, & \text{elsewhere} \end{cases} = A \cos(2\pi\ell n/N) \mathcal{R}_N(n)$$

where  $\ell$  is an integer. Notice that  $x(n)$  contains *exactly*  $\ell$  periods (or cycles) of the cosine waveform in  $N$  samples. This is a windowed cosine sequence containing *no leakage*.

1. Show that the DFT  $X(k)$  is a real sequence given by

$$X(k) = \frac{AN}{2} \delta(k - \ell) + \frac{AN}{2} \delta(k - N + \ell); \quad 0 \leq k \leq (N - 1), \quad 0 < \ell < N$$

2. Show that if  $\ell = 0$ , then the DFT  $X(k)$  is given by

$$X(k) = AN\delta(k); \quad 0 \leq k \leq (N - 1)$$

3. Explain clearly how these results should be modified if  $\ell < 0$  or  $\ell > N$ .
4. Verify the results of parts 1, 2, and 3 using the following sequences. Plot the real parts of the DFT sequences using the `stem` function.
  - (a)  $x_1(n) = 3 \cos(0.04\pi n) \mathcal{R}_{200}(n)$
  - (b)  $x_2(n) = 5\mathcal{R}_{50}(n)$
  - (c)  $x_3(n) = [1 + 2 \cos(0.5\pi n) + \cos(\pi n)] \mathcal{R}_{100}(n)$
  - (d)  $x_4(n) = \cos(25\pi n/16) \mathcal{R}_{64}(n)$
  - (e)  $x_5(n) = [4 \cos(0.1\pi n) - 3 \cos(1.9\pi n)] \mathcal{R}_{40}(n)$

**P5.35** Let  $x(n) = A \cos(\omega_0 n) \mathcal{R}_N(n)$ , where  $\omega_0$  is a real number.

1. Using the properties of the DFT, show that the real and the imaginary parts of  $X(k)$  are given by

$$\begin{aligned} X(k) &= X_R(k) + jX_I(k) \\ X_R(k) &= (A/2) \cos\left[\frac{\pi(N-1)}{N}(k - f_0 N)\right] \frac{\sin[\pi(k - f_0 N)]}{\sin[\pi(k - f_0 N)/N]} \\ &\quad + (A/2) \cos\left[\frac{\pi(N-1)}{N}(k + f_0 N)\right] \frac{\sin[\pi(k - N + f_0 N)]}{\sin[\pi(k - N + f_0 N)/N]} \\ X_I(k) &= -(A/2) \sin\left[\frac{\pi(N-1)}{N}(k - f_0 N)\right] \frac{\sin[\pi(k - f_0 N)]}{\sin[\pi(k - f_0 N)/N]} \\ &\quad - (A/2) \sin\left[\frac{\pi(N-1)}{N}(k + f_0 N)\right] \frac{\sin[\pi(k - N + f_0 N)]}{\sin[\pi(k - N + f_0 N)/N]} \end{aligned}$$

2. This result implies that the original frequency  $\omega_0$  of the cosine waveform has *leaked* into other frequencies that form the harmonics of the time-limited sequence, and hence it is called the leakage property of cosines. It is a natural result due to the fact that bandlimited periodic cosines are sampled over noninteger periods. Explain this result using the periodic extension  $\tilde{x}(n)$  of  $x(n)$  and the result in Problem P5.34.1.
3. Verify the leakage property using  $x(n) = \cos(5\pi n/99) \mathcal{R}_{200}(n)$ . Plot the real and the imaginary parts of  $X(k)$  using the `stem` function.

**P5.36** Let

$$x(n) = \begin{cases} A \sin(2\pi\ell n/N), & 0 \leq n \leq N-1 \\ 0, & \text{elsewhere} \end{cases} = A \sin(2\pi\ell n/N) \mathcal{R}_N(n)$$

where  $\ell$  is an integer. Notice that  $x(n)$  contains *exactly*  $\ell$  periods (or cycles) of the sine waveform in  $N$  samples. This is a windowed sine sequence containing *no leakage*.

1. Show that the DFT  $X(k)$  is a purely imaginary sequence given by

$$X(k) = \frac{AN}{2j} \delta(k - \ell) - \frac{AN}{2j} \delta(k - N + \ell); \quad 0 \leq k \leq (N - 1), \quad 0 < \ell < N$$

2. Show that if  $\ell = 0$ , then the DFT  $X(k)$  is given by

$$X(k) = 0; \quad 0 \leq k \leq (N - 1)$$

3. Explain clearly how these results should be modified if  $\ell < 0$  or  $\ell > N$ .
4. Verify the results of parts 1, 2, and 3 using the following sequences. Plot the imaginary parts of the DFT sequences using the `stem` function.
  - (a)  $x_1(n) = 3 \sin(0.04\pi n) \mathcal{R}_{200}(n)$
  - (b)  $x_2(n) = 5 \sin 10\pi n \mathcal{R}_{50}(n)$
  - (c)  $x_3(n) = [2 \sin(0.5\pi n) + \sin(\pi n)] \mathcal{R}_{100}(n)$
  - (d)  $x_4(n) = \sin(25\pi n/16) \mathcal{R}_{64}(n)$
  - (e)  $x_5(n) = [4 \sin(0.1\pi n) - 3 \sin(1.9\pi n)] \mathcal{R}_{20}(n)$

**P5.37** Let  $x(n) = A \sin(\omega_0 n) \mathcal{R}_N(n)$ , where  $\omega_0$  is a real number.

1. Using the properties of the DFT, show that the real and the imaginary parts of  $X(k)$  are given by

$$\begin{aligned} X(k) &= X_R(k) + jX_I(k) \\ X_R(k) &= -(A/2) \sin \left[ \frac{\pi(N-1)}{N} (k - f_0 N) \right] \frac{\sin [\pi (k - f_0 N)]}{\sin [\pi (k - f_0 N)/N]} \\ &\quad + (A/2) \sin \left[ \frac{\pi(N-1)}{N} (k + f_0 N) \right] \frac{\sin [\pi (k - N + f_0 N)]}{\sin [\pi (k - N + f_0 N)/N]} \\ X_I(k) &= -(A/2) \cos \left[ \frac{\pi(N-1)}{N} (k - f_0 N) \right] \frac{\sin [\pi (k - f_0 N)]}{\sin [\pi (k - f_0 N)/N]} \\ &\quad + (A/2) \cos \left[ \frac{\pi(N-1)}{N} (k + f_0 N) \right] \frac{\sin [\pi (k - N + f_0 N)]}{\sin [\pi (k - N + f_0 N)/N]} \end{aligned}$$

2. This result is the leakage property of sines. Explain it using the periodic extension  $\tilde{x}(n)$  of  $x(n)$  and the result in Problem P5.36.1.
3. Verify the leakage property using  $x(n) = \sin(5\pi n/99) \mathcal{R}_{100}(n)$ . Plot the real and the imaginary parts of  $X(k)$  using the `stem` function.

**P5.38** An analog signal  $x_a(t) = 2 \sin(4\pi t) + 5 \cos(8\pi t)$  is sampled at  $t = 0.01n$  for  $n = 0, 1, \dots, N - 1$  to obtain an  $N$ -point sequence  $x(n)$ . An  $N$ -point DFT is used to obtain an estimate of the magnitude spectrum of  $x_a(t)$ .

1. From the following values of  $N$ , choose the one that will provide the accurate estimate of the spectrum of  $x_a(t)$ . Plot the real and imaginary parts of the DFT spectrum  $X(k)$ .
  - (a)  $N = 40$ ,
  - (b)  $N = 50$ ,
  - (c)  $N = 60$ .

2. From the following values of  $N$ , choose the one that will provide the least amount of leakage in the spectrum of  $x_a(t)$ . Plot the real and imaginary parts of the DFT spectrum  $X(k)$ .
- (a)  $N = 90$ ,    (b)  $N = 95$ ,    (c)  $N = 99$ .

**P5.39** Using (5.49), determine and draw the signal flow graph for the  $N = 8$  point, radix-2 decimation-in-frequency FFT algorithm. Using this flow graph, determine the DFT of the sequence

$$x(n) = \cos(\pi n/2), \quad 0 \leq n \leq 7$$

**P5.40** Using (5.49), determine and draw the signal flow graph for the  $N = 16$  point, radix-4 decimation-in-time FFT algorithm. Using this flow graph, determine the DFT of the sequence

$$x(n) = \cos(\pi n/2), \quad 0 \leq n \leq 15$$

**P5.41** Let  $x(n)$  be a uniformly distributed random number between  $[-1, 1]$  for  $0 \leq n \leq 10^6$ . Let

$$h(n) = \sin(0.4\pi n), \quad 0 \leq n \leq 100$$

1. Using the `conv` function, determine the output sequence  $y(n) = x(n) * h(n)$ .
2. Consider the overlap-and-save method of block convolution along with the FFT algorithm to implement high-speed block convolution. Using this approach, determine  $y(n)$  with FFT sizes of 1024, 2048, and 4096.
3. Compare these approaches in terms of the convolution results and their execution times.

# CHAPTER

---

# 6

## Implementation of Discrete-Time Filters

---

In earlier chapters, we studied the theory of discrete systems in both the time and frequency domains. We will now use this theory for the processing of digital signals. To process signals, we have to design and implement systems called *filters* (or spectrum analyzers in some contexts). The filter design issue is influenced by such factors as the type of the filter (i.e., IIR or FIR) and the form of its implementation (structures). Hence, before we discuss the design issue, we first concern ourselves with how these filters can be implemented in practice. This is an important concern because different filter structures dictate different design strategies.

IIR filters, as designed and used in DSP, can be modeled by rational system functions or, equivalently, by difference equations. Such filters are termed *autoregressive moving average (ARMA)* or, more generally, as *recursive* filters. Although ARMA filters include moving average filters that are FIR filters, we will treat FIR filters separately from IIR filters for both design and implementation purposes.

In addition to describing various filter structures, we also begin to consider problems associated with quantization effects when finite-precision arithmetic is used in the implementation. Digital hardware contains processing elements that use finite-precision arithmetic. When filters are implemented either in hardware or in software, filter coefficients as well as filter operations are subjected to the effects of these finite-precision operations. In this chapter, we treat the effects on filter frequency response

characteristics due to coefficient quantization. In Chapter 10, we will consider the round-off noise effects in the digital filter implementations.

We begin with a description of basic building blocks that are used to describe filter structures. In the subsequent sections, we briefly describe IIR, FIR, and lattice filter structures, respectively, and provide MATLAB functions to implement these structures. This is followed by a brief treatment of the representation of numbers and the resulting error characteristics, which is then used to analyze coefficient quantization effects.

## 6.1 BASIC ELEMENTS

---

Since our filters are LTI systems, we need the following three elements to describe digital filter structures. These elements are shown in Figure 6.1.

1. **Adder:** This element has two inputs and one output and is shown in Figure 6.1a. Note that the addition of three or more signals is implemented by successive two-input adders.
2. **Multiplier (gain):** This is a single-input, single-output element and is shown in Figure 6.1b. Note that the multiplication by 1 is understood and hence not explicitly shown.
3. **Delay element (shifter or memory):** This element delays the signal passing through it by one sample, as shown in Figure 6.1c. It is implemented by using a shift register.

Using these basic elements, we can now describe various structures of both IIR and FIR filters. MATLAB is a convenient tool in the development of these structures that require operations on polynomials.

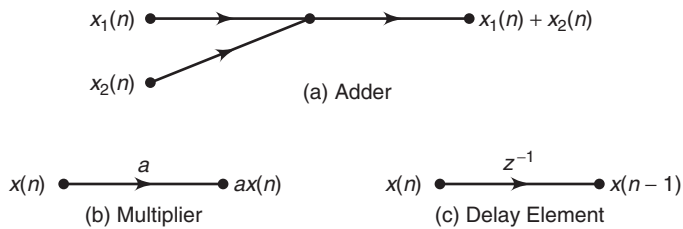


**FIGURE 6.1** Three basic elements

## 6.2 IIR FILTER STRUCTURES

---

The system function of an IIR filter is given by

$$H(z) = \frac{B(z)}{A(z)} = \frac{\sum_{n=0}^M b_n z^{-n}}{\sum_{n=0}^N a_n z^{-n}} = \frac{b_0 + b_1 z^{-1} + \cdots + b_M z^{-M}}{1 + a_1 z^{-1} + \cdots + a_N z^{-N}}; a_0 = 1 \quad (6.1)$$

where  $b_n$  and  $a_n$  are the coefficients of the filter. We have assumed without loss of generality that  $a_0 = 1$ . The order of such an IIR filter is called  $N$  if  $a_N \neq 0$ . The difference equation representation of an IIR filter is expressed as

$$y(n) = \sum_{m=0}^M b_m x(n-m) - \sum_{m=1}^N a_m y(n-m) \quad (6.2)$$

Three different structures can be used to implement an IIR filter:

1. **Direct form:** In this form, the difference equation (6.2) is implemented directly as given. There are two parts to this filter, namely the moving average part and the recursive part (or equivalently, the numerator and denominator parts). Therefore, this implementation leads to two versions: direct form I and direct form II structures.
2. **Cascade form:** In this form, the system function  $H(z)$  in equation (6.1) is factored into smaller second-order sections, called *biquads*. The system function is then represented as a *product* of these biquads. Each biquad is implemented in a direct form, and the entire system function is implemented as a *cascade* of biquad sections.
3. **Parallel form:** This is similar to the cascade form, but after factorization, a partial fraction expansion is used to represent  $H(z)$  as a *sum* of smaller second-order sections. Each section is again implemented in a direct form, and the entire system function is implemented as a *parallel* network of sections.

We will briefly discuss these forms in this section. IIR filters are generally described using the rational form version (or the direct form structure) of the system function. Hence we will provide MATLAB functions for converting direct form structures to cascade and parallel form structures.

### 6.2.1 DIRECT FORM

As the name suggests, the difference equation (6.2) is implemented as given using delays, multipliers, and adders. For the purpose of illustration, let  $M = N = 4$ . Then the difference equation is

$$\begin{aligned} y(n) = & b_0 x(n) + b_1 x(n-1) + b_2 x(n-2) + b_3 x(n-3) + b_4 x(n-4) \\ & - a_1 y(n-1) - a_2 y(n-2) - a_3 y(n-3) - a_4 y(n-4) \end{aligned}$$

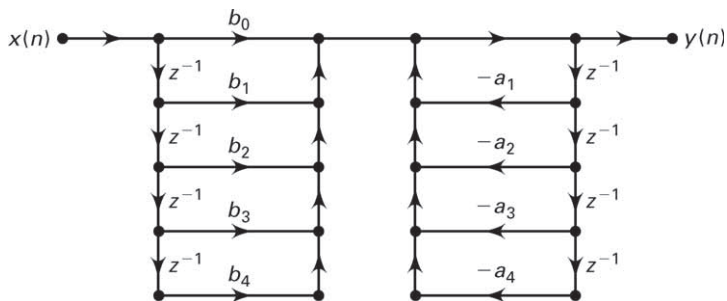


**FIGURE 6.2** Direct form I structure

which can be implemented as shown in Figure 6.2. This block diagram is called *direct form I* structure.

The direct form I structure implements each part of the rational function  $H(z)$  separately with a cascade connection between them. The numerator part is a tapped delay line followed by the denominator part, which is a feedback tapped delay line. Thus there are two separate delay lines in this structure, and hence it requires eight delay elements. We can reduce this delay element count or eliminate one delay line by interchanging the order in which the two parts are connected in the cascade. Now the two delay lines are close to each other, connected by a unity gain branch. Therefore, one delay line can be removed, and this reduction leads to a canonical structure called *direct form II* structure, shown in Figure 6.3. It should be noted that both direct forms are equivalent from the input-output point of view. Internally, however, they have different signals.

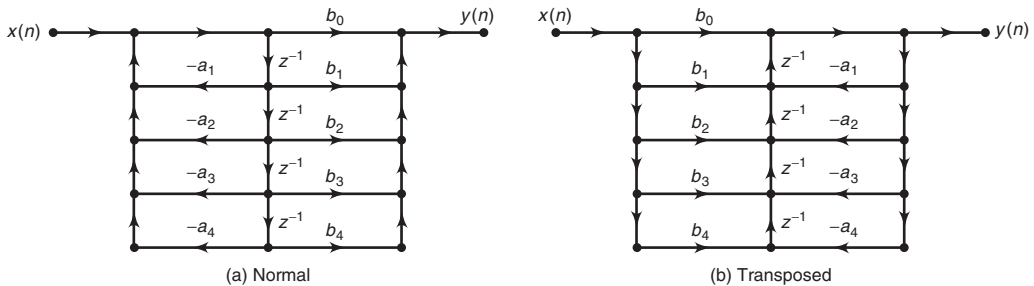


**FIGURE 6.3** Direct form II structure

### 6.2.2 TRANSPOSED STRUCTURE

An equivalent structure to the direct form can be obtained using a procedure called *transposition*. In this operation, three steps are performed:

1. All path arrow directions are reversed.
2. All branch nodes are replaced by adder nodes, and all adder nodes are replaced by branch nodes.
3. The input and output nodes are interchanged.

The resulting structure is called the *transposed direct form* structure. The transposed direct form II structure is shown in Figure 6.3b. Problem P6.3 explains this equivalent structure.

### 6.2.3 MATLAB IMPLEMENTATION

In MATLAB, the direct form structure is described by two row vectors: **b** containing the  $\{b_n\}$  coefficients and **a** containing the  $\{a_n\}$  coefficients. The **filter** function, which is discussed in Chapter 2, implements the transposed direct form II structure.

### 6.2.4 CASCADE FORM

In this form, the system function  $H(z)$  is written as a product of second-order sections with real coefficients. This is done by factoring the numerator and denominator polynomials into their respective roots and then combining either a complex conjugate root pair or any two real roots into second-order polynomials. In the remainder of this chapter, we assume that  $N$  is an even integer. Then

$$\begin{aligned} H(z) &= \frac{b_0 + b_1 z^{-1} + \cdots + b_N z^{-N}}{1 + a_1 z^{-1} + \cdots + a_N z^{-N}} \\ &= b_0 \frac{1 + \frac{b_1}{b_0} z^{-1} + \cdots + \frac{b_N}{b_0} z^{-N}}{1 + a_1 z^{-1} + \cdots + a_N z^{-N}} \\ &= b_0 \prod_{k=1}^K \frac{1 + B_{k,1} z^{-1} + B_{k,2} z^{-2}}{1 + A_{k,1} z^{-1} + A_{k,2} z^{-2}} \end{aligned} \quad (6.3)$$

where  $K$  is equal to  $\frac{N}{2}$  and  $B_{k,1}$ ,  $B_{k,2}$ ,  $A_{k,1}$ , and  $A_{k,2}$  are real numbers representing the coefficients of second-order sections. The second-order section

$$H_k(z) = \frac{Y_{k+1}(z)}{Y_k(z)} = \frac{1 + B_{k,1} z^{-1} + B_{k,2} z^{-2}}{1 + A_{k,1} z^{-1} + A_{k,2} z^{-2}}; \quad k = 1, \dots, K$$

with

$$Y_1(z) = b_0 X(z); \quad Y_{K+1}(z) = Y(z)$$

is called the  $k$ th biquad section. The input to the  $k$ th biquad section is the output from the  $(k - 1)$ th biquad section, and the output from the

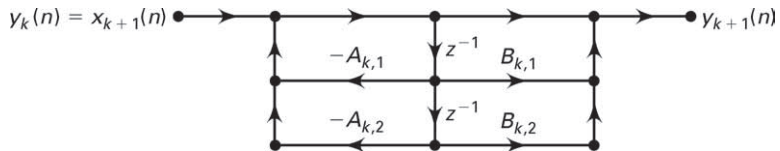


**FIGURE 6.4** Biquad section structure

$k$ th biquad is the input to the  $(k+1)$ th biquad. Now each biquad section  $H_k(z)$  can be implemented in direct form II, as shown in Figure 6.4. The entire filter is then implemented as a cascade of biquads.

As an example, consider  $N = 4$ . Figure 6.5 shows a cascade form structure for this fourth-order IIR filter.

### 6.2.5 MATLAB IMPLEMENTATION

Given the coefficients  $\{b_n\}$  and  $\{a_n\}$  of the direct form filter, we have to obtain the coefficients  $b_0$ ,  $\{B_{k,i}\}$ , and  $\{A_{k,i}\}$ . This is done by the following function `dir2cas`.

```

function [b0,B,A] = dir2cas(b,a)
% DIRECT form to CASCADE form conversion (cplxpair version)
%
% [b0,B,A] = dir2cas(b,a)
% b0 = gain coefficient
% B = K by 3 matrix of real coefficients containing bk's
% A = K by 3 matrix of real coefficients containing ak's
% b = numerator polynomial coefficients of DIRECT form
% a = denominator polynomial coefficients of DIRECT form

% Compute gain coefficient b0
b0 = b(1); b = b/b0; a0 = a(1); a = a/a0; b0 = b0/a0;
%
M = length(b); N = length(a);
if N > M
    b = [b zeros(1,N-M)];

```

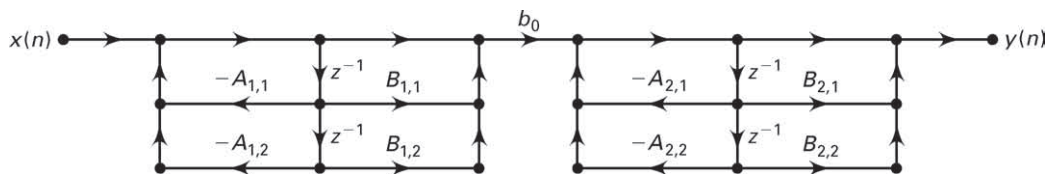


**FIGURE 6.5** Cascade form structure for  $N = 4$

```

elseif M > N
a = [a zeros(1,M-N)]; N = M;
else
NM = 0;
end
%
K = floor(N/2); B = zeros(K,3); A = zeros(K,3);
if K*2 == N
b = [b 0]; a = [a 0];
end
%
broots = cplxpair(roots(b)); aroots = cplxpair(roots(a));
for i=1:2:2*K
Brow = broots(i:1:i+1,:); Brow = real(poly(Brow));
B(fix((i+1)/2),:) = Brow;
Arow = aroots(i:1:i+1,:); Arow = real(poly(Arow));
A(fix((i+1)/2),:) = Arow;
end

```

This function converts the **b** and **a** vectors into  $K \times 3$  size **B** and **A** matrices. It begins by computing  $b_0$ , which is equal to  $b_0/a_0$  (assuming  $a_0 \neq 1$ ). It then makes the vectors **b** and **a** of equal length by zero-padding the shorter vector. This ensures that each biquad has a nonzero numerator and denominator. Next, it computes the roots of the  $B(z)$  and  $A(z)$  polynomials. Using the **cplxpair** function, these roots are ordered in complex conjugate pairs. Now every pair is converted back into a second-order numerator or denominator polynomial using the **poly** function. The SP toolbox function, **tf2sos** (transfer function to second-order section), also performs a similar operation.

The cascade form is implemented using the following **casfiltr** function.

```

function y = casfiltr(b0,B,A,x)
% CASCADE form realization of IIR and FIR filters
% -----
% y = casfiltr(b0,B,A,x);
% y = output sequence
% b0 = gain coefficient of CASCADE form
% B = K by 3 matrix of real coefficients containing bk's
% A = K by 3 matrix of real coefficients containing ak's
% x = input sequence
%
[K,L] = size(B);
N = length(x); w = zeros(K+1,N); w(1,:) = x;

```

```

for i = 1:1:K
    w(i+1,:) = filter(B(i,:),A(i,:),w(i,:));
end
y = b0*w(K+1,:);

```

This function employs the `filter` function in a loop using the coefficients of each biquad stored in `B` and `A` matrices. The input is scaled by `b0`, and the output of each filter operation is used as an input to the next filter operation. The output of the final filter operation is the overall output.

The following MATLAB function, `cas2dir`, converts a cascade form to a direct form. This is a simple operation that involves multiplication of several second-order polynomials. For this purpose, the MATLAB function `conv` is used in a loop over  $K$  factors. The SP toolbox function `sos2tf` also performs a similar operation.

```

function [b,a] = cas2dir(b0,B,A)
% CASCADE-to-DIRECT form conversion
%
% [b,a] = cas2dir(b0,B,A)
% b = numerator polynomial coefficients of DIRECT form
% a = denominator polynomial coefficients of DIRECT form
% b0 = gain coefficient
% B = K by 3 matrix of real coefficients containing bk's
% A = K by 3 matrix of real coefficients containing ak's
%
[K,L] = size(B);
b = [1]; a = [1];
for i=1:1:K
    b=conv(b,B(i,:)); a=conv(a,A(i,:));
end
b = b*b0;

```

- EXAMPLE 6.1** A filter is described by the following difference equation:

$$\begin{aligned}
 16y(n) + 12y(n-1) + 2y(n-2) - 4y(n-3) - y(n-4) \\
 = x(n) - 3x(n-1) + 11x(n-2) - 27x(n-3) + 18x(n-4)
 \end{aligned}$$

Determine its cascaded form structure.

**Solution**

MATLAB script:

```
>> b=[1 -3 11 -27 18]; a=[16 12 2 -4 -1];
>> [b0,B,A]=dir2cas(b,a)
b0 = 0.0625
B =
    1.0000   -0.0000    9.0000
    1.0000   -3.0000    2.0000
A =
    1.0000   1.0000    0.5000
    1.0000  -0.2500   -0.1250
```

The resulting structure is shown in Figure 6.6. To check that our cascade structure is correct, let us compute the first eight samples of the impulse response using both forms.

```
>> delta = impseq(0,0,7)
delta =
    1     0     0     0     0     0     0     0
>> format long
>> hcas=casfiltr(b0,B,A,delta)
hcas =
    Columns 1 through 4
    0.062500000000000   -0.234375000000000   0.855468750000000   -2.284179687500000
    Columns 5 through 8
    2.676513671875000   -1.522644042968750   0.289840698242190   0.49931716918945
>> hdir=filter(b,a,delta)
hdir =
    Columns 1 through 4
    0.062500000000000   -0.234375000000000   0.855468750000000   -2.284179687500000
    Columns 5 through 8
    2.676513671875000   -1.522644042968750   0.289840698242190   0.49931716918945
```

□

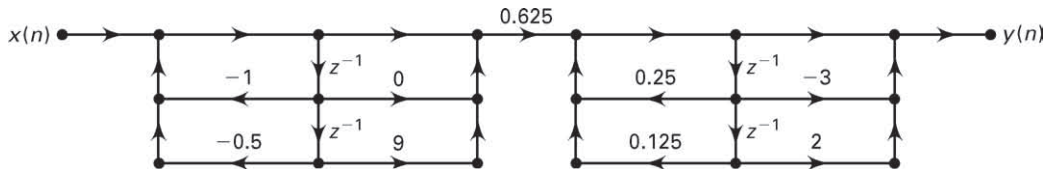


**FIGURE 6.6** Cascade structure in Example 6.1

### 6.2.6 PARALLEL FORM

In this form, the system function  $H(z)$  is written as a sum of second-order sections using partial fraction expansion.

$$\begin{aligned}
 H(z) &= \frac{B(z)}{A(z)} = \frac{b_0 + b_1 z^{-1} + \cdots + b_M z^{-M}}{1 + a_1 z^{-1} + \cdots + a_N z^{-N}} \\
 &= \frac{\hat{b}_0 + \hat{b}_1 z^{-1} + \cdots + \hat{b}_{N-1} z^{1-N}}{1 + a_1 z^{-1} + \cdots + a_N z^{-N}} + \underbrace{\sum_0^{M-N} C_k z^{-k}}_{\text{Only if } M \geq N} \\
 &= \sum_{k=1}^K \frac{B_{k,0} + B_{k,1} z^{-1}}{1 + A_{k,1} z^{-1} + A_{k,2} z^{-2}} + \underbrace{\sum_0^{M-N} C_k z^{-k}}_{\text{Only if } M \geq N} \quad (6.4)
 \end{aligned}$$

where  $K$  is equal to  $\frac{N}{2}$  and  $B_{k,0}$ ,  $B_{k,1}$ ,  $A_{k,1}$ , and  $A_{k,2}$  are real numbers representing the coefficients of second-order sections. The second-order section

$$H_k(z) = \frac{Y_k(z)}{X(z)} = \frac{B_{k,0} + B_{k,1} z^{-1}}{1 + A_{k,1} z^{-1} + A_{k,2} z^{-2}}; \quad k = 1, \dots, K$$

with

$$Y_k(z) = H_k(z)X(z), \quad Y(z) = \sum Y_k(z), \quad M < N$$

is the  $k$ th proper rational biquad section. The filter input is available to all biquad sections as well as to the polynomial section if  $M \geq N$  (which is an FIR part). The output from these sections is summed to form the filter output. Now each biquad section  $H_k(z)$  can be implemented in direct form II. Due to the summation of subsections, a parallel structure can be built to realize  $H(z)$ . As an example, consider  $M = N = 4$ . Figure 6.7 shows a parallel form structure for this fourth-order IIR filter.

### 6.2.7 MATLAB IMPLEMENTATION

The following function `dir2par` converts the direct form coefficients  $\{b_n\}$  and  $\{a_n\}$  into parallel form coefficients  $\{B_{k,i}\}$  and  $\{A_{k,i}\}$ .

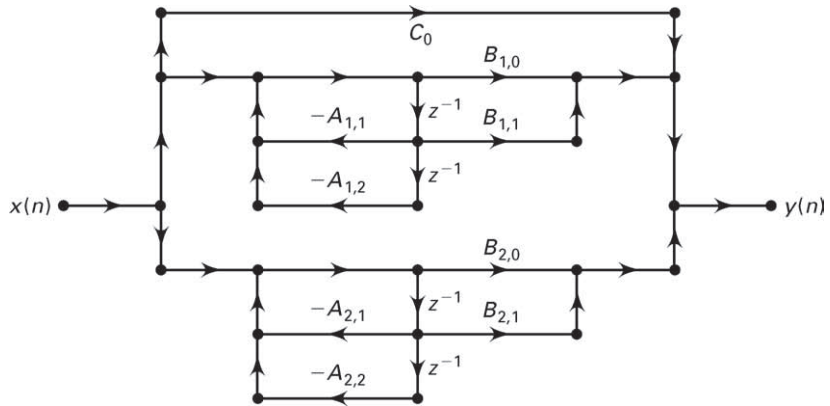


**FIGURE 6.7** Parallel form structure for  $N = 4$

```

function [C,B,A] = dir2par(b,a)
% DIRECT form to PARALLEL form conversion
% -----
% [C,B,A] = dir2par(b,a)
% C = polynomial part when length(b) >= length(a)
% B = K by 2 matrix of real coefficients containing bk's
% A = K by 3 matrix of real coefficients containing ak's
% b = numerator polynomial coefficients of DIRECT form
% a = denominator polynomial coefficients of DIRECT form
%
M = length(b); N = length(a);

[r1,p1,C] = residuez(b,a);
p = cplxpair(p1,10000000*eps); I = cplxcomp(p1,p); r = r1(I);

K = floor(N/2); B = zeros(K,2); A = zeros(K,3);
if K*2 == N; %N even, order of A(z) odd, one factor is first order
for i=1:2:N-2
Brow = r(i:1:i+1,:); Arow = p(i:1:i+1,:);
[Brow,Arow] = residuez(Brow,Arow,[]);
B(fix((i+1)/2),:) = real(Brow); A(fix((i+1)/2),:) = real(Arow);
end
[Brow,Arow] = residuez(r(N-1),p(N-1),[]);
B(K,:) = [real(Brow) 0]; A(K,:) = [real(Arow) 0];
else
for i=1:2:N-1

```

```
Brow = r(i:1:i+1,:); Arow = p(i:1:i+1,:);
[Brow,Arow] = residuez(Brow,Arow,[]);
B(fix((i+1)/2),:) = real(Brow); A(fix((i+1)/2),:) = real(Arow);
end
end
```

The **dir2cas** function first computes the *z*-domain partial fraction expansion using the **residuez** function. We need to arrange pole-and-residue pairs into complex conjugate pole-and-residue pairs followed by real pole-and-residue pairs. To do this, the **cplxpair** function from MATLAB can be used; it sorts a complex array into complex conjugate pairs. However, two consecutive calls to this function, one each for pole and residue arrays, will not guarantee that poles and residues will correspond to each other. Therefore, a new **cplxcomp** function is developed, which compares two shuffled complex arrays and returns the index of one array, which can be used to rearrange another array.

```
function I = cplxcomp(p1,p2)
% I = cplxcomp(p1,p2)
% Compares two complex pairs which contain the same scalar elements
% but (possibly) at different indices. This routine should be
% used after CPLXPAIR routine for rearranging pole vector and its
% corresponding residue vector.
% p2 = cplxpair(p1)
%
I=[];
for j=1:1:length(p2)
    for i=1:1:length(p1)
        if (abs(p1(i)-p2(j)) < 0.0001)
            I=[I,i];
        end
    end
end
I=I';
```

After collecting these pole-and-residue pairs, the **dir2cas** function computes the numerator and denominator of the biquads by employing the **residuez** function in the reverse fashion.

These parallel form coefficients are then used in the function **parfiltr**, which implements the parallel form. The **parfiltr** function uses the **filter** function in a loop using the coefficients of each biquad stored in the **B** and **A** matrices. The input is first filtered through the FIR part **C** and stored in the first row of a **w** matrix. Then the outputs of all biquad filters are computed for the same input and stored as subsequent

rows in the  $w$  matrix. Finally, all the columns of the  $w$  matrix are summed to yield the output.

```
function y = parfiltr(C,B,A,x)
% PARALLEL form realization of IIR filters
%
% [y] = parfiltr(C,B,A,x);
% y = output sequence
% C = polynomial (FIR) part when M >= N
% B = K by 2 matrix of real coefficients containing bk's
% A = K by 3 matrix of real coefficients containing ak's
% x = input sequence
%
[K,L] = size(B); N = length(x); w = zeros(K+1,N);
w(1,:) = filter(C,1,x);
for i = 1:1:K
    w(i+1,:) = filter(B(i,:),A(i,:),x);
end
y = sum(w);
```

To obtain a direct form from a parallel form, the function `par2dir` can be used. It computes poles and residues of each proper biquad and combines these into system poles and residues. Another call of the `residuez` function in reverse order computes the numerator and denominator polynomials.

```
function [b,a] = par2dir(C,B,A)
% PARALLEL-to-DIRECT form conversion
%
% [b,a] = par2dir(C,B,A)
% b = numerator polynomial coefficients of DIRECT form
% a = denominator polynomial coefficients of DIRECT form
% C = polynomial part of PARALLEL form
% B = K by 2 matrix of real coefficients containing bk's
% A = K by 3 matrix of real coefficients containing ak's
%
[K,L] = size(A); R = [] ; P = [] ;

for i=1:1:K
[r,p,k]=residuez(B(i,:),A(i,:)); R = [R;r]; P = [P;p];
end
[b,a] = residuez(R,P,C); b = b(:)'; a = a(:)';
```

- **EXAMPLE 6.2** Consider the filter given in Example 6.1.

$$\begin{aligned} 16y(n) + 12y(n-1) + 2y(n-2) - 4y(n-3) - y(n-4) \\ = x(n) - 3x(n-1) + 11x(n-2) - 27x(n-3) + 18x(n-4) \end{aligned}$$

Now determine its parallel form.

**Solution**

MATLAB script:

```
>> b=[1 -3 11 -27 18]; a=[16 12 2 -4 -1];
>> [C,B,A]=dir2par(b,a)
C =
-18
B =
-10.0500 -3.9500
28.1125 -13.3625
A =
1.0000 1.0000 0.5000
1.0000 -0.2500 -0.1250
```

The resulting structure is shown in Figure 6.8. To check our parallel structure, let us compute the first eight samples of the impulse response using both forms.

```
>> format long; delta = impseq(0,0,7); hpar=parfiltr(C,B,A,delta)
hpar =
Columns 1 through 4
0.06250000000000 -0.23437500000000 0.85546875000000 -2.28417968750000
```

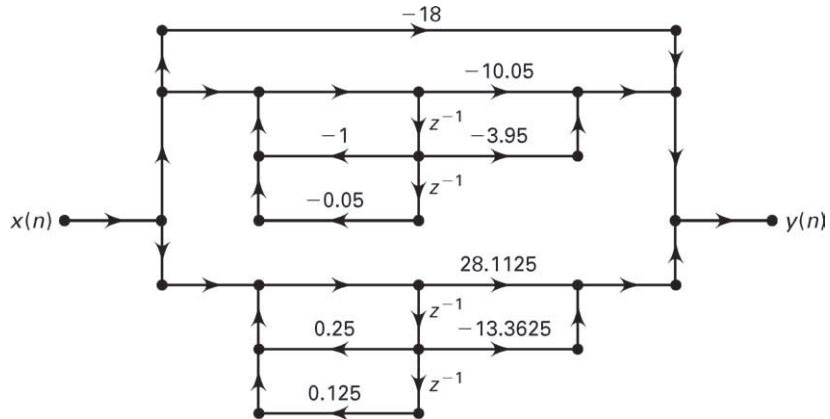


**FIGURE 6.8** Parallel form structure in Example 6.2

```

Columns 5 through 8
2.67651367187500 -1.52264404296875 0.28984069824219 0.49931716918945
>> hdir = filter(b,a,delta)
hdir =
Columns 1 through 4
0.06250000000000 -0.23437500000000 0.85546875000000 -2.28417968750000
Columns 5 through 8
2.67651367187500 -1.52264404296875 0.28984069824219 0.49931716918945

```

□

- **EXAMPLE 6.3** What would be the overall direct, cascade, or parallel form if a structure contains a combination of these forms? Consider the block diagram shown in Figure 6.9.

**Solution**

This structure contains a cascade of two parallel sections. The first parallel section contains two biquads, while the second one contains three biquads. We will have to convert each parallel section into a direct form using the `par2dir` function, giving us a cascade of two direct forms. The overall direct form can be computed by convolving the corresponding numerator and denominator polynomials. The overall cascade and parallel forms can now be derived from the direct form.

MATLAB script:

```

>> C0=0; B1=[2 4;3 1]; A1=[1 1 0.9; 1 0.4 -0.4];
>> B2=[0.5 0.7;1.5 2.5;0.8 1]; A2=[1 -1 0.8;1 0.5 0.5;1 0 -0.5];
>> [b1,a1]=par2dir(C0,B1,A1)
b1 =
      5.0000    8.8000    4.5000   -0.7000

```

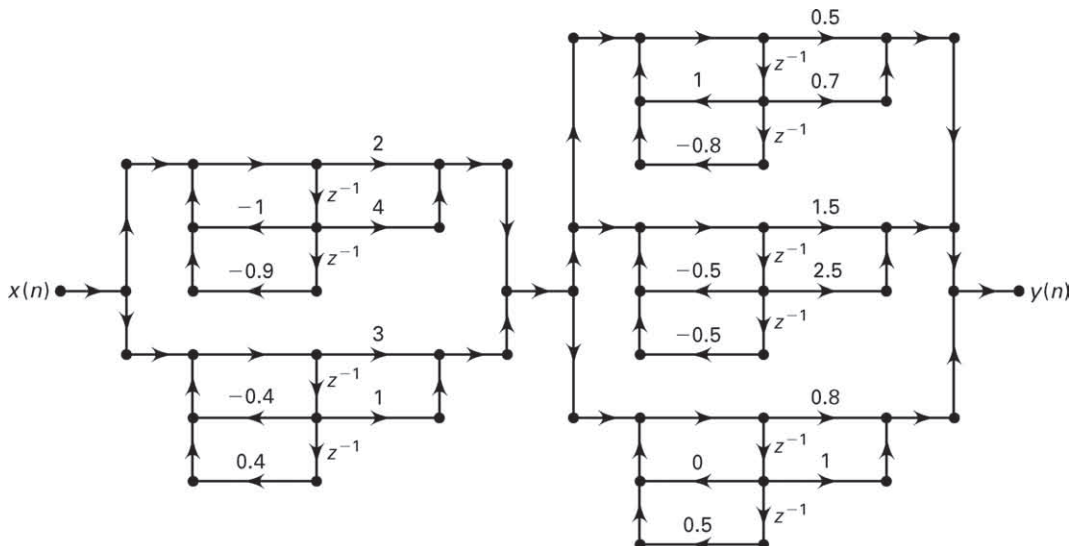


**FIGURE 6.9** Block diagram in Example 6.3

```

a1 =
    1.0000    1.4000    0.9000   -0.0400   -0.3600
>> [b2,a2]=par2dir(C0,B2,A2)
b2 =
    2.8000    2.5500   -1.5600    2.0950    0.5700   -0.7750
a2 =
    1.0000   -0.5000    0.3000    0.1500    0.0000    0.0500   -0.2000
>> b=conv(b1,b2) % Overall direct form numerator
b =
    Columns 1 through 7
    14.0000    37.3900   27.2400    6.2620   12.4810   11.6605   -5.7215
    Columns 8 through 9
    -3.8865     0.5425
>> a=conv(a1,a2) % Overall direct form denominator
a =
    Columns 1 through 7
    1.0000    0.9000    0.5000    0.0800    0.1400    0.3530   -0.2440
    Columns 8 through 11
    -0.2890   -0.1820   -0.0100    0.0720
>> [b0,Bc,Ac]=dir2cas(b,a) % Overall cascade form
b0 =
    14.0000
Bc =
    1.0000    1.8836    1.1328
    1.0000   -0.6915    0.6719
    1.0000    2.0776    0.8666
    1.0000        0        0
    1.0000   -0.5990    0.0588
Ac =
    1.0000    1.0000    0.9000
    1.0000    0.5000    0.5000
    1.0000   -1.0000    0.8000
    1.0000    1.5704    0.6105
    1.0000   -1.1704    0.3276
>> [C0,Bp,Ap]=dir2par(b,a) % Overall parallel form
C0 = []
Bp =
    -20.4201   -1.6000
    24.1602    5.1448
    2.4570    3.3774
   -0.8101   -0.2382
    8.6129   -4.0439
Ap =
    1.0000    1.0000    0.9000
    1.0000    0.5000    0.5000
    1.0000   -1.0000    0.8000
    1.0000    1.5704    0.6105
    1.0000   -1.1704    0.3276

```

This example shows that by using the MATLAB functions developed in this section, we can probe and construct a wide variety of structures.  $\square$

## 6.3 FIR FILTER STRUCTURES

---

A finite-duration impulse response filter has a system function of the form

$$H(z) = b_0 + b_1 z^{-1} + \cdots + b_{M-1} z^{1-M} = \sum_{n=0}^{M-1} b_n z^{-n} \quad (6.5)$$

Hence the impulse response  $h(n)$  is

$$h(n) = \begin{cases} b_n, & 0 \leq n \leq M-1 \\ 0, & \text{else} \end{cases} \quad (6.6)$$

and the difference equation representation is

$$y(n) = b_0 x(n) + b_1 x(n-1) + \cdots + b_{M-1} x(n-M+1) \quad (6.7)$$

which is a linear convolution of finite support.

The order of the filter is  $M - 1$ , and the *length* of the filter (which is equal to the number of coefficients) is  $M$ . The FIR filter structures are always stable, and they are relatively simple compared to IIR structures. Furthermore, FIR filters can be designed to have a linear-phase response, which is desirable in some applications.

We will consider the following four structures.

- 1. Direct form:** In this form, the difference equation (6.7) is implemented directly as given.
- 2. Cascade form:** In this form, the system function  $H(z)$  in (6.5) is factored into second-order factors, which are then implemented in a cascade connection.
- 3. Linear-phase form:** When an FIR filter has a linear-phase response, its impulse response exhibits certain symmetry conditions. In this form, we exploit these symmetry relations to reduce multiplications by about half.
- 4. Frequency-sampling form:** This structure is based on the DFT of the impulse response  $h(n)$  and leads to a parallel structure. It is also suitable for a design technique based on the sampling of frequency response  $H(e^{j\omega})$ .

We will briefly describe these four forms along with some examples. The MATLAB function `dir2cas` developed in the previous section is also applicable for the cascade form.

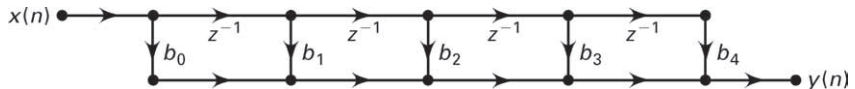


**FIGURE 6.10** Direct form FIR structure

### 6.3.1 DIRECT FORM

The difference equation (6.7) is implemented as a tapped delay line since there are no feedback paths. Let  $M = 5$  (i.e., a fourth-order FIR filter); then

$$y(n) = b_0x(n) + b_1x(n - 1) + b_2x(n - 2) + b_3x(n - 3) + b_4x(n - 4)$$

The direct form structure is given in Figure 6.10. Note that since the denominator is equal to unity, there is only one direct form structure.

### 6.3.2 MATLAB IMPLEMENTATION

In MATLAB, the direct form FIR structure is described by the row vector  $\mathbf{b}$  containing the  $\{b_n\}$  coefficients. The structure is implemented by the `filter` function, in which the vector  $\mathbf{a}$  is set to the scalar value 1, as discussed in Chapter 2.

### 6.3.3 CASCADE FORM

This form is similar to that of the IIR form. The system function  $H(z)$  is converted into products of second-order sections with real coefficients. These sections are implemented in direct form and the entire filter as a cascade of second-order sections. From (6.5),

$$\begin{aligned} H(z) &= b_0 + b_1z^{-1} + \cdots + b_{M-1}z^{-M+1} \\ &= b_0 \left( 1 + \frac{b_1}{b_0}z^{-1} + \cdots + \frac{b_{M-1}}{b_0}z^{-M+1} \right) \\ &= b_0 \prod_{k=1}^K (1 + B_{k,1}z^{-1} + B_{k,2}z^{-2}) \end{aligned} \quad (6.8)$$

where  $K$  is equal to  $\lfloor \frac{M}{2} \rfloor$  and  $B_{k,1}$  and  $B_{k,2}$  are real numbers representing the coefficients of second-order sections. For  $M = 7$ , the cascade form is shown in Figure 6.11.

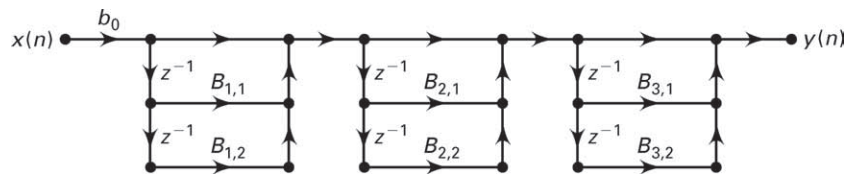


**FIGURE 6.11** Cascade form FIR structure

### 6.3.4 MATLAB IMPLEMENTATION

Although it is possible to develop a new MATLAB function for the FIR cascade form, we will use our `dir2cas` function by setting the denominator vector `a` equal to 1. Similarly, `cas2dir` can be used to obtain the direct form from the cascade form.

### 6.3.5 LINEAR-PHASE FORM

For frequency-selective filters (e.g., lowpass filters), it is generally desirable to have a phase response that is a linear function of frequency; that is, we want

$$\angle H(e^{j\omega}) = \beta - \alpha\omega, \quad -\pi < \omega \leq \pi \quad (6.9)$$

where  $\beta = 0$  or  $\pm\pi/2$  and  $\alpha$  is a constant. For a causal FIR filter with impulse response over  $[0, M-1]$  interval, the linear-phase condition (6.9) imposes the following symmetry conditions on the impulse response  $h(n)$  (see Problem P6.15):

$$h(n) = h(M-1-n); \quad \beta = 0, \alpha = \frac{M-1}{2}, \quad 0 \leq n \leq M-1 \quad (6.10)$$

$$h(n) = -h(M-1-n); \quad \beta = \pm\pi/2, \alpha = \frac{M-1}{2}, \quad 0 \leq n \leq M-1 \quad (6.11)$$

An impulse response that satisfies (6.10) is called a *symmetric impulse response* and that in (6.11) is called an *antisymmetric impulse response*. These symmetry conditions can now be exploited in a structure called the linear-phase form.

Consider the difference equation given in (6.7) with a symmetric impulse response in (6.10). We have

$$\begin{aligned} y(n) &= b_0x(n) + b_1x(n-1) + \cdots + b_1x(n-M+2) + b_0x(n-M+1) \\ &= b_0[x(n) + x(n-M+1)] + b_1[x(n-1) + x(n-M+2)] + \cdots \end{aligned}$$

The block diagram implementation of this difference equation is shown in Figure 6.12 for both odd and even  $M$ .

Clearly, this structure requires 50% fewer multiplications than the direct form. A similar structure can be derived for an antisymmetric impulse response.

### 6.3.6 MATLAB IMPLEMENTATION

The linear-phase structure is essentially a direct form drawn differently to save on multiplications. Hence in MATLAB, representation of the linear-phase structure is equivalent to the direct form.

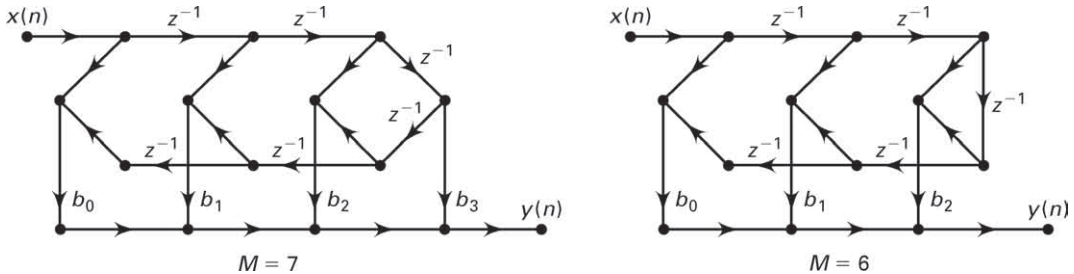


FIGURE 6.12 Linear-phase form FIR structures (symmetric impulse response)

- EXAMPLE 6.4** An FIR filter is given by the system function

$$H(z) = 1 + 16 \frac{1}{16} z^{-4} + z^{-8}$$

Determine and draw the direct, linear-phase, and cascade form structures.

- a. **Direct form:** The difference equation is given by

$$y(n) = x(n) + 16.0625x(n - 4) + x(n - 8)$$

and the direct form structure is shown in Figure 6.13(a).

- b. **Linear-phase form:** The difference equation can be written in the form

$$y(n) = [x(n) + x(n - 8)] + 16.0625x(n - 4)$$

and the resulting structure is shown in Figure 6.13b.

- c. **Cascade form:** We use the following MATLAB script.

```
>> b=[1,0,0,0,16+1/16,0,0,0,1]; [b0,B,A] = dir2cas(b,1)
```

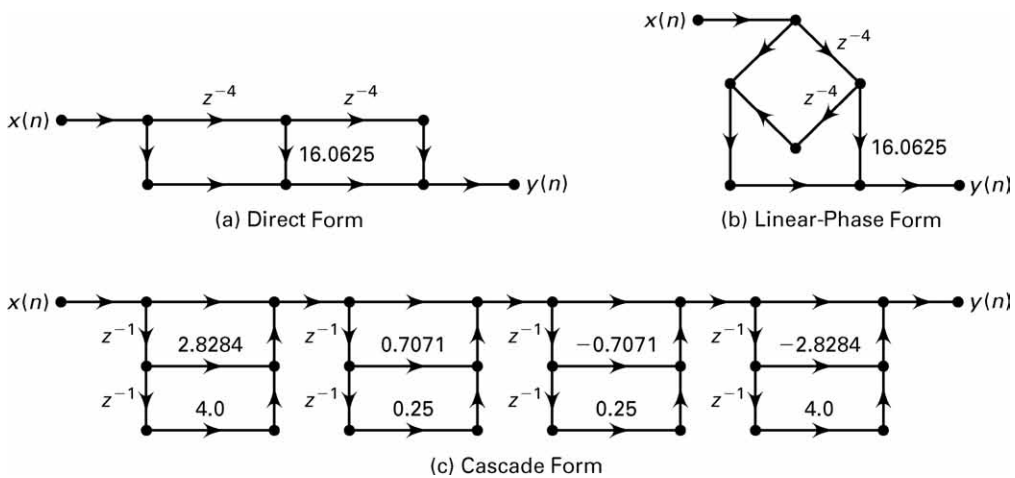


FIGURE 6.13 FIR filter structures in Example 6.4

```
b0 = 1
B =
    1.0000    2.8284    4.0000
    1.0000    0.7071    0.2500
    1.0000   -0.7071    0.2500
    1.0000   -2.8284    4.0000
A =
    1      0      0
    1      0      0
    1      0      0
    1      0      0
```

The cascade form structure is shown in Figure 6.13c. □

- **EXAMPLE 6.5** For the filter in Example 6.4, what would be the structure if we desire a cascade form containing linear-phase components with real coefficients?

### Solution

We are interested in cascade sections that have symmetry and real coefficients. From the properties of linear-phase FIR filters (see Chapter 7), if such a filter has an arbitrary zero at  $z = r\angle\theta$ , then there must be three other zeros at  $(1/r)\angle\theta$ ,  $r\angle -\theta$ , and  $(1/r)\angle -\theta$  to have real filter coefficients. We can now make use of this property. First we will determine the zero locations of the given eighth-order polynomial. Then we will group four zeros that satisfy this property to obtain one (fourth-order) linear-phase section. There are two such sections, which we will connect in cascade.

MATLAB script:

```
>> b=[1,0,0,0,16+1/16,0,0,0,1]; broots=roots(b)
broots =
-1.4142 + 1.4142i
-1.4142 - 1.4142i
1.4142 + 1.4142i
1.4142 - 1.4142i
-0.3536 + 0.3536i
-0.3536 - 0.3536i
0.3536 + 0.3536i
0.3536 - 0.3536i
>> B1=real(poly([broots(1),broots(2),broots(5),broots(6)]))
B1 =
    1.0000    3.5355    6.2500    3.5355    1.0000
>> B2=real(poly([broots(3),broots(4),broots(7),broots(8)]))
B2 =
    1.0000   -3.5355    6.2500   -3.5355    1.0000
```

The structure is shown in Figure 6.14. □

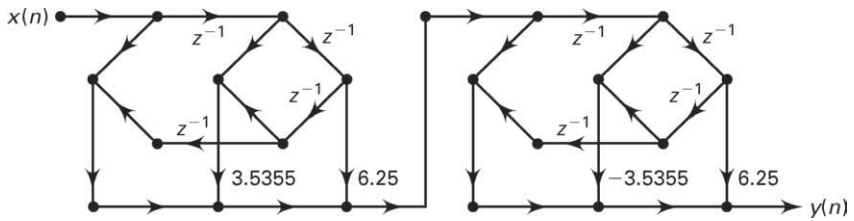


**FIGURE 6.14** Cascade of FIR linear-phase elements

### 6.3.7 FREQUENCY-SAMPLING FORM

In this form, we use the fact that the system function  $H(z)$  of an FIR filter can be reconstructed from its samples on the unit circle. From our discussions on the DFT in Chapter 5, we recall that these samples are in fact the  $M$ -point DFT values  $\{H(k), 0 \leq k \leq M-1\}$  of the  $M$ -point impulse response  $h(n)$ . Therefore, we have

$$H(z) = \mathcal{Z}[h(n)] = \mathcal{Z}[\text{IDFT}\{H(k)\}]$$

Using this procedure, we obtain [see (5.17) in Chapter 5]

$$H(z) = \left( \frac{1 - z^{-M}}{M} \right) \sum_{k=0}^{M-1} \frac{H(k)}{1 - W_M^{-k} z^{-1}} \quad (6.12)$$

This shows that the DFT  $H(k)$ , rather than the impulse response  $h(n)$  (or the difference equation), is used in this structure. Also note that the FIR filter described by (6.12) has a recursive form similar to an IIR filter because (6.12) contains both poles and zeros. The resulting filter is an FIR filter since the poles at  $W_M^{-k}$  are canceled by the roots of

$$1 - z^{-M} = 0$$

The system function in (6.12) leads to a parallel structure, as shown in Figure 6.15 for  $M = 4$ .

One problem with the structure in Figure 6.15 is that it requires a complex arithmetic implementation. Since an FIR filter is almost always a real-valued filter, it is possible to obtain an alternate realization in which only real arithmetic is used. This realization is derived using the symmetry properties of the DFT and the  $W_M^{-k}$  factor. Then (6.12) can be expressed as (see Problem P6.18)

$$H(z) = \frac{1 - z^{-M}}{M} \left\{ \sum_{k=1}^L 2|H(k)|H_k(z) + \frac{H(0)}{1 - z^{-1}} + \frac{H(M/2)}{1 + z^{-1}} \right\} \quad (6.13)$$

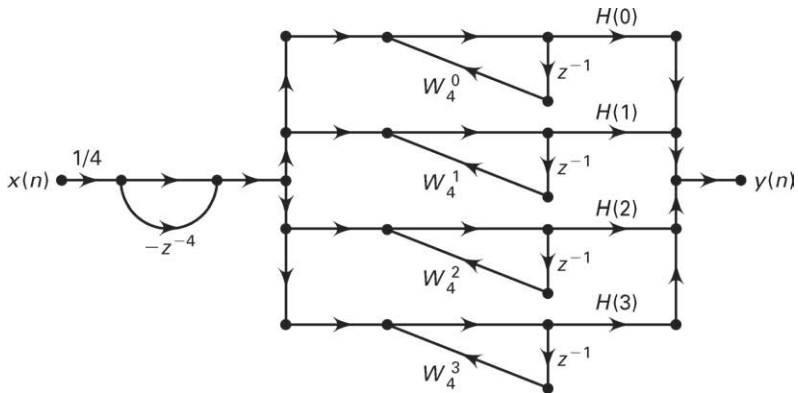


**FIGURE 6.15** Frequency-sampling structure for  $M = 4$

where  $L = \frac{M-1}{2}$  for  $M$  odd,  $L = \frac{M}{2} - 1$  for  $M$  even, and  $\{H_k(z), k = 1, \dots, L\}$  are second-order sections given by

$$H_k(z) = \frac{\cos[\angle H(k)] - z^{-1} \cos[\angle H(k) - \frac{2\pi k}{M}]}{1 - 2z^{-1} \cos(\frac{2\pi k}{M}) + z^{-2}} \quad (6.14)$$

Note that the DFT samples  $H(0)$  and  $H(M/2)$  are real-valued and that the third term on the right-hand side of (6.13) is absent if  $M$  is odd. Using (6.13) and (6.14), we show a frequency-sampling structure in Figure 6.16 for  $M = 4$  containing real coefficients.

### 6.3.8 MATLAB IMPLEMENTATION

Given the impulse response  $h(n)$  or the DFT  $H(k)$ , we have to determine the coefficients in (6.13) and (6.14). The following MATLAB function, `dir2fs`, converts a direct form  $h(n)$  to the frequency-sampling form by directly implementing (6.13) and (6.14).

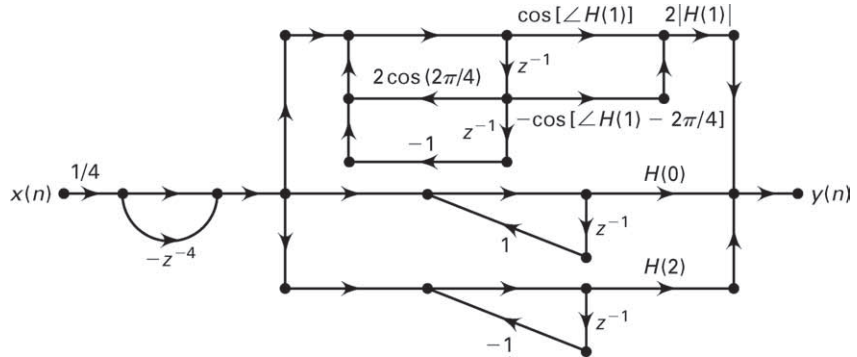


**FIGURE 6.16** Frequency-sampling structure for  $M = 4$  with real coefficients

```

function [C,B,A] = dir2fs(h)
% Direct form to frequency-sampling form conversion
% -----
% [C,B,A] = dir2fs(h)
% C = row vector containing gains for parallel sections
% B = matrix containing numerator coefficients arranged in rows
% A = matrix containing denominator coefficients arranged in rows
% h = impulse response vector of an FIR filter
%
M = length(h); H = fft(h,M);
magH = abs(H); phaH = angle(H)';
% Check even or odd M
if (M == 2*floor(M/2))
    L = M/2-1; % M is even
    A1 = [1,-1,0;1,1,0]; C1 = [real(H(1)),real(H(L+2))];
else
    L = (M-1)/2; % M is odd
    A1 = [1,-1,0]; C1 = [real(H(1))];
end
k = [1:L]';
% Initialize B and A arrays
B = zeros(L,2); A = ones(L,3);
% Compute denominator coefficients
A(1:L,2) = -2*cos(2*pi*k/M); A = [A;A1];
% Compute numerator coefficients
B(1:L,1) = cos(phaH(2:L+1));
B(1:L,2) = -cos(phaH(2:L+1)-(2*pi*k/M));
% Compute gain coefficients
C = [2*magH(2:L+1),C1]';

```

In this function, the impulse response values are supplied through the *h* array. After conversion, the *C* array contains the gain values for each parallel section. The gain values for the second-order parallel sections are given first, followed by  $H(0)$  and  $H(M/2)$  (if  $M$  is even). The *B* matrix contains the numerator coefficients, which are arranged in length-2 row vectors for each second-order section. The *A* matrix contains the denominator coefficients, which are arranged in length-3 row vectors for the second-order sections corresponding to those in *B*, followed by the coefficients for the first-order sections.

A practical problem with the structure in Figure 6.16 is that it has poles on the unit circle, which makes this filter critically unstable. If the filter is not excited by one of the pole frequencies, then the output is bounded. We can avoid this problem by sampling  $H(z)$  on a circle  $|z| = r$ ,

where the radius  $r$  is very close to 1 but is less than 1 (e.g.,  $r = 0.99$ ), which results in

$$H(z) = \frac{1 - r^M z^{-M}}{M} \sum_{k=0}^{M-1} \frac{H(k)}{1 - r W_M^{-k} z^{-k}}; \quad H(k) = H(re^{j2\pi k/M}) \quad (6.15)$$

Now approximating  $H(re^{j2\pi k/M}) \approx H(e^{j2\pi k/M})$  for  $r \approx 1$ , we can obtain a stable structure similar to the one in Figure 6.16 containing real values. This is explored in Problem P6.19.

- **EXAMPLE 6.6** Let  $h(n) = \begin{matrix} 1, 2, 3, 2, 1 \\ \uparrow \end{matrix} / 9$ . Determine and draw the frequency-sampling form.

**Solution** MATLAB script:

```
>> h = [1,2,3,2,1]/9; [C,B,A] = dir2fs(h)
C =
    0.5818
    0.0849
    1.0000
B =
   -0.8090    0.8090
    0.3090   -0.3090
A =
    1.0000   -0.6180    1.0000
    1.0000    1.6180    1.0000
    1.0000   -1.0000        0
```

Since  $M = 5$  is odd, there is only one first-order section. Hence

$$H(z) = \frac{1 - z^{-5}}{5} \left[ 0.5818 \frac{-0.809 + 0.809z^{-1}}{1 - 0.618z^{-1} + z^{-2}} + 0.0849 \frac{0.309 - 0.309z^{-1}}{1 + 1.618z^{-1} + z^{-2}} + \frac{1}{1 - z^{-1}} \right]$$

The frequency-sampling form is shown in Figure 6.17. □

- **EXAMPLE 6.7** The frequency samples of a 32-point linear-phase FIR filter are given by

$$|H(k)| = \begin{cases} 1, & k = 0, 1, 2 \\ 0.5, & k = 3 \\ 0, & k = 4, 5, \dots, 15 \end{cases}$$

Determine its frequency-sampling form, and compare its computational complexity with the linear-phase form.

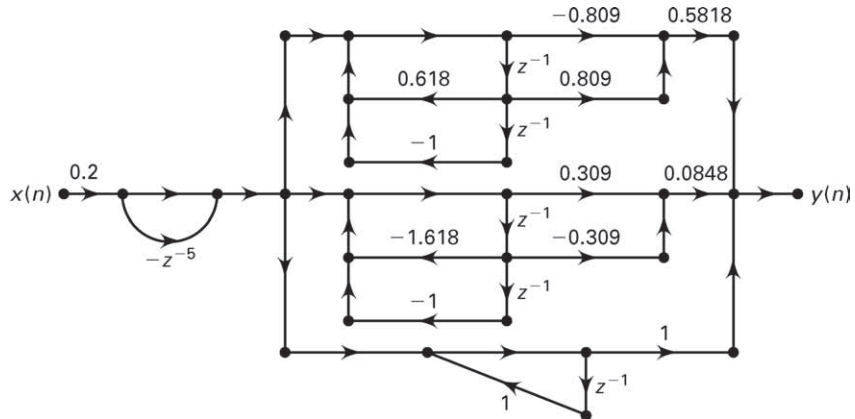


**FIGURE 6.17** Frequency-sampling structure in Example 6.6

### Solution

In this example, since the samples of the DFT  $H(k)$  are given, we could use (6.13) and (6.14) directly to determine the structure. However, we will use the `dir2fs` function for which we will have to determine the impulse response  $h(n)$ . Using the symmetry property and the linear-phase constraint, we assemble the DFT  $H(k)$  as

$$\begin{aligned} H(k) &= |H(k)| e^{j\angle H(k)}, \quad k = 0, 1, \dots, 31 \\ |H(k)| &= |H(32-k)|, \quad k = 1, 2, \dots, 31; \quad H(0) = 1 \\ \angle H(k) &= -\frac{31}{2} \frac{2\pi}{32} k = -\angle H(32-k), \quad k = 0, 1, \dots, 31 \end{aligned}$$

Now the IDFT of  $H(k)$  will result in the desired impulse response.

MATLAB script:

```
>> M = 32; alpha = (M-1)/2;
>> magHk = [1,1,1,0.5,zeros(1,25),0.5,1,1];
>> k1 = 0:15; k2 = 16:M-1;
>> angHk = [-alpha*(2*pi)/M*k1, alpha*(2*pi)/M*(M-k2)];
>> H = magHk.*exp(j*angHk); h = real(ifft(H,M)); [C,B,A] = dir2fs(h)
```

```
C =
    2.0000
    2.0000
    1.0000
    0.0000
    0.0000
    0.0000
    0.0000
    0
```

```
0.0000
0.0000
0.0000
0.0000
0.0000
0.0000
0.0000
1.0000
0
B =
-0.9952    0.9952
0.9808   -0.9808
-0.9569    0.9569
-0.8944    0.3162
0.9794   -0.7121
0.8265    0.2038
-0.6754    0.8551
1.0000    0.0000
0.6866   -0.5792
0.5191    0.9883
-0.4430    0.4993
-0.8944   -0.3162
-0.2766    0.3039
0.9343    0.9996
-0.9077   -0.8084
A =
1.0000   -1.9616    1.0000
1.0000   -1.8478    1.0000
1.0000   -1.6629    1.0000
1.0000   -1.4142    1.0000
1.0000   -1.1111    1.0000
1.0000   -0.7654    1.0000
1.0000   -0.3902    1.0000
1.0000    0.0000    1.0000
1.0000    0.3902    1.0000
1.0000    0.7654    1.0000
1.0000    1.1111    1.0000
1.0000    1.4142    1.0000
1.0000    1.6629    1.0000
1.0000    1.8478    1.0000
1.0000    1.9616    1.0000
1.0000   -1.0000      0
1.0000    1.0000      0
```

Note that only four gain coefficients are nonzero. Hence the frequency-sampling form is

$$H(z) = \frac{1 - z^{-32}}{32} \left[ 2 \frac{-0.9952 + 0.9952z^{-1}}{1 - 1.9616z^{-1} + z^{-2}} + 2 \frac{0.9808 - 0.9808z^{-1}}{1 - 1.8478z^{-1} + z^{-2}} + \right. \\ \left. \frac{-0.9569 + 0.9569z^{-1}}{1 - 1.6629z^{-1} + z^{-2}} + \frac{1}{1 - z^{-1}} \right]$$

To determine the computational complexity, note that since  $H(0) = 1$ , the first-order section requires no multiplication, whereas the three second-order sections require three multiplications each for a total of nine multiplications per output sample. The total number of additions is 13. To implement the linear-phase structure would require 16 multiplications and 31 additions per output sample. Therefore, the frequency-sampling structure of this FIR filter is more efficient than the linear-phase structure.  $\square$

## 6.4 OVERVIEW OF FINITE-PRECISION NUMERICAL EFFECTS

---

Until now, we have considered digital filter designs and implementations in which both the filter coefficients and the filter operations such as additions and multiplications were expressed using infinite-precision numbers. When discrete-time systems are implemented in hardware or in software, all parameters and arithmetic operations are implemented using finite-precision numbers, and hence their effect is unavoidable.

Consider a typical digital filter implemented as a direct form II structure, which is shown in Figure 6.18a. When finite-precision representation is used in its implementation, there are three possible considerations that affect the overall quality of its output. We have to

1. quantize the filter coefficients  $\{a_k, b_k\}$  to obtain their finite word-length representations  $\{\hat{a}_k, \hat{b}_k\}$ ,
2. quantize the input sequence  $x(n)$  to obtain  $\hat{x}(n)$ , and
3. consider all internal arithmetic that must be converted to their next best representations.

Thus the output,  $y(n)$ , is also a quantized value  $\hat{y}(n)$ . This gives us a new filter realization,  $\hat{H}(z)$ , which is shown in Figure 6.18b. We hope that this new filter  $\hat{H}(z)$  and its output  $\hat{y}(n)$  are as close as possible to the original filter  $H(z)$  and the original output  $y(n)$ .

Since the quantization operation is a nonlinear operation, the overall analysis that takes into account all three effects described above is very difficult and tedious. Therefore, we will study each of these effects separately as though it were the only one acting at the time. This makes the analysis easier and the results more interpretable.

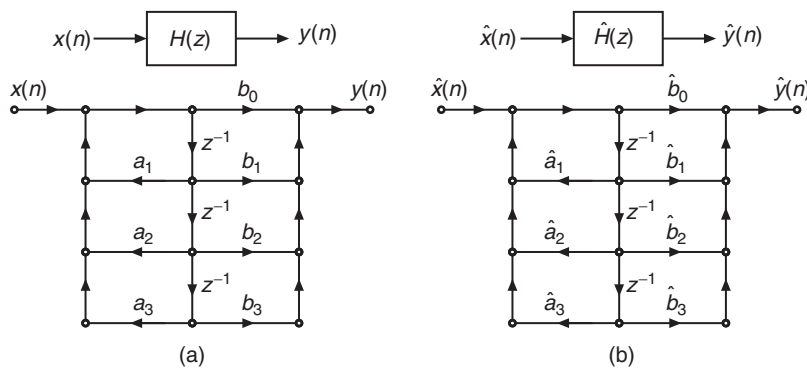


**FIGURE 6.18** Direct form II digital filter implementation: (a) infinite precision, (b) finite precision

We begin by discussing the number representation in a computer—more accurately, a central processing unit (CPU). This leads to the process of number quantization and the resulting error characterization. We then analyze the effects of filter coefficient quantization on digital filter frequency responses. The effects of multiplication and addition quantization (collectively known as arithmetic round-off errors) on filter output are discussed in Chapter 10.

## 6.5 REPRESENTATION OF NUMBERS

In computers, numbers (real-valued or complex-valued, integers or fractions) are represented using binary digits (*bits*), which take the value of either a 0 or a 1. The finite word-length arithmetic needed for processing these numbers is implemented using two different approaches, depending on the ease of implementation and the accuracy as well as dynamic range needed in processing. The *fixed-point* arithmetic is easy to implement but has only a fixed dynamic range and accuracy (i.e., very large numbers or very small numbers). The *floating-point* arithmetic, on the other hand, has a wide dynamic range and a variable accuracy (relative to the magnitude of a number) but is more complicated to implement and analyze.

Since a computer can operate only on a binary variable (e.g., a 1 or a 0), positive numbers can straightforwardly be represented using binary numbers. The problem arises as to how to represent the negative numbers. There are three different formats used in each of these arithmetics: *sign-magnitude* format, *one's-complement* format, and *two's-complement* format. In discussing and analyzing these representations, we will mostly consider a binary number system containing bits. However, this discussion and analysis is also valid for any radix numbering system—for example, the hexadecimal, octal, or decimal system.

In the following discussion, we will first begin with fixed-point signed integer arithmetic. A  $B$ -bit binary representation of an integer  $x$  is given by<sup>1</sup>

$$x \equiv b_{B-1} b_{B-2} \dots b_0 = b_{B-1} \times 2^{B-1} + b_{B-2} \times 2^{B-2} + \dots + b_0 \times 2^0 \quad (6.16)$$

where each bit  $b_i$  represents either a 0 or a 1. This representation will help us to understand the advantages and disadvantages of each signed format and to develop simple MATLAB functions. We will then extend these concepts to fractional real numbers for both fixed-point and floating-point arithmetic.

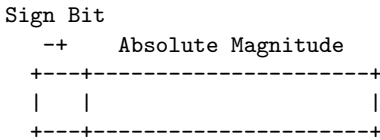
### 6.5.1 FIXED-POINT SIGNED INTEGER ARITHMETIC

In this arithmetic, positive numbers are coded using their binary representation. For example, using 3 bits, we can represent numbers from 0 to 7 as

0	1	2	3	4	5	6	7
000	001	010	011	100	101	110	111

Thus, with 8 bits the numbers represented can be 0 to 255, with 10 bits we can represent the numbers from 0 to 1023, and with 16 bits the range covered is 0 to 65535. For negative numbers, the following three formats are used: sign-magnitude, one's-complement, and two's-complement.

**Sign-magnitude format** In this format, positive numbers are represented using bits as before. However, the leftmost bit (also known as the most-significant bit, or MSB) is used as the sign bit (0 is +, and 1 is -), and the remaining bits hold the absolute magnitude of the number as shown here:



This system has thus two different codes for 0, one for the positive 0, the other one for the negative 0. For example, using 3 bits, we can represent numbers from -3 to 3 as

-3	-2	-1	-0	0	1	2	3
111	110	101	100	000	001	010	011

Thus, 8 bits cover the interval  $[-127, +127]$ , while 16 bits cover  $[-32, 767, +32, 767]$ . If we use  $B$  bits in the sign-magnitude format, then we can represent integers from  $-(2^{B-1} - 1)$  to  $+(2^{B-1} - 1)$  only.

<sup>1</sup>Here the letter  $b$  is used to represent a binary bit. It is also used for filter coefficients  $\{b_k\}$ . Its use in the text should be clear from the context.

This format has two drawbacks. First, there are two representations for 0. Second, the arithmetic using the sign-magnitude format requires one rule to compute addition, another rule to compute subtraction, and a way to compare two magnitudes to determine their relative value before subtraction.

**MATLAB Implementation** MATLAB is a 64-bit floating-point computation engine that provides results in decimal numbers. Therefore, fixed-point binary operations must be simulated in MATLAB. It provides the function `dec2bin` to convert a positive decimal integer into a B-bit representation, which is a symbol (or a code) and not a number. Hence it cannot be used in computation. Similarly, the function `bin2dec` converts a B-bit binary character code into a decimal integer. For example, `dec2bin(3,3)` gives 011 and `bin2dec('111')` results in 7. To obtain a sign-magnitude format, a sign bit must be prefixed. Similarly, to convert a sign-magnitude format, the leading bit must be used to impart a positive or negative value. These functions are explored in Problem P9.1.

**One's-complement format** In this format, the negation (or complementation) of an integer  $x$  is obtained by complementing every bit (i.e., a 0 is replaced by 1 and a 1 by 0) in the binary representation of  $x$ . Suppose the  $B$ -bit binary representation of  $x$  is  $b_{B-1} b_{B-2} \dots b_0$ ; then the B-bit *one's-complement*,  $\bar{x}$ , of  $x$  is given by

$$\bar{x} \triangleq \bar{b}_{B-1} \bar{b}_{B-2} \dots \bar{b}_0$$

where each bit  $\bar{b}_i$  is a complement of bit  $b_i$ . Clearly then

$$x + \bar{x} \equiv 11 \dots 1 = 2^B - 1 \quad (6.17)$$

The MSB of the representation once again represents the sign bit, because the positive integer has the MSB of 0 so that its negation (or a negative integer) has the MSB of 1. The remaining bits represent either the number  $x$  (if positive) or its one's-complement (if negative). Thus, using (6.17) the one's-complement format representation<sup>2</sup> is given by

$$x_{(1)} \triangleq \begin{cases} x, & x \geq 0 \\ |\bar{x}|, & x < 0 \end{cases} = \begin{cases} x, & x \geq 0 \\ 2^B - 1 - |x|, & x < 0 \end{cases} = \begin{cases} x, & x \geq 0 \\ 2^B - 1 + x, & x < 0 \end{cases} \quad (6.18)$$

Clearly, if  $B$  bits are available, then we can represent only integers from  $(-2^{B-1}+1)$  to  $(+2^{B-1}-1)$ , which is similar to the sign-magnitude format.

<sup>2</sup>The one's-complement format refers to the representation of positive and negative numbers, whereas the one's-complement of a number refers to the negation of that number.

For example, using 3 bits, we can represent numbers from  $-3$  to  $3$  as

-3	-2	-1	-0	0	1	2	3
-----	-----	-----	-----	-----	-----	-----	-----
100	101	110	111	000	001	010	011

which is a different bit arrangement for negative numbers compared to the sign-magnitude format.

The advantage of this format is that subtraction can be achieved by adding the complement, which is very easy to obtain by simply complementing a number's bits. However, there are many drawbacks. There are still two different codes for 0, the addition is a bit tricky to implement, and overflow management requires addition of the overflow bit to the least significant bit (or  $2^0$ ).

**MATLAB Implementation** The one's-complement of a positive integer  $x$  using  $B$  bits can be obtained by using the built-in function `bitcmp(x,B)`, which complements the number's bits. The result is a decimal number between 0 and  $2^B - 1$ . As before, the `dec2bin` can be used to obtain the binary code. Using (6.18), we can develop the MATLAB function `OnesComplement`, which obtains the one's-complement format representation. It uses the sign of a number to determine when to use one's-complement and can use scalar as well as vector values. The result is a decimal equivalent of the representation.

```
function y = OnesComplement(x,B)
% y = OnesComplement(x,B)
% -----
% Decimal equivalent of
% sign-magnitude format integer to b-bit ones'-complement format conversion
%
% x: integer between -2^(B-1) < x < 2^(B-1) (sign-magnitude)
% y: integer between 0 <= y <= 2^b-1 (1's-complement)

if any((x <= -2^(B-1) | (x >= 2^(B-1))))
    error('Numbers must satisfy -2^(B-1) < x < 2^(B-1)')
end
s = sign(x); % sign of x (-1 if x<0, 0 if x=0, 1 if x>0)
sb = (s < 0); % sign-bit (0 if x>=0, 1 if x<0);
y = (1-sb).*x + sb.*bitcmp(abs(x),B);
```

- **EXAMPLE 6.8** Using the function `OnesComplement`, obtain one's-complement format representation of integers from  $-7$  to  $7$  using 4 bits.

**Solution**

MATLAB script:

```
>> x = -7:7
x =
-7   -6   -5   -4   -3   -2   -1    0    1    2    3    4    5    6    7
>> y = OnesComplement(x,4)
y =
 8    9   10   11   12   13   14    0    1    2    3    4    5    6    7
```

Note that the number 15 is missing since we do not have  $-0$  in our original array.  $\square$

**Two's-complement format** The disadvantage of having two codes for the number 0 is eliminated in this format. Positive numbers are coded as usual. The  $B$ -bit two's-complement,  $\tilde{x}$ , of a positive integer  $x$  is given by

$$\tilde{x} = \bar{x} + 1 = 2^B - x \quad \text{or} \quad x + \tilde{x} = 2^B \quad (6.19)$$

where the second equality is obtained from (6.18). Once again, the MSB of the representation provides the sign bit. Thus using (6.19), the two's-complement format representation<sup>3</sup> is given by

$$x_{(2)} = \begin{cases} x, & x \geq 0 \\ -|x|, & x < 0 \end{cases} = \begin{cases} x, & x \geq 0 \\ 2^B - |x|, & x < 0 \end{cases} = \begin{cases} x, & x \geq 0 \\ 2^B + x, & x < 0 \end{cases} \quad (6.20)$$

Thus in  $B$ -bit two's-complement format negative numbers are obtained by adding  $2^B$  to them. Clearly, if  $B$  bits are available, then we can represent  $2^B$  integers from  $(-2^{B-1})$  to  $(+2^{B-1} - 1)$ . For example, using 3 bits, we can represent numbers from  $-4$  to  $3$  as

-4	-3	-2	-1	0	1	2	3
-+-+-	-+-+-	-+-+-	-+-+-	-+-+-	-+-+-	-+-+-	-+-+-
100	101	110	111	000	001	010	011

This format, by shifting to the right (e.g., by incrementing) the code of the negative numbers, straightforwardly removes the problem of having two codes for 0 and gives access to an additional negative number at the left of the line. Thus 4 bits go from  $-8$  to  $+7$ , 8 bits cover the interval  $[-127, +127]$ , and 16 bits cover  $[-32768, +32767]$ .

<sup>3</sup>Again, the two's-complement format refers to the representation of positive and negative numbers, whereas the two's-complement of a number refers to the negation of that number.

**MATLAB Implementation** Using (6.20), we can develop the MATLAB function `TwosComplement`, which obtains the two's-complement format representation. We can use the `bitcmp` function and then add 1 to the result to obtain the two's-complement. However, we will use the last equality in (6.20) to obtain the two's-complement since this approach will also be useful for fractional numbers. The function can use scalar as well as vector values. The result is a decimal equivalent of the two's-complement representation. As before, the `dec2bin` can be used to obtain the binary code.

```
function y = TwosComplement(x,b)
% y = TwosComplement(x,b)
%
% Decimal equivalent of
% sign-magnitude format integer to b-bit ones'-complement format conversion
%
% x: integer between -2^(b-1) <= x < 2^(b-1) (sign-magnitude)
% y: integer between 0 <= y <= 2^b-1 (two's-complement)
if any((x < -2^(b-1) | (x >= 2^(b-1))))
    error('Numbers must satisfy -2^(b-1) <= x < 2^(b-1)')
end
s = sign(x); % Sign of x (-1 if x<0, 0 if x=0, 1 if x>0)
sb = (s < 0); % Sign-bit (0 if x>=0, 1 if x<0);
y = (1-sb).*x + sb.*((2^b)+x); % or y = (1-sb).*x + sb.*bitcmp(abs(x),b)+1;
```

- **EXAMPLE 6.9** Using the function `TwosComplement`, obtain the two's-complement format representation of integers from  $-8$  to  $7$  using 4 bits.

**Solution** MATLAB script:

```
>> x = -8:7
x =
   -8   -7   -6   -5   -4   -3   -2   -1    0    1    2    3    4    5    6    7
>> y = TwosComplement(x,4)
y =
    8    9    10   11   12   13   14   15    0    1    2    3    4    5    6    7
>> y = dec2bin(y,4); disp(sprintf('%s',[y';char(ones(1,16)*32)]))
1000 1001 1010 1011 1100 1101 1110 1111 0000 0001 0010 0011 0100 0101 0110 0111
```

□

The two's-complement format has many interesting characteristics and advantages. These will be given after we discuss the next format—namely, the ten's-complement.

**Ten's-complement format** This is a representation for decimal integers. We will describe it so that we can explore characteristics of two's-complement through decimal integers, which is much easier to understand. Following (6.19), the  $N$ -digit ten's-complement of a positive integer  $x$  is given by

$$\tilde{x} = 10^N - x \quad \text{or} \quad x + \tilde{x} = 10^N \quad (6.21)$$

Using (6.21), the  $N$ -digit ten's-complement format representation is given by

$$x_{(10^N)} \triangleq \begin{cases} x, & x \geq 0 \\ |\tilde{x}|, & x < 0 \end{cases} = \begin{cases} x, & x \geq 0 \\ 10^N - |x|, & x < 0 \end{cases} = \begin{cases} x, & x \geq 0 \\ 10^N + x, & x < 0 \end{cases} \quad (6.22)$$

Thus in  $N$ -digit ten's-complement format (which is sometimes referred to as  $10^N$ -complement format), negative numbers are obtained by adding  $10^N$  to them. Clearly, when  $N$  digits are available, we can represent  $10^N$  integers from  $(-\frac{10^N}{2})$  to  $(+\frac{10^N}{2} - 1)$ . For example, using one digit, we can represent numbers from  $-5$  to  $4$  as

-5	-4	-3	-2	-1	0	1	2	3	4
-----+-----+-----+-----+-----+-----+-----+-----+									
5	6	7	8	9	0	1	2	3	4

- **EXAMPLE 6.10** Using the two-digit ten's-complement, i.e., hundred's-complement format, perform the following operations:  
 1.  $16 - 32$ , 2.  $32 - 16$ , 3.  $-30 - 40$ , 4.  $40 + 20 - 30$ , 5.  $-40 - 20 + 30$ .

### Solution

1.  $16 - 32$

First, we note that  $16 - 32 = -16$ . If we use the usual subtraction rule to proceed from right to left generating carries in the process, we cannot complete the operation. To use the hundred's-complement format, we first note that in the hundred's-complement format we have

$$16_{(100)} = 16, \quad -16_{(100)} = 100 - 16 = 84, \quad \text{and} \quad -32_{(100)} = 100 - 32 = 68$$

Hence  $16 - 32 \equiv 16 + 68 = 84 \equiv -16$  in the sign-magnitude format, as expected.

2.  $32 - 16$

In this case, the hundred's-complement format gives

$$32 + 84 = 116 \equiv 16$$

in the sign-magnitude format by ignoring the generated carry digit. This is because the sign bits were different; therefore, the operation cannot generate an overflow. Hence we check for overflow only if the sign bits are same.

3.  $-30 - 40$

In this case, the hundred's-complement format gives

$$(100 - 30) + (100 - 40) = 70 + 60 = 130$$

Since the sign bits were the same, an overflow is generated and the result is invalid.

$$4. \quad 40 + 20 - 30$$

This is an example of more than one addition or subtraction. Since the final result is well within the range, the overflow can be ignored—that is,

$$40 + 20 + (100 - 30) = 40 + 20 + 70 = 130 \equiv 30$$

which is a correct result.

$$5. \quad -40 - 20 + 30$$

In this case, we have

$$(100 - 40) + (100 - 20) + 30 = 60 + 80 + 30 = 170 \equiv -30$$

in the sign-magnitude format, which is, again, a correct result.  $\square$

**MATLAB Implementation** Using (6.22), one can develop the MATLAB function, `TensComplement`, which obtains ten's-complement format representation. It is similar to the `TwosComplement` function and is explored in Problem P6.23.

**Advantages of two's-complement format** Using the results of the Example 6.10, we now state the benefits of the two's-complement format. These also hold (with obvious modifications) for the ten's-complement format.

1. It provides for all  $2^{B+1}$  distinct representations for a  $B$ -bit fractional representation. There is only one representation for zero.
2. This complement is compatible with our notion of negation: the complement of a complement is the number itself.
3. It unifies the subtraction and addition operations (subtractions are essentially additions).
4. In a sum of more than two numbers, the internal overflows do not affect the final result so long as the result is within the range (i.e., adding two positive numbers gives a positive result, and adding two negative numbers gives a negative result).

Hence in most A/D converters and processors, negative numbers are represented using two's-complement format. Almost all current processors implement signed arithmetic using this format and provide special functions (e.g., an overflow flag) to support it.

**Excess- $2^{B-1}$  format** This format is used in describing the exponent of floating-point arithmetic; hence it is briefly discussed here. In excess- $2^{B-1}$  signed format (also known as a *biased* format), all positive and

negative integers between  $-2^{B-1}$  and  $2^{B-1} - 1$  are given by

$$x_{(e)} \stackrel{\Delta}{=} 2^{B-1} + x \quad (6.23)$$

For example, using 3 bits, we can represent the numbers from  $-4$  to  $3$  as

-4	-3	-2	-1	0	1	2	3
-	-	-	-	-	-	-	-
000	001	010	011	100	101	110	111

Notice that this format is very similar to the two's-complement format, but the sign bit is complemented. The arithmetic for this format is similar to that of the two's-complement format. It is used in the exponent of floating-point number representation.

### 6.5.2 GENERAL FIXED-POINT ARITHMETIC

Using the discussion of integer arithmetic from the last section as a guide, we can extend the fixed-point representation to arbitrary real (integer and fractional) numbers. We assume that a given infinite-precision real number  $x$  is approximated by a binary number  $\hat{x}$  with the following bit arrangement:

$$\hat{x} = \underset{\substack{\uparrow \\ \text{Sign bit}}}{\pm} \underbrace{\text{xx} \cdots \text{x}}_{\substack{\text{"L"} \\ \text{Integer bits}}} \blacktriangle \underbrace{\text{xx} \cdots \text{x}}_{\substack{\text{"B"} \\ \text{Fraction bits}}} \quad (6.24)$$

where the sign bit  $\pm$  is 0 for positive numbers and 1 for negative numbers,  $x$  represents either a 0 or a 1, and  $\blacktriangle$  represents the *binary point*. This representation is in fact the sign-magnitude format for real numbers, as we will see. The total *word length* of the number  $\hat{x}$  is then equal to  $L + B + 1$  bits.

- **EXAMPLE 6.11** Let  $L = 4$  and  $B = 5$ , which means  $\hat{x}$  is a 10-bit number. Represent 11010 $\blacktriangle$ 01110 in decimal.

**Solution**

$$\begin{aligned} \hat{x} &= -(1 \times 2^3 + 0 \times 2^2 + 1 \times 2^1 + 0 \times 2^0 + 0 \times 2^{-1} + 1 \times 2^{-2} + 1 \times 2^{-3} + 1 \times 2^{-4} + 0 \times 2^{-5}) \\ &= -10.4375 \end{aligned}$$

in decimal. □

In many A/D converters and processors, the real numbers are scaled so that the fixed-point representation is in the  $(-1, 1)$  range. This has the advantage that the multiplication of two fractions is always a fraction

and, as such, there is no overflow. Hence we will consider the following representation:

$$\hat{x} = A(\pm \underbrace{\text{xxxxxx} \cdots \text{x}}_{B \text{ fraction bits}}) \quad (6.25)$$

where  $A$  is a positive *scaling factor*.

- EXAMPLE 6.12** Represent the number  $\hat{x} = -10.4375$  in Example 6.11 using a fraction-only arrangement.

**Solution** Choose  $A = 2^4 = 16$  and  $B = 9$ . Then

$$\hat{x} = -10.4375 = 16(1\blacktriangle 101001110)$$

Hence by properly choosing  $A$  and  $B$ , one can obtain any fraction-only representation.

*Note:* The scalar  $A$  need not be a power of two. In fact, by choosing any real number  $A$  we can obtain an arbitrary range. The power-of-two choice for  $A$ , however, makes hardware implementation a little easier.  $\square$

As discussed in the previous section, there are three main formats for fixed-point arithmetic, depending on how negative numbers are obtained. For all these formats, positive numbers have exactly the same representation. In the following, we assume the fraction-only arrangement.

**Sign-magnitude format** As the name suggests, the magnitude is given by the  $B$ -bit fraction, and the sign is given by the MSB. Thus

$$\hat{x} = \begin{cases} 0\blacktriangle x_1 x_2 \cdots x_B & \text{if } x \geq 0 \\ 1\blacktriangle x_1 x_2 \cdots x_B & \text{if } x < 0 \end{cases} \quad (6.26)$$

For example, when  $B = 2$ ,  $\hat{x} = +1/4$  is represented by  $\hat{x} = 0\blacktriangle 01$ , and  $\hat{x} = -1/4$  is represented by  $\hat{x} = 1\blacktriangle 01$ .

**One's-complement format** In this format, the positive numbers have the same representation as the sign-magnitude format. When the number is negative, then its magnitude is given by its bit-complement arrangement. Thus

$$\hat{x} = \begin{cases} 0\blacktriangle x_1 x_2 \cdots x_B & \text{if } x \geq 0 \\ 1\blacktriangle \bar{x}_1 \bar{x}_2 \cdots \bar{x}_B & \text{if } x < 0 \end{cases} \quad (6.27)$$

For example, when  $B = 2$ ,  $\hat{x} = +1/4$  is represented by  $\hat{x} = 0\blacktriangle 01$ , and  $\hat{x} = -1/4$  is represented by  $\hat{x} = 1\blacktriangle 10$ .

**Two's-complement format** Once again, the positive numbers have the same representation. Negative numbers are obtained by first complementing the magnitude and then modulo-2 adding 1 to the last bit or the *least-significant bit* (LSB). Stated differently, two's-complement is formed by subtracting the magnitude of the number from 2. Thus

$$\hat{x} = \begin{cases} 0\blacktriangle x_1 x_2 \cdots x_B & \text{if } x \geq 0 \\ 2 - |x| = 1\blacktriangle \bar{x}_1 \bar{x}_2 \cdots \bar{x}_B \oplus 0\blacktriangle 00 \cdots 1 = 1\blacktriangle y_1 y_2 \cdots y_B & \text{if } x < 0 \end{cases} \quad (6.28)$$

where  $\oplus$  represents modulo-2 addition and bit  $y$  is, in general, different from bit  $\bar{x}$ . For example, when  $B = 2$ ,  $\hat{x} = +1/4$  is represented by  $\hat{x} = 0\blacktriangle 01$ , and  $\hat{x} = -1/4$  is represented by  $\hat{x} = 1\blacktriangle 10 \oplus 0\blacktriangle 01 = 1\blacktriangle 11$ .

- **EXAMPLE 6.13** Let  $B = 3$ ; then  $\hat{x}$  is a 4-bit number (sign plus 3 bits). Provide all possible values that  $\hat{x}$  can take in each of the three formats.

**Solution** There are  $2^4 = 16$  possible values that  $\hat{x}$  can take for each of the three formats, as shown in the following table.

Binary	Sign-Magnitude	one's	two's
0 $\blacktriangle$ 111	7/8	7/8	7/8
0 $\blacktriangle$ 110	6/8	6/8	6/8
0 $\blacktriangle$ 101	5/8	5/8	5/8
0 $\blacktriangle$ 100	4/8	4/8	4/8
0 $\blacktriangle$ 011	3/8	3/8	3/8
0 $\blacktriangle$ 010	2/8	2/8	2/8
0 $\blacktriangle$ 001	1/8	1/8	1/8
0 $\blacktriangle$ 000	0	0	0
1 $\blacktriangle$ 000	-0	-7/8	-1
1 $\blacktriangle$ 001	-1/8	-6/8	-7/8
1 $\blacktriangle$ 010	-2/8	-5/8	-6/8
1 $\blacktriangle$ 011	-3/8	-4/8	-5/8
1 $\blacktriangle$ 100	-4/8	-3/8	-4/8
1 $\blacktriangle$ 101	-5/8	-2/8	-3/8
1 $\blacktriangle$ 110	-6/8	-1/8	-2/8
1 $\blacktriangle$ 111	-7/8	-0	-1/8

□

In Example 6.13, observe that the bit arrangement is exactly the same as in the integer case for 4 bits. The only difference is in the position of the binary point. Thus the MATLAB programs developed in the previous section can easily be used with proper modifications. The MATLAB

function `sm2oc` converts a decimal sign-magnitude fraction into its one's-complement format, while the function `oc2sm` performs the inverse operation. These functions are explored in Problem P6.24. Similarly, MATLAB functions `sm2tc` and `tc2sm` convert a decimal sign-magnitude fraction into its two's-complement format and vice versa, respectively; they are explored in Problem P6.25.

### 6.5.3 FLOATING-POINT ARITHMETIC

In many applications, the range of numbers needed is very large. For example, in physics one might need, at the same time, the mass of the sun (e.g.,  $2.10^{30}$  kg) and the mass of the electron (e.g.,  $9.10^{-31}$  kg). These two numbers cover a range of over  $10^{60}$ . For fixed-point arithmetic, we would need 62-digit numbers (or 62-digit precision). However, even the mass of the sun is not accurately known with a precision of 5 digits, and there is almost no measurement in physics that could be made with a precision of 62 digits. One could then imagine making all calculations with a precision of 62 digits and throwing away 50 or 60 of them before printing out the final results. This would be wasteful of both CPU time and memory space. So what is needed is a system for representing numbers in which the range of expressible numbers is independent of the number of significant digits.

**Decimal numbers** The floating-point representation for a decimal number  $x$  is based on expressing the number in the scientific notation:

$$x = \pm M \times 10^{\pm E}$$

where  $M$  is called the *mantissa* and  $E$  is the *exponent*. However, there are different possible representations of the same number, depending on the actual position of the decimal point—for example,

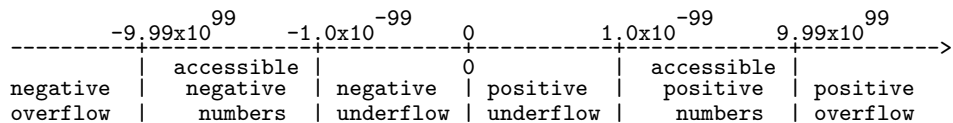
$$1234 = 0.1234 \times 10^4 = 1.234 \times 10^3 = 12.34 \times 10^2 = \dots$$

To fix this problem, a floating-point number is always stored using a unique representation, which has only one nonzero digit to the left of the decimal point. This representation of a floating-point number is called a *normalized form*. The normalized form of the preceding number is  $1.234 \times 10^3$ , because it is the only representation resulting in a unique nonzero digit to the left of the decimal point. The digit arrangement for the normalized form is given by

$$\hat{x} = \begin{array}{c} \text{sign of } M \\ \downarrow \\ \pm \end{array} \quad \begin{array}{c} \text{x} \blacktriangle \underbrace{\text{xx} \cdots \text{x}}_{N\text{-bit } M} \end{array} \quad \begin{array}{c} \text{sign of } E \\ \downarrow \\ \pm \end{array} \quad \begin{array}{c} \underbrace{\text{xx} \cdots \text{x}}_{L\text{-bit } E} \end{array} \quad (6.29)$$

For the negative numbers, we have the same formats as the fixed-point representations, including the ten's-complement format.

The number of digits used in the exponent determine the range of representable numbers, whereas the number of digits used in the mantissa determine the precision of the numbers. For example, if the mantissa is expressed using two digits plus the sign, and the exponent is expressed using two digits plus the sign, then the real number line will be covered as



The range of accessible floating-point numbers with a given representation can be large, but it is still finite. In the preceding example (e.g., with two digits for the mantissa and two digits for the exponent), there are only  $9 \times 10 \times 10 \times 199 = 179,100$  positive numbers, and as many negative numbers, plus the number zero, for a total of 358,201 numbers that can be represented.

**Binary numbers** Although the fraction-only fixed-point arithmetic does not have any overflow problems when two numbers are multiplied, it does suffer from overflow problems when two numbers are added. Also, the fixed-point numbers have limited dynamic range. Both of these aspects are unacceptable for an intensive computational job. These limitations can be removed by making the binary point ▲ floating rather than fixed.

The floating-point bit arrangement for binary-number representation is similar to that for the decimal numbers. In practice, however, two exceptions are made. The exponent is expressed using  $L$ -bit excess- $2^{L-1}$  format, and the  $B$ -bit normalized mantissa is a fractional number with a 1 following the binary point. Note that the sign bit is the MSB of the bit pattern. Thus the  $B$ -bit mantissa and  $L$ -bit exponent (for a total of  $B + L + 1$  word length) bit pattern is given by (note the reversal of the mantissa and exponent places)

$$\hat{x} = \underset{\substack{\downarrow \\ \text{Sign of } M}}{\pm} \underbrace{\text{xx} \cdots \text{x}}_{\substack{\text{L-bit } E}} \blacktriangle \underbrace{1\text{x} \cdots \text{x}}_{\substack{\text{B-bit } M}} \quad (6.30)$$

where exponent  $E$  is adjusted so that we have a normalized mantissa—that is,  $1/2 \leq M < 1$ . Hence the first bit after the binary point is always 1. The decimal equivalent of  $\hat{x}$  is given by

$$\hat{x} = \pm M \times 2^E \quad (6.31)$$

For the negative numbers, we can have the same formats as the fixed-point representations for the mantissa including two's-complement format.

However, the most widely used format for the mantissa is the sign-magnitude one.

- EXAMPLE 6.14** Consider a 32-bit floating-point word with the following arrangement:

$$\hat{x} = \pm \underbrace{xx \cdots x}_{\text{8-bit } E} \Delta \underbrace{1x \cdots x}_{\text{23-bit } M}$$

Determine the decimal equivalent of

010000011110000000000000000000000000000

## Solution

Since the exponent is 8-bit, it is expressed in excess- $2^7$  or in excess-128 format. Then the bit pattern can be partitioned into

The sign bit is 0, which means that the number is positive. The exponent code is 131, which means that its decimal value is  $131 - 128 = 3$ . Thus the bit pattern represents the decimal number  $\hat{x} = +\left(2^{-1} + 2^{-2}\right)(2^3) = 2^2 + 2^1 = 6$ .  $\square$

- EXAMPLE 6.15** Let  $\hat{x} = -0.1875$ . Represent  $\hat{x}$  using the format given in (6.30), in which  $B = 11$ ,  $L = 4$  (for a total of 16 bits), and sign-magnitude format is used for the mantissa.

## Solution

We can write

$$\hat{x} = -0.1875 = -0.75 \times 2^{-2}$$

Hence the exponent is  $-2$ , the mantissa is  $0.75$ , and the sign is negative. The 4-bit exponent, in excess-8 format, is expressed as  $8 - 2 = 6$  or with bit pattern  $0110$ . The mantissa is expressed as  $1100000000$ . Since  $\hat{x}$  is negative, the bit pattern is

$$\hat{x} \equiv 1011011000000000$$

1

The advantages of the floating-point representation are that it has a large dynamic range and that its resolution, defined as the interval between two consecutive representable levels, is proportional to the magnitude. The disadvantages include no representation for the number 0 and the fact that the arithmetic operations are more complicated than their fixed-point representations.

**IEEE 754 standard** In the early days of the digital computer revolution, each processor design had its own internal representation for floating-point numbers. Since floating-point arithmetic is more complicated to implement, some of these designs did incorrect arithmetic. Therefore, in 1985 IEEE issued a standard (IEEE standard 754-1985, or IEEE-754 for short) to allow floating-point data exchange among different computers and to provide hardware designers with a model known to be correct. Currently, almost all manufacturers design main processors or a dedicated coprocessor for floating-point operations using the IEEE-754 standard representation.

The IEEE-754 standard defines three formats for binary numbers: a 32-bit single-precision format, a 64-bit double-precision format, and an 80-bit temporary format (which is used internally by the processors or arithmetic coprocessors to minimize rounding errors).

We will briefly describe the 32-bit single-precision standard. This standard has many similarities with the floating-point representation discussed above, but there are also differences. Remember, this is another model advocated by IEEE. The form of this model is

$$\hat{x} = \begin{array}{c} \text{sign of } M \\ \downarrow \\ \pm \end{array} \underbrace{\text{xx}\cdots\text{x}}_{\text{8-bit E}} \blacktriangle \underbrace{\text{xx}\cdots\text{x}}_{\text{23-bit M}} \quad (6.32)$$

The mantissa's value is called the *significand* in this standard. Features of this model are as follows:

- If the sign bit is 0, the number is positive; if the sign bit is 1, the number is negative.
- The exponent is coded in 8-bit excess-127 (and not 128) format. Hence the uncoded exponents are between  $-127$  and  $128$ .
- The mantissa is in 23-bit binary. A normalized mantissa always starts with a bit 1, followed by the binary point, followed by the rest of the 23-bit mantissa. However, the leading bit 1, which is always present in a normalized mantissa, is hidden (not stored) and needs to be restored for computation. Again, note that this is different from the usual definition of the normalized mantissa. If all the 23 bits representing the mantissa are set to 0, the significand is 1 (remember the implicit leading 1). If all 23 bits are set to 1, the significand is almost 2 (in fact  $2 - 2^{-23}$ ). All IEEE 754 normalized numbers have a significand that is in the interval  $1 \leq M < 2$ .
- The smallest normalized number is  $2^{-126}$ , and the largest normalized number is almost  $2^{128}$ . The resulting positive decimal range is roughly  $10^{-38}$  to  $10^{38}$  with a similar negative range.
- If  $E = 0$  and  $M = 0$ , then the representation is interpreted as a *denormalized* number (i.e., the hidden bit is 0) and is assigned a value

of  $\pm 0$ , depending on the sign bit (called the *soft zero*). Thus 0 has two representations.

- If  $E = 255$  and  $M \neq 0$ , then the representation is interpreted as a *not-a-number* (abbreviated as NaN). MATLAB assigns a variable NaN when this happens—for example,  $0/0$ .
- If  $E = 255$  and  $M = 0$ , then the representation is interpreted as  $\pm\infty$ . MATLAB assigns a variable inf when this happens—for example,  $1/0$ .

- EXAMPLE 6.16** Consider the bit pattern given in Example 6.14. Assuming IEEE-754 format, determine its decimal equivalent.

**Solution**

The sign bit is 0 and the exponent code is 131, which means that the exponent is  $131 - 127 = 4$ . The significand is  $1 + 2^{-1} + 2^{-2} = 1.75$ . Hence the bit pattern represents

$$\hat{x} = +(1 + 2^{-1} + 2^{-2})(2^4) = 2^4 + 2^3 + 2^2 = 28$$

which is different from the number in Example 6.14.

MATLAB employs the 64-bit double-precision IEEE-754 format for all its number representations and the 80-bit temporary format for its internal computations. Hence all calculations that we perform in MATLAB are in fact floating-point computations. Simulating a different floating-point format in MATLAB would be much more complicated and would not add any more insight to our understanding than the native format. Hence we will not consider a MATLAB simulation of floating-point arithmetic as we did for fixed-point.

## 6.6 THE PROCESS OF QUANTIZATION AND ERROR CHARACTERIZATIONS

---

From the discussion of number representations in the previous section, it should be clear that a general infinite-precision real number must be assigned to one of the finite representable numbers, given a specific structure for the finite-length register (i.e., the arithmetic as well as the format). Usually, in practice, there are two different operations by which this assignment is made to the nearest number or level: the *truncation* operation and the *rounding* operation. These operations affect the accuracy as well as general characteristics of digital filters and DSP operations.

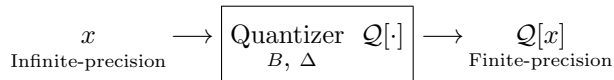
We assume, without loss of generality, that there are  $B + 1$  bits in the fixed-point (fractional) arithmetic or in the mantissa of floating-point

arithmetic including the sign bit. Then the resolution ( $\Delta$ ) is given by

$$\Delta = 2^{-B} \begin{cases} \text{absolute in the case of fixed-point arithmetic} \\ \text{relative in the case of floating-point arithmetic} \end{cases} \quad (6.33)$$

### 6.6.1 FIXED-POINT ARITHMETIC

The quantizer block diagram in this case is given by



where  $B$ , the number of fractional bits, and  $\Delta$ , the resolution, are the parameters of the quantizer. We will denote the finite word-length number, after quantization, by  $Q[x]$  for an input number  $x$ . Let the quantization error be given by

$$e \triangleq Q[x] - x \quad (6.34)$$

We will analyze this error for both the truncation and the rounding operations.

**Truncation operation** In this operation, the number  $x$  is truncated beyond  $B$  significant bits (i.e., the rest of the bits are eliminated) to obtain  $Q_T[x]$ . In MATLAB, to obtain a  $B$ -bit truncation, we have to first scale the number  $x$  upward by  $2^B$ , then use the `fix` function on the scaled number, and finally scale the result down by  $2^{-B}$ . Thus the MATLAB statement `xhat = fix(x*2^B)/2^B;` implements the desired operation. We will now consider each of the three formats.

**Sign-magnitude format** If the number  $x$  is positive, then after truncation  $Q_T[x] \leq x$  since some value in  $x$  is lost. Hence quantizer error for truncation denoted by  $e_T$  is less than or equal to 0 or  $e_T \leq 0$ . However, since there are  $B$  bits in the quantizer, the maximum error in terms of magnitude is

$$|e_T| = 0 \blacktriangleunderbrace{00 \cdots 0}_{B \text{ bits}} 111 \cdots = 2^{-B} \text{ (decimal)} \quad (6.35)$$

or

$$-2^{-B} \leq e_T \leq 0, \quad \text{for } x \geq 0 \quad (6.36)$$

Similarly, if the  $x < 0$  then after truncation  $Q_T[x] \geq x$  since  $Q_T[x]$  is less negative, or  $e_T \geq 0$ . The largest magnitude of this error is again  $2^{-B}$ , or

$$0 \leq e_T \leq 2^{-B}, \quad \text{for } x < 0 \quad (6.37)$$

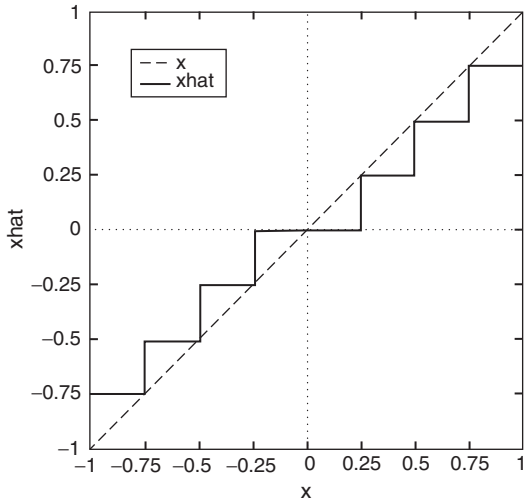


**FIGURE 6.19** Truncation error characteristics in the sign-magnitude format

- **EXAMPLE 6.17** Let  $-1 < x < 1$ , and let  $B = 2$ . Using MATLAB, verify the truncation error characteristics.

**Solution**

The resolution is  $\Delta = 2^{-2} = 0.25$ . Using the following MATLAB script, we can verify the truncation error  $e_T$  relations given in (6.36) and (6.37).

```
x = [-1+2^(-10):2^(-10):1-2^(-10)]; % Sign-Mag numbers between -1 and 1
B = 2; % Number of bits for truncation
xhat = fix(x*2^B)/2^B % Truncation
plot(x,x,'g',x,xhat,'r','linewidth',1); % Plot
```

The resulting plots of  $x$  and  $\hat{x}$  are shown in Figure 6.19. Note that the plot of  $\hat{x}$  has a staircase shape and that it satisfies (6.36) and (6.37). □

**One's-complement format** For  $x \geq 0$ , we have the same characteristics for  $e_T$  as in sign-magnitude format—that is,

$$-2^{-B} \leq e_T \leq 0, \quad \text{for } x \geq 0 \quad (6.38)$$

For  $x < 0$ , the representation is obtained by complementing all bits, including the sign bit. To compute the maximum error, let

$$x = 1 \blacktriangle b_1 b_2 \cdots b_B 000 \cdots = -\{\blacktriangle (1 - b_1)(1 - b_2) \cdots (1 - b_B) 111 \cdots\}$$

After truncation, we obtain

$$\mathcal{Q}_T[x] = 1 \blacktriangle b_1 b_2 \cdots b_B = -\{\blacktriangle (1 - b_1)(1 - b_2) \cdots (1 - b_B)\}$$

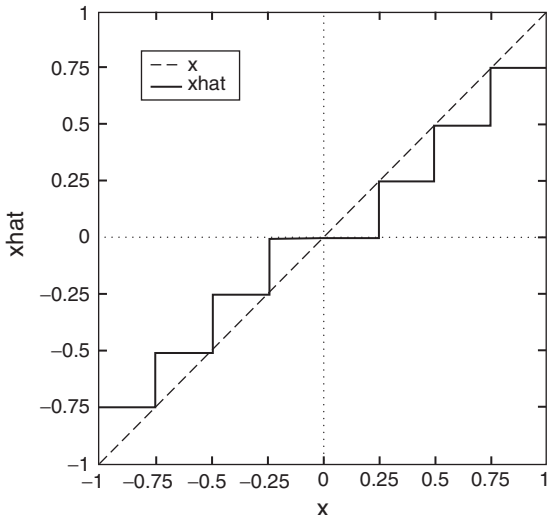


**FIGURE 6.20** Truncation error characteristics in the one's-complement format

Clearly,  $x$  is more negative than  $Q_T[x]$  or  $x \leq Q_T[x]$  or  $e_T \geq 0$ . In fact, the maximum truncation error is

$$e_{T\max} = 0.100\cdots 0111\cdots = 2^{-B} \text{ (decimal)}$$

Hence

$$0 \leq e_T \leq 2^{-B}, \quad \text{for } x < 0 \quad (6.39)$$

- **EXAMPLE 6.18** Again let  $-1 < x < 1$  and  $B = 2$  with the resolution  $\Delta = 2^{-2} = 0.25$ . Using MATLAB, verify the truncation error  $e_T$  relations given in (6.38) and (6.39).

#### Solution

The MATLAB script uses functions `sm2oc` and `oc2sm`, which are explored in Problem P6.24.

```

x = [-1+2^(-10):2^(-10):1-2^(-10)]; % Sign-Magnitude numbers between -1 and 1
B = 2; % Select bits for truncation
y = sm2oc(x,B); % Sign-mag to one's complement
yhat = fix(y*2^B)/2^B; % Truncation
xhat = oc2sm(yhat,B); % One's-complement to sign-mag
plot(x,x,'g',x,xhat,'r','linewidth',1); % Plot

```

The resulting plots of  $x$  and  $\hat{x}$  are shown in Figure 6.20. Note that the plot of  $\hat{x}$  is identical to the plot in Figure 6.19 and that it satisfies (6.38) and (6.39). □

**Two's-complement format** Once again, for  $x \geq 0$ , we have

$$-2^{-B} \leq e_T \leq 0, \quad \text{for } x \geq 0 \quad (6.40)$$

For  $x < 0$ , the representation is given by  $2 - |x|$  where  $|x|$  is the magnitude. Hence the magnitude of  $x$  is given by

$$|x| = 2 - x \quad (6.41)$$

with  $x = 1\Delta b_1 b_2 \cdots b_B b_{B+1} \cdots$ . After truncation to  $B$  bits, we obtain  $Q_T[x] = 1\Delta b_1 b_2 \cdots b_B$ , the magnitude of which is

$$|Q_T[x]| = 2 - Q_T[x] \quad (6.42)$$

From (6.41) and (6.42),

$$\begin{aligned} |Q_T[x]| - |x| &= x - Q_T[x] = 1\Delta b_1 b_2 \cdots b_B b_{B+1} \cdots - 1\Delta b_1 b_2 \cdots b_B \\ &= 0\Delta 00 \cdots 0 b_{B+1} \cdots \end{aligned} \quad (6.43)$$

The largest change in magnitude from (6.43) is

$$0\Delta 00 \cdots 0111 \cdots = 2^{-B} \text{ (decimal)} \quad (6.44)$$

Since the change in the magnitude is positive, then after truncation  $Q_T[x]$  becomes more negative, which means that  $Q_T[x] \leq x$ . Hence

$$-2^{-B} \leq e_T \leq 0, \quad \text{for } x < 0 \quad (6.45)$$

- **EXAMPLE 6.19** Again consider  $-1 < x < 1$  and  $B = 2$  with the resolution  $\Delta = 2^{-2} = 0.25$ . Using MATLAB, verify the truncation error  $e_T$  relations given in (6.40) and (6.45).

#### Solution

The MATLAB script uses functions `sm2tc` and `tc2sm`, which are explored in Problem P6.25.

```

x = [-1+2^(-10):2^(-10):1-2^(-10)]; % Sign-magnitude numbers between -1 and 1
B = 2; % Select bits for truncation
y = sm2tc(x); % Sign-mag to two's complement
yhat = fix(y*2^B)/2^B; % Truncation
xq = tc2sm(yq); % Two's-complement to sign-mag
plot(x,x,'g',x,xhat,'r','linewidth',1); % Plot

```

The resulting plots of  $x$  and  $\hat{x}$  are shown in Figure 6.21. Note that the plot of  $\hat{x}$  is also a staircase graph but is below the  $x$  graph and that it satisfies (6.40) and (6.45). □

Collecting results (6.36)–(6.40) and (6.45) along with those in Figures 6.19–6.21, we conclude that the truncation characteristics for fixed-point arithmetic are the same for the sign-magnitude and the one's-complement formats but are different for the two's-complement format.

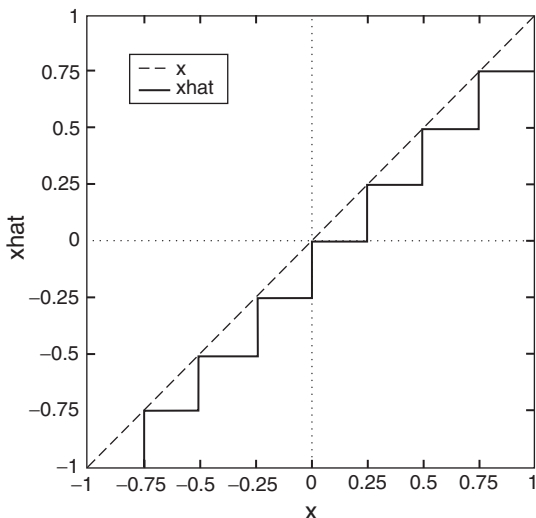


**FIGURE 6.21** Truncation error characteristics in the two's-complement format

**Rounding operation** In this operation, the real number  $x$  is rounded to the nearest representable level, which we will refer to as  $Q_R[x]$ . In MATLAB, to obtain a  $B$ -bit rounding approximation, we have to first scale the number  $x$  up by  $2^B$ , then use the `round` function on the scaled number, and finally scale the result down by  $2^{-B}$ . Thus the MATLAB statement `xhat = round(x*2^B)/2^B;` implements the desired operation.

Since the quantization step or resolution is  $\Delta = 2^{-B}$ , the magnitude of the maximum error is

$$|e_R|_{\max} = \frac{\Delta}{2} = \frac{1}{2}2^{-B} \quad (6.46)$$

Hence for all three formats, the quantizer error due to rounding, denoted by  $e_R$ , satisfies

$$-\frac{1}{2}2^{-B} \leq e_R \leq \frac{1}{2}2^{-B} \quad (6.47)$$

- **EXAMPLE 6.20** Demonstrate the rounding operations and the corresponding error characteristics on the signal of Examples 6.17–6.19 using the three formats.

### Solution

Since the rounding operation assigns values that can be larger than the unquantized values, which can create problems for the two's- and one's-complement formats, we will restrict the signal over the interval  $[-1, 1 - 2^{-B-1}]$ . The following MATLAB script shows the two's-complement format rounding, but other scripts are similar (readers are encouraged to verify).

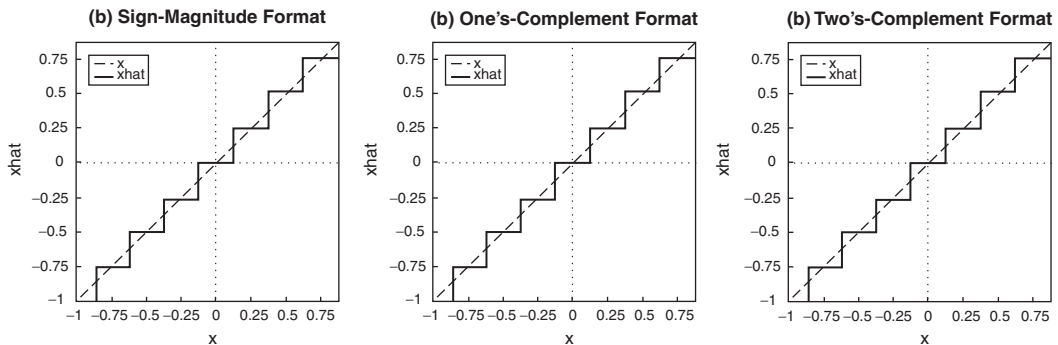


**FIGURE 6.22** Rounding error characteristics in the fixed-point representation

```
B = 2; % Select bits for rounding
x = [-1:2^(-10):1-2^(-B-1)]; % Sign-magnitude numbers between -1 and 1
y = sm2tc(x); % Sign-mag to two's complement
yq = round(y*2^B)/2^B; % Rounding
xq = tc2sm(yq); % Two's-complement to sign-mag
```

The resulting plots for the sign-magnitude, one's-, and two's-complement formats are shown in Figure 6.22. These plots do satisfy (6.47).  $\square$

Comparing the error characteristics of the truncation and rounding operations given in Figures 6.19 through 6.22, it is clear that the rounding operation is a superior one for the quantization error. This is because the error is symmetric with respect to zero (or equal positive and negative distribution) and because the error is the same across all three formats. Hence we will mostly consider the rounding operation for the floating-point arithmetic as well as for further analysis.

### 6.6.2 FLOATING-POINT ARITHMETIC

In this arithmetic, the quantizer affects only the mantissa  $M$ . However, the number  $x$  is represented by  $M \times 2^E$  where  $E$  is the exponent. Hence the quantizer errors are multiplicative and depend on the magnitude of  $x$ . Therefore, the more appropriate measure of error is the relative error rather than the absolute error,  $(Q[x] - x)$ . Let us define the relative error,  $\varepsilon$ , as

$$\varepsilon \triangleq \frac{Q[x] - x}{x} \quad (6.48)$$

Then the quantized value  $Q[x]$  can be written as

$$Q[x] = x + \varepsilon x = x(1 + \varepsilon) \quad (6.49)$$

When  $\mathcal{Q}[x]$  is due to the rounding operation, then the *error in the mantissa* is between  $[-\frac{1}{2}2^{-B}, \frac{1}{2}2^{-B}]$ . In this case, we will denote the relative error by  $\varepsilon_R$ . Then from (6.31), the absolute error,  $\mathcal{Q}_R[x] - x = \varepsilon_R x$ , is between

$$\left(-\frac{1}{2}2^{-B}\right)2^E \leq \varepsilon_R x \leq \left(\frac{1}{2}2^{-B}\right)2^E \quad (6.50)$$

Now for a given  $E$ , and since the mantissa is between  $\frac{1}{2} \leq M < 1$  (this is not the IEEE-754 model), the number  $x$  is between

$$2^{E-1} \leq x < 2^E \quad (6.51)$$

Hence from (6.50) and using the smallest value in (6.51), we obtain

$$-2^{-B} \leq \varepsilon_R \leq 2^{-B} \quad (6.52)$$

This relative error relation, (6.52), will be used in subsequent analysis.

## 6.7 QUANTIZATION OF FILTER COEFFICIENTS

---

We now study the finite word-length effects on the filter responses, pole-zero locations, and stability when the filter coefficients are quantized. We will separately discuss the issues relating to IIR and FIR filters since we can obtain simpler results for FIR filters. We begin with the case of IIR filters.

### 6.7.1 IIR FILTERS

Consider a general IIR filter described by

$$H(z) = \frac{\sum_{k=0}^M b_k z^{-k}}{1 + \sum_{k=1}^N a_k z^{-k}} \quad (6.53)$$

where  $a_k$ s and  $b_k$ s are the filter coefficients. Now assume that these coefficients are represented by their finite-precision numbers  $\hat{a}_k$ s and  $\hat{b}_k$ s. Then we get a new filter system function

$$H(z) \rightarrow \hat{H}(z) \triangleq \frac{\sum_{k=0}^M \hat{b}_k z^{-k}}{1 + \sum_{k=1}^N \hat{a}_k z^{-k}} \quad (6.54)$$

Since this is a new filter, we want to know how “different” this filter is from the original one  $H(z)$ . Various aspects can be compared; for example, we may want to compare their magnitude responses, or phase responses, or change in their pole-zero locations, and so on. A general analytical expression to compute this change in all these aspects is difficult to derive. This is where MATLAB can be used to investigate this change and its overall effect on the usability of the filter.

### 6.7.2 EFFECT ON POLE-ZERO LOCATIONS

One aspect can be reasonably analyzed, which is the movement of filter poles when  $a_k$  is changed to  $\hat{a}_k$ . This can be used to check the stability of IIR filters. A similar movement of zeros to changes in numerator coefficients can also be analyzed.

To evaluate this movement, consider the denominator polynomial of  $H(z)$  in (6.53),

$$D(z) \triangleq 1 + \sum_{k=1}^N a_k z^{-k} = \prod_{\ell=1}^N (1 - p_\ell z^{-1}) \quad (6.55)$$

where  $\{p_\ell\}$ s are the poles of  $H(z)$ . We will regard  $D(z)$  as a function  $D(p_1, \dots, p_N)$  of poles  $\{p_1, \dots, p_N\}$  where each pole  $p_\ell$  is a function of the filter coefficients  $\{a_1, \dots, a_N\}$ —that is,  $p_\ell = f_\ell(a_1, \dots, a_N)$ ,  $\ell = 1, \dots, N$ . Then the change in the denominator  $D(z)$  due to a change in the  $k$ th coefficient  $a_k$  is given by

$$\left( \frac{\partial D(z)}{\partial a_k} \right) = \left( \frac{\partial D(z)}{\partial p_1} \right) \left( \frac{\partial p_1}{\partial a_k} \right) + \left( \frac{\partial D(z)}{\partial p_2} \right) \left( \frac{\partial p_2}{\partial a_k} \right) + \dots + \left( \frac{\partial D(z)}{\partial p_N} \right) \left( \frac{\partial p_N}{\partial a_k} \right) \quad (6.56)$$

where, from (6.55),

$$\left( \frac{\partial D(z)}{\partial p_i} \right) = \frac{\partial}{\partial p_i} \left[ \prod_{\ell=1}^N (1 - p_\ell z^{-1}) \right] = -z^{-1} \prod_{\ell \neq i} (1 - p_\ell z^{-1}) \quad (6.57)$$

From (6.57), note that  $\left. \left( \frac{\partial D(z)}{\partial p_i} \right) \right|_{z=p_\ell} = 0$  for  $\ell \neq i$ . Hence from (6.56) we obtain

$$\left. \left( \frac{\partial D(z)}{\partial a_k} \right) \right|_{z=p_\ell} = \left. \left( \frac{\partial D(z)}{\partial p_\ell} \right) \right|_{z=p_\ell} \left( \frac{\partial p_\ell}{\partial a_k} \right) \quad \text{or} \quad \left( \frac{\partial p_\ell}{\partial a_k} \right) = \frac{\left. \left( \frac{\partial D(z)}{\partial a_k} \right) \right|_{z=p_\ell}}{\left. \left( \frac{\partial D(z)}{\partial p_\ell} \right) \right|_{z=p_\ell}} \quad (6.58)$$

Now

$$\left. \left( \frac{\partial D(z)}{\partial a_k} \right) \right|_{z=p_\ell} = \frac{\partial}{\partial a_k} \left( 1 + \sum_{i=1}^N a_i z^{-i} \right) \Bigg|_{z=p_\ell} = z^{-k} \Big|_{z=p_\ell} = p_\ell^{-k} \quad (6.59)$$

From (6.57), (6.58), and (6.59), we obtain

$$\left( \frac{\partial p_\ell}{\partial a_k} \right) = \frac{p_\ell^{-k}}{-z^{-1} \prod_{i \neq \ell} (1 - p_i z^{-1}) \Big|_{z=p_\ell}} = -\frac{p_\ell^{N-k}}{\prod_{i \neq \ell} (p_\ell - p_i)} \quad (6.60)$$

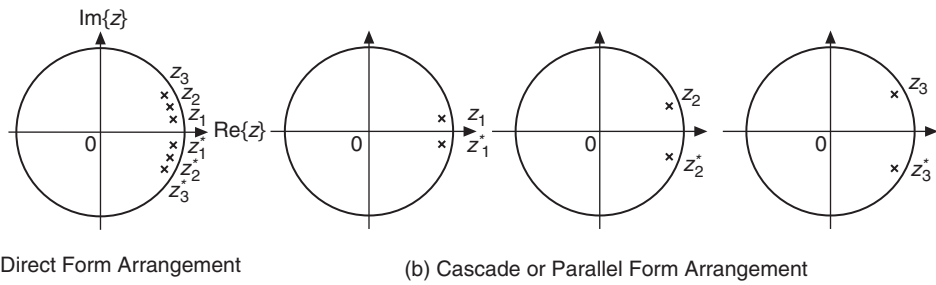


**FIGURE 6.23** *z*-plane plots of tightly clustered poles of a digital filter

Finally, the total perturbation error  $\Delta p_\ell$  can be expressed as

$$\Delta p_\ell = \sum_{k=1}^N \frac{\partial p_\ell}{\partial a_k} \Delta a_k \quad (6.61)$$

This formula measures the movement of the  $\ell$ th pole,  $p_\ell$ , to changes in each of the coefficient  $\{a_k\}$ ; hence it is known as a *sensitivity* formula. It shows that if the coefficients  $\{a_k\}$  are such that if the poles  $p_\ell$  and  $p_i$  are very close for some  $\ell, i$ , then  $(p_\ell - p_i)$  is very small and as a result the filter is very sensitive to the changes in filter coefficients. A similar result can be obtained for the sensitivity of zeros to changes in the parameters  $\{b_k\}$ .

To investigate this further in the light of various filter realizations, consider the *z*-plane plot shown in Figure 6.23(a), where poles are tightly clustered. This situation arises in wideband frequency selective filters such as lowpass or highpass filters. Now if we were to realize this filter using the direct form (either I or II), then the filter has all these tightly clustered poles, which makes the direct form realization very sensitive to coefficient changes due to finite word length. Thus the direct form realizations will suffer severely from coefficient quantization effects.

On the other hand, if we were to use either the cascade or the parallel forms, then we would realize the filter using second-order sections containing widely separated poles, as shown in Figure 6.23(b). Thus each second-order section will have low sensitivity in that its pole locations will be perturbed only slightly. Consequently, we expect that the overall system function  $H(z)$  will be perturbed only slightly. Thus the cascade or the parallel forms, when realized properly, will have low sensitivity to the changes or errors in filter coefficients.

- **EXAMPLE 6.21** Consider a digital resonator that is a second-order IIR filter given by

$$H(z) = \frac{1}{1 - (2r \cos \theta) z^{-1} + r^2 z^{-2}} \quad (6.62)$$

Analyze its sensitivity to pole locations when a 3-bit sign-magnitude format is used for the coefficient representation.

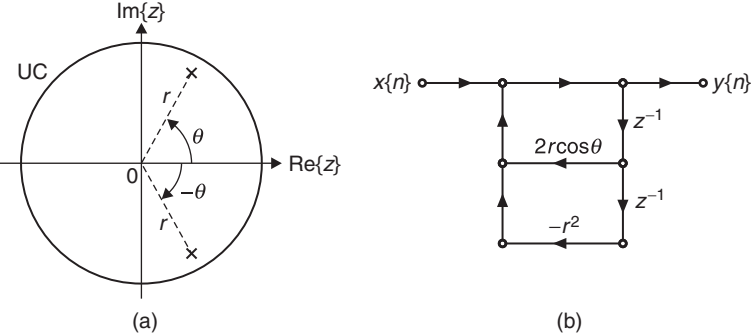


**FIGURE 6.24** Digital filter in Example 6.21: (a) pole-zero plot, (b) filter realization

### Solution

The filter has two complex-conjugate poles at

$$p_1 = re^{j\theta} \quad \text{and} \quad p_2 = re^{-j\theta} = p_1^*$$

For a proper operation as a resonator, the poles must be close to the unit circle—that is,  $r \simeq 1$  (but  $r < 1$ ). Then the resonant frequency  $\omega_r \simeq \theta$ . The zero-pole diagram is shown in Figure 6.24 along with the filter realization. Let  $r = 0.9$  and  $\theta = \pi/3$ . Then from (6.62),

$$a_1 = -2r \cos \theta = -0.9 \quad \text{and} \quad a_2 = r^2 = 0.81$$

We now represent  $a_1$  and  $a_2$ , each using 3-bit sign-magnitude format representation—that is,

$$a_k = \pm \bullet b_1 b_2 b_3 = \pm (b_1 2^{-1} + b_2 2^{-2} + b_3 2^{-3}), \quad k = 1, 2$$

where  $b_j$  represents the  $j$ th bit and  $\bullet$  represents the binary point. Then for the closest representation, we must have

$$\hat{a}_1 = 1\bullet 111 = -0.875 \quad \text{and} \quad \hat{a}_2 = 0\bullet 110 = +0.75$$

Hence  $|\Delta a_1| = 0.025$  and  $|\Delta a_2| = 0.06$ . Consider the sensitivity formula (6.61), in which

$$\begin{aligned} \frac{\partial p_1}{\partial a_1} &= -\frac{p_1^{2-1}}{(p_1 - p_1^*)} = \frac{-p_1}{2 \operatorname{Im}\{p_1\}} = \frac{-re^{j\theta}}{2r(\sin \theta)} = \frac{e^{j\pi/3}}{\sqrt{3}}, \text{ and} \\ \frac{\partial p_1}{\partial a_2} &= -\frac{p_1^{2-2}}{(p_1 - p_1^*)} = \frac{-1}{2 \operatorname{Im}\{p_1\}} = \frac{1}{0.9\sqrt{3}} \end{aligned}$$

Using (6.61), we obtain

$$\begin{aligned} |\Delta p_1| &\leq \left| \frac{\partial p_1}{\partial a_1} \right| |\Delta a_1| + \left| \frac{\partial p_1}{\partial a_2} \right| |\Delta a_2| \\ &= \frac{1}{\sqrt{3}} (0.025) + \frac{1}{0.9\sqrt{3}} (0.06) = 0.0529 \end{aligned} \quad (6.63)$$

To determine the exact locations of the changed poles, consider the changed denominator

$$\hat{D}(z) = 1 - 0.875z^{-1} + 0.75z^{-2} = (1 - 0.866e^{j0.331\pi}z^{-1})(1 - 0.866e^{-j0.331\pi}z^{-1})$$

Thus the changed pole locations are  $\hat{p}_1 = 0.866e^{j0.331\pi} = \hat{p}_2^*$ . Then  $|\Delta p_1| = |0.9e^{j\pi/3} - 0.866e^{j0.331\pi}| = 0.0344$ , which agrees with (6.63).  $\square$

**Analysis using MATLAB** To investigate the effect of coefficient quantization on filter behavior, MATLAB is an ideal vehicle. Using functions developed in previous sections, we can obtain quantized coefficients and then study such aspects as pole-zero movements, frequency response, or impulse response. We will have to represent all filter coefficients using the same number of integer and fraction bits. Hence, instead of quantizing each coefficient separately, we will develop the function **QCoeff** for coefficient quantization. This function implements quantization using rounding operation on sign-magnitude format. Although similar functions can be written for truncation as well as for other formats, we will analyze the effects using the **Qcoeff** function as explained previously.

```
function [y,L,B] = QCoeff(x,N)
% [y,L,B] = QCoeff(x,N)
%     Coefficient quantization using N=1+L+B bit representation
%         with rounding operation
%     y: quantized array (same dim as x)
%     L: number of integer bits
%     B: number of fractional bits
%     x: a scalar, vector, or matrix
%     N: total number of bits

xm = abs(x);
L = max(max(0,fix(log2(xm(:)+eps)+1))); % Integer bits
if (L > N)
    errmsg = [' *** N must be at least ',num2str(L), ' ***']; error(errmsg);
end
B = N-L; % Fractional bits
y = xm./(2^L); y = round(y.*((2^N)); % Rounding to N bits
y = sign(x).*y*(2^(-B)); % L+B+1 bit representation
```

The **Qcoeff** function represents each coefficient in the **x** array using  $N+1$ -bit (including the sign bit) representation. First, it determines the number of bits **L** needed for integer representation for the magnitude-wise largest coefficient, and then it assigns  $N-L$  bits to the fraction part. The resulting number is returned in **B**. Thus all coefficients have the same bit pattern  $L+B+1$ . Clearly,  $N \geq L$ .

- EXAMPLE 6.22** Consider the digital resonator in Example 6.21. Determine the change in the pole locations using MATLAB.

**Solution**

The filter coefficients,  $a_1 = -0.9$  and  $a_2 = 0.81$ , can be quantized using

```
>> x = [-0.9,0.81]; [y,L,B] = Qcoeff(x,3)
y = -0.8750    0.7500
L = 0
B = 3
```

as expected. Now using the following MATLAB script, we can determine the change in the location of the poles.

```
% Unquantized parameters
r = 0.9; theta = pi/3; a1 = -2*r*cos(theta); a2 = r*r;
p1 = r*exp(j*theta); p2 = p1';
% Quantized parameters: N = 3;
[ahat,L,B] = Qcoeff([a1,a2],3); rhat = sqrt(ahat(2));
thetahat = acos(-ahat(1)/(2*rhat)); p1hat = rhat*exp(j*thetahat); p2 = p1';
% Changes in pole locations
Dp1 = abs(p1-p1hat)
Dp1 = 0.0344
```

This is the same as before.

- EXAMPLE 6.23** Consider the following IIR filter with 10 poles closely packed at a radius of  $r = 0.9$  around angles  $\pm 45^\circ$  with a separation of  $5^\circ$ . Due to large number of poles, the denominator coefficients have values that require 6 bits for the integer part. Using 9 bits for the fractional part for a total of 16-bit representation, we compute and plot the new locations of poles:

```
r = 0.9; theta = (pi/180)*[-55:5:-35,35:5:55]';
p = r*exp(j*theta); a = poly(p); b = 1;

% Direct form: quantized coefficients
N = 15; [ahat,L,B] = Qcoeff(a,N);
TITLE = sprintf('"%i-bit (1+%i+%i) Precision',N+1,L,B);

% Comparison of pole-zero plots
subplot(1,2,1); [HZ,HP,Hl] = zplane(1,a);
set(HZ,'color','g','linewidth',1); set(HP,'color','g','linewidth',1);
set(Hl,'color','w'); axis([-1.1,1.1,-1.1,1.1]);
title('Infinite Precision','fontsize',10,'fontweight','bold');
```

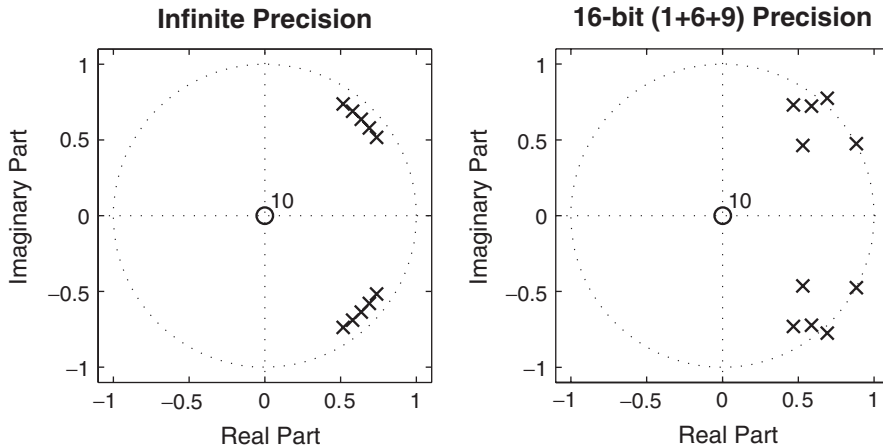


**FIGURE 6.25** Pole-zero plots for direct form structure in Example 6.23

```

subplot(1,2,2); [HZhat,HPhat,Hlhat] = zplane(1,ahat);
set(HZhat,'color','r','linewidth',1); set(HPhat,'color','r','linewidth',1);
set(Hlhat,'color','w'); title(TITLE,'fontsize',10,'fontweight','bold');
axis([-1.1,1.1,-1.1,1.1]);

```

Figure 6.25 shows the pole-zero plots for filters with both infinite and 16-bit precision coefficients. Clearly, with 16-bit word length, the resulting filter is completely different from the original one and is unstable. To investigate the effect of finite word length on the cascade form structure, we first converted the direct form coefficients into the cascade form coefficients using the `dir2cas` function, quantized the resulting set of coefficients, and then converted back to the direct form for pole-zero plotting. We show results for two different word lengths. In the first case, we used the same 16-bit word length. Since the cascade coefficients have smaller integer parts that require only one integer bit, the number of fractional bits is 14. In the second case, we used 9 fractional bits (same as those in the direct form) for a total word length of 11 bits.

```

% Cascade form: quantized coefficients: same N
[b0,B0,A0] = dir2cas(b,a); [BAhat1,L1,B1] = Qcoeff([B0,A0],N);
TITLE1 = sprintf('%i-bit (1+%i+i) Precision',N+1,L1,B1);
Bhat1 = BAhat1(:,1:3); Ahat1 = BAhat1(:,4:6);
[bhat1,ahat1] = cas2dir(b0,Bhat1,Ahat1);

subplot(1,2,1); [HZhat1,HPhat1,Hlhat1] = zplane(bhat1,ahat1);
set(HZhat1,'color','g','linewidth',1); set(HPhat1,'color','g','linewidth',1);
set(Hlhat1,'color','w'); axis([-1.1,1.1,-1.1,1.1]);
title(TITLE1,'fontsize',10,'fontweight','bold');

```

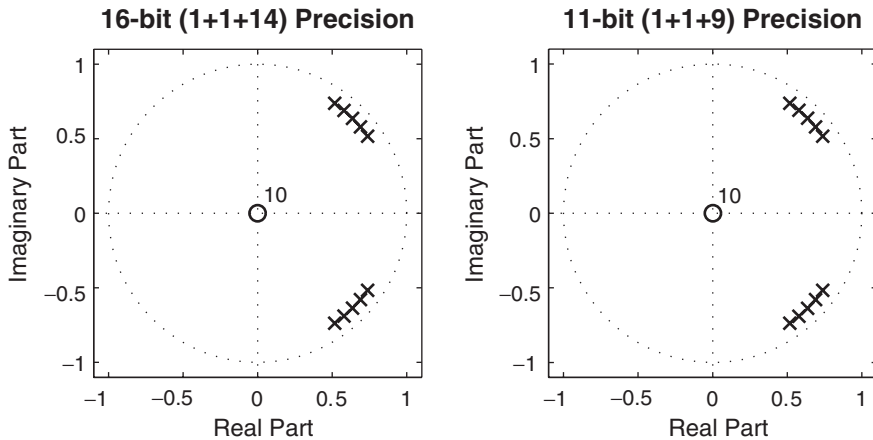


**FIGURE 6.26** Pole-zero plots for cascade form structure in Example 6.23

```
% Cascade form: quantized coefficients: same B (N=L1+B)
N1 = L1+B; [BAhat2,L2,B2] = Qcoeff([B0,A0],N1);
TITLE2 = sprintf('%i-bit (1+%i+i) Precision',N1+1,L2,B2);
Bhat2 = BAhat2(:,1:3); Ahat2 = BAhat2(:,4:6);
[bhat2,ahat2] = cas2dir(b0,Bhat2,Ahat2);

subplot(1,2,2); [HZhat2,HPhat2,Hlhat2] = zplane(bhat2,ahat2);
set(HZhat2,'color','r','linewidth',1); set(HPhat2,'color','r','linewidth',1);
set(Hlhat2,'color','w'); title(TITLE2,'fontsize',10,'fontweight','bold');
axis([-1.1,1.1,-1.1,1.1]);
```

The results are shown in Figure 6.26. We observe that not only for 16-bit representation but also for 11-bit representation, the resulting filter is essentially the same as the original one and is stable. Clearly, the cascade form structure has better finite-word-length properties than the direct form structure.  $\square$

### 6.7.3 EFFECTS ON FREQUENCY RESPONSE

The frequency response of the IIR filter in (6.38) is given by

$$H(e^{j\omega}) = \frac{\sum_{k=0}^M b_k e^{-j\omega k}}{1 + \sum_{k=1}^N a_k e^{-j\omega k}} \quad (6.64)$$

When the coefficients  $\{a_k\}$  and  $\{b_k\}$  are quantized to  $\{\hat{a}_k\}$  and  $\{\hat{b}_k\}$ , respectively, the new frequency response is given by

$$\hat{H}(e^{j\omega}) = \frac{\sum_{k=0}^M \hat{b}_k e^{-j\omega k}}{1 + \sum_{k=1}^N \hat{a}_k e^{-j\omega k}} \quad (6.65)$$

One can perform analysis similar to that for the movement of poles to obtain maximum change in the magnitude or phase responses due to changes in filter coefficients. However, such an analysis is very complicated and may not add any new insight. Hence we will study these effects using MATLAB. We provide the following two examples.

- EXAMPLE 6.24** Compute and plot magnitude responses of filter structures given for the filter in Example 6.23.

**Solution**

The filter is a bandpass filter with 10 tightly clustered poles implemented using the direct and the cascade forms. For the direct form structure, we compute the magnitude response for infinite precision as well as for 16-bit quantization. For the cascade form structure, we use 16-bit and 11-bit representations.

```
r = 0.9; theta = (pi/180)*[-55:5:-35,35:5:55]';
p = r*exp(j*theta); a = poly(p); b = 1;
w = [0:500]*pi/500; H = freqz(b*1e-4,a,w);
magH = abs(H); magHdb = 20*log10(magH);

% Direct form: quantized coefficients
N = 15; [ahat,L,B] = Qcoeff(a,N);
TITLE = sprintf('%i-bit (1+%i+i) Precision (DF)',N+1,L,B);
Hhat = freqz(b*1e-4,ahat,w); magHhat = abs(Hhat);

% Cascade form: quantized coefficients: Same N
[b0,B0,A0] = dir2cas(b,a);
[BAhat1,L1,B1] = Qcoeff([B0,A0],N);
TITLE1 = sprintf('%i-bit (1+%i+i) Precision (CF)',N+1,L1,B1);
Bhat1 = BAhat1(:,1:3); Ahat1 = BAhat1(:,4:6);
[bhat1,ahat1] = cas2dir(b0,Bhat1,Ahat1);
Hhat1 = freqz(b*1e-4,ahat1,w); magHhat1 = abs(Hhat1);

% Cascade form: quantized coefficients: Same B (N=L1+B)
N1 = L1+B; [BAhat2,L2,B2] = Qcoeff([B0,A0],N1);
TITLE2 = sprintf('%i-bit (1+%i+i) Precision (CF)',N1+1,L2,B2);
Bhat2 = BAhat2(:,1:3); Ahat2 = BAhat2(:,4:6);
[bhat2,ahat2] = cas2dir(b0,Bhat2,Ahat2);
Hhat2 = freqz(b*1e-4,ahat2,w); magHhat2 = abs(Hhat2);

% Comparison of Magnitude Plots
Hf_1 = figure('paperunits','inches','paperposition',[0,0,6,4]);
subplot(2,2,1); plot(w/pi,magH,'g','linewidth',2); axis([0,1,0,0.7]);
% xlabel('Digital Frequency in \pi units','fontsize',10);
ylabel('Magnitude Response','fontsize',10);
title('Infinite Precision (DF)','fontsize',10,'fontweight','bold');
subplot(2,2,2); plot(w/pi,magHhat,'r','linewidth',2); axis([0,1,0,0.7]);
```

```
% xlabel('Digital Frequency in \pi units','fontsize',10);
ylabel('Magnitude Response','fontsize',10);
title(TITLE,'fontsize',10,'fontweight','bold');
subplot(2,2,3); plot(w/pi,maghhat1,'r','linewidth',2); axis([0,1,0,0.7]);
xlabel('Digital Frequency in \pi units','fontsize',10);
ylabel('Magnitude Response','fontsize',10);
title(TITLE1,'fontsize',10,'fontweight','bold');
subplot(2,2,4); plot(w/pi,maghhat2,'r','linewidth',2); axis([0,1,0,0.7]);
xlabel('Digital Frequency in \pi units','fontsize',10);
ylabel('Magnitude Response','fontsize',10);
title(TITLE2,'fontsize',10,'fontweight','bold');
```

The plots are shown in Figure 6.27. The top row shows plots for the direct form, and the bottom row shows those for the cascade form. As expected, the magnitude plot of the direct form is severely distorted for 16-bit representation, while those for the cascade form are preserved even for 11-bit word length. □

- **EXAMPLE 6.25** An eighth-order bandpass filter was obtained using the elliptic filter design approach. This and other design methods will be discussed in Chapter 8. The MATLAB functions needed for this design are shown in the script below. This design produces direct form filter coefficients  $b_k$  and  $a_k$ , using 64-bit floating-point arithmetic, which gives the precision of 15 decimals and hence can be considered as *unquantized* coefficients. Table 6.1 shows these filter coefficients.

Represent the unquantized filter coefficients using 16-bit and 8-bit word lengths. Plot the filter log-magnitude responses and pole-zero locations for both the infinite and finite word-length coefficients.

**TABLE 6.1** Unquantized IIR filter coefficients used in Example 6.25

$k$	$b_k$	$a_k$
0	0.021985541264351	1.0000000000000000
1	0.0000000000000000	-0.0000000000000004
2	-0.032498273955222	2.344233276056572
3	0.0000000000000000	-0.0000000000000003
4	0.046424673058794	2.689868616770005
5	0.0000000000000000	0.0000000000000001
6	-0.032498273955221	1.584557559015230
7	0.0000000000000000	0.0000000000000001
8	0.021985541264351	0.413275250482975

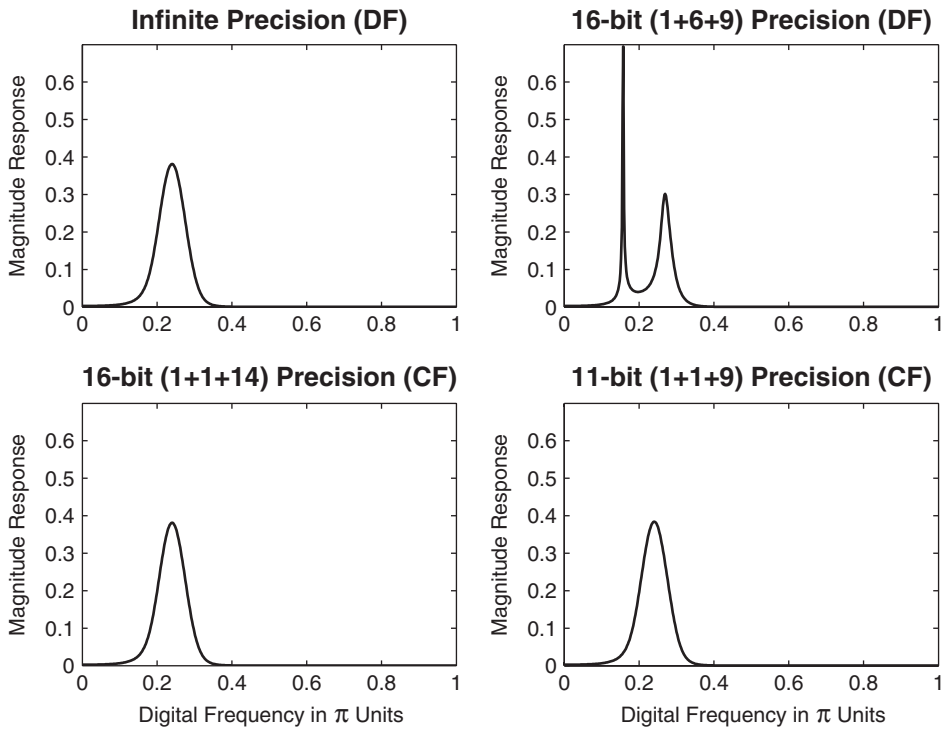


**FIGURE 6.27** Magnitude plots for direct and cascade form structures in Example 6.24

### Solution

Unlike the previous example, some of the filter coefficient values (specifically those of the autoregressive part) are greater than 1 and hence require bits for the integer part. This assignment is done for all coefficients since, in practice, the same bit-pattern is used for the filter representation. These and other steps are given in the following MATLAB script.

```
% The following 3 lines produce filter coefficients shown in Table 6.1.
wp = [0.35,0.65]; ws = [0.25,0.75]; Rp = 1; As = 50;
[N, wn] = ellipord(wp, ws, Rp, As);
[b,a] = ellip(N,Rp,As,wn);
w = [0:500]*pi/500; H = freqz(b,a,w); magH = abs(H);
magHdb = 20*log10(magH);

% 16-bit word-length quantization
N1 = 15; [bahat,L1,B1] = QCoeff([b;a],N1);
TITLE1 = sprintf('%i-bits (1+%i+i)',N1+1,L1,B1);
bhat1 = bahat(1,:); ah1 = bahat(2,:);
Hhat1 = freqz(bhat1,ah1,w); magHhat1 = abs(Hhat1);
magHhat1db = 20*log10(magHhat1); zhat1 = roots(bhat1);
```

```
% 8-bit word-length quantization
N2 = 7; [bahat,L2,B2] = QCoeff([b;a],N2);
TITLE2 = sprintf('%i-bits (1+%i+%i)',N2+1,L2,B2);
bhat2 = bahat(1,:); ahat2 = bahat(2,:);
Hhat2 = freqz(bhat2,ahat2,w); magHhat2 = abs(Hhat2);
magHhat2db = 20*log10(magHhat2); zhat2 = roots(bhat2);

% Plots
Hf_1 = figure('paperunits','inches','paperposition',[0,0,6,5]);

% Comparison of log-magnitude responses: 16 bits
subplot(2,2,1); plot(w/pi,magHdb,'g','linewidth',1.5); axis([0,1,-80,5]);
hold on; plot(w/pi,magHhat1db,'r','linewidth',1); hold off;
xlabel('Digital Frequency in \pi units','fontsize',10);
ylabel('Decibels','fontsize',10);
title(['Log-Mag plot: ',TITLE1],'fontsize',10,'fontweight','bold');

% Comparison of pole-zero plots: 16 bits
subplot(2,2,3); [HZ,HP,H1] = zplane([b],[a]); axis([-2,2,-2,2]); hold on;
set(HZ,'color','g','linewidth',1,'markersize',4);
set(HP,'color','g','linewidth',1,'markersize',4);
plot(real(zhat1),imag(zhat1),'r+','linewidth',1);
title(['PZ Plot: ',TITLE1],'fontsize',10,'fontweight','bold');
hold off;

% Comparison of log-magnitude responses: 8 bits
subplot(2,2,2); plot(w/pi,magHdb,'g','linewidth',1.5); axis([0,1,-80,5]);
hold on; plot(w/pi,magHhat2db,'r','linewidth',1); hold off;
xlabel('Digital Frequency in \pi units','fontsize',10);
ylabel('Decibels','fontsize',10);
title(['Log-Mag plot: ',TITLE2],'fontsize',10,'fontweight','bold');

% Comparison of pole-zero plots: 8 bits
subplot(2,2,4); [HZ,HP,H1] = zplane([b],[a]); axis([-2,2,-2,2]); hold on;
set(HZ,'color','g','linewidth',1,'markersize',4);
set(HP,'color','g','linewidth',1,'markersize',4);
plot(real(zhat2),imag(zhat2),'r+','linewidth',1);
title(['PZ Plot: ',TITLE2],'fontsize',10,'fontweight','bold');
hold off;
```

The log-magnitude responses and zero-pole locations of the resulting filters are plotted in Figure 6.28 along with those of the original filter. When 16 bits are used, the resulting filter is virtually indistinguishable from the original one. However, when 8 bits are used, the filter behavior is severely distorted. The filter is still stable, but it does not satisfy the design specifications.  $\square$

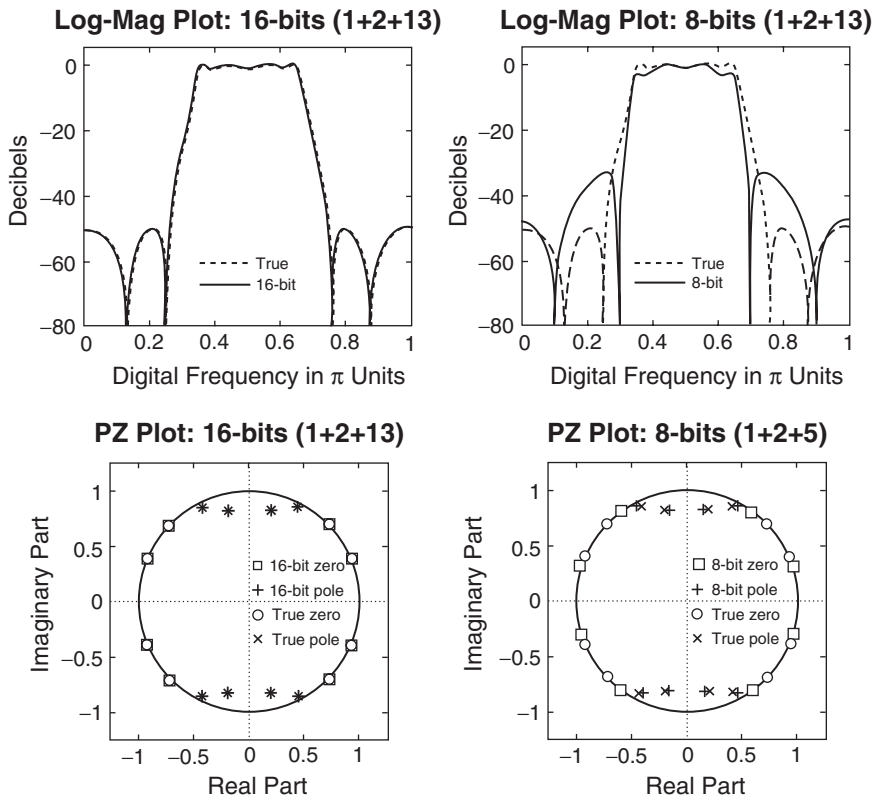


**FIGURE 6.28** Plots for the IIR filter in Example 6.25

#### 6.7.4 FIR FILTERS

A similar analysis can be done for FIR filters. Let the impulse response of an FIR filter be  $h(n)$  with system response

$$H(z) = \sum_{n=0}^{M-1} h(n)z^{-n} \quad (6.66)$$

Then

$$\Delta H(z) = \sum_{n=0}^{M-1} \Delta h(n)z^{-n} \quad (6.67)$$

where  $\Delta H(z)$  is the change due to change in the impulse response  $h(n)$ . Hence

$$\Delta H(e^{j\omega}) = \sum_{n=0}^{M-1} \Delta h(n) e^{-j\omega n} \quad \text{or} \quad |\Delta H(e^{j\omega})| \leq \sum_{n=0}^{M-1} |\Delta h(n)| \quad (6.68)$$

Now, if each coefficient is quantized to  $B$  fraction bits (i.e., total register length is  $B + 1$ ), then

$$|\Delta h(n)| \leq \frac{1}{2} 2^{-B}$$

Therefore,

$$|\Delta H(e^{j\omega})| \leq \frac{1}{2} 2^{-B} M = \frac{M}{2} 2^{-B} \quad (6.69)$$

Thus the change in frequency response depends not only on the number of bits used but also on the length  $M$  of the filter. For large  $M$  and small  $b$ , this difference can be significant and can destroy the desirable behavior of the filter, as we see in the following example.

- EXAMPLE 6.26** An order-30 lowpass FIR filter is designed using the `firpm` function. This and other FIR filter design functions will be discussed in Chapter 7. The resulting filter coefficients are symmetric and are shown in Table 6.2. We will consider these coefficients as essentially unquantized. The coefficients are quantized to 16 bits (15 fractional plus 1 sign bit) and to 8 bits (7 fractional and 1 sign bit). The resulting filter frequency responses and pole-zero plots are determined and compared. These and other relevant steps are shown in the following MATLAB script.

**TABLE 6.2** *Unquantized FIR filter coefficients used in Example 6.26*

$k$	$b_k$	$k$
0	0.000199512328641	30
1	-0.002708453461401	29
2	-0.002400461099957	28
3	0.003546543555809	27
4	0.008266607456720	26
5	0.000012109690648	25
6	-0.015608300819736	24
7	-0.012905580320708	23
8	0.017047710292001	22
9	0.036435951059014	21
10	0.000019292305776	20
11	-0.065652005307521	19
12	-0.057621325403582	18
13	0.090301607282890	17
14	0.300096964940136	16
15	0.400022084144842	15

```
% Filter coefficients given in Table 6.2 are computed using the firpm function
b = firpm(30,[0,0.3,0.5,1],[1,1,0,0]);
w = [0:500]*pi/500; H = freqz(b,1,w); magH = abs(H);
```

```

magHdb = 20*log10(magH);
N1 = 15; [bhat1,L1,B1] = Qcoeff(b,N1);
TITLE1 = sprintf('%i-bits (1+%i+i)',N1+1,L1,B1);
Hhat1 = freqz(bhat1,1,w); magHhat1 = abs(Hhat1);
magHhat1db = 20*log10(magHhat1);
zhat1 = roots(bhat1);

N2 = 7; [bhat2,L2,B2] = Qcoeff(b,N2);
TITLE2 = sprintf('%i-bits (1+%i+i)',N2+1,L2,B2);
Hhat2 = freqz(bhat2,1,w); magHhat2 = abs(Hhat2);
magHhat2db = 20*log10(magHhat2);
zhat2 = roots(bhat2);

% Plots
Hf_1 = figure('paperunits','inches','paperposition',[0,0,6,5]);

% Comparison of log-magnitude responses: 16 bits
subplot(2,2,1); plot(w/pi,magHdb,'g','linewidth',1.5); axis([0,1,-80,5]);
hold on; plot(w/pi,magHhat1db,'r','linewidth',1); hold off;
xlabel('Digital Frequency in \pi units','fontsize',10);
ylabel('Decibels','fontsize',10);
title(['Log-Mag plot: ',TITLE1],'fontsize',10,'fontweight','bold');

% Comparison of pole-zero plots: 16 bits
subplot(2,2,3); [HZ,HP,Hl] = zplane([b],[1]); axis([-2,2,-2,2]); hold on;
set(HZ,'color','g','linewidth',1,'markersize',4);
set(HP,'color','g','linewidth',1,'markersize',4);
plot(real(zhat1),imag(zhat1),'r+','linewidth',1);
title(['PZ Plot: ',TITLE1],'fontsize',10,'fontweight','bold');
hold off;

% Comparison of log-magnitude responses: 8 bits
subplot(2,2,2); plot(w/pi,magHdb,'g','linewidth',1.5); axis([0,1,-80,5]);
hold on; plot(w/pi,magHhat2db,'r','linewidth',1); hold off;
xlabel('Digital Frequency in \pi units','fontsize',10);
ylabel('Decibels','fontsize',10);
title(['Log-Mag plot: ',TITLE2],'fontsize',10,'fontweight','bold');

% Comparison of pole-zero plots: 8 bits
subplot(2,2,4); [HZ,HP,Hl] = zplane([b],[1]); axis([-2,2,-2,2]); hold on;
set(HZ,'color','g','linewidth',1,'markersize',4);
set(HP,'color','g','linewidth',1,'markersize',4);
plot(real(zhat2),imag(zhat2),'r+','linewidth',1);
title(['PZ Plot: ',TITLE2],'fontsize',10,'fontweight','bold');
hold off;

```

The log-magnitude responses and zero-pole locations of the resulting filters are computed and plotted in Figure 6.29 along with those of the original filter.

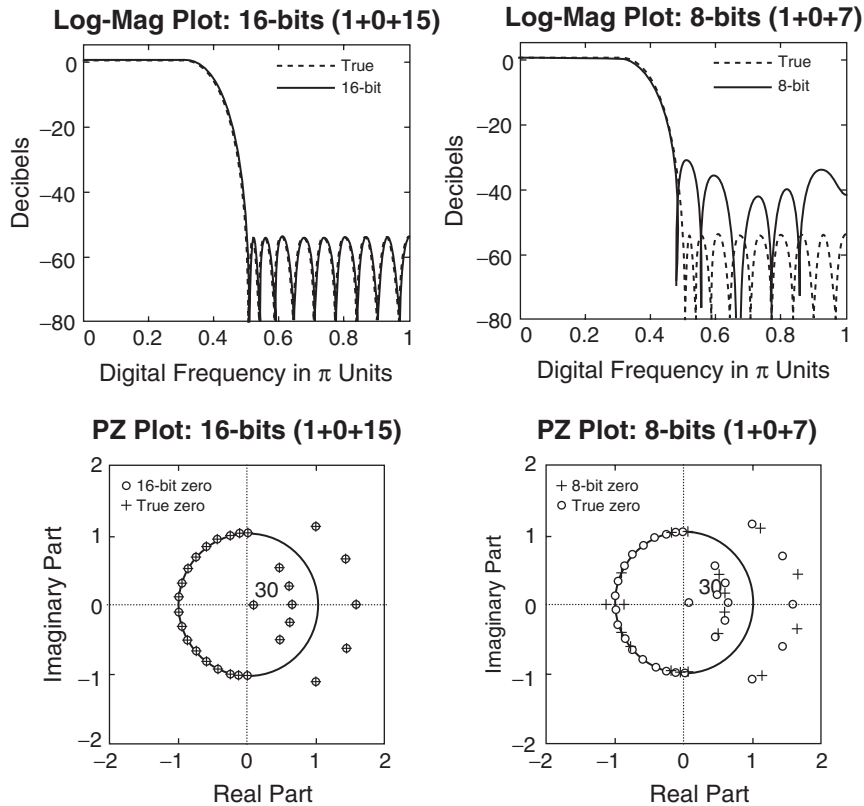


**FIGURE 6.29** Plots for the FIR filter in Example 6.26

When 16 bits are used, the resulting filter is virtually indistinguishable from the original one. However, when 8 bits are used, the filter behavior is severely distorted and the filter does not satisfy the design specifications.  $\square$

## 6.8 PROBLEMS

---

- P6.1** Draw direct form I block diagram structures for each of the following LTI systems with input node  $x(n)$  and output node  $y(n)$ .

1.  $y(n) = x(n) + 2x(n-1) + 3x(n-2)$
2.  $H(z) = \frac{1}{1 - 1.7z^{-1} + 1.53z^{-2} - 0.648z^{-3}}$
3.  $y(n) = 1.7y(n-1) - 1.36y(n-2) + 0.576y(n-3) + x(n)$
4.  $y(n) = 1.6y(n-1) + 0.64y(n-2) + x(n) + 2x(n-1) + x(n-2)$
5.  $H(z) = \frac{1 - 3z^{-1} + 3z^{-2} + z^{-3}}{1 + 0.2z^{-1} - 0.14z^{-2} + 0.44z^{-3}}$

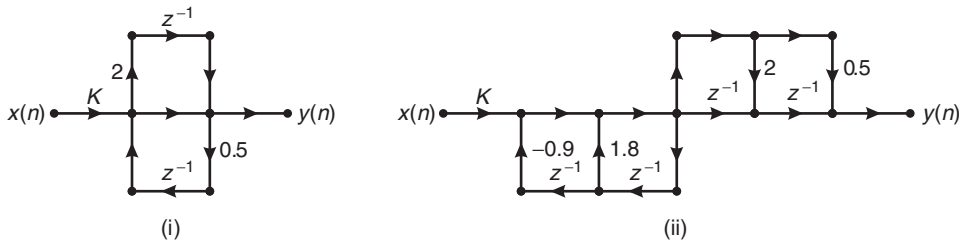


FIGURE P6.1 Block diagrams for Problem 6.2

**P6.2** Two block diagrams are shown in Figure P6.1. Answer the following for each structure.

1. Determine the system function  $H(z) = Y(z)/X(z)$ .
2. Is the structure canonical (i.e., with the least number of delays)? If not, draw a canonical structure.
3. Determine the value of  $K$  so that  $H(e^{j0}) = 1$ .

**P6.3** Consider the LTI system described by

$$y(n) = a y(n-1) + b x(n) \quad (6.70)$$

1. Draw a block diagram of this system with input node  $x(n)$  and output node  $y(n)$ .
2. Now perform the following two operations on the structure drawn in part 1: (i) reverse all arrow directions and (ii) interchange the input node with the output node. Notice that the branch node becomes the adder node and vice versa. Redraw the block diagram so that input node is on the left side and the output node is on the right side. This is the *transposed* block diagram.
3. Determine the difference equation representation of your transposed structure in part 2, and verify that it is the same equation as (6.70).

**P6.4** Consider the LTI system given by

$$H(z) = \frac{1 - 2.818z^{-1} + 3.97z^{-2} - 2.8180z^{-3} + z^{-4}}{1 - 2.536z^{-1} + 3.215z^{-2} - 2.054z^{-3} + 0.6560z^{-4}} \quad (6.71)$$

1. Draw the normal direct form I structure block diagram.
2. Draw the transposed direct form I structure block diagram.
3. Draw the normal direct form II structure block diagram. Observe that it looks very similar to that in part 2.
4. Draw the transposed direct form II structure block diagram. Observe that it looks very similar to that in part 1.

**P6.5** Consider the LTI system given in Problem P6.4.

1. Draw a cascade structure containing second-order normal direct form II sections.
2. Draw a cascade structure containing second-order transposed direct form II sections.
3. Draw a parallel structure containing second-order normal direct form II sections.
4. Draw a parallel structure containing second-order transposed direct form II sections.

**P6.6** A causal linear time-invariant system is described by

$$y(n) = \sum_{k=0}^4 \cos(0.1\pi k)x(n-k) - \sum_{k=1}^5 (0.8)^k \sin(0.1\pi k)y(n-k)$$

Determine and draw the block diagrams of the following structures. Compute the response of the system to

$$x(n) = [1 + 2(-1)^n], \quad 0 \leq n \leq 50$$

in each case, using the following structures.

1. Normal direct form I
2. Transposed direct form II
3. Cascade form containing second-order normal direct form II sections
4. Parallel form containing second-order transposed direct form II sections

**P6.7** An IIR filter is described by system function

$$H(z) = 2 \left( \frac{1 + 0z^{-1} + z^{-2}}{1 - 0.8z^{-1} + 0.64z^{-2}} \right) + \left( \frac{2 - z^{-1}}{1 - 0.75z^{-1}} \right) + \left( \frac{1 + 2z^{-1} + z^{-2}}{1 + 0.81z^{-2}} \right)$$

Determine and draw the following structures.

1. Transposed direct form I
2. Normal direct form II
3. Cascade form containing transposed second-order direct form II sections
4. Parallel form containing normal second-order direct form II sections

**P6.8** An IIR filter is described by the system function

$$H(z) = \left( \frac{-14.75 - 12.9z^{-1}}{1 - \frac{7}{8}z^{-1} + \frac{3}{32}z^{-2}} \right) + \left( \frac{24.5 + 26.82z^{-1}}{1 - z^{-1} + \frac{1}{2}z^{-2}} \right) \left( \frac{1 + 2z^{-1} + z^{-2}}{1 + 0.81z^{-2}} \right)$$

Determine and draw the following structures.

1. Normal direct form I
2. Normal direct form II
3. Cascade form containing transposed second-order direct form II sections
4. Parallel form containing transposed second-order direct form II sections

**P6.9** A linear time-invariant system with system function

$$H(z) = \frac{0.05 - 0.01z^{-1} - 0.13z^{-2} + 0.13z^{-4} + 0.01z^{-5} - 0.05z^{-6}}{1 - 0.77z^{-1} + 1.59z^{-2} - 0.88z^{-3} + 1.2z^{-4} - 0.35z^{-5} + 0.31z^{-6}}$$

is to be implemented using a flow graph of the form shown in Figure P6.2.

1. Fill in all the coefficients in the diagram.
2. Is your solution unique? Explain.

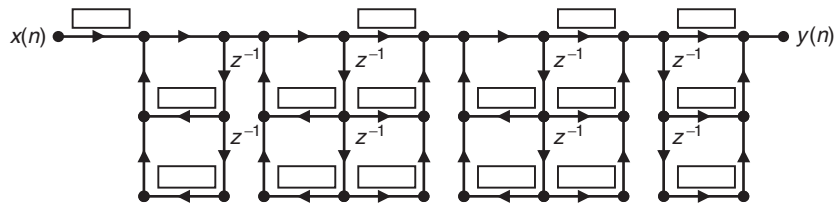


**FIGURE P6.2** Structure for Problem 6.9

**P6.10** A linear time-invariant system with system function

$$H(z) = \frac{0.051 + 0.088z^{-1} + 0.06z^{-2} - 0.029z^{-3} - 0.069z^{-4} - 0.046z^{-5}}{1 - 1.34z^{-1} + 1.478z^{-2} - 0.789z^{-3} + 0.232z^{-4}}$$

is to be implemented using a flow graph of the form shown in Figure P6.3. Fill in all the coefficients in the diagram.

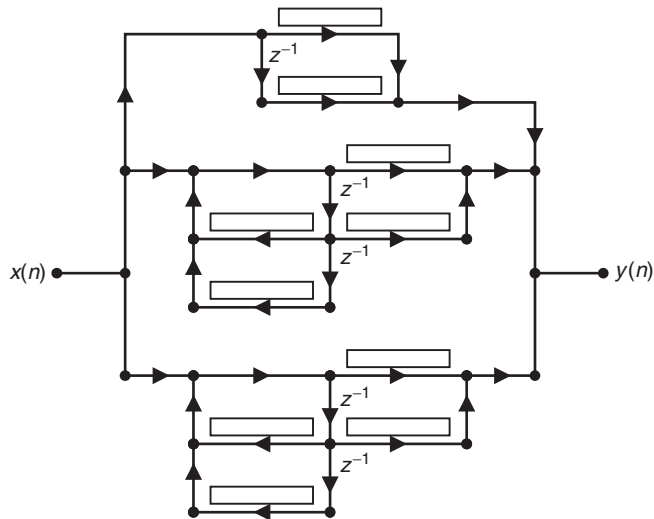


**FIGURE P6.3** Structure for Problem 6.10

**P6.11** Consider the linear time-invariant system given in Problem P6.9.

$$H(z) = \frac{0.05 - 0.01z^{-1} - 0.13z^{-2} + 0.13z^{-4} + 0.01z^{-5} - 0.05z^{-6}}{1 - 0.77z^{-1} + 1.59z^{-2} - 0.88z^{-3} + 1.2z^{-4} - 0.35z^{-5} + 0.31z^{-6}}$$

It is to be implemented using a flow graph of the form shown in Figure P6.4.

1. Fill in all the coefficients in the diagram.
2. Is your solution unique? Explain.

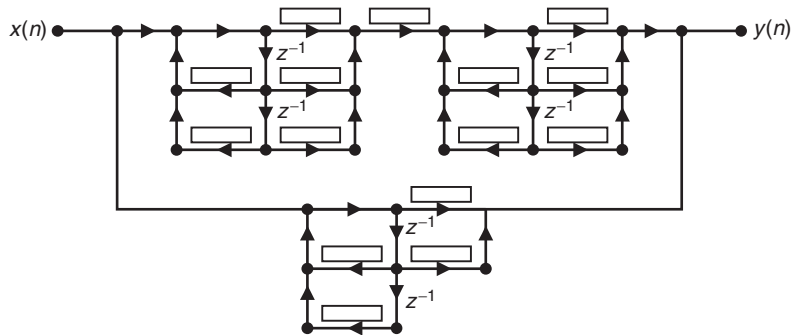


**FIGURE P6.4** Structure for Problem 6.11

**P6.12** The filter structure shown in Figure P6.5 contains a parallel connection of cascade sections. Determine and draw the overall

1. direct form (normal) structure,
2. direct form (transposed) structure,
3. cascade form structure containing second-order sections,
4. parallel form structure containing second-order sections.

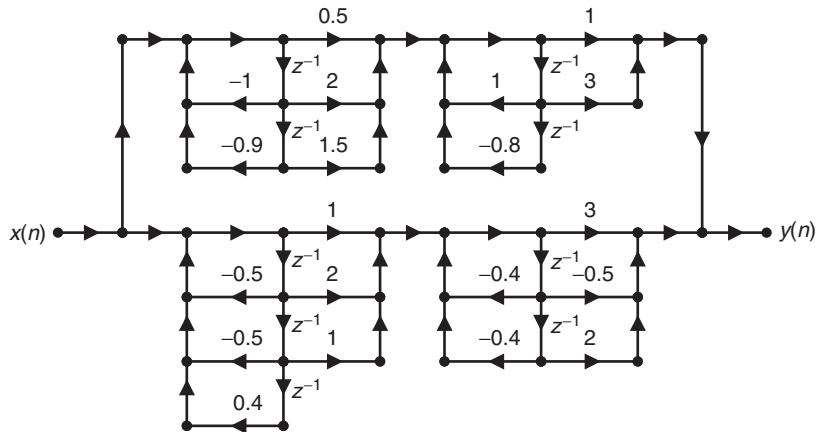


**FIGURE P6.5** Structure for Problem 6.12

**P6.13** In the filter structure shown in Figure P6.6, systems  $H_1(z)$  and  $H_2(z)$  are subcomponents of a larger system  $H(z)$ . The system function  $H_1(z)$  is given in the parallel form

$$H_1(z) = 2 + \frac{0.2 - 0.3z^{-1}}{1 + 0.9z^{-1} + 0.9z^{-2}} + \frac{0.4 + 0.5z^{-1}}{1 - 0.8z^{-1} + 0.8z^{-2}}$$

and the system function  $H_2(z)$  is given in the cascade form

$$H_2(z) = \left( \frac{2 + z^{-1} - z^{-2}}{1 + 1.7z^{-1} + 0.72z^{-2}} \right) \left( \frac{3 + 4z^{-1} + 5z^{-2}}{1 - 1.5z^{-1} + 0.56z^{-2}} \right)$$

1. Express  $H(z)$  as a rational function.
2. Draw the block diagram of  $H(z)$  as a cascade form structure.
3. Draw the block diagram of  $H(z)$  as a parallel form structure.

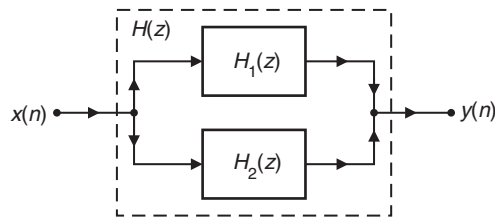


**FIGURE P6.6** Structure for Problem 6.13

**P6.14** The digital filter structure shown in Figure P6.7 is a cascade of two parallel sections and corresponds to a tenth-order IIR digital filter system function

$$H(z) = \frac{1 - 2.2z^{-2} + 1.6368z^{-4} - 0.48928z^{-6} + 5395456 \times 10^{-8}z^{-8} - 147456 \times 10^{-8}z^{-10}}{1 - 1.65z^{-2} + 0.8778z^{-4} - 0.17281z^{-6} + 1057221 \times 10^{-8}z^{-8} - 893025 \times 10^{-10}z^{-10}}$$

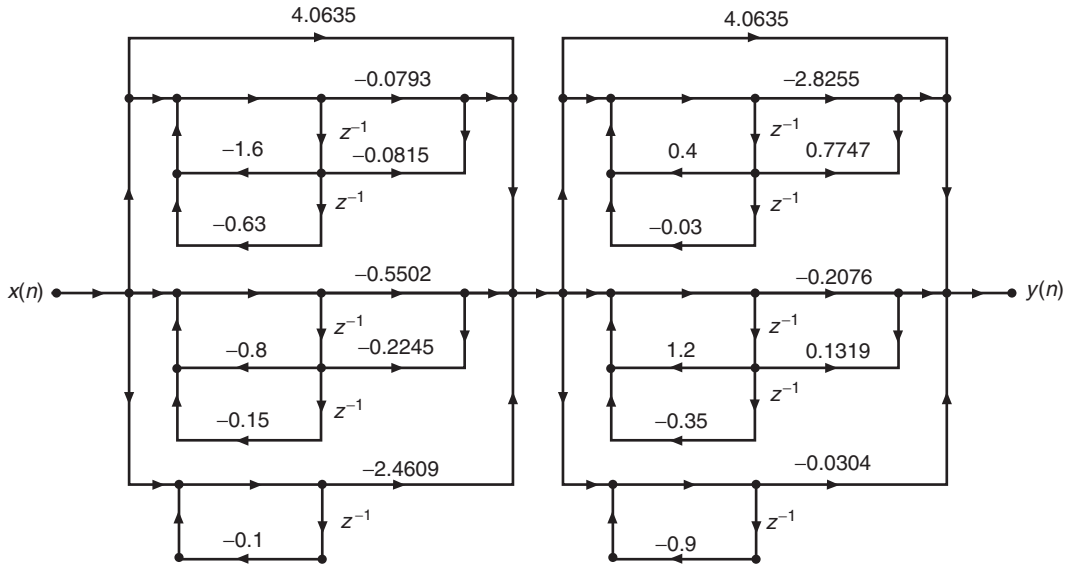


**FIGURE P6.7** Structure for Problem 6.14

1. Due to an error in labeling, two of the multiplier coefficients (rounded to four decimals) in this structure have incorrect values. Locate these two multipliers and determine their correct values.
2. Determine and draw an overall cascade structure containing second-order sections and which contains the least number of multipliers.

**P6.15** As described in this chapter, a linear-phase FIR filter is obtained by requiring certain symmetry conditions on its impulse responses.

1. In the case of symmetrical impulse response, we have  $h(n) = h(M - 1 - n)$ ,  $0 \leq n \leq M - 1$ . Show that the resulting phase response is linear in  $\omega$  and is given by

$$\angle H(e^{j\omega}) = -\left(\frac{M-1}{2}\right)\omega, \quad -\pi < \omega \leq \pi$$

2. Draw the linear-phase structures for this form when  $M = 5$  and  $M = 6$ .
3. In the case of antisymmetrical impulse response, we have  $h(n) = -h(M - 1 - n)$ ,  $0 \leq n \leq M - 1$ . Show that the resulting phase response is given by

$$\angle H(e^{j\omega}) = \pm\frac{\pi}{2} - \left(\frac{M-1}{2}\right)\omega, \quad -\pi < \omega \leq \pi$$

4. Draw the linear-phase structures for this form when  $M = 5$  and  $M = 6$ .

**P6.16** An FIR filter is described by the difference equation

$$y(n) = \sum_{k=0}^6 e^{-0.9|k-3|} x(n-k)$$

Determine and draw the block diagrams of the following structures.

1. Direct form
2. Linear-phase form
3. Cascade form
4. Frequency-sampling form

**P6.17** A linear time-invariant system is given by the system function

$$H(z) = 2 + 3z^{-1} + 5z^{-2} - 3z^{-3} + 4z^{-5} + 8z^{-7} - 7z^{-8} + 4z^{-9}$$

Determine and draw the block diagrams of the following structures.

1. Direct form
2. Cascade form
3. Frequency-sampling form

**P6.18** Using the conjugate symmetry property of the DFT

$$H(k) = \begin{cases} H(0), & k = 0 \\ H^*(M-k), & k = 1, \dots, M-1 \end{cases}$$

and the conjugate symmetry property of the  $W_M^{-k}$  factor, show that (6.12) can be put in the form (6.13) and (6.14) for real FIR filters.

**P6.19** To avoid poles on the unit circle in the frequency-sampling structure, one samples  $H(z)$  at  $z_k = re^{j2\pi k/M}$ ,  $k = 0, \dots, M-1$  where  $r \approx 1$  (but  $< 1$ ), as discussed in Section 6.3.

1. Using

$$H(re^{j2\pi k/M}) \approx H(k)$$

show that the frequency-sampling structure is given by

$$H(z) = \frac{1 - (rz)^{-M}}{M} \left\{ \sum_{k=1}^L 2|H(k)|H_k(z) + \frac{H(0)}{1 - rz^{-1}} + \frac{H(M/2)}{1 + rz^{-1}} \right\}$$

where

$$H_k(z) = \frac{\cos[\angle H(k)] - rz^{-1} \cos[\angle H(k) - \frac{2\pi k}{M}]}{1 - 2rz^{-1} \cos(\frac{2\pi k}{M}) + r^2 z^{-2}}, \quad k = 1, \dots, L$$

and  $M$  is even.

2. Modify the MATLAB function `dir2fs` (which was developed in Section 6.3) to implement this frequency-sampling form. The format of this function should be

```
[C,B,A,rM] = dir2fs(h,r)
% Direct form to frequency-sampling form conversion
%
% [C,B,A,rM] = dir2fs(h,r)
% C = Row vector containing gains for parallel sections
% B = Matrix containing numerator coefficients arranged in rows
% A = Matrix containing denominator coefficients arranged in rows
% rM = r^M factor needed in the feedforward loop
% h = impulse response vector of an FIR filter
% r = radius of the circle over which samples are taken (r<1)
%
```

3. Determine the frequency sampling structure for the impulse response given in Example 6.6 using this function.

**P6.20** Consider the following system function of an FIR filter:

$$H(z) = 1 - 4z^{-1} + 6.4z^{-2} - 5.12z^{-3} + 2.048z^{-4} - 0.32768z^{-5}$$

1. Provide block diagram structures in the following forms.
  - (a) Normal and transposed direct forms
  - (b) Cascade of five first-order sections
  - (c) Cascade of one first-order section and two second-order sections
  - (d) Cascade of one second-order section and one third-order section
  - (e) Frequency-sampling structure with real coefficients
2. The computational complexity of a digital filter structure can be given by the total number of multiplications and the total number of 2-input additions that are required per output point. Assume that  $x(n)$  is real and that multiplication by 1 is not counted as a multiplication. Compare the computational complexity of each of these structures.

**P6.21** A causal digital filter is described by the following zeros:

$$\begin{aligned} z_1 &= 0.5 e^{j60^\circ}, & z_2 &= 0.5 e^{-j60^\circ}, & z_3 &= 2 e^{j60^\circ}, & z_4 &= 2 e^{-j60^\circ}, \\ z_5 &= 0.25 e^{j30^\circ}, & z_6 &= 0.25 e^{-j30^\circ}, & z_7 &= 4 e^{j30^\circ}, & z_8 &= 4 e^{-j30^\circ} \end{aligned}$$

and poles:  $\{p_i\}_{i=1}^8 = 0$ .

1. Determine the phase response of this filter, and show that it is a linear-phase FIR filter.
2. Determine the impulse response of the filter.
3. Draw a block diagram of the filter structure in the direct form.
4. Draw a block diagram of the filter structure in the linear-phase form.

**P6.22** MATLAB provides the built-in functions `dec2bin` and `bin2dec` to convert nonnegative decimal integers into binary codes and vice versa, respectively.

1. Develop a function `B = sm2bin(D)` to convert a sign-magnitude format decimal integer  $D$  into its binary representation  $B$ . Verify your function on the following numbers:
  - (a)  $D = 1001$
  - (b)  $D = -63$
  - (c)  $D = -449$
  - (d)  $D = 978$
  - (e)  $D = -205$

2. Develop a function  $D = \text{bin2sm}(B)$  to convert a binary representation  $B$  into its sign-magnitude format decimal integer  $D$ . Verify your function on the following representations:
- (a)  $B = 1010$       (b)  $B = 011011011$       (c)  $B = 11001$   
(d)  $B = 1010101$       (e)  $B = 011011$

**P6.23** Using the function `TwosComplement` as a model, develop a function  $y = \text{TensComplement}(x, N)$  that converts a sign-magnitude format integer  $x$  into the  $N$ -digit ten's-complement integer  $y$ .

1. Verify your function using the following integers:
- (a)  $x = 1234, N = 6$       (b)  $x = -603, N = 4$       (c)  $x = -843, N = 5$   
(d)  $x = -1978, N = 6$       (e)  $x = 50, N = 3$
2. Using the ten's-complement format, perform the following arithmetic operations. In each case, choose an appropriate value on  $N$  for the meaningful result.
- (a)  $123 + 456 - 789$       (b)  $648 + 836 - 452$       (c)  $2001 + 3756$   
(d)  $-968 + 4539$       (e)  $888 - 666 + 777$

Verify your results using decimal operations.

**P6.24** The function `OnesComplement` developed in this chapter converts signed integers into one's-complement-format decimal representations. In this problem, we will develop functions that will operate on fractional numbers.

1. Develop a MATLAB function  $y = \text{sm2oc}(x, B)$  that converts the sign-magnitude format fraction  $x$  into the  $B$ -bit one's-complement-format decimal equivalent number  $y$ . Verify your function on the following numbers. In each case, the numbers to be considered are both positive and negative. Also, in each case select the appropriate number of bits  $B$ .
- (a)  $x = \pm 0.5625$       (b)  $x = \pm 0.40625$       (c)  $x = \pm 0.953125$   
(d)  $x = \pm 0.1328125$       (e)  $x = \pm 0.7314453125$
2. Develop a MATLAB function  $x = \text{oc2sm}(y, B)$  that converts the  $B$ -bit one's-complement-format decimal equivalent number  $y$  into the sign-magnitude-format fraction  $x$ . Verify your function on the following fractional binary representations:
- (a)  $y = 1\bullet 10110$       (b)  $y = 0.\bullet 011001$       (c)  $y = 1\bullet 00110011$   
(d)  $y = 1\bullet 11101110$       (e)  $y = 0\bullet 00010001$

**P6.25** The function `TwosComplement` developed in this chapter converts signed integers into two's-complement-format decimal representations. In this problem, we will develop functions that will operate on fractional numbers.

1. Develop a MATLAB function  $y = \text{sm2tc}(x, B)$  that converts the sign-magnitude-format fraction  $x$  into the  $B$ -bit two's-complement-format decimal equivalent number  $y$ . Verify your function on the following numbers. In each case, the numbers to be considered are both positive and negative. Also, in each case select the appropriate number of bits  $B$ .
- (a)  $x = \pm 0.5625$       (b)  $x = \pm 0.40625$       (c)  $x = \pm 0.953125$   
(d)  $x = \pm 0.1328125$       (f)  $x = \pm 0.7314453125$

Compare your representations with those in Problem P6.24, part 1.

2. Develop a MATLAB function  $x = \text{tc2sm}(y, B)$  that converts the  $B$ -bit two's-complement-format decimal equivalent number  $y$  into the sign-magnitude-format fraction  $x$ . Verify your function on the following fractional binary representations:
- (a)  $y = 1\Delta 10110$       (b)  $y = 0\Delta 011001$       (c)  $y = 1\Delta 00110011$   
 (d)  $y = 1\Delta 11101110$       (e)  $y = 0\Delta 00010001$

Compare your representations with those in Problem P6.24, part 2.

**P6.26** Determine the 10-bit sign-magnitude, one's-complement, and two's-complement representation of the following decimal numbers:

- (a) 0.12345      (b) -0.56789      (c) 0.38452386      (d) -0.762349      (e) -0.90625

**P6.27** Consider a 32-bit floating-point number representation with a 6-bit exponent and a 25-bit mantissa.

1. Determine the value of the smallest number that can be represented.
2. Determine the value of the largest number that can be represented.
3. Determine the dynamic range of this floating-point representation and compare it with the dynamic range of a 32-bit fixed-point signed integer representation.

**P6.28** Show that the magnitudes of floating-point numbers in a 32-bit IEEE standard range from  $1.18 \times 10^{-38}$  to  $3.4 \times 10^{38}$ .

**P6.29** Compute and plot the truncation error characteristics when  $B = 4$  for the sign-magnitude, one's-complement, and two's-complement formats.

**P6.30** Consider the third-order elliptic lowpass filter.

$$H(z) = \frac{0.1214 (1 - 1.4211z^{-1} + z^{-2}) (1 + z^{-1})}{(1 - 1.4928z^{-1} + 0.8612z^{-2})(1 - 0.6183z^{-1})}$$

1. If the filter is realized using a direct form structure, determine its pole sensitivity.
2. If the filter is realized using a cascade form structure, determine its pole sensitivity.

**P6.31** Consider the filter described by the difference equation

$$y(n) = \frac{1}{\sqrt{2}}y(n-1) - x(n) + \sqrt{2}x(n-1) \quad (6.72)$$

1. Show that this filter is an allpass filter, that is,  $|H(e^{j\omega})|$  is a constant over the entire frequency range  $-\pi \leq \omega \leq \pi$ . Verify your answer by plotting the magnitude response  $|H(e^{j\omega})|$  over the normalized frequency range  $0 \leq \omega/\pi \leq 1$ . Use `subplot(3,1,1)`.
2. Round the coefficients of the difference equation in (6.72) to three decimals. Is the filter still allpass? Verify your answer by plotting the resulting magnitude response,  $|\hat{H}_1(e^{j\omega})|$ , over the normalized frequency range  $0 \leq \omega/\pi \leq 1$ . Use `subplot(3,1,2)`.
3. Round the coefficients of the difference equation in (6.72) to two decimals. Is the filter still allpass? Verify your answer by plotting the resulting magnitude response,  $|\hat{H}_2(e^{j\omega})|$ , over the normalized frequency range  $0 \leq \omega/\pi \leq 1$ . Use `subplot(3,1,3)`.
4. Explain why the magnitude  $|\hat{H}_1(e^{j\omega})|$  is "different" from the magnitude  $|\hat{H}_2(e^{j\omega})|$ .

**P6.32** An IIR lowpass filter designed to meet the specifications of 0.5 dB ripple in the passband, 60 dB ripple in the stopband, a passband edge frequency  $\omega_p = 0.25\pi$ , and a stopband edge frequency  $\omega_s = 0.3\pi$  is obtained using the following MATLAB script.

```
wp = 0.25*pi; ws = 0.3*pi; Rp = 0.5; As = 60;
[N, Wn] = ellipord(wp/pi, ws/pi, Rp, As);
[b,a] = ellip(N,Rp,As,Wn);
```

The filter coefficients  $b_k$  and  $a_k$  are in the arrays **b** and **a**, respectively, and can be considered to have infinite precision.

1. Using infinite precision, plot the log-magnitude and phase responses of the designed filter. Use two rows and one column of subplots.
2. Quantize the direct form coefficients to four decimals (by rounding). Now plot the log-magnitude and phase responses of the resulting filter. Use two rows and one column of subplots.
3. Quantize the direct form coefficients to three decimals (by rounding). Now plot the log-magnitude and phase responses of the resulting filter. Use two rows and one column of subplots.
4. Comment on the plots in parts 1, 2, and 3.

**P6.33** Consider the digital lowpass filter used in Problem P6.32.

1. Using infinite precision and cascade form realization, plot the log-magnitude and phase responses of the designed filter. Use two rows and one column of subplots.
2. Quantize the cascade form coefficients to four decimals (by rounding). Now plot the log-magnitude and phase responses of the resulting filter. Use two rows and one column of subplots.
3. Quantize the cascade form coefficients to three decimals (by rounding). Now plot the log-magnitude and phase responses of the resulting filter. Use two rows and one column of subplots.
4. Comment on the plots in the above three parts and compare them with the similar plots in Problem P6.32.

**P6.34** A length-32 linear-phase FIR bandpass filter that satisfies the requirements of 60 dB stopband attenuation, lower stopband edge frequency  $\omega_{s1} = 0.2\pi$ , and upper stopband edge frequency  $\omega_{s2} = 0.8\pi$  is obtained using the following MATLAB script.

```
ws1 = 0.2*pi; ws2 = 0.8*pi; As = 60;
M = 32; Df = 0.2115;
fp1 = ws1/pi+Df; fp2 = ws2/pi-Df;
h = firpm(M-1,[0,ws1/pi,fp1,fp2,ws2/pi,1],[0,0,1,1,0,0]);
```

The filter impulse response  $h(n)$  is in the array **h** and can be considered to have infinite precision.

1. Using infinite precision, plot the log-magnitude and amplitude responses of the designed filter. Use two rows and one column of subplots.
2. Quantize the direct form coefficients to four decimals (by rounding). Now plot the log-magnitude and amplitude responses of the resulting filter. Use two rows and one column of subplots.

3. Quantize the direct form coefficients to three decimals (by rounding). Now plot the log-magnitude and amplitude responses of the resulting filter. Use two rows and one column of subplots.
4. Comment on the plots in parts 1, 2, and 3.
5. Based on the results of this problem, determine how many significant *bits* (and not decimals) are needed in practice to represent FIR direct form realizations.

**P6.35** The digital filter structure shown in Figure P6.8 is a cascade of two parallel sections and corresponds to a tenth-order IIR digital filter system function

$$H(z) = \frac{1 - 2.2z^{-2} + 1.6368z^{-4} - 0.48928z^{-6} + 5395456 \times 10^{-8}z^{-8} - 147456 \times 10^{-8}z^{-10}}{1 - 1.65z^{-2} + 0.8778z^{-4} - 0.17281z^{-6} + 1057221 \times 10^{-8}z^{-8} - 893025 \times 10^{-10}z^{-10}}$$

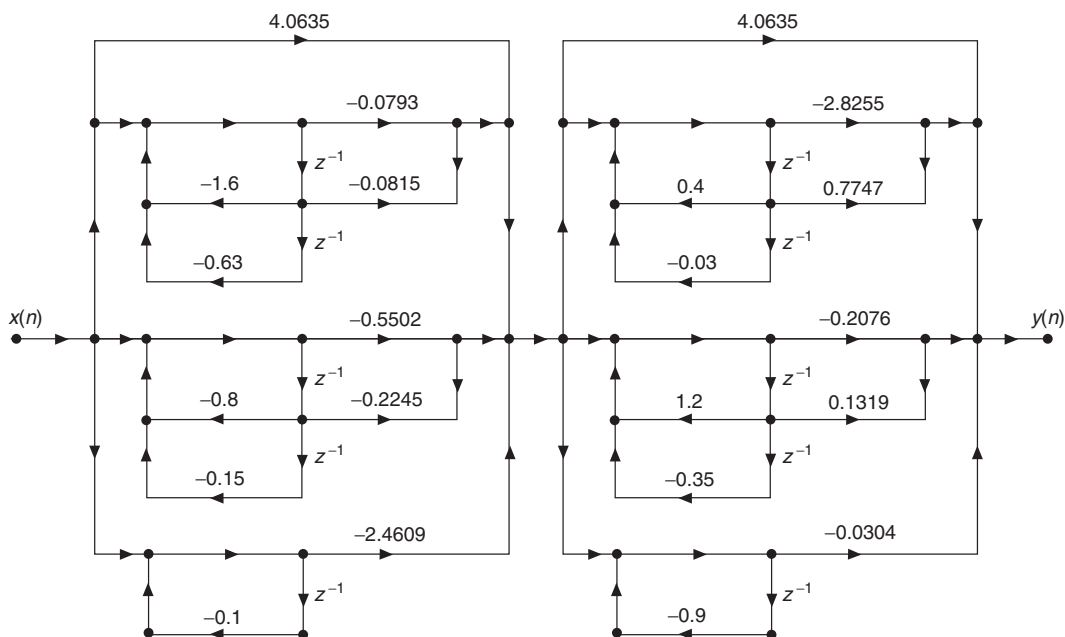


**FIGURE P6.8** Structure for Problem P6.35

1. Due to an error in labeling, two of the multiplier coefficients (rounded to four decimals) in this structure have incorrect values. Locate these two multipliers and determine their correct values.
2. By inspecting the pole locations of the system function  $H(z)$ , you should realize that this structure is sensitive to the coefficient quantization. Suggest, with justification, an alternative structure that in *your opinion* is least sensitive to coefficient quantization.

**P6.36** An IIR bandstop digital filter that satisfies the requirements:

$$\begin{aligned} 0.95 &\leq |H(e^{j\omega})| \leq 1.05, & 0 \leq |\omega| \leq 0.25\pi \\ 0 &\leq |H(e^{j\omega})| \leq 0.01, & 0.35\pi \leq |\omega| \leq 0.65\pi \\ 0.95 &\leq |H(e^{j\omega})| \leq 1.05, & 0.75\pi \leq |\omega| \leq \pi \end{aligned}$$

can be obtained using the following MATLAB script:

```
wp = [0.25,0.75]; ws = [0.35,0.65]; delta1 = 0.05; delta2 = 0.01;
[Rp,As] = delta2db(delta1,delta2);
[N, wn] = cheb2ord(wp, ws, Rp, As);
[b,a] = cheby2(N,As,wn,'stop');
```

The filter coefficients  $b_k$  and  $a_k$  are in the arrays **b** and **a**, respectively, and can be considered to have infinite precision.

1. Using infinite precision, provide the log-magnitude response plot and the pole-zero plot of the designed filter.
2. Assuming direct-form structure and a 12-bit representation for filter coefficients, provide the log-magnitude response plot and the pole-zero plot of the designed filter. Use the **Qcoeff** function.
3. Assuming cascade-form structure and a 12-bit representation for filter coefficients, provide the log-magnitude response plot and the pole-zero plot of the designed filter. Use the **Qcoeff** function.

**P6.37** An IIR lowpass digital filter that satisfies the specifications:

$$\begin{aligned} \text{passband edge: } & 0.4\pi, \quad R_p = 0.5 \text{ dB} \\ \text{stopband edge: } & 0.6\pi, \quad A_s = 50 \text{ dB} \end{aligned}$$

can be obtained using the following MATLAB script:

```
wp = 0.4; ws = 0.6; Rp = 0.5; As = 50;
[N, wn] = buttord(wp, ws, Rp, As);
[b,a] = butter(N,wn);
```

The filter coefficients  $b_k$  and  $a_k$  are in the arrays **b** and **a**, respectively, and can be considered to have infinite precision.

1. Using infinite precision, provide the magnitude response plot and the pole-zero plot of the designed filter.
2. Assuming direct-form structure and a 10-bit representation for filter coefficients, provide the magnitude response plot and the pole-zero plot of the designed filter. Use the **Qcoeff** function.
3. Assuming cascade-form structure and a 10-bit representation for filter coefficients, provide the magnitude response plot and the pole-zero plot of the designed filter. Use the **Qcoeff** function.

**P6.38** An IIR highpass digital filter that satisfies the specifications:

$$\begin{aligned} \text{stopband edge: } & 0.4\pi, \quad A_s = 60 \text{ dB} \\ \text{passband edge: } & 0.6\pi, \quad R_p = 0.5 \text{ dB} \end{aligned}$$

can be obtained using the following MATLAB script:

```
wp = 0.6; ws = 0.4; Rp = 0.5; As = 60;
[N,wn] = ellipord(wp, ws, Rp, As);
[b,a] = ellip(N,Rp,As,wn,'high');
```

The filter coefficients  $b_k$  and  $a_k$  are in the arrays **b** and **a**, respectively, and can be considered to have infinite precision.

1. Using infinite precision, provide the magnitude response plot and the pole-zero plot of the designed filter.
2. Assuming direct-form structure and a 10-bit representation for filter coefficients, provide the magnitude response plot and the pole-zero plot of the designed filter. Use the **Qcoeff** function.
3. Assuming parallel-form structure and a 10-bit representation for filter coefficients, provide the magnitude response plot and the pole-zero plot of the designed filter. Use the **Qcoeff** function.

**P6.39** A bandstop linear-phase FIR filter that satisfies the specifications:

$$\begin{array}{ll} \text{lower stopband edge: } & 0.4\pi \\ \text{upper stopband edge: } & 0.6\pi \quad A_s = 50 \text{ dB} \\ \text{lower passband edge: } & 0.3\pi \\ \text{upper passband edge: } & 0.7\pi \quad R_p = 0.2 \text{ dB} \end{array}$$

can be obtained using the following MATLAB script:

```
wp1 = 0.3; ws1 = 0.4; ws2 = 0.6; wp2 = 0.7; Rp = 0.2; As = 50;
[delta1,delta2] = db2delta(Rp,As);
b = firpm(44,[0,wp1,ws1,ws2,wp2,1],[1,1,0,0,1,1],...
           [delta2/delta1,1,delta2/delta1]);
```

The filter impulse response  $h(n)$  is in the array **b** and can be considered to have infinite precision.

**P6.40** A bandpass linear-phase FIR filter that satisfies the specifications:

$$\begin{array}{lll} 0 & \leq & |H(e^{j\omega})| \leq 0.01, \quad 0 \leq \omega \leq 0.25\pi \\ 0.95 & \leq & |H(e^{j\omega})| \leq 1.05, \quad 0.35\pi \leq \omega \leq 0.65\pi \\ 0 & \leq & |H(e^{j\omega})| \leq 0.01, \quad 0.75\pi \leq \omega \leq \pi \end{array}$$

can be obtained using the following MATLAB script:

```
ws1 = 0.25; wp1 = 0.35; wp2 = 0.65; ws2 = 0.75;
delta1 = 0.05; delta2 = 0.01;
b = firpm(40,[0,ws1,wp1,wp2,ws2,1],[0,0,1,1,0,0],...
           [1,delta2/delta1,1]);
```

The filter impulse response  $h(n)$  is in the array **b** and can be considered to have infinite precision.

# CHAPTER 7

## FIR Filter Design

We now turn our attention to the inverse problem of designing systems from the given specifications. It is an important as well as difficult problem. In digital signal processing, there are two important types of systems. The first type of systems perform signal filtering in the time domain and hence are called *digital filters*. The second type of systems provide signal representation in the frequency domain and are called *spectrum analyzers*. In Chapter 5, we described signal representations using the DFT. In this and the next chapter, we will study several basic design algorithms for both FIR and IIR filters. These designs are mostly of the *frequency selective* type; that is, we will design primarily multiband lowpass, highpass, bandpass, and bandstop filters. In FIR filter design, we will also consider systems like differentiators or Hilbert transformers, which, although not frequency-selective filters, nevertheless follow the design techniques being considered. More sophisticated filter designs are based on arbitrary frequency-domain specifications and require tools that are beyond the scope of this book.

We first begin with some preliminary issues related to design philosophy and design specifications. These issues are applicable to both FIR and IIR filter designs. We will then study FIR filter design algorithms in the rest of this chapter. In Chapter 8, we will provide a similar treatment for IIR filters.

## 7.1 PRELIMINARIES

---

The design of a digital filter is carried out in three steps:

- **Specifications:** Before we can design a filter, we must have some specifications. These specifications are determined by the applications.
- **Approximations:** Once the specifications are defined, we use various concepts and mathematics that we studied so far to come up with a filter description that approximates the given set of specifications. This step is the topic of filter design.
- **Implementation:** The product of the above step is a filter description in the form of a difference equation, a system function  $H(z)$ , or an impulse response  $h(n)$ . From this description, we implement the filter in hardware or through software on a computer as we discussed in Chapter 6.

In this and the next chapter, we will discuss in detail only the second step, which is the conversion of specifications into a filter description.

In many applications like speech or audio signal processing, digital filters are used to implement frequency-selective operations. Therefore, specifications are required in the frequency domain in terms of the desired magnitude and phase response of the filter. Generally, a linear phase response in the passband is desirable. In the case of FIR filters, it is possible to have exact linear phase, as we have seen in Chapter 6. In the case of IIR filters, a linear phase in the passband is not achievable. Hence we will consider *magnitude-only* specifications.

The magnitude specifications are given in one of two ways. The first approach is called *absolute specifications*, which provide a set of requirements on the magnitude response function  $|H(e^{j\omega})|$ . These specifications are generally used for FIR filters. IIR filters are specified in a somewhat different way, which we will discuss in Chapter 8. The second approach is called *relative specifications*, which provide requirements in *decibels* (dB), given by

$$\text{dB scale} = -20 \log_{10} \frac{|H(e^{j\omega})|}{|H(e^{j\omega})|_{\max}} \geq 0$$

This approach is the most popular one in practice and is used for both FIR and IIR filters. To illustrate these specifications, we will consider a lowpass filter design as an example.

### 7.1.1 ABSOLUTE SPECIFICATIONS

A typical absolute specification of a lowpass filter is shown in Figure 7.1a, in which

- band  $[0, \omega_p]$  is called the *passband* and  $\delta_1$  is the tolerance (or ripple) that we are willing to accept in the ideal passband response,

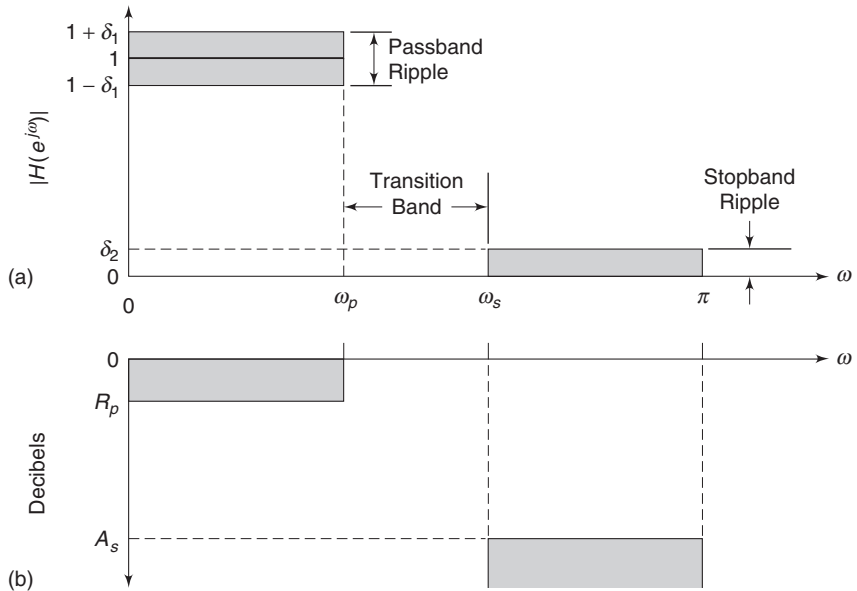


**FIGURE 7.1** FIR filter specifications: (a) absolute (b) relative

- band  $[\omega_s, \pi]$  is called the *stopband* and  $\delta_2$  is the corresponding tolerance (or ripple), and
- band  $[\omega_p, \omega_s]$  is called the *transition band* that imposes no restrictions on the magnitude response.

### 7.1.2 RELATIVE (DB) SPECIFICATIONS

A typical relative specification of a lowpass filter is shown in Figure 7.1b, in which

- $R_p$  is the passband ripple in dB, and
- $A_s$  is the stopband attenuation in dB.

The parameters given in these two specifications are obviously related. Since  $|H(e^{j\omega})|_{\max}$  in absolute specifications is equal to  $(1 + \delta_1)$ , we have

$$R_p = -20 \log_{10} \frac{1 - \delta_1}{1 + \delta_1} > 0 (\approx 0) \quad (7.1)$$

and

$$A_s = -20 \log_{10} \frac{\delta_2}{1 + \delta_1} > 0 (\gg 1) \quad (7.2)$$

- **EXAMPLE 7.1** In a certain filter's specifications, the passband ripple is 0.25 dB and the stopband attenuation is 50 dB. Determine  $\delta_1$  and  $\delta_2$ .

**Solution**

Using (7.1), we obtain

$$R_p = 0.25 = -20 \log_{10} \frac{1 - \delta_1}{1 + \delta_1} \Rightarrow \delta_1 = 0.0144$$

Using (7.2), we obtain

$$A_s = 50 = -20 \log_{10} \frac{\delta_2}{1 + \delta_1} = -20 \log_{10} \frac{\delta_2}{1 + 0.0144} \Rightarrow \delta_2 = 0.0032 \quad \square$$

- EXAMPLE 7.2** Given the passband tolerance  $\delta_1 = 0.01$  and the stopband tolerance  $\delta_2 = 0.001$ , determine the passband ripple  $R_p$  and the stopband attenuation  $A_s$ .

**Solution**

From (7.1), the passband ripple is

$$R_p = -20 \log_{10} \frac{1 - \delta_1}{1 + \delta_1} = 0.1737 \text{ dB}$$

and from (7.2), the stopband attenuation is

$$A_s = -20 \log_{10} \frac{\delta_2}{1 + \delta_1} = 60 \text{ dB} \quad \square$$

Problem P7.1 develops MATLAB functions to convert one set of specifications into another.

These specifications were given for a lowpass filter. Similar specifications can also be given for other types of frequency-selective filters, such as highpass or bandpass. However, the most important design parameters are *frequency-band tolerances* (or ripples) and *band-edge frequencies*. Whether the given band is a passband or a stopband is a relatively minor issue. Therefore, in describing design techniques, we will concentrate on a lowpass filter. In the next chapter, we will discuss how to transform a lowpass filter into other types of frequency-selective filters. Hence it makes more sense to develop techniques for a lowpass filter so that we can compare these techniques. However, we will also provide examples of other types of filters. In light of this discussion, our design goal is the following.

**Problem statement** Design a lowpass filter (i.e., obtain its system function  $H(z)$  or its difference equation) that has a passband  $[0, \omega_p]$  with tolerance  $\delta_1$  (or  $R_p$  in dB) and a stopband  $[\omega_s, \pi]$  with tolerance  $\delta_2$  (or  $A_s$  in dB).

In this chapter, we turn our attention to the design and approximation of FIR digital filters. These filters have several design and implementation advantages:

- The phase response can be exactly linear.
- They are relatively easy to design since there are no stability problems.
- They are efficient to implement.
- The DFT can be used in their implementation.

As we discussed in Chapter 6, we are generally interested in linear-phase frequency-selective FIR filters. Linear-phase response filters have several advantages:

- The design problem contains only real arithmetic and not complex arithmetic
- Linear-phase filters provide no delay distortion and only a fixed amount of delay
- For the filter of length  $M$  (or order  $M - 1$ ), the number of operations are of the order of  $M/2$ , as we discussed in the linear-phase filter implementation

We first begin with a discussion of the properties of the linear-phase FIR filters, which are required in design algorithms. Then we will discuss three design techniques—namely, the window design, the frequency-sampling design, and the optimal equiripple design techniques for linear-phase FIR filters.

## 7.2 PROPERTIES OF LINEAR-PHASE FIR FILTERS

---

In this section, we discuss shapes of impulse and frequency responses and locations of system function zeros of linear-phase FIR filters. Let  $h(n)$ ,  $0 \leq n \leq M - 1$ , be the impulse response of length (or duration)  $M$ . Then the system function is

$$H(z) = \sum_{n=0}^{M-1} h(n)z^{-n} = z^{-(M-1)} \sum_{n=0}^{M-1} h(n)z^{M-1-n}$$

which has  $(M - 1)$  poles at the origin  $z = 0$  (trivial poles) and  $(M - 1)$  zeros located anywhere in the  $z$ -plane. The frequency response function is

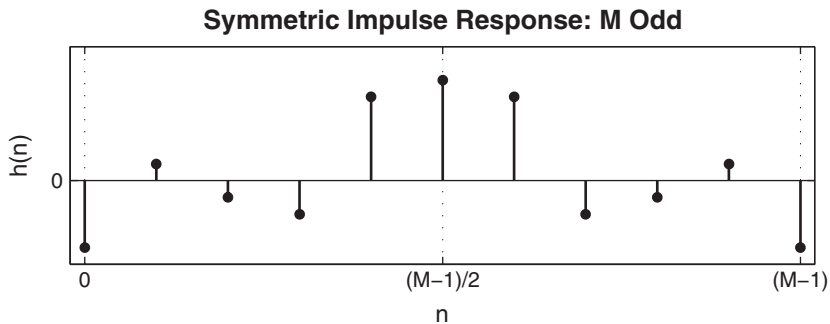
$$H(e^{j\omega}) = \sum_{n=0}^{M-1} h(n)e^{-j\omega n}, \quad -\pi < \omega \leq \pi$$

Now we will discuss specific requirements on the forms of  $h(n)$  and  $H(e^{j\omega})$  as well as requirements on the specific locations of  $(M - 1)$  zeros that the linear-phase constraint imposes.

### 7.2.1 IMPULSE RESPONSE $h(n)$

We impose a linear-phase constraint

$$\angle H(e^{j\omega}) = -\alpha\omega, \quad -\pi < \omega \leq \pi$$

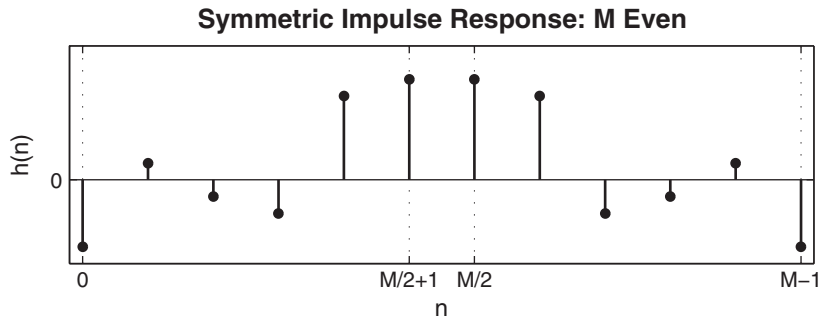


where  $\alpha$  is a *constant phase delay*. Then we know from Chapter 6 that  $h(n)$  must be symmetric, that is,

$$h(n) = h(M-1-n), \quad 0 \leq n \leq (M-1) \text{ with } \alpha = \frac{M-1}{2} \quad (7.3)$$

Hence  $h(n)$  is symmetric about  $\alpha$ , which is the index of symmetry. There are two possible types of symmetry:

- *M odd.* In this case,  $\alpha = (M-1)/2$  is an integer. The impulse response is as shown above.
- *M even.* In this case,  $\alpha = (M-1)/2$  is not an integer. The impulse response is as shown here.



We also have a second type of “linear-phase” FIR filter if we require that the phase response  $\angle H(e^{j\omega})$  satisfy the condition

$$\angle H(e^{j\omega}) = \beta - \alpha\omega$$

which is a straight line, but not through the origin. In this case,  $\alpha$  is not a constant phase delay, but

$$\frac{d\angle H(e^{j\omega})}{d\omega} = -\alpha$$

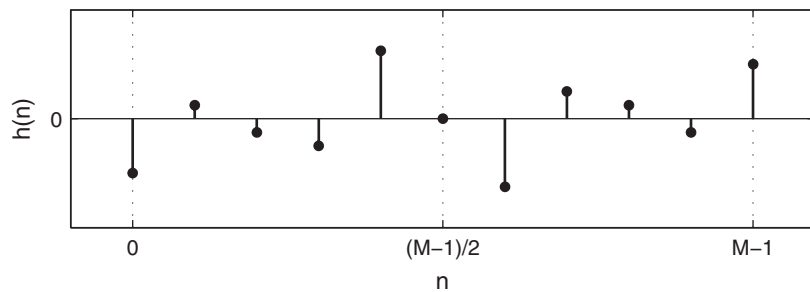
is constant, which is the group delay. Therefore,  $\alpha$  is called a *constant group delay*. In this case, as a group, frequencies are delayed at a constant rate. But some frequencies may get delayed more and others delayed less. For this type of linear phase, one can show that

$$h(n) = -h(M-1-n), \quad 0 \leq n \leq (M-1); \quad \alpha = \frac{M-1}{2}, \quad \beta = \pm \frac{\pi}{2} \quad (7.4)$$

This means that the impulse response  $h(n)$  is *antisymmetric*. The index of symmetry is still  $\alpha = (M-1)/2$ . Once again, we have two possible types, one for  $M$  odd and one for  $M$  even.

- $M$  odd. In this case,  $\alpha = (M-1)/2$  is an integer and the impulse response is as shown.

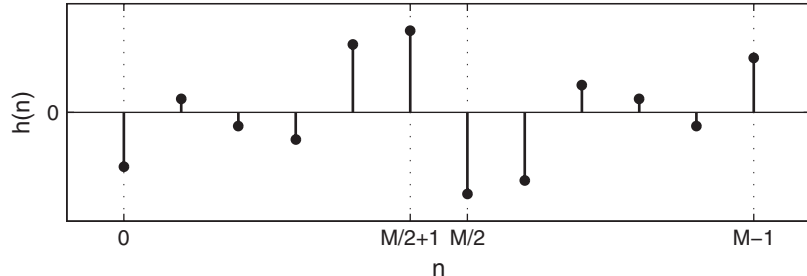
**Antisymmetric Impulse Response: M Odd**



Note that the sample  $h(\alpha)$  at  $\alpha = (M-1)/2$  must necessarily be equal to zero, that is,  $h((M-1)/2) = 0$ .

- $M$  even. In this case,  $\alpha = (M-1)/2$  is not an integer and the impulse response is as shown.

**Antisymmetric Impulse Response: M Even**



### 7.2.2 FREQUENCY RESPONSE $H(e^{j\omega})$

When the cases of symmetry and antisymmetry are combined with odd and even  $M$ , we obtain four types of linear-phase FIR filters. Frequency response functions for each of these types have some peculiar expressions and shapes. To study these responses, we write  $H(e^{j\omega})$  as

$$H(e^{j\omega}) = H_r(\omega) e^{j(\beta - \alpha\omega)}; \quad \beta = \pm \frac{\pi}{2}, \alpha = \frac{M-1}{2} \quad (7.5)$$

where  $H_r(\omega)$  is an *amplitude response* function and not a magnitude response function. The amplitude response is a real function, but unlike the magnitude response, which is always positive, the amplitude response may be both positive and negative. The phase response associated with the magnitude response is a *discontinuous* function, while that associated with the amplitude response is a *continuous linear* function. To illustrate the difference between these two types of responses, consider the following example.

- **EXAMPLE 7.3** Let the impulse response be  $h(n) = \{1, 1, 1\}$ . Determine and draw frequency responses.

**Solution**

The frequency response function is

$$\begin{aligned} H(e^{j\omega}) &= \sum_0^2 h(n) e^{j\omega n} = 1 + 1e^{-j\omega} + e^{-j2\omega} = \{e^{j\omega} + 1 + e^{-j\omega}\} e^{-j\omega} \\ &= \{1 + 2 \cos \omega\} e^{-j\omega} \end{aligned}$$

From this, the magnitude and the phase responses are

$$|H(e^{j\omega})| = |1 + 2 \cos \omega|, \quad 0 < \omega \leq \pi$$

$$\angle H(e^{j\omega}) = \begin{cases} -\omega, & 0 < \omega < 2\pi/3 \\ \pi - \omega, & 2\pi/3 < \omega < \pi \end{cases}$$

since  $\cos \omega$  can be both positive and negative. In this case, the phase response is *piecewise linear*. On the other hand, the amplitude and the corresponding phase responses are

$$\begin{aligned} H_r(\omega) &= 1 + 2 \cos \omega, & -\pi < \omega \leq \pi \\ \angle H(e^{j\omega}) &= -\omega, \end{aligned}$$

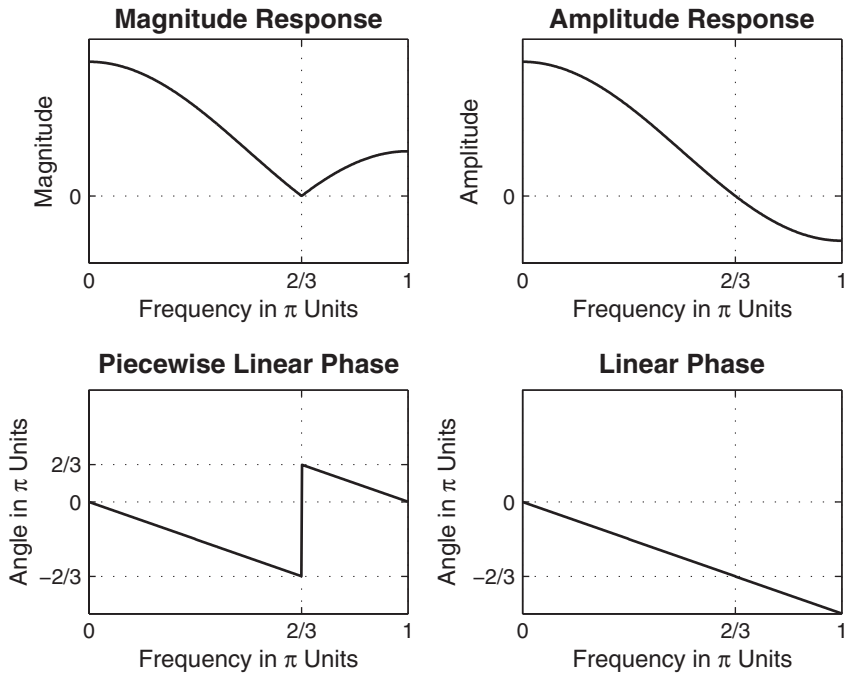


FIGURE 7.2 Frequency responses in Example 7.3

In this case, the phase response is *truly linear*. These responses are shown in Figure 7.2. From this example, the difference between the magnitude and the amplitude (or between the piecewise linear and the linear-phase) responses should be clear.  $\square$

**Type-1 linear-phase FIR filter: Symmetrical impulse response,  $M$  odd** In this case,  $\beta = 0$ ,  $\alpha = (M - 1)/2$  is an integer and  $h(n) = h(M - 1 - n)$ ,  $0 \leq n \leq M - 1$ . Then we can show (see Problem P7.2) that

$$H(e^{j\omega}) = \left[ \sum_{n=0}^{(M-1)/2} a(n) \cos \omega n \right] e^{-j\omega(M-1)/2} \quad (7.6)$$

where sequence  $a(n)$  is obtained from  $h(n)$  as

$$\begin{aligned} a(0) &= h\left(\frac{M-1}{2}\right) && \text{(the middle sample)} \\ a(n) &= 2h\left(\frac{M-1}{2} - n\right), \quad 1 \leq n \leq \frac{M-3}{2} \end{aligned} \quad (7.7)$$

Comparing (7.5) with (7.6), we have

$$H_r(\omega) = \sum_{n=0}^{(M-1)/2} a(n) \cos \omega n \quad (7.8)$$

**Type-2 linear-phase FIR filter: Symmetrical impulse response, M even** In this case, again  $\beta = 0$ ,  $h(n) = h(M - 1 - n)$ ,  $0 \leq n \leq M - 1$ , but  $\alpha = (M - 1)/2$  is not an integer. Then we can show (see Problem P7.3) that

$$H(e^{j\omega}) = \left[ \sum_{n=1}^{M/2} b(n) \cos \left\{ \omega \left( n - \frac{1}{2} \right) \right\} \right] e^{-j\omega(M-1)/2} \quad (7.9)$$

where

$$b(n) = 2h\left(\frac{M}{2} - n\right), \quad n = 1, 2, \dots, \frac{M}{2} \quad (7.10)$$

Hence

$$H_r(\omega) = \sum_{n=1}^{M/2} b(n) \cos \left\{ \omega \left( n - \frac{1}{2} \right) \right\} \quad (7.11)$$

*Note:* At  $\omega = \pi$ , we get

$$H_r(\pi) = \sum_{n=1}^{M/2} b(n) \cos \left\{ \pi \left( n - \frac{1}{2} \right) \right\} = 0$$

regardless of  $b(n)$  or  $h(n)$ . Hence we cannot use this type (i.e., symmetric  $h(n)$ ,  $M$  even) for highpass or bandstop filters.

**Type-3 linear-phase FIR filter: Antisymmetric impulse response, M odd** In this case,  $\beta = \pi/2$ ,  $\alpha = (M - 1)/2$  is an integer,  $h(n) = -h(M - 1 - n)$ ,  $0 \leq n \leq M - 1$ , and  $h((M - 1)/2) = 0$ . Then we can show (see Problem P7.4) that

$$H(e^{j\omega}) = \left[ \sum_{n=1}^{(M-1)/2} c(n) \sin \omega n \right] e^{j[\frac{\pi}{2} - (\frac{M-1}{2})\omega]} \quad (7.12)$$

where

$$c(n) = 2h \left( \frac{M-1}{2} - n \right), \quad n = 1, 2, \dots, \frac{M-1}{2} \quad (7.13)$$

and

$$H_r(\omega) = \sum_{n=1}^{(M-1)/2} c(n) \sin \omega n \quad (7.14)$$

*Note:* At  $\omega = 0$  and  $\omega = \pi$ , we have  $H_r(\omega) = 0$ , regardless of  $c(n)$  or  $h(n)$ . Furthermore,  $e^{j\pi/2} = j$ , which means that  $jH_r(\omega)$  is purely imaginary. Hence this type of filter is not suitable for designing a lowpass filter or a highpass filter. However, this behavior is suitable for approximating ideal digital Hilbert transformers and differentiators. An ideal Hilbert transformer [79] is an allpass filter that imparts a  $90^\circ$  phase shift on the input signal. It is frequently used in communication systems for modulation purposes. Differentiators are used in many analog and digital systems to take the derivative of a signal.

**Type-4 linear-phase FIR filter: Antisymmetric impulse response,  $M$  even** This case is similar to Type-2. We have (see Problem P7.5)

$$H(e^{j\omega}) = \left[ \sum_{n=1}^{M/2} d(n) \sin \left\{ \omega \left( n - \frac{1}{2} \right) \right\} \right] e^{j[\frac{\pi}{2} - \omega(M-1)/2]} \quad (7.15)$$

where

$$d(n) = 2h \left( \frac{M}{2} - n \right), \quad n = 1, 2, \dots, \frac{M}{2} \quad (7.16)$$

and

$$H_r(\omega) = \sum_{n=1}^{M/2} d(n) \sin \left\{ \omega \left( n - \frac{1}{2} \right) \right\} \quad (7.17)$$

*Note:* At  $\omega = 0$ ,  $H_r(0) = 0$  and  $e^{j\pi/2} = j$ . Hence this type is also suitable for designing digital Hilbert transformers and differentiators.

### 7.2.3 MATLAB IMPLEMENTATION

The MATLAB function `freqz` computes the frequency response from which we can determine the magnitude response but not the amplitude response. The SP toolbox now provides the function `zerophase` that can compute the amplitude response. However, it is easy to write simple functions to compute amplitude responses for each of the four types. We provide four functions to do this.

## 1. Hr\_type1:

```

function [Hr,w,a,L] = Hr_Type1(h);
% Computes amplitude response Hr(w) of a Type-1 LP FIR filter
%
% [Hr,w,a,L] = Hr_Type1(h)
% Hr = amplitude response
% w = 500 frequencies between [0 pi] over which Hr is computed
% a = type-1 LP filter coefficients
% L = order of Hr
% h = type-1 LP filter impulse response
%
M = length(h); L = (M-1)/2;
a = [h(L+1) 2*h(L:-1:1)]; % 1x(L+1) row vector
n = [0:1:L]; % (L+1)x1 column vector
w = [0:1:500] '*pi/500; Hr = cos(w*n)*a';

```

## 2. Hr\_type2:

```

function [Hr,w,b,L] = Hr_Type2(h);
% Computes amplitude response of a Type-2 LP FIR filter
%
% [Hr,w,b,L] = Hr_Type2(h)
% Hr = amplitude response
% w = frequencies between [0 pi] over which Hr is computed
% b = type-2 LP filter coefficients
% L = order of Hr
% h = type-2 LP impulse response
%
M = length(h); L = M/2;
b = 2*[h(L:-1:1)]; n = [1:1:L]; n = n-0.5;
w = [0:1:500] '*pi/500; Hr = cos(w*n)*b';

```

## 3. Hr\_type3:

```

function [Hr,w,c,L] = Hr_Type3(h);
% Computes amplitude response Hr(w) of a Type-3 LP FIR filter
%
% [Hr,w,c,L] = Hr_Type3(h)
% Hr = amplitude response
% w = frequencies between [0 pi] over which Hr is computed
% c = type-3 LP filter coefficients
% L = order of Hr
% h = type-3 LP impulse response
%
M = length(h); L = (M-1)/2;
c = [2*h(L+1:-1:1)]; n = [0:1:L];
w = [0:1:500] '*pi/500; Hr = sin(w*n)*c';

```

#### 4. Hr\_type4:

```

function [Hr,w,d,L] = Hr_Type4(h);
% Computes amplitude response of a Type-4 LP FIR filter
%
% [Hr,w,d,L] = Hr_Type4(h)
% Hr = amplitude response
% w = frequencies between [0 pi] over which Hr is computed
% d = type-4 LP filter coefficients
% L = order of d
% h = type-4 LP impulse response
%
M = length(h); L = M/2;
d = 2*[h(L:-1:1)]; n = [1:1:L]; n = n-0.5;
w = [0:1:500] *pi/500; Hr = sin(w*n)*d';

```

These four functions can be combined into one function, called `ampl_res`, that can be written to determine the type of the linear-phase filter and to implement the appropriate amplitude response expression. This is explored in Problem P7.6. The use of these functions is described in Examples 7.4 through 7.7.

The `zerophase` function from the SP toolbox is similar in use to the `freqz` function. The invocation `[Hr, w, phi] = zerophase(b, a)` returns the amplitude response in `Hr`, evaluated at 512 values around the top half of the unit circle in the array `w` and the continuous phase response in `phi`. Thus this function can be used for both FIR and IIR filters. Other invocations are also available.

#### 7.2.4 ZERO LOCATIONS

Recall that for an FIR filter there are  $(M - 1)$  (trivial) poles at the origin and  $(M - 1)$  zeros located somewhere in the  $z$ -plane. For linear-phase FIR filters, these zeros possess certain symmetries that are due to the symmetry constraints on  $h(n)$ . It can be shown (see reference [79] and Problem P7.7) that if  $H(z)$  has a zero at

$$z = z_1 = re^{j\theta}$$

then for the linear-phase constraint, there must be a zero at

$$z = \frac{1}{z_1} = \frac{1}{r}e^{-j\theta}$$

For a real-valued filter, we also know that if  $z_1$  is complex, then there must be a conjugate zero at  $z_1^* = re^{-j\theta}$ , which implies that there must be a

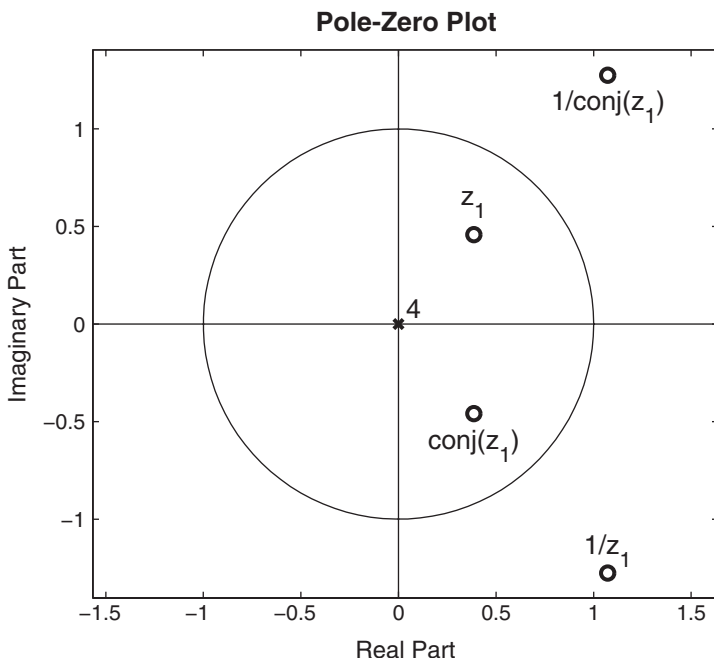


**FIGURE 7.3** A general zero constellation

zero at  $1/z_1^* = (1/r) e^{j\theta}$ . Thus a general zero constellation is a quadruplet

$$re^{j\theta}, \quad \frac{1}{r}e^{j\theta}, \quad re^{-j\theta}, \quad \text{and} \quad \frac{1}{r}e^{-j\theta}$$

as shown in Figure 7.3. Clearly, if  $r = 1$ , then  $1/r = 1$ , and hence the zeros are on the unit circle and occur in pairs

$$e^{j\theta} \quad \text{and} \quad e^{-j\theta}$$

If  $\theta = 0$  or  $\theta = \pi$ , then the zeros are on the real line and occur in pairs

$$r \quad \text{and} \quad \frac{1}{r}$$

Finally, if  $r = 1$  and  $\theta = 0$  or  $\theta = \pi$ , the zeros are either at  $z = 1$  or  $z = -1$ . These symmetries can be used to implement cascade forms with linear-phase sections.

In the following examples, we illustrate the preceding properties of linear-phase FIR filters.

- **EXAMPLE 7.4** Let  $h(n) = \{-4, 1, -1, -2, 5, \overset{\uparrow}{6}, 5, -2, -1, 1, -4\}$ . Determine the amplitude response  $H_r(\omega)$  and the locations of the zeros of  $H(z)$ .

**Solution**

Since  $M = 11$ , which is odd, and since  $h(n)$  is symmetric about  $\alpha = (11-1)/2 = 5$ , this is a Type-1 linear-phase FIR filter. From (7.7), we have

$$\begin{aligned} a(0) &= h(\alpha) = h(5) = 6, \quad a(1) = 2h(5-1) = 10, \quad a(2) = 2h(5-2) = -4 \\ a(3) &= 2h(5-3) = -2, \quad a(4) = 2h(5-4) = 2, \quad a(5) = 2h(5-5) = -8 \end{aligned}$$

From (7.8), we obtain

$$\begin{aligned} H_r(\omega) &= a(0) + a(1) \cos \omega + a(2) \cos 2\omega + a(3) \cos 3\omega + a(4) \cos 4\omega + a(5) \cos 5\omega \\ &= 6 + 10 \cos \omega - 4 \cos 2\omega - 2 \cos 3\omega + 2 \cos 4\omega - 8 \cos 5\omega \end{aligned}$$

MATLAB script:

```
>> h = [-4,1,-1,-2,5,6,5,-2,-1,1,-4];
>> M = length(h); n = 0:M-1;
>> [Hr,w,a,L] = Hr_Type1(h);
>> a,L
a = 6     10     -4     -2      2     -8
L = 5
>> % plotting commands follow
```

The plots and the zero locations are shown in Figure 7.4. From these plots, we observe that there are no restrictions on  $H_r(\omega)$  either at  $\omega = 0$  or at  $\omega = \pi$ . There is one zero-quadruplet constellation and three zero pairs.  $\square$

- EXAMPLE 7.5** Let  $h(n) = \{-4, 1, -1, -2, 5, \overset{\uparrow}{6}, 6, 5, -2, -1, 1, -4\}$ . Determine the amplitude response  $H_r(\omega)$  and the locations of the zeros of  $H(z)$ .

**Solution**

This is a Type-2 linear-phase FIR filter since  $M = 12$  and since  $h(n)$  is symmetric with respect to  $\alpha = (12-1)/2 = 5.5$ . From (7.10), we have

$$\begin{aligned} b(1) &= 2h\left(\frac{12}{2} - 1\right) = 12, \quad b(2) = 2h\left(\frac{12}{2} - 2\right) = 10, \quad b(3) = 2h\left(\frac{12}{2} - 3\right) = -4 \\ b(4) &= 2h\left(\frac{12}{2} - 4\right) = -2, \quad b(5) = 2h\left(\frac{12}{2} - 5\right) = 2, \quad b(6) = 2h\left(\frac{12}{2} - 6\right) = -8 \end{aligned}$$

Hence from (7.11) we obtain

$$\begin{aligned} H_r(\omega) &= b(1) \cos \left[ \omega \left( 1 - \frac{1}{2} \right) \right] + b(2) \cos \left[ \omega \left( 2 - \frac{1}{2} \right) \right] + b(3) \cos \left[ \omega \left( 3 - \frac{1}{2} \right) \right] \\ &\quad + b(4) \cos \left[ \omega \left( 4 - \frac{1}{2} \right) \right] + b(5) \cos \left[ \omega \left( 5 - \frac{1}{2} \right) \right] + b(6) \cos \left[ \omega \left( 6 - \frac{1}{2} \right) \right] \\ &= 12 \cos \left( \frac{\omega}{2} \right) + 10 \cos \left( \frac{3\omega}{2} \right) - 4 \cos \left( \frac{5\omega}{2} \right) - 2 \cos \left( \frac{7\omega}{2} \right) \\ &\quad + 2 \cos \left( \frac{9\omega}{2} \right) - 8 \cos \left( \frac{11\omega}{2} \right) \end{aligned}$$

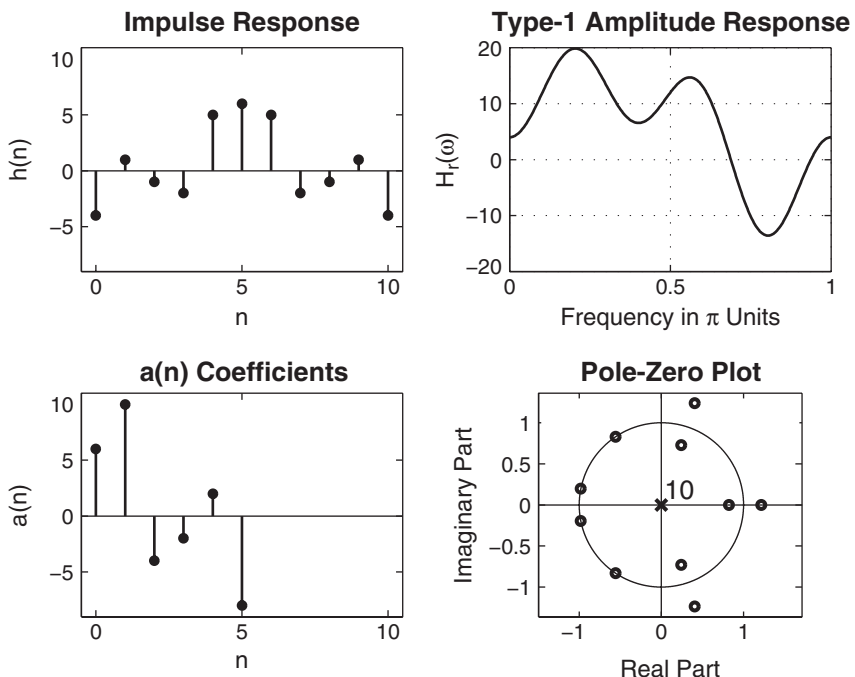


**FIGURE 7.4** Plots in Example 7.4

MATLAB script:

```
>> h = [-4,1,-1,-2,5,6,6,5,-2,-1,1,-4];
>> M = length(h); n = 0:M-1; [Hr,w,b,L] = Hr_Type2(h);
>> b,L
b = 12      10      -4      -2      2      -8
L = 6
>> % plotting commands follow
```

The plots and the zero locations are shown in Figure 7.5. From these plots, we observe that  $H_r(\omega)$  is zero at  $\omega = \pi$ . There is one zero-quadruplet constellation, three zero pairs, and one zero at  $\omega = \pi$ , as expected.  $\square$

- EXAMPLE 7.6** Let  $h(n) = \{-4, 1, -1, -2, 5, 0, -5, 2, 1, -1, 4\}$ . Determine the amplitude response  $H_r(\omega)$  and the locations of the zeros of  $H(z)$ .

#### Solution

Since  $M=11$ , which is odd, and since  $h(n)$  is antisymmetric about  $\alpha = (11-1)/2 = 5$ , this is a Type-3 linear-phase FIR filter. From (7.13), we have

$$\begin{aligned} c(0) &= h(\alpha) = h(5) = 0, \quad c(1) = 2h(5-1) = 10, \quad c(2) = 2h(5-2) = -4 \\ c(3) &= 2h(5-3) = -2, \quad c(4) = 2h(5-4) = 2, \quad c(5) = 2h(5-5) = -8 \end{aligned}$$

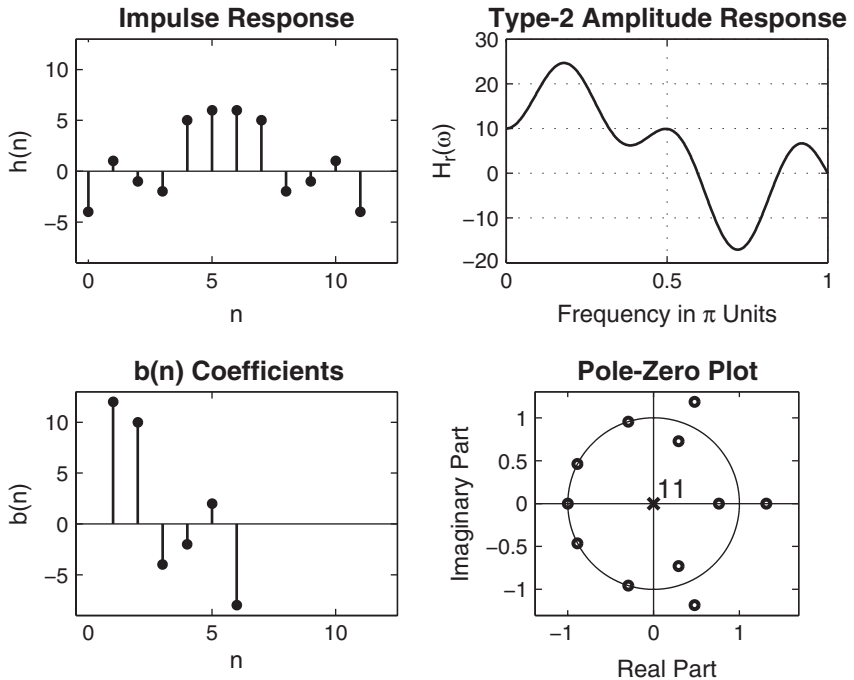


**FIGURE 7.5** Plots in Example 7.5

From (7.14), we obtain

$$\begin{aligned} H_r(\omega) &= c(0) + c(1) \sin \omega + c(2) \sin 2\omega + c(3) \sin 3\omega + c(4) \sin 4\omega + c(5) \sin 5\omega \\ &= 0 + 10 \sin \omega - 4 \sin 2\omega - 2 \sin 3\omega + 2 \sin 4\omega - 8 \sin 5\omega \end{aligned}$$

MATLAB script:

```
>> h = [-4,1,-1,-2,5,0,-5,2,1,-1,4];
>> M = length(h); n = 0:M-1; [Hr,w,c,L] = Hr_Type3(h);
>> c,L
a = 0      10      -4      -2      2      -8
L = 5
>> % plotting commands follow
```

The plots and the zero locations are shown in Figure 7.6. From these plots, we observe that  $H_r(\omega) = 0$  at  $\omega = 0$  and at  $\omega = \pi$ . There is one zero-quadruplet constellation, two zero pairs, and zeros at  $\omega = 0$  and  $\omega = \pi$ , as expected.  $\square$

- EXAMPLE 7.7** Let  $h(n) = \{ -4, 1, -1, -2, 5, \overset{\uparrow}{6}, -6, -5, 2, 1, -1, 4 \}$ . Determine the amplitude response  $H_r(\omega)$  and the locations of the zeros of  $H(z)$ .

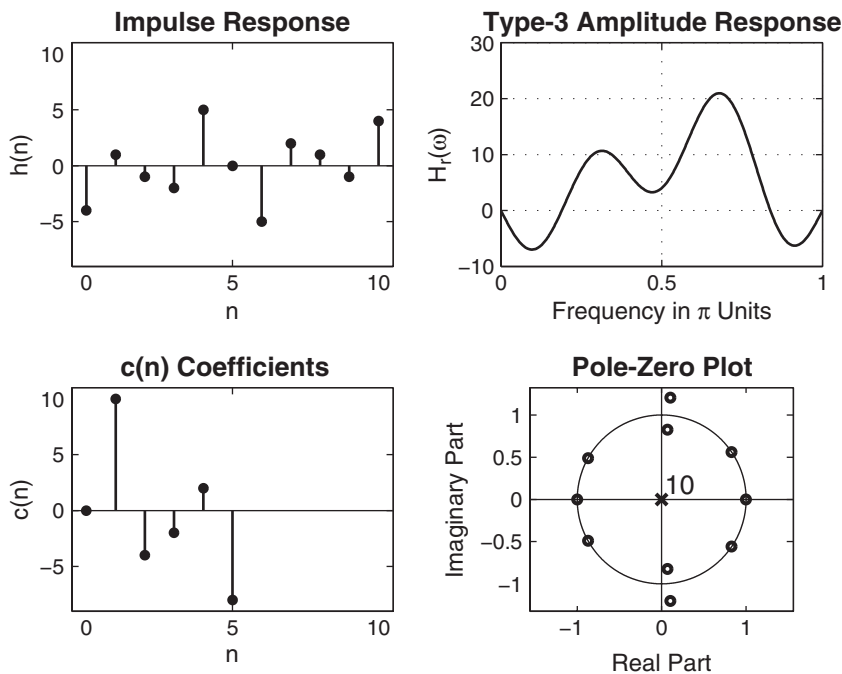


FIGURE 7.6 Plots in Example 7.6

### Solution

This is a Type-4 linear-phase FIR filter since  $M = 12$  and since  $h(n)$  is anti-symmetric with respect to  $\alpha = (12 - 1)/2 = 5.5$ . From (7.16), we have

$$\begin{aligned} d(1) &= 2h\left(\frac{12}{2} - 1\right) = 12, \quad d(2) = 2h\left(\frac{12}{2} - 2\right) = 10, \quad d(3) = 2h\left(\frac{12}{2} - 3\right) = -4 \\ d(4) &= 2h\left(\frac{12}{2} - 4\right) = -2, \quad d(5) = 2h\left(\frac{12}{2} - 5\right) = 2, \quad d(6) = 2h\left(\frac{12}{2} - 6\right) = -8 \end{aligned}$$

Hence from (7.17), we obtain

$$\begin{aligned} H_r(\omega) &= d(1) \sin\left[\omega\left(1 - \frac{1}{2}\right)\right] + d(2) \sin\left[\omega\left(2 - \frac{1}{2}\right)\right] + d(3) \sin\left[\omega\left(3 - \frac{1}{2}\right)\right] \\ &\quad + d(4) \sin\left[\omega\left(4 - \frac{1}{2}\right)\right] + d(5) \sin\left[\omega\left(5 - \frac{1}{2}\right)\right] + d(6) \sin\left[\omega\left(6 - \frac{1}{2}\right)\right] \\ &= 12 \sin\left(\frac{\omega}{2}\right) + 10 \sin\left(\frac{3\omega}{2}\right) - 4 \sin\left(\frac{5\omega}{2}\right) - 2 \sin\left(\frac{7\omega}{2}\right) \\ &\quad + 2 \sin\left(\frac{9\omega}{2}\right) - 8 \sin\left(\frac{11\omega}{2}\right) \end{aligned}$$

MATLAB script:

```
>> h = [-4,1,-1,-2,5,6,-6,-5,2,1,-1,4];
>> M = length(h); n = 0:M-1; [Hr,w,d,L] = Hr_Type4(h);
>> d,L
d = 12      10      -4      -2      2      -8
L = 6
>> % plotting commands follow
```

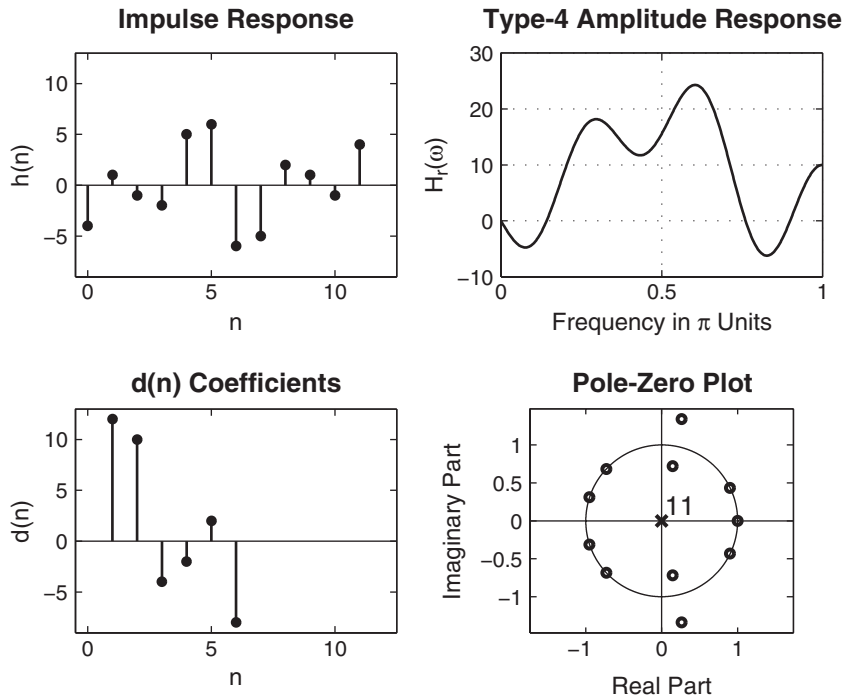


**FIGURE 7.7** Plots in Example 7.7

The plots and the zero locations are shown in Figure 7.7. From these plots, we observe that  $H_r(\omega)$  is zero at  $\omega = 0$ . There is one zero-quadruplet constellation, three zero pairs, and one zero at  $\omega = 0$ , as expected.  $\square$

## 7.3 WINDOW DESIGN TECHNIQUE

The basic idea behind the window design is to choose a proper ideal frequency-selective filter (which always has a noncausal, infinite-duration impulse response) and then to truncate (or window) its impulse response to obtain a linear-phase and causal FIR filter. Therefore, the emphasis in this method is on selecting an appropriate *windowing* function and an appropriate *ideal* filter. We will denote an ideal frequency-selective filter by  $H_d(e^{j\omega})$ , which has a unity magnitude gain and linear-phase characteristics over its passband, and zero response over its stopband. An ideal LPF of bandwidth  $\omega_c < \pi$  is given by

$$H_d(e^{j\omega}) = \begin{cases} 1 \cdot e^{-j\alpha\omega}, & |\omega| \leq \omega_c \\ 0, & \omega_c < |\omega| \leq \pi \end{cases} \quad (7.18)$$

where  $\omega_c$  is also called the *cutoff frequency* and  $\alpha$  is called the sample *delay*. (Note that from the DTFT properties,  $e^{-j\alpha\omega}$  implies shift in the positive  $n$  direction or delay.) The impulse response of this filter is of infinite duration and is given by

$$\begin{aligned} h_d(n) &= \mathcal{F}^{-1}[H_d(e^{j\omega})] = \frac{1}{2\pi} \int_{-\pi}^{\pi} H_d(e^{j\omega}) e^{j\omega n} d\omega \quad (7.19) \\ &= \frac{1}{2\pi} \int_{-\omega_c}^{\omega_c} 1 \cdot e^{-j\alpha\omega} e^{j\omega n} d\omega \\ &= \frac{\sin[\omega_c(n - \alpha)]}{\pi(n - \alpha)} \end{aligned}$$

Note that  $h_d(n)$  is symmetric with respect to  $\alpha$ , a fact useful for linear-phase FIR filters.

To obtain an FIR filter from  $h_d(n)$ , one has to truncate  $h_d(n)$  on both sides. To obtain a causal and linear-phase FIR filter  $h(n)$  of length  $M$ , we must have

$$h(n) = \begin{cases} h_d(n), & 0 \leq n \leq M-1 \\ 0, & \text{elsewhere} \end{cases} \quad \text{and} \quad \alpha = \frac{M-1}{2} \quad (7.20)$$

This operation is called “windowing.” In general,  $h(n)$  can be thought of as being formed by the product of  $h_d(n)$  and a window function  $w(n)$  as follows:

$$h(n) = h_d(n)w(n) \quad (7.21)$$

where

$$w(n) = \begin{cases} \text{some symmetric function with respect to } n \\ \alpha \text{ over } 0 \leq n \leq M-1 \\ 0, \text{ otherwise} \end{cases}$$

Depending on how we define  $w(n)$ , we obtain different window designs. For example, in (7.20)

$$w(n) = \begin{cases} 1, & 0 \leq n \leq M-1 \\ 0, & \text{otherwise} \end{cases} = \mathcal{R}_M(n)$$

which is the *rectangular window* defined earlier.

In the frequency domain, the causal FIR filter response  $H(e^{j\omega})$  is given by the periodic convolution of  $H_d(e^{j\omega})$  and the window response  $W(e^{j\omega})$ ; that is,

$$H(e^{j\omega}) = H_d(e^{j\omega}) \odot W(e^{j\omega}) = \frac{1}{2\pi} \int_{-\pi}^{\pi} W(e^{j\lambda}) H_d(e^{j(\omega-\lambda)}) d\lambda \quad (7.22)$$

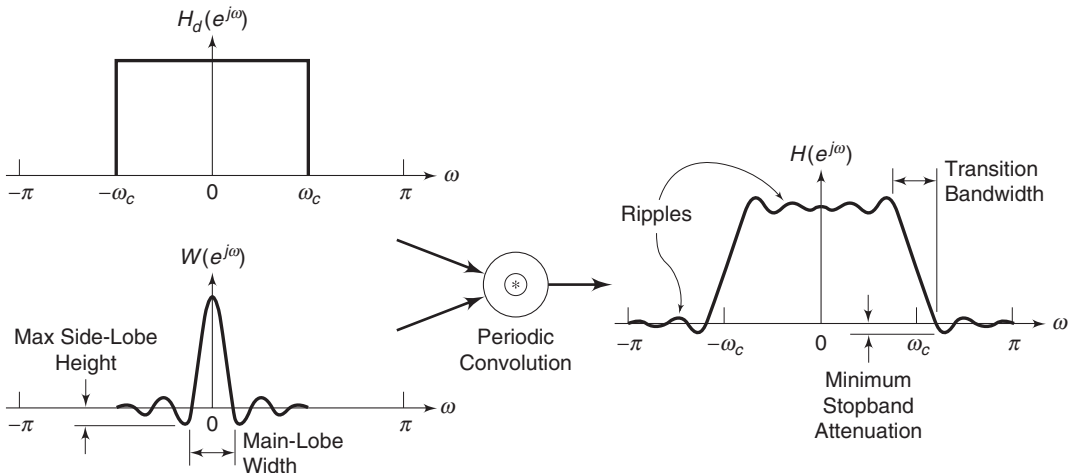


**FIGURE 7.8** Windowing operation in the frequency domain

This is shown pictorially in Figure 7.8 for a typical window response, from which we have the following observations.

1. Since the window  $w(n)$  has a finite length equal to  $M$ , its response has a *peaky main-lobe* whose width is proportional to  $1/M$  and has side-lobes of smaller heights.
2. The periodic convolution (7.22) produces a smeared version of the ideal response  $H_d(e^{j\omega})$ .
3. The main lobe produces a transition band in  $H(e^{j\omega})$  whose width is responsible for the transition width. This width is then proportional to  $1/M$ . The wider the main lobe, the wider will be the transition width.
4. The side lobes produce ripples that have similar shapes in both the passband and stopband.

**Basic window design idea** For the given filter specifications, choose the filter length  $M$  and a window function  $w(n)$  for the narrowest main-lobe width and the smallest side-lobe attenuation possible.

From observation 4, we note that the passband tolerance  $\delta_1$  and the stopband tolerance  $\delta_2$  cannot be specified independently. We generally take care of  $\delta_2$  alone, which results in  $\delta_2 = \delta_1$ . We now briefly describe various well-known window functions. We will use the rectangular window as an example to study their performances in the frequency domain.

### 7.3.1 RECTANGULAR WINDOW

This is the simplest window function but provides the worst performance from the viewpoint of stopband attenuation. It was defined earlier by

$$w(n) = \begin{cases} 1, & 0 \leq n \leq M-1 \\ 0, & \text{otherwise} \end{cases} \quad (7.23)$$

Its frequency response function is

$$W(e^{j\omega}) = \left[ \frac{\sin(\frac{\omega M}{2})}{\sin(\frac{\omega}{2})} \right] e^{-j\omega \frac{M-1}{2}} \Rightarrow W_r(\omega) = \frac{\sin(\frac{\omega M}{2})}{\sin(\frac{\omega}{2})}$$

which is the amplitude response. From (7.22), the actual amplitude response  $H_r(\omega)$  is given by

$$H_r(\omega) \simeq \frac{1}{2\pi} \int_{-\pi}^{\omega + \omega_c} W_r(\lambda) d\lambda = \frac{1}{2\pi} \int_{-\pi}^{\omega + \omega_c} \frac{\sin(\frac{\omega M}{2})}{\sin(\frac{\omega}{2})} d\lambda, \quad M \gg 1 \quad (7.24)$$

This implies that the running integral of the window amplitude response (or *integrated* amplitude response) is necessary in the accurate analysis of the transition bandwidth and the stopband attenuation. Figure 7.9 shows the rectangular window function  $w(n)$ , its amplitude response  $W(\omega)$ , the amplitude response in dB, and the integrated amplitude response (7.24) in dB. From the observation of plots in Figure 7.9, we can make several observations.

1. The amplitude response  $W_r(\omega)$  has the first zero at  $\omega = \omega_1$ , where

$$\frac{\omega_1 M}{2} = \pi \quad \text{or} \quad \omega_1 = \frac{2\pi}{M}$$

Hence the width of the main lobe is  $2\omega_1 = 4\pi/M$ . Therefore, the *approximate transition bandwidth* is  $4\pi/M$ .

2. The magnitude of the first side lobe (which is also the peak side-lobe magnitude) is approximately at  $\omega = 3\pi/M$  and is given by

$$\left| W_r \left( \omega = \frac{3\pi}{M} \right) \right| = \left| \frac{\sin(\frac{3\pi}{2})}{\sin(\frac{3\pi}{2M})} \right| \simeq \frac{2M}{3\pi} \quad \text{for } M \gg 1$$

Comparing this with the main-lobe amplitude, which is equal to  $M$ , the *peak side-lobe magnitude* is

$$\frac{2}{3\pi} = 21.22\% \equiv 13 \text{ dB}$$

below the main-lobe magnitude of 0 dB.

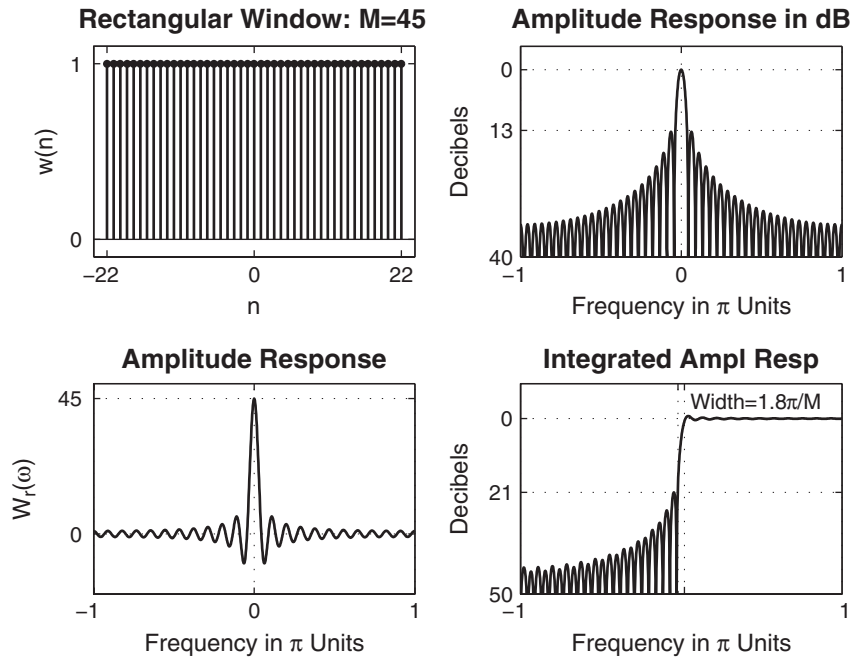


**FIGURE 7.9** Rectangular window:  $M = 45$

3. The integrated amplitude response has the first side-lobe magnitude at 21 dB. This results in the *minimum stopband attenuation* of 21 dB irrespective of the window length  $M$ .
4. Using the minimum stopband attenuation, the transition bandwidth can be accurately computed. It is shown in the accumulated amplitude response plot in Figure 7.9. This computed *exact transition bandwidth* is

$$\omega_s - \omega_p = \frac{1.8\pi}{M}$$

which is less than half the approximate bandwidth of  $4\pi/M$ .

Clearly, this is a simple window operation in the time domain and an easy function to analyze in the frequency domain. However, there are two main problems. First, the minimum stopband attenuation of 21 dB is insufficient in practical applications. Second, the rectangular windowing being a direct truncation of the infinite length  $h_d(n)$ , it suffers from the *Gibbs phenomenon*. If we increase  $M$ , the width of each side lobe will decrease, but the area under each lobe will remain constant. Therefore, the *relative amplitudes* of side lobes will remain constant, and the minimum stopband attenuation will remain at 21 dB. This implies that all ripples will bunch up near the band edges. This is shown in Figure 7.10.

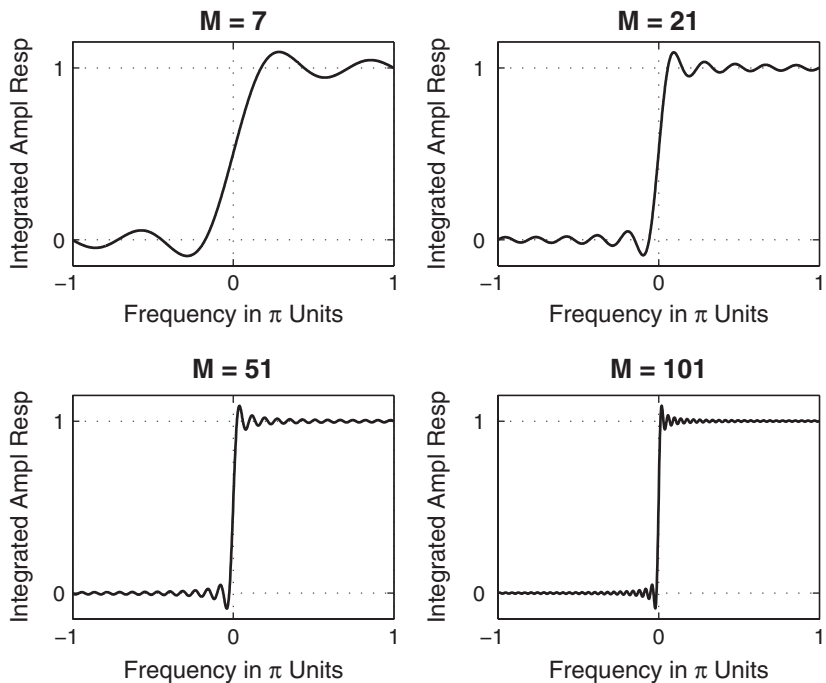


**FIGURE 7.10** Gibbs phenomenon

Since the rectangular window is impractical in many applications, we consider other fixed window functions that provide a fixed amount of attenuation. These window functions bear the names of the people who first proposed them. Although these window functions can also be analyzed similar to the rectangular window, we present their results using MATLAB simulations.

### 7.3.2 BARTLETT WINDOW

Since the Gibbs phenomenon results from the fact that the rectangular window has a sudden transition from 0 to 1 (or 1 to 0), Bartlett suggested a more gradual transition in the form of a triangular window, which is given by

$$w(n) = \begin{cases} \frac{2n}{M-1}, & 0 \leq n \leq \frac{M-1}{2} \\ 2 - \frac{2n}{M-1}, & \frac{M-1}{2} \leq n \leq M-1 \\ 0, & \text{otherwise} \end{cases} \quad (7.25)$$

This window and its frequency-domain responses are shown in Figure 7.11.

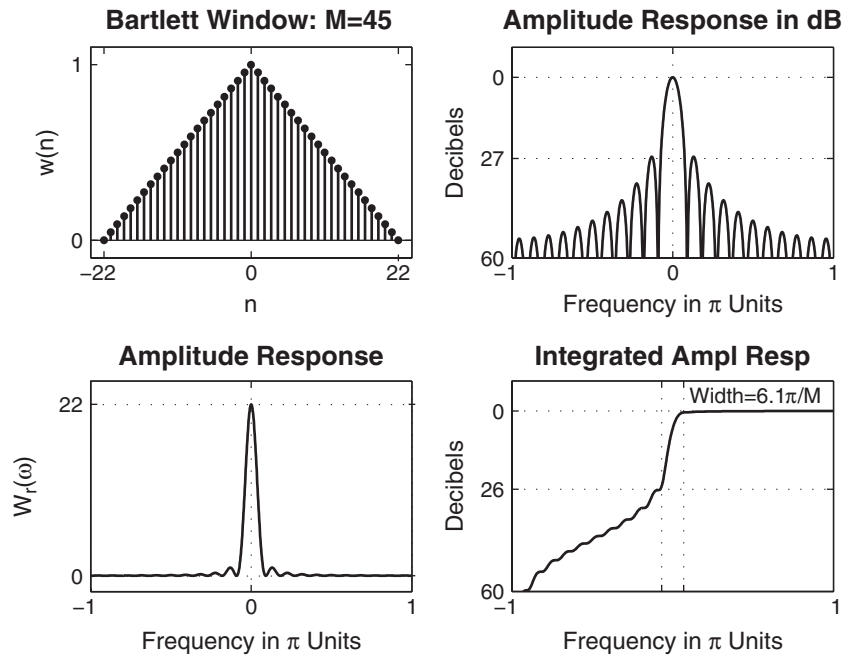


**FIGURE 7.11** Bartlett window:  $M = 45$

### 7.3.3 HANN WINDOW

This is a raised cosine window function given by

$$w(n) = \begin{cases} 0.5 \left[ 1 - \cos \left( \frac{2\pi n}{M-1} \right) \right], & 0 \leq n \leq M-1 \\ 0, & \text{otherwise} \end{cases} \quad (7.26)$$

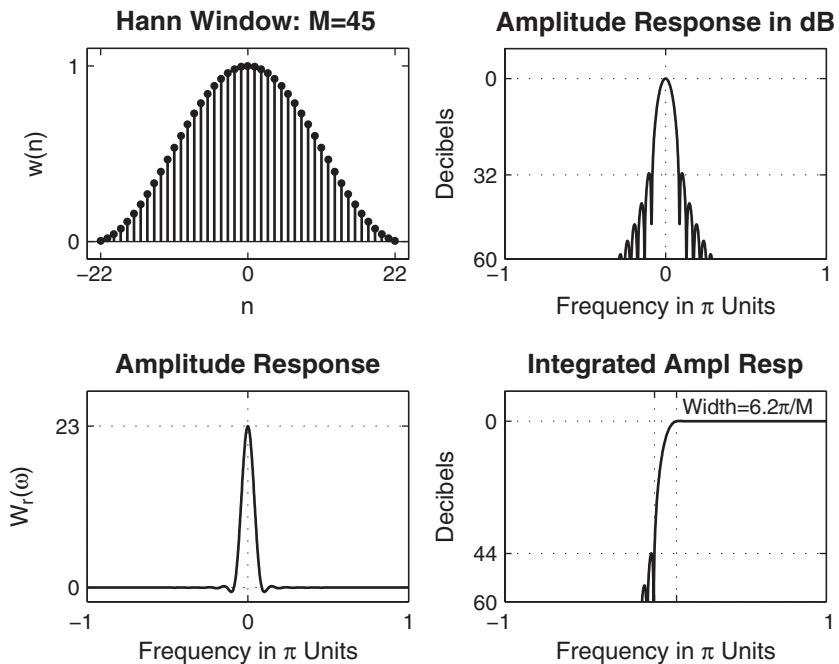
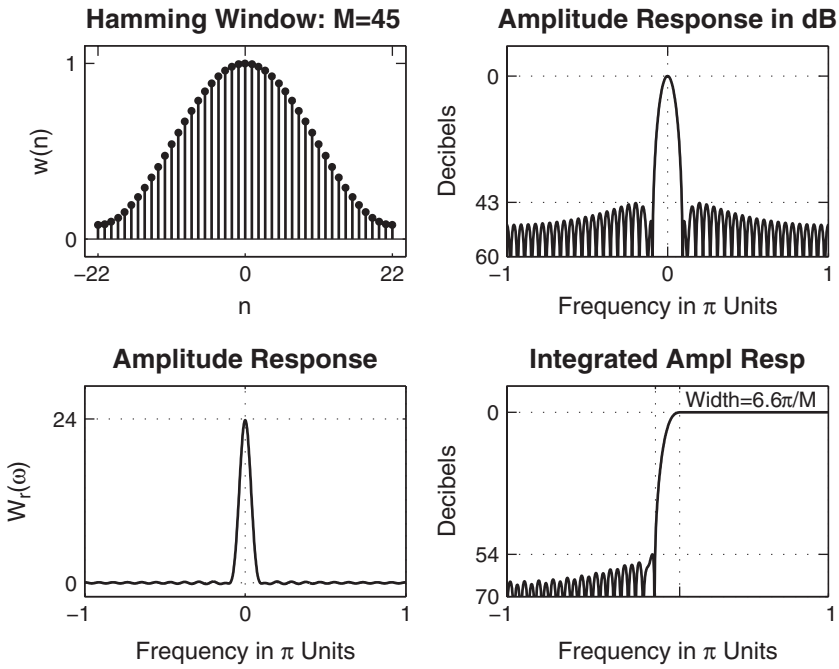
This window and its frequency-domain responses are shown in Figure 7.12.

### 7.3.4 HAMMING WINDOW

This window is similar to the Hann window except that it has a small amount of discontinuity and is given by

$$w(n) = \begin{cases} 0.54 - 0.46 \cos \left( \frac{2\pi n}{M-1} \right), & 0 \leq n \leq M-1 \\ 0, & \text{otherwise} \end{cases} \quad (7.27)$$

This window and its frequency-domain responses are shown in Figure 7.13.

FIGURE 7.12 *Hann window:  $M = 45$* FIGURE 7.13 *Hamming window:  $M = 45$*

### 7.3.5 BLACKMAN WINDOW

This window is also similar to the previous two but contains a second harmonic term and is given by

$$w(n) = \begin{cases} 0.42 - 0.5 \cos\left(\frac{2\pi n}{M-1}\right) + 0.08 \cos\left(\frac{4\pi n}{M-1}\right), & 0 \leq n \leq M-1 \\ 0, & \text{otherwise} \end{cases} \quad (7.28)$$

This window and its frequency-domain responses are shown in Figure 7.14.

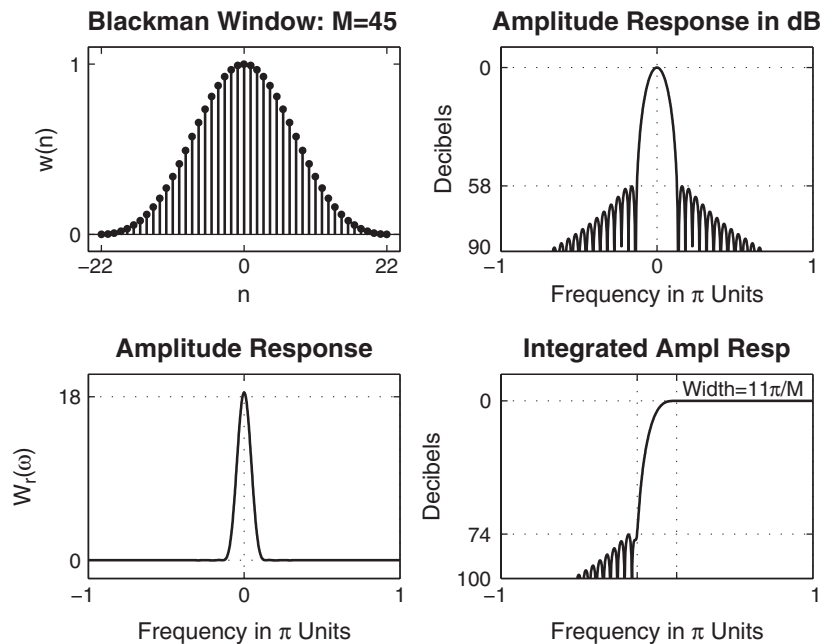


**FIGURE 7.14** Blackman window:  $M = 45$

In Table 7.1, we provide a summary of fixed window function characteristics in terms of their transition widths (as a function of  $M$ ) and their minimum stopband attenuations in dB. Both the approximate as well as the exact transition bandwidths are given. Note that the transition widths and the stopband attenuations increase as we go down the table. The Hamming window appears to be the best choice for many applications.

### 7.3.6 KAISER WINDOW

This is an adjustable window function that is widely used in practice. The window function is due to J.F. Kaiser and is given by

$$w(n) = \frac{I_0 \left[ \beta \sqrt{1 - (1 - \frac{2n}{M-1})^2} \right]}{I_0 [\beta]}, \quad 0 \leq n \leq M-1 \quad (7.29)$$

**TABLE 7.1** Summary of commonly used window function characteristics

Window Name	Transition Approximate	Width $\Delta\omega$ Exact Values	Min. Stopband Attenuation
Rectangular	$\frac{4\pi}{M}$	$\frac{1.8\pi}{M}$	21 dB
Bartlett	$\frac{8\pi}{M}$	$\frac{6.1\pi}{M}$	25 dB
Hann	$\frac{8\pi}{M}$	$\frac{6.2\pi}{M}$	44 dB
Hamming	$\frac{8\pi}{M}$	$\frac{6.6\pi}{M}$	53 dB
Blackman	$\frac{12\pi}{M}$	$\frac{11\pi}{M}$	74 dB

where  $I_0[\cdot]$  is the *modified zero-order Bessel* function given by

$$I_0(x) = 1 + \sum_{k=0}^{\infty} \left[ \frac{(x/2)^k}{k!} \right]^2$$

which is positive for all real values of  $x$ . The parameter  $\beta$  controls the minimum stopband attenuation  $A_s$  and can be chosen to yield different transition widths for near-optimum  $A_s$ . This window can provide different transition widths for the same  $M$ , which is something other fixed windows lack. For example:

- If  $\beta = 5.658$ , then the transition width is equal to  $7.8\pi/M$ , and the minimum stopband attenuation is equal to 60 dB. This is shown in Figure 7.15.
- If  $\beta = 4.538$ , then the transition width is equal to  $5.8\pi/M$ , and the minimum stopband attenuation is equal to 50 dB.

Hence the performance of this window is comparable to that of the Hamming window. In addition, the Kaiser window provides flexible transition bandwidths. Due to the complexity involved in the Bessel functions, the design equations for this window are not easy to derive. Fortunately, Kaiser has developed *empirical* design equations, which we provide here without proof. Given  $\omega_p$ ,  $\omega_s$ ,  $R_p$ , and  $A_s$ , the parameters  $M$  and  $\beta$  are given by

$$\text{Transition width} = \Delta\omega = \omega_s - \omega_p \quad (7.30a)$$

$$\text{Filter length } M \simeq \frac{A_s - 7.95}{2.285\Delta\omega} + 1 \quad (7.30b)$$

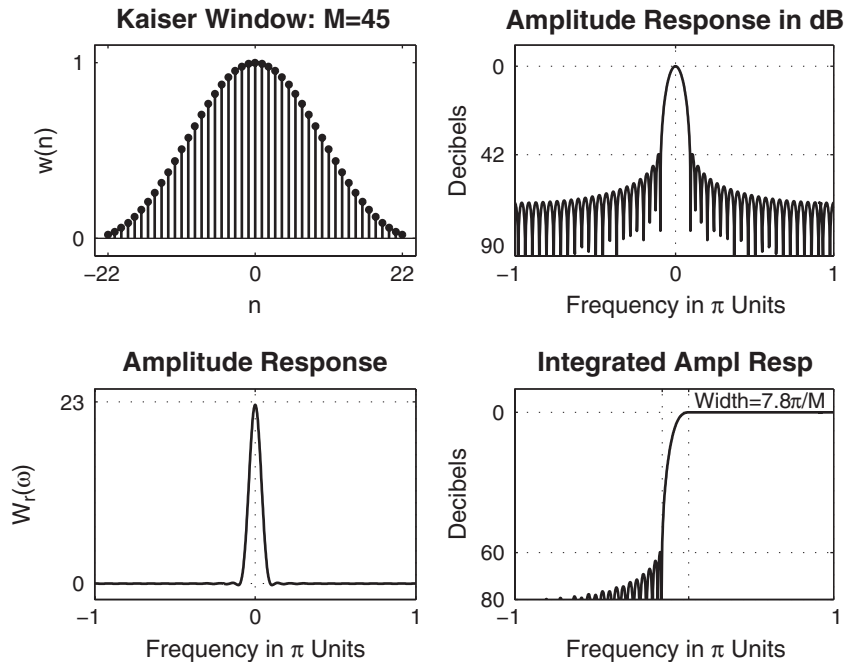


**FIGURE 7.15** Kaiser window:  $M = 45$ ,  $\beta = 5.658$

$$\text{Parameter } \beta = \begin{cases} 0.1102(A_s - 8.7), & A_s \geq 50 \\ 0.5842(A_s - 21)^{0.4} \\ + 0.07886(A_s - 21), & 21 < A_s < 50 \end{cases} \quad (7.30c)$$

### 7.3.7 MATLAB IMPLEMENTATION

MATLAB provides several functions to implement window functions discussed in this section. A brief description of these functions follow.

- `w=boxcar(M)` returns the  $M$ -point rectangular window function in array `w`.
- `w=bartlett(M)` returns the  $M$ -point Bartlett window function in array `w`.
- `w=hann(M)` returns the  $M$ -point Hann window function in array `w`.
- `w=hamming(M)` returns the  $M$ -point Hamming window function in array `w`.
- `w=blackman(M)` returns the  $M$ -point Blackman window function in array `w`.
- `w=kaiser(M,beta)` returns the `beta`-valued  $M$ -point rectangular window function in array `w`.

Using these functions, we can use MATLAB to design FIR filters based on the window technique, which also requires an ideal lowpass impulse response  $h_d(n)$ . Therefore, it is convenient to have a simple routine that creates  $h_d(n)$  as shown here.

```
function hd = ideal_lp(wc,M);
% Ideal lowpass filter computation
%
% [hd] = ideal_lp(wc,M)
%   hd = ideal impulse response between 0 to M-1
%   wc = cutoff frequency in radians
%   M = length of the ideal filter
%
alpha = (M-1)/2; n = [0:1:(M-1)];
m = n - alpha; fc = wc/pi; hd = fc*sinc(fc*m);
```

To display the frequency-domain plots of digital filters, MATLAB provides the `freqz` function, which we used in earlier chapters. Using this function, we have developed a modified version, called `freqz_m`, which returns the magnitude response in absolute as well as in relative dB scale, the phase response, and the group delay response. We will need the group delay response in the next chapter.

```
function [db,mag,pha,grd,w] = freqz_m(b,a);
% Modified version of freqz subroutine
%
% [db,mag,pha,grd,w] = freqz_m(b,a);
%   db = relative magnitude in dB computed over 0 to pi radians
%   mag = absolute magnitude computed over 0 to pi radians
%   pha = phase response in radians over 0 to pi radians
%   grd = group delay over 0 to pi radians
%   w = 501 frequency samples between 0 to pi radians
%   b = numerator polynomial of H(z) (for FIR: b=h)
%   a = denominator polynomial of H(z) (for FIR: a=[1])
%
[H,w] = freqz(b,a,1000,'whole');
H = (H(1:1:501))'; w = (w(1:1:501))';
mag = abs(H); db = 20*log10((mag+eps)/max(mag));
pha = angle(H); grd = grpdelay(b,a,w);
```

### 7.3.8 DESIGN EXAMPLES

We now provide several examples of FIR filter design using window techniques and MATLAB functions.

- EXAMPLE 7.8** Design a digital FIR lowpass filter with the following specifications:

$$\omega_p = 0.2\pi, \quad R_p = 0.25 \text{ dB}$$

$$\omega_s = 0.3\pi, \quad A_s = 50 \text{ dB}$$

Choose an appropriate window function from Table 7.1. Determine the impulse response and provide a plot of the frequency response of the designed filter.

**Solution**

Both the Hamming and Blackman windows can provide attenuation of more than 50 dB. Let us choose the Hamming window, which provides the smaller transition band and hence has the smaller order. Although we do not use the passband ripple value of  $R_p = 0.25$  dB in the design, we will have to check the actual ripple from the design and verify that it is indeed within the given tolerance. The design steps are given in the following MATLAB script.

```
>> wp = 0.2*pi; ws = 0.3*pi; tr_width = ws - wp;
>> M = ceil(6.6*pi/tr_width) + 1
M = 67
>> n=[0:1:M-1];
>> wc = (ws+wp)/2, % Ideal LPF cutoff frequency
>> hd = ideal_lp(wc,M); w_ham = (hamming(M))'; h = hd .* w_ham;
>> [db,mag,pha,grd,w] = freqz_m(h,[1]); delta_w = 2*pi/1000;
>> Rp = -(min(db(1:1:wp/delta_w+1))); % Actual passband ripple
Rp = 0.0394
>> As = -round(max(db(ws/delta_w+1:1:501))) % Min stopband attenuation
As = 52
% plotting commands follow
```

Note that the filter length is  $M = 67$ , the actual stopband attenuation is 52 dB, and the actual passband ripple is 0.0394 dB. Clearly, the passband ripple is satisfied by this design. This practice of verifying the passband ripple is strongly recommended. The time- and the frequency-domain plots are shown in Figure 7.16.  $\square$

- EXAMPLE 7.9** For the design specifications given in Example 7.8, choose the Kaiser window to design the necessary lowpass filter.

**Solution**

The design steps are given in the following MATLAB script.

```
>> wp = 0.2*pi; ws = 0.3*pi; As = 50; tr_width = ws - wp;
>> M = ceil((As-7.95)/(2.285*tr_width)+1) + 1
M = 61
>> n=[0:1:M-1]; beta = 0.1102*(As-8.7)
beta = 4.5513
>> wc = (ws+wp)/2; hd = ideal_lp(wc,M);
>> w_kai = (kaiser(M,beta))'; h = hd .* w_kai;
>> [db,mag,pha,grd,w] = freqz_m(h,[1]); delta_w = 2*pi/1000;
>> As = -round(max(db(ws/delta_w+1:1:501))) % Min stopband attenuation
As = 52
% plotting commands follow
```

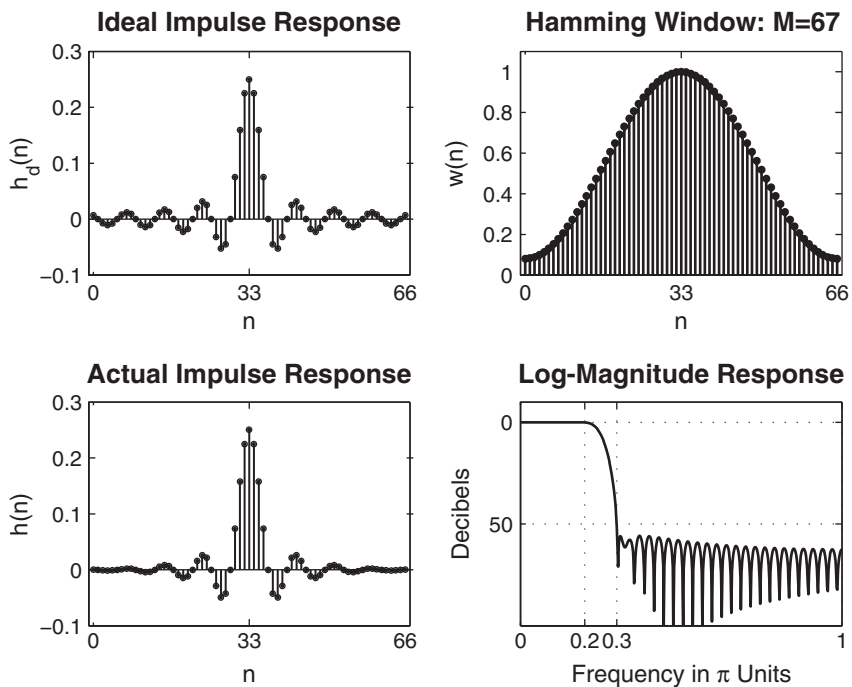


**FIGURE 7.16** Lowpass filter plots for Example 7.8

Note that the Kaiser window parameters are  $M = 61$  and  $\beta = 4.5513$  and that the actual stopband attenuation is 52 dB. The time- and the frequency-domain plots are shown in Figure 7.17.  $\square$

**EXAMPLE 7.10** Let us design the following digital bandpass filter.

lower stopband edge:  $\omega_{1s} = 0.2\pi$ ,  $A_s = 60$  dB

lower passband edge:  $\omega_{1p} = 0.35\pi$ ,  $R_p = 1$  dB

upper passband edge:  $\omega_{2p} = 0.65\pi$   $R_p = 1$  dB

upper stopband edge:  $\omega_{2s} = 0.8\pi$   $A_s = 60$  dB

These quantities are shown in Figure 7.18.

### Solution

There are two transition bands, namely,  $\Delta\omega_1 \triangleq \omega_{1p} - \omega_{1s}$  and  $\Delta\omega_2 \triangleq \omega_{2s} - \omega_{2p}$ . These two bandwidths must be the same in the window design; that is, there is no independent control over  $\Delta\omega_1$  and  $\Delta\omega_2$ . Hence  $\Delta\omega_1 = \Delta\omega_2 = \Delta\omega$ . For this design, we can use either the Kaiser window or the Blackman window. Let us

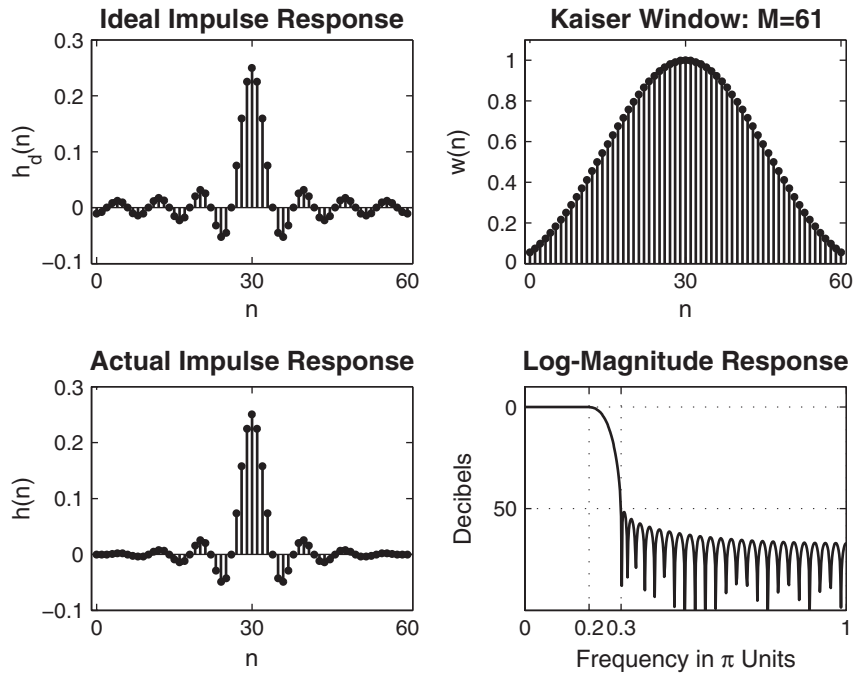


**FIGURE 7.17** Lowpass filter plots for Example 7.9

use the Blackman Window. We will also need the ideal bandpass filter impulse response  $h_d(n)$ . Note that this impulse response can be obtained from two ideal lowpass magnitude responses, provided they have the same phase response. This is shown in Figure 7.19. Therefore, the MATLAB routine `ideal_bp(wc,M)` is sufficient to determine the impulse response of an ideal bandpass filter. The design steps are given in the following MATLAB script.

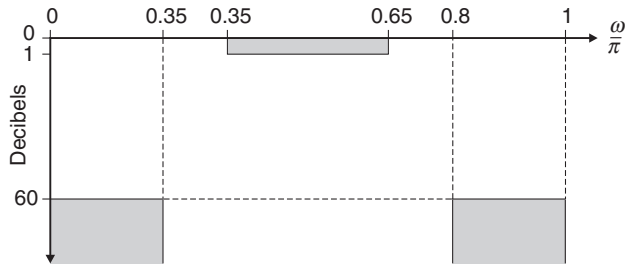


**FIGURE 7.18** Bandpass filter specifications in Example 7.10

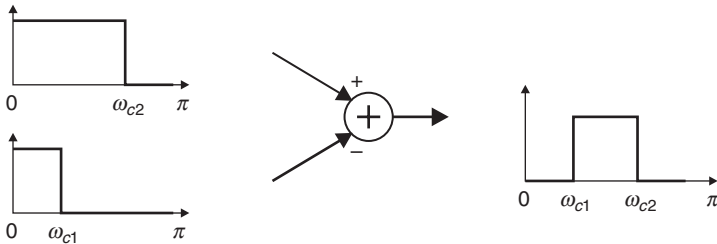


**FIGURE 7.19** Ideal bandpass filter from two lowpass filters

```

>> ws1 = 0.2*pi; wp1 = 0.35*pi; wp2 = 0.65*pi; ws2 = 0.8*pi; As = 60;
>> tr_width = min((wp1-ws1),(ws2-wp2)); M = ceil(11*pi/tr_width) + 1
M = 75
>> n=[0:1:M-1]; wc1 = (ws1+wp1)/2; wc2 = (wp2+ws2)/2;
>> hd = ideal_lp(wc2,M) - ideal_lp(wc1,M);
>> w_bla = (blackman(M))'; h = hd .* w_bla;
>> [db,mag,pha,grd,w] = freqz_m(h,[1]); delta_w = 2*pi/1000;
>> Rp = -min(db(wp1/delta_w+1:1:wp2/delta_w)) % Actual passband ripple
Rp = 0.0030
>> As = -round(max(db(ws2/delta_w+1:1:501))) % Min stopband attenuation
As = 75
% plotting commands follow

```

Note that the Blackman window length is  $M = 75$  and that the actual stopband attenuation is 75 dB. The time- and the frequency-domain plots are shown in Figure 7.20.  $\square$

- **EXAMPLE 7.11** The frequency response of an ideal bandstop filter is given by

$$H_e(e^{j\omega}) = \begin{cases} 1, & 0 \leq |\omega| < \pi/3 \\ 0, & \pi/3 \leq |\omega| \leq 2\pi/3 \\ 1, & 2\pi/3 < |\omega| \leq \pi \end{cases}$$

Using a Kaiser window, design a bandstop filter of length 45 with stopband attenuation of 60 dB.

### Solution

Note that in these design specifications, the transition bandwidth is not given. It will be determined by the length  $M = 45$  and the parameter  $\beta$  of the Kaiser window. From the design equations (7.30b), we can determine  $\beta$  from  $A_s$ ; that is,

$$\beta = 0.1102 \times (A_s - 8.7)$$

The ideal bandstop impulse response can also be determined from the ideal lowpass impulse response using a method similar to Figure 7.19. We can now

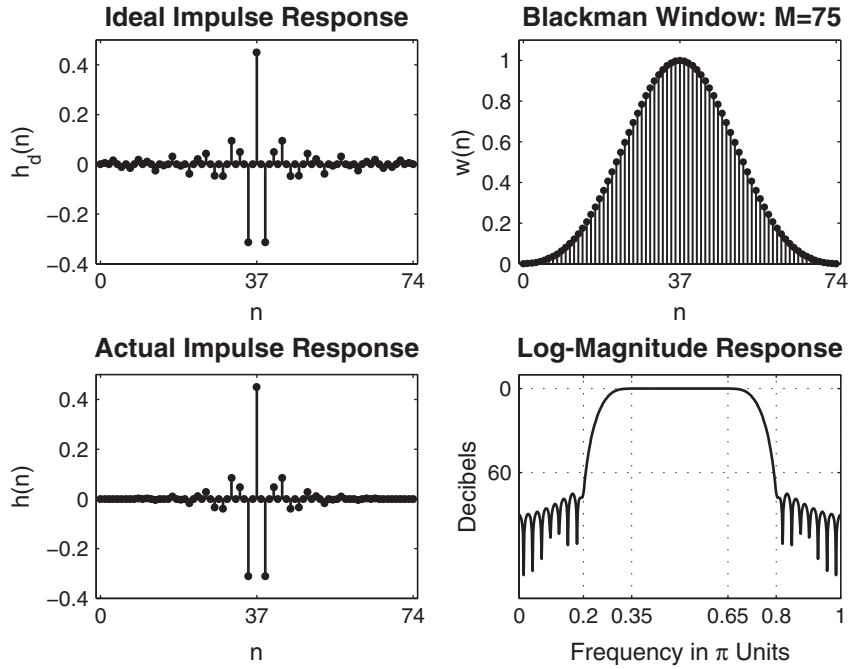


**FIGURE 7.20** Bandpass filter plots in Example 7.10

implement the Kaiser window design and check for the minimum stopband attenuation. This is shown in the following MATLAB script.

```
>> M = 45; As = 60; n=[0:1:M-1];
>> beta = 0.1102*(As-8.7)
beta = 5.6533
>> w_kai = (kaiser(M,beta))'; wc1 = pi/3; wc2 = 2*pi/3;
>> hd = ideal_lp(wc1,M) + ideal_lp(pi,M) - ideal_lp(wc2,M);
>> h = hd .* w_kai; [db,mag,pha,grd,w] = freqz_m(h,[1]);
```

The  $\beta$  parameter is equal to 5.6533, and, from the magnitude plot in Figure 7.21, we observe that the minimum stopband attenuation is smaller than 60 dB. Clearly, we have to increase  $\beta$  to increase the attenuation to 60 dB. The required value was found to be  $\beta = 5.9533$ .

```
>> M = 45; As = 60; n=[0:1:M-1];
>> beta = 0.1102*(As-8.7)+0.3
beta = 5.9533
>> w_kai = (kaiser(M,beta))'; wc1 = pi/3; wc2 = 2*pi/3;
>> hd = ideal_lp(wc1,M) + ideal_lp(pi,M) - ideal_lp(wc2,M);
>> h = hd .* w_kai; [db,mag,pha,grd,w] = freqz_m(h,[1]);
>> plotting commands follow
```

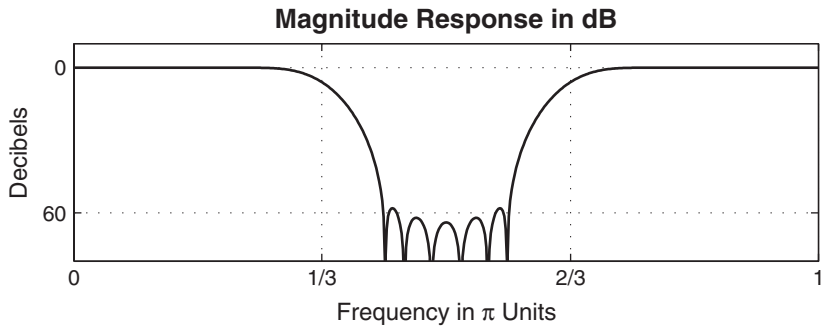


**FIGURE 7.21** Bandstop filter magnitude response in Example 7.11 for  $\beta = 5.6533$

The time- and the frequency-domain plots are shown in Figure 7.22, in which the designed filter satisfies the necessary requirements.  $\square$

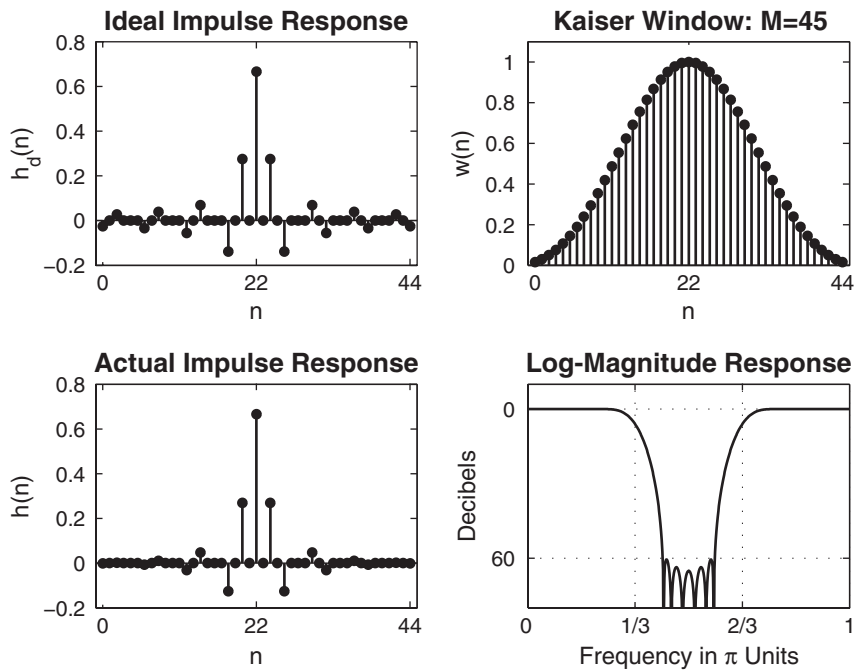


**FIGURE 7.22** Bandstop filter plots in Example 7.11:  $\beta = 5.9533$

$\square$  **EXAMPLE 7.12** The frequency response of an ideal digital differentiator is given by

$$H_d(e^{j\omega}) = \begin{cases} j\omega, & 0 < \omega \leq \pi \\ -j\omega, & -\pi < \omega < 0 \end{cases} \quad (7.31)$$

Using a Hamming window of length 21, design a digital FIR differentiator. Plot the time- and the frequency-domain responses.

**Solution**

The ideal impulse response of a digital differentiator with linear phase is given by

$$\begin{aligned} h_d(n) &= \mathcal{F}[H_d(e^{j\omega})e^{-j\alpha\omega}] = \frac{1}{2\pi} \int_{-\pi}^{\pi} H_d(e^{j\omega})e^{-j\alpha\omega} e^{j\omega n} d\omega \\ &= \frac{1}{2\pi} \int_{-\pi}^0 (-j\omega) e^{-j\alpha\omega} e^{j\omega n} d\omega + \frac{1}{2\pi} \int_0^{\pi} (j\omega) e^{-j\alpha\omega} e^{j\omega n} d\omega \\ &= \begin{cases} \frac{\cos \pi(n - \alpha)}{(n - \alpha)}, & n \neq \alpha \\ 0, & n = \alpha \end{cases} \end{aligned}$$

This impulse response can be implemented in MATLAB, along with the Hamming window to design the required differentiator. Note that if  $M$  is an even number, then  $\alpha = (M - 1)/2$  is not an integer and  $h_d(n)$  will be zero for all  $n$ . Hence  $M$  must be an odd number, and this will be a Type-3 linear-phase FIR filter. However, the filter will not be a full-band differentiator, since  $H_r(\pi) = 0$  for Type-3 filters.

```
>> M = 21; alpha = (M-1)/2; n = 0:M-1;
>> hd = (cos(pi*(n-alpha)))./(n-alpha); hd(alpha+1)=0;
>> w_ham = (hamming(M))';
h = hd .* w_ham; [Hr,w,P,L] = Hr_Type3(h);
% plotting commands follow
```

The plots are shown in Figure 7.23. □

□ **EXAMPLE 7.13** Design a length-25 digital Hilbert transformer using a Hann window.

**Solution**

The ideal frequency response of a linear-phase Hilbert transformer is given by

$$H_d(e^{j\omega}) = \begin{cases} -je^{-j\alpha\omega}, & 0 < \omega < \pi \\ +je^{-j\alpha\omega}, & -\pi < \omega < 0 \end{cases} \quad (7.32)$$

After inverse transformation, the ideal impulse response is given by

$$h_d(n) = \begin{cases} \frac{2 \sin^2 \pi(n - \alpha)/2}{\pi(n - \alpha)}, & n \neq \alpha \\ 0, & n = \alpha \end{cases}$$

which can be easily implemented in MATLAB. Note that since  $M = 25$ , the designed filter is of Type-3.

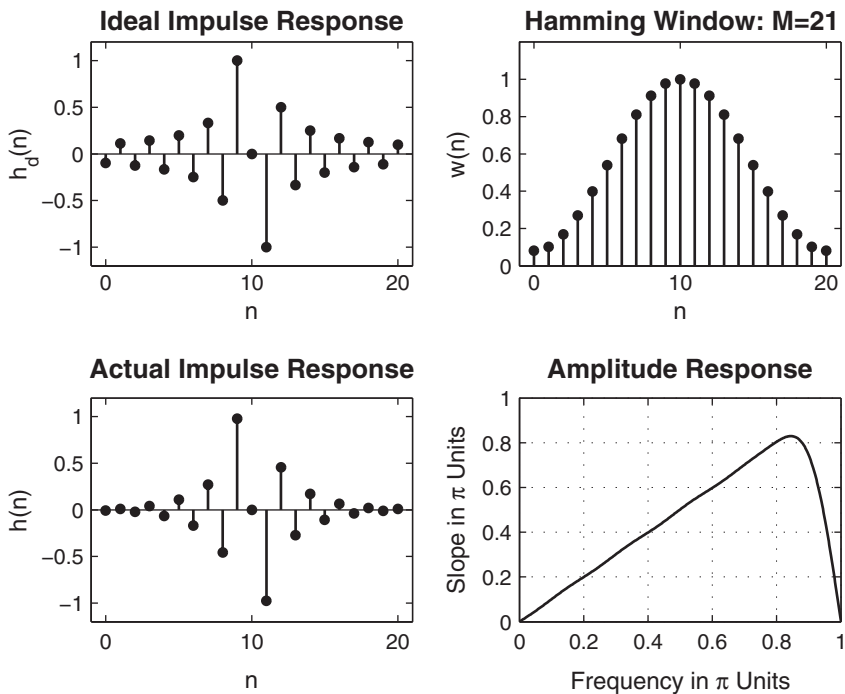


**FIGURE 7.23** FIR differentiator design in Example 7.12

MATLAB script:

```
>> M = 25; alpha = (M-1)/2; n = 0:M-1;
>> hd = (2/pi)*((sin(pi/2)*(n-alpha)).^2)./(n-alpha); hd(alpha+1)=0;
>> w_han = (hann(M))';
>> h = hd .* w_han; [Hr,w,P,L] = Hr_Type3(h);
>> plotting commands follow
```

The plots are shown in Figure 7.24. Observe that the amplitude response is plotted over  $-\pi \leq \omega \leq \pi$ .  $\square$

The SP toolbox provides a function called **fir1**, which designs conventional lowpass, highpass, and other multiband FIR filters using the window technique. This function's syntax has several forms, including:

- **$h = \text{fir1}(N, wc)$**  designs an  $N$ th-order ( $N = M - 1$ ) lowpass FIR filter and returns the impulse response in vector  $h$ . By default this is a Hamming-window based, linear-phase design with a normalized cutoff frequency in  $wc$  that is a number between 0 and 1, where 1 corresponds to  $\pi$  rad/sample. If  $wc$  is a two-element vector, that is,

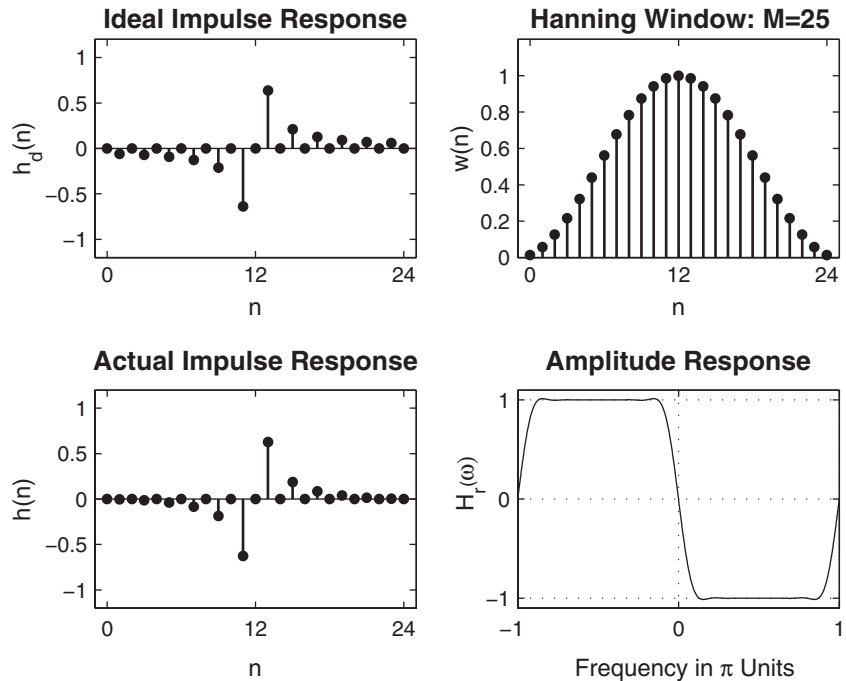


**FIGURE 7.24** FIR Hilbert transformer design in Example 7.13

`wc = [wc1 wc2]`, then `fir1` returns a bandpass filter with passband cutoffs `wc1` and `wc2`. If `wc` is a multi-element (more than two) vector, then `fir1` returns a multiband filter with cutoffs given in `wc`.

- `h = fir1(N,wc,'ftype')` specifies a filter type, where '`ftype`' is:
  - a. '`high`' for a highpass filter with cutoff frequency `Wn`.
  - b. '`stop`' for a bandstop filter, if `Wc = [wc1 wc2]`. The stopband frequency range is specified by this interval.
  - c. '`DC-1`' to make the first band of a multiband filter a passband.
  - d. '`DC-0`' to make the first band of a multiband filter a stopband.
- `h = fir1(N,wc,'ftype',window)` or `h = fir1(N,wc,window)` uses the vector `window` of length `N+1` obtained from one of the specified MATLAB window functions. The default window function used is the Hamming window.

To design FIR filters using the Kaiser window, the SP toolbox provides the function `kaiserord`, which estimates window parameters that can be used in the `fir1` function. The basic syntax is

```
[N,wc,beta,ftype] = kaiserord(f,m,ripple);
```

The function computes the window order  $N$ , the cutoff frequency vector  $wc$ , parameter  $\beta$  in **beta**, and the filter type **ftype** as discussed. The vector **f** is a vector of normalized band edges and **m** is a vector specifying the desired amplitude on the bands defined by **f**. The length of **f** is twice the length of **m**, minus 2; that is, **f** does not contain 0 or 1. The vector **ripple** specifies tolerances in each band (not in decibels). Using the estimated parameters, the Kaiser window array can be computed and used in the **fir1** function.

To design FIR filters using window technique with arbitrary-shaped magnitude response, the SP toolbox provides the function **fir2**, which also incorporates the frequency-sampling technique. It is explained in the following section.

## 7.4 FREQUENCY-SAMPLING DESIGN TECHNIQUE

---

In this design approach, we use the fact that the system function  $H(z)$  can be obtained from the samples  $H(k)$  of the frequency response  $H(e^{j\omega})$ . Furthermore, this design technique fits nicely with the frequency-sampling structure that we discussed in Chapter 6. Let  $h(n)$  be the impulse response of an  $M$ -point FIR filter, let  $H(k)$  be its  $M$ -point DFT, and let  $H(z)$  be its system function. Then from (6.12), we have

$$H(z) = \sum_{n=0}^{M-1} h(n) z^{-n} = \frac{1 - z^{-M}}{M} \sum_{k=0}^{M-1} \frac{H(k)}{1 - z^{-1} e^{j2\pi k/M}} \quad (7.33)$$

and

$$H(e^{j\omega}) = \frac{1 - e^{-j\omega M}}{M} \sum_{k=0}^{M-1} \frac{H(k)}{1 - e^{-j\omega} e^{j2\pi k/M}} \quad (7.34)$$

with

$$H(k) = H\left(e^{j2\pi k/M}\right) = \begin{cases} H(0), & k = 0 \\ H^*(M-k), & k = 1, \dots, M-1 \end{cases}$$

For a linear-phase FIR filter, we have

$$h(n) = \pm h(M-1-n), \quad n = 0, 1, \dots, M-1$$

where the positive sign is for the Type-1 and Type-2 linear-phase filters, while the negative sign is for the Type-3 and Type-4 linear-phase filters. Then  $H(k)$  is given by

$$H(k) = H_r\left(\frac{2\pi k}{M}\right) e^{j\angle H(k)} \quad (7.35)$$

where

$$H_r\left(\frac{2\pi k}{M}\right) = \begin{cases} H_r(0), & k = 0 \\ H_r\left(\frac{2\pi(M-k)}{M}\right), & k = 1, \dots, M-1 \end{cases} \quad (7.36)$$

and

$$\angle H(k) = \begin{cases} -\left(\frac{M-1}{2}\right)\left(\frac{2\pi k}{M}\right), & k = 0, \dots, \left\lfloor \frac{M-1}{2} \right\rfloor \\ +\left(\frac{M-1}{2}\right)\frac{2\pi}{M}(M-k), & k = \left\lfloor \frac{M-1}{2} \right\rfloor + 1, \dots, M-1 \end{cases} \quad (\text{Type-1 \& -2}) \quad (7.37)$$

or

$$\angle H(k) = \begin{cases} \left(\pm\frac{\pi}{2}\right) - \left(\frac{M-1}{2}\right)\left(\frac{2\pi k}{M}\right), & k = 0, \dots, \left\lfloor \frac{M-1}{2} \right\rfloor \\ -\left(\pm\frac{\pi}{2}\right) + \left(\frac{M-1}{2}\right)\frac{2\pi}{M}(M-k), & k = \left\lfloor \frac{M-1}{2} \right\rfloor + 1, \dots, M-1 \end{cases} \quad (\text{Type-3 \& -4}) \quad (7.38)$$

Finally, we have

$$h(n) = \text{IDFT}[H(k)] \quad (7.39)$$

Note that several textbooks (e.g., [71, 79, 83]) provide explicit formulas to compute  $h(n)$ , given  $H(k)$ . We will use MATLAB's `ifft` function to compute  $h(n)$  from (7.39).

**Basic idea** Given an ideal filter  $H_d(e^{j\omega})$ , choose the filter length  $M$  and then sample  $H_d(e^{j\omega})$  at  $M$  equispaced frequencies between 0 and  $2\pi$ . The actual response  $H(e^{j\omega})$  is the interpolation of the samples  $H(k)$  given by (7.34). This is shown in Figure 7.25. The impulse response is given by (7.39). Similar steps apply to other frequency-selective filters. Furthermore, this idea can also be extended for approximating arbitrary frequency-domain specifications.

From Figure 7.25, we observe the following:

1. The approximation error—that is, the difference between the ideal and the actual response—is zero at the sampled frequencies.
2. The approximation error at all other frequencies depends on the shape of the ideal response; that is, the sharper the ideal response, the larger the approximation error.
3. The error is larger near the band edges and smaller within the band.

There are two design approaches. In the first approach, we use the basic idea literally and provide no constraints on the approximation error;

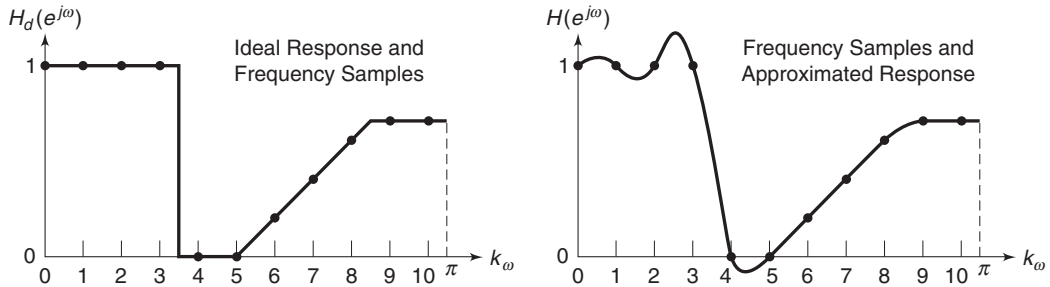


**FIGURE 7.25** Pictorial description of frequency-sampling technique

that is, we accept whatever error we get from the design. This approach is called a *naive design* method. In the second approach, we try to minimize error in the stopband by varying values of the transition band samples. It results in a much better design called an *optimum design* method.

#### 7.4.1 NAIVE DESIGN METHOD

In this method, we set  $H(k) = H_d(e^{j2\pi k/M})$ ,  $k = 0, \dots, M - 1$ , and use (7.35) through (7.39) to obtain the impulse response  $h(n)$ .

- **EXAMPLE 7.14** Consider the lowpass filter specifications from Example 7.8:

$$\omega_p = 0.2\pi, R_p = 0.25 \text{ dB}$$

$$\omega_s = 0.3\pi, A_s = 50 \text{ dB}$$

Design an FIR filter using the frequency-sampling approach.

#### Solution

Let us choose  $M = 20$  so that we have a frequency sample at  $\omega_p$ , that is, at  $k = 2$ ,

$$\omega_p = 0.2\pi = \frac{2\pi}{20}2$$

and the next sample at  $\omega_s$ , that is, at  $k = 3$ ,

$$\omega_s = 0.3\pi = \frac{2\pi}{20}3$$

Thus we have three samples in the passband  $[0 \leq \omega \leq \omega_p]$  and seven samples in the stopband  $[\omega_s \leq \omega \leq \pi]$ . From (7.36), we have

$$H_r(k) = [1, 1, 1, \underbrace{0, \dots, 0}_{15 \text{ zeros}}, 1, 1]$$

Since  $M = 20$ ,  $\alpha = \frac{20-1}{2} = 9.5$  and since this is a Type-2 linear-phase filter, from (7.37) we have

$$\angle H(k) = \begin{cases} -9.5 \frac{2\pi}{20} k = -0.95\pi k, & 0 \leq k \leq 9 \\ +0.95\pi(20-k), & 10 \leq k \leq 19 \end{cases}$$

Now, from (7.35), we assemble  $H(k)$  and from (7.39) determine the impulse response  $h(n)$ . The MATLAB script follows.

```
>> M = 20; alpha = (M-1)/2; l = 0:M-1; wl = (2*pi/M)*l;
>> Hrs = [1,1,1,zeros(1,15),1,1]; %Ideal amp res sampled
>> Hdr = [1,1,0,0]; wdl = [0,0.25,0.25,1]; %Ideal amp res for plotting
>> k1 = 0:floor((M-1)/2); k2 = floor((M-1)/2)+1:M-1;
>> angH = [-alpha*(2*pi)/M*k1, alpha*(2*pi)/M*(M-k2)];
>> H = Hrs.*exp(j*angH); h = real(ifft(H,M));
>> [db,mag,pha,grd,w] = freqz_m(h,1); [Hr,ww,a,L] = Hr_Type2(h);
>> plotting commands follow
```

The time- and the frequency-domain plots are shown in Figure 7.26. Observe that the minimum stopband attenuation is about 16 dB, which is clearly unacceptable. If we increase  $M$ , then there will be samples in the transition band, for which we do not precisely know the frequency response. Therefore, the naive design method is seldom used in practice.  $\square$

#### 7.4.2 OPTIMUM DESIGN METHOD

To obtain more attenuation, we will have to increase  $M$  and make the transition band samples free samples—that is, we vary their values to obtain the largest attenuation for the given  $M$  and the transition width. This problem is known as an optimization problem, and it is solved using linear programming techniques. We demonstrate the effect of transition band sample variation on the design using the following example.

- EXAMPLE 7.15** Using the optimum design method, design a better lowpass filter of Example 7.14.

**Solution**

Let us choose  $M = 40$  so that we have one sample in the transition band  $0.2\pi < \omega < 0.3\pi$ . Since  $\omega_1 \stackrel{\triangle}{=} 2\pi/40$ , the transition band samples are at  $k = 5$  and at  $k = 40 - 5 = 35$ . Let us denote the value of these samples by  $T_1$ ,  $0 < T_1 < 1$ ; then the sampled amplitude response is

$$H_r(k) = [1, 1, 1, 1, 1, T_1, \underbrace{0, \dots, 0}_{29 \text{ zeros}}, T_1, 1, 1, 1, 1]$$

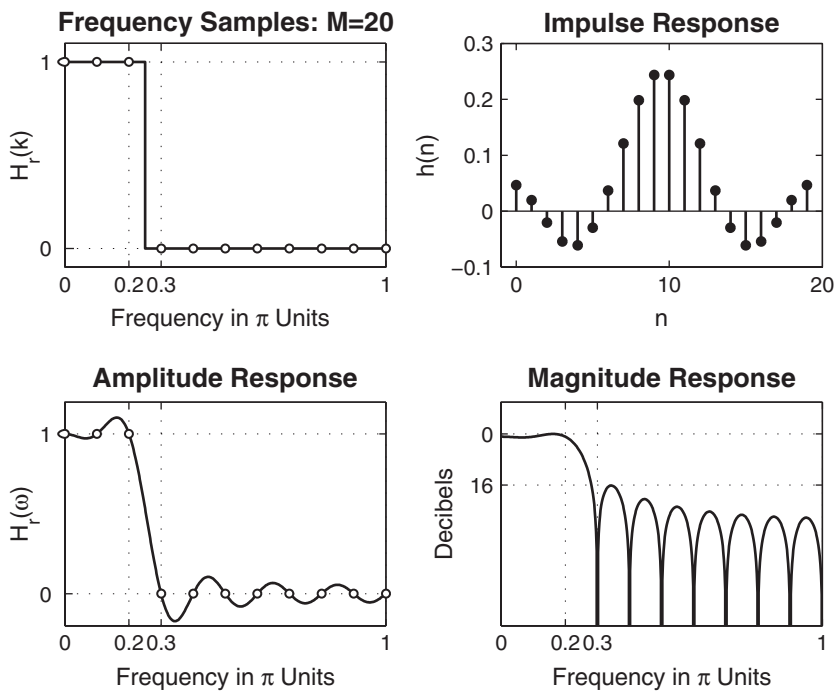


**FIGURE 7.26** Naive frequency sampling design method in Example 7.14

Since  $\alpha = \frac{40-1}{2} = 19.5$ , the samples of the phase response are

$$\angle H(k) = \begin{cases} -19.5 \frac{2\pi}{40} k = -0.975\pi k, & 0 \leq k \leq 19 \\ +0.975\pi(40-k), & 20 \leq k \leq 39 \end{cases}$$

Now we can vary  $T_1$  to get the best minimum stopband attenuation. This will result in the widening of the transition width. We first see what happens when  $T_1 = 0.5$  using the following MATLAB script.

```
% T1 = 0.5
>> M = 40; alpha = (M-1)/2;
>> Hrs = [ones(1,5),0.5,zeros(1,29),0.5,ones(1,4)];
>> k1 = 0:floor((M-1)/2); k2 = floor((M-1)/2)+1:M-1;
>> angH = [-alpha*(2*pi)/M*k1, alpha*(2*pi)/M*(M-k2)];
>> H = Hrs.*exp(j*angH);
>> h = real(ifft(H,M));
```

From the plots of this design in Figure 7.27, we observe that the minimum stopband attenuation is now 30 dB, which is better than the naive design attenuation but is still not at the acceptable level of 50 dB. The best value for  $T_1$

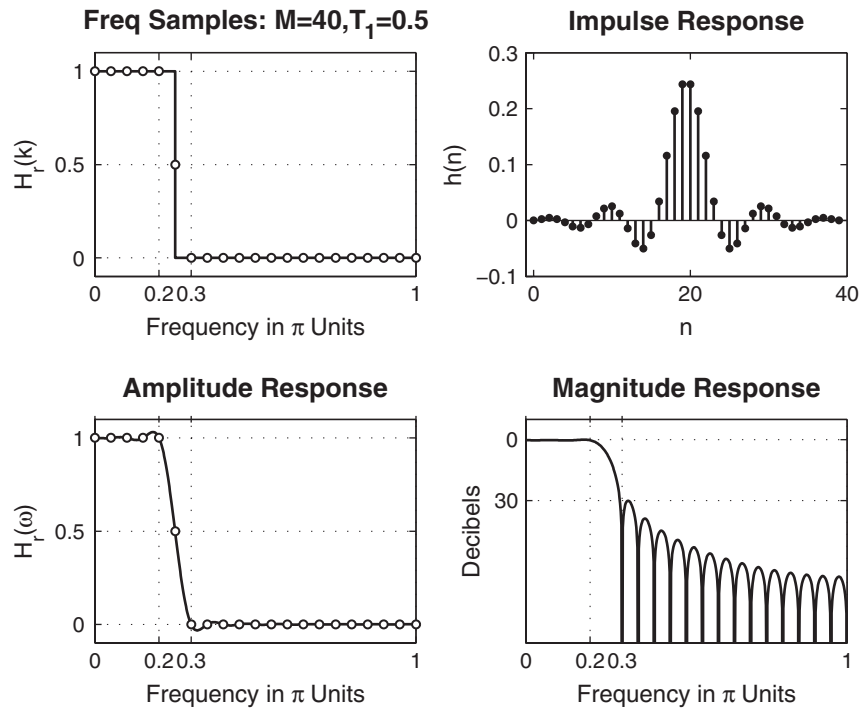


**FIGURE 7.27** Optimum frequency design method:  $T_1 = 0.5$  in Example 7.15

was obtained by varying it manually (although more efficient linear programming techniques are available, these were not used in this case), and the near optimum solution was found at  $T_1 = 0.39$ . The resulting filter is obtained using the following MATLAB script.

```
% T1 = 0.39
>> M = 40; alpha = (M-1)/2;
>> Hrs = [ones(1,5),0.39,zeros(1,29),0.39,ones(1,4)];
>> k1 = 0:floor((M-1)/2); k2 = floor((M-1)/2)+1:M-1;
>> angH = [-alpha*(2*pi)/M*k1, alpha*(2*pi)/M*(M-k2)];
>> H = Hrs.*exp(j*angH); h = real(ifft(H,M));
```

From the plots in Figure 7.28, we observe that the optimum stopband attenuation is 43 dB. It is obvious that to further increase the attenuation, we will have to vary more than one sample in the transition band.  $\square$

Clearly, this method is superior in that by varying one sample we can get a much better design. In practice, the transition bandwidth is

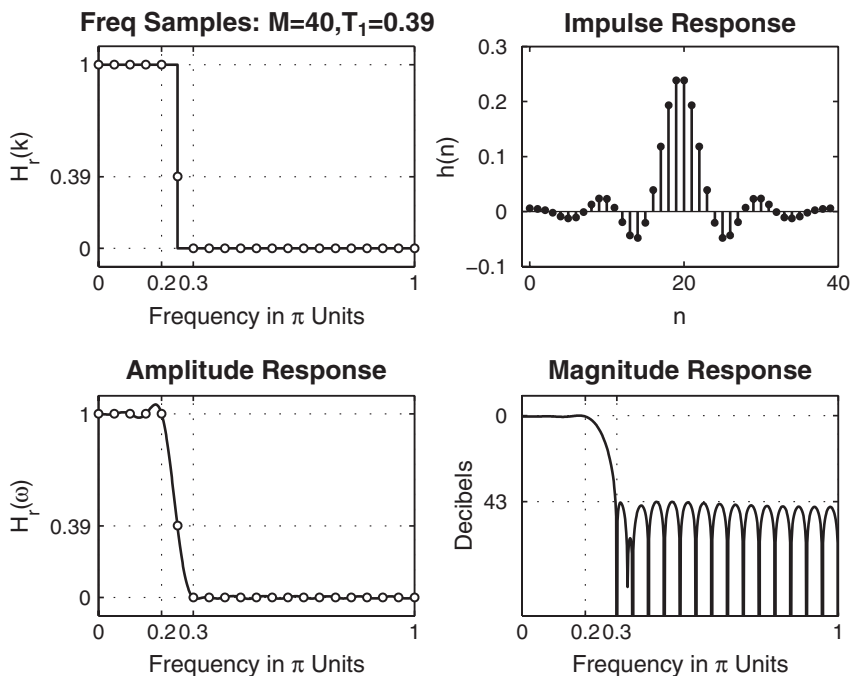


**FIGURE 7.28** Optimum frequency design method:  $T_1 = 0.39$  in Example 7.15

generally small, containing either one or two samples. Hence we need to optimize at most two samples to obtain the largest minimum stopband attenuation. This is also equivalent to minimizing the maximum side-lobe magnitudes in the absolute sense. Hence this optimization problem is also called a *minimax* problem. This problem is solved by Rabiner et al. [83], and the solution is available in the form of tables of transition values. A selected number of tables are also available in [79, Appendix B]. This problem can also be solved in MATLAB, but it would require the use of the Optimization toolbox. We will consider a more general version of this problem in the next section. We now illustrate the use of these tables in the following examples.

- **EXAMPLE 7.16** Let us revisit our lowpass filter design in Example 7.14. We will solve it using two samples in the transition band so that we can get a better stopband attenuation.

#### Solution

Let us choose  $M = 60$  so that there are two samples in the transition band. Let the values of these transition band samples be  $T_1$  and  $T_2$ . Then  $H_r(\omega)$  is given by

$$H(\omega) = [\underbrace{1, \dots, 1}_{7 \text{ ones}}, T_1, T_2, \underbrace{0, \dots, 0}_{43 \text{ zeros}}, T_2, T_1, \underbrace{1, \dots, 1}_{6 \text{ ones}}]$$

From tables in [79, Appendix B],  $T_1 = 0.5925$  and  $T_2 = 0.1099$ . Using these values, we use MATLAB to compute  $h(n)$ .

```
>> M = 60; alpha = (M-1)/2; l = 0:M-1; wl = (2*pi/M)*l;
>> Hrs = [ones(1,7),0.5925,0.1099,zeros(1,43),0.1099,0.5925,ones(1,6)];
>> Hdr = [1,1,0,0]; wdl = [0,0.2,0.3,1];
>> k1 = 0:floor((M-1)/2); k2 = floor((M-1)/2)+1:M-1;
>> angH = [-alpha*(2*pi)/M*k1, alpha*(2*pi)/M*(M-k2)];
>> H = Hrs.*exp(j*angH); h = real(ifft(H,M));
>> [db,mag,pha,grd,w] = freqz_m(h,1); [Hr,ww,a,L] = Hr_Type2(h);
```

The time- and the frequency-domain plots are shown in Figure 7.29. The minimum stopband attenuation is now at 63 dB, which is acceptable.  $\square$

- EXAMPLE 7.17** Design the bandpass filter of Example 7.10 using the frequency sampling technique. The design specifications are as follows.

lower stopband edge:  $\omega_{1s} = 0.2\pi$ ,  $A_s = 60$  dB

lower passband edge:  $\omega_{1p} = 0.35\pi$ ,  $R_p = 1$  dB

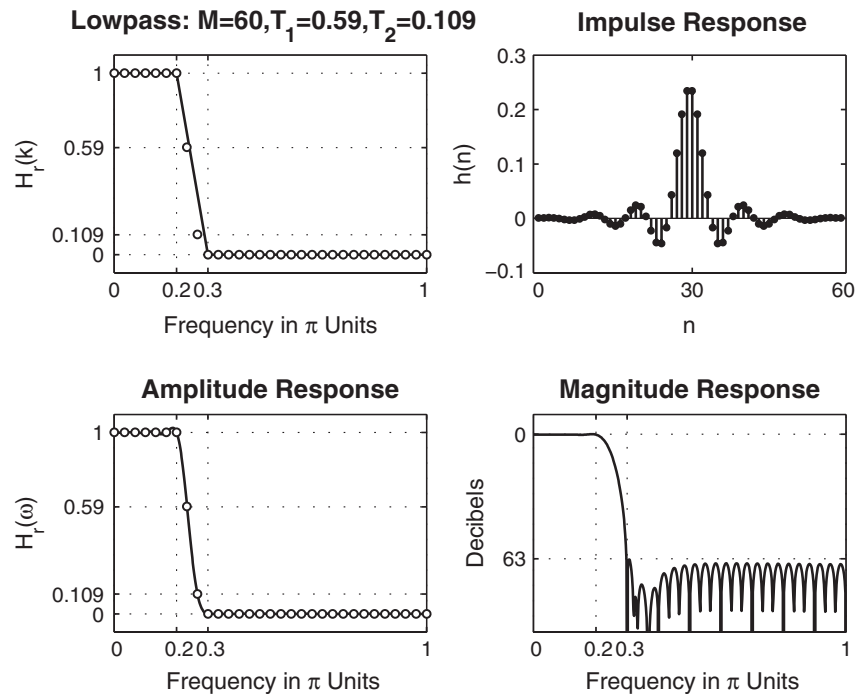


**FIGURE 7.29** Lowpass filter design plots in Example 7.16

upper passband edge:  $\omega_{2p} = 0.65\pi$   $R_p = 1$  dB

upper stopband edge:  $\omega_{2s} = 0.8\pi$   $A_s = 60$  dB

### Solution

Let us choose  $M = 40$  so that we have two samples in the transition band. Let the frequency samples in the lower transition band be  $T_1$  and  $T_2$ . Then the samples of the amplitude response are

$$H_r(\omega) = [0, \dots, 0, T_1, T_2, \underbrace{1, \dots, 1}_7, T_2, T_1, \underbrace{0, \dots, 0}_9, T_1, T_2, \underbrace{1, \dots, 1}_7, T_2, T_1, \underbrace{0, \dots, 0}_4]$$

The optimum values of  $T_1$  and  $T_2$  for  $M = 40$  and seven samples in the passband [79, Appendix B] are

$$T_1 = 0.109021, \quad T_2 = 0.59417456$$

MATLAB script:

```
>> M = 40; alpha = (M-1)/2; l = 0:M-1; wl = (2*pi/M)*l;
>> T1 = 0.109021; T2 = 0.59417456;
>> Hrs=[zeros(1,5),T1,T2,ones(1,7),T2,T1,zeros(1,9),T1,T2,ones(1,7),T2,T1,zeros(1,4)];
>> Hdr = [0,0,1,1,0,0]; wdl = [0,0.2,0.35,0.65,0.8,1];
>> k1 = 0:floor((M-1)/2); k2 = floor((M-1)/2)+1:M-1;
>> angH = [-alpha*(2*pi)/M*k1, alpha*(2*pi)/M*(M-k2)];
>> H = Hrs.*exp(j*angH); h = real(ifft(H,M));
>> [db,mag,pha,grd,w] = freqz_m(h,1); [Hr,ww,a,L] = Hr_Type2(h);
```

The plots in Figure 7.30 show an acceptable bandpass filter design. □

### □ EXAMPLE 7.18 Design the following highpass filter.

Stopband edge:  $\omega_s = 0.6\pi$   $A_s = 50$  dB

Passband edge:  $\omega_p = 0.8\pi$   $R_p = 1$  dB

### Solution

Recall that for a highpass filter  $M$  must be odd (or Type-1 filter). Hence we will choose  $M = 33$  to get two samples in the transition band. With this choice of  $M$  it is not possible to have frequency samples at  $\omega_s$  and  $\omega_p$ . The samples of the amplitude response are

$$H_r(k) = [\underbrace{0, \dots, 0}_{11}, T_1, T_2, \underbrace{1, \dots, 1}_8, T_2, T_1, \underbrace{0, \dots, 0}_{10}]$$

while the phase response samples are

$$\angle H(k) = \begin{cases} -\frac{33-1}{2} \frac{2\pi}{33} k = -\frac{32}{33}\pi k, & 0 \leq k \leq 16 \\ +\frac{32}{33}\pi(33-k), & 17 \leq k \leq 32 \end{cases}$$

The optimum values of transition samples are  $T_1 = 0.1095$  and  $T_2 = 0.598$ . Using these values, the MATLAB design is given in the following script.

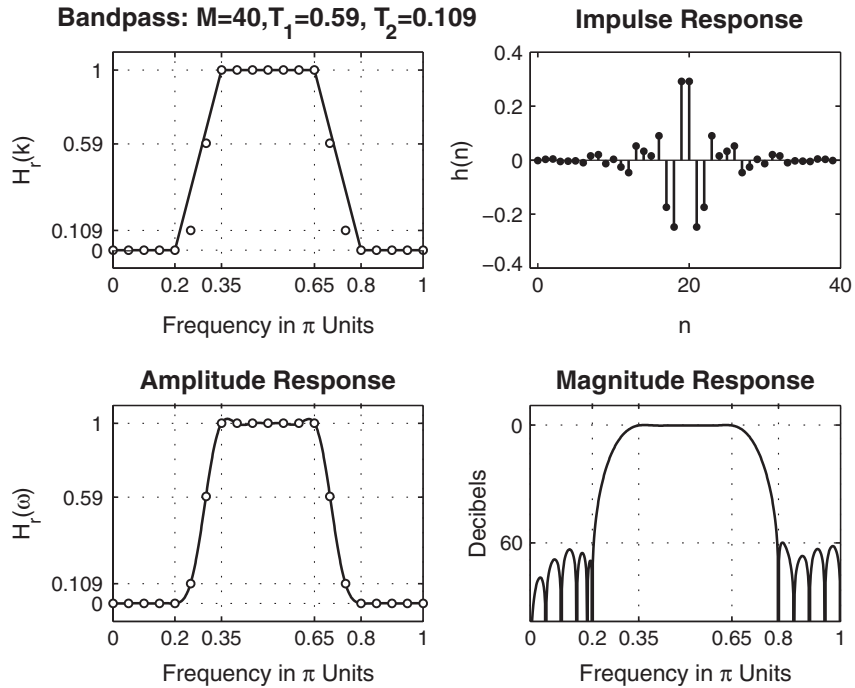


**FIGURE 7.30** Bandpass filter design plots in Example 7.17

```
>> M = 33; alpha = (M-1)/2; l = 0:M-1; wl = (2*pi/M)*l;
>> T1 = 0.1095; T2 = 0.598;
>> Hrs = [zeros(1,11),T1,T2,ones(1,8),T2,T1,zeros(1,10)];
>> Hdr = [0,0,1,1]; wdl = [0,0.6,0.8,1];
>> k1 = 0:floor((M-1)/2); k2 = floor((M-1)/2)+1:M-1;
>> angH = [-alpha*(2*pi)/M*k1, alpha*(2*pi)/M*(M-k2)];
>> H = Hrs.*exp(j*angH); h = real(ifft(H,M));
>> [db,mag,pha,grd,w] = freqz_m(h,1); [Hr,ww,a,L] = Hr_Type1(h);
```

The time- and the frequency-domain plots of the design are shown in Figure 7.31.  $\square$

- EXAMPLE 7.19** Design a 33-point digital differentiator based on the ideal differentiator of (7.31) given in Example 7.12.

#### Solution

From (7.31), the samples of the (imaginary-valued) amplitude response are given by

$$jH_r(k) = \begin{cases} +j\frac{2\pi}{M}k, & k = 0, \dots, \left\lfloor \frac{M-1}{2} \right\rfloor \\ -j\frac{2\pi}{M}(M-k), & k = \left\lfloor \frac{M-1}{2} \right\rfloor + 1, \dots, M-1 \end{cases}$$

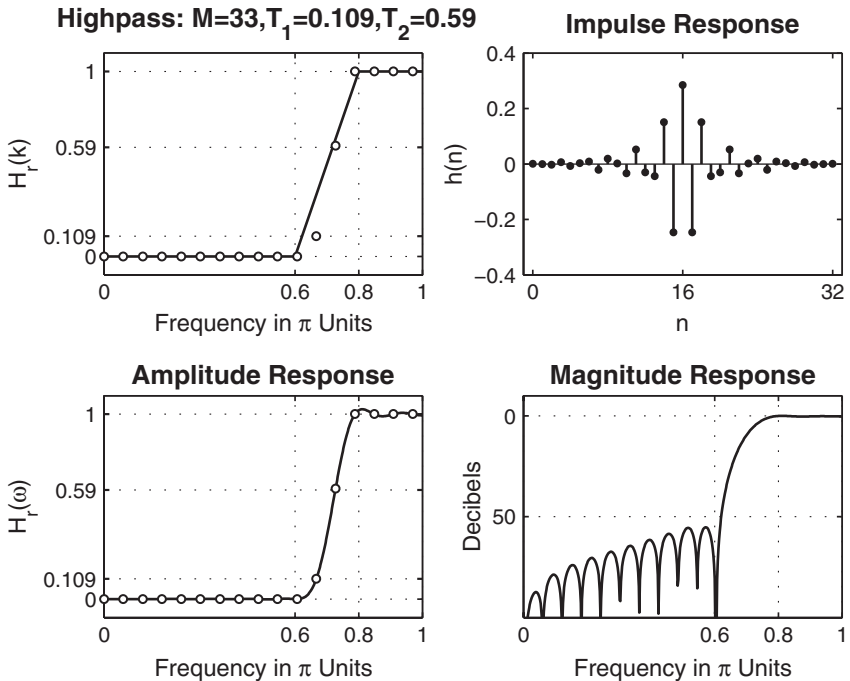


**FIGURE 7.31** Highpass filter design plots in Example 7.18

and for linear phase the phase samples are

$$\angle H(k) = \begin{cases} -\frac{M-1}{2} \frac{2\pi}{M} k = -\frac{M-1}{M} \pi k, & k = 0, \dots, \left\lfloor \frac{M-1}{2} \right\rfloor \\ +\frac{M-1}{M} \pi (M-k), & k = \left\lfloor \frac{M-1}{2} \right\rfloor + 1, \dots, M-1 \end{cases}$$

Therefore,

$$H(k) = j H_r(k) e^{j \angle H(k)}, \quad 0 \leq k \leq M-1 \quad \text{and} \quad h(n) = \text{IDFT}[H(k)]$$

MATLAB script:

```
>> M = 33; alpha = (M-1)/2; Dw = 2*pi/M; l = 0:M-1; wl = Dw*l;
>> k1 = 0:floor((M-1)/2); k2 = floor((M-1)/2)+1:M-1;
>> Hrs = [j*Dw*k1, -j*Dw*(M-k2)];
>> angH = [-alpha*Dw*k1, alpha*Dw*(M-k2)];
>> H = Hrs.*exp(j*angH); h = real(ifft(H,M)); [Hr,ww,a,P]=Hr_Type3(h);
```

The time- and the frequency-domain plots are shown in Figure 7.32. We observe that the differentiator is not a full-band differentiator.  $\square$

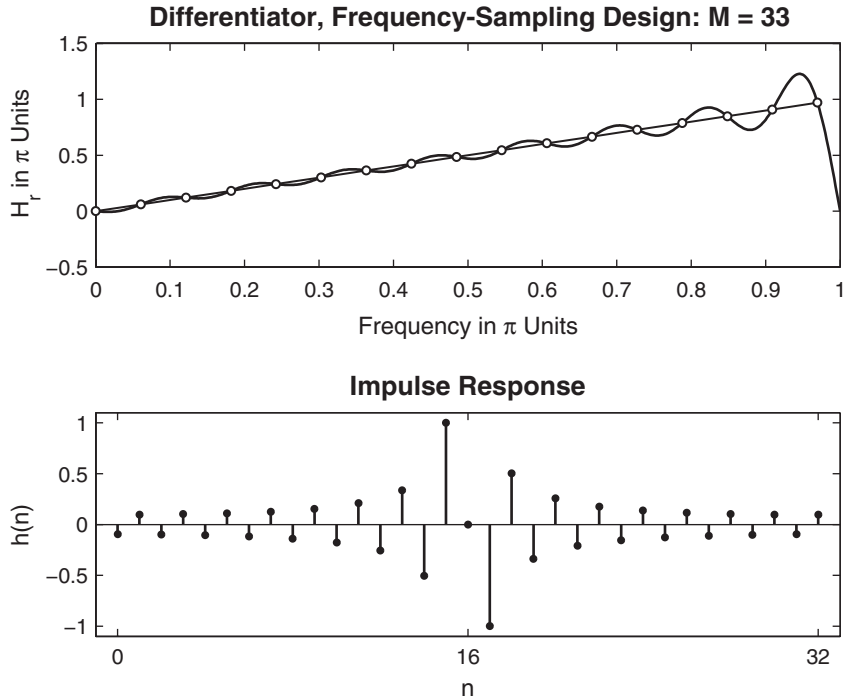


**FIGURE 7.32** Differentiator design plots in Example 7.19

- **EXAMPLE 7.20** Design a 51-point digital Hilbert transformer based on the ideal Hilbert transformer of (7.32).

**Solution**

From (7.32), the samples of the (imaginary-valued) amplitude response are given by

$$jH_r(k) = \begin{cases} -j, & k = 1, \dots, \left\lfloor \frac{M-1}{2} \right\rfloor \\ 0, & k = 0 \\ +j, & k = \left\lfloor \frac{M-1}{2} \right\rfloor + 1, \dots, M-1 \end{cases}$$

Since this is a Type-3 linear-phase filter, the amplitude response will be zero at  $\omega = \pi$ . Hence to reduce the ripples, we should choose the two samples (in transition bands) near  $\omega = \pi$ , optimally between 0 and  $j$ . Using our previous experience, we could select this value as  $0.39j$ . The samples of the phase response are selected similar to those in Example 7.19.

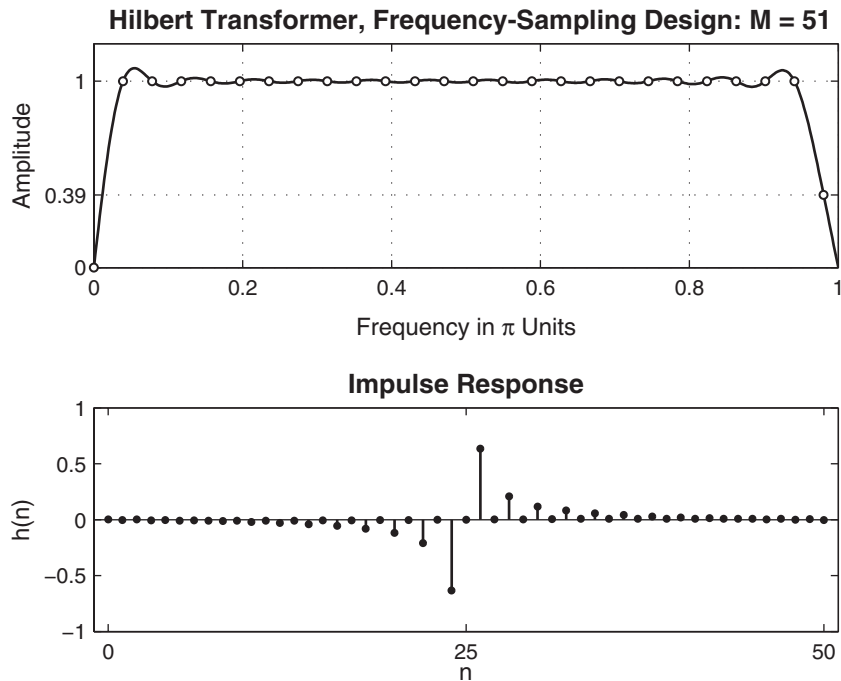


**FIGURE 7.33** Digital Hilbert transformer design plots in Example 7.20

MATLAB script:

```
>> M = 51; alpha = (M-1)/2; Dw = 2*pi/M; l = 0:M-1; wl = Dw*l;
>> k1 = 0:floor((M-1)/2); k2 = floor((M-1)/2)+1:M-1;
>> Hrs = [0,-j*ones(1,(M-3)/2),-0.39j,0.39j,j*ones(1,(M-3)/2)];
>> angH = [-alpha*Dw*k1, alpha*Dw*(M-k2)];
>> H = Hrs.*exp(j*angH); h = real(ifft(H,M)); [Hr,ww,a,P]=Hr_Type3(h);
```

The plots in Figure 7.33 show the effect of the transition band samples. □

The SP toolbox provides a function called **fir2**, which combines the frequency-sampling technique with the window technique to design arbitrary-shaped magnitude response FIR filters. After computing the filter impulse response using the naive design method, **fir2** then applies a selected window to minimize ripples near the band-edge frequencies. This function's syntax also has several forms, including:

- **h = fir2(N,f,m)** designs an  $N$ th-order ( $N = M-1$ ) lowpass FIR filter and returns the impulse response in vector **h**. The desired magnitude

response of the filter is supplied in vectors  $f$  and  $m$ , which must be of the same length. The vector  $f$  contains normalized frequencies in the range from 0 to 1, where 1 corresponds to  $\pi$  rad/sample. The first value of  $f$  must be 0 and the last value 1. The vector  $m$ , contains the samples of the desired magnitude response at the values specified in  $f$ . The desired frequency response is then interpolated onto a dense, evenly spaced grid of length 512. Thus this syntax corresponds to the naive design method.

- $h = \text{fir2}(N, f, m, \text{window})$  uses the vector  $\text{window}$  of length  $N+1$  obtained from one of the specified MATLAB window functions. The default window function used is the Hamming window.
- $h = \text{fir2}(N, f, m, npt)$  or  $h = \text{fir2}(N, f, m, npt, \text{window})$  specifies the number of points  $npt$  for the grid onto which  $\text{fir2}$  interpolates the frequency response. The default  $npt$  value is 512.

Note that the  $\text{fir2}$  does not implement the classic optimum frequency-sampling method. By incorporating window design,  $\text{fir2}$  has found an alternative (and somewhat clever) approach to do away with the optimum transition band values and the associated tables. By densely sampling values in the entire band, interpolation errors are reduced (but not minimized), and stopband attenuation is increased to an acceptable level. However, the basic design is contaminated by the window operation; hence, the frequency response does not go through the original sampled values. It is more suitable for designing FIR filters with arbitrary-shaped frequency responses.

The type of frequency-sampling filter that we considered is called a Type-A filter, in which the sampled frequencies are

$$\omega_k = \frac{2\pi}{M}k, \quad 0 \leq k \leq M - 1$$

There is a second set of uniformly spaced samples given by

$$\omega_k = \frac{2\pi}{M}\left(k + \frac{1}{2}\right), \quad 0 \leq k \leq M - 1$$

This is called a Type-B filter, for which a frequency-sampling structure is also available. The expressions for the magnitude response  $H(e^{j\omega})$  and the impulse response  $h(n)$  are somewhat more complicated and are available in Proakis and Manolakis [79]. Their design can also be done in MATLAB using the approach discussed in this section.

## 7.5 OPTIMAL EQUIRIPPLE DESIGN TECHNIQUE

The last two techniques—namely, the window design and the frequency-sampling design—were easy to understand and implement. However, they have some disadvantages. First, we cannot specify the band frequencies  $\omega_p$  and  $\omega_s$  precisely in the design; that is, we have to accept whatever values we obtain after the design. Second, we cannot specify both  $\delta_1$  and  $\delta_2$  ripple factors simultaneously. Either we have  $\delta_1 = \delta_2$  in the window design method, or we can optimize only  $\delta_2$  in the frequency-sampling method. Finally, the approximation error—that is, the difference between the ideal response and the actual response—is not uniformly distributed over the band intervals. It is higher near the band edges and smaller in the regions away from band edges. By distributing the error uniformly, we can obtain a lower-order filter satisfying the same specifications. Fortunately, a technique exists that can eliminate these three problems. This technique is somewhat difficult to understand and requires a computer for its implementation.

For linear-phase FIR filters, it is possible to derive a set of conditions for which it can be proved that the design solution is optimal in the sense of *minimizing the maximum approximation error* (sometimes called the *minimax* or the *Chebyshev* error). Filters that have this property are called *equiripple* filters because the approximation error is uniformly distributed in both the passband and the stopband. This results in lower-order filters.

In the following, we first formulate a minimax optimal FIR design problem and discuss the total number of maxima and minima (collectively called *extrema*) that one can obtain in the amplitude response of a linear-phase FIR filter. Using this, we then discuss a general equiripple FIR filter design algorithm, which uses polynomial interpolation for its solution. This algorithm is known as the Parks–McClellan algorithm, and it incorporates the Remez exchange algorithm for polynomial solution. This algorithm is available as a subroutine on many computing platforms. In this section, we will use MATLAB to design equiripple FIR filters.

### 7.5.1 DEVELOPMENT OF THE MINIMAX PROBLEM

Earlier in this chapter, we showed that the frequency response of the four cases of linear-phase FIR filters can be written in the form

$$H(e^{j\omega}) = e^{j\beta} e^{-j\frac{M-1}{2}\omega} H_r(\omega)$$

where the values for  $\beta$  and the expressions for  $H_r(\omega)$  are given in Table 7.2.

**TABLE 7.2** Amplitude response and  $\beta$ -values for linear-phase FIR filters

Linear-phase FIR Filter Type	$\beta$	$H_r(e^{j\omega})$
Type-1: $M$ odd, symmetric $h(n)$	0	$\sum_0^{(M-1)/2} a(n) \cos \omega n$
Type-2: $M$ even, symmetric $h(n)$	0	$\sum_1^{M/2} b(n) \cos [\omega(n - 1/2)]$
Type-3: $M$ odd, antisymmetric $h(n)$	$\frac{\pi}{2}$	$\sum_1^{(M-1)/2} c(n) \sin \omega n$
Type-4: $M$ even, antisymmetric $h(n)$	$\frac{\pi}{2}$	$\sum_1^{M/2} d(n) \sin [\omega(n - 1/2)]$

Using simple trigonometric identities, each expression for  $H_r(\omega)$  can be written as a product of a fixed function of  $\omega$  (call this  $Q(\omega)$ ) and a function that is a sum of cosines (call this  $P(\omega)$ ). For details, see Proakis and Manolakis [79] and Problems P7.2–P7.5. Thus

$$H_r(\omega) = Q(\omega)P(\omega) \quad (7.40)$$

where  $P(\omega)$  is of the form

$$P(\omega) = \sum_{n=0}^L \alpha(n) \cos \omega n \quad (7.41)$$

and  $Q(\omega)$ ,  $L$ ,  $P(\omega)$  for the four cases are given in Table 7.3.

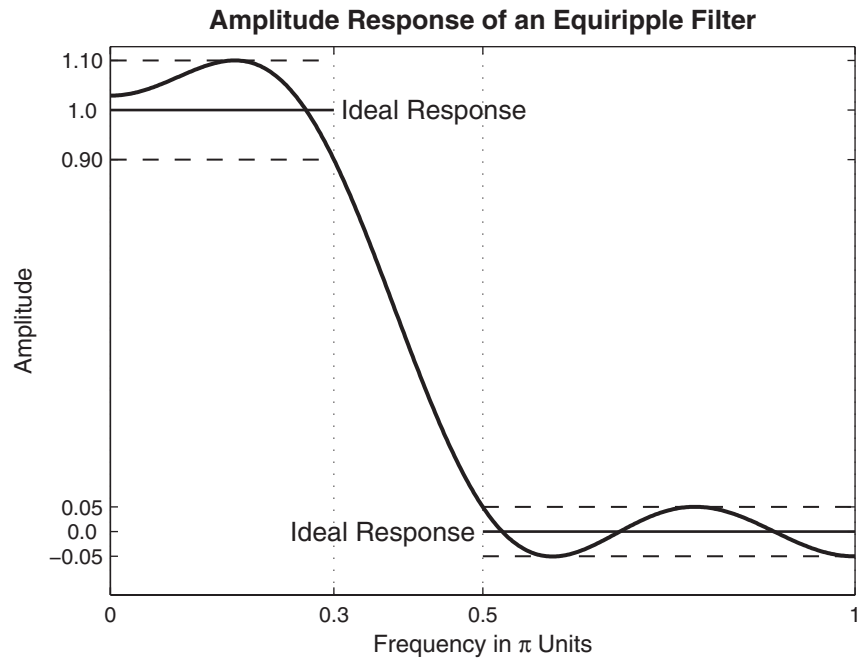
**TABLE 7.3**  $Q(\omega)$ ,  $L$ , and  $P(\omega)$  for linear-phase FIR filters

LP FIR Filter Type	$Q(\omega)$	$L$	$P(\omega)$
Type-1	1	$\frac{M-1}{2}$	$\sum_0^L a(n) \cos \omega n$
Type-2	$\cos \frac{\omega}{2}$	$\frac{M}{2} - 1$	$\sum_0^L \tilde{b}(n) \cos \omega n$
Type-3	$\sin \omega$	$\frac{M-3}{2}$	$\sum_0^L \tilde{c}(n) \cos \omega n$
Type-4	$\sin \frac{\omega}{2}$	$\frac{M}{2} - 1$	$\sum_0^L \tilde{d}(n) \cos \omega n$

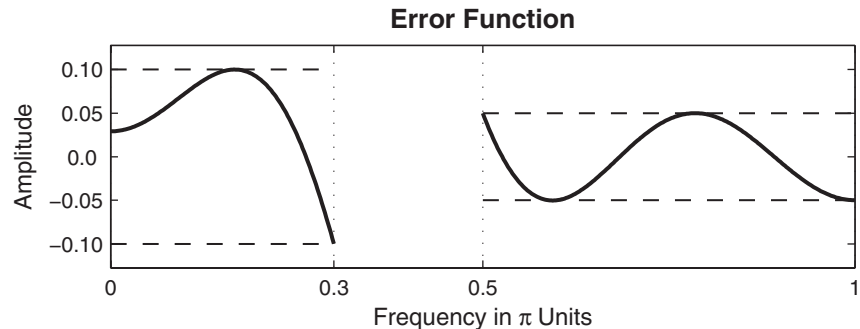
The purpose of the previous analysis was to have a *common form* for  $H_r(\omega)$  across all four cases. It makes the problem formulation much easier. To formulate our problem as a Chebyshev approximation problem, we have to define the desired amplitude response  $H_{dr}(\omega)$  and a weighting function  $W(\omega)$ , both defined over passbands and stopbands. The weighting function is necessary so that we can have an independent control over  $\delta_1$  and  $\delta_2$ . The weighted error is defined as

$$E(\omega) \stackrel{\Delta}{=} W(\omega) [H_{dr}(\omega) - H_r(\omega)], \quad \omega \in \mathcal{S} \stackrel{\Delta}{=} [0, \omega_p] \cup [\omega_s, \pi] \quad (7.42)$$

These concepts are made clear in the following set of figures. It shows a typical equiripple filter response along with its ideal response.



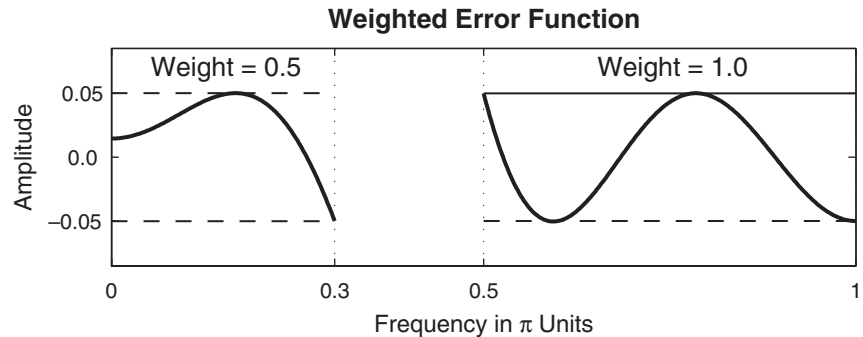
The error  $[H_{dr}(\omega) - H_r(\omega)]$  response is shown here.



Now if we choose

$$W(\omega) = \begin{cases} \frac{\delta_2}{\delta_1}, & \text{in the passband} \\ 1, & \text{in the stopband} \end{cases} \quad (7.43)$$

then the weighted error  $E(\omega)$  response is



Thus the maximum error in both the passband and stopband is  $\delta_2$ . Therefore, if we succeed in minimizing the maximum weighted error to  $\delta_2$ , we automatically also satisfy the specification in the passband to  $\delta_1$ . Substituting  $H_r(\omega)$  from (7.40) into (7.42), we obtain

$$\begin{aligned} E(\omega) &= W(\omega) [H_{dr}(\omega) - Q(\omega) P(\omega)] \\ &= W(\omega) Q(\omega) \left[ \frac{H_{dr}(\omega)}{Q(\omega)} - P(\omega) \right], \quad \omega \in \mathcal{S} \end{aligned}$$

If we define

$$\hat{W}(\omega) \triangleq W(\omega) Q(\omega) \quad \text{and} \quad \hat{H}_{dr}(\omega) \triangleq \frac{H_{dr}(\omega)}{Q(\omega)}$$

then we obtain

$$E(\omega) = \hat{W}(\omega) [\hat{H}_{dr}(\omega) - P(\omega)], \quad \omega \in \mathcal{S} \quad (7.44)$$

Thus we have a common form of  $E(\omega)$  for all four cases.

**Problem statement** The Chebyshev approximation problem can now be defined as follows:

Determine the set of coefficients  $a(n)$  or  $\tilde{b}(n)$  or  $\tilde{c}(n)$  or  $\tilde{d}(n)$  [or equivalently  $a(n)$  or  $b(n)$  or  $c(n)$  or  $d(n)$ ] to minimize the maximum absolute value of  $E(\omega)$  over the passband and stopband, that is,

$$\min_{\text{over coeff.}} \left[ \max_{\omega \in S} |E(\omega)| \right] \quad (7.45)$$

Now we have succeeded in specifying the exact  $\omega_p$ ,  $\omega_s$ ,  $\delta_1$ , and  $\delta_2$ . In addition, the error can now be distributed uniformly in both the passband and stopband.

### 7.5.2 CONSTRAINT ON THE NUMBER OF EXTREMA

Before we give the solution to this above problem, we will first discuss the following issue: How many local maxima and minima exist in the error function  $E(\omega)$  for a given  $M$ -point filter? This information is used by the Parks–McClellan algorithm to obtain the polynomial interpolation. The answer is in the expression  $P(\omega)$ . From (7.41),  $P(\omega)$  is a trigonometric function in  $\omega$ . Using trigonometric identities of the form

$$\begin{aligned}\cos(2\omega) &= 2\cos^2(\omega) - 1 \\ \cos(3\omega) &= 4\cos^3(\omega) - 3\cos(\omega) \\ &\vdots \quad = \quad \vdots\end{aligned}$$

$P(\omega)$ , given in (7.41) can be converted to a trigonometric polynomial in  $\cos(\omega)$ , as follows

$$P(\omega) = \sum_{n=0}^L \beta(n) \cos^n \omega \quad (7.46)$$

□ **EXAMPLE 7.21** Let  $h(n) = \frac{1}{15}[1, 2, 3, 4, 3, 2, 1]$ . Then  $M = 7$  and  $h(n)$  is symmetric, which means that we have a Type-1 linear-phase filter. Hence  $L = (M - 1)/2 = 3$ . Now from (7.7),

$$\alpha(n) = a(n) = 2h(3 - n), \quad 1 \leq n \leq 2; \quad \text{and} \quad \alpha(0) = a(0) = h(3)$$

or  $\alpha(n) = \frac{1}{15}[4, 6, 4, 2]$ . Hence

$$\begin{aligned}P(\omega) &= \sum_0^3 \alpha(n) \cos n\omega = \frac{1}{15}(4 + 6\cos\omega + 4\cos 2\omega + 2\cos 3\omega) \\ &= \frac{1}{15}\{4 + 6\cos\omega + 4(2\cos^2\omega - 1) + 2(4\cos^3\omega - 3\cos\omega)\} \\ &= 0 + 0 + \frac{8}{15}\cos^2\omega + \frac{8}{15}\cos^3\omega = \sum_0^3 \beta(n) \cos^n \omega\end{aligned}$$

$$\text{or } \beta(n) = \left[0, 0, \frac{8}{15}, \frac{8}{15}\right]. \quad \square$$

From (7.46), we note that  $P(\omega)$  is an  $L$ th-order polynomial in  $\cos(\omega)$ . Since  $\cos(\omega)$  is a *monotone* function in the *open* interval  $0 < \omega < \pi$ , then it follows that the  $L$ th-order polynomial  $P(\omega)$  in  $\cos(\omega)$  should behave like an ordinary  $L$ th-order polynomial  $P(x)$  in  $x$ . Therefore,  $P(\omega)$  has

at most (i.e., no more than)  $(L - 1)$  local extrema in the open interval  $0 < \omega < \pi$ . For example,

$$\cos^2(\omega) = \frac{1 + \cos 2\omega}{2}$$

has only one minimum at  $\omega = \pi/2$ . However, it has three extrema in the closed interval  $0 \leq \omega \leq \pi$  (i.e., a maximum at  $\omega = 0$ , a minimum at  $\omega = \pi/2$ , and a maximum at  $\omega = \pi$ ). Thus if we include the end points  $\omega = 0$  and  $\omega = \pi$ , then  $P(\omega)$  has at most  $(L + 1)$  local extrema in the closed interval  $0 \leq \omega \leq \pi$ . Finally, we would like the filter specifications to be met exactly at band edges  $\omega_p$  and  $\omega_s$ . Then the specifications can be met at no more than  $(L + 3)$  extremal frequencies in the  $0 \leq \omega \leq \pi$  interval.

**Conclusion** The error function  $E(\omega)$  has at most  $(L + 3)$  extrema in  $\mathcal{S}$ .

- **EXAMPLE 7.22** Let us plot the amplitude response of the filter given in Example 7.21 and count the total number of extrema in the corresponding error function.

**Solution**

The impulse response is

$$h(n) = \frac{1}{15}[1, 2, 3, 4, 3, 2, 1], \quad M = 7 \quad \text{or} \quad L = 3$$

and  $\alpha(n) = \frac{1}{15}[4, 6, 4, 2]$  and  $\beta(n) = [0, 0, \frac{8}{15}, \frac{8}{15}]$  from Example 7.21. Hence

$$P(\omega) = \frac{8}{15} \cos^2 \omega + \frac{8}{15} \cos^3 \omega$$

which is shown in Figure 7.34. Clearly,  $P(\omega)$  has  $(L - 1) = 2$  extrema in the open interval  $0 < \omega < \pi$ . Also shown in Figure 7.34 is the error function, which has  $(L + 3) = 6$  extrema. □

Let us now turn our attention to the problem statement and equation (7.45). It is a well-known problem in *approximation theory*, and the solution is given by the following important theorem.

■ **THEOREM 1**

**Alternation Theorem**

Let  $\mathcal{S}$  be any closed subset of the closed interval  $[0, \pi]$ . In order that  $P(\omega)$  be the unique minimax approximation to  $H_{dr}(\omega)$  on  $\mathcal{S}$ , it is necessary and sufficient that the error function  $E(\omega)$  exhibit at least  $(L + 2)$  “alternations” or extremal frequencies in  $\mathcal{S}$ ; that is, there must exist  $(L + 2)$  frequencies  $\omega_i$  in  $\mathcal{S}$  such that

$$\begin{aligned} E(\omega_i) = -E(\omega_{i-1}) &= \pm \max_S |E(\omega)| \\ &\triangleq \pm \delta, \forall \omega_0 < \omega_1 < \dots < \omega_{L+1} \in \mathcal{S} \end{aligned} \tag{7.47}$$

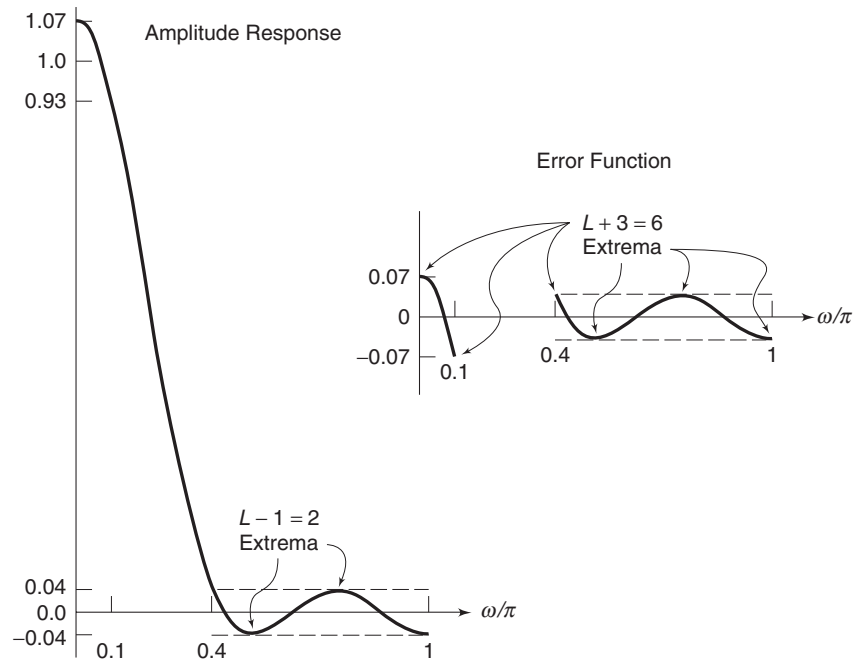


**FIGURE 7.34** Amplitude response and the error function in Example 7.22

Combining this theorem with our earlier conclusion, we infer that the optimal equiripple filter has either  $(L + 2)$  or  $(L + 3)$  alternations in its error function over  $\mathcal{S}$ . Most of the equiripple filters have  $(L + 2)$  alternations. However, for some combinations of  $\omega_p$  and  $\omega_s$ , we can get filters with  $(L + 3)$  alternations. These filters have one extra ripple in their response and hence are called *extraripple* filters.

### 7.5.3 PARKS–McCLELLAN ALGORITHM

The alternation theorem ensures that the solution to our minimax approximation problem exists and is unique, but it does not tell us how to obtain this solution. We know neither the order  $M$  (or equivalently,  $L$ ), nor the extremal frequencies  $\omega_i$ , nor the parameters  $\{\alpha(n)\}$ , nor the maximum error  $\delta$ . Parks and McClellan [74] provided an iterative solution using the Remez exchange algorithm. It assumes that the filter length  $M$  (or  $L$ ) and the ratio  $\delta_2/\delta_1$  are known. If we choose the weighting function as in (7.43), and if we choose the order  $M$  correctly, then  $\delta = \delta_2$  when the solution is obtained. Clearly,  $\delta$  and  $M$  are related; the larger the  $M$ , the smaller the  $\delta$ . In the filter specifications,  $\delta_1$ ,  $\delta_2$ ,  $\omega_p$ , and  $\omega_s$  are given.

Therefore,  $M$  has to be assumed. Fortunately, a simple formula, due to Kaiser, exists for approximating  $M$ . It is given by

$$\hat{M} = \frac{-20 \log_{10} \sqrt{\delta_1 \delta_2} - 13}{2.285 \Delta\omega} + 1; \quad \Delta\omega = \omega_s - \omega_p \quad (7.48)$$

The Parks–McClellan algorithm begins by guessing ( $L + 2$ ) extremal frequencies  $\{\omega_i\}$  and estimating the maximum error  $\delta$  at these frequencies. It then fits an  $L$ th-order polynomial (7.46) through points given in (7.47). Local maximum errors are determined over a finer grid, and the extremal frequencies  $\{\omega_i\}$  are adjusted at these new extremal values. A new  $L$ th-order polynomial is fit through these new frequencies, and the procedure is repeated. This iteration continues until the optimum set  $\{\omega_i\}$  and the global maximum error  $\delta$  are found. The iterative procedure is guaranteed to converge, yielding the polynomial  $P(\omega)$ . From (7.46), coefficients  $\beta(n)$  are determined. Finally, the coefficients  $a(n)$  as well as the impulse response  $h(n)$  are computed. This algorithm is available in MATLAB as the **firpm** function, which is described shortly.

Since we approximated  $M$ , the maximum error  $\delta$  may not be equal to  $\delta_2$ . If this is the case, then we have to increase  $M$  (if  $\delta > \delta_2$ ) or decrease  $M$  (if  $\delta < \delta_2$ ) and use the **firpm** algorithm again to determine a new  $\delta$ . We repeat this procedure until  $\delta \leq \delta_2$ . The optimal equiripple FIR filter, which satisfies all the three requirements discussed earlier, is now determined.

#### 7.5.4 MATLAB IMPLEMENTATION

The Parks–McClellan algorithm is available in MATLAB as a function called **firpm**, the most general syntax of which is

```
[h] = firpm(N,f,m,weights,fptype)
```

There are several versions of this syntax:

- `[h] = firpm(N,f,m)` designs an  $N$ th-order (note that the length of the filter is  $M = N + 1$ ) FIR digital filter whose frequency response is specified by the arrays `f` and `m`. The filter coefficients (or the impulse response) are returned in array `h` of length  $M$ . The array `f` contains band-edge frequencies in units of  $\pi$ , that is,  $0.0 \leq f \leq 1.0$ . These frequencies must be in increasing order, starting with 0.0 and ending with 1.0. The array `m` contains the desired magnitude response at frequencies specified in `f`. The lengths of `f` and `m` arrays must be the same and must be an even number. The weighting function used in each band

is equal to unity, which means that the tolerances ( $\delta_i$ 's) in every band are the same.

- `[h] = firpm(N,f,m,weights)` is similar to the preceding case except that the array `weights` specifies the weighting function in each band.
- `[h] = firpm(N,f,m,ftype)` is similar to the first case except that when `ftype` is the string ‘differentiator’ or ‘hilbert’, it designs digital differentiators or digital Hilbert transformers, respectively. For the digital Hilbert transformer, the lowest frequency in the `f` array should not be 0, and the highest frequency should not be 1. For the digital differentiator, the `m` vector does not specify the desired slope in each band but the desired magnitude.
- `[h] = firpm(N,f,m,weights,ftype)` is similar to the above case except that the array `weights` specifies the weighting function in each band.

To estimate the filter order  $N$ , the SP toolbox provides the function `firpmord`, which also estimates other parameters that can be used in the `firpm` function. The basic syntax is

```
[N,f0,m0,weights] = firpmord(f,m,delta);
```

The function computes the window order `N`, the normalized frequency band edges in `f0`, amplitude response in `a0`, and the band weights in `weights`. The vector `f` is a vector of normalized band edges and `m` is a vector specifying the desired amplitude on the bands defined by `f`. The length of `f` is 2 less than twice the length of `m`; that is, `f` does not contain 0 or 1. The vector `delta` specifies tolerances in each band (not in decibels). The estimated parameters can now be used in the `firpm` function.

As explained during the description of the Parks–McClellan algorithm, we have to first guess the order of the filter using (7.48) to use the function `firpm`. After we obtain the filter coefficients in array `h`, we have to check the minimum stopband attenuation and compare it with the given  $A_s$  and then increase (or decrease) the filter order. We have to repeat this procedure until we obtain the desired  $A_s$ . We illustrate this procedure in the following several MATLAB examples. These examples also use the ripple conversion function `db2delta`, which is developed in Problem P7.1.

- **EXAMPLE 7.23** Let us design the lowpass filter described in Example 7.8 using the Parks–McClellan algorithm. The design parameters are

$$\begin{aligned}\omega_p &= 0.2\pi, \quad R_p = 0.25 \text{ dB} \\ \omega_s &= 0.3\pi, \quad A_s = 50 \text{ dB}\end{aligned}$$

We provide a MATLAB script to design this filter.

```

>> wp = 0.2*pi; ws = 0.3*pi; Rp = 0.25; As = 50;
>> [delta1,delta2] = db2delta(Rp,As);
>> [N,f,m,weights] = firpmord([wp,ws]/pi,[1,0],[delta1,delta2]);
>> h = firpm(N,f,m,weights);
>> [db,mag,pha,grd,w] = freqz_m(h,[1]);
>> delta_w = 2*pi/1000; wsi=ws/delta_w+1; wpi = wp/delta_w;
>> Asd = -max(db(wsi:1:501))
Asd = 47.8404
>> N = N+1
N = 43
>> h = firpm(N,f,m,weights); [db,mag,pha,grd,w] = freqz_m(h,[1]);
>> Asd = -max(db(wsi:1:501))
Asd = 48.2131
>> N = N+1
N = 44
>> h = firpm(N,f,m,weights); [db,mag,pha,grd,w] = freqz_m(h,[1]);
>> Asd = -max(db(wsi:1:501))
Asd = 48.8689
>> N = N+1
N = 45
>> h = firpm(N,f,m,weights); [db,mag,pha,grd,w] = freqz_m(h,[1]);
>> Asd = -max(db(wsi:1:501))
Asd = 49.8241
>> N = N+1
N = 46
>> h = firpm(N,f,m,weights); [db,mag,pha,grd,w] = freqz_m(h,[1]);
>> Asd = -max(db(wsi:1:501))
Asd = 51.0857
>> M = N+1
M = 47

```

Note that we stopped this iterative procedure when the computed stopband attenuation exceeded the given stopband attenuation  $A_s$  and the optimal value of  $M$  was found to be 47. This value is considerably lower than the window design techniques ( $M = 61$  for a Kaiser window) or the frequency-sampling technique ( $M = 60$ ). In Figure 7.35, we show the time- and the frequency-domain plots of the designed filter along with the error function in both the passband and the stopband to illustrate the equiripple behavior.

- EXAMPLE 7.24** Let us design the bandpass filter described in Example 7.10 using the Parks-McClellan algorithm. The design parameters are

$$\begin{aligned}\omega_{1s} &= 0.2\pi & R_p &= 1 \text{ dB} \\ \omega_{1p} &= 0.35\pi & & \\ \omega_{2p} &= 0.65\pi & A_s &= 60 \text{ dB} \\ \omega_{2s} &= 0.8\pi & &\end{aligned}$$

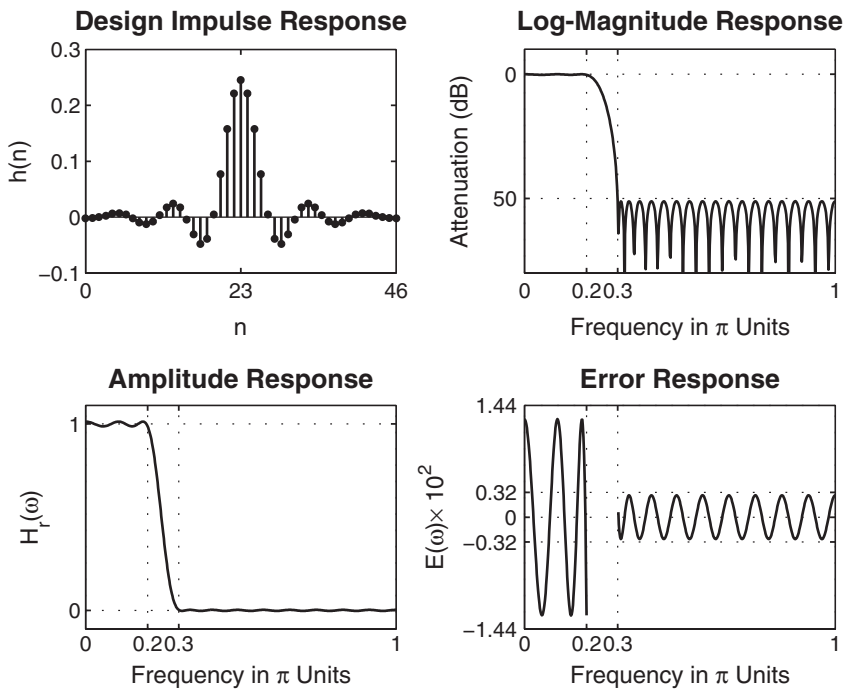


FIGURE 7.35 Plots for equiripple lowpass FIR filter in Example 7.23

### Solution

The following MATLAB script shows how to design this filter.

```

>> ws1 = 0.2*pi; wp1 = 0.35*pi; wp2 = 0.65*pi; ws2 = 0.8*pi;
>> Rp = 1.0; As = 60;
>> [delta1,delta2] = db2delta(Rp,As);
>> f = [ws1,wp1,wp2,ws2]/pi; m = [0,1,0]; delta = [delta2,delta1,delta2];
>> [N,f,m,weights] = firpmord(f,m,delta); N
N = 26
>> h = firpm(N,f,m,weights);
>> [db,mag,pha,grd,w] = freqz_m(h,[1]);
>> delta_w=2*pi/1000;
>> ws1i=floor(ws1/delta_w)+1; wp1i = floor(wp1/delta_w)+1;
>> ws2i=floor(ws2/delta_w)+1; wp2i = floor(wp2/delta_w)+1;
>> Asd = -max(db(1:1:ws1i));
Asd = 54.7756
>> N = N+1;
>> h = firpm(N,f,m,weights);
>> [db,mag,pha,grd,w] = freqz_m(h,[1]);
>> Asd = -max(db(1:1:ws1i))

```

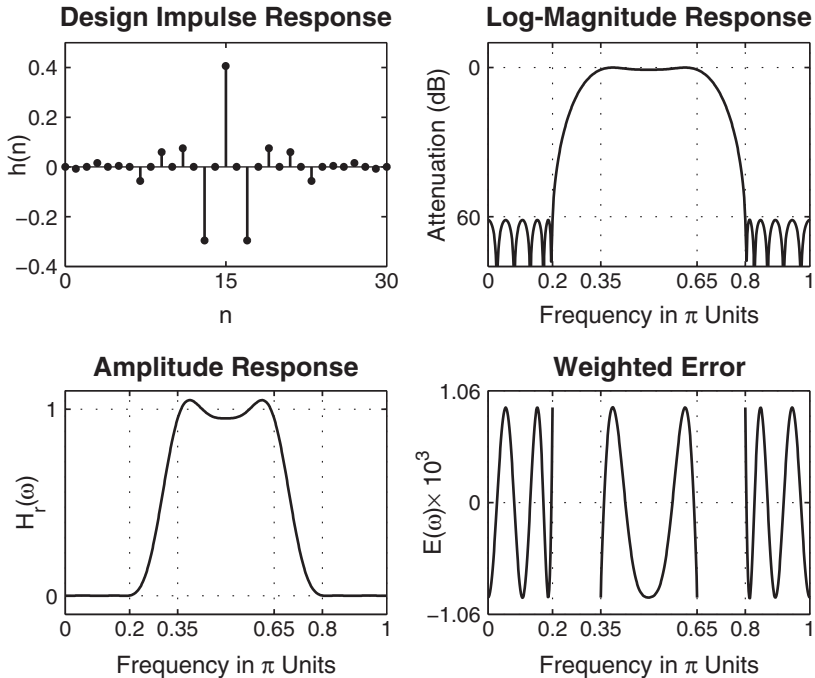


**FIGURE 7.36** Plots for equiripple bandpass FIR filter in Example 7.24

```

Asd = 56.5910
>> N = N+1;
>> h = firpm(N,f,m,weights);
>> [db,mag,pha,grd,w] = freqz_m(h,[1]);
Asd = -max(db(1:1:ws1i))
>> Asd = 61.2843
>> M = N+1
M = 29

```

The optimal value of  $M$  was found to be 29. The time- and the frequency-domain plots of the designed filter are shown in Figure 7.36.  $\square$

- $\square$  **EXAMPLE 7.25** Design a highpass filter that has the following specifications:

$$\omega_s = 0.6\pi, \quad A_s = 50 \text{ dB}$$

$$\omega_p = 0.75\pi, \quad R_p = 0.5 \text{ dB}$$

**Solution**

Since this is a highpass filter, we must ensure that the length  $M$  is an odd number. This is shown in the following MATLAB script.

```

>> ws = 0.6*pi; wp = 0.75*pi; Rp = 0.5; As = 50;
>> [delta1,delta2] = db2delta(Rp,As);
>> [N,f,m,weights] = firpmord([ws,wp]/pi,[0,1],[delta2,delta1]); N
N = 26
>> h = firpm(N,f,m,weights);
>> [db,mag,pha,grd,w] = freqz_m(h,[1]);
>> delta_w = 2*pi/1000; wsi=ws/delta_w; wpi = wp/delta_w;
>> Asd = -max(db(1:1:wsi))
Asd = 49.5918
>> N = N+2;
>> h = firpm(N,f,m,weights);
>> [db,mag,pha,grd,w] = freqz_m(h,[1]);
>> Asd = -max(db(1:1:wsi))
>> Asd = 50.2253
>> M = N+1
M = 29

```

Note also that we increased the value of  $N$  by two to maintain its even value. The optimum  $M$  was found to be 29. The time- and the frequency-domain plots of the designed filter are shown in Figure 7.37.  $\square$

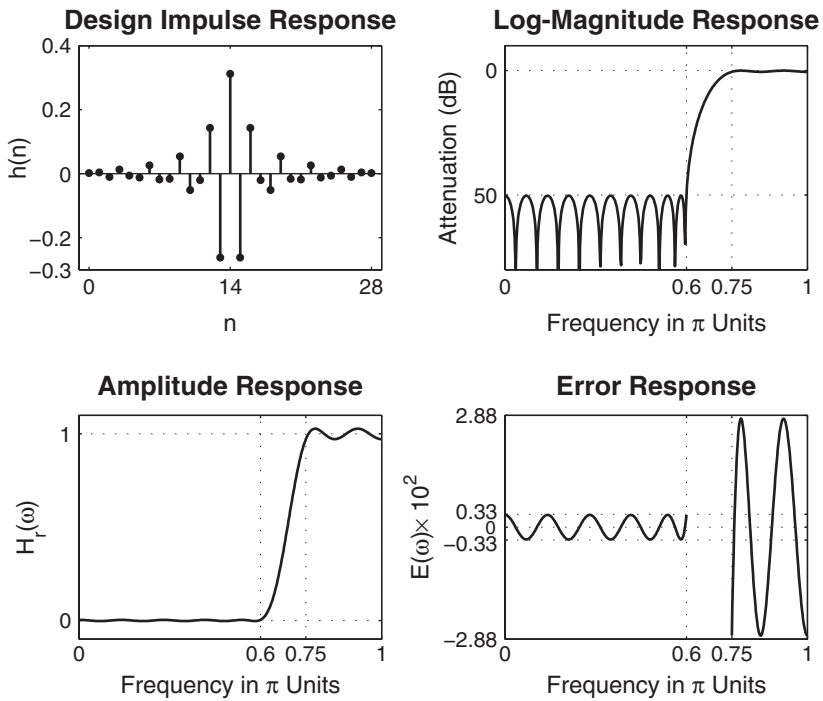


**FIGURE 7.37** Plots for equiripple highpass FIR filter in Example 7.25

- EXAMPLE 7.26** In this example, we will design a “staircase” filter, which has 3 bands with different ideal responses and different tolerances in each band. The design specifications are as follows.

Band-1:  $0 \leq \omega \leq 0.3\pi$ , Ideal gain = 1, Tolerance  $\delta_1 = 0.01$

Band-2:  $0.4\pi \leq \omega \leq 0.7\pi$ , Ideal gain = 0.5, Tolerance  $\delta_2 = 0.005$

Band-3:  $0.8\pi \leq \omega \leq \pi$ , Ideal gain = 0, Tolerance  $\delta_3 = 0.001$

### Solution

The following MATLAB script describes the design procedure.

```
>> w1 = 0; w2 = 0.3*pi; delta1 = 0.01;
>> w3 = 0.4*pi; w4 = 0.7*pi; delta2 = 0.005;
>> w5 = 0.8*pi; w6 = pi; delta3 = 0.001;
>> weights = [delta3/delta1 delta3/delta2 1];
>> Dw = min((w3-w2), (w5-w3));
>> M = ceil((-20*log10((delta1*delta2*delta3)^(1/3))-13)/(2.285*Dw)+1)
>> M = 51
>> f = [0 w2/pi w3/pi w4/pi w5/pi 1];
>> m = [1 1 0.5 0.5 0 0];
>> h = firpm(M-1,f,m,weights);
>> [db,mag,pha,grd,w] = freqz_m(h,[1]);
>> delta_w = 2*pi/1000;
>> w1i=floor(w1/delta_w)+1; w2i = floor(w2/delta_w)+1;
>> w3i=floor(w3/delta_w)+1; w4i = floor(w4/delta_w)+1;
>> w5i=floor(w5/delta_w)+1; w6i = floor(w6/delta_w)+1;
>> Asd = -max(db(w5i:w6i))
Asd = 62.0745
>> M = M-1; h = firpm(M-1,f,m,weights);
>> [db,mag,pha,grd,w] = freqz_m(h,[1]);
>> Asd = -max(db(w5i:w6i))
Asd = 60.0299
>> M = M-1; h = firpm(M-1,f,m,weights);
>> [db,mag,pha,grd,w] = freqz_m(h,[1]);
>> Asd = -max(db(w5i:w6i))
Asd = 60.6068
>> M
M = 49
```

The time- and the frequency-domain plots of the designed filter are shown in Figure 7.38.  $\square$

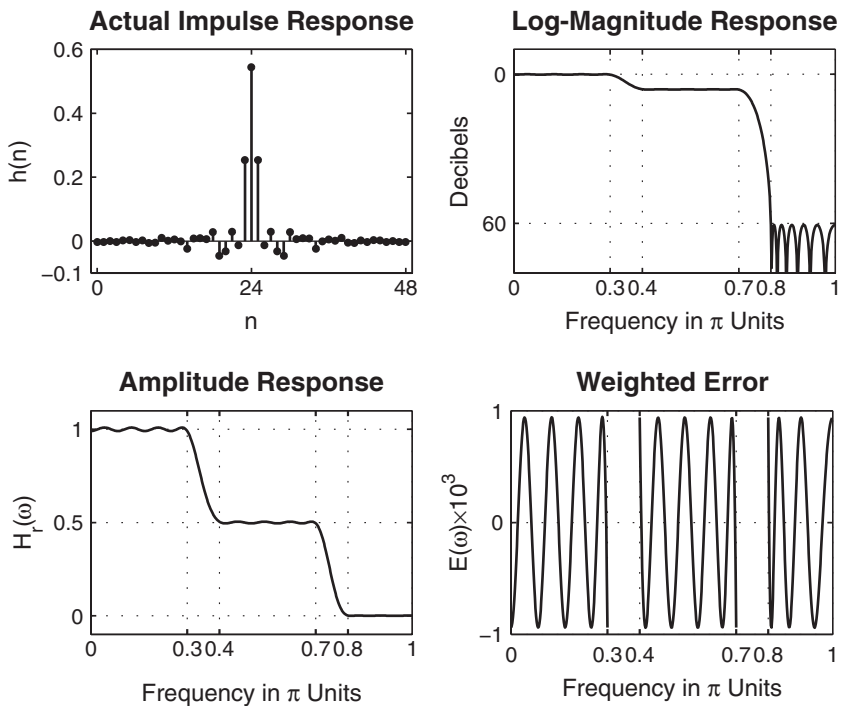


**FIGURE 7.38** Plots for equiripple staircase FIR filter in Example 7.26

- **EXAMPLE 7.27** In this example, we will design a digital differentiator with different slopes in each band. The specifications are as follows.

Band-1:  $0 \leq \omega \leq 0.2\pi$ , Slope = 1 sam/cycle

Band-2:  $0.4\pi \leq \omega \leq 0.6\pi$ , Slope = 2 sam/cycle

Band-3:  $0.8\pi \leq \omega \leq \pi$ , Slope = 3 sam/cycle

#### Solution

We need desired magnitude response values in each band. These can be obtained by multiplying band-edge frequencies in cycles/sam by the slope values in sam/cycle.

$$\text{Band-1: } 0 \leq f \leq 0.1, \text{ Slope} = 1 \text{ sam/cycle} \Rightarrow 0.0 \leq |H| \leq 0.1$$

$$\text{Band-2: } 0.2 \leq f \leq 0.3, \text{ Slope} = 2 \text{ sam/cycle} \Rightarrow 0.4 \leq |H| \leq 0.6$$

$$\text{Band-3: } 0.4 \leq f \leq 0.5, \text{ Slope} = 3 \text{ sam/cycle} \Rightarrow 1.2 \leq |H| \leq 1.5$$

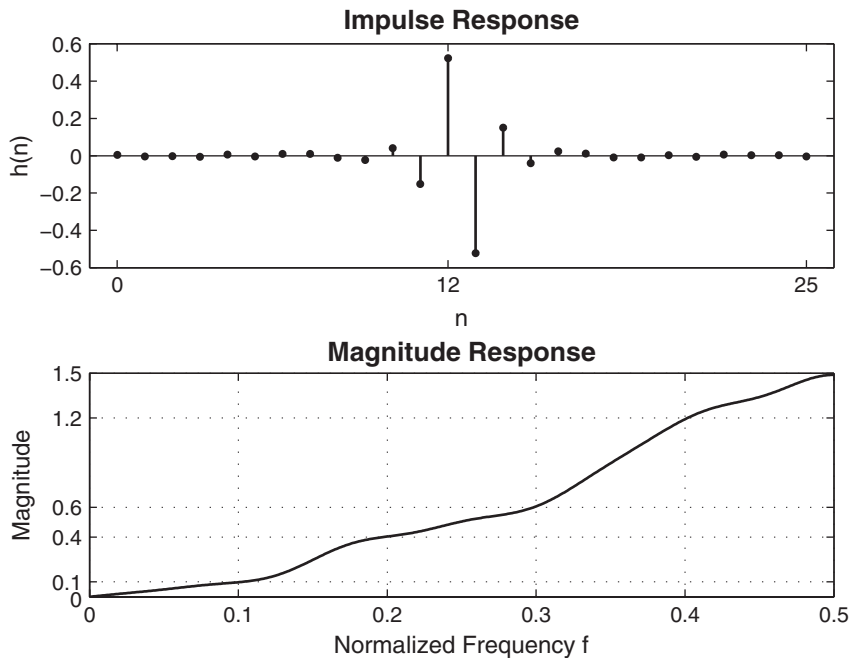


**FIGURE 7.39** Plots of the differentiator in Example 7.27

Let the weights be equal in all bands. MATLAB script:

```
>> f = [0 0.2 0.4 0.6 0.8 1]; % In w/pi units
>> m = [0,0.1,0.4,0.6,1.2,1.5]; % Magnitude values
>> h = firpm(25,f,m,'differentiator');
>> [db,mag,pha,grd,w] = freqz_m(h,[1]);
% Plot commands follow
```

The frequency-domain response is shown in Figure 7.39. □

□ **EXAMPLE 7.28** Finally, we design a Hilbert transformer over the band  $0.05\pi \leq \omega \leq 0.95\pi$ .

#### Solution

Since this is a wideband Hilbert transformer, we will choose an odd length for our filter (i.e., a Type-3 filter). Let us choose  $M = 51$ . MATLAB script:

```
>> f = [0.05,0.95]; m = [1 1]; h = firpm(50,f,m,'hilbert');
>> [db,mag,pha,grd,w] = freqz_m(h,[1]);
% Plot commands follow
```

The plots of this Hilbert transformer are shown in Figure 7.40. □

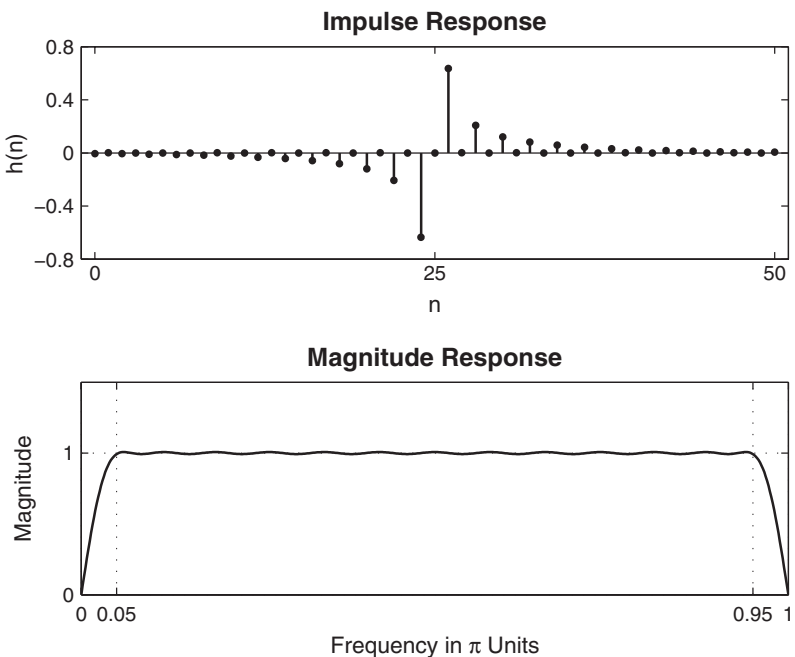


**FIGURE 7.40** Plots of the Hilbert transformer in Example 7.28

## 7.6 PROBLEMS

---

**P7.1** The absolute and relative (dB) specifications for a lowpass filter are related by (7.1) and (7.2). In this problem, we will develop a simple MATLAB function to convert one set of specifications into another.

1. Write a MATLAB function to convert absolute specifications  $\delta_1$  and  $\delta_2$  into the relative specifications  $R_p$  and  $A_s$  in dB. The format of the function should be

```
function [Rp,As] = delta2db(delta1,delta2)
% Converts absolute specs delta1 and delta2 into dB specs Rp and As
% [Rp,As] = delta2db(delta1,delta2)
```

- Verify your function using the specifications given in Example 7.2.
2. Write a MATLAB function to convert relative (dB) specifications  $R_p$  and  $A_s$  into the absolute specifications  $\delta_1$  and  $\delta_2$ . The format of the function should be

```
function [delta1,delta2] = db2delta(Rp,As)
% Converts dB specs Rp and As into absolute specs delta1 and delta2
% [delta1,delta2] = db2delta(Rp,As)
```

Verify your function using the specifications given in Example 7.1.

**P7.2** The Type-1 linear-phase FIR filter is characterized by

$$h(n) = h(M - 1 - n), \quad 0 \leq n \leq M - 1, \quad M \text{ odd}$$

Show that its amplitude response  $H_r(\omega)$  is given by

$$H_r(\omega) = \sum_{n=0}^L a(n) \cos(\omega n), \quad L = \frac{M-1}{2}$$

where coefficients  $\{a(n)\}$  are obtained as defined in (7.7).

**P7.3** The Type-2 linear-phase FIR filter is characterized by

$$h(n) = h(M - 1 - n), \quad 0 \leq n \leq M - 1, \quad M \text{ even}$$

1. Show that its amplitude response  $H_r(\omega)$  is given by

$$H_r(\omega) = \sum_{n=1}^{M/2} b(n) \cos\left\{\omega\left(n - \frac{1}{2}\right)\right\}$$

where coefficients  $\{b(n)\}$  are obtained as defined in (7.10).

2. Show that  $H_r(\omega)$  can be further expressed as

$$H_r(\omega) = \cos\left(\frac{\omega}{2}\right) \sum_{n=0}^L \tilde{b}(n) \cos(\omega n), \quad L = \frac{M}{2} - 1$$

where coefficients  $\tilde{b}(n)$  are given by

$$\begin{aligned} b(1) &= \tilde{b}(0) + \frac{1}{2}\tilde{b}(1), \\ b(n) &= \frac{1}{2} [\tilde{b}(n-1) + \tilde{b}(n)], \quad 2 \leq n \leq \frac{M}{2} - 1, \\ b\left(\frac{M}{2}\right) &= \frac{1}{2}\tilde{b}\left(\frac{M}{2} - 1\right). \end{aligned}$$

**P7.4** The Type-3 linear-phase FIR filter is characterized by

$$h(n) = -h(M - 1 - n), \quad 0 \leq n \leq M - 1, \quad M \text{ odd}$$

1. Show that its amplitude response  $H_r(\omega)$  is given by

$$H_r(\omega) = \sum_{n=1}^{(M-1)/2} c(n) \sin(\omega n)$$

where coefficients  $\{c(n)\}$  are obtained as defined in (7.13).

2. Show that  $H_r(\omega)$  can be further expressed as

$$H_r(\omega) = \sin(\omega) \sum_{n=0}^L \tilde{c}(n) \cos(\omega n), \quad L = \frac{M-3}{2}$$

where coefficients  $\tilde{c}(n)$  are given by

$$\begin{aligned} c(1) &= \tilde{c}(0) - \frac{1}{2}\tilde{c}(1), \\ c(n) &= \frac{1}{2} [\tilde{c}(n-1) - \tilde{c}(n)], \quad 2 \leq n \leq \frac{M-3}{2}, \\ c\left(\frac{M-1}{2}\right) &= \frac{1}{2}\tilde{c}\left(\frac{M-3}{2}\right). \end{aligned}$$

**P7.5** The Type-4 linear-phase FIR filter is characterized by

$$h(n) = -h(M-1-n), \quad 0 \leq n \leq M-1, \quad M \text{ even}$$

1. Show that its amplitude response  $H_r(\omega)$  is given by

$$H_r(\omega) = \sum_{n=1}^{M/2} d(n) \sin \left\{ \omega \left( n - \frac{1}{2} \right) \right\}$$

- where coefficients  $\{d(n)\}$  are obtained as defined in (7.16).
2. Show that the above  $H_r(\omega)$  can be further expressed as

$$H_r(\omega) = \sin \left( \frac{\omega}{2} \right) \sum_{n=0}^L \tilde{d}(n) \cos(\omega n), \quad L = \frac{M}{2} - 1$$

where coefficients  $\tilde{d}(n)$  are given by

$$\begin{aligned} d(1) &= \tilde{d}(0) - \frac{1}{2}\tilde{d}(1), \\ d(n) &= \frac{1}{2} [\tilde{d}(n-1) - \tilde{d}(n)], \quad 2 \leq n \leq \frac{M}{2} - 1, \\ d\left(\frac{M}{2}\right) &= \frac{1}{2}\tilde{d}\left(\frac{M}{2} - 1\right). \end{aligned}$$

**P7.6** Write a MATLAB function to compute the amplitude response  $H_r(\omega)$  given a linear phase impulse response  $h(n)$ . The format of this function should be

```
function [Hr,w,P,L] = Ampl_Res(h);
% Computes amplitude response Hr(w) and its polynomial P of order L,
% given a linear-phase FIR filter impulse response h.
% The type of filter is determined automatically by the subroutine.
%
% [Hr,w,P,L] = Ampl_Res(h)
% Hr = amplitude response
% w = frequencies between [0 pi] over which Hr is computed
% P = polynomial coefficients
% L = Order of P
% h = Linear-phase filter impulse response
```

The function should first determine the type of the linear-phase FIR filter and then use the appropriate `Hr_Type#` function discussed in this chapter. It should also check if the given  $h(n)$  is of a linear-phase type. Verify your function on sequences given here.

$$h_I(n) = (0.9)^{|n-5|} \cos[\pi(n-5)/12] [u(n) - u(n-11)]$$

$$h_{II}(n) = (0.9)^{|n-4.5|} \cos[\pi(n-4.5)/11] [u(n) - u(n-10)]$$

$$h_{III}(n) = (0.9)^{|n-5|} \sin[\pi(n-5)/12] [u(n) - u(n-11)]$$

$$h_{IV}(n) = (0.9)^{|n-4.5|} \sin[\pi(n-4.5)/11] [u(n) - u(n-10)]$$

$$h(n) = (0.9)^n \cos[\pi(n-5)/12] [u(n) - u(n-11)]$$

**P7.7** Prove the following properties of linear-phase FIR filters.

1. If  $H(z)$  has four zeros at  $z_1 = re^{j\theta}$ ,  $z_2 = \frac{1}{r}e^{-j\theta}$ ,  $z_3 = re^{-j\theta}$ , and  $z_4 = \frac{1}{r}e^{j\theta}$ , then  $H(z)$  represents a linear-phase FIR filter.
2. If  $H(z)$  has two zeros at  $z_1 = e^{j\theta}$  and  $z_2 = e^{-j\theta}$ , then  $H(z)$  represents a linear-phase FIR filter.
3. If  $H(z)$  has two zeros at  $z_1 = r$  and  $z_2 = \frac{1}{r}$ , then  $H(z)$  represents a linear-phase FIR filter.
4. If  $H(z)$  has a zero at  $z_1 = 1$  or a zero at  $z_1 = -1$ , then  $H(z)$  represents a linear-phase FIR filter.
5. For each of the sequences given in Problem P7.6, plot the locations of zeros. Determine which sequences imply linear-phase FIR filters.

**P7.8** A notch filter is an LTI system, which is used to eliminate an arbitrary frequency  $\omega = \omega_0$ . The ideal linear-phase notch filter frequency response is given by

$$H_d(e^{j\omega}) = \begin{cases} 0, & |\omega| = \omega_0; \\ 1 \cdot e^{-j\alpha\omega}, & \text{otherwise.} \end{cases} \quad (\alpha \text{ is a delay in samples})$$

1. Determine the ideal impulse response,  $h_d(n)$ , of the ideal notch filter.
2. Using  $h_d(n)$ , design a linear-phase FIR notch filter using a length 51 rectangular window to eliminate the frequency  $\omega_0 = \pi/2$  rad/sample. Plot the amplitude response of the resulting filter.
3. Repeat part 2 using a length 51 Hamming window. Compare your results.

**P7.9** Design a linear-phase bandpass filter using the Hann window design technique. The specifications are

lower stopband edge:  $0.2\pi$   $A_s = 40$  dB

upper stopband edge:  $0.75\pi$

lower passband edge:  $0.35\pi$   $R_p = 0.25$  dB

upper passband edge:  $0.55\pi$

Plot the impulse response and the magnitude response (in dB) of the designed filter. Do not use the `fir1` function.

**P7.10** Design a bandstop filter using the Hamming window design technique. The specifications are

lower stopband edge:  $0.4\pi$   $A_s = 50$  dB

upper stopband edge:  $0.6\pi$

lower passband edge:  $0.3\pi$   $R_p = 0.2$  dB

upper passband edge:  $0.7\pi$

Plot the impulse response and the magnitude response (in dB) of the designed filter. Do not use the **fir1** function.

**P7.11** Design a bandpass filter using the Hamming window design technique. The specifications are

$$\begin{aligned} \text{lower stopband edge: } & 0.3\pi & A_s = 50 \text{ dB} \\ \text{upper stopband edge: } & 0.6\pi \\ \text{lower passband edge: } & 0.4\pi & R_p = 0.5 \text{ dB} \\ \text{upper passband edge: } & 0.5\pi \end{aligned}$$

Plot the impulse response and the magnitude response (in dB) of the designed filter. Do not use the **fir1** function.

**P7.12** Design a highpass filter using one of the fixed window functions. The specifications are

$$\begin{aligned} \text{stopband edge: } & 0.4\pi, A_s = 50 \text{ dB} \\ \text{passband edge: } & 0.6\pi, R_p = 0.004 \text{ dB} \end{aligned}$$

Plot the zoomed magnitude response (in dB) of the designed filter in the passband to verify the passband ripple  $R_p$ . Do not use the **fir1** function.

**P7.13** Using the Kaiser window method, design a linear-phase FIR digital filter that meets the following specifications:

$$\begin{aligned} 0.975 \leq |H(e^{j\omega})| & \leq 1.025, & 0 \leq \omega \leq 0.25\pi \\ 0 \leq |H(e^{j\omega})| & \leq 0.005, & 0.35\pi \leq \omega \leq 0.65\pi \\ 0.975 \leq |H(e^{j\omega})| & \leq 1.025, & 0.75\pi \leq \omega \leq \pi \end{aligned}$$

Determine the minimum-length impulse response  $h(n)$  of such a filter. Provide a plot containing subplots of the amplitude response and the magnitude response in dB. Do not use the **fir1** function.

**P7.14** We wish to use the Kaiser window method to design a linear-phase FIR digital filter that meets the following specifications:

$$\begin{aligned} 0 \leq |H(e^{j\omega})| & \leq 0.01, & 0 \leq \omega \leq 0.25\pi \\ 0.95 \leq |H(e^{j\omega})| & \leq 1.05, & 0.35\pi \leq \omega \leq 0.65\pi \\ 0 \leq |H(e^{j\omega})| & \leq 0.01, & 0.75\pi \leq \omega \leq \pi \end{aligned}$$

Determine the minimum-length impulse response  $h(n)$  of such a filter. Provide a plot containing subplots of the amplitude response and the magnitude response in dB. Do not use the **fir1** function.

**P7.15** Design the staircase filter of Example 7.26 using the Kaiser window approach. The specifications are as follows.

$$\begin{aligned} \text{Band-1: } & 0 \leq \omega \leq 0.3\pi, \text{ Ideal gain} = 1, & \delta_1 = 0.01 \\ \text{Band-2: } & 0.4\pi \leq \omega \leq 0.7\pi, \text{ Ideal gain} = 0.5, & \delta_2 = 0.005 \\ \text{Band-3: } & 0.8\pi \leq \omega \leq \pi, \text{ Ideal gain} = 0, & \delta_3 = 0.001 \end{aligned}$$

Compare the filter length of this design with that of Example 7.26. Provide a plot of the magnitude response in dB. Do not use the **fir1** function.

**P7.16** Design a bandpass filter using a fixed window design technique that has the minimum length and that satisfies the following specifications:

$$\left. \begin{array}{l} \text{lower stopband edge} = 0.3\pi \\ \text{upper stopband edge} = 0.6\pi \end{array} \right\} A_s = 40 \text{ dB}$$

$$\left. \begin{array}{l} \text{lower passband edge} = 0.4\pi \\ \text{upper passband edge} = 0.5\pi \end{array} \right\} R_p = 0.5 \text{ dB}$$

Provide a plot of the log-magnitude response in dB and `stem` plot of the impulse response.

**P7.17** Repeat Problem P7.9 using the `fir1` function.

**P7.18** Repeat Problem P7.10 using the `fir1` function.

**P7.19** Repeat Problem P7.11 using the `fir1` function.

**P7.20** Repeat Problem P7.12 using the `fir1` function.

**P7.21** Repeat Problem P7.13 using the `fir1` function.

**P7.22** Repeat Problem P7.14 using the `fir1` function.

**P7.23** Consider an ideal lowpass filter with the cutoff frequency  $\omega_c = 0.3\pi$ . We want to approximate this filter using a frequency-sampling design in which we choose 40 samples.

1. Choose the sample at  $\omega_c$  equal to 0.5, and use the naive design method to compute  $h(n)$ . Determine the minimum stopband attenuation.
2. Now vary the sample at  $\omega_c$ , and determine the optimum value to obtain the largest minimum stopband attenuation.
3. Plot the magnitude responses in dB of the preceding two designs in one plot; comment on the results.

**P7.24** Design the bandstop filter of Problem P7.10 using the frequency-sampling method. Choose the order of the filter appropriately so that there are two samples in the transition band. Use optimum values for these samples. Compare your results with those obtained using the `fir2` function.

**P7.25** Design the bandpass filter of Problem P7.11 using the frequency-sampling method. Choose the order of the filter appropriately so that there are two samples in the transition band. Use optimum values for these samples. Compare your results with those obtained using the `fir2` function.

**P7.26** Design the highpass filter of Problem P7.12 using the frequency-sampling method. Choose the order of the filter appropriately so that there are two samples in the transition band. Use optimum values. Compare your results with those obtained using the `fir2` function.

**P7.27** Consider the filter specifications given in Figure P7.1. Use the `fir2` function and a Hamming window to design a linear-phase FIR filter via the frequency-sampling method. Experiment with the filter length to achieve the required design. Plot the amplitude response of the resulting filter.

**P7.28** Design a bandpass filter using the frequency-sampling method. Choose the order of the filter appropriately so that there is one sample in the transition band. Use optimum value for this sample. The specifications are as follows:

$$\left. \begin{array}{l} \text{lower stopband edge} = 0.3\pi \\ \text{upper stopband edge} = 0.7\pi \end{array} \right\} A_s = 40 \text{ dB}$$

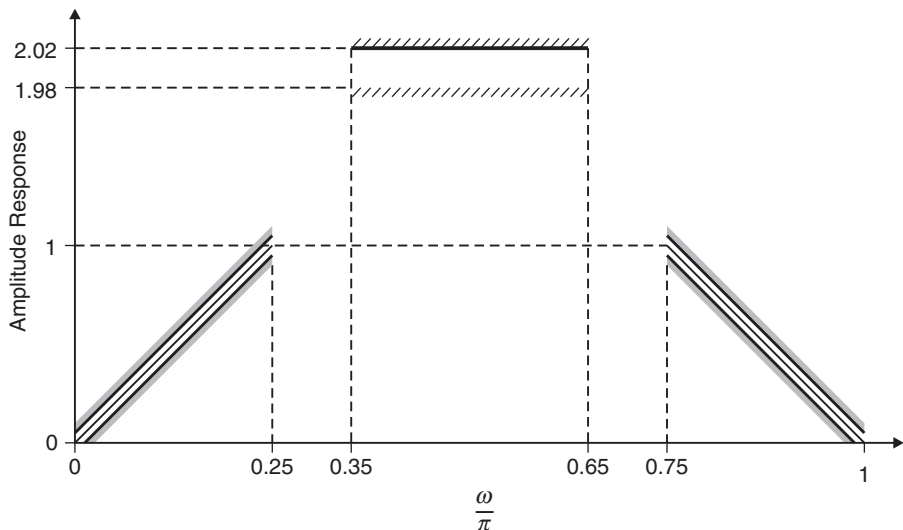


**FIGURE P7.1** Filter specifications for Problem P7.27

$$\left. \begin{array}{l} \text{lower passband edge} = 0.4\pi \\ \text{upper passband edge} = 0.6\pi \end{array} \right\} R_p = 0.5 \text{ dB.}$$

Provide a plot of the log-magnitude response in dB and `stem` plot of the impulse response.

**P7.29** The frequency response of an ideal bandpass filter is given by

$$H_d(e^{j\omega}) = \begin{cases} 0, & 0 \leq |\omega| \leq \pi/3 \\ 1, & \pi/3 \leq |\omega| \leq 2\pi/3 \\ 0, & 2\pi/3 \leq |\omega| \leq \pi \end{cases}$$

1. Determine the coefficients of a 25-tap filter based on the Parks–McClellan algorithm with stopband attenuation of 50 dB. The designed filter should have the smallest possible transition width.
2. Plot the amplitude response of the filter using the function developed in Problem P7.6.

**P7.30** Consider the bandstop filter given in Problem P7.10.

1. Design a linear-phase bandstop FIR filter using the Parks–McClellan algorithm. Note that the length of the filter must be odd. Provide a plot of the impulse response and the magnitude response in dB of the designed filter.
2. Plot the amplitude response of the designed filter and count the total number of extrema in stopband and passbands. Verify this number with the theoretical estimate of the total number of extrema.
3. Compare the order of this filter with those of the filters in Problems P7.10 and P7.24.
4. Verify the operation of the designed filter on the following signal:

$$x(n) = 5 - 5 \cos\left(\frac{\pi n}{2}\right); \quad 0 \leq n \leq 300$$

**P7.31** Using the Parks–McClellan algorithm, design a 25-tap FIR differentiator with slope equal to 1 sample/cycle.

1. Choose the frequency band of interest between  $0.1\pi$  and  $0.9\pi$ . Plot the impulse response and the amplitude response.
2. Generate 100 samples of the sinusoid

$$x(n) = 3 \sin(0.25\pi n), \quad n = 0, \dots, 100$$

and process through the preceding FIR differentiator. Compare the result with the theoretical “derivative” of  $x(n)$ . Note: Don’t forget to take the 12-sample delay of the FIR filter into account.

**P7.32** Design a lowest-order equiripple linear-phase FIR filter to satisfy the specifications given in Figure P7.2. Provide a plot of the amplitude response and a plot of the impulse response.

**P7.33** A digital signal  $x(n)$  contains a sinusoid of frequency  $\pi/2$  and a Gaussian noise  $w(n)$  of zero mean and unit variance; that is,

$$x(n) = 2 \cos \frac{\pi n}{2} + w(n)$$

We want to filter out the noise component using a 50th-order causal and linear-phase FIR filter.

1. Using the Parks–McClellan algorithm, design a narrow bandpass filter with passband width of no more than  $0.02\pi$  and stopband attenuation of at least 30 dB. Note that no other parameters are given and that you have to choose the remaining parameters for the `firpm` function to satisfy the requirements. Provide a plot of the log-magnitude response in dB of the designed filter.
2. Generate 200 samples of the sequence  $x(n)$  and processed through the preceding filter to obtain the output  $y(n)$ . Provide subplots of  $x(n)$  and  $y(n)$  for  $100 \leq n \leq 200$  on one plot and comment on your results.

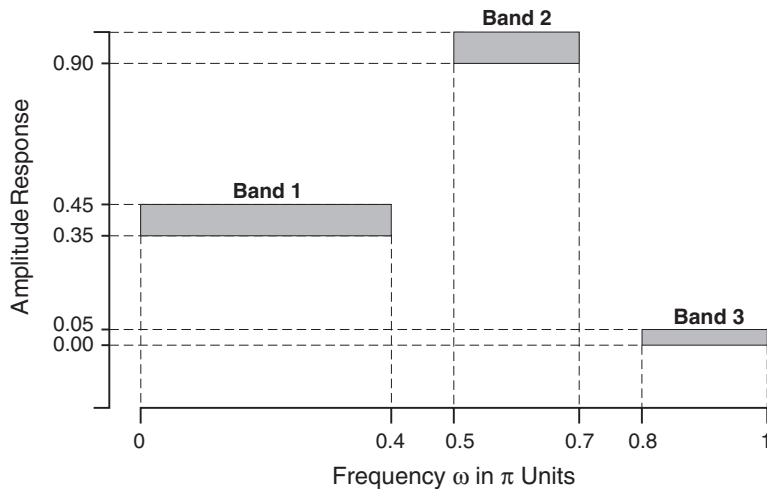


**FIGURE P7.2** Filter specifications for Problem P7.32

**P7.34** Design a minimum-order linear-phase FIR filter, using the Parks–McClellan algorithm, to satisfy the requirements given in Figure P7.1.

1. Provide a plot of the amplitude response with grid lines and axis labeling as shown in Figure P7.1.
2. Generate the following signals:

$$x_1(n) = \cos(0.25\pi n), \quad x_2(n) = \cos(0.5\pi n), \quad x_3(n) = \cos(0.75\pi n); \quad 0 \leq n \leq 100$$

Process these signals through this filter to obtain the corresponding output signals  $y_1(n)$ ,  $y_2(n)$ , and  $y_3(n)$ . Provide stem plots of all input and output signals in one figure.

**P7.35** Design a minimum-order linear-phase FIR filter, using the Parks–McClellan algorithm, to satisfy the requirements given in Figure P7.3. Provide a plot of the amplitude response with grid lines and axis labeling as shown in Figure P7.3.

**P7.36** The specifications on the amplitude response (not to scale) of an FIR filter are given in Figure P7.4.

1. Using a window design approach and a *fixed* window function, design a minimum-length linear-phase FIR filter to satisfy the given requirements. Provide a plot of the amplitude response with grid lines as shown in Figure P7.4.
2. Using a window design approach and the Kaiser window function, design a minimum-length linear-phase FIR filter to satisfy the given requirements. Provide a plot of the amplitude response with grid lines as shown in Figure P7.4.
3. Using a frequency-sampling design approach and with no more than two samples in the transition bands, design a minimum-length linear-phase FIR filter to satisfy the given requirements. Provide a plot of the amplitude response with grid lines as shown in Figure P7.4.
4. Using the Parks–McClellan design approach, design a minimum-length linear-phase FIR filter to satisfy the given requirements. Provide a plot of the amplitude response with grid lines as shown in Figure P7.4.
5. Compare the preceding four design methods in terms of
  - the *order* of the filter,

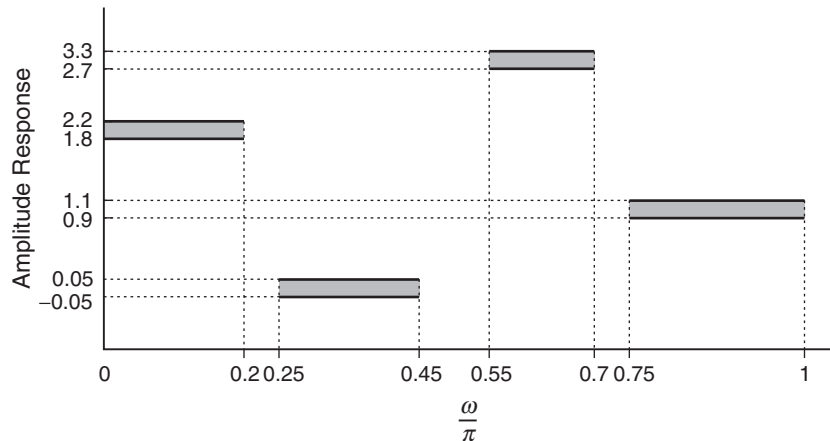


**FIGURE P7.3** Filter specifications for Problem P7.35

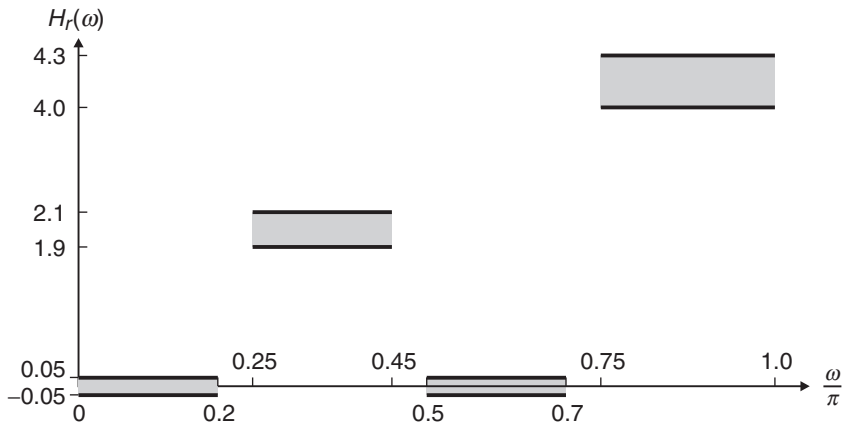


**FIGURE P7.4** Filter specifications for Problem P7.36

- the *exact* band-edge frequencies,
- the *exact* tolerances in each band.

**P7.37** Design a minimum-order linear-phase FIR filter, using the Parks–McClellan algorithm, to satisfy the requirements given in Figure P7.5. Provide a plot of the amplitude response with grid lines as shown in Figure P7.5.

**P7.38** Design a minimum-length linear-phase bandpass filter of Problem P7.9 using the Parks–McClellan algorithm.

1. Plot the impulse response and the magnitude response in dB of the designed filter in one figure plot.
2. Plot the amplitude response of the designed filter and count the total number of extrema in passband and stopbands. Verify this number with the theoretical estimate of the total number of extrema.
3. Compare the order of this filter with that of the filter in Problem P7.9.

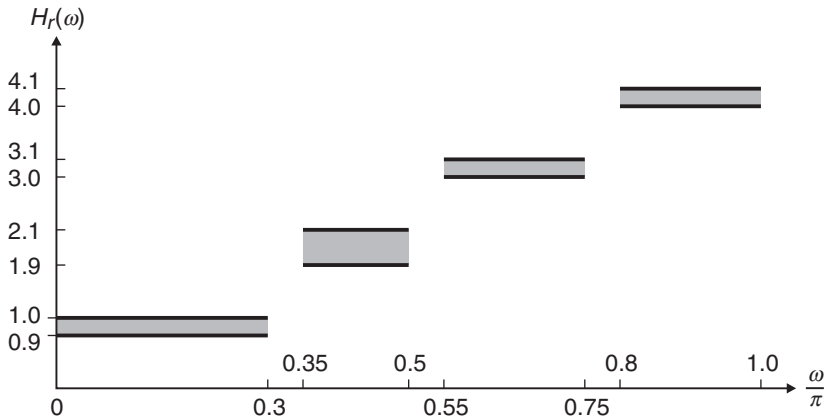


**FIGURE P7.5** Filter specifications for Problem P7.37

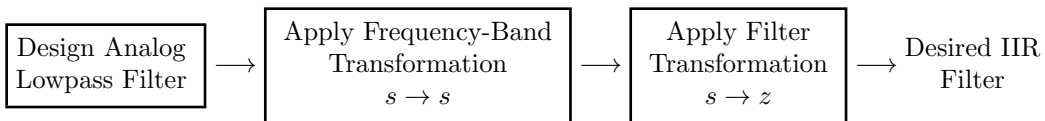
# CHAPTER

# 8

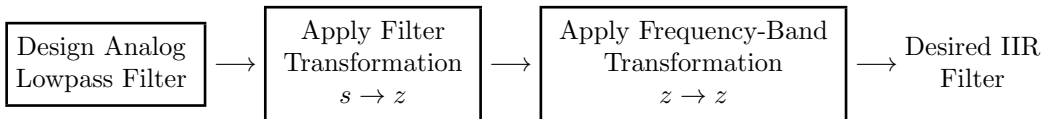
## IIR Filter Design

IIR filters have infinite-duration impulse responses, and hence they can be matched to analog filters, all of which generally have infinitely long impulse responses. Therefore, the basic technique of IIR filter design transforms well-known analog filters into digital filters using *complex-valued* mappings. The advantage of this technique lies in the fact that both analog filter design (AFD) tables and the mappings are available extensively in the literature. This basic technique is called the A/D (analog-to-digital) filter transformation. However, the AFD tables are available only for lowpass filters. We also want to design other frequency-selective filters (highpass, bandpass, bandstop, etc.). To do this, we need to apply frequency-band transformations to lowpass filters. These transformations are also complex-valued mappings, and they are also available in the literature. There are two approaches to this basic technique of IIR filter design:

Approach 1:



Approach 2:



The first approach is used in MATLAB to design IIR filters. A straightforward use of these MATLAB functions does not provide any insight into the design methodology. Therefore, we will study the second approach because it involves the frequency-band transformation in the digital domain. Hence in this IIR filter design technique, we will follow the following steps:

- Design analog lowpass filters.
- Study and apply filter transformations to obtain digital lowpass filters.
- Study and apply frequency-band transformations to obtain other digital filters from digital lowpass filters.

The main problem with these approaches is that we have no control over the phase characteristics of the IIR filter. Hence IIR filter designs will be treated as *magnitude-only* designs. More sophisticated techniques, which can simultaneously approximate both the magnitude and the phase responses, require advanced optimization tools and hence will not be covered in this book.

We begin with a discussion on the analog filter specifications and the properties of the magnitude-squared response used in specifying analog filters. Next, before we delve into basic techniques for general IIR filters, we consider the design of special types of digital filters—for example, resonators, notch filters, comb filters, and so on. This is followed by a brief description of the characteristics of three widely used analog filters: *Butterworth*, *Chebyshev*, and *elliptic* filters. Finally, we will study transformations to convert these prototype analog filters into different frequency-selective digital filters and conclude this chapter with several IIR filter designs using MATLAB.

## 8.1 SOME PRELIMINARIES

---

We discuss two preliminary issues in this section. First, we consider the magnitude-squared response specifications, which are more typical of analog (and hence of IIR) filters. These specifications are given on the *relative linear scale*. Second, we study the properties of the magnitude-squared response.

### 8.1.1 RELATIVE LINEAR SCALE

Let  $H_a(j\Omega)$  be the frequency response of an analog filter. Then the lowpass filter specifications on the magnitude-squared response are given by

$$\begin{aligned} \frac{1}{1 + \epsilon^2} &\leq |H_a(j\Omega)|^2 \leq 1, \quad |\Omega| \leq \Omega_p \\ 0 &\leq |H_a(j\Omega)|^2 \leq \frac{1}{A^2}, \quad \Omega_s \leq |\Omega| \end{aligned} \tag{8.1}$$

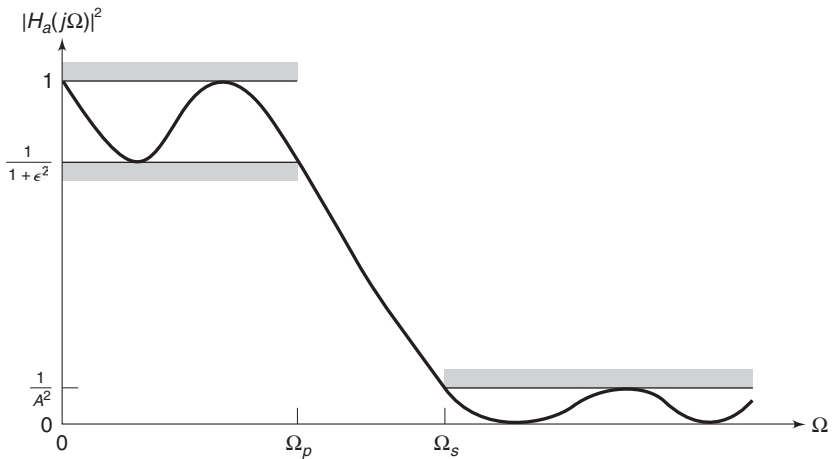


**FIGURE 8.1** Analog lowpass filter specifications

where  $\epsilon$  is a passband *ripple parameter*,  $\Omega_p$  is the passband cutoff frequency in rad/sec,  $A$  is a stopband *attenuation parameter*, and  $\Omega_s$  is the stopband cutoff in rad/sec. These specifications are shown in Figure 8.1, from which we observe that  $|H_a(j\Omega)|^2$  must satisfy

$$\begin{aligned} |H_a(j\Omega_p)|^2 &= \frac{1}{1+\epsilon^2} && \text{at } \Omega = \Omega_p \\ |H_a(j\Omega_s)|^2 &= \frac{1}{A^2} && \text{at } \Omega = \Omega_s \end{aligned} \quad (8.2)$$

The parameters  $\epsilon$  and  $A$  are related to parameters  $R_p$  and  $A_s$ , respectively, of the dB scale. These relations are given by

$$R_p = -10 \log_{10} \frac{1}{1+\epsilon^2} \implies \epsilon = \sqrt{10^{R_p/10} - 1} \quad (8.3)$$

and

$$A_s = -10 \log_{10} \frac{1}{A^2} \implies A = 10^{A_s/20} \quad (8.4)$$

The ripples,  $\delta_1$  and  $\delta_2$ , of the absolute scale are related to  $\epsilon$  and  $A$  by

$$\frac{1-\delta_1}{1+\delta_1} = \sqrt{\frac{1}{1+\epsilon^2}} \implies \epsilon = \frac{2\sqrt{\delta_1}}{1-\delta_1}$$

and

$$\frac{\delta_2}{1+\delta_1} = \frac{1}{A} \implies A = \frac{1+\delta_1}{\delta_2}$$

### 8.1.2 PROPERTIES OF $|H_a(j\Omega)|^2$

Analog filter specifications (8.1), which are given in terms of the magnitude-squared response, contain no phase information. Now to evaluate the  $s$ -domain system function  $H_a(s)$ , consider

$$H_a(j\Omega) = H_a(s)|_{s=j\Omega}$$

Then we have

$$|H_a(j\Omega)|^2 = H_a(j\Omega)H_a^*(j\Omega) = H_a(j\Omega)H_a(-j\Omega) = H_a(s)H_a(-s)|_{s=j\Omega}$$

or

$$H_a(s)H_a(-s) = |H_a(j\Omega)|^2 \Big|_{\Omega=s/j} \quad (8.5)$$

Therefore, the poles and zeros of the magnitude-squared function are distributed in a *mirror-image symmetry* with respect to the  $j\Omega$  axis. Also for real filters, poles and zeros occur in complex conjugate pairs (or mirror-image symmetry with respect to the real axis). A typical pole-zero pattern of  $H_a(s)H_a(-s)$  is shown in Figure 8.2. From this pattern, we can construct  $H_a(s)$ , which is the system function of our analog filter. We want  $H_a(s)$  to represent a *causal* and *stable* filter. Then all poles of  $H_a(s)$  must lie within the left half-plane. Thus we assign all left-half poles of  $H_a(s)H_a(-s)$  to  $H_a(s)$ . However, zeros of  $H_a(s)$  can lie anywhere in the  $s$ -plane. Therefore, they are not uniquely determined unless they all are on the  $j\Omega$  axis. We will choose the zeros of  $H_a(s)H_a(-s)$  lying left to or on the  $j\Omega$  axis as the zeros of  $H_a(s)$ . The resulting filter is then called a *minimum-phase* filter.

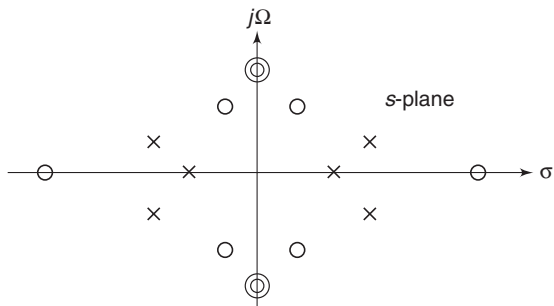


**FIGURE 8.2** Typical pole-zero pattern of  $H_a(s)H_a(-s)$

## 8.2 SOME SPECIAL FILTER TYPES

In this section, we consider the design of several special types of digital filters and describe their frequency response characteristics. We begin by describing the design and characteristics of a digital resonator.

### 8.2.1 DIGITAL RESONATORS

A digital resonator is a special two-pole bandpass filter with a pair of complex-conjugate poles located very near the unit circle, as shown in the left plot of Figure 8.3. The magnitude of the frequency response of the filter is shown in the top right plot of Figure 8.3. The name *resonator* refers to the fact that the filter has a large magnitude response in the vicinity of the pole position. The angle of the pole location determines the resonant frequency of the filter. Digital resonators are useful in many applications, including simple bandpass filtering and speech generation.

Let us consider the design of a digital resonator with a resonant peak at or near  $\omega = \omega_0$ . Hence we select the pole position as

$$p_{1,2} = re^{\pm j\omega_0} \quad (8.6)$$

### Digital Resonator Responses

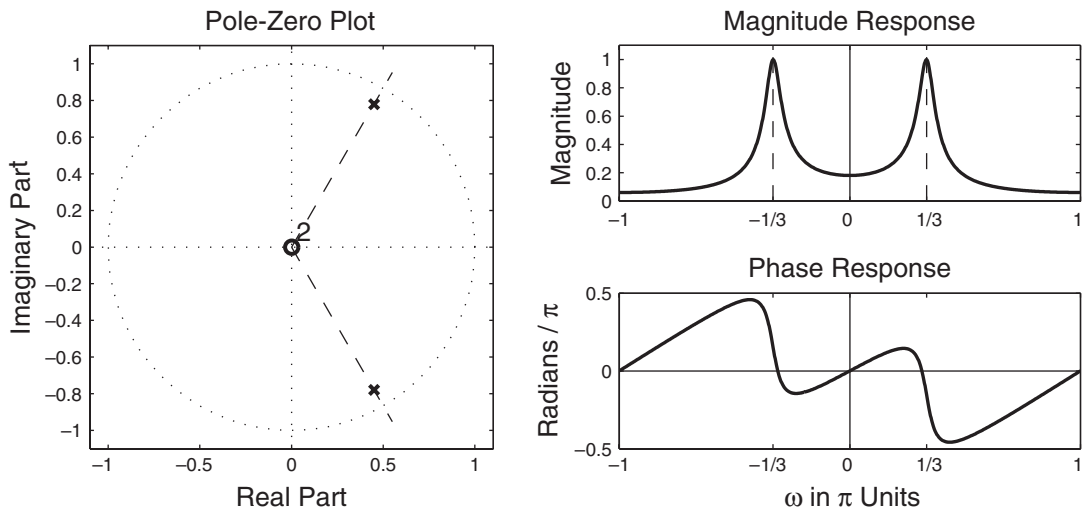


**FIGURE 8.3** Pole positions and frequency response of a digital resonator with  $r = 0.9$  and  $\omega_0 = \pi/3$

The corresponding system function is

$$\begin{aligned} H(z) &= \frac{b_0}{(1 - re^{j\omega_0}z^{-1})(1 - re^{-j\omega_0}z^{-1})} \\ &= \frac{b_0}{1 - (2r \cos \omega_0)z^{-1} + r^2 z^{-2}} \end{aligned} \quad (8.7)$$

where  $b_0$  is a gain parameter. The frequency response of the resonator is

$$H(e^{j\omega}) = \frac{b_0}{[1 - re^{-j(\omega - \omega_0)}][1 - re^{-j(\omega + \omega_0)}]} \quad (8.8)$$

Since  $|H(e^{j\omega})|$  has its peak at or near  $\omega = \omega_0$ , we select the gain parameter  $b_0$  so that  $|H(e^{j\omega_0})| = 1$ . Hence

$$\begin{aligned} |H(e^{j\omega_0})| &= \frac{b_0}{|(1 - r)(1 - re^{-j2\omega_0})|} \\ &= \frac{b_0}{(1 - r)\sqrt{1 + r^2 - 2r \cos 2\omega_0}} \end{aligned} \quad (8.9)$$

Consequently, the desired gain parameter is

$$b_0 = (1 - r)\sqrt{1 + r^2 - 2r \cos 2\omega_0} \quad (8.10)$$

The magnitude of the frequency response  $H(\omega)$  may be expressed as

$$|H(e^{j\omega})| = \frac{b_0}{D_1(\omega)D_2(\omega)} \quad (8.11)$$

where  $D_1(\omega)$  and  $D_2(\omega)$  are given as

$$D_1(\omega) = \sqrt{1 + r^2 - 2r \cos(\omega - \omega_0)} \quad (8.12a)$$

$$D_2(\omega) = \sqrt{1 + r^2 - 2r \cos(\omega + \omega_0)} \quad (8.12b)$$

For a given value of  $r$ ,  $D_1(\omega)$  takes its minimum value  $(1 - r)$  at  $\omega = \omega_0$ , and the product  $D_1(\omega)D_2(\omega)$  attains a minimum at the frequency

$$\omega_r = \cos^{-1} \left( \frac{1 + r^2}{2r} \cos \omega_0 \right) \quad (8.13)$$

which defines precisely the resonant frequency of the filter. Note that when  $r$  is very close to unity,  $\omega_r \approx \omega_0$ , which is the angular position of the pole. Furthermore, as  $r$  approaches unity, the resonant peak becomes sharper (narrower) because  $D_1(\omega)$  changes rapidly in the vicinity of  $\omega_0$ .

A quantitative measure of the width of the peak is the 3 dB bandwidth of the filter, denoted as  $\Delta(\omega)$ . For values of  $r$  close to unity,

$$\Delta\omega \approx 2(1 - r) \quad (8.14)$$

Figure 8.3 illustrates the magnitude and phase responses of a digital resonator with  $\omega_0 = \pi/3$ ,  $r = 0.90$ . Note that the phase response has its greatest rate of change near the resonant frequency  $\omega_r \approx \omega_0 = \pi/3$ .

This resonator has two zeros at  $z = 0$ . Instead of placing zeros at the origin, an alternative choice is to locate the zeros at  $z = 1$  and  $z = -1$ . This choice completely eliminates the response of the filter at the frequencies  $\omega = 0$  and  $\omega = \pi$ , which may be desirable in some applications. The corresponding resonator has the system function

$$\begin{aligned} H(z) &= \frac{G(1 - z^{-1})(1 + z^{-1})}{(1 - re^{j\omega_0}z^{-1})(1 - re^{-j\omega_0}z^{-1})} \\ &= G \frac{1 - z^{-2}}{1 - (2r \cos \omega_0)z^{-1} + r^2 z^{-2}} \end{aligned} \quad (8.15)$$

and the frequency response characteristic

$$H(e^{j\omega}) = G \frac{1 - e^{-j2\omega}}{[1 - re^{j(\omega_0 - \omega)}][1 - re^{-j(\omega_0 + \omega)}]} \quad (8.16)$$

where  $G$  is a gain parameter that is selected so that  $|H(e^{j\omega_0})| = 1$ .

The introduction of zeros at  $z = \pm 1$  alters both the magnitude and phase response of the resonator. The magnitude response may be expressed as

$$|H(e^{j\omega})| = G \frac{N(\omega)}{D_1(\omega)D_2(\omega)} \quad (8.17)$$

where  $N(\omega)$  is defined as

$$N(\omega) = \sqrt{2(1 - \cos 2\omega)} \quad (8.18)$$

Due to the presence of the zeros at  $z = \pm 1$ , the resonant frequency of the resonator is altered from the expression given by (8.13). The bandwidth of the filter is also altered. Although exact values for these two parameters are rather tedious to derive, we can easily compute the frequency response when the zeros are at  $z = \pm 1$  and  $z = 0$  and compare the results.

Figure 8.4 illustrates the magnitude and phase responses for the cases  $z = \pm 1$  and  $z = 0$ , for pole location at  $\omega = \pi/3$  and  $r = 0.90$ . We observe that the resonator with  $z = \pm 1$  has a slightly smaller bandwidth than the resonator with zeros at  $z = 0$ . In addition, there appears to be a very small shift in the resonant frequency between the two cases.

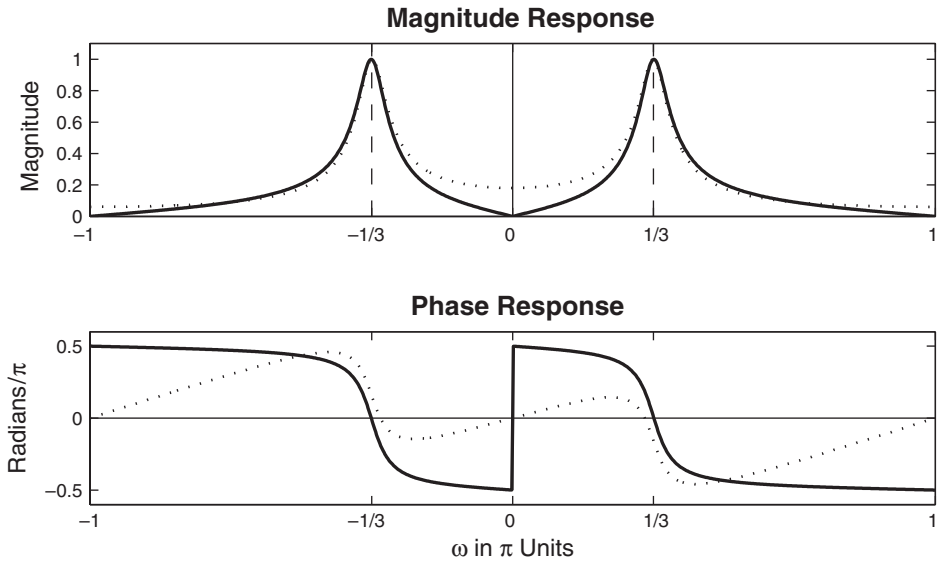


**FIGURE 8.4** Magnitude and phase responses of digital resonator with zeros at  $z = \pm 1$  (solid lines) and  $z = 0$  (dotted lines) for  $r = 0.9$  and  $\omega_0 = \pi/3$

### 8.2.2 NOTCH FILTERS

A notch filter is a filter that contains one or more deep notches or, ideally, perfect nulls in its frequency response. Figure 8.5 illustrates the frequency response of a notch filter with a null at the frequency  $\omega = \omega_0$ . Notch filters are useful in many applications where specific frequency components must be eliminated. For example, instrumentation systems require that the power line frequency of 60 Hz and its harmonics be eliminated.

To create a null in the frequency response of a filter at a frequency  $\omega_0$ , we simply introduce a pair of complex-conjugate zeros on the unit circle at the angle  $\omega_0$ . Hence the zeros are selected as

$$z_{1,2} = e^{\pm j\omega_0} \quad (8.19)$$

Then the system function for the notch filter is

$$\begin{aligned} H(z) &= b_0(1 - e^{j\omega_0}z^{-1})(1 - e^{-j\omega_0}z^{-1}) \\ &= b_0(1 - (2 \cos \omega_0)z^{-1} + z^{-2}) \end{aligned} \quad (8.20)$$

where  $b_0$  is a gain factor. Figure 8.6 illustrates the magnitude response of a notch filter having a null at  $\omega = \pi/4$ .

The major problem with this notch filter is that the notch has a relatively large bandwidth, which means that other frequency components

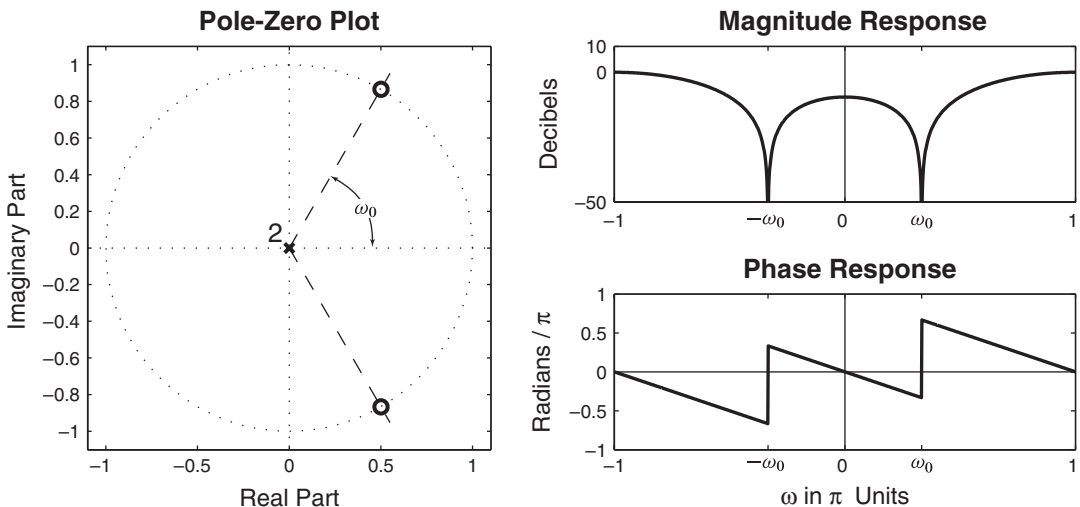


**FIGURE 8.5** Frequency response of a typical notch filter

around the desired null are severely attenuated. To reduce the bandwidth of the null, we may resort to the more sophisticated, longer FIR filter designed according to the optimum equiripple design method described in Chapter 7. Alternatively, we could attempt to improve the frequency response of the filter by introducing poles in the system function.

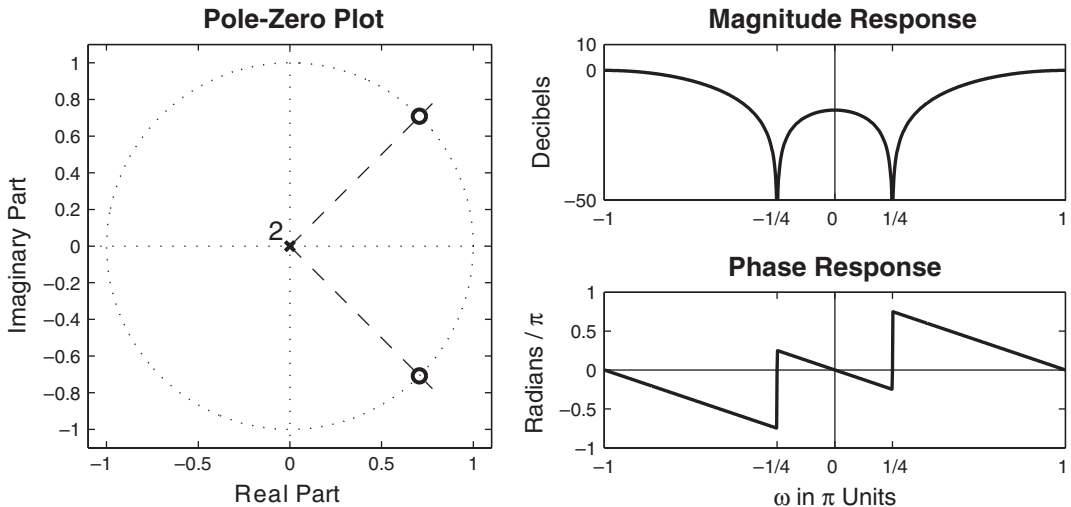


**FIGURE 8.6** Frequency response of a notch filter with  $\omega_0 = \pi/4$

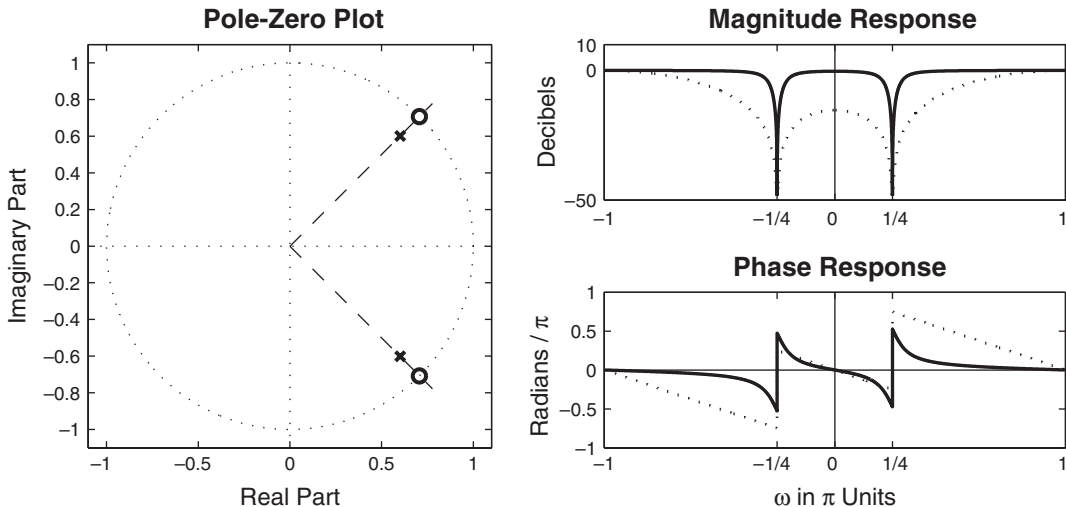


**FIGURE 8.7** Magnitude and phase responses of notch filter with poles (solid lines) and without poles (dotted lines) for  $\omega_0 = \pi/4$  and  $r = 0.85$

In particular, suppose that we select the poles at

$$p_{1,2} = re^{\pm j\omega_0} \quad (8.21)$$

Hence the system function becomes

$$H(z) = b_0 \frac{1 - (2 \cos \omega_0)z^{-1} + z^2}{1 - (2r \cos \omega_0)z^{-1} + r^2 z^{-2}} \quad (8.22)$$

The magnitude of the frequency response  $|H(e^{j\omega})|$  of this filter is illustrated in Figure 8.7 for  $\omega_0 = \pi/4$  and  $r = 0.85$ . Also plotted in this figure is the frequency response without the poles. We observe that the effect of the pole is to introduce a resonance in the vicinity of the null and, thus, to reduce the bandwidth of the notch. In addition to reducing the bandwidth of the notch, the introduction of a pole in the vicinity of the null may result in a small ripple in the passband of the filter due to the resonance created by the pole.

### 8.2.3 COMB FILTERS

In its simplest form, a comb filter may be viewed as a notch filter in which the nulls occur periodically across the frequency band, hence the analogy to an ordinary comb that has periodically spaced teeth. Comb filters are used in many practical systems, including the rejections of power-line harmonics and the suppression of clutter from fixed objects in moving-target indicator (MTI) radars.

We can create a comb filter by taking our FIR filter with system function

$$H(z) = \sum_{k=0}^M h(k)z^{-k} \quad (8.23)$$

and replacing  $z$  by  $z^L$ , where  $L$  is a positive integer. Thus the new FIR filter has the system function

$$H_L(z) = \sum_{k=0}^M h(k)z^{-kL} \quad (8.24)$$

If the frequency response of the original FIR filter is  $H(e^{j\omega})$ , the frequency response of the filter given by (8.24) is

$$H_L(e^{j\omega}) = \sum_{k=0}^M h(k)e^{-jkL\omega} = H(e^{jL\omega}) \quad (8.25)$$

Consequently, the frequency response characteristic  $H_L(e^{j\omega})$  is an  $L$ -order repetition of  $H(e^{j\omega})$  in the range  $0 \leq \omega \leq 2\pi$ . Figure 8.8 illustrates the relationship between  $H_L(e^{j\omega})$  and  $H(e^{j\omega})$  for  $L = 4$ . The introduction of a pole at each notch may be used to narrow the bandwidth of each notch, as just described.

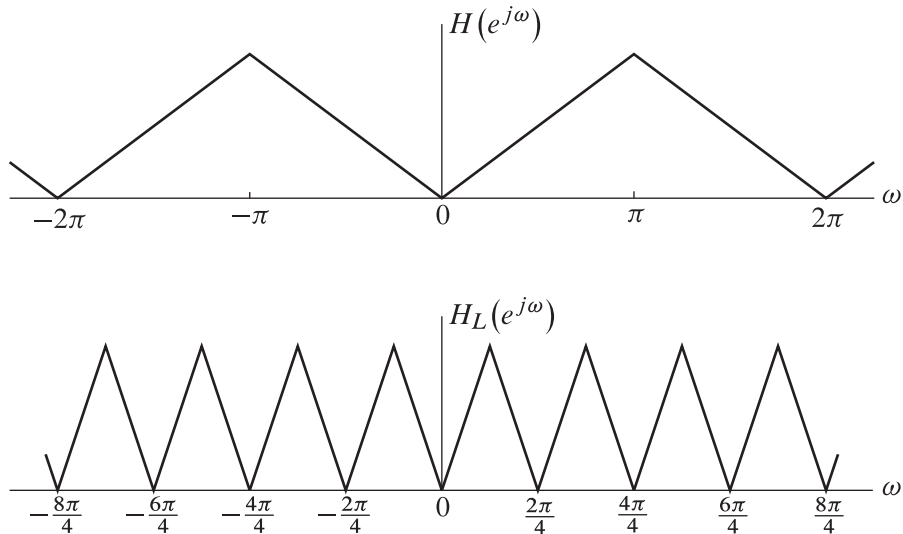


**FIGURE 8.8** Comb filters with frequency response  $H_L(e^{j\omega})$  obtained from  $H(e^{j\omega})$  for  $L = 4$

### 8.2.4 ALLPASS FILTERS

An *allpass filter* is characterized by a system function that has a constant magnitude response for all frequencies, that is,

$$|H(e^{j\omega})| = 1, \quad 0 \leq \omega \leq \pi \quad (8.26)$$

A simple example of an allpass system is a system that introduces a pure delay to an input signal, that is,

$$H(z) = z^{-k} \quad (8.27)$$

This system passes all frequency components of an input signal without any frequency-dependent attenuation. It simply delays all frequency components by  $k$  samples.

A more general characterization of an allpass filter is one having a system function of the form

$$H(z) = \frac{a_N + a_{N-1}z^{-1} + \cdots + a_1z^{-N+1} + z^{-N}}{1 + a_1z^{-1} + \cdots + a_{N-1}z^{-N+1} + a_Nz^{-N}} \quad (8.28)$$

which may be expressed in the compact form as

$$H(z) = z^{-N} \frac{A(z^{-1})}{A(z)} \quad (8.29)$$

where

$$A(z) = \sum_{k=0}^N a_k z^{-k}, \quad a_0 = 1 \quad (8.30)$$

We observe that

$$|H(e^{j\omega})|^2 = H(z)H(z^{-1})|_{z=e^{j\omega}} = 1 \quad (8.31)$$

for all frequencies. Hence the system is allpass.

From the form of  $H(z)$  given by (8.28), we observe that if  $z_0$  is a pole of  $H(z)$ , then  $1/z_0$  is a zero of  $H(z)$ . That is, the poles and zeros are reciprocals of one another. Figure 8.9 illustrates the typical pole-zero pattern for a single-pole, single-zero filter and a two-pole, two-zero filter. Graphs of the magnitude and phase characteristics of these two filters are shown in Figure 8.10 for  $a = 0.6$  and  $r = 0.9$ ,  $\omega_0 = \pi/4$ , where  $A(z)$  for the two filters is, respectively, given as

$$A(z) = 1 + az^{-1} \quad (8.32a)$$

$$A(z) = 1 - (2r \cos \omega_0)z^{-1} + r^2 z^{-2} \quad (8.32b)$$

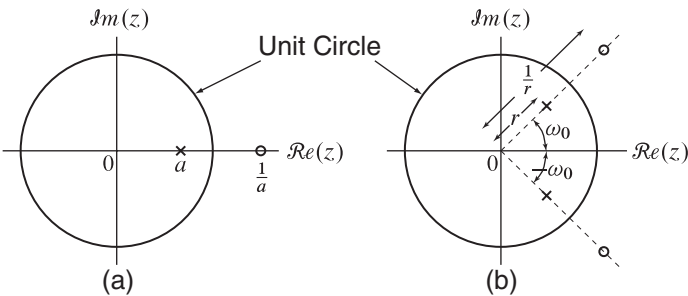


**FIGURE 8.9** Pole-zero locations for (a) one-pole and (b) two-pole allpass filter

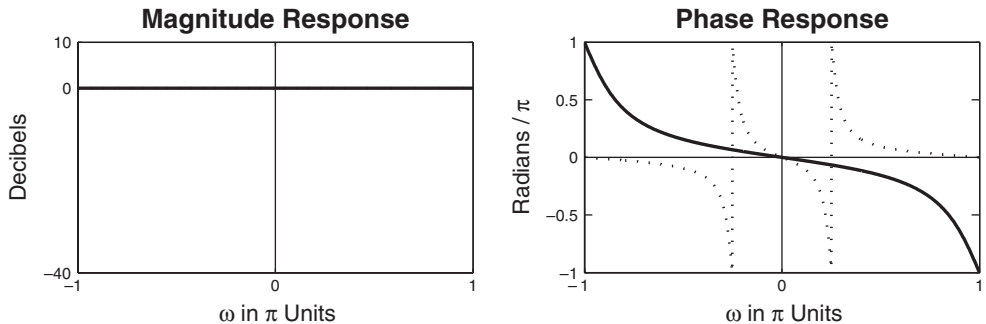


**FIGURE 8.10** Magnitude and phase responses for one-pole (solid line) and two-pole (dotted line) allpass filters

The general form for the system function of an allpass filter with real coefficients may be expressed in factored form as

$$H(z) = \prod_{k=1}^{N_R} \frac{z^{-1} - \alpha_k}{1 - \alpha_k z^{-1}} \prod_{k=1}^{N_C} \frac{(z^{-1} - \beta_k)(z^{-1} - \beta_k^*)}{(1 - \beta_k z^{-1})(1 - \beta_k^* z^{-1})} \quad (8.33)$$

where  $N_R$  is the number of real poles and zeros and  $N_C$  is the number of complex-conjugate pairs of poles and zeros. For a causal and stable system, we require that  $|\alpha_k| < 1$  and  $|\beta_k| < 1$ .

Allpass filters are usually employed as phase equalizers. When placed in cascade with a system that has an undesirable phase response, a phase equalizer is designed to compensate for the poor phase characteristics of the system and thus result in an overall linear phase system.

### 8.2.5 DIGITAL SINUSOIDAL OSCILLATORS

A digital sinusoidal oscillator can be viewed as a limiting form of a two-pole resonator for which the complex-conjugate poles are located on the

unit circle. From our previous discussion of resonators, the system function for a resonator with poles at  $re \pm j\omega_0$  is

$$H(z) = \frac{b_0}{1 - (2r \cos \omega_0)z^{-1} + r^2 z^{-2}} \quad (8.34)$$

When we set  $r = 1$  and select the gain parameter  $b_0$  as

$$b_0 = A \sin \omega_0 \quad (8.35)$$

the system function becomes

$$H(z) = \frac{A \sin \omega_0}{1 - (2 \cos \omega_0)z^{-1} + z^{-2}} \quad (8.36)$$

and the corresponding impulse response of the system becomes

$$h(n) = A \sin((n+1)\omega_0) u(n) \quad (8.37)$$

Thus this system generates a sinusoidal signal of frequency  $\omega_0$  when excited by an impulse  $\delta(n) = 1$ .

The block diagram representation of the system function given by (8.36) is illustrated in Figure 8.11. The corresponding difference equation for this system is

$$y(n) = (2 \cos \omega_0) y(n-1) - y(n-2) + b_0 \delta(n) \quad (8.38)$$

where  $b_0 = A \sin \omega_0$ .

Note that the sinusoidal oscillation obtained from the difference equation in (8.38) can also be obtained by setting the input to zero and setting the initial conditions to  $y(-1) = 0$ ,  $y(-2) = -A \sin \omega_0$ . Thus the zero-input response to the second-order system described by the homogeneous difference equation

$$y(n) = (2 \cos \omega_0) y(n-1) - y(n-2) \quad (8.39)$$

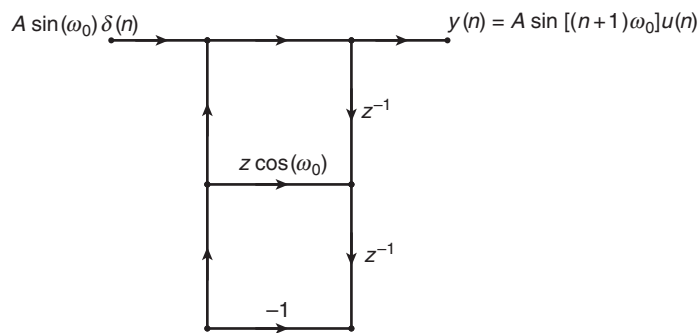


**FIGURE 8.11** Digital sinusoidal oscillator

with initial conditions  $y(-1) = 0$ ,  $y(-2) = -A \sin \omega_0$  is exactly the same as the response of (8.38) to an impulse excitation. In fact, the homogeneous difference equation in (8.39) can be obtained directly from the trigonometric identity

$$\sin \alpha + \sin \beta = 2 \sin\left(\frac{\alpha + \beta}{2}\right) \cos\left(\frac{\alpha - \beta}{2}\right) \quad (8.40)$$

where, by definition,  $\alpha = (n+1)\omega_0$ ,  $\beta = (n-1)\omega_0$ , and  $y(n) = \sin(n+1)\omega_0$ .

In practical applications involving modulation of two sinusoidal carrier signals in phase quadrature, there is a need to generate the sinusoids  $A \sin \omega_0 n$  and  $A \cos \omega_0 n$ . These quadrature carrier signals can be generated by the so-called coupled-form oscillator, which can be obtained with the aid of the trigonometric formulas

$$\cos(\alpha + \beta) = \cos \alpha \cos \beta - \sin \alpha \sin \beta \quad (8.41)$$

$$\sin(\alpha + \beta) = \sin \alpha \cos \beta + \cos \alpha \sin \beta \quad (8.42)$$

where by definition,  $\alpha = n\omega_0$ ,  $\beta = \omega_0$ ,  $y_c(n) = \cos(n+1)\omega_0$ , and  $y_s(n) = \sin(n+1)\omega_0$ . Thus, with substitution of these quantities into the two trigonometric identities, we obtain the two coupled difference equations

$$y_c(n) = (\cos \omega_0) y_c(n-1) - (\sin \omega_0) y_s(n-1) \quad (8.43)$$

$$y_s(n) = (\sin \omega_0) y_c(n-1) + (\cos \omega_0) y_s(n-1) \quad (8.44)$$

The structure for the realization of the coupled-form oscillator is illustrated in Figure 8.12. Note that this is a two-output system that does not require any input excitation, but it does require setting the initial conditions  $y_c(-1) = A \cos \omega_0$  and  $y_s(-1) = -A \sin \omega_0$  in order to begin its self-sustaining oscillations.

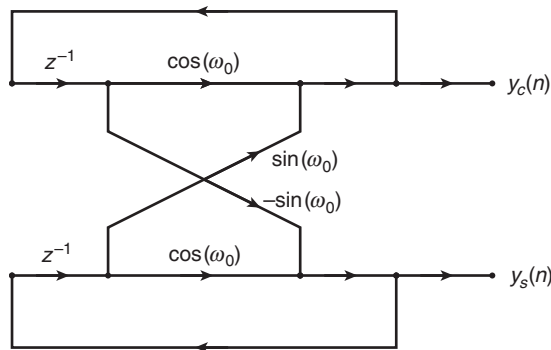


**FIGURE 8.12** Realization of the coupled form oscillator

## 8.3 CHARACTERISTICS OF PROTOTYPE ANALOG FILTERS

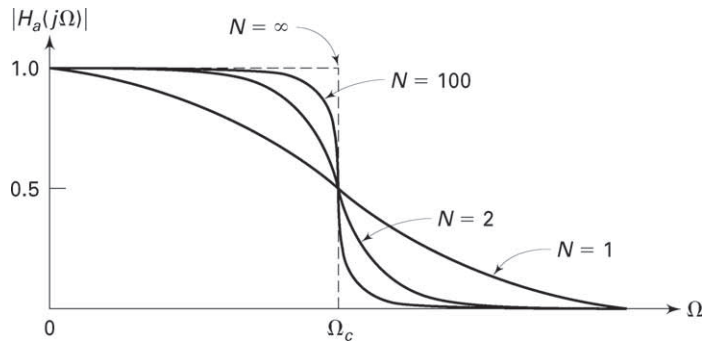
IIR filter design techniques rely on existing analog filters to obtain digital filters. We designate these analog filters as *prototype* filters. Three prototypes are widely used in practice. In this section, we briefly summarize the characteristics of the lowpass versions of these prototypes: Butterworth lowpass, Chebyshev lowpass (Type I and II), and Elliptic lowpass. Although we will use MATLAB functions to design these filters, it is necessary to learn the characteristics of these filters so that we can use proper parameters in MATLAB functions to obtain correct results.

### 8.3.1 BUTTERWORTH LOWPASS FILTERS

This filter is characterized by the property that its magnitude response is flat in both passband and stopband. The magnitude-squared response of an  $N$ th-order lowpass filter is given by

$$|H_a(j\Omega)|^2 = \frac{1}{1 + \left(\frac{\Omega}{\Omega_c}\right)^{2N}} \quad (8.45)$$

where  $N$  is the order of the filter and  $\Omega_c$  is the cutoff frequency in rad/sec. The plot of the magnitude-squared response is as follows.



From this plot, we can observe the following properties:

- At  $\Omega = 0$ ,  $|H_a(j0)|^2 = 1$  for all  $N$ .
- At  $\Omega = \Omega_c$ ,  $|H_a(j\Omega_c)|^2 = \frac{1}{2}$  for all  $N$ , which implies a 3 dB attenuation at  $\Omega_c$ .
- $|H_a(j\Omega)|^2$  is a monotonically decreasing function of  $\Omega$ .

- $|H_a(j\Omega)|^2$  approaches an ideal lowpass filter as  $N \rightarrow \infty$ .
- $|H_a(j\Omega)|^2$  is *maximally flat* at  $\Omega = 0$  since derivatives of all orders exist and are equal to zero.

To determine the system function  $H_a(s)$ , we put (8.45) in the form of (8.5) to obtain

$$H_a(s)H_a(-s) = |H_a(j\Omega)|^2 \Big|_{\Omega=s/j} = \frac{1}{1 + \left(\frac{s}{j\Omega_c}\right)^{2N}} = \frac{(j\Omega)^{2N}}{s^{2N} + (j\Omega_c)^{2N}} \quad (8.46)$$

The roots of the denominator polynomial (or poles of  $H_a(s)H_a(-s)$ ) from (8.46) are given by

$$p_k = (-1)^{\frac{1}{2N}}(j\Omega) = \Omega_c e^{j\frac{\pi}{2N}(2k+N+1)}, \quad k = 0, 1, \dots, 2N-1 \quad (8.47)$$

An interpretation of (8.47) is that

- there are  $2N$  poles of  $H_a(s)H_a(-s)$ , which are equally distributed on a circle of radius  $\Omega_c$  with angular spacing of  $\pi/N$  radians;
- for  $N$  odd the poles are given by  $p_k = \Omega_c e^{jk\pi/N}$ ,  $k = 0, 1, \dots, 2N-1$ ;
- for  $N$  even the poles are given by  $p_k = \Omega_c e^{j(\frac{\pi}{2N} + \frac{k\pi}{N})}$ ,  $k = 0, 1, \dots, 2N-1$ ;
- the poles are symmetrically located with respect to the  $j\Omega$  axis;
- a pole never falls on the imaginary axis, and falls on the real axis only if  $N$  is odd.

As an example, the poles of third- and fourth-order Butterworth filters are shown in Figure 8.13.

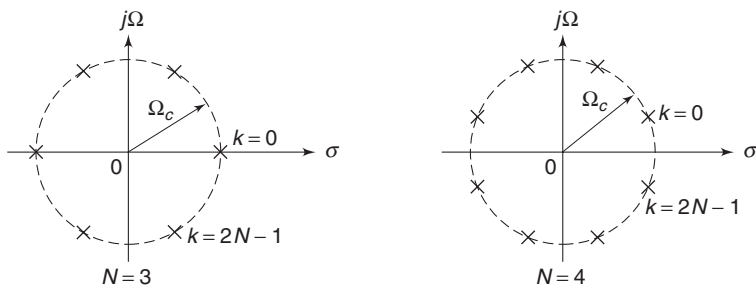


**FIGURE 8.13** Pole plots for Butterworth filters

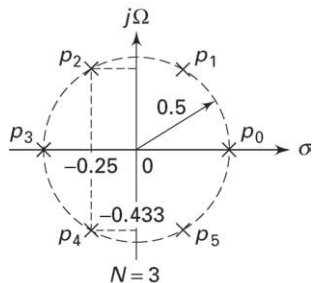


**FIGURE 8.14** Pole plot for Example 8.1

A stable and causal filter  $H_a(s)$  can now be specified by selecting poles in the left half-plane, and  $H_a(s)$  can be written in the form

$$H_a(s) = \frac{\Omega_c^N}{\prod_{\text{LHP poles}} (s - p_k)} \quad (8.48)$$

- **EXAMPLE 8.1** Given that  $|H_a(j\Omega)|^2 = \frac{1}{1 + 64\Omega^6}$ , determine the analog filter system function  $H_a(s)$ .

#### Solution

From the given magnitude-squared response,

$$|H_a(j\Omega)|^2 = \frac{1}{1 + 64\Omega^6} = \frac{1}{1 + \left(\frac{\Omega}{0.5}\right)^{2(3)}}$$

Comparing this with expression (8.45), we obtain  $N = 3$  and  $\Omega_c = 0.5$ . The poles of  $H_a(s)H_a(-s)$  are as shown in Figure 8.14.

Hence

$$\begin{aligned} H_a(j\Omega) &= \frac{\Omega_c^3}{(s - p_2)(s - p_3)(s - p_4)} \\ &= \frac{1/8}{(s + 0.25 - j0.433)(s + 0.5)(s + 0.25 + j0.433)} \\ &= \frac{0.125}{(s + 0.5)(s^2 + 0.5s + 0.25)} \end{aligned}$$

□

### 8.3.2 MATLAB IMPLEMENTATION

MATLAB provides a function called `[z,p,k]=buttap(N)` to design a *normalized* (i.e.,  $\Omega_c = 1$ ) Butterworth analog prototype filter of order  $N$ ,

which returns zeros in  $z$  array, poles in  $p$  array, and the gain value  $k$ . However, we need an unnormalized Butterworth filter with arbitrary  $\Omega_c$ . From Example 8.1, we observe that there are no zeros and that the poles of the unnormalized filter are on a circle with radius  $\Omega_c$  instead of on a unit circle. This means that we have to scale the array  $p$  of the normalized filter by  $\Omega_c$  and the gain  $k$  by  $\Omega_c^N$ . In the following function, called `U_buttap(N,Omegac)`, we design the unnormalized Butterworth analog prototype filter.

```
function [b,a] = u_buttap(N,Omegac);
% Unnormalized Butterworth analog lowpass filter prototype
%
% [b,a] = u_buttap(N,Omegac);
%     b = numerator polynomial coefficients of Ha(s)
%     a = denominator polynomial coefficients of Ha(s)
%     N = Order of the Butterworth Filter
% Omegac = Cutoff frequency in radians/sec
%
[z,p,k] = buttap(N);
p = p*Omegac;
k = k*Omegac^N;
B = real(poly(z));
b0 = k; b = k*B; a = real(poly(p));
```

This function provides a direct form (or numerator-denominator) structure. Often, we also need a cascade form structure. In Chapter 6, we have already studied how to convert a direct form into a cascade form. The following `sdir2cas` function describes the procedure that is suitable for analog filters.

```
function [C,B,A] = sdir2cas(b,a);
% DIRECT form to CASCADE form conversion in s-plane
%
% [C,B,A] = sdir2cas(b,a)
%   C = gain coefficient
%   B = K by 3 matrix of real coefficients containing bk's
%   A = K by 3 matrix of real coefficients containing ak's
%   b = numerator polynomial coefficients of DIRECT form
%   a = denominator polynomial coefficients of DIRECT form
%
Na = length(a)-1; Nb = length(b)-1;
```

```
% Compute gain coefficient C
b0 = b(1); b = b/b0; a0 = a(1); a = a/a0; C = b0/a0;
%
% Denominator second-order sections:
p= cplxpair(roots(a)); K = floor(Na/2);
if K*2 == Na      % Computation when Na is even
    A = zeros(K,3);
    for n=1:2:Na
        Arow = p(n:1:n+1,:); Arow = poly(Arow);
        A(fix((n+1)/2),:) = real(Arow);
    end

elseif Na == 1    % Computation when Na = 1
    A = [0 real(poly(p))];

else             % Computation when Na is odd and > 1
    A = zeros(K+1,3);
    for n=1:2:2*K
        Arow = p(n:1:n+1,:); Arow = poly(Arow);
        A(fix((n+1)/2),:) = real(Arow);
    end
    A(K+1,:) = [0 real(poly(p(Na)))];
end

% Numerator second-order sections:
z = cplxpair(roots(b)); K = floor(Nb/2);
if Nb == 0          % Computation when Nb = 0
    B = [0 0 poly(z)];

elseif K*2 == Nb    % Computation when Nb is even
    B = zeros(K,3);
    for n=1:2:Nb
        Brow = z(n:1:n+1,:); Brow = poly(Brow);
        B(fix((n+1)/2),:) = real(Brow);
    end

elseif Nb == 1      % Computation when Nb = 1
    B = [0 real(poly(z))];

else               % Computation when Nb is odd and > 1
    B = zeros(K+1,3);
    for n=1:2:2*K
        Brow = z(n:1:n+1,:); Brow = poly(Brow);
        B(fix((n+1)/2),:) = real(Brow);
    end
    B(K+1,:) = [0 real(poly(z(Nb)))];
end
```

- EXAMPLE 8.2** Design a third-order Butterworth analog prototype filter with  $\Omega_c = 0.5$  given in Example 8.1.

**Solution**

MATLAB script:

```
>> N = 3; OmegaC = 0.5; [b,a] = u_buttap(N,OmegaC);
>> [C,B,A] = sdir2cas(b,a)
C = 0.1250
B = 0      0      1
A = 1.0000  0.5000  0.2500
          0      1.0000  0.5000
```

The cascade form coefficients agree with those in Example 8.1. □

### 8.3.3 DESIGN EQUATIONS

The analog lowpass filter is specified by the parameters  $\Omega_p$ ,  $R_p$ ,  $\Omega_s$ , and  $A_s$ . Therefore, the essence of the design in the case of Butterworth filter is to obtain the order  $N$  and the cutoff frequency  $\Omega_c$ , given these specifications. We want

- at  $\Omega = \Omega_p$ ,  $-10 \log_{10} |H_a(j\Omega)|^2 = R_p$ , or

$$-10 \log_{10} \left( \frac{1}{1 + \left( \frac{\Omega_p}{\Omega_c} \right)^{2N}} \right) = R_p$$

- and
- at  $\Omega = \Omega_s$ ,  $-10 \log_{10} |H_a(j\Omega)|^2 = A_s$ , or

$$-10 \log_{10} \left( \frac{1}{1 + \left( \frac{\Omega_s}{\Omega_c} \right)^{2N}} \right) = A_s$$

Solving these two equations for  $N$  and  $\Omega_c$ , we have

$$N = \frac{\log_{10} [(10^{R_p/10} - 1) / (10^{A_s/10} - 1)]}{2 \log_{10} (\Omega_p/\Omega_s)}$$

In general,  $N$  will not be an integer. Since we want  $N$  to be an integer, we must choose

$$N = \left\lceil \frac{\log_{10} [(10^{R_p/10} - 1) / (10^{A_s/10} - 1)]}{2 \log_{10} (\Omega_p/\Omega_s)} \right\rceil \quad (8.49)$$

where the operation  $\lceil x \rceil$  means “choose the smallest integer larger than  $x$ ”—for example,  $\lceil 4.5 \rceil = 5$ . Since the actual  $N$  chosen is larger than required, specifications can be either met or exceeded either at  $\Omega_p$  or at  $\Omega_s$ . To satisfy the specifications exactly at  $\Omega_p$ ,

$$\Omega_c = \frac{\Omega_p}{\sqrt[2N]{(10^{R_p/10} - 1)}} \quad (8.50)$$

or, to satisfy the specifications exactly at  $\Omega_s$ ,

$$\Omega_c = \frac{\Omega_s}{\sqrt[2N]{(10^{A_s/10} - 1)}} \quad (8.51)$$

**EXAMPLE 8.3** Design a lowpass Butterworth filter to satisfy the following specifications.

Passband cutoff:  $\Omega_p = 0.2\pi$ ; Passband ripple:  $R_p = 7$  dB

Stopband cutoff:  $\Omega_s = 0.3\pi$ ; Stopband ripple:  $A_s = 16$  dB

**Solution**

From (8.49),

$$N = \left\lceil \frac{\log_{10} \left[ (10^{0.7} - 1) / (10^{1.6} - 1) \right]}{2 \log_{10} (0.2\pi/0.3\pi)} \right\rceil = \lceil 2.79 \rceil = 3$$

To satisfy the specifications exactly at  $\Omega_p$ , from (8.50) we obtain

$$\Omega_c = \frac{0.2\pi}{\sqrt[6]{(10^{0.7} - 1)}} = 0.4985$$

To satisfy specifications exactly at  $\Omega_s$ , from (8.51) we obtain

$$\Omega_c = \frac{0.3\pi}{\sqrt[6]{(10^{1.6} - 1)}} = 0.5122$$

Now we can choose any  $\Omega_c$  between the above two numbers. Let us choose  $\Omega_c = 0.5$ . We have to design a Butterworth filter with  $N = 3$  and  $\Omega_c = 0.5$ , which we did in Example 8.1. Hence

$$H_a(j\Omega) = \frac{0.125}{(s + 0.5)(s^2 + 0.5s + 0.25)}$$

□

### 8.3.4 MATLAB IMPLEMENTATION

The preceding design procedure can be implemented in MATLAB as a simple function. Using the `U_buttap` function, we provide the `afd_but` function to design an analog Butterworth lowpass filter, given its specifications. This function uses (8.50).

```
function [b,a] = afd_but(Wp,Ws,Rp,As);
% Analog lowpass filter design: Butterworth
%
% [b,a] = afd_but(Wp,Ws,Rp,As);
% b = numerator coefficients of Ha(s)
% a = denominator coefficients of Ha(s)
% Wp = passband-edge frequency in rad/sec; Wp > 0
% Ws = stopband-edge frequency in rad/sec; Ws > Wp > 0
% Rp = passband ripple in +dB; (Rp > 0)
% As = stopband attenuation in +dB; (As > 0)
%
if Wp <= 0
    error('Passband edge must be larger than 0')
end
if Ws <= Wp
    error('Stopband edge must be larger than Passband edge')
end
if (Rp <= 0) | (As < 0)
    error('PB ripple and/or SB attenuation must be larger than 0')
end

N = ceil((log10((10^(Rp/10)-1)/(10^(As/10)-1)))/(2*log10(Wp/Ws)));
fprintf('\n*** Butterworth Filter Order = %2.0f \n',N)
OmegaC = Wp/((10^(Rp/10)-1)^(1/(2*N)));
[b,a]=u_buttap(N,OmegaC);
```

To display the frequency-domain plots of analog filters, we provide a function called `freqs_m`, which is a modified version of a function `freqs` provided by MATLAB. This function computes the magnitude response in absolute as well as in relative dB scale and the phase response. This function is similar to the `freqz_m` function discussed earlier. One main difference between them is that in the `freqs_m` function the responses are computed up to a maximum frequency  $\Omega_{\max}$ .

```
function [db,mag,pha,w] = freqs_m(b,a,wmax);
% Computation of s-domain frequency response: Modified version
%
% [db,mag,pha,w] = freqs_m(b,a,wmax);
```

```
% db = relative magnitude in db over [0 to wmax]
% mag = absolute magnitude over [0 to wmax]
% pha = phase response in radians over [0 to wmax]
% w = array of 500 frequency samples between [0 to wmax]
% b = numerator polynomial coefficents of Ha(s)
% a = denominator polynomial coefficents of Ha(s)
% wmax = maximum frequency in rad/sec over which response is desired
%
w = [0:1:500]*wmax/500; H = freqs(b,a,w);
mag = abs(H); db = 20*log10((mag+eps)/max(mag)); pha = angle(H);
```

The impulse response  $h_a(t)$  of the analog filter is computed using MATLAB's **impulse** function.

- EXAMPLE 8.4** Design the analog Butterworth lowpass filter specified in Example 8.3 using MATLAB.

**Solution**

MATLAB script:

```
>> Wp = 0.2*pi; Ws = 0.3*pi; Rp = 7; As = 16;
>> Ripple = 10 ^ (-Rp/20); Attn = 10 ^ (-As/20);
>> % Analog filter design:
>> [b,a] = afd_butte(Wp,Ws,Rp,As);
*** Butterworth Filter Order = 3
>> % Calculation of second-order sections:
>> [C,B,A] = sdir2cas(b,a)
C = 0.1238
B = 0      0      1
A = 1.0000    0.4985    0.2485
          0      1.0000    0.4985
>> % Calculation of frequency response:
>> [db,mag,pha,w] = freqs_m(b,a,0.5*pi);
>> % Calculation of impulse response:
>> [ha,x,t] = impulse(b,a);
```

The system function is given by

$$H_a(s) = \frac{0.1238}{(s^2 + 0.4985s + 0.2485)(s + 0.4985)}$$

This  $H_a(s)$  is slightly different from the one in Example 8.3 because in that example we used  $\Omega_c = 0.5$ , while in the **afd.butte** function  $\Omega_c$  is chosen to satisfy the specifications at  $\Omega_p$ . The filter plots are shown in Figure 8.15.  $\square$

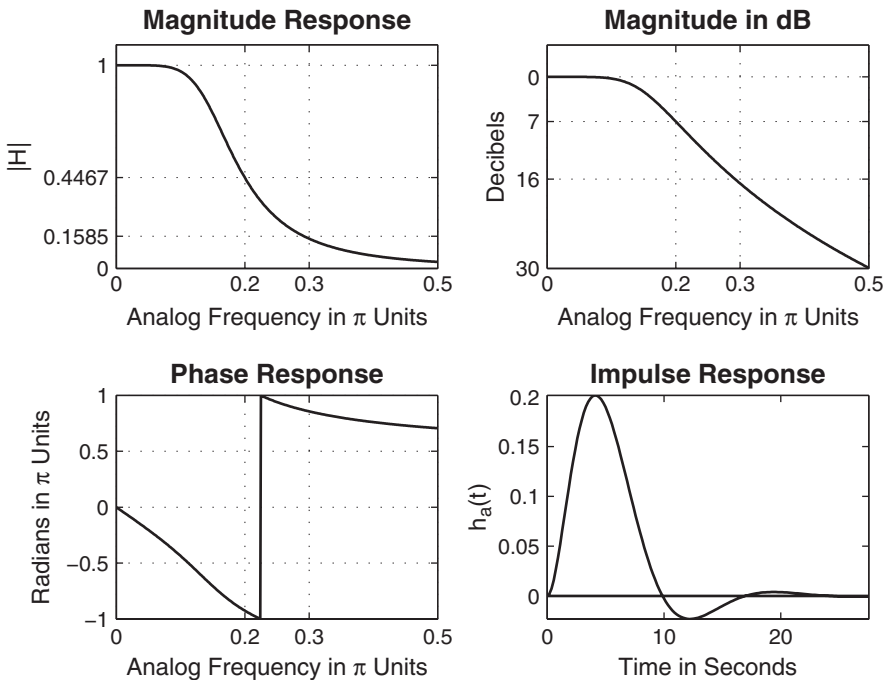


FIGURE 8.15 Butterworth analog filter in Example 8.4

### 8.3.5 CHEBYSHEV LOWPASS FILTERS

There are two types of Chebyshev filters. The Chebyshev-I filters have *equiripple response in the passband*, while the Chebyshev-II filters have *equiripple response in the stopband*. Butterworth filters have monotonic response in both bands. Recall our discussions regarding equiripple FIR filters. We noted that by choosing a filter that has an equiripple rather than a monotonic behavior, we can obtain a lower-order filter. Therefore, Chebyshev filters provide lower order than Butterworth filters for the same specifications.

The magnitude-squared response of a Chebyshev-I filter is

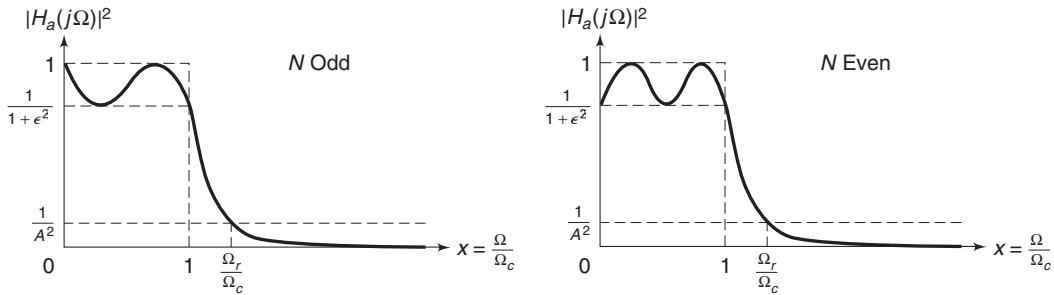
$$|H_a(j\Omega)|^2 = \frac{1}{1 + \epsilon^2 T_N^2 \left( \frac{\Omega}{\Omega_c} \right)} \quad (8.52)$$

where  $N$  is the order of the filter,  $\epsilon$  is the passband ripple factor, which is related to  $R_p$ , and  $T_N(x)$  is the  $N$ th-order Chebyshev polynomial given by

$$T_N(x) = \begin{cases} \cos(N \cos^{-1}(x)), & 0 \leq x \leq 1 \\ \cosh(\cosh^{-1}(x)), & 1 < x < \infty \end{cases} \quad \text{where } x = \frac{\Omega}{\Omega_c}$$

The equiripple response of the Chebyshev filters is due to this polynomial  $T_N(x)$ . Its key properties are (a) for  $0 < x < 1$ ,  $T_N(x)$  oscillates between  $-1$  and  $1$ , and (b) for  $1 < x < \infty$ ,  $T_N(x)$  increases monotonically to  $\infty$ .

There are two possible shapes of  $|H_a(j\Omega)|^2$ , one for  $N$  odd and one for  $N$  even as shown here. Note that  $x = \Omega/\Omega_c$  is the normalized frequency.



From these two response plots we observe the following properties:

- At  $x = 0$  (or  $\Omega = 0$ ),  $|H_a(j0)|^2 = 1$  for  $N$  odd,  
 $|H_a(j0)|^2 = \frac{1}{1 + \epsilon^2}$  for  $N$  even.
- At  $x = 1$  (or  $\Omega = \Omega_c$ ),  $|H_a(j1)|^2 = \frac{1}{1 + \epsilon^2}$  for all  $N$ .
- For  $0 \leq x \leq 1$  (or  $0 \leq \Omega \leq \Omega_c$ ),  $|H_a(jx)|^2$  oscillates between  $1$  and  $\frac{1}{1 + \epsilon^2}$ .
- For  $x > 1$  (or  $\Omega > \Omega_c$ ),  $|H_a(jx)|^2$  decreases monotonically to  $0$ .
- At  $x = \Omega_r$ ,  $|H_a(jx)|^2 = \frac{1}{A^2}$ .

To determine a causal and stable  $H_a(s)$ , we must find the poles of  $H_a(s)H_a(-s)$  and select the left half-plane poles for  $H_a(s)$ . The poles of  $H_a(s)H_a(-s)$  are obtained by finding the roots of

$$1 + \epsilon^2 T_N^2 \left( \frac{s}{j\Omega_c} \right)$$

The solution of this equation is tedious if not difficult to obtain. It can be shown that if  $p_k = \sigma_k + j\Omega_k$ ,  $k = 0, \dots, N - 1$  are the (left half-plane) roots of these polynomial, then

$$\begin{aligned}\sigma_k &= (a\Omega_c) \cos \left[ \frac{\pi}{2} + \frac{(2k+1)\pi}{2N} \right] \\ \Omega_k &= (b\Omega_c) \sin \left[ \frac{\pi}{2} + \frac{(2k+1)\pi}{2N} \right] \quad k = 0, \dots, N-1\end{aligned}\tag{8.53}$$

where

$$a = \frac{1}{2} \left( \sqrt[N]{\alpha} - \sqrt[N]{1/\alpha} \right), \quad b = \frac{1}{2} \left( \sqrt[N]{\alpha} + \sqrt[N]{1/\alpha} \right), \quad \text{and} \quad \alpha = \frac{1}{\epsilon} + \sqrt{1 + \frac{1}{\epsilon^2}}\tag{8.54}$$

These roots fall on an ellipse with major axis  $b\Omega_c$  and minor axis  $a\Omega_c$ . Now the system function is given by

$$H_a(s) = \frac{K}{\prod_k (s - p_k)}\tag{8.55}$$

where  $K$  is a normalizing factor chosen to make

$$H_a(j0) = \begin{cases} 1, & N \text{ odd}, \\ \frac{1}{\sqrt{1 + \epsilon^2}}, & N \text{ even} \end{cases}\tag{8.56}$$

### 8.3.6 MATLAB IMPLEMENTATION

MATLAB provides a function called `[z,p,k]=cheb1ap(N,Rp)` to design a *normalized* Chebyshev-I analog prototype filter of order  $N$  and passband ripple  $R_p$  and that returns zeros in  $z$  array, poles in  $p$  array, and the gain value  $k$ . We need an unnormalized Chebyshev-I filter with arbitrary  $\Omega_c$ . This is achieved by scaling the array  $p$  of the normalized filter by  $\Omega_c$ . Similar to the Butterworth prototype, this filter has no zeros. The new gain  $k$  is determined using (8.56), which is achieved by scaling the old  $k$  by the ratio of the unnormalized to the normalized denominator polynomials evaluated at  $s = 0$ . In the following function, called `U_chb1ap(N,Rp,Omegac)`, we design an unnormalized Chebyshev-I analog prototype filter that returns  $H_a(s)$  in the direct form.

```

function [b,a] = u_chb1ap(N,Rp,Omegac);
% Unnormalized Chebyshev-1 analog lowpass filter prototype
%
% [b,a] = u_chb1ap(N,Rp,Omegac);
%     b = numerator polynomial coefficients
%     a = denominator polynomial coefficients
%     N = order of the elliptic filter
%     Rp = passband ripple in dB; Rp > 0
%     Omegac = cutoff frequency in radians/sec
%
[z,p,k] = cheb1ap(N,Rp); a = real(poly(p)); aNn = a(N+1);
p = p*Omegac; a = real(poly(p)); aNu = a(N+1);
k = k*aNu/aNn;
b0 = k; B = real(poly(z)); b = k*B;

```

### 8.3.7 DESIGN EQUATIONS

Given  $\Omega_p$ ,  $\Omega_s$ ,  $R_p$ , and  $A_s$ , three parameters are required to determine a Chebyshev-I filter:  $\epsilon$ ,  $\Omega_c$ , and  $N$ . From equations (8.3) and (8.4), we obtain

$$\epsilon = \sqrt{10^{0.1R_p} - 1} \quad \text{and} \quad A = 10^{A_s/20}$$

From these properties, we have

$$\Omega_c = \Omega_p \quad \text{and} \quad \Omega_r = \frac{\Omega_s}{\Omega_p} \quad (8.57)$$

The order  $N$  is given by

$$g = \sqrt{(A^2 - 1) / \epsilon^2} \quad (8.58)$$

$$N = \left\lceil \frac{\log_{10} \left[ g + \sqrt{g^2 - 1} \right]}{\log_{10} \left[ \Omega_r + \sqrt{\Omega_r^2 - 1} \right]} \right\rceil \quad (8.59)$$

Now using (8.54), (8.53), and (8.55), we can determine  $H_a(s)$ .

- EXAMPLE 8.5** Design a lowpass Chebyshev-I filter to satisfy the following specifications.

Passband cutoff:  $\Omega_p = 0.2\pi$ ; Passband ripple:  $R_p = 1$  dB

Stopband cutoff:  $\Omega_s = 0.3\pi$ ; Stopband ripple:  $A_s = 16$  dB

#### Solution

First, compute the necessary parameters.

$$\epsilon = \sqrt{10^{0.1(1)} - 1} = 0.5088 \quad A = 10^{16/20} = 6.3096$$

$$\Omega_c = \Omega_p = 0.2\pi \quad \Omega_r = \frac{0.3\pi}{0.2\pi} = 1.5$$

$$g = \sqrt{(A^2 - 1) / \epsilon^2} = 12.2429 \quad N = 4$$

Now we can determine  $H_a(s)$ .

$$\alpha = \frac{1}{\epsilon} + \sqrt{1 + \frac{1}{\epsilon^2}} = 4.1702$$

$$a = 0.5 \left( \sqrt[n]{\alpha} - \sqrt[n]{1/\alpha} \right) = 0.3646$$

$$b = 0.5 \left( \sqrt[n]{\alpha} + \sqrt[n]{1/\alpha} \right) = 1.0644$$

There are four poles for  $H_a(s)$ :

$$p_{0,3} = (a\Omega_c) \cos \left[ \frac{\pi}{2} + \frac{\pi}{8} \right] \pm (b\Omega_c) \sin \left[ \frac{\pi}{2} + \frac{\pi}{8} \right] = -0.0877 \pm j0.6179$$

$$p_{1,2} = (a\Omega_c) \cos \left[ \frac{\pi}{2} + \frac{3\pi}{8} \right] \pm (b\Omega_c) \sin \left[ \frac{\pi}{2} + \frac{3\pi}{8} \right] = -0.2117 \pm j0.2559$$

Hence

$$H_a(s) = \frac{K}{\prod_{k=0}^3 (s - p_k)} = \frac{\overbrace{0.89125 \times .1103 \times .3895}^{0.03829}}{(s^2 + 0.1754s + 0.3895)(s^2 + 0.4234s + 0.1103)}$$

Note that the numerator is such that

$$H_a(j0) = \frac{1}{\sqrt{1 + \epsilon^2}} = 0.89125$$

□

### 8.3.8 MATLAB IMPLEMENTATION

Using the `U_chb1ap` function, we provide a function called `afd_chb1` to design an analog Chebyshev-II lowpass filter, given its specifications. This is shown below and uses the procedure described in Example 8.5.

```
function [b,a] = afd_chb1(Wp,Ws,Rp,As);
% Analog lowpass filter design: Chebyshev-1
% -----
% [b,a] = afd_chb1(Wp,Ws,Rp,As);
% b = numerator coefficients of Ha(s)
% a = denominator coefficients of Ha(s)
% Wp = passband-edge frequency in rad/sec; Wp > 0
% Ws = stopband-edge frequency in rad/sec; Ws > Wp > 0
% Rp = passband ripple in +dB; (Rp > 0)
% As = stopband attenuation in +dB; (As > 0)
```

```

%
if Wp <= 0
    error('Passband edge must be larger than 0')
end
if Ws <= Wp
    error('Stopband edge must be larger than Passband edge')
end
if (Rp <= 0) | (As < 0)
    error('PB ripple and/or SB attenuation must be larger than 0')
end

ep = sqrt(10^(Rp/10)-1); A = 10^(As/20);
OmegaC = Wp; OmegaR = Ws/Wp; g = sqrt(A*A-1)/ep;
N = ceil(log10(g+sqrt(g*g-1))/log10(OmegaR+sqrt(OmegaR*OmegaR-1)));
fprintf('\n*** Chebyshev-1 Filter Order = %2.0f \n',N)
[b,a]=u_chb1ap(N,Rp,OmegaC);

```

- EXAMPLE 8.6** Design the analog Chebyshev-I lowpass filter given in Example 8.5 using MATLAB.

**Solution**

MATLAB script:

```

>> Wp = 0.2*pi; Ws = 0.3*pi; Rp = 1; As = 16;
>> Ripple = 10 ^ (-Rp/20); Attn = 10 ^ (-As/20);
>> % Analog filter design:
>> [b,a] = afd_chb1(Wp,Ws,Rp,As);
*** Chebyshev-1 Filter Order = 4
>> % Calculation of second-order sections:
>> [C,B,A] = sdir2cas(b,a)
C = 0.0383
B = 0      0      1
A = 1.0000  0.4233  0.1103
      1.0000  0.1753  0.3895
>> % Calculation of frequency response:
>> [db,mag,pha,w] = freqs_m(b,a,0.5*pi);
>> % Calculation of impulse response:
>> [ha,x,t] = impulse(b,a);

```

The specifications are satisfied by a fourth-order Chebyshev-I filter whose system function is

$$H_a(s) = \frac{0.0383}{(s^2 + 4233s + 0.1103)(s^2 + 0.1753s + 0.3895)}$$

The filter plots are shown in Figure 8.16.

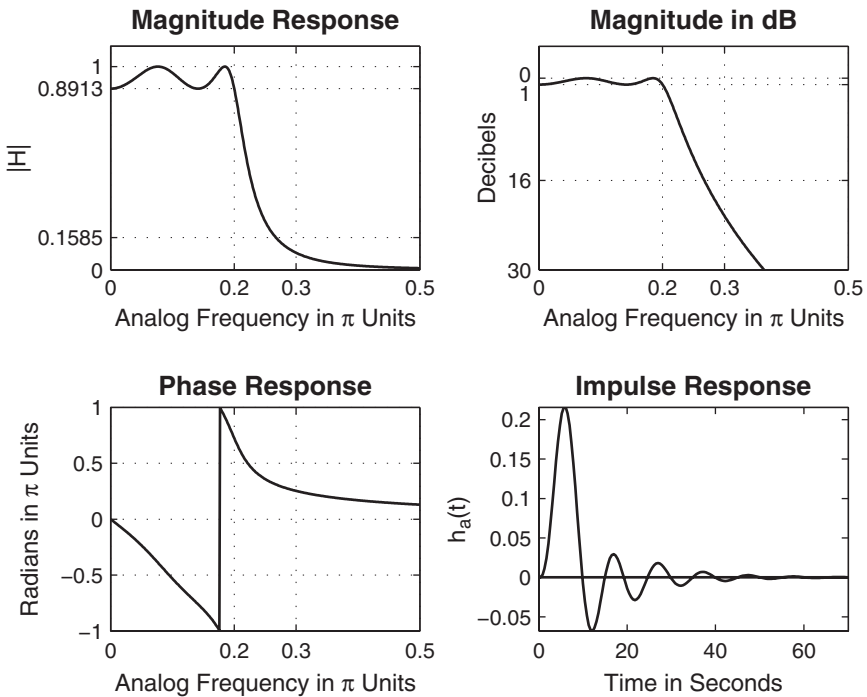


**FIGURE 8.16** Chebyshev-I analog filter in Example 8.6

A Chebyshev-II filter is related to the Chebyshev-I filter through a simple transformation. It has a monotone passband and an equiripple stopband, which implies that this filter has both poles and zeros in the  $s$ -plane. Therefore, the group delay characteristics are better (and the phase response more linear) in the passband than those of the Chebyshev-I prototype. If we replace the term  $\epsilon^2 T_N^2(\Omega/\Omega_c)$  in (8.52) by its reciprocal and also the argument  $x = \Omega/\Omega_c$  by its reciprocal, we obtain the magnitude-squared response of Chebyshev-II as

$$|H_a(j\Omega)|^2 = \frac{1}{1 + [\epsilon^2 T_N^2(\Omega_c/\Omega)]^{-1}} \quad (8.60)$$

One approach to designing a Chebyshev-II filter is to design the corresponding Chebyshev-I first and then apply these transformations. We will not discuss the details of this filter but will use a function from MATLAB to design a Chebyshev-II filter.

### 8.3.9 MATLAB IMPLEMENTATION

MATLAB provides a function called `[z,p,k]=cheb2ap(N,As)` to design a *normalized* Chebyshev-II analog prototype filter of order  $N$  and passband ripple  $As$  and that returns zeros in  $z$  array, poles in  $p$  array, and the gain

value  $k$ . We need an unnormalized Chebyshev-I filter with arbitrary  $\Omega_c$ . This is achieved by scaling the array  $p$  of the normalized filter by  $\Omega_c$ . Since this filter has zeros, we also have to scale the array  $z$  by  $\Omega_c$ . The new gain  $k$  is determined using (8.56), which is achieved by scaling the old  $k$  by the ratio of the unnormalized to the normalized rational functions evaluated at  $s = 0$ . In the following function, called `U_chb2ap(N,As,Omegac)`, we design an unnormalized Chebyshev-II analog prototype filter that returns  $H_a(s)$  in the direct form.

```
function [b,a] = u_chb2ap(N,As,Omegac);
% Unnormalized Chebyshev-2 analog lowpass filter prototype
%
% [b,a] = u_chb2ap(N,As,Omegac);
%     b = numerator polynomial coefficients
%     a = denominator polynomial coefficients
%     N = order of the Elliptic Filter
%     As = stopband Ripple in dB; As > 0
% Omegac = cutoff frequency in radians/sec
%
[z,p,k] = cheb2ap(N,As);
a = real(poly(p)); aNn = a(N+1);
p = p*Omegac; a = real(poly(p)); aNu = a(N+1);
b = real(poly(z)); M = length(b); bNn = b(M);
z = z*Omegac; b = real(poly(z)); bNu = b(M);
k = k*(aNn*bNn)/(aNn*bNu);
b0 = k; b = k*b;
```

The design equations for the Chebyshev-II prototype are similar to those of the Chebyshev-I except that  $\Omega_c = \Omega_s$  since the ripples are in the stopband. Therefore, we can develop a MATLAB function similar to the `afd_chb1` function for the Chebyshev-II prototype.

```
function [b,a] = afd_chb2(Wp,Ws,Rp,As);
% Analog lowpass filter design: Chebyshev-2
%
% [b,a] = afd_chb2(Wp,Ws,Rp,As);
%     b = numerator coefficients of Ha(s)
%     a = denominator coefficients of Ha(s)
%     Wp = passband-edge frequency in rad/sec; Wp > 0
%     Ws = stopband-edge frequency in rad/sec; Ws > Wp > 0
%     Rp = passband ripple in +dB; (Rp > 0)
%     As = stopband attenuation in +dB; (As > 0)
%
if Wp <= 0
    error('Passband edge must be larger than 0')
end
```

```

if Ws <= Wp
    error('Stopband edge must be larger than Passband edge')
end
if (Rp <= 0) | (As < 0)
    error('PB ripple and/or SB attenuation must be larger than 0')
end

ep = sqrt(10^(Rp/10)-1); A = 10^(As/20);
OmegaC = Wp; OmegaR = Ws/Wp; g = sqrt(A*A-1)/ep;
N = ceil(log10(g+sqrt(g*g-1))/log10(OmegaR+sqrt(OmegaR*OmegaR-1)));
fprintf('\n*** Chebyshev-2 Filter Order = %2.0f \n',N)
[b,a]=u_chb2ap(N,As,Ws);

```

- **EXAMPLE 8.7** Design a Chebyshev-II analog lowpass filter to satisfy the specifications given in Example 8.5:

Passband cutoff:  $\Omega_p = 0.2\pi$ ; Passband ripple:  $R_p = 1$  dB

Stopband cutoff:  $\Omega_s = 0.3\pi$ ; Stopband ripple:  $A_s = 16$  dB

**Solution**

MATLAB script:

```

>> Wp = 0.2*pi; Ws = 0.3*pi; Rp = 1; As = 16;
>> Ripple = 10 ^ (-Rp/20); Attn = 10 ^ (-As/20);
>> % Analog filter design:
>> [b,a] = afd_chb2(Wp,Ws,Rp,As);
*** Chebyshev-2 Filter Order = 4
>> % Calculation of second-order sections:
>> [C,B,A] = sdir2cas(b,a)
C = 0.1585
B = 1.0000      0      6.0654
          1.0000      0      1.0407
A = 1.0000      1.9521      1.4747
          1.0000      0.3719      0.6784
>> % Calculation of frequency response:
>> [db,mag,pha,w] = freqs_m(b,a,0.5*pi);
>> % Calculation of impulse response:
>> [ha,x,t] = impulse(b,a);

```

The specifications are satisfied by a fourth-order Chebyshev-II filter whose system function is

$$H_a(s) = \frac{0.1585 (s^2 + 6.0654) (s^2 + 1.0407)}{(s^2 + 1.9521s + 1.4747) (s^2 + 0.3719s + 0.6784)}$$

The filter plots are shown in Figure 8.17.

□

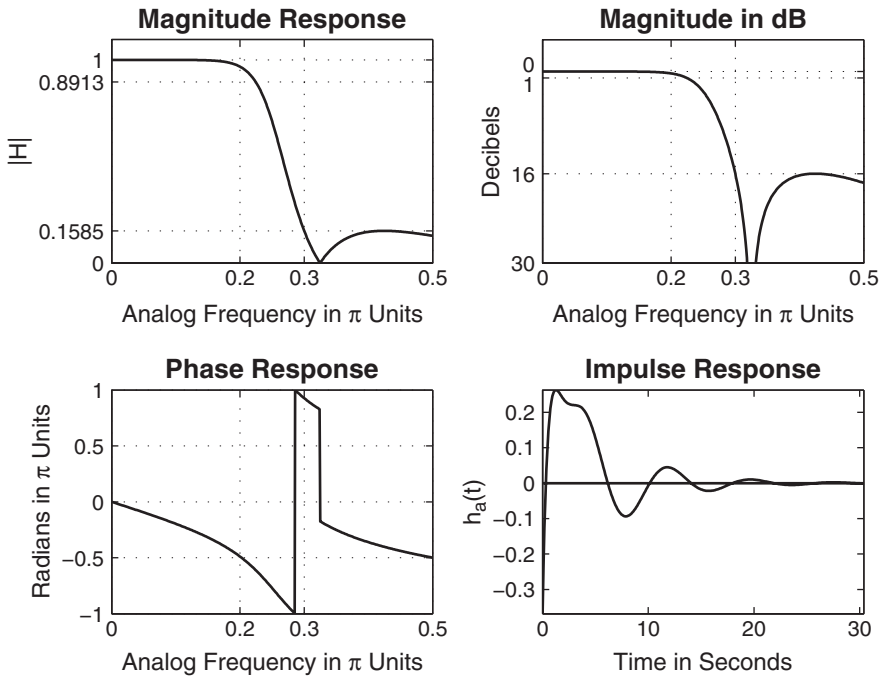


**FIGURE 8.17** Chebyshev-II analog filter in Example 8.7

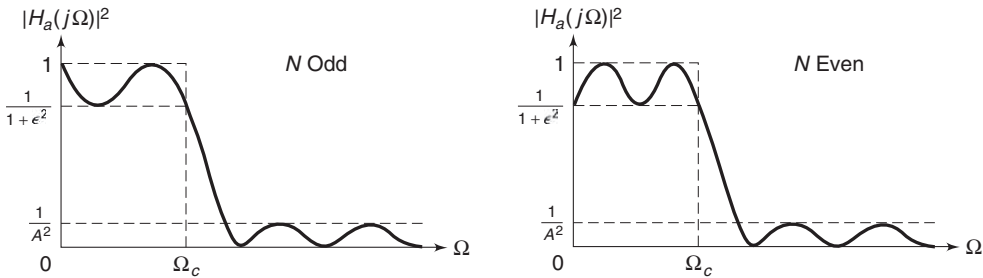
### 8.3.10 ELLIPTIC LOWPASS FILTERS

These filters exhibit equiripple behavior in the passband as well as in the stopband. They are similar in magnitude response characteristics to the FIR equiripple filters. Therefore, elliptic filters are optimum filters in that they achieve the minimum order  $N$  for the given specifications (or alternately, achieve the sharpest transition band for the given order  $N$ ). These filters, for obvious reasons, are very difficult to analyze and, therefore, to design. It is not possible to design them using simple tools, and often programs or tables are needed to design them.

The magnitude-squared response of elliptic filters is given by

$$|H_a(j\Omega)|^2 = \frac{1}{1 + \epsilon^2 U_N^2 \left( \frac{\Omega}{\Omega_c} \right)} \quad (8.61)$$

where  $N$  is the order,  $\epsilon$  is the passband ripple (which is related to  $R_p$ ), and  $U_N(\cdot)$  is the  $N$ th-order Jacobian elliptic function. The analysis of this function, even on a superficial level, is beyond the scope of this book. Note the similarity between the preceding response (8.61) and that of the Chebyshev filters given by (8.52). Typical responses for odd and even  $N$  are as follows:



### 8.3.11 COMPUTATION OF FILTER ORDER $N$

Even though the analysis of (8.61) is difficult, the order calculation formula is very compact and is available in many textbooks [71, 79, 83]. It is given by

$$N = \frac{K(k)K(\sqrt{1-k_1^2})}{K(k_1)K(\sqrt{1-k^2})} \quad (8.62)$$

where

$$k = \frac{\Omega_p}{\Omega_s}, \quad k_1 = \frac{\epsilon}{\sqrt{A^2 - 1}}$$

and

$$K(x) = \int_0^{\pi/2} \frac{d\theta}{\sqrt{1-x^2 \sin^2 \theta}}$$

is the complete elliptic integral of the first kind. MATLAB provides the function `ellipke` to numerically compute the above integral, which we will use to compute  $N$  and to design elliptic filters.

### 8.3.12 MATLAB IMPLEMENTATION

MATLAB provides a function called `[z, p, k] = ellipap(N, Rp, As)` to design a *normalized* elliptic analog prototype filter of order  $N$ , passband ripple  $Rp$ , and stopband attenuation  $As$ , and that returns zeros in `z` array, poles in `p` array, and the gain value `k`. We need an unnormalized elliptic filter with arbitrary  $\Omega_c$ . This is achieved by scaling the arrays `p` and `z` of the normalized filter by  $\Omega_c$  and the gain `k` by the ratio of the unnormalized to the normalized rational functions evaluated at  $s = 0$ . In the following function, called `U_elipap(N, Rp, As, Omegac)`, we design an unnormalized elliptic analog prototype filter that returns  $H_a(s)$  in the direct form.

```

function [b,a] = u_elipap(N,Rp,As,Omegac);
% Unnormalized elliptic analog lowpass filter prototype
%
% [b,a] = u_elipap(N,Rp,As,Omegac);
%     b = numerator polynomial coefficients
%     a = denominator polynomial coefficients
%     N = order of the elliptic filter
%     Rp = passband ripple in dB; Rp > 0
%     As = stopband attenuation in dB; As > 0
% Omegac = cutoff frequency in radians/sec
%
[z,p,k] = ellipap(N,Rp,As);
a = real(poly(p)); aNn = a(N+1);
p = p*Omegac; a = real(poly(p)); aNu = a(N+1);
b = real(poly(z)); M = length(b); bNn = b(M);
z = z*Omegac; b = real(poly(z)); bNu = b(M);
k = k*(aNn*bNn)/(aNn*bNu);
b0 = k; b = k*b;

```

Using the `U_elipap` function, we provide a function called `afd_elip` to design an analog elliptic lowpass filter, given its specifications. This follows and uses the filter order computation formula given in (8.62).

```

function [b,a] = afd_elip(Wp,Ws,Rp,As);
% Analog lowpass filter design: Elliptic
%
% [b,a] = afd_elip(Wp,Ws,Rp,As);
%     b = numerator coefficients of Ha(s)
%     a = denominator coefficients of Ha(s)
%     Wp = passband-edge frequency in rad/sec; Wp > 0
%     Ws = stopband-edge frequency in rad/sec; Ws > Wp > 0
%     Rp = passband ripple in +dB; (Rp > 0)
%     As = stopband attenuation in +dB; (As > 0)
%
if Wp <= 0
    error('Passband edge must be larger than 0')
end
if Ws <= Wp
    error('Stopband edge must be larger than Passband edge')
end
if (Rp <= 0) | (As < 0)
    error('PB ripple and/or SB attenuation must be larger than 0')
end

ep = sqrt(10^(Rp/10)-1); A = 10^(As/20);
OmegaC = Wp; k = Wp/Ws; k1 = ep/sqrt(A*A-1);

```

```

capk = ellipke([k.^2 1-k.^2]); % Version 4.0 code
capk1 = ellipke([(k1.^2) 1-(k1.^2)]); % Version 4.0 code
N = ceil(capk(1)*capk1(2)/(capk(2)*capk1(1)));
fprintf('\n*** Elliptic Filter Order = %2.0f \n',N)
[b,a]=u_elipap(N,Rp,As,OmegaC);

```

- **EXAMPLE 8.8** Design an analog elliptic lowpass filter to satisfy the following specifications of Example 8.5:

$$\Omega_p = 0.2\pi, R_p = 1 \text{ dB}$$

$$\Omega_s = 0.3\pi, A_s = 16 \text{ dB}$$

**Solution**

MATLAB script:

```

>> Wp = 0.2*pi; Ws = 0.3*pi; Rp = 1; As = 16;
>> Ripple = 10 ^ (-Rp/20); Attn = 10 ^ (-As/20);
>> % Analog filter design:
>> [b,a] = afd_elip(Wp,Ws,Rp,As);
*** Elliptic Filter Order = 3
>> % Calculation of second-order sections:
>> [C,B,A] = sdir2cas(b,a)
C = 0.2740
B = 1.0000      0      0.6641
A = 1.0000      0.1696    0.4102
          0      1.0000    0.4435
>> % Calculation of frequency response:
>> [db,mag,pha,w] = freqs_m(b,a,0.5*pi);
>> % Calculation of impulse response:
>> [ha,x,t] = impulse(b,a);

```

The specifications are satisfied by a third-order elliptic filter whose system function is

$$H_a(s) = \frac{0.274(s^2 + 0.6641)}{(s^2 + 0.1696s + 0.4102)(s + 0.4435)}$$

The filter plots are shown in Figure 8.18. □

### 8.3.13 PHASE RESPONSES OF PROTOTYPE FILTERS

Elliptic filters provide optimal performance in the magnitude-squared response but have highly nonlinear phase response in the passband (which is undesirable in many applications). Even though we decided not to worry

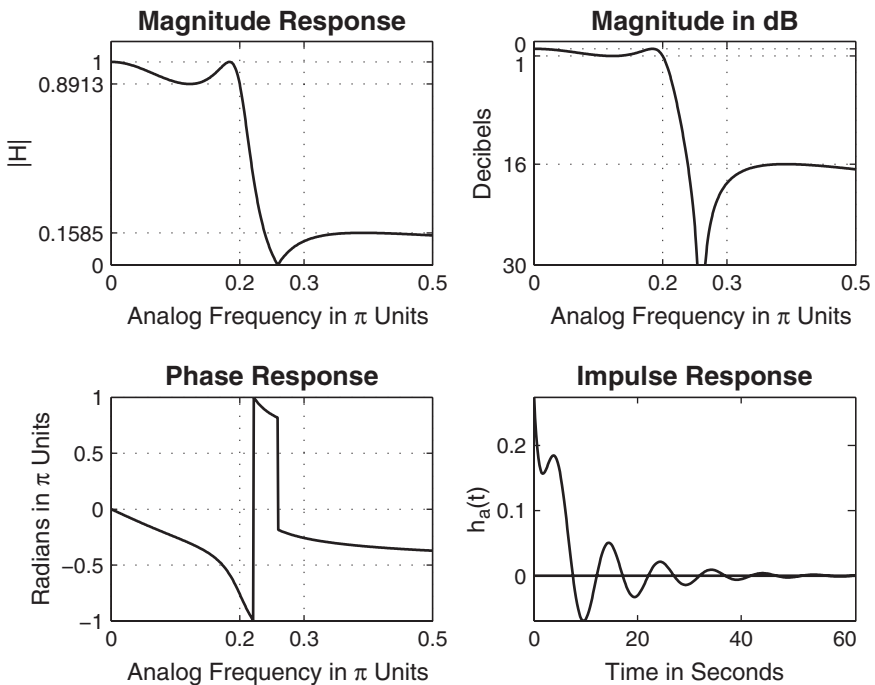


**FIGURE 8.18** Elliptic analog lowpass filter in Example 8.8

about phase response in our designs, phase is still an important issue in the overall system. At the other end of the performance scale are the Butterworth filters, which have maximally flat magnitude response and require a higher-order  $N$  (more poles) to achieve the same stopband specification. However, they exhibit a fairly linear phase response in their passband. The Chebyshev filters have phase characteristics that lie somewhere in between. Therefore, in practical applications, we do consider Butterworth as well as Chebyshev filters, in addition to elliptic filters. The choice depends on both the filter order (which influences processing speed and implementation complexity) and the phase characteristics (which control the distortion).

## 8.4 ANALOG-TO-DIGITAL FILTER TRANSFORMATIONS

After discussing different approaches to the design of analog filters, we are now ready to transform them into digital filters. These transformations are complex-valued mappings that are extensively studied in

the literature. These transformations are derived by preserving different aspects of analog and digital filters. If we want to preserve the shape of the impulse response from analog to digital filter, then we obtain a technique called *impulse invariance* transformation. If we want to convert a differential equation representation into a corresponding difference equation representation, then we obtain a *finite difference approximation* technique. Numerous other techniques are also possible. One technique, called *step invariance*, preserves the shape of the step response; this is explored in Problem P8.24. Another technique that is similar to the impulse invariance is the matched- $z$  transformation, which matches the pole-zero representation. It is described at the end of this section and is explored in Problem P8.26. The most popular technique used in practice is called a *Bilinear* transformation, which preserves the system function representation from analog to digital domain. In this section, we will study in detail impulse invariance and bilinear transformations, both of which can be easily implemented in MATLAB.

#### 8.4.1 IMPULSE INVARIANCE TRANSFORMATION

In this design method, we want the digital filter impulse response to look “similar” to that of a frequency-selective analog filter. Hence we sample  $h_a(t)$  at some sampling interval  $T$  to obtain  $h(n)$ ; that is,

$$h(n) = h_a(nT)$$

The parameter  $T$  is chosen so that the shape of  $h_a(t)$  is “captured” by the samples. Since this is a sampling operation, the analog and digital frequencies are related by

$$\omega = \Omega T \text{ or } e^{j\omega} = e^{j\Omega T}$$

Since  $z = e^{j\omega}$  on the unit circle and  $s = j\Omega$  on the imaginary axis, we have the following transformation from the  $s$ -plane to the  $z$ -plane:

$$z = e^{sT} \quad (8.63)$$

The system functions  $H(z)$  and  $H_a(s)$  are related through the frequency-domain aliasing formula (3.27):

$$H(z) = \frac{1}{T} \sum_{k=-\infty}^{\infty} H_a \left( s - j \frac{2\pi}{T} k \right)$$

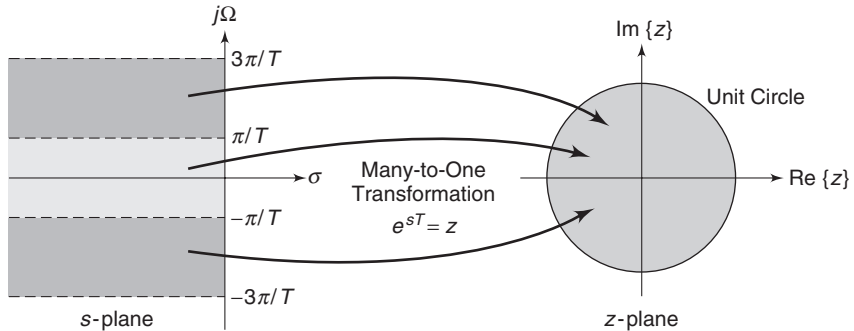


**FIGURE 8.19** Complex-plane mapping in impulse invariance transformation

The complex plane transformation under the mapping (8.63) is shown in Figure 8.19, from which we have the following observations.

1. Using  $\sigma = \text{Re}(s)$ , we note that

$\sigma < 0$  maps into  $|z| < 1$  (inside of the UC)

$\sigma = 0$  maps onto  $|z| = 1$  (on the UC)

$\sigma > 0$  maps into  $|z| > 1$  (outside of the UC)

2. All semi-infinite strips (shown above) of width  $2\pi/T$  map into  $|z| < 1$ . Thus this mapping is not unique but a *many-to-one* mapping.
3. Since the entire left half of the  $s$ -plane maps into the unit circle, a causal and stable analog filter maps into a causal and stable digital filter.
4. If  $H_a(j\Omega) = H_a(j\omega/T) = 0$  for  $|\Omega| \geq \pi/T$ , then

$$H(e^{j\omega}) = \frac{1}{T} H_a(j\omega/T), \quad |\omega| \leq \pi$$

and there will be no aliasing. However, no analog filter of finite order can be exactly band-limited. Therefore some aliasing error will occur in this design procedure, and hence the sampling interval  $T$  plays a minor role in this design method.

#### 8.4.2 DESIGN PROCEDURE

Given the digital lowpass filter specifications  $\omega_p$ ,  $\omega_s$ ,  $R_p$ , and  $A_s$ , we want to determine  $H(z)$  by first designing an equivalent analog filter and then mapping it into the desired digital filter. The steps required for this procedure are as follows.

1. Choose  $T$  and determine the analog frequencies

$$\Omega_p = \frac{\omega_p}{T_p} \quad \text{and} \quad \Omega_s = \frac{\omega_s}{T}$$

2. Design an analog filter  $H_a(s)$  using the specifications  $\Omega_p$ ,  $\Omega_s$ ,  $R_p$ , and  $A_s$ . This can be done using any one of the three (Butterworth, Cheby-shev, or elliptic) prototypes of the previous section.
3. Using partial fraction expansion, expand  $H_a(s)$  into

$$H_a(s) = \sum_{k=1}^N \frac{R_k}{s - p_k}$$

4. Now transform analog poles  $\{p_k\}$  into digital poles  $\{e^{p_k T}\}$  to obtain the digital filter:

$$H(z) = \sum_{k=1}^N \frac{R_k}{1 - e^{p_k T} z^{-1}} \quad (8.64)$$

□ **EXAMPLE 8.9** Transform

$$H_a(s) = \frac{s + 1}{s^2 + 5s + 6}$$

into a digital filter  $H(z)$  using the impulse invariance technique in which  $T = 0.1$ .

**Solution**

We first expand  $H_a(s)$  using partial fraction expansion:

$$H_a(s) = \frac{s + 1}{s^2 + 5s + 6} = \frac{2}{s + 3} - \frac{1}{s + 2}$$

The poles are at  $p_1 = -3$  and  $p_2 = -2$ . Then from (8.64) and using  $T = 0.1$ , we obtain

$$H(z) = \frac{2}{1 - e^{-3T} z^{-1}} - \frac{1}{1 - e^{-2T} z^{-1}} = \frac{1 - 0.8966z^{-1}}{1 - 1.5595z^{-1} + 0.6065z^{-2}}$$

It is easy to develop a MATLAB function to implement the impulse invariance mapping. Given a rational function description of  $H_a(s)$ , we can use the **residue** function to obtain its pole-zero description. Then each analog pole is mapped into a digital pole using (8.63). Finally, the **residuez** function can be used to convert  $H(z)$  into rational function form. This procedure is given in the function **imp\_invr**.

```
function [b,a] = imp_invr(c,d,T)
% Impulse invariance transformation from analog to digital filter
%
% [b,a] = imp_invr(c,d,T)
% b = numerator polynomial in z^(-1) of the digital filter
% a = denominator polynomial in z^(-1) of the digital filter
% c = numerator polynomial in s of the analog filter
```

```
% d = denominator polynomial in s of the analog filter
% T = sampling (transformation) parameter
%
[R,p,k] = residue(c,d); p = exp(p*T);
[b,a] = residuez(R,p,k); b = real(b'); a = real(a');
```

A similar function called **impinvar** is available in the SP toolbox of MATLAB.

□

- **EXAMPLE 8.10** We demonstrate the use of the **imp\_invr** function on the system function from Example 8.9.

**Solution** MATLAB script:

```
>> c = [1,1]; d = [1,5,6]; T = 0.1;
>> [b,a] = imp_invr(c,d,T)
b = 1.0000 -0.8966
a = 1.0000 -1.5595 0.6065
```

The digital filter is

$$H(z) = \frac{1 - 0.8966z^{-1}}{1 - 1.5595z^{-1} + 0.6065z^{-2}}$$

as expected. In Figure 8.20, we show the impulse responses and the magnitude responses (plotted up to the sampling frequency  $1/T$ ) of the analog and the resulting digital filter. Clearly, the aliasing in the frequency domain is evident.

□

In the next several examples, we illustrate the impulse invariance design procedure on all three prototypes.

- **EXAMPLE 8.11** Design a lowpass digital filter using a Butterworth prototype to satisfy

$$\omega_p = 0.2\pi, R_p = 1 \text{ dB}$$

$$\omega_s = 0.3\pi, A_s = 15 \text{ dB}$$

**Solution** The design procedure is described in the following MATLAB script.

```
>> % Digital filter specifications:
>> wp = 0.2*pi; % Digital passband freq in Hz
>> ws = 0.3*pi; % Digital stopband freq in Hz
>> Rp = 1; % Passband ripple in dB
>> As = 15; % Stopband attenuation in dB
```

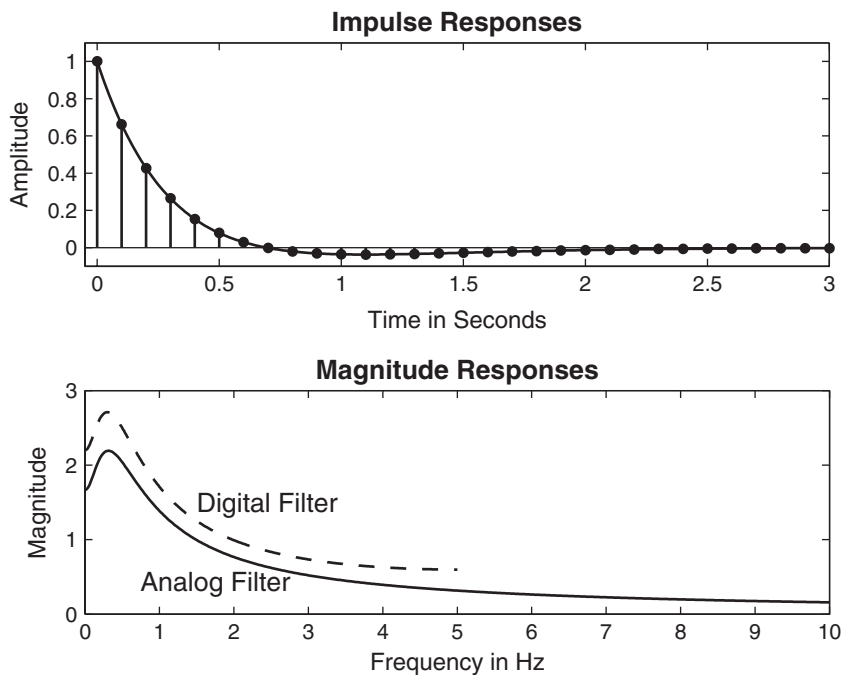


**FIGURE 8.20** Impulse and frequency response plots in Example 8.10

```
>> % Analog prototype specifications: Inverse mapping for frequencies
>> T = 1; % Set T=1
>> OmegaP = wp / T; % Prototype passband freq
>> OmegaS = ws / T; % Prototype stopband freq

>> % Analog Butterworth prototype filter calculation:
>> [cs,ds] = afd_but(PrototypeP, PrototypeS,Rp,As);
*** Butterworth Filter Order = 6

>> % Impulse invariance transformation:
>> [b,a] = imp_invr(cs,ds,T); [C,B,A] = dir2par(b,a)
C =
B = 1.8557 -0.6304
      -2.1428  1.1454
      0.2871 -0.4466
A = 1.0000 -0.9973  0.2570
      1.0000 -1.0691  0.3699
      1.0000 -1.2972  0.6949
```

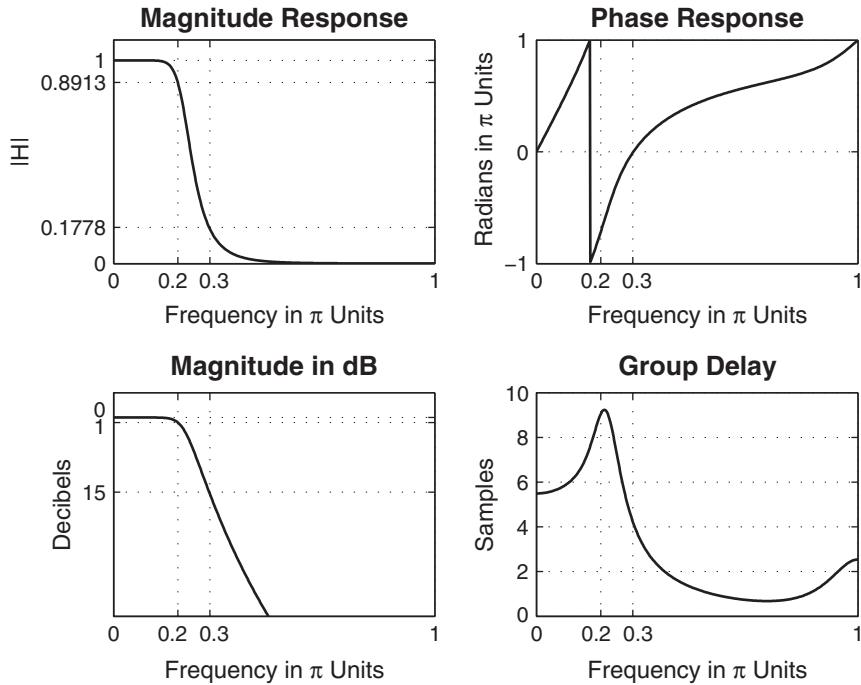


**FIGURE 8.21** Digital Butterworth lowpass filter using impulse invariance design

The desired filter is a sixth-order Butterworth filter whose system function  $H(z)$  is given in the parallel form

$$H(z) = \frac{1.8587 - 0.6304z^{-1}}{1 - 0.9973z^{-1} + 0.257z^{-2}} + \frac{-2.1428 + 1.1454z^{-1}}{1 - 1.0691z^{-1} + 0.3699z^{-2}} \\ + \frac{0.2871 - 0.4463z^{-1}}{1 - 1.2972z^{-1} + 0.6449z^{-2}}$$

The frequency response plots are given in Figure 8.21. □

- **EXAMPLE 8.12** Design a lowpass digital filter using a Chebyshev-I prototype to satisfy

$$\omega_p = 0.2\pi, R_p = 1 \text{ dB}$$

$$\omega_s = 0.3\pi, A_s = 15 \text{ dB}$$

**Solution**

The design procedure is described in the following MATLAB script.

```

>> % Digital filter specifications:
>> wp = 0.2*pi;                                % Digital passband freq in rad
>> ws = 0.3*pi;                                % Digital stopband freq in rad
>> Rp = 1;                                     % Passband ripple in dB
>> As = 15;                                    % Stopband attenuation in dB

>> % Analog prototype specifications: Inverse mapping for frequencies
>> T = 1;                                       % Set T=1
>> OmegaP = wp / T;                            % Prototype passband freq
>> OmegaS = ws / T;                            % Prototype stopband freq
>> % Analog Chebyshev-1 prototype filter calculation:
>> [cs,ds] = afd_chb1(OmegaP,OmegaS,Rp,As);
*** Chebyshev-1 Filter Order = 4

>> % Impulse invariance transformation:
>> [b,a] = imp_invr(cs,ds,T);   [C,B,A] = dir2par(b,a)
C =
B = -0.0833   -0.0246
      0.0833    0.0239
A =  1.0000   -1.4934    0.8392
      1.0000   -1.5658    0.6549

```

The desired filter is a fourth-order Chebyshev-I filter whose system function  $H(z)$  is

$$H(z) = \frac{-0.0833 - 0.0246z^{-1}}{1 - 1.4934z^{-1} + 0.8392z^{-2}} + \frac{-0.0833 + 0.0239z^{-1}}{1 - 1.5658z^{-1} + 0.6549z^{-2}}$$

The frequency response plots are given in Figure 8.22. □

- EXAMPLE 8.13** Design a lowpass digital filter using a Chebyshev-II prototype to satisfy

$$\omega_p = 0.2\pi, R_p = 1 \text{ dB}$$

$$\omega_s = 0.3\pi, A_s = 15 \text{ dB}$$

**Solution**

Recall that the Chebyshev-II filter is equiripple in the stopband. This means that this analog filter has a response that does not go to zero at high frequencies in the stopband. Therefore, after impulse invariance transformation, the aliasing

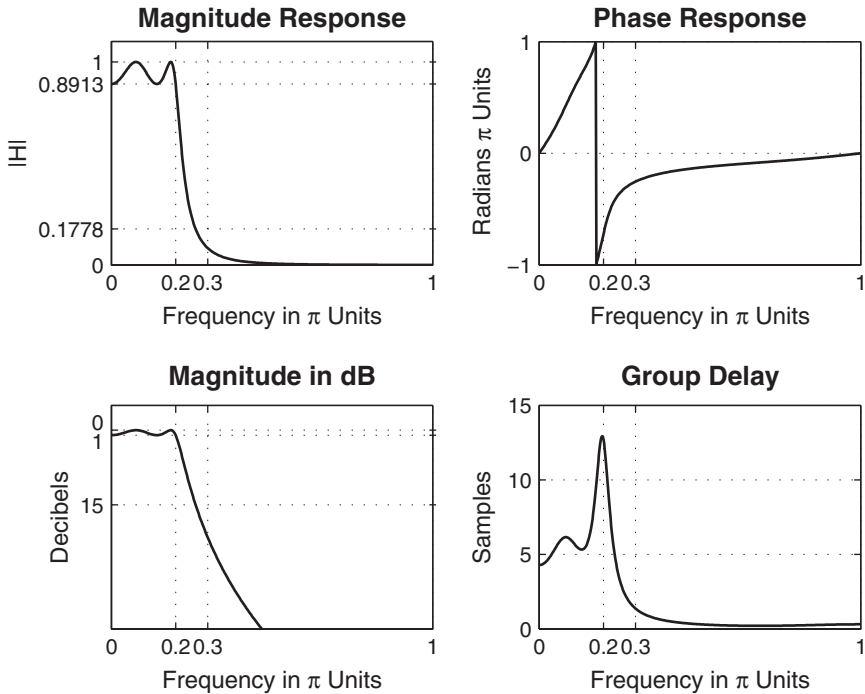


**FIGURE 8.22** Digital Chebyshev-I lowpass filter using impulse invariance design

effect will be significant; this can degrade the passband response. The MATLAB script follows:

```
>> % Digital filter specifications:
>> wp = 0.2*pi; % Digital passband freq in rad
>> ws = 0.3*pi; % Digital stopband freq in rad
>> Rp = 1; % Passband ripple in dB
>> As = 15; % Stopband attenuation in dB

>> % Analog prototype specifications: Inverse mapping for frequencies
>> T = 1; % Set T=1
>> OmegaP = wp / T; % Prototype passband freq
>> OmegaS = ws / T; % Prototype stopband freq

>> % Analog Chebyshev-1 prototype filter calculation:
>> [cs,ds] = afd_chb2(OmegaP,OmegaS,Rp,As);
*** Chebyshev-2 Filter Order = 4

>> % Impulse invariance transformation:
>> [b,a] = imp_invr(cs,ds,T); [C,B,A] = dir2par(b,a);
```

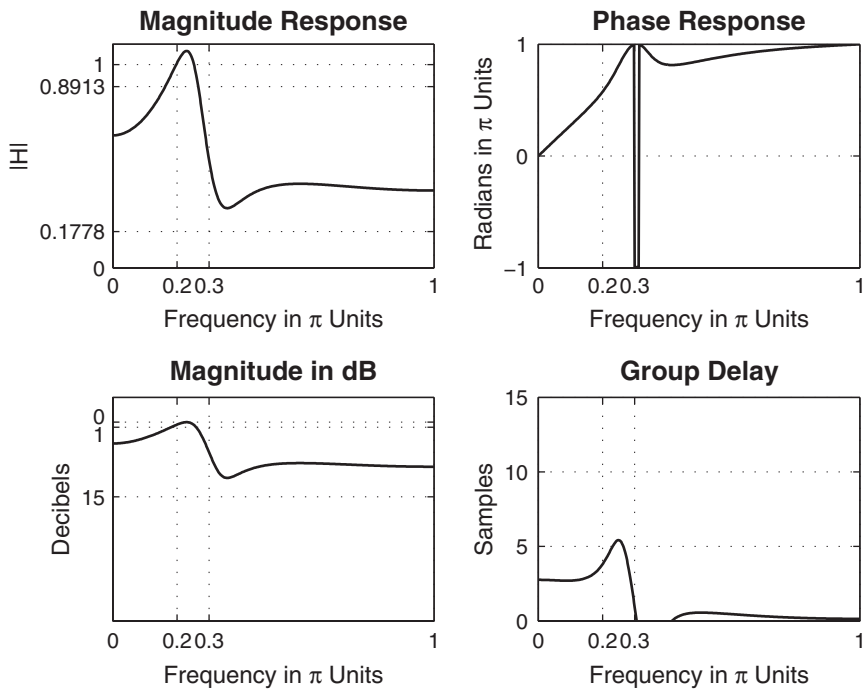


**FIGURE 8.23** Digital Chebyshev-II lowpass filter using impulse invariance design

From the frequency response plots in Figure 8.23, we clearly observe the passband as well as stopband degradation. Hence the impulse invariance design technique has failed to produce a desired digital filter.  $\square$

- **EXAMPLE 8.14** Design a lowpass digital filter using an elliptic prototype to satisfy

$$\omega_p = 0.2\pi, R_p = 1 \text{ dB}$$

$$\omega_s = 0.3\pi, A_s = 15 \text{ dB}$$

#### Solution

The elliptic filter is equiripple in both bands. Hence this situation is similar to that of the Chebyshev-II filter, and we should not expect a good digital filter. MATLAB script:

```
>> % Digital filter specifications:
>> wp = 0.2*pi; % Digital passband freq in rad
>> ws = 0.3*pi; % Digital stopband freq in rad
>> Rp = 1; % Passband ripple in dB
>> As = 15; % Stopband attenuation in dB
```

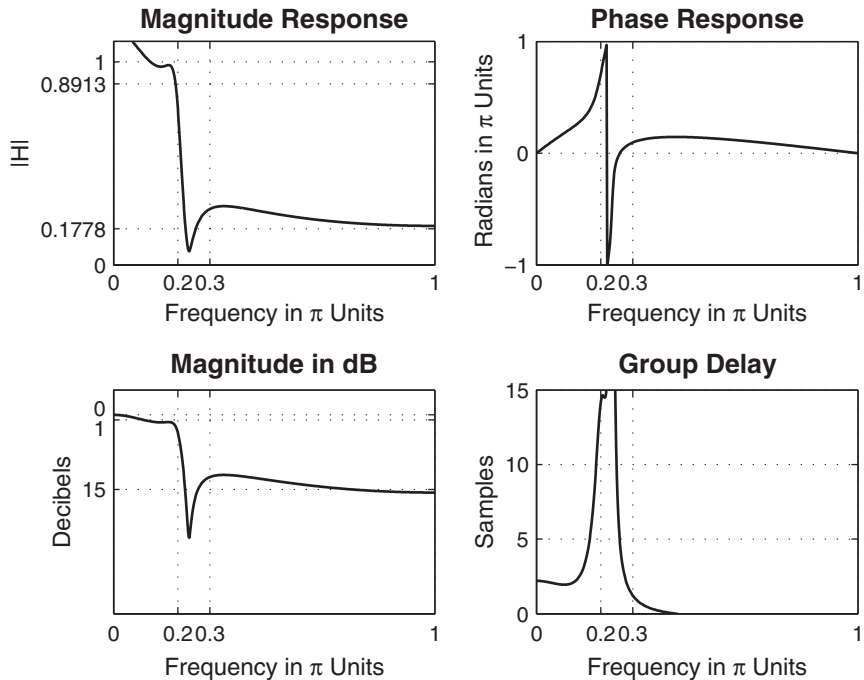


**FIGURE 8.24** Digital elliptic lowpass filter using impulse invariance design

```

>> % Analog prototype specifications: Inverse mapping for frequencies
>> T = 1;                                % Set T=1
>> OmegaP = wp / T;                      % Prototype passband freq
>> OmegaS = ws / T;                      % Prototype stopband freq

>> % Analog elliptic prototype filter calculation:
>> [cs,ds] = afd_elip(OmegaP,OmegaS,Rp,As);
*** Elliptic Filter Order = 3

>> % Impulse invariance transformation:
>> [b,a] = imp_invr(cs,ds,T);  [C,B,A] = dir2par(b,a);

```

From the frequency response plots in Figure 8.24, we clearly observe that once again the impulse invariance design technique has failed.  $\square$

The advantages of the impulse invariance mapping are that it is a stable design and that the frequencies  $\Omega$  and  $\omega$  are linearly related. But the disadvantage is that we should expect some aliasing of the analog frequency response, and in some cases this aliasing is intolerable. Consequently, this design method is useful only when the analog filter

is essentially band-limited to a lowpass or bandpass filter in which there are no oscillations in the stopband.

#### 8.4.3 BILINEAR TRANSFORMATION

This mapping is the best transformation method; it involves a well-known function given by

$$s = \frac{2}{T} \frac{1 - z^{-1}}{1 + z^{-1}} \implies z = \frac{1 + sT/2}{1 - sT/2} \quad (8.65)$$

where  $T$  is a parameter. Another name for this transformation is the *linear fractional* transformation because when cleared of fractions, we obtain

$$\frac{T}{2}sz + \frac{T}{2}s - z + 1 = 0$$

which is linear in each variable if the other is fixed, or *bilinear* in  $s$  and  $z$ . The complex plane mapping under (8.65) is shown in Figure 8.25, from which we have the following observations.

1. Using  $s = \sigma + j\Omega$  in (8.65), we obtain

$$z = \left(1 + \frac{\sigma T}{2} + j\frac{\Omega T}{2}\right) / \left(1 - \frac{\sigma T}{2} - j\frac{\Omega T}{2}\right) \quad (8.66)$$

Hence

$$\sigma < 0 \implies |z| = \left| \frac{1 + \frac{\sigma T}{2} + j\frac{\Omega T}{2}}{1 - \frac{\sigma T}{2} - j\frac{\Omega T}{2}} \right| < 1$$

$$\sigma = 0 \implies |z| = \left| \frac{1 + j\frac{\Omega T}{2}}{1 - j\frac{\Omega T}{2}} \right| = 1$$

$$\sigma > 0 \implies |z| = \left| \frac{1 + \frac{\sigma T}{2} + j\frac{\Omega T}{2}}{1 - \frac{\sigma T}{2} - j\frac{\Omega T}{2}} \right| > 1$$

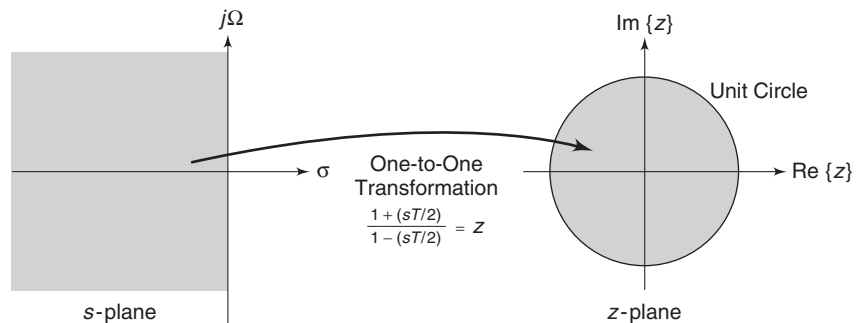


**FIGURE 8.25** Complex-plane mapping in bilinear transformation

2. The entire left half-plane maps into the inside of the unit circle. Hence this is a stable transformation.
3. The imaginary axis maps onto the unit circle in a one-to-one fashion. Hence there is no aliasing in the frequency domain.

Substituting  $\sigma = 0$  in (8.66), we obtain

$$z = \frac{1 + j\frac{\Omega T}{2}}{1 - j\frac{\Omega T}{2}} = e^{j\omega}$$

since the magnitude is 1. Solving for  $\omega$  as a function of  $\Omega$ , we obtain

$$\omega = 2 \tan^{-1} \left( \frac{\Omega T}{2} \right) \quad \text{or} \quad \Omega = \frac{2}{T} \tan \left( \frac{\omega}{2} \right) \quad (8.67)$$

This shows that  $\Omega$  is nonlinearly related to (or warped into)  $\omega$  but that there is no aliasing. Hence, in (8.67), we will say that  $\omega$  is prewarped into  $\Omega$ .

- EXAMPLE 8.15** Transform  $H_a(s) = \frac{s+1}{s^2+5s+6}$  into a digital filter using the bilinear transformation. Choose  $T = 1$ .

#### Solution

Using (8.65), we obtain

$$\begin{aligned} H(z) &= H_a \left( \frac{2}{T} \frac{1-z^{-1}}{1+z^{-1}} \Big|_{T=1} \right) = H_a \left( 2 \frac{1-z^{-1}}{1+z^{-1}} \right) \\ &= \frac{2 \frac{1-z^{-1}}{1+z^{-1}} + 1}{\left( 2 \frac{1-z^{-1}}{1+z^{-1}} \right)^2 + 5 \left( 2 \frac{1-z^{-1}}{1+z^{-1}} \right) + 6} \end{aligned}$$

Simplifying,

$$H(z) = \frac{3 + 2z^{-1} - z^{-2}}{20 + 4z^{-1}} = \frac{0.15 + 0.1z^{-1} - 0.05z^{-2}}{1 + 0.2z^{-1}}$$

□

MATLAB provides a function called `bilinear` to implement this mapping. Its invocation is similar to the `imp_invr` function, but it also takes several forms for different input-output quantities. The SP toolbox manual should be consulted for more details. Its use is shown in the following example.

- **EXAMPLE 8.16** Transform the system function  $H_a(s)$  in Example 8.15 using the `bilinear` function.

**Solution**

MATLAB script:

```
>> c = [1,1]; d = [1,5,6]; T = 1; Fs = 1/T;
>> [b,a] = bilinear(c,d,Fs)
b = 0.1500    0.1000   -0.0500
a = 1.0000    0.2000   0.0000
```

The filter is

$$H(z) = \frac{0.15 + 0.1z^{-1} - 0.05z^{-2}}{1 + 0.2z^{-1}}$$

as before. □

#### 8.4.4 DESIGN PROCEDURE

Given digital filter specifications  $\omega_p$ ,  $\omega_s$ ,  $R_p$ , and  $A_s$ , we want to determine  $H(z)$ . The design steps in this procedure are the following.

1. Choose a value for  $T$ . This is arbitrary, and we may set  $T = 1$ .
2. Pre-warp the cutoff frequencies  $\omega_p$  and  $\omega_s$ ; that is, calculate  $\Omega_p$  and  $\Omega_s$  using (8.67):

$$\Omega_p = \frac{2}{T} \tan\left(\frac{\omega_p}{2}\right), \quad \Omega_s = \frac{2}{T} \tan\left(\frac{\omega_s}{2}\right) \quad (8.68)$$

3. Design an analog filter  $H_a(s)$  to meet the specifications  $\Omega_p$ ,  $\Omega_s$ ,  $R_p$ , and  $A_s$ . We have already described how to do this in the previous section.
4. Finally, set

$$H(z) = H_a\left(\frac{2}{T} \frac{1-z^{-1}}{1+z^{-1}}\right)$$

and simplify to obtain  $H(z)$  as a rational function in  $z^{-1}$ .

In the next several examples, we demonstrate this design procedure on our analog prototype filters.

- **EXAMPLE 8.17** Design the digital Butterworth filter of Example 8.11. The specifications are

$$\omega_p = 0.2\pi, R_p = 1 \text{ dB}$$

$$\omega_s = 0.3\pi, A_s = 15 \text{ dB}$$

**Solution**

MATLAB script:

```

>> % Digital filter specifications:
>> wp = 0.2*pi;                                % Digital passband freq in rad
>> ws = 0.3*pi;                                % Digital stopband freq in rad
>> Rp = 1;                                     % Passband ripple in dB
>> As = 15;                                    % Stopband attenuation in dB
>> % Analog prototype specifications: Inverse mapping for frequencies
>> T = 1; Fs = 1/T;                             % Set T=1
>> OmegaP = (2/T)*tan(wp/2);                   % Pre-warp prototype passband freq
>> OmegaS = (2/T)*tan(ws/2);                   % Pre-warp prototype stopband freq
>> % Analog Butterworth prototype filter calculation:
>> [cs,ds] = afd_but(2,T,wp,As);
*** Butterworth Filter Order = 6
>> % Bilinear transformation:
>> [b,a] = bilinear(cs,ds,Fs);    [C,B,A] = dir2cas(b,a)
C = 5.7969e-004
B = 1.0000    2.0183    1.0186
      1.0000    1.9814    0.9817
      1.0000    2.0004    1.0000
A = 1.0000   -0.9459    0.2342
      1.0000   -1.0541    0.3753
      1.0000   -1.3143    0.7149

```

The desired filter is once again a sixth-order filter and has six zeros. Since the sixth-order zero of  $H_a(s)$  at  $s = -\infty$  is mapped to  $z = -1$ , these zeros should be at  $z = -1$ . Due to the finite precision of MATLAB, these zeros are not exactly at  $z = -1$ . Hence the system function should be

$$H(z) = \frac{0.00057969 (1 + z^{-1})^6}{(1 - 0.9459z^{-1} + 0.2342z^{-2})(1 - 1.0541z^{-1} + 0.3753z^{-2})(1 - 1.3143z^{-1} + 0.7149z^{-2})}$$

The frequency response plots are given in Figure 8.26. Comparing these plots with those in Figure 8.21, we observe that these two designs are very similar.

□

- **EXAMPLE 8.18** Design the digital Chebyshev-I filter of Example 8.12. The specifications are

$$\omega_p = 0.2\pi, R_p = 1 \text{ dB}$$

$$\omega_s = 0.3\pi, A_s = 15 \text{ dB}$$

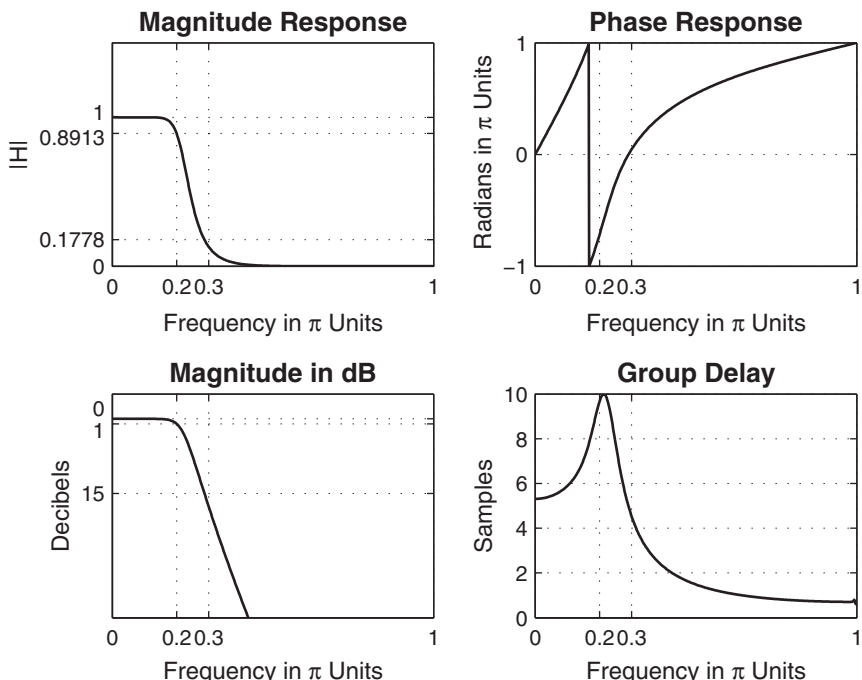


**FIGURE 8.26** Digital Butterworth lowpass filter using bilinear transformation

Solution

MATLAB script:

```

>> % Digital filter specifications:
>> wp = 0.2*pi;                                % Digital passband freq in rad
>> ws = 0.3*pi;                                % Digital stopband freq in rad
>> Rp = 1;                                     % Passband ripple in dB
>> As = 15;                                    % Stopband attenuation in dB
>> % Analog prototype specifications: Inverse mapping for frequencies
>> T = 1; Fs = 1/T;                             % Set T=1
>> OmegaP = (2/T)*tan(wp/2);                   % Prewarp prototype passband freq
>> OmegaS = (2/T)*tan(ws/2);                   % Prewarp prototype stopband freq
>> % Analog Chebyshev-1 prototype filter calculation:
>> [cs,ds] = afd_chb1(OmegaP,OmegaS,Rp,As);
*** Chebyshev-1 Filter Order = 4
>> % Bilinear transformation:
>> [b,a] = bilinear(cs,ds,Fs);    [C,B,A] = dir2cas(b,a)
C = 0.0018
B = 1.0000    2.0000    1.0000
          1.0000    2.0000    1.0000
A = 1.0000   -1.4996    0.8482
          1.0000   -1.5548    0.6493

```

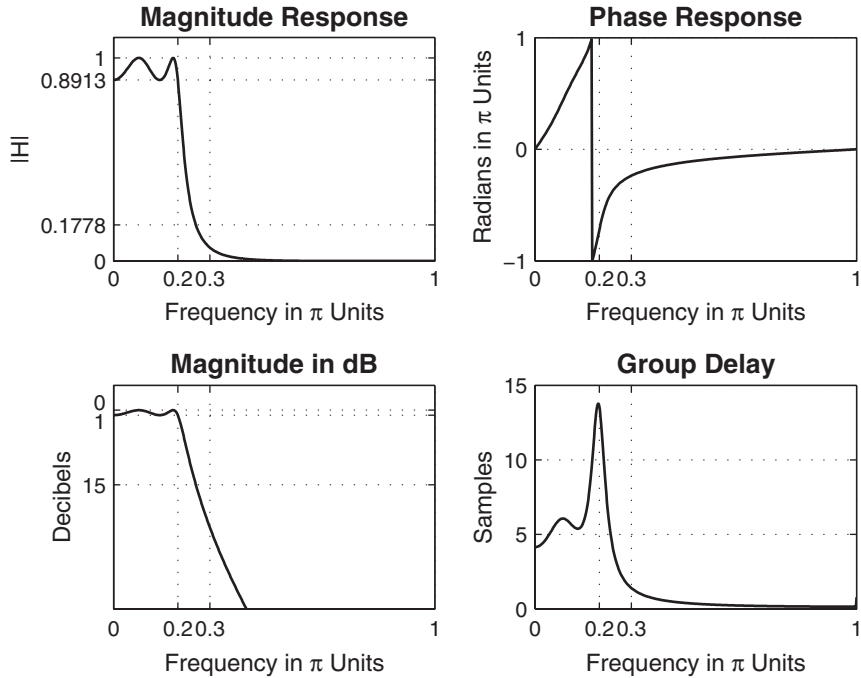


**FIGURE 8.27** Digital Chebyshev-I lowpass filter using bilinear transformation

The desired filter is a fourth-order filter and has four zeros at  $z = -1$ . The system function is

$$H(z) = \frac{0.0018 (1 + z^{-1})^4}{(1 - 1.4996z^{-1} + 0.8482z^{-2})(1 - 1.5548z^{-1} + 0.6493z^{-2})}$$

The frequency response plots are given in Figure 8.27, which are similar to those in Figure 8.22.  $\square$

- EXAMPLE 8.19** Design the digital Chebyshev-II filter of Example 8.13. The specifications are

$$\omega_p = 0.2\pi, R_p = 1 \text{ dB}$$

$$\omega_s = 0.3\pi, A_s = 15 \text{ dB}$$

**Solution**

MATLAB script:

```

>> % Digital filter specifications:
>> wp = 0.2*pi;                                % Digital passband freq in rad
>> ws = 0.3*pi;                                % Digital stopband freq in rad
>> Rp = 1;                                     % Passband ripple in dB
>> As = 15;                                    % Stopband attenuation in dB
>> % Analog prototype specifications: Inverse mapping for frequencies
>> T = 1; Fs = 1/T;                             % Set T=1
>> OmegaP = (2/T)*tan(wp/2);                   % Prewarp prototype passband freq
>> OmegaS = (2/T)*tan(ws/2);                   % Prewarp prototype stopband freq
>> % Analog Chebyshev-2 Prototype Filter Calculation:
>> [cs,ds] = afd_chb2(OmegaP,OmegaS,Rp,As);
*** Chebyshev-2 Filter Order = 4
>> % Bilinear transformation:
>> [b,a] = bilinear(cs,ds,Fs);    [C,B,A] = dir2cas(b,a)
C = 0.1797
B = 1.0000    0.5574    1.0000
        1.0000   -1.0671    1.0000
A = 1.0000    -0.4183    0.1503
        1.0000   -1.1325    0.7183

```

The desired filter is again a fourth-order filter with system function

$$H(z) = \frac{0.1797 (1 + 0.5574z^{-1} + z^{-2}) (1 - 1.0671z^{-1} + z^{-2})}{(1 - 0.4183z^{-1} + 0.1503z^{-2}) (1 - 1.1325z^{-1} + 0.7183z^{-2})}$$

The frequency response plots are given in Figure 8.28. Note that the bilinear transformation has properly designed the Chebyshev-II digital filter.  $\square$

- $\square$  **EXAMPLE 8.20** Design the digital elliptic filter of Example 8.14. The specifications are

$$\omega_p = 0.2\pi, R_p = 1 \text{ dB}$$

$$\omega_s = 0.3\pi, A_s = 15 \text{ dB}$$

**Solution**

MATLAB script:

```

>> % Digital filter specifications:
>> wp = 0.2*pi;                                % Digital passband freq in rad
>> ws = 0.3*pi;                                % Digital stopband freq in rad
>> Rp = 1;                                     % Passband ripple in dB
>> As = 15;                                    % Stopband attenuation in dB
>> % Analog prototype specifications: Inverse mapping for frequencies
>> T = 1; Fs = 1/T;                             % Set T=1

```

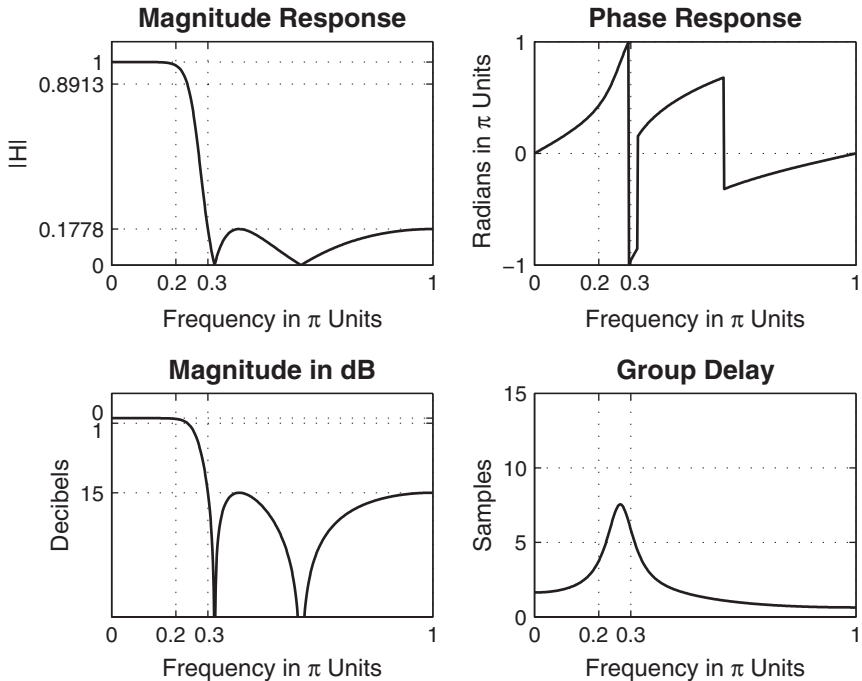


**FIGURE 8.28** Digital Chebyshev-II lowpass filter using bilinear transformation

```

>> OmegaP = (2/T)*tan(wp/2); % Prewarp prototype passband freq
>> OmegaS = (2/T)*tan(ws/2); % Prewarp prototype stopband freq
>> % Analog elliptic prototype filter calculation:
>> [cs,ds] = afd_elip(OmegaP,OmegaS,Rp,As);
*** Elliptic Filter Order = 3
>> % Bilinear transformation:
>> [b,a] = bilinear(cs,ds,Fs); [C,B,A] = dir2cas(b,a)
C = 0.1214
B = 1.0000   -1.4211   1.0000
           1.0000   1.0000    0
A = 1.0000   -1.4928   0.8612
           1.0000   -0.6183    0

```

The desired filter is a third-order filter with system function

$$H(z) = \frac{0.1214 (1 - 1.4211z^{-1} + z^{-2}) (1 + z^{-1})}{(1 - 1.4928z^{-1} + 0.8612z^{-2})(1 - 0.6183z^{-1})}$$

The frequency response plots are given in Figure 8.29. Note that the bilinear transformation has again properly designed the elliptic digital filter.  $\square$

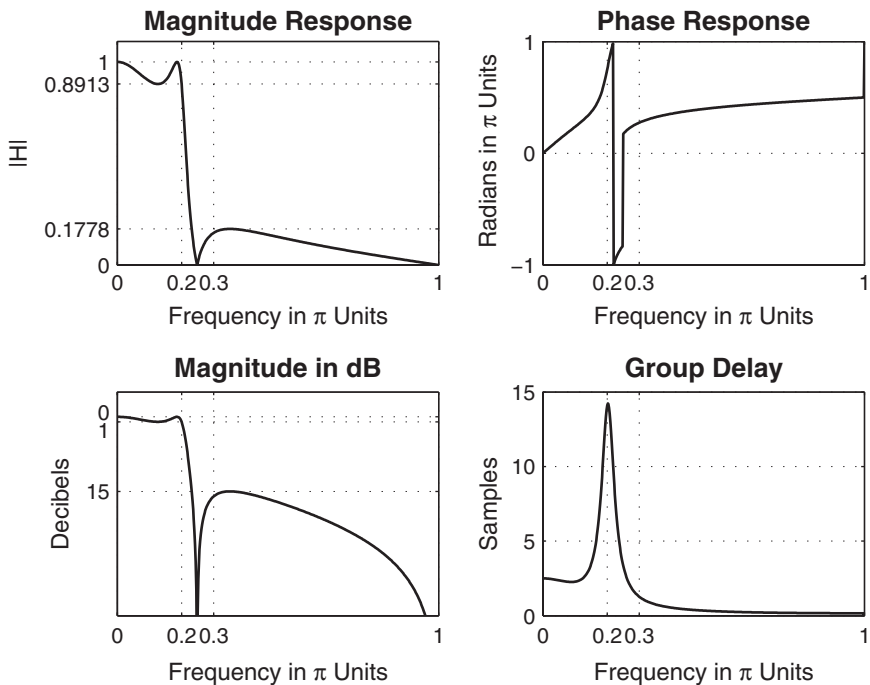


**FIGURE 8.29** Digital elliptic lowpass filter using bilinear transformation

The advantages of this mapping are that (a) it is a stable design, (b) there is no aliasing, and (c) there is no restriction on the type of filter that can be transformed. Therefore, this method is used exclusively in computer programs including MATLAB, as we shall see next.

#### 8.4.5 MATCHED- $z$ TRANSFORMATION

In this method of filter transformation, zeros and poles of  $H_a(s)$  are directly mapped into zeros and poles in the  $z$ -plane using an exponential function. Given a root (zero or pole) at the location  $s = a$  in the  $s$ -plane, we map it in the  $z$ -plane at  $z = e^{aT}$  where  $T$  is a sampling interval. Thus the system function  $H_a(s)$  with zeros  $\{z_k\}$  and poles  $\{p_\ell\}$  is mapped into the digital filter system function  $H(z)$  as

$$H_a(s) = \frac{\prod_{k=1}^M (s - z_k)}{\prod_{\ell=1}^N (s - p_\ell)} \rightarrow H(z) = \frac{\prod_{k=1}^M (1 - e^{z_k T} z^{-1})}{\prod_{\ell=1}^N (1 - e^{p_\ell T} z^{-1})} \quad (8.69)$$

Clearly, the  $z$ -transform system function is “matched” to the  $s$ -domain system function.

Note that this technique appears to be similar to the impulse invariance mapping in that the pole locations are identical and aliasing

is unavoidable. However, these two techniques differ in zero locations. Also, the matched- $z$  transformation does not preserve either the impulse response or the frequency response characteristics. Hence it is suitable when designing using pole-zero placement, but it is generally unsuitable when the frequency-domain specifications are given.

## 8.5 LOWPASS FILTER DESIGN USING MATLAB

---

In this section, we will demonstrate the use of MATLAB's filter design functions to design digital lowpass filters. These functions use the bilinear transformation because of its desirable advantages as discussed in the previous section. These functions are as follows.

1. **[b,a]=butter(N,wn)**

This function designs an  $N$ th-order lowpass digital Butterworth filter and returns the filter coefficients in length  $N + 1$  vectors **b** and **a**. The filter order is given by (8.49), and the cutoff frequency **wn** is determined by the prewarping formula (8.68). However, in MATLAB all digital frequencies are given in *units of  $\pi$* . Hence **wn** is computed by using the following relation:

$$\omega_n = \frac{2}{\pi} \tan^{-1} \left( \frac{\Omega_c T}{2} \right)$$

The use of this function is given in Example 8.21.

2. **[b,a]=cheby1(N,Rp,wn)**

This function designs an  $N$ th-order lowpass digital Chebyshev-I filter with **Rp** decibels of ripple in the passband. It returns the filter coefficients in length  $N + 1$  vectors **b** and **a**. The filter order is given by (8.59), and the cutoff frequency **wn** is the digital passband frequency in units of  $\pi$ ; that is,

$$\omega_n = \omega_p / \pi$$

The use of this function is given in Example 8.22.

3. **[b,a]=cheby2(N,As,wn)**

This function designs an  $N$ th-order lowpass digital Chebyshev-II filter with the stopband attenuation **As** decibels. It returns the filter coefficients in length  $N + 1$  vectors **b** and **a**. The filter order is given by (8.59), and the cutoff frequency **wn** is the digital stopband frequency in units of  $\pi$ ; that is,

$$\omega_n = \omega_s / \pi$$

The use of this function is given in Example 8.23.

4. **[b,a]=ellip(N,Rp,As,wn)**

This function designs an  $N$ th-order lowpass digital elliptic filter with the passband ripple of  $R_p$  decibels and a stopband attenuation of  $A_s$  decibels. It returns the filter coefficients in length  $N + 1$  vectors **b** and **a**. The filter order is given by (8.62), and the cutoff frequency **wn** is the digital passband frequency in units of  $\pi$ ; that is,

$$\omega_n = \omega_p / \pi$$

The use of this function is given in Example 8.24.

All these above functions can also be used to design other frequency-selective filters, such as highpass and bandpass. We will discuss their additional capabilities in Section 8.6.

There is also another set of filter functions—namely, the **buttord**, **cheb1ord**, **cheb2ord**, and **ellipord** functions—that can provide filter order  $N$  and filter cutoff frequency  $\omega_n$ , given the specifications. These functions are available in the Signal Processing toolbox. In the examples to follow, we will determine these parameters using the formulas given earlier. We will discuss the filter-order functions in the next section.

In the following examples, we will redesign the same lowpass filters of previous examples and compare their results. The specifications of the lowpass digital filter are

$$\omega_p = 0.2\pi, R_p = 1 \text{ dB}$$

$$\omega_s = 0.3\pi, A_s = 15 \text{ dB}$$

□ **EXAMPLE 8.21** Digital Butterworth lowpass filter design:

```
>> % Digital filter specifications:
>> wp = 0.2*pi; % Digital passband freq in rad
>> ws = 0.3*pi; % Digital stopband freq in rad
>> Rp = 1; % Passband ripple in dB
>> As = 15; % Stopband attenuation in dB

>> % Analog Prototype Specifications:
>> T = 1; % Set T=1
>> OmegaP = (2/T)*tan(wp/2); % Prewarp prototype passband freq
>> OmegaS = (2/T)*tan(ws/2); % Prewarp prototype stopband freq
>> % Analog Prototype Order Calculation:
>> N =ceil((log10((10^(Rp/10)-1)/(10^(As/10)-1)))/(2*log10(OmegaP/OmegaS)));
>> fprintf('\n*** Butterworth Filter Order = %2.0f \n',N)
** Butterworth Filter Order = 6
>> OmegaC = OmegaP/((10^(Rp/10)-1)^(1/(2*N))); % Analog BF prototype cutoff
>> wn = 2*atan((OmegaC*T)/2); % Digital BF cutoff freq
```

```
>> % Digital butterworth filter design:
>> wn = wn/pi; % Digital BF cutoff in pi units
>> [b,a]=butter(N,wn); [b0,B,A] = dir2cas(b,a)
C = 5.7969e-004
B = 1.0000    2.0297    1.0300
      1.0000    1.9997    1.0000
      1.0000    1.9706    0.9709
A = 1.0000   -0.9459    0.2342
      1.0000   -1.0541    0.3753
      1.0000   -1.3143    0.7149
```

The system function is

$$H(z) = \frac{0.00057969 (1 + z^{-1})^6}{(1 - 0.9459z^{-1} + 0.2342z^{-2})(1 - 1.0541z^{-1} + 0.3753z^{-2})(1 - 1.3143z^{-1} + 0.7149z^{-2})}$$

which is the same as in Example 8.17. The frequency-domain plots were shown in Figure 8.26.  $\square$

$\square$  EXAMPLE 8.22 Digital Chebyshev-I lowpass filter design:

```
>> % Digital filter specifications:
>> wp = 0.2*pi; % Digital passband freq in rad
>> ws = 0.3*pi; % Digital stopband freq in rad
>> Rp = 1; % Passband ripple in dB
>> As = 15; % Stopband attenuation in dB

>> % Analog prototype specifications:
>> T = 1; % Set T=1
>> OmegaP = (2/T)*tan(wp/2); % Prewarp prototype passband freq
>> OmegaS = (2/T)*tan(ws/2); % Prewarp prototype stopband freq

>> % Analog prototype order calculation:
>> ep = sqrt(10^(Rp/10)-1); % Passband ripple factor
>> A = 10^(As/20); % Stopband attenuation factor
>> OmegaC = OmegaP; % Analog prototype cutoff freq
>> OmegaR = OmegaS/OmegaP; % Analog prototype transition ratio
>> g = sqrt(A*A-1); % Analog prototype intermediate cal.
>> N = ceil(log10(g+sqrt(g*g-1))/log10(OmegaR+sqrt(OmegaR*OmegaR-1)));
>> fprintf('\n*** Chebyshev-1 Filter Order = %.2f\n',N)
*** Chebyshev-1 Filter Order = 4
>> % Digital Chebyshev-I Filter Design:
>> wn = wp/pi; % Digital passband freq in pi units
>> [b,a]=cheby1(N,Rp,wn); [b0,B,A] = dir2cas(b,a)
```

```
b0 = 0.0018
B = 1.0000    2.0000    1.0000
          1.0000    2.0000    1.0000
A = 1.0000   -1.4996    0.8482
          1.0000   -1.5548    0.6493
```

The system function is

$$H(z) = \frac{0.0018 (1 + z^{-1})^4}{(1 - 1.4996z^{-1} + 0.8482z^{-2})(1 - 1.5548z^{-1} + 0.6493z^{-2})}$$

which is the same as in Example 8.18. The frequency-domain plots were shown in Figure 8.27.  $\square$

$\square$  **EXAMPLE 8.23** Digital Chebyshev-II lowpass filter design:

```
>> % Digital filter specifications:
>> wp = 0.2*pi;                                % Digital passband freq in rad
>> ws = 0.3*pi;                                % Digital stopband freq in rad
>> Rp = 1;                                     % Passband ripple in dB
>> As = 15;                                    % Stopband attenuation in dB

>> % Analog prototype specifications:
>> T = 1;                                       % Set T=1
>> OmegaP = (2/T)*tan(wp/2);                   % Prewarp prototype passband freq
>> OmegaS = (2/T)*tan(ws/2);                   % Prewarp prototype stopband freq

>> % Analog prototype order calculation:
>> ep = sqrt(10^(Rp/10)-1);                  % Passband ripple factor
>> A = 10^(As/20);                            % Stopband attenuation factor
>> OmegaC = OmegaP;                           % Analog prototype cutoff freq
>> OmegaR = OmegaS/OmegaP;                    % Analog prototype transition ratio
>> g = sqrt(A*A-1)/ep;                      % Analog prototype intermediate cal.
>> N = ceil(log10(g+sqrt(g*g-1))/log10(OmegaR+sqrt(OmegaR*OmegaR-1)));
>> fprintf('\n*** Chebyshev-2 Filter Order = %2.0f \n',N)
*** Chebyshev-2 Filter Order = 4

>> % Digital Chebyshev-II filter design:
>> wn = ws/pi;                                % Digital stopband freq in pi units
>> [b,a]=cheby2(N,As,wn); [b0,B,A] = dir2cas(b,a)
b0 = 0.1797
B = 1.0000    0.5574    1.0000
          1.0000   -1.0671    1.0000
A = 1.0000   -0.4183    0.1503
          1.0000   -1.1325    0.7183
```

The system function is

$$H(z) = \frac{0.1797(1 + 0.5574z^{-1} + z^{-2})(1 - 1.0671z^{-1} + z^{-2})}{(1 - 0.4183z^{-1} + 0.1503z^{-2})(1 - 1.1325z^{-1} + 0.7183z^{-2})}$$

which is the same as in Example 8.19. The frequency-domain plots were shown in Figure 8.28.  $\square$

**EXAMPLE 8.24** Digital elliptic lowpass filter design:

```
>> % Digital filter specifications:
>> wp = 0.2*pi;                                % Digital passband freq in rad
>> ws = 0.3*pi;                                % Digital stopband freq in rad
>> Rp = 1;                                     % Passband ripple in dB
>> As = 15;                                    % Stopband attenuation in dB

>> % Analog prototype specifications:
>> T = 1;                                       % Set T=1
>> OmegaP = (2/T)*tan(wp/2);                   % Prewarp prototype passband freq
>> OmegaS = (2/T)*tan(ws/2);                   % Prewarp prototype stopband freq

>> % Analog elliptic filter order calculations:
>> ep = sqrt(10^(Rp/10)-1);                    % Passband ripple factor
>> A = 10^(As/20);                            % Stopband attenuation factor
>> OmegaC = OmegaP;                           % Analog prototype cutoff freq
>> k = OmegaP/OmegaS;                         % Analog prototype transition ratio
>> k1 = ep/sqrt(A*A-1);                      % Analog prototype intermediate cal.
>> capk = ellipke([k.^2 1-k.^2]);
>> capk1 = ellipke([(k1.^2) 1-(k1.^2)]);
>> N = ceil(capk1(1)*capk1(2)/(capk2*capk1(1)));
>> fprintf('\n*** Elliptic Filter Order = %2.0f \n',N)
*** Elliptic Filter Order = 3

>> % Digital elliptic filter design:
>> wn = wp/pi;                                 % Digital passband freq in pi units
>> [b,a]=ellip(N,Rp,As,wn);      [b0,B,A] = dir2cas(b,a)
b0 = 0.1214
B = 1.0000   -1.4211    1.0000
          1.0000        0
A = 1.0000   -1.4928    0.8612
          1.0000   -0.6183        0
```

The system function is

$$H(z) = \frac{0.1214(1 - 1.4211z^{-1} + z^{-2})(1 + z^{-1})}{(1 - 1.4928z^{-1} + 0.8612z^{-2})(1 - 0.6183z^{-1})}$$

which is the same as in Example 8.20. The frequency-domain plots were shown in Figure 8.29.  $\square$

**TABLE 8.1** Comparison of four prototype filters

Prototype	Order $N$	Actual $R_p$	Actual $A_s$
Butterworth	6	1	17.6
Chebyshev-I	4	1	23.6
Chebyshev-II	4	0.15	15
Elliptic	3	1	16

### 8.5.1 COMPARISON OF FOUR PROTOTYPE FILTERS

In Examples 8.17–8.20, we designed a lowpass digital filter using the bilinear mapping on four different prototype analog filters satisfying the specifications  $\omega_p = 0.2\pi$ ,  $R_p = 1$  dB,  $\omega_s = 0.3\pi$ , and  $A_s = 15$  dB. Let us now compare their performance in terms of order  $N$ , the actual passband ripple  $R_p$  measured at  $\omega_p$ , and the actual stopband attenuation  $A_s$  measured at  $\omega_s$ . This comparison is shown in Table 8.1. The Butterworth, Chebyshev-I, and elliptic filters satisfy  $R_p$  specification exactly at  $\omega_p$  but exceed  $A_s$  specification at  $\omega_s$  while the Chebyshev-II filter performs exactly opposite.

Clearly, the elliptic prototype gives the best design in terms of the smallest order while satisfying magnitude specifications almost exactly. However, if we compare phase responses of all four filters, then the elliptic design has the most nonlinear phase response in the passband, while Butterworth has the least nonlinear phase response.

## 8.6 FREQUENCY-BAND TRANSFORMATIONS

In the preceding two sections, we designed digital lowpass filters from their corresponding analog filters. Certainly, we would like to design other types of frequency-selective filters, such as highpass, bandpass, and bandstop. This is accomplished by transforming the frequency axis (or band) of a lowpass filter so that it behaves as another frequency-selective filter. These transformations on the complex variable  $z$  are very similar to bilinear transformations, and the design equations are algebraic. The procedure to design a general frequency-selective filter is to first design a *digital prototype* (of fixed bandwidth—say, unit bandwidth) lowpass filter and then to apply these algebraic transformations. In this section, we will describe the basic philosophy behind these mappings and illustrate their mechanism through examples. MATLAB provides functions that incorporate frequency-band transformation in the  $s$ -plane. We will first demonstrate the use of the  $z$ -plane mapping and then illustrate the use of MATLAB functions. Typical specifications for most commonly used types of frequency-selective digital filters are shown in Figure 8.30.

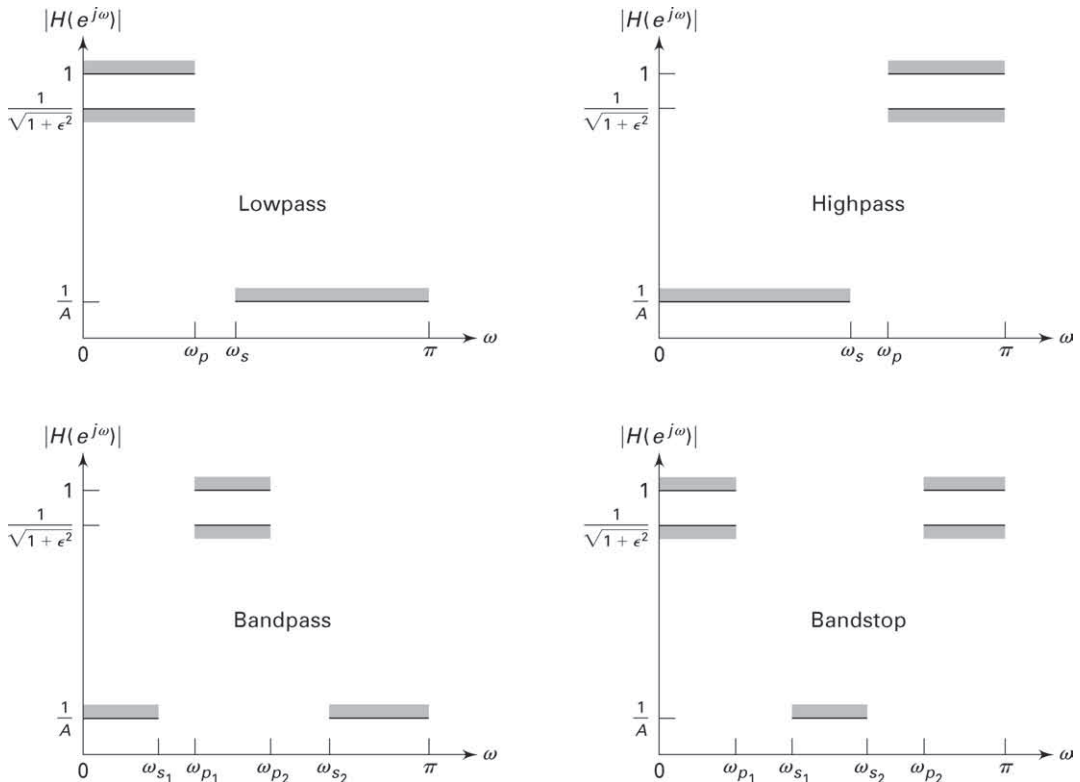


**FIGURE 8.30** Specifications of frequency-selective filters

Let  $H_{LP}(Z)$  be the given prototype lowpass digital filter, and let  $H(z)$  be the desired frequency-selective digital filter. Note that we are using two different frequency variables,  $Z$  and  $z$ , with  $H_{LP}$  and  $H$ , respectively. Define a mapping of the form

$$Z^{-1} = G(z^{-1})$$

such that

$$H(z) = H_{LP}(Z)|_{Z^{-1}=G(z^{-1})}$$

To do this, we simply replace  $Z^{-1}$  everywhere in  $H_{LP}$  by the function  $G(z^{-1})$ . Given that  $H_{LP}(Z)$  is a stable and causal filter, we also want  $H(z)$  to be stable and causal. This imposes the following requirements.

1.  $G(\cdot)$  must be a rational function in  $z^{-1}$  so that  $H(z)$  is implementable.
2. The unit circle of the  $Z$ -plane must map onto the unit circle of the  $z$ -plane.
3. For stable filters, the inside of the unit circle of the  $Z$ -plane must also map onto the inside of the unit circle of the  $z$ -plane.

Let  $\omega'$  and  $\omega$  be the frequency variables of  $Z$  and  $z$ , respectively—that is,  $Z = e^{j\omega'}$  and  $z = e^{j\omega}$  on their respective unit circles. Then requirement 2 above implies that

$$|Z^{-1}| = |G(z^{-1})| = |G(e^{-j\omega})| = 1$$

and

$$e^{-j\omega'} = |G(e^{-j\omega})| e^{j\angle G(e^{-j\omega})}$$

or

$$-\omega' = \angle G(e^{-j\omega})$$

The general form of the function  $G(\cdot)$  that satisfies these requirements is a rational function of the *allpass* type given by

$$Z^{-1} = G(z^{-1}) = \pm \prod_{k=1}^n \frac{z^{-1} - \alpha_k}{1 - \alpha_k z^{-1}}$$

where  $|\alpha_k| < 1$  for stability and to satisfy requirement 3.

Now by choosing an appropriate order  $n$  and the coefficients  $\{\alpha_k\}$ , we can obtain a variety of mappings. The most widely used transformations are given in Table 8.2. We will now illustrate the use of this table for designing a highpass digital filter.

- **EXAMPLE 8.25** In Example 8.22 we designed a Chebyshev-I lowpass filter with specifications

$$\omega_p' = 0.2\pi, \quad R_p = 1 \text{ dB}$$

$$\omega_s' = 0.3\pi, \quad A_s = 15 \text{ dB}$$

and determined its system function

$$H_{LP}(Z) = \frac{0.001836(1 + Z^{-1})^4}{(1 - 1.4996Z^{-1} + 0.8482Z^{-2})(1 - 1.5548Z^{-1} + 0.6493Z^{-2})}$$

Design a highpass filter with these tolerances but with passband beginning at  $\omega_p = 0.6\pi$ .

### Solution

We want to transform the given lowpass filter into a highpass filter such that the cutoff frequency  $\omega_p' = 0.2\pi$  is mapped onto the cutoff frequency  $\omega_p = 0.6\pi$ . From Table 8.2,

$$\alpha = -\frac{\cos[(0.2\pi + 0.6\pi)/2]}{\cos[(0.2\pi - 0.6\pi)/2]} = -0.38197 \quad (8.70)$$

Hence

$$\begin{aligned} H_{LP}(z) &= H(Z)|_{Z=-\frac{z^{-1}-0.38197}{1-0.38197z^{-1}}} \\ &= \frac{0.02426(1 - z^{-1})^4}{(1 + 0.5661z^{-1} + 0.7657z^{-2})(1 + 1.0416z^{-1} + 0.4019z^{-2})} \end{aligned}$$

which is the desired filter. The frequency response plots of the lowpass filter and the new highpass filter are shown in Figure 8.31. □

**TABLE 8.2** Frequency transformation for digital filters (prototype lowpass filter has cutoff frequency  $\omega'_c$ )

Type of Transformation	Transformation	Parameters
Lowpass	$z^{-1} \rightarrow \frac{z^{-1} - \alpha}{1 - \alpha z^{-1}}$	$\omega_c = \text{cutoff frequency of new filter}$ $\alpha = \frac{\sin[(\omega'_c - \omega_c)/2]}{\sin[(\omega'_c + \omega_c)/2]}$
Highpass	$z^{-1} \rightarrow -\frac{z^{-1} + \alpha}{1 + \alpha z^{-1}}$	$\omega_c = \text{cutoff frequency of new filter}$ $\alpha = -\frac{\cos[(\omega'_c + \omega_c)/2]}{\cos[(\omega'_c - \omega_c)/2]}$
Bandpass	$z^{-1} \rightarrow -\frac{z^{-2} - \alpha_1 z^{-1} + \alpha_2}{\alpha_2 z^{-2} - \alpha_1 z^{-1} + 1}$	$\omega_\ell = \text{lower cutoff frequency}$ $\omega_u = \text{upper cutoff frequency}$ $\alpha_1 = -2\beta K/(K+1)$ $\alpha_2 = (K-1)/(K+1)$ $\beta = \frac{\cos[(\omega_u + \omega_\ell)/2]}{\cos[(\omega_u - \omega_\ell)/2]}$ $K = \cot \frac{\omega_u - \omega_\ell}{2} \tan \frac{\omega'_c}{2}$
Bandstop	$z^{-1} \rightarrow \frac{z^{-2} - \alpha_1 z^{-1} + \alpha_2}{\alpha_2 z^{-2} - \alpha_1 z^{-1} + 1}$	$\omega_\ell = \text{lower cutoff frequency}$ $\omega_u = \text{upper cutoff frequency}$ $\alpha_1 = -2\beta/(K+1)$ $\alpha_2 = (K-1)/(K+1)$ $\beta = \frac{\cos[(\omega_u + \omega_\ell)/2]}{\cos[(\omega_u - \omega_\ell)/2]}$ $K = \tan \frac{\omega_u - \omega_\ell}{2} \tan \frac{\omega'_c}{2}$

From this example, it is obvious that to obtain the rational function of a new digital filter from the prototype lowpass digital filter, we should be able to implement rational function substitutions from Table 8.2. This appears to be a difficult task, but since these are algebraic functions, we can use the `conv` function repetitively for this purpose. The following `zmapping` function illustrates this approach.

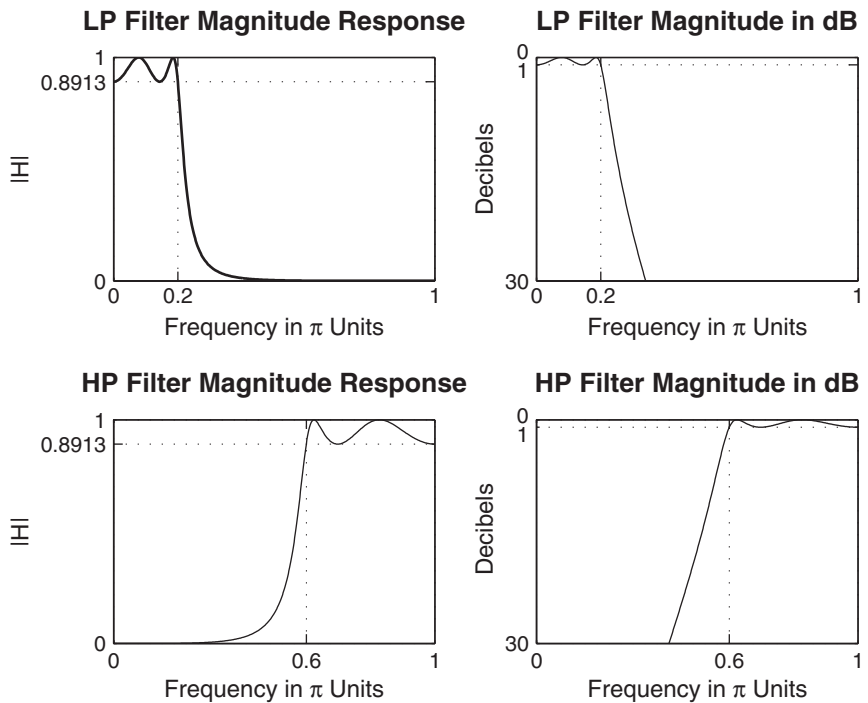


**FIGURE 8.31** Magnitude response plots for Example 8.25

```

function [bz,az] = zmapping(bZ,aZ,Nz,Dz)
% Frequency-band transformation from Z-domain to z-domain
%
% [bz,az] = zmapping(bZ,aZ,Nz,Dz)
% performs:
%      b(z)   b(Z) |
%      ----- = -----| N(z)
%      a(z)   a(Z) |@Z = -----
%                           D(z)
%
bNzord = (length(bZ)-1)*(length(Nz)-1);
aDzord = (length(aZ)-1)*(length(Dz)-1);
bzord = length(bZ)-1; azord = length(aZ)-1;
bz = zeros(1,bNzord+1);
for k = 0:bzord
    pln = [1];
    for l = 0:k-1
        pln = conv(pln,Nz);
    end
    pld = [1];
    for m = 0:l-1
        pld = conv(pld,Dz);
    end
    bz(k+1) = sum(bz.*pld);
    az(k+1) = sum(az.*pln);
end

```

```

for l = 0:bzord-k-1
    pld = conv(pld,Dz);
end
bz = bz+bZ(k+1)*conv(pln,pld);
end
az = zeros(1,aDzord+1);
for k = 0:azord
    pln = [1];
    for l = 0:k-1
        pln = conv(pln,Nz);
    end
    pld = [1];
    for l = 0:azord-k-1
        pld = conv(pld,Dz);
    end
    az = az+aZ(k+1)*conv(pln,pld);
end

```

- EXAMPLE 8.26** Use the `zmapping` function to perform the lowpass-to-highpass transformation in Example 8.25.

### Solution

First we will design the lowpass digital filter in MATLAB using the bilinear transformation procedure and then use the `zmapping` function.

MATLAB script:

```

>> % Digital lowpass filter specifications:
>> wplp = 0.2*pi;                                % Digital passband freq in rad
>> wsdp = 0.3*pi;                                % Digital stopband freq in rad
>> Rp = 1;                                         % Passband ripple in dB
>> As = 15;                                         % Stopband attenuation in dB

>> % Analog prototype specifications: Inverse mapping for frequencies
>> T = 1; Fs = 1/T;                                 % Set T=1
>> OmegaP = (2/T)*tan(wplp/2);                    % Prewarp prototype passband freq
>> OmegaS = (2/T)*tan(wsdp/2);                    % Prewarp prototype stopband freq

>> % Analog Chebyshev prototype filter calculation:
>> [cs,ds] = afd_chb1(OmegaP,OmegaS,Rp,As);
** Chebyshev-1 Filter Order = 4

>> % Bilinear transformation:
>> [blp,alp] = bilinear(cs,ds,Fs);

```

```

>> % Digital highpass filter cutoff frequency:
>> wphp = 0.6*pi;                                % Passband-edge frequency

>> % LP-to-HP frequency-band transformation:
>> alpha = -(cos((wplp+wphp)/2))/(cos((wplp-wphp)/2))
alpha = -0.3820

>> Nz = -[alpha,1]; Dz = [1,alpha];
>> [bhp,ahp] = zmapping(blp,alp,Nz,Dz);   [C,B,A] = dir2cas(bhp,ahp)
C = 0.0243
B = 1.0000    -2.0000    1.0000
          1.0000    -2.0000    1.0000
A = 1.0000    1.0416    0.4019
          1.0000    0.5561    0.7647

```

The system function of the highpass filter is

$$H(z) = \frac{0.0243(1-z^{-1})^4}{(1+0.5661z^{-1}+0.7647z^{-2})(1+1.0416z^{-1}+0.4019z^{-2})}$$

which is essentially identical to that in Example 8.25.  $\square$

### 8.6.1 DESIGN PROCEDURE

In Example 8.26, a lowpass prototype digital filter was available to transform into a highpass filter so that a particular band-edge frequency was properly mapped. In practice, we have to first design a prototype lowpass digital filter whose specifications should be obtained from specifications of other frequency-selective filters as given in Figure 8.30. We will now show that the lowpass prototype filter specifications can be obtained from the transformation formulas given in Table 8.2.

Let us use the highpass filter of Example 8.25 as an example. The passband-edge frequencies were transformed using the parameter  $\alpha = -0.38197$  in (8.70). What is the stopband-edge frequency of the highpass filter, say  $\omega_s$ , corresponding to the stopband edge  $\omega'_s = 0.3\pi$  of the prototype lowpass filter? This can be answered by (8.70). Since  $\alpha$  is fixed for the transformation, we set the equation

$$\alpha = -\frac{\cos[(0.3\pi + \omega_s)/2]}{\cos[(0.3\pi - \omega_s)/2]} = -0.38197$$

This is a transcendental equation whose solution can be obtained iteratively from an initial guess. It can be done using MATLAB, and the solution is

$$\omega_s = 0.4586\pi$$

Now, in practice, we will know the desired highpass frequencies  $\omega_s$  and  $\omega_p$ , and we are required to find the prototype lowpass cutoff frequencies  $\omega'_s$  and  $\omega'_p$ . We can choose the passband frequency  $\omega'_p$  with a reasonable value—say,  $\omega'_p = 0.2\pi$ —and determine  $\alpha$  from  $\omega_p$  using the formula from Table 8.2. Now  $\omega'_s$  can be determined (for our highpass filter example) from  $\alpha$  and

$$Z = -\frac{z^{-1} + \alpha}{1 + \alpha z^{-1}}$$

where  $Z = e^{j\omega'_s}$  and  $z = e^{j\omega_s}$ , or

$$\omega'_s = \angle \left( -\frac{e^{-j\omega_s} + \alpha}{1 + \alpha e^{-j\omega_s}} \right) \quad (8.71)$$

Continuing our highpass filter example, let  $\omega_p = 0.6\pi$  and  $\omega_s = 0.4586\pi$  be the band-edge frequencies. Let us choose  $\omega'_p = 0.2\pi$ . Then  $\alpha = -0.38197$  from (8.70), and from (8.71)

$$\omega'_s = \angle \left( -\frac{e^{-j0.4586\pi} - 0.38197}{1 - 0.38197 e^{-j-0.38197}} \right) = 0.3\pi$$

as expected. Now we can design a digital lowpass filter and transform it into a highpass filter using the `zmapping` function to complete our design procedure. For designing a highpass Chebyshev-I digital filter, the above procedure can be incorporated into a MATLAB function called the `cheb1hpf` function, shown here.

```
function [b,a] = cheb1hpf(wp,ws,Rp,As)
% IIR highpass filter design using Chebyshev-1 prototype
% function [b,a] = cheb1hpf(wp,ws,Rp,As)
%   b = numerator polynomial of the highpass filter
%   a = denominator polynomial of the highpass filter
%   wp = passband frequency in radians
%   ws = stopband frequency in radians
%   Rp = passband ripple in dB
%   As = stopband attenuation in dB
%
% Determine the digital lowpass cutoff frequencies:
wplp = 0.2*pi;
alpha = -(cos((wplp+wp)/2))/(cos((wplp-wp)/2));
wslp = angle(-exp(-j*ws)+alpha)/(1+alpha*exp(-j*ws));
%
```

```
% Compute analog lowpass prototype specifications:
T = 1; Fs = 1/T;
OmegaP = (2/T)*tan(wplp/2);
OmegaS = (2/T)*tan(wsdp/2);

% Design analog Chebyshev prototype lowpass filter:
[cs,ds] = afd_chb1(OmegaP,OmegaS,Rp,As);

% Perform bilinear transformation to obtain digital lowpass
[blp,alp] = bilinear(cs,ds,Fs);

% Transform digital lowpass into highpass filter
Nz = -[alpha,1]; Dz = [1,alpha];
[b,a] = zmapping(blp,alp,Nz,Dz);
```

We will demonstrate this procedure in the following example.

- EXAMPLE 8.27 Design a highpass digital filter to satisfy

$$\begin{aligned}\omega_p &= 0.6\pi, & R_p &= 1 \text{ dB} \\ \omega_s &= 0.4586\pi, & A_s &= 15 \text{ dB}\end{aligned}$$

Use the Chebyshev-I prototype.

### Solution

MATLAB script:

```
>> % Digital highpass filter specifications:
>> wp = 0.6*pi; % Digital passband freq in rad
>> ws = 0.4586*pi; % Digital stopband freq in rad
>> Rp = 1; % Passband ripple in dB
>> As = 15; % Stopband attenuation in dB

>> [b,a] = cheb1hpf(wp,ws,Rp,As); [C,B,A] = dir2cas(b,a)
C = 0.0243
B = 1.0000 -2.0000 1.0000
      1.0000 -2.0000 1.0000
A = 1.0000 1.0416 0.4019
      1.0000 0.5561 0.7647
```

The system function is

$$H(z) = \frac{0.0243(1 - z^{-1})^4}{(1 + 0.5661z^{-1} + 0.7647z^{-2})(1 + 1.0416z^{-1} + 0.4019z^{-2})}$$

which is identical to that in Example 8.26. □

This highpass filter design procedure can be easily extended to other frequency-selective filters using the transformation functions in Table 8.2. These design procedures are explored in Problems P8.34, P8.36, P8.38, and P8.40. We now describe MATLAB's filter design functions for designing arbitrary frequency-selective filters.

### 8.6.2 MATLAB IMPLEMENTATION

In the preceding section, we discussed four MATLAB functions to design digital lowpass filters. These same functions can also be used to design highpass, bandpass, and bandstop filters. The frequency-band transformations in these functions are done in the  $s$ -plane; that is, they use Approach-1 discussed on page 370. For the purpose of illustration, we will use the function **butter**. It can be used with the following variations in its input arguments.

- `[b,a] = BUTTER(N,wn,'high')` designs an Nth-order *highpass* filter with digital 3 dB cutoff frequency `wn` in units of  $\pi$ .
- `[b,a] = BUTTER(N,wn,)` designs an order 2N *bandpass* filter if `wn` is a two-element vector, `wn=[w1 w2]`, with 3 dB passband  $w_1 < w < w_2$  in units of  $\pi$ .
- `[b,a] = BUTTER(N,wn,'stop')` is an order 2N *bandstop* filter if `wn=[w1 w2]` with 3 dB stopband  $w_1 < w < w_2$  in units of  $\pi$ .

To design any frequency-selective Butterworth filter, we need to know the order `N` and the 3 dB cutoff frequency vector `wn`. In this chapter, we described how to determine these parameters for lowpass filters. However, these calculations are more complicated for bandpass and bandstop filters. In their SP toolbox, MATLAB provides a function called **buttord** to compute these parameters. Given the specifications,  $\omega_p$ ,  $\omega_s$ ,  $R_p$ , and  $A_s$ , this function determines the necessary parameters. Its syntax is

```
[N,wn] = buttord(wp,ws,Rp,As)
```

The parameters `wp` and `ws` have some restrictions, depending on the type of filter:

- For lowpass filters `wp < ws`.
- For highpass filters `wp > ws`.
- For bandpass filters `wp` and `ws` are two-element vectors, `wp=[wp1, wp2]` and `ws=[ws1, ws2]`, such that  $ws_1 < wp_1 < wp_2 < ws_2$ .
- For bandstop filters `wp1 < ws1 < ws2 < wp2`.

Now using the **buttord** function in conjunction with the **butter** function, we can design any Butterworth IIR filter. Similar discussions apply

for `cheby1`, `cheby2`, and `ellip` functions with appropriate modifications. We illustrate the use of these functions through the following examples.

- **EXAMPLE 8.28** In this example, we will design a Chebyshev-I highpass filter whose specifications were given in Example 8.27.

**Solution** MATLAB script:

```
>> % Digital filter specifications:           % Type: Chebyshev-I highpass
>> ws = 0.4586*pi;                          % Dig. stopband-edge frequency
>> wp = 0.6*pi;                            % Dig. passband-edge frequency
>> Rp = 1;                                 % Passband ripple in dB
>> As = 15;                                % Stopband attenuation in dB

>> % Calculations of Chebyshev-I filter parameters:
>> [N,wn] = cheb1ord(wp/pi,ws/pi,Rp,As);

>> % Digital Chebyshev-I highpass filter design:
>> [b,a] = cheby1(N,Rp,wn,'high');

>> % Cascade form realization:
>> [b0,B,A] = dir2cas(b,a)
b0 = 0.0243
B = 1.0000   -1.9991    0.9991
      1.0000   -2.0009    1.0009
A = 1.0000    1.0416    0.4019
      1.0000    0.5561    0.7647
```

The cascade form system function

$$H(z) = \frac{0.0243(1 - z^{-1})^4}{(1 + 0.5661z^{-1} + 0.7647z^{-2})(1 + 1.0416z^{-1} + 0.4019z^{-2})}$$

is identical to the filter designed in Example 8.27, which demonstrates that the two approaches described on page 370 are identical. The frequency-domain plots are shown in Figure 8.32. □

- **EXAMPLE 8.29** In this example, we will design an elliptic bandpass filter whose specifications are given in the following MATLAB script.

```
>> % Digital filter specifications:           % Type: Elliptic bandpass
>> ws = [0.3*pi 0.75*pi];                  % Dig. stopband-edge frequency
>> wp = [0.4*pi 0.6*pi];                  % Dig. passband-edge frequency
>> Rp = 1;                                 % Passband ripple in dB
>> As = 40;                                % Stopband attenuation in dB
```

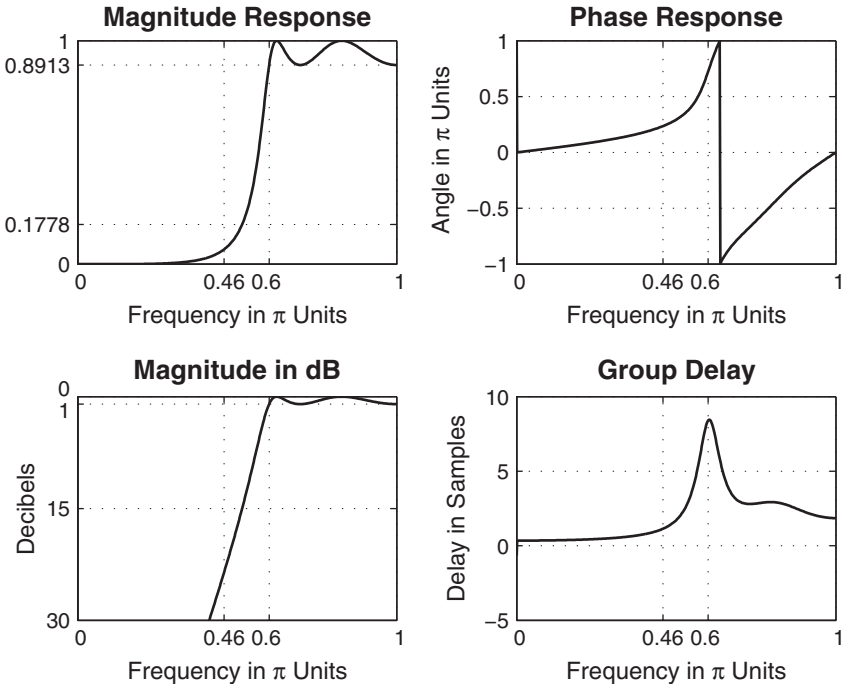


FIGURE 8.32 Digital Chebyshev-I highpass filter in Example 8.28

```

>> % Calculations of elliptic filter parameters:
>> [N,wn] = ellipord(wp/pi,ws/pi,Rp,As);

>> % Digital elliptic bandpass filter design:
>> [b,a] = ellip(N,Rp,As,wn);

>> % Cascade form realization:
>> [b0,B,A] = dir2cas(b,a)
b0 = 0.0197
B = 1.0000    1.5066    1.0000
          1.0000    0.9268    1.0000
          1.0000   -0.9268    1.0000
          1.0000   -1.5066    1.0000
A = 1.0000    0.5963    0.9399
          1.0000    0.2774    0.7929
          1.0000   -0.2774    0.7929
          1.0000   -0.5963    0.9399

```

Note that the designed filter is a tenth-order filter. The frequency-domain plots are shown in Figure 8.33. □

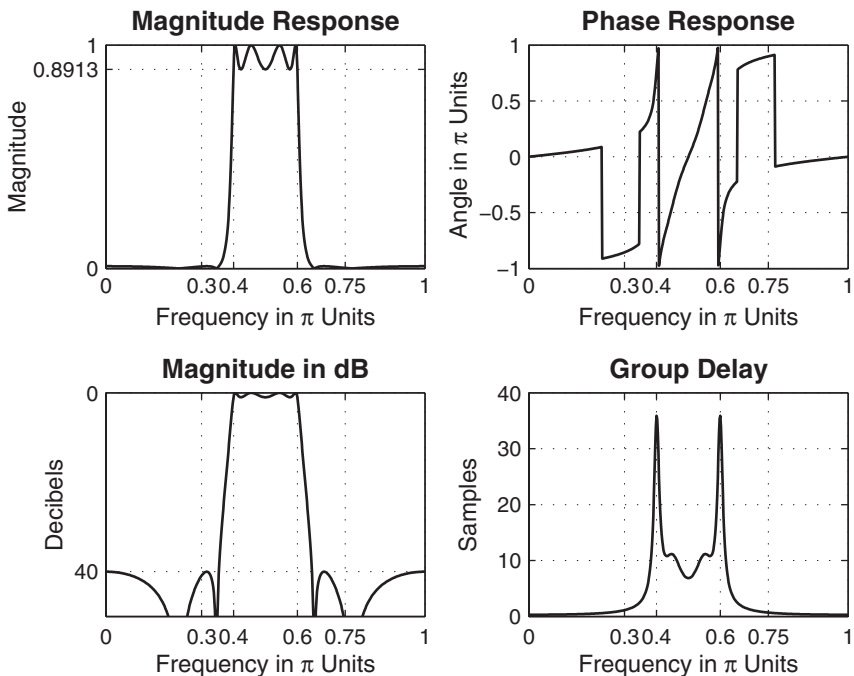


**FIGURE 8.33** Digital elliptic bandpass filter in Example 8.29

- **EXAMPLE 8.30** Finally, we will design a Chebyshev-II bandstop filter whose specifications are given in the following MATLAB script.

```

>> % Digital filter specifications:           % Type: Chebyshev-II bandstop
>> ws = [0.4*pi 0.7*pi];                   % Dig. stopband-edge frequency
>> wp = [0.25*pi 0.8*pi];                 % Dig. passband-edge frequency
>> Rp = 1;                                  % Passband ripple in dB
>> As = 40;                                 % Stopband attenuation in dB

>> % Calculations of Chebyshev-II filter parameters:
>> [N,wn] = cheb2ord(wp/pi,ws/pi,Rp,As);

>> % Digital Chebyshev-II bandstop filter design:
>> [b,a] = cheby2(N,As,ws/pi,'stop');

>> % Cascade form realization:
>> [b0,B,A] = dir2cas(b,a)
b0 = 0.1558
B = 1.0000    1.1456    1.0000
          1.0000    0.8879    1.0000
          1.0000    0.3511    1.0000
          1.0000   -0.2434    1.0000
          1.0000   -0.5768    1.0000

```

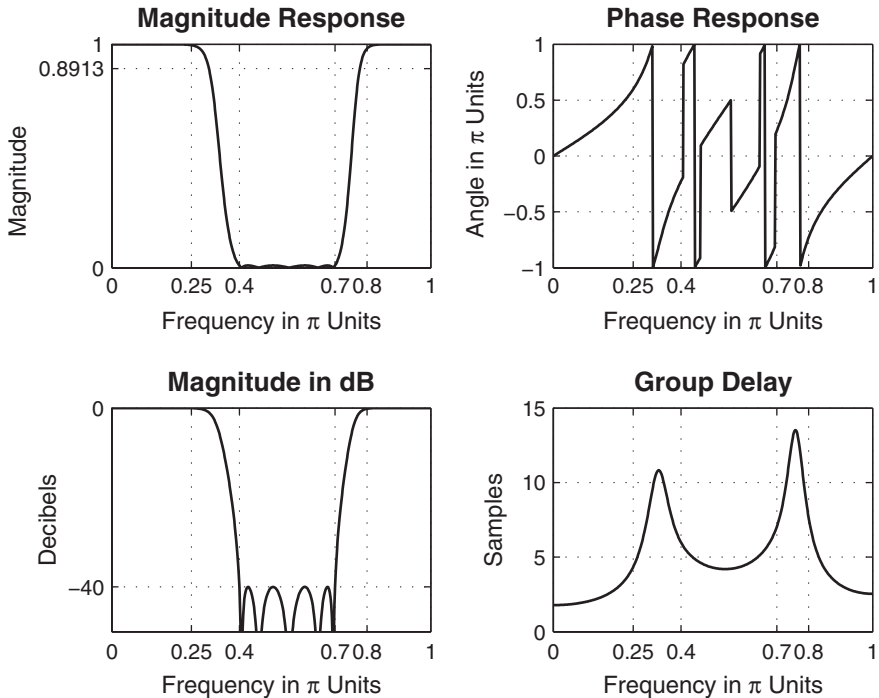


**FIGURE 8.34** Digital Chebyshev-II bandstop filter in Example 8.30

<b>A =</b>	1.0000	1.3041	0.8031
	1.0000	0.8901	0.4614
	1.0000	0.2132	0.2145
	1.0000	-0.4713	0.3916
	1.0000	-0.8936	0.7602

This is also a tenth-order filter. The frequency domain plots are shown in Figure 8.34. □

## 8.7 PROBLEMS

---

**P8.1** A digital resonator is to be designed with  $\omega_0 = \pi/4$  that has two zeros at  $z = 0$ .

1. Compute and plot the frequency response of this resonator for  $r = 0.8, 0.9$ , and  $0.99$ .
2. For each case in part 1, determine the 3 dB bandwidth and the resonant frequency  $\omega_r$  from your magnitude plots.
3. Check if your results in part 2 are in agreement with the theoretical results.

**P8.2** A digital resonator is to be designed with  $\omega_0 = \pi/4$  that has two zeros at  $z = 1$  and  $z = -1$ .

1. Compute and plot the frequency response of this resonator for  $r = 0.8, 0.9$ , and  $0.99$ .
2. For each case in part 1 determine the 3 dB bandwidth and the resonant frequency  $\omega_r$  from your magnitude plots.
3. Compare your results in part 2 with (8.48) and (8.47), respectively.

**P8.3** We want to design a digital resonator with the following requirements: a 3 dB bandwidth of  $0.05$  rad, a resonant frequency of  $0.375$  cycles/sam, and zeros at  $z = 1$  and  $z = -1$ . Using trial-and-error approach, determine the difference equation of the resonator.

**P8.4** A notch filter is to be designed with a null at the frequency  $\omega_0 = \pi/2$ .

1. Compute and plot the frequency response of this notch filter for  $r = 0.7, 0.9$ , and  $0.99$ .
2. For each case in part 1, determine the 3 dB bandwidth from your magnitude plots.
3. By trial-and-error approach, determine the value of  $r$  if we want the 3 dB bandwidth to be  $0.04$  radians at the null frequency  $\omega_0 = \pi/2$ .

**P8.5** Repeat Problem P8.4 for a null at  $\omega_0 = \pi/6$ .

**P8.6** A speech signal with bandwidth of  $4$  kHz is sampled at  $8$  kHz. The signal is corrupted by sinusoids with frequencies  $1$  kHz,  $2$  kHz, and  $3$  kHz.

1. Design an IIR filter using notch filter components that eliminates these sinusoidal signals.
2. Choose the gain of the filter so that the maximum gain is equal to  $1$ , and plot the log-magnitude response of your filter.
3. Load the `handel` sound file in MATLAB, and add the preceding three sinusoidal signals to create a corrupted sound signal. Now filter the corrupted sound signal using your filter and comment on its performance.

**P8.7** Consider the system function of an IIR lowpass filter

$$H(z) = K \frac{1 + z^{-1}}{1 - 0.9z^{-1}} \quad (8.72)$$

where  $K$  is a constant that can be adjusted to make the maximum gain response equal to  $1$ . We obtain the system function of an  $L$ th-order comb filter  $H_L(z)$  using  $H_L(z) = H(z^L)$ .

1. Determine the value of  $K$  for the system function in (8.72).
2. Using the  $K$  value from part 1, determine and plot the log-magnitude response of the comb filter for  $L = 6$ .
3. Describe the shape of your plot in part 2.

**P8.8** Consider the system function of an IIR highpass filter

$$H(z) = K \frac{1 - z^{-1}}{1 - 0.9z^{-1}} \quad (8.73)$$

where  $K$  is a constant that can be adjusted to make the maximum gain response equal to  $1$ . We obtain the system function of an  $L$ th-order comb filter  $H_L(z)$  using  $H_L(z) = H(z^L)$ .

1. Determine the value of  $K$  for the system function in (8.73).
2. Using the  $K$  value from part 1, determine and plot the log-magnitude response of the comb filter for  $L = 6$ .
3. Describe the shape of your plot in part 2.

**P8.9** (Adapted from [72]) As discussed in Chapter 1, echos and reverberations of a signal  $x(n)$  can be obtained by scaling and delaying, that is,

$$y(n) = \sum_{k=0}^{\infty} \alpha_k x(n - kD) \quad (8.74)$$

where  $D$  is a positive integer for minimum delay and  $\alpha_k > \alpha_{k-1} > 0$ .

1. Consider the IIR comb filter given by

$$H(z) = \frac{1}{1 - az^{-D}} \quad (8.75)$$

Determine its impulse response. Explain why this filter can be used as a reverberator.

2. Consider the cascade of three allpass comb filters

$$H(z) = \frac{z^{D_1} - a_1}{1 - a_1 z^{-D_1}} \times \frac{z^{D_2} - a_2}{1 - a_2 z^{-D_2}} \times \frac{z^{D_3} - a_3}{1 - a_3 z^{-D_3}} \quad (8.76)$$

which can be used as a practical digital reverberator. Compute and plot the impulse response of this reverberator for  $D_1 = 50$ ,  $a_1 = 0.7$ ;  $D_2 = 41$ ,  $a_2 = 0.665$ ; and  $D_3 = 32$ ,  $a_3 = 0.63175$ .

3. Repeat part 2 for  $D_1 = 53$ ,  $a_1 = 0.7$ ;  $D_2 = 40$ ,  $a_2 = 0.665$ ; and  $D_3 = 31$ ,  $a_3 = 0.63175$ . How does the shape of this reverberator differ from the one in part 2? Which is a good reverberator?

**P8.10** Consider the first-order allpass system function given by

$$H(z) = \frac{a + z^{-1}}{1 + az^{-1}}, \quad 0 < a < 1 \quad (8.77)$$

The phase-delay of a system is defined as  $\Phi(\omega) \triangleq -\angle H(e^{j\omega})/\omega$  and is measured in samples.

1. Show that the phase-delay of the system in (8.77) at low frequencies is given by

$$\Phi(\omega) \approx \frac{1-a}{1+a} \quad \text{for } a \approx 1 \quad (8.78)$$

2. Plot the phase-delay over  $-\pi/2 \leq \omega \leq \pi/2$  for  $a = 0.9$ ,  $0.95$ , and  $0.99$  to verify Problem P8.10. Comment on the accuracy of the results.
3. Design a first-order allpass system that has phase delay of 0.01 samples. Plot its magnitude and phase-delay responses.

**P8.11** Consider the second-order allpass system function given by

$$H(z) = \frac{a_2 + a_1 z^{-1} + z^{-2}}{1 + a_1 z^{-1} + a_2 z^{-2}} \quad (8.79)$$

The phase-delay of a system is defined as  $\Phi(\omega) \triangleq -\angle H(e^{j\omega})/\omega$  and is measured in samples.

It can be shown that if we choose

$$a_1 = 1 \left( \frac{2-d}{1+d} \right), \quad a_2 = \frac{(2-d)(1-d)}{(2+d)(1+d)} \quad (8.80)$$

then phase-delay  $\Phi(\omega)$  at low frequencies is approximated by  $d$  in samples. Verify this result by plotting  $\Phi(\omega)$  over  $-\pi/2 \leq \omega \leq \pi/2$  for  $d = 0.1$ ,  $d = 0.05$ , and  $d = 0.01$ .

- P8.12** Design an analog Butterworth lowpass filter that has a 0.25 dB or better ripple at 500 rad/sec and at least 50 dB of attenuation at 2000 rad/sec. Determine the system function in a rational function form. Plot the magnitude response, the log-magnitude response in dB, the phase response, and the impulse response of the filter.
- P8.13** Design an analog Butterworth lowpass filter that has a 0.5 dB or better ripple at 10 kHz and at least 45 dB of attenuation at 20 kHz. Determine the system function in a cascade form. Plot the magnitude response, the log-magnitude response in dB, the group-delay, and the impulse response of the filter.
- P8.14** Design a lowpass analog Chebyshev-I filter with an acceptable ripple of 1 dB for  $|\Omega| \leq 10$  and an attenuation of 50 dB or greater beyond  $|\Omega| = 15$  rad/sec. Determine the system function in a rational function form. Plot the magnitude response, the log-magnitude response in dB, the group-delay, and the impulse response of the filter.
- P8.15** Design a lowpass analog Chebyshev-I filter with the following characteristics:
- a passband ripple of 0.5 dB,
  - passband cutoff frequency of 4 kHz, and
  - stopband attenuation of 45 dB or greater beyond 20 kHz.
- Determine the system function in a cascade form. Plot the magnitude response, the log-magnitude response in dB, the phase response, and the impulse response of the filter.
- P8.16** A signal  $x_a(t)$  contains two frequencies, 10 kHz and 15 kHz. We want to suppress the 15 kHz component to 50 dB attenuation while passing the 10 kHz component with less than 0.25 dB attenuation. Design a minimum-order Chebyshev-II analog filter to perform this filtering operation. Plot the log-magnitude response, and verify the design.
- P8.17** Design an analog Chebyshev-II lowpass filter that has a 0.25 dB or better ripple at 250 Hz and at least 40 dB of attenuation at 400 Hz. Plot the magnitude response, the log-magnitude response in dB, the group-delay, and the impulse response of the filter.
- P8.18** A signal  $x_a(t)$  contains two frequencies, 10 kHz and 15 kHz. We want to suppress the 15 kHz component to 50 dB attenuation while passing the 10 kHz component with less than 0.25 dB attenuation. Design a minimum-order elliptic analog filter to perform this filtering operation. Plot the log-magnitude response and verify the design. Compare your design with the Chebyshev-II design in Problem P8.16.
- P8.19** Design an analog elliptic lowpass filter that has a 0.25 dB or better ripple at 500 rad/sec and at least 50 dB of attenuation at 2000 rad/sec. Determine the system function in a rational function form. Plot the magnitude response, the log-magnitude response in dB, the phase response, and the impulse response of the filter. Compare your design with the Butterworth design in Problem P8.12.
- P8.20** Write a MATLAB function to design analog lowpass filters. The format of this function should be

```

function [b,a] =afd(type,Fp,Fs,Rp,As)
%
% function [b,a] =afd(type,Fp,Fs,Rp,As)
%   Designs analog lowpass filters
% type = 'butter' or 'cheby1' or 'cheby2' or 'ellip'
% Fp = passband cutoff in Hz
% Fs = stopband cutoff in Hz
% Rp = passband ripple in dB
% As = stopband attenuation in dB

```

Use the **afd.butt**, **afd.chb1**, **afd.chb2**, and **afd.ellip** functions developed in this chapter. Check your function using specifications given in Problems P8.12 through P8.17.

- P8.21** We want to design a Chebyshev-I prototype lowpass digital filter operating at a sampling rate of 8 kHz with a passband edge of 3.2 kHz, a passband ripple of 0.5 dB, and a minimum stopband attenuation of 45 dB at 3.8 kHz.

1. Using the impulse invariance transformation with  $T = 1$  sec, design the digital filter. Plot the magnitude and the log-magnitude responses as functions of analog frequency in kHz.
2. Repeat part 1 using  $T = 1/8000$  sec.
3. Compare the above two designs in parts 1 and 2 in terms of their frequency responses. Comment on the effect of  $T$  on the impulse invariance design.

- P8.22** Design a Butterworth digital lowpass filter to satisfy the following specifications.

$$\text{passband edge: } 0.4\pi, \quad R_p = 0.5 \text{ dB}$$

$$\text{stopband edge: } 0.6\pi, \quad A_s = 50 \text{ dB}$$

Use the impulse invariance method with  $T = 2$ . Determine the system function in the rational form, and plot the log-magnitude response in dB. Plot the impulse response  $h(n)$  and the impulse response  $h_a(t)$  of the analog prototype and compare their shapes.

- P8.23** Write a MATLAB function to design digital lowpass filters based on the impulse invariance transformation. The format of this function should be

```

function [b,a] =dlpfid_ii(type,wp,ws,Rp,As,T)
%
% function [b,a] =dlpfid_ii(type,wp,ws,Rp,As,T)
%   Designs digital lowpass filters using impulse invariance
% type = 'butter' or 'cheby1'
% wp = passband cutoff in Hz
% ws = stopband cutoff in Hz
% Rp = passband ripple in dB
% As = stopband attenuation in dB
% T = sampling interval

```

Use the **afd** function developed in Problem P8.20. Check your function on specifications given in Problems P8.21 and P8.22.

- P8.24** In this problem, we will develop a technique called the *step invariance* transformation. In this technique, the step response of an analog prototype filter is preserved in the resulting digital filter; that is, if  $v_a(t)$  is the step response of the prototype and if  $v(n)$  is the step response of the digital filter, then

$$v(n) = v_a(t)|_{t=nT}, \quad T : \text{sampling interval}$$

Note that the frequency-domain quantities are related by

$$V_a(s) \stackrel{\triangle}{=} \mathcal{L}[v_a(t)] = H_a(s)/s$$

and

$$V(z) \stackrel{\triangle}{=} \mathcal{Z}[v(n)] = H(z) \frac{1}{1 - z^{-1}}$$

Hence the step invariance transformation steps are as follows.

Given  $H_a(s)$ ,

- divide  $H_a(s)$  by  $s$  to obtain  $V_a(s)$ ,
- find residues  $\{R_k\}$  and poles  $\{p_k\}$  of  $V_a(s)$ ,
- transform analog poles  $\{p_k\}$  into digital poles  $\{e^{p_k T}\}$  where  $T$  is arbitrary,
- determine  $V(z)$  from residues  $\{R_k\}$  and poles  $\{e^{p_k T}\}$ , and finally
- determine  $H(z)$  by multiplying  $V(z)$  by  $(1 - z^{-1})$ .

Use the above procedure to develop a MATLAB function to implement the step invariance transformation. The format of this function should be

```
function [b,a] =stp_inv(c,d,T)
% Step invariance transformation from analog to digital filter
% [b,a] =stp_inv(c,d,T)
% b = numerator polynomial in z^(-1) of the digital filter
% a = denominator polynomial in z^(-1) of the digital filter
% c = numerator polynomial in s of the analog filter
% d = denominator polynomial in s of the analog filter
% T = sampling (transformation) parameter
```

- P8.25** Design the lowpass Butterworth digital filter of Problem P8.22 using the step invariance method. Plot the log-magnitude response in dB and compare it with that in Problem P8.22. Plot the step response  $v(n)$  and the impulse response  $v_a(t)$  of the analog prototype and compare their shapes.

- P8.26** In this chapter, we discussed a filter transformation technique called the matched- $z$  transformation. Using (8.69), write a MATLAB function called `mzt` that maps the analog system function  $H_a(s)$  into the digital system function  $H(z)$ . The format of the function should be

```

function [b,a] = mzt(c,d,T)
% Matched-z transformation from analog to digital filter
% [b,a] = MZT(c,d,T)
% b = numerator polynomial in z^(-1) of the digital filter
% a = denominator polynomial in z^(-1) of the digital filter
% c = numerator polynomial in s of the analog filter
% d = denominator polynomial in s of the analog filter
% T = sampling interval (transformation parameter)

```

Using this function, transform

$$H_a(s) = \frac{s+1}{s^2 + 5s + 6}$$

into a digital filter  $H(z)$  for the sampling intervals (in seconds)  $T = 0.05$ ,  $T = 0.1$ , and  $T = 0.2$ . In each case, obtain a plot similar to that in Figure 8.20 and comment on the performance of this technique.

**P8.27** Consider an analog Butterworth lowpass filter that has a 1 dB or better ripple at 100 Hz and at least 30 dB of attenuation at 150 Hz. Transform this filter into a digital filter using the matched- $z$  transformation technique in which  $F_s = 1000$  Hz. Plot the magnitude and phase response of the resulting digital filter and determine the exact band-edge frequencies for the given dB specifications. Comment on the results.

**P8.28** Consider an analog Chebyshev-I lowpass filter that has a 0.5 dB or better ripple at 500 Hz and at least 40 dB of attenuation at 700 Hz. Transform this filter into a digital filter using the matched- $z$  transformation technique in which  $F_s = 2000$  Hz. Plot the magnitude and phase response of the resulting digital filter and determine the exact band-edge frequencies for the given dB specifications. Comment on the results.

**P8.29** Consider an analog Chebyshev-II lowpass filter that has a 0.25 dB or better ripple at 1500 Hz and at least 80 dB of attenuation at 2000 Hz. Transform this filter into a digital filter using the matched- $z$  transformation technique in which  $F_s = 8000$  Hz. Plot the magnitude and phase response of the resulting digital filter, and determine the exact band-edge frequencies for the given dB specifications. Comment on the results. Is this a satisfactory design?

**P8.30** Consider the design of the lowpass Butterworth filter of Problem P8.22.

1. Use the bilinear transformation technique outlined in this chapter and the `bilinear` function. Plot the log-magnitude response in dB. Compare the impulse responses of the analog prototype and the digital filter.
2. Use the `butter` function and compare this design with the one in part 1.

**P8.31** Consider the design of the digital Chebyshev-1 filter of Problem P8.21.

1. Use the bilinear transformation technique outlined in this chapter and the `bilinear` function. Plot the log-magnitude response in dB. Compare the impulse responses of the analog prototype and the digital filter.
2. Use the `cheby1` function and compare this design with the one above.

**P8.32** Design a digital lowpass filter using elliptic prototype to satisfy the requirements

passband edge:  $0.3\pi$ ,  $R_p = 0.25$  dB

stopband edge:  $0.4\pi$ ,  $A_s = 50$  dB

Use the **bilinear** as well as the **ellip** function and compare your designs.

**P8.33** Design a digital lowpass filter to satisfy the specifications

passband edge:  $0.45\pi$ ,  $R_p = 0.5$  dB

stopband edge:  $0.5\pi$ ,  $A_s = 60$  dB

1. Use the **butter** function and determine the order  $N$  and the actual minimum stopband attenuation in dB.
2. Use the **cheby1** function and determine the order  $N$  and the actual minimum stopband attenuation in dB.
3. Use the **cheby2** function and determine the order  $N$  and the actual minimum stopband attenuation in dB.
4. Use the **ellip** function and determine the order  $N$  and the actual minimum stopband attenuation in dB.
5. Compare the orders, the actual minimum stopband attenuations, and the group delays in each of the above designs.

**P8.34** Write a MATLAB function to determine the lowpass prototype digital filter frequencies from an highpass digital filter specifications using the procedure outlined in this chapter. The format of this function should be

```
function [wpLP,wsLP,alpha] = hp2lpfre(wphp,wshp)
% Band-edge frequency conversion from highpass to lowpass digital filter
% [wpLP,wsLP,a] = hp2lpfre(wphp,wshp)
% wpLP = passband edge for the lowpass prototype
% wsLP = stopband edge for the lowpass prototype
% alpha = lowpass-to-highpass transformation parameter
% wphp = passband edge for the highpass
% wshp = stopband edge for the highpass
```

Using this function, develop a MATLAB function to design a highpass digital filter using the bilinear transformation. The format of this function should be

```
function [b,a] = dhpfd_b1(type,wp,ws,Rp,As)
% IIR highpass filter design using bilinear transformation
% [b,a] = dhpfd_b1(type,wp,ws,Rp,As)
% type = 'butter' or 'cheby1' or 'cheby2' or 'ellip'
% b = numerator polynomial of the highpass filter
% a = denominator polynomial of the highpass filter
% wp = passband frequency in radians
% ws = stopband frequency in radians (wp < ws)
% Rp = passband ripple in dB
% As = stopband attenuation in dB
```

Verify your function using the specifications in Example 8.27.

**P8.35** Design a highpass filter to satisfy the specifications

$$\begin{aligned} \text{stopband edge: } & 0.4\pi, A_s = 60 \text{ dB} \\ \text{passband edge: } & 0.6\pi, R_p = 0.5 \text{ dB} \end{aligned}$$

1. Use the `dhpfd.bl` function of Problem P8.34 and the Chebyshev-I prototype to design this filter. Plot the log-magnitude response in dB of the designed filter.
2. Use the `cheby1` function for design and plot the log-magnitude response in dB. Compare these two designs.

**P8.36** Write a MATLAB function to determine the lowpass prototype digital filter frequencies from an arbitrary lowpass digital filter specifications using the functions given in Table 8.2 and the procedure outlined for highpass filters. The format of this function should be

```
function [wpLP,wsLP,alpha] = lp2lpfre(wplp,wslp)
% Band-edge frequency conversion from lowpass to lowpass digital filter
% [wpLP,wsLP,a] = lp2lpfre(wplp,wslp)
% wpLP = passband edge for the lowpass prototype
% wsLP = stopband edge for the lowpass prototype
% alpha = lowpass-to-highpass transformation parameter
% wplp = passband edge for the given lowpass
% wslp = stopband edge for the given lowpass
```

Using this function, develop a MATLAB function to design a lowpass filter from a prototype lowpass digital filter using the bilinear transformation. The format of this function should be

```
function [b,a] = dlpfd_bl(type,wp,ws,Rp,As)
% IIR lowpass filter design using bilinear transformation
% [b,a] = dlpfd_bl(type,wp,ws,Rp,As)
% type = 'butter' or 'cheby1' or 'chevy2' or 'ellip'
% b = numerator polynomial of the bandpass filter
% a = denominator polynomial of the bandpass filter
% wp = passband frequency in radians
% ws = stopband frequency in radians
% Rp = passband ripple in dB
% As = stopband attenuation in dB
```

Verify your function using the designs in Problem P8.33.

**P8.37** Design a bandpass digital filter using the `Cheby2` function. The specifications are

$$\begin{aligned} \text{lower stopband edge: } & 0.3\pi \quad A_s = 50 \text{ dB} \\ \text{upper stopband edge: } & 0.6\pi \\ \text{lower passband edge: } & 0.4\pi \quad R_p = 0.5 \text{ dB} \\ \text{upper passband edge: } & 0.5\pi \end{aligned}$$

Plot the impulse response and the log-magnitude response in dB of the designed filter.

**P8.38** Write a MATLAB function to determine the lowpass prototype digital filter frequencies from a bandpass digital filter specifications using the functions given in Table 8.2 and the procedure outlined for highpass filters. The format of this function should be

```

function [wpLP,wsLP,alpha] = bp2lpfre(wpbp,wsblp)
% Band-edge frequency conversion from bandpass to lowpass digital filter
% [wpLP,wsLP,a] = bp2lpfre(wpbp,wsbp)
% wpLP = passband edge for the lowpass prototype
% wsLP = stopband edge for the lowpass prototype
% alpha = lowpass-to-highpass transformation parameter
% wpbp = passband-edge frequency array [wp_lower, wp_upper] for the bandpass
% wsbp = passband-edge frequency array [ws_lower, ws_upper] for the bandpass

```

Using this function, develop a MATLAB function to design a bandpass filter from a prototype lowpass digital filter using the bilinear transformation. The format of this function should be

```

function [b,a] = dbpfdbl(type,wp,ws,Rp,As)
% IIR bandpass filter design using bilinear transformation
% [b,a] = dbpfdbl(type,wp,ws,Rp,As)
% type = 'butter' or 'cheby1' or 'chevy2' or 'ellip'
% b = numerator polynomial of the bandpass filter
% a = denominator polynomial of the bandpass filter
% wp = passband frequency array [wp_lower, wp_upper] in radians
% ws = stopband frequency array [wp_lower, wp_upper] in radians
% Rp = passband ripple in dB
% As = stopband attenuation in dB

```

Verify your function using the design in Problem P8.37.

- P8.39** We wish to use the Chebyshev-I prototype to design a bandstop digital IIR filter that meets the following specifications:

$$\begin{aligned} 0.95 &\leq |H(e^{j\omega})| \leq 1.05, \quad 0 \leq |\omega| \leq 0.25\pi \\ 0 &\leq |H(e^{j\omega})| \leq 0.01, \quad 0.35\pi \leq |\omega| \leq 0.65\pi \\ 0.95 &\leq |H(e^{j\omega})| \leq 1.05, \quad 0.75\pi \leq |\omega| \leq \pi \end{aligned}$$

Use the `cheby1` function and determine the system function  $H(z)$  of such a filter. Provide a plot containing subplots of the log-magnitude response in dB and the impulse response.

- P8.40** Write a MATLAB function to determine the lowpass prototype digital filter frequencies from a bandstop digital filter specifications using the functions given in Table 8.2 and the procedure outlined for highpass filters. The format of this function should be

```

function [wpLP,wsLP,alpha] = bs2lpfre(wpbp,wsblp)
% Band-edge frequency conversion from bandstop to lowpass digital filter
% [wpLP,wsLP,a] = bs2lpfre(wpbp,wsbp)
% wpLP = passband edge for the lowpass prototype
% wsLP = stopband edge for the lowpass prototype
% alpha = lowpass-to-highpass transformation parameter
% wpbp = passband-edge frequency array [wp_lower, wp_upper] for the bandstop
% wsbp = passband-edge frequency array [ws_lower, ws_upper] for the bandstop

```

Using this function, develop a MATLAB function to design a bandstop filter from a prototype lowpass digital filter using the bilinear transformation. The format of this function should be

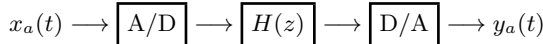
```
function [b,a] = db5fd_b1(type,wp,ws,Rp,As)
% IIR bandstop filter design using bilinear transformation
% [b,a] = db5fd_b1(type,wp,ws,Rp,As)
% type = 'butter' or 'cheby1' or 'chevy2' or 'ellip'
% b = numerator polynomial of the bandstop filter
% a = denominator polynomial of the bandstop filter
% wp = passband frequency array [wp_lower, wp_upper] in radians
% ws = stopband frequency array [ws_lower, ws_upper] in radians
% Rp = passband ripple in dB
% As = stopband attenuation in dB
```

Verify your function using the design in Problem P8.39.

**P8.41** An analog signal

$$x_a(t) = 3 \sin(40\pi t) + 3 \cos(50\pi t)$$

is to be processed by a



system in which the sampling frequency is 100 sam/sec.

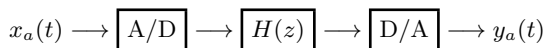
1. Design a minimum-order IIR digital filter that will pass the first component of  $x_a(t)$  with attenuation of less than 1 dB and suppress the second component to at least 50 dB. The filter should have a monotone passband and an equiripple stopband. Determine the system function in rational function form and plot the log-magnitude response.
2. Generate 500 samples (sampled at 100 sam/sec) of the signal  $x_a(t)$  and process through the designed filter to obtain the output sequence. Interpolate this sequence (using any one of the interpolating techniques discussed in Chapter 3) to obtain  $y_a(t)$ . Plot the input and the output signals and comment on your results.

**P8.42** Using the bilinear transformation method, design a tenth-order elliptic bandstop filter to remove the digital frequency  $\omega = 0.44\pi$  with bandwidth of  $0.08\pi$ . Choose a reasonable value for the stopband attenuation. Plot the magnitude response. Generate 201 samples of the sequence

$$x(n) = \sin[0.44\pi n], \quad n = 0, \dots, 200$$

and process thorough the bandstop filter. Comment on your results.

**P8.43** Design a digital highpass filter  $H(z)$  to be used in a



structure to satisfy the following requirements:

- sampling rate of 10 KHz,
  - stopband edge of 1.5 KHz with attenuation of 40 dB,
  - passband edge of 2 KHz with ripple of 1 dB,
  - equiripple passband and stopband, and
  - bilinear transformation method.
1. Plot the magnitude response of the overall analog filter over the [0, 5 KHz] interval.
  2. Plot the magnitude response of the digital lowpass prototype.
  3. What limitations must be placed on the input signals so that the preceding structure truly acts as a highpass filter to them?

**P8.44** The filter specifications shown in Figure P8.1 can be considered a combination of a bandpass and a highpass specifications. Design a minimum-order IIR digital filter to satisfy these specifications. Provide a plot of the magnitude response with grid lines as shown in Figure P8.1. From your design and plot determine the order of the filter and the exact band-edge frequencies.

**P8.45** The filter specifications shown in Figure P8.2 can be considered as a combination of a lowpass and a bandpass specifications. Design a minimum-order IIR digital filter to satisfy these specifications. Provide a plot of the magnitude response with grid lines as shown in Figure P8.2. From your design and plot determine the order of the filter and the exact band-edge frequencies.

**P8.46** Design a minimum-order IIR digital filter to satisfy the following specifications:

- a passband over the  $[0.35\pi, 0.5\pi]$  interval,
- stopbands over the  $[0, 0.3\pi]$  and  $[0.6\pi, \pi]$  intervals,
- passband ripple of 1 dB,

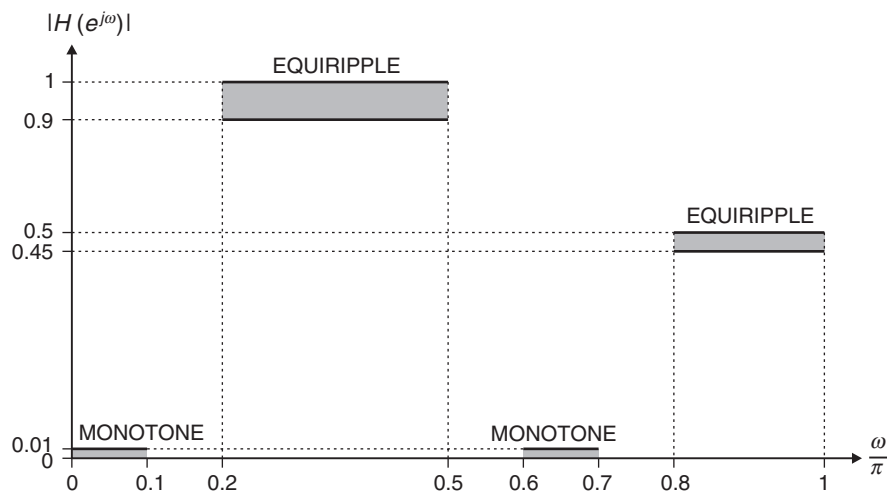


**FIGURE P8.1** Filter specifications for Problem P8.44

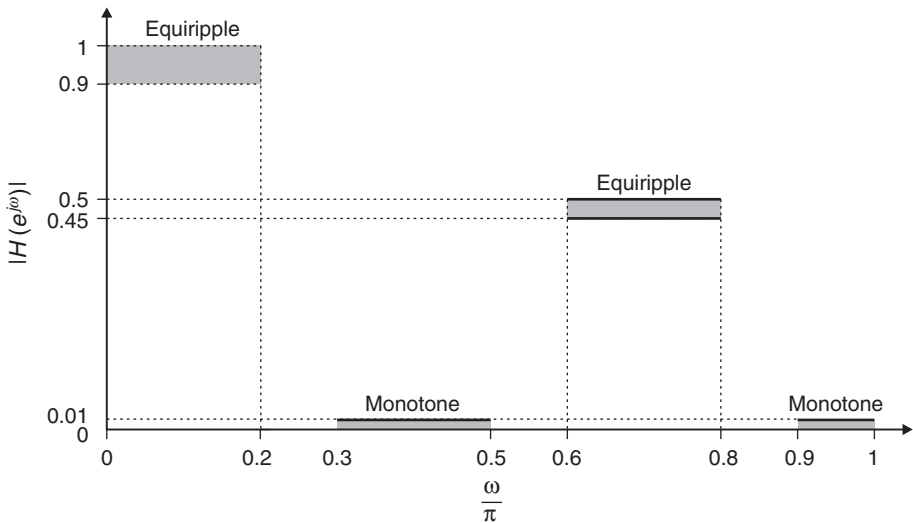


**FIGURE P8.2** Filter specifications for Problem P8.45

- stopband attenuation of 40 dB, and
- equiripple passbands and stopband.

Determine the system function  $H(z)$  of the designed filter in the rational function form. Provide a plot of the log-magnitude response in dB. From your design and plot, answer the following questions.

1. What is the order of the filter?
2. From your plot what are the exact band-edge frequencies for the given passband and stopband attenuations?
3. Why is there a discrepancy between the specification frequencies and the exact frequencies?

# CHAPTER 9

---

## Sampling Rate Conversion

---

In many practical applications of digital signal processing, one is faced with the problem of changing the sampling rate of a signal, either increasing it or decreasing it by some amount. The process of converting a signal from a given rate to a different rate is called *sampling rate conversion*. In turn, systems that employ multiple sampling rates in the processing of digital signals are called *multirate digital signal processing systems*. In this chapter, we describe sampling rate conversion and multirate signal processing in the digital domain.

As an example, consider the system shown in Figure 9.1, in which an analog signal  $x_a(t)$  is sampled using the sampling rate of  $F_s = \frac{1}{T}$  samples/second. The resulting digital signal  $x(n)$  is subsequently filtered using a lowpass filter (LPF) with a cutoff frequency of  $\omega_c$ .

Thus the output signal  $y(n)$  has all its energy in the band  $0 \leq \omega \leq \omega_c = 2\pi f_c$ . According to the sampling theorem, such a signal may be represented by the rate of  $2f_c/T$  samples/second instead of its existing rate of  $F_s = 1/T$ . Note that  $|f_c| \leq 0.5$ . However, if  $f_c \ll 0.5$ , then  $2f_c/T \ll F_s$ . Hence it would seem more advantageous to lower the sampling frequency to a value closer to  $2f_c/T$  and perform signal processing operations at this lower rate.

Other applications include the need for an optimal interpolation in computer tomography and efficient multistage designs of narrowband low-pass filters.

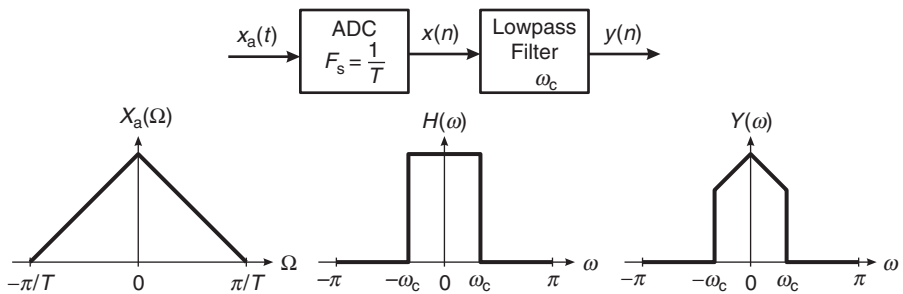


**FIGURE 9.1** A typical signal processing system

## 9.1 INTRODUCTION

---

The idea of interpolation is a very familiar concept to most of us and has its origin in numerical analysis. Typically, interpolation is performed on a table of numbers representing a mathematical function. Such a table may be printed in a handbook or stored in a computer memory device. The interpolation, often simply a linear (or straight line) approximation, creates an error called the *interpolation error*. The main difference between interpolation in digital signal processing and interpolation in numerical analysis is that we will assume that the given data is bandlimited to some band of frequencies and develop schemes that are optimal on this basis, whereas a numerical analyst typically assumes that the data consists of samples of polynomials (or very nearly so) and develops schemes to minimize the resulting error.

To motivate this concept of interpolation in signal processing, it is helpful to think of an underlying (or original) analog signal  $x_a(t)$  that was sampled to produce the given discrete signal  $x(n)$ . If the  $x_a(t)$  was sampled at the minimum required rate, then, according to the sampling theorem, it can be recovered completely from the samples  $x(n)$ . If we now sample this recovered analog signal, at, say, twice the old rate, we have succeeded in doubling the sampling rate or interpolating by a factor of 2 with zero interpolation error. Specifically, we have the following.

$$\text{Original discrete signal: } x(n) = x_a(nT) \quad (9.1)$$

$$\text{Reconstructed analog signal: } x_a(t) = \sum_k x_a(kT) \frac{\sin[\pi(t - kT)/T]}{\pi(t - kT)/T} \quad (9.2)$$

$$\begin{aligned} \text{Resampled analog signal: } x_a\left(m \frac{T}{2}\right) &= \sum_k x_a(kT) \frac{\sin [\pi (m \frac{T}{2} - kT) / T]}{\pi (m \frac{T}{2} - kT) / T} \\ &= \sum_k x_a(kT) \frac{\sin [\pi (\frac{m}{2} - k)]}{\pi (\frac{m}{2} - k)} \end{aligned} \quad (9.3)$$

$$\text{resulting in high-rate discrete signal: } y(m) \triangleq x_a\left(m \frac{T}{2}\right) \quad (9.4)$$

In this formulation of ideal interpolation, the discrete signal was converted to the analog signal and then back to the discrete signal at twice the rate. In the subsequent sections, we will study how to avoid this roundabout approach and perform sampling rate conversion completely in the digital domain.

The process of sampling rate conversion in the digital domain can be viewed as a linear filtering operation, as illustrated in Figure 9.2a. The input signal  $x(n)$  is characterized by the sampling rate  $F_x = 1/T_x$ , and the output signal  $y(m)$  is characterized by the sampling rate  $F_y = 1/T_y$ , where  $T_x$  and  $T_y$  are the corresponding sampling intervals. In our treatment, the ratio  $F_y/F_x$  is constrained to be rational

$$\frac{F_y}{F_x} = \frac{I}{D} \quad (9.5)$$

where  $D$  and  $I$  are relatively prime integers. We shall show that the linear filter is characterized by a time-variant impulse response, denoted

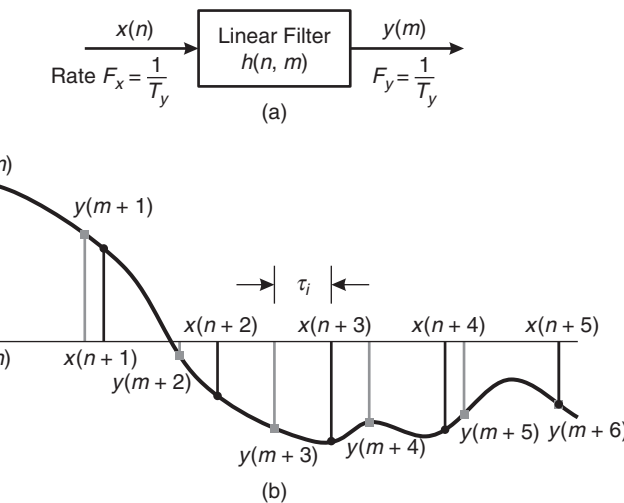


**FIGURE 9.2** Sampling rate conversion viewed as a linear filtering process

as  $h(n, m)$ . Hence the input  $x(n)$  and the output  $y(m)$  are related by the superposition summation for time-variant systems.

The sampling rate conversion process can also be understood from the point of view of digital resampling of the same analog signal. Let  $x_a(t)$  be the analog signal that is sampled at the first rate  $F_x$  to generate  $x(n)$ . The goal of rate conversion is to obtain another sequence  $y(m)$  directly from  $x(n)$ , which is equal to the sampled values of  $x_a(t)$  at a second rate  $F_y$ . As is depicted in Figure 9.2b,  $y(m)$  is a time-shifted version of  $x(n)$ . Such a time shift can be realized by using a linear filter that has a flat magnitude response and a linear phase response (i.e., it has a frequency response of  $e^{-j\omega\tau_i}$ , where  $\tau_i$  is the time delay generated by the filter). If the two sampling rates are not equal, the required amount of time shifting will vary from sample to sample, as shown in Figure 9.2b. Thus the rate converter can be implemented using a set of linear filters that have the same flat magnitude response but generate different time delays.

Before considering the general case of sampling rate conversion, we shall consider two special cases. One is the case of sampling rate reduction by an integer factor  $D$ , and the second is the case of a sampling rate increase by an integer factor  $I$ . The process of reducing the sampling rate by a factor  $D$  (downsampling by  $D$ ) is called *decimation*. The process of increasing the sampling rate by an integer factor  $I$  (upsampling by  $I$ ) is called *interpolation*.

## 9.2 DECIMATION BY A FACTOR $D$

---

The basic operation required in decimation is the downsampling of the *high-rate* signal  $x(n)$  into a *low-rate* signal  $y(m)$ . We will develop the time- and frequency-domain relationships between these two signals to understand the frequency-domain aliasing in  $y(m)$ . We will then study the condition needed for error-free decimation and the system structure required for its implementation.

### 9.2.1 THE DOWNSAMPLER

Note that the downsampled signal  $y(m)$  is obtained by selecting one out of  $D$  samples of  $x(n)$  and throwing away the other  $(D - 1)$  samples out of every  $D$  samples—that is,

$$y(m) = x(n)|_{n=mD} = x(mD); \quad n, m, D \in \{\text{integers}\} \quad (9.6)$$

The block diagram representation of (9.6) is shown in Figure 9.3. This downsampling element changes the rate of processing and thus is fundamentally different from other block diagram elements that we have used

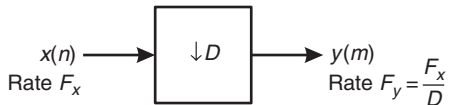


**FIGURE 9.3** A downsampling element

previously. In fact, we can show that a system containing a downsampling element is shift varying. However, this fact does not prohibit the frequency-domain analysis of  $y(m)$  in terms of  $x(n)$ , as we shall see later.

- **EXAMPLE 9.1** Using  $D = 2$  and  $x(n) = \{1, 2, 3, 4, 3, 2, 1\}$ , verify that the downampler is time varying.

**Solution**

The downsampled signal is  $y(m) = \{1, \overset{\uparrow}{3}, 3, 1\}$ . If we now delay  $x(n)$  by one sample, we get  $x(n - 1) = \{0, 1, \overset{\uparrow}{2}, 3, 4, 3, 2, 1\}$ . The corresponding downsampled signal is  $y_1(m) = \{0, 2, \overset{\uparrow}{4}, 2\}$ , which is different from  $y(m - 1)$ . □

**MATLAB Implementation** MATLAB provides the function `[y] = downsample(x,D)` that downsamples input array  $x$  into output array  $y$  by keeping every  $D$ th sample starting with the first sample. An optional third parameter “`phase`” specifies the sample offset which must be an integer between 0 and  $(D-1)$ . For example,

```
>> x = [1,2,3,4,3,2,1]; y = downsample(x,2)
y =
    1      3      3      1
```

downsamples by a factor of 2 starting with the first sample. However,

```
>> x = [1,2,3,4,3,2,1]; y = downsample(x,2,1)
y =
    2      4      2
```

produces an entirely different sequence by downsampling, starting with the second sample (i.e., offset by 1).

**The frequency-domain representation of the downsampled signal  $y(m)$**  We now express  $Y(\omega)$  in terms of  $X(\omega)$  using  $z$ -transform relations. Toward this, we introduce a high-rate sequence  $\bar{x}(n)$ , which is given by

$$\bar{x}(n) \triangleq \begin{cases} x(n), & n = 0, \pm D, \pm 2D, \dots \\ 0, & \text{elsewhere} \end{cases} \quad (9.7)$$

Clearly,  $\bar{x}(n)$  can be viewed as a sequence obtained by multiplying  $x(n)$  with a periodic train of impulses  $p(n)$ , with period  $D$ , as illustrated in Figure 9.4. The discrete Fourier series representation of  $p(n)$  is

$$p(n) \triangleq \begin{cases} 1, & n = 0, \pm D, \pm 2D, \dots \\ 0, & \text{elsewhere} \end{cases} = \frac{1}{D} \sum_{\ell=0}^{D-1} e^{j \frac{2\pi}{D} \ell n} \quad (9.8)$$

Hence we can write

$$\bar{x}(n) = x(n)p(n) \quad (9.9)$$

and

$$y(m) = \bar{x}(mD) = x(mD)p(mD) = x(mD) \quad (9.10)$$

as shown in (9.6). Figure 9.4 shows an example of sequences  $x(n)$ ,  $\bar{x}(n)$ , and  $y(m)$  defined in (9.7)–(9.10).

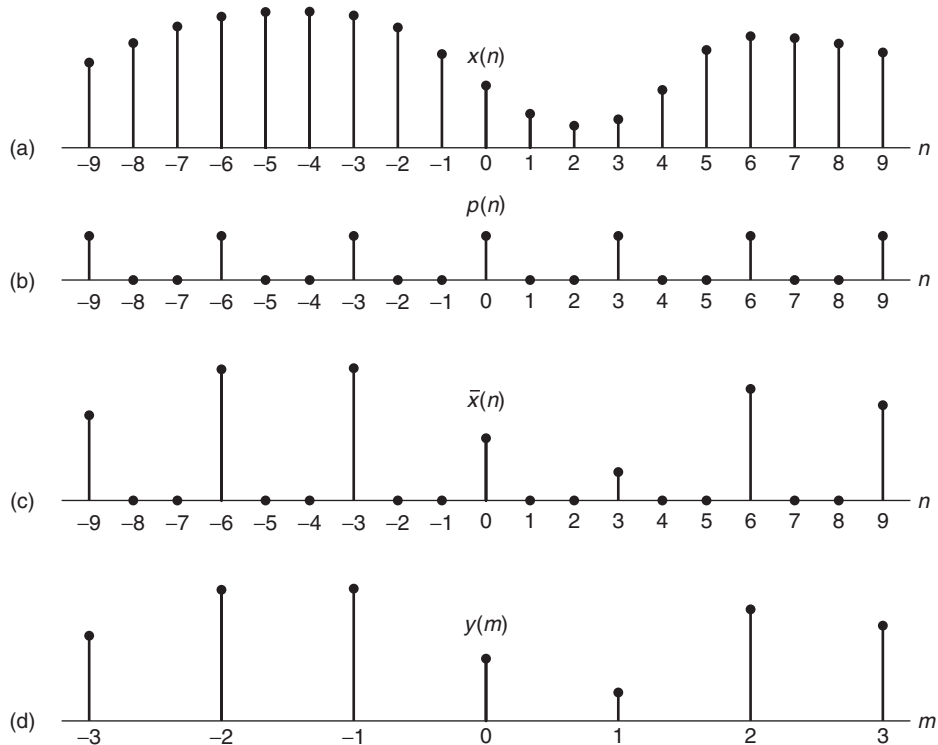


**FIGURE 9.4** Operation of downsampling: (a) original signal  $x(n)$ , (b) periodic impulse train  $p(n)$  with period  $D = 3$ , (c) multiplication of  $x(n)$  with  $p(n)$ , and (d) downsampled signal  $y(m)$

Now the  $z$ -transform of the output sequence  $y(m)$  is

$$\begin{aligned} Y(z) &= \sum_{m=-\infty}^{\infty} y(m)z^{-m} = \sum_{m=-\infty}^{\infty} \bar{x}(mD)z^{-m} \\ Y(z) &= \sum_{m=-\infty}^{\infty} \bar{x}(m)z^{-m/D} \end{aligned} \quad (9.11)$$

where the last step follows from the fact that  $\bar{x}(m) = 0$ , except at multiples of  $D$ . By making use of the relations in (9.7) and (9.8) in (9.11), we obtain

$$\begin{aligned} Y(z) &= \sum_{m=-\infty}^{\infty} x(m) \left[ \frac{1}{D} \sum_{k=0}^{D-1} e^{j2\pi mk/D} \right] z^{-m/D} \\ &= \frac{1}{D} \sum_{k=0}^{D-1} \sum_{m=-\infty}^{\infty} x(m) (e^{-j2\pi k/D} z^{1/D})^{-m} \\ &= \frac{1}{D} \sum_{k=0}^{D-1} X(e^{-j2\pi k/D} z^{1/D}) \end{aligned} \quad (9.12)$$

The key steps in obtaining the  $z$ -transform representation (9.12), for the  $(D \downarrow 1)$  downampler, are as follows:

- the introduction of the high-rate sequence  $\bar{x}(n)$ , which has  $(D-1)$  zeros in between the retained values  $x(nD)$ , and
- the impulse-train representation (9.8) for the periodic sampling series that relates  $x(n)$  to  $\bar{x}(n)$ .

By evaluating  $Y(z)$  on the unit circle, we obtain the spectrum of the output signal  $y(m)$ . Since the rate of  $y(m)$  is  $F_y = 1/T_y$ , the frequency variable, which we denote as  $\omega_y$ , is in radians and is relative to the sampling rate  $F_y$ ,

$$\omega_y = \frac{2\pi F}{F_y} = 2\pi F T_y \quad (9.13)$$

Since the sampling rates are related by the expression

$$F_y = \frac{F_x}{D} \quad (9.14)$$

it follows that the frequency variables  $\omega_y$  and

$$\omega_x = \frac{2\pi F}{F_x} 2\pi F T_x \quad (9.15)$$

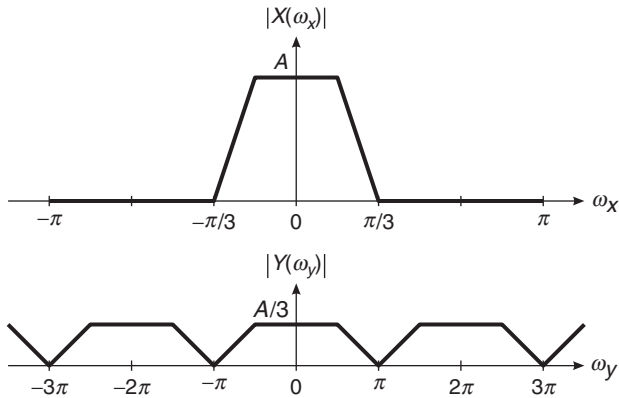


**FIGURE 9.5** Spectra of  $x(n)$  and  $y(m)$  in no-aliasing case

are related by

$$\omega_y = D\omega_x \quad (9.16)$$

Thus, as expected, the frequency range  $0 \leq |\omega_x| \leq \pi/D$  is stretched into the corresponding frequency range  $0 \leq |\omega_y| \leq \pi$  by the downsampling process.

We conclude that the spectrum  $Y(\omega_y)$ , which is obtained by evaluating (9.12) on the unit circle, can be expressed as<sup>1</sup>

$$Y(\omega_y) = \frac{1}{D} \sum_{k=0}^{D-1} X\left(\frac{\omega_y - 2\pi k}{D}\right) \quad (9.17)$$

which is an aliased version of the spectrum  $X(\omega_x)$  of  $x(n)$ . To avoid aliasing error, one needs the spectrum  $X(\omega_x)$  to be less than full band or bandlimited (note that this bandlimitedness is in the digital frequency domain). In fact, we must have

$$X(\omega_x) = 0 \quad \text{for} \quad \frac{\pi}{D} \leq |\omega_x| \leq \pi \quad (9.18)$$

Then

$$Y(\omega_y) = \frac{1}{D} X\left(\frac{\omega_y}{D}\right), |\omega_y| \leq \pi \quad (9.19)$$

and no aliasing error is present. An example of this for  $D = 3$  is shown in Figure 9.5.

<sup>1</sup>In this chapter, we will make a slight change in our notation for the DTFT. We will use  $X(\omega)$  to denote the spectrum of  $x(n)$  instead of the previously used notation  $X(e^{j\omega})$ . Although this change does conflict with the  $z$ -transform notation, the meaning should be clear from the context. This change is made for the sake of clarity and visibility of variables.

*Comments:*

1. The sampling theorem interpretation for (9.19) is that the sequence  $x(n)$  was originally sampled at  $D$  times higher rate than required; therefore, downsampling by  $D$  simply reduces the effective sampling rate to the minimum required to prevent aliasing.
2. Equation (9.18) expresses the requirement for *zero decimation error* in the sense that no information is lost—i.e., there is no irreversible aliasing error in the frequency domain.
3. The argument  $\frac{\omega_y}{D}$  occurs because in our notation  $\omega$  is expressed in rad/sample. Thus the frequency of  $y(m)$  expressed in terms of the higher-rate sequence  $x(n)$  must be divided by  $D$  to account for the slower rate of  $y(m)$ .
4. Note that there is a factor  $\frac{1}{D}$  in (9.19). This factor is required to make the inverse Fourier transform work out properly and is entirely consistent with the spectra of the sampled analog signals.

### 9.2.2 THE IDEAL DECIMATOR

In general, (9.18) will not be exactly true, and the  $(D \downarrow 1)$  downampler would cause irreversible aliasing error. To avoid aliasing, we must first reduce the bandwidth of  $x(n)$  to  $F_{x,\max} = F_x/2D$ , or equivalently, to  $\omega_{x,\max} = \pi/D$ . Then we may downsample by  $D$  and thus avoid aliasing.

The decimation process is illustrated in Figure 9.6. The input sequence  $x(n)$  is passed through a lowpass filter, characterized by the impulse response  $h(n)$  and a frequency response  $H_D(\omega_x)$ , which ideally satisfies the condition

$$H_D(\omega_x) = \begin{cases} 1, & |\omega_x| \leq \pi/D \\ 0, & \text{otherwise} \end{cases} \quad (9.20)$$

Thus the filter eliminates the spectrum of  $X(\omega_x)$  in the range  $\pi/D < \omega_x < \pi$ . Of course, the implication is that only the frequency components of  $x(n)$  in the range  $|\omega_x| \leq \pi/D$  are of interest in further processing of the signal.

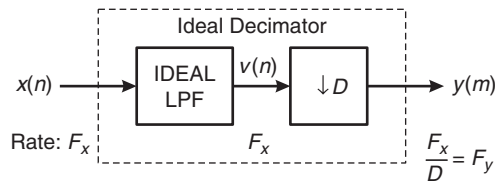


**FIGURE 9.6** Ideal decimation by a factor  $D$

The output of the filter is a sequence  $v(n)$  given as

$$v(n) \triangleq \sum_{k=0}^{\infty} h(k)x(n-k) \quad (9.21)$$

which is then downsampled by the factor  $D$  to produce  $y(m)$ . Thus

$$y(m) = v(mD) = \sum_{k=0}^{\infty} h(k)x(mD - k) \quad (9.22)$$

Although the filtering operation on  $x(n)$  is linear and time invariant, the downsampling operation in combination with the filtering results also in a time-variant system.

The frequency-domain characteristics of the output sequence  $y(m)$  obtained through the filtered signal  $v(n)$  can be determined by following the analysis steps given before—that is, by relating the spectrum of  $y(m)$  to the spectrum of the input sequence  $x(n)$ . Using these steps, we can show that

$$Y(z) = \frac{1}{D} \sum_{k=0}^{D-1} H\left(e^{-j2\pi k/D} z^{1/D}\right) X\left(e^{-j2\pi k/D} z^{1/D}\right) \quad (9.23)$$

or that

$$Y(\omega_y) = \frac{1}{D} \sum_{k=0}^{D-1} H\left(\frac{\omega_y - 2\pi k}{D}\right) X\left(\frac{\omega_y - 2\pi k}{D}\right) \quad (9.24)$$

With a properly designed filter  $H_D(\omega)$ , the aliasing is eliminated and, consequently, all but the first term in (9.24) vanish. Hence

$$Y(\omega_y) = \frac{1}{D} H_D\left(\frac{\omega_y}{D}\right) X\left(\frac{\omega_y}{D}\right) = \frac{1}{D} X\left(\frac{\omega_y}{D}\right) \quad (9.25)$$

for  $0 \leq |\omega_y| \leq \pi$ . The spectra for the sequences  $x(n)$ ,  $h(n)$ ,  $v(n)$ , and  $y(m)$  are illustrated in Figure 9.7.

**MATLAB Implementation** MATLAB provides the function `y = decimate(x,D)` that resamples the sequence in array `x` at  $1/D$  times the original sampling rate. The resulting resampled array `y` is  $D$  times shorter—that is, `length(y) = length(x)/D`. The ideal lowpass filter given in (9.20) is not possible in the MATLAB implementation; however, fairly accurate approximations are used. The default lowpass filter used in the function is an eighth-order Chebyshev type-I lowpass filter with the cutoff frequency of  $0.8\pi/D$ . Using additional optional arguments, the filter order can be changed or an FIR filter of specified order and cutoff frequency can be used.

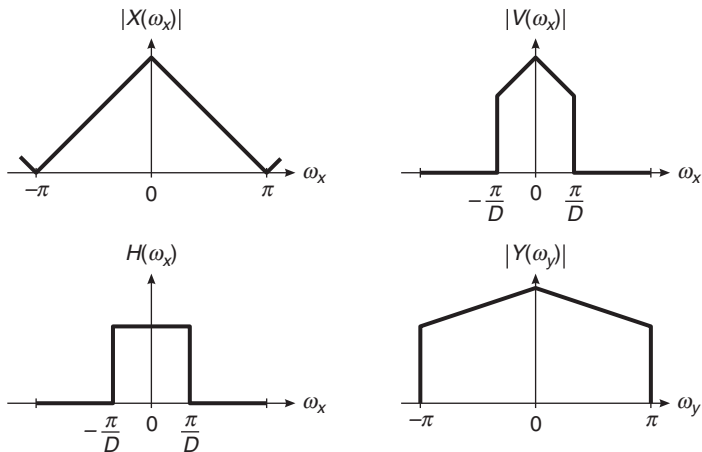


**FIGURE 9.7** Spectra of signals in the decimation of  $x(n)$  by a factor  $D$

- **EXAMPLE 9.2** Let  $x(n) = \cos(0.125\pi n)$ . Generate a large number of samples of  $x(n)$  and decimate them using  $D = 2, 4$ , and  $8$  to show the results of decimation.

### Solution

We will plot the middle segments of the signals to avoid end-effects due to the default lowpass filter in the `decimate` function. The following MATLAB script shows details of these operations, and Figure 9.7 shows the plots of the sequences.

```

n = 0:2048; k1 = 256; k2 = k1+32; m = 0:(k2-k1);
Hf1 = figure('units','inches','position',[1,1,6,4],...
    'paperunits','inches','paperposition',[0,0,6,4]);

% (a) Original signal
x = cos(0.125*pi*n); subplot(2,2,1);
Ha = stem(m,x(m+k1+1),'g','filled'); axis([-1,33,-1.1,1.1]);
set(Ha,'markersize',2); ylabel('Amplitude');
title('Original Sequence x(n)', 'fontsize',TF);
set(gca,'xtick',[0,16,32]); set(gca,'ytick',[-1,0,1]);

% (b) Decimation by D = 2
D = 2; y = decimate(x,D); subplot(2,2,2);
Hb = stem(m,y(m+k1/D+1),'c','filled'); axis([-1,33,-1.1,1.1]);
set(Hb,'markersize',2); ylabel('Amplitude');
title('Decimated by D = 2', 'fontsize',TF);
set(gca,'xtick',[0,16,32]); set(gca,'ytick',[-1,0,1]);

```

```
% (c) Decimation by D = 4
D = 4; y = decimate(x,D); subplot(2,2,3);
Hc = stem(m,y(m+k1/D+1),'r','filled'); axis([-1,33,-1.1,1.1]);
set(Hc,'markersize',2); ylabel('Amplitude');
title('Decimated by D = 4','fontsize',TF);
set(gca,'xtick',[0,16,32]); set(gca,'ytick',[-1,0,1]);
xlabel('n');

% (d) Decimation by D = 8
D = 8; y = decimate(x,D); subplot(2,2,4);
Hd = stem(m,y(m+k1/D+1),'m','filled'); axis([-1,33,-1.1,1.1]);
set(Hd,'markersize',2); ylabel('Amplitude');
title('Decimated by D = 8','fontsize',TF);
set(gca,'xtick',[0,16,32]); set(gca,'ytick',[-1,0,1]);
xlabel('n');
```

From Figure 9.8, we observe that the decimated sequences for  $D = 2$  and  $D = 4$  are correct and represent the original sinusoidal sequence  $x(n)$  at lower sampling rates. However, the sequence for  $D = 8$  is almost zero because the

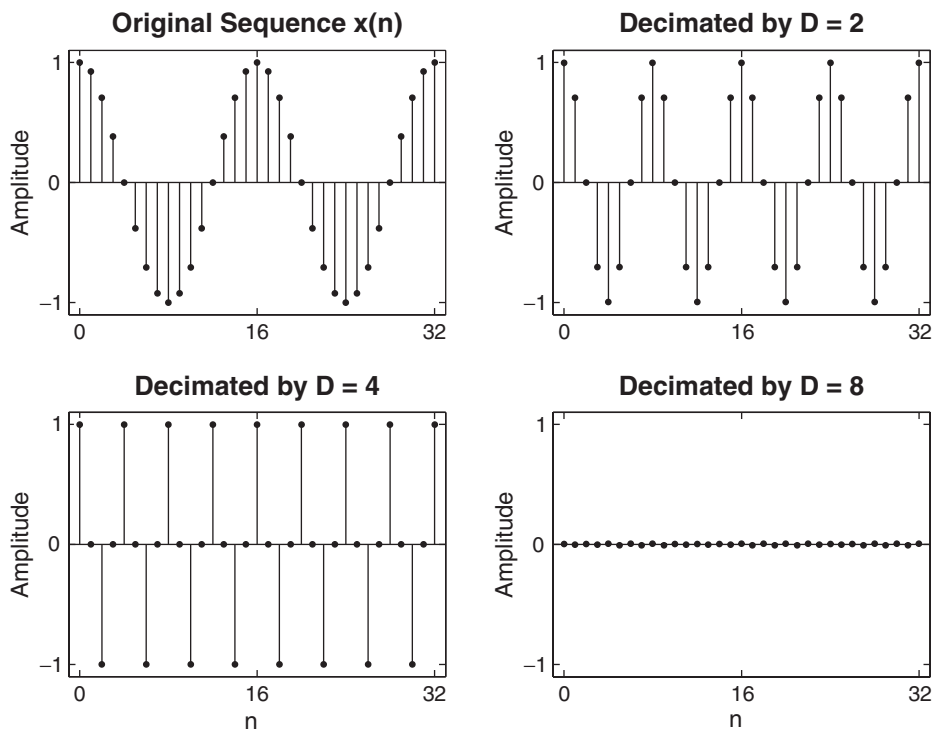


**FIGURE 9.8** Original and decimated signals in Example 9.2

lowpass filter has attenuated  $x(n)$  prior to downsampling. Recall that the cutoff frequency of the lowpass filter is set to  $0.8\pi/D = 0.1\pi$ , which eliminates  $x(n)$ . If we had used the downsampling operation on  $x(n)$  instead of decimation, the resulting sequence would be  $y(m) = 1$ , which is an aliased signal. Thus the lowpass filtering is necessary.  $\square$

## 9.3 INTERPOLATION BY A FACTOR $I$

An increase in the sampling rate by an integer factor of  $I$ —that is,  $F_y = IF_x$ —can be accomplished by interpolating  $I - 1$  new samples between successive values of the signal. The interpolation process can be accomplished in a variety of ways. We shall describe a process that preserves the spectral shape of the signal sequence  $x(n)$ . This process can be accomplished in two steps. The first step creates an intermediate signal at the high rate  $F_y$  by interlacing zeros in between nonzero samples in an operation called *upsampling*. In the second step, the intermediate signal is filtered to “fill in” zero-interlaced samples to create the interpolated high-rate signal. As before, we will first study the time- and frequency-domain characteristics of the upsampled signal and then introduce the interpolation system.

### 9.3.1 THE UPSAMPLER

Let  $v(m)$  denote the intermediate sequence with a rate  $F_y = IF_x$ , which is obtained from  $x(n)$  by adding  $I - 1$  zeros between successive values of  $x(n)$ . Thus

$$v(m) = \begin{cases} x(m/I), & m = 0, \pm I, \pm 2I, \dots \\ 0, & \text{otherwise} \end{cases} \quad (9.26)$$

and its sampling rate is identical to the rate of  $v(m)$ . The block diagram of the upsampler is shown in Figure 9.9. Again, any system containing the upsampler is a time-varying system (Problem P9.1).

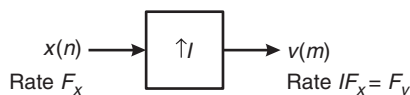


**FIGURE 9.9** An upsampling element

- $\square$  **EXAMPLE 9.3** Let  $I = 2$  and  $x(n) = \{1, 2, 3, 4\}$ . Verify that the upsampler is time varying.

**Solution**

The upsampled signal is  $v(m) = \{1, 0, 2, 0, 3, 0, 4, 0\}$ . If we now delay  $x(n)$  by one sample, we get  $x(n-1) = \{0, 1, 2, 3, 4\}$ . The corresponding upsampled signal is  $v_1(m) = \{0, 0, 1, 0, 2, 0, 3, 0, 4, 0\} = v(m-2)$  and not  $v(m-1)$ .  $\square$

**MATLAB Implementation** MATLAB provides the function `[v] = upsample(x,I)` that upsamples input array  $x$  into output  $v$  by inserting  $(I-1)$  zeros between input samples. An optional third parameter, “phase,” specifies the sample offset, which must be an integer between 0 and  $(I-1)$ . For example,

```
>> x = [1,2,3,4]; v = upsample(x,3)
v =
    1     0     0     2     0     0     3     0     0     4     0     0
```

upsamples by a factor of 2 starting with the first sample. However,

```
>> v = upsample(x,3,1)
v =
    0     1     0     0     2     0     0     3     0     0     4     0
>> v = upsample(x,3,2)
v =
    0     0     1     0     0     2     0     0     3     0     0     4
```

produces two different signals by upsampling, starting with the second and the third sample (i.e., offset by 1), respectively. Note that the lengths of the upsampled signals are  $I$  times the length of the original signal.

**The frequency-domain representation of the upsampled signal  $y(m)$**  The sequence  $v(m)$  has a  $z$ -transform

$$V(z) = \sum_{m=-\infty}^{\infty} v(m)z^{-m} = \sum_{m=-\infty}^{\infty} v(m)z^{-mI} = X(z^I) \quad (9.27)$$

The corresponding spectrum of  $v(m)$  is obtained by evaluating (9.27) on the unit circle. Thus

$$V(\omega_y) = X(\omega_y I) \quad (9.28)$$

where  $\omega_y$  denotes the frequency variable relative to the new sampling rate  $F_y$  (i.e.,  $\omega_y = 2\pi F/F_y$ ). Now the relationship between sampling rates is  $F_y = IF_x$ , and hence the frequency variables  $\omega_x$  and  $\omega_y$  are related according to the formula

$$\omega_y = \frac{\omega_x}{I} \quad (9.29)$$

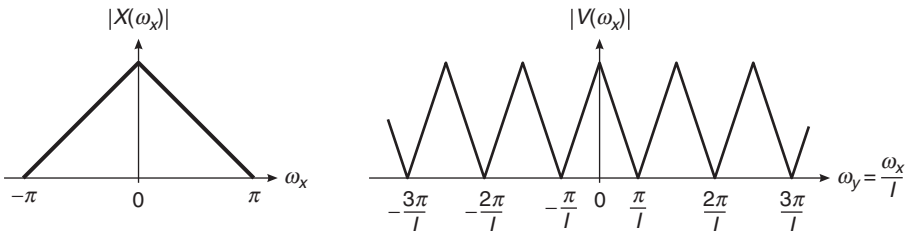


**FIGURE 9.10** Spectra of  $x(n)$  and  $v(m)$  where  $V(\omega_y) = X(\omega_y I)$

The spectra  $X(\omega_x)$  and  $V(\omega_y)$  are illustrated in Figure 9.10. We observe that the sampling rate increase, obtained by the addition of  $I - 1$  zero samples between successive values of  $x(n)$ , results in a signal whose spectrum  $V(\omega_y)$  is an  $I$ -fold periodic repetition of the input signal spectrum  $X(\omega_x)$ .

### 9.3.2 THE IDEAL INTERPOLATOR

Since only the frequency components of  $x(n)$  in the range  $0 \leq \omega_y \leq \pi/I$  are unique, the images of  $X(\omega)$  above  $\omega_y = \pi/I$  should be rejected by passing the sequence  $v(m)$  through a lowpass filter with a frequency response  $H_I(\omega_y)$  that ideally has the characteristic

$$H_I(\omega_y) = \begin{cases} C, & 0 \leq |\omega_y| \leq \pi/I \\ 0, & \text{otherwise} \end{cases} \quad (9.30)$$

where  $C$  is a scale factor required to properly normalize the output sequence  $y(m)$ . Consequently, the output spectrum is

$$Y(\omega_y) = \begin{cases} CX(\omega_y I), & 0 \leq |\omega_y| \leq \pi/I \\ 0, & \text{otherwise} \end{cases} \quad (9.31)$$

The scale factor  $C$  is selected so that the output  $y(m) = x(m/I)$  for  $m = 0, \pm I, \pm 2I, \dots$ . For mathematical convenience, we select the point  $m = 0$ . Thus

$$y(0) = \frac{1}{2\pi} \int_{-\pi}^{\pi} Y(\omega_y) d\omega_y = \frac{C}{2\pi} \int_{-\pi/I}^{\pi/I} X(\omega_y I) d\omega_y \quad (9.32)$$

Since  $\omega_y = \omega_x/I$ , (9.32) can be expressed as

$$y(0) = \frac{C}{I} \frac{1}{2\pi} \int_{-\pi}^{\pi} X(\omega_x) d\omega_x = \frac{C}{I} x(0) \quad (9.33)$$

therefore  $C = I$  is the desired normalization factor.

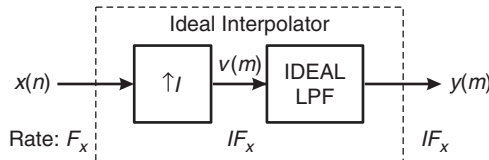


**FIGURE 9.11** Ideal interpolation by a factor  $I$

Finally, we indicate that the output sequence  $y(m)$  can be expressed as a convolution of the sequence  $v(n)$  with the unit sample response  $h(n)$  of the lowpass filter. Thus

$$y(m) = \sum_{k=-\infty}^{\infty} h(m-k)v(k) \quad (9.34)$$

Since  $v(k) = 0$  except at multiples of  $I$ , where  $v(kI) = x(k)$ , (9.34) becomes

$$y(m) = \sum_{k=-\infty}^{\infty} h(m-kI)x(k) \quad (9.35)$$

The ideal interpolator is shown in Figure 9.11.

**MATLAB Implementation** MATLAB provides the function `[y,h] = interp(x,I)` that resamples the signal in array `x` at `I` times the original sampling rate. The resulting resampled array `y` is `I` times longer—that is, `length(y) = I*length(x)`. The ideal lowpass filter given in (9.30) is approximated by a symmetric filter impulse response, `h`, which is designed internally. It allows the original samples to pass through unchanged and interpolates between so that the mean square error between them and their ideal values is minimized. The third optional parameter, `L`, specifies the length of the symmetric filter as `2*L*I+1`, and the fourth optional parameter, `cutoff`, specifies the cutoff frequency of the input signal in  $\pi$  units. The default values are `L = 5` and `cutoff = 0.5`. Thus, if `I = 2`, then the length of the symmetric filter is 21 for the default `L = 5`.

- **EXAMPLE 9.4** Let  $x(n) = \cos(\pi n)$ . Generate samples of  $x(n)$  and interpolate them using  $I = 2$ , 4, and 8 to show the results of interpolation.

#### Solution

We will plot the middle segments of the signals to avoid end-effects due to the default lowpass filter in the `interp` function. The following MATLAB script shows details of these operations, and Figure 9.12 shows the plots of the sequences.

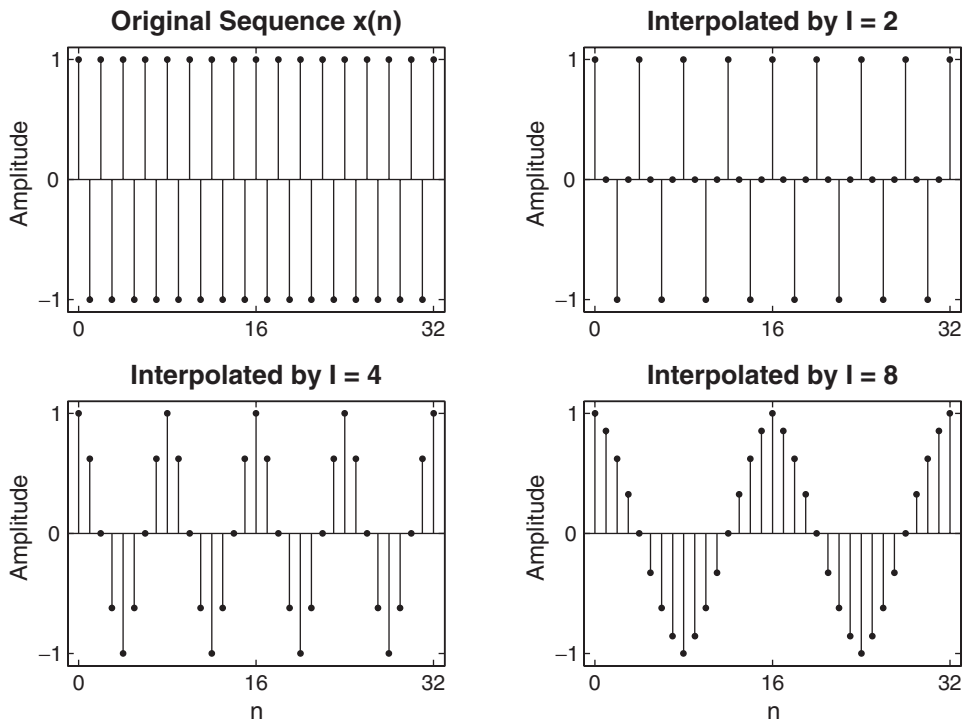


**FIGURE 9.12** Original and interpolated signals in Example 9.4

```

n = 0:256; k1 = 64; k2 = k1+32; m = 0:(k2-k1);
Hf1 = figure('units','inches','position',[1,1,6,4],...
    'paperunits','inches','paperposition',[0,0,6,4]);

% (a) Original signal
x = cos(pi*n); subplot(2,2,1);
Ha = stem(m,x(m+k1+1),'g','filled'); axis([-1,33,-1.1,1.1]);
set(Ha,'markersize',2); ylabel('Amplitude');
title('Original Sequence x(n)', 'fontsize',TF);
set(gca,'xtick',[0,16,32]); set(gca,'ytick',[-1,0,1]);

% (b) Interpolation by I = 2
I = 2; y = interp(x,I); subplot(2,2,2);
Hb = stem(m,y(m+k1*I+1),'c','filled'); axis([-1,33,-1.1,1.1]);
set(Hb,'markersize',2); ylabel('Amplitude');
title('Interpolated by I = 2', 'fontsize',TF);
set(gca,'xtick',[0,16,32]); set(gca,'ytick',[-1,0,1]);

```

```
% (c) Interpolation by I = 4
I = 4; y = interp(x,I); subplot(2,2,3);
Hc = stem(m,y(m+k1*I+1),'r','filled'); axis([-1,33,-1.1,1.1]);
set(Hc,'markersize',2); ylabel('Amplitude');
title('Interpolated by I = 4','fontsize',TF);
set(gca,'xtick',[0,16,32]); set(gca,'ytick',[-1,0,1]);
xlabel('n');

% (d) Interpolation by I = 8
I = 8; y = interp(x,I); subplot(2,2,4);
Hd = stem(m,y(m+k1*I+1),'m','filled'); axis([-1,33,-1.1,1.1]);
set(Hd,'markersize',2); ylabel('Amplitude');
title('Interpolated by I = 8','fontsize',TF);
set(gca,'xtick',[0,16,32]); set(gca,'ytick',[-1,0,1]);
xlabel('n');
```

From Figure 9.11, we observe that the interpolated sequences for all three values of  $I$  are appropriate and represent the original sinusoidal signal  $x(n)$  at higher sampling rates. In the case of  $I = 8$ , the resulting sequence does not appear to be perfectly sinusoidal in shape. This is due to the fact that the frequency response of the designed lowpass filter is not close to that of an ideal filter.  $\square$

- EXAMPLE 9.5** Examine the frequency response of the lowpass filter used in the interpolation of the signal in Example 10.4.

#### Solution

The second optional argument in the `interp` function provides the impulse response from which we can compute the frequency response, as shown in the following MATLAB script.

```
n = 0:256; x = cos(pi*n); w = [0:100]*pi/100;
Hf1 = figure('units','inches','position',[1,1,6,4],...
    'paperunits','inches','paperposition',[0,0,6,4]);

% (a) Interpolation by I = 2, L = 5;
I = 2; [y,h] = interp(x,I); H = freqz(h,1,w); H = abs(H);
subplot(2,2,1); plot(w/pi,H,'g'); axis([0,1,0,I+0.1]); ylabel('Magnitude');
title('I = 2, L = 5','fontsize',TF);
set(gca,'xtick',[0,0.5,1]); set(gca,'ytick',[0:1:I]);

% (b) Interpolation by I = 4, L = 5;
I = 4; [y,h] = interp(x,I); H = freqz(h,1,w); H = abs(H);
subplot(2,2,2); plot(w/pi,H,'g'); axis([0,1,0,I+0.2]); ylabel('Magnitude');
title('I = 4, L = 5','fontsize',TF);
set(gca,'xtick',[0,0.25,1]); set(gca,'ytick',[0:1:I]);
```

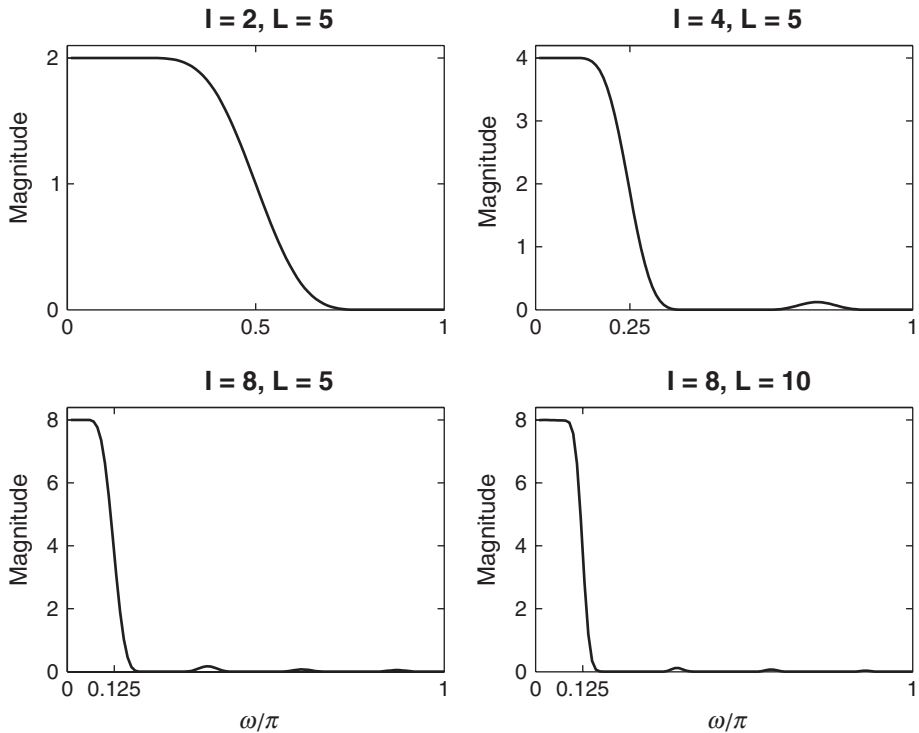


**FIGURE 9.13** Filter frequency responses in Example 9.5

```
% (c) Interpolation by I = 8, L = 5;
I = 8; [y,h] = interp(x,I); H = freqz(h,1,w); H = abs(H);
subplot(2,2,3); plot(w/pi,H,'g'); axis([0,1,0,I+0.4]); ylabel('Magnitude');
title('I = 8, L = 5','fontsize',TF); xlabel('\omega/\pi','fontsize',10)
set(gca,'xtick',[0,0.125,1]); set(gca,'ytick',[0:2:I]);

% (d) Interpolation by I = 8, L = 10;
I = 8; [y,h] = interp(x,I,10); H = freqz(h,1,w); H = abs(H);
subplot(2,2,4); plot(w/pi,H,'g'); axis([0,1,0,I+0.4]); ylabel('Magnitude');
title('I = 8, L = 10','fontsize',TF); xlabel('\omega/\pi','fontsize',10)
set(gca,'xtick',[0,0.125,1]); set(gca,'ytick',[0:2:I]);
```

The frequency response plots are shown in Figure 9.13. The first three plots are for  $L = 5$ , and, as expected, the filters are all lowpass with passband edges approximately around  $\pi/I$  frequencies and the gain of  $I$ . Also note that the filters do not have sharp transitions and thus are not good approximations to the ideal filter. The last plot shows the response for  $L = 10$ , which indicates a more sharp transition, which is to be expected. Any value beyond  $L = 10$  results in an unstable filter design and hence should be avoided.  $\square$

## 9.4 SAMPLING RATE CONVERSION BY A RATIONAL FACTOR $I/D$

Having discussed the special cases of decimation (downsampling by a factor  $D$ ) and interpolation (upsampling by a factor  $I$ ), we now consider the general case of sampling rate conversion by a rational factor  $I/D$ . Basically, we can achieve this sampling rate conversion by first performing interpolation by the factor  $I$  and then decimating the output of the interpolator by the factor  $D$ . In other words, a sampling rate conversion by the rational factor  $I/D$  is accomplished by cascading an interpolator with a decimator, as illustrated in Figure 9.14.

We emphasize that the importance of performing the interpolation first and the decimation second is to preserve the desired spectral characteristics of  $x(n)$ . Furthermore, with the cascade configuration illustrated in Figure 9.14, the two filters with impulse response  $\{h_u(k)\}$  and  $\{h_d(k)\}$  are operated at the same rate—namely,  $IF_x$ —and hence can be combined into a single lowpass filter with impulse response  $h(k)$ , as illustrated in Figure 9.15. The frequency response  $H(\omega_v)$  of the combined filter must incorporate the filtering operations for both interpolation and decimation, and hence it should ideally possess the frequency-response characteristic

$$H(\omega_v) = \begin{cases} I, & 0 \leq |\omega_v| \leq \min(\pi/D, \pi/I) \\ 0, & \text{otherwise} \end{cases} \quad (9.36)$$

where  $\omega_v = 2\pi F/F_v = 2\pi F/IF_x = \omega_x/I$ .

**Explanation of (9.36)** Note that  $V(\omega_v)$  and hence  $W(\omega_v)$  in Figure 9.15 are periodic with period  $2\pi/I$ . Thus

- if  $D < I$ , then filter  $H(\omega_v)$  allows a full period through and there is no net lowpass filtering;
- if  $D > I$ , then filter must first truncate the fundamental period of  $W(\omega_v)$  to avoid aliasing error in the  $(D \downarrow 1)$  decimation stage to follow.

Putting these two observations together, we can state that when  $D/I < 1$ , we have net interpolation and no smoothing is required by

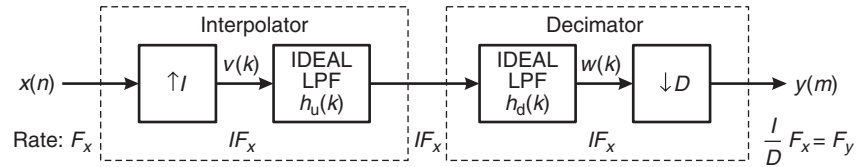


**FIGURE 9.14** Cascade of interpolator and decimator for sampling rate conversion by a rational factor  $I/D$

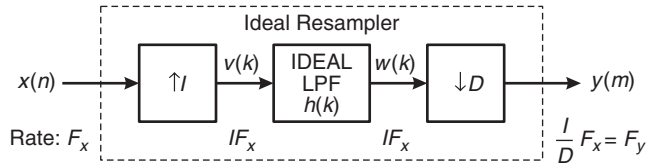


**FIGURE 9.15** Method for sampling rate conversion by a factor  $I/D$

$H(\omega_v)$  other than to extract the fundamental period of  $W(\omega_v)$ . In this respect,  $H(\omega_v)$  acts as a lowpass filter as in the ideal interpolator. On the other hand, if  $D/I > 1$ , then we have net decimation. Hence it is necessary to first truncate even the fundamental period of  $W(\omega_v)$  to get the frequency band down to  $[-\pi/D, \pi/D]$  and to avoid aliasing in the decimation that follows. In this respect,  $H(\omega_v)$  acts as a smoothing filter in the ideal decimator. When  $D$  or  $I$  is equal to 1, the general decimator/interpolator in Figure 9.15 along with (9.36) reduces to the ideal interpolator or decimator as a special case, respectively.

In the time domain, the output of the upsampler is the sequence

$$v(k) = \begin{cases} x(k/I), & k = 0, \pm I, \pm 2I, \dots \\ 0, & \text{otherwise} \end{cases} \quad (9.37)$$

and the output of the linear time-invariant filter is

$$w(k) = \sum_{\ell=-\infty}^{\infty} h(k-\ell)v(\ell) = \sum_{\ell=-\infty}^{\infty} h(k-\ell I)x(\ell) \quad (9.38)$$

Finally, the output of the sampling rate converter is the sequence  $\{y(m)\}$ , which is obtained by downsampling the sequence  $\{w(k)\}$  by a factor of  $D$ . Thus

$$y(m) = w(mD) = \sum_{\ell=-\infty}^{\infty} h(mD - \ell I)x(\ell) \quad (9.39)$$

It is illuminating to express (9.39) in a different form by making a change in variable. Let

$$\ell = \left\lfloor \frac{mD}{I} \right\rfloor - n \quad (9.40)$$

where the notation  $\lfloor r \rfloor$  denotes the largest integer contained in  $r$ . With this change in variable, (9.39) becomes

$$y(m) = \sum_{n=-\infty}^{\infty} h\left(mD - \left\lfloor \frac{mD}{I} \right\rfloor I + nI\right) x\left(\left\lfloor \frac{mD}{I} \right\rfloor - n\right) \quad (9.41)$$

We note that

$$mD - \left\lfloor \frac{mD}{I} \right\rfloor I = (mD) \bmod I = ((mD))_I$$

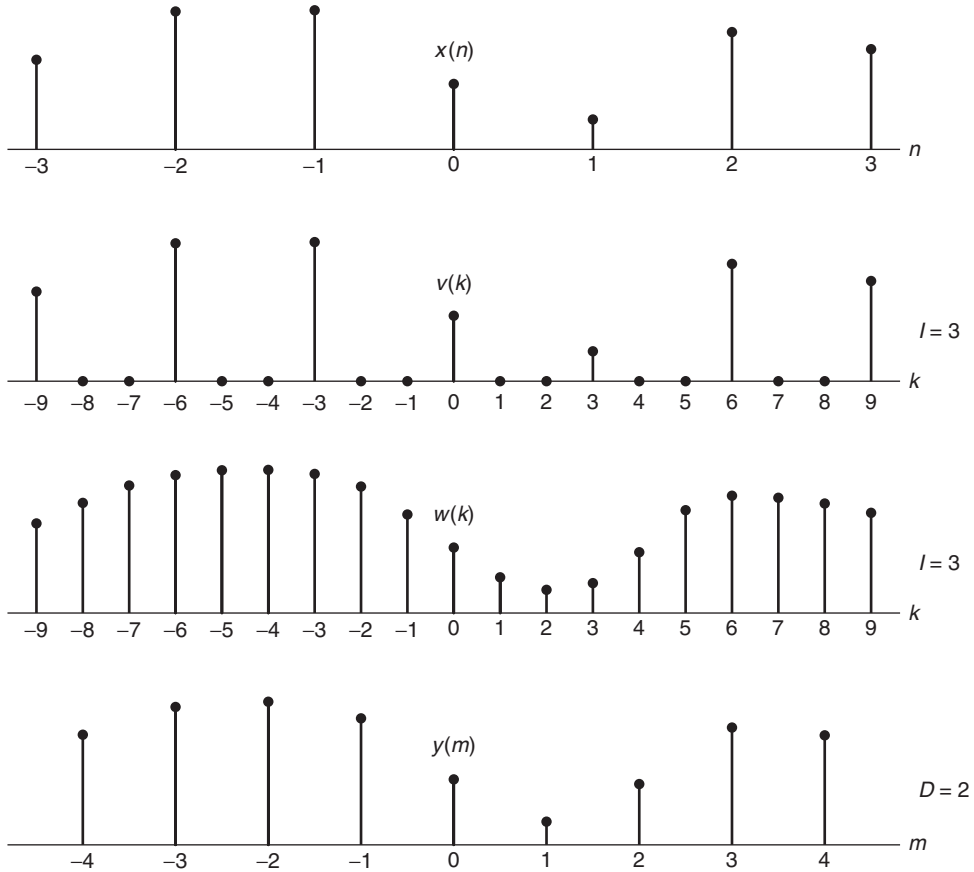


**FIGURE 9.16** Examples of signals  $x(n)$ ,  $v(k)$ ,  $w(k)$ , and  $y(m)$  in the sampling rate converter of Figure 9.15 for  $I = 3$  and  $D = 2$

Consequently, (9.41) can be expressed as

$$y(m) = \sum_{n=-\infty}^{\infty} h[nI + ((mD))_I] x\left(\left\lfloor \frac{mD}{I} \right\rfloor - n\right) \quad (9.42)$$

These operations are shown in Figure 9.16 for  $I = 3$  and  $D = 2$ .

It is apparent from (9.41) and Figure 9.16 that the output  $y(m)$  is obtained by passing the input sequence  $x(n)$  through a time-variant filter with impulse response

$$g(n, m) = h[nI + ((mD))_I] \quad -\infty < m, n < \infty \quad (9.43)$$

where  $h(k)$  is the impulse response of the time-invariant lowpass filter operating at the sampling rate  $IF_x$ . We further observe that for any integer  $k$ ,

$$\begin{aligned} g(n, m + kI) &= h[nI + ((mD + kDI))_I] = h[nI + ((mD))_I] \\ &= g(n, m) \end{aligned} \quad (9.44)$$

Hence  $g(n, m)$  is periodic in the variable  $m$  with period  $I$ .

Regarding the computational complexity of the lowpass filter in the general resampler, we note that it has a nonzero input only every  $I$  samples and the output is required only every  $D$  samples. If we use an FIR implementation for this lowpass filter, we need only compute its output one out of every  $D$  samples. However, if we instead use IIR implementation, we would generally have to compute intermediate outputs also because of the recursive nature of the filter. However, both types of filter benefit from the computational savings due to their sparse input.

**The frequency-domain representation of the resampled signal  $y(m)$**  The frequency-domain relationships can be obtained by combining the results of the interpolation and decimation process. Thus the spectrum at the output of the linear filter with impulse response  $h(k)$  is

$$\begin{aligned} V(\omega_v) &= H(\omega_v)X(\omega_v I) \\ &= \begin{cases} IX(\omega_v I), & 0 \leq |\omega_v| \leq \min(\pi/D, \pi/I) \\ 0, & \text{otherwise} \end{cases} \end{aligned} \quad (9.45)$$

The spectrum of the output sequence  $y(m)$ , obtained by decimating the sequence  $v(n)$  by a factor of  $D$ , is

$$Y(\omega_y) = \frac{1}{D} \sum_{k=0}^{D-1} V\left(\frac{\omega_y - 2\pi k}{D}\right) \quad (9.46)$$

where  $\omega_y = D\omega_v$ . Since the linear filter prevents aliasing as implied by (9.45), the spectrum of the output sequence given by (9.46) reduces to

$$Y(\omega_y) = \begin{cases} \frac{I}{D} X\left(\frac{\omega_y}{D}\right), & 0 \leq |\omega_y| \leq \min(\pi, \frac{\pi D}{I}) \\ 0, & \text{otherwise} \end{cases} \quad (9.47)$$

**MATLAB Implementation** MATLAB provides the function `[y,h]=resample(x,I,D)` that resamples the signal in array `x` at  $I/D$  times the original sampling rate. The resulting resampled array `y` is  $I/D$  times longer (or the ceiling of it if the ratio is not an integer)—that is, `length(y) = ceil(I/D)*length(x)`. The function approximates the anti-aliasing (lowpass) filter given in (9.36) by an FIR filter, `h`, designed (internally) using the Kaiser window. It also compensates for the filter's delay.

The length of the FIR filter  $h$  that `resample` uses is proportional to the fourth (optional) parameter  $L$  that has the default value of 10. For  $L = 0$ , `resample` performs a nearest-neighbor interpolation. The fifth optional parameter `beta` (default value 5) can be used to specify the Kaiser window stopband attenuation parameter  $\beta$ . The filter characteristics can be studied using the impulse response  $h$ .

- EXAMPLE 9.6** Consider the sequence  $x(n) = \cos(0.125\pi n)$  discussed in Example 9.2. Change its sampling rate by  $3/2$ ,  $3/4$ , and  $5/8$ .

**Solution**

The following MATLAB script shows the details.

```
n = 0:2048; k1 = 256; k2 = k1+32; m = 0:(k2-k1);
% (a) Original signal
x = cos(0.125*pi*n);
% (b) Sample rate conversion by 3/2: I= 3, D = 2
I = 3; D = 2; y = resample(x,I,D);
% (c) Sample rate conversion by 3/4: I= 3, D = 4
I = 3; D = 4; y = resample(x,I,D);
% (d) Sample rate conversion by 5/8: I= 5, D = 8
I = 5; D = 8; y = resample(x,I,D);
% Plotting commands follow
```

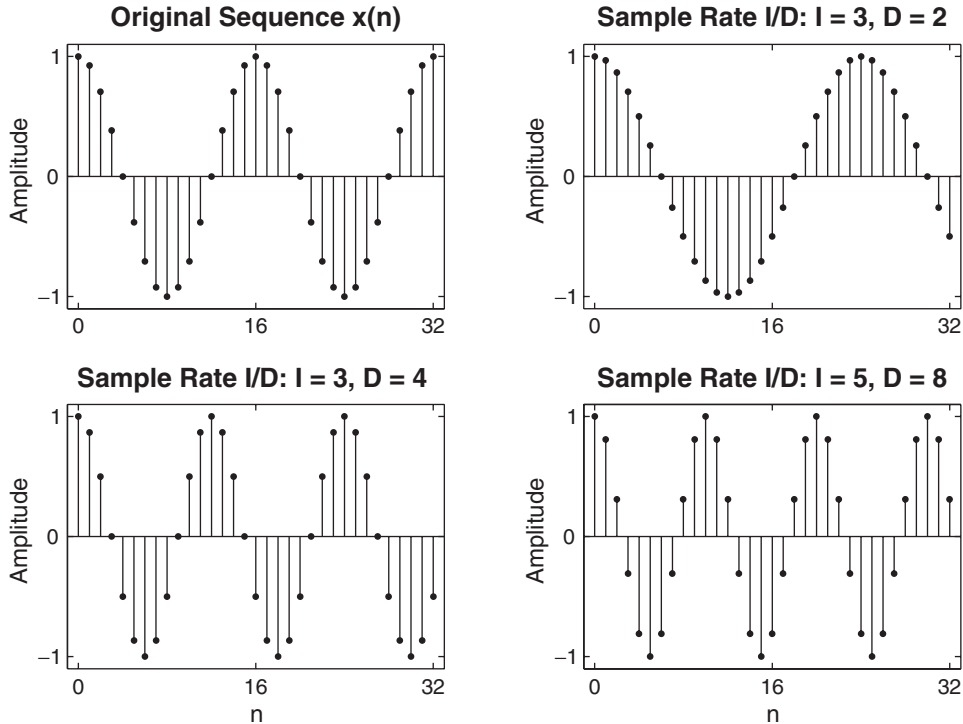


**FIGURE 9.17** Original and resampled signals in Example 9.6

The resulting plots are shown in Figure 9.17. The original  $x(n)$  signal has 16 samples in one period of the cosine waveform. Since the first sampling rate conversion by  $3/2$  is greater than 1, the overall effect is to interpolate  $x(n)$ . The resulting signal has  $16 \times 3/2 = 24$  samples in one period. The other two sampling rate conversion factors are less than 1; thus the overall effect is to decimate  $x(n)$ . The resulting signals have  $16 \times 3/4 = 12$  and  $16 \times 5/8 = 10$  samples per period, respectively.  $\square$

## 9.5 FIR FILTER DESIGNS FOR SAMPLING RATE CONVERSION

In practical implementations of sampling rate converters, we must replace the ideal lowpass filters of equations (9.20), (9.30), and (9.36) by a practical finite-order filter. The lowpass filter can be designed to have linear phase, a specified passband ripple, and stopband attenuation. Any of the standard, well-known FIR filter design techniques (e.g., window method, frequency-sampling method) can be used to carry out this design. We consider linear-phase FIR filters for this purpose because of their ease of design and because they fit very nicely into a decimator stage where only one of  $D$  outputs is required [see the discussion following (9.44) on page 480]. We will first discuss integer interpolators, followed by integer decimators and then the rational resamplers. The main emphasis will be on the specifications of these FIR lowpass filters, since the design problem has already been considered in Chapter 7.

### 9.5.1 FIR INTEGER INTERPOLATION

Replacing the ideal filter of the system given on page 473 with an FIR filter, we obtain the system shown in Figure 9.18. The relevant equation that relates the Fourier transforms  $V(\omega)$  and  $X(\omega)$  is (9.28), repeated here for convenience:

$$V(\omega) = X(\omega I) \quad (9.48)$$

Considering the frequency compression by  $I$  and the required amplitude scale factor of  $I$ , the ideal lowpass filter was determined in (9.30) and (9.33) to be

$$H_I(\omega) = \begin{cases} I, & |\omega| < \pi/I \\ 0, & \text{otherwise} \end{cases} \quad (9.49)$$

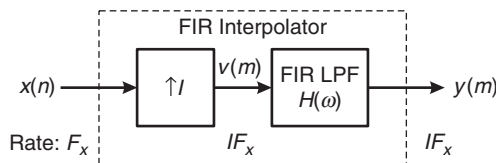


**FIGURE 9.18** An FIR integer interpolator

**MATLAB Implementation** To design a linear-phase FIR filter for use in interpolation (and, as we shall see later, for decimation) operation, MATLAB provides the function `h = intfilt(I,L,alpha)`. When used on a sequence interspersed with  $I-1$  consecutive zeros between every  $I$  samples, the function performs ideal bandlimited interpolation using the nearest  $2*L$  nonzero samples. It assumes that the bandwidth of the signal  $x(n)$  is `alpha` times  $\pi$  radians/sample—that is, `alpha=1` means the full signal bandwidth. The length of the filter impulse response array `h` is  $2*I*L-1$ . The designed filter is identical to that used by the `interp` function. Therefore, the parameter `L` should be chosen carefully to avoid numerical instability. It should be a smaller value for higher `I` value but no more than 10.

- **EXAMPLE 9.7** Design a linear-phase FIR interpolation filter to interpolate a signal by a factor of 4, using the bandlimited method.

**Solution**

We will explore the `intfilt` function for the design using  $L = 5$  and study the effect of `alpha` on the filter design. The following MATLAB script provides the detail.

```
I = 4; L = 5;
% (a) Full signal bandwidth: alpha = 1
alpha = 1; h = intfilt(I,L,alpha);
[Hr,w,a,L] = Hr_Type1(h); Hr_min = min(Hr); w_min = find(Hr == Hr_min);
H = abs(freqz(h,1,w)); Hdb = 20*log10(H/max(H)); min_attn = Hdb(w_min);
% (b) Partial signal bandwidth: alpha = 0.75
alpha = 0.75; h = intfilt(I,L,alpha);
[Hr,w,a,L] = Hr_Type1(h); Hr_min = max(Hr(end/2:end)); w_min = find(Hr == Hr_min);
H = abs(freqz(h,1,w)); Hdb = 20*log10(H/max(H)); min_attn = Hdb(w_min);
% Plotting commands follow
```

The plots are shown in Figure 9.19. For the full bandwidth case of `alpha = 1`, the filter has more ripple in both the passband and the stopband with the minimum stopband attenuation of 22 dB. This is because the filter transition band is very narrow. For `alpha = 0.75`, the filter specifications are more lenient, and hence its response is well behaved with minimum stopband attenuation of 40 dB. Note that we do not have complete control over other design parameters. These issues are discussed in more detail further along in this section. □

In the following example, we design a linear-phase equiripple FIR interpolation filter using the Parks–McClellan algorithm.

- **EXAMPLE 9.8** Design an interpolator that increases the input sampling rate by a factor of  $I = 5$ . Use the `firpm` algorithm to determine the coefficients of the FIR filter that has 0.1 dB ripple in the passband and is down by at least 30 dB in the stopband. Choose reasonable values for band-edge frequencies.

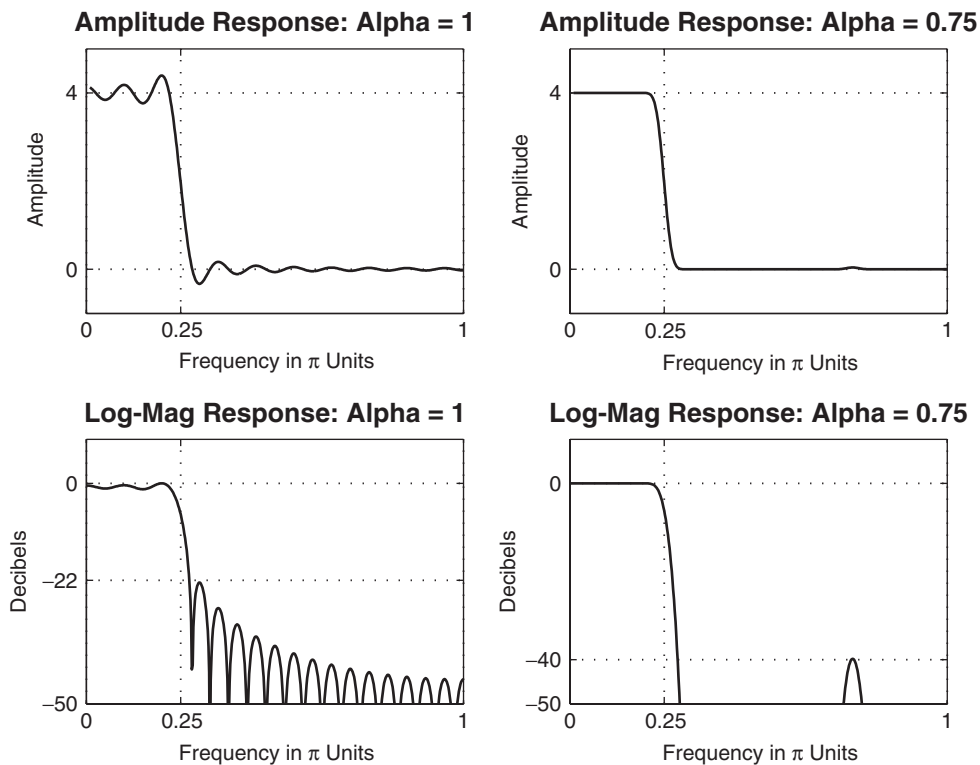


**FIGURE 9.19** FIR interpolation filter design plots for  $I = 4$  and  $L = 5$

### Solution

The passband cutoff frequency should be  $\omega_p = \pi/I = 0.2\pi$ . To get a reasonable value for the filter length, we choose the transition width of  $0.12\pi$ , which gives stopband cutoff frequency of  $\omega_s = 0.32\pi$ . Note that the nominal gain of the filter in the passband should be equal to  $I = 5$ , which means that the ripple values computed using the decibel values are scaled by 5. A filter of length  $M = 31$  achieves the design specifications given above. The details are given in the following MATLAB script.

```
I = 5; Rp = 0.1; As = 30; wp = pi/I; ws = wp+pi*0.12;
[delta1,delta2] = db2delta(Rp,As); weights = [delta2/delta1,1];
F = [0,wp,ws,pi]/pi; A = [I,I,0,0];
h = firpm(30,F,A,weights); n = [0:length(h)-1];
[Hr,w,a,L] = Hr_Type1(h); Hr_min = min(Hr); w_min = find(Hr == Hr_min);
H = abs(freqz(h,1,w)); Hdb = 20*log10(H/max(H)); min_attn = Hdb(w_min);
```

The responses of the designed FIR filter are given in Figure 9.20. Even though this filter passes the original signal, it is possible that some of the

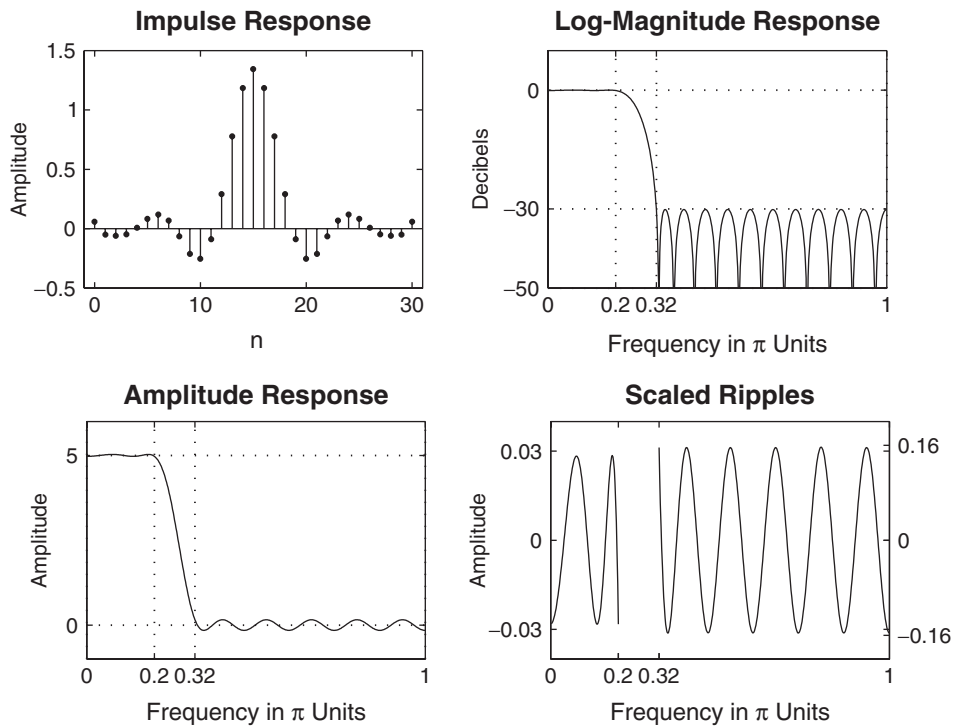


**FIGURE 9.20** Responses of the FIR interpolation filter in Example 9.8

neighboring spectral energy may also leak through if the signal is of full bandwidth of  $\pi$  radians. Hence we need better design specifications, which are discussed further along in this section.  $\square$

**MATLAB Implementation** To use the FIR filter for interpolation purposes (such as the one designed in Example 9.8), MATLAB has provided a general function, `upfirdn`, that can be used for interpolation and decimation as well as for resampling purposes. Unlike other functions discussed in this chapter, `upfirdn` incorporates the user-defined FIR filter (which need not be linear phase) in the operation. When invoked as  $y = \text{upfirdn}(x, h, I)$ , the function upsamples the input data in the array  $x$  by a factor of the integer  $I$  and then filters the upsampled signal data with the impulse response sequence given in the array  $h$  to produce the output array  $y$ , thus implementing the system in Figure 9.18.

- EXAMPLE 9.9** Let  $x(n) = \cos(0.5\pi n)$ . Increase the input sampling rate by a factor of  $I = 5$ , using the filter designed in Example 9.8.

**Solution**

The steps are given in the following MATLAB script.

```
% Given Parameters:
I = 5; Rp = 0.1; As = 30; wp = pi/I; ws = 0.32*pi;
[delta1,delta2] = db2delta(Rp,As); weights = [delta2/delta1,1];
n = [0:50]; x = cos(0.5*pi*n);
n1 = n(1:17); x1 = x(17:33); % For plotting purposes
% Input signal plotting commands follow
% Interpolation with Filter Design: Length M = 31
M = 31; F = [0,wp,ws,pi]/pi; A = [I,I,0,0];
h = firpm(M-1,F,A,weights); y = upfirdn(x,h,I);
delay = (M-1)/2; % Delay imparted by the filter
m = delay+1:1:50*I+delay+1; y = y(m); m = 1:81; y = y(81:161); % for plotting
% Output signal plotting commands follow
```

The signal stem plots are shown in Figure 9.21. The upper left-hand plot shows a segment of the input signal  $x(n)$ , and the upper right-hand plot shows the interpolated signal  $y(n)$  using the filter of length 31. The plot is corrected for

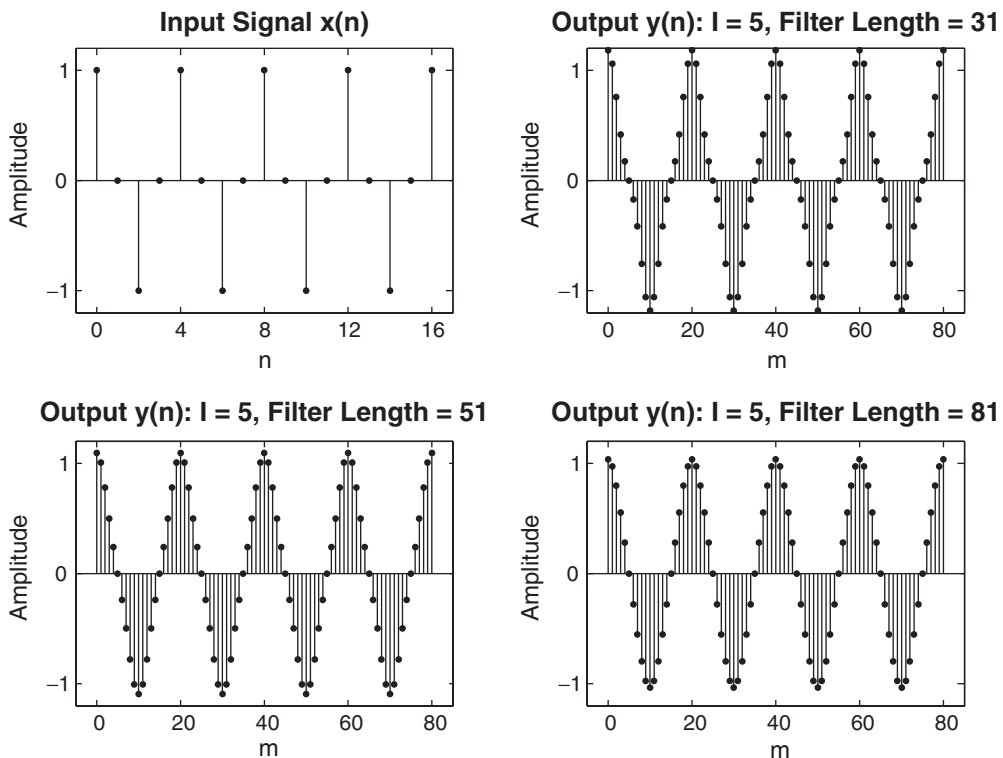


**FIGURE 9.21** Signal plots in Example 9.9

filter delay and the effect of its transient response. It is somewhat surprising that the interpolated signal is not what it should be. The signal peak is more than 1, and the shape is distorted. A careful observation of the filter response plot in Figure 9.20 reveals that the broad transition width and a smaller attenuation has allowed some of the spectral energy to leak, creating a distortion.

To investigate this further, we designed filters with larger orders of 51 and 81, as detailed in the following MATLAB script.

```
% Interpolation with Filter Design: Length M = 51
M = 51; F = [0,wp,ws,pil]/pi; A = [I,I,0,0];
h = firpm(M-1,F,A,weights); y = upfirdn(x,h,I);
delay = (M-1)/2; % Delay imparted by the filter
m = delay+1:1:50*I+delay+1; y = y(m); m = 1:81; y = y(81:161);
% Plotting commands follow
% Interpolation with Filter Design: Length M = 81
M = 81; F = [0,wp,ws,pil]/pi; A = [I,I,0,0];
h = firpm(M-1,F,A,weights); y = upfirdn(x,h,I);
delay = (M-1)/2; % Delay imparted by the filter
m = delay+1:1:50*I+delay+1; y = y(m); m = 1:81; y = y(81:161);
% Plotting commands follow
```

The resulting signals are shown in lower plots in Figure 9.21. Clearly, for large orders, the filter has better lowpass characteristics. The signal peak value approaches 1, and its shape approaches the cosine waveform. Thus a good filter design is critical even in a simple signal case.  $\square$

### 9.5.2 DESIGN SPECIFICATIONS

When we replace  $H_I(\omega)$  by a finite-order FIR filter  $H(\omega)$ , we must allow for a transition band; thus the filter cannot have a passband edge up to  $\pi/I$ . Toward this, we define

- $\omega_{x,p}$  as the highest frequency of the signal  $x(n)$  that we want to preserve, and
- $\omega_{x,s}$  as the full signal bandwidth of  $x(n)$ ,—that is, there is no energy in  $x(n)$  above the frequency  $\omega_{x,s}$ .

Thus we have  $0 < \omega_{x,p} < \omega_{x,s} < \pi$ . Note that the parameters  $\omega_{x,p}$  and  $\omega_{x,s}$ , as defined, are *signal parameters*, not filter parameters; they are shown in Figure 9.22a. The filter parameters will be defined based on  $\omega_{x,p}$  and  $\omega_{x,s}$ .

From equation (9.48), these signal parameter frequencies for  $v(m)$  become  $\omega_{x,p}/I$  and  $\omega_{x,s}/I$ , respectively, because the frequency scale is compressed by the factor  $I$ . This is shown in Figure 9.22b. A linear-phase

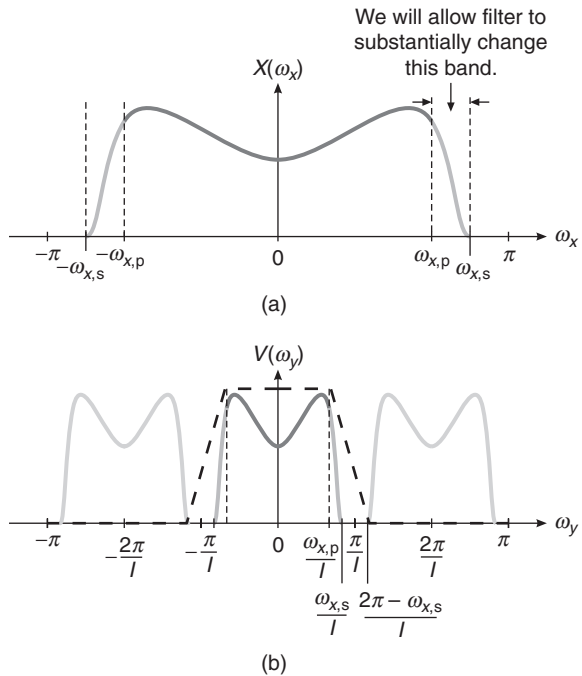


**FIGURE 9.22** Frequency parameters: (a) signal, (b) filter

FIR filter can now be designed to pass frequencies up to  $\omega_{x,p}/I$  and to suppress frequencies starting at  $(2\pi - \omega_{x,s})/I$ . Let

$$\omega_p = \left(\frac{\omega_{x,p}}{I}\right) \quad \text{and} \quad \omega_s = \left(\frac{2\pi - \omega_{x,s}}{I}\right) \quad (9.50)$$

be the passband and stopband edge frequencies, respectively, of the low-pass linear-phase FIR filter given by

$$H(\omega) = H_r(\omega)e^{j\theta(\omega)} \quad (9.51)$$

where  $H_r(\omega)$  is the real-valued amplitude response and  $\theta(\omega)$  is the unwrapped phase response. Then we have the following filter design specifications:

$$\frac{1}{I}H_r(\omega) \leq 1 \pm \delta_1 \quad \text{for } |\omega| \in [0, \omega_p]$$
  

$$\frac{1}{I}H_r(\omega) \leq \pm \delta_2 \quad \text{for } |\omega| \in [\omega_s, \pi]$$

(9.52)

where  $\omega_p$  and  $\omega_s$  are as given in (9.50) and  $\delta_1$  and  $\delta_2$  are the passband and stopband ripple parameters, respectively, of the lowpass FIR filter.

*Comment:* Instead of beginning the stopband at  $\pi/I$ , we were able to shift it to  $(2\pi - \omega_s)/I$ . If  $\omega_{x,s} \ll \pi$ , then this will be an important consideration to lower filter order. However, in the worst-case scenario of  $\omega_{x,s} = \pi$ , the stopband will begin at  $\frac{\pi}{I}$ , which is the same as in the ideal lowpass filter of (9.49). Almost always,  $\omega_{x,s} < \pi$ , and we can then choose  $\omega_{x,p}$  as close to  $\omega_{x,s}$  as we want. However, this will reduce the size of the transition band, which means a higher filter order.

- **EXAMPLE 9.10** Design a better FIR lowpass filter for sampling rate increase by a factor of  $I = 5$  for the signal in Example 9.9.

### Solution

Since  $x(n) = \cos(0.5\pi n)$ , the signal bandwidth and bandwidth to be preserved are the same—that is,  $\omega_{x,p} = \omega_{x,s} = 0.5\pi$ . Thus, from (9.50),  $\omega_p = 0.5\pi/5 = 0.1\pi$  and  $\omega_s = (2\pi - 0.5\pi)/5 = 0.3\pi$ . We will design the filter for  $R_p = 0.01$  and  $A_s = 50$  dB. The resulting filter order is 32, which is 2 higher than the one in Example 9.9 but with much superior attenuation. The details are given below.

```
% Given Parameters:
n = [0:50]; wxp = 0.5*pi; x = cos(wxp*n);
n1 = n(1:9); x1 = x(9:17); % for plotting purposes
I = 5; I = 5; Rp = 0.01; As = 50; wp = wxp/I; ws = (2*pi-wxp)/I;
[delta1,delta2] = db2delta(Rp,As); weights = [delta2/delta1,1];
[N,Fo,Ao,weights] = firpmord([wp,ws]/pi,[1,0],[delta1,delta2],2);N = N+2;
% Input signal plotting commands follow
% Interpolation with Filter Design: Length M = 31
h = firpm(N,Fo,I*Ao,weights); y = upfirdn(x,h,I);
delay = (N)/2; % Delay imparted by the filter
m = delay+1:1:50*I+delay+1; y = y(m); m = 0:40; y = y(81:121);
% Output signal plotting commands follow
[Hr,w,a,L] = Hr_Type1(h); Hr_min = min(Hr); w_min = find(Hr == Hr_min);
H = abs(freqz(h,1,w)); Hdb = 20*log10(H/max(H)); min_attn = Hdb(w_min);
% Filter design plotting commands follow
```

The signal stem plots and filter design plots are shown in Figure 9.23. The designed filter has a minimum stopband attenuation of 53 dB, and the resulting interpolation is accurate even with the filter order of 32. □

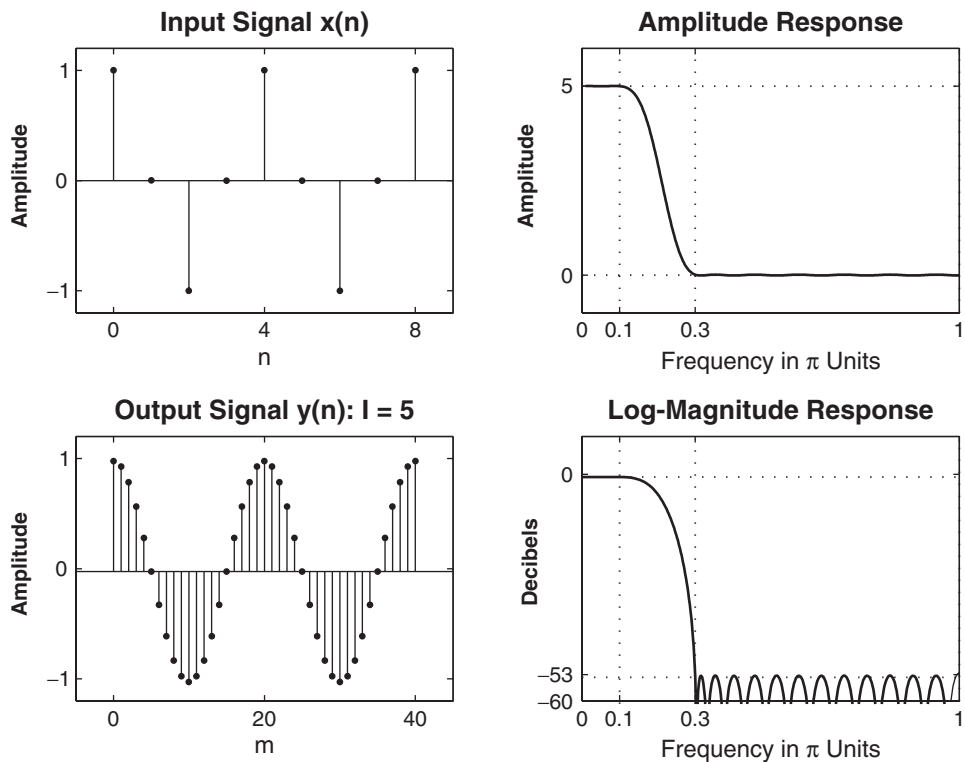


**FIGURE 9.23** Signal plots and filter design plots in Example 9.10

### 9.5.3 FIR INTEGER DECIMATION

Consider the system in Figure 9.6 on page 466 in which the ideal lowpass filter is replaced by an FIR filter  $H(\omega)$ , which then results in the system shown in Figure 9.24. The relationship between  $Y(\omega_y)$  and  $X(\omega)$  is given by (9.24), which is repeated here for convenience:

$$Y(\omega_y) = \frac{1}{D} \sum_{k=0}^{D-1} H\left(\omega - \frac{2\pi k}{D}\right) X\left(\omega - \frac{2\pi k}{D}\right); \quad \omega = \frac{\omega_y}{D} \quad (9.53)$$

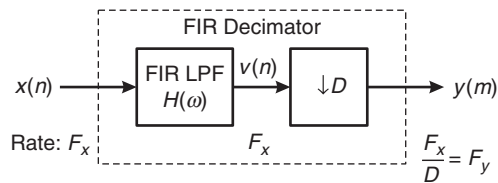


**FIGURE 9.24** An FIR integer decimator

which is nothing but the aliased sum of the  $H(\omega)X(\omega)$ . Thus the condition necessary to avoid aliasing is

$$H(\omega)X(\omega) = 0 \quad \text{for} \quad \frac{\pi}{D} \leq |\omega| \leq \pi \quad (9.54)$$

Then

$$Y(\omega_y) = \frac{1}{D}X(\omega)H(\omega) \quad (9.55)$$

as in (9.25), where the ideal filtering was accomplished with  $H_D(\omega)$  as given in (9.20).

- **EXAMPLE 9.11** Design a decimator that downsamples an input signal  $x(n)$  by a factor  $D = 2$ . Use the `firpm` algorithm to determine the coefficients of the FIR filter that has a 0.1 dB ripple in the passband and is down by at least 30 dB in the stopband. Choose reasonable values for band-edge frequencies.

#### Solution

The passband cutoff frequency should be  $\omega_p = \pi/D = 0.5\pi$ . To get a reasonable value for the filter length, we choose the transition width of  $0.1\pi$ , which gives stopband a cutoff frequency of  $\omega_s = 0.3\pi$ . A filter of length  $M = 37$  achieves the preceding design specifications. The details are given in the following MATLAB script.

```
% Filter Design
D = 2; Rp = 0.1; As = 30; wp = pi/D; ws = wp+0.1*pi;
[delta1,delta2] = db2delta(Rp,As);
[N,F,A,weights] = firpmord([wp,ws]/pi,[1,0],[delta1,delta2],2);
h = firpm(N,F,A,weights); n = [0:length(h)-1];
[Hr,w,a,L] = Hr_Type1(h); Hr_min = min(Hr); w_min = find(Hr == Hr_min);
H = abs(freqz(h,1,w)); Hdb = 20*log10(H/max(H)); min_attn = Hdb(w_min);
% Plotting commands follow
```

The responses of the designed FIR filter are given in Figure 9.25. This filter passes the signal spectrum over the passband  $[0, \pi/2]$  without any distortion. However, since the transition width is not very narrow, it is possible that some of the signal over the transition band may alias into the band of interest. Also, the 30 db attenuation may allow a small fraction of the signal spectrum from the stopband into the passband after downsampling. Therefore, we need a better approach for filter specifications, as discussed further along in this section. □

**MATLAB Implementation** As discussed, the `upfirdn` function can also be used for implementing the user-designed FIR filter in the decimation operation. When invoked as  $y = \text{upfirdn}(x,h,1,D)$ , the function filters the signal data in the array  $x$  with the impulse response given in the array  $h$  and then downsamples the filtered data by the integer factor  $D$  to produce the output array  $y$ , thus implementing the system in Figure 9.24.

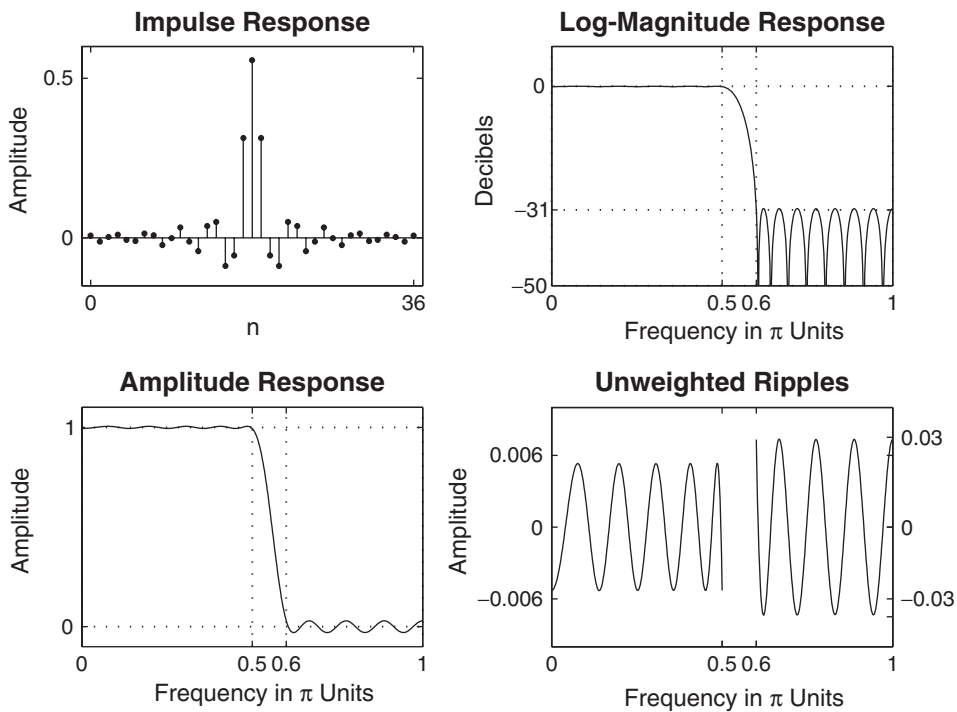


FIGURE 9.25 Responses of the FIR decimation filter in Example 9.11

- **EXAMPLE 9.12** Using the filter designed in Example 9.11, decimate sinusoidal signals  $x_1(n) = \cos(\pi n/8)$  and  $x_2(n) = \cos(\pi n/2)$  with frequencies within the passband of the filter. Verify the performance of the FIR filter and the results of the decimation.

#### Solution

The following MATLAB script provides the details.

```
% Given Parameters:
D = 2; Rp = 0.1; As = 30; wp = pi/D; ws = wp+0.1*pi;
% Filter Design
[delta1,delta2] = db2delta(Rp,As);
[N,F,A,weights] = firpmord([wp,ws]/pi,[1,0],[delta1,delta2],2);
h = firpm(N,F,A,weights); delay = N/2; % Delay imparted by the filter
% Input signal x1(n) = cos(2*pi*n/16)
n = [0:256]; x = cos(pi*n/8);
n1 = n(1:33); x1 = x(33:65); % for plotting purposes
% Input signal plotting commands follow
% Decimation of x1(n): D = 2
y = upfirdn(x,h,1,D);
```

```

m = delay+1:1:128/D+delay+1; y = y(m); m = 0:16; y = y(16:32);
% Output signal plotting commands follow
% Input signal x2(n) = cos(8*pi*n/16)
n = [0:256]; x = cos(8*pi*n/(16));
n1 = n(1:33); x1 = x(33:65); % for plotting purposes
% Input signal plotting commands follow
% Decimation of x2(n): D = 2
y = upfirdn(x,[h],1,D); %y = downsample(conv(x,h),2);
m = delay+1:1:128/D+delay+1; y = y(m); m = 0:16; y = y(16:32);
% Output signal plotting commands follow

```

The signal stem plots are shown in Figure 9.26. The left-side plots show the signal  $x_1(n)$  and the corresponding decimated signal  $y_1(n)$ , and the right-side plots show the same for  $x_2(n)$  and  $y_2(n)$ . In both cases, the decimation appears to be correct. If we had chosen any frequency above  $\pi/2$ , then the filter would have attenuated or eliminated the signal.  $\square$

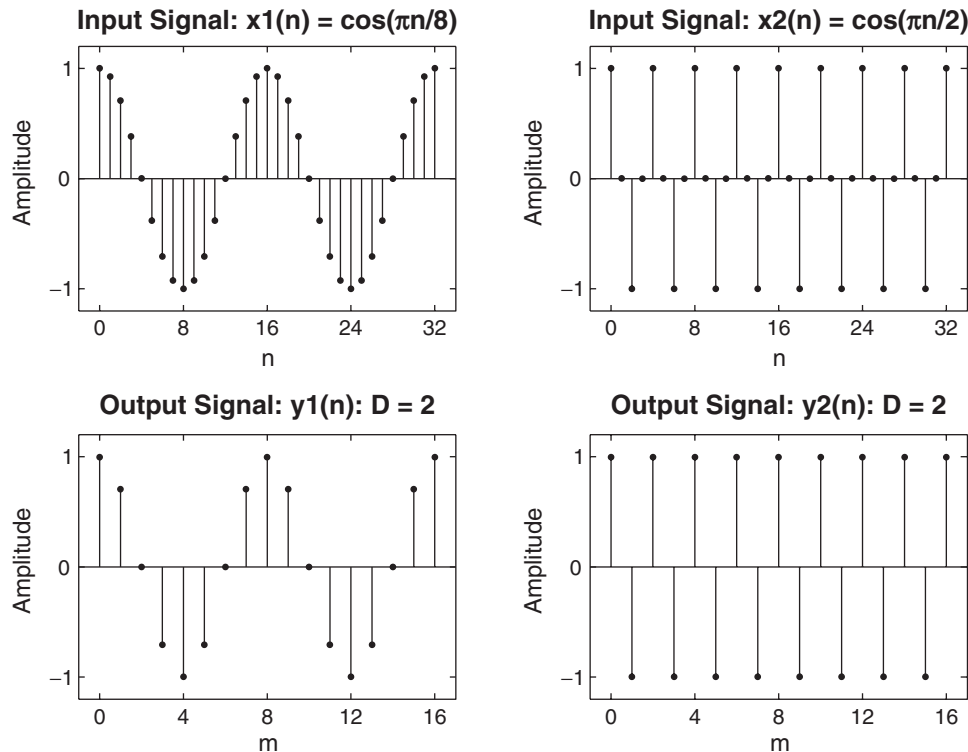


**FIGURE 9.26** Signal plots in Example 9.12

### 9.5.4 DESIGN SPECIFICATIONS

When we replace the ideal lowpass filter  $H_D(\omega)$  by a finite-order FIR filter  $H(\omega)$ , we must allow for a transition band. Again we define

- $\omega_{x,p}$  as the signal bandwidth to be preserved, and
- $\omega_{x,s}$  as the frequency above which aliasing error is tolerated.

Then we have  $0 < \omega_{x,p} \leq \omega_{x,s} \leq \pi/D$ . If we choose  $\omega_{x,s} = \pi/D$ , then the decimator will give no aliasing error. If we choose  $\omega_{x,s} = \omega_{x,p}$ , then the band above the signal band will contain aliasing errors. With these definitions and observations, we can now specify the desired filter specifications. The filter must pass frequencies up to  $\omega_{x,p}$ , and its stopband must begin at  $(\frac{2\pi}{D} - \omega_{x,s})$  and continue up to  $\pi$ . Then none of the  $k \neq 0$  terms in (9.53)—that is, the “aliases”—will cause appreciable distortion in the band up to  $\omega_{x,s}$ . Let

$$\omega_p = \omega_{x,p} \quad \text{and} \quad \omega_s = \left( \frac{2\pi}{D} - \omega_{x,s} \right) \quad (9.56)$$

be the passband and stopband edge frequencies, respectively, of the low-pass linear-phase FIR filter given in (9.51). Then we have the following filter design specifications:

$$H_r(\omega) \leq 1 \pm \delta_1 \quad \text{for } |\omega| \in [0, \omega_p]$$

$$H_r(\omega) \leq \pm \delta_2 \quad \text{for } |\omega| \in [\omega_s, \pi]$$

(9.57)

where  $\omega_p$  and  $\omega_s$  are as given in (9.56) and  $\delta_1$  and  $\delta_2$  are the passband and stopband ripple parameters of the lowpass FIR filter, respectively. Note that it does not matter what the spectrum  $X(\omega)$  is. We simply require that the product  $X(\omega)H(\omega)$  be very small beginning at  $\omega_l = 2\pi/D - \omega_{x,s}$  so that  $k \neq 0$  terms in (9.53) do not provide significant contribution in the band  $[-\omega_{x,s}, \omega_{x,s}]$ , which is required to be free of aliasing.

**Significance of  $\delta_1$  and  $\delta_2$**  The filter ripple parameters  $\delta_1$  and  $\delta_2$  have the following significance, which must be taken into consideration while specifying their values:

- The passband ripple  $\delta_1$  measures the ripple in the passband and hence controls the distortion in the signal bandwidth  $\omega_p$ .
- The stopband ripple  $\delta_2$  controls the amount of aliased energy (also called leakage) that gets into the band up to  $\omega_{x,s}$ .

There are  $(D - 1)$  contributions due to  $k \neq 0$  terms in (9.53). These are expected to add incoherently (i.e., have peaks at different locations), so the overall peak error should be about  $\delta_2$ . The actual error depends on how  $X(\omega)$  varies over the rest of the band  $|\omega| > \omega_{x,p}$ . Clearly, the filter stopband ripple  $\delta_2$  controls the aliasing error in the signal passband. Therefore, *both  $\delta_1$  and  $\delta_2$  affect the decimated signal in its passband.*

*Comment:* Comparing the FIR decimator filter specifications (9.57) to those for the FIR interpolator in (9.52), we see a high degree of similarity. In fact, a filter designed to decimate by factor  $D$  can also be used to interpolate by the factor  $I = D$ , as we see from the following example. This means that the function `intfilt` can also be used to design FIR filters for decimation.

- **EXAMPLE 9.13** To design a decimate by  $D$  stage, we need values for  $\omega_{x,p}$  and  $\omega_{x,s}$  (remember that these are signal parameters). Assume  $\omega_{x,p} = \pi/(2D)$ , which satisfies the constraint  $\omega_{x,p} \leq \pi/D$  and is exactly half the decimated bandwidth. Let  $\omega_{x,s} = \omega_{x,p}$ . Then the FIR lowpass filter must pass frequencies up to  $\omega_p = \pi/(2D)$  and stop frequencies above  $\omega_s = 2\pi/D - \pi/(2D) = 3\pi/(2D)$ .

Now consider the corresponding interpolation problem. We want to interpolate by  $I$ . We again choose  $\omega_{x,s} = \omega_{x,p}$ , but now the range is  $\omega_{x,p} < \pi$ . If we take exactly half this band, we get  $\omega_{x,p} = \pi/2$ . Then according to the specifications (9.52) for the interpolation, we want the filter to pass frequencies up to  $\pi/2I$  and to stop above  $3\pi/2I$ . Thus for  $I = D$ , we have the same filter specifications, so the same filter could serve both the decimation and interpolation problems. □

- **EXAMPLE 9.14** Design a decimation FIR filter for the signal  $x_1(n)$  in Example 9.12 that has a better stopband attenuation of  $A_s = 50$  dB and a lower filter order.

#### Solution

The signal bandwidth is  $\omega_{x,p} = \pi/8$ , and we will choose  $\omega_{x,s} = \pi/D = \pi/2$ . Then  $\omega_p = \pi/8$  and  $\omega_s = (2\pi/D) - \omega_{x,s} = \pi/2$ . With these parameters the optimum FIR filter length is 13, which is much lower than the previous one of 37 with a higher attenuation.

MATLAB script:

```
% Given Parameters:
D = 2; Rp = 0.1; As = 50; wxp = pi/8; wxs = pi/D; wp = wxp; ws = (2*pi/D)-wxs;
% Filter Design
[delta1,delta2] = db2delta(Rp,As);
[N,F,A,weights] = firpmord([wp,ws]/pi,[1,0],[delta1,delta2],2); N = ceil(N/2)*2;
h = firpm(N,F,A,weights); delay = N/2; % Delay imparted by the filter
```

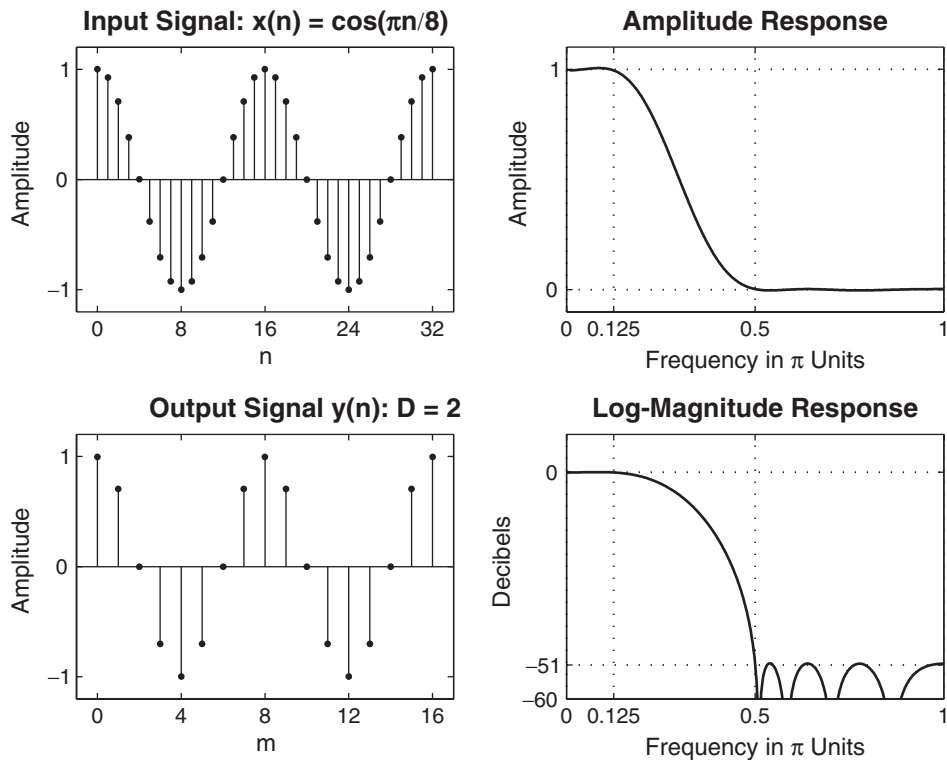


**FIGURE 9.27** Signal plots and filter design plots in Example 9.14

```
% Input signal x(n) = cos(2*pi*n/16)
n = [0:256]; x = cos(pi*n/8);
n1 = n(1:33); x1 = x(33:65); % for plotting purposes
% Input signal plotting commands follow
% Decimation of x(n): D = 2
y = upfirdn(x,h,1,D);
m = delay+1:1:128/D+delay+1; y1 = y(m); m = 0:16; y1 = y1(14:30);
% Output signal plotting commands follow
% Filter Design Plots
[Hr,w,a,L] = Hr_Type1(h); Hr_min = min(Hr); w_min = find(Hr == Hr_min);
H = abs(freqz(h,1,w)); Hdb = 20*log10(H/max(H)); min_attn = Hdb(w_min);
% Filter design plotting commands follow
```

The signal stem plots and the filter responses are shown in Figure 9.27. The designed filter achieves an attenuation of 51 dB, and the decimated signal is correct.  $\square$

### 9.5.5 FIR RATIONAL-FACTOR RATE CONVERSION

Replacing the ideal filter of the system given on page 478 with an FIR filter  $H(\omega)$ , we obtain the system shown in Figure 9.28. In this case, the relevant ideal lowpass filter is given by (9.36), which is repeated here for convenience:

$$H(\omega) = \begin{cases} I, & 0 \leq |\omega| \leq \min(\pi/D, \pi/I) \\ 0, & \text{otherwise} \end{cases} \quad (9.58)$$

For the signal  $x(n)$ , we define

- $\omega_{x,p}$  as the signal bandwidth that should be preserved,
- $\omega_{x,s_1}$  as the overall signal bandwidth, and
- $\omega_{x,s_2}$  as the signal bandwidth that is required to be free of aliasing error after resampling.

Then we have

$$0 < \omega_{x,p} \leq \omega_{x,s_2} \leq \frac{I\pi}{D} \quad \text{and} \quad \omega_{x,s_1} \leq \pi \quad (9.59)$$

Now, for the interpolation part, the lowpass filter must pass frequencies up to  $\omega_{x,p}/I$  and attenuate frequencies starting at  $(2\pi/I - \omega_{x,s_1}/I)$ . The decimation part of the filter must again pass frequencies up to  $\omega_{x,p}/I$  but attenuate frequencies above  $(2\pi/D - \omega_{x,s_2}/I)$ . Therefore, the stopband must start at the lower of these two values. Defining filter cutoff frequencies as

$$\omega_p = \left( \frac{\omega_{x,p}}{I} \right) \quad \text{and} \quad \omega_s = \min \left[ \frac{2\pi}{I} - \frac{\omega_{x,s_1}}{I}, \frac{2\pi}{D} - \frac{\omega_{x,s_2}}{I} \right] \quad (9.60)$$

and the corresponding ripple parameters as  $\delta_1$  and  $\delta_2$ , we have the following filter specifications:

$$\frac{1}{I} H_r(\omega) \leq 1 \pm \delta_1 \quad \text{for } |\omega| \in [0, \omega_p]$$
  

$$\frac{1}{I} H_r(\omega) \leq \pm \delta_2 \quad \text{for } |\omega| \in [\omega_s, \pi]$$

(9.61)

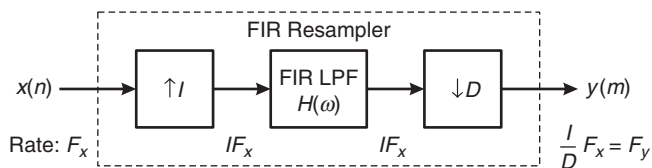


**FIGURE 9.28** An FIR rational-factor resampler

where  $H_r(\omega)$  is the amplitude response. Note that if we set  $\omega_{x,s_1} = \pi$  and  $\omega_{x,s_2} = I\pi/D$ , which are their maximum values, then we get the ideal cutoff frequency  $\max[\pi/I, \pi/D]$ , as given before in (9.36).

**MATLAB Implementation** Clearly, the `upfirdn` function implements all the necessary operations needed in the rational sampling rate conversion system shown in Figure 9.28. When invoked as `y = upfirdn(x,h,I,D)`, it performs a cascade of three operations: upsampling the input data array `x` by a factor of the integer `I`, FIR filtering the upsampled signal data with the impulse response sequence given in the array `h`, and, finally, down-sampling the result by a factor of the integer `D`. Using a well-designed filter, we have complete control over the sampling rate conversion operation.

- **EXAMPLE 9.15** Design a sampling rate converter that increases the sampling rate by a factor of 2.5. Use the `firpm` algorithm to determine the coefficients of the FIR filter that has 0.1 dB ripple in the passband and is down by at least 30 dB in the stopband.

#### Solution

The FIR filter that meets the specifications of this problem is exactly the same as the filter designed in Example 9.8. Its bandwidth is  $\pi/5$ . □

- **EXAMPLE 9.16** A signal  $x(n)$  has a total bandwidth of  $0.9\pi$ . It is resampled by a factor of  $4/3$  to obtain  $y(m)$ . We want to preserve the frequency band up to  $0.8\pi$  and require that the band up to  $0.7\pi$  be free of aliasing. Using the Parks–McClellan algorithm, determine the coefficients of the FIR filter that has 0.1 dB ripple in the passband and 40 dB attenuation in the stopband.

#### Solution

The overall signal bandwidth is  $\omega_{x,s_1} = 0.9\pi$ , the bandwidth to be preserved is  $\omega_{x,p} = 0.8\pi$ , and the bandwidth above which aliasing is tolerated is  $\omega_{x,s_2} = 0.7\pi$ . From (9.60) and using  $I = 4$  and  $D = 3$ , the FIR filter design parameters are  $\omega_p = 0.2\pi$  and  $\omega_s = 0.275\pi$ . With these parameters, along with the passband ripple of 0.1 dB and stopband attenuation of 40 dB, the optimum FIR filter length is 58. The details and computation of design plots follow.

```
% Given Parameters:
I = 4; D = 3; Rp = 0.1; As = 40;
wpx = 0.8*pi; wxs1 = 0.9*pi; wxs2 = 0.7*pi;
% Computed Filter Parameters
wp = wpx/I; ws = min((2*pi/I-wxs1/I),(2*pi/D-wxs2/I));
% Filter Design
[delta1,delta2] = db2delta(Rp,As);
[N,F,A,weights] = firpmord([wp,ws]/pi,[1,0],[delta1,delta2],2);
N = ceil(N/2)*2+1; h = firpm(N,F,I*A,weights);
[Hr,w,a,L] = Ampl_res(h); Hr_min = min(Hr); w_min = find(Hr == Hr_min);
H = abs(freqz(h,1,w)); Hdb = 20*log10(H/max(H)); min_attn = Hdb(w_min);
% Plotting commands follow
```

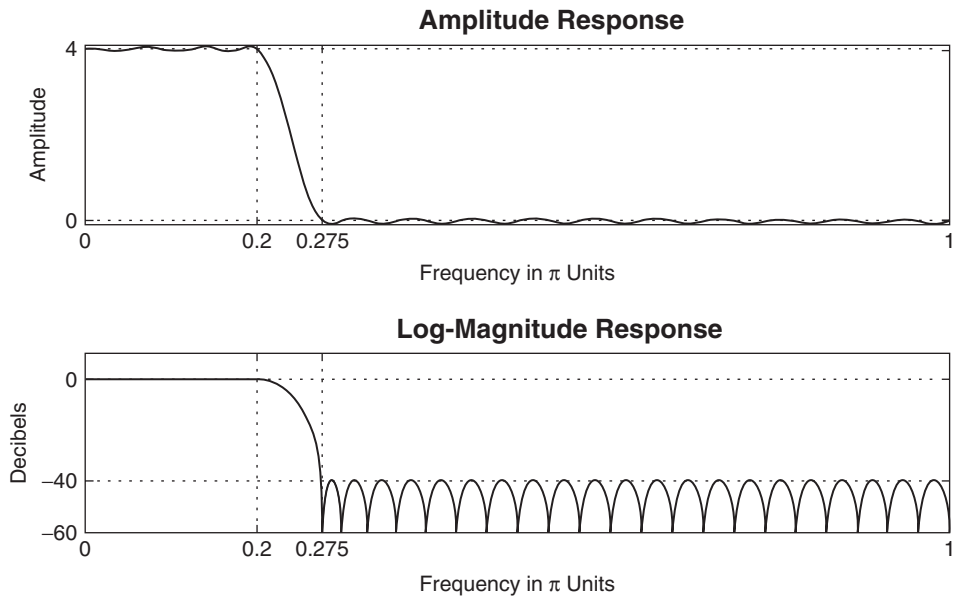


**FIGURE 9.29** The filter design plots in Example 9.16

The filter responses are shown in Figure 9.29, which shows that the designed filter achieves the attenuation of 40 dB.  $\square$

### 9.5.6 FIR FILTERS WITH MULTIPLE STOPBANDS

We now discuss the use of multiple stopbands in the design of FIR integer interpolators when the low sampling rate is more than two times that required. Let us refer back to the Figure 9.22b on page 488, which illustrates a typical spectrum  $V(\omega)$  in integer interpolators. We could use a lowpass filter with multiple stopbands of bandwidth  $\omega_s/I$  centered at  $2\pi k/I$  for  $k \neq 0$ . For  $I = 4$ , such a spectrum is shown in Figure 9.30(a), and the corresponding filter specifications are shown in Figure 9.30b.

Clearly, these filter specifications differ from those given in (9.52) on page 488 in that the stopband is no longer one contiguous interval. Now, if  $\omega_s < \pi/2$ , then there is a practical advantage to using this multiband design because it results in a lower-order filter [9]. For  $\pi \geq \omega_s > \pi/2$ , the single-band lowpass filter specification (9.52) is easier and works as well.

Similar advantages can be obtained for FIR integer decimators. We again find that we can substitute a multiple-stopband lowpass filter for the single-stopband design given in (9.57). With reference to the

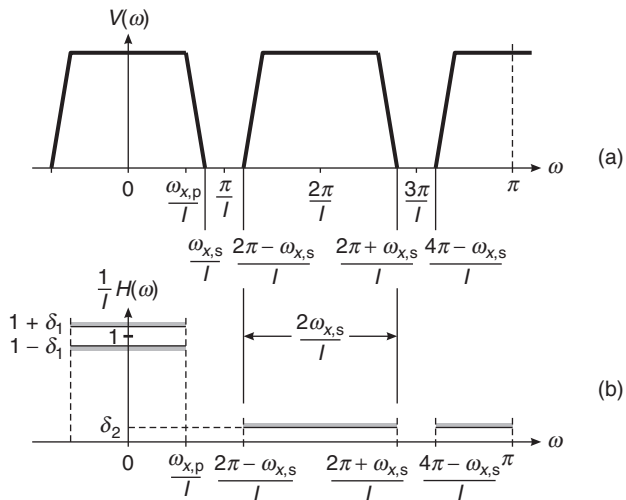


**FIGURE 9.30** Multiple-stopband design: (a) signal spectrum, (b) filter specifications

signal specifications on page 494, we note that only part of the bands  $[\pi/D, 3\pi/D], [3\pi/D, 5\pi/D], \dots$  and so on will get aliased into  $[-\omega_s, +\omega_s]$ . Therefore, the multiple stopbands are given by  $[(2\pi/D) - \omega_s, (2\pi/D) + \omega_s], [(4\pi/D) - \omega_s, (4\pi/D) + \omega_s], \dots$ , centered at  $2\pi k/D$ ,  $k \neq 0$ . Once again, there are practical advantages when  $\omega_s < \pi/2M$ .

## 9.6 FIR FILTER STRUCTURES FOR SAMPLING RATE CONVERSION

As indicated in the discussion in Section 9.4, sampling rate conversion by a factor  $I/D$  can be achieved by first increasing the sampling rate by  $I$ , accomplished by inserting  $I - 1$  zeros between successive values of the input signal  $x(n)$ , followed by linear filtering of the resulting sequence to eliminate the unwanted images of  $X(\omega)$ , and finally by downsampling the filtered signal by the factor  $D$ . In this section, we consider the design and implementation of the linear filter. We begin with the simplest structure, which is the direct form FIR filter structure, and develop its computationally efficient implementation. We then consider another computationally efficient structure called the *polyphase* structure, which is used in the implementation of the MATLAB functions `resample` and `upfirdn`. Finally, we close this section by discussing the time-variant filter structures for the general case of sampling rate conversion.

### 9.6.1 DIRECT FORM FIR FILTER STRUCTURES

In principle, the simplest realization of the filter is the direct form FIR structure with system function

$$H(z) = \sum_{k=0}^{M-1} h(k)z^{-k} \quad (9.62)$$

where  $h(k)$  is the unit sample response of the FIR filter. After designing the filter as discussed in the previous section, we will have the filter parameters  $h(k)$ , which allow us to implement the FIR filter directly, as shown in Figure 9.31.

Although the direct form FIR filter realization illustrated in Figure 9.31 is simple, it is also very inefficient. The inefficiency results from the fact that the upsampling process introduces  $I - 1$  zeros between successive points of the input signal. If  $I$  is large, most of the signal components in the FIR filter are zero. Consequently, most of the multiplications and additions result in zeros. Furthermore, the downsampling process at the output of the filter implies that only one out of every  $D$  output samples is required at the output of the filter. Consequently, only one out of every  $D$  possible values at the output of the filter should be computed.

To develop a more efficient filter structure, let us begin with a decimator that reduces the sampling rate by an integer factor  $D$ . From our previous discussion, the decimator is obtained by passing the input sequence

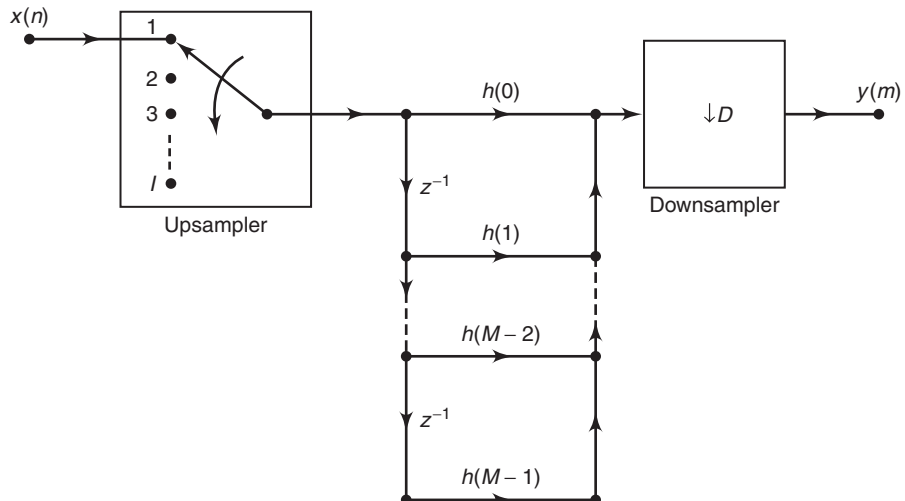


**FIGURE 9.31** Direct form realization of FIR filter in sampling rate conversion by a factor  $I/D$

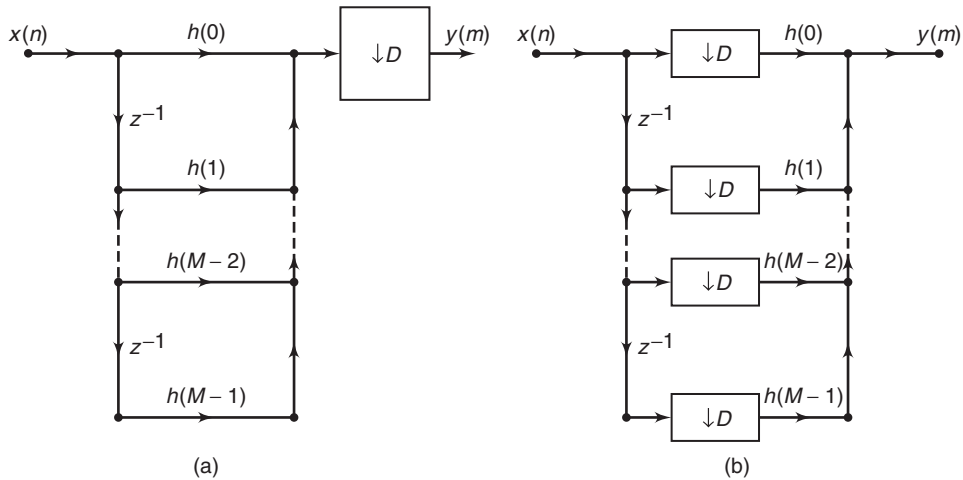


**FIGURE 9.32** Decimation by a factor  $D$ : (a) standard realization, (b) efficient realization

$x(n)$  through an FIR filter and then downsampling the filter output by a factor  $D$ , as illustrated in Figure 9.32a. In this configuration, the filter is operating at the high sampling rate  $F_x$ , while only one out of every  $D$  output samples is actually needed. The logical solution to this inefficiency problem is to embed the downsampling operation within the filter, as illustrated in the filter realization given in Figure 9.32b. In this filter structure, all the multiplications and additions are performed at the lower sampling rate  $F_x/D$ . Thus we have achieved the desired efficiency. Additional reduction in computation can be achieved by exploiting the symmetry characteristics of  $\{h(k)\}$ . Figure 9.33 illustrates an efficient realization of the decimator in which the FIR filter has linear phase and hence  $\{h(k)\}$  is symmetric.

Next, let us consider the efficient implementation of an interpolator, which is realized by first inserting  $I - 1$  zeros between samples of  $x(n)$  and then filtering the resulting sequence. The direct form realization is illustrated in Figure 9.34. The major problem with this structure is that the filter computations are performed at the high sampling rate of  $IF_x$ . The desired simplification is achieved by first using the transposed form of the FIR filter, as illustrated in Figure 9.35a, and then embedding the upsampler within the filter, as shown in Figure 9.35b. Thus all the filter multiplications are performed at the low rate  $F_x$ , while the upsampling process introduces  $I - 1$  zeros in each of the filter branches of the structure shown in Figure 9.35b. The reader can easily verify that the two filter structures in Figure 9.35 are equivalent.

It is interesting to note that the structure of the interpolator, shown in Figure 9.35b, can be obtained by transposing the structure of the

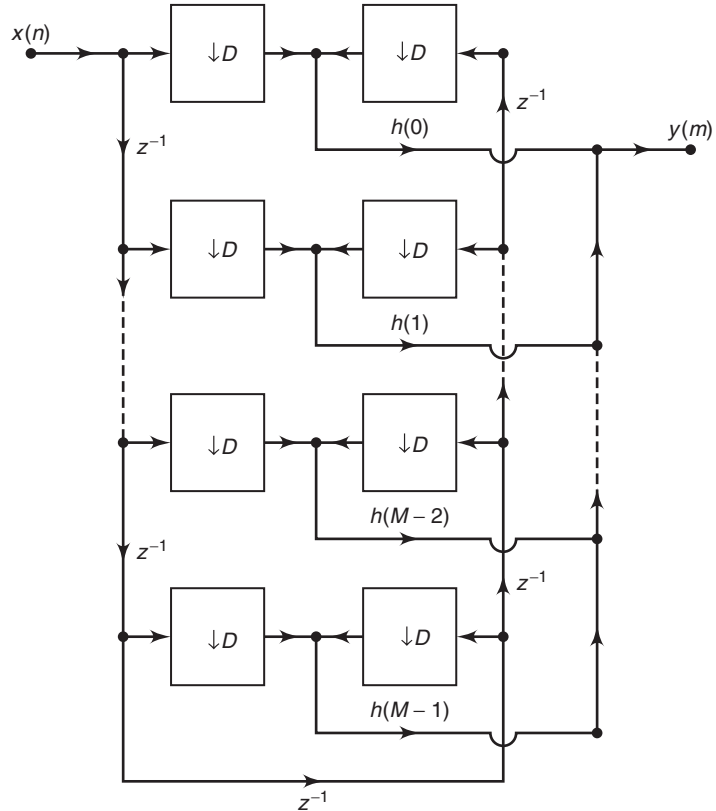


**FIGURE 9.33** Efficient realization of a decimator that exploits the symmetry in the FIR filter

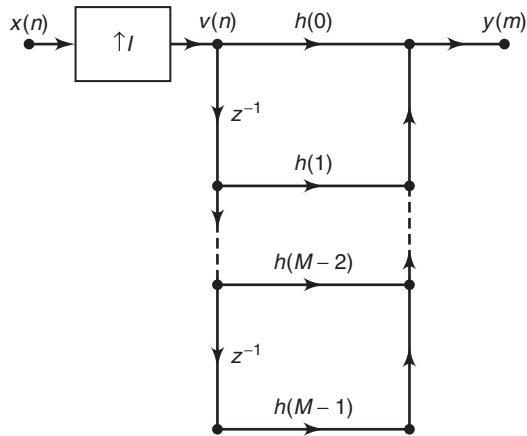


**FIGURE 9.34** Direct form realization of FIR filter in interpolation by a factor I

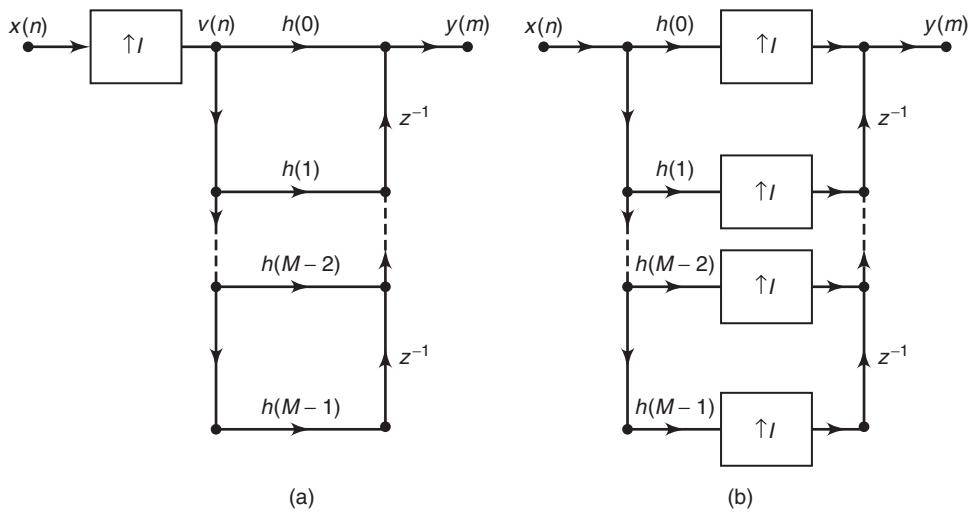


**FIGURE 9.35** Efficient realization of an interpolator

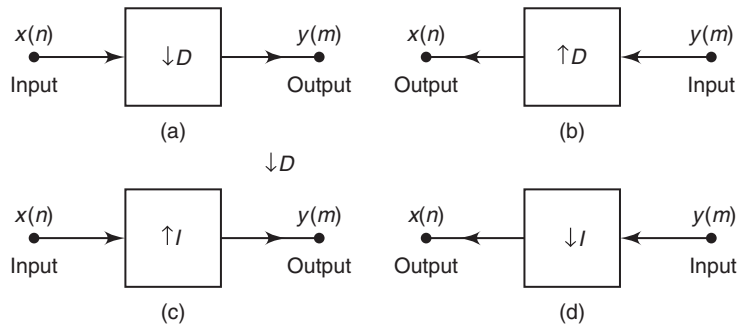


**FIGURE 9.36** Duality relationships obtained through transpositions

decimator shown in Figure 9.32. We observe that the transpose of a decimator is an interpolator, and vice versa. These relationships are illustrated in Figure 9.36, where part b is obtained by transposing part a and part d is obtained by transposing part c. Consequently, a decimator is the dual of an interpolator, and vice versa. From these relationships, it follows that there is an interpolator whose structure is the dual of the decimator shown in Figure 9.33, which exploits the symmetry in  $h(n)$ .

### 9.6.2 POLYPHASE FILTER STRUCTURE

The computational efficiency of the filter structure shown in Figure 9.35 can also be achieved by reducing the large FIR filter of length  $M$  into a set of smaller filters of length  $K = M/I$ , where  $M$  is selected to be a

multiple of  $I$ . To demonstrate this point, let us consider the interpolator given in Figure 9.34. Since the upsampling process inserts  $I - 1$  zeros between successive values of  $x(n)$ , only  $K$  out of the  $M$  input values stored in the FIR filter at any one time are nonzero. At one time instant, these nonzero values coincide and are multiplied by the filter coefficients  $h(0), h(I), h(2I), \dots, h(M - I)$ . In the following time instant, the nonzero values of the input sequence coincide and are multiplied by the filter coefficients  $h(1), h(I + 1), h(2I + 1)$ , and so on. This observation leads us to define a set of smaller filters, called polyphase filters, with unit sample responses

$$p_k(n) = h(k + nI); \quad k = 0, 1, \dots, I - 1, \quad n = 0, 1, \dots, K - 1 \quad (9.63)$$

where  $K = M/I$  is an integer.

From this discussion, it follows that the set of  $I$  polyphase filters can be arranged as a parallel realization, and the output of each filter can be selected by a commutator, as illustrated in Figure 9.37. The rotation of the commutator is in the counterclockwise direction, beginning with the point at  $m = 0$ . Thus the polyphase filters perform the computations at the low sampling rate  $F_x$ , and the rate conversion results from the fact that  $I$  output samples are generated, one from each of the filters, for each input sample.

The decomposition of  $\{h(k)\}$  into the set of  $I$  subfilters with impulse response  $p_k(n)$ ,  $k = 0, 1, \dots, I - 1$ , is consistent with our previous observation that the input signal was being filtered by a periodically time-variant linear filter with impulse response

$$g(n, m) = h(nI + (mD)_I) \quad (9.64)$$

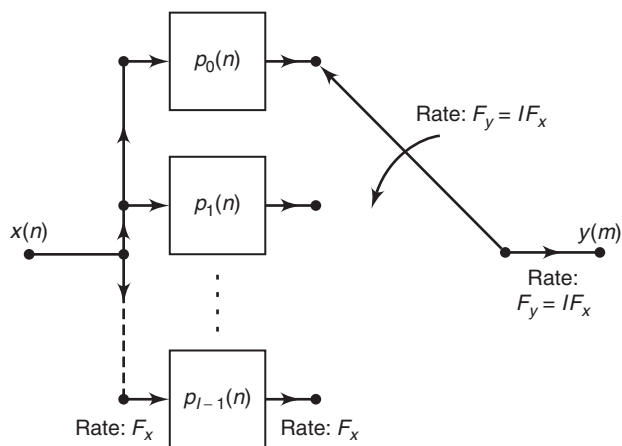


**FIGURE 9.37** Interpolation by use of polyphase filters

where  $D = 1$  in the case of the interpolator. We noted previously that  $g(n, m)$  varies periodically with period  $I$ . Consequently, a different set of coefficients is used to generate the set of  $I$  output samples  $y(m), m = 0, 1, \dots, I - 1$ .

Additional insight can be gained about the characteristics of the set of polyphase subfilters by noting that  $p_k(n)$  is obtained from  $h(n)$  by decimation with a factor  $I$ . Consequently, if the original filter frequency response  $H(\omega)$  is flat over the range  $0 \leq |\omega| \leq \omega/I$ , each of the polyphase subfilters possesses a relatively flat response over the range  $0 \leq |\omega| \leq \pi$  (i.e., the polyphase subfilters are basically allpass filters and differ primarily in their phase characteristics). This explains the reason for using the term *polyphase* in describing these filters.

The polyphase filter can also be viewed as a set of  $I$  subfilters connected to a common delay line. Ideally, the  $k$ th subfilter will generate a forward time shift of  $(k/I)T_x$ , for  $k = 0, 1, 2, \dots, I - 1$ , relative to the zeroth subfilter. Therefore, if the zeroth filter generates zero delay, the frequency response of the  $k$ th subfilter is

$$p_k(\omega) = e^{j\omega k/I}$$

A time shift of an integer number of input sampling intervals (e.g.,  $kT_x$ ) can be generated by shifting the input data in the delay line by  $I$  samples and using the same subfilters. By combining these two methods, we can generate an output that is shifted forward by an amount  $(k + i/I)T_x$  relative to the previous output.

By transposing the interpolator structure in Figure 9.37, we obtain a commutator structure for a decimator based on the parallel bank of polyphase filters, as illustrated in Figure 9.38. The unit sample responses of the polyphase filters are now defined as

$$p_k(n) = h(k + nD); \quad k = 0, 1, \dots, D - 1, \quad n = 0, 1, \dots, K - 1 \quad (9.65)$$

where  $K = M/D$  is an integer when  $M$  is selected to be a multiple of  $D$ . The commutator rotates in a counterclockwise direction, starting with the filter  $p_0(n)$  at  $m = 0$ .

Although the two commutator structures for the interpolator and the decimator just described rotate in a counterclockwise direction, it is also possible to derive an equivalent pair of commutator structures having a clockwise rotation. In this alternative formulation, the sets of polyphase filters are defined to have impulse responses

$$p_k(n) = h(nI - k), \quad k = 0, 1, \dots, I - 1 \quad (9.66)$$

and

$$p_k(n) = h(nD - k), \quad k = 0, 1, \dots, D - 1 \quad (9.67)$$

for the interpolator and decimator, respectively.

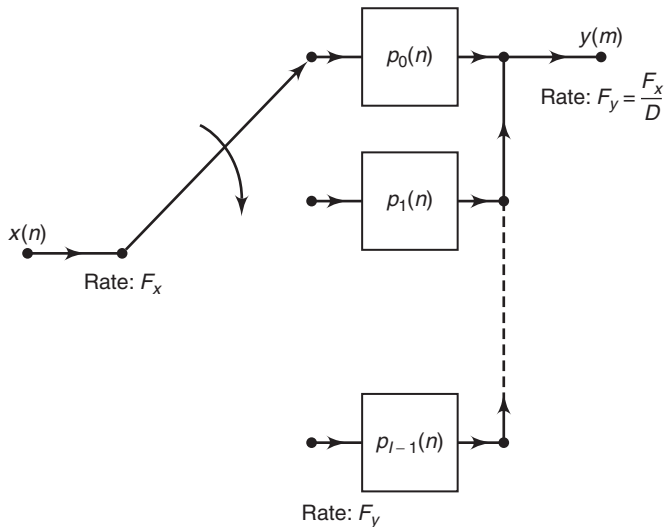


**FIGURE 9.38** Decimation by use of polyphase filters

- **EXAMPLE 9.17** For the decimation filter designed in Example 9.11, determine the polyphase filter coefficients  $\{p_k(n)\}$  in terms of the FIR filter coefficients  $\{h(n)\}$ .

**Solution**

The polyphase filters obtained from  $h(n)$  have impulse responses

$$p_k(n) = h(2n + k) \quad k = 0, 1; \quad n = 0, 1, \dots, 14$$

Note that  $p_0(n) = h(2n)$  and  $p_1(n) = h(2n + 1)$ . Hence one filter consists of the even-numbered samples of  $h(n)$ , and the other filter consists of the odd-numbered samples of  $h(n)$ . □

- **EXAMPLE 9.18** For the interpolation filter designed in Example 9.8, determine the polyphase filter coefficients  $\{p_k(n)\}$  in terms of the filter coefficients  $\{h(n)\}$ .

**Solution**

The polyphase filters obtained from  $h(n)$  have impulse responses

$$p_k(n) = h(5n + k) \quad k = 0, 1, 2, 3, 4$$

Consequently, each filter has length 6. □

### 9.6.3 TIME-VARIANT FILTER STRUCTURES

Having described the filter implementation for a decimator and an interpolator, let us now consider the general problem of sampling rate conversion by the factor  $I/D$ . In the general case of sampling rate conversion

by a factor  $I/D$ , the filtering can be accomplished by means of the linear time-variant filter described by the response function

$$g(n, m) = h[nI - ((mD))_I] \quad (9.68)$$

where  $h(n)$  is the impulse response of the lowpass FIR filter, which, ideally, has the frequency response specified by (9.36). For convenience, we select the length of the FIR filter  $\{h(n)\}$  to be a multiple of  $I$  (i.e.,  $M = KI$ ). As a consequence, the set of coefficients  $\{g(n, m)\}$  for each  $m = 0, 1, 2, \dots, I-1$ , contains  $K$  elements. Since  $g(n, m)$  is also periodic with period  $I$ , as demonstrated in (9.44), it follows that the output  $y(m)$  can be expressed as

$$y(m) = \sum_{n=0}^{K-1} g\left(n, m - \left\lfloor \frac{m}{I} \right\rfloor I\right) x\left(\left\lfloor \frac{mD}{I} \right\rfloor - n\right) \quad (9.69)$$

Conceptually, we can think of performing the computations specified by (9.69) by processing blocks of data of length  $K$  by a set of  $K$  filter coefficients  $g(n, m - [m/I] I), n = 0, 1, \dots, K-1$ . There are  $I$  such sets of coefficients, one set for each block of  $I$  output points of  $y(m)$ . For each block of  $I$  output points, there is a corresponding block of  $D$  input points of  $x(n)$  that enter in the computation.

The block processing algorithm for computing (9.69) can be visualized as illustrated in Figure 9.39. A block of  $D$  input samples is buffered and shifted into a second buffer of length  $K$ , one sample at a time. The shifting from the input buffer to the second buffer occurs at a rate of one

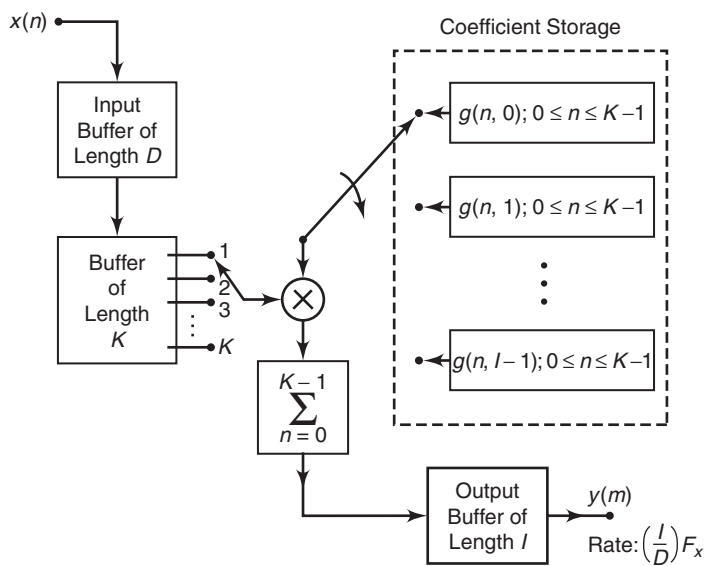


**FIGURE 9.39** Efficient implementation of sampling rate conversion by block processing

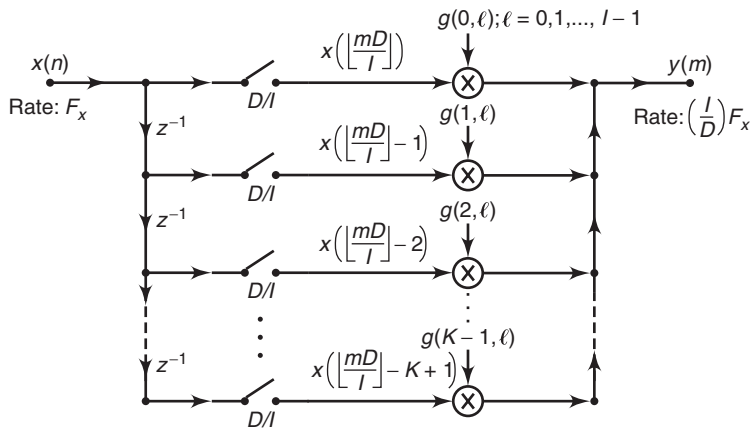


**FIGURE 9.40** Efficient realization of sampling rate conversion by a factor  $I/D$

sample each time the quantity  $\lfloor mD/I \rfloor$  increases by 1. For each output sample  $y(l)$ , the samples from the second buffer are multiplied by the corresponding set of filter coefficients  $g(n, l)$  for  $n = 0, 1, \dots, K - 1$ , and the  $K$  products are accumulated to give  $y(l)$ , for  $l = 0, 1, \dots, I - 1$ . Thus this computation produces  $I$  outputs. It is then repeated for a new set of  $D$  input samples, and so on.

An alternative method for computing the output of the sampling rate converter, specified by (9.69), is by means of an FIR filter structure with periodically varying filter coefficients. Such a structure is illustrated in Figure 9.40. The input samples  $x(n)$  are passed into a shift register that operates at the sampling rate  $F_x$  and is of length  $K = M/I$ , where  $M$  is the length of the time-invariant FIR filter specified by the frequency response given by (9.36). Each stage of the register is connected to a hold-and-sample device that serves to couple the input sampling rate  $F_x$  to the output sampling rate  $F_y = (I/D)F_x$ . The sample at the input to each hold-and-sample device is held until the next input sample arrives and then is discarded. The output samples on the hold-and-sample device are taken at times  $mD/I$ ,  $m = 0, 1, 2, \dots$ . When both the input and output sampling times coincide (i.e., when  $mD/I$  is an integer), the input to the hold-and-sample is changed first; then the output samples the new input. The  $K$  outputs from the  $K$  hold-and-sample devices are multiplied by the periodically time-varying coefficients  $g(n, m - \lfloor m/I \rfloor I)$ , for  $n = 0, 1, \dots, K - 1$ , and the resulting products are summed to yield  $y(m)$ . The computations at the output of the hold-and-sample devices are repeated at the output sampling rate of  $F_y = (I/D)F_x$ .

Finally, rate conversion by a rational factor  $I/D$  can also be performed by use of a polyphase filter having  $I$  subfilters. If we assume that the  $m$ th sample  $y(m)$  is computed by taking the output of the  $i_m$ th subfilter with input data  $x(n), x(n - 1), \dots, x(n - K + 1)$ , in the delay line, the next

sample  $y(m + 1)$  is taken from the  $(i_{m+1})$ st subfilter after shifting  $l_{m+1}$  new samples in the delay lines where  $i_{m+1} = (i_m + D)_{\text{mod}I}$  and  $l_{m+1}$  is the integer part of  $(i_m + D)/I$ . The integer  $i_{m+1}$  should be saved to be used in determining the subfilter from which the next sample is taken.

- EXAMPLE 9.19** For the sampling rate converter designed in Example 9.15, specify the set of time-varying coefficients  $\{g(n, m)\}$  used in the realization of the converter based on the structure given in Figure 9.19. Also, specify the corresponding implementation based in polyphase filters.

### Solution

The coefficients of the filter are given by (9.43):

$$g(n, m) = h(nI + (mD)_I) = h\left(nI + mD - \left\lfloor \frac{D}{I}m \right\rfloor I\right)$$

By substituting  $I = 5$  and  $D = 2$ , we obtain

$$g(n, m) = h\left(5n + 2m - 5 \left\lfloor \frac{2m}{5} \right\rfloor\right)$$

By evaluating  $g(n, m)$  for  $n = 0, 1, \dots, 5$  and  $m = 0, 1, \dots, 4$ , we obtain the following coefficients for the time-variant filter:

$$\begin{aligned} g(0, m) &= \{h(0) \quad h(2) \quad h(4) \quad h(1) \quad h(3)\} \\ g(1, m) &= \{h(5) \quad h(7) \quad h(9) \quad h(6) \quad h(8)\} \\ g(2, m) &= \{h(10) \quad h(12) \quad h(14) \quad h(11) \quad h(13)\} \\ g(3, m) &= \{h(15) \quad h(17) \quad h(19) \quad h(16) \quad h(18)\} \\ g(4, m) &= \{h(20) \quad h(22) \quad h(24) \quad h(21) \quad h(23)\} \\ g(5, m) &= \{h(25) \quad h(27) \quad h(29) \quad h(26) \quad h(28)\} \end{aligned}$$

A polyphase filter implementation would employ five subfilters, each of length 6. To decimate the output of the polyphase filters by a factor of  $D = 2$  simply means that we take every other output from the polyphase filters. Thus the first output  $y(0)$  is taken from  $p_0(n)$ , the second output  $y(1)$  is taken from  $p_2(n)$ , the third output is taken from  $p_4(n)$ , the fourth output is taken from  $p_1(n)$ , the fifth output is taken from  $p_3(n)$ , and so on.  $\square$

## 9.7 PROBLEMS

---

- P9.1** Consider the upsampler with input  $x(n)$  and output  $v(m)$  given in (9.26). Show that the upsampler is a linear but time-varying system.
- P9.2** Let  $x(n) = 0.9^n u(n)$ . The signal is applied to a downampler that reduces the rate by a factor of 2 to obtain the signal  $y(m)$ .
1. Determine and plot the spectrum  $X(\omega)$ .
  2. Determine and plot the spectrum  $Y(\omega)$ .
  3. Show that the spectrum in part (2) is simply the DTFT of  $x(2n)$ .

**P9.3** Consider a signal with spectrum

$$X(\omega) = \begin{cases} \text{nonzero, } |\omega| \leq \omega_0 \\ 0, \quad \omega_0 < |\omega| \leq \pi \end{cases}$$

1. Show that the signal  $x(n)$  can be recovered from its samples  $x(mD)$  if the sampling frequency  $\omega_s \triangleq 2\pi/D \geq 2\omega_0$ .
2. Sketch the spectra of  $x(n)$  and  $x(mD)$  for  $D = 4$ .
3. Show that  $x(n)$  can be reconstructed from the bandlimited interpolation

$$x(n) = \sum_{k=-\infty}^{\infty} x(kD) \operatorname{sinc}[f_c(n - kD)]; \quad \omega_0 < 2\pi f_c < \omega_s - \omega_0, f_c = \frac{1}{D}$$

**P9.4** Using the function `downsample`, study the operation of factor-of-4 downsampling on the following sequences. Use the `stem` function to plot the original and the downsampled sequences. Experiment using the default offset value of zero and the offset value equal to 2. Comment on any differences.

1.  $x_1(n) = \cos(0.15\pi n)$ ,  $0 \leq n \leq 100$
2.  $x_2(n) = \sin(0.1\pi n) + \sin(0.4\pi n)$ ,  $0 \leq n \leq 100$
3.  $x_3(n) = 1 - \cos(0.25\pi n)$ ,  $0 \leq n \leq 100$
4.  $x_4(n) = 0.1n$ ,  $0 \leq n \leq 100$
5.  $x_5(n) = \{0, 1, 2, 3, 4, 5, 4, 3, 2, 1\}_{\text{PERIODIC}}$ ,  $0 \leq n \leq 100$

**P9.5** Repeat Problem P9.4 using the factor-of-5 downampler.

**P9.6** Using the `fir2` function, generate a 101-length sequence  $x(n)$  whose frequency-domain sampled-values are 0.5 at  $\omega = 0$ , 1 at  $\omega = 0.1\pi$ , 1 at  $\omega = 0.2$ , 0 at  $\omega = 0.22\pi$ , and 0 at  $\omega = \pi$ .

1. Compute and plot the DTFT magnitude of  $x(n)$ .
2. Downsample  $x(n)$  by a factor of 2, and plot the DTFT of the resulting sequence.
3. Downsample  $x(n)$  by a factor of 4, and plot the DTFT of the resulting sequence.
4. Downsample  $x(n)$  by a factor of 5, and plot the DTFT of the resulting sequence.
5. Comment on your results.

**P9.7** Using the function `decimate`, study the operation of factor-of-4 decimation on the following sequences. Use the `stem` function to plot the original and the decimated sequences. Experiment, using both the default IIR and FIR decimation filters. Comment on any differences.

1.  $x_1(n) = \sin(0.15\pi n)$ ,  $0 \leq n \leq 100$
2.  $x_2(n) = \cos(0.1\pi n) + \cos(0.4\pi n)$ ,  $0 \leq n \leq 100$
3.  $x_3(n) = 1 - \cos(0.25\pi n)$ ,  $0 \leq n \leq 100$
4.  $x_4(n) = 0.1n$ ,  $0 \leq n \leq 100$
5.  $x_5(n) = \{0, 1, 2, 3, 4, 5, 4, 3, 2, 1\}_{\text{PERIODIC}}$ ,  $0 \leq n \leq 100$

**P9.8** Repeat Problem P9.7 using the 4th-order IIR filter and the 15th-order FIR decimation filters. Comment on any performance differences.

**P9.9** Repeat Problem P9.7 using the factor-of-5 decimation. Comment on any differences.

**P9.10** Repeat Problem P9.9 using the 4th-order IIR filter and the 15th-order FIR decimation filters. Comment on any differences.

- P9.11** Using the `fir2` function, generate a 101-length sequence  $x(n)$  whose frequency-domain sampled-values are 0.5 at  $\omega = 0$ , 1 at  $\omega = 0.1\pi$ , 1 at  $\omega = 0.2$ , 0 at  $\omega = 0.22\pi$ , and 0 at  $\omega = \pi$ .
1. Compute and plot the DTFT of  $x(n)$ .
  2. Decimate  $x(n)$  by a factor of 2, and plot the DTFT of the resulting sequence.
  3. Decimate  $x(n)$  by a factor of 4, and plot the DTFT of the resulting sequence.
  4. Decimate  $x(n)$  by a factor of 5, and plot the DTFT of the resulting sequence.
  5. Comment on your results.
- P9.12** Using the function `upsample`, study the operation of factor-of-4 upsampling on the following sequences. Use the `stem` function to plot the original and the upsampled sequences. Experiment using the default offset value of zero and the offset value equal to 2.
1.  $x_1(n) = \sin(0.6\pi n)$ ,  $0 \leq n \leq 100$
  2.  $x_2(n) = \sin(0.8\pi n) + \cos(0.5\pi n)$ ,  $0 \leq n \leq 100$
  3.  $x_3(n) = 1 + \cos(\pi n)$ ,  $0 \leq n \leq 100$
  4.  $x_4(n) = 0.2n$ ,  $0 \leq n \leq 100$
  5.  $x_5(n) = \{1, 1, 1, 1, 0, 0, 0, 0, 0, 0\}$  PERIODIC,  $0 \leq n \leq 100$
- P9.13** Using the `fir2` function, generate a 91-length sequence  $x(n)$  whose frequency-domain sampled-values are 0 at  $\omega = 0$ , 0.5 at  $\omega = 0.1\pi$ , 1 at  $\omega = 0.2$ , 1 at  $\omega = 0.7\pi$ , 0.5 at  $\omega = 0.75\pi$ , 0 at  $\omega = 0.8\pi$ , and 0 at  $\omega = \pi$ .
1. Compute and plot the DTFT magnitude of  $x(n)$ .
  2. Upsample  $x(n)$  by a factor of 2, and plot the DTFT magnitude of the resulting sequence.
  3. Upsample  $x(n)$  by a factor of 3, and plot the DTFT magnitude of the resulting sequence.
  4. Upsample  $x(n)$  by a factor of 4, and plot the DTFT magnitude of the resulting sequence.
  5. Comment on your results.
- P9.14** Using the function `interp`, study the operation of factor-of-4 interpolation on the sequences of Problem P9.12. Use the `stem` function to plot the original and the interpolated sequences. Experiment, using the filter length parameter values equal to 3 and 5. Comment on any differences in performance of the interpolation.
- P9.15** Provide the frequency response plots of the lowpass filters used in the interpolators of Problem P9.14.
- P9.16** Repeat Problem P9.14, using the factor-of-3 interpolation.
- P9.17** Provide the frequency response plots of the lowpass filters used in the interpolators of Problem P9.16.
- P9.18** Repeat Problem P9.14, using the factor-of-5 interpolation.
- P9.19** Provide the frequency response plots of the lowpass filters used in the interpolators of Problem P9.18.
- P9.20** Using the `fir2` function generate a 91-length sequence  $x(n)$  whose frequency-domain sampled-values are 0 at  $\omega = 0$ , 0.5 at  $\omega = 0.1\pi$ , 1 at  $\omega = 0.2$ , 1 at  $\omega = 0.7\pi$ , 0.5 at  $\omega = 0.75\pi$ , 0 at  $\omega = 0.8\pi$ , and 0 at  $\omega = \pi$ .

1. Compute and plot the DTFT of  $x(n)$ .
2. Interpolate  $x(n)$  by a factor of 2, and plot the DTFT of the resulting sequence.
3. Interpolate  $x(n)$  by a factor of 3, and plot the DTFT of the resulting sequence.
4. Interpolate  $x(n)$  by a factor of 4, and plot the DTFT of the resulting sequence.
5. Comment on your results.

**P9.21** Consider two sequences  $x_1(n)$  and  $x_2(n)$ , which appear to be related:

$$x_1(n) = \max(10 - |n|, 0) \quad \text{and} \quad x_2(n) = \min(|n|, 10)$$

Use the `resample` function with default parameters.

1. Resample the sequence  $x_1(n)$  at 3/2 times the original rate to obtain  $y_1(m)$ , and provide the `stem` plots of both sequences.
2. Resample the sequence  $x_2(n)$  at 3/2 times the original rate to obtain  $y_2(m)$ , and provide the `stem` plots of both sequences.
3. Explain why the resampled plot of  $y_2(n)$  has inaccuracies near the boundaries that  $y_1(n)$  does not have.
4. Plot the frequency response of the filter used in the resampling operation.

**P9.22** Let  $x(n) = \cos(0.1\pi n) + 0.5 \sin(0.2\pi n) + 0.25 \cos(0.4\pi n)$ . Use the `resample` function with default parameters.

1. Resample the sequence  $x(n)$  at 4/5 times the original rate to obtain  $y_1(m)$ , and provide the `stem` plots of both sequences.
2. Resample the sequence  $x(n)$  at 5/4 times the original rate to obtain  $y_2(m)$ , and provide the `stem` plots of both sequences.
3. Resample the sequence  $x(n)$  at 2/3 times the original rate to obtain  $y_3(m)$ , and provide the `stem` plots of both sequences.
4. Explain which of the three output sequences retain the “shape” of the original sequence  $x(n)$ .

**P9.23** Let  $x(n) = \{0, 0, 0, 1, 1, 1, 0, 0, 0\}_{\text{PERIODIC}}$  be a periodic sequence with period 10. Use the `resample` function for the following parts to resample the sequence  $x(n)$  at 3/5 times the original rate. Consider the length of the input sequence to be 80.

1. Use the filter length parameter `L` equal to zero to obtain  $y_1(m)$ , and provide the `stem` plots of  $x(n)$  and  $y_1(m)$  sequences.
2. Use the default value of the filter length parameter `L` to obtain  $y_2(m)$ , and provide the `stem` plots of  $x(n)$  and  $y_2(m)$  sequences.
3. Use the filter length parameter `L` equal to 15 to obtain  $y_3(m)$ , and provide the `stem` plots of  $x(n)$  and  $y_3(m)$  sequences.

**P9.24** Using the `fir2` function, generate a 101-length sequence  $x(n)$  whose frequency-domain sampled-values are 0 at  $\omega = 0$ , 0.5 at  $\omega = 0.1\pi$ , 1 at  $\omega = 0.2\pi$ , 1 at  $\omega = 0.5\pi$ , 0.5 at  $\omega = 0.55\pi$ , 0 at  $\omega = 0.6\pi$ , and 0 at  $\omega = \pi$ .

1. Compute and plot the DTFT of  $x(n)$ .
2. Resample  $x(n)$  by a factor of 4/3, and plot the DTFT of the resulting sequence.
3. Resample  $x(n)$  by a factor of 3/4, and plot the DTFT of the resulting sequence.
4. Resample  $x(n)$  by a factor of 4/5, and plot the DTFT of the resulting sequence.
5. Comment on your results.

**P9.25** We want to design a linear-phase FIR filter to increase the input sampling rate by a factor of 3 using the `intfilt` function.

1. Assuming full bandwidth of the signal to be interpolated, determine the impulse response of the required FIR filter. Plot its amplitude response and the log-magnitude response in dB. Experiment with the length parameter  $L$  to obtain a reasonable stopband attenuation.
2. Assuming that bandwidth of the signal to be interpolated is  $\pi/2$ , determine the impulse response of the required FIR filter. Plot its amplitude response and the log-magnitude response in decibels. Again, experiment with the length parameter  $L$  to obtain a reasonable stopband attenuation.

**P9.26** We want to design a linear-phase FIR filter to increase the input sampling rate by a factor of 5 using the `intfilt` function.

1. Assuming full bandwidth of the signal to be interpolated, determine the impulse response of the required FIR filter. Plot its amplitude response and the log-magnitude response in decibels. Experiment with the length parameter  $L$  to obtain a reasonable stopband attenuation.
2. Assuming that bandwidth of the signal to be interpolated is  $4\pi/5$ , determine the impulse response of the required FIR filter. Plot its amplitude response and the log-magnitude response in decibels. Again, experiment with the length parameter  $L$  to obtain a reasonable stopband attenuation.

**P9.27** Using the Parks–McClellan algorithm, design an interpolator that increases the input sampling rate by a factor of  $I = 2$ .

1. Determine the coefficients of the FIR filter that has 0.5 dB ripple in the passband and 50 dB attenuation in the stopband. Choose reasonable values for the band-edge frequencies.
2. Provide plots of the impulse and the log-magnitude responses.
3. Determine the corresponding polyphase structure for implementing the filter.
4. Let  $x(n) = \cos(0.4\pi n)$ . Generate 100 samples of  $x(n)$ , and process it using this filter to interpolate by  $I = 2$  to obtain  $y(m)$ . Provide the `stem` plots of the both sequences.

**P9.28** Using the Parks–McClellan algorithm, design an interpolator that increases the input sampling rate by a factor of  $I = 3$ .

1. Determine the coefficients of the FIR filter that has 0.1 dB ripple in the passband and 40 dB attenuation in the stopband. Choose reasonable values for the band-edge frequencies.
2. Provide plots of the impulse and the log-magnitude responses.
3. Determine the corresponding polyphase structure for implementing the filter.
4. Let  $x(n) = \cos(0.3\pi n)$ . Generate 100 samples of  $x(n)$  and process it using this filter to interpolate by  $I = 3$  to obtain  $y(m)$ . Provide the `stem` plots of both sequences.

**P9.29** A signal  $x(n)$  is to be interpolated by a factor of 3. It has a bandwidth of  $0.4\pi$ , but we want to preserve frequency band up to  $0.3\pi$  in the interpolated signal. Using the Parks–McClellan algorithm, we want to design such an interpolator.

1. Determine the coefficients of the FIR filter that has 0.1 dB ripple in the passband and 40 dB attenuation in the stopband.
2. Provide plots of the impulse and the log-magnitude responses.

3. Let  $x(n) = \cos(0.3\pi n) + 0.5 \sin(0.4\pi n)$ . Generate 100 samples of  $x(n)$ , and process it using this filter to interpolate by  $I = 3$  to obtain  $y(m)$ . Provide the `stem` plots of both sequences.
- P9.30** A signal  $x(n)$  is to be interpolated by a factor of 4. It has a bandwidth of  $0.7\pi$ , but we want to preserve frequency band up to  $0.6\pi$  in the interpolated signal. Using the Parks–McClellan algorithm, we want to design such an interpolator.
1. Determine the coefficients of the FIR filter that has 0.5 dB ripple in the passband and 50 dB attenuation in the stopband.
  2. Provide plots of the impulse and the log-magnitude responses.
  3. Let  $x(n) = \sin(0.5\pi n) + \cos(0.7\pi n)$ . Generate 100 samples of  $x(n)$  and process it using this filter to interpolate by  $I = 4$  to obtain  $y(m)$ . Provide the `stem` plots of both sequences.
- P9.31** Using the Parks–McClellan algorithm, design a decimator that downsamples an input signal  $x(n)$  by a factor of  $D = 5$ .
1. Determine the coefficients of the FIR filter that has 0.1 dB ripple in the passband and 30 dB attenuation in the stopband. Choose reasonable values for the band-edge frequencies.
  2. Provide plots of the impulse and the log-magnitude responses.
  3. Determine the corresponding polyphase structure for implementing the filter.
  4. Using the `fir2` function, generate a 131-length sequence  $x(n)$  whose frequency-domain sampled-values are 1 at  $\omega = 0$ , 0.9 at  $\omega = 0.1\pi$ , 1 at  $\omega = 0.2\pi$ , 1 at  $\omega = 0.5\pi$ , 0.5 at  $\omega = 0.55\pi$ , 0 at  $\omega = 0.6\pi$ , and 0 at  $\omega = \pi$ . Process  $x(n)$  using this filter to decimate it by a factor of 5 to obtain  $y(m)$ . Provide the spectral plots of both sequences.
- P9.32** Using the Parks–McClellan algorithm, design a decimator that downsamples an input signal  $x(n)$  by a factor of  $D = 3$ .
1. Determine the coefficients of the FIR filter that has 0.5 dB ripple in the passband and 30 dB attenuation in the stopband. Choose reasonable values for the band-edge frequencies.
  2. Provide plots of the impulse and the log-magnitude responses.
  3. Let  $x_1(n) = \sin(0.2\pi n) + 0.2 \cos(0.5\pi n)$ . Generate 500 samples of  $x_1(n)$ , and process it using this to decimate by  $D = 3$  to obtain  $y_1(m)$ . Provide the `stem` plots of both sequences.
  4. Using the `fir2` function, generate a 131-length sequence  $x_2(n)$  whose frequency-domain sampled-values are 1 at  $\omega = 0$ , 0.8 at  $\omega = 0.15\pi$ , 1 at  $\omega = 0.3\pi$ , 1 at  $\omega = 0.4\pi$ , 0.5 at  $\omega = 0.45\pi$ , 0 at  $\omega = 0.5\pi$ , and 0 at  $\omega = \pi$ . Process  $x_2(n)$ , using this filter to decimate it by a factor of 3 to obtain  $y_2(m)$ . Provide the spectral plots of both sequences.
- P9.33** A signal  $x(n)$  is to be decimated by a factor of  $D = 2$ . It has a bandwidth of  $0.4\pi$ , and we will tolerate aliasing this frequency  $0.45\pi$  in the decimated signal. Using the Parks–McClellan algorithm, we want to design such a decimator.
1. Determine the coefficients of the FIR filter that has 0.1 dB ripple in the passband and 45 dB attenuation in the stopband.
  2. Provide plots of the impulse and the log-magnitude responses.
  3. Let  $x_1(n) = \cos(0.4\pi n) + 2 \sin(0.45\pi n)$ . Generate 200 samples of  $x_1(n)$ , and process it using this filter to decimate by  $D = 2$  to obtain  $y_1(m)$ . Provide the `stem` plots of both sequences.

4. Using the `fir2` function, generate a 151-length sequence  $x_2(n)$  whose frequency-domain sampled-values are 1 at  $\omega = 0$ , 0.9 at  $\omega = 0.2\pi$ , 1 at  $\omega = 0.4\pi$ , 0.5 at  $\omega = 0.45\pi$ , 0 at  $\omega = 0.5\pi$ , and 0 at  $\omega = \pi$ . Process  $x_2(n)$ , using this filter to decimate it by a factor of 2 to obtain  $y_2(m)$ . Provide the spectral plots of both sequences.

**P9.34** A signal  $x(n)$  is to be decimated by a factor of  $D = 3$ . It has a bandwidth of  $0.25\pi$ , and we will tolerate aliasing this frequency  $0.3\pi$  in the decimated signal. Using the Parks–McClellan algorithm, we want to design such a decimator.

1. Determine the coefficients of the FIR filter that has 0.1 dB ripple in the passband and 40 dB attenuation in the stopband.
2. Provide plots of the impulse and the log-magnitude responses.
3. Let  $x_1(n) = \cos(0.2\pi n) + 2 \sin(0.3\pi n)$ . Generate 300 samples of  $x_1(n)$ , and process it using this filter to decimate by  $D = 3$  to obtain  $y_1(m)$ . Provide the `stem` plots of both sequences.
4. Using the `fir2` function, generate a 151-length sequence  $x_2(n)$  whose frequency-domain sampled-values are 1 at  $\omega = 0$ , 1 at  $\omega = 0.1\pi$ , 1 at  $\omega = 0.25\pi$ , 0.5 at  $\omega = 0.3\pi$ , 0 at  $\omega = 0.35\pi$ , and 0 at  $\omega = \pi$ . Process  $x_2(n)$ , using this filter to decimate it by a factor of 3 to obtain  $y_2(m)$ . Provide the spectral plots of both sequences.

**P9.35** Design a sampling rate converter that reduces the sampling rate by a factor of  $2/5$ .

1. Using the Parks–McClellan algorithm, determine the coefficients of the FIR filter that has 0.1 dB ripple in the passband and 30 dB attenuation in the stopband. Choose reasonable values for the band-edge frequencies.
2. Provide plots of the impulse and the log-magnitude responses.
3. Specify the sets of the time-varying coefficients  $g(m, n)$  and the corresponding coefficients in the polyphase filter realization.
4. Let  $x(n) = \sin(0.35\pi n) + 2 \cos(0.45\pi n)$ . Generate 500 samples of  $x(n)$  and process it using this filter to resample by  $2/5$  to obtain  $y(m)$ . Provide the `stem` plots of both sequences.

**P9.36** Design a sampling rate converter that increases the sampling rate by a factor of  $7/4$ .

1. Using the Parks–McClellan algorithm, determine the coefficients of the FIR filter that has 0.1 dB ripple in the passband and 40 dB attenuation in the stopband. Choose reasonable values for the band-edge frequencies.
2. Provide plots of the impulse and the log-magnitude responses.
3. Specify the sets of the time-varying coefficients  $g(m, n)$  and the corresponding coefficients in the polyphase filter realization.
4. Let  $x(n) = 2 \sin(0.35\pi n) + \cos(0.95\pi n)$ . Generate 500 samples of  $x(n)$  and process it, using this filter to resample by  $7/4$  to obtain  $y(m)$ . Provide the `stem` plots of both sequences.

**P9.37** A signal  $x(n)$  is to be resampled by a factor of  $3/2$ . It has a total bandwidth of  $0.8\pi$ , but we want to preserve frequencies only up to  $0.6\pi$  and require that the band up to  $0.75\pi$  be free of aliasing in the resampled signal.

1. Using the Parks–McClellan algorithm, determine the coefficients of the FIR filter that has 0.5 dB ripple in the passband and 50 dB attenuation in the stopband.
2. Provide plots of the impulse and the log-magnitude responses.

3. Using the `fir2` function, generate a 101-length sequence  $x(n)$  whose frequency-domain sampled-values are 0.7 at  $\omega = 0$ , 1 at  $\omega = 0.3\pi$ , 1 at  $\omega = 0.7\pi$ , 0.5 at  $\omega = 0.75\pi$ , 0 at  $\omega = 0.8\pi$ , and 0 at  $\omega = \pi$ . Process  $x(n)$  using this filter to resample it by 3/2 to obtain  $y(m)$ . Provide the spectral plots of both sequences.

**P9.38** A signal  $x(n)$  is to be resampled by a factor of 4/5. It has a total bandwidth of  $0.8\pi$ , but we want to preserve frequencies only up to  $0.5\pi$  and require that the band up to  $0.75\pi$  be free of aliasing in the resampled signal.

1. Using the Parks–McClellan algorithm, determine the coefficients of the FIR filter that has 0.1 dB ripple in the passband and 40 dB attenuation in the stopband.
2. Provide plots of the impulse and the log-magnitude responses.
3. Using the `fir2` function, generate a 101-length sequence  $x(n)$  whose frequency-domain sampled-values are 0.7 at  $\omega = 0$ , 1 at  $\omega = 0.3\pi$ , 1 at  $\omega = 0.7\pi$ , 0.5 at  $\omega = 0.75\pi$ , 0 at  $\omega = 0.8\pi$ , and 0 at  $\omega = \pi$ . Process  $x(n)$ , using this filter to resample it by 4/5 to obtain  $y(m)$ . Provide the spectral plots of both sequences.

**P9.39** A signal  $x(n)$  is to be resampled by a factor of 5/2. It has a total bandwidth of  $0.8\pi$ , but we want to preserve frequencies only up to  $0.7\pi$  and require that the band up to  $0.75\pi$  be free of aliasing in the resampled signal.

1. Using the Parks–McClellan algorithm, determine the coefficients of the FIR filter that has 0.5 dB ripple in the passband and 50 dB attenuation in the stopband.
2. Provide plots of the impulse and the log-magnitude responses.
3. Using the `fir2` function, generate a 101-length sequence  $x(n)$  whose frequency-domain sampled-values are 0.7 at  $\omega = 0$ , 1 at  $\omega = 0.3\pi$ , 1 at  $\omega = 0.7\pi$ , 0.5 at  $\omega = 0.75\pi$ , 0 at  $\omega = 0.8\pi$ , and 0 at  $\omega = \pi$ . Process  $x(n)$  using this filter to resample it by a 5/2 to obtain  $y(m)$ . Provide the spectral plots of both sequences.

**P9.40** A signal  $x(n)$  is to be resampled by a factor of 3/8. It has a total bandwidth of  $0.5\pi$ , but we want to preserve frequencies only up to  $0.3\pi$  and require that the band up to  $0.35\pi$  be free of aliasing in the resampled signal.

1. Using the Parks–McClellan algorithm, determine the coefficients of the FIR filter that has 0.1 dB ripple in the passband and 40 dB attenuation in the stopband.
2. Provide plots of the impulse and the log-magnitude responses.
3. Using the `fir2` function, generate a 101-length sequence  $x(n)$  whose frequency-domain sampled-values are 1 at  $\omega = 0$ , 1 at  $\omega = 0.25\pi$ , 1 at  $\omega = 0.5\pi$ , 0.5 at  $\omega = 0.55\pi$ , 0 at  $\omega = 0.6\pi$ , and 0 at  $\omega = \pi$ . Process  $x(n)$  using this filter to resample it by 3/8 to obtain  $y(m)$ . Provide the spectral plots of both sequences.

# CHAPTER **10**

---

## Round-Off Effects in Digital Filters

---

In the latter part of Chapter 6, we discussed the finite-precision number representations for the purpose of implementing filtering operations on digital hardware. In particular, we focused on the process of number quantization, the resulting error characterizations, and the effects of filter coefficient quantization on filter specifications and responses. In this chapter, we further extend the effects of finite-precision numerical effects to the filtering aspects in signal processing.

We begin by discussing analog-to-digital (A/D) conversion noise using the number representations and quantization error characteristics developed in Chapter 6. We then analyze the multiplication and addition quantization (collectively known as arithmetic round-off error) models. The effects of these errors on filter output are discussed as two topics: correlated errors called *limit cycles* and uncorrelated *round-off noise*.

### 10.1 ANALYSIS OF A/D QUANTIZATION NOISE

---

From the quantizer characteristics obtained in Chapter 6, it is obvious that the quantized value  $\mathcal{Q}[x]$  is a nonlinear operation on the value  $x$ . Hence the exact analysis of the finite word-length effects in digital filters is generally difficult and one has to consider less ideal analysis techniques that work well in practice.

One such technique is the statistical modeling technique. It converts the nonlinear analysis problem into a linear one and allows us to examine

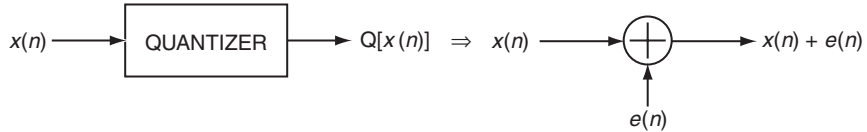


**FIGURE 10.1** Statistical model of a quantizer

output-error characteristics. In this technique, we assume that the quantized value  $Q[x]$  is a sum of the exact value  $x$  and the quantization error  $e$ , which is assumed to be a random variable. When  $x(n)$  is applied as an input sequence to the quantizer, the error  $e(n)$  is assumed to be a random sequence. We then develop a statistical model for this random sequence to analyze its effects through a digital filter.

For the purpose of analysis, we assume that the quantizer employs fixed-point two's-complement number format representation. Using the results given previously, we can extend this analysis to other formats as well.

### 10.1.1 STATISTICAL MODEL

We model the quantizer block on the input as a signal-plus-noise operation—that is, from (6.46),

$$Q[x(n)] = x(n) + e(n) \quad (10.1)$$

where  $e(n)$  is a random sequence that describes the quantization error sequence and is termed the *quantization noise*. This is shown in Figure 10.1.

**Model assumptions** For the model in (10.1) to be mathematically convenient and hence practically useful, we have to assume *reasonable* statistical properties for the sequences involved. That these assumptions are practically reasonable can be ascertained using simple MATLAB examples, as we shall see. We assume that the error sequence,  $e(n)$  has the following characteristics:<sup>1</sup>

1. The sequence  $e(n)$  is a sample sequence from a stationary random process  $\{e(n)\}$ .
2. This random process  $\{e(n)\}$  is *uncorrelated* with sequence  $x(n)$ .
3. The process  $\{e(n)\}$  is an independent process (i.e., the samples are independent of each other).
4. The probability density function (pdf),  $f_E(e)$ , of sample  $e(n)$  for each  $n$  is uniformly distributed over the interval of width  $\Delta = 2^{-B}$ , which is the quantizer resolution.

<sup>1</sup>The review of random variables, processes, and the associated terminology is given in Chapter 13.

These assumptions are reasonable in practice if the sequence  $x(n)$  is sufficiently random to traverse many quantization steps in going from time  $n$  to  $n + 1$ .

### 10.1.2 ANALYSIS USING MATLAB

To investigate the statistical properties of the error samples, we will have to generate a large number of these samples and plot their distribution using a histogram (or a probability bar graph). Furthermore, we have to design the sequence  $x(n)$  so that its samples do not repeat; otherwise, the error samples will also repeat, which will result in an inaccurate analysis. This can be guaranteed either by choosing a well-defined aperiodic sequence or a random sequence.

We will quantize  $x(n)$  using *B-bit rounding* operation. A similar implementation can be developed for the truncation operation. Since all three error characteristics are exactly the same under the rounding operation, we will choose the sign-magnitude format for ease in implementation. After quantization, the resulting error samples  $e(n)$  are uniformly distributed over the  $[-\frac{\Delta}{2}, \frac{\Delta}{2}]$  interval. Let  $e_1(n)$  be the normalized error given by

$$e_1(n) \triangleq \frac{e(n)}{\Delta} = e(n) 2^B \Rightarrow e_1(n) \in [-1/2, 1/2] \quad (10.2)$$

Then  $e_1(n)$  is uniform over the interval  $[-\frac{1}{2}, +\frac{1}{2}]$ , as shown in Figure 10.2a. Thus the histogram interval will be uniform across all  $B$ -bit values, which will make its computation and plotting easier. This interval will be divided into 128 bins for the purpose of plotting.

To determine the sample independence, we consider the histogram of the sequence

$$e_2(n) \triangleq \frac{e_1(n) + e_1(n - 1)}{2} \quad (10.3)$$

which is the average of two consecutive normalized error samples. If  $e_1(n)$  is uniformly distributed between  $[-1/2, 1/2]$ , then, for sample independence,  $e_2(n)$  must have a triangle-shaped distribution between  $[-1/2, 1/2]$ , as shown in Figure 10.2b. We will again generate a 128-bin histogram for  $e_2(n)$ . These steps are implemented in the following MATLAB function.

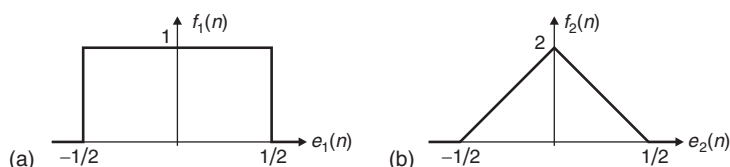


**FIGURE 10.2** Probability distributions of the normalized errors  $e_1(n)$  and  $e_2(n)$

```

function [H1,H2,Q, estat] = StatModelR(xn,B,N);
% Statistical Model (Rounding) for A/D Quantization error and its Distribution
% -----
% [H1,H2,Q] = StatModelR(xn,B,N);
%   OUT: H1 = normalized histogram of e1
%         H2 = normalized histogram of e2
%         Q = normalized histogram bins
%   estat = row vector: [[e1avg,e1std,e2avg,e2std]
% IN:  B = bits to quantize
%      N = number of samples of x(n)
%      xn = samples of the sequence
% Plot variables
bM = 7; DbM = 2^bM;                                % Bin parameter
M = round((DbM)/2);                                % Half number of bins
bins = [-M+0.5:1:M-0.5];                           % Bin values from -M to M
Q = bins/(DbM);                                    % Normalized bins
% Quantization error analysis
xq = (round(xn*(2^B)))/(2^B);                      % Quantized to B bits
e1 = xq-xn; clear xn xq;                           % Quantization error
e2 = 0.5*(e1(1:N-1)+e1(2:N));                     % Average of two adj errors
e1avg = mean(e1); e1std = std(e1);                 % Mean & std dev of the error e1
e2avg = mean(e2); e2std = std(e2);                 % Mean & std dev of the error e2
estat = [e1avg,e1std,e2avg,e2std];
% Probability distribution of e1
e1 = floor(e1*(2^(B+bM)));                        % Normalized e1 (int between -M & M)
e1 = sort([e1,-M-1:1:M]);                           %
H1 = diff(find(diff(e1)))-1; clear e1;            % Error histogram
if length(H1) == DbM+1
    H1(DbM) = H1(DbM)+H1(DbM+1);
    H1 = H1(1:DbM);
end
H1 = H1/N;                                         % Normalized histogram
% Probability distribution of e2
e2 = floor(e2*(2^(B+bM)));                        % Normalized e2 (int between -M & M)
e2 = sort([e2,-M-1:1:M]);                           %
H2 = diff(find(diff(e2)))-1; clear e2;            % Error histogram
if length(H2) == DbM+1
    H2(DbM) = H2(DbM)+H2(DbM+1);
    H2 = H2(1:DbM);
end
H2 = H2/N;                                         % Normalized histogram

```

To validate the model assumptions, we consider the following two examples. In the first example, an aperiodic sinusoidal sequence is quantized to  $B$  bits, and in the second example, a random sequence is quantized to  $B$  bits. The resulting quantization errors are analyzed for their distribution properties and for their sample independence for various values of  $B$ .

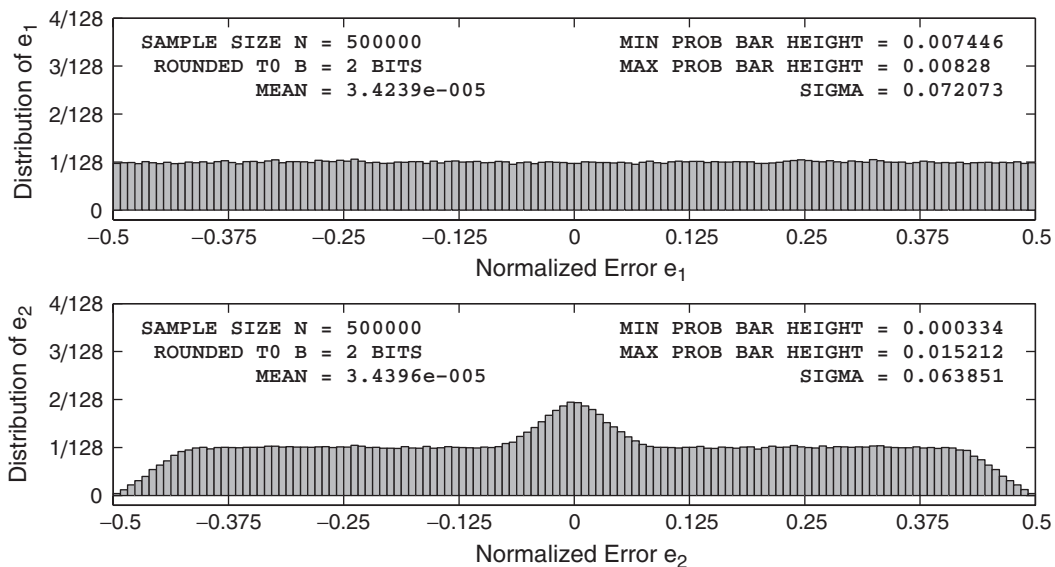


**FIGURE 10.3** A/D quantization error distribution for the sinusoidal signal in Example 10.1,  $B = 2$  bits

Through these examples, we hope to learn how small error  $e$  must be (or equivalently, how large  $B$  must be) for the above assumptions to be valid.

- **EXAMPLE 10.1** Let  $x(n) = \frac{1}{3}\{\sin(n/11) + \sin(n/31) + \cos(n/67)\}$ . This sequence is not periodic, and hence its samples never repeat using infinite-precision representation. However, since the sequence is of sinusoidal nature, its continuous envelope is periodic and the samples are continuously distributed over the fundamental period of this envelope. Determine the error distributions for  $B = 2$  and 6 bits.

#### Solution

To minimize statistical variations, the sample size must be large. We choose 500,000 samples. The following MATLAB script computes the distributions for  $B = 2$  bits.

```
clear; close all;
% Example parameters
B = 2; N = 500000; n = [1:N];
xn = (1/3)*(sin(n/11)+sin(n/31)+cos(n/67)); clear n;
% Quantization error analysis
[H1,H2,Q, estat] = StatModelR(xn,B,N); % Compute histograms
H1max = max(H1); H1min = min(H1); % Max and Min of H1
H2max = max(H2); H2min = min(H2); % Max and Min of H2
```

The plots of the resulting histogram are shown in Figure 10.3. Clearly, even though the error samples appear to be uniformly distributed, the samples are not independent. The corresponding plots for  $B = 6$  bits are shown in

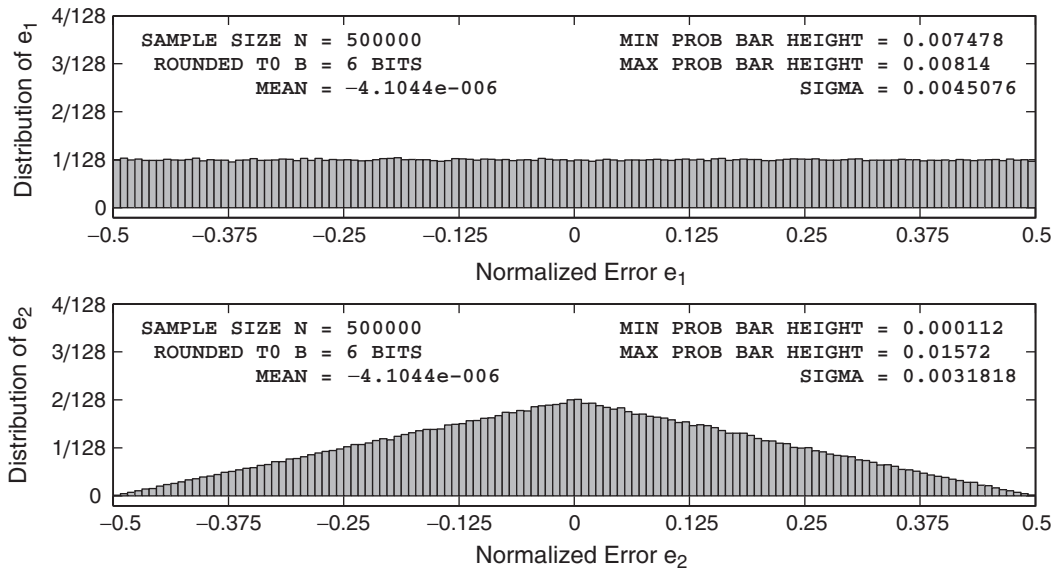


**FIGURE 10.4** Quantization error distribution for the sinusoidal signal in Example 10.1,  $B = 6$  bits

Figure 10.4, from which we observe that the quantization error sequence appears to satisfy the model assumptions for  $B \geq 6$  bits.  $\square$

- EXAMPLE 10.2** Let  $x(n)$  be an independent and identically distributed random sequence whose samples are uniformly distributed over the  $[-1, 1]$  interval. Determine the error distributions for  $B = 2$  and 6 bits.

#### Solution

We again choose 500,000 samples to minimize any statistical variations. The following MATLAB fragment computes the distributions for  $B = 2$  bits.

```
clear; close all;
% Example parameters
B = 2; N = 500000; xn = (2*rand(1,N)-1);
% Quantization error analysis
[H1,H2,Q, estat] = StatModelR(xn,B,N);    % Compute histograms
H1max = max(H1); H1min = min(H1); % Max and Min of H1
H2max = max(H2); H2min = min(H2); % Max and Min of H2
```

The plots of the resulting histogram are shown in Figure 10.5. The corresponding plots for  $B = 6$  bits are shown in Figure 10.6. From these plots, we observe that even for  $B = 2$  bits the quantization error samples are independent and uniformly distributed.  $\square$

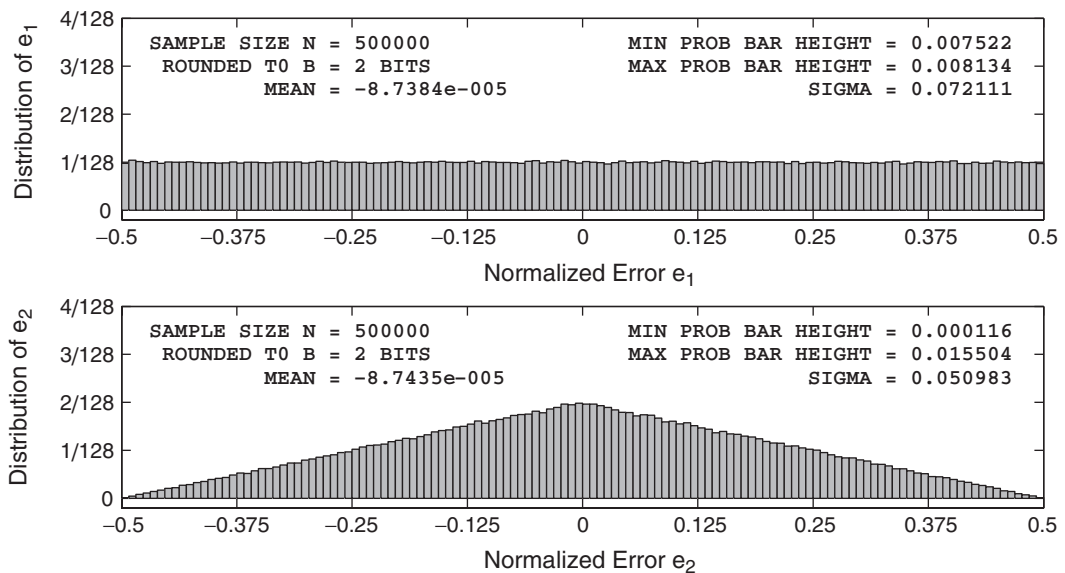


**FIGURE 10.5** A/D quantization error distribution for the random signal in Example 10.2,  $B = 2$  bits

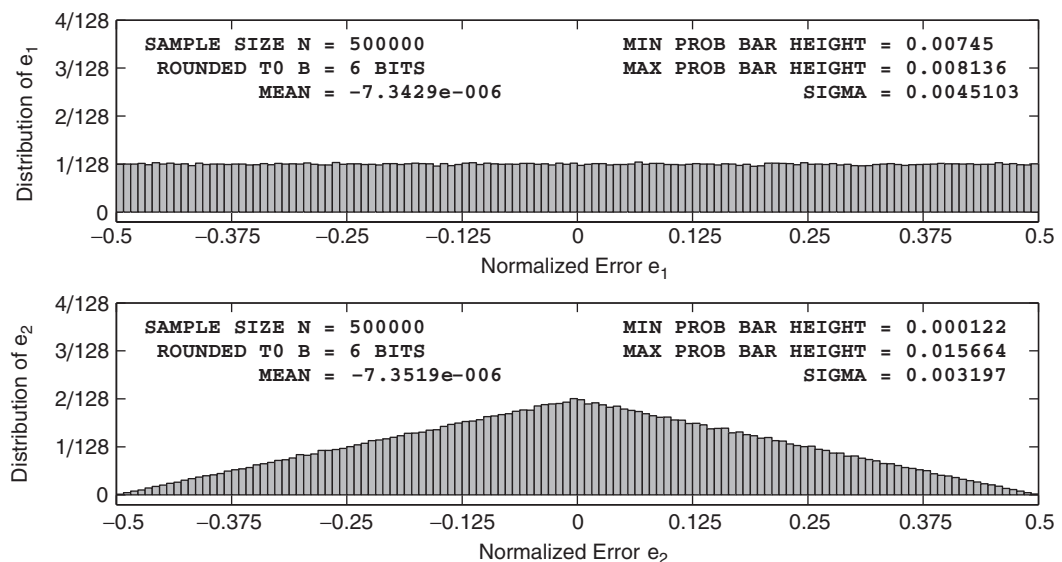


**FIGURE 10.6** Quantization error distribution for the random signal in Example 10.2,  $B = 6$  bits

Since practical signals processed using a DSP chip are typically random in nature (or can be modeled as such), we conclude from these two examples that the statistical model, with its stated assumptions, is a very good model.

### 10.1.3 STATISTICS OF A/D QUANTIZATION NOISE

We now develop a second-order statistical description of the error sequence  $e(n)$  for both the truncation and rounding operations.

### 10.1.4 TRUNCATION

From (6.57), the pdf  $f_{E_T}(e)$  of  $e_T(n)$  is uniform over  $[-\Delta, 0]$ , as shown in Figure 10.7a. Then the average of  $e_T(n)$  is given by

$$m_{e_T} \stackrel{\Delta}{=} E[e_T(n)] = -\Delta/2 \quad (10.4)$$

and the variance is

$$\begin{aligned} \sigma_{e_T}^2 &\stackrel{\Delta}{=} E[(e_T(n) - m_{e_T})^2] = \int_{-\Delta}^0 (e - \Delta/2)^2 f_{E_T}(e) de \\ &= \int_{-\Delta/2}^{\Delta/2} e^2 \left(\frac{1}{\Delta}\right) de = \frac{\Delta^2}{12} \end{aligned} \quad (10.5)$$

Using  $\Delta = 2^{-B}$ , we obtain

$$\sigma_{e_T}^2 = \frac{2^{-2B}}{12} \quad \text{or} \quad \sigma_{e_T} = \frac{2^{-B}}{2\sqrt{3}} \quad (10.6)$$

**Rounding** From (6.59), the pdf  $f_{E_R}(e)$  of  $e_R(n)$  is uniform over  $[-\Delta/2, \Delta/2]$ , as shown in Figure 10.7b. Then the average of  $e_R(n)$  is given by

$$m_{e_R} \stackrel{\Delta}{=} [Ee_R] = 0 \quad (10.7)$$

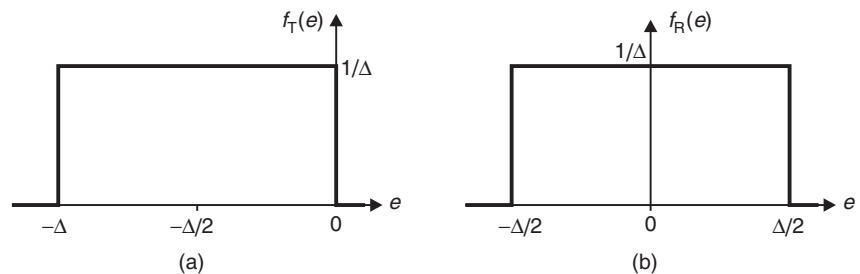


**FIGURE 10.7** Probability density functions: (a) truncation and (b) rounding

and the variance is

$$\begin{aligned}\sigma_{e_R}^2 &\stackrel{\Delta}{=} E[(e_R(n) - m_{e_R})^2] = \int_{-\Delta/2}^{\Delta/2} e^2 f_{E_R}(e) de = \int_{-\Delta/2}^{\Delta/2} e^2 \left(\frac{1}{\Delta}\right) de \\ &= \frac{\Delta^2}{12}\end{aligned}\quad (10.8)$$

Using (6.45), we obtain

$$\sigma_{e_R}^2 = \frac{2^{-2B}}{12} \quad \text{or} \quad \sigma_{e_R} = \frac{2^{-B}}{2\sqrt{3}} \quad (10.9)$$

Since the samples of the sequence  $e_R(n)$  are assumed to be independent of each other, the variance of  $[e_R(n) + e_R(n-1)]/2$  is given by

$$\text{var}\left[\frac{e_R(n) + e_R(n-1)}{2}\right] = \frac{1}{4} \left(\frac{2^{-2B}}{12} + \frac{2^{-2B}}{12}\right) = \frac{2^{-2B}}{24} = \frac{1}{2} \sigma_{e_R}^2 \quad (10.10)$$

or the standard deviation is  $\sigma_{e_R}/\sqrt{2}$ .

From the model assumptions and (10.6) or (10.9), the covariance of the error sequence (which is an independent sequence) is given by

$$E[e(m)e(n)] \stackrel{\Delta}{=} C_e(m-n) \stackrel{\Delta}{=} C_e(\ell) = \frac{2^{-2B}}{12} \delta(\ell) \quad (10.11)$$

where  $\ell \stackrel{\Delta}{=} m-n$  is called the lag variable. Such an error sequence is also known as a white noise sequence.

### 10.1.5 MATLAB IMPLEMENTATION

In MATLAB, the sample mean and standard deviation are computed using the functions `mean` and `std`, respectively. The last argument of the function `StatModelR` is a vector containing sample means and standard deviations of unnormalized errors  $e(n)$  and  $[e(n) + e(n-1)]/2$ . Thus these values can be compared with the theoretical values obtained from the statistical model.

- **EXAMPLE 10.3** The plots in Example 10.1 also indicate the sample means and standard deviations of the errors  $e(n)$  and  $[e(n) + e(n-1)]/2$ . For  $B = 2$ , these computed values are shown in Figure 10.3. Since  $e(n)$  is uniformly distributed over the interval  $[-2^{-3}, 2^{-3}]$ , its mean value is 0, and so is the mean of  $[e(n) + e(n-1)]/2$ . The computed values are  $3.4239 \times 10^{-5}$  and  $3.4396 \times 10^{-5}$ , respectively, which agree fairly well with the model. The standard deviation of  $e(n)$ , from (10.9), is 0.072169, while that from the top plot in Figure 10.3 is 0.072073, which again agrees closely with the model. The standard deviation of the average of the two consecutive samples, from (10.10), is 0.051031, and from the bottom plot in Figure 10.3 it is 0.063851, which clearly does not agree with the model. Hence the samples of  $e(n)$  for  $B = 2$  are not independent. This was confirmed by the bottom plot in Figure 10.3.

Similarly, for  $B = 6$  computed statistical values are shown in Figure 10.4. The computed values of the two means are  $-4.1044 \times 10^{-6}$ , which agree very well with the model. The standard deviation of  $e(n)$ , from (10.9), is 0.0045105, while that from the top plot in Figure 10.4 is 0.0045076, which again agrees closely with the model. The standard deviation of the average of the two consecutive samples, from (10.10), is 0.0031894, while from the bottom plot in Figure 10.4 it is 0.00318181, which clearly agrees with the model. Hence the samples of  $e(n)$  for  $B = 6$  are independent. This was also confirmed by the bottom plot in Figure 10.4.  $\square$

Similar calculations can be carried out for the signal in Example 10.2. The details are left to the reader.

#### 10.1.6 A/D QUANTIZATION NOISE THROUGH DIGITAL FILTERS

Let a digital filter be described by the impulse response,  $h(n)$ , or the frequency response,  $H(e^{j\omega})$ . When a quantized input,  $Q[x(n)] = x(n) + e(n)$ , is applied to this system, we can determine the effects of the error sequence  $e(n)$  on the filter output as it propagates through the filter, assuming infinite-precision arithmetic implementation in the filter. We are generally interested in the mean and variance of this output-noise sequence, which we can obtain using linear system theory concepts. Details of these results are given in Section 13.5.

Referring to Figure 10.8, let the output of the filter be  $\hat{y}(n)$ . Using LTI properties and the statistical independence between  $x(n)$  and  $e(n)$ , the output  $\hat{y}(n)$  can be expressed as the sum of two components. Let  $y(n)$  be the (true) output due to  $x(n)$  and let  $q(n)$  be the response due to  $e(n)$ . Then we can show that  $q(n)$  is also a random sequence with mean

$$m_q \triangleq E[q(n)] = m_e \sum_{-\infty}^{\infty} h(n) = m_e H(e^{j0}) \quad (10.12)$$

where the term  $H(e^{j0})$  is termed the *DC gain* of the filter. For truncation,  $m_{e_T} = -\Delta/2$ , which gives

$$m_{q_T} = -\frac{\Delta}{2} H(e^{j0}) \quad (10.13)$$

For rounding,  $m_{e_R} = 0$  or

$$m_{q_R} = 0 \quad (10.14)$$

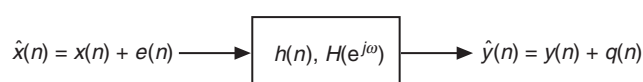


**FIGURE 10.8** Noise through digital filter

We can also show that the variance of  $q(n)$ , for both the truncation and rounding, is given by

$$\sigma_q^2 = \sigma_e^2 \sum_{-\infty}^{\infty} |h(n)|^2 = \frac{\sigma_e^2}{2\pi} \int_{-\pi}^{\pi} |H(e^{j\omega})|^2 d\omega \quad (10.15)$$

The *variance gain* from the input to the output (also known as the *normalized output variance*) is the ratio

$$\frac{\sigma_q^2}{\sigma_e^2} = \sum_{-\infty}^{\infty} |h(n)|^2 = \frac{1}{2\pi} \int_{-\pi}^{\pi} |H(e^{j\omega})|^2 d\omega \quad (10.16)$$

For a real and stable filter, using the substitution  $z = e^{j\omega}$ , the integral in (10.16) can be further expressed as a complex contour integral

$$\frac{1}{2\pi} \int_{-\pi}^{\pi} |H(e^{j\omega})|^2 d\omega = \frac{1}{2\pi j} \oint_{UC} H(z)H(z^{-1})z^{-1} dz \quad (10.17)$$

where UC is the unit circle and can be computed using residues (or the inverse  $\mathcal{Z}$ -transform) as

$$\frac{1}{2\pi} \int_{-\pi}^{\pi} |H(e^{j\omega})|^2 d\omega = \sum [\text{Res of } H(z)H(z^{-1})z^{-1} \text{ inside UC}] \quad (10.18a)$$

$$= \mathcal{Z}^{-1} [H(z)H(z^{-1})] \Big|_{n=0} \quad (10.18b)$$

### 10.1.7 MATLAB IMPLEMENTATION

Computation of the variance-gain for the A/D quantization noise can be carried out in MATLAB using (10.16) and (10.18). For FIR filters, we can perform exact calculations using the time-domain expression in (10.16). In the case of IIR filters, exact calculations can only be done using (10.18) in special cases, as we shall see (fortunately, this works for most practical filters). The approximate computations can always be done using the time-domain expression.

Let the FIR filter be given by the coefficients  $\{b_k\}_0^{M-1}$ . Then using the time-domain expression in (10.16), the variance-gain is given by

$$\frac{\sigma_q^2}{\sigma_e^2} = \sum_{k=0}^{M-1} |b_k|^2 \quad (10.19)$$

Let an IIR filter be given by the system function

$$H(z) = \frac{\sum_{\ell=0}^{N-1} b_\ell z^{-\ell}}{1 + \sum_{k=1}^{N-1} a_k z^{-k}} \quad (10.20)$$

with impulse response  $h(n)$ . If we assume that the filter is real, causal, and stable and has only simple poles, then using the partial fraction expansion, we can write

$$H(z) = R_0 + \sum_{k=1}^{N-1} \frac{R_k}{z - p_k} \quad (10.21)$$

where  $R_0$  is the constant term and  $R_k$ 's are the residues at the pole locations  $p_k$ . This expansion can be computed using the **residue** function. Note that both poles and the corresponding residues are either real-valued or occur in complex-conjugate pairs. Then using (10.18a), we can show that (see [68] and also Problem P10.3)

$$\frac{\sigma_q^2}{\sigma_e^2} = R_0^2 + \sum_{k=1}^{N-1} \sum_{\ell=1}^{N-1} \frac{R_k R_\ell^*}{1 - p_k p_\ell^*} \quad (10.22)$$

The variance-gain expression in (10.22) is applicable for most practical filters since rarely do they have multiple poles. The approximate value of the variance-gain for IIR filters is given by

$$\frac{\sigma_q^2}{\sigma_e^2} \simeq \sum_{k=0}^{K-1} |h(n)|^2, \quad K \gg 1 \quad (10.23)$$

where  $K$  is chosen so that the impulse response values (magnitudewise) are almost zero beyond  $K$  samples. The following MATLAB function, **VarGain**, computes variance-gain using (10.19) or (10.22).

```
function Gv = VarGain(b,a)
% Computation of variance-gain for the output noise process
% of digital filter described by b(z)/a(z)
% Gv = VarGain(b,a)
a0 = a(1); a = a/a0; b = b/a0; M = length(b); N = length(a);
if N == 1
    Gv = sum(b.*b); % FIR Filter
    return
else
    % IIR Filter
    [R,p,P] = residue(b,a);
    if length(P) > 1
        error('*** Variance Gain Not computable ***');
    elseif length(P) == 1
        Gv = P*P;
    else
        Gv = 0;
    end
    Rnum = R*R'; pden = 1-p*p';
    H = Rnum./pd़en; Gv = Gv + real(sum(H(:)));
end
```

It should be noted that the actual output noise variance is obtained by multiplying the A/D quantization noise variance by the variance-gain.

- EXAMPLE 10.4** Consider an eighth-order IIR filter with poles at  $p_k = r e^{j2\pi k/8}$ ,  $k = 0, \dots, 7$ . If  $r$  is close to 1, then the filter has four narrowband peaks. Determine the variance-gain for this filter when  $r = 0.9$  and  $r = 0.99$ .

**Solution**

The following MATLAB script illustrates calculations for  $r = 0.9$ , which implements exact as well as approximate approaches.

```
% Filter Parameters
N = 8; r = 0.9; b = 1; pl = r*exp(j*2*pi*[0:N-1]/N); a = real(poly(pl));

% Variance-gain (Exact)
Vg = VarGain(b,a)
Vg =
    1.02896272593178

% Variance-gain (approximate)
x = [1,zeros(1,10000)]; % Unit sample sequence
h = filter(b,a,x);      % Impulse response
VgCheck = sum(h.*h)
VgCheck =
    1.02896272593178
```

Clearly, both approaches give the same variance-gain, which for  $r = 0.9$  is about 3% above unity. For  $r = 0.99$  the calculations are

```
% Filter Parameters
N = 8; r = 0.99; b = 1; pl = r*exp(j*2*pi*[0:N-1]/N); a = real(poly(pl));
% Variance-gain (Exact)
Vg = VarGain(b,a)
Vg =
    6.73209233071894
```

The variance-gain is more than 673%, which means that when poles are close to the unit circle, the filter output can be very noisy.  $\square$

## 10.2 ROUND-OFF EFFECTS IN IIR DIGITAL FILTERS

---

With our insight into the quantizer operation and its simpler statistical model, we are now ready to delve into the analysis of finite word-length effects in both IIR and FIR digital filters. We have already studied the effects of input signal quantization and filter coefficient quantization on filter behavior. We will now turn our attention to the effects of arithmetic operation quantization on filter output responses (in terms of signal-to-noise ratios). For this study, we will consider both fixed-point and floating-point arithmetic. We first consider the effects on IIR filters since, due to feedback paths, the results are more complicated—yet more interesting—than those in FIR filters. The effects on FIR filters are studied in the next section.

We will restrict ourselves to the rounding operation of the quantizer due to its superior statistical qualities (no bias or average value). From (6.59), we know that, for the rounding operation, the quantizer error,  $e_R$ , has the same characteristics across all three number representation formats. Hence for MATLAB simulation purposes, we will consider the sign-magnitude format because it is easy to program and simulate for arithmetic operation. However, in practice, two's-complement format number representation has advantages over the others in terms of hardware implementation.

Digital filter implementation requires arithmetic operations of multiplication and addition. If two  $B$ -bit fractional numbers are multiplied, the result is a  $2B$ -bit fractional number that must be quantized to  $B$  bits. Similarly, if two  $B$ -bit fractional numbers are added, the sum could be more than 1, which results in an *overflow* (which in itself is a nonlinear characteristic), or the sum must be corrected using a *saturation* strategy, which is also nonlinear. Thus a finite word-length implementation of the filter is a highly nonlinear filter and must be analyzed carefully for any meaningful results.

In this section, we will consider two approaches to deal with errors due to finite word-length representation. The first type of error can occur when error samples become *correlated* with each other due to the nonlinearity of the quantizer. This is called *limit-cycle behavior*, and it can exist only in IIR filters. We will analyze this problem using the nonlinear quantizer model rather than the statistical model of the quantizer. In the second type of error, we assume that more nonlinear effects in the quantizer have been suppressed. Then, using the statistical model of the quantizer, we develop a quantization noise model for IIR filters that is more useful in predicting the finite word-length effects.

### 10.2.1 LIMIT CYCLES

Digital filters are linear systems, but when quantizers are incorporated in their implementation, they become nonlinear systems. For nonlinear systems, it is possible to have an output sequence even when there is no input. Limit cycles is one such behavior that creates an oscillatory periodic output that is highly undesirable.

#### DEFINITION 1 *Limit cycle*

A zero-input limit cycle is a nonzero periodic output sequence produced by nonlinear elements or quantizers in the feedback loop of a digital filter.  $\square$

There are two types of limit cycles. The *granular* limit cycles are due to nonlinearities in multiplication quantization and are of low amplitude. The *overflow* limit cycles are a result of overflow in addition and can have large amplitudes.

### 10.2.2 GRANULAR LIMIT CYCLES

This type of limit cycle can easily be demonstrated with a simple rounding quantizer following a multiplication. We illustrate with the following example.

- **EXAMPLE 10.5** Consider a simple first-order IIR filter given by

$$y(n) = \alpha y(n-1) + x(n); \quad y(-1) = 0, \quad n \geq 0 \quad (10.24)$$

Let  $\alpha = -\frac{1}{2}$ ; then this is a highpass filter, since its pole is near  $z = -1$ . Determine the output  $y(n)$  when  $x(n) = \frac{7}{8}\delta(n)$ , assuming a 3-bit quantizer in the multiplier.

**Solution**

After multiplication by  $\alpha$ , we have to quantize the result. Let the output due to this quantization be  $\hat{y}(n)$ . Then the actual implementable digital filter is

$$\hat{y}(n) = \mathcal{Q} \left[ -\frac{1}{2} \hat{y}(n-1) \right] + x(n); \quad \hat{y}(-1) = 0, \quad n \geq 0 \quad (10.25)$$

We assume that the input in (10.24) is quantized and that there is no overflow due to addition. Let  $B = 3$  (i.e., we have 3 fraction bits and 1 sign bit), and let  $x(n) = \frac{7}{8}\delta(n)$ . Now  $\alpha = -\frac{1}{2}$  is represented by 1 $\blacktriangle$ 110 in two's-complement format. Hence the output sequence is obtained as

$$\begin{aligned} \hat{y}(0) &= x(0) &= +\frac{7}{8} : 0\blacktriangle111 \\ \hat{y}(1) &= \mathcal{Q}[\alpha \hat{y}(0)] = \mathcal{Q} \left[ -\frac{1}{2} \left( +\frac{7}{8} \right) \right] = \mathcal{Q} \left[ -\frac{7}{16} \right] = -\frac{1}{2} : 1\blacktriangle100 \\ \hat{y}(2) &= \mathcal{Q}[\alpha \hat{y}(1)] = \mathcal{Q} \left[ -\frac{1}{2} \left( -\frac{1}{2} \right) \right] = \mathcal{Q} \left[ +\frac{1}{4} \right] = +\frac{1}{4} : 0\blacktriangle010 \\ \hat{y}(3) &= \mathcal{Q}[\alpha \hat{y}(2)] = \mathcal{Q} \left[ -\frac{1}{2} \left( +\frac{1}{4} \right) \right] = \mathcal{Q} \left[ -\frac{1}{8} \right] = -\frac{1}{8} : 1\blacktriangle111 \quad (10.26) \\ \hat{y}(4) &= \mathcal{Q}[\alpha \hat{y}(3)] = \mathcal{Q} \left[ -\frac{1}{2} \left( -\frac{1}{8} \right) \right] = \mathcal{Q} \left[ +\frac{1}{16} \right] = +\frac{1}{16} : 0\blacktriangle001 \\ \hat{y}(5) &= \mathcal{Q}[\alpha \hat{y}(4)] = \mathcal{Q} \left[ -\frac{1}{2} \left( +\frac{1}{16} \right) \right] = \mathcal{Q} \left[ -\frac{1}{16} \right] = -\frac{1}{16} : 1\blacktriangle111 \\ &\vdots && \vdots && \vdots \end{aligned}$$

Thus  $\hat{y}(n) = \pm \frac{1}{8}$  for  $n \geq 5$ . The desired output  $y(n)$  is

$$y(n) = \left\{ \frac{7}{8}, -\frac{7}{16}, \frac{7}{32}, -\frac{7}{64}, \frac{7}{128}, \dots, \rightarrow 0 \right\} \quad (10.27)$$

Hence the error sequence is

$$e(n) = \hat{y}(n) - y(n) = \left\{ 0, -\frac{1}{16}, \frac{1}{32}, -\frac{1}{64}, \frac{9}{128}, \dots, \rightarrow \pm \frac{1}{8} \right\} \quad (10.28)$$

This shows that the error  $e(n)$  slowly builds up to  $\pm \frac{1}{8}$ . Hence the error is *asymptotically periodic* with period 2.  $\square$

From Example 10.5, it is clear that, in the steady state, the system has poles on the unit circle and hence the nonlinear system has effectively become a linear system [37]. This implies that, effectively, for the system in (10.24)

$$\mathcal{Q}[\alpha \hat{y}(n-1)] = \begin{cases} \hat{y}(n-1), & \alpha > 0 \\ -\hat{y}(n-1), & \alpha < 0 \end{cases} \quad (10.29)$$

Also due to the rounding operation, the quantization error is bounded by  $\pm \Delta/2$ , where  $\Delta = 2^{-B}$  is the quantization step, or

$$|\mathcal{Q}[\alpha \hat{y}(n-1)] - \alpha \hat{y}(n-1)| \leq \frac{\Delta}{2} \quad (10.30)$$

From (10.29) and (10.30), we conclude that

$$|\hat{y}(n-1)| \leq \frac{\Delta}{2(1 - |\alpha|)} \quad (10.31)$$

which is the amplitude range of limit-cycle oscillations and is called a *dead band*. For the system in Example 10.5,  $B = 3$  and  $\alpha = -\frac{1}{2}$ . Hence the dead-band range is  $\pm \frac{1}{8}$ , which agrees with (10.31). If the output  $\hat{y}(n-1)$  gets trapped in this band when the input is zero, the filter exhibits the granular limit cycle. From (10.29), the period of the oscillation is either 1 or 2.

**Analysis using MATLAB** In our previous MATLAB simulations, we did not worry about the quantization in multiplication or addition operations because the emphasis was on either signal quantization or on filter coefficient quantization. The important operation that we have to consider is the arithmetic overflow characteristics. We assume that the represented numbers are in fractional two's-complement format. Then in practice, two overflow characteristics are used: a two's-complement overflow, which is a modulo (periodic) function, and a saturation, which is a limiting function. These characteristics are shown in Figure 10.9.

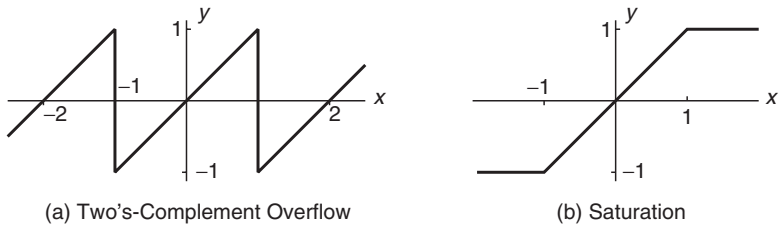


**FIGURE 10.9** Overflow characteristics used in Qfix

To simulate these two effects, we provide the function  $y = \text{Qfix}(x, B, \text{'Qmode'}, \text{'Omode'})$ . This function performs a fixed-point two's-complement format quantization using  $(B+1)$ -bit representation so that the resulting number  $y$  is between  $-1 \leq y < 1$ . The quantization mode,  $\text{Qmode}$ , is either a rounding or a truncation operation. The overflow characteristic is provided in  $\text{Omode}$ . Using this function, we can study both types of limit cycles.

```

function [y] = QFix(x,B,Qmode,Omode)
% Fixed-point Arithmetic using (B+1)-bit Representation
%
%
%   [y] = QFix(x,B,Qmode,Omode)
%       y: decimal equivalent of quantized x with values in [-1,1]
%       x: a real number array
%       B: Number of fractional bits
%   Qmode: quantizer mode
%           'round': Two's-complement rounding characteristics
%           'trunc': Two's complement truncation characteristics
%   Omode: overflow mode
%           'satur': Saturation limiter
%           'twosc': Two's-complement overflow
% Quantization operation
if strcmp(lower(Qmode), 'round');
    y = round(x.* (2^B));
elseif strcmp(lower(Qmode), 'trunc');
    y = floor(x.* (2^B));
else
    error('Use Qmode = "round" or "trunc"');
end;
y = y*(2^(-B)); % (B+1)-bit representation
%
% Overflow operation
if strcmp(lower(Omode), 'satur');
    y = min(y,1-2^(-B)); y = max(-1,y); % Saturation
elseif strcmp(lower(Omode), 'twosc');
    y = 2*(mod(y/2-0.5,1)-0.5); % Overflow
else error('Use Omode = "satur" or "twosc"');
end;
```

- EXAMPLE 10.6** In this example, simulate the results for the system given in Example 10.5 using the `Qfix` function with  $B = 3$  bits. In addition, also examine limit-cycle behavior for the truncation operation in the multiplier and for the case when the system is a lowpass filter with coefficient  $\alpha = 0.5$ .

**Solution**

MATLAB script:

```
% Highpass filter, rounding operation in multiplier
a = -0.5; yn1 = 0; m = 0:10; y = [yn1, zeros(1,length(m))];
x = 0.875*impseq(m(1),m(1)-1,m(end));
for n = m+2
    yn1 = y(n-1);
    y(n) = QFix(a*yn1,3,'round','satur') + x(n);
end
% Plotting commands follow
% Lowpass filter, rounding operation in multiplier
a = 0.5; yn1 = 0; m = 0:10; y = [yn1, zeros(1,length(m))];
x = 0.875*impseq(m(1),m(1)-1,m(end));
for n = m+2
    yn1 = y(n-1);
    y(n) = QFix(a*yn1,3,'round','satur') + x(n);
end
% Plotting commands follow
% Highpass filter, Truncation operation in multiplier
a = -0.5; yn1 = 0; m = 0:10; y = [yn1, zeros(1,length(m))];
x = 0.875*impseq(m(1),m(1)-1,m(end));
for n = m+2
    yn1 = y(n-1);
    y(n) = QFix(a*yn1,3,'trunc','satur') + x(n);
end
% Plotting commands follow
```

The resulting plots are shown in Figure 10.10. The output signal in the left plot agrees with that in Example 10.5 and has an asymptotic period of two samples. The middle plot for  $\alpha = 0.5$  (lowpass filter) shows that the limit cycle has a period of one sample with amplitude of  $\frac{1}{8}$ . Finally, the right plot shows that the limit cycles vanish for the truncation operation. This behavior for the truncation operation is also exhibited for lowpass filters.  $\square$

In the case of second-order and higher-order digital filters, granular limit cycles not only exist but also are of various types. These cycles in second-order filters can be analyzed, and dead-band as well as frequency of oscillations can be estimated. For example, if the recursive all-pole filter is implemented with rounding quantizers in the multipliers as

$$\hat{y}(n) = \mathcal{Q}[a_1\hat{y}(n-1)] + \mathcal{Q}[a_2\hat{y}(n-2)] + x(n) \quad (10.32)$$

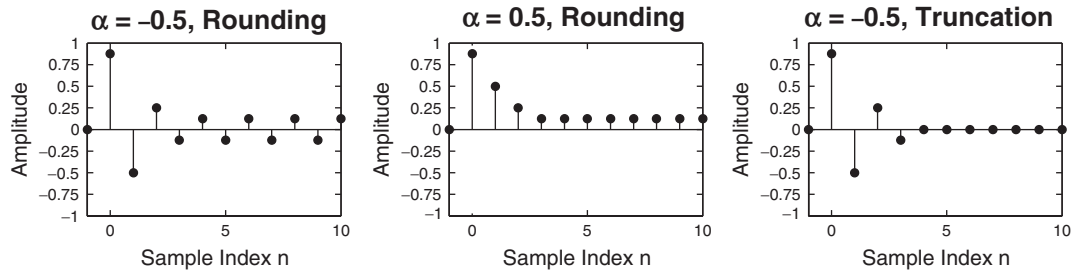


**FIGURE 10.10** Granular limit cycles in Example 10.6

where  $\hat{y}(n)$  is the quantized output, then using the analysis similar to that of the 1-order case, the dead-band region is given by

$$\hat{y}(n-2) \leq \frac{\Delta}{2(1-|a_2|)} \quad (10.33)$$

with  $a_1$  determining the frequency of oscillations. For more details, see Proakis and Manolakis [79]. We provide the following example to illustrate granular limit cycles in second-order filters using 3-bit quantizers.

- **EXAMPLE 10.7** Consider the second-order recursive filter

$$y(n) = 0.875y(n-1) - 0.75y(n-2) + x(n) \quad (10.34)$$

with zero initial conditions. This filter has two complex-conjugate poles and hence is a bandpass filter. Let the input be  $x(n) = 0.375\delta(n)$ . Analyze the limit cycle behavior using a 3-bit quantizer.

#### Solution

In the filter implementation, the coefficient products are quantized, which results in

$$\hat{y}(n) = Q[0.875\hat{y}(n-1)] - Q[0.75\hat{y}(n-2)] + x(n) \quad (10.35)$$

where  $\hat{y}(n)$  is the quantized output. We simulate (10.35) in MATLAB using both the rounding and truncation operations.

```
% Bandpass filter
a1 = 0.875; a2 = -0.75;
% Rounding operation in multipliers
yn1 = 0; yn2 = 0;
m = 0:20; y = [yn2,yn1,zeros(1,length(m))];
x = 0.375*impseq(m(1),m(1)-2,m(end));
for n = m+3
    yn1 = y(n-1); yn2 = y(n-2);
    y(n) = QFix(a1*yn1,3,'round','satur')+QFix(a2*yn2,3,'round','satur')+x(n);
end
% Plotting commands follow
% Truncation operation in multipliers
```

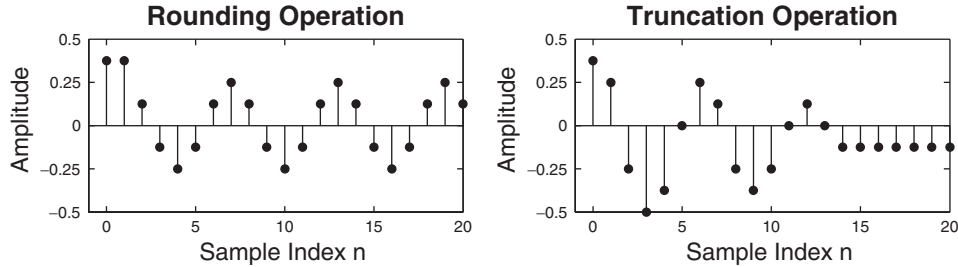


**FIGURE 10.11** Granular limit cycles in Example 10.7

```

yn1 = 0; yn2 = 0;
m = 0:20; y = [yn2,yn1,zeros(1,length(m))];
x = 0.375*impseq(m(1),m(1)-2,m(end));
for n = m+3
    yn1 = y(n-1); yn2 = y(n-2);
    y(n) = QFix(a1*yn1,3,'trunc','satur')+QFix(a2*yn2,3,'trunc','satur')+x(n);
end
% Plotting commands follow

```

The resulting plots are shown in Figure 10.11. The round-off limit cycles have a period of six samples and amplitude of 0.25, which agrees with (10.33). Unlike in the case of first-order filters, the limit cycles for the second-order exist even when truncation is used in the quantizer.  $\square$

### 10.2.3 OVERFLOW LIMIT CYCLES

This type of limit cycle is also a zero-input behavior that gives an oscillatory output. It is due to overflow in the addition even if we ignore multiplication or product quantization in the filter implementation. This is a more serious limit cycle because the oscillations can cover the entire dynamic range of the quantizer. It can be avoided in practice by using the saturation characteristics instead of overflow in the quantizer. In the following example, we simulate both granular and overflow limit cycles in a second-order filter, in addition to infinite-precision implementation.

- EXAMPLE 10.8** To obtain overflow in addition, we will consider the second-order filter with large coefficient values and initial conditions (magnitude-wise) excited by a zero input:

$$y(n) = 0.875y(n-1) - 0.875y(n-2); \quad y(-1) = -0.875, \quad y(-2) = 0.875 \quad (10.36)$$

The overflow in the addition is obtained by placing the quantizer after the additions as

$$\hat{y}(n) = \mathcal{Q}[0.875\hat{y}(n-1) - 0.875\hat{y}(n-2)]; \quad \hat{y}(-1) = -0.875, \quad \hat{y}(-2) = 0.875 \quad (10.37)$$

where  $\hat{y}(n)$  is the quantized output. We first simulate the infinite-precision operation of (10.36) and compare its output with the granular limit-cycle implementation in (10.35) and with the overflow limit-cycle in (10.37). We use the rounding operation. The details are in the following MATLAB script.

```
M = 100; B = 3; A = 1-2^(-B);
a1 = A; a2 = -A; yn1 = -A; yn2 = A;
m = 0:M; y = [yn2,yn1,zeros(1,length(m))];
% Infinite precision
for n = m+3
    yn1 = y(n-1); yn2 = y(n-2);
    y(n) = a1*yn1 + a2*yn2;
end
% Plotting commands follow
% Granular limit cycle
for n = m+3
    yn1 = y(n-1); yn2 = y(n-2);
    y(n) = QFix(a1*yn1,B,'round','satur')+QFix(a2*yn2,B,'round','satur');
    y(n) = QFix(y(n),B,'round','satur');
end
% Plotting commands follow
% Overflow limit cycle
for n = m+3
    yn1 = y(n-1); yn2 = y(n-2);
    y(n) = a1*yn1 + a2*yn2;
    y(n) = QFix(y(n),B,'round','twosc');
end
% Plotting commands follow
```

The resulting plots are shown in Figure 10.12. As expected, the infinite-precision implementation has no limit cycles. The granular limit cycles are of smaller amplitudes. Clearly, the overflow limit cycles have large amplitudes spanning the  $-1$  to  $1$  range of the quantizers.  $\square$

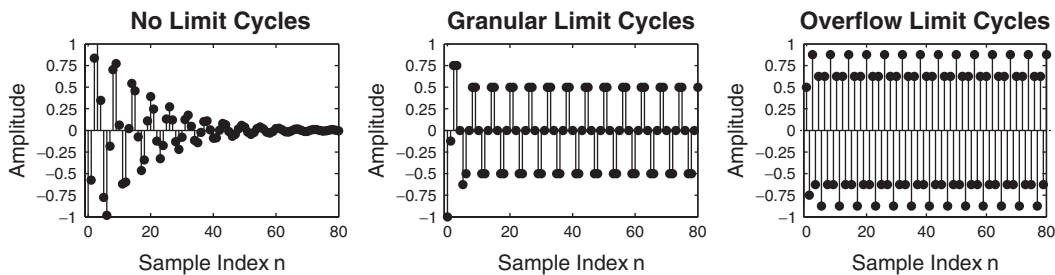


**FIGURE 10.12** Comparison of limit cycles in Example 10.8

As shown in these examples, the limit-cycle behaviors of many different filters can be studied for different quantizer characteristics using the MATLAB function `QFix`.

#### 10.2.4 MULTIPLICATION QUANTIZATION ERROR

A multiplier element in the filter implementation can introduce additional quantization errors since multiplication of two  $B$ -bit fractional numbers results in a  $2B$ -bit fraction and must be quantized to a  $B$ -bit fraction. Consider a multiplier in fixed-point arithmetic with  $B = 8$ . The number  $\frac{1}{\sqrt{3}}$  is represented as 0.578125 in decimal. The square of 0.578125 rounded to 8 bits is 0.3359375 (which should not be confused with  $1/3$  rounded to 8 bits, which is 0.33203125). The additional error in the squaring operation is

$$0.3359375 - (0.578125)^2 = 0.001708984375$$

This additional error is termed as the *multiplication quantization error*. Its statistically equivalent model is similar to that of the A/D quantization error model, as shown in Figure 10.13.

**Statistical model** Consider the  $B$ -bit quantizer block following the multiplier element shown in Figure 10.13a. The sequence  $x(n)$  and the constant  $c$  are quantized to  $B$  fractional bits prior to multiplication (as would be the case in a typical implementation). The multiplied sequence  $\{cx(n)\}$  is quantized to obtain  $y(n)$ . We want to replace the quantizer by a simpler linear system model shown in Figure 10.13b, in which  $y(n) = cx(n) + e(n)$ , where  $e(n)$  is a multiplication quantization error. For analysis purposes we assume that the conditions on  $e(n)$  are similar to those for the A/D quantization error:

1. The random signal  $e(n)$  is *uncorrelated* with the sequence  $x(n)$  for rounding operation (or two's-complement truncation operation) in the quantizer.
2. The signal  $e(n)$  is an independent process (i.e., the samples are independent of each other).
3. The probability density function (pdf)  $f_E(e)$  of  $e(n)$  for each  $n$  is uniformly distributed over the interval of width  $\Delta = 2^{-B}$ , which is the quantizer resolution.

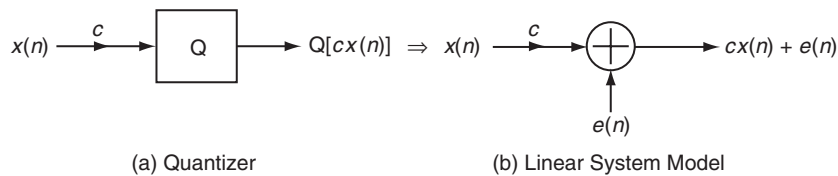


**FIGURE 10.13** Linear system model for multiplication quantization error

We will emphasize the rounding operation for the rest of this section. Based on the above model assumptions, the results given in (10.7), (10.9), and (10.10) are also applicable for the multiplication quantization error  $e(n)$ .

We offer the following two MATLAB examples to illustrate this model. A more thorough investigation of this error can be found in Rabiner and Gold [83].

- **EXAMPLE 10.9** Consider the sequence given in Example 10.1, which is repeated here:

$$x(n) = \frac{1}{3} [\sin(n/11) + \sin(n/31) + \cos(n/67)]$$

This signal is multiplied by  $c = 1/\sqrt{2}$ , quantized to  $B$  bits, and the resulting multiplication is quantized to  $B$  bits with rounding. Using the `StatModelR` function and 500,000 samples, compute and analyze normalized errors  $e_1(n)$  and  $e_2(n)$ , defined in (10.2) and (10.3), respectively.

**Solution** The following MATLAB script computes error distribution, for  $B = 6$  bits.

```
clear; close all;
% Example parameters
B = 6; N = 500000; n = [1:N]; bM = 7;
xn = (1/3)*(sin(n/11)+sin(n/31)+cos(n/67)); clear n;
c = 1/sqrt(2);
% Signal and coefficient quantization
xq = (round(xn*(2^B)))/(2^B); c = (round(c*(2^B)))/(2^B);
cxq = c*xq; % Multiplication of constant and signal
% Quantization error analysis
[H1,H2,Q, estat] = StatModelR(cxq,B,N);
H1max = max(H1); H1min = min(H1); % Max and min of H1
H2max = max(H2); H2min = min(H2); % Max and min of H2
```

The plots of the resulting histogram are shown in Figure 10.14. For the sinusoidal signal, when  $B = 6$  bits, the error samples are not uniformly distributed and the samples are not independent. The means of  $e(n)$  and  $[e(n) + e(n-1)]/2$  are small. Their standard deviations are 0.0045105 and 0.0031059, which do not agree with (10.10). The corresponding plots for  $B = 12$  bits are shown in Figure 10.15, from which we observe that the quantization error sequence appears to satisfy the model assumptions for  $B \geq 12$  bits. The means of  $e(n)$  and  $[e(n) + e(n-1)]/2$  are very small, and their standard deviations agree closely with (10.10). □

- **EXAMPLE 10.10** Let  $x(n)$  be an independent and identically distributed random sequence whose samples are uniformly distributed over the  $[-1, 1]$  interval. Using 500,000 samples to minimize any statistical variations, analyze normalized errors.

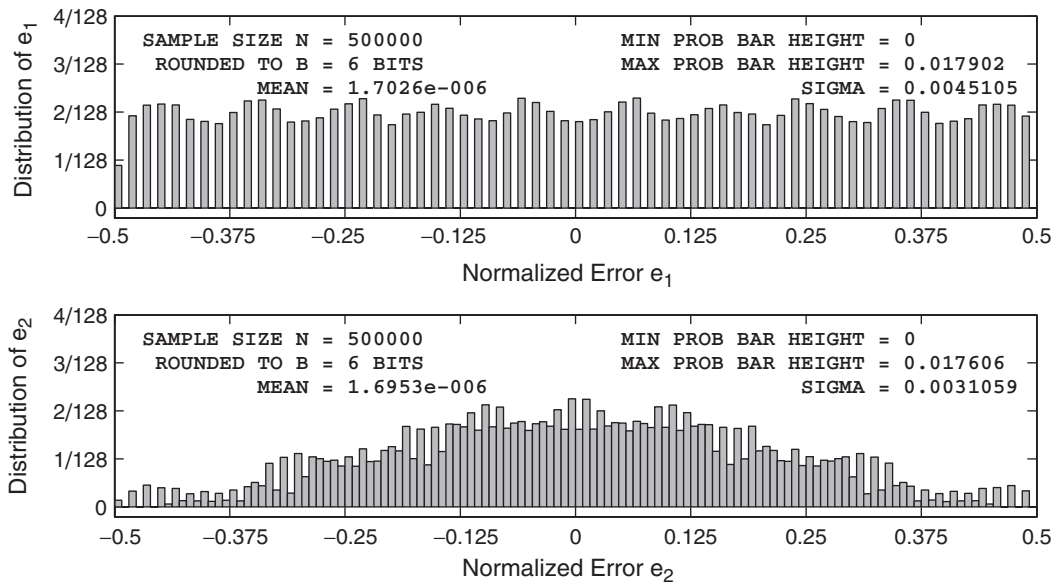


**FIGURE 10.14** Multiplication quantization error distribution for the sinusoidal signal in Example 10.9,  $B = 6$  bits

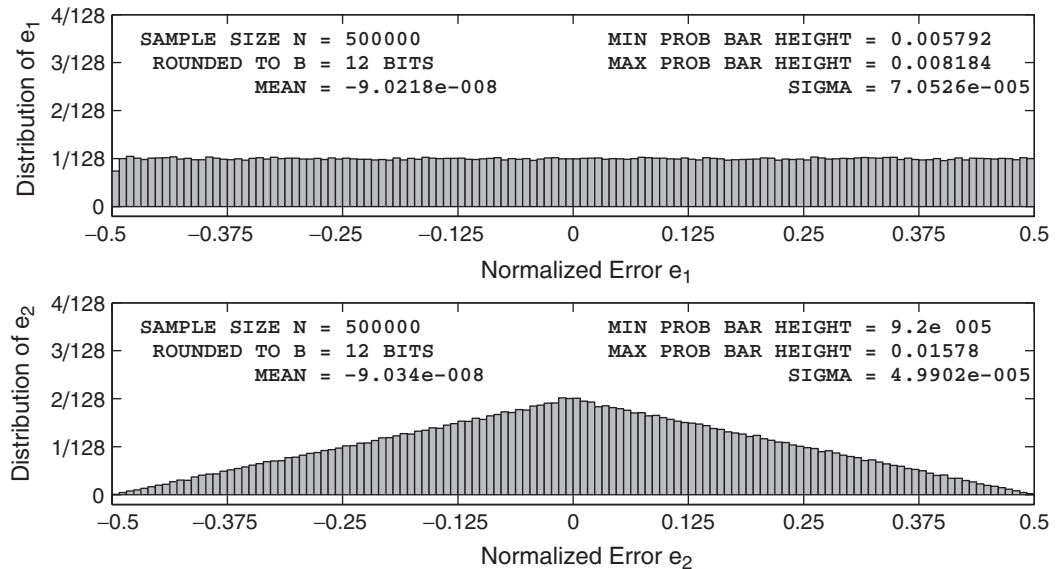


**FIGURE 10.15** Multiplication quantization error distribution for the sinusoidal signal in Example 10.9,  $B = 12$  bits

**Solution**

The following MATLAB script computes the distributions for  $B = 6$  bits.

```
clear; close all;
% Example parameters
B = 6; N = 500000; xn = (2*rand(1,N)-1); bM = 7; c = 1/sqrt(2);
% Signal and coefficient quantization
xq = (round(xn*(2^B)))/(2^B); c = (round(c*(2^B)))/(2^B);
cxq = c*xq; % Multiplication of constant and signal
% Quantization error analysis
[H1,H2,Q, estat] = StatModelR(cxq,B,N);
H1max = max(H1); H1min = min(H1); % Max and min of H1
H2max = max(H2); H2min = min(H2); % Max and min of H2
```

The plots of the resulting histogram are shown in Figure 10.16. Even for  $B = 6$  bits, the error samples appear to be uniformly distributed (albeit in discrete fashion) and are independent of each other. The corresponding plots for  $B = 12$  bits are shown in Figure 10.17. It is clear for  $B = 12$  bits that the quantization error samples are independent and uniformly distributed. Readers should verify the statistics of these errors given in (10.7), (10.9), and (10.10).  $\square$

From these two examples, we conclude that the statistical model for the multiplication quantization error, with its stated assumptions, is a very good model for random signals when the number of bits in the quantizer is large enough.

### 10.2.5 STATISTICAL ROUND-OFF NOISE—FIXED-POINT ARITHMETIC

In this and the next section, we will consider the round-off effects on IIR filters using the multiplication quantization error model developed in the previous section. Since we emphasize the rounding operation, this model is also known as a round-off noise model. We will limit ourselves to the first- and second-order filters since practical realizations involve first- or second-order sections.

**First-order filter** Consider the first-order filter shown in Figure 10.18a. When a quantizer  $Q[\cdot]$  is introduced after the multiplier, the resulting filter model is shown in Figure 10.18b, which is a nonlinear system. When  $Q[\cdot]$  is a quantizer based on the round-off characteristics, then its effect is to add a zero-mean, stationary white noise sequence  $e(n)$  at the multiplier output as shown in Figure 10.18c.

Let  $q(n)$  be the response due to  $e(n)$ , and let  $h_e(n)$  be the noise impulse response (i.e., between  $e(n)$  and  $q(n)$ ). For the system in Figure 10.18c,

$$h_e(n) = h(n) = \alpha^n u(n) \quad (10.38)$$

Using (10.12) and (10.7), the mean of  $q(n)$  is

$$m_q = m_e \sum_0^{\infty} h_e(n) = 0 \quad (10.39)$$

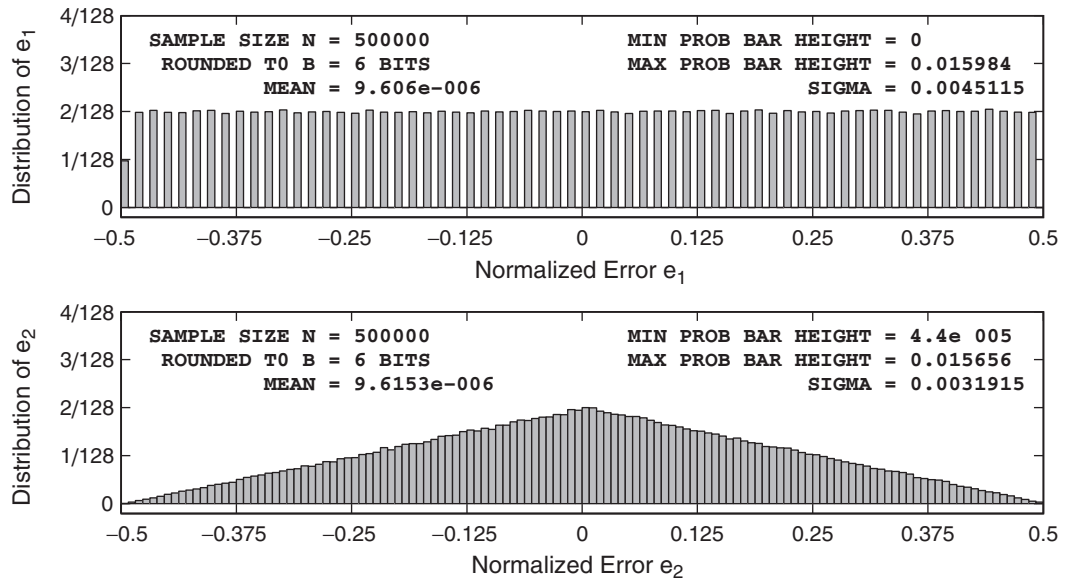


**FIGURE 10.16** Multiplication quantization error distribution for the random signal in Example 10.10,  $B = 6$  bits

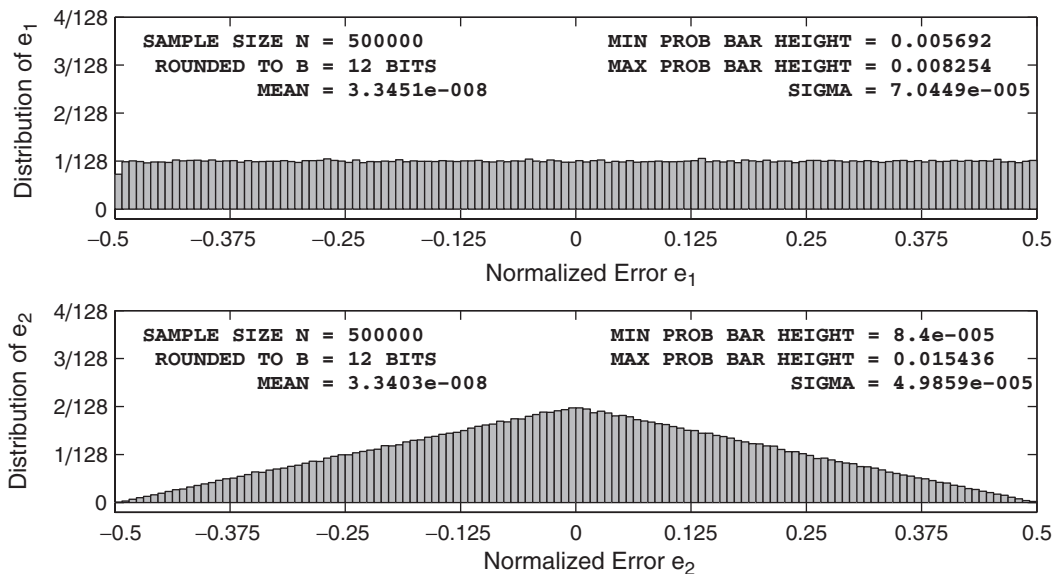


**FIGURE 10.17** Multiplication quantization error distribution for the random signal in Example 10.10,  $B = 12$  bits

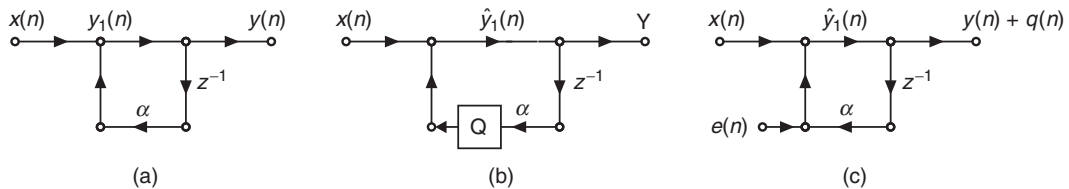


**FIGURE 10.18** First-order IIR filter: (a) structure, (b) structure with quantizer, (c) round-off noise model

Similarly, using (10.15), the variance of  $q(n)$  is

$$\sigma_q^2 = \sigma_e^2 \left( \sum_0^{\infty} |h_e(n)|^2 \right) \quad (10.40)$$

Substituting  $\sigma_e^2 = 2^{-2B}/12$  for rounding and  $h_e(n)$  from (10.38), we obtain

$$\sigma_q^2 = \frac{2^{-2B}}{12} \left( \sum_0^{\infty} |\alpha^n|^2 \right) = \frac{2^{-2B}}{12} \sum_0^{\infty} (|\alpha|^2)^n = \frac{2^{-2B}}{12(1 - |\alpha|^2)} \quad (10.41)$$

which is the output noise power due to rounding following the multiplication.

However, we also have to prevent a possible overflow following the adder. Let  $y_1(n)$  be the signal at the output of the adder in Figure 10.18a, which in this case is equal to  $y(n)$ . Now the upper bound on  $y_1(n)$  is

$$|y_1(n)| = |y(n)| = \left| \sum_0^{\infty} h(k) x(n-k) \right| \leq \sum_0^{\infty} |h(k)| |x(n-k)| \quad (10.42)$$

Let the input sequence be bounded by  $X_{\max}$  (i.e.,  $|x(n)| \leq X_{\max}$ ). Then

$$|y_1(n)| \leq X_{\max} \sum_0^{\infty} |h(k)| \quad (10.43)$$

Since  $y_1(n)$  is represented by  $B$  fraction bits, we have  $|y_1(n)| \leq 1$ . The condition (10.43) can be satisfied by requiring

$$X_{\max} = \frac{1}{\sum_0^{\infty} |h(k)|} = \frac{1}{1/(1 - |\alpha|)} = 1 - |\alpha| \quad (10.44)$$

Thus to prevent overflow,  $x(n)$  must satisfy

$$-(1 - |\alpha|) \leq x(n) \leq (1 - |\alpha|) \quad (10.45)$$

Thus the input must be scaled before it is applied to the filter as shown in Figure 10.19.

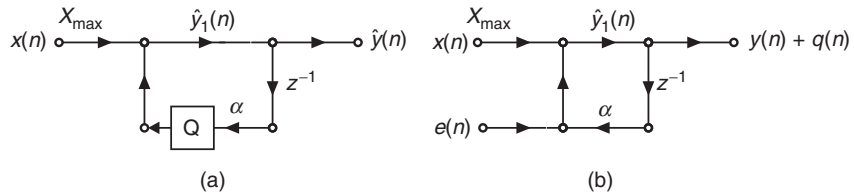


**FIGURE 10.19** Scaled first-order IIR filter: (a) structure with quantizer, (b) round-off noise model

**Signal-to-noise ratio** We will now compute the finite word-length effect in terms of the output signal-to-noise ratio (SNR). We assume that there is no overflow at the output by properly scaling  $x(n)$ . Let  $x(n)$  be a stationary white sequence, uniformly distributed between  $[-(1 - |\alpha|), (1 - |\alpha|)]$ . Then

$$m_x = 0 \quad \text{and} \quad \sigma_x^2 = \frac{(1 - |\alpha|)^2}{3} \quad (10.46)$$

Therefore,  $y(n)$  is also a stationary random sequence with mean  $m_y = 0$  and

$$\sigma_y^2 = \sigma_x^2 \sum_0^\infty |h(n)|^2 = \frac{(1 - |\alpha|)^2}{3} \frac{1}{1 - |\alpha|^2} = \frac{(1 - |\alpha|)^2}{3(1 - |\alpha|^2)} \quad (10.47)$$

Using (10.41) and (10.47), the output SNR is

$$\begin{aligned} \text{SNR} &\triangleq \frac{\sigma_y^2}{\sigma_q^2} = \frac{(1 - |\alpha|)^2}{3(1 - |\alpha|^2)} \frac{12(1 - |\alpha|^2)}{2^{-2B}} \\ &= 4(2^{2B})(1 - |\alpha|)^2 = 2^{2(B+1)}(1 - |\alpha|)^2 \end{aligned} \quad (10.48)$$

or the SNR in dB is

$$\text{SNR}_{\text{dB}} \stackrel{\Delta}{=} 10 \log_{10}(\text{SNR}) = 6.02 + 6.02B + 20 \log_{10}(1 - |\alpha|) \quad (10.49)$$

Let  $\delta = 1 - |\alpha|$ , which is the distance of the pole from the unit circle. Then

$$\text{SNR}_{\text{dB}} = 6.02 + 6.02B + 20 \log_{10}(\delta) \quad (10.50)$$

which is a very informative result. First, it shows that the SNR is directly proportional to  $B$  and increases by about 6 dB for each additional bit added to the word length. Second, the SNR is also directly proportional to the distance  $\delta$ . The smaller the  $\delta$  (or nearer the pole to the unit circle), the smaller is the SNR, which is a consequence of the filter characteristics. As an example, if  $B = 6$  and  $\delta = 0.05$ , then  $\text{SNR} = 16.12$  dB, and if  $B = 12$  and  $\delta = 0.1$ , then  $\text{SNR} = 58.26$  dB.

### 10.2.6 ANALYSIS USING MATLAB

To analyze the properties of the round-off errors in IIR filters, we will simulate them using the MATLAB function `QFix` with quantization mode '`'round'` and overflow mode '`'satur'`'. If proper scaling to avoid overflow is performed, then only the multiplier output needs to be quantized at each  $n$  without worrying about the overflow. However, we will still saturate the final sum to avoid any unforeseen problems. In previous simulations, we could perform the quantization operations on vectors (i.e., perform parallel processing). Since IIR filters are recursive filters and since each error is fed back into the system, vector operation is generally not possible. Hence the filter output will be computed sequentially from the first to the last sample. For a large number of samples, this implementation will slow the execution speed in MATLAB since MATLAB is optimized for vector calculations. However, for newer fast processors, the execution time is within a few seconds. These simulation steps are detailed in the following example.

- **EXAMPLE 10.11** Consider the model given in Figure 10.19b. We will simulate this model in MATLAB and investigate its output error characteristics. Let  $a = 0.9$ , which will be quantized to  $B$  bits. The input signal is uniformly distributed over the  $[-1, +1]$  interval and is also quantized to  $B$  bits prior to filtering. The scaling factor  $X_{\max}$  is computed from (10.44). Using 100,000 signal samples and  $B = 6$  bits, the following MATLAB script computes the true output  $y(n)$ , the quantized output  $\hat{y}(n)$ , the output error  $q(n)$ , and the output SNR.

```

close all; clc;

% Example Parameters
B = 6; % # of fractional bits
N = 100000; % # of samples
xn = (2*rand(1,N)-1); % Input sequence - uniform distribution
a = 0.9; % Filter parameter
Xm = 1-abs(a); % Scaling factor

% Local variables
bM = 7; DbM = 2^bM; % Bin parameter
BB = 2^B; % Useful factor in quantization
M = round(DbM/2); % Half number of bins
bins = [-M+0.5:1:M-0.5]; % Bin values from -M to M
Q = bins/DbM; % Normalized bins
YTN = 2^(-bM); % Ytick marks interval
YLM = 4*YTN; % Yaxis limit

% Quantize the input and the filter coefficients
xn = QFix(Xm*xn,B,'round','satur'); % Scaled input quant to B bits
a = QFix(a,B,'round','satur'); % a quantized to B bits

```

```
% Filter output without multiplication quantization
yn = filter(1,[1,-a],xn); % Output using filter routine

% Filter output with multiplication quantization
yq = zeros(1,N); % Initialize quantized output array
yq(1) = xn(1); % Calculation of the first sample yq(1)
for I = 2:N;
    A1Y = QFix(a*yq(I-1),B,'round','satur'); % Quantization of a*y(n-1)
    yq(I) = QFix(A1Y+xn(I),B,'round','satur'); % I-th sample yq(I)
end

% Output Error Analysis
en = yn-yq; % Output error sequence
varyn = var(yn); varen = var(en); % Signal and noise power
eemax = max(en); eemin = min(en); % Maximum and minimum of the error
enmax = max(abs([eemax,eemin])); % Absolute maximum range of the error
enavg = mean(en); enstd = std(en); % Mean and std dev of the error
en = round(en*(2^bM)/(2*enmax)+0.5); % Normalized en (integer between -M & M)
en = sort([en,-M:1:(M+1)]); %
H = diff(find(diff(en)))-1; % Error histogram
H = H/N; % Normalized histogram
Hmax = max(H); Hmin = min(H); % Max and min of the normalized histogram

% Output SNRs
SNR_C = 10*log10(varyn/varen); % Computed SNR
SNR_T = 6.02 + 6.02*B + 20*log10(Xm); % Theoretical SNR
```

The part of the script not shown above also computes and plots the normalized histogram of the output error and prints the statistical values in the plot, as shown in Figure 10.20. The error appears to have a Gaussian distribution, which is to be expected. The exact value of the output SNR is 22.14 dB, which agrees with the computed value of 22.21 dB. Similar results done for  $B = 12$  bits are shown in Figure 10.21. Again, the simulation results agree with the model results.  $\square$

**Second-order filter** Similar analysis can be done for second-order filters with poles near the unit circle. Let the two poles be at complex locations  $re^{j\theta}$  and  $re^{-j\theta}$ . Then the system function of the filter is given by

$$H(z) = \frac{1}{(1 - re^{j\theta}z^{-1})(1 - re^{-j\theta}z^{-1})} = \frac{1}{1 - 2r \cos(\theta) z^{-1} + r^2 z^{-2}} \quad (10.51)$$

with impulse response

$$h(n) = \frac{r^n \sin\{(n+1)\theta\}}{\sin(\theta)} u(n) \quad (10.52)$$

The difference equation from (10.51) is given by

$$y(n) = x(n) - a_1 y(n-1) - a_2 y(n-2); \quad a_1 = -2r \cos(\theta), \quad a_2 = r^2 \quad (10.53)$$

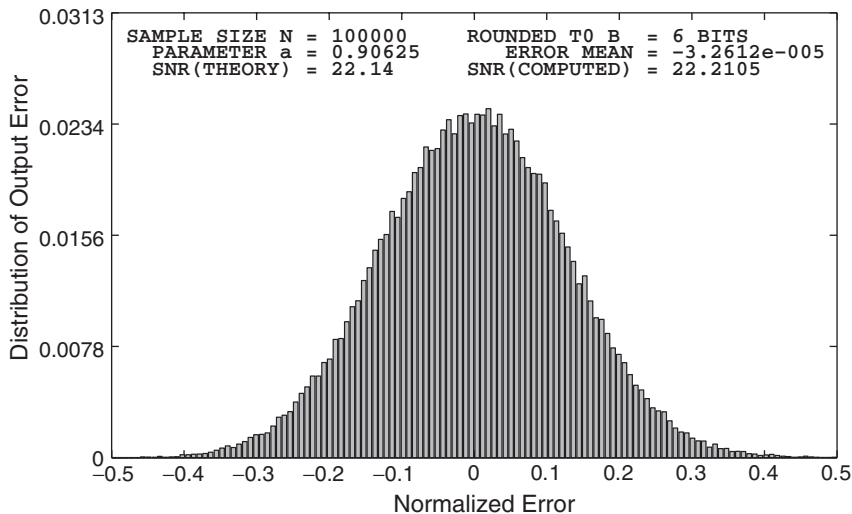


**FIGURE 10.20** Multiplication quantization effects in the first-order IIR filter in Example 10.11,  $B = 6$  bits

which requires two multiplications and two additions, as shown in Figure 10.22a. Thus there are two noise sources and two possible locations for overflow. The round-off noise model for quantization following

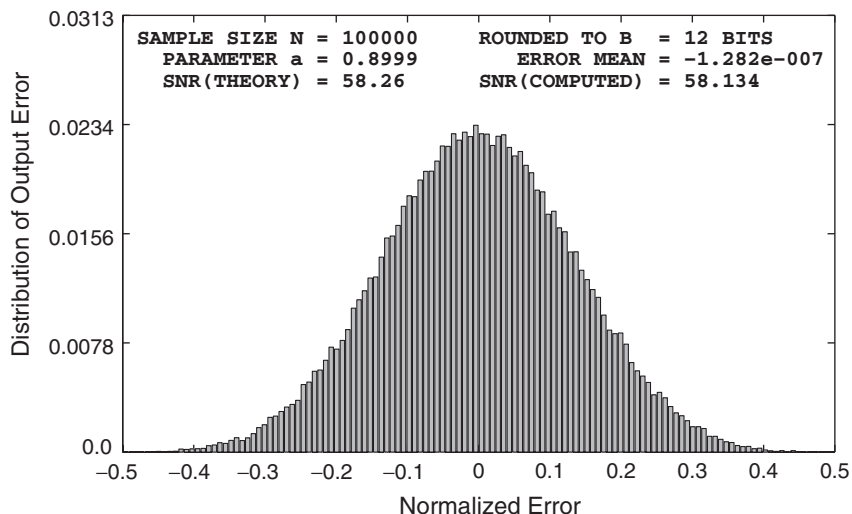


**FIGURE 10.21** Multiplication quantization effects in the first-order IIR filter in Example 10.11,  $B = 12$  bits

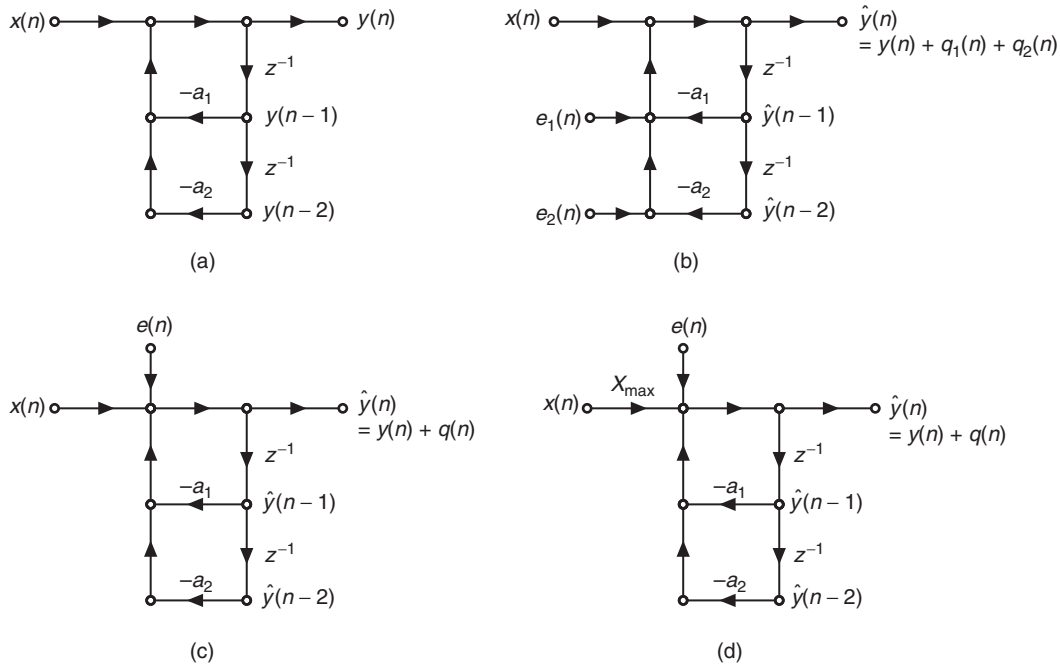


**FIGURE 10.22** Second-order IIR filter: (a) structure, (b) round-off noise model, (c) simplified model, (d) scaled simplified model

the two multipliers is shown in Figure 10.22b, where the responses  $q_1(n)$  and  $q_2(n)$  are due to noise sources  $e_1(n)$  and  $e_2(n)$ , respectively. We can combine two noise sources into one. However, to avoid overflow, we have to scale signals at the input of each adder, which can complicate this consolidation of sources.

In modern DSP chips, the intermediate results of multiply-add operations are stored in a multiply-accumulate (MAC) unit that has a double-precision register to accumulate sums. The final sum (which for Figure 10.22b is at the output of the top adder) is quantized to obtain  $\hat{y}(n)$ . This implementation not only reduces the total multiplication quantization noise but also makes the resulting analysis easier. Assuming this modern implementation, the resulting simplified model is shown in Figure 10.22c, where  $e(n)$  is the single noise source that is uniformly distributed between  $[-2^{-(B+1)}, 2^{-(B+1)}]$  and  $q(n)$  is the response due to  $e(n)$ . Note that  $e(n) \neq e_1(n) + e_2(n)$  and that  $q(n) \neq q_1(n) + q_2(n)$ . The only overflow that we have to worry about is at the output of the top adder, which can be controlled by scaling the input sequence  $x(n)$  as shown in Figure 10.22d. Now the round-off noise analysis can be carried out in a fashion similar to that of the first-order filter. The details, however, are more involved due to the impulse response in (10.52).

**Signal-to-noise ratio** Referring to Figure 10.22d, the noise impulse response  $h_e(n)$  is equal to  $h(n)$ . Hence the output round-off noise power is given by

$$\sigma_q^2 = \sigma_e^2 \sum_{n=0}^{\infty} |h(n)|^2 = \frac{2^{-2B}}{12} \sum_{n=0}^{\infty} |h(n)|^2 \quad (10.54)$$

Since  $x(n)$  is quantized, we have  $|x(n)| \leq 1$ . It is then scaled by  $X_{\max}$  to avoid overflow in the adder. Hence the output signal power is given by

$$\sigma_y^2 = X_{\max}^2 \sigma_x^2 \sum_{n=0}^{\infty} |h(n)|^2 = \frac{X_{\max}^2}{3} \sum_{n=0}^{\infty} |h(n)|^2 \quad (10.55)$$

assuming that  $x(n)$  is uniformly distributed over  $[-1, +1]$ . Hence the output SNR is given by

$$\text{SNR} = \frac{\sigma_y^2}{\sigma_q^2} = 4(2^{2B}) X_{\max}^2 = 2^{2(B+1)} X_{\max}^2 \quad (10.56)$$

or

$$\text{SNR}_{\text{dB}} = 6.02 + 6.02B + 20 \log_{10} X_{\max} \quad (10.57)$$

Following (10.43), (10.44), and (10.45), the scaling factor  $X_{\max}$  is given by

$$X_{\max} = \frac{1}{\sum_{n=0}^{\infty} |h(n)|} \quad (10.58)$$

which is not easy to compute. However, lower and upper bounds on  $X_{\max}$  are easy to obtain. From (10.52), the upper bound on the denominator of (10.58) is given by

$$\sum_{n=0}^{\infty} |h(n)| = \frac{1}{\sin \theta} \sum_{n=0}^{\infty} r^n |\sin[(n+1)\theta]| \leq \frac{1}{\sin \theta} \sum_{n=0}^{\infty} r^n = \frac{1}{(1-r) \sin \theta} \quad (10.59)$$

or the lower bound on  $X_{\max}$  is given by

$$X_{\max} \geq (1-r) \sin \theta \quad (10.60)$$

The lower bound on the denominator of (10.58) is obtained by noting that

$$|H(e^{j\omega})| = \left| \sum_{n=0}^{\infty} h(n) e^{-jn\omega} \right| \leq \sum_{n=0}^{\infty} |h(n)|$$

Now from (10.51), the magnitude  $|H(e^{j\omega})|$  is given by

$$|H(e^{j\omega})| = \left| \frac{1}{1 - 2r \cos(\theta)e^{-j\omega} + r^2 e^{-j2\omega}} \right|$$

which has the maximum value at the resonant frequency  $\omega = \theta$ , which can be easily obtained. Hence

$$\sum_{n=0}^{\infty} |h(n)| \geq |H(e^{j\theta})| = \frac{1}{(1-r)\sqrt{1+r^2 - 2r \cos(2\theta)}} \quad (10.61)$$

or the upper bound on  $X_{\max}$  is given by

$$X_{\max} \leq (1-r)\sqrt{1+r^2 - 2r \cos(2\theta)} \quad (10.62)$$

Substituting (10.60) and (10.62) in (10.56), the output SNR is upper and lower bounded by

$$2^{2(B+1)}(1-r)^2 \sin^2 \theta \leq \text{SNR} \leq 2^{2(B+1)}(1-r)^2(1+r^2 - 2r \cos 2\theta) \quad (10.63)$$

Substituting  $1-r = \delta \ll 1$  and after some simplification, we obtain

$$2^{2(B+1)}\delta^2 \sin^2 \theta \leq \text{SNR} \leq 4 \left(2^{2(B+1)}\right) \delta^2 \sin^2 \theta \quad (10.64)$$

or the difference between the upper and lower SNR bounds is about 6 dB. Once again, the output SNR is directly proportional to  $B$  and  $\delta$ . Furthermore, it also depends on the angle  $\theta$ . Some of these observations are investigated in Example 10.12.

### 10.2.7 ANALYSIS USING MATLAB

We will again simulate round-off errors using the MATLAB function `QFix` with quantization mode '`round`' and overflow mode '`satur`'. Since a MAC architecture is assumed, we do not have to quantize the intermediate results and worry about overflow. Only the final sum needs to be quantized with saturation. These operations are also simulated in sequential fashion, which has an impact on execution speed. The simulation steps for the second-order filter are detailed in the following example.

- EXAMPLE 10.12** Consider the model given in Figure 10.22d. We will simulate this model in MATLAB and investigate its output error characteristics. Let  $r = 0.9$  and  $\theta = \pi/3$ , from which filter parameters are computed and quantized to  $B$  bits. The input signal is uniformly distributed over the  $[-1, +1]$  interval and is also quantized to  $B$  bits prior to filtering. The scaling factor  $X_{\max}$  is determined using (10.58), which can be obtained in MATLAB by computing the impulse response for a sufficiently large number of samples. Using 100,000 signal samples and  $B = 6$  bits, the following MATLAB script computes the true output SNR, the computed SNR, and the lower and upper bounds of the SNR.

```

close all; clc;

% Example Parameters
B = 12; % # of fractional bits
N = 100000; % # of samples
xn = (2*rand(1,N)-1); % Input sequence - Uniform
r = 0.9; theta = pi/3;% Pole locations

% Computed Parameters
p1 = r*exp(j*theta); % Poles
p2 = conj(p1); %
a = poly([p1,p2]); % Filter parameters
hn = filter(1,a,[1,zeros(1,1000)]); % Imp res
Xm = 1/sum(abs(hn)); % Scaling factor
Xm_L = (1-r)*sin(theta); % Lower bound
Xm_U = (1-r)*sqrt(1+r*r-2*r*cos(2*theta)); % Upper bound

% Local variables
bM = 7; DbM = 2^bM; % Bin parameter
BB = 2^B; % Useful factor in quantization
M = round(DbM/2); % Half number of bins
bins = [-M+0.5:1:M-0.5]; % Bin values from -M to M
Q = bins/DbM; % Normalized bins
YTN = 2^(-bM); % Ytick marks interval
YLM = 4*YTN; % Yaxis limit

% Quantize the input and the filter coefficients
xn = QFix(Xm*xn,B,'round','satur'); % Scaled input quant B bits
a = QFix(a,B,'round','satur'); % a quantized to B bits
a1 = a(2); a2 = a(3);

% Filter output without multiplication quantization
yn = filter(1,a,xn); % output using filter routine

% Filter output with multiplication quantization
yq = zeros(1,N); % Initialize quantized output array
yq(1) = xn(1); % sample yq(1)
yq(2) = QFix((xn(2)-a1*yq(1)),B,'round','satur'); % sample yq(2)
for I = 3:N;
    yq(I) = xn(I)-a1*yq(I-1)-a2*yq(I-2); % Unquantized sample
    yq(I) = QFix(yq(I),B,'round','satur'); % Quantized sample
end

% Output Error Analysis
en = yn-yq; % Output error sequence
varyn = var(yn); varen = var(en); % Signal and noise power
eemax = max(en); eemin = min(en); % Maximum and minimum of the error

```

```

enmax = max(abs([eemax,eemin])); % Absolute maximum range of the error
enavg = mean(en); enstd = std(en); % Mean and std dev of the error
en = round(en*(2^bM)/(2*enmax)+0.5); % Normalized en (integer between -M & M)
en = sort([en,-M:1:(M+1)]);
H = diff(find(diff(en))-1); % Error histogram
H = H/N; % Normalized histogram
Hmax = max(H); Hmin = min(H); % Max and Min of the normalized histogram

% Output SNRs
SNR_C = 10*log10(varyn/varen); % Computed SNR
SNR_T = 6.02 + 6.02*B + 20*log10(Xm); % Theoretical SNR
SNR_L = 6.02 + 6.02*B + 20*log10(Xm_L); % Lower SNR bound
SNR_U = 6.02 + 6.02*B + 20*log10(Xm_U); % Upper SNR bound

```

The part of the script not shown above also computes and plots the normalized histogram of the output error and prints the statistical values in the plot, as shown in Figure 10.23. The error again has a Gaussian distribution. The exact value of the output SNR is 25.22 dB, which agrees with the computed value of 25.11 dB and lies between the lower bound of 20.89 dB and the upper bound of 26.47 dB. Similar results done for  $B = 12$  bits are shown in Figure 10.24. Again, the simulation results agree with the model results.  $\square$

### 10.2.8 HIGHER-ORDER FILTERS

The analysis of the quantization effects in a second-order filter can be applied directly to higher-order filters based on a parallel realization.

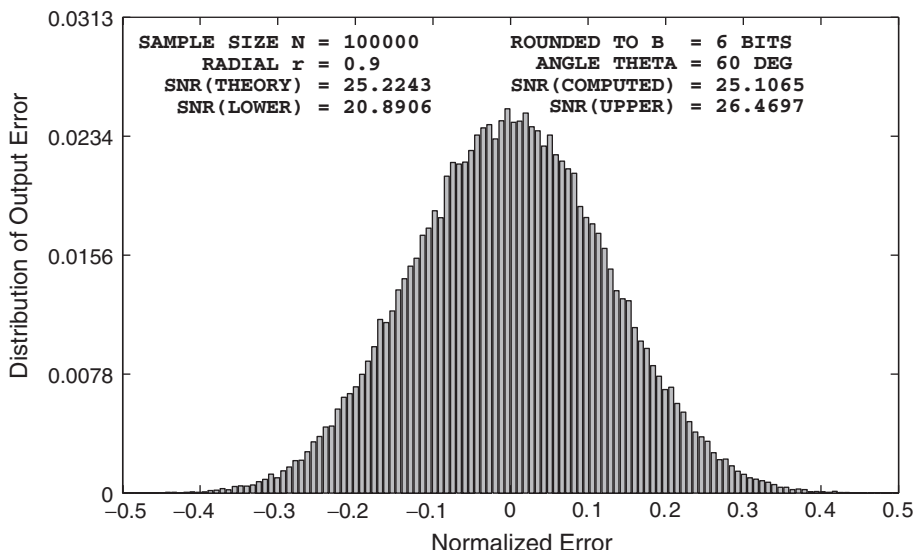


**FIGURE 10.23** Multiplication quantization effects in the first-order IIR filter in Example 10.12,  $B = 6$  bits

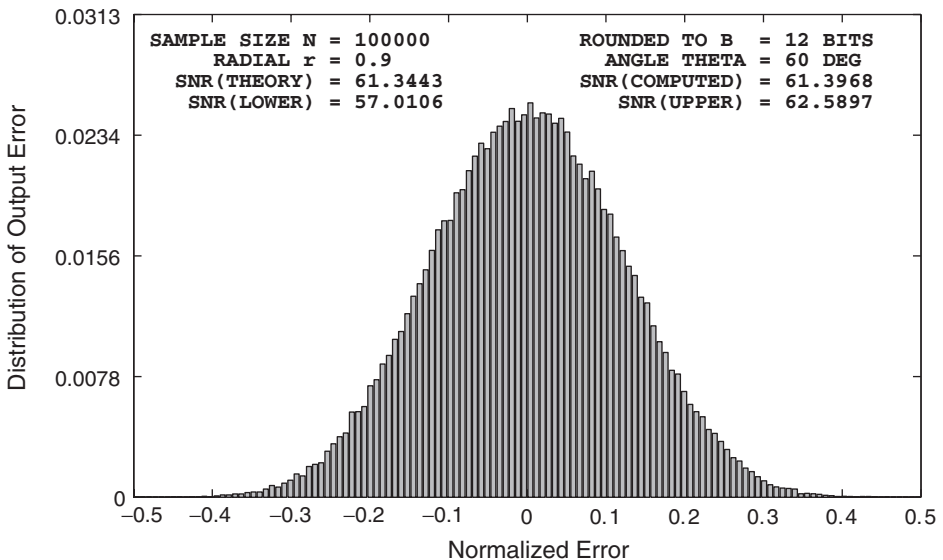


**FIGURE 10.24** Multiplication quantization effects in the first-order IIR filter in Example 10.12,  $B = 12$  bits

In this case, each second-order filter section is independent of all the other sections, and therefore the total quantization noise power at the output of the parallel structure is simply the linear sum of the quantization noise powers of each of the individual sections. On the other hand, the cascade realization is more difficult to analyze because the noise generated in any second-order filter section is filtered by the succeeding sections. To minimize the total noise power at the output of the high-order filter, a reasonable strategy is to place the sections in the order of decreasing maximum frequency gain. In this case, the noise power generated in the early high-gain section is not boosted significantly by the latter sections. Using the MATLAB techniques developed in the previous sections, it is easier to simulate finite word-length implementations and determine the output SNR for a given cascade structure.

### 10.2.9 STATISTICAL ROUND-OFF NOISE—FLOATING-POINT ARITHMETIC

As stated in Chapter 6, the floating-point arithmetic gives an error that is relative to the magnitude rather than an absolute error. This results in a multiplicative noise rather than additive noise—that is, from (6.61),

$$\mathcal{Q}[x(n)] = x(n) + \varepsilon(n)x(n) = x(n)\{1 + \varepsilon(n)\} \quad (10.65)$$

with

$$-2^{-B} < \varepsilon(n) \leq 2^{-B} \quad (10.66)$$

for a  $(B + 1)$ -bit mantissa. Hence the mean of the relative error is  $m_\varepsilon = 0$  and its variance is

$$\sigma_\varepsilon^2 = \frac{2^{-2B}}{3} \quad (10.67)$$

Since MATLAB is implemented in IEEE-754 floating-point arithmetic, all simulations that we perform are IEEE-754 floating-point calculations. It is difficult (if not impossible) to simulate arbitrary floating-point arithmetic in MATLAB. Therefore, we give theoretical results only.

**First-order filter** Consider a first-order filter as before and shown in Figure 10.25a. For the finite word-length analysis with floating-point arithmetic we need quantizers after both multiplication and addition to account for rounding off in the mantissa, as shown in Figure 10.25b. Hence there are two noise sources in the the statistical model, as shown in Figure 10.25c, where  $e_1(n)$  is the noise source in the multiplier,  $e_2(n)$  is the noise source in the adder,  $\hat{g}(n)$  is an adder sequence prior to quantization, and  $\hat{y}(n)$  is the quantized output. Now

$$e_1(n) = \varepsilon_1(n) \alpha \hat{y}(n - 1) \quad (10.68a)$$

$$e_2(n) = \varepsilon_2(n) \hat{g}(n) \quad (10.68b)$$

where  $\varepsilon_1(n)$  and  $\varepsilon_2(n)$  are the relative errors in the corresponding quantizers. The exact analysis even for the first-order case is tedious; hence we make a few practically reasonable approximations. If the absolute values of the errors are small, then we have  $\hat{y}(n - 1) \approx y(n - 1)$  and  $\hat{g}(n) \approx g(n)$ ; hence from (10.68a) we obtain

$$e_1(n) \approx \alpha \varepsilon_1(n) y(n - 1) \quad (10.69a)$$

$$e_2(n) \approx \varepsilon_2(n) y(n) \quad (10.69b)$$

Furthermore, we make the following assumption about the noise sources:

1.  $\varepsilon_1(n)$  and  $\varepsilon_2(n)$  are white noise sources.
2.  $\varepsilon_1(n)$  and  $\varepsilon_2(n)$  are uncorrelated with each other.

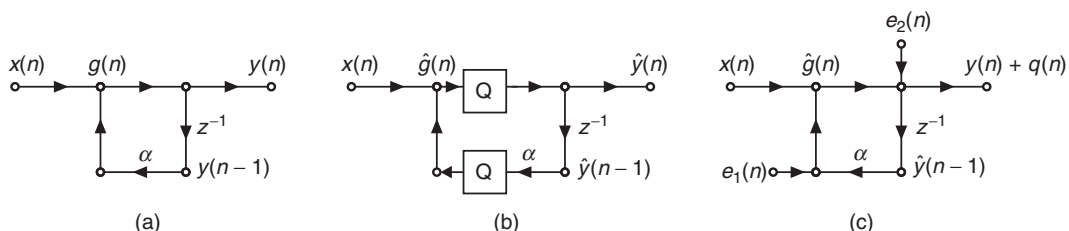


**FIGURE 10.25** First-order IIR filter: (a) structure, (b) finite word-length model for floating-point arithmetic, (c) statistical model for floating-point arithmetic

3.  $\varepsilon_1(n)$  and  $\varepsilon_2(n)$  are uncorrelated with the input  $x(n)$ .
4.  $\varepsilon_1(n)$  and  $\varepsilon_2(n)$  are uniformly distributed between  $-2^{-B}$  and  $2^{-B}$ .

Let  $x(n)$  be a zero-mean, stationary random sequence. Then  $y(n)$  is also a zero-mean, stationary sequence. Hence from (10.69),

$$\sigma_{e_1}^2 = |\alpha|^2 \sigma_{\varepsilon_1}^2 \sigma_y^2 \quad (10.70a)$$

$$\sigma_{e_2}^2 = \sigma_{\varepsilon_2}^2 \sigma_y^2 \quad (10.70b)$$

Let the error in the output due to  $e_1(n)$  be  $q_1(n)$ , and let that due to  $e_2(n)$  be  $q_2(n)$ . Let  $h_1(n)$  and  $h_2(n)$  be the corresponding noise impulse responses. Note that  $h_1(n) = h_2(n) = h(n) = \alpha^n u(n)$ . Then the total error  $q(n)$  is

$$q(n) = q_1(n) + q_2(n) \quad (10.71)$$

with

$$\sigma_q^2 = \sigma_{q_1}^2 + \sigma_{q_2}^2 \quad (10.72)$$

where

$$\sigma_{q_1}^2 = \sigma_{e_1}^2 \sum_0^{\infty} |h_1(n)|^2 \quad \text{and} \quad \sigma_{q_2}^2 = \sigma_{e_2}^2 \sum_0^{\infty} |h_2(n)|^2 \quad (10.73)$$

Hence using (10.72), (10.73), and (10.70),

$$\sigma_q^2 = (\sigma_{e_1}^2 + \sigma_{e_2}^2) \left( \frac{1}{1 - |\alpha|^2} \right) = \sigma_y^2 \left( \frac{1}{1 - |\alpha|^2} \right) (|\alpha|^2 \sigma_{\varepsilon_1}^2 + \sigma_{\varepsilon_2}^2) \quad (10.74)$$

Using  $\sigma_{\varepsilon_1}^2 = \sigma_{\varepsilon_2}^2 = 2^{-2B}/3$ , we obtain

$$\sigma_q^2 = \sigma_y^2 \left( \frac{2^{-2B}}{3} \right) \left( \frac{1 + |\alpha|^2}{1 - |\alpha|^2} \right) \quad (10.75)$$

Therefore,

$$\text{SNR} = \frac{\sigma_y^2}{\sigma_q^2} = 3 (2^{2B}) \left( \frac{1 - |\alpha|^2}{1 + |\alpha|^2} \right) \quad (10.76)$$

or

$$\text{SNR}_{\text{dB}} = 4.77 + 6.02B + 10 \log_{10}(1 - |\alpha|^2) - 10 \log_{10}(1 + |\alpha|^2) \quad (10.77)$$

which is also a very informative result. Some comments are in order.

1. The SNR in (10.76) was derived without assuming any input statistics, Hence the result is valid for a large class of inputs including white-noise, narrow-band, or wide-band signals. The floating-point arithmetic does not have to worry about the scaling or limiting input values, since it can handle a large dynamic range.

2. Using  $0 < \delta = 1 - |\alpha| \ll 1$ , the SNR in (10.77) can be put in the form

$$\text{SNR}_{\text{dB}} \approx 4.77 + 6.02B + 10 \log_{10}(\delta) = O(\delta) \quad (10.78)$$

This is to be compared with the fixed-point result (10.50), where  $\text{SNR} \approx O(\delta^2)$ . Thus the floating-point result is less sensitive to the distance of the pole to the unit circle.

3. In floating-point arithmetic, the output noise variance,  $\sigma_q^2$ , in (10.75) is proportional to  $\sigma_y^2$ . Thus, if the input signal is scaled up, so is the noise variance since  $\sigma_y^2$  is also scaled up. Hence the SNR remains constant. This again should be compared with the fixed-point case (10.41), in which  $\sigma_q^2$  is independent of the input signal. Hence if the signal level increases, then  $\sigma_y^2$  increases, which increases the SNR.

**Second-order filter** Similar analysis can be done for the second-order filter with poles close to the unit circle. If the poles are given by  $re^{\pm j\theta}$ , then we can show that (see [71])

$$\text{SNR} = \frac{\sigma_y^2}{\sigma_q^2} \approx 3(2^{2B}) \frac{4\delta \sin^{2\theta}}{3 + 4\cos\theta} \approx O(\delta) \quad (10.79)$$

where  $\delta = 1 - r$ . This again is an approximate result that works very well in practice. In this case again, the SNR depends on  $\delta$  rather than on  $\delta^2$  as in the fixed-point case.

## 10.3 ROUND-OFF EFFECTS IN FIR DIGITAL FILTERS

---

We will now turn our attention to the finite word-length effects in FIR digital filters. As before, we will consider the fixed-point and floating-point cases separately. We will then conclude this section with some representative examples.

### 10.3.1 FIXED-POINT ARITHMETIC

We will consider the effects on two realizations: direct form and cascade form. There is no parallel form realization for FIR filters, since we do not have a partial fraction expansion, except for the frequency-sampling realization, which can be analyzed using IIR filter techniques. The analysis of FIR filters is much simpler than that for IIR because there are no feedback paths. One consequence of this is the absence of limit cycles.

**Direct-form realization** Consider an FIR filter of length  $M$  (i.e., there are  $M$  samples in the impulse response), which is realized using the direct form as shown in Figure 10.26a. The filter coefficients are the samples of the impulse response  $h(n)$ . We have to introduce quantizers in the vertical branches. If we use the implementation in which each multiplier output is quantized, then we obtain the model shown in Figure 10.26b. On the other hand, if we implement the filter in a typical DSP chip, then the final sum is quantized, as shown in Figure 10.26c. We will separately consider the effects of round-off noise and scaling (to avoid overflow).

**Round-off noise** Let the output of the filter in Figure 10.26b due to round-off errors be  $\hat{y}(n) = y(n) + q(n)$ . Then

$$q(n) = \sum_{k=0}^{M-1} e_k(n) \quad (10.80)$$

where  $e_k(n)$  are the noise sources introduced in each vertical branch to account for the rounding operations. Since these noise sources are all independent and identical, the noise power in  $q(n)$  is given by

$$\sigma_q^2 = \sum_0^{M-1} \sigma_{e_k}^2 = M \sigma_e^2 = M \left( \frac{2^{-2B}}{12} \right) = \frac{M}{3} 2^{-2(B+1)} \quad (10.81)$$

In Figure 10.26c, the output due to the rounding operation is  $\hat{y}(n) = y(n) + e(n)$ . Hence the noise power in this case is given by

$$\sigma_q^2 = \sigma_e^2 = \frac{1}{3} 2^{-2(B+1)} \quad (10.82)$$

which is smaller by a factor of  $M$  compared to (10.81), as expected.

**Scaling to avoid overflow** We assume that the fixed-point numbers have the two's-complement form representation, which is a reasonable assumption. Then we will have to check only the overflow of the total sum. Thus this analysis is the same for both implementations in Figure 10.26 and is similar to that for the IIR filter in (10.42)–(10.44). The upper-bound on  $y(n)$  is obtained as

$$|y(n)| = \left| \sum h(k) x(n-k) \right| \leq X_{\max} \sum |h(n)| \quad (10.83)$$

where  $X_{\max}$  is the upper-bound on  $x(n)$ . To guarantee that  $|y(n)| \leq 1$ , we need the scaling factor  $X_{\max}$  on  $x(n)$  as

$$X_{\max} \leq \frac{1}{\sum |h(n)|} \quad (10.84)$$

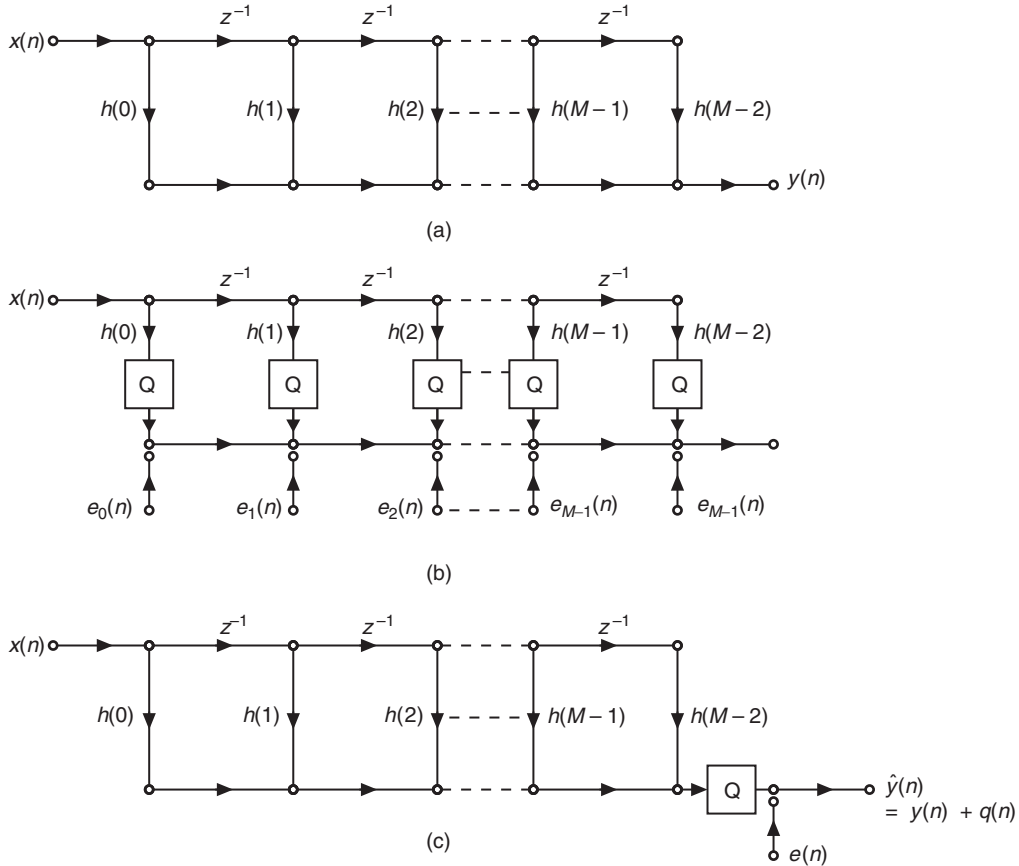


**FIGURE 10.26** Direct form FIR filter: (a) structure, (b) round-off noise model with quantizers after each multiplier, (c) round-off noise mode with one quantizer after the final sum

which is the most conservative scaling factor. There are other scaling factors, depending on the applications—for example, the narrowband signals use

$$X_{\max} \leq \frac{1}{\max |H(e^{j\omega})|}$$

and wideband random signals use

$$X_{\max} \leq \frac{1}{4\sigma_x \sqrt{\sum |h(n)|^2}}$$

Using (10.84) and assuming that  $x(n)$  is uniformly distributed over  $[-X_{\max}, +X_{\max}]$ , the input signal power is given by

$$\sigma_x^2 = \frac{X_{\max}^2}{3} = \frac{1}{3(\sum |h(n)|)^2} \quad (10.85)$$

Furthermore, assuming that  $x(n)$  is also a white sequence, the output signal power is given by

$$\sigma_y^2 = \sigma_x^2 \sum |h(n)|^2 = \frac{1}{3} \frac{\sum |h(n)|^2}{(\sum |h(n)|)^2} \quad (10.86)$$

Thus the output SNR is

$$\text{SNR} = \frac{\sigma_y^2}{\sigma_q^2} = \frac{2^{2(B+1)}}{A} \left[ \frac{\sum |h(n)|^2}{(\sum |h(n)|)^2} \right] \quad (10.87)$$

where  $A = M$  for the model in Figure 10.26b or  $A = 1$  for the model in Figure 10.26c. The corresponding SNR in dB is

$$\text{SNR}_{\text{dB}} = 6.02 + 6.02B + 10 \log_{10} \left( \frac{\sum |h(n)|^2}{(\sum |h(n)|)^2} \right) - 10 \log_{10} A \quad (10.88)$$

### 10.3.2 ANALYSIS USING MATLAB

This simulation in MATLAB can be done in parallel fashion since there is no feedback path for the multiplication quantization errors. Using the function `Qfix` function with '`round`' mode, we will compute the quantized multiplier output. In the case of  $M$  quantizers, assuming two's-complement format, we will use the '`twosc`' mode for each quantizer. Only the final sum will be quantized and saturated. In the case of one quantizer, we need the '`satur`' mode. These simulation steps are detailed in the following example.

- **EXAMPLE 10.13** Let a fourth-order ( $M = 5$ ) FIR filter be given by

$$H(z) = 0.1 + 0.2z^{-1} + 0.4z^{-2} + 0.2z^{-3} + 0.1z^{-4} \quad (10.89)$$

which is implemented as a direct form with  $B = 12$  fractional bit quantizers. Compute SNRs for models in Figure 10.26b and 10.26c and verify them using MATLAB simulations.

#### Solution

We will need the quantities  $\sum |h(n)|^2$  and  $(\sum |h(n)|)^2$ . These quantities should be computed using 12-bit quantization of the filter coefficients. These values

using the quantized numbers are  $\sum |h(n)|^2 = 0.2599$  and  $(\sum |h(n)|)^2 = 1$ . Using (10.88), the output SNR is 65.42 dB for five multipliers and is 72.41 dB for one multiplier. The following MATLAB script evaluates these and other quantities.

```
% Example Parameters
B = 12; % # of fractional bits
N = 100000; % # of samples
xn = (2*rand(1,N)-1); % Input sequence - uniform distribution
h = [0.1,0.2,0.4,0.2,0.1]; % Filter parameters
M = length(h);

% Local variables
bM = 7; DbM = 2^bM; % Bin parameter
BB = 2^B; % Useful factor in quantization
K = round(DbM/2); % Half number of bins
bins = [-K+0.5:1:K-0.5]; % Bin values from -K to K
Q = bins/DbM; % Normalized bins
YTN = 2^(-bM); % Ytick marks interval
YLM = 4*YTN; % Yaxis limit

% Quantize the input and the filter coefficients
h = QFix(h,B,'round','satur'); % h quantized to B bits
Xm = 1/sum(abs(h)); % Scaling factor
xn = QFix(Xm*xn,B,'round','satur'); % Scaled Input quant to B bits

% Filter output without multiplication quantization
yn = filter(h,1,xn); % output using filter routine

% Filter output with multi quant (5 multipliers)
x1 = [zeros(1,1),xn(1:N-1)]; x2 = [zeros(1,2),xn(1:N-2)];
x3 = [zeros(1,3),xn(1:N-3)]; x4 = [zeros(1,4),xn(1:N-4)];
h0x0 = QFix(h(1)*xn,B,'round','twosc');
h1x1 = QFix(h(2)*x1,B,'round','twosc');
h2x2 = QFix(h(3)*x2,B,'round','twosc');
h3x3 = QFix(h(4)*x3,B,'round','twosc');
h4x4 = QFix(h(5)*x4,B,'round','twosc');
yq = h0x0+h1x1+h2x2+h3x3+h4x4;
yq = QFix(yq,B,'round','satur');

% Output Error Analysis
qn = yn-yq; % Outout error sequence
varyn = var(yn); varqn = var(qn); % Signal and noise power
qqmax = max(qn); qqmin = min(qn); % Maximun and minimum of the error
qnmax = max(abs([qqmax,qqmin])); % Absolute maximum range of the error
qnavg = mean(qn); qnstd = std(qn); % Mean and std dev of the error
```

```

qn = round(qn*(2^bM)/(2*qnmax)+0.5); % Normalized en (integer between -K & K)
qn = sort([qn,-K:1:(K+1)]); %
H = diff(find(diff(qn))-1); % Error histogram
H = H/N; % Normalized histogram
Hmax = max(H); Hmin = min(H); % Max and Min of the normalized histogram

% Output SNRs
SNR_C = 10*log10(varyn/varqn); % Computed SNR
SNR_T = 6.02 + 6.02*B + 10*log10(sum(h.*h)/Xm^2) - 10*log10(M); % Theoretical SNR

% Filter output with multi quant (1 multiplier)
yq = QFix(yn,B,'round','satur');

% Output Error Analysis
qn = yn-yq; % Outout error sequence
varyn = var(yn); varqn = var(qn); % Signal and noise power
qqmax = max(qn); qqmin = min(qn); % Maximun and minimum of the error
qnmax = max(abs([qqmax,qqmin])); % Absolute maximum range of the error
qnavg = mean(qn); qnstd = std(qn); % Mean and std dev of the error
qn = round(qn*(2^bM)/(2*qnmax)+0.5); % Normalized en (integer between -K & K)
qn = sort([qn,-K:1:(K+1)]); %
H = diff(find(diff(qn))-1); % Error histogram
H = H/N; % Normalized histogram
Hmax = max(H); Hmin = min(H); % Max and min of the normalized histogram

% Output SNRs
SNR_C = 10*log10(varyn/varqn); % Computed SNR
SNR_T = 6.02 + 6.02*B + 10*log10(sum(h.*h)/Xm^2); % Theoretical SNR

```

The computed and theoretical SNRs as well as output error histograms for the two models are shown in Figure 10.27. The top plot shows the histogram when five multipliers are used. The output error has Gaussian-like distribution with SNR equal to 65.42 dB, which agrees with the theoretical value. The bottom plot show the histogram when one multiplier is used. As expected, the error is uniformly distributed with SNR equal to 72.43 dB, which also agrees with the theoretical one. □

**Cascade-form realization** Let the filter be realized by a cascade of  $K$ , second-order ( $M = 3$ ) sections given by

$$H(z) = \sum_{i=1}^K H_i(z) \quad \text{where } H_i(z) = \beta_{0i} + \beta_{1i} z^{-1} + \beta_{2i} z^{-2} \quad (10.90)$$

as shown in Figure 10.28. The overall length of the filter is  $M = 2K + 1$ . Figure 10.28 also shows the finite word-length model for the cascade form,

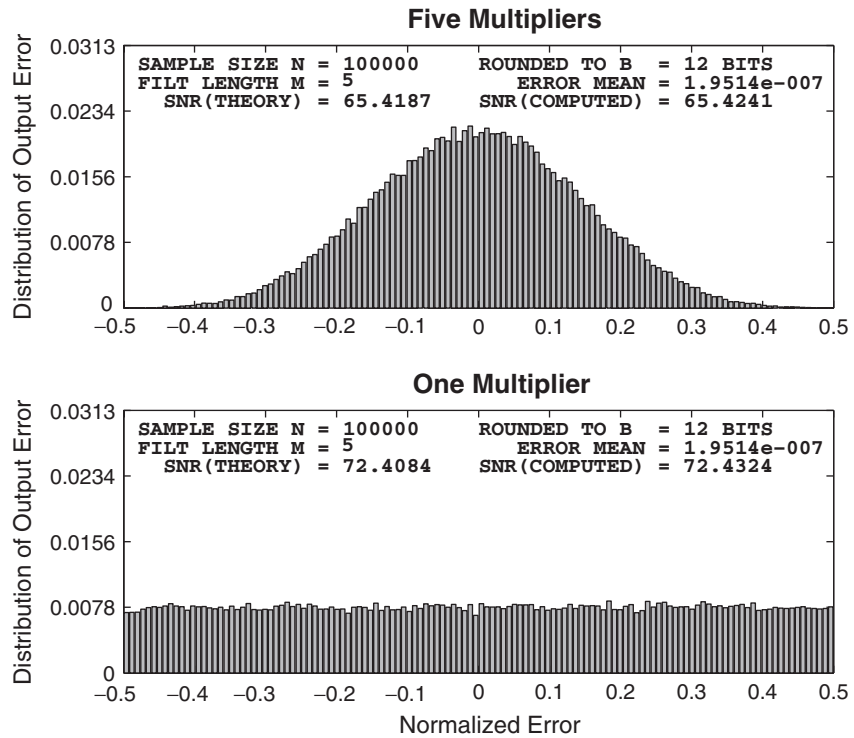


**FIGURE 10.27** Multiplication quantization effects for the direct form FIR filter in Example 10.13

in which quantization noise sources,  $e_i(n)$   $1 \leq i \leq K$ , at each section's output are incorporated. Let  $y(n)$  be the output due to input  $x(n)$ , and let  $q(n)$  be the output due to all noise sources. We make the following reasonable assumptions:

1. The sections are implemented using the MAC (multiply-accumulate) architecture so that there is only one independent noise source in each section that contributes to  $e_i(n)$ . The other possibility of three multipliers in each section is straightforward.

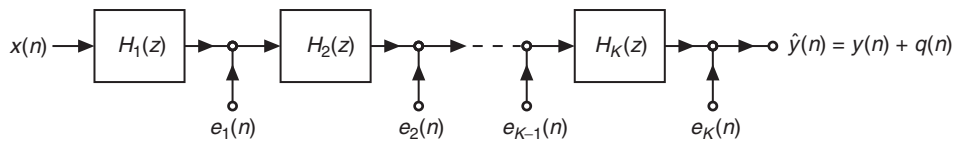


**FIGURE 10.28** Cascade form FIR filter structure with noise sources inserted for multiplication quantization

2. The noise sources are independent of each other—that is,

$$e_i(n) \perp e_j(n) \quad \text{for } i \neq j$$

3. Each noise source is a white-noise source with  $\sigma_{e_i}^2 = 2^{-2B}/12$ .

We will now consider the issues of round-off noise and scaling (to prevent overflow) for the cascade form realization.

**Round-off noise** Let the noise impulse response at the output from the  $e_i(n)$  node be denoted by  $g_i(n)$ . Then the length of  $g_i(n)$  is equal to  $(M - 2i)$ . Let  $q_i(n)$  be the output noise due to  $e_i(n)$ . Then its power is given by

$$\sigma_{q_i}^2 = \sigma_{e_i}^2 \sum_0^{M-2i} |g_i(n)|^2 = \frac{2^{-2B}}{12} \sum_0^{M-2i} |g_i(n)|^2 \quad (10.91)$$

Since  $q(n) = \sum_{i=1}^K q_i(n)$ , we obtain the total noise power as

$$\sigma_q^2 = \sum_{i=1}^K \sigma_{q_i}^2 = \frac{2^{-2B}}{12} \left( \sum_{i=1}^K \sum_{n=1}^{M-2i} |g_i(n)|^2 \right) \quad (10.92)$$

The expression  $\sum_{i=1}^K \sum_{n=1}^{M-2i} |g_i(n)|^2$  shows that the error power depends on the order of the cascade connections. It has been shown that for the majority of the orderings the noise power is approximately the same.

**Scaling to prevent overflow** From Figure 10.28, we note that one must prevent overflow at each node. Let  $h_k(n)$  be the impulse response at each node  $k$ ; then we need a scaling constant  $X_{\max}$  as

$$X_{\max} = \frac{1}{\max_k \sum |h_k(n)|}$$

so that  $|y(n)| \leq 1$ . Clearly, this is a very conservative value. A better approach is to scale the impulse responses of every section  $\{h_i(n)\}$  so that  $\sum |h_i| = 1$  for each  $i$ . Hence the output of every section is limited between  $-1$  and  $+1$  if the input  $x(n)$  is distributed over the same interval. Assuming that  $x(n)$  is uniformly distributed over  $[-1, +1]$  and is white, the output signal power is

$$\sigma_y^2 = \sigma_x^2 \sum_0^{M-1} |h(n)|^2 = \frac{1}{3} \sum_0^{M-1} |h(n)|^2 \quad (10.93)$$

where  $h(n)$  is the overall impulse response of the filter. Let  $\hat{g}_i$  be the corresponding scaled impulse responses in (10.92). Now the output SNR can be computed as either

$$\text{SNR} = \frac{\sigma_y^2}{\sigma_q^2} = 2^{2(B+1)} \frac{\sum_0^{M-1} |h(n)|^2}{\left( \sum_{i=1}^K \sum_{n=1}^{M-2i} |\hat{g}_i(n)|^2 \right)} \quad (10.94)$$

or

$$\text{SNR}_{\text{dB}} = 6.02(B+1) + 10 \log_{10} \left( \sum_0^{M-1} |h(n)|^2 \right) - 10 \log_{10} \left( \sum_{i=1}^K \sum_{n=1}^{M-2i} |\hat{g}_i(n)|^2 \right) \quad (10.95)$$

### 10.3.3 ANALYSIS USING MATLAB

Using the **casfiltr** function, we can compute the output of the infinite-precision cascade structure. Using the scaling approach outlined above, each second-order section can be scaled and used in the simulation of quantized outputs. Again, all calculations can be done in vector fashion, which improves the execution speed. These and other simulation steps are detailed in the following example.

- **EXAMPLE 10.14** Consider the fourth-order FIR filter given in Example 10.13. Its cascade form realization has two sections along with a gain constant  $b_0$ , which can be obtained using the **dir2cas** function:

$$H_1(z) = 1 + 1.4859z^{-1} + 2.8901z^{-2}, \quad H_2(z) = 1 + 0.5141z^{-1} + 0.3460z^{-2}, \text{ and } b_0 = 0.1 \quad (10.96)$$

Note that some of these coefficients are greater than 1, which will cause problems with coefficient quantization when only  $B$  fractional bits are used. Hence we need to scale each section as explained. The scaled values are

$$\hat{H}_1(z) = 0.1860 + 0.2764z^{-1} + 0.5376z^{-2}, \quad \hat{H}_2(z) = 0.5376 + 0.2764z^{-1} + 0.1860z^{-2} \quad (10.97)$$

and  $\hat{b}_0 = 1$ . Thus we do not need to scale the input. Now  $\hat{g}_1(n) = \hat{h}_2(n)$  and  $\hat{g}_2(n) = 1$  in (10.94). Thus from (10.95), the output SNR is 70.96 dB, which compares well with the one-multiplier direct form implementation (72.41 dB). These calculations and error histogram plotting are illustrated in the following MATLAB script.

```
% Example Parameters
B = 12; % # of fractional bits
N = 100000; % # of samples
xn = (2*rand(1,N)-1); % Input sequence - uniform distribution
h = [0.1,0.2,0.4,0.2,0.1]; % Filter parameters
M = length(h); % Filter length
[b0,Bh,Ah] = dir2cas(h,1); % Cascade sections
h1 = Bh(1,:); % Section-1
h2 = Bh(2,:); % Section-2
h1 = h1/sum(h1); % Scaled so Gain=1
h2 = h2/sum(h2); % Scaled so Gain=1
```

```
% Local variables
bM = 7; DbM = 2^bM;      % Bin parameter
BB = 2^B;                  % Useful factor in quantization
K = round(DbM/2);         % Half number of bins
bins = [-K+0.5:1:K-0.5];  % Bin values from -K to K
Q = bins/DbM;              % Normalized bins
YTN = 2^(-bM);             % Ytick marks interval
YLM = 20*YTN;               % Yaxis limit
% Quantize the input and the filter coefficients
h1 = QFix(h1,B,'round','satur'); % h1 quantized to B bits
h2 = QFix(h2,B,'round','satur'); % h1 quantized to B bits
xn = QFix(xn,B,'round','satur'); % Input quantized to B bits
% Filter output without multiplication quantization
yn = casfiltr(b0,Bh,Ah,xn); % output using Casfiltr routine
% Filter output with multi quant (1 multiplier/section)
xq = QFix(xn,B,'round','satur'); % Section-1 scaled input
wn = filter(h1,1,xq);           % Sec-1 unquantized output
wq = QFix(wn,B,'round','satur'); % Sec-1 quantized output
wq = QFix(wq,B,'round','satur'); % Section-2 scaled input
yq = filter(h2,1,wq);           % Sec-2 unquantized output
yq = QFix(yq,B,'round','satur'); % Sec-2 quantized output
% Output Error Analysis
qn = yn-yq;                   % Outout error sequence
varyn = var(yn); varqn = var(qn); % Signal and noise power
qqmax = max(qn); qqmin = min(qn); % Maximun and minimum of the error
qnmax = max(abs([qqmax,qqmin])); % Absolute maximum range of the error
qnavg = mean(qn); qnstd = std(qn); % Mean and std dev of the error
qn = round(qn*(2^bM)/(2*qnmax)+0.5); % Normalized en (integer between -K & K)
qn = sort([qn,-K:1:(K+1)]);          %
H = diff(find(diff(qn)))-1;          % Error histogram
H = H/N;                            % Normalized histogram
Hmax = max(H); Hmin = min(H);        % Max and min of the normalized histogram
% Output SNRs
SNR_C = 10*log10(varyn/varqn); % Computed SNR
SNR_T = 6.02*(B+1) + 10*log10(sum(h.*h)) ...
- 10*log10(1+sum(h2.*h2)); % Theoretical SNR
```

The plot is shown in Figure 10.29. The error distribution appears to have a Gaussian envelope, but the error is not continuously distributed. This behavior indicates that the output error takes only a fixed set of values, which is due to a particular set of coefficient values. The computed SNR is 70.85 dB, which agrees with the above theoretical value. Thus our assumptions are reasonable.  $\square$

#### 10.3.4 FLOATING-POINT ARITHMETIC

Analysis for the floating-point arithmetic is more complicated and tedious. Hence we will consider only the direct form realization with simplified

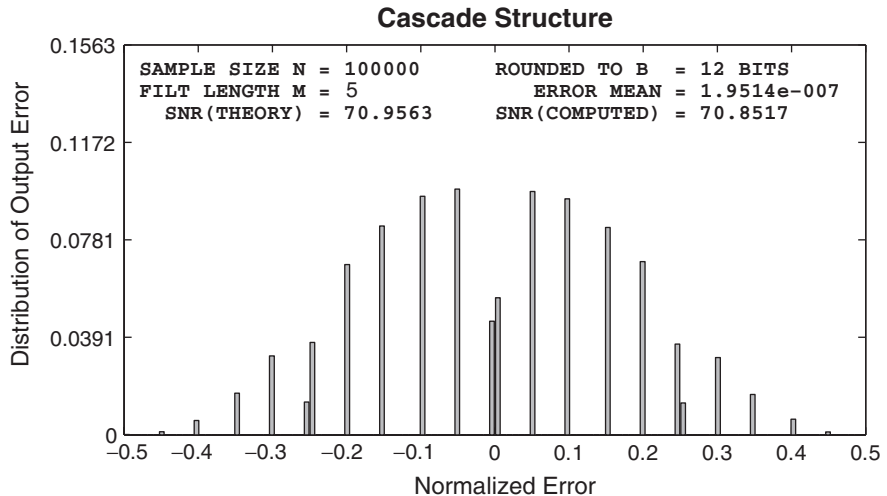


**FIGURE 10.29** Multiplication quantization effects for the cascade form FIR filter in Example 10.14

assumptions. Figure 10.30 shows a direct form realization with a floating-point arithmetic model. In this realization,  $\{\eta_i(n)\}$ ,  $1 \leq i \leq M - 1$  are the relative errors in adders and  $\{\varepsilon_i(n)\}$ ,  $0 \leq i \leq M - 1$  are the relative errors in multipliers, with  $|\eta_i| \leq 2^{-2B}$  and  $|\varepsilon_i| \leq 2^{-2B}$ .

Let  $A(n, k)$  be the gain from the  $k$ th multiplier to the output node, which is given by

$$A(n, k) = \begin{cases} (1 + \varepsilon_k(n)) \prod_{r=k}^{M-1} (1 + \eta_r(n)), & k \neq 0 \\ (1 + \varepsilon_0(n)) \prod_{r=k}^{M-1} (1 + \eta_r(n)), & k = 0 \end{cases} \quad (10.98)$$

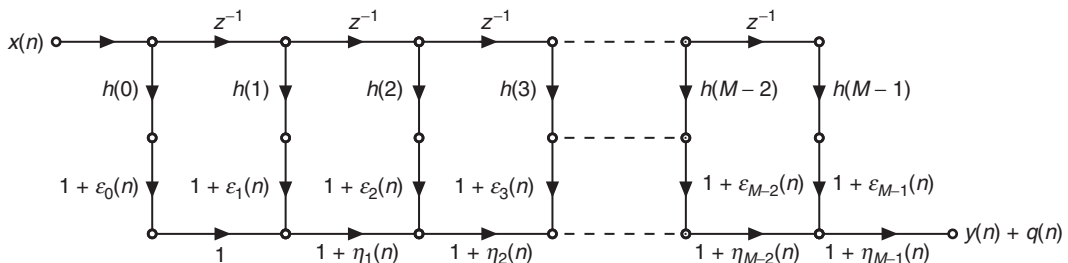


**FIGURE 10.30** Multiplication quantization model for direct form floating-point implementation of an FIR filter

Let  $\hat{y}(n) \triangleq y(n) + q(n)$  be the overall output where  $y(n)$  is the output due to the input  $x(n)$  and  $q(n)$  is the output due to noise sources. Then

$$\hat{y}(n) = \sum_{k=0}^{M-1} A(n, k) h(k) x(n - k) \quad (10.99)$$

Subtracting  $y(n) = \sum_{k=0}^{M-1} h(k) x(n - k)$  from (10.99), we obtain

$$q(n) = \sum_{k=0}^{M-1} \{A(n, k) - 1\} h(k) x(n - k) \quad (10.100)$$

Now from (10.98), the average value of  $A(n, k)$  is  $E[A(n, k)] = 1$ , and the average power of  $A(n, k)$  is

$$\begin{aligned} E[A^2(n, k)] &= \left(1 + \frac{1}{3} 2^{-2B}\right)^{M+1-k} \\ &\approx 1 + (M+1-k) \frac{2^{-2B}}{3} \quad \text{for small } 2^{-2B} \end{aligned} \quad (10.101)$$

Assuming that the input signal  $x(n)$  is also a white sequence with variance  $\sigma_x^2$ , then from (10.101) the noise power is given by

$$\sigma_q^2 = \frac{(M+1)2^{-2B}}{3} \sigma_x^2 \sum_{k=0}^{M-1} |h(k)|^2 \left(1 - \frac{k}{M+1}\right) \quad (10.102)$$

Since  $(1 - \frac{k}{M+1}) \leq 1$  and using  $\sigma_y^2 = \sigma_x^2 \sum_{k=0}^{M-1} |h(k)|^2$ , the noise power  $\sigma_q^2$  is upper bounded by

$$\sigma_q^2 \leq (M+1) \frac{2^{-2B}}{3} \sigma_y^2 \quad (10.103)$$

or the SNR is lower bounded by

$$\text{SNR} \geq \frac{3}{M+1} 2^{2B} \quad (10.104)$$

Equation (10.104) shows that it is best to compute products in order of increasing magnitude.

- **EXAMPLE 10.15** Again consider the fourth-order FIR filter given in Example 10.13 in which  $M = 5$ ,  $B = 12$ , and  $h(n) = \{0.1, 0.2, 0.4, 0.2, 0.1\}$ . From (10.104), the SNR is lower bounded by

$$\text{SNR}_{dB} \geq 10 \log_{10} \left( \frac{3}{M+1} 2^{24} \right) = 69.24 \text{ dB}$$

and the approximate value from (10.102) is 71 dB, which is comparable to the fixed-point value of 72 dB. Note that the fixed-point results would degrade with

less than optimum scaling (e.g., if signal amplitude were 10 dB down), whereas the floating-point SNR would remain the same. To counter this, one could put a variable scaling factor  $A$  on the fixed-point system, which is then getting close to the full floating-point system. In fact, floating-point is nothing but fixed-point with variable scaling—that is, a scaling by a power of two (or shifting) at each multiplication and addition.  $\square$

## 10.4 PROBLEMS

---

- P10.1** Let  $x(n) = 0.5[\cos(n/17) + \sin(n/23)]$ . For the following parts, use 500,000 samples of  $x(n)$  and the **StatModelR** function.

1. Quantize  $x(n)$  to  $B = 2$  bits, and plot the resulting distributions for the error signals  $e_1(n)$  and  $e_2(n)$ . Comment on these plots.
2. Quantize  $x(n)$  to  $B = 4$  bits, and plot the resulting distributions for the error signals  $e_1(n)$  and  $e_2(n)$ . Comment on these plots.
3. Quantize  $x(n)$  to  $B = 6$  bits, and plot the resulting distributions for the error signals  $e_1(n)$  and  $e_2(n)$ . Comment on these plots.

- P10.2** Let  $x(n) = \frac{1}{3} [\cos(0.1\pi n) + \sin(0.2\pi n) + \sin(0.4\pi n)]$ . For the following parts, use 500,000 samples of  $x(n)$  and the **StatModelR** function.

1. Quantize  $x(n)$  to  $B = 2$  bits, and plot the resulting distributions for the error signals  $e_1(n)$  and  $e_2(n)$ . Comment on these plots.
2. Quantize  $x(n)$  to  $B = 4$  bits, and plot the resulting distributions for the error signals  $e_1(n)$  and  $e_2(n)$ . Comment on these plots.
3. Quantize  $x(n)$  to  $B = 6$  bits, and plot the resulting distributions for the error signals  $e_1(n)$  and  $e_2(n)$ . Comment on these plots.

- P10.3** Let a real, causal, and stable IIR filter be given by

$$H(z) = R_0 + \sum_{k=1}^{N-1} \frac{R_k}{z - p_k} \quad (10.105)$$

where all poles are distinct. Using (10.16), (10.18a), and (10.105), show that

$$\frac{\sigma_q^2}{\sigma_e^2} = R_0^2 + \sum_{k=1}^{N-1} \sum_{\ell=1}^{N-1} \frac{R_k R_\ell^*}{1 - p_k p_\ell^*}$$

- P10.4** Consider the lowpass digital filter designed in Problem P6.39. The input to this filter is an independent and identically distributed Gaussian sequence with zero-mean and variance equal to 0.1.

1. Determine the variance of the filter output process using the **VarGain** function.
2. Determine numerically the variance of the output process by generating 500,000 samples of the input sequence. Comment on your results.

- P10.5** Design an elliptic bandpass digital filter that has a lower stopband of  $0.3\pi$ , a lower passband of  $0.4\pi$ , an upper passband of  $0.5\pi$ , and an upper stopband of  $0.65\pi$ .

The passband ripple is 0.1 dB and the stopband attenuation is 50 dB. The input signal is a random sequence whose components are independent and uniformly distributed between  $-1$  and  $1$ .

1. Determine the variance of the filter output process using the `VarGain` function.
  2. Determine numerically the variance of the output process by generating 500,000 samples of the input sequence. Comment on your results.
- P10.6** Consider the first-order recursive system  $y(n) = 0.75y(n - 1) + 0.125\delta(n)$  with zero initial conditions. The filter is implemented in 4-bit (including sign) fixed-point two's-complement fractional arithmetic. Products are rounded to 3 bits.
1. Determine and plot the first 20 samples of the output using saturation limiter for the addition. Does the filter go into a limit cycle?
  2. Determine and plot the first 20 samples of the output using two's-complement overflow for the addition. Does the filter go into a limit cycle?
- P10.7** Repeat Problem P10.6 when products are truncated to 3 bits.
- P10.8** Consider the second-order recursive system  $y(n) = 0.125\delta(n) - 0.875y(n - 2)$  with zero initial conditions. The filter is implemented in 5-bit (including sign) fixed-point two's-complement fractional arithmetic. Products are rounded to 4 bits.
1. Determine and plot the first 30 samples of the output using a saturation limiter for the addition. Does the filter go into a limit cycle?
  2. Determine and plot the first 30 samples of the output using two's-complement overflow for the addition. Does the filter go into a limit cycle?
- P10.9** Repeat Problem P10.8 when products are truncated to 4 bits.
- P10.10** Let  $x(n) = \frac{1}{4}[\sin(n/11) + \cos(n/13) + \sin(n/17) + \cos(n/19)]$  and  $c = 0.7777$ . For the following parts, use 500,000 samples of  $x(n)$  and the `StatModelR` function.
1. Quantize  $cx(n)$  to  $B = 4$  bits, and plot the resulting distributions for the error signals  $e_1(n)$  and  $e_2(n)$ . Comment on these plots.
  2. Quantize  $cx(n)$  to  $B = 8$  bits, and plot the resulting distributions for the error signals  $e_1(n)$  and  $e_2(n)$ . Comment on these plots.
  3. Quantize  $cx(n)$  to  $B = 12$  bits, and plot the resulting distributions for the error signals  $e_1(n)$  and  $e_2(n)$ . Comment on these plots.
- P10.11** Let  $x(n)$  be a random sequence uniformly distributed between  $-1$  and  $1$ , and let  $c = 0.7777$ . For the following parts, use 500,000 samples of  $x(n)$  and the `StatModelR` function.
1. Quantize  $cx(n)$  to  $B = 4$  bits, and plot the resulting distributions for the error signals  $e_1(n)$  and  $e_2(n)$ . Comment on these plots.
  2. Quantize  $cx(n)$  to  $B = 8$  bits, and plot the resulting distributions for the error signals  $e_1(n)$  and  $e_2(n)$ . Comment on these plots.
  3. Quantize  $cx(n)$  to  $B = 12$  bits, and plot the resulting distributions for the error signals  $e_1(n)$  and  $e_2(n)$ . Comment on these plots.
- P10.12** Consider an LTI system with the input  $x(n)$  and output  $y(n)$

$$y(n) = b_0x(n) + b_1x(n - 1) + a_1y(n - 1) \quad (10.106)$$

1. Draw the direct form I structure for the above system.
2. Let  $e_{b_0}(n)$  denote the multiplication quantization error resulting from the product  $b_0x(n)$ ,  $e_{b_1}(n - 1)$  from the product  $b_1x(n - 1)$ , and  $e_{a_1}(n - 1)$  from the product

$a_1 y(n-1)$  in the direct form I realization. Draw an equivalent structure that contains only one noise source.

3. Draw an equivalent system that can be used to study multiplication quantization error for the system in (10.106). The input to this system should be the noise source in part 2, and the output should be the overall output error  $q(n)$ .
4. Using the model in part 3, determine an expression for the variance of the output error  $e(n)$ .

**P10.13** Let the system be given by  $y(n) = a y(n-1) + x(n)$ . Let  $a = 0.7$ , which is quantized to  $B$  (fractional) bits in the filter realization. Let the input sequence be  $x(n) = \sin(n/11)$ , which is properly scaled to avoid overflow in the adder and quantized to  $B$  bits prior to filtering. The multiplications in the filtering operations are also quantized to  $B$  bits.

1. Let  $B = 5$ . Generate 100,000 samples of  $x(n)$ , and filter through the system with multiplication quantization. Compute the true output, the quantized output, the output error, and the output SNR. Plot the normalized histogram, and comment on the results.
2. Let  $B = 10$ . Generate 100,000 samples of  $x(n)$  and filter through the system with multiplication quantization. Compute the true output, the quantized output, the output error, and the output SNR. Plot the normalized histogram, and comment on the results.

**P10.14** Let the system be given by  $y(n) = a y(n-1) + x(n)$ . Let  $a = 0.333$ , which is quantized to  $B$  (fractional) bits in the filter realization. Let the input sequence be  $x(n) = \sin(n/11)$ , which is properly scaled to avoid overflow in the adder and quantized to  $B$  bits prior to filtering. The multiplications in the filtering operations are also quantized to  $B$  bits.

1. Let  $B = 5$ . Generate 100,000 samples of  $x(n)$ , and filter through the system with multiplication quantization. Compute the true output, the quantized output, the output error, and the output SNR. Plot the normalized histogram and comment on the results.
2. Let  $B = 10$ . Generate 100,000 samples of  $x(n)$ , and filter through the system with multiplication quantization. Compute the true output, the quantized output, the output error, and the output SNR. Plot the normalized histogram and comment on the results.

**P10.15** Consider the second-order IIR filter given in (10.51) with  $r = 0.8$  and  $\theta = \pi/4$ . The input to this filter is  $x(n) = \sin(n/23)$ .

1. Investigate the multiplication quantization error behavior of this filter for  $B = 5$  bits. Determine the true output SNR, the computed output SNR, and the upper and lower bounds of the SNR. Plot the normalized histogram of the output error.
2. Investigate the multiplication quantization error behavior of this filter for  $B = 10$  bits. Determine the true output SNR, the computed output SNR, and the upper and lower bounds of the SNR. Plot the normalized histogram of the output error.

**P10.16** Consider the second-order IIR filter given in (10.51) with  $r = 0.8$  and  $\theta = 2\pi/3$ . The input to this filter is  $x(n) = \sin(n/23)$ .

1. Investigate the multiplication quantization error behavior of this filter for  $B = 5$  bits. Determine the true output SNR, the computed output SNR, and the upper and lower bounds of the SNR. Plot the normalized histogram of the output error.

2. Investigate the multiplication quantization error behavior of this filter for  $B = 10$  bits. Determine the true output SNR, the computed output SNR, and the upper and lower bounds of the SNR. Plot the normalized histogram of the output error.

**P10.17** Consider a fifth-order FIR system given by

$$H(z) = 0.1 + 0.2z^{-1} + 0.3z^{-2} + 0.3z^{-3} + 0.2z^{-4} + 0.1z^{-5}$$

which is implemented in a direct form using  $B = 10$  bits. Input to the filter is a random sequence whose samples are independent and identically distributed over  $[-1, 1]$ .

1. Investigate the multiplication quantization errors when all six multipliers are used in the implementation. Plot the normalized histogram of the output error.
2. Investigate the multiplication quantization errors when one multiplier is used in the implementation. Plot the normalized histogram of the output error.

**P10.18** Consider a fourth-order FIR system given by

$$H(z) = 0.1 + 0.2z^{-1} + 0.3z^{-2} + 0.2z^{-3} + 0.1z^{-4}$$

which is implemented in a cascade form containing second-order sections. Input to the filter is a random sequence whose samples are independent and identically distributed over  $[-1, 1]$ .

1. Investigate the multiplication quantization errors when  $B = 6$  bits is used in the implementation. Plot the normalized histogram of the output error.
2. Investigate the multiplication quantization errors when  $B = 12$  bits is used in the implementation. Plot the normalized histogram of the output error.

# CHAPTER **11**

---

## Applications in Adaptive Filtering

---

In Chapters 7 and 8, we described methods for designing FIR and IIR digital filters to satisfy some desired specifications. Our goal was to determine the coefficients of the digital filter that met the desired specifications.

In contrast to the filter design techniques considered in those two chapters, there are many digital signal processing applications in which the filter coefficients cannot be specified *a priori*. For example, let us consider a high-speed modem that is designed to transmit data over telephone channels. Such a modem employs a filter called a channel equalizer to compensate for the channel distortion. The modem must effectively transmit data through communication channels that have different frequency response characteristics and hence result in different distortion effects. The only way in which this is possible is if the channel equalizer has *adjustable coefficients* that can be optimized to minimize some measure of the distortion, on the basis of measurements performed on the characteristics of the channel. Such a filter with adjustable parameters is called an *adaptive filter*—in this case, an *adaptive equalizer*.

Numerous applications of adaptive filters have been described in the literature. Some of the more noteworthy applications include (1) adaptive antenna systems, in which adaptive filters are used for beam steering and for providing nulls in the beam pattern to remove undesired interference [97], (2) digital communication receivers, in which adaptive filters are used to provide equalization of intersymbol interference and for channel

identification [81], (3) adaptive noise canceling techniques, in which an adaptive filter is used to estimate and eliminate a noise component in some desired signal [96, 34, 15], and (4) system modeling, in which an adaptive filter is used as a model to estimate the characteristics of an unknown system. These are just a few of the best-known examples on the use of adaptive filters.

Although both IIR and FIR filters have been considered for adaptive filtering, the FIR filter is by far the most practical and widely used. The reason for this preference is quite simple. The FIR filter has only adjustable zeros, and hence it is free of stability problems associated with adaptive IIR filters that have adjustable poles as well as zeros. We should not conclude, however, that adaptive FIR filters are always stable. On the contrary, the stability of the filter depends critically on the algorithm for adjusting its coefficients.

Of the various FIR filter structures that we may use, the direct form and the lattice form are the ones often used in adaptive filtering applications. The direct form FIR filter structure with adjustable coefficients  $h(0), h(1), \dots, h(N-1)$  is illustrated in Figure 11.1. The FIR lattice structures are discussed in Chapter 14 and have adjustable parameters  $K_n$ , called reflection coefficients, shown in Figure 14.15.

An important consideration in the use of an adaptive filter is the criterion for optimizing the adjustable filter parameters. The criterion must not only provide a meaningful measure of filter performance, but it must also result in a practically realizable algorithm.

One criterion that provides a good measure of performance in adaptive filtering applications is the least-squares criterion, and its counterpart in a statistical formulation of the problem, namely, the mean-square-error (MSE) criterion. The least-squares (and MSE) criterion results in a quadratic performance index as a function of the filter coefficients, and hence it possesses a single minimum. The resulting algorithms for adjusting the coefficients of the filter are relatively easy to implement.

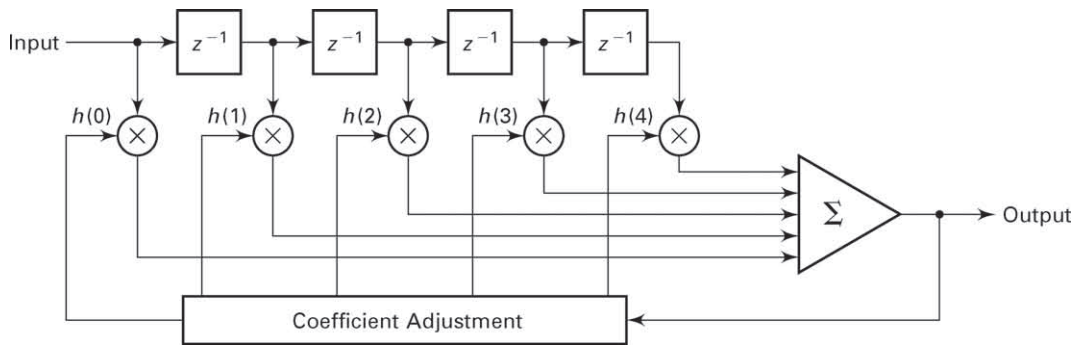


**FIGURE 11.1** Direct form adaptive FIR filter

In this chapter, we describe a basic algorithm, called the *least-mean-square* (LMS) *algorithm*, to adaptively adjust the coefficients of an FIR filter. The adaptive filter structure that will be implemented is the direct form FIR filter structure with adjustable coefficients  $h(0), h(1), \dots, h(N - 1)$ , as illustrated in Figure 11.1. After we describe the LMS algorithm, we apply it to several practical systems in which adaptive filters are employed.

## 11.1 LMS ALGORITHM FOR COEFFICIENT ADJUSTMENT

---

Suppose we have an FIR filter with adjustable coefficients  $\{h(k), 0 \leq k \leq N - 1\}$ . Let  $\{x(n)\}$  denote the input sequence to the filter, and let the corresponding output be  $\{y(n)\}$ , where

$$y(n) = \sum_{k=0}^{N-1} h(k)x(n-k), \quad n = 0, \dots, M \quad (11.1)$$

Suppose that we also have a desired sequence  $\{d(n)\}$  with which we can compare the FIR filter output. Then we can form the error sequence  $\{e(n)\}$  by taking the difference between  $d(n)$  and  $y(n)$ , that is,

$$e(n) = d(n) - y(n), \quad n = 0, \dots, M \quad (11.2)$$

The coefficients of the FIR filter will be selected to minimize the sum of squared errors. Thus we have

$$\begin{aligned} \mathcal{E} &= \sum_{n=0}^M e^2(n) = \sum_{n=0}^M \left[ d(n) - \sum_{k=0}^{N-1} h(k)x(n-k) \right]^2 \\ &= \sum_{n=0}^M d^2(n) - 2 \sum_{k=0}^{N-1} h(k)r_{dx}(k) + \sum_{k=0}^{N-1} \sum_{\ell=0}^{N-1} h(k)h(\ell)r_{xx}(k-\ell) \end{aligned} \quad (11.3)$$

where, by definition,

$$r_{dx}(k) = \sum_{n=0}^M d(n)x(n-k), \quad 0 \leq k \leq N-1 \quad (11.4)$$

$$r_{xx}(k) = \sum_{n=0}^M x(n)x(n+k), \quad 0 \leq k \leq N-1 \quad (11.5)$$

We call  $\{r_{dx}(k)\}$  the cross-correlation between the desired output sequence  $\{d(n)\}$  and the input sequence  $\{x(n)\}$ , and  $\{r_{xx}(k)\}$  is the autocorrelation sequence of  $\{x(n)\}$ .

The sum of squared errors  $\mathcal{E}$  is a quadratic function of the FIR filter coefficients. Consequently, the minimization of  $\mathcal{E}$  with respect to the filter coefficients  $\{h(k)\}$  results in a set of linear equations. By differentiating  $\mathcal{E}$  with respect to each of the filter coefficients, we obtain

$$\frac{\partial \mathcal{E}}{\partial h(m)} = 0, \quad 0 \leq m \leq N - 1 \quad (11.6)$$

and hence

$$\sum_{k=0}^{N-1} h(k) r_{xx}(k-m) = r_{dx}(m), \quad 0 \leq m \leq N - 1 \quad (11.7)$$

This is the set of linear equations that yield the optimum filter coefficients.

To solve the set of linear equations directly, we must first compute the autocorrelation sequence  $\{r_{xx}(k)\}$  of the input signal and the cross-correlation sequence  $\{r_{dx}(k)\}$  between the desired sequence  $\{d(n)\}$  and the input sequence  $\{x(n)\}$ .

The LMS algorithm provides an alternative computational method for determining the optimum filter coefficients  $\{h(k)\}$  without explicitly computing the correlation sequences  $\{r_{xx}(k)\}$  and  $\{r_{dx}(k)\}$ . The algorithm is basically a recursive gradient (steepest-descent) method that finds the minimum of  $\mathcal{E}$  and thus yields the set of optimum filter coefficients.

We begin with any arbitrary choice for the initial values of  $\{h(k)\}$ —say,  $\{h_0(k)\}$ . For example, we may begin with  $h_0(k) = 0$ ,  $0 \leq k \leq N - 1$ . Then after each new input sample  $\{x(n)\}$  enters the adaptive FIR filter, we compute the corresponding output—say,  $\{y(n)\}$ —form the error signal  $e(n) = d(n) - y(n)$ , and update the filter coefficients according to the equation

$$h_n(k) = h_{n-1}(k) + \Delta \cdot e(n) \cdot x(n-k), \quad 0 \leq k \leq N - 1, \quad n = 0, 1, \dots \quad (11.8)$$

where  $\Delta$  is called the step-size parameter,  $x(n-k)$  is the sample of the input signal located at the  $k$ th tap of the filter at time  $n$ , and  $e(n)x(n-k)$  is an approximation (estimate) of the negative of the gradient for the  $k$ th filter coefficient. This is the LMS recursive algorithm for adjusting the filter coefficients adaptively so as to minimize the sum of squared errors  $\mathcal{E}$ .

The step-size parameter  $\Delta$  controls the rate of convergence of the algorithm to the optimum solution. A large value of  $\Delta$  leads to large step-size adjustments and thus to rapid convergence, while a small value of  $\Delta$  results in slower convergence. However, if  $\Delta$  is made too large the algorithm becomes unstable. To ensure stability,  $\Delta$  must be chosen [81]

to be in the range

$$0 < \Delta < \frac{1}{10NP_x} \quad (11.9)$$

where  $N$  is the length of the adaptive FIR filter and  $P_x$  is the power in the input signal, which can be approximated by

$$P_x \approx \frac{1}{1+M} \sum_{n=0}^M x^2(n) = \frac{r_{xx}(0)}{M+1} \quad (11.10)$$

The mathematical justification of equations (11.9) and (11.10) and the proof that the LMS algorithm leads to the solution for the optimum filter coefficients is given in more advanced treatments of adaptive filters. The interested reader may refer to the books by Haykin [30] and Proakis and Manolakis [79].

### 11.1.1 MATLAB IMPLEMENTATION

The LMS algorithm (11.8) can easily be implemented in MATLAB. Given the input sequence  $\{x(n)\}$ , the desired sequence  $\{d(n)\}$ , step size  $\Delta$ , and the desired length of the adaptive FIR filter  $N$ , we can use (11.1), (11.2), and (11.8) to determine the adaptive filter coefficients  $\{h(n), 0 \leq n \leq N - 1\}$  recursively. This is shown in the following function, called `lms`.

```
function [h,y] = lms(x,d,delta,N)
% LMS Algorithm for Coefficient Adjustment
%
% [h,y] = lms(x,d,delta,N)
%     h = estimated FIR filter
%     y = output array y(n)
%     x = input array x(n)
%     d = desired array d(n), length must be same as x
% delta = step size
%     N = length of the FIR filter
%
M = length(x); y = zeros(1,M);
h = zeros(1,N);
for n = N:M
    x1 = x(n:-1:n-N+1);
    y = h * x1';
    e = d(n) - y;
    h = h + delta*e*x1;
end
```

In addition, the `lms` function provides the output  $\{y(n)\}$  of the adaptive filter.

We will apply the LMS algorithm to several practical applications involving adaptive filtering.

## 11.2 SYSTEM IDENTIFICATION OR SYSTEM MODELING

---

To formulate the problem, let us refer to Figure 11.2. We have an unknown linear system that we wish to identify. The unknown system may be an all-zero (FIR) system or a pole-zero (IIR) system. The unknown system will be approximated (modeled) by an FIR filter of length  $N$ . Both the unknown system and the FIR model are connected in parallel and are excited by the same input sequence  $\{x(n)\}$ . If  $\{y(n)\}$  denotes the output of the model and  $\{d(n)\}$  denotes the output of the unknown system, the error sequence is  $\{e(n) = d(n) - y(n)\}$ . If we minimize the sum of squared errors, we obtain the same set of linear equations as in (11.7). Therefore, the LMS algorithm given by (11.8) may be used to adapt the coefficients of the FIR model so that its output approximates the output of the unknown system.

### 11.2.1 PROJECT 11.1: SYSTEM IDENTIFICATION

There are three basic modules that are needed to perform this project.

1. A noise signal generator that generates a sequence of random numbers with zero mean value. For example, we may generate a sequence of uniformly distributed random numbers over the interval  $[-a, a]$ . Such a sequence of uniformly distributed numbers has an average value of zero and a variance of  $a^2/3$ . This signal sequence, call it  $\{x(n)\}$ , will be used as the input to the unknown system and the adaptive FIR model. In this case, the input signal  $\{x(n)\}$  has power  $P_x = a^2/3$ . In MATLAB this can be implemented using the `rand` function.

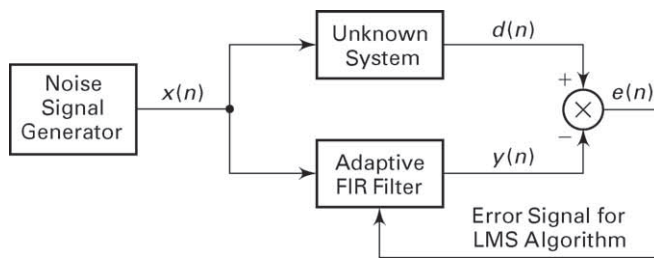


**FIGURE 11.2** Block diagram of system identification or system modeling problem

2. An unknown system module that may be selected is an IIR filter and implemented by its difference equation. For example, we may select an IIR filter specified by the second-order difference equation

$$d(n) = a_1 d(n-1) + a_2 d(n-2) + x(n) + b_1 x(n-1) + b_2 x(n-2) \quad (11.11)$$

where the parameters  $\{a_1, a_2\}$  determine the positions of the poles and  $\{b_1, b_2\}$  determine the positions of the zeros of the filter. These parameters are input variables to the program. This can be implemented by the `filter` function.

3. An adaptive FIR filter module where the FIR filter has  $N$  tap coefficients that are adjusted by means of the LMS algorithm. The length  $N$  of the filter is an input variable to the program. This can be implemented using the `lms` function given in the previous section.

The three modules are configured as shown in Figure 11.2. From this project, we can determine how closely the impulse response of the FIR model approximates the impulse response of the unknown system after the LMS algorithm has converged.

To monitor the convergence rate of the LMS algorithm, we may compute a short-term average of the squared error  $e^2(n)$  and plot it. That is, we may compute

$$\text{ASE}(m) = \frac{1}{K} \sum_{k=n+1}^{n+K} e^2(k) \quad (11.12)$$

where  $m = n/K = 1, 2, \dots$ . The averaging interval  $K$  may be selected to be (approximately)  $K = 10N$ . The effect of the choice of the step-size parameter  $\Delta$  on the convergence rate of the LMS algorithm may be observed by monitoring the  $\text{ASE}(m)$ .

Besides the main part of the program, you should also include, as an aside, the computation of the impulse response of the unknown system, which can be obtained by exciting the system with a unit sample sequence  $\delta(n)$ . This actual impulse response can be compared with that of the FIR model after convergence of the LMS algorithm. The two impulse responses can be plotted for the purpose of comparison.

## 11.3 SUPPRESSION OF NARROWBAND INTERFERENCE IN A WIDEBAND SIGNAL

---

Let us assume that we have a signal sequence  $\{x(n)\}$  that consists of a desired wideband signal sequence—say,  $\{w(n)\}$ —corrupted by an additive narrowband interference sequence  $\{s(n)\}$ . The two sequences are uncorrelated. This problem arises in digital communications and in signal

detection, where the desired signal sequence  $\{w(n)\}$  is a spread-spectrum signal, while the narrowband interference represents a signal from another user of the frequency band or some intentional interference from a jammer who is trying to disrupt the communication or detection system.

From a filtering point of view, our objective is to design a filter that suppresses the narrowband interference. In effect, such a filter should place a notch in the frequency band occupied by the interference. In practice, however, the frequency band of the interference might be unknown. Moreover, the frequency band of the interference may vary slowly in time.

The narrowband characteristics of the interference allow us to estimate  $s(n)$  from past samples of the sequence  $x(n) = s(n) + w(n)$  and to subtract the estimate from  $x(n)$ . Since the bandwidth of  $\{s(n)\}$  is narrow compared to the bandwidth of  $\{w(n)\}$ , the samples of  $\{s(n)\}$  are highly correlated. On the other hand, the wideband sequence  $\{w(n)\}$  has a relatively narrow correlation.

The general configuration of the interference suppression system is shown in Figure 11.3. The signal  $x(n)$  is delayed by  $D$  samples, where the delay  $D$  is chosen sufficiently large so that the wideband signal components  $w(n)$  and  $w(n - D)$ , which are contained in  $x(n)$  and  $x(n - D)$ , respectively, are uncorrelated. The output of the adaptive FIR filter is the estimate

$$\hat{s}(n) = \sum_{k=0}^{N-1} h(k)x(n - k - D) \quad (11.13)$$

The error signal that is used in optimizing the FIR filter coefficients is  $e(n) = x(n) - \hat{s}(n)$ . The minimization of the sum of squared errors again leads to a set of linear equations for determining the optimum coefficients. Due to the delay  $D$ , the LMS algorithm for adjusting the coefficients recursively becomes

$$h_n(k) = h_{n-1}(k) + \Delta e(n)x(n - k - D), \quad n = 1, 2, \dots \quad k = 0, 1, \dots, N - 1 \quad (11.14)$$

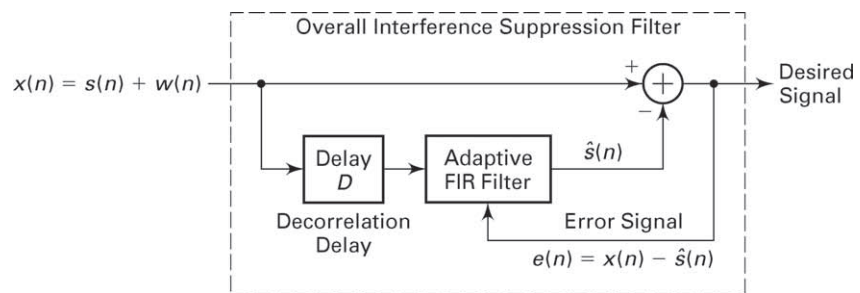


**FIGURE 11.3** Adaptive filter for estimating and suppressing a narrowband interference

### 11.3.1 PROJECT 11.2: SUPPRESSION OF SINUSOIDAL INTERFERENCE

Three basic modules are required to perform this project.

1. A noise signal generator module that generates a wideband sequence  $\{w(n)\}$  of random numbers with zero mean value. In particular, we may generate a sequence of uniformly distributed random numbers using the `rand` function as previously described in the project on system identification. The signal power is denoted as  $P_w$ .
2. A sinusoidal signal generator module that generates a sine wave sequence  $s(n) = A \sin \omega_0 n$ , where  $0 < \omega_0 < \pi$  and  $A$  is the signal amplitude. The power of the sinusoidal sequence is denoted as  $P_s$ .
3. An adaptive FIR filter module using the `lms` function, where the FIR filter has  $N$  tap coefficients that are adjusted by the LMS algorithm. The length  $N$  of the filter is an input variable to the program.

The three modules are configured as shown in Figure 11.4. In this project, the delay  $D = 1$  is sufficient, since the sequence  $\{w(n)\}$  is a white noise (spectrally flat or uncorrelated) sequence. The objective is to adapt the FIR filter coefficients and then to investigate the characteristics of the adaptive filter.

It is interesting to select the interference signal to be much stronger than the desired signal  $w(n)$ , for example,  $P_s = 10P_w$ . Note that the power  $P_x$  required in selecting the step-size parameter in the LMS algorithm is  $P_x = P_s + P_w$ . The frequency response characteristic  $H(e^{j\omega})$  of the adaptive FIR filter with coefficients  $\{h(k)\}$  should exhibit a resonant peak at the frequency of the interference. The frequency response of the interference suppression filter is  $H_s(e^{j\omega}) = 1 - H(e^{j\omega})$ , which should then exhibit a notch at the frequency of the interference.

It is interesting to plot the sequences  $\{w(n)\}$ ,  $\{s(n)\}$ , and  $\{x(n)\}$ . It is also interesting to plot the frequency responses  $H(e^{j\omega})$  and  $H_s(e^{j\omega})$  after the LMS algorithm has converged. The short-time average squared error  $ASE(m)$ , defined by (11.12), may be used to monitor the convergence characteristics of the LMS algorithm. The effect of the length of the adaptive filter on the quality of the estimate should be investigated.

The project may be generalized by adding a second sinusoid of a different frequency. Then  $H(e^{j\omega})$  should exhibit two resonant peaks, provided

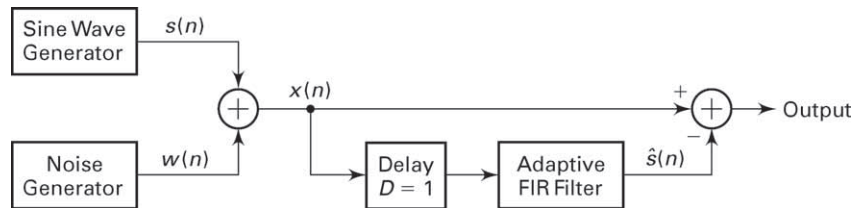


**FIGURE 11.4** Configuration of modules for experiment on interference suppression

the frequencies are sufficiently separated. Investigate the effect of the filter length  $N$  on the resolution of two closely spaced sinusoids.

## 11.4 ADAPTIVE LINE ENHANCEMENT

---

In the preceding section, we described a method for suppressing a strong narrowband interference from a wideband signal. An adaptive line enhancer (ALE) has the same configuration as the interference suppression filter in Figure 11.3, except that the objective is different.

In the adaptive line enhancer,  $\{s(n)\}$  is the desired signal and  $\{w(n)\}$  represents a wideband noise component that masks  $\{s(n)\}$ . The desired signal  $\{s(n)\}$  may be a spectral line (a pure sinusoid) or a relatively narrowband signal. Usually, the power in the wideband signal is greater than that in the narrowband signal—that is,  $P_w > P_s$ . It is apparent that the ALE is a self-tuning filter that has a peak in its frequency response at the frequency of the input sinusoid or in the frequency band occupied by the narrowband signal. By having a narrow bandwidth FIR filter, the noise outside the frequency band of the signal is suppressed, and thus the spectral line is enhanced in amplitude relative to the noise power in  $\{w(n)\}$ .

### 11.4.1 PROJECT 11.3: ADAPTIVE LINE ENHANCEMENT

This project requires the same software modules as those used in the project on interference suppression. Hence the description given in the preceding section applies directly. One change is that in the ALE, the condition is that  $P_w > P_s$ . Second, the output signal from the ALE is  $\{s(n)\}$ . Repeat the project described in the previous section under these conditions.

## 11.5 ADAPTIVE CHANNEL EQUALIZATION

---

The speed of data transmission over telephone channels is usually limited by channel distortion that causes intersymbol interference (ISI). At data rates below 2400 bits, the ISI is relatively small and is usually not a problem in the operation of a modem. However, at data rates above 2400 bits, an adaptive equalizer is employed in the modem to compensate for the channel distortion and thus to allow for highly reliable high-speed data transmission. In telephone channels, filters are used throughout the system to separate signals in different frequency bands. These filters cause amplitude and phase distortion. The adaptive equalizer is basically an adaptive FIR filter with coefficients that are adjusted by means of the LMS algorithm to correct for the channel distortion.

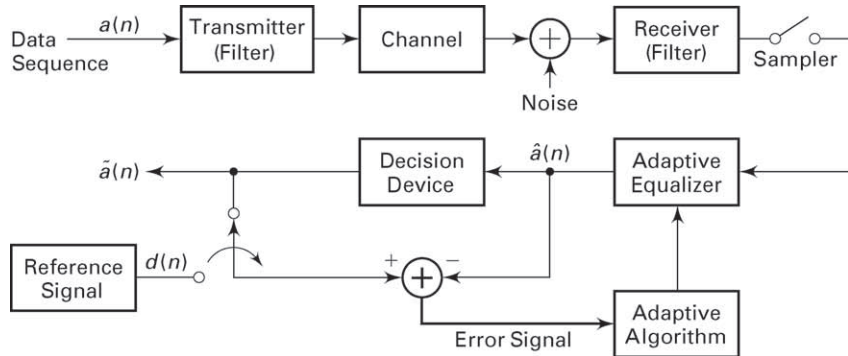


**FIGURE 11.5** Application of adaptive filtering to adaptive channel equalization

A block diagram showing the basic elements of a modem transmitting data over a channel is given in Figure 11.5. Initially, the equalizer coefficients are adjusted by transmitting a short training sequence, usually less than 1 second in duration. After the short training period, the transmitter begins to transmit the data sequence  $\{a(n)\}$ . To track the possible slow time variations in the channel, the equalizer coefficients must continue to be adjusted in an adaptive manner while receiving data. This is usually accomplished, as illustrated in Figure 11.5, by treating the decisions at the output of the decision device as correct and by using the decisions in place of the reference  $\{d(n)\}$  to generate the error signal. This approach works quite well when decision errors occur infrequently, such as less than one error in 100 data symbols. The occasional decision errors cause only a small misadjustment in the equalizer coefficients.

### 11.5.1 PROJECT 11.4: ADAPTIVE CHANNEL EQUALIZATION

The objective of this project is to investigate the performance of an adaptive equalizer for data transmission over a channel that causes inter-symbol interference. The basic configuration of the system to be simulated is shown in Figure 11.6. As we observe, five basic modules are required. Note that we have avoided carrier modulation and demodulation, which is required in a telephone channel modem. This is done to simplify the simulation program. However, all processing involves complex arithmetic operations.

The five modules are as follows.

1. The data generator module is used to generate a sequence of complex-valued information symbols  $\{a(n)\}$ . In particular, employ four equally probable symbols  $s + js$ ,  $s - js$ ,  $-s + js$ , and  $-s - js$ , where  $s$  is a scale factor that may be set to  $s = 1$ , or it can be an input parameter.

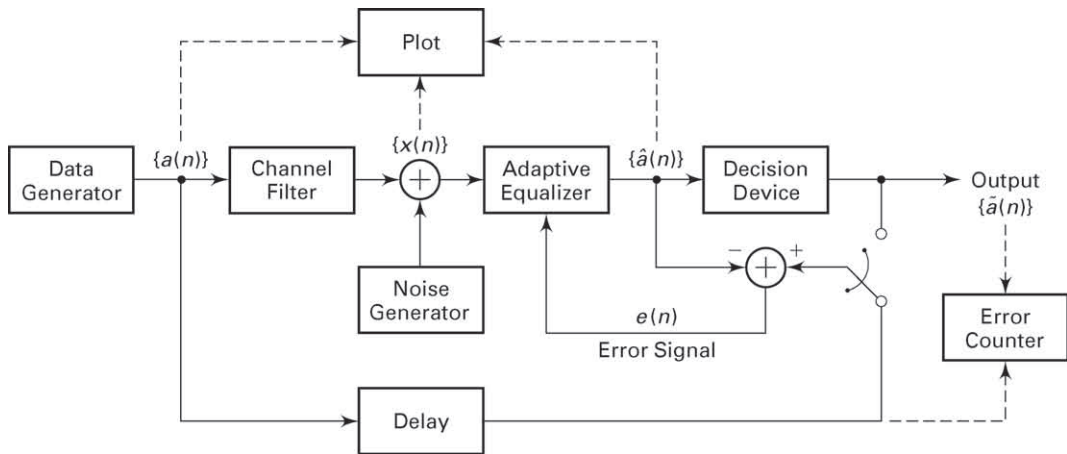


**FIGURE 11.6** Experiment for investigating the performance of an adaptive equalizer

2. The channel filter module is an FIR filter with coefficients  $\{c(n), 0 \leq n \leq K - 1\}$  that simulates the channel distortion. For distortionless transmission, set  $c(0) = 1$  and  $c(n) = 0$  for  $1 \leq n \leq K - 1$ . The length  $K$  of the filter is an input parameter.
3. The noise generator module is used to generate additive noise that is usually present in any digital communication system. If we are modeling noise that is generated by electronic devices, the noise distribution should be Gaussian with zero mean. Use the `randn` function.
4. The adaptive equalizer module is an FIR filter with tap coefficients  $\{h(k), 0 < k < N - 1\}$ , which are adjusted by the LMS algorithm. However, due to the use of complex arithmetic, the recursive equation in the LMS algorithm is slightly modified to

$$h_n(k) = h_{n-1}(k) + \Delta e(n)x^*(n - k) \quad (11.15)$$

- where the asterisk denotes the complex conjugate.
5. The decision device module takes the estimate  $\hat{a}(n)$  and quantizes it to one of the four possible signal points on the basis of the following decision rule:

$$\begin{aligned} \text{Re } [\hat{a}(n)] > 0 \text{ and } \text{Im } [\hat{a}(n)] > 0 &\longrightarrow 1+j \\ \text{Re } [\hat{a}(n)] > 0 \text{ and } \text{Im } [\hat{a}(n)] < 0 &\longrightarrow 1-j \\ \text{Re } [\hat{a}(n)] < 0 \text{ and } \text{Im } [\hat{a}(n)] > 0 &\longrightarrow -1+j \\ \text{Re } [\hat{a}(n)] < 0 \text{ and } \text{Im } [\hat{a}(n)] < 0 &\longrightarrow -1-j \end{aligned}$$

The effectiveness of the equalizer in suppressing the ISI introduced by the channel filter may be seen by plotting the following relevant

sequences in a two-dimensional (real–imaginary) display. The data generator output  $\{a(n)\}$  should consist of four points with values  $\pm 1 \pm j$ . The effect of channel distortion and additive noise may be viewed by displaying the sequence  $\{x(n)\}$  at the input to the equalizer. The effectiveness of the adaptive equalizer may be assessed by plotting its output  $\{\hat{a}(n)\}$  after convergence of its coefficients. The short-time average squared error ASE( $n$ ) may also be used to monitor the convergence characteristics of the LMS algorithm. Note that a delay must be introduced into the output of the data generator to compensate for the delays that the signal encounters due to the channel filter and the adaptive equalizer. For example, this delay may be set to the largest integer closest to  $(N + K)/2$ . Finally, an error counter may be used to count the number of symbol errors in the received data sequence, and the ratio for the number of errors to the total number of symbols (error rate) may be displayed. The error rate may be varied by changing the level of the ISI and the level of the additive noise.

It is suggested that simulations be performed for the following three channel conditions.

- a. No ISI:  $c(0) = 1, c(n) = 0, 1 \leq n \leq K - 1$
- b. Mild ISI:  $c(0) = 1, c(1) = 0.2, c(2) = -0.2, c(n) = 0, 3 \leq n \leq K - 1$
- c. Strong ISI:  $c(0) = 1, c(1) = 0.5, c(2) = 0.5, c(n) = 0, 3 \leq n \leq K - 1$

The measured error rate may be plotted as a function of the signal-to-noise ratio (SNR) at the input to the equalizer, where SNR is defined as  $P_s/P_n$ , where  $P_s$  is the signal power, given as  $P_s = s^2$ , and  $P_n$  is the noise power of the sequence at the output of the noise generator.

# CHAPTER **12**

---

## **Applications in Communications**

---

Today MATLAB finds widespread use in the simulation of a variety of communication systems. In this chapter, we shall focus on several applications dealing with waveform representation and coding, especially speech coding, and with digital communications. In particular, we shall describe several methods for digitizing analog waveforms, with specific application to speech coding and transmission. These methods are pulse-code modulation (PCM), differential PCM and adaptive differential PCM (ADPCM), delta modulation (DM) and adaptive delta modulation (ADM), and linear predictive coding (LPC). A project is formulated involving each of these waveform-encoding methods for simulation using MATLAB.

The last three topics treated in this chapter deal with signal-detection applications that are usually encountered in the implementation of a receiver in a digital communication system. For each of these topics, we describe a project that involves the implementations via simulation of the detection scheme in MATLAB.

### **12.1 PULSE-CODE MODULATION**

---

Pulse-code modulation is a method for quantizing an analog signal for the purpose of transmitting or storing the signal in digital form. PCM is widely used for speech transmission in telephone communications and for telemetry systems that employ radio transmission. We shall concentrate our attention on the application of PCM to speech signal processing.

Speech signals transmitted over telephone channels are usually limited in bandwidth to the frequency range below 4 kHz. Hence the Nyquist rate for sampling such a signal is less than 8 kHz. In PCM, the analog speech signal is sampled at the nominal rate of 8 kHz (samples per second), and each sample is quantized to one of  $2^b$  levels and represented digitally by a sequence of  $b$  bits. Thus the bit rate required to transmit the digitized speech signal is  $8000b$  bits per second.

The quantization process may be modeled mathematically as

$$\tilde{s}(n) = s(n) + q(n) \quad (12.1)$$

where  $\tilde{s}(n)$  represents the quantized value of  $s(n)$  and  $q(n)$  represents the quantization error, which we treat as an additive noise. Assuming that a uniform quantizer is used and the number of levels is sufficiently large, the quantization noise is well characterized statistically by the uniform probability density function

$$p(q) = \frac{1}{\Delta}, \quad -\frac{\Delta}{2} \leq q \leq \frac{\Delta}{2} \quad (12.2)$$

where the step size of the quantizer is  $\Delta = 2^{-b}$ . The mean square value of the quantization error is

$$E(q^2) = \frac{\Delta^2}{12} = \frac{2^{-2b}}{12} \quad (12.3)$$

Measured in decibels, the mean square value of the noise is

$$10 \log \left( \frac{\Delta^2}{12} \right) = 10 \log \left( \frac{2^{-2b}}{12} \right) = -6b - 10.8 \text{ dB} \quad (12.4)$$

We observe that the quantization noise decreases by 6 dB/bit used in the quantizer. High-quality speech requires a minimum of 12 bits per sample and hence a bit rate of 96,000 bits per second (bps) or 96 kbps.

Speech signals have the characteristic that small signal amplitudes occur more frequently than large signal amplitudes. However, a uniform quantizer provides the same spacing between successive levels throughout the entire dynamic range of the signal. A better approach is to use a nonuniform quantizer, which provides more closely spaced levels at the low signal amplitudes and more widely spaced levels at the large signal amplitudes. For a nonuniform quantizer with  $b$  bits, the resulting quantization error has a mean square value that is smaller than that given by (12.4). A nonuniform quantizer characteristic is usually obtained by passing the signal through a nonlinear device that compresses the signal amplitude, followed by a uniform quantizer. For example, a logarithmic compressor employed in United States and Canadian telecommunications

systems, called a  $\mu$ -law compressor, has an input-output magnitude characteristic of the form

$$y = \frac{\ln(1 + \mu|s|)}{\ln(1 + \mu)} \operatorname{sgn}(s); \quad |s| \leq 1, |y| \leq 1 \quad (12.5)$$

where  $s$  is the normalized input,  $y$  is the normalized output,  $\operatorname{sgn}(\cdot)$  is the sign function, and  $\mu$  is a parameter that is selected to give the desired compression characteristic.

In the encoding of speech waveforms, the value of  $\mu = 255$  has been adopted as a standard in the United States and Canada. This value results in about a 24 dB reduction in the quantization noise power relative to uniform quantization. Consequently, an 8-bit quantizer used in conjunction with a  $\mu = 255$  logarithmic compressor produces the same quality speech as a 12-bit uniform quantizer with no compression. Thus the compressed PCM speech signal has a bit rate of 64 kbps.

The logarithmic compressor standard used in European telecommunication systems is called  $A$ -law and is defined as

$$y = \begin{cases} \frac{1 + \ln(A|s|)}{1 + \ln A} \operatorname{sgn}(s), & \frac{1}{A} \leq |s| \leq 1 \\ \frac{A|s|}{1 + \ln A} \operatorname{sgn}(s), & 0 \leq |s| \leq \frac{1}{A} \end{cases} \quad (12.6)$$

where  $A$  is chosen as 87.56. Although (12.5) and (12.6) are different nonlinear functions, the two compression characteristics are very similar. Figure 12.1 illustrates these two compression functions. Note their strong similarity.

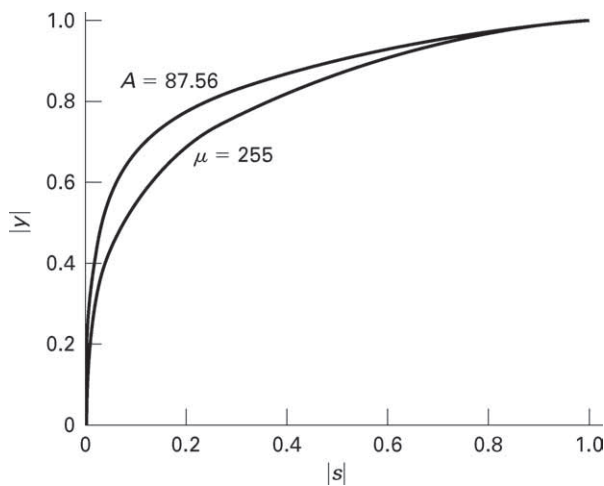


**FIGURE 12.1** Comparison of  $\mu$ -law and  $A$ -law nonlinearities

In the reconstruction of the signal from the quantized values, the decoder employs an inverse logarithmic relation to expand the signal amplitude. For example, in  $\mu$ -law the inverse relation is given by

$$|s| = \frac{(1 + \mu)^{|y|} - 1}{\mu}; \quad |y| \leq 1, |s| \leq 1 \quad (12.7)$$

The combined compressor-expander pair is termed a *compander*.

### 12.1.1 PROJECT 12.1: PCM

The purpose of this project is to gain an understanding of PCM compression (linear to logarithmic) and PCM expansion (logarithmic to linear). Write the following three MATLAB functions for this project:

1. a  $\mu$ -law compressor function to implement (12.5) that accepts a zero-mean normalized ( $|s| \leq 1$ ) signal and produces a compressed zero-mean signal with  $\mu$  as a free parameter that can be specified,
2. a quantizer function that accepts a zero-mean input and produces an integer output after  $b$ -bit quantization that can be specified, and
3. a  $\mu$ -law expander to implement (12.7) that accepts an integer input and produces a zero-mean output for a specified  $\mu$  parameter.

For simulation purposes, generate a large number of samples (10,000 or more) of the following sequences: (a) a sawtooth sequence, (b) an exponential pulse train sequence, (c) a sinusoidal sequence, and (d) a random sequence with small variance. Care must be taken to generate nonperiodic sequences by choosing their normalized frequencies as irrational numbers (i.e., sample values should not repeat). For example, a sinusoidal sequence can be generated using

$$s(n) = 0.5 \sin(n/33), \quad 0 \leq n \leq 10,000$$

From our discussions in Chapter 2, this sequence is nonperiodic, yet it has a periodic envelope. Other sequences can also be generated in a similar fashion. Process these signals through the above  $\mu$ -law compressor, quantizer, and expander functions as shown in Figure 12.2, and compute

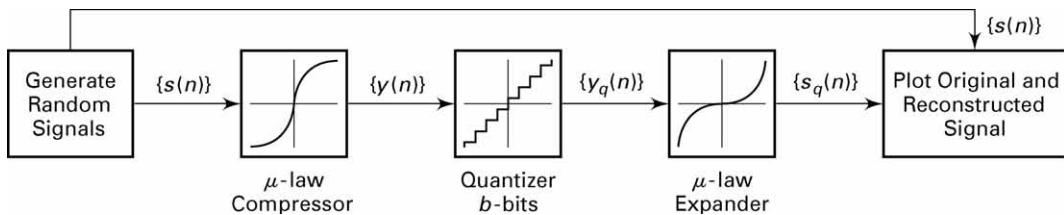


**FIGURE 12.2** PCM project

the signal-to-quantization noise ratio (SQNR) in dB as

$$\text{SQNR} = 10 \log_{10} \left( \frac{\sum_{n=1}^N s^2(n)}{\sum_{n=1}^N (s(n) - s_q(n))^2} \right)$$

For different  $b$ -bit quantizers, systematically determine the value of  $\mu$  that maximizes the SQNR. Also plot the input and output waveforms, and comment on the results.

## 12.2 DIFFERENTIAL PCM (DPCM)

---

In PCM, each sample of the waveform is encoded independently of all the other samples. However, most signals, including speech, sampled at the Nyquist rate or faster exhibit significant correlation between successive samples. In other words, the average change in amplitude between successive samples is relatively small. Consequently, an encoding scheme that exploits the redundancy in the samples will result in a lower bit rate for the speech signal.

A relatively simple solution is to encode the differences between successive samples rather than the samples themselves. Since differences between samples are expected to be smaller than the actual sampled amplitudes, fewer bits are required to represent the differences. A refinement of this general approach is to predict the current sample based on the previous  $p$  samples. To be specific, let  $s(n)$  denote the current sample of speech, and let  $\hat{s}(n)$  denote the predicted value of  $s(n)$ , defined as

$$\hat{s}(n) = \sum_{i=1}^p a(i) s(n-i) \quad (12.8)$$

Thus  $\hat{s}(n)$  is a weighted linear combination of the past  $p$  samples, and the  $a(i)$  are the predictor (filter) coefficients. The  $a(i)$  are selected to minimize some function of the error between  $s(n)$  and  $\hat{s}(n)$ .

A mathematically and practically convenient error function is the sum of squared errors. With this as the performance index for the predictor, we select the  $a(i)$  to minimize

$$\begin{aligned} \mathcal{E}_p &\stackrel{\Delta}{=} \sum_{n=1}^N e^2(n) = \sum_{n=1}^N \left[ s(n) - \sum_{i=1}^p a(i) s(n-i) \right]^2 \\ &= r_{ss}(0) - 2 \sum_{i=1}^p a(i) r_{ss}(i) + \sum_{i=1}^p \sum_{j=1}^p a(i) a(j) r_{ss}(i-j) \end{aligned} \quad (12.9)$$

where  $r_{ss}(m)$  is the autocorrelation function of the sampled signal sequence  $s(n)$ , defined as

$$r_{ss}(m) = \sum_{i=1}^N s(i)s(i+m) \quad (12.10)$$

Minimization of  $\mathcal{E}_p$  with respect to the predictor coefficients  $\{a_i(n)\}$  results in the set of linear equations, called the normal equations,

$$\sum_{i=1}^p a(i)r_{ss}(i-j) = r_{ss}(j), \quad j = 1, 2, \dots, p \quad (12.11)$$

or in the matrix form,

$$\mathbf{R}\mathbf{a} = \mathbf{r} \implies \mathbf{a} = \mathbf{R}^{-1}\mathbf{r} \quad (12.12)$$

where  $\mathbf{R}$  is the autocorrelation matrix,  $\mathbf{a}$  is the coefficient vector, and  $\mathbf{r}$  is the autocorrelation vector. Thus the values of the predictor coefficients are established.

Having described the method for determining the predictor coefficients, let us now consider the block diagram of a practical DPCM system, shown in Figure 12.3. In this configuration, the predictor is implemented with the feedback loop around the quantizer. The input to the predictor is denoted as  $\hat{s}(n)$ , which represents the signal sample  $s(n)$  modified by the quantization process, and the output of the predictor is

$$\hat{s} = \sum_{i=1}^p a(i)\hat{s}(n-i) \quad (12.13)$$

The difference

$$e(n) = s(n) - \hat{s}(n) \quad (12.14)$$

is the input to the quantizer, and  $\tilde{e}(n)$  denotes the output. Each value of the quantized prediction error  $\tilde{e}(n)$  is encoded into a sequence of binary

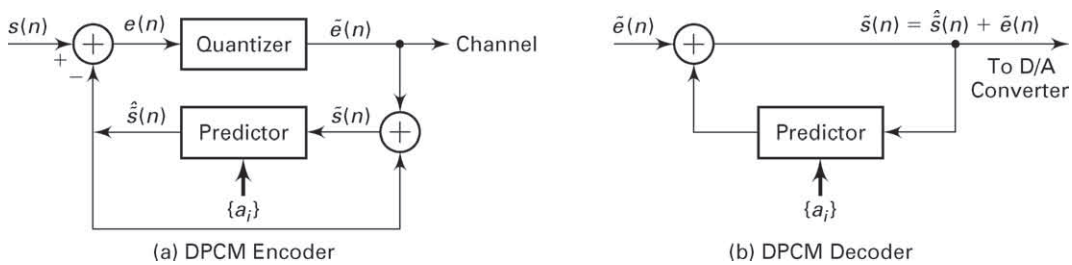


**FIGURE 12.3** Block diagram of a DPCM transcoder: (a) encoder, (b) decoder

digits and transmitted over the channel to the receiver. The quantized error  $\tilde{e}(n)$  is also added to the predicted value  $\hat{s}(n)$  to yield  $\tilde{s}(n)$ .

At the receiver, the same predictor that was used at the transmitting end is synthesized, and its output  $\hat{s}(n)$  is added to  $\tilde{e}(n)$  to yield  $\tilde{s}(n)$ . The signal  $\tilde{s}(n)$  is the desired excitation for the predictor and also the desired output sequence from which the reconstructed signal  $s(t)$  is obtained by filtering, as shown in Figure 12.3b.

The use of feedback around the quantizer, as described, ensures that the error in  $\tilde{s}(n)$  is simply the quantization error  $q(n) = \tilde{e}(n) - e(n)$  and that there is no accumulation of previous quantization errors in the implementation of the decoder. That is,

$$q(n) = \tilde{e}(n) - e(n) = \tilde{e}(n) - s(n) + \hat{s}(n) = \tilde{s}(n) - s(n) \quad (12.15)$$

Hence  $\tilde{s}(n) = s(n) + q(n)$ . This means that the quantized sample  $\tilde{s}(n)$  differs from the input  $s(n)$  by the quantization error  $q(n)$  independent of the predictor used. Therefore, the quantization errors do not accumulate.

In the DPCM system illustrated in Figure 12.3, the estimate or predicted value  $\tilde{s}(n)$  of the signal sample  $s(n)$  is obtained by taking a linear combination of past values  $\tilde{s}(n-k)$ ,  $k = 1, 2, \dots, p$ , as indicated by (12.13). An improvement in the quality of the estimate is obtained by including linearly filtered past values of the quantized error. Specifically, the estimate of  $s(n)$  may be expressed as

$$\hat{s}(n) = \sum_{i=1}^p a(i) \tilde{s}(n-i) + \sum_{i=1}^m b(i) \tilde{e}(n-i) \quad (12.16)$$

where  $b(i)$  are the coefficients of the filter for the quantized error sequence  $\tilde{e}(n)$ . The block diagram of the encoder at the transmitter and the decoder at the receiver are shown in Figure 12.4. The two sets of coefficients  $a(i)$  and  $b(i)$  are selected to minimize some function of the error  $e(n) = \tilde{s}(n) - s(n)$ , such as the sum of squared errors.

By using a logarithmic compressor and a 4-bit quantizer for the error sequence  $e(n)$ , DPCM results in high-quality speech at a rate of 32 kbps, which is a factor of 2 lower than logarithmic PCM.

### 12.2.1 PROJECT 12.2: DPCM

The objective of this project is to gain understanding of the DPCM encoding and decoding operations. For simulation purposes, generate correlated random sequences using a pole-zero signal model of the form

$$s(n) = a(1)s(n-1) + b_0x(n) + b_1x(n-1) \quad (12.17)$$

where  $x(n)$  is a zero-mean unit variance Gaussian sequence. This can be done using the **filter** function. The sequences developed in Project 12.1

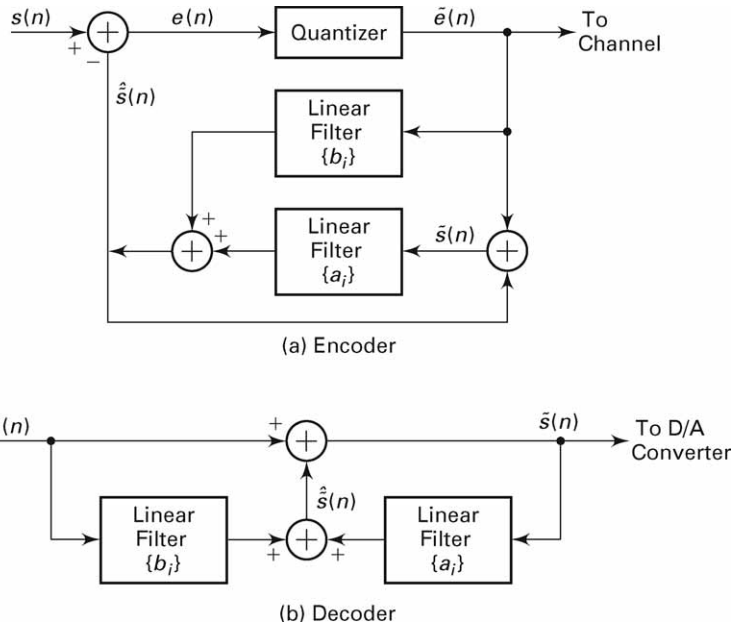


**FIGURE 12.4** DPCM modified by the linearly filtered error sequence

can also be used for simulation. Develop the following three MATLAB modules for this project:

1. a model predictor function to implement (12.12), given the input signal  $s(n)$ ;
2. a DPCM encoder function to implement the block diagram of Figure 12.3a, which accepts a zero-mean input sequence and produces a quantized  $b$ -bit integer error sequence, where  $b$  is a free parameter; and
3. a DPCM decoder function of Figure 12.3b, which reconstructs the signal from the quantized error sequence.

Experiment with several  $p$ -order prediction models for a given signal and determine the optimum order. Compare this DPCM implementation with the PCM system of Project 12.1 (at the end of the chapter) and comment on the results. Extend this implementation to include an  $m$ th-order moving average filter as indicated in (12.16).

## 12.3 ADAPTIVE PCM AND DPCM (ADPCM)

In general, the power in a speech signal varies slowly with time. PCM and DPCM encoders, however, are designed on the basis that the speech signal power is constant, and hence the quantizer is fixed. The efficiency

and performance of these encoders can be improved by having them adapt to the slowly time-variant power level of the speech signal.

In both PCM and DPCM, the quantization error  $q(n)$  resulting from a uniform quantizer operating on a slowly varying power level input signal will have a time-variant variance (quantization noise power). One improvement that reduces the dynamic range of the quantization noise is the use of an adaptive quantizer.

Adaptive quantizers can be classified as feedforward or feedback. A feedforward adaptive quantizer adjusts its step size for each signal sample, based on a measurement of the input speech signal variance (power). For example, the estimated variance, based as a sliding window estimator, is

$$\hat{\sigma}_{n+1}^2 = \frac{1}{M} \sum_{k=n+1-M}^{n+1} s^2(k) \quad (12.18)$$

Then the step size for the quantizer is

$$\Delta(n+1) = \Delta(n)\hat{\sigma}_{n+1} \quad (12.19)$$

In this case, it is necessary to transmit  $\Delta(n+1)$  to the decoder in order for it to reconstruct the signal.

A feedback-adaptive quantizer employs the output of the quantizer in the adjustment of the step size. In particular, we may set the step size as

$$\Delta(n+1) = \alpha(n)\Delta(n) \quad (12.20)$$

where the scale factor  $\alpha(n)$  depends on the previous quantizer output. For example, if the previous quantizer output is small, we may select  $\alpha(n) < 1$  in order to provide for finer quantization. On the other hand, if the quantizer output is large, then the step size should be increased to reduce the possibility of signal clipping. Such an algorithm has been successfully used in the encoding of speech signals. Figure 12.5 illustrates such a (3-bit) quantizer in which the step size is adjusted recursively according to the relation

$$\Delta(n+1) = \Delta(n) \cdot M(n)$$

where  $M(n)$  is a multiplication factor whose value depends on the quantizer level for the sample  $s(n)$  and  $\Delta(n)$  is the step size of the quantizer for processing  $s(n)$ . Values of the multiplication factors optimized for speech encoding have been given by [39]. These values are displayed in Table 12.1 for 2-, 3-, and 4-bit quantization for PCM and DPCM.

In DPCM, the predictor can also be made adaptive. Thus in ADPCM, the coefficients of the predictor are changed periodically to reflect the changing signal statistics of the speech. The linear equations given by (12.11) still apply, but the short-term autocorrelation function of  $s(n)$ ,  $r_{ss}(m)$  changes with time.

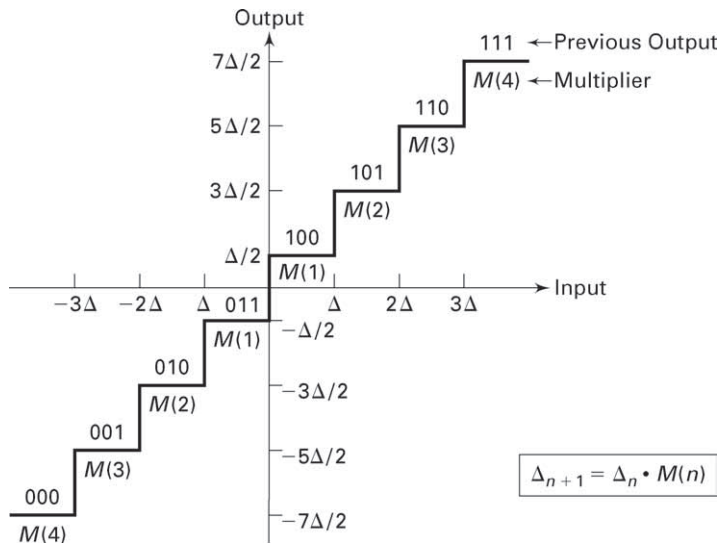


**FIGURE 12.5** Example of a quantizer with an adaptive step size ([39])

**TABLE 12.1** Multiplication factors for adaptive step-size adjustment ([39])

	PCM			DPCM		
	2	3	4	2	3	4
M(1)	0.60	0.85	0.80	0.80	0.90	0.90
M(2)	2.20	1.00	0.80	1.60	0.90	0.90
M(3)		1.00	0.80		1.25	0.90
M(4)		1.50	0.80		1.70	0.90
M(5)			0.80			1.20
M(6)			0.80			1.60
M(7)			0.80			2.00
M(8)			0.80			2.40

### 12.3.1 ADPCM STANDARD

Figure 12.6 illustrates, in block diagram form, a 32 kbps ADPCM encoder and decoder that has been adopted as an international (CCITT) standard for speech transmission over telephone channels. The ADPCM encoder is designed to accept 8-bit PCM compressed signal samples at 64 kbps, and by means of adaptive prediction and adaptive 4-bit quantization to reduce the bit rate over the channel to 32 kbps. The ADPCM decoder accepts the 32 kbps data stream and reconstructs the signal in the form of an 8-bit compressed PCM at 64 kbps. Thus we have a configuration shown in Figure 12.7, where the ADPCM encoder/decoder is embedded into a PCM system. Although the ADPCM encoder/decoder

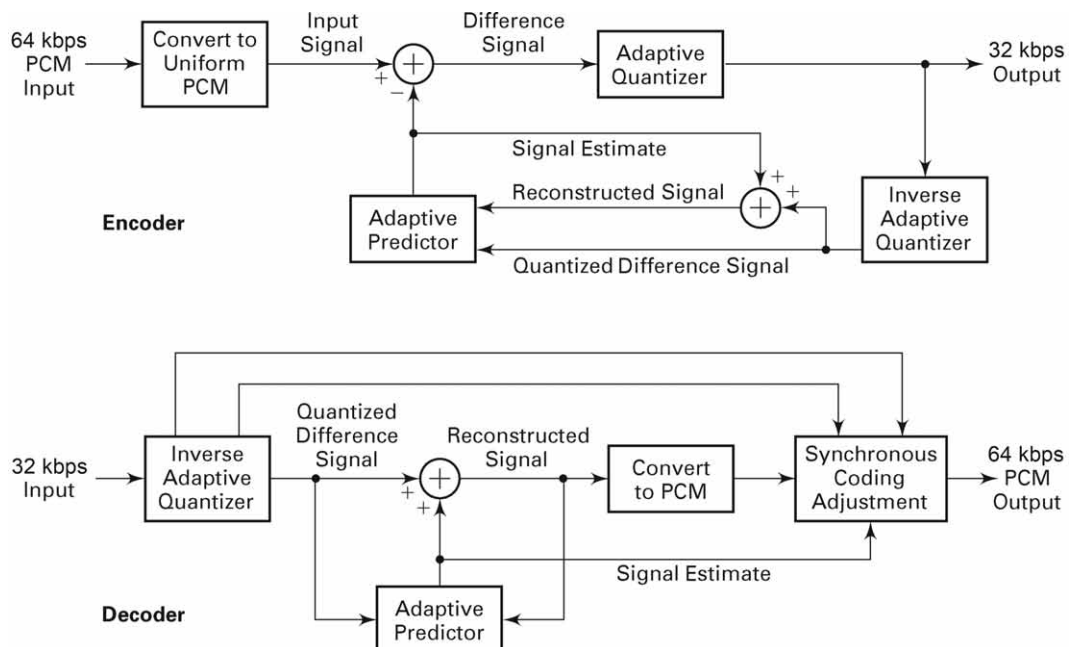


**FIGURE 12.6** ADPCM block diagram

could be used directly on the speech signal, the interface to the PCM system is necessary in practice in order to maintain compatibility with existing PCM systems that are widely used in the telephone network.

The ADPCM encoder accepts the 8-bit PCM compressed signal and expands it to a 14-bit-per-sample linear representation for processing. The predicted value is subtracted from this 14-bit linear value to produce a difference signal sample that is fed to the quantizer. Adaptive quantization is performed on the difference signal to produce a 4-bit output for transmission over the channel.

Both the encoder and decoder update their internal variables, based only on the ADPCM values that are generated. Consequently, an ADPCM

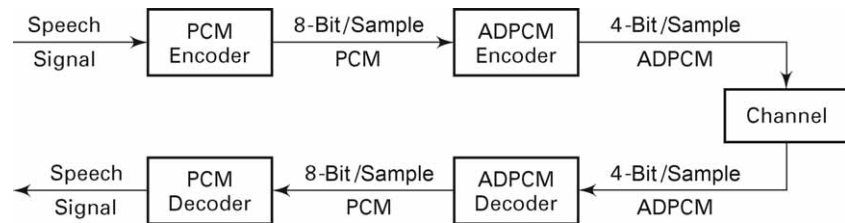


**FIGURE 12.7** ADPCM interface to PCM system

decoder, including an inverse adaptive quantizer, is embedded in the encoder so that all internal variables are updated, based on the same data. This ensures that the encoder and decoder operate in synchronism without the need to transmit any information on the values of internal variables.

The adaptive predictor computes a weighted average of the last six dequantized difference values and the last two predicted values. Hence this predictor is basically a two-pole ( $p = 2$ ) and six-zero ( $m = 6$ ) filter governed by the difference equation given by (12.16). The filter coefficients are updated adaptively for every new input sample.

At the receiving decoder and at the decoder that is embedded in the encoder, the 4-bit transmitted ADPCM value is used to update the inverse adaptive quantizer, whose output is a dequantized version of the difference signal. This dequantized value is added to the value generated by the adaptive predictor to produce the reconstructed speech sample. This signal is the output of the decoder, which is converted to compressed PCM format at the receiver.

### 12.3.2 PROJECT 12.3: ADPCM

The objective of this project is to gain familiarity with, and understanding of, ADPCM and its interface with a PCM encoder/decoder (transcoder). As described, the ADPCM transcoder is inserted between the PCM compressor and the PCM expander as shown in Figure 12.7. Use the already developed MATLAB PCM and DPCM modules for this project.

The input to the PCM-ADPCM transcoder system can be supplied from internally generated waveform data files, just as in the case of the PCM project. The output of the transcoder can be plotted. Comparisons should be made between the output signal from the PCM-ADPCM transcoder with the signal from the PCM transcoder (PCM Project 12.1), and with the original input signal.

## 12.4 DELTA MODULATION (DM)

Delta modulation may be viewed as a simplified form of DPCM in which a two-level (1-bit) quantizer is used in conjunction with a fixed first-order predictor. The block diagram of a DM encoder-decoder is shown in Figure 12.8. We note that

$$\hat{s}(n) = \tilde{s}(n - 1) = \hat{s}(n - 1) + \tilde{e}(n - 1) \quad (12.21)$$

Since

$$q(n) = \tilde{e}(n) - e(n) = \tilde{e}(n) - [s(n) - \hat{s}(n)]$$

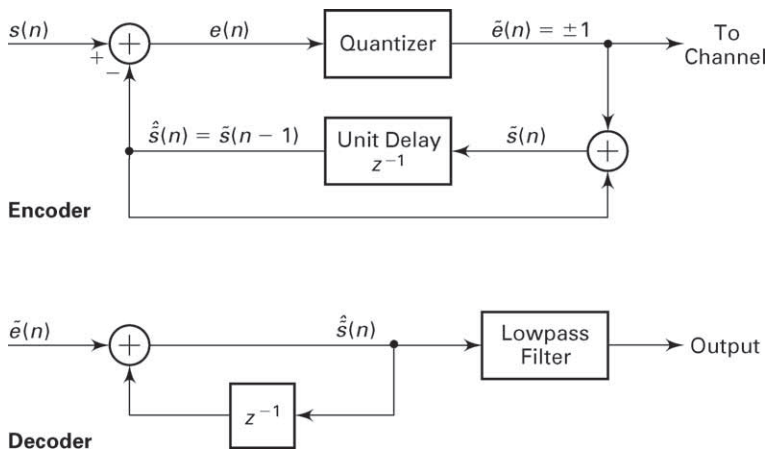


**FIGURE 12.8** Block diagram of a delta modulation system

it follows that

$$\hat{s}(n) = s(n - 1) + q(n - 1) \quad (12.22)$$

Thus the estimated (predicted) value of  $s(n)$  is really the previous sample  $s(n - 1)$  modified by the quantization noise  $q(n - 1)$ . We also note that the difference equation in (12.21) represents an integrator with an input  $\tilde{e}(n)$ . Hence an equivalent realization of the one-step predictor is an accumulator with an input equal to the quantized error signal  $\tilde{e}(n)$ . In general, the quantized error signal is scaled by some value—say,  $\Delta_1$ —which is called the step size. This equivalent realization is illustrated in Figure 12.9. In effect, the encoder shown in Figure 12.9 approximates a waveform  $s(t)$

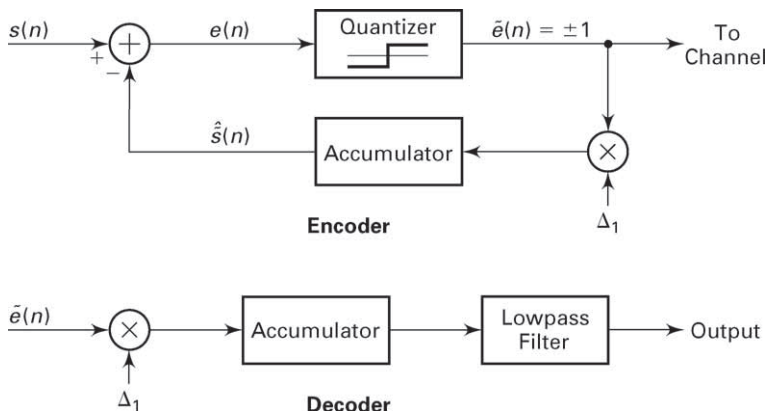


**FIGURE 12.9** An equivalent realization of a delta modulation system

by a linear staircase function. In order for the approximation to be relatively good, the waveform  $s(t)$  must change slowly relative to the sampling rate. This requirement implies that the sampling rate must be several (a factor of at least 5) times the Nyquist rate. A lowpass filter is usually incorporated into the decoder to smooth out discontinuities in the reconstructed signal.

#### 12.4.1 ADAPTIVE DELTA MODULATION (ADM)

At any given sampling rate, the performance of the DM encoder is limited by two types of distortion, as shown in Figure 12.10. One is called slope-overload distortion. It is due to the use of a step size  $\Delta_1$  that is too small to follow portions of the waveform that have a steep slope. The second type of distortion, called granular noise, results from using a step size that is too large in parts of the waveform having a small slope. The need to minimize both of these two types of distortion results in conflicting requirements in the selection of the step size  $\Delta_1$ .

An alternative solution is to employ a variable size that adapts itself to the short-term characteristics of the source signal. That is, the step size is increased when the waveform has a steep slope and decreased when the waveform has a relatively small slope.

A variety of methods can be used to set adaptively the step size in every iteration. The quantized error sequence  $\tilde{e}(n)$  provides a good indication of the slope characteristics of the waveform being encoded. When the quantized error  $\tilde{e}(n)$  is changing signs between successive iterations, this is an indication that the slope of the waveform in the locality is relatively small. On the other hand, when the waveform has a steep slope, successive values of the error  $\tilde{e}(n)$  are expected to have identical signs. From these observations, it is possible to devise algorithms that decrease or increase the step size, depending on successive values of  $\tilde{e}(n)$ . A relatively simple rule devised by [38] is to vary adaptively the step size according to the relation

$$\Delta(n) = \Delta(n-1) K^{\tilde{e}(n)\tilde{e}(n-1)}, \quad n = 1, 2, \dots \quad (12.23)$$

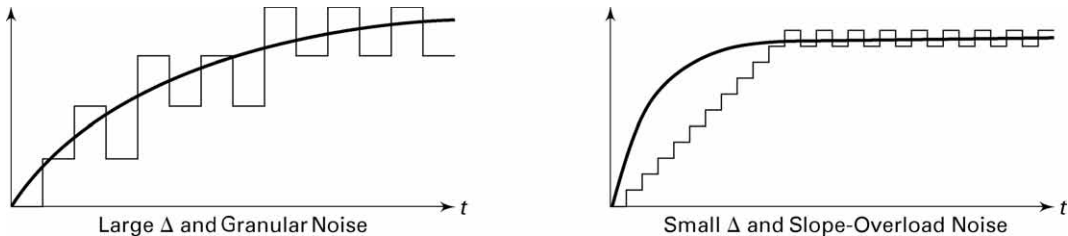


**FIGURE 12.10** Two types of distortion in the DM encoder

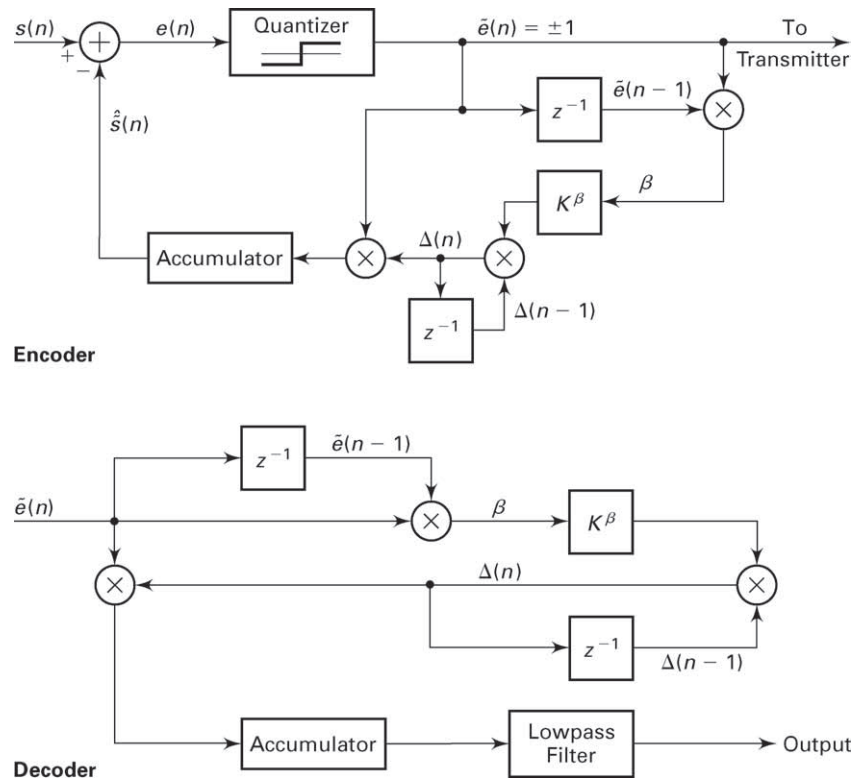


**FIGURE 12.11** An example of a delta modulation system with adaptive step size

where  $K \geq 1$  is a constant that is selected to minimize the total distortion. A block diagram of a DM encoder-decoder that incorporates this adaptive algorithm is illustrated in Figure 12.11.

Several other variations of adaptive DM encoding have been investigated and described in the technical literature. A particularly effective and popular technique first proposed by [27] is called *continuously variable slope delta modulation* (CVSD). In CVSD, the adaptive step-size parameter may be expressed as

$$\Delta(n) = \alpha\Delta(n-1) + k_1 \quad (12.24)$$

if  $\tilde{e}(n)$ ,  $\tilde{e}(n-1)$ , and  $\tilde{e}(n-2)$  have the same sign; otherwise,

$$\Delta(n) = \alpha\Delta(n-1) + k_2 \quad (12.25)$$

The parameters  $\alpha$ ,  $k_1$ , and  $k_2$  are selected such that  $0 < \alpha < 1$  and  $k_1 > k_2 > 0$ . For more discussion on this and other variations of adaptive

DM, the interested reader is referred to the papers by Jayant [39] and Flanagan et al. [15] and to the extensive references contained in these papers.

#### 12.4.2 PROJECT 12.4: DM AND ADM

The purpose of this project is to gain an understanding of delta modulation and adaptive delta modulation for coding of waveforms. This project involves writing MATLAB functions for the DM encoder and decoder as shown in Figure 12.9, and for the ADM encoder and decoder shown in Figure 12.11. The lowpass filter at the decoder can be implemented as a linear-phase FIR filter. For example, a Hanning filter that has the impulse response

$$h(n) = \frac{1}{2} \left[ 1 - \cos \left( \frac{2\pi n}{N-1} \right) \right], \quad 0 \leq n \leq N-1 \quad (12.26)$$

may be used, where the length  $N$  may be selected in the range  $5 \leq N \leq 15$ .

The input to the DM and ADM systems can be supplied from the waveforms generated in Project 12.1 except that the sampling rate should be higher by a factor of 5 to 10. The output of the decoder can be plotted. Comparisons should be made between the output signal from the DM and ADM decoders and the original input signal.

## 12.5 LINEAR PREDICTIVE CODING (LPC) OF SPEECH

The linear predictive coding (LPC) method for speech analysis and synthesis is based on modeling the vocal tract as a linear all-pole (IIR) filter having the system function

$$H(z) = \frac{G}{1 + \sum_{k=1}^p a_p(k) z^{-k}} \quad (12.27)$$

where  $p$  is the number of poles,  $G$  is the filter gain, and  $\{a_p(k)\}$  are the parameters that determine the poles. There are two mutually exclusive excitation functions to model voiced and unvoiced speech sounds. On a short-time basis, voiced speech is periodic with a fundamental frequency  $F_0$ , or a pitch period  $1/F_0$ , which depends on the speaker. Thus voiced speech is generated by exciting the all-pole filter model by a periodic impulse train with a period equal to the desired pitch period. Unvoiced speech sounds are generated by exciting the all-pole filter model by the output of a random-noise generator. This model is shown in Figure 12.12.

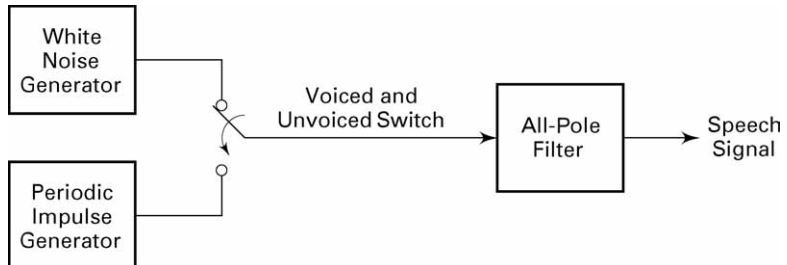


**FIGURE 12.12** Block diagram model for the generation of a speech signal

Given a short-time segment of a speech signal, usually about 20 ms or 160 samples at an 8 kHz sampling rate, the speech encoder at the transmitter must determine the proper excitation function, the pitch period for voiced speech, the gain parameter  $G$ , and the coefficients  $a_p(k)$ . A block diagram that illustrates the speech encoding system is given in Figure 12.13. The parameters of the model are determined adaptively from the data and encoded into a binary sequence and transmitted to the receiver. At the receiver, the speech signal is synthesized from the model and the excitation signal.

The parameters of the all-pole filter model are easily determined from the speech samples by means of linear prediction. To be specific, the output of the FIR linear prediction filter is

$$\hat{s}(n) = - \sum_{k=1}^p a_p(k) s(n-k) \quad (12.28)$$

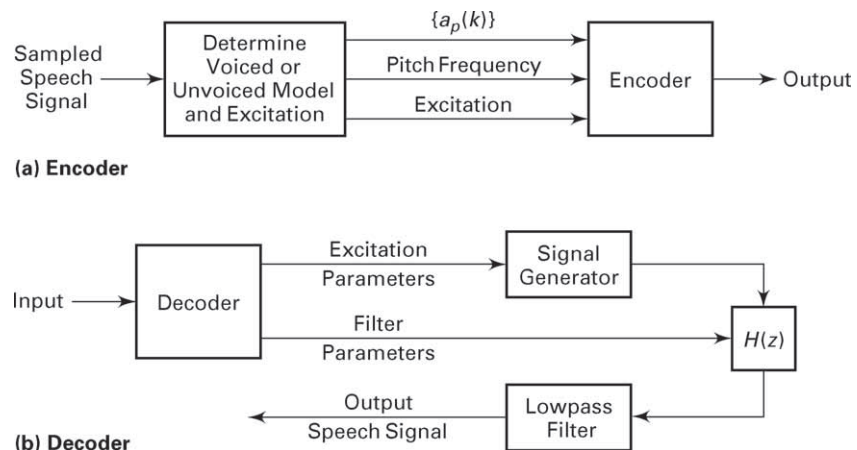


**FIGURE 12.13** Encoder and decoder for LPC

and the corresponding error between the observed sample  $s(n)$  and the predicted value  $\hat{s}(n)$  is

$$e(n) = s(n) + \sum_{k=1}^p a_p(k) s(n-k) \quad (12.29)$$

By minimizing the sum of squared errors, that is,

$$\mathcal{E} = \sum_{n=0}^N e^2(n) = \sum_{n=0}^N \left[ s(n) + \sum_{k=1}^p a_p(k) s(n-k) \right]^2 \quad (12.30)$$

we can determine the pole parameters  $\{a_p(k)\}$  of the model. The result of differentiating  $\mathcal{E}$  with respect to each of the parameters and equating the result to zero is a set of  $p$  linear equations

$$\sum_{k=1}^p a_p(k) r_{ss}(m-k) = -r_{ss}(m), \quad m = 1, 2, \dots, p \quad (12.31)$$

where  $r_{ss}(m)$  is the autocorrelation of the sequence  $s(n)$  defined as

$$r_{ss}(m) = \sum_{n=0}^N s(n)s(n+m) \quad (12.32)$$

The linear equation (12.31) can be expressed in matrix form as

$$\mathbf{R}_{ss}\mathbf{a} = -\mathbf{r}_{ss} \quad (12.33)$$

where  $\mathbf{R}_{ss}$  is a  $p \times p$  autocorrelation matrix,  $\mathbf{r}_{ss}$  is a  $p \times 1$  autocorrelation vector, and  $\mathbf{a}$  is a  $p \times 1$  vector of model parameters. Hence

$$\mathbf{a} = -\mathbf{R}_{ss}^{-1}\mathbf{r}_{ss} \quad (12.34)$$

These equations can also be solved recursively and most efficiently, without resorting to matrix inversion, by using the Levinson–Durbin algorithm [54]. However, in MATLAB it is convenient to use the matrix inversion. The all-pole filter parameters  $\{a_p(k)\}$  can be converted to the all-pole lattice parameters  $\{K_i\}$  (called the reflection coefficients) using the MATLAB function `dir2latc` developed in Chapter 6.

The gain parameter of the filter can be obtained by noting that its input-output equation is

$$s(n) = -\sum_{k=1}^p a_p(k) s(n-k) + Gx(n) \quad (12.35)$$

where  $x(n)$  is the input sequence. Clearly,

$$Gx(n) = s(n) + \sum_{k=1}^p a_p(k) s(n-k) = e(n)$$

Then

$$G^2 \sum_{n=0}^{N-1} x^2(n) = \sum_{n=0}^{N-1} e^2(n) \quad (12.36)$$

If the input excitation is normalized to unit energy by design, then

$$G^2 = \sum_{n=0}^{N-1} e^2(n) = r_{ss}(0) + \sum_{k=1}^p a_p(k) r_{ss}(k) \quad (12.37)$$

Thus  $G^2$  is set equal to the residual energy resulting from the least-squares optimization.

Once the LPC coefficients are computed, we can determine whether the input speech frame is voiced, and if so, what the pitch is. This is accomplished by computing the sequence

$$r_e(n) = \sum_{k=1}^p r_a(k) r_{ss}(n-k) \quad (12.38)$$

where  $r_a(k)$  is defined as

$$r_a(k) = \sum_{i=1}^p a_p(i) a_p(i+k) \quad (12.39)$$

which is the autocorrelation sequence of the prediction coefficients. The pitch is detected by finding the peak of the normalized sequence  $r_e(n)/r_e(0)$  in the time interval that corresponds to 3 to 15 ms in the 20 ms sampling frame. If the value of this peak is at least 0.25, the frame of speech is considered voiced with a pitch period equal to the value of  $n = N_p$ , where  $r_e(N_p)/r_e(0)$  is a maximum. If the peak value is less than 0.25, the frame of speech is considered unvoiced and the pitch is zero.

The values of the LPC coefficients, the pitch period, and the type of excitation are transmitted to the receiver, where the decoder synthesizes the speech signal by passing the proper excitation through the all-pole filter model of the vocal tract. Typically, the pitch period requires 6 bits, and the gain parameter may be represented by 5 bits after its dynamic range is compressed logarithmically. If the prediction coefficients were to be coded, they would require between 8 to 10 bits per coefficient for accurate representation. The reason for such high accuracy is that relatively small changes in the prediction coefficients result in a large change in the pole positions of the filter model. The accuracy requirements are lessened by transmitting the reflection coefficients  $\{K_i\}$ , which have a smaller dynamic range—that is,  $|K_i| < 1$ . These are adequately represented by 6 bits per coefficient. Thus for a tenth-order predictor, the total number of bits assigned to the model parameters per frame is 72. If the model

parameters are changed every 20  $\mu$ sec, the resulting bit rate is 3,600 bps. Since the reflection coefficients are usually transmitted to the receiver, the synthesis filter at the receiver is implemented as an all-pole lattice filter, described in Chapter 6.

#### 12.5.1 PROJECT 12.5: LPC

The objective of this project is to analyze a speech signal through an LPC coder and then to synthesize it through the corresponding PLC decoder. Use several .wav sound files (sampled at 8000 sam/sec rate), which are available in MATLAB for this purpose. Divide speech signals into short-time segments (with lengths between 120 and 150 samples) and process each segment to determine the proper excitation function (voiced or unvoiced), the pitch period for voiced speech, the coefficients  $\{a_p(k)\}$  ( $p \leq 10$ ), and the gain  $G$ . The decoder that performs the synthesis is an all-pole lattice filter whose parameters are the reflection coefficients that can be determined from  $\{a_p(k)\}$ . The output of this project is a synthetic speech signal that can be compared with the original speech signal. The distortion effects due to LPC analysis/synthesis may be assessed qualitatively.

## 12.6 DUAL-TONE MULTIFREQUENCY (DTMF) SIGNALS

DTMF is the generic name for push-button telephone signaling that is equivalent to the Touch Tone system in use within the Bell System. DTMF also finds widespread use in electronic mail systems and telephone banking systems in which the user can select options from a menu by sending DTMF signals from a telephone.

In a DTMF signaling system, a combination of a high-frequency tone and a low-frequency tone represent a specific digit or the characters \* and #. The eight frequencies are arranged as shown in Figure 12.14, to accommodate a total of 16 characters, 12 of which are assigned as shown, while the other four are reserved for future use.

DTMF signals are easily generated in software and detected by means of digital filters, also implemented in software, that are tuned to the eight frequency tones. Usually, DTMF signals are interfaced to the analog world via a *codec* (coder/decoder) chip or by linear A/D and D/A converters. Codec chips contain all the necessary A/D and D/A, sampling, and filtering circuitry for a bidirectional analog/digital interface.

The DTMF tones may be generated either mathematically or from a look-up table. In a hardware implementation (e.g., in a digital signal

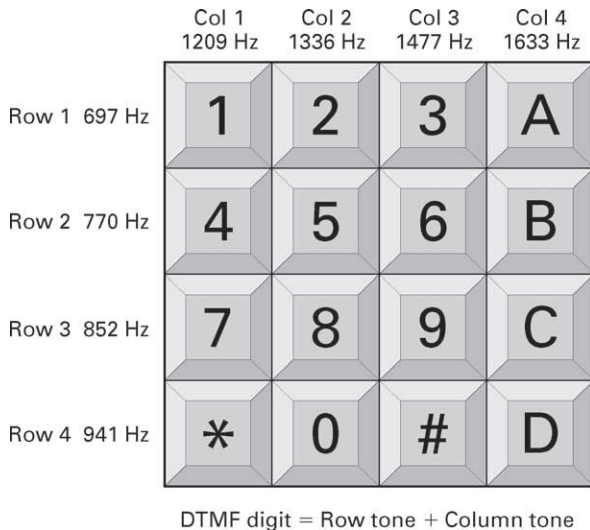


**FIGURE 12.14** DTMF digits

processor), digital samples of two sine waves are generated mathematically, scaled, and added together. The sum is logarithmically compressed and sent to the codec for conversion to an analog signal. At an 8 kHz sampling rate, the hardware must output a sample every 125 ms. In this case, a sine look-up table is not used, because the values of the sine wave can be computed quickly without using the large amount of data memory that a table look-up would require. For simulation and investigation purposes, the look-up table might be a good approach in MATLAB.

At the receiving end, the logarithmically compressed, 8-bit digital data words from the codec are received and logarithmically expanded to their 16-bit linear format. Then the tones are detected to decide on the transmitted digit. The detection algorithm can be a DFT implementation using the FFT algorithm or a filter bank implementation. For the relatively small number of tones to be detected, the filter bank implementation is more efficient. We now describe the use of the Goertzel algorithm to implement the eight tuned filters.

Recall from the discussion in Chapter 5 that the DFT of an  $N$ -point data sequence  $\{x(n)\}$  is

$$X(k) = \sum_{n=0}^{N-1} x(n)W_N^{nk}, \quad k = 0, 1, \dots, N-1 \quad (12.40)$$

If the FFT algorithm is used to perform the computation of the DFT, the number of computations (complex multiplications and additions) is  $N \log_2 N$ . In this case, we obtain all  $N$  values of the DFT at once.

However, if we desire to compute only  $M$  points of the DFT, where  $M < \log_2 N$ , then a direct computation of the DFT is more efficient. The Goertzel algorithm, which is now described, is basically a linear filtering approach to the computation of the DFT and provides an alternative to direct computation.

### 12.6.1 THE GOERTZEL ALGORITHM

The Goertzel algorithm exploits the periodicity of the phase factors  $\{W_N^k\}$  and allows us to express the computation of the DFT as a linear filtering operation. Since  $W_N^{-kN} = 1$ , we can multiply the DFT by this factor. Thus

$$X(k) = W_N^{-kN} X(k) = \sum_{m=0}^{N-1} x(m) W_N^{-k(N-m)} \quad (12.41)$$

We note that (12.41) is in the form of a convolution. Indeed, if we define the sequence  $y_k(n)$  as

$$y_k(n) = \sum_{m=0}^{N-1} x(m) W_N^{-k(n-m)} \quad (12.42)$$

then it is clear that  $y_k(n)$  is the convolution of the finite-duration input sequence  $x(n)$  of length  $N$  with a filter that has an impulse response

$$h_k(n) = W_N^{-kn} u(n) \quad (12.43)$$

The output of this filter at  $n = N$  yields the value of the DFT at the frequency  $\omega_k = 2\pi k/N$ . That is,

$$X(k) = y_k(n)|_{n=N} \quad (12.44)$$

as can be verified by comparing (12.41) with (12.42).

The filter with impulse response  $h_k(n)$  has the system function

$$H_k(z) = \frac{1}{1 - W_N^{-k} z^{-1}} \quad (12.45)$$

This filter has a pole on the unit circle at the frequency  $\omega_k = 2\pi k/N$ . Thus the entire DFT can be computed by passing the block of input data into a parallel bank of  $N$  single-pole filters (resonators), where each filter has a pole at the corresponding frequency of the DFT.

Instead of performing the computation of the DFT as in (12.42), via convolution, we can use the difference equation corresponding to the filter given by (12.45) to compute  $y_k(n)$  recursively. Thus we have

$$y_k(n) = W_N^{-k} y_k(n-1) + x(n), \quad y_k(-1) = 0 \quad (12.46)$$

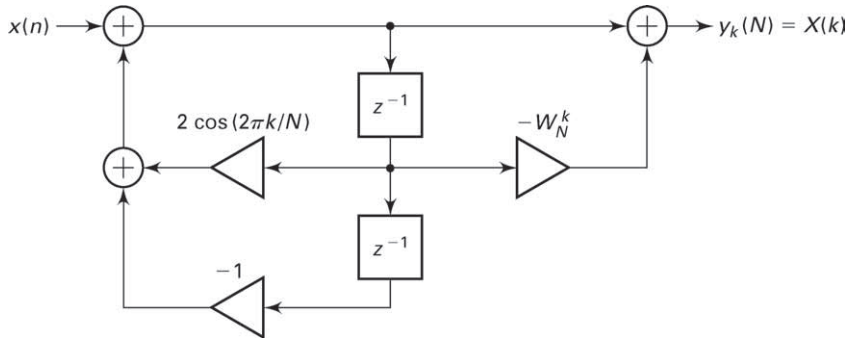


**FIGURE 12.15** Realization of two-pole resonator for computing the DFT

The desired output is  $X(k) = y_k(N)$ . To perform this computation, we can compute once and store the phase factor  $W_N^{-k}$ .

The complex multiplications and additions inherent in (12.46) can be avoided by combining the pairs of resonators possessing complex conjugate poles. This leads to two-pole filters with system functions of the form

$$H_k(z) = \frac{1 - W_N^k z^{-1}}{1 - 2 \cos(2\pi k/N) z^{-1} + z^{-2}} \quad (12.47)$$

The realization of the system illustrated in Figure 12.15 is described by the difference equations

$$v_k(n) = 2 \cos \frac{2\pi k}{N} v_k(n-1) - v_k(n-2) + x(n) \quad (12.48)$$

$$y_k(n) = v_k(n) - W_N^k v_k(n-1) \quad (12.49)$$

with initial conditions  $v_k(-1) = v_k(-2) = 0$ . This is the Goertzel algorithm.

The recursive relation in (12.48) is iterated for  $n = 0, 1, \dots, N$ , but the equation in (12.49) is computed only once, at time  $n = N$ . Each iteration requires one real multiplication and two additions. Consequently, for a real input sequence  $x(n)$ , this algorithm requires  $N + 1$  real multiplications to yield not only  $X(k)$  but also, due to symmetry, the value of  $X(N - k)$ .

We can now implement the DTMF decoder by use of the Goertzel algorithm. Since there are eight possible tones to be detected, we require eight filters of the type given by (12.47), with each filter tuned to one of the eight frequencies. In the DTMF detector, there is no need to compute the complex value  $X(k)$ ; the magnitude  $|X(k)|$  or the magnitude-squared value  $|X(k)|^2$  will suffice. Consequently, the final step in the computation of the DFT value involving the numerator term (feedforward part of the

filter computation) can be simplified. In particular, we have

$$\begin{aligned}|X(k)|^2 &= |y_k(N)|^2 = \left|v_k(N) - W_N^k v_k(N-1)\right|^2 \\&= v_k^2(N) + v_k^2(N-1) - \left(2 \cos \frac{2\pi k}{N}\right) v_k(N) v_k(N-1)\end{aligned}\quad (12.50)$$

Thus complex-valued arithmetic operations are completely eliminated in the DTMF detector.

### 12.6.2 PROJECT 12.6: DTMF SIGNALING

The objective of this project is to gain an understanding of the DTMF tone generation software and the DTMF decoding algorithm (the Goertzel algorithm). Design the following MATLAB modules:

1. a tone generation function that accepts an array containing dialing digits and produces a signal containing appropriate tones (from Figure 12.14) of 0.5 sec duration for each digit at 8 kHz sampling frequency,
2. a dial-tone generator generating samples of  $(350 + 440)$  Hz frequency at 8 kHz sampling interval for a specified amount of duration, and
3. a decoding function to implement (12.50) that accepts a DTMF signal and produces an array containing dialing digits.

Generate several dialing list arrays containing a mix of digits and dial tones. Experiment with the tone generation and detection modules and comment on your observations. Use MATLAB's sound generation capabilities to listen to the tones and to observe the frequency components of the generated tones.

## 12.7 BINARY DIGITAL COMMUNICATIONS

---

Digitized speech signals that have been encoded via PCM, ADPCM, DM, and LPC are usually transmitted to the decoder by means of digital modulation. A binary digital communications system employs two signal waveforms—say,  $s_1(t) = s(t)$  and  $s_2(t) = -s(t)$ —to transmit the binary sequence representing the speech signal. The signal waveform  $s(t)$ , which is nonzero over the interval  $0 \leq t \leq T$ , is transmitted to the receiver if the data bit is a 1, and the signal waveform  $-s(t)$ ,  $0 \leq t \leq T$  is transmitted if the data bit is a 0. The time interval  $T$  is called the signal interval, and the bit rate over the channel is  $R = 1/T$  bits per second. A typical signal waveform  $s(t)$  is a rectangular pulse—that is,  $s(t) = A$ ,  $0 \leq t \leq T$ —which has energy  $A^2T$ .

In practice, the signal waveforms transmitted over the channel are corrupted by additive noise and other types of channel distortions that ultimately limit the performance of the communications system. As a measure of performance, we normally use the average probability of error, which is often called the bit error rate.

### 12.7.1 PROJECT 12.7: BINARY DATA COMMUNICATIONS SYSTEM

The purpose of this project is to investigate the performance of a binary data communications system on an additive noise channel by means of simulation. The basic configuration of the system to be simulated is shown in Figure 12.16. Five MATLAB functions are required.

1. A binary data generator module that generates a sequence of independent binary digits with equal probability.
2. A modulator module that maps a binary digit 1 into a sequence of  $M$  consecutive +1's, and maps a binary digit 0 into a sequence of  $M$  consecutive -1's. Thus the  $M$  consecutive +1's represent a sampled version of the rectangular pulse.
3. A noise generator that generates a sequence of uniformly distributed numbers over the interval  $(-a, a)$ . Each noise sample is added to a corresponding signal sample.
4. A demodulator module that sums the  $M$  successive outputs of the noise corrupted sequence +1's or -1's received from the channel. We assume that the demodulator is time synchronized so that it knows the beginning and end of each waveform.
5. A detector and error-counting module. The detector compares the output of the modulator with zero and decides in favor of 1 if the output is greater than zero and in favor of zero if the output is less than zero. If the output of the detector does not agree with the transmitted bit from the transmitter, an error is counted by the counter. The error rate depends on the ratio (called signal-to-noise ratio) of the size of  $M$  to the additive noise power, which is  $P_n = a^2/3$ .

The measured error rate can be plotted for different signal-to-noise ratios, either by changing  $M$  and keeping  $P_n$  fixed or vice versa.

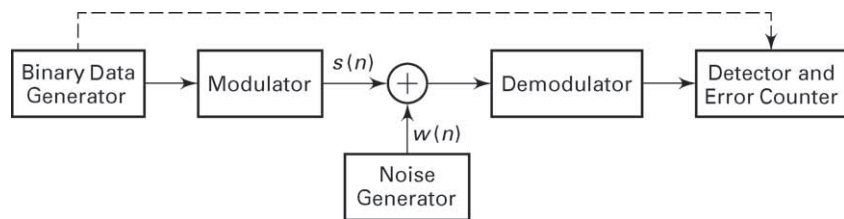


**FIGURE 12.16** Model of binary data communications system

## 12.8 SPREAD-SPECTRUM COMMUNICATIONS

Spread-spectrum signals are often used in the transmission of digital data over communication channels that are corrupted by interference due to intentional jamming or from other users of the channel (e.g., cellular telephones and other wireless applications). In applications other than communications, spread-spectrum signals are used to obtain accurate range (time delay) and range rate (velocity) measurements in radar and navigation. For the sake of brevity, we shall limit our discussion to the use of spread spectrum for digital communications. Such signals have the characteristic that their bandwidth is much greater than the information rate in bits per second.

In combatting intentional interference (jamming), it is important to the communicators that the jammer who is trying to disrupt their communication does not have prior knowledge of the signal characteristics. To accomplish this, the transmitter introduces an element of unpredictability or randomness (pseudo-randomness) in each of the possible transmitted signal waveforms, which is known to the intended receiver, but not to the jammer. As a consequence, the jammer must transmit an interfering signal without knowledge of the pseudo-random characteristics of the desired signal.

Interference from other users arises in multiple-access communications systems in which a number of users share a common communications channel. At any given time, a subset of these users may transmit information simultaneously over a common channel to corresponding receivers. The transmitted signals in this common channel may be distinguished from one another by superimposing a different pseudo-random pattern, called a *multiple-access code*, in each transmitted signal. Thus a particular receiver can recover the transmitted data intended for it by knowing the pseudo-random pattern—that is, the key used by the corresponding transmitter. This type of communication technique, which allows multiple users to simultaneously use a common channel for data transmission, is called *code division multiple access* (CDMA).

The block diagram shown in Figure 12.17 illustrates the basic elements of a spread-spectrum digital communications system. It differs

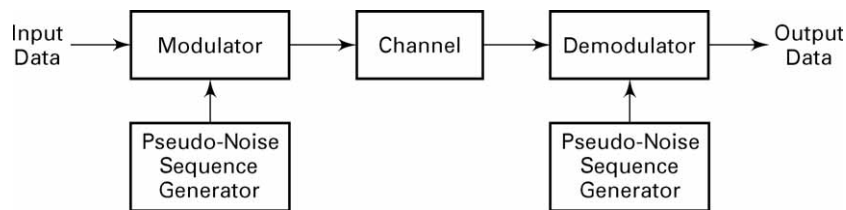


**FIGURE 12.17** Basic spread-spectrum digital communications system

from a conventional digital communications system by the inclusion of two identical pseudo-random pattern generators, one that interfaces with the modulator at the transmitting end and a second that interfaces with the demodulator at the receiving end. The generators generate a pseudo-random or *pseudo-noise* (PN) binary-valued sequence ( $\pm 1$ 's), which is impressed on the transmitted signal at the modulator and removed from the received signal at the demodulator.

Synchronization of the PN sequence generated at the demodulator with the PN sequence contained in the incoming received signal is required in order to demodulate the received signal. Initially, prior to the transmission of data, synchronization is achieved by transmitting a short fixed PN sequence to the receiver for purposes of establishing synchronization. After time synchronization of the PN generators is established, the transmission of data commences.

### 12.8.1 PROJECT 12.8: BINARY SPREAD-SPECTRUM COMMUNICATIONS

The objective of this project is to demonstrate the effectiveness of a PN spread-spectrum signal in suppressing sinusoidal interference. Let us consider the binary communication system described in Project 12.7, and let us multiply the output of the modulator by a binary ( $\pm 1$ ) PN sequence. The same binary PN sequence is used to multiply the input to the demodulator and thus to remove the effect of the PN sequence in the desired signal. The channel corrupts the transmitted signal by the addition of a

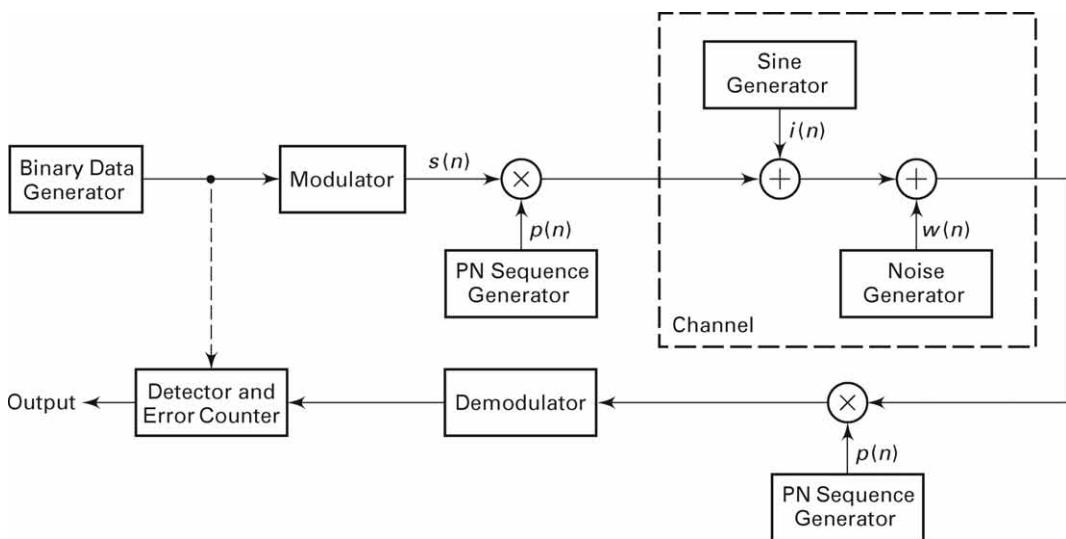


**FIGURE 12.18** Block diagram of binary PN spread-spectrum system for simulation experiment

wideband noise sequence  $\{w(n)\}$  and a sinusoidal interference sequence of the form  $i(n) = A \sin \omega_0 n$ , where  $0 < \omega_0 < \pi$ . We may assume that  $A \geq M$ , where  $M$  is the number of samples per bit from the modulator. The basic binary spread spectrum system is shown in Figure 12.18. As can be observed, this is just the binary digital communication system shown in Figure 12.16, to which we have added the sinusoidal interference and the PN sequence generators. The PN sequence may be generated by using a random number generator to generate a sequence of equally probable  $\pm 1$ 's.

Execute the simulated system with and without the use of the PN sequence, and measure the error rate under the condition that  $A \geq M$  for different values of  $M$ , such as  $M = 50, 100, 500, 1000$ . Explain the effect of the PN sequence on the sinusoidal interference signal. Thus explain why the PN spread-spectrum system outperforms the conventional binary communication system in the presence of the sinusoidal jamming signal.

# CHAPTER **13**

---

## Random Processes

---

The main focus in the first ten chapters was on characterizing, processing, and filtering deterministic signals—that is, signals defined using exact mathematical expressions or through their Fourier spectra. In the real world, there are signals that cannot be completely described as deterministic or that have random fluctuations (or variations) around known waveforms. Speech signals, audio signals, video signals, and so on, fall under the first category, while noisy signals, received radar signals, and communication signals fall under the second category. Such signals are known as *random processes* or *random signals* and can be thought of as a collection or ensemble of sample signals with associated probabilistic description. Therefore, we need a statistical approach to characterize them and to process them.

In Chapters 14 and 15, we will consider the processing of random signals. Although linear filtering of a sample waveform from the ensemble of the process is akin to convolution operation in the time domain or filtering in the frequency domain, the emphasis will be on estimating parameters from observations, detecting signals in noisy environments and designing optimal filters for satisfying a given optimality criteria.

In this chapter, we provide an overview of various analytical concepts to define randomness of measurements or waveform variations and provide sound techniques to calculate the response of linear filters to random signals. We begin with the relevant probability theory of random variables by defining probability functions and statistical averages, and continue with pairs of random variables. We extend these concepts to random

signals, describe them in terms of second-order statistics, and then delve into stationary and ergodic processes, correlations, and power spectra. We also show how this theory can be applied to processing of random signals through an LTI system using both the time and frequency domains. Finally, we discuss a few representative random processes, including Gaussian, Markov, white noise, and filtered noise processes.

## 13.1 RANDOM VARIABLE

---

When we make measurements of certain variables over a collection of objects—for example, height in meters or weight in kilograms of a population—we obtain numbers that fluctuate over a range of values. Such measurements are called random measurements, the act of measurement is called a random experiment, and the variables are termed random variables. Even if we consider repeating the same random experiment—say, rolling a six-sided die—again and again, the outcomes vary and cannot be predicted. In the context of signal processing, the value of a noisy signal at each instant cannot be determined precisely and hence must be considered as a random value.

Even though the numerical outcomes of these random experiments vary widely every time we repeat them, there appears to be some pattern of their relative likelihood of obtaining these values. Such patterns can be understood and quantified using probability measure. For example, if we toss a *fair* coin, we will not know if the outcome of the toss is a head or a tail. But if we repeat this toss a large number of times, we will observe that the total number of head/tail outcomes are approximately equal.

### 13.1.1 PROBABILITY FUNCTIONS

Consider a random variable under measurement such as a noisy voltage source. We will use capital letters such as  $X$  to denote a random variable and lowercase  $x$  to denote its measured value. Thus  $x$  is a value on a real line  $\mathbb{R}$ . We divide this line into small intervals of length  $\Delta x$  and count the number of voltage values, say,  $N_x$ , that fall into  $\Delta x$  at each  $x$ . If  $N$  is the total number of times we measure the random voltage  $X$ , then  $N_x/N$  is the approximate *probability* of observing voltage value  $x$  and  $(N_x/N)/\Delta x$  is approximately the *probability density* of the random variable  $X$  at  $x$ . We will denote this probability density function (pdf) as  $f_X(x)$  and formally define it by

$$f_X(x) = \lim_{\substack{\Delta x \rightarrow 0 \\ N \rightarrow \infty}} \left( \frac{N_x}{N\Delta x} \right) \quad (13.1)$$

The probability that the random voltage  $X$  takes values over the range  $x_1 < X < x_2$  is given by integrating  $f_X(x) dx$  over the interval, or

$$\Pr\{x_1 < X < x_2\} = \int_{x_1}^{x_2} f_X(x) dx \quad (13.2)$$

The pdf has to satisfy important properties for it to be a valid function. It cannot be negative or imaginary, and every measurement must yield some real value signifying

$$\int_{-\infty}^{\infty} f_X(x) dx = 1 \quad (13.3)$$

Another useful probability function is the cumulative distribution function (CDF), which is the probability that the random variable  $X$  takes a value less than or equal to some specified value  $x$ . It is denoted by  $F_X(x)$  and is defined as

$$F_X(x) = \int_{-\infty}^x f_X(u) du \quad (13.4)$$

This function also has to satisfy properties such as non-negativeness with increasing  $x$  and, from (13.4), and (13.3),

$$F_X(-\infty) = 0, \quad F_X(\infty) = 1 \quad (13.5)$$

**Discrete Random Variable** So far, we described a *continuous random variable* that assumes values in a continuous range over  $\mathbb{R}$ . If the random variable  $X$  takes a set of discrete values  $\{x_i\}$  with probabilities  $p_i$ ,  $i = 1, 2, \dots$  such that  $\sum_i p_i = 1$ , then the random variable  $X$  is called a *discrete random variable*. In this case, we can obtain its pdf using impulse functions and CDF using step functions:

$$f_X(x) = \sum_i p_i \delta(x - x_i) \quad (13.6a)$$

$$F_X(x) = \sum_i p_i u(x - x_i) \quad (13.6b)$$

Finally, we note that, in the general case, a random variable can take a continuous range of values as well as a discrete set of values. Such a random variable is called a *mixed random variable*. The pdf description using impulse functions is sufficient to describe any type of random variable.

**Histogram as a pdf Approximation** Given  $N$  observations of a random variable  $X$ , we have denoted  $N_x$  as the number of values of  $X$  that fall into the small interval  $\Delta x$  at  $x = x_i$ . Then the plot of  $N_x$  vs.  $x$  is called the *histogram* of the observed values and the plot of the ratio

$$P_X(x) = \frac{N_x}{N \Delta x} \quad (13.7)$$

vs.  $x$  is called the *normalized histogram* and is a good approximation of the pdf  $f_X(x)$  of  $X$  from (13.1). MATLAB provides a function,  $\text{Nx} = \text{histc}(x, \text{edges})$ , that provides counts in  $\text{Nx}$ , given observed values  $x$  and bin edges. Using this function, we can design a MATLAB function, which we will call  $\text{pdf1}$ , that computes the pdf as a normalized histogram from the observed values. It is shown below and its use is given in Example 13.1.

```

function [Px,xc] = pdf1(x,xmin,xmax,M)
% pdf1: Normalized Histogram as 1-D Probability Density
%       Function (pdf)
% [Px,xc] = pdf1(x,xmin,xmax,M)
%       Px: normalized histogram over the range [xmin, xmax]
%       xc: histogram bin centers
%       x: data (observation) values
%       xmin: minimum range value
%       xmax: maximum range value
%       M: number of bins
N = length(x);                                % Observation count
edges = linspace(xmin,xmax,M);                % Histogram boundaries
Dx = (xmax-xmin)/(M-1);                      % Delta_x
xc = [xmin,edges(1:M-1)+Dx/2,xmax];          % Bin centers
edges = [-inf,edges,inf];                      % Augment boundaries
Nx = histc(x,edges); Nx = Nx(1:end-1);        % Histogram
Px = Nx/(N*Dx);                             % Normalized Histogram
end

```

- EXAMPLE 13.1** In Section 13.1.3, we will discuss the pdf of a random variable that is sinusoidally distributed. In this random variable, the observed values are taken from a sine waveform over one complete cycle. Thus, to demonstrate use of the  $\text{pdf1}$  function, consider the signal

$$x(t) = \sin(2\pi t), 0 \leq t \leq 1$$

We will take large samples of this waveform and consider them as the observed values for computing and plotting the normalized histogram. The following MATLAB script illustrates the approach.

```

>> N = 1000000; % Number of observations
>> n = 0:1:N; % Time index
>> x = sin(2*pi*n/N); % Observations
>> [Px,xc] = pdf1(x,-1,1,100); % Normalized Histogram
>> plot(xc(2:end-1),Px(2:end-1),'linewidth',1);
>> axis([-1.1,1.1,0,3.5]);
>> xlabel('Range of {\it x}', 'fontsize', 9);
>> ylabel('Relative Histogram', 'fontsize', 9);

```

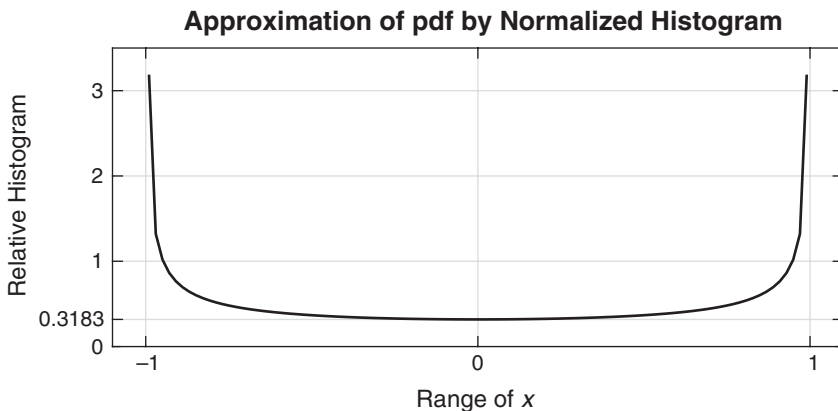


**FIGURE 13.1** Normalized histogram of sinusoidally distributed samples

```
>> set(gca,'xtick',[-1,0,1], 'ytick',[0,1/pi,1,2,3,4]); grid;
>> title('Approximation of pdf by Normalized Histogram',...
    'fontsize',10,'fontweight','bold');
```

The resulting histogram is shown in Figure 13.1, which agrees with the pdf of the sinusoidal distribution shown in Figure 13.6, which will be derived later. □

### 13.1.2 STATISTICAL AVERAGES

As explained in the discussion leading up to (13.1), the pdf completely describes the random variable  $X$  in a probabilistic sense. However, in practice it is not always possible to obtain such a function when we have measurements from an arbitrary random quantity. The pdf contains much more information about the random variable than we actually need in practice. A random variable can also be described by characteristic numbers called *moments*. These moments are computed using *statistical averaging* and form a countable (or discrete) set, whereas the pdf is uncountable (or continuous).

The analytic calculation of averages is facilitated by the pdf. Assume that we want to calculate the statistical average of the random variable  $X$  from a large number of measurements. We denote this average by  $E[X]$ , which means “the expectation of  $X$ .” Again we divide the real line  $\mathbb{R}$  into fine intervals of width  $dx$ . Then for a large number of measurements, the quantity  $f_X(x) dx$  corresponds to the probability of  $dx$  containing the value  $x$ . Thus in the limit as the number of observations become very large, the average of  $X$  is given by

$$E[X] = \int_{-\infty}^{\infty} x f_X(x) dx \quad (13.8)$$

In a similar fashion, we can calculate the average of some function of the random variable  $X$ , such as a power  $X^n$  or an exponential  $\exp(X)$ , from a large number of measurements. Let  $g(x)$  be such a function of  $x$ . Then its average is given by

$$E[g(X)] = \int_{-\infty}^{\infty} g(x) f_X(x) dx \quad (13.9)$$

The averages of positive powers,  $g(X) = E[X^n]$ , are particularly useful. These averages are the moments of  $X$  referred to above. We will denote these moments by  $\xi_X(n)$ , given by

$$\xi_X(n) = \int_{-\infty}^{\infty} x^n f_X(x) dx \quad (13.10)$$

Clearly,  $\xi_X(0) = 1$ , while the first moment

$$\xi_X(1) \stackrel{\Delta}{=} \mu_X = \int_{-\infty}^{\infty} x f_X(x) dx \quad (13.11)$$

is the statistical average or *mean* of  $X$ . The second moment

$$\xi_X(2) = \int_{-\infty}^{\infty} x^2 f_X(x) dx \quad (13.12)$$

is the *mean-squared* value of  $X$ . If  $X$  represents a random voltage, then  $\mu_X$  represents the average (or dc) value and  $\xi_X(2)$  represents the average total power consumed across unit impedance.

Another useful set of statistical averages is the set of *central moments* of  $X$ , defined by

$$M_X(n) \stackrel{\Delta}{=} E[(X - \mu_X)^n] = \int_{-\infty}^{\infty} (x - \mu_X)^n f_X(x) dx \quad (13.13)$$

Clearly,  $M_X(0) = 1$  and  $M_X(1) = 0$ . The second central moment  $M_X(2)$  is the most important one and is called the variance of the random variable distribution. It is denoted by  $\sigma_X^2$  and related to the mean  $\mu_X$  and the mean-squared value  $\xi_X(2)$  by

$$\sigma_X^2 = M_X(2) = \int_{-\infty}^{\infty} (x - \mu_X)^2 f_X(x) dx = \xi_X(2) - \mu_X^2 \quad (13.14)$$

The square root of the variance is called the *standard deviation* or the *root-mean-squared* (rms) value and gives the average spread of random measurements from their mean value. Again, if  $X$  represents a random voltage, then  $\sigma_X^2$  represents the average ac power consumed across unit impedance.

### 13.1.3 RANDOM VARIABLE MODELS

Although a random variable is completely described by its pdf, it is not always possible to know this function for every random measurement. In Example 13.1, we showed how to approximate a pdf using normalized histogram given a set of measurements. Another approach is to assume a particular form (or shape) for the pdf based on how the random measurements are created. These forms are called *models*, and there are several such models that are used in practice. We will consider the following three models used often in Chapters 14 and 15.

#### **Uniform Distribution**

In this model, a random variable  $X$  is uniformly distributed (or equally likely) over a finite range of  $a \leq x \leq b$  and is denoted by  $U(a, b)$ . Its pdf is given by

$$f_X(x) = \begin{cases} \frac{1}{b-a}, & a \leq x \leq b, \\ 0, & \text{otherwise,} \end{cases} \sim U(a, b) \quad (13.15)$$

and its CDF is given by

$$F_X(x) = \begin{cases} 0, & x < a \\ \frac{x-a}{b-a}, & a \leq x \leq b \\ 1, & x > b \end{cases} \quad (13.16)$$

These probability functions are shown in Figure 13.2. The mean of the uniform distribution is given by

$$\mu_X = \int_a^b \frac{x}{b-a} dx = \frac{a+b}{2} \quad (13.17)$$

while the mean-squared value is given by

$$\xi_X(2) = \int_a^b \frac{x^2}{b-a} dx = \frac{b^2 + ab + a^2}{3} \quad (13.18)$$

Hence the variance is given by

$$\sigma_X^2 = \xi_X(2) - \mu_X^2 = \frac{(b-a)^2}{12} \quad (13.19)$$

The case of  $a = 0$  and  $b = 1$  is called the standard uniform distribution, denoted by  $U(0, 1)$ .

**MATLAB Implementation** MATLAB provides the function `x=rand(N,1)`, which generates a column vector containing  $N$  standard uniform

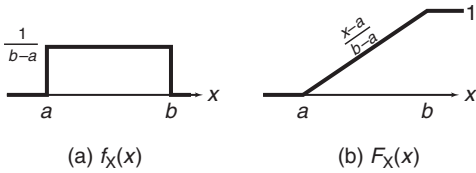


**FIGURE 13.2** Uniform distribution: (a) pdf, (b) CDF

random numbers each of which is uniform over the interval  $[0, 1]$ . These numbers are independent of each other; that is, generation of each one of them does not affect the occurrence of any other (this concept is discussed in Section 13.2.1). To obtain the uniformly distributed random numbers according to (13.15), we make a simple change of variable  $X = (b-a)Y + a$  where  $Y$  is  $U(0, 1)$ :

```
>> x = (b-a)*rand(N,1)+a;
```

The uniform distribution is useful in generating random sinusoidal waveforms with uniformly distributed phase angles.

### Gaussian Distribution

This is a very popular distribution model in many applications. In this model, the distribution has two parameters,  $\mu$  and  $\sigma$ , and is denoted by  $N(\mu, \sigma^2)$ . Its pdf is given by

$$f_X(x) = \frac{1}{\sigma\sqrt{2\pi}} e^{-(x-\mu)^2/2\sigma^2} \sim N(\mu, \sigma^2) \quad (13.20)$$

and the CDF is given by

$$F_X(x) = \frac{1}{2} \left[ 1 + \operatorname{erf} \left( \frac{x-\mu}{\sqrt{2\sigma^2}} \right) \right] \quad (13.21)$$

where

$$\operatorname{erf}(x) = \frac{2}{\sqrt{\pi}} \int_0^x e^{-\lambda^2} d\lambda \quad (13.22)$$

is called the *error function*, which is extensively tabulated since the above integral does not have a closed-form expression. It is available in MATLAB as the **erf(x)** function. The Gaussian probability functions are shown in Figure 13.3.

The mean of the Gaussian distribution is given by the parameter  $\mu$ , while its variance is given by the parameter  $\sigma^2$ —that is,

$$\mu_X = \mu \quad \text{and} \quad \sigma_X^2 = \sigma^2 \quad (13.23)$$

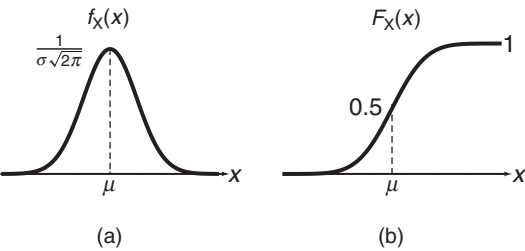


**FIGURE 13.3** Gaussian distribution: (a) pdf, (b) CDF

Thus the Gaussian distribution is completely described by its first two moments. It should be noted that although  $X$  takes values over the entire real line  $\mathbb{R}$ , these values are mostly concentrated around its mean  $\mu$  with spread given by  $\sigma$ . The case of  $\mu = 0$  and  $\sigma^2 = 1$  is the normalized distribution, or *Normal* distribution, denoted by  $N(0, 1)$ , although the terms “Gaussian” and “Normal” are used synonymously in the literature.

**MATLAB Implementation** MATLAB provides the function  $x = \text{randn}(N, 1)$ , which generates a column vector containing  $N$  independent and Normally distributed random numbers with mean 0 and variance 1. To obtain arbitrary Gaussian distributed random numbers with mean  $\mu$  and variance  $\sigma^2$ , we make a simple change of variable  $X = \sigma Y + \mu$  where  $Y$  is Normal:

```
>> x = sigma*randn(N,1)+mu;
```

### Transformation of a Random Variable

In signal processing, we perform operations on random signals. This means that we transform random signal values, which are random variables, into other ones using a function or transformation. In a simple operation, one random variable with known pdf is mapped into another one, and we wish to calculate the pdf of the transformed random variable. Let  $X$  be the given random variable with pdf  $f_X(x)$ , and let  $Y$  be the new random variable obtained through the function  $Y = g(X)$ . We wish to determine the pdf  $f_Y(y)$ . If the transformation function  $g(\cdot)$  is invertible, then we have  $x = g^{-1}(y) \triangleq h(y)$  and  $f_Y(y) dy = f_X(h(y)) h'(y) dy$ . Then by direct substitution, we have

$$f_Y(y) dy = f_X(x) dx = f_X(h(y)) h'(y) dy \quad (13.24)$$

where  $h'(y) = dh(y)/dy$  is the derivative of the inverse function. Hence

$$f_Y(y) = f_X(h(y)) h'(y) \quad (13.25)$$

If  $g(x)$  is not invertible, then  $h(y)$  has multiple values and we sum the right-hand side of (13.25) over all the multiple values. Another approach, using uniformly distributed random number, is illustrated in the following example.

- **EXAMPLE 13.2** Uniformly distributed random numbers in the range  $(0, 1)$  can be used to generate other random numbers with the prescribed probability distribution function. Consider a random variable  $Y$  that has a linear pdf given by

$$f_Y(y) = \begin{cases} \frac{1}{2}y, & 0 \leq y \leq 2 \\ 0, & \text{otherwise} \end{cases} \quad (13.26)$$

with CDF

$$F_Y(y) = \begin{cases} 0, & y < 0 \\ \frac{1}{4}y^2, & 0 \leq y \leq 2 \\ 1, & y > 2 \end{cases} \quad (13.27)$$

These functions are shown in Figure 13.4.

Since the range of  $F_Y(y)$  is the interval  $(0, 1)$ , we begin by generating a uniformly distributed random variable  $X$  in the range  $(0, 1)$  and set

$$F_Y(y) = \frac{1}{4}y^2 = x \Rightarrow y = 2\sqrt{x} \quad (13.28)$$

Thus we generate a random variable  $Y$  with the linear pdf shown in Figure 13.4(a). This can be verified using the `pdf1` function as shown below. The plot of the resulting pdf is shown in Figure 13.5.

```
>> N = 1000000; x = rand(N,1); % Uniform distribution
>> y = 2*sqrt(x); % Transformed random variable
>> [Py,yc] = pdf1(y,0,2,100); % Normalized Histogram
>> plot(yc,Py,'linewidth',1); axis([-0.1,2.1,0,1.1]);
>> % Plotting commands follow
```

□

### Sinusoidal Distribution

One application of random variable transformation is in obtaining the sinusoidal distribution, which is useful in many communication signals. It was mentioned in Example 13.1. Let

$$X = A \sin(\Theta) \quad (13.29)$$

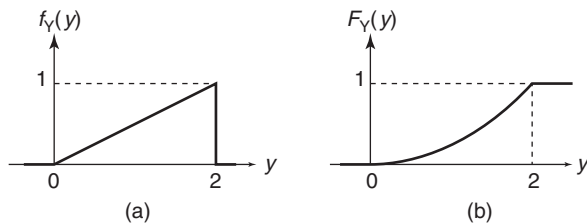


**FIGURE 13.4** Linear distribution: (a) pdf, (b) CDF

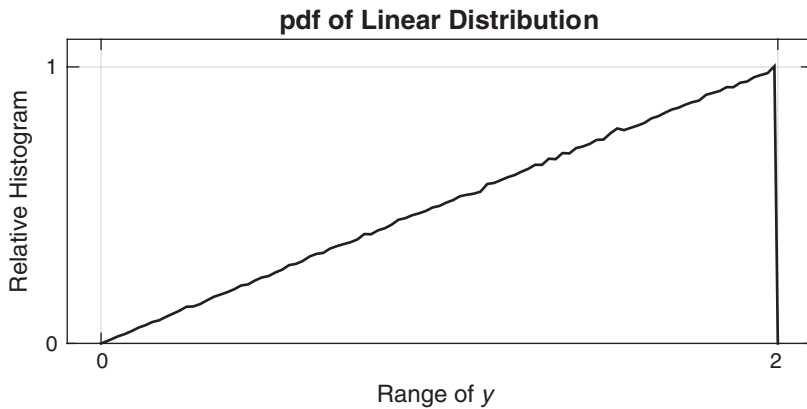


**FIGURE 13.5** Normalized histogram of linearly distributed samples

where the random variable  $\Theta$  is uniformly distributed between 0 and  $2\pi$  radians. Then  $X$  is said to be sinusoidally distributed with amplitude  $A$ . The pdf of  $\Theta$  is given by

$$f_{\Theta}(\theta) = \begin{cases} \frac{1}{2\pi}, & 0 \leq \theta < 2\pi \\ 0, & \text{otherwise} \end{cases} \quad (13.30)$$

Since  $g(\Theta) = A \sin(\Theta)$  in (13.29), the inverse function is given by

$$\Theta = h(X) = \sin^{-1}\left(\frac{X}{A}\right) \quad (13.31)$$

with

$$h'(x) = \frac{1}{\sqrt{A^2 - x^2}} \quad (13.32)$$

Also the  $h(X)$  function is not unique and has two values for  $\theta$  for each value of  $x$  in the range  $-A \leq x \leq A$ . Hence we must add two contributions of the right-hand side in (13.25) to obtain

$$f_X(x) = \begin{cases} \frac{1}{\pi\sqrt{A^2 - x^2}}, & -A \leq x \leq A \\ 0, & \text{otherwise} \end{cases} \quad (13.33)$$

The corresponding CDF is given by

$$F_X(x) = \int_{-A}^x \frac{d\lambda}{\pi\sqrt{A^2 - \lambda^2}} = \frac{1}{\pi} \left[ \frac{\pi}{2} + \sin^{-1}\left(\frac{x}{A}\right) \right] \quad (13.34)$$

These functions are shown in Figure 13.6.

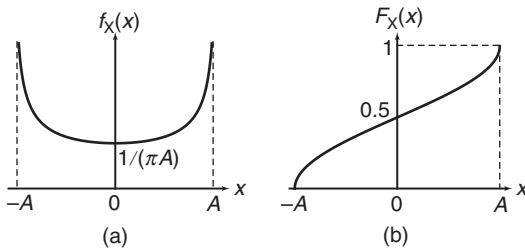


**FIGURE 13.6** Sinusoidal distribution: (a) pdf, (b) CDF

The mean of  $X$ , using the symmetry of its pdf, is given by

$$\mu_X = \xi_X(1) = \int_{-A}^A \frac{x \, dx}{\pi \sqrt{A^2 - x^2}} = 0 \quad (13.35)$$

and the variance, which is also its mean-squared value, is given by

$$\sigma_X^2 = \xi_X(2) = \int_{-A}^A \frac{x^2 \, dx}{\pi \sqrt{A^2 - x^2}} = \frac{A^2}{2} \quad (13.36)$$

**MATLAB Implementation** It is easy to generate sinusoidally distributed random numbers by first generating uniformly distributed numbers and then transforming them using (13.29). Assuming previously defined  $A$  and  $N$ , the following MATLAB fragment generates sinusoidally distributed random numbers.

```
>> theta = 2*pi*rand(N,1);
>> x = A*sin(theta);
```

#### 13.1.4 ESTIMATION OF THE MEAN OF RANDOM VARIABLE

Suppose we have  $N$  statistically independent observations  $x_1, x_2, \dots, x_N$  of a random variable  $X$ . We wish to estimate the mean value of  $X$  from the  $N$  observations. The estimate of the mean value is denoted by  $\hat{\mu}_X$  and is computed as

$$\hat{\mu}_X = \frac{1}{N} \sum_{n=1}^N x_k \quad (13.37)$$

Because  $\hat{\mu}_X$  is a sum of random variables, it is also a random variable. We note that the expected value of the estimate  $\hat{\mu}_X$  is

$$E[\hat{\mu}_X] = \frac{1}{N} \sum_{n=1}^N E[x_k] = \frac{1}{N} (\mu_X) N = \mu_X \quad (13.38)$$

where  $\mu_X$  is the actual mean of  $X$ . Thus the estimate  $\hat{\mu}_X$  is said to be *unbiased*.

The variance of the estimate  $\hat{\mu}_X$  is a measure of the spread or dispersion of  $\hat{\mu}_X$  relative to its mean value. The variance of  $\hat{\mu}_X$  is denoted by  $\sigma_{\hat{\mu}}^2$  and is given by

$$\begin{aligned}\sigma_{\hat{\mu}}^2 &= E[(\hat{\mu}_X - \mu_X)^2] = E[\hat{\mu}_X^2] - 2E[\hat{\mu}_X]\mu_X + \mu_X^2 \\ &= E[\hat{\mu}_X^2] - \mu_X^2\end{aligned}\quad (13.39)$$

But the  $E[\hat{\mu}_X^2]$  is

$$E[\hat{\mu}_X^2] = \frac{1}{N^2} \sum_{n=1}^N \sum_{k=1}^N E[x_n x_k] = \frac{\sigma_X^2}{N} + \mu_X^2 \quad (13.40)$$

where  $\sigma_X^2$  is the actual variance of  $X$ . Therefore, the variance of  $\hat{\mu}_X$  is

$$\sigma_{\hat{\mu}}^2 = \frac{\sigma_X^2}{N} \quad (13.41)$$

Note that as  $N \rightarrow \infty$ , the variance of the estimate tends to zero. Thus the estimate  $\hat{\mu}_X$  is said to be *consistent*.

**MATLAB Implementation** The built-in MATLAB function `mean(X)` computes the average or mean value of the elements in the array  $X$ . If  $X$  is a matrix, then `mean(X)` contains the mean value of each column of  $X$ . This function implements the estimate given in (13.37). Similarly, the `var(X)` computes the variance of the values in  $X$ .

- **EXAMPLE 13.3** Generate 10 samples of a random variable  $X$  that is uniformly distributed in the interval  $[0, 2]$ . Compute the estimate  $\hat{\mu}_X$  of the mean value of  $X$ , and compare the result with the true mean value,  $\mu_X = 1$ , of  $X$ . Repeat this experiment 100 times, and compute and plot the resulting estimates. Also compute the mean value and the variance of the estimates, and compare the result with the true mean value of  $X$ .

### Solution

The following MATLAB script shows the generation of random variables and estimation of mean as well as its display from 10 samples.

```
>> a = 0; b = 2; % Uniform random variable parameters
>> mu_X = (a+b)/2; % True mean value
>> N = 10; % Number of values
>> x = (b-a)*rand(N,1)+a; % Random data values
>> mu_hat = mean(x); % Mean estimate
>> disp(['True Mean value of X is: ',num2str(mu_X,2)]);
True Mean value of X is: 1
>> disp(['      Estimated Mean is: ',num2str(mu_hat,2)]);
      Estimated Mean is: 0.94
```

The above script indicates that the estimated mean is very close to the true mean even for 10 samples. The following script repeats the above experiment 100 times and computes as well as plots the results.

```
>> M = 100; % Number of experiments
>> x = (b-a)*rand(N,M)+a; % M experiments, each N values
>> mu_hat = mean(x); % Mean estimate of each column
>> mean_muhat = mean(mu_hat); % Mean of the estimates
>> var_muhat = var(mu_hat); % Variance of the estimates
>> disp(['      Mean value of the estimate is: ',...
    num2str(mean_muhat,2)]);
      Mean value of the estimate is: 1
>> disp(['Estimated variance of the estimate is: ',...
    num2str(var_muhat,2)]);
      Variance of the estimate is: 0.034
>> disp(['      True variance of the estimate is: ',...
    num2str(var_mutrue,2)]);
      True variance of the estimate is: 0.033
% Plotting commands follow
```

This shows that the mean of the estimates is equal to the true mean and that its variance is very small and close to the true variance. The plot of the estimates is shown in Figure 13.7.  $\square$

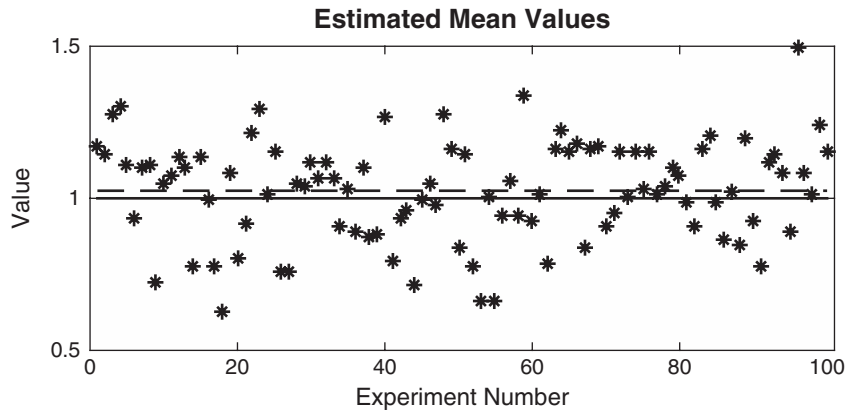


**FIGURE 13.7** The estimated means in Example 13.3 are denoted by asterisks. The horizontal dashed line represents the plot of  $\hat{\mu}_X$ , and the horizontal solid line is the true mean of the uniform random variable.

## 13.2 A PAIR OF RANDOM VARIABLES

---

So far, we discussed one random variable as a model to describe a single value of a random signal (say, at some fixed time). This description was in terms of a density function that gave probabilistic information as to relative numbers of occurrence at different amplitudes and in terms of statistical averages such as means and variances. The latter description also allowed us to relate average signal power quantities to moments.

However, we also want to know how fast or slow these random quantities may be changing over time—that is, their frequency of change. This is important for frequency-selective operations like filtering. Since one random variable cannot provide this time (or frequency) dependent information, we have to consider two random values separated by some finite time. This leads us to the case of a pair of random variables and the statistical knowledge afforded by them. It turns out that this additional statistical information is sufficient for many practical applications.

### 13.2.1 JOINT PROBABILITY FUNCTIONS

The generalization of one random variable to two random variables leads to the extension of the one-dimensional real line  $\mathbb{R}$  to the two-dimensional real plane  $\mathbb{R}^2$ . Let  $(X, Y)$  be a pair of random variables. Then it is obvious to note that the pair  $(X, Y)$  takes values in a small area  $\Delta x \Delta y$  around  $(x, y)$  when  $X$  takes values in  $\Delta x$  around  $x$  and  $Y$  takes values in  $\Delta y$  around  $y$ . Thus, analogous to one random variable, we define the *joint probability density function*  $f_{XY}(x, y)$  as the limiting value of relative number of occurrences  $N_{xy}/N$  in  $\Delta x \Delta y$  when the number of observations  $N$  approach infinity, or

$$f_{XY}(x, y) \triangleq \lim_{\substack{\Delta x, \Delta y \rightarrow 0 \\ N \rightarrow \infty}} \left( \frac{N_{xy}}{N \Delta x \Delta y} \right) \quad (13.42)$$

The *joint cumulative distribution function* is then the probability of the semi-infinite quarter-plane  $\{X \leq x, Y \leq y\}$  and is given by

$$F_{XY}(x, y) = \int_{\lambda=-\infty}^x \int_{\nu=-\infty}^y f_{XY}(\lambda, \nu) d\lambda d\nu \quad (13.43)$$

or

$$f_{XY} = \frac{\partial^2 F_{XY}(x, y)}{\partial x \partial y} \quad (13.44)$$

The probability that  $X$  falls in the range  $\{x_1 \leq X \leq x_2\}$  and  $Y$  falls in the range  $\{y_1 \leq Y \leq y_2\}$  is given by

$$\Pr\{x_1 \leq X \leq x_2, y_1 \leq Y \leq y_2\} = \int_{x_1}^{x_2} \int_{y_1}^{y_2} f_{XY}(x, y) dx dy \quad (13.45)$$

Once again, the above joint probability functions must satisfy axiomatic properties such as non-negativity, nondecreasing monotonicity (for joint CDF), and

$$F_{XY}(-\infty, -\infty) = F_{XY}(-\infty, y) = F_{XY}(x, -\infty) = 0 \quad (13.46a)$$

$$F_{XY}(\infty, \infty) = \int_{-\infty}^{\infty} \int_{-\infty}^{\infty} f_{XY}(x, y) dx dy = 1 \quad (13.46b)$$

### Marginal Probability Functions

These functions define probabilities of one random variable without regard to the other one and are the same as those for one random variable but defined using the joint functions. Thus we have two such marginal distributions,

$$F_X(x) = F_{XY}(x, \infty) = \int_{\lambda=-\infty}^x \left( \int_{-\infty}^{\infty} f_{XY}(\lambda, y) dy \right) d\lambda = \int_{-\infty}^x f_X(\lambda) d\lambda \quad (13.47a)$$

$$F_Y(y) = F_{XY}(\infty, y) = \int_{\nu=-\infty}^y \left( \int_{-\infty}^{\infty} f_{XY}(x, \nu) dx \right) d\nu = \int_{-\infty}^y f_Y(\nu) d\nu \quad (13.47b)$$

and from (13.47) two marginal densities,

$$f_X(x) = \int_{-\infty}^{\infty} f_{XY}(x, y) dy \quad (13.48a)$$

$$f_Y(y) = \int_{-\infty}^{\infty} f_{XY}(x, y) dx \quad (13.48b)$$

### Conditional Probability Functions

As opposed to the marginal functions, these functions for one random variable are defined based on the observation or knowledge of the value of the other random variable and are also very useful in practice. The *conditional* pdf of  $X$  conditioned on the observation of  $Y = y$  is denoted by  $f_{X|Y}(x|y)$  and is defined as

$$f_{X|Y}(x|y) \triangleq \frac{f_{XY}(x, y)}{f_Y(y)} \quad (13.49)$$

Similarly, we have conditional pdf of  $Y$  given  $X$  as

$$f_{Y|X}(y|x) \triangleq \frac{f_{XY}(x, y)}{f_X(x)} \quad (13.50)$$

From (13.49) and (13.50), we obtain

$$f_{XY}(x, y) = f_{X|Y}(x|y)f_Y(y) = f_{Y|X}(y|x)f_X(x) \quad (13.51)$$

and from (13.51), we obtain

$$f_{X|Y}(x|y) = \frac{f_{Y|X}(y|x)f_X(x)}{f_Y(y)} \quad (13.52a)$$

$$f_{Y|X}(y|x) = \frac{f_{X|Y}(x|y)f_Y(y)}{f_X(x)} \quad (13.52b)$$

The results in (13.52) are known as *Bayes rules* and are useful in detection and estimation theory.

### **Statistical Independence**

Although the marginal probability functions for random variable  $X$  were obtained without regard to  $Y$ , the occurrence of  $Y$  can still affect the occurrence of  $X$ . On the other hand, if the conditional pdf of  $X$  given  $Y$  does not depend on  $Y$  and reduces to the marginal pdf of  $X$  or vice versa, we will say that random variables  $X$  and  $Y$  are statistically (or mutually) independent, or *independent* for short. Thus when  $X$  and  $Y$  are independent, we have

$$f_{X|Y}(x|y) = f_X(x) \quad \text{and} \quad f_{Y|X}(y|x) = f_Y(y) \quad (13.53)$$

Hence from (13.49) or (13.50),

$$f_{XY}(x, y) = f_X(x)f_Y(y) \quad (13.54)$$

Similarly, we can also show a similar relationship for cumulative distribution functions when  $X$  and  $Y$  are independent, that is,

$$F_{XY}(x, y) = F_X(x)F_Y(y) \quad (13.55)$$

**Histogram as a Joint pdf Approximation** Given observations of  $N$  random variable pairs ( $XY$ ), let  $N_{xy}$  denote the number of pairs that fall into the small area  $\Delta_{xy}$  at  $(x, y)$ . Then the three-dimensional plot of  $N_{xy}$  vs.  $(x, y)$  is a two-variable histogram of the observed values, and the three-dimensional plot of the ratio

$$P_{XY}(x, y) \triangleq \frac{N_{xy}}{N\Delta_{xy}} \quad (13.56)$$

vs.  $(x, y)$  is the normalized histogram and is a good approximation to the joint pdf  $f_{XY}(x, y)$ . MATLAB provides a function, `Nxy = hist3([x,y], nbins)`, that provides counts in `Nxy` given observed pairs `[x,y]` and an `nbins(1) × nbins(2)` grid of bins. Using this function, one can design a MATLAB function, which we will call `pdf2`, that computes the pdf as a normalized histogram from the observed pairs. The design of this function is left as an exercise.

**Scatter-plot as a pdf Plot** Another visual depiction of the joint pdf is obtained by using a scatter-plot which is a two-dimensional picture. It is obtained by plotting  $(x, y)$  pairs as dots in the plane. Dot density indicates value of the pdf; higher density means higher value and vice versa. The scatter-plot shape also gives the approximate support of the pdf. Its use is illustrated in Example 13.5.

### Transformations of Pairs of Random Variables

We have discussed the transformation of one random variable into another and calculations of its pdf. In a similar fashion a somewhat more involved signal processing operation would transform two random variables with known joint pdf into either one or two new random variables. An application of the first operation would be the case of a signal in additive noise and that of the second one would be converting cartesian coordinates into polar coordinates. In each case we are interested in obtaining the density functions of the new random variables.

**One Function** Let  $f_{XY}(x, y)$  be the joint pdf of a pair of random variables  $(X, Y)$  and let  $W = g(X, Y)$  be the new random variable. There are several approaches to determine the pdf of  $W$ . One easy to understand approach is to first determine the CDF of  $W$  using the function  $g(\cdot, \cdot)$  and then differentiate it to obtain its pdf. Toward this, the CDF of  $W$  can be expressed in terms of  $X$  and  $Y$  as

$$\begin{aligned} F_W(w) &= \Pr\{W \leq w\} = \Pr\{g(X, Y) \leq w\} \\ &= \iint_{g(x,y) \leq w} f_{XY}(x, y) dx dy \end{aligned} \quad (13.57)$$

where the inequality  $g(X, Y) \leq w$  defines a region in the  $(x, y)$  plane over which integration is performed. The pdf of  $W$  is now given by

$$f_W(w) = \frac{d}{dw} \left( \iint_{g(x,y) \leq w} f_{XY}(x, y) dx dy \right) \quad (13.58)$$

Although elegant in its simplicity, the integral, depending on the joint pdf and the function  $g(\cdot, \cdot)$ , may or may not be analytically tractable.

One particularly important application of this approach is when the transformation is just the sum of two random variables, for example the signal plus noise case. Let  $W = X + Y$ . Then from (13.57)

$$F_W(w) = \iint_{x+y \leq w} f_{XY}(x, y) dx dy = \int_{y=-\infty}^{\infty} \int_{x=-\infty}^{w-y} f_{XY}(x, y) dx dy \quad (13.59)$$

Differentiating (13.59) and using the Leibnitz's rule<sup>1</sup> from calculus, we obtain

$$\begin{aligned} f_W(w) &= \int_{y=-\infty}^{\infty} \frac{d}{dw} \left( \int_{x=-\infty}^{w-y} f_{XY}(x, y) dx \right) dy \\ &= \int_{y=-\infty}^{\infty} f_{XY}(w-y, y) dy \end{aligned} \quad (13.60)$$

A further special case is when  $X$  and  $Y$  are independent in which case, using (13.54), we obtain

$$f_W(w) = \int_{y=-\infty}^{\infty} f_X(w-y) f_Y(y) dy = f_X(w) * f_Y(w) \quad (13.61)$$

which is a convolution integral. This is a very significant result.

- **EXAMPLE 13.4** Let  $X \sim U(0, 1)$  and  $Y \sim U(0, 1)$  be two uniformly distributed, independent random variables and let  $W = X+Y$ . Then from (13.61) the pdf of  $W$  is given by

$$\begin{aligned} f_W(w) &= (u(w) - u(w-1)) * (u(w) - u(w-1)) \\ &= (1 - |w-1|)(u(w) - u(w-2)) \end{aligned} \quad (13.62)$$

which is a triangle between 0 and 2. To verify (13.62), we will generate a large number of random numbers for  $X$  and  $Y$ , add them to obtain the corresponding numbers for  $W$ , and then use the `pdf1` function to obtain the pdf  $f_W(w)$ . The following MATLAB script illustrates these steps.

```
>> N = 1000000;
>> x = rand(N,1); y = rand(N,1); >> w = x+y;
>> [Pw,wc] = pdf1(w,0,2,100);
>> % Plotting commands follow
```

Plot of the resulting pdf is shown in Figure 13.8. □

**Two Functions** This second transformation case is an extension of the one random variable result (13.25) to two dimensions. Let two functions of the two random variables  $X$  and  $Y$  be

$$W = g_1(X, Y) \quad \text{and} \quad V = g_2(X, Y) \quad (13.63)$$

<sup>1</sup>Leibnitz's rule states that

$$\frac{\partial}{\partial x} \int_{a(x)}^{b(x)} f(x, y) dy = \frac{\partial b}{\partial x} f(x, b(x)) - \frac{\partial a}{\partial x} f(a(x), x) + \int_{a(x)}^{b(x)} \frac{\partial}{\partial x} f(x, y) dy.$$

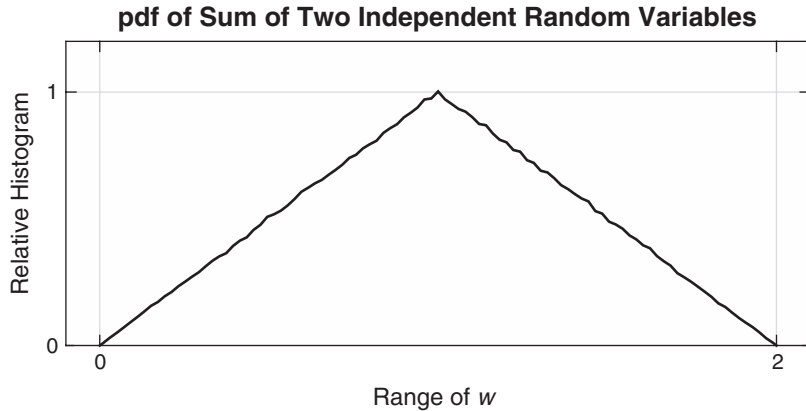


**FIGURE 13.8** Normalized histogram of sum of two uniformly distributed random variables

and assuming that this  $2 \times 2$  mapping is invertible, then we also have the inverse functions

$$X = h_1(W, V) \quad \text{and} \quad Y = h_2(W, V) \quad (13.64)$$

Under the mappings (13.64) let the infinitesimal area  $dw dv$  in the  $(w, v)$  plane be mapped into area  $A_{x,y}$  in the  $(x, y)$  plane so that the following probabilities are equal

$$f_{WV}(w, v) dw dv = f_{XY}(h_1, h_2) A_{x,y} \quad (13.65)$$

in which

$$A_{x,y} = \left| J \begin{pmatrix} x & y \\ w & v \end{pmatrix} \right| dw dv = \left| \det \begin{bmatrix} \frac{\partial x}{\partial w} & \frac{\partial x}{\partial v} \\ \frac{\partial y}{\partial w} & \frac{\partial y}{\partial v} \end{bmatrix} \right| dw dv \quad (13.66)$$

where  $J(\cdot)$  is called the *Jacobian* of the transformation and represents the slope plane in two dimensions. Substituting (13.66) in (13.65) we obtain the desired result

$$f_{WV}(w, v) = f_{XY}(h_1(W, V), h_2(W, V)) \times \left| \det \begin{bmatrix} \frac{\partial x}{\partial w} & \frac{\partial x}{\partial v} \\ \frac{\partial y}{\partial w} & \frac{\partial y}{\partial v} \end{bmatrix} \right| \quad (13.67)$$

As in the one variable case, if the given  $2 \times 2$  transformation is not invertible then the inverse mapping has multiple roots and contribution from each root should be added to complete the joint pdf  $f_{WV}(w, v)$ .

- **EXAMPLE 13.5** Let random variables  $X$  and  $Y$  be independent and identically distributed with uniform distribution  $U(0, 1)$ . Define  $W = X + Y$  and  $V = X - Y$ . Then

$$X = \frac{W + V}{2} \triangleq h_1(W, V) \quad \text{and} \quad Y = \frac{W - V}{2} \triangleq h_2(W, V)$$

and

$$\left| J \begin{pmatrix} x & y \\ w & v \end{pmatrix} \right| = \left| \det \begin{bmatrix} \frac{1}{2} & \frac{1}{2} \\ \frac{1}{2} & -\frac{1}{2} \end{bmatrix} \right| = \frac{1}{2}$$

Hence

$$f_{WV}(w, v) = \frac{1}{2} f_{XY}\left(\frac{w+v}{2}, \frac{w-v}{2}\right) = \frac{1}{2} f_X\left(\frac{w+v}{2}\right) f_Y\left(\frac{w-v}{2}\right) \quad (13.68)$$

due to independence. Since  $X$  and  $Y$  are  $U(0, 1)$ , the joint pdf  $f_{WV}(w, v)$  from (13.68) is also uniform with value of  $\frac{1}{2}$  over a diamond-shaped region bounded by four straight lines:  $w + v = 0$ ,  $w - v = -2$ ,  $w + v = 2$ , and  $w - v = 0$ . This can be verified using a scatter-plot as shown in the MATLAB script below.

```
>> x = rand(10000,1); y = rand(10000,1);
>> w = x+y; v = x-y;
>> plot([-0.2,2.2],[0,0],'k','linewidth',0.75); hold on;
>> plot([0,0],[-1.1,1.1],'k','linewidth',0.75);
>> plot(w,v,'.','markersize',2); axis equal;
>> axis([-0.2,2.2,-1.1,1.2]);
>> set(gca,'xtick',[0,1,2],'ytick',[-1,0,1]); grid;
>> xlabel('Range of {\\it w}', 'fontsize',9);
>> ylabel('Range of {\\it v}', 'fontsize',9);
>> title('Scatter-Plot: W = X+Y, V = X-Y',...
>>      'fontsize',10,'fontweight','bold');
```

The resulting scatter-plot is shown in Figure 13.9. □

### 13.2.2 JOINT STATISTICAL AVERAGES

These averages, or *joint moments*, are now doubly countable and require two arguments. They are given by averaging the product of integer powers of  $X$  and  $Y$ , or

$$\xi_{XY}(m, n) \triangleq E[X^m Y^n] = \iint_{-\infty}^{\infty} x^m y^n f_{XY}(x, y) dx dy \quad (13.69)$$

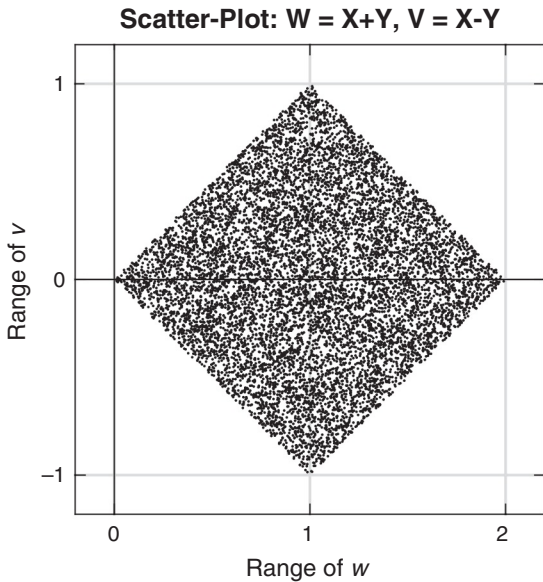


**FIGURE 13.9** Scatter-plot of  $W = X + Y$  vs.  $V = X - Y$  for  $X \sim U(0, 1)$  and  $Y \sim U(0, 1)$

Clearly,  $\xi_{XY}(0, 0) = 1$ , while the means of  $X$  and  $Y$  are given by

$$\xi_{XY}(1, 0) = \xi_X(1) = \mu_X = \iint_{-\infty}^{\infty} xf_{XY}(x, y) dx dy = \int_{-\infty}^{\infty} xf_X(x) dx \quad (13.70)$$

and

$$\xi_{XY}(0, 1) = \xi_Y(1) = \mu_Y = \iint_{-\infty}^{\infty} yf_{XY}(x, y) dx dy = \int_{-\infty}^{\infty} yf_Y(y) dy \quad (13.71)$$

as we have shown before. However,  $\xi_{XY}(1, 1)$  defines a new joint moment denoted by

$$R_{XY} \triangleq \xi_{XY}(1, 1) = E[XY] = \iint_{-\infty}^{\infty} xyf_{XY}(x, y) dx dy \quad (13.72)$$

which is called the *correlation* between  $X$  and  $Y$ . It measures the *average linear relationship* between the two random variables.

Similar to the above moments, we can define the *joint central moments* by subtracting the mean values before averaging as

$$\begin{aligned} M_{XY}(m, n) &\triangleq E[(X - \mu_X)^m (Y - \mu_Y)^n] \\ &= \int_{-\infty}^{\infty} (x - \mu_X)^m (y - \mu_Y)^n f_{XY}(x, y) dx dy \end{aligned} \quad (13.73)$$

Again,  $M_{XY}(0, 0) = 1$  and  $M_{XY}(1, 0) = M_{XY}(0, 1) = 0$ . The variances of  $X$  and  $Y$  are given by

$$\begin{aligned} M_{XY}(2, 0) = M_X(2) = \sigma_X^2 &= \int_{-\infty}^{\infty} (x - \mu_X)^2 f_{XY}(x, y) dx dy \\ &= \int_{-\infty}^{\infty} (x - \mu_X)^2 f_X(x) dx \end{aligned} \quad (13.74)$$

and

$$\begin{aligned} M_{XY}(0, 2) = M_Y(2) = \sigma_Y^2 &= \int_{-\infty}^{\infty} (y - \mu_Y)^2 f_{XY}(x, y) dx dy \\ &= \int_{-\infty}^{\infty} (y - \mu_Y)^2 f_Y(y) dy \end{aligned} \quad (13.75)$$

as we have shown before. However,  $M_{XY}(1, 1)$  defines a new joint central moment denoted by

$$C_{XY} \triangleq M_{XY}(1, 1) = \int_{-\infty}^{\infty} (x - \mu_X)(y - \mu_Y) f_{XY}(x, y) dx dy \quad (13.76)$$

which is called the *covariance* between  $X$  and  $Y$ . It measures the *average linear relationship* between the two random variables after their means have been subtracted out. Note that from (13.76), it is straightforward to show that

$$C_{XY} = R_{XY} - \mu_X \mu_Y \quad (13.77)$$

### **Important Concepts**

Through the joint moments of correlation and covariance, we now discuss new important relationships between two random variables.

**Uncorrelated Random Variables** If the covariance  $C_{XY}$  between  $X$  and  $Y$  is zero, then from (13.77) we have

$$R_{XY} = \mu_X^2 \mu_Y^2 \quad \text{or} \quad E[XY] = E[X]E[Y] \quad (13.78)$$

and we will say that random variables  $X$  and  $Y$  are *uncorrelated* with each other. This is a *weaker* condition between  $X$  and  $Y$  compared to their independence, (13.54), which is a stronger condition. This is because independence always implies zero correlation between  $X$  and  $Y$ , while the inverse is not always true. In Section 13.2.3, we will show that for Gaussian random variables zero correlation also implies independence.

For uncorrelated random variables  $X$  and  $Y$ , it is easy to show that the variance of the sum of two random variables is the sum of their variances, that is,

$$\sigma_{X+Y}^2 = \sigma_X^2 + \sigma_Y^2 \quad (13.79)$$

**Orthogonal Random Variables** Consider the expectation  $E[(X+Y)^2]$ . Since expectation is a *linear operator*, we have

$$\begin{aligned} E[(X+Y)^2] &= E[X^2 + Y^2 + 2XY] = E[X^2] + E[Y^2] + 2E[XY] \\ &= E[X^2] + E[Y^2] + 2R_{XY} \end{aligned} \quad (13.80)$$

If the correlation  $R_{XY} = 0$ , then from (13.80) we have

$$E[(X+Y)^2] = E[X^2] + E[Y^2] \quad (13.81)$$

which suggests that  $X$  and  $Y$  are perpendicular to each other if  $X$  and  $Y$  are considered vectors in a Cartesian space. Thus we will say that if correlation is zero, then  $X$  and  $Y$  are *orthogonal* to each other. We note that this condition holds when  $X$  and  $Y$  are uncorrelated and either  $X$  or  $Y$  or both have zero mean.

**Correlation Coefficient** Finally, we define a *normalized covariance* between random variables so that we can compare average linear dependencies between pairs of random variables. This normalized covariance is called the *correlation coefficient* and is defined by

$$\rho_{XY} \triangleq \frac{C_{XY}}{\sigma_X \sigma_Y} \quad (13.82)$$

Clearly, if  $\rho_{XY} = 0$ , then the covariance  $C_{XY} = 0$  and  $X$  and  $Y$  are uncorrelated. If  $\rho_{XY} = 1$ , we will say that  $X$  and  $Y$  are *perfectly correlated* and *agree* with each other, on the average. However, if  $\rho_{XY} = -1$ , we will still say that  $X$  and  $Y$  are perfectly correlated but *disagree* with each other, on the average.

### 13.2.3 BIVARIATE GAUSSIAN DISTRIBUTION

One of the well-known and often-used models for two random variables is the two-dimensional jointly Gaussian distribution. It is completely described by the first two joint moments of random variables  $X$  and  $Y$  and

in its most general form is characterized by five parameters and its pdf given by

$$\begin{aligned} N(\mu_X, \mu_Y; \sigma_X, \sigma_Y; \rho_{XY}) &\triangleq f_{XY}(x, y) = \frac{1}{2\pi\sigma_X\sigma_Y\sqrt{1-\rho_{XY}^2}} \times \\ &\exp\left[\frac{-1}{2(1-\rho_{XY}^2)}\left\{\left(\frac{x-\mu_X}{\sigma_X}\right)^2 - 2\rho_{XY}\left(\frac{x-\mu_X}{\sigma_X}\right)\left(\frac{y-\mu_Y}{\sigma_Y}\right) + \left(\frac{y-\mu_Y}{\sigma_Y}\right)^2\right\}\right] \end{aligned} \quad (13.83)$$

This is a unimodal bell-shaped surface and is shown in Figure 13.10 for various values of  $\sigma_X$ ,  $\sigma_Y$ , and  $\rho_{XY}$  and for  $\mu_X = \mu_Y = 0$ . The contours of constant-density values are also superimposed on the density surface for clarity. We observe that in Figure 13.10a contours are circular; in Figure 13.10b contours are elliptical with the major axis rotated 45° with the  $x$ -axis; in Figure 13.10c contours are also elliptic but the major axis rotated more than 45°; and in Figure 13.10d contours are elliptic but the major axis rotated more than 45° in the clockwise direction. The density surfaces are symmetric with respect to the rotated axis. The non-zero values of the means simply move the center of the surface to a new location.

Using direct integration of  $f_{XY}(x, y)$  in (13.83), we can show that the marginal densities are given by

$$f_X(x) = \int_{-\infty}^{\infty} f_{XY}(x, y) dy = \frac{1}{\sigma_X\sqrt{2\pi}} \exp\left[\frac{-1}{2}\left(\frac{x-\mu_X}{\sigma_X}\right)^2\right] = N(\mu_X, \sigma_X^2) \quad (13.84a)$$

$$f_Y(y) = \int_{-\infty}^{\infty} f_{XY}(x, y) dx = \frac{1}{\sigma_Y\sqrt{2\pi}} \exp\left[\frac{-1}{2}\left(\frac{y-\mu_Y}{\sigma_Y}\right)^2\right] = N(\mu_Y, \sigma_Y^2) \quad (13.84b)$$

which are marginal Gaussian random variables. Hence  $f_{XY}(x, y)$  in (13.83) is known as the *jointly* Gaussian or bivariate Gaussian distribution.

It should further be noted that if  $\rho_{XY} = 0$ , that is, if the covariance is zero so that  $X$  and  $Y$  are uncorrelated, then from (13.83) we have

$$\begin{aligned} f_{XY}(x, y) &= \frac{1}{2\pi\sigma_X\sigma_Y} \exp\left[\frac{-1}{2}\left\{\left(\frac{x-\mu_X}{\sigma_X}\right)^2 + \left(\frac{y-\mu_Y}{\sigma_Y}\right)^2\right\}\right] \\ &= \frac{1}{\sigma_X\sqrt{2\pi}} \exp\left[\frac{-1}{2}\left(\frac{x-\mu_X}{\sigma_X}\right)^2\right] \\ &\quad \times \frac{1}{\sigma_Y\sqrt{2\pi}} \exp\left[\frac{-1}{2}\left(\frac{y-\mu_Y}{\sigma_Y}\right)^2\right] = f_X(x)f_Y(y) \end{aligned} \quad (13.85)$$

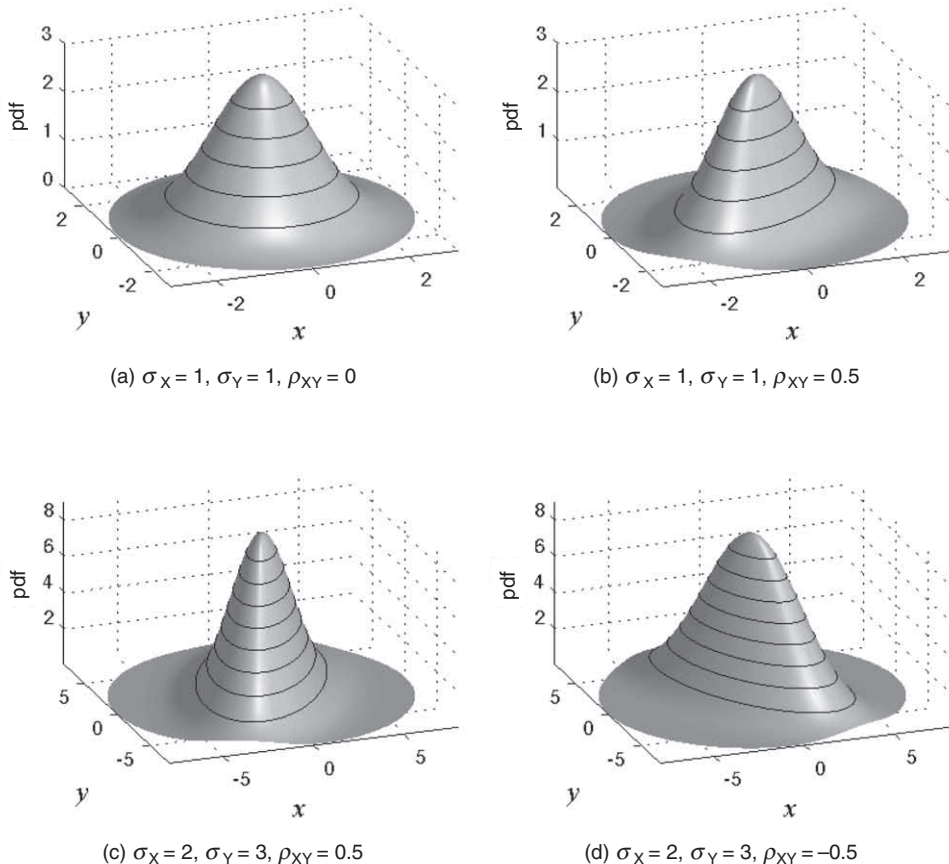


**FIGURE 13.10** Bivariate Gaussian distributions for various values of  $\sigma_X$ ,  $\sigma_Y$ , and  $\rho_{XY}$  and for  $\mu_X = \mu_Y = 0$

which implies independence between  $X$  and  $Y$ . Hence, only in the case of the Gaussian distribution, zero correlation between  $X$  and  $Y$  implies independence.

**Useful Properties** Based on our discussion so far on Gaussian random variables, it should be obvious that they possess some unique and important properties. We enumerate these properties, along with those that were not discussed:

1. A Gaussian random variable is completely described by its first two moments, which means that higher-order moments can be obtained in terms of its first two moments.
2. The sum of two Gaussian random variable is also Gaussian.

3. In fact, any linear combination of a number of Gaussian random variables is also Gaussian.
4. The product of two Gaussian density functions also results in a Gaussian function.
5. The convolution of two Gaussian functions also results in a Gaussian function.
6. A countable sum of independent random variables, irrespective of their distribution functions, results in a Gaussian distribution under some very general conditions. This result is known as the *Central Limit theorem*. Hence a Gaussian distribution is also a *stable* distribution for finite means and variances.
7. If Gaussian random variables are mutually uncorrelated, then they are also mutually independent.

Other random variable models do not possess all these properties.

- EXAMPLE 13.6** Generate samples of bivariate Gaussian random variables,  $X_1$  and  $X_2$ , having specified mean values  $\mu_1$  and  $\mu_2$ , variances  $\sigma_1^2$  and  $\sigma_2^2$ , respectively, and a correlation coefficient  $\rho$  between the two.

### Solution

First, we generate samples of two statistically independent, zero-mean, and unit-variance Gaussian random variables by using the method described in Section 13.1.3. Let us denote these random variable values by the vector notation

$$\mathbf{Y} = \begin{bmatrix} y_1 \\ y_2 \end{bmatrix} \quad (13.86)$$

Next, we assemble the desired  $(2 \times 2)$  covariance matrix

$$\mathbf{C}_X = \begin{bmatrix} \sigma_1^2 & \rho\sigma_1\sigma_2 \\ \rho\sigma_1\sigma_2 & \sigma_2^2 \end{bmatrix} \quad (13.87)$$

and factor it as

$$\mathbf{C}_X = \mathbf{C}_X^{\frac{1}{2}} (\mathbf{C}_X^{\frac{1}{2}})^T \quad (13.88)$$

We now define the linearly transformed  $(2 \times 1)$  vector  $\mathbf{X}$  as

$$\mathbf{X} \triangleq \begin{bmatrix} X_1 \\ X_2 \end{bmatrix} = \mathbf{C}_X^{\frac{1}{2}} \mathbf{Y} + \boldsymbol{\mu}_X, \quad \boldsymbol{\mu}_X \triangleq \begin{bmatrix} \mu_1 \\ \mu_2 \end{bmatrix} \quad (13.89)$$

Then the covariance of  $\mathbf{X}$  is

$$\begin{aligned} E[(\mathbf{X} - \boldsymbol{\mu}_X)(\mathbf{X} - \boldsymbol{\mu}_X)^T] &= E[\mathbf{C}_X^{\frac{1}{2}} \mathbf{Y} \mathbf{Y}^T (\mathbf{C}_X^{\frac{1}{2}})^T] \\ &= \mathbf{C}_X^{\frac{1}{2}} E[\mathbf{Y} \mathbf{Y}^T] (\mathbf{C}_X^{\frac{1}{2}})^T = \mathbf{C}_X^{\frac{1}{2}} \mathbf{I} (\mathbf{C}_X^{\frac{1}{2}})^T \\ &= \mathbf{C}_X \end{aligned} \quad (13.90)$$

as expected. The most difficult step in this process is the factorization of the covariance matrix  $\mathbf{C}_X$ , which can be implemented in MATLAB using the matrix square-root function `sqrtm`. The following MATLAB script generates 1000 samples of the bivariate Gaussian distribution for  $\mu_1 = 2$ ,  $\mu_2 = 1$ ,  $\sigma_1 = 1$ ,  $\sigma_2 = 2$ ,

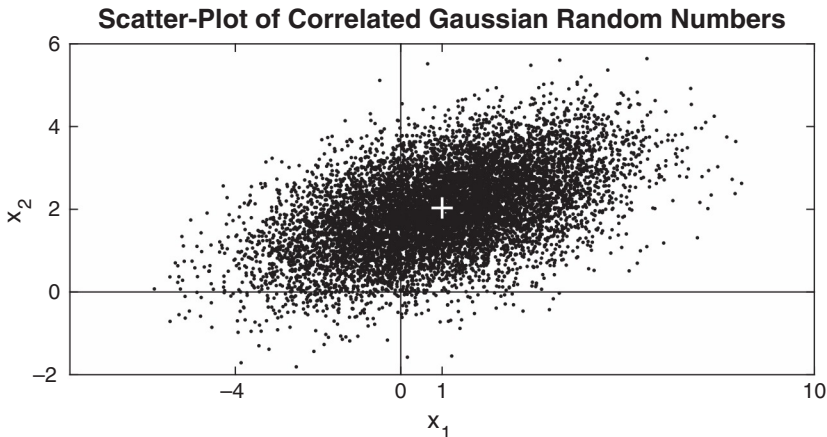


**FIGURE 13.11** Scatter-plot of Gaussian random numbers in Example 13.6

and  $\rho = 0.5$ . The scatter-plot of the resulting samples is shown in Figure 13.11, in which the distribution center is shown as the “+” symbol.

```

mu1 = 1; mu2 = 2; % Mean parameters
sd1 = 2; sd2 = 1; % Standard deviations
var1 = sd1^2; var2 = sd2^2; % Variances
rho = 0.5; % Correlation coefficient
Cx = [var1, rho*sd1*sd2; rho*sd1*sd2, var2]; % Cov matrix
% Generate 1000 unit Gaussian random-2 vectors
N = 10000; M = 2; Y = randn(N,M);
% Generate correlated non-zero mean Gaussian random-2 vectors
X = sqrtm(Cx)*Y'+ [mu1;mu2]*ones(1,N); X = X';
% Plotting commands follow

```

□

To generate multivariate Gaussian random numbers, we can extend the approach of Example 13.6 to arbitrary-size ( $> 2$ ) vectors. The following MATLAB function,  $X=\text{randnMV}(N,\mu,C)$ , generates  $N$  multivariate Gaussian random vectors in  $X$  given the mean vector  $\mu$  in  $\mu$  and the covariance matrix  $C$  in  $C$ .

```

function X = randnMV(N,mu,C)
% randnMV: multivariate Gaussian random vector generator
% Generates N vectors in X given mean mu and covariance matrix C
% mu should be a Mx1 column vector; C should be MxM
% Generated X is NxM
% X = randnMV(N,mu,C)
%
mu = mu(:); M = length(mu);
Y = randn(N,M);
X = sqrtm(C)*Y'+ mu*ones(1,N); X = X';
end

```

### 13.3 RANDOM SIGNALS

---

A random signal or process can be thought of as a collection of waveforms (or time-varying values) with some assigned probability. Similarly, we can think of the value of a random signal at each time instant as a random variable with an assigned pdf. Thus a random signal is a collection of random variables in the temporal space as well as a collection of sample waveforms in the ensemble space. This understanding is crucial in dealing with its probabilistic (or statistical) description as well as for its processing through linear systems.

A random process can be continuous in time (random signals) or discrete in time (random sequences). We will mostly discuss random signals, but the derived results will also apply to random sequences with obvious modifications that we will also state. In keeping with our random variable terminology, we will denote a random signal by  $X(t)$  and its realization or sample waveform by  $x(t)$ . Thus we have a new temporal variable in our random object.

If a time instance  $t$  is fixed (i.e., when we assign a known value), then  $X(t)$  is a random variable and hence has a pdf  $f_X(x; t)$  or moment functions such as a mean  $\mu_X(t)$ , mean-squared value, and variance  $\sigma_X^2(t)$  given by

$$\mu_X(t) = E[X(t)] = \int_{x=-\infty}^{\infty} x f_X(x; t) dx, \quad (13.91a)$$

$$E[X^2(t)] = \int_{x=-\infty}^{\infty} x^2 f_X(x; t) dx, \quad (13.91b)$$

$$\sigma_X^2(t) = E[(X(t) - \mu_X(t))^2] = E[X^2(t)] - \mu_X^2(t) \quad (13.91c)$$

Then all the concepts that we discussed in Section 13.1 apply at each time instance of  $X(t)$ .

If we have two fixed time instances—say,  $t_1$  and  $t_2$ —then  $X(t_1)$  and  $X(t_2)$  are a pair of random variables with joint pdf  $f_X(x_1, x_2; t_1, t_2)$  or joint moment functions such as correlation  $R_{XX}(t_1, t_2)$  and covariance  $C_{XX}(t_1, t_2)$  given by<sup>2</sup>

$$R_{XX}(t_1, t_2) = E[X(t_1)X(t_2)] = \iint_{-\infty}^{\infty} x_1 x_2 f_X(x_1, x_2; t_1, t_2) dx_1 dx_2 \quad (13.92a)$$

$$C_{XX}(t_1, t_2) = R_{XX}(t_1, t_2) - \mu_X(t_1)\mu_X(t_2) \quad (13.92b)$$

in addition to their marginal densities or moments. Since the pair of random variables  $X(t_1)$  and  $X(t_2)$  are from the same process  $X(t)$ , we will

<sup>2</sup>We will assume real-valued random signals. For complex-valued signals, the second term in the expectation requires complex-conjugation.

henceforth call  $R_{XX}(t_1, t_2)$  the *autocorrelation function* and  $C_{XX}(t_1, t_2)$  the *autocovariance function*. Now the concepts that we discussed in Section 13.2 can be used for each such pair from  $\mathbf{X}(t)$ .

- **EXAMPLE 13.7** A random process is given by

$$\mathbf{X}(t) = \mathbf{A}e^{-t}u(t) \quad (13.93)$$

which is a causal exponential signal whose amplitude  $\mathbf{A} \sim U(0, 1)$  is a uniformly distributed random variable over  $(0, 1)$ . The marginal density of  $\mathbf{X}(t)$  for  $t \geq 0$ , using the transformation of random variable formula (13.25), is given by

$$\begin{aligned} f_{\mathbf{X}}(x; t) &= f_{\mathbf{A}}(xe^t)e^t \quad (\text{since } h(x) = xe^t \text{ and } h'(x) = e^t) \\ &= e^t(u(x) - u(x - e^{-t})) \sim U(0, e^{-t}) \end{aligned} \quad (13.94)$$

which is a uniform distribution between 0 and  $e^{-t}$  at each  $t \geq 0$ . Note that as  $t \rightarrow \infty$ , this pdf becomes a narrower pulse with increasing amplitude and in the limit becomes  $f_{\mathbf{X}}(x; \infty) = \delta(x)$ , which means that  $\mathbf{X}(\infty)$  is a deterministic number zero. The first two moments of  $\mathbf{X}(t)$ , using (13.91) and the moments of uniform distribution, are given by

$$\mu_{\mathbf{X}}(t) = E[\mathbf{A}e^{-t}u(t)] = E[\mathbf{A}]e^{-t}u(t) = \frac{1}{2}e^{-t}u(t), \quad (13.95a)$$

$$E[\mathbf{X}^2(t)] = E[\mathbf{A}^2]e^{-2t}u(t) = \frac{1}{3}e^{-2t}u(t), \quad (13.95b)$$

$$\sigma_{\mathbf{X}}(t) = E[\mathbf{X}^2(t)] - \mu_{\mathbf{X}}^2(t) = \frac{1}{12}e^{-2t}u(t) \quad (13.95c)$$

To determine the joint pdf  $f_{\mathbf{X}}(x_1, x_2; t_1, t_2)$ , note that since the random variable  $\mathbf{A}$  is time independent, the random variables  $\mathbf{X}(t_1)$  and  $\mathbf{X}(t_2)$ , for  $t_1, t_2 \geq 0$ , are linearly dependent, that is,

$$\mathbf{X}(t_2) = X(t_1)e^{-(t_2-t_1)} \quad (13.96)$$

This means that the joint pdf  $f_{\mathbf{X}}(x_1, x_2; t_1, t_2)$  is singular; that is, it contains an impulse plane in the  $(x_1, x_2)$  domain. Now consider

$$f_{\mathbf{X}}(x_1, x_2; t_1, t_2) = f_{\mathbf{X}}(x_2|x_1; t_1, t_2)f_{\mathbf{X}}(x_1; t_1) \quad (13.97)$$

where from (13.94)  $f_{\mathbf{X}}(x_1; t_1) \sim U(0, e^{-t_1})$  and from (13.96),

$$f_{\mathbf{X}}(x_2|x_1; t_1, t_2) = \delta(x_2 - x_1 e^{-(t_2-t_1)}) \quad (13.98)$$

which is the singular function that represents an impulse plane at an angle given by the slope  $e^{-(t_2-t_1)}$ . Substituting (13.98) in (13.97), the joint pdf is given by

$$f_{\mathbf{X}}(x_1, x_2; t_1, t_2) = e^{t_1}(u(x_1) - u(x_1 - e^{-t_1}))\delta(x_2 - x_1 e^{-(t_2-t_1)}), \quad t_1, t_2 \geq 0 \quad (13.99)$$

From (13.92) and (13.95), the autocorrelation and autocovariance functions are given by

$$R_{XX}(t_1, t_2) = E[\mathbf{A}e^{-t_1}\mathbf{A}e^{-t_2}] = E[\mathbf{A}^2]e^{-(t_1+t_2)} = \frac{1}{3}e^{-(t_1+t_2)}, \quad (13.100a)$$

$$C_{XX}(t_1, t_2) = R_{XX}(t_1, t_2) - \mu_{\mathbf{X}}(t_1)\mu_{\mathbf{X}}(t_2) = \frac{1}{12}e^{-(t_1+t_2)} \quad (13.100b)$$

□

- **EXAMPLE 13.8** Consider a sinusoidal random process given by

$$X(t) = A \cos(\Omega_0 t + \Theta) \quad (13.101)$$

where  $\Omega_0$  is a fixed frequency, the amplitude random variable  $A$  is linearly distributed with pdf

$$f_A(a) = \begin{cases} 2a, & 0 \leq a \leq 1 \\ 0, & \text{otherwise} \end{cases} \quad (13.102)$$

and the phase random variable  $\Theta \sim U(0, 2\pi)$ . These two random variables are statistically independent. The mean of  $X(t)$  is given by

$$\mu_X(t) = E[X(t)] = E[A \cos(\Omega_0 t + \Theta)] = E[A]E[\cos(\Omega_0 t + \Theta)] = 0 \quad (13.103)$$

since the average of cosine waveform over one full cycle is zero. The autocorrelation of  $X(t)$  is given by

$$\begin{aligned} R_{XX}(t_1, t_2) &= E[X(t_1)X(t_2)] = E[A \cos(\Omega_0 t_1 + \Theta)A \cos(\Omega_0 t_2 + \Theta)] \\ &= E[A^2]E[\cos(\Omega_0 t_1 + \Theta)\cos(\Omega_0 t_2 + \Theta)] \end{aligned} \quad (13.104)$$

The first expectation on the right of (13.104) is computed as

$$E[A^2] = \int_0^1 a^2 (2a) da = \frac{1}{2} \quad (13.105)$$

while the second expectation is given by

$$\begin{aligned} E[\cos(\Omega_0 t_1 + \Theta)\cos(\Omega_0 t_2 + \Theta)] &= \frac{1}{2} \left\{ E[\cos(\Omega_0(t_1 - t_2)) \right. \\ &\quad \left. + \cos(\Omega_0(t_1 + t_2) + 2\Theta)] \right\} \\ &= \frac{1}{2} \cos(\Omega_0(t_1 - t_2)) \end{aligned} \quad (13.106)$$

where we have used the trigonometric identity on product of two cosine functions. Substituting (13.105) and (13.106) in (13.104), we obtain

$$R_{XX}(t_1, t_2) = \frac{1}{4} \cos(\Omega_0(t_1 - t_2)) \quad (13.107)$$

□

**Cross-correlation Functions** If  $Y(t)$  is another random process defined in the same random experiment, then its linear interaction with  $X(t)$  can be described using the joint pdf  $f_{XY}(x, y; t_1, t_2)$  or the cross moments in addition to its own marginal pdf and auto moments. We define the *cross-correlation* function  $R_{XY}(t_1, t_2)$  and *cross-covariance* function  $C_{XY}(t_1, t_2)$  between  $X(t)$  and  $Y(t)$  as

$$R_{XY}(t_1, t_2) = E[X(t_1)Y(t_2)] = \iint_{-\infty}^{\infty} xy f_{XY}(x, y; t_1, t_2) dx dy \quad (13.108a)$$

$$C_{XY}(t_1, t_2) = R_{XY}(t_1, t_2) - \mu_X(t_1)\mu_Y(t_2) \quad (13.108b)$$

These functions will be useful later in the calculations of linear system input/output correlations and covariances.

### 13.3.1 STATIONARITY

For a general random signal, the statistical quantities such as densities or moments vary or change with time, as in Example 13.7. However, for some random signals it is possible to have these quantities be time invariant, as in Example 13.8. In many applications, we model a random signal that exhibits this time-invariant statistical behavior. It simplifies storage and processing complexities. We will discuss two types of this time-invariance property of random signals, collectively known as *stationarity*.

#### ***Strict-Sense Stationarity***

In this type of stationarity, all orders of joint density functions or, alternatively, all orders of joint moments are time invariant, that is, the first-order densities are independent of time

$$f_{\mathbf{X}}(x; t) = f_{\mathbf{X}}(x) \quad (13.109)$$

and the joint densities are independent of time  $t$  but depend only on the relative interval  $\tau$  between the two time instances

$$f_{\mathbf{X}}(x_1, x_2; t_1 = t + \tau, t_2 = t) = f_{\mathbf{X}}(x_1, x_2; \tau = t_1 - t_2) \quad (13.110)$$

and so on, for all orders. This also means that

$$\mu_{\mathbf{X}}(t) = \mu_{\mathbf{X}}, \quad \mathbb{E}[X^2(t)] = \xi_X(2) \quad (13.111a)$$

$$R_{\mathbf{XX}}(t_1, t_2) = R_{\mathbf{XX}}(t_1 - t_2) \quad (13.111b)$$

$$C_{\mathbf{XX}}(t_1, t_2) = C_{\mathbf{XX}}(t_1 - t_2) \quad (13.111c)$$

and so on, for all higher-order moments. This is the strongest form of stationarity since it requires time independence for all orders of pdf and moments. Hence the name *strict-sense stationarity*, which is not always easy to achieve.

#### ***Wide-Sense Stationarity***

In many practical applications, we need or use only up to second-order statistical quantities of a random signal. Therefore, why not require time-invariance only for the first two orders of moments? This leads to a weaker but workable form of stationarity called *wide-sense stationarity*, or WSS. We will say that a random signal  $\mathbf{X}(t)$  is WSS if it satisfies the following three conditions:

$$\mathbb{E}[X^2(t)] = \xi_X(2) < \infty \quad (\text{finite average power}), \quad (13.112a)$$

$$\mu_{\mathbf{X}}(t) = \mu_{\mathbf{X}} \quad (\text{a constant}), \quad (13.112b)$$

$$R_{\mathbf{XX}}(t + \tau, t) = R_{\mathbf{XX}}(\tau) \quad (\text{function of } \tau \text{ only}) \quad (13.112c)$$

The variable  $\tau$  is called the *lag* time variable since the random variable  $X(t)$  lags  $X(t + \tau)$  in time by  $\tau$  seconds. Clearly, the autocovariance function  $C_{XX}(t, t + \tau)$  also exhibits a similar time-invariance as in (13.112c),

$$C_{XX}(t + \tau, t) = C_{XX}(\tau) \quad (13.113)$$

Note that the random process in Example 13.7 is nonstationary since both its first- and second-order moments are functions of time, whereas the random process in Example 13.8 is WSS since its mean is constant and its autocorrelation function depends only on  $(t_1 - t_2)$ , which, from (13.107), can be written as

$$R_{XX}(t + \tau, t) = R_{XX}(\tau) = \frac{1}{4} \cos(\Omega_0 \tau) \quad (13.114)$$

In the rest of the chapter, we will mostly deal with WSS random signals. Therefore, if we state that a random signal has a constant mean and an autocorrelation function that depends on a single time variable, then the reader can infer that the signal is WSS.

Finally, if  $X(t)$  and  $Y(t)$  are jointly WSS, then their cross-correlation and cross-covariance functions depend only on the lag variable  $\tau$ ; that is,

$$R_{XY}(t + \tau, t) = R_{XY}(\tau) \quad \text{and} \quad C_{XY}(t + \tau, t) = C_{XY}(\tau) \quad (13.115)$$

### 13.3.2 ERGODICITY

Up to this point we treated a random signal as random variables at each  $t$  and computed averages using the ensemble space. Thus we assumed that we have had access to a very large number of waveforms so that we could obtain averages, at each  $t$ , as weighted (by pdf) sums over ensemble as explained in (13.8). However, in reality we have only one temporal sample waveform,  $x(t)$ , available to us for measurement and analysis. Using our time integrating meters such as voltmeters, ammeters, or wattmeters we could determine averages over a sufficiently long period of time. We then wonder whether these time averages would give us the same ensemble averages so that we can replace ensemble expectations by the temporal integrals.

After a considerable thought, we conclude that, in general, we can not state that the two methods that we have described above to compute statistical averages will yield the same result even when the processes are stationary. Therefore, we introduce a new concept called *ergodicity* that would allow us to equate statistics computed over a long time using one sample waveform to those computed over ensemble of values at each  $t$ . We will call such processes as *ergodic* processes and, by necessity, these processes must be stationary. However, not all stationary processes are ergodic. By ergodicity we basically imply that using any one sample waveform we have observed all possible variabilities and undulations in the random process that are inherent in the ensemble of waveforms.

To begin with, consider the computation of the mean value. Let  $X(t)$  be WSS with mean  $\mu_X$  and let  $x(t)$  be its sample waveform. We will denote the temporal average of  $x(t)$  using angular brackets:

$$\langle x(t) \rangle \triangleq \lim_{T \rightarrow \infty} \frac{1}{2T} \int_{-T}^T x(t) dt \quad (13.116)$$

where the measurement interval is  $2T$ . If this average is equal to  $\mu_X$ , we will say that  $X(t)$  is *ergodic in the mean*.<sup>3</sup>

Now consider the temporal averaging to compute the autocorrelation function  $R_{XX}(\tau)$  given an arbitrary sample waveform  $x(t)$ :

$$\mathcal{R}_{xx}(\tau) \triangleq \langle x(t + \tau)x(t) \rangle \triangleq \lim_{T \rightarrow \infty} \frac{1}{2T} \int_{-T}^T x(t + \tau)x(t) dt \quad (13.117)$$

If  $\mathcal{R}_{xx}(\tau) = R_{XX}(\tau)$  for each  $\tau$ , then we will say that  $X(t)$  is *ergodic in the autocorrelation*. If  $\tau = 0$ , then we have  $\mathcal{R}_{xx}(0)$  as the average power in watts from (13.116). Thus if  $\mathcal{R}_{xx}(0) = R_{XX}(0)$ , then  $X(t)$  is *ergodic in the average power*.

- **EXAMPLE 13.9** Consider the random process  $X(t) = A \cos(\Omega_0 t + \Theta)$  in which amplitude  $A$  and frequency  $\Omega_0$  are constants while  $\Theta \sim U(0, 2\pi)$  is the random phase. Then its first two moments are given by

$$\mu_X(t) = E[A \cos(\Omega_0 t + \Theta)] = AE[\cos(\Omega_0 t + \Theta)] = 0 = \mu_X \quad (13.118a)$$

$$\begin{aligned} R_{XX}(t_1, t_2) &= E[A \cos(\Omega_0 t_1 + \Theta) A \cos(\Omega_0 t_2 + \Theta)] \\ &= A^2 E[\cos(\Omega_0 t_1 + \Theta) \cos(\Omega_0 t_2 + \Theta)] \\ &= \frac{1}{2} A^2 \cos(\Omega_0(t_1 - t_2)) \end{aligned} \quad (13.118b)$$

following the steps used in obtaining (13.106). Clearly,  $X(t)$  is WSS. Consider the temporal averaging in (13.116),

$$\langle x(t) \rangle \triangleq \lim_{T \rightarrow \infty} \frac{1}{2T} \int_{-T}^T A \cos(\Omega_0 t + \theta) dt = 0 = \mu_X \quad (13.119)$$

by choosing  $T = 2\pi/\Omega_0$ . Thus  $X(t)$  is ergodic in the mean. Now consider the temporal averaging in (13.117),

$$\begin{aligned} \mathcal{R}_{xx}(\tau) &= \lim_{T \rightarrow \infty} \frac{1}{2T} \int_{-T}^T A \cos(\Omega_0(t + \tau) + \theta) A \cos(\Omega_0 t + \theta) dt \\ &= A^2 \lim_{T \rightarrow \infty} \frac{1}{2T} \int_{-T}^T \frac{1}{2} (\cos(\Omega_0 \tau) + \cos(\Omega_0(2t + \tau) + \theta)) dt \\ &= \frac{1}{2} A^2 \cos(\Omega_0 \tau) = R_{XX}(\tau) \end{aligned} \quad (13.120)$$

<sup>3</sup>This equivalence requires certain conditions on the autocorrelation function  $R_{XX}(\tau)$  depending on the convergence concept used. These issues are beyond the scope of this book.

Thus  $X(t)$  is also ergodic in the autocorrelation at each  $\tau$ . In particular, it is ergodic in the average power.  $\square$

- $\square$  **EXAMPLE 13.10** Consider the random process  $X(t) = A \cos(\Omega_0 t + \Theta)$  given in Example 13.8, which is a WSS process. Its mean and autocorrelation were computed as  $\mu_X = 0$  and  $R_{XX}(\tau) = \frac{1}{4} \cos(\Omega_0 \tau)$ . This process is ergodic in the mean but not in the autocorrelation since its temporal average, for any observed value  $a$  of the random variable  $A$ , is given by

$$\begin{aligned}\mathcal{R}_{xx}(\tau) &= \lim_{T \rightarrow \infty} \frac{1}{2T} \int_{-T}^T a \cos(\Omega_0(t + \tau) + \theta) a \cos(\Omega_0 t + \theta) dt \\ &= a^2 \lim_{T \rightarrow \infty} \frac{1}{2T} \int_{-T}^T \frac{1}{2} (\cos(\Omega_0 \tau) + \cos(\Omega_0(2t + \tau) + \theta)) dt \\ &= \frac{1}{2} a^2 \cos(\Omega_0 \tau) \neq R_{XX}(\tau)\end{aligned}\quad (13.121)$$

 $\square$ 

### 13.3.3 RANDOM SEQUENCES

The results and the concepts that we have discussed so far for random signals also apply to random sequences that are discrete-time random processes. We will denote random sequences by  $X(n)$  where  $n$  is a sample index, which we assume is uniformly spaced in time. Then at each  $n$ , the value  $X(n)$  is a random variable with pdf  $f_X(x; n)$ , while the first two moments are given by

$$\mu_X(n) = E[X(n)] = \int_{-\infty}^{\infty} x f_X(x; n) dx, \quad (13.122a)$$

$$E[X^2(n)] = \int_{-\infty}^{\infty} x^2 f_X(x; n) dx, \quad (13.122b)$$

$$\sigma_X^2(n) = E[X^2(n)] - \mu_X^2(n) \quad (13.122c)$$

If two time indices,  $m$  and  $n$ , are fixed, then values  $X(m)$  and  $X(n)$  represent a pair of random variables with joint pdf  $f_X(x_1, x_2; m, n)$ . Then the autocorrelation and autocovariance sequences, respectively, are given by

$$R_{XX}(m, n) = E[X(m)X(n)] = \iint_{-\infty}^{\infty} x_1 x_2 f_X(x_1, x_2; m, n) dx_1 dx_2, \quad (13.123a)$$

$$C_{XX}(m, n) = R_{XX}(m, n) - \mu_X(m)\mu_X(n) \quad (13.123b)$$

If  $\mathbf{Y}(n)$  is another random sequence defined along with  $\mathbf{X}(m)$  with joint pdf  $f_{\mathbf{XY}}(x, y; m, n)$ , then their cross-correlation and cross-covariance sequences, respectively, are given by

$$R_{\mathbf{XY}}(m, n) = E[\mathbf{X}(m)\mathbf{Y}(n)] = \iint_{-\infty}^{\infty} xy f_{\mathbf{XY}}(x, y; m, n) dx dy, \quad (13.124a)$$

$$C_{\mathbf{XY}}(m, n) = R_{\mathbf{XY}}(m, n) - \mu_{\mathbf{X}}(m)\mu_{\mathbf{Y}}(n) \quad (13.124b)$$

A random sequence  $\mathbf{X}(n)$  is WSS if

$$E[\mathbf{X}^2(n)] = \xi_X(2) < \infty, \quad (13.125a)$$

$$\mu_{\mathbf{X}}(n) = \mu_{\mathbf{X}}, \quad (13.125b)$$

$$R_{\mathbf{XX}}(n + \ell, n) = R_{\mathbf{XX}}(\ell) \quad \text{or} \quad C_{\mathbf{XX}}(n + \ell, n) = C_{\mathbf{XX}}(\ell) \quad (13.125c)$$

where  $\ell$  is called the lag index variable. Similarly, two mutually WSS random sequences have cross-correlation and cross-covariance sequences that are functions of  $\ell$ .

Finally, for an ergodic random sequence  $\mathbf{X}(n)$ , we can compute its statistical averages using the temporal arithmetic averages from a sample waveform  $x(n)$  as

$$\mu_{\mathbf{X}} = \langle x(n) \rangle \triangleq \lim_{N \rightarrow \infty} \frac{1}{2N+1} \sum_{n=-N}^N x(n), \quad (13.126a)$$

$$R_{\mathbf{XX}}(\ell) = \langle x(n + \ell)x(n) \rangle \triangleq \lim_{N \rightarrow \infty} \frac{1}{2N+1} \sum_{n=-N}^N x(n + \ell)x(n) \quad (13.126b)$$

**MATLAB Implementation** The SP Toolbox provides the function

```
[Rxy,lags]=xcorr(x,y,maxlags,'option')
```

that estimates cross-correlation values  $R_{xy}$  at lag indices  $lags$  between two data vectors  $x$  and  $y$ . The correlation values are computed up to the  $maxlag$  index using four  $option$  cases: '`'none'`' (default), '`'biased'`', '`'unbiased'`', and '`'coeff'`', which are described below. It also computes the autocorrelation values using the invocation

```
[Rxy,lags]=xcorr(x,maxlags,'option')
```

When both  $x$  and  $y$  are zero-mean arrays, obtained by subtracting their respective means, then `xcorr` computes the covariance values.

By default, **xcorr** computes estimated correlations, with no normalization, given by

$$\hat{R}_{XY}(\ell) = \begin{cases} \sum_{n=0}^{N-\ell} x(n+\ell)y(n), & \ell \geq 0 \\ \hat{R}_{XY}(-\ell), & \ell < 0 \end{cases} \quad (13.127)$$

where  $N$  is the **maxlag** index. The elements of the output vector **Rxy** are then given by

$$R_{XY}(m) = \hat{R}_{XY}(m - N - 1), \quad m = 1, 2, \dots, 2N + 1 \quad (13.128)$$

The parameter ‘option’ has the following choices:

- ‘**biased**’: Biased estimate of the cross-correlation function given by

$$\hat{R}_{XY,\text{biased}}(\ell) = \left( \frac{1}{N} \right) \hat{R}_{XY}(\ell) \quad (13.129)$$

- ‘**unbiased**’: Unbiased estimate of the cross-correlation function given by

$$\hat{R}_{XY,\text{unbiased}}(\ell) = \left( \frac{1}{N - |\ell|} \right) \hat{R}_{XY}(\ell) \quad (13.130)$$

- ‘**coeff**’: Normalizes the sequence so the autocorrelations at zero lag are identically equal to 1.
- ‘**none**’: Uses the raw, unscaled cross-correlations (default).

- **EXAMPLE 13.11** In Section 13.6.3 and in Example 13.22, we will discuss how to generate a random process with the autocorrelation sequence of  $\rho^{|\ell|}$ . Samples of such a process are available in the MATLAB data file **x.mat**. Determine and plot the autocorrelation sequence for this process over the maximum lag of 10.

#### Solution

The following MATLAB script loads the data file, uses the **xcorr** function to compute autocorrelations, and then plots the random sequence and its autocorrelation. The resulting plots are shown in Figure 13.12. From the autocorrelation plot, we can conclude that the correlation coefficient  $\rho$  is approximately equal to 0.7.

```
>> load x; maxlag = 10;
>> [Rx,lags] = xcorr(x,maxlag,'coeff');
>> % Plotting commands follow
```

□

## 13.4 POWER SPECTRAL DENSITY

In our previous discussions in Section 13.1.2, we related average dc and ac powers in a stationary random signal to the first and second moments

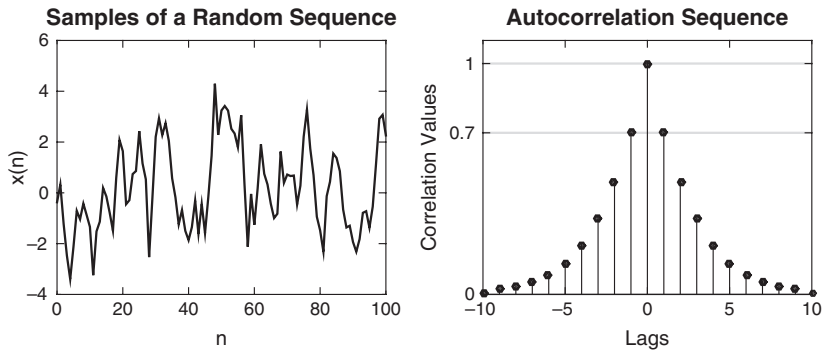


**FIGURE 13.12** Plots of the random process and its autocorrelation in Example 13.11

of a random variable at each  $t$ . We further would like to know how the average ac power is distributed along the frequency scale so that we can design appropriate frequency selective or optimal filters. As we explain in this section, this power distribution can be gleaned from the analysis of the pairs of random variables and, in particular, from the autocorrelation function. The result is a new term called *power spectral density*, or PSD.

To develop this result, we will need the use of Fourier analysis. We studied and used Fourier transforms of continuous- and discrete-time signals in previous chapters where signals were mostly deterministic and satisfied certain convergence conditions such as finite power or absolute integrability. It is difficult to establish that random signals can satisfy these conditions. To alleviate this seemingly difficult mathematical problem, we will consider a truncated version of the random signal for which the Fourier transform certainly exists for each sample waveform. Then we will take the ensemble average to remove randomness and a limiting operation in time (toward infinity) to remove truncation in order to obtain the desired result.

Let  $\mathbf{X}_T(t)$  be a finite-duration random signal derived from the WSS random process  $\mathbf{X}(t)$

$$\mathbf{X}_T(t) \triangleq \begin{cases} \mathbf{X}(t), & -T \leq t \leq T \\ 0, & \text{otherwise} \end{cases} \quad (13.131)$$

and let  $X_T(j\Omega)$  be its continuous-time Fourier transform (CTFT), which exists.<sup>4</sup> The relevant CTFT pairs are given by

$$X_T(j\Omega) = \int_{-\infty}^{\infty} \mathbf{X}_T(t) e^{-j\Omega t} dt = \int_{-T}^{T} \mathbf{X}(t) e^{-j\Omega t} dt, \quad (13.132a)$$

$$\mathbf{X}_T(t) = \frac{1}{2\pi} \int_{-\infty}^{\infty} X_T(j\Omega) e^{j\Omega t} d\Omega \quad (13.132b)$$

<sup>4</sup>Note the difference in font representation: sans-serif  $\mathbf{X}$  for random variable and roman-italic  $X$  for CTFT.

where  $\Omega$  is the analog radian frequency in rad/sec. Note that  $X_T(j\Omega)$  is a random variable. The energy in the truncated random signal  $\mathbf{X}_T(t)$  is given by

$$E_{\mathbf{X}_T} \triangleq \int_{-T}^T \mathbf{X}^2(t) dt = \int_{-\infty}^{\infty} \mathbf{X}_T^2(t) dt \quad (13.133)$$

The time-averaged power across 1 ohm resistance is then given by

$$P_{\mathbf{X}_T} = \frac{1}{2T} \int_{-\infty}^{\infty} \mathbf{X}_T^2(t) dt = \frac{1}{2T(2\pi)} \int_{-\infty}^{\infty} |X_T(j\Omega)|^2 d\Omega \quad (13.134)$$

where for the second equality we have used Parseval's theorem for CTFT. Clearly, the term  $P_{\mathbf{X}_T}$  is a random variable since it contains random quantities. Hence we will take an ensemble average to obtain the average power in the truncated random process as

$$\overline{P_{\mathbf{X}_T}} \triangleq E[P_{\mathbf{X}_T}] = \frac{1}{2T(2\pi)} \int_{-\infty}^{\infty} E[|X_T(j\Omega)|^2] d\Omega \quad (13.135)$$

Finally, we take the limit as  $T \rightarrow \infty$  to obtain the average power in the original *untruncated* random process

$$\begin{aligned} \overline{P_{\mathbf{X}}} &\triangleq \lim_{T \rightarrow \infty} \left\{ \frac{1}{2T(2\pi)} \int_{-\infty}^{\infty} E[|X_T(j\Omega)|^2] d\Omega \right\} \\ &= \frac{1}{2\pi} \int_{-\infty}^{\infty} \lim_{T \rightarrow \infty} \frac{E[|X_T(j\Omega)|^2]}{2T} d\Omega \end{aligned} \quad (13.136)$$

A close examination of the quantity inside the integral in (13.136) above reveals that it is a power density term since the left-hand side is an average power. We denote this term as

$$S_{\mathbf{XX}}(\Omega) \triangleq \lim_{T \rightarrow \infty} \frac{E[|X_T(j\Omega)|^2]}{2T} \quad (13.137)$$

and refer to it as *power spectral density* (PSD) since it is a power density as a function of frequency.

It remains to be shown that the PSD is related to the autocorrelation function through the CTFT. Toward this, consider the numerator in (13.137), which from (13.132a) can be written as

$$\begin{aligned} E[|X_T(j\Omega)|^2] &= E \left[ \int_{-T}^T \int_{-T}^T \mathbf{X}(t_1) \mathbf{X}(t_2) e^{-j\Omega(t_1-t_2)} dt_1 dt_2 \right] \\ &= \int_{-T}^T \int_{-T}^T E[\mathbf{X}(t_1) \mathbf{X}(t_2)] e^{-j\Omega(t_1-t_2)} dt_1 dt_2 \\ &= \int_{-T}^T \int_{-T}^T R_{\mathbf{XX}}(t_1 - t_2) e^{-j\Omega(t_1-t_2)} dt_1 dt_2 \end{aligned} \quad (13.138)$$

where in the last equality we have used the fact that  $X(t)$  is a WSS process. Since the integrand in (13.138) depends only on  $(t_1 - t_2)$ , we make the change of variables  $\tau = t_1 - t_2$  and  $\lambda = t_1 + t_2$  and integrate along  $\lambda$  to transform the double integral into a single integral

$$\mathbb{E} \left[ |X_T(j\Omega)|^2 \right] = \int_{-2T}^{2T} R_{XX}(\tau)(2T - |\tau|) e^{-j\Omega\tau} d\tau \quad (13.139)$$

Finally, substituting (13.139) into (13.137) and taking the limit, we obtain

$$\begin{aligned} S_{XX}(\Omega) &= \lim_{T \rightarrow \infty} \int_{-2T}^{2T} R_{XX}(\tau) \left(1 - \frac{|\tau|}{2T}\right) e^{-j\Omega\tau} d\tau \\ &= \int_{-\infty}^{\infty} R_{XX}(\tau) e^{-j\Omega\tau} d\tau \end{aligned} \quad (13.140)$$

which shows that the PSD  $S_{XX}(\Omega)$  is a CTFT of the autocorrelation function  $R_{XX}(\tau)$ . This important result is known as the *Wiener–Khinchin theorem*. The autocorrelation function can be obtained from the PSD using the inverse CTFT

$$R_{XX}(\tau) = \frac{1}{2\pi} \int_{-\infty}^{\infty} S_{XX}(\Omega) e^{j\Omega\tau} d\Omega \quad (13.141)$$

It should be noted that the total average power in the WSS random process  $X(t)$  is given by

$$\overline{P_X} = \frac{1}{2\pi} \int_{-\infty}^{\infty} S_{XX}(\Omega) d\Omega \quad (13.142)$$

which from (13.141) is equal to  $R_{XX}(0) = \mathbb{E}[X^2(t)] = \mu_X^2 + \sigma_X^2$ . This is the sum of the dc and ac powers. Although it is tempting to conclude that the dc power is equal to  $\mu_X^2$  and ac power is equal to  $\sigma_X^2$ , this is not always true unless the process is also ergodic. However, if the process has a dc power, then the PSD function will have an impulse at the origin  $\Omega = 0$  with area equal to the dc power. Likewise, if the PSD function has impulses at nonzero frequencies, then the process is known as a *harmonic process*.

### **Properties of the PSD and Autocorrelation Functions**

The PSD  $S_{XX}(\Omega)$  function possesses several important properties:

1.  $S_{XX}(\Omega)$  is a real-valued function even for complex-valued random processes.
2.  $S_{XX}(\Omega)$  is an even function for real-valued processes or conjugate even for complex-valued processes.
3.  $S_{XX}(\Omega)$  is a non-negative function.

Through the CTFT relations, the autocorrelation function  $R_{XX}(\tau)$  also possesses equivalent properties:

1.  $R_{XX}(\tau)$  is a conjugate symmetric function.
2. For real-valued random processes,  $R_{XX}(\tau)$  is real and even.
3.  $R_{XX}(\tau)$  is a non-negative definite function.

**EXAMPLE 13.12** Let  $R_{XX}(\tau) = e^{-\alpha|\tau|}$ ,  $\alpha > 0$ . Determine the PSD  $S_{XX}(\Omega)$ .

**Solution**

Using (13.140), we have

$$\begin{aligned} S_{XX}(\Omega) &= \int_{-\infty}^{\infty} e^{-\alpha|\tau|} e^{-j\Omega\tau} d\tau \\ &= \int_{-\infty}^0 e^{\alpha\tau} e^{-j\Omega\tau} d\tau + \int_0^{\infty} e^{-\alpha\tau} e^{-j\Omega\tau} d\tau \\ &= \frac{1}{\alpha - j\Omega} + \frac{1}{\alpha + j\Omega} = \frac{2\alpha}{\alpha^2 + \Omega^2} \end{aligned} \quad (13.143)$$

The autocorrelation function  $R_{XX}(\tau)$  and the PSD  $S_{XX}(\Omega)$  are plotted in Figure 13.13.

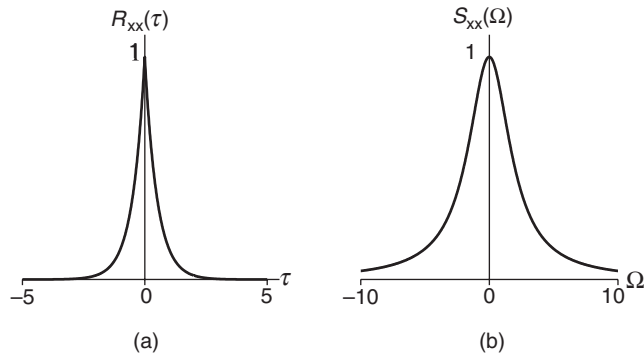


**FIGURE 13.13** Plots of (a) autocorrelation and (b) PSD in Example 13.12

#### Cross-Spectral Density Function

Analogous to the PSD (which we will also call an auto-PSD) function, we can also define the cross-spectral density (CSD) function as the Fourier transform of the cross-correlation function. Let  $X(t)$  and  $Y(t)$  be jointly WSS random signals with cross-correlation  $R_{XY}(\tau)$ . Then the CSD function is given by

$$S_{XY}(\Omega) \triangleq \int_{-\infty}^{\infty} R_{XY}(\tau) e^{-j\Omega\tau} d\tau \quad (13.144)$$

This function does not have a connotation as a power density function and, in general, is a complex-valued function. However, it is useful in analysis.

### 13.4.1 PSD OF RANDOM SEQUENCES

A similar discussion and analysis applies to random sequences. The PSD of a WSS random sequence  $X[n]$  and its autocorrelation are related by the discrete-time Fourier transform (DTFT) relations

$$S_{XX}(\omega) = \sum_{\ell=-\infty}^{\infty} R_{XX}(\ell) e^{-j\omega\ell}, \quad (13.145a)$$

$$R_{XX}(\ell) = \frac{1}{2\pi} \int_{-\pi}^{\pi} S_{XX}(\omega) e^{j\omega\ell} d\omega \quad (13.145b)$$

where  $\omega$  is the digital radian frequency in radians/sample. Note that in this case, the PSD  $S_{XX}(\omega)$  is periodic in  $\omega$  with a period of  $2\pi$ . The total average power in  $X[n]$  is then given by

$$\overline{P_X} = R_{XX}(0) = \frac{1}{2\pi} \int_{-\pi}^{\pi} S_{XX}(\omega) d\omega \quad (13.146)$$

Also note that the PSD and the autocorrelation functions of a random sequence follows similar properties given for random signals above. Finally, for jointly WSS random sequences  $X(n)$  and  $Y(n)$  with cross-correlation  $R_{XY}(\ell)$ , we define the CSD function by

$$S_{XY}(\omega) \triangleq \sum_{\ell=-\infty}^{\infty} R_{XY}(\ell) e^{-j\omega\ell} \quad (13.147)$$

- EXAMPLE 13.13** Let the autocorrelation of a random sequence  $X(n)$  be given by  $R_{XX}(\ell) = (\frac{1}{2})^{|\ell|}$  for all  $\ell$ . Determine its PSD  $S_{XX}(\omega)$ .

**Solution**

Using (13.145a), we obtain

$$\begin{aligned} S_{XX}(\omega) &= \sum_{\ell=-\infty}^{\infty} \left(\frac{1}{2}\right)^{|\ell|} e^{-j\omega\ell} = \sum_{\ell=-\infty}^{-1} \left(\frac{1}{2}\right)^{-\ell} e^{-j\omega\ell} + \sum_{\ell=0}^{\infty} \left(\frac{1}{2}\right)^{\ell} e^{-j\omega\ell} \\ &= \sum_{\ell=1}^{\infty} \left(\frac{1}{2}e^{j\omega}\right)^{\ell} + \sum_{\ell=0}^{\infty} \left(\frac{1}{2}e^{-j\omega}\right)^{\ell} = \frac{\frac{1}{2}e^{j\omega}}{1 - \frac{1}{2}e^{j\omega}} + \frac{1}{1 - \frac{1}{2}e^{-j\omega}} \\ &= \frac{3}{5 - 4\cos(\omega)} \end{aligned} \quad (13.148)$$

The plots of the autocorrelation  $R_{XX}(\ell)$  and PSD  $S_{XX}(\omega)$  are shown in Figure 13.14.

- EXAMPLE 13.14** Let the PSD of a random sequence  $X(n)$  be given by

$$S_{XX}(\omega) = \frac{16}{17 + 8\cos(\omega)}, \quad -\pi < \omega \leq \pi \quad (13.149)$$

Determine its autocorrelation sequence  $R_{XX}(\ell)$ .

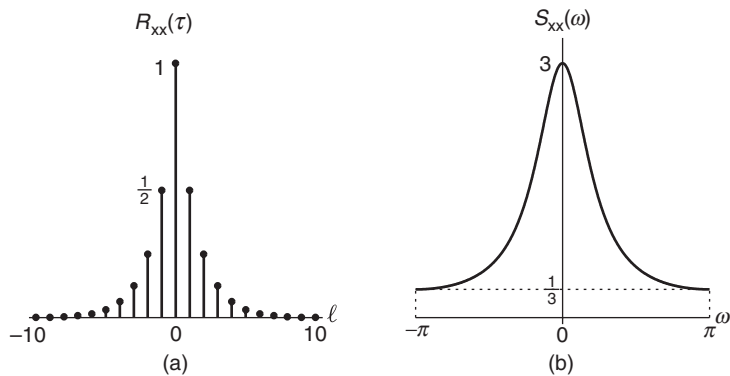


**FIGURE 13.14** Plots of (a) autocorrelation and (b) PSD in Example 13.13

### Solution

Using (13.145b), we obtain

$$R_{xx}(\ell) = \frac{1}{2\pi} \int_{-\pi}^{\pi} \frac{16}{17 + 8 \cos(\omega)} e^{j\omega\ell} d\omega \quad (13.150)$$

which is not easy to evaluate. Therefore, we will use the inverse  $z$ -transform approach by converting  $S_{xx}(\omega)$  in (13.149) into an equivalent  $z$ -domain function  $\tilde{S}_{xx}(z)$ , called the *complex PSD*. This is done by using

$$\cos(\omega) = \frac{e^{j\omega} + e^{-j\omega}}{2} = \frac{z + z^{-1}}{2} \Big|_{z=e^{j\omega}} \quad (13.151)$$

Substituting (13.151) in (13.149), we have

$$\begin{aligned} \tilde{S}_{xx}(z) &= \frac{16}{17 + 8(z + z^{-1})/2} = \frac{16z}{4z^2 + 17z + 4} \\ &= \frac{4z}{(z + \frac{1}{4})(z + 4)}, \quad \text{ROC: } \frac{1}{4} < |z| < 4 \end{aligned} \quad (13.152)$$

since the unit circle must be in the ROC. Now using partial fraction expansion followed by the use of Table 4.1 ( $z$ -transform pairs), we can obtain  $R_{xx}(\ell)$ . From (13.152),

$$\tilde{S}_{xx}(z) = \frac{4z}{(z + \frac{1}{4})(z + 4)} = \frac{16}{15} \left( \frac{z}{z + \frac{1}{4}} - \frac{z}{z + 4} \right), \quad \frac{1}{4} < |z| < 4 \quad (13.153)$$

Hence

$$\begin{aligned} R_{xx}(\ell) &= \frac{16}{15} \left( -\frac{1}{4} \right)^{\ell} u(\ell) + \frac{16}{15} (-4)^{\ell} u[-\ell - 1] \\ &= \frac{16}{15} \left( -\frac{1}{4} \right)^{|\ell|}, \quad \text{for all } \ell \end{aligned} \quad (13.154)$$

The plots of the PSD  $s_x(\omega)$  and autocorrelation  $R_{xx}(\ell)$  are shown in Figure 13.15.  $\square$

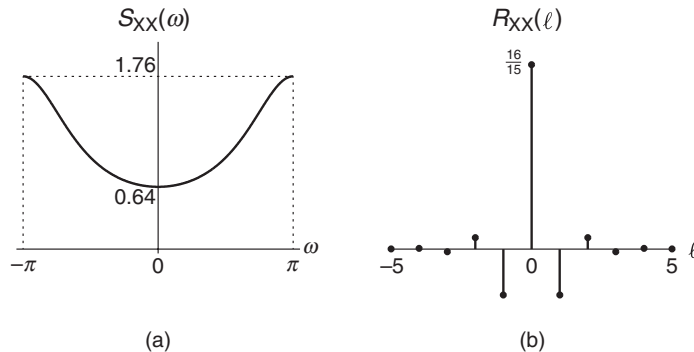


**FIGURE 13.15** Plots of (a) PSD and (b) autocorrelation in Example 13.14

**MATLAB Implementation** The SP Toolbox provides several functions, such as `pwelch` and `cpsd`, to estimate PSD and CSD functions, respectively, from data vectors. These functions use techniques from spectral estimation theory, a topic that is beyond the scope of this book. Since we have used the `xcorr` function to estimate autocorrelation lag values, we will compute the FFT of a large number of suitably zero-padded autocorrelations as a preferred implementation of the PSD estimate.

Since the autocorrelation values being transformed are still finite in number (and not infinite as the theory requires), this computation amounts to windowing the original autocorrelation sequence by a rectangular window. This may result in some of the computed PSD values becoming negative, which violates one of the PSD properties. Therefore, we will use a window function whose DTFT is always non-negative. Such windows are known as *lag* windows, and one such window is the Bartlett (or triangular) window. It should be noted that there are other choices available in literature for lag-windows. One side-effect of using nonrectangular window is some loss of resolution in the spectral estimates. However, this loss can be mitigated by using a large number of autocorrelation lags. The following PSD function incorporates the above discussed approach.

```

function [Sx,omega] = PSD(Rx,maxlag,Nfft)
%PSD Computation of PSD using Autocorrelation Lags
% [Sx,omega] = PSD(Rx,lags,Nfft)
% Sx: Computed PSD values
% omega: digital frequency array in pi units from -1 to 1
% Rx: autocorrelations from -maxlag to +maxlag
% maxlag: maximum lag index (must be >= 10)
% Nfft: FFT size (must be >= 512)
Nfft2 = Nfft/2;
M = 2*maxlag+1; % Bartlett window length

```

```

Rx = bartlett(M).*Rx(:); % Windowed autocorrelations
Rxxp = [zeros(Nfft2-maxlag,1);Rx;zeros(Nfft2-maxlag-1,1)];
Rxxp = ifftshift(Rxxp); %Zero-padding and circular shifting
Sx = fftshift(real(fft(Rxxp))); % PSD
Sx = [Sx;Sx(1)]; % Circular shifting
omega = linspace(-1,1,Nfft+1); % Frequencies in units of pi
end

```

- EXAMPLE 13.15** In Example 13.11 we computed autocorrelation sequence  $R_{XX}(\ell)$ ,  $-10 \leq \ell \leq 10$ , of a random sequence from its observed values. Compute its PSD numerically.

**Solution**

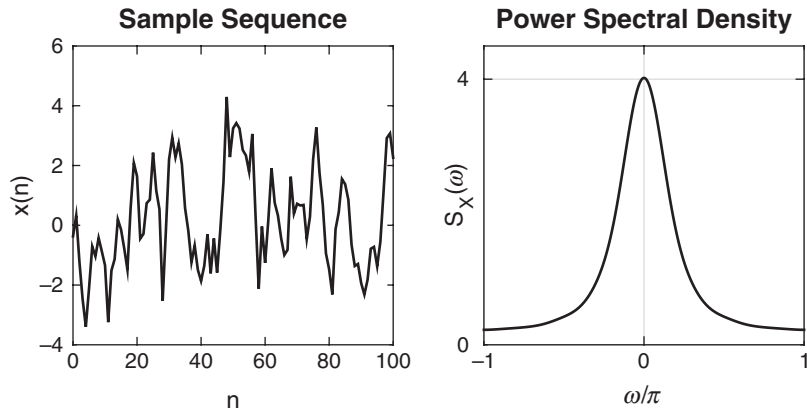
We will demonstrate the use of the PSD function in the following MATLAB script.

```

>> load x; maxlag = 10; %Load random sequence data
>> [Rx,lags] = xcorr(x,maxlag,'coeff'); % Compute ACRS
>> [Sx,omega] = PSD(Rx,maxlag,512); % Compute PSD
>> % Plotting commands follow

```

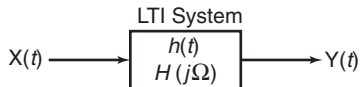
The resulting plots are shown in Figure 13.16.



**FIGURE 13.16** Plots of a sample sequence and its PSD in Example 13.15

## 13.5 STATIONARY RANDOM PROCESSES THROUGH LTI SYSTEMS

One of the important aspects of signal processing is the filtering of signals through linear systems. In previous chapters, we studied how to filter deterministic signals through linear and time-invariant (LTI) systems to

**FIGURE 13.17** Filtering of random process

obtain the output response in both the time domain and the frequency domain. Now we want to consider filtering of stationary random processes. What do we mean exactly by this filtering?

To obtain this meaning, we appeal to the ensemble description of the random process, which is that it is a collection of sample waveforms. When each input sample waveform is processed through the system, it produces a filtered sample function. Thus at the output, we also have an ensemble of sample waveforms or an output random process. The individual sample waveform filtering aspect is well understood and can be implemented with filter structures from Chapter 6. What we really are interested in is how do we characterize the output random process in terms of its second-order statistical averages. This is the meaning that we seek. A complete description of the output process in terms of its joint densities is difficult to obtain even for simple systems.

Let the input random signal be a WSS process  $X(t)$  with a known mean  $\mu_X$  and an autocorrelation function  $R_{XX}(\tau)$ . It is applied as an input to a LTI system with impulse response  $h(t)$  or frequency response function  $H(j\Omega)$ . Let the output process be  $Y(t)$ . This system set up is shown in Figure 13.17. The output process, symbolically, is given by the convolution integral

$$Y(t) = X(t) * h(t) = \int_{\lambda=-\infty}^{\infty} X(\lambda)h(t-\lambda) d\lambda \quad (13.155)$$

while the frequency response function  $H(j\Omega)$  is given by

$$H(j\Omega) = \int_{-\infty}^{\infty} h(t)e^{-j\Omega t} dt \quad (13.156)$$

We want to determine the mean and autocorrelation function of the output process  $Y(t)$  as well as the cross-correlation between the output and input processes and also want to examine if  $Y(t)$  is a stationary process.

**Computation of Output Mean Function** The mean of  $Y(t)$  from (13.155) is given by

$$\begin{aligned} \mu_Y(t) &= E[Y(t)] = \int_{\lambda=-\infty}^{\infty} E[X(\lambda)]h(t-\lambda) d\lambda \\ &= \int_{\lambda=-\infty}^{\infty} \mu_X h(t-\lambda) d\lambda = \left( \int_{\lambda=-\infty}^{\infty} h(\lambda) d\lambda \right) \mu_X \end{aligned} \quad (13.157)$$

Note that the integral in the parenthesis is a constant, which from (13.156) is equal to  $H(j0)$ , or the dc-gain value. Hence the output mean is given by

$$\mu_Y(t) = \left( \int_{\lambda=-\infty}^{\infty} h(\lambda) d\lambda \right) \mu_X = H(j0)\mu_X = \mu_Y \quad (13.158)$$

which also is a constant. Thus the output mean is the input mean scaled by the dc-gain of the LTI system, which makes sense.

**Computation of Cross-Correlation and CSD Functions** Consider the cross-correlation between the output  $Y(t + \tau)$  and  $X(t)$ . Using (13.155), we obtain

$$\begin{aligned} R_{YX}(t + \tau, t) &= E[Y(t + \tau)X(t)] = E \left[ \int_{\lambda=-\infty}^{\infty} h(\lambda)X(t + \tau - \lambda)X(t) d\lambda \right] \\ &= \int_{t_1=-\infty}^{\infty} h(\lambda)E[X(t + \tau - \lambda)X(t)] d\lambda \\ &= \int_{t_1=-\infty}^{\infty} h(\lambda)R_{XX}(\tau - \lambda) d\lambda \end{aligned} \quad (13.159)$$

where in the last equality we have used the stationarity of  $X(t)$ . The integral in (13.159) can be identified as a convolution between  $h(\tau)$  and  $R_{XX}(\tau)$ , that is,

$$R_{YX}(t + \tau, t) = h(\tau) * R_{XX}(\tau) = R_{YX}(\tau) \quad (13.160)$$

Thus the cross-correlation function is time invariant. After taking Fourier transform of (13.160), the CSD function between the output and the input is given by

$$S_{YX}(\Omega) = H(j\Omega)S_{XX}(\Omega) \quad (13.161)$$

In a similar fashion, we can compute the cross-correlation and CSD between the *input* and the *output*. The results are

$$R_{XY}(\tau) = h(-\tau) * R_{XX}(\tau) \quad (13.162a)$$

$$S_{XY}(\Omega) = H^*(j\Omega)S_{XX}(\Omega) \quad (13.162b)$$

### **Computation of the Output Autocorrelation and PSD Functions**

Now consider the autocorrelation function of the output  $Y(t)$ . Again using (13.155), we obtain

$$\begin{aligned} R_{YY}(t + \tau, t) &= E[Y(t + \tau)Y(t)] = E\left[\int_{\lambda=-\infty}^{\infty} Y(t + \tau)h(\lambda)X(t - \lambda) d\lambda\right] \\ &= \int_{\lambda=-\infty}^{\infty} h(\lambda)E[Y(t + \tau)X(t - \lambda)] d\lambda \\ &= \int_{\lambda=-\infty}^{\infty} h(\lambda)R_{YX}(\tau + \lambda) d\lambda = \int_{\lambda=-\infty}^{\infty} h(-\lambda)R_{YX}(\tau - \lambda) d\lambda \end{aligned} \quad (13.163)$$

where we have used the fact that the cross-correlation  $R_{YX}(\tau)$  is time invariant. The integral in (13.163) can be identified as a convolution between  $h(-\tau)$  and  $R_{YX}(\tau)$ , that is,

$$R_{YY}(t + \tau, t) = h(-\tau) * R_{YX}(\tau) = R_{YY}(\tau) \quad (13.164)$$

Clearly, the autocorrelation  $R_{YY}(\tau)$  is also time invariant. Substituting  $R_{YX}(\tau)$  from (13.160) in (13.164), we obtain

$$R_{YY}(\tau) = h(\tau) * h(-\tau) * R_{XX}(\tau) \quad (13.165)$$

After taking Fourier transform of (13.165), the output PSD is given by

$$S_{YY}(\Omega) = |H(j\Omega)|^2 S_{XX}(\Omega) \quad (13.166)$$

which is also a real and non-negative function, thus emphasizing that it is a valid PSD function.

The first convolution term in (13.165) is unique to the LTI system and can be pre-computed. It is referred to as the *system autocorrelation function* and is denoted by

$$R_h(\tau) \triangleq h(\tau) * h(-\tau) \quad (13.167)$$

which implies

$$R_{YY}(\tau) = R_h(\tau) * R_{XX}(\tau) \quad (13.168)$$

The Fourier transform of  $R_h(\tau)$  is referred to as the *system power-spectral function* and is denoted by

$$S_H(\Omega) = |H(j\Omega)|^2 \quad (13.169)$$

which implies

$$S_{YY}(\Omega) = S_H(\Omega)S_{XX}(\Omega) \quad (13.170)$$

Starting with the cross-correlation function  $R_{XY}(\tau)$ , we can obtain the same result given in (13.165). The corresponding expressions are

$$R_{YY}(\tau) = h(\tau) * R_{XY}(\tau) = h(\tau) * h(-\tau) * R_{XX}(\tau) \quad (13.171a)$$

$$S_{YY}(\Omega) = H(j\Omega)S_{XY}(\Omega) = |H(j\Omega)|^2 S_{XX}(\Omega) \quad (13.171b)$$

In conclusion, since the mean  $\mu_Y$  is a constant and the autocorrelation  $R_{YY}(\tau)$  is time invariant, the output process  $Y(t)$  is also a WSS process. *Thus the LTI filtering of a WSS process will always result in a WSS process.*

- **EXAMPLE 13.16** A WSS random process  $X(t)$  with mean  $\mu_X = 2$  and autocovariance  $C_{XX}(\tau) = 4\delta(\tau)$  is applied as an input to a stable LTI system with impulse response

$$h(t) = e^{-t}u(t) \quad (13.172)$$

The output of this system is the random process  $Y(t)$ . Determine the following quantities.

1. The mean  $\mu_Y$ .

**Solution**

Using (13.158), the mean of  $Y(t)$  is given by

$$\mu_Y = \mu_X \int_{-\infty}^{\infty} h(t) dt = 2 \int_0^{\infty} e^{-t} dt = 2 \quad (13.173)$$

2. The cross-correlation  $R_{XY}(\tau)$  and the cross-covariance  $C_{XY}(\tau)$ .

**Solution**

The autocorrelation of  $X(t)$  is given by

$$R_{XX}(\tau) = \mu_X^2 + C_{XX}(\tau) = 4 + 4\delta(\tau) \quad (13.174)$$

Now using (13.162a), we have

$$\begin{aligned} R_{XY}(\tau) &= h(-\tau) * R_{XX}(\tau) = e^{\tau}u(-\tau) * [4 + 4\delta(\tau)] \\ &= 4 \int_{-\infty}^0 e^{\tau} d\tau + 4e^{\tau}u(-\tau) = 4 + 4e^{\tau}u(-\tau) \end{aligned} \quad (13.175)$$

Since  $R_{XY}(\tau) = \mu_X\mu_Y + C_{XY}(\tau)$ , the cross-covariance,  $C_{XY}(\tau)$ , from (13.175) is given by

$$C_{XY}(\tau) = 4e^{\tau}u(-\tau) \quad (13.176)$$

3. The autocorrelation  $R_{XX}(\tau)$  and the autocovariance  $C_{XX}(\tau)$ .

**Solution**

From (13.167), the system autocorrelation function is given by

$$\begin{aligned} R_h(\tau) &= h(\tau) * h(-\tau) = [e^{-\tau}u(\tau)] * [e^{\tau}u(-\tau)] \\ &= \begin{cases} \int_{-\infty}^{\tau} e^{\lambda}e^{-(\tau-\lambda)} d\lambda, & \tau < 0, \\ \int_{-\infty}^0 e^{\lambda}e^{-(\tau-\lambda)} d\lambda, & \tau \geq 0, \end{cases} = \begin{cases} \frac{1}{2}e^{\tau}, & \tau < 0, \\ \frac{1}{2}e^{-\tau}, & \tau \geq 0, \end{cases} = \frac{1}{2}e^{-|\tau|} \end{aligned} \quad (13.177)$$

Now from (13.168), (13.174), and (13.177), the output autocorrelation is given by

$$\begin{aligned} R_{YY}(\tau) &= R_h(\tau) * R_{XX}(\tau) = \frac{1}{2} e^{-|\tau|} * [4 + 4\delta(\tau)] \\ &= 2 \int_{-\infty}^{\infty} e^{|\tau|} d\tau + 2e^{-|\tau|} = 4 + 2e^{-|\tau|} \end{aligned} \quad (13.178)$$

Since  $\mu_Y = 2$ , the autocovariance  $C_{YY}(\tau)$  is given by

$$C_{YY}(\tau) = R_{YY}(\tau) - \mu_Y^2 = 2e^{-|\tau|} \quad (13.179)$$

From these calculations, note that cross quantities undergo operations identical to those for the auto quantities.  $\square$

- EXAMPLE 13.17** Repeat Example 13.16 using the frequency domain approach by computing the PSD and CSD quantities.

### Solution

The frequency response function is given by

$$H(j\Omega) = \mathcal{F}[e^{-t}u(t)] = \frac{1}{1+j\Omega} \quad (13.180)$$

From (13.158), the mean  $\mu_Y$  is

$$\mu_Y = \mu_X H(j0) = 2(1) = 2 \quad (13.181)$$

From (13.174), the input PSD is

$$S_{XX}(\Omega) = \mathcal{F}[4 + 4\delta(\tau)] = 8\pi\delta(\Omega) + 4 \quad (13.182)$$

Now from (13.162b), the CSD between  $X(t)$  and  $Y(t)$  is given by

$$\begin{aligned} S_{XY}(\Omega) &= H^*(j\Omega)S_{XX}(\Omega) = \frac{8\pi\delta(\Omega) + 4}{1 - j\Omega} \\ &= 8\pi\delta(\Omega) + \frac{4}{1 - j\Omega} \end{aligned} \quad (13.183)$$

Hence, after inverse Fourier transformation, we obtain

$$R_{XY}(\tau) = 4 + 4e^{\tau}u(-\tau) \quad (13.184)$$

as before in (13.175). From (13.169) and (13.170), the PSD  $S_{YY}(\Omega)$  is given by

$$\begin{aligned} S_{YY}(\Omega) &= |H(j\Omega)|^2 S_{XX}(\Omega) = \frac{8\pi\delta(\Omega) + 4}{1 + \Omega^2} \\ &= 8\pi\delta(\Omega) + \frac{4}{1 + \Omega^2} \end{aligned} \quad (13.185)$$

In Example 13.12 and in (13.143), we obtained the Fourier transform pair

$$e^{-a|\tau|}, \quad a > 0 \quad \xleftrightarrow{\mathcal{F}} \quad \frac{2a}{a^2 + \Omega^2} \quad (13.186)$$

Using  $a = 1$  in (13.186), we obtain the inverse Fourier transform of the second term in (13.186). Hence

$$R_{YY}(\tau) = 4 + 2e^{-|\tau|} \quad (13.187)$$

as before in (13.178).  $\square$

### 13.5.1 DISCRETE-TIME LTI SYSTEMS

Similar results apply to the discrete-time LTI systems driven by WSS random sequences. Let  $h(n)$  be the impulse response of the system, and let  $H(e^{j\omega})$  be the frequency response function, that is,

$$H(e^{j\omega}) = \sum_{n=-\infty}^{\infty} h(n)e^{-jn\omega} \quad (13.188)$$

Let  $X(n)$  be the input WSS process with mean  $\mu_X$ , autocorrelation sequence  $R_{XX}(\ell)$ , and auto PSD  $S_{XX}(\omega)$ . Let  $Y(n)$  be the resulting output process. Then  $Y(n)$  is also WSS with the following statistical quantities.

Output Mean

$$\mu_Y = \left( \sum_{n=-\infty}^{\infty} h(n) \right) \mu_X = \underbrace{H(e^{j0})}_{\text{dc-gain}} \mu_X \quad (13.189)$$

Cross-correlations between input and output

$$R_{YX}(\ell) = h(\ell) * R_{XX}(\ell), \quad (13.190a)$$

$$R_{XY}(\ell) = h(-\ell) * R_{XX}(\ell) \quad (13.190b)$$

CSD functions between input and output

$$S_{YX}(\omega) = H(e^{j\omega}) S_{XX}(\omega) \quad (13.191a)$$

$$S_{XY}(\omega) = H(e^{-j\omega}) S_{XX}(\omega) \quad (13.191b)$$

Autocorrelations between input and output

$$R_{YY}(\ell) = h(-\ell) * R_{YX}(\ell) = h(\ell) * R_{XY}(\ell) \quad (13.192a)$$

$$= \underbrace{h(\ell) * h(-\ell)}_{\triangleq R_h(\ell)} * R_{XX}(\ell) = R_h(\ell) * R_{XX}(\ell) \quad (13.192b)$$

$$\triangleq R_h(\ell)$$

Auto PSD functions between input and output

$$S_{YY}(\omega) = H(e^{-j\omega})S_{YX}(\omega) = H(e^{j\omega})S_{XY}(\omega) \quad (13.193a)$$

$$= \underbrace{|H(e^{j\omega})|^2}_{\triangleq S_H(\omega)} S_{XX}(\omega) = S_H(\omega)S_{XX}(\omega) \quad (13.193b)$$

Average power in the output

$$E\{X^2(n)\} = R_{XX}[0] = \frac{1}{2\pi} \int_{-\pi}^{\pi} S_{XX}(\omega) d\omega \quad (13.194)$$

- EXAMPLE 13.18** Let  $X(n)$  be a WSS random sequence with mean and autocovariance sequence given by

$$\mu_X = 1 \quad \text{and} \quad C_{XX}(\ell) = \begin{cases} 1, 2, 3, 2, 1 \\ \uparrow \end{cases} \quad (13.195)$$

It is applied as an input to a stable LTI system given by the impulse response

$$h(n) = \begin{cases} 1, 1, 1, 1 \\ \uparrow \end{cases} \quad (13.196)$$

Determine the following quantities.

1. The mean  $\mu_Y$ .

**Solution**

From (13.189), we obtain

$$\mu_Y = \left( \sum_{\ell=-\infty}^{\infty} h(\ell) \right) \mu_X = (1 + 1 + 1 + 1)(1) = 4 \quad (13.197)$$

2. The cross-covariance  $C_{YX}(\ell)$  and cross-correlation  $R_{Y,X}(\ell)$ .

**Solution**

The cross-covariance sequences follow operations similar to those in (13.190). Thus  $C_{YX}(\ell)$  is given by

$$\begin{aligned} C_{YX}(\ell) &= h(\ell) * C_{XX}(\ell) = \begin{cases} 1, 1, 1, 1 \\ \uparrow \end{cases} * \begin{cases} 1, 2, 3, 2, 1 \\ \uparrow \end{cases} \\ &= \begin{cases} 1, 3, 6, 8, 8, 6, 3, 1 \\ \uparrow \end{cases} \end{aligned} \quad (13.198)$$

which is computed using MATLAB as shown in the following script.

```

>> h = [1,1,1,1]; nh = [0:3];
>> Cx = [1,2,3,2,1]; lCx = [-2:2];
>> [Cyx,lCyx] = conv_m(Cx,lCx,h,nh)
Cyx =
    1      3      6      8      8      6      3      1
lCyx =
   -2     -1      0      1      2      3      4      5

```

The cross-correlation  $R_{YX}(\ell)$  is then given by

$$\begin{aligned}
R_{YX}(\ell) &= C_{YX}(\ell) + \mu_Y \mu_X = \{1, 3, 6, \underset{\uparrow}{8}, 8, 6, 3, 1\} + 4 \\
&= \{\dots, 4, 4, 5, 7, \underset{\uparrow}{10}, 12, 12, 10, 7, 5, 4, 4 \dots\}
\end{aligned} \tag{13.199}$$

3. The autocovariance  $C_{YY}(\ell)$  and autocorrelation  $R_{YY}(\ell)$ .

### Solution

The autocovariance sequences also follow operations similar to those in (13.192). Thus  $C_{YY}(\ell)$  is given by

$$\begin{aligned}
C_{YY}(\ell) &= h(-\ell) * C_{YX}(\ell) = \{1, 1, 1, \underset{\uparrow}{1}\} * \{1, 3, 6, \underset{\uparrow}{8}, 8, 6, 3, 1\} \\
&= \{1, 4, 10, 18, 25, \underset{\uparrow}{28}, 25, 18, 10, 4, 1\}
\end{aligned} \tag{13.200}$$

which is also computed using MATLAB as shown below.

```

>> [Cy,lCy] = conv_m(Cyx,lCyx,h,-fliplr(nh))
Cy =
    1      4     10     18     25     28     25     18     10      4      1
lCy =
   -5     -4     -3     -2     -1      0      1      2      3      4      5

```

Finally, the autocorrelation  $R_{YY}(\ell)$  is given by

$$\begin{aligned}
R_{YY}(\ell) &= C_{YY}(\ell) + \mu_Y^2 = \{1, 4, 10, 18, 25, \underset{\uparrow}{28}, 25, 18, 10, 4, 1\} + 16 \\
&= \{\dots, 16, 16, 17, 20, 26, 34, \underset{\uparrow}{41}, 44, 41, 34, 26, 20, 17, 16, 16 \dots\}
\end{aligned} \tag{13.201}$$

□

- **EXAMPLE 13.19** A zero-mean stationary random process with PSD  $S_{XX}(\omega) = 1$  is passed through a linear filter with impulse response

$$h(n) = \begin{cases} (0.95)^n, & n \geq 0 \\ 0, & n < 0 \end{cases} \tag{13.202}$$

Determine the PSD  $S_{YY}(\omega)$  and the autocorrelation  $R_{YY}(\ell)$  of the output process  $Y(n)$ .

**Solution**

It is easily seen that

$$\begin{aligned} H(e^{j\omega}) &= \sum_{n=0}^{\infty} h(n)e^{-jn\omega} = \sum_{n=0}^{\infty} (0.95e^{-j\omega})^n \\ &= \frac{1}{1 - 0.95e^{-j\omega}} \end{aligned} \quad (13.203)$$

from which we obtain

$$|H(e^{j\omega})|^2 = \frac{1}{|1 - 0.95e^{-j\omega}|^2} = \frac{1}{1.9025 - 1.9 \cos(\omega)} \quad (13.204)$$

Therefore, the PSD of the output is

$$S_{YY}(\omega) = |H(e^{j\omega})|^2 S_{XX}(\omega) = \frac{1}{1.9025 - 1.9 \cos(\omega)} \quad (13.205)$$

Note that  $S_{YY}(\omega)$  is periodic with period  $2\pi$ . We can determine the autocorrelation  $R_{YY}(\ell)$  using the inverse  $z$ -transform approach of Example 13.14. However, in this example, we will use MATLAB to numerically compute samples of  $R_{YY}(\ell)$ . This computation is similar to the one used in the PSD function to compute  $S_{XX}(\omega)$  from samples of  $R_{XX}(\ell)$  except for the windowing. Details are given in the following MATLAB script.

```
>> N = 1024; omega = linspace(-1,1,N+1)*pi; % Frequency samples
>> Sy = 1./(.9025-1.9*cos(omega));
>> % Autocorrelation sequence
>> Sy = fftshift(Sy(1:end-1)); % Circular shift; origin at the beginning
>> Ry = real(ifft(Sy)); % Autocorrelation samples
>> Ry = ifftshift(Ry); % Circular shift; origin at the center
>> Ry = [Ry,Ry(1)]; % Sample symmetry for plotting
>> Rymax = max(Ry); % Ry[0] value
>> fprintf(' Ry[0] = %7.4f\n',Rymax);
Ry[0] = 10.2564
>> Ry = Ry/Rymax; % Normalized autocorrelation
>> fprintf(' rho = %4.2f\n',Ry(N/2));
rho = 0.95
```

From the resulting printout, note that the maximum autocorrelation is  $R_{YY}(0) = 10.2564$  while the normalized autocorrelation at lag  $\ell = \pm 1$  is equal to 0.95. Since  $10.2564 = 1/(1 - 0.95^2)$ , we infer that the autocorrelation sequence is

$$R_{YY}(\ell) = \frac{\rho^{|\ell|}}{1 - \rho^2}, \quad \rho = 0.95 \quad (13.206)$$

Figure 13.18 shows plots of the PSD  $S_{YY}(\omega)$  and the first  $\pm 10$  lag values of the autocorrelation  $R_{YY}(\ell)$ , which confirms our inference in (13.206).  $\square$

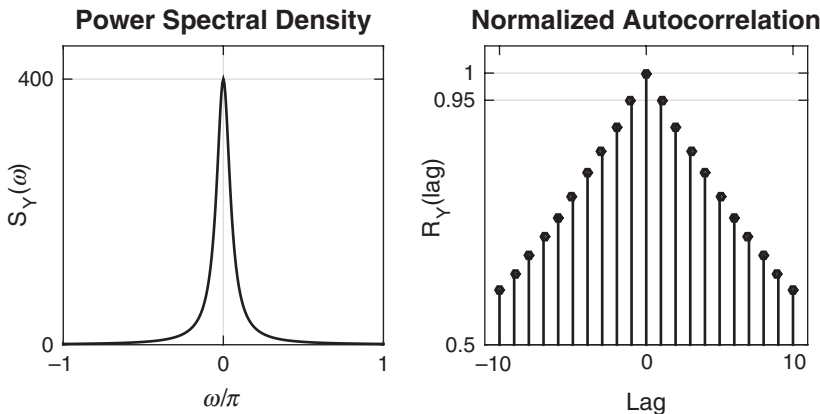


**FIGURE 13.18** Plots of the PSD and first 10 lag samples of the normalized  $R_{YY}(\ell)$  in Example 13.19

## 13.6 USEFUL RANDOM PROCESSES

---

After studying random processes through their statistical and spectral descriptions as well as analyzing their input-output behavior through LTI systems, we now consider a few representative and useful random process models that will be needed in Chapters 14 and 15. One important model is that of the Gaussian random process which needs only second-order statistical averages to describe it completely. Another important model is that of the idealized noise signal called the *white noise* process. The term noise is generally used to describe unwanted signals that tend to disturb and distort the transmission and processing of signals—for example, in communication systems—and over which we have limited control. Using white noise process and appropriately designed LTI systems we can generate other types of random processes such as Markov processes, lowpass and bandpass processes, and so on. We will also consider a few discrete-time processes.

### 13.6.1 GAUSSIAN PROCESS

Gaussian processes play an important role in many applications, in particular, in communication systems. We have discussed useful properties of the Gaussian distribution in Section 13.2.3. These properties make Gaussian processes mathematically tractable and easy to deal with. Another crucial reason why Gaussian distribution is necessary can be found in the ever-present thermal noise that is produced by the random movement of agitated electrons in electrical devices.

To understand this Gaussian behavior, consider a resistor. The free electrons in a resistor move as a result of thermal agitation. This movement is random and can be in any direction. However, their velocity is proportional to the ambient temperature; the higher the temperature, the higher the velocity. This movement generates a current with a random value. We can model each electron as a tiny current source whose current is a random variable with positive or negative values. The total current generated (which is the thermal noise) is the sum of all these current sources. Quantum mechanics suggests that the electron movements (i.e., current sources) are statistically independent. Thus the thermal noise is a sum of a large number of IID random sources. Using the central limit theorem, we conclude that this total current has a Gaussian distribution.

A random process  $\mathbf{X}(t)$  is a Gaussian process if for all  $n$  and all time instances  $(t_1, t_2, \dots, t_n)$ , the  $n$  random variables  $\{\mathbf{X}(t_i)\}_{i=1}^n$  are jointly Gaussian with pdf given by

$$f_{\mathbf{X}}(\mathbf{x}) = \frac{1}{(2\pi)^{n/2} [\det(\mathbf{C}_{\mathbf{X}})]^{1/2}} \exp \left[ -\frac{1}{2} (\mathbf{x} - \boldsymbol{\mu}_{\mathbf{X}})^T \mathbf{C}_{\mathbf{XX}}^{-1} (\mathbf{x} - \boldsymbol{\mu}_{\mathbf{X}}) \right] \quad (13.207)$$

where the vector  $\mathbf{x} = [x_1, \dots, x_n]^T$  denotes the values taken by the  $n$  random variables  $\mathbf{X}(t_i) \stackrel{\triangle}{=} \mathbf{X}_i$ ,  $\boldsymbol{\mu}_{\mathbf{X}}$  denotes the mean vector containing the means,  $E[\mathbf{X}_i] = \mu_i \stackrel{\triangle}{=} \boldsymbol{\mu}_{\mathbf{X}}(t_i)$ , of the random variables  $\mathbf{X}_i$ , and  $\mathbf{C}_{\mathbf{XX}}$  denotes the autocovariance matrix of the  $n$  random variables with elements

$$C_{\mathbf{XX}}(t_k, t_\ell) = E[(\mathbf{X}_k - \mu_k)(\mathbf{X}_\ell - \mu_\ell)] \quad (13.208)$$

The superscript  $T$  denotes the transpose of a vector or a matrix, and the term  $\mathbf{C}^{-1}$  denotes the inverse of matrix  $\mathbf{C}$ .

From the above definition of the Gaussian random process, it should be obvious that at any  $t$ ,  $\mathbf{X}(t)$  is Gaussian with mean  $\boldsymbol{\mu}_{\mathbf{X}}(t)$  and variance  $C_{\mathbf{XX}}(t, t)$ . Similarly, if  $t_1 \neq t_2$  are two time instances, then  $\mathbf{X}(t_1)$  and  $\mathbf{X}(t_2)$  are jointly Gaussian with means  $\boldsymbol{\mu}_{\mathbf{X}}(t_1)$  and  $\boldsymbol{\mu}_{\mathbf{X}}(t_2)$ , variances  $C_{\mathbf{XX}}(t_1, t_1)$  and  $C_{\mathbf{XX}}(t_2, t_2)$ , and correlation coefficient  $\rho_{\mathbf{X}}(t_1, t_2) = C_{\mathbf{XX}}(t_1, t_2)/\sqrt{C_{\mathbf{XX}}(t_1, t_1)C_{\mathbf{XX}}(t_2, t_2)}$ , and so on. Thus the Gaussian random process is completely described in the probabilistic sense. Furthermore, if it is a stationary random process, then  $\boldsymbol{\mu}_{\mathbf{X}}(t) = \boldsymbol{\mu}_{\mathbf{X}}$  and  $C_{\mathbf{XX}}(t + \tau, t) = C_{\mathbf{XX}}(\tau)$ .

Finally, since Gaussianity is preserved under linear transformation, if a Gaussian process  $\mathbf{X}(t)$  is passed through a LTI system, the output is also a Gaussian process. The effect of the system operation is simply to change the mean function  $\boldsymbol{\mu}_{\mathbf{X}}(t) \rightarrow \boldsymbol{\mu}_{\mathbf{Y}}(t)$  and the covariance function  $C_{\mathbf{XX}}(t_1, t_2) \rightarrow C_{\mathbf{YY}}(t_1, t_2)$ .

- EXAMPLE 13.20** Let  $X(t)$  be a Gaussian random process with mean  $\mu_X(t) = 3$  and autocovariance  $C_{XX}(t_1, t_2) = 4e^{-0.2|t_1-t_2|}$ .

1. Determine the probability that  $X(5) \leq 2$ .

**Solution**

Note that  $X(t)$  is a stationary random process with mean  $\mu_X = 3$  and variance  $\sigma_X^2 = C_{XX}(t, t) = 4$ . Thus from (13.21) and (13.22), we obtain

$$\begin{aligned}\Pr[X(5) \leq 2] &= F_{X(5)}(2) = \frac{1}{2} \left[ 1 + \operatorname{erf} \left( \frac{2-3}{\sqrt{2(4)}} \right) \right] \\ &= \frac{1}{2} \left[ 1 + \operatorname{erf} \left( \frac{-1}{2\sqrt{2}} \right) \right] = 0.3085\end{aligned}\quad (13.209)$$

which is computed using the MATLAB fragment

```
>> Pr = 0.5*(1+erf(-1/sqrt(2*4)));
>> fprintf('Pr[X(5)<=2] = %6.4f\n',Pr);
Pr[X(5)<=2] = 0.3085
```

2. Determine the probability that  $|X(8) - X(5)| \leq 1$ .

**Solution**

Let  $Y = X(8) - X(5)$  be a random variable. Then  $Y$  is Gaussian with mean 0 and variance

$$\begin{aligned}\sigma_Y^2 &= C_{XX}(8, 8) + C_{XX}(5, 5) - 2C_{XX}(5, 5) = 4 + 4 - 8e^{-0.6} \\ &= 3.608\end{aligned}\quad (13.210)$$

Hence

$$\begin{aligned}\Pr[|X(8) - X(5)| \leq 1] &= \Pr[|Y| \leq 1] = F_Y(1) - F_Y(-1) \\ &= \frac{1}{2} \left[ 1 + \operatorname{erf} \left( \frac{1}{\sqrt{2 \cdot 3.608}} \right) \right] - \frac{1}{2} \left[ 1 + \operatorname{erf} \left( \frac{-1}{\sqrt{2 \cdot 3.608}} \right) \right] \\ &= 0.4014\end{aligned}\quad (13.211)$$

which is also computed using MATLAB as shown below.

```
>> Pr = 0.5*(1+erf(1/sqrt(2*3.608))) ...
- 0.5*(1+erf(-1/sqrt(2*3.608)));
>> fprintf('Pr[|X(8)-X(5)|<=1] = %6.4f\n\n',Pr);
Pr[|X(8)-X(5)|<=1] = 0.4014
```

□

### 13.6.2 WHITE NOISE PROCESS

This is an idealization of the thermal noise generated in electronic devices that helps in analysis immensely. Recall the discussion leading up to the Gaussian process in the previous section. Using quantum mechanical

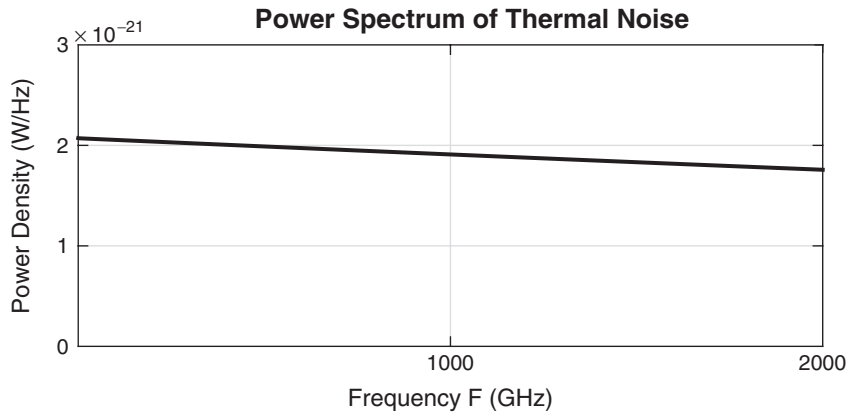


**FIGURE 13.19** Power spectrum of thermal noise at room temperature,  $T = 300 \text{ K}$

analysis, it can be shown that the thermal noise is a *zero-mean stationary process* with a PSD given by

$$S_{\text{TN}}(2\pi F) = \frac{\hbar F}{2(e^{\hbar F/kT} - 1)}, \quad F \text{ in Hz} \quad (13.212)$$

where  $\hbar$  is Planck's constant (equal to  $6.6 \times 10^{-34}$  joules-sec.),  $k$  is Boltzmann's constant (equal to  $1.38 \times 10^{-23}$  joules/kelvin), and  $T$  is the absolute temperature in degrees kelvin (K). A plot of this PSD is shown in Figure 13.19. It achieves its maximum at  $F = 0$  with the value of  $kT/2$ . The spectrum goes to zero as  $F \rightarrow \infty$ , but the rate of decrease is very slow. For example, at room temperature ( $T = 300 \text{ K}$ ), the PSD  $S_{\text{TN}}(2\pi F)$  drops to only 90% of the peak value at about 2000 GHz, well beyond the frequencies used in the conventional systems, including communication and radar systems.

Since the thermal noise process has a PSD that is approximately constant over a large range of frequencies, one simple approach to approximate (13.212) is to consider an *ideal process* that has PSD which is exactly constant over the entire frequency range. Such a process will have an infinite power, and hence it may not be a meaningful physical process. However, this idealization is equivalent in usefulness to the impulse function, which also has infinite power.

The noise analysis in systems is usually based on this idealized form of noise called *white noise* (WN), which is a zero-mean stationary process. The adjective white is used in the same sense as that of the white light, which contains equal amounts of all frequencies within the visible

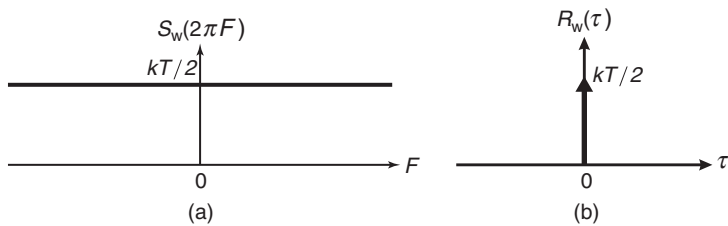


**FIGURE 13.20** Characteristics of white noise: (a) power spectral density, (b) autocorrelation function

electromagnetic spectrum. The white noise will be denoted by  $W(t)$  and is defined in terms of its PSD as

$$S_{WW}(2\pi F) = \frac{N_0}{2}, \frac{\text{watts}}{\text{Hz}} \quad \text{or} \quad S_{WW}(\Omega) = \frac{N_0}{4\pi}, \frac{\text{watts}}{\text{rad/sec}} \quad (13.213)$$

This PSD is shown in Figure 13.20 and is sometimes referred to as the *two-sided power spectral density*, emphasizing that this spectrum extends to both positive and negative frequencies. The parameter  $N_0$  is expressed as

$$N_0 = kT, \quad \text{watts per Hz} \quad (13.214)$$

so that  $S_{WW}(2\pi F)$  matches the thermal PSD at  $F = 0$ . The autocorrelation function of  $W(t)$  is given by

$$R_{WW}(\tau) = \frac{N_0}{2} \delta(\tau) \quad (13.215)$$

which reinforces the fact that white noise is an unrealistic process. This autocorrelation function is also shown in Figure 13.20. Clearly, the samples  $W(t_1)$  and  $W(t_2)$  of white noise for  $t_1 \neq t_2$  are uncorrelated. If  $W(t)$  is also Gaussian (since thermal noise is Gaussian), then it is called a white Gaussian noise (WGN) process. In this case, the components of the process (i.e., random variables at each  $t$ ) are also independent. Such a process is called an *independent process*.

#### Discrete-Time White Noise Process

In a similar fashion, a discrete-time white noise process  $W(n)$  is defined as a zero-mean stationary random sequence with PSD

$$S_{WW}(2\pi f) = \sigma_W^2 \quad \text{or} \quad S_{WW}(\omega) = \frac{\sigma_W^2}{2\pi}, \quad f = \frac{\omega}{2\pi} \quad (13.216)$$

where  $\sigma_W^2$  is the variance of  $W(n)$ . The autocorrelation of  $W(n)$  is then given by

$$R_{WW}(\ell) = \sigma_W^2 \delta(\ell) \quad (13.217)$$

In addition, if  $W(n)$  is also Gaussian at each  $n$ , then it is termed a WGN process, which is also an independent process. Sample sequences for independent WN processes are easy to generate in MATLAB using the `randn` or `rand` functions. For example,

```
>> Wn = randn(N,1);
```

generates  $N$  samples of unit variance WGN process, while

```
>> Wn = rand(N,1);
```

generates  $N$  samples of unit variance independent WN process.

- EXAMPLE 13.21** Generate 10,000 samples of a WGN random process with variance  $\sigma_W^2 = 4$ . Numerically estimate autocorrelation lag values  $R_{WW}(\ell)$ ,  $-20 \leq \ell \leq 20$  and use these to compute the PSD  $S_{WW}(2\pi f)$ . Repeat this procedure over 100 sample sequences to reduce variability of estimates and average  $R_{WW}(\ell)$  and  $S_{WW}(2\pi f)$  over these sample functions and plot the resulting quantities.

#### Solution

We will use the `randn` function to generate WGN samples, the `xcorr` function to estimate autocorrelation lag values, and the `PSD` function to compute the PSD. These steps and averaging operations are illustrated in the following MATLAB script.

```
>> M = 100; % Number of sample sequences to average over
>> N = 10000; % Number of samples in each sequence
>> varW = 4; % Variance of the process
>> sigW = sqrt(varW); % Standard deviation
>> maxlag = 20; % Maximum number of lag values
>> Nfft = 1024; Nfft2 = Nfft/2; % FFT size
>> Rws = zeros(2*maxlag+1,1)'; % Rw initialization
>> Sws = zeros(Nfft+1,1); % Sw initialization
>> ell = -maxlag:maxlag; % Lag indices for plotting
>> f = linspace(-0.5,0.5,Nfft+1); % Frequency grid for plotting
>> % Loop over M Sample Sequences
>> for k = 1:M
>>     % Generate 10000 samples of WGN Process
>>     wn = sigW*randn(N,1)';
>>     % Compute ACRS
>>     [Rw,lags] = xcorr(wn, maxlag,'unbiased');
>>     Rws = Rw+Rws; % Sum autocorrelations
>>     Sw = PSD(Rw',maxlag,Nfft); % Compute PSD
>>     Sws = Sw+Sws; % Sum PSD values
>> end
```

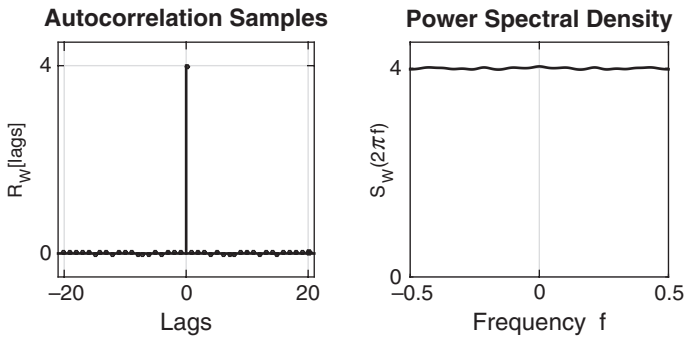


**FIGURE 13.21** Plots of the autocorrelation  $R_{WW}(\ell)$  and PSD  $S_{WW}(2\pi f)$  in Example 13.21

```
>> Rw = Rsum/M; % Average autocorrelations
>> Sw = Ssum /M; % Average PSD
>> % Plotting commands follow
```

The resulting plots of  $R_{WW}(\ell)$  and  $S_{WW}(2\pi f)$  are shown in Figure 13.21. The white noise property of the generated random numbers is quite obvious from these plots.  $\square$

### 13.6.3 MARKOV PROCESS

In some applications, it is advantageous to model a random process whose future values depend only on the present value. This reduces storage as well as processing complexities. Such a process is called a *Markov process*, and it is a process whose past has no influence on the future given that its present is specified; that is, if  $t_n > t_{n-1}$ , then the conditional distribution of a Markov process  $X(t)$  based on the infinite past

$$\Pr\{X(t_n) \leq x_n | X(t), t \leq t_{n-1}\} = \Pr\{X(t_n) \leq x_n | X(t_{n-1})\} \quad (13.218)$$

depends on its immediate past. It further follows that if  $t_1 < t_2 < \dots < t_n$ , then

$$\Pr\{X(t_n) \leq x_n | X(t_{n-1}), X(t_{n-2}), \dots, X(t_1)\} = \Pr\{X(t_n) \leq x_n | X(t_{n-1})\} \quad (13.219)$$

If  $X(t)$  is a Gaussian process, then it is called a *Gauss–Markov process*. It can be shown that continuous-time LTI systems described by linear, constant-coefficient differential equations and driven by a WGN process generate Gauss–Markov processes.

#### Discrete-Time Markov Process

Similarly, discrete-time LTI systems described by linear, constant-coefficient difference equations and driven by WGN sequence generate

Gauss–Markov sequences. Hence the simplest method for generating a Gauss–Markov sequence is to use the first-order auto-regressive AR system

$$\mathbf{X}(n) = \rho\mathbf{X}(n-1) + \mathbf{W}(n) \quad (13.220)$$

where  $\mathbf{W}(n)$  is an independent, zero-mean WGN sequence and the filter coefficient  $\rho$  represents the correlation coefficient between  $\mathbf{X}(n)$  and  $\mathbf{X}(n-1)$ , that is,

$$\begin{aligned} \mathbb{E}[\mathbf{X}(n)\mathbf{X}(n-1)] &= \mathbb{E}[(\rho\mathbf{X}(n-1) + \mathbf{W}(n))\mathbf{X}(n-1)] \\ &= \rho\mathbb{E}[\mathbf{X}^2(n-1)] = \rho\sigma_{\mathbf{X}}^2(n-1) \end{aligned} \quad (13.221)$$

Thus in this process, we have to store only one past value to generate the next correlated value.

- EXAMPLE 13.22** Generate 10,000 samples of a Gauss–Markov process  $\mathbf{X}(n)$  that has correlation coefficient  $\rho = 0.7$  and average power of 100 watts.

### Solution

We will use (13.220) with  $\rho = 0.7$  to generate samples of  $\mathbf{X}(n)$  from  $\mathbf{W}(n)$ . To generate the WGN  $\mathbf{W}(n)$ , we will need its variance  $\sigma_{\mathbf{W}}^2$ . Following the steps used in Example 13.14, we can show that the autocorrelation of  $\mathbf{X}(n)$  in (13.220) is given by

$$R_{\mathbf{XX}}(\ell) = \left( \frac{\sigma_{\mathbf{W}}^2}{1 - \rho^2} \right) \rho^{|\ell|} = \left( \frac{\sigma_{\mathbf{W}}^2}{0.51} \right) 0.7^{|\ell|} \quad (13.222)$$

The average power in  $\mathbf{X}(n)$  is then given by

$$R_{\mathbf{XX}}[0] = \frac{\sigma_{\mathbf{W}}^2}{0.51} \quad (13.223)$$

Hence for  $R_{\mathbf{XX}}[0] = 100$ , we obtain  $\sigma_{\mathbf{W}}^2 = 51$ . Now we will generate samples of  $\mathbf{W}(n)$  using the `randn` function and filter those samples using (13.220) to obtain samples of  $\mathbf{X}(n)$ . The following MATLAB script provides these steps.

```
>> N = 10000; varW = 51;
>> wn = sqrt(varW)*randn(N,1);
>> rho = 0.7; b = 1; a = [1,-rho];
>> xn = filter(b,a,wn);
```

The resulting samples were used in Example 13.11. Plots of these samples and the normalized autocorrelation are shown in Figure 13.12.  $\square$

### 13.6.4 FILTERED NOISE PROCESS

Even if we model the thermal noise as a white noise process at the input of a communication receiver system, it gets processed, or, more correctly, filtered, by subsequent stages of operations in the receiver. At each stage, a *correlated* noise process is generated, known as a color noise process, or *colored process* for short. If the frequency response function of the receiver is  $H(j\Omega)$  and the input is WGN  $W(t)$  with PSD  $S_{WW}(\Omega) = N_0/(4\pi)$ , then the colored process  $X(t)$  is also zero mean with PSD

$$S_{XX}(\Omega) = \frac{N_0}{4\pi} |H(j\Omega)|^2 \quad (13.224)$$

Generally, the stages in the receiver are bandpass systems, and hence the filtered noise is a bandpass process. However, the information signals generally have lowpass power distribution. We now consider both processes below.

#### *Lowpass Process*

A random process  $X(t)$  is called lowpass if its power spectrum is large in the vicinity of  $F = 0$  Hz and small (approaching 0) at high frequencies. In other words, a lowpass random process has most of its power concentrated at low frequencies. The discrete-time random process generated in Example 13.22 is a lowpass process whose PSD is shown in Figure 13.16.

A lowpass random process  $X(t)$  is *bandlimited* if its power spectrum is given by  $S_{XX}(j\Omega) = 0$  for  $|\Omega| > 2\pi B$ . The parameter  $B$  is called the bandwidth in Hz of the random process. It can be generated by filtering the WN process through a lowpass filter. Similarly, an *ideal* bandlimited lowpass process can be generated by filtering a WN process through an ideal filter with frequency response function

$$H(j\Omega) = \begin{cases} 1, & |\Omega| \leq 2\pi B \\ 0, & |\Omega| > 2\pi B \end{cases} \quad (13.225)$$

It has the PSD (in watts per radian) given by

$$S_{XX}(\Omega) = \begin{cases} N_0/(4\pi), & |\Omega| \leq 2\pi B \\ 0, & |\Omega| > 2\pi B \end{cases} \quad (13.226)$$

which is shown in Figure 13.22(a), from which the average power in this process is  $\overline{P_X} = \frac{N_0}{4\pi}(4\pi B) = N_0 B$  watts. The autocorrelation function is given by

$$R_{XX}(\tau) = N_0 B \operatorname{sinc}(2B\tau) \quad (13.227)$$

It is also shown in Figure 13.22. Thus from the zero-crossings, we conclude that every random variables pair in the ideal bandlimited lowpass process, separated by  $\tau = 1/2B$  lag interval, is uncorrelated (due to zero mean) or is independent if  $X(t)$  is also Gaussian.

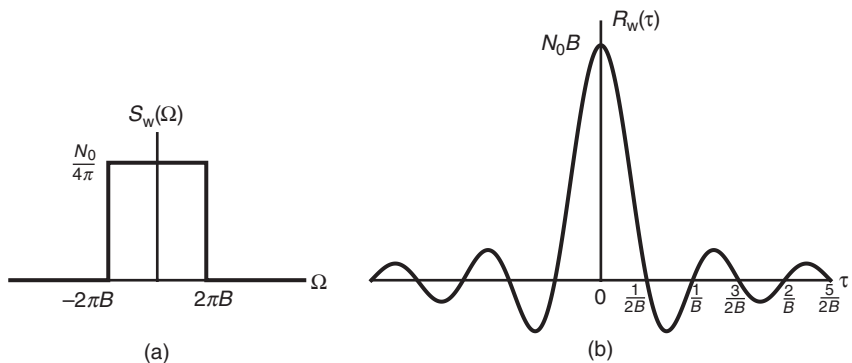


**FIGURE 13.22** Ideal lowpass process: (a) PSD, (b) autocorrelation function

- **EXAMPLE 13.23** Consider the problem of generating samples of a bandlimited lowpass process by filtering a discrete-time WGN process through a properly designed IIR elliptic filter that approximates the ideal filter in (13.225). Obtain samples  $X(n)$  of a lowpass process  $X(t)$  that is bandlimited to 3 KHz using a fifth-order elliptic filter. Choose a sampling rate of 20 KHz.

#### Solution

First, we will design a fifth-order elliptic filter by setting passband cutoff frequency to  $\omega_p = (3/20)2\pi = 0.3\pi$ . To approximate the ideal lowpass filter, we will choose passband ripple of 0.1 dB and stopband attenuation of 50 dB, which are quite reasonable. Now using the `ellip` function, we obtain the required low-pass filter that can be used in filtering WGN samples to obtain samples of the bandlimited lowpass process. The following MATLAB script gives all the necessary details.

```

M = 100; % Number of sample sequences to average over
N = 10000; % Number of samples in each sequence
varW = 4; % Variance of the input WGN process
sigW = sqrt(varW); % Standard deviation
maxlag = 50; % Maximum number of lag values
Nfft = 2048; Nfft2 = Nfft/2; % FFT size
Rxsum = zeros(2*maxlag+1,1)'; % Contains Autoc sum for averaging
Sxsum = zeros(Nfft+1,1); % Contains PSD sum for averaging
ell = -maxlag:maxlag; % Lag indices
f = linspace(-0.5,0.5,Nfft+1); % Frequency grid
% Approximation to Ideal LPF using Elliptic Filter
omp = 0.3; % Passband cutoff in pi units
Rp = 0.1; % Passband ripple in dB
As = 50; % Stopband attenuation in dB
Nellip = 5; % Order of the elliptic filter
[b,a] = ellip(Nellip,Rp,As,omp); % Elliptic filter coefficients
% Loop over M Sample Sequences

```

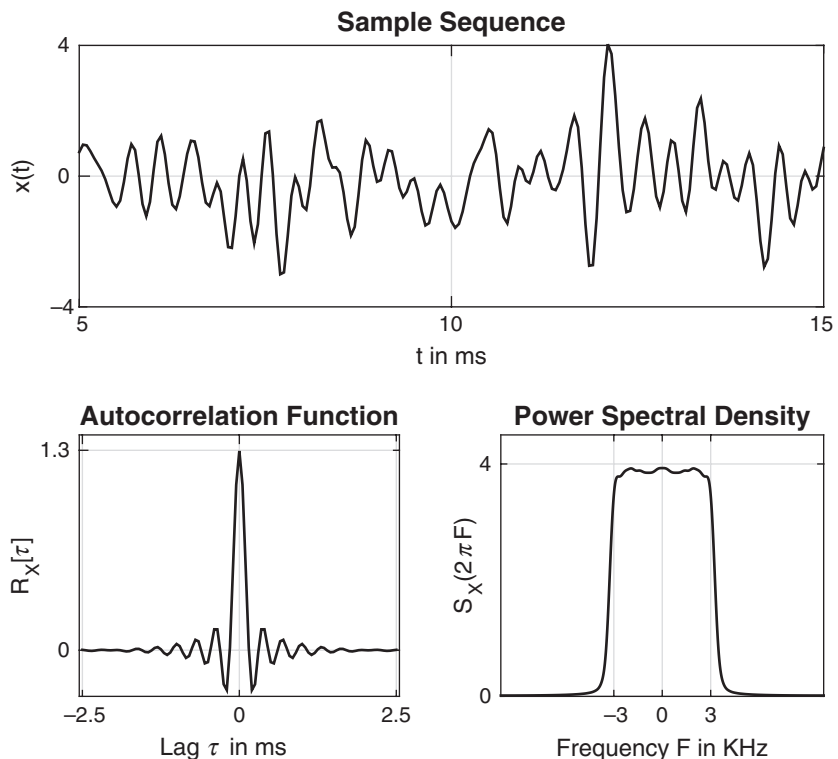


**FIGURE 13.23** A few illustrative samples, the autocorrelation values, and the PSD function of a generated bandlimited lowpass process

```

for k = 1:M
    % Generate 10000 samples of WGN Process
    wn = sigW*randn(N,1)';
    xn = filter(b,a,wn); % Filtered WGN using lowpass filter
    % Compute ACRS
    [Rx,lags] = xcorr(xn, maxlag,'unbiased');
    Rxsum = Rx+Rxsum;
    Sx = PSD(Rx,maxlag,Nfft); % Compute PSD
    Sxsum = Sx+Sxsum;
end
Rx = Rxsum/M;
Sx = Sxsum/M;
% Plotting commands follow

```

The top plot in Figure 13.23 shows few samples of the generated process, while the bottom plots show its autocorrelation and PSD functions, respectively.

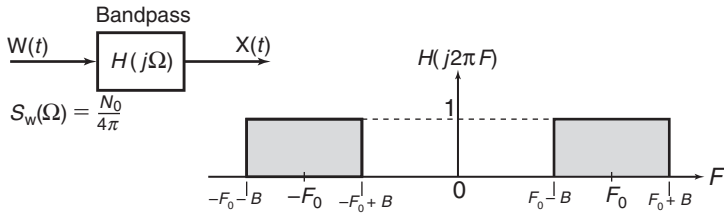


**FIGURE 13.24** White noise filtered through an ideal bandpass filter

The autocorrelation function plot clearly shows the sinc function shape, while the PSD plot is bandlimited to 3 KHz.  $\square$

### Bandpass Process

A random process is called a *bandpass* process if its power spectrum is large in a band of frequencies centered in the neighborhood of a central frequency  $\pm F_0$  and relatively small outside of this band of frequencies. A random process is called *narrowband bandpass* if its bandwidth  $B \ll F_0$ .

Let  $X(t)$  be the output of an ideal bandpass filter  $H(j\Omega)$  whose input is a WGN process  $W(t)$  with PSD  $S_{WW}(\Omega) = N_0/(4\pi)$ . The ideal bandpass filter has a bandwidth of  $B$  Hz that is located at frequencies around  $F_0$  Hz as shown in Figure 13.24 and is given by

$$H(j\Omega) = \begin{cases} 1, & |\Omega - \Omega_0| \leq 2\pi B \\ 0, & \text{otherwise} \end{cases} \quad (13.228)$$

Since the thermal noise is white and Gaussian, the filtered noise  $X(t)$  is Gaussian but *not* white. The PSD of the filtered noise is given by

$$\begin{aligned} S_{XX}(\Omega) &= |H(j\Omega)|^2 S_{WW}(\Omega) \\ &= \frac{N_0}{4\pi} H(j\Omega) = \begin{cases} \frac{N_0}{4\pi}, & |\Omega - \Omega_0| \leq 2\pi B \\ 0, & \text{otherwise} \end{cases} \end{aligned} \quad (13.229)$$

and the average power in the filtered process  $X(t)$  is given by

$$\overline{P_X} = 2 \times \frac{N_0}{4\pi} \times 4\pi B = 2N_0B \quad \text{watts} \quad (13.230)$$

- $\square$  **EXAMPLE 13.24** In this example, we will use the procedure of Example 13.23 to obtain samples of an approximated bandlimited bandpass process. Generate samples  $X(n)$  of a bandpass process  $X(t)$  that is bandlimited between 3 and 6 KHz using a tenth-order bandpass elliptic filter. Choose sampling rate of 20 KHz.

#### Solution

Again, we will first design a tenth-order elliptic filter by setting passband cutoff frequencies to  $\omega_{p1} = (3/20)2\pi = 0.3\pi$  and  $\omega_{p2} = (6/20)2\pi = 0.6\pi$ . To approximate the ideal bandpass filter, we will choose passband ripple of 0.1 dB

and stopband attenuation of 50 dB, which are quite reasonable. The stopband cutoff frequencies will be set by the order of the filter. Now using the `ellip` function, we obtain the required bandpass filter that can be used in filtering WGN samples to obtain samples of the bandlimited bandpass process. The following MATLAB script gives all the necessary details. A representative segment of the bandpass process, its autocorrelation, and the resulting PSD functions are shown in Figure 13.25.

```

M = 100; % Number of sample sequences to average over
N = 10000; % Number of samples in each sequence
varW = 1; % Variance of the input WGN process
sigW = sqrt(varW); % Standard deviation
maxlag = 50; % Maximum number of lag values
Nfft = 2048; Nfft2 = Nfft/2; % FFT size
Rxsum = zeros(2*maxlag+1,1)'; % Contains Autoc sum for averaging
Sxsum = zeros(Nfft+1,1); % Contains PSD sum for averaging
ell = -maxlag:maxlag; % Lag indices
f = linspace(-0.5,0.5,Nfft+1); % Frequencies in cycles/sam
Fs = 20; % Sampling rate in KHz
F = f*Fs; % Frequencies in KHz
% Approximation to ideal BPF using elliptic filter
omp1 = 0.3; % Lower Passband cutoff in pi units
omp2 = 0.6; % Upper Passband cutoff in pi units
Rp = 0.1; % Passband ripple in dB
As = 50; % Stopband attenuation in dB
Nellip = 5; % Order of the resulting elliptic filter is 2*N
[b,a] = ellip(Nellip,Rp,As,[omp1,omp2]); % Elliptic filter coefficients
% Loop over M sample sequences
for k = 1:M
    % Generate 10000 samples of WGN Process
    wn = sigW*randn(N,1)';
    xn = filter(b,a,wn); % Filtered WGN using lowpass filter
    % Compute ACRS
    [Rx,lags] = xcorr(xn, maxlag,'unbiased');
    Rxsum = Rx+Rxsum;
    Sx = PSD(Rx,maxlag,Nfft); % Compute PSD
    Sxsum = Sx+Sxsum;
end
Rx = Rxsum/M;
Sx = Sxsum/M;
% Plotting commands follow

```



Bandpass processes are suitable for representing modulated signals. In a communication system, the information-bearing signal is usually a lowpass random process that modulates a carrier for transmission over

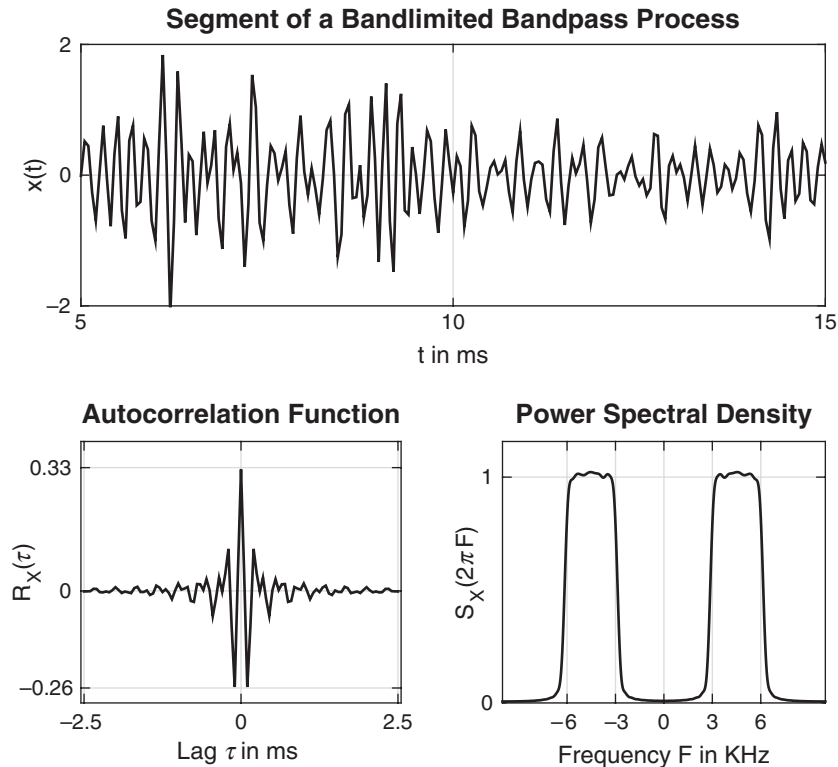


**FIGURE 13.25** A segment of the process, its autocorrelation, and the resulting PSD functions of a generated bandlimited bandpass process in Example 13.24

a bandpass (narrowband) communication channel. Thus the modulated signal is a bandpass random process.

A bandpass random process  $X(t)$  can be represented in terms of low-pass processes as

$$X(t) = X_c(t) \cos(2\pi F_0 t) - X_s(t) \sin(2\pi F_0 t) \quad (13.231)$$

where  $X_c(t)$  and  $X_s(t)$  are called the *in-phase* and *quadrature* components of  $X(t)$ . These random processes  $X_c(t)$  and  $X_s(t)$  are lowpass processes. Furthermore, there is an important relationship among these  $X(t)$ ,  $X_c(t)$ , and  $X_s(t)$  processes, given below without proof:

■ **THEOREM 1** If  $X(t)$  is a zero-mean, stationary random process, then processes  $X_c(t)$  and  $X_s(t)$  are also zero-mean, jointly stationary processes.

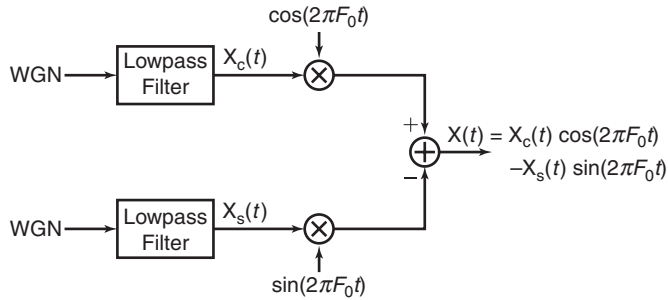


**FIGURE 13.26** Generation of a bandpass random process

In fact, it can be easily proved that (see [82]) the autocorrelation functions of  $X_c(t)$  and  $X_s(t)$  are identical and may be expressed as

$$R_{X_c}(\tau) = R_{X_s}(\tau) = R_{XX}(\tau) \cos(2\pi F_0 \tau) + \hat{R}_{XX}(\tau) \sin(2\pi F_0 \tau) \quad (13.232)$$

where  $R_{XX}(\tau)$  is the autocorrelation function of the bandpass process  $X(t)$  and  $\hat{R}_{XX}(\tau)$  is the Hilbert transform of  $R_X(\tau)$ , which is defined as

$$\hat{R}_{XX}(\tau) = \frac{1}{\pi} \int_{-\infty}^{\infty} \frac{R_{XX}(\tau)}{\tau - t} dt \quad (13.233)$$

The cross-correlation function of  $X_c(t)$  and  $X_s(t)$  can be expressed as

$$R_{X_{cs}}(\tau) = R_{XX}(\tau) \sin(2\pi F_0 \tau) - \hat{R}_{XX}(\tau) \cos(2\pi F_0 \tau) \quad (13.234)$$

- **EXAMPLE 13.25** Generate samples of a Gaussian bandpass random process by first generating samples of two statistically independent Gaussian random processes  $X_c(t)$  and  $X_s(t)$  and then using these to modulate the quadrature carriers  $\cos(2\pi F_0 t)$  and  $\sin(2\pi F_0 t)$ , as shown in Figure 13.26.

#### Solution

On a digital computer or in MATLAB, samples of the lowpass processes  $X_c(t)$  and  $X_s(t)$  are generated by filtering two independent Gaussian white noise sequences by two identical lowpass filters. Thus we obtain the samples  $X_c(n)$  and  $X_s(n)$ , corresponding to the sampled values of  $X_c(t)$  and  $X_s(t)$ . Then  $X_c(n)$  modulates the sampled carrier  $\cos(2\pi F_0 nT)$ , and  $X_s(n)$  modulates the quadrature carrier  $\sin(2\pi F_0 nT)$ , where  $T$  is the appropriate sampling interval.

The MATLAB script for these computations is given below. For illustrative purposes, we have selected the lowpass filter to have a system function

$$H(z) = \frac{1}{1 - 0.9z^{-1}} \quad (13.235)$$

Also, we selected  $T = 0.001$  sec or sampling rate of 1000 sam/sec and  $F_0 = 200$  Hz. A representative segment of the bandpass process, its autocorrelation, and the resulting PSD are shown in Figure 13.27.

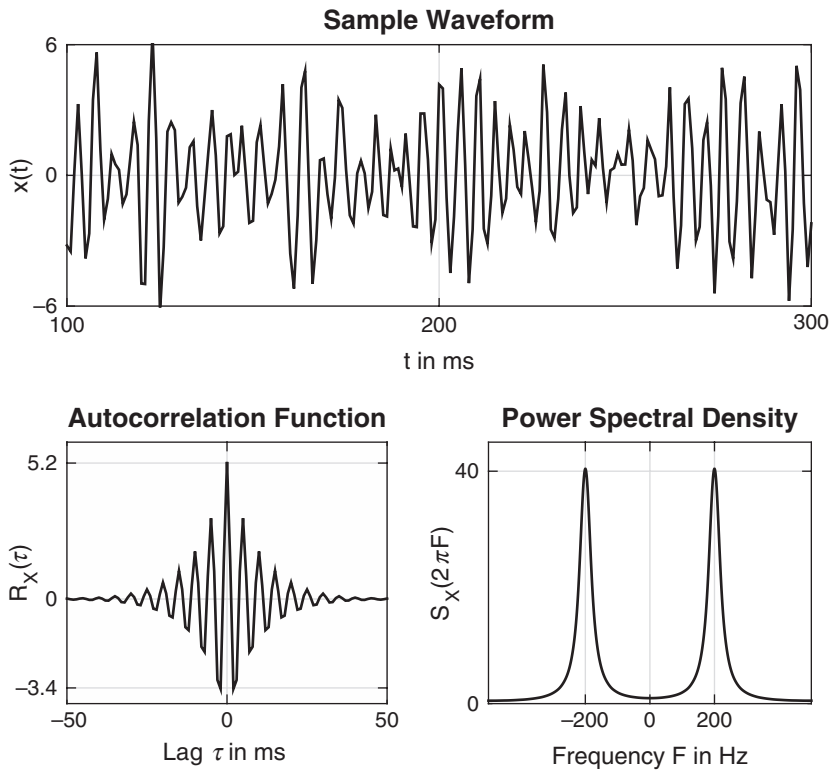


**FIGURE 13.27** A segment of the process, its autocorrelation, and the resulting PSD functions of a generated bandpass process in Example 13.25

```

M = 100; % Number of sample sequences to average over
N = 10000; % Number of samples in each sample sequence
varW = 1; % Variance of the input WGN process
sigW = sqrt(varW); % Standard deviation
maxlag = 50; % Maximum number of lag values
Nfft = 2048; Nfft2 = Nfft/2; % FFT size
Rxsum = zeros(2*maxlag+1,1)'; % Contains Autoc sum for averaging
Sxsum = zeros(Nfft+1,1); % Contains PSD sum for averaging
ell = -maxlag:maxlag; % Lag indices
f = linspace(-0.5,0.5,Nfft+1); % Frequency grid
Fs = 1000; % Sampling rate in Khz
F = f*Fs; % Frequencies in KHz
F0 = 200; % Carrier frequency in Hz
T = 1/Fs; % Sampling interval
t = (0:N-1)*T; % Sampled time instances

```

```
% Lowpass filter for illustration
b = 1; a = [1,-0.9];
% Loop over M Sample Sequences
for k = 1:M
    % Generate 10000 samples of WGN process
    wcn = sigW*randn(N,1)'; % Input WGN for Xc(n)
    wsn = sigW*randn(N,1)'; % Input WGN for Xs(n)
    xcn = filter(b,a,wcn); % WGN -> lowpass filter -> Xc(n)
    xsn = filter(b,a,wsn); % WGN -> lowpass filter -> Xs(n)
    xn = xcn.*cos(2*pi*F0*t) - xsn.*sin(2*pi*F0*t); % BP process
    % Compute ACRS
    [Rx,lags] = xcorr(xn, maxlag,'unbiased');
    Rxsum = Rx+Rxsum;
    Sx = PSD(Rx,maxlag,Nfft); % Compute PSD
    Sxsum = Sx+Sxsum;
end
Rx = Rxsum/M; Sx = Sxsum/M;
% Plotting commands follow
```



## 13.7 SUMMARY AND REFERENCES

---

In this chapter, we have presented probabilistic and statistical description of signals with randomly varying waveforms and provided tools and techniques to process them through LTI systems. We began in Section 13.1 with the concept of a random variable as a model for single random measurement. We described it using probability functions, the most important one being the marginal probability density function (pdf). We developed MATLAB function `pdf1` to simulate the pdf using normalized histogram. For practical simplicity, we emphasized statistical averages (or moments) of mean and variance to describe the random variable and provided tools to estimate its mean value using several observed measurements. We discussed few useful random variable models including uniform and Gaussian distributions.

In Section 13.2, we extended this treatment to a pair of random variables using the joint pdf and the joint moments of correlation and covariance. We showed the use of scatter-plots to simulate the joint density function in MATLAB. The important model for the random variable pair (namely, the bivariate Gaussian distribution) was discussed in detail, including enumeration of its unique and important properties.

The major focus of this chapter was on random signals, or stochastic processes. To this end, in Section 13.3, we modeled the random signal value  $X(t)$  at each fixed time instance  $t$ , as a random variable and at two fixed-time instances,  $t_1$  and  $t_2$ , the two random measurements

$(X(t_1), X(t_2))$  as a pair of random variables. This allowed us to extend and apply concepts such as the marginal and joint densities, the mean and variance, and the correlations and covariances to random processes in a straightforward manner. The means and variances became temporal functions while *autocorrelations* and *autocovariances* became joint temporal functions. In practice, we are interested in statistical quantities that do not vary with time, so we focused on *stationary* processes in which means were constant and auto moments were functions of lag variable  $\tau = t_1 - t_2$ . Also, for practical considerations, we discussed *ergodic* processes that allowed us to estimate mean and autocorrelation from the observation of a single sample waveform. We extended these ideas to discrete-time random processes or random sequences. The use of `xcorr` function in MATLAB was illustrated through several examples.

One of the most useful parameters in signal description is its average power. In Section 13.4, we developed the Wiener–Khinchin theorem that related the autocorrelation function of a stationary process to the power spectral density through Fourier transform and allowed us to obtain average signal power in the frequency domain. This concept was extended to random sequences as well. In Section 13.5, we discussed filtering of stationary random processes and sequences through LTI systems. We developed formulas to obtain output means and autocorrelations using convolutions with the impulse response in the time domain. Likewise, we obtained formulas to compute output psd functions using the frequency response function in the frequency domain.

In Section 13.6, we discussed several useful practical random processes and how to obtain their samples through simple linear filtering. The Gaussian process was an extension of the bivariate Gaussian distribution to multivariate distribution at several arbitrary time instances. The white noise process was developed as an idealized model to describe thermal noise in electrical components. This noise process was further filtered through recursive equations to obtain Markov processes and through lowpass and bandpass filters to obtain lowpass and bandpass processes, respectively. Finally, we showed how to generate bandlimited lowpass and bandpass processes filtering white noise processes through carefully designed elliptic filters.

The material presented in this chapter is available in many excellent textbooks written over the period of last 50 years. One of the best sources for insightful exposition of probability and stochastic processes is the book by Papoulis and Pillai [73], now in its fourth edition. For graduate students, books by Stark and Woods [90] and Leon-Garcia [53] are good choices. For reading at the undergraduate level, books by Miller and Childers [67], and Yates and Goodman [99] are sufficient. This material is also available either as a single chapter or a part of a chapter in many books, including Proakis and Salehi [82], Oppenheim and Schafer [71], Manolakis and Ingle [60], and Manolakis, Ingle, and Kogon [61].

# CHAPTER **14**

---

## Linear Prediction and Optimum Linear Filters

---

The design of filters to perform signal estimation is a problem that frequently arises in the design of communication systems and control systems, in geophysics, and in many other disciplines. In this chapter, we treat the problem of optimum filter design from a statistical viewpoint. The filters are constrained to be linear and the optimization criterion is based on the minimization of the mean square error. As a consequence, only the second-order statistics (autocorrelation and cross-correlation functions) of a stationary process are required in the determination of optimum filters.

Included in this treatment is the design of optimum filters for linear prediction. Linear prediction is a particularly important topic in digital signal processing, with applications in a variety of areas, such as speech signal processing, image processing, and noise suppression in communication systems. As we shall observe, the determination of the optimum filter for linear prediction requires the solution of a set of linear equations that have special symmetry. To solve these linear equations, we describe two algorithms, Levinson–Durbin and Schur, which provide the solution to the equations through computationally efficient procedures that exploit the symmetry properties.

The last section of this chapter treats an important class of optimum filters called Wiener filters, which are widely used in many applications involving the estimation of signals corrupted with additive noise.

## 14.1 INNOVATIONS REPRESENTATION OF A STATIONARY RANDOM PROCESS

---

In this section, we demonstrate that a wide-sense stationary random process may be represented as the output of a causal and causally invertible linear system excited by a white noise process. The condition that the system is causally invertible also allows us to represent the wide-sense stationary random process by the output of the inverse system, which is a white noise process.

Let us consider a wide-sense stationary process  $X(n)$  with autocorrelation sequence  $\{R_{XX}(m)\}$  and power spectral density<sup>1</sup>  $S_{XX}(f)$ ,  $|f| \leq \frac{1}{2}$ . We assume that  $S_{XX}(f)$  is real and continuous for all  $|f| \leq \frac{1}{2}$ . The  $z$ -transform of the autocorrelation sequence  $\{R_{XX}(m)\}$  was termed the complex PSD and is given by<sup>2</sup>

$$S_{XX}(z) = \sum_{m=-\infty}^{\infty} R_{XX}(m)z^{-m} \quad (14.1)$$

from which we obtain the power spectral density  $S_{XX}(f)$  by evaluating  $S_{XX}(z)$  on the unit circle—that is, by substituting  $z = \exp(j2\pi f)$ .

Now, let us assume that  $\log S(z)$  is analytic (possesses derivatives of all orders) in an annular region in the  $z$ -plane that includes the unit circle, that is,  $r_1 < |z| < r_2$  where  $r_1 < 1$  and  $r_2 > 1$ . Then  $\log S_{XX}(z)$  may be expanded in a Laurent series of the form

$$\log S_{XX}(z) = \sum_{m=-\infty}^{\infty} v(m)z^{-m} \quad (14.2)$$

where the  $v(m)$  are the coefficients in the series expansion. We may view  $\{v(m)\}$  as the sequence with  $z$ -transform  $V(z) = \log S_{XX}(z)$ . Equivalently, we may evaluate  $\log S_{XX}(z)$  on the unit circle,

$$\log S_{XX}(z)|_{z=e^{j2\pi f}} = \log S_{XX}(f) = \sum_{m=-\infty}^{\infty} v(m)e^{-j2\pi fm} \quad (14.3)$$

<sup>1</sup>In this chapter, we slightly abuse our Chapter 13 notation of  $S_{XX}(2\pi f)$  for PSD and denote it by  $S_{XX}(f)$  for simplicity.

<sup>2</sup>Again, for simplicity we use  $S_{XX}(z)$  instead of  $\tilde{S}_{XX}(z)$  to denote a complex PSD, as was done in Chapter 13. It should be noted that  $S_{XX}(\omega)$ ,  $S_{XX}(f)$ , and  $S_{XX}(z)$  all refer to the same basic PSD function but with different frequency argument dependencies. The exact dependency should be clear from the context.

so that the  $v(m)$  are the Fourier coefficients in the Fourier series expansion of the periodic function  $\log S_{XX}(f)$ . Hence

$$v(m) = \int_{-\frac{1}{2}}^{\frac{1}{2}} [\log S_{XX}(f)] e^{j2\pi f m} df, \quad m = 0, \pm 1, \dots \quad (14.4)$$

We observe that  $v(m) = v(-m)$ , since  $S_{XX}(f)$  is a real and even function of  $f$ .

From (14.2), it follows that

$$\begin{aligned} S_{XX}(z) &= \exp \left[ \sum_{m=-\infty}^{\infty} v(m) z^{-m} \right] \\ &= \exp \left[ \sum_{m=-\infty}^{-1} v(m) z^{-m} + v(0) + \sum_{m=1}^{\infty} v(m) z^{-m} \right] \\ &\stackrel{\triangle}{=} \sigma_W^2 H(z) H(z^{-1}) \end{aligned} \quad (14.5)$$

where, by definition,  $\sigma_W^2 = \exp[v(0)]$  and

$$H(z) = \exp \left[ \sum_{m=1}^{\infty} v(m) z^{-m} \right], \quad |z| > r_1 \quad (14.6)$$

If (14.5) is evaluated on the unit circle, we have the equivalent representation of the power spectral density as

$$S_{XX}(f) = \sigma_W^2 |H(f)|^2 \quad (14.7)$$

We note that

$$\begin{aligned} \log S_{XX}(f) &= \log \sigma_W^2 + \log H(f) + \log H^*(f) \\ &= \sum_{m=-\infty}^{\infty} v(m) e^{-j2\pi f m} \end{aligned}$$

From the definition of  $H(z)$  given by (14.6), it is clear that the causal part of the Fourier series in (14.3) is associated with  $H(z)$  and that the anticausal part is associated with  $H(z^{-1})$ .

The filter with system function  $H(z)$  given by (14.6) is analytic in the region  $|z| > r_1 < 1$ . Hence, in this region, it has a Taylor series expansion as a causal system of the form

$$H(z) = \sum_{n=0}^{\infty} h(n) z^{-n} \quad (14.8)$$

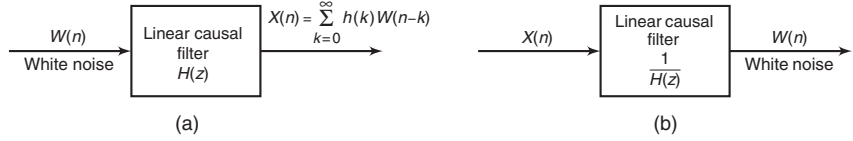


**FIGURE 14.1** Filters for generating (a) the random process  $X(n)$  from white noise and (b) the inverse filter

The output of this filter to a white noise input sequence  $W(n)$  with power spectral density  $\sigma_W^2$  is a stationary random process  $X(n)$  with power spectral density  $S_{XX}(f) = \sigma_W^2 |H(f)|^2$ . Conversely, the stationary random process  $X(n)$  with power spectral density  $S_{XX}(f)$  may be transformed into a white noise process by passing  $X(n)$  through a linear filter with system function  $1/H(z)$ . We call this filter a *noise-whitening filter*. Its output, denoted by  $W(n)$ , is called the *innovations process* associated with the stationary random process  $X(n)$ . These two relationships are illustrated in Figure 14.1, where  $x(n)$  and  $w(n)$  are sample sequences of the stationary random processes  $X(n)$  and  $W(n)$ , respectively.

The representation of stationary stochastic process  $X(n)$  as the output of an IIR filter with system function  $H(z)$  as given by (14.8) and excited by a white noise sequence  $W(n)$  is called the *Wold representation*.

- **EXAMPLE 14.1** The autocorrelation function of a wide-sense stationary random process is given by

$$R_{XX}(m) = 5\left(\frac{1}{2}\right)^{|m|}$$

- a. Determine  $S_{XX}(z)$  and its factors  $\sigma_W^2$ ,  $H(z)$ , and  $H(z^{-1})$  as given in (14.5).
- b. Plot  $R_{XX}(m)$  and  $S_{XX}(f)$  for  $|f| \leq \frac{1}{2}$ . Note that

$$S_{XX}(f) = \sum_{m=-\infty}^{\infty} R_{XX}(m) e^{-j2\pi fm} \text{ and}$$

$$R_{XX}(m) = \int_{-\frac{1}{2}}^{\frac{1}{2}} S_{XX}(f) e^{j2\pi fm} df$$

- c. Implement the filter  $H(z)$  to generate an output sequence  $x(n)$  for  $0 \leq n \leq 10,000$ , when the input sequence  $w(n)$  is a sample sequence of a white, zero-mean Gaussian noise sequence with variance  $\sigma_W^2$ . Compute and plot the autocorrelation  $\hat{R}_{XX}(m)$  for  $|m| \leq 50$  and the power density spectrum  $\hat{S}_{XX}(f)$  of the output sequence  $x(n)$ . Compare these plots with the analytic

results of part (b) and comment on similarities and differences. The *biased* estimates  $\hat{R}_{xx}(m)$  and  $\hat{S}_{xx}(f)$  are defined as follows:

$$\begin{aligned}\hat{R}_{xx}(m) &= \frac{1}{N} \sum_{n=0}^{N-m-1} x^*(n)x(n+m), \quad 0 \leq m \leq N-1 \\ \hat{S}_{xx}(f) &= \sum_{m=-(N-1)}^{N-1} R_{xx}(m)e^{-j2\pi fm}, \quad |f| \leq \frac{1}{2}\end{aligned}$$

### Solution

Note that this example is similar to Example 13.13.

- a. The  $z$ -transform of  $R_{xx}(m)$  is

$$\begin{aligned}S_{xx}(z) &= \sum_{m=-\infty}^{\infty} R_{xx}(m)z^{-m} = 5 \left[ \sum_{m=-\infty}^{-1} \left(\frac{1}{2}\right) z^{-m} + \sum_{m=0}^{\infty} \left(\frac{1}{2}\right)^m z^{-m} \right] \\ &= \frac{15}{4} \left[ \frac{1}{(1 - \frac{1}{2}z^{-1})(1 - \frac{1}{2}z)} \right], \quad \frac{1}{2} < |z| < 2\end{aligned}$$

Therefore,  $\sigma_w^2 = \frac{15}{4}$  and  $H(z) = \frac{1}{1 - \frac{1}{2}z^{-1}}$

- b. The PSD  $S_{xx}(f)$  is given by

$$\begin{aligned}S_{xx}(f) &= \sum_{m=-\infty}^{\infty} R_{xx}(m)e^{-j2\pi fm} = 5 \sum_{m=-\infty}^{\infty} \left(\frac{1}{2}\right)^{|m|} e^{-j2\pi fm} \\ &= \frac{15}{5 - 4 \cos(2\pi f)}\end{aligned}$$

using (13.148). Plots of  $R_{xx}(m)$  and  $S_{xx}(f)$  are shown in Figure 14.2.

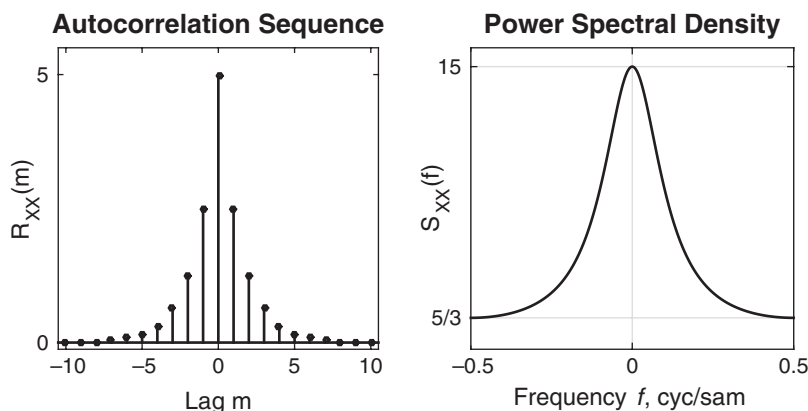


**FIGURE 14.2** Plots of autocorrelation  $R_{xx}(m)$  and PSD  $S_{xx}(f)$  in Example 14.1(b)

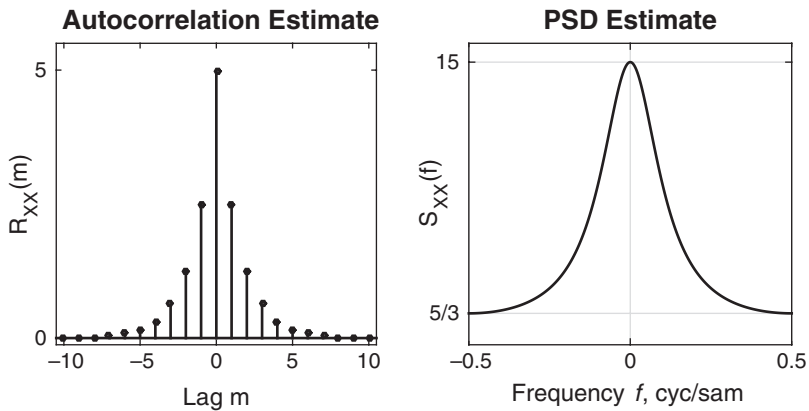


**FIGURE 14.3** Plots of the estimated autocorrelation sequence  $\hat{R}_{XX}(m)$  and PSD  $\hat{S}_{XX}(f)$  in Example 14.1(c)

c. The difference equation for the filter  $H(z)$  is

$$x(n) = \frac{1}{2}x(n-1) + w(n)$$

where  $w(n)$  is a sample sequence from a white Gaussian noise process with variance  $\sigma_w^2 = \frac{15}{4}$ . Plots of the estimated autocorrelation  $\hat{R}_{XX}(m)$  and its Fourier transform  $\hat{S}_{XX}(f)$  are shown in Figure 14.3 which were obtained using the procedures discussed in Chapter 13. We observe that these plots are similar to those of part (b).  $\square$

#### 14.1.1 RATIONAL POWER SPECTRA

Let us now restrict our attention to the case where the power spectral density of the stationary random process  $X(n)$  is a rational function, expressed as

$$S_{XX}(z) = \sigma_w^2 \frac{B(z)B(z^{-1})}{A(z)A(z^{-1})}, \quad r_1 < |z| < r_2 \quad (14.9)$$

where the polynomials  $B(z)$  and  $A(z)$  have roots that fall inside the unit circle in the  $z$ -plane. Then the linear filter  $H(z)$  for generating the random process  $X(n)$  from the white noise sequence  $W(n)$  is also rational, and is expressed as

$$H(z) = \frac{B(z)}{A(z)} = \frac{\sum_{k=0}^q b_k z^{-k}}{1 + \sum_{k=1}^p a_k z^{-k}}, \quad |z| > r_1 \quad (14.10)$$

where  $b_k$  and  $a_k$  are the filter coefficients that determine the location of the zeros and poles of  $H(z)$ , respectively. Thus  $H(z)$  is a causal, stable,

and minimum phase linear system. Its reciprocal  $1/H(z)$  is also a causal, stable, and minimum phase linear system. Therefore, the random process  $X(n)$  uniquely represents the statistical properties of the innovations process  $W(n)$ , and vice versa.

For the linear system with the rational system function  $H(z)$  given by (14.10), the output process  $X(n)$  is related to the input process  $W(n)$  by the difference equation

$$X(n) + \sum_{k=1}^p a_k X(n-k) = \sum_{k=0}^q b_k W(n-k) \quad (14.11)$$

We distinguish among three specific cases:

**Autoregressive (AR) Process:**  $b_0 = 1, b_k = 0, k > 0$ .

In this case, the linear filter  $H(z) = 1/A(z)$  is an all-pole filter, and the difference equation for the input-output relationship is

$$X(n) + \sum_{k=1}^p a_k X(n-k) = W(n) \quad (14.12)$$

In turn, the noise-whitening filter for generating the innovations process is an all-zero filter.

**Moving Average (MA) Process:**  $a_k = 0, k \geq 1$ .

In this case, the linear filter  $H(z) = B(z)$  is an all-zero filter, and the difference equation for the input-output relationship is

$$X(n) = \sum_{k=0}^q b_k W(n-k) \quad (14.13)$$

The noise-whitening filter for the MA process is an all-pole filter.

**Autoregressive, Moving Average (ARMA) Process.** In this case, the linear filter  $H(z) = B(z)/A(z)$  has both finite poles and zeros in the  $z$ -plane, and the corresponding difference equation is given by (14.11). The inverse system for generating the innovations process from  $X(n)$  is also a pole-zero system of the form  $1/H(z) = A(z)/B(z)$ .

□ **EXAMPLE 14.2** Consider an ARMA process  $X(n)$  generated by the difference equation

$$X(n) = 1.6X(n-1) - 0.63X(n-2) + W(n) + 0.9W(n-1)$$

where  $W(n)$  is a white noise sequence with unit variance.

- Determine the system function  $H(z)$  and the system function of the noise whitening filter and its poles and zeros. Is the noise whitening filter stable?
- Determine and plot the power spectrum density  $S_{XX}(f)$  for  $|f| \leq \frac{1}{2}$ .

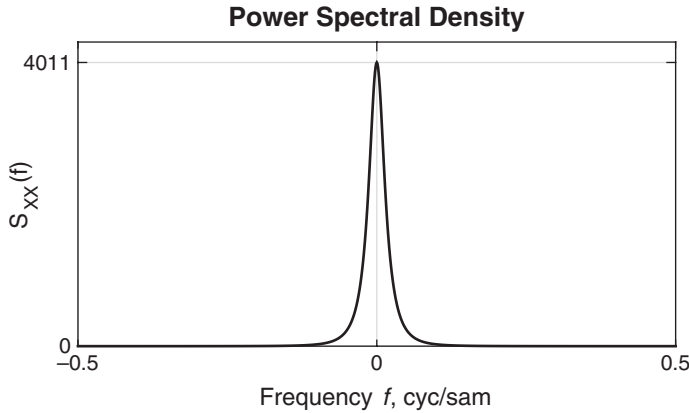


**FIGURE 14.4** Plot of power spectral density  $\hat{S}_{xx}(f)$  in Example 14.2(b)

**Solution**

- a. The system function is given by

$$H(z) = \frac{1 + 0.9z^{-1}}{1 - 1.6z^{-1} + 0.63z^{-2}}$$

$$\text{Whitening filter: } B(z) = H(z)^{-1} = \frac{1 - 1.6z^{-1} + 0.63z^{-2}}{1 + 0.9z^{-1}}$$

$$\text{zeros: } z_{1,2} = 0.7, 0.9$$

$$\text{poles: } p_1 = -0.9$$

Yes, the noise whitening filter is stable, since  $|p_1| < 1$ .

- b. The power spectral density is

$$S_{xx}(f) = \sigma_w^2 |H(f)|^2 = \frac{|1 + 0.9e^{-j2\pi f}|^2}{|1 - 1.6e^{j2\pi f} + 0.63e^{j4\pi f}|^2}$$

since  $\sigma_w^2 = 1$ . A plot of  $S_{xx}(f)$  is shown in Figure 14.4. □

- **EXAMPLE 14.3** An ARMA process has an autocorrelation  $R_{xx}(m)$ , where its  $z$ -transform is given as

$$S_{xx}(z) = 9 \frac{(z - \frac{1}{3})(z - 3)}{(z - \frac{1}{2})(z - 2)}, \quad \frac{1}{2} < |z| < 2$$

- a. Determine the filter  $H(z)$  for generating an output sequence  $x(n)$  from a white noise input sample sequence  $w(n)$ . Is  $H(z)$  unique? Explain.  
 b. Implement the filter  $H(z)$  to generate an output sequence  $x(n)$  for  $0 \leq n \leq 10,000$ , when the input sequence  $w(n)$  is a sample sequence from a white, zero-mean Gaussian noise sequence with unit variance. Compute and plot the autocorrelation estimates  $\hat{R}_{xx}(m)$  for  $|m| \leq 50$  and the power spectral density estimates  $\hat{S}_{xx}(f)$  for  $|f| \leq \frac{1}{2}$  from the output sequence  $x(n)$ .

- c. Determine a stable linear whitening filter for the sequence generated in part (b). Pass the sequence  $x(n)$  generated in part (b) through the noise-whitening filter for  $0 \leq n \leq 10,000$ . Compute the autocorrelation  $\hat{R}_{YY}(m)$  for  $|m| \leq 50$  and the power spectral density  $\hat{S}_{YY}(f)$  for  $|f| \leq \frac{1}{2}$ , where  $y(n)$  is the output of the noise-whitening filter. Plot  $\hat{R}_{YY}(m)$  and  $\hat{S}_{YY}(f)$ , and comment on the results.

**Solution**

- a. The complex PSD can be put in the form

$$S_{XX}(z) = \frac{27}{2} \frac{(1 - \frac{1}{3}z^{-1})(1 - \frac{1}{3}z)}{(1 - \frac{1}{2}z^{-1})(1 - \frac{1}{2}z)}$$

For a stable system, denominator  $\left(1 - \frac{1}{2}z^{-1}\right)$  must be chosen. However, either numerator factor may be used:

$$H(z) = \underbrace{\frac{\left(1 - \frac{1}{3}z^{-1}\right)}{\left(1 - \frac{1}{2}z^{-1}\right)}}_{\text{Min. phase}} \quad \text{or} \quad H(z) = \frac{\left(1 - \frac{1}{3}z\right)}{\left(1 - \frac{1}{2}z^{-1}\right)}$$

- b. We use the minimum phase system function  $H(z)$  to generate the sequence

$$x(n) = \frac{1}{2}x(n-1) + w(n) - \frac{1}{3}w(n-1)$$

We compute the *unbiased* autocorrelation sequence estimate

$$\hat{R}_{XX}(m) = \frac{1}{N-m} \sum_{n=0}^{N-1-m} x(n)x(n-m), \quad |m| \leq 50$$

and from it the estimate of the power spectral density

$$\hat{S}_{XX}(f) = \sum_{m=-N}^N \hat{R}_{XX}(m)e^{-j2\pi fm}$$

Graphs of  $\hat{R}_{XX}(m)$  and  $\hat{S}_{XX}(f)$  are shown in Figure 14.5.

- c. The stable whitening filter is the minimum phase system with system function

$$A(z) = \frac{1 - \frac{1}{2}z^{-1}}{1 - \frac{1}{3}z^{-1}}$$

Thus we generate the sequence

$$y(n) = \frac{1}{3}y(n-1) + x(n) - \frac{1}{2}x(n-1)$$

and compute the estimates  $\hat{R}_{YY}(m)$  and  $\hat{S}_{YY}(f)$ , which are illustrated in Figure 14.6.  $\square$

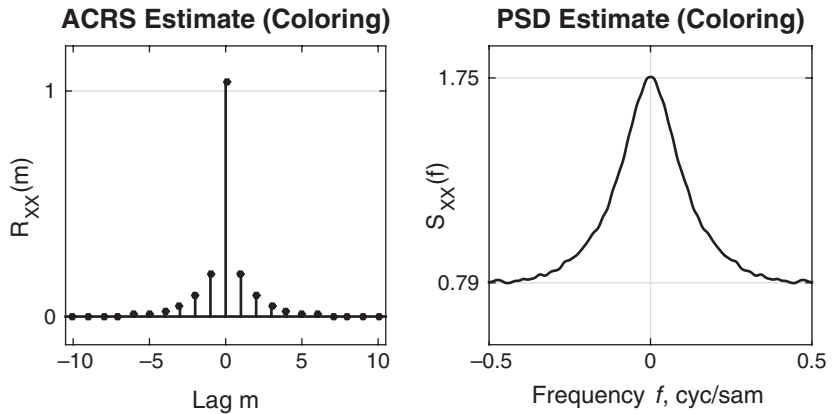


**FIGURE 14.5** Plots of the estimated autocorrelation sequence  $\hat{R}_{xx}(m)$  and PSD  $\hat{S}_{xx}(f)$  in Example 14.3(b)

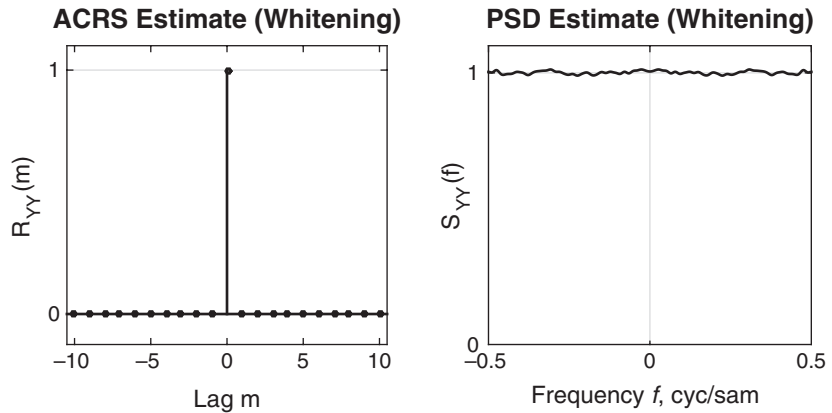


**FIGURE 14.6** Plots of the estimated autocorrelation sequence  $\hat{R}_{yy}(m)$  and PSD  $\hat{S}_{yy}(f)$  in Example 14.3(c)

#### 14.1.2 RELATIONSHIPS BETWEEN THE FILTER PARAMETERS AND THE AUTOCORRELATION SEQUENCE

When the power spectral density of the stationary random process is a rational function, there is a basic relationship that exists between the autocorrelation sequence  $R_{xx}(m)$  and the parameters  $a_k$  and  $b_k$  of the linear filter  $H(z)$  that generates the process by filtering the white noise sequence  $W(n)$ . This relationship may be obtained by multiplying

the difference equation in (14.11) by  $\mathbf{X}^*(n - m)$  and taking the expected value of both sides of the resulting equation. Thus we have

$$\begin{aligned} & \mathbb{E}[\mathbf{X}(n)\mathbf{X}^*(n - m)] \\ &= -\sum_{k=1}^p a_k \mathbb{E}[\mathbf{X}(n - k)\mathbf{X}^*(n - m)] + \sum_{k=0}^q b_k \mathbb{E}[\mathbf{W}(n - k)\mathbf{X}^*(n - m)] \end{aligned} \quad (14.14)$$

Hence

$$R_{\mathbf{XX}}(m) = -\sum_{k=1}^p a_k R_{\mathbf{XX}}(m - k) + \sum_{k=0}^q b_k R_{\mathbf{WX}}(m - k) \quad (14.15)$$

where  $R_{\mathbf{WX}}(m)$  is the cross-correlation sequence between  $\mathbf{W}(n)$  and  $\mathbf{X}(n)$ .

The cross-correlation  $R_{\mathbf{WX}}(m)$  is related to the filter impulse response. That is,

$$\begin{aligned} R_{\mathbf{WX}}(m) &= \mathbb{E}[\mathbf{X}^*(n)\mathbf{W}(n + m)] \\ &= \mathbb{E}\left[\sum_{k=0}^{\infty} h(k)\mathbf{W}^*(n - k)\mathbf{W}(n + m)\right] \\ &= \sigma_W^2 h(-m) \end{aligned} \quad (14.16)$$

where, in the last step, we have used the fact that the sequence  $\mathbf{W}(n)$  is white. Hence

$$R_{\mathbf{WX}}(m) = \begin{cases} 0, & m > 0 \\ \sigma_W^2 h(-m), & m \leq 0 \end{cases} \quad (14.17)$$

By combining (14.17) with (14.15), we obtain the desired relationship,

$$R_{\mathbf{XX}}(m) = \begin{cases} -\sum_{k=1}^p a_k R_{\mathbf{XX}}(m - k), & m > q \\ -\sum_{k=1}^p a_k R_{\mathbf{XX}}(m - k) + \sigma_W^2 \sum_{k=0}^{1-m} h(k)b_{k+m}, & 0 \leq m \leq q \\ R_{\mathbf{XX}}^*(-m), & m < 0 \end{cases} \quad (14.18)$$

This represents a nonlinear relationship between  $R_{\mathbf{XX}}(m)$  and the parameters  $a_k$ ,  $b_k$ . The relationship in (14.18) applies, in general, to the ARMA process. For an AR process, (14.18) simplifies to

$$R_{\mathbf{XX}}(m) = \begin{cases} -\sum_{k=1}^p a_k R_{\mathbf{XX}}(m - k), & m > 0 \\ -\sum_{k=1}^p a_k R_{\mathbf{XX}}(m - k) + \sigma_W^2, & m = 0 \\ R_{\mathbf{XX}}^*(-m), & m < 0 \end{cases} \quad (14.19)$$

Thus we have a linear relationship between  $R_{XX}(m)$  and the  $a_k$  parameters. These equations are called the Yule–Walker equations and may be expressed in the matrix form

$$\begin{bmatrix} R_{XX}(0) & R_{XX}(-1) & R_{XX}(-2) & \dots & R_{XX}(-p) \\ R_{XX}(1) & R_{XX}(0) & R_{XX}(-1) & \dots & R_{XX}(-p+1) \\ \vdots & \vdots & \vdots & \ddots & \vdots \\ R_{XX}(p) & R_{XX}(p-1) & R_{XX}(p-2) & \dots & R_{XX}(0) \end{bmatrix} \begin{bmatrix} 1 \\ a_1 \\ a_2 \\ \vdots \\ a_p \end{bmatrix} = \begin{bmatrix} \sigma_W^2 \\ 0 \\ 0 \\ \vdots \\ 0 \end{bmatrix} \quad (14.20)$$

This correlation matrix is Toeplitz and, hence, can be efficiently inverted by use of the algorithms described in Section 14.3.

Finally, by setting  $a_k = 0$ ,  $1 \leq k \leq p$ , and  $h(k) = b_k$ ,  $0 \leq k \leq q$ , in (14.18), we obtain the relationship for the autocorrelation sequence in the case of a MA process, namely,

$$R_{XX}(m) = \begin{cases} \sum_{k=0}^{q-m} b_k b_{k+m}, & 0 \leq m \leq q \\ 0, & m > q \\ R_{XX}^*(-m), & m < 0 \end{cases} \quad (14.21)$$

**EXAMPLE 14.4** A moving average (MA) process is described by the difference equation

$$X(n) = W(n) - 2W(n-1) + W(n-2) \quad (14.22)$$

where  $W(n)$  is a white noise sequence with variance  $\sigma_W^2 = 1$ .

- a. Determine and plot the autocorrelation  $R_{XX}(m)$  and power spectral density  $S_{XX}(f)$ .
- b. Generate the output sequence  $x(n)$ ,  $0 \leq n \leq 10,000$ , when  $w(n)$  is a sample sequence of a white, zero-mean Gaussian noise sequence with unit variance. Compute and plot the autocorrelation estimates  $\hat{R}_{XX}(m)$  of the sequence  $X(n)$  for  $|m| \leq 50$  and the corresponding power spectral density  $\hat{S}_{XX}(f)$  for  $|f| \leq \frac{1}{2}$ . Compare these plots with those in part (a) and comment on any similarities and differences.

### Solution

- a. From (14.22) and using  $E[W(n)] = 0$ , we have  $E[X(n)] = 0$ . Hence we obtain

$$R_{XX}(m) = \sigma_W^2 \sum_{k=0}^q b_k b_{k+m}, \quad 0 \leq m \leq q$$

With  $q = 2$ ,  $b_0 = 1$ ,  $b_1 = -2$ ,  $b_2 = 1$  and from (14.21), the autocorrelation values are given by

$$R_{XX}(0) = \sigma_W^2 \sum_{k=0}^2 b_k^2 = 6\sigma_W^2 = 6,$$

$$R_{XX}(\pm 1) = \sigma_W^2 \sum_{k=0}^1 b_k b_{k+1} = -4\sigma_W^2 = -4,$$

$$R_{XX}(\pm 2) = \sigma_W^2 \sum_{k=0}^0 b_k b_{k+2} = \sigma_W^2 = 1, \text{ and}$$

$$R_{XX}(m) = 0, \quad |m| \geq 3$$

The PSD is given by

$$\begin{aligned} S_{XX}(f) &= \sum_{m=-2}^2 R_{XX}(m) e^{-j2\pi f m} \\ &= (1)e^{-j2\pi f(-2)} + (-4)e^{-j2\pi f(-1)} + (6)e^{-j2\pi f(0)} \\ &\quad + (-4)e^{-j2\pi f(1)} + (1)e^{-j2\pi f(2)} \\ &= 6 - 8\cos(2\pi f) + 2\cos(4\pi f) \end{aligned}$$

The plots of  $R_{XX}(m)$  and  $S_{XX}(f)$  are shown in Figure 14.7.

- b.** Using the difference equation

$$x(n) = w(n) - 2w(n-1) + w(n-2)$$

we compute  $x(n)$  for  $0 \leq n \leq 10,000$  and estimate the autocorrelation and power spectral density. These functions are plotted in Figure 14.8. They closely resemble the function  $R_{XX}(m)$  and  $S_{XX}(f)$  computed in part (a).  $\square$

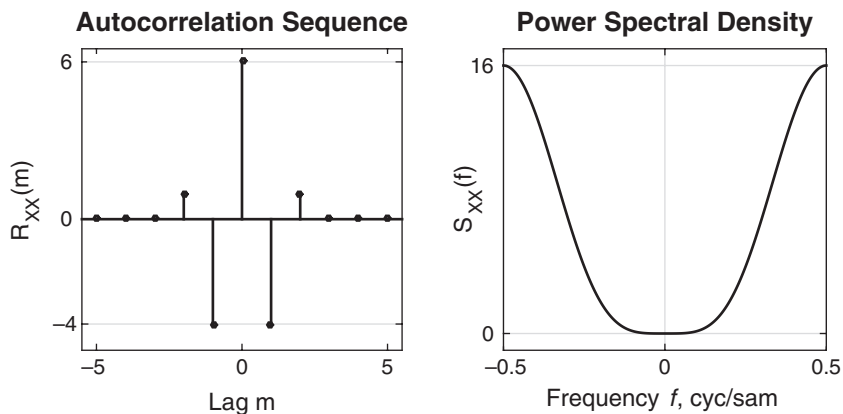


**FIGURE 14.7** Plots of autocorrelation  $R_{XX}(m)$  and PSD  $S_{XX}(f)$  in Example 14.4(a)

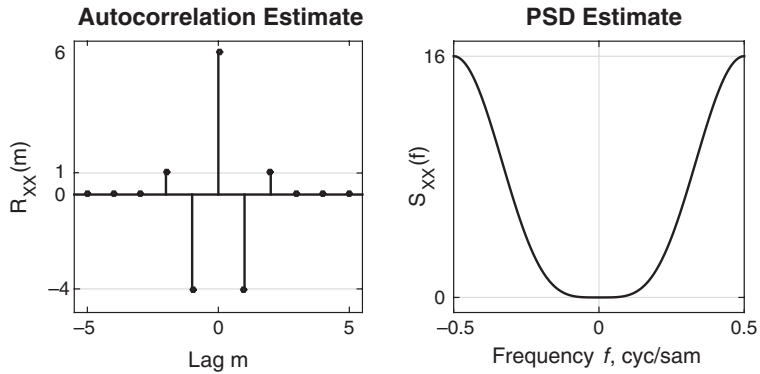


**FIGURE 14.8** Plots of the estimated autocorrelation  $\hat{R}_{XX}(m)$  and PSD  $\hat{S}_{XX}(f)$  in Example 14.4(b)

- **EXAMPLE 14.5** An AR process is described by the difference equation

$$X(n) = X(n-1) - 0.6X(n-2) + W(n) \quad (14.23)$$

where  $W(n)$  is a zero-mean, white noise process with variance  $\sigma_W^2$ .

- Use the Yule–Walker equations to solve for the values of the autocorrelations  $R_{XX}(m)$ .
- Determine the  $z$ -transform of the autocorrelation  $R_{XX}(m)$  and plot the power spectral density  $S_{XX}(f)$  for  $|f| \leq \frac{1}{2}$ .
- Generate the output sequence  $x(n)$ ,  $0 \leq n \leq 10,000$ , when  $w(n)$  is a sample sequence from a white, zero-mean Gaussian noise process with unit variance. Compute and plot the autocorrelation estimates  $\hat{R}_{XX}(m)$  of the sequence  $x(n)$  for  $|m| \leq 50$  and the corresponding power spectral density estimate  $\hat{S}_{XX}(f)$  for  $|f| \leq \frac{1}{2}$ . Compare  $\hat{S}_{XX}(f)$  with  $S_{XX}(f)$  plotted in part (b).

**Solution**

- The Yule–Walker equations are given by

$$\begin{bmatrix} R_{XX}(0) & R_{XX}(1) & R_{XX}(2) \\ R_{XX}(1) & R_{XX}(0) & R_{XX}(1) \\ R_{XX}(2) & R_{XX}(1) & R_{XX}(0) \end{bmatrix} \begin{bmatrix} 1 \\ -1 \\ 0.6 \end{bmatrix} = \begin{bmatrix} 1 \\ 0 \\ 0 \end{bmatrix} \sigma_W^2$$

or

$$\begin{bmatrix} 1 & -1 & 0.6 \\ -1 & 1.6 & 0 \\ 0.6 & -1 & 1 \end{bmatrix} \begin{bmatrix} R_{XX}(0) \\ R_{XX}(1) \\ R_{XX}(2) \end{bmatrix} = \begin{bmatrix} 1 \\ 0 \\ 0 \end{bmatrix} \sigma_W^2$$

Solving,

$$R_{XX}(0) = 2.5641\sigma_W^2, \quad R_{XX}(1) = 1.6026\sigma_W^2, \quad R_{XX}(2) = 0.06416\sigma_W^2$$

For  $m \geq 3$ , we have

$$R_{XX}(m) = R_{XX}(m-1) - 0.6R_{XX}(m-2)$$

and finally, for  $m < 0$ , we have

$$R_{XX}(m) = R_{XX}(-m)$$

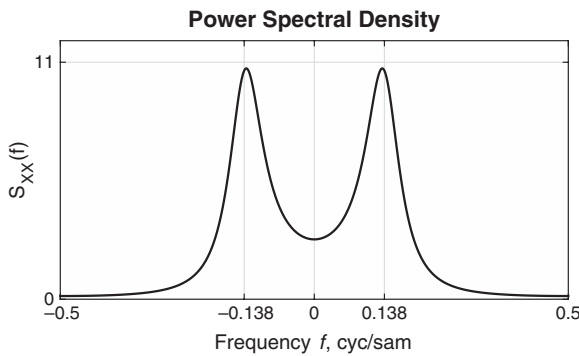


**FIGURE 14.9** Plot of power spectral density  $S_{xx}(f)$  in Example 14.5(b)

b. The  $z$ -transform of the autocorrelation  $R_{xx}(m)$ , from (14.5), is

$$\begin{aligned} S_{xx}(z) &= \sum_{m=-\infty}^{\infty} R_{xx}(m)z^{-m} = \sigma_w^2 H(z)H(z^{-1}) \\ &= \sigma_w^2 \frac{1}{(1-z^{-1}+0.6z^{-2})(1-z+0.6z^2)} \end{aligned}$$

and  $S_{xx}(f)$  is

$$S_{xx}(f) = \frac{\sigma_w^2}{|1 - e^{-j2\pi f} + 0.6e^{-j4\pi f}|^2}$$

The PSD  $S_{xx}(f)$  is plotted in Figure 14.9.

- c. The estimated autocorrelation  $\hat{R}_{xx}(m)$  and the power spectral density  $\hat{S}_{xx}(f)$  are plotted in Figure 14.10. The estimate  $\hat{S}_{xx}(f)$  is a close approximation to  $S_{xx}(f)$  shown in Figure 14.9.  $\square$

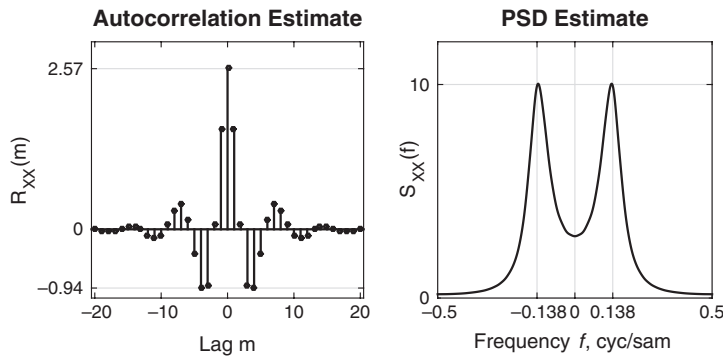


**FIGURE 14.10** Plots of the estimated autocorrelation  $\hat{R}_{xx}(m)$  and PSD  $\hat{S}_{xx}(f)$  in Example 14.5(c)

## 14.2 FORWARD AND BACKWARD LINEAR PREDICTION

---

Linear prediction is an important topic in digital signal processing, with many practical applications. In this section, we consider the problem of linearly predicting the value of a stationary random process either forward or backward in time. This formulation leads to lattice filter structures, and to some interesting connections to parametric signal models.

### 14.2.1 FORWARD LINEAR PREDICTION

Let us begin with the problem of predicting a future value of a stationary random process  $X(n)$  from observation of past values of the process. We will denote its observed values by  $x(n)$ . In particular, we consider the *one-step forward linear predictor*, which forms the prediction of the value  $x(n)$  by a weighted linear combination of the past values  $x(n - 1), x(n - 2), \dots, x(n - p)$ . Hence the linearly predicted values of  $X(n)$  is the process  $\hat{X}(n)$  with observed values given by

$$\hat{x}(n) = - \sum_{k=1}^p a_p(k)x(n - k) \quad (14.24)$$

where the  $-a_p(k)$  represent the weights in the linear combination. These weights are called the *prediction coefficients* of the one-step forward linear predictor of *order p*. (The negative sign in the definition of  $\hat{x}(n)$  is for mathematical convenience and conforms with current practice in the technical literature.)

The difference between the value of  $X(n)$  and the predicted value  $\hat{X}(n)$  is called the *forward prediction error* process, denoted by  $F_p(n)$ , with observed values given by

$$\begin{aligned} f_p(n) &= x(n) - \hat{x}(n) \\ &= x(n) + \sum_{k=1}^p a_p(k)x(n - k) \end{aligned} \quad (14.25)$$

We view linear prediction as being equivalent to linear filtering when the predictor is embedded in the linear filter, as shown in Figure 14.11. This is called a *prediction-error filter* with input sequence  $x(n)$  and output sequence  $f_p(n)$ . An equivalent realization for the prediction-error filter is shown in Figure 14.12. This realization is a direct form FIR filter with system function

$$A_p(z) = \sum_{k=0}^p a_p(k)z^{-k} \quad (14.26)$$

where, by definition,  $a_p(0) = 1$ .

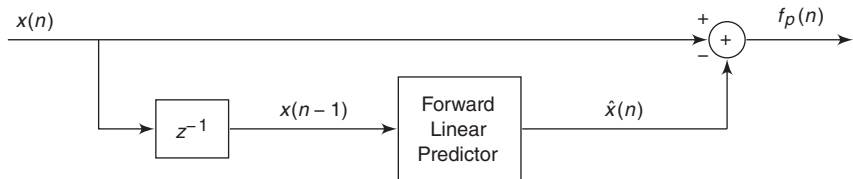


**FIGURE 14.11** Forward linear prediction

There is another realization of an FIR filter that takes the form of a lattice structure. To describe this structure and to relate it to the direct form FIR filter structure, let us begin with a predictor of order  $p = 1$ . The output of such a filter is

$$f_1(n) = x(n) + a_1(1)x(n - 1) \quad (14.27)$$

This output can be obtained from the single-stage lattice filter, illustrated in Figure 14.13, by exciting both inputs by  $x(n)$  and selecting the output from the top branch. Thus the output is exactly that given by (14.27) if we select  $K_1 = a_1(1)$ . The parameter  $K$  in the lattice filter is called a *reflection coefficient*.

Next, let us consider a predictor of order  $p = 2$ . In this case, the output of the direct form FIR filter is

$$f_2(n) = x(n) + a_2(1)x(n - 1) + a_2(2)x(n - 2) \quad (14.28)$$

By cascading two lattice stages as shown in Figure 14.14, it is possible to obtain the same output as (14.28). Indeed, the two outputs from the first stage are

$$\begin{aligned} f_1(n) &= x(n) + K_1x(n - 1) \\ g_1(n) &= K_1^*x(n) + x(n - 1) \end{aligned} \quad (14.29)$$

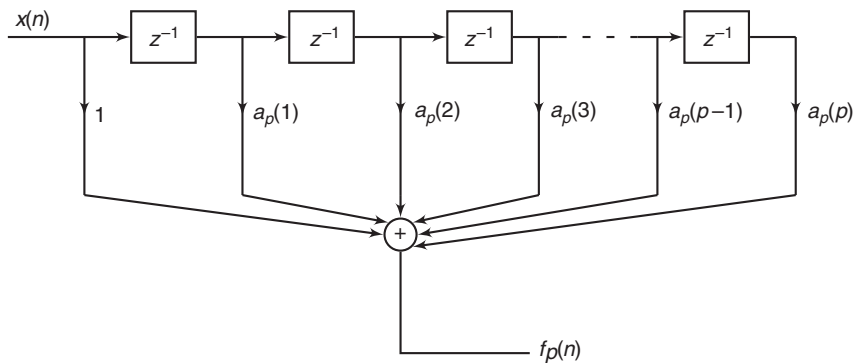


**FIGURE 14.12** Prediction-error filter

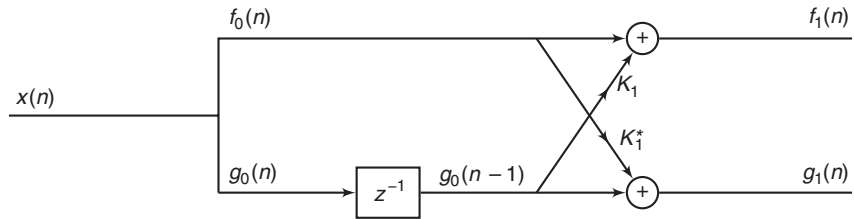


FIGURE 14.13 Single-stage lattice filter

The two outputs from the second stage are

$$\begin{aligned} f_2(n) &= f_1(n) + K_2 g_1(n-1) \\ g_2(n) &= K_2^* f_1(n) + g_1(n-1) \end{aligned} \quad (14.30)$$

If we focus our attention on  $f_2(n)$  and substitute for  $f_1(n)$  and  $g_1(n-1)$  from (14.29) into (14.30), we obtain

$$\begin{aligned} f_2(n) &= x(n) + K_1 x(n-1) + K_2 [K_1^* x(n-1) + x(n-2)] \\ &= x(n) + (K_1 + K_1^* K_2) x(n-1) + K_2 x(n-2) \end{aligned} \quad (14.31)$$

Now (14.31) is identical to the output of the direct form FIR filter given by (14.28), if we equate the coefficients. Thus

$$a_2(2) = K_2, \quad a_2(1) = K_1 + K_1^* K_2 \quad (14.32)$$

or equivalently,

$$K_2 = a_2(2), \quad K_1 = a_1(1) \quad (14.33)$$

By continuing this process, one can easily demonstrate by induction the equivalence between an  $m$ th-order direct form FIR filter and an  $m$ th-order or  $m$ -stage lattice filter. The lattice filter is generally described by the following set of *order-recursive equations*:

$$\begin{aligned} f_0(n) &= g_0(n) = x(n) \\ f_m(n) &= f_{m-1}(n) + K_m g_{m-1}(n-1), \quad m = 1, 2, \dots, p \\ g_m(n) &= K_m^* f_{m-1}(n) + g_{m-1}(n-1), \quad m = 1, 2, \dots, p \end{aligned} \quad (14.34)$$

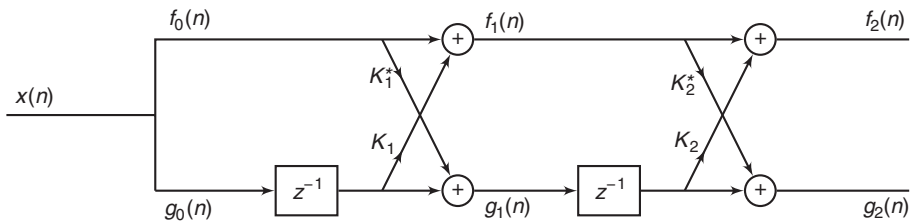
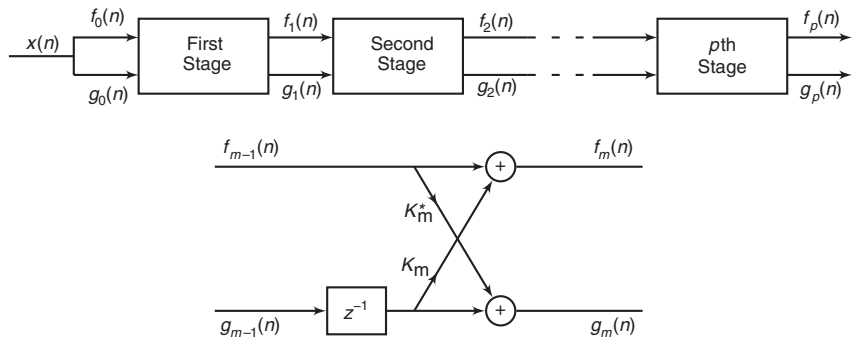


FIGURE 14.14 Two-stage lattice filter



**FIGURE 14.15** *p*-stage lattice filter

Then the output of the  $p$ -stage lattice filter is identical to the output of a  $p$ -order direct form FIR filter. Figure 14.15 illustrates a  $p$ -stage lattice filter in block-diagram form, along with a typical stage that shows the computations given by (14.34).

As a consequence of the equivalence between the direct form prediction-error FIR filter and the FIR lattice filter, the output of the  $p$ -stage lattice filter is expressed as

$$f_p(n) = \sum_{k=0}^p a_p(k)x(n-k), \quad a_p(0) = 1 \quad (14.35)$$

Since (14.35) is a convolution sum, the  $z$ -transform relationship is

$$F_p(z) = A_p(z)X(z) \quad (14.36)$$

or equivalently,

$$A_p(z) = \frac{F_p(z)}{X(z)} = \frac{F_p(z)}{F_0(z)} \quad (14.37)$$

The mean-square value of the forward linear prediction error process  $F_p(n)$  is

$$\begin{aligned} \mathcal{E}_p^f &= E[|F_p(n)|^2] \\ &= R_{XX}(0) + 2\operatorname{Re} \left[ \sum_{k=1}^p a_p^*(k)R_{XX}(k) \right] + \sum_{k=1}^p \sum_{\ell=1}^p a_p^*(\ell)a_p(k)R_{XX}(\ell-k) \end{aligned} \quad (14.38)$$

$\mathcal{E}_p^f$  is a quadratic function of the predictor coefficients, and its minimization leads to the set of linear equations

$$R_{XX}(\ell) = - \sum_{k=1}^p a_p(k)R_{XX}(\ell-k), \quad \ell = 1, 2, \dots, p \quad (14.39)$$

These are called the *normal equations* for the coefficients of the linear predictor. The minimum mean-square prediction error is simply

$$\min [\xi_p^f] \equiv E_p^f = R_{XX}(0) + \sum_{k=1}^p a_p(k)R_{XX}(-k) \quad (14.40)$$

In the following section, we extend the above development to the problem of predicting the value of a time series in the opposite direction, namely, backward in time.

- **EXAMPLE 14.6** Consider the AR(3) process generated by the equation

$$x(n) = \frac{14}{24}x(n-1) + \frac{9}{24}x(n-2) - \frac{1}{24}x(n-3) + w(n)$$

where  $w(n)$  is a sample sequence of a white noise sequence with variance  $\sigma_W^2$ .

- Determine the coefficient of the optimum  $p = 3$  linear predictor.
- Determine the autocorrelation sequence  $R_{XX}(m)$ ,  $0 \leq m \leq 5$ .

### Solution

- The coefficients of the optimum  $p = 3$  are obtained using

$$A(z) = \frac{1}{1 - \frac{14}{24}z^{-1} - \frac{9}{24}z^{-2} + \frac{1}{24}z^{-3}}$$

Thus the optimum whitening filter of order 3 will have  $z$ -transform

$$B(z) = 1 - \frac{14}{24}z^{-1} - \frac{9}{24}z^{-2} + \frac{1}{24}z^{-3}$$

- For an AR process, we have

$$R_{XX}(m) = \begin{cases} -\sum_{k=1}^p a_k R_{XX}(m-k), & m > 0 \\ -\sum_{k=1}^p a_k R_{XX}(m-k) + \sigma_W^2, & m = 0 \\ R_{XX}^*(-m), & m < 0 \end{cases}$$

Since we know the  $\{a_k\}$ , we can solve for  $R_{XX}$ ,  $m = 0, 1, 2, 3$ . Then we can obtain  $R_{XX}(m)$  for  $m > 3$ , by the previous recursions. Start with

$$\begin{bmatrix} 1 & -\frac{14}{24} & -\frac{9}{24} & \frac{1}{24} \\ -\frac{14}{24} & \frac{15}{24} & \frac{1}{24} & 0 \\ -\frac{9}{24} & -\frac{13}{24} & 1 & 0 \\ \frac{1}{24} & -\frac{9}{24} & -\frac{14}{24} & 1 \end{bmatrix} \begin{bmatrix} R_{XX}(0) \\ R_{XX}(1) \\ R_{XX}(2) \\ R_{XX}(3) \end{bmatrix} = \begin{bmatrix} \sigma_W^2 \\ 0 \\ 0 \\ 0 \end{bmatrix}$$

which gives

$$\begin{aligned} R_{XX}(0) &= 4.9377\sigma_W^2, & R_{XX}(1) &= 4.3287\sigma_W^2, \\ R_{XX}(2) &= 4.1964\sigma_W^2, & R_{XX}(3) &= 3.8654\sigma_W^2 \end{aligned}$$

Using  $R_{XX}(m) = -\sum_{k=1}^p a_k R_{XX}(m-k)$ ,  $m > 0$ , we obtain  $R_{XX}(4) = 3.65\sigma_W^2$  and  $R_{XX}(5) = 3.46\sigma_W^2$ . □

### 14.2.2 BACKWARD LINEAR PREDICTION

Let us assume that we have the data sequence  $x(n), x(n - 1), \dots, x(n - p + 1)$  from a stationary random process  $X(n)$  and we wish to predict the value  $x(n - p)$  of the process. In this case, we employ a *one-step backward linear predictor* of order  $p$ . Hence

$$\hat{x}(n - p) = - \sum_{k=0}^{p-1} b_p(k)x(n - k) \quad (14.41)$$

The difference between the value  $x(n - p)$  and the estimate  $\hat{x}(n - p)$  is called the *backward prediction error*, denoted by  $g_p(n)$ ,

$$\begin{aligned} g_p(n) &= x(n - p) + \sum_{k=0}^{p-1} b_p(k)x(n - k) \\ &= \sum_{k=0}^p b_p(k)x(n - k), \quad b_p(p) = 1 \end{aligned} \quad (14.42)$$

The backward linear predictor may be realized either by a direct form FIR filter structure similar to the structure shown in Figure 14.11, or as a lattice structure. The lattice structure shown in Figure 14.15 provides the backward as well as the forward linear predictor. To prove this point, let us consider the output of this lattice filter from the lower branch. This output is given as

$$g_1(n) = K_1^*x(n) + x(n - 1) \quad (14.43)$$

Hence the weighting coefficient of the backward predictor is  $b_1(0) = K_1^*$ .

In the two-stage lattice shown in Figure 14.14, the output of the second stage from the bottom branch is

$$g_2(n) = K_2^*f_1(n) + g_1(n - 1) \quad (14.44)$$

If we substitute from (14.29) for  $f_1(n)$  and  $g_1(n - 1)$ , we obtain

$$g_2(n) = K_2^*x(n) + (K_1^* + K_1 K_2^*)x(n - 1) + x(n - 2) \quad (14.45)$$

Hence the weighting coefficients in the backward linear predictor are identical to the (complex conjugate) coefficients for the forward linear predictor, but they occur in reverse order. Thus we have

$$b_p(k) = a_p^*(p - k), \quad k = 0, 1, \dots, p \quad (14.46)$$

In the  $z$ -domain, the convolution sum in (14.42) becomes

$$G_p(z) = B_p(z)X(z) \quad (14.47)$$

or equivalently,

$$B_p(z) = \frac{G_p(z)}{X(z)} = \frac{G_p(z)}{G_0(z)} \quad (14.48)$$

where  $B_p(z)$  represents the system function of the FIR filter with coefficients  $b_p(k)$ .

Since  $b_p(k) = a_p^*(p - k)$ ,  $B_p(z)$  is related to  $A_p(z)$  as follows:

$$\begin{aligned} B_p(z) &= \sum_{k=0}^p b_p(k)z^{-k} = \sum_{k=0}^p a_p^*(p - k)z^{-k} \\ &= z^{-p} \sum_{k=0}^p a_p^*(k)z^k = z^{-p} A_p^*(z^{-1}) \end{aligned} \quad (14.49)$$

The relationship in (14.49) implies that the zeros of the FIR filter with system function  $B_p(z)$  are simply the (conjugate) reciprocals of the zeros of  $A_p(z)$ . Hence  $B_p(z)$  is called the reciprocal or *reverse polynomial* of  $A_p(z)$ .

Finally, let us consider the minimization of the mean-square error in a backward linear predictor. The backward prediction-error process is denoted by  $G_p(n)$  with sample sequence  $g_p(n)$  given by

$$\begin{aligned} g_p(n) &= x(n - p) + \sum_{k=0}^{p-1} b_p(k)x(n - k) \\ &= x(n - p) + \sum_{k=1}^p a_p^*(k)x(n - p + k) \end{aligned} \quad (14.50)$$

and its mean-square value given by

$$\mathcal{E}_p^b = E[|G_p(n)|^2] \quad (14.51)$$

The minimization of  $\mathcal{E}_p^b$  with respect to the prediction coefficients yields the same set of linear equations as in (14.39). Hence, the minimum mean-square error is

$$\min[\mathcal{E}_p^b] \equiv E_p^b = E_p^f \quad (14.52)$$

which is given by (14.40).

### 14.2.3 CONVERSIONS BETWEEN FIR FILTER COEFFICIENTS AND LATTICE REFLECTION COEFFICIENTS

Now that we have established these interesting relationships between the direct form FIR filter and the FIR lattice filter, let us return to the

recursive lattice equations in (14.34) and transform them to the  $z$ -domain. Thus we have

$$F_0(z) = G_0(z) = X(z) \quad (14.53a)$$

$$F_m(z) = F_{m-1}(z) + K_m z^{-1} G_{m-1}(z), \quad m = 1, 2, \dots, p \quad (14.53b)$$

$$G_m(z) = K_m^* F_{m-1}(z) + z^{-1} G_{m-1}(z), \quad m = 1, 2, \dots, p \quad (14.53c)$$

If we divide each equation by  $X(z)$ , we obtain the desired results in the form

$$A_0(z) = B_0(z) = 1 \quad (14.54a)$$

$$A_m(z) = A_{m-1}(z) + K_m z^{-1} B_{m-1}(z), \quad m = 1, 2, \dots, p \quad (14.54b)$$

$$B_m(z) = K_m^* A_{m-1}(z) + z^{-1} B_{m-1}(z), \quad m = 1, 2, \dots, p \quad (14.54c)$$

Thus a lattice filter is described in the  $z$ -domain by the matrix equation

$$\begin{bmatrix} A_m(z) \\ B_m(z) \end{bmatrix} = \begin{bmatrix} 1 & K_m z^{-1} \\ K_m^* & z^{-1} \end{bmatrix} \begin{bmatrix} A_{m-1}(z) \\ B_{m-1}(z) \end{bmatrix} \quad (14.55)$$

The relations in (14.54) for  $A_m(z)$  and  $B_m(z)$  allow us to obtain the direct form FIR filter coefficients  $a_m(k)$  from the reflection coefficients  $K_m$ , and vice versa. We illustrate the procedure in the following example.

- EXAMPLE 14.7** Given a three-stage lattice filter with coefficients  $K_1 = \frac{1}{4}$ ,  $K_2 = \frac{1}{2}$ ,  $K_3 = \frac{1}{3}$ , determine the FIR filter coefficients for the direct form structure.

### Solution

We solve the problem recursively, beginning with (14.54) for  $m = 1$ . Thus we have

$$\begin{aligned} A_1(z) &= A_0(z) + K_1 z^{-1} B_0(z) = 1 + K_1 z^{-1} \\ &= 1 + \frac{1}{4} z^{-1} \end{aligned}$$

Hence the coefficients of an FIR filter corresponding to the single-stage lattice are  $a_1(0) = 1$ ,  $a_1(1) = K_1$ . Since  $B_m(z)$  is the reverse polynomial of  $A_m(z)$ , we have

$$B_1(z) = \frac{1}{4} + z^{-1}$$

Next, we add the second stage to the lattice. For  $m = 2$ , (14.54) yields

$$\begin{aligned} A_2(z) &= A_1(z) + K_2 z^{-1} B_1(z) \\ &= 1 + \frac{3}{8} z^{-1} + \frac{1}{2} z^{-2} \end{aligned}$$

Hence the FIR filter parameters corresponding to the two-stage lattice are  $a_2(0) = 1$ ,  $a_2(1) = \frac{3}{8}$ , and  $a_2(2) = \frac{1}{2}$ . Also,

$$B_2(z) = \frac{1}{2} + \frac{3}{8} z^{-1} + z^{-2}$$

Finally, the addition of the third stage to the lattice results in the polynomial

$$\begin{aligned} A_3(z) &= A_2(z) + K_3 z^{-1} B_2(z) \\ &= 1 + \frac{13}{24} z^{-1} + \frac{5}{8} z^{-2} + \frac{1}{3} z^{-3} \end{aligned}$$

Consequently, the desired direct form FIR filter is characterized by the coefficients

$$a_3(0) = 1, \quad a_3(1) = \frac{13}{24}, \quad a_3(2) = \frac{5}{8}, \quad a_3(3) = \frac{1}{3}$$

□

As this example illustrates, the lattice structure with parameters  $K_1, K_2, \dots, K_p$  corresponds to a class of  $p$  direct form FIR filters with system functions  $A_1(z), A_2(z), \dots, A_p(z)$ . It is interesting to note that a characterization of this class of  $p$  FIR filters in direct form requires  $p(p+1)/2$  filter coefficients. In contrast, the lattice form characterization requires only the  $p$  reflection coefficients  $\{K_i\}$ . The reason that the lattice provides a more compact representation for the class of  $p$  FIR filters is that appending stages to the lattice does not alter the parameters of the previous stages. On the other hand, appending the  $p$ th stage to a lattice with  $(p-1)$  stages results in an FIR filter with system function  $A_p(z)$  that has coefficients totally different from the coefficients of the lower-order FIR filter with system function  $A_{p-1}(z)$ .

A formula for recursively determining the filter coefficients  $a_p(k)$ ,  $1 \leq k \leq p$ , can be derived easily from polynomial relationships (14.54). We have

$$A_m(z) = A_{m-1}(z) + K_m z^{-1} B_{m-1}(z) \quad (14.56a)$$

$$\sum_{k=0}^m a_m(k) z^{-k} = \sum_{k=0}^{m-1} a_{m-1}(k) z^{-k} + K_m \sum_{k=0}^{m-1} a_{m-1}^*(m-1-k) z^{-(k+1)} \quad (14.56b)$$

By equating the coefficients of equal powers of  $z^{-1}$ , and recalling that  $a_m(0) = 1$  for  $m = 1, 2, \dots, p$ , we obtain the desired recursive equation for the FIR filter coefficients in the form

$$\begin{aligned} a_m(0) &= 1 \\ a_m(m) &= K_m \\ \vdots &\quad \vdots \\ a_m(k) &= a_{m-1}(k) + K_m a_{m-1}^*(m-k) \\ &= a_{m-1}(k) + a_m(m) a_{m-1}^*(m-k), \quad 1 \leq k \leq m-1, \quad m = 1, 2, \dots, p \end{aligned} \quad (14.57)$$

**MATLAB Implementation** The following MATLAB function, `latc2fir`, implements (14.56a). Note that the product  $K_m z^{-1} B_{m-1}(z)$  is obtained by convolving the two corresponding arrays, whereas the polynomial  $B_m(z)$  is obtained by using a `fliplr` operation on the  $A_m(z)$  polynomial.

```
function [a] = latc2fir(K,a0)
% Lattice form to FIR direct form conversion
%
% -----
% [a] = latc2fir(K,b0)
% a = FIR direct form coefficients (prediction coefficients)
% K = lattice filter coefficients (reflection coefficients)
% a0 = overall gain if \= 1 (optional)
%
if nargin == 1
    a0 = 1;
end
p = length(K);
B = 1; A = 1;
for m=1:1:p
    A = [A,0]+conv([0,K(m)],B);
    B = fliplr(A);
end
a = a0*A;
end
```

To verify the `latc2fir` function, consider the lattice reflection coefficients used in Example 14.7 above:

```
>> K = [1/4,1/2,1/3];
>> a = latc2fir(K)
a =
    1           13/24          5/8           1/3
```

Clearly, we obtain the same FIR filter coefficients.

The formula for conversion from the direct form FIR filter coefficients  $a_p(k)$  to the lattice reflection coefficients  $K_i$  is also very simple. For the  $p$ -stage lattice, we immediately obtain the reflection coefficient  $K_p = a_p(p)$ . To obtain  $K_{p-1}, \dots, K_1$ , we need the polynomials  $A_m(z)$  for  $m = p - 1, \dots, 1$ . From (14.55), we obtain

$$A_{m-1}(z) = \frac{A_m(z) - K_m B_m(z)}{1 - |K_m|^2}, \quad m = p, \dots, 1 \quad (14.58)$$

which is just a step-down recursion. Thus we compute all lower-degree polynomials  $A_m(z)$  beginning with  $A_{p-1}(z)$  and obtain the desired lattice

reflection coefficients from the relation  $K_m = a_m(m)$ . We observe that the procedure works as long as  $K_m \neq 1$  for  $m = 1, 2, \dots, p - 1$ . From this step-down recursion for the polynomials, it is relatively easy to obtain a formula for recursively and directly computing  $K_m, m = p - 1, \dots, 1$ . For  $m = p - 1, \dots, 1$ , we have

$$\begin{aligned} K_m &= a_m(m) \\ a_{m-1}(k) &= \frac{a_m(k) - K_m b_m(k)}{1 - |K_m|^2} \\ &= \frac{a_m(k) - a_m(m)a_m^*(m-k)}{1 - |a_m(m)|^2} \end{aligned} \quad (14.59)$$

which is just the recursion in the Schur–Cohn stability test for the polynomial  $A_m(z)$ .

**MATLAB Implementation** Given the coefficients  $\{a_p(k)\}$  of the direct form, we can obtain the lattice filter coefficients  $\{K_i\}$  using (14.58) and (14.59). This is done by the following MATLAB function, `fir2latc`. Note that the equation to compute  $B_m(z)$  in (14.58) implies that the polynomial  $B_m(z)$  is a `fliplr` operation on the  $A_m(z)$  polynomial.

```
function [K,a0] = fir2latc(a)
% FIR Direct form to All-Zero Lattice form Conversion
%
% -----
% [K,a0] = fir2latc(b)
%   K = lattice filter coefficients (reflection coefficients)
%   a0 = first coefficient (or gain) of A(z), useful if \leq 1
%   a = FIR direct form coefficients (prediction coefficients)
p = length(a)-1;
K = zeros(1,p);
a0 = a(1);
if a0 == 0
    error('a(1) is equal to zero')
end
A = a/a0;
for m=p+1:-1:2
    K(m-1) = A(m);
    B = fliplr(A);
    A = (A-K(m-1)*B)/(1-K(m-1)*K(m-1));
    A = A(1:m-1);
end
end
```

Finally, the lattice filter can be implemented using (14.34), which is done by the `latcfilt` function, as shown here.

```

function [y] = latcfilter(K,x,a0)
% LATTICE form realization of FIR filters
%
% -----
% y = latcfilter(K,x,a0)
%   y = output sequence
%   K = LATTICE filter (reflection) coefficient array
%   x = input sequence
%   a0 = Overall Gain (optional)
%
if nargin == 1
    a0 = 1;
end
Nx = length(x)-1;
x = a0*x;
p = length(K); %K = K(2:M+1);
fg = [x; [0 x(1:Nx)]];
for m = 1:p
    fg = [1,K(m);K(m),1]*fg;
    fg(2,:) = [0 fg(2,1:Nx)];
end
y = fg(1,:);
end

```

The SP Toolbox provides several functions that are similar in functionality to the functions developed in this section. The function  $K = \text{tf2latc}(a)$  computes the FIR lattice reflection coefficients in array  $K$  given the FIR filter (or prediction) coefficients in array  $a$ , normalized by  $a(1)$ . Similarly, the function  $a = \text{latc2tf}(K)$  produces a general FIR filter coefficient array  $a$  from the lattice reflection coefficients in  $K$  with  $a(1)=1$ . Finally, the function  $[f,g] = \text{latcfilt}(K,x)$  implements the lattice filter shown in Figure 14.15. It filters the input array  $x$  with the FIR lattice coefficients in the array  $K$ . The forward lattice filter output (or forward prediction error) is in array  $f$ , and the backward lattice filter output (or backward prediction error) is in array  $g$ . If  $|K| \leq 1$ ,  $f$  corresponds to the minimum-phase output and  $g$  corresponds to the maximum-phase output (see Section 14.4).

- EXAMPLE 14.8** An FIR filter is characterized by its system function

$$H(z) \equiv A_3(z) = 1 + \frac{13}{24}z^{-1} + \frac{5}{8}z^{-2} + \frac{1}{3}z^{-3}$$

Determine the lattice coefficients and sketch the lattice filter structure corresponding to the FIR filter.

**Solution**

We follow the step-down procedure given in (14.58).

- $m = 3$ :

$$A_3(z) = 1 + \frac{13}{24}z^{-1} + \frac{5}{8}z^{-2} + \frac{1}{3}z^{-3}, \quad K_3 = \frac{1}{3}$$

$$B_3(z) = \frac{1}{3} + \frac{5}{8}z^{-1} + \frac{13}{24}z^{-2} + z^{-3}.$$

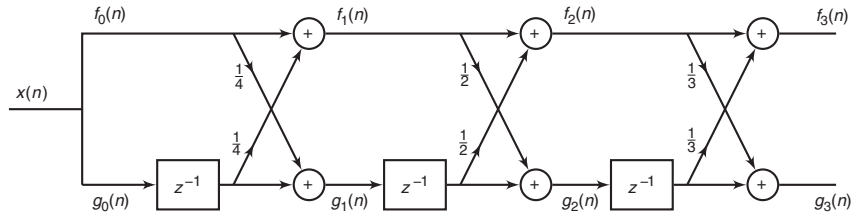


FIGURE 14.16 Lattice filter diagram in Example 14.8

- $m = 2$ :

$$A_2(z) = \frac{A_3(z) - K_3 B_3(z)}{1 - K_3^2} = 1 + \frac{3}{8}z^{-1} + \frac{1}{2}z^{-2}, \quad K_2 = \frac{1}{2}$$

$$B_2(z) = \frac{1}{2} + \frac{3}{8}z^{-1} + z^{-3}.$$

- $m = 1$ :

$$A_1(z) = \frac{A_2(z) - K_2 B_2(z)}{1 - K_2^2} = 1 + \frac{1}{4}z^{-1}, \quad K_1 = \frac{1}{4}$$

We can also use the `fir2latc` function:

```
>> a = [1,13/24,5/8,1/3];
>> [K] = fir2latc(a)
K =
    1/4           1/2           1/3
```

The resulting lattice filter structure is shown in Figure 14.16. □

□ **EXAMPLE 14.9** The reflection coefficient of an FIR lattice filter are

$$K_1 = \frac{1}{2}, \quad K_2 = -\frac{1}{3}, \quad K_3 = 1$$

- Determine the system function  $H(z)$  of the FIR filter.
- Determine the zeros of the FIR filter and sketch the pattern in the  $z$ -plane.
- Repeat when  $K_3 = -1$ . Comment your results.

**Solution**

- The system function is obtained using the following steps:

$$A_1(z) = 1 + K_1 z^{-1} = 1 + \frac{1}{2}z^{-1},$$

$$B_1(z) = \frac{1}{2} + z^{-1},$$

$$A_2(z) = A_1(z) + K_2 B_1(z)z^{-1} = 1 + \frac{1}{3}z^{-1} - \frac{1}{3}z^{-2},$$

$$B_2(z) = -\frac{1}{3} + \frac{1}{3}z^{-1} + z^{-2},$$

$$H(z) = A_3(z) = A_2(z) + K_3 z^{-1} B_2(z) = 1 + z^{-3}$$

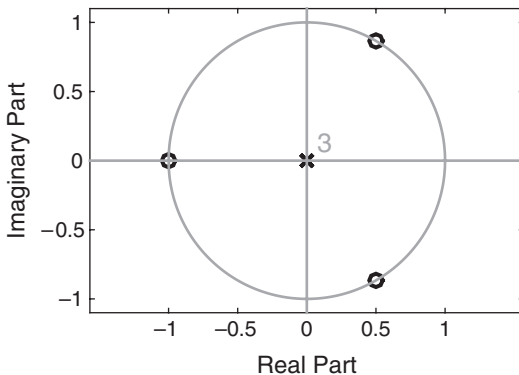


**FIGURE 14.17** Pole-zero plot in Example 14.9(b)

Use of the `latc2fir` function gives

```
>> K = [1/2,-1/3,1];
>> a = latc2fir(K)
a =
    1.0000    0.0000    0.0000    1.0000
```

- b. The zeros are located at  $z_1 = -1$  and at  $z_{2,3} = e^{\pm j\pi/3}$ . The pole-zero plot is shown in Figure 14.17.
- c. If  $K_3 = -1$ , then we have

$$H(z) = A_2(z) - z^{-1}B_2(z) = 1 + \frac{2}{3}z^{-1} - \frac{2}{3}z^{-2} - z^{-3}$$

Use of the `latc2fir` function gives

```
>> K = [1/2,-1/3,-1];
>> a = latc2fir(K)
a =
    1.0000    0.6667   -0.6667   -1.0000
>> zeros = roots(a)'; mag_zeros = abs(zeros)
mag_zeros =
    1.0000    1.0000    1.0000
>> pha_zeros = angle(zeros)/pi
pha_zeros =
    0    -0.8136    0.8136
```

The zeros are then located at  $z_1 = 1$ ,  $z_{2,3} = e^{\pm j0.8136\pi}$ . The pole-zero plot is shown in Figure 14.18.  $\square$

As indicated previously, the recursive equation in (14.59) breaks down if any of the lattice parameters  $|K_m| = 1$ . If this occurs, it is indicative that

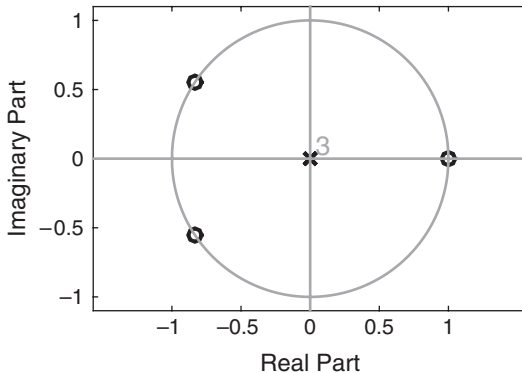


**FIGURE 14.18** Pole-zero plot in Example 14.9(c)

the polynomial  $A_{m-1}(z)$  has a root located on the unit circle. This was clearly evident in Figures 14.17 and 14.18. Such a root may be factored out from  $A_{m-1}(z)$ , and the iterative process in (14.59) can be carried out for the reduced-order system.

- **EXAMPLE 14.10** Use the recursive equation (14.59) to determine the FIR lattice filter parameters for the AR(3) process given in Example 14.6.

**Solution** In this case,  $p = 3$  and  $a_3(3) = \frac{1}{24}$ ,  $a_3(2) = -\frac{9}{24}$ ,  $a_3(1) = -\frac{14}{24}$ . The recursive equation for the reflection coefficient is

$$a_{m-1}(k) = \frac{a_m(k) - a_m(m)a^*(m-k)}{1 - |a_m(m)|^2}, \quad m = p-1, \dots, 1$$

with  $K_m = a_m(m)$ .

From these, we obtain the reflection coefficient  $K_3 = 0.0417$ ,  $K_2 = -0.3513$ , and  $K_1 = -0.8767$ . For verification, we use

```
>> a = [1,-14/24,-9/24,1/24];
>> K = dir2latc(a)
K =
    1.0000   -0.8767   -0.3513    0.0417
```

□

#### 14.2.4 OPTIMUM REFLECTION COEFFICIENTS FOR THE LATTICE FORWARD AND BACKWARD PREDICTORS

In Sections 14.2.1 and 14.2.2, we derived the set of linear equations that provide the predictor coefficients that minimize the mean-square value of

the prediction error. In this section, we consider the problem of optimizing the reflection coefficients in the lattice predictor.

The forward prediction error process in the lattice filter is expressed as

$$\mathsf{F}_m(n) = \mathsf{F}_{m-1}(n) + K_m \mathsf{G}_{m-1}(n-1) \quad (14.60)$$

The minimization of  $E[|\mathsf{F}_m(n)|^2]$  with respect to the reflection coefficient  $K_m$  yields the result

$$K_m = \frac{-E[\mathsf{F}_{m-1}(n)\mathsf{G}_{m-1}^*(n-1)]}{E[|\mathsf{G}_{m-1}(n-1)|^2]} \quad (14.61)$$

or equivalently,

$$K_m = \frac{-E[\mathsf{F}_{m-1}(n)\mathsf{G}_{m-1}^*(n-1)]}{\sqrt{E_{m-1}^f E_{m-1}^b}} \quad (14.62)$$

where

$$E_{m-1}^f = E_{m-1}^b = E[|\mathsf{G}_{m-1}(n-1)|^2] = E[|\mathsf{F}_{m-1}(n)|^2]$$

We observe that the optimum choice of the reflection coefficients in the lattice predictor is the negative of the (normalized) cross-correlation coefficients between the forward and backward errors in the lattice.<sup>3</sup> Since it is apparent from (14.61) that  $|K_m| \leq 1$ , it follows that the minimum mean-square value of the prediction error, which may be expressed recursively as

$$E_m^f = (1 - |K_m|^2) E_{m-1}^f \quad (14.63)$$

is a monotonically decreasing sequence.

#### 14.2.5 RELATIONSHIP OF AN AR PROCESS TO LINEAR PREDICTION

The parameters of an AR( $p$ ) process are intimately related to a predictor of order  $p$  for the same process. To see the relationship, we recall that in an AR( $p$ ) process, the autocorrelation sequence  $R_{XX}(m)$  is related to the parameters  $a_k$  by the Yule–Walker equations given in (14.19) or (14.20). The corresponding equations for the predictor of order  $p$  are given by (14.39) and (14.40).

A direct comparison of these two sets of relations reveals that there is a one-to-one correspondence between the parameters  $a_k$  of the AR( $p$ )

<sup>3</sup>The normalized cross-correlation coefficients between the forward and backward error in the lattice (i.e.,  $-K_m$ ) are often called the *partial correlation* (PARCOR) coefficients.

process and the predictor coefficients  $a_p(k)$  of the  $p$ th-order predictor. In fact, if the underlying process  $x(n)$  is AR( $p$ ), the prediction coefficients of the  $p$ th-order predictor will be identical to  $a_k$ . Furthermore, the minimum MSE in the  $p$ th-order predictor  $E_p^f$  will be identical to  $\sigma_W^2$ , the variance of the white noise process. In this case, the prediction-error filter is a noise-whitening filter that produces the innovations sequence  $W(n)$ .

- EXAMPLE 14.11** In Section 14.2.5, we indicated that the noise-whitening filter  $A_p(z)$  for a causal AR( $p$ ) process is a forward linear prediction-error filter of order  $p$ . Show that the backward linear prediction-error filter of order  $p$  is the noise-whitening filter of the corresponding anticausal AR( $p$ ) process.

**Solution**

For the backward linear prediction-error filter,

$$\hat{x}(n-p) = -\sum_{k=0}^{p-1} b_p(k)x(n-k) \quad \text{where} \quad b_p(k) = a_p^*(p-k), \quad k = 0, \dots, p$$

Thus

$$\begin{aligned} \hat{x}(n-p) &= -\sum_{k=0}^{p-1} a_p^*(p-k)x(n-k) \quad \text{set} \quad p-k=l \\ &= -\sum_{l=1}^p a_p^*(l)x(n-p+l) = \{x(n-p+1), \dots, x(n)\} \\ &\quad * \{a_p^*(-p), \dots, a_p^*(-1)\} \end{aligned}$$

that is, the convolution of  $\{x(n)\}$  with the anticausal sequence  $\{a_p^*(-p), \dots, a_p^*(-1)\}$ .  $\square$

### 14.3 SOLUTION OF THE NORMAL EQUATIONS

---

In the previous section, we observed that the minimization of the mean-square value of the forward prediction error resulted in a set of linear equations for the coefficients of the predictor given by (14.39). These equations, called the *normal equations*, may be expressed in the compact form

$$\sum_{k=0}^p a_p(k)R_{xx}(\ell-k) = 0, \quad \ell = 1, 2, \dots, p, \quad a_p(0) = 1 \quad (14.64)$$

The resulting minimum MSE (MMSE) is given by (14.40). If we augment (14.40) to the normal equations given by (14.64), we obtain

the set of augmented normal equations, which may be expressed as

$$\sum_{k=0}^p a_p(k) R_{XX}(\ell - k) = \begin{cases} E_p^f, & \ell = 0 \\ 0, & \ell = 1, 2, \dots, p \end{cases} \quad (14.65)$$

We also noted that if the random process is an AR( $p$ ) process, the MMSE  $E_p^f = \sigma_W^2$ . In this section, we describe two computationally efficient algorithms for solving the normal equations. The Levinson–Durbin algorithm, originally due to Levinson [54] and modified by Durbin [14], is suitable for serial processing and has a computation complexity of  $O(p^2)$ . The second algorithm, due to Schur [88], also computes the reflection coefficients in  $O(p^2)$  operations, but with parallel processors the computations can be performed in  $O(p)$  time units. Both algorithms exploit the Toeplitz symmetry property inherent in the autocorrelation matrix. We begin by describing the Levinson–Durbin algorithm.

#### 14.3.1 LEVINSON–DURBIN ALGORITHM

The Levinson–Durbin algorithm is a computationally efficient algorithm for solving the normal equations in (14.64) for the prediction coefficients. This algorithm exploits the special symmetry in the autocorrelation matrix

$$\mathbf{T}_p = \begin{bmatrix} R_{XX}(0) & R_{XX}^*(1) & \cdots & R_{XX}^*(p-1) \\ R_{XX}(1) & R_{XX}(0) & \cdots & R_{XX}^*(p-2) \\ \vdots & \vdots & & \vdots \\ R_{XX}(p-1) & R_{XX}(p-2) & \cdots & R_{XX}(0) \end{bmatrix} \quad (14.66)$$

Note that  $\mathbf{T}_p(i, j) = \mathbf{T}_p(i - j)$ , so that the autocorrelation matrix is a Toeplitz matrix. Since  $\mathbf{T}_p(i, j) = \mathbf{T}_p^*(j, i)$ , the matrix is also Hermitian.

The key to the Levinson–Durbin solution method, which exploits the Toeplitz property of the matrix, is to proceed recursively, beginning with a predictor of order  $m = 1$  (one coefficient), we increase the order recursively, using the lower-order solutions to obtain the solution to the next-higher order. Thus the solution to the first-order predictor, obtained by solving (14.64), is

$$a_1(1) = -\frac{R_{XX}(1)}{R_{XX}(0)} \quad (14.67)$$

and the resulting MMSE is

$$\begin{aligned} E_1^f &= R_{XX}(0) + a_1(1)R_{XX}(-1) \\ &= R_{XX}(0) \left[ 1 - |a_1(1)|^2 \right] \end{aligned} \quad (14.68)$$

Recall that  $a_1(1) = K_1$ , the first reflection coefficient in the lattice filter.

The next step is to solve for the coefficients  $a_2(1)$ ,  $a_2(2)$  of the second-order predictor and express the solution in terms of  $a_1(1)$ . The two equations obtained from (14.64) are

$$\begin{aligned} a_2(1)R_{XX}(0) + a_2(2)R_{XX}^*(1) &= -R_{XX}(1) \\ a_2(1)R_{XX}(1) + a_2(2)R_{XX}^*(0) &= -R_{XX}(2) \end{aligned} \quad (14.69)$$

By using the solution in (14.67) to eliminate  $R_{XX}(1)$ , we obtain the solution

$$\begin{aligned} a_2(2) &= -\frac{R_{XX}(2) + a_1(1)R_{XX}(1)}{R_{XX}(0) \left[ 1 - |a_1(1)|^2 \right]} \\ &= -\frac{R_{XX}(2) + a_1(1)R_{XX}(1)}{E_1^f} \\ a_2(1) &= a_1(1) + a_2(2)a_1^*(1) \end{aligned} \quad (14.70)$$

Thus we have obtained the coefficients of the second-order predictor. Again, we note that  $a_2(2) = K_2$ , the second reflection coefficient in the lattice filter.

Proceeding in this manner, we may express the coefficients of the  $m$ th-order predictor in terms of the coefficients of the  $(m-1)$ th-order predictor. Thus we may write the coefficient vector  $\mathbf{a}_m$  as the sum of two vectors, namely,

$$\mathbf{a}_m = \begin{bmatrix} a_m(1) \\ a_m(2) \\ \vdots \\ a_m(m) \end{bmatrix} = \begin{bmatrix} \mathbf{a}_{m-1} \\ \dots \\ 0 \end{bmatrix} + \begin{bmatrix} \mathbf{d}_{m-1} \\ \dots \\ K_m \end{bmatrix} \quad (14.71)$$

where  $\mathbf{a}_{m-1}$  is the predictor coefficient vector of the  $(m-1)$ th-order predictor and the vector  $\mathbf{d}_{m-1}$  and the scalar  $K_m$  are to be determined. Let us also partition the  $m \times m$  autocorrelation matrix  $\mathbf{T}_m$  as

$$\mathbf{T}_m = \begin{bmatrix} \mathbf{T}_{m-1} & \mathbf{R}_{m-1}^{b*} \\ \mathbf{R}_{m-1}^b & R_{XX}(0) \end{bmatrix} \quad (14.72)$$

where  $\mathbf{R}_{m-1}^b = [R_{XX}(m-1) R_{XX}(m-2) \dots R_{XX}(1)] = (\mathbf{R}_{m-1}^b)^t$ , the asterisk (\*) denotes the complex conjugate,  $\mathbf{R}_m^t$  denotes the transpose of  $\mathbf{R}_m$ , and the superscript b on  $\mathbf{R}_{m-1}$  denotes the vector  $\mathbf{R}_{m-1}^t = [R_{XX}(1) R_{XX}(2) \dots R_{XX}(m-1)]$ , with elements taken in reverse order.

The solution to the equation  $\mathbf{T}_m \mathbf{a}_m = -\mathbf{R}_m$  may be expressed as

$$\begin{bmatrix} \mathbf{T}_{m-1} & \mathbf{R}_{m-1}^{b*} \\ \mathbf{R}_{m-1}^b & R_{XX}(0) \end{bmatrix} \left( \begin{bmatrix} \mathbf{a}_{m-1} \\ 0 \end{bmatrix} + \begin{bmatrix} \mathbf{d}_{m-1} \\ K_m \end{bmatrix} \right) = - \begin{bmatrix} \mathbf{R}_{m-1} \\ R_{XX}(m) \end{bmatrix} \quad (14.73)$$

This is the key step in the Levinson–Durbin algorithm. From (14.73), we obtain two equations,

$$\mathbf{T}_{m-1}\mathbf{a}_{m-1} + \mathbf{T}_{m-1}\mathbf{d}_{m-1} + K_m \mathbf{R}_{m-1}^{\text{b}*} = -\mathbf{R}_{m-1} \quad (14.74)$$

$$\mathbf{R}_{m-1}^{\text{bt}} \mathbf{a}_{m-1} + \mathbf{R}_{m-1}^{\text{bt}} \mathbf{d}_{m-1} + K_m \mathbf{R}_{\mathbf{XX}}(0) = -R_{\mathbf{XX}}(m) \quad (14.75)$$

Since  $\mathbf{T}_{m-1}\mathbf{a}_{m-1} = -\mathbf{R}_{m-1}$ , (14.74) yields the solution

$$\mathbf{d}_{m-1} = -K_m \mathbf{T}_{m-1}^{-1} \mathbf{R}_{m-1}^{\text{b}*} \quad (14.76)$$

But  $\mathbf{R}_{m-1}^{\text{b}*}$  is just  $\mathbf{R}_{m-1}$  with elements taken in reverse order and conjugated; therefore, the solution in (14.76) is simply

$$\mathbf{d}_{m-1} = K_m \mathbf{a}_{m-1}^{\text{b}*} = K_m \begin{bmatrix} a_{m-1}^*(m-1) \\ a_{m-1}^*(m-2) \\ \vdots \\ a_{m-1}^*(1) \end{bmatrix} \quad (14.77)$$

The scalar equation (14.75) can now be used to solve for  $K_m$ . If we eliminate  $\mathbf{d}_{m-1}$  in (14.75), we obtain

$$K_m [R_{\mathbf{XX}}(0) + \mathbf{R}_{m-1}^{\text{bt}} \mathbf{a}_{m-1}^{\text{b}*}] + \mathbf{R}_{m-1}^{\text{bt}} \mathbf{a}_{m-1} = -R_{\mathbf{XX}}(m)$$

Hence

$$K_m = -\frac{R_{\mathbf{XX}}(m) + \mathbf{R}_{m-1}^{\text{bt}} \mathbf{a}_{m-1}}{R_{\mathbf{XX}}(0) + \mathbf{R}_{m-1}^{\text{bt}} \mathbf{a}_{m-1}^{\text{b}*}} \quad (14.78)$$

Therefore, by substituting the solutions in (14.77) and (14.78) into (14.71), we obtain the desired recursion for the predictor coefficients in the Levinson–Durbin algorithm as

$$a_m(m) = K_m = -\frac{R_{\mathbf{XX}}(m) + \mathbf{R}_{m-1}^{\text{bt}} \mathbf{a}_{m-1}}{R_{\mathbf{XX}}(0) + \mathbf{R}_{m-1}^{\text{bt}} \mathbf{a}_{m-1}^{\text{b}*}} = -\frac{R_{\mathbf{XX}}(m) + \mathbf{R}_{m-1}^{\text{bt}} \mathbf{a}_{m-1}}{E_{m-1}^f} \quad (14.79)$$

$$\begin{aligned} a_m(k) &= a_{m-1}(k) + K_m a_{m-1}^*(m-k) \\ &= a_{m-1}(k) + a_m(m) a_{m-1}^*(m-k), \quad k = 1, 2, \dots, m-1 \\ &\quad m = 1, 2, \dots, p \end{aligned} \quad (14.80)$$

Note that the recursive relation in (14.80) is identical to the recursive relation in (14.57) for the predictor coefficients, which was obtained from the polynomials  $A_m(z)$  and  $B_m(z)$ . Furthermore,  $K_m$  is the reflection coefficient in the  $m$ th-stage of the lattice predictor. This development clearly illustrates that the Levinson–Durbin algorithm produces the reflection coefficients for the optimum lattice predictor as well as the coefficients of the optimum direct form FIR predictor.

Finally, let us determine the expression for the MMSE. For the  $m$ th-order predictor, we have

$$\begin{aligned}
 E_m^f &= R_{\mathbf{X}\mathbf{X}}(0) + \sum_{k=1}^m a_m(k)R_{\mathbf{X}\mathbf{X}}(-k) \\
 &= R_{\mathbf{X}\mathbf{X}}(0) + \sum_{k=1}^m [a_{m-1}(k) + a_m(m)a_{m-1}^*(m-k)]R_{\mathbf{X}\mathbf{X}}(-k) \\
 &= E_{m-1}^f[1 - |a_m(m)|^2] = E_{m-1}^f \left(1 - |K_m|^2\right) \quad m = 1, 2, \dots, p
 \end{aligned} \tag{14.81}$$

where  $E_0^f = R_{\mathbf{X}\mathbf{X}}(0)$ . Since the reflection coefficients satisfy the property that  $|K_m| \leq 1$ , the MMSE for the sequence of predictors satisfies the condition

$$E_0^f \geq E_1^f \geq E_2^f \geq \dots \geq E_p^f \tag{14.82}$$

This concludes the derivation of the Levinson–Durbin algorithm for the solution of the linear equations  $\mathbf{T}_m \mathbf{a}_m = -\mathbf{R}_m$ , for  $m = 0, 1, \dots, p$ . We observe that the linear equations have the special property that the vector on the right-hand side also appears as a vector in  $\mathbf{T}_m$ . In the more general case, where the vector on the right-hand side is some other vector—say,  $\mathbf{c}_m$ —the set of linear equations can be solved recursively by introducing a second recursive equation to solve the more general linear equations  $\mathbf{T}_m \mathbf{b}_m = \mathbf{c}_m$ . The result is a generalized Levinson–Durbin algorithm.

The Levinson–Durbin recursion given by (14.80) require  $\mathcal{O}(m)$  multiplications and additions (operations) to go from stage  $m$  to stage  $m + 1$ . Therefore, for  $p$  stages, it will require of the order of  $1 + 2 + 3 + \dots + p(p + 1)/2$ , or  $\mathcal{O}(p^2)$  operations to solve for the prediction or reflection coefficients, compared with  $\mathcal{O}(p^3)$  operations if we do not exploit the Toeplitz property of the correlation matrix.

If the Levinson–Durbin algorithm is implemented on a serial computer or signal processor, the required computation time is of the order of  $\mathcal{O}(p^2)$  time units. On the other hand, if the processing is performed on a parallel-processing machine utilizing as many processors as necessary to exploit the full parallelism in the algorithm, the multiplications as well as the additions required to compute (14.80) can be carried out simultaneously. In that case, the computation can be performed in  $\mathcal{O}(p)$  time units. However, the computation in (14.79) for the reflection coefficients takes additional time. Certainly the inner products involving the vectors  $\mathbf{a}_{m-1}$  and  $\mathbf{R}_{m-1}^b$  can be computed simultaneously by employing parallel processors. However, the addition of these products cannot be done simultaneously but, instead, requires  $\mathcal{O}(\log p)$  time units. Hence the computations in the Levinson–Durbin algorithm, when performed by  $p$  parallel processors, can be accomplished in  $\mathcal{O}(p \log p)$  time units.

**MATLAB Implementation** The SP Toolbox provides the function `levinson` that implements the Levinson–Durbin algorithm. Its invocation is

```
[a,E,K] = levinson(Rx,p)
```

in which the input array `Rx` contains autocorrelation sequence for positive lags starting with lag 0. The linear predictor coefficients of order `p` are computed in array `a` along with `p`th-order prediction error in `E` and the corresponding reflection coefficients in array `K`.

- **EXAMPLE 14.12** The autocorrelation sequence of a random process is

$$R_{XX}(m) = \begin{cases} 1, & m = 0 \\ -0.5, & m = \pm 1 \\ 0.625, & m = \pm 2 \\ -0.6875, & m = \pm 3 \\ 0, & \text{otherwise} \end{cases}$$

Use the Levinson–Durbin algorithm to determine the system function  $A_m(z)$  for the prediction-error filter for  $m = 1, 2, 3$ , the reflection coefficients, and the corresponding mean sequence prediction error.

### Solution

Use the Levinson–Durbin algorithm: For  $m = 1$  we have

$$a_1(1) = -\frac{R_{XX}(1)}{R_{XX}(0)} = K_1 = \frac{1}{2}$$

Therefore,  $A_1(z) = 1 + \frac{1}{2}z^{-1}$  and  $E_1 = R_{XX}(0)(1 - a_1^2(1)) = \frac{3}{4}$ . For  $m = 2$ ,

$$a_2(2) = -\frac{R_{XX}(2) + a_1(1)R_{XX}(1)}{E_1} = K_2 = -\frac{1}{2}$$

and

$$a_2(1) = a_1(1) + a_2(2)a_1(1) = \frac{1}{4}$$

Therefore,  $A_2(z) = 1 + \frac{1}{4}z^{-1} - \frac{1}{2}z^{-2}$  and  $E_2 = (1 - a_2^2(2))E_1 = \frac{9}{16}$ . Finally, for  $m = 3$ ,

$$\begin{aligned} a_3(3) &= -\frac{R_{XX}(3) + a_2(1)R_{XX}(2) + a_2(2)R_{XX}(1)}{E_2} = K_3 = \frac{1}{2} \\ a_3(2) &= a_2(2) + a_3(3)a_2(1) = -\frac{3}{8} \\ a_3(1) &= a_2(1) + a_3(3)a_2(2) = 0 \end{aligned}$$

Hence

$$A_3(x) = 1 - \frac{3}{8}z^{-2} + \frac{1}{2}z^{-3} \quad E_3 = (1 - a_3^2(3))E_2 = \frac{27}{64} = 0.4219$$

We will verify the above results using the `levinson` function:

```
>> Rx = [1,-0.5,0.625,-0.6875];
>> [a,E,K] = levinson(Rx)
a =
    1.0000      0   -0.3750   0.5000
E =
    0.4219
K =
    0.5000
   -0.5000
    0.5000
```

□

- **EXAMPLE 14.13** Repeat Example 14.12 for an AR process with autocorrelation

$$R_{XX}(m) = a^{|m|} \cos \frac{\pi m}{2}, \quad 0 < a < 1$$

**Solution**

From the given autocorrelation  $R_{XX}(m)$ , we will need first four values:

$$\begin{aligned} R_{XX}(0) &= a^{|0|} \cos(0) = 1, & R_{XX}(1) &= a^{|1|} \cos(\pi/2) = 0, \\ R_{XX}(2) &= a^{|2|} \cos(\pi) = -a^2, & R_{XX}(3) &= a^{|3|} \cos(3\pi/2) = 0 \end{aligned}$$

Now consider the recursion.

- $m = 1$ :

$$a_1(1) = -\frac{R_{XX}(1)}{R_{XX}(0)} = 0 \Rightarrow K_1 = 0;$$

$$A_1(z) = 1;$$

$$E_1 = R_{XX}(0)(1 - a_1^2(1)) = R_{XX}(0) = 1$$

- $m = 2$ :

$$a_2(2) = -\frac{R_{XX}(2) + a_1(1)R_{XX}(1)}{E_1} = a^2$$

$$a_2(1) = a_1(1) + a_2(2)a_1(1) = 0 \Rightarrow K_2 = a^2;$$

$$A_2(z) = 1 + a^2 z^{-2};$$

$$\begin{aligned} E_2 &= E_1(1 - a_2^2(2)) = E_1(1 - a^4) \\ &= 1 - a^4 \end{aligned}$$

- $m = 3$ :

$$a_3(3) = -\frac{R_{XX}(3) + a_2(1)R_{XX}(2) + a_2(2)R_{XX}(1)}{E_2} = 0$$

$$a_3(2) = a_2(2) + a_3(3)a_2(1) = a^2$$

$$a_3(1) = a_2(1) + a_3(3)a_2(2) = 0 \Rightarrow K_3 = 0;$$

$$A_3(z) = 1 + a^2 z^{-2};$$

$$E_3 = E_2 = 1 - a^4$$

□

In the following section, we describe another algorithm, due to Schur [88], that avoids the computation of inner products and, hence, is more suitable for parallel computation of the reflection coefficients.

### 14.3.2 THE SCHUR ALGORITHM

The Schur algorithm is intimately related to a recursive test for determining the positive definiteness of a correlation matrix. To be specific, let us consider the autocorrelation matrix  $\mathbf{T}_{p+1}$  associated with the augmented normal equations given by (14.65). From the elements of this matrix, we form the function

$$D_0(z) = \frac{R_{XX}(1)z^{-1} + R_{XX}(2)z^{-2} + \cdots + R_{XX}(p)z^{-p}}{R_{XX}(0) + R_{XX}(1)z^{-1} + \cdots + R_{XX}(p)z^{-p}} \quad (14.83)$$

and the sequence of functions  $D_m(z)$  defined recursively as

$$D_m(z) = \frac{D_{m-1}(z) - D_{m-1}(\infty)}{z^{-1}[1 - D_{m-1}^*(\infty)D_{m-1}(z)]}, \quad m = 1, 2, \dots \quad (14.84)$$

Schur's theorem states that a necessary and sufficient condition for the correlation matrix to be positive definite is that  $|D_m(\infty)| < 1$  for  $m = 1, 2, \dots, p$ .

Let us demonstrate that the condition for positive definiteness of the autocorrelation matrix  $\mathbf{T}_{p+1}$  is equivalent to the condition that the reflection coefficients in the equivalent lattice filter satisfy the condition  $|K_m| < 1$ ,  $m = 1, 2, \dots, p$ .

First, we note that  $D_0(\infty) = 0$ . Then from (14.84), we have

$$D_1(z) = \frac{R_{XX}(1) + R_{XX}(2)z^{-1} + \cdots + R_{XX}(p)z^{-p+1}}{R_{XX}(0) + R_{XX}(1)z^{-1} + \cdots + R_{XX}(p)z^{-p}} \quad (14.85)$$

Hence  $D_1(\infty) = R_{XX}(1)/R_{XX}(0)$ . We observe  $D_1(\infty) = -K_1$ .

Second, we compute  $D_2(z)$  according to (14.84) and evaluate the result at  $z = \infty$ . Thus, we obtain

$$D_2(\infty) = \frac{R_{XX}(2) + K_1R_{XX}(1)}{R_{XX}(0)(1 - |K_1|^2)}$$

Again, we observe that  $D_2(\infty) = -K_2$ . By continuing this procedure, we find that  $D_m(\infty) = -K_m$ , for  $m = 1, 2, \dots, p$ . Hence the condition  $|D_m(\infty)|$  for  $m = 1, 2, \dots, p$  is identical to the condition  $|K_m| < 1$  for  $m = 1, 2, \dots, p$ , which ensures the positive definiteness of the autocorrelation matrix  $\mathbf{T}_{p+1}$ .

Since the reflection coefficients can be obtained from the sequence of functions  $D_m(z)$ ,  $m = 1, 2, \dots, p$ , we have another method for solving the normal equations. We call this method the *Schur algorithm*.

**Schur Algorithm Derivation** Let us first rewrite  $D_m(z)$  as

$$D_m(z) = \frac{P_m(z)}{Q_m(z)}, \quad m = 0, 1, \dots, p \quad (14.86)$$

where

$$P_0(z) = R_{XX}(1)z^{-1} + R_{XX}(2)z^{-2} + \dots + R_{XX}(p)z^{-p} \quad (14.87a)$$

$$Q_0(z) = R_{XX}(0) + R_{XX}(1)z^{-1} + \dots + R_{XX}(p)z^{-p} \quad (14.87b)$$

Since  $K_0 = 0$  and  $K_m = -D_m(\infty)$  for  $m = 1, 2, \dots, p$ , the recursive Equation (14.84) implies the following recursive equations for the polynomials  $P_m(z)$  and  $Q_m(z)$ :

$$\begin{bmatrix} P_m(z) \\ Q_m(z) \end{bmatrix} = \begin{bmatrix} 1 & K_{m-1} \\ K_{m-1}^* z^{-1} & z^{-1} \end{bmatrix} \begin{bmatrix} P_{m-1}(z) \\ Q_{m-1}(z) \end{bmatrix}, \quad m = 1, 2, \dots, p \quad (14.88)$$

Thus we have

$$\begin{aligned} P_1(z) &= P_0(z) = R_{XX}(1)z^{-1} + R_{XX}(2)z^{-2} + \dots + R_{XX}(p)z^{-p} \\ Q_1(z) &= z^{-1}Q_0(z) = R_{XX}(0)z^{-1} + R_{XX}(1)z^{-2} + \dots + R_{XX}(p)z^{-p-1} \end{aligned} \quad (14.89)$$

and

$$K_1 = -\left. \frac{P_1(z)}{Q_1(z)} \right|_{z=\infty} = -\frac{R_{XX}(1)}{R_{XX}(0)} \quad (14.90)$$

Next, the reflection coefficient  $K_2$  is obtained by determining  $P_2(z)$  and  $Q_2(z)$  from (14.88), dividing  $P_2(z)$  by  $Q_2(z)$ , and evaluating the result at  $z = \infty$ . Thus we find that

$$\begin{aligned} P_2(z) &= P_1(z) + K_1 Q_1(z) \\ &= [R_{XX}(2) + K_1 R_{XX}(1)]z^{-2} + \dots + [R_{XX}(p) + K_1 R_{XX}(p-1)]z^{-p} \\ &\quad + K_1 R_{XX}(p)z^{-p-1} \\ Q_2(z) &= z^{-1}[Q_1(z) + K_1^* P_1(z)] \\ &= [R_{XX}(0) + K_1^* R_{XX}(1)]z^{-2} + \dots + [R_{XX}(p-1) + K_1^* R_{XX}(p)]z^{-p-1} \\ &\quad + R_{XX}(p)z^{-p-2} \end{aligned} \quad (14.91)$$

Thus we observe that the recursive equation in (14.88) is equivalent to (14.84).

Based on these relationships, the Schur algorithm is described by the following recursive procedure.

**Initialization:** Form the  $2 \times (p+1)$  generator matrix

$$\mathbf{G}_0 = \begin{bmatrix} 0 & R_{XX}(1) & R_{XX}(2) & \cdots & R_{XX}(p) \\ R_{XX}(0) & R_{XX}(1) & R_{XX}(2) & \cdots & R_{XX}(p) \end{bmatrix} \quad (14.92)$$

where the elements of the first row are the coefficients of  $P_0(Z)$  and the elements of the second row are the coefficients of  $Q_0(z)$ .

**Step 1.** Shift the second row of the generator matrix to the right by one place and discard the last element of this row, and place a zero in the vacant position. You will obtain the new generator matrix

$$\mathbf{G}_1 = \begin{bmatrix} 0 & R_{XX}(1) & R_{XX}(2) & \cdots & R_{XX}(p) \\ 0 & R_{XX}(0) & R_{XX}(1) & \cdots & R_{XX}(p-1) \end{bmatrix} \quad (14.93)$$

The (negative) ratio of the elements in the second column yields the reflection coefficient  $K_1 = -R_{XX}(1)/R_{XX}(0)$ .

**Step 2.** Multiply the generator matrix by the  $2 \times 2$  matrix

$$\mathbf{V}_1 = \begin{bmatrix} 1 & K_1 \\ K_1^* & 1 \end{bmatrix} \quad (14.94)$$

to obtain  $\mathbf{V}_1 \mathbf{G}_1$ :

$$\mathbf{V}_1 \mathbf{G}_1 = \begin{bmatrix} 0 & 0 & R_{XX}(2) + K_1 R_{XX}(1) & \cdots & R_{XX}(p) + K_1 R_{XX}(p-1) \\ 0 & R_{XX}(0) + K_1^* R_{XX}(1) & \cdots & \cdots & R_{XX}(p-1) + K_1^* R_{XX}(p) \end{bmatrix} \quad (14.95)$$

**Step 3.** Shift the second row of  $\mathbf{V}_1 \mathbf{G}_1$  by one place to the right and, thus, form the new generator matrix

$$\mathbf{G}_2 = \begin{bmatrix} 0 & 0 & R_{XX}(2) + K_1 R_{XX}(1) & \cdots & R_{XX}(p) + K_1 R_{XX}(p-1) \\ 0 & 0 & R_{XX}(0) + K_1^* R_{XX}(1) & \cdots & R_{XX}(p-2) + K_1^* R_{XX}(p-1) \end{bmatrix} \quad (14.96)$$

The negative ratio of the elements in the third column of  $\mathbf{G}_2$  yields  $K_2$ .

Steps 2 and 3 are repeated until we have solved for all  $p$  reflection coefficients. In general, the  $2 \times 2$  matrix in step  $m$  is

$$\mathbf{V}_m = \begin{bmatrix} 1 & K_m \\ K_m^* & 1 \end{bmatrix} \quad (14.97)$$

and multiplication of  $\mathbf{V}_m$  by  $\mathbf{G}_m$  yields  $\mathbf{V}_m \mathbf{G}_m$ . In Step 3, we shift the second row of  $\mathbf{V}_m \mathbf{G}_m$  one place to the right and, thus, we obtain the new generator matrix  $\mathbf{G}_{m+1}$ .

Observe that the shifting operation of the second row in each iteration is equivalent to multiplication by the delay operator  $z^{-1}$  in the second recursive equation in (14.88).

Also, note that the division of the polynomial  $P_m(z)$  by the polynomial  $Q_m(z)$  and the evaluation of the quotient at  $z = \infty$  are equivalent to dividing the elements in the  $(m+1)$ th column of  $\mathbf{G}_m$ . The computation of the  $p$  reflection coefficients can be accomplished by use of parallel processors in  $o(p)$  time units. We describe a pipelined architecture for performing these computations below.

- **EXAMPLE 14.14** An AR(3) process  $x(n)$  is characterized by the autocorrelation sequence

$$R_{xx}(0) = 1, R_{xx}(1) = \frac{1}{2}, R_{xx}(2) = \frac{1}{8}, R_{xx}(3) = \frac{1}{64}$$

Use the Schur algorithm to determine the three reflection coefficients  $K_1$ ,  $K_2$ , and  $K_3$ .

**Solution**

Following the above steps in the Schur algorithm, we obtain the following.

- Initialization:

$$G_0 = \begin{bmatrix} 0 & \frac{1}{2} & \frac{1}{8} & \frac{1}{64} \\ 1 & \frac{1}{2} & \frac{1}{8} & \frac{1}{64} \end{bmatrix}$$

- Step 1:

$$G_1 = \begin{bmatrix} 0 & \frac{1}{2} & \frac{1}{8} & \frac{1}{64} \\ 0 & 1 & \frac{1}{2} & \frac{1}{8} \end{bmatrix} \Rightarrow K_1 = -\frac{1}{2},$$

$$V_1 = \begin{bmatrix} 1 & -\frac{1}{2} \\ -\frac{1}{2} & 1 \end{bmatrix}, \quad V_1 G_1 = \begin{bmatrix} 0 & 0 & -\frac{1}{8} & -\frac{3}{64} \\ 0 & \frac{3}{4} & \frac{7}{16} & \frac{15}{128} \end{bmatrix}$$

- Step 2:

$$G_2 = \begin{bmatrix} 0 & 0 & -\frac{1}{8} & -\frac{3}{64} \\ 0 & 0 & \frac{3}{4} & \frac{7}{16} \end{bmatrix} \Rightarrow K_2 = \frac{2}{3},$$

$$V_2 = \begin{bmatrix} 1 & \frac{2}{3} \\ \frac{2}{3} & 1 \end{bmatrix}, \quad V_2 G_2 = \begin{bmatrix} 0 & 0 & 0 & \frac{47}{192} \\ 0 & 0 & \frac{2}{3} & \frac{13}{32} \end{bmatrix}$$

- Step 3:

$$G_3 = \begin{bmatrix} 0 & 0 & 0 & \frac{47}{192} \\ 0 & 0 & 0 & \frac{2}{3} \end{bmatrix} \Rightarrow K_3 = -\frac{47}{128}$$

Hence the reflection coefficients are

$$K_1 = -\frac{1}{2}, \quad K_2 = \frac{2}{3}, \quad \text{and} \quad K_3 = -\frac{47}{128}$$

□

- **EXAMPLE 14.15** Repeat Example 14.14 for an AR process characterized by the autocorrelation

$$R_{xx}(m) = a^{|m|} \cos \frac{\pi m}{2}$$

**Solution**

The first four autocorrelation values are

$$R_{xx}(0) = 1, \quad R_{xx}(1) = 0, \quad R_{xx}(2) = -a^2, \quad \text{and} \quad R_{xx}(3) = 0$$

Again following the steps in the Schur algorithm, we obtain the following.

- Initialization:

$$G_0 = \begin{bmatrix} 0 & 0 & -a^2 & 0 \\ 1 & 0 & -a^2 & 0 \end{bmatrix}$$

- Step 1:

$$G_1 = \begin{bmatrix} 0 & 0 & -a^2 & 0 \\ 0 & 1 & 0 & -a^2 \end{bmatrix} \Rightarrow K_1 = -\frac{0}{1} = 0,$$

$$V_1 = \begin{bmatrix} 1 & 0 \\ 0 & 1 \end{bmatrix}, \quad V_1 G_1 = G_1 = \begin{bmatrix} 0 & 0 & -a^2 & 0 \\ 0 & 1 & 0 & -a^2 \end{bmatrix}$$

- Step 2:

$$G_2 = \begin{bmatrix} 0 & 0 & -a^2 & 0 \\ 0 & 0 & 1 & 0 \end{bmatrix} \Rightarrow K_2 = a^2,$$

$$V_2 = \begin{bmatrix} 1 & a^2 \\ a^2 & 1 \end{bmatrix}, \quad V_2 G_2 = \begin{bmatrix} 0 & 0 & 0 & 0 \\ 0 & 0 & 1-a^4 & 0 \end{bmatrix}$$

- Step 3:

$$G_3 = \begin{bmatrix} 0 & 0 & 0 & 0 \\ 0 & 0 & 0 & 1-a^4 \end{bmatrix} \Rightarrow K_3 = 0$$

Hence the reflection coefficients are

$$K_1 = 0, \quad K_2 = a^2, \quad \text{and} \quad K_3 = 0$$

as obtained in Example 14.13. □

Another way of demonstrating the relationship of the Schur algorithm to the Levinson–Durbin algorithm and the corresponding lattice predictor is to determine the output of the lattice filter that is obtained when the input sequence is the correlation sequence  $\{R_{XX}(m), m = 0, 1, \dots\}$ . Thus the first input to the lattice filter is  $R_{XX}(0)$ , the second input is  $R_{XX}(1)$ , and so on; in other words,  $f_0(n) = R_{XX}(n)$ . After the delay in the first stage, we have  $g_0(n-1) = R_{XX}(n-1)$ . Hence, for  $n = 1$ , the ratio  $f_0(1)/g_0(0) = R_{XX}(1)/R_{XX}(0)$ , which is the negative of the reflection coefficient  $K_1$ . Alternatively, we may express this relationship as

$$f_0(1) + K_1 g_0(0) = R_{XX}(1) + K_1 R_{XX}(0) = 0$$

Furthermore,  $g_0(0) = R_{XX}(0) = E_0^f$ . At time  $n = 2$ , the input to the second stage is, according to (14.34),

$$f_1(2) = f_0(2) + K_1 g_0(1) = R_{XX}(2) + K_1 R_{XX}(1)$$

and after the unit of delay in the second stage, we have

$$g_1(1) = K_1^* f_0(1) + g_0(0) = K_1^* R_{XX}(1) + R_{XX}(0)$$

Now the ratio  $f_1(2)/g_1(1)$  is

$$\frac{f_1(2)}{g_1(1)} = \frac{R_{XX}(2) + K_1 R_{XX}(1)}{R_{XX}(0) + K_1^* R_{XX}(1)} = \frac{R_{XX}(2) + K_1 R_{XX}(1)}{E_1^f} = -K_2$$

Hence

$$\begin{aligned} f_1(2) + K_2 g_1(1) &= 0 \\ g_1(1) &= E_1^f \end{aligned}$$

By continuing in this way, we can show that at the input to the  $m$ th lattice stage the ratio  $f_{m-1}(m)/g_{m-1}(m-1) = -K_m$  and  $g_{m-1}(m-1) = E_{m-1}^f$ . Consequently, the lattice filter coefficients obtained from the Levinson algorithm are identical to the coefficients obtained from the Schur algorithm. Furthermore, the lattice filter structure provides a method for computing the reflection coefficients in the lattice predictor.

**A Pipelined Architecture for Implementing the Schur Algorithm**  
 Kung and Hu [52] developed a pipelined lattice-type processor for implementing the Schur algorithm. The processor consists of a cascade of  $p$  lattice-type stages, where each stage consists of two processing elements (PEs), which we designate as upper PEs, denoted by  $A_1, A_2, \dots, A_p$ , and lower PEs, denoted by  $B_1, B_2, \dots, B_p$ , as shown in Figure 14.19.

The PE designated as  $A_1$  is assigned the task of performing divisions. The remaining PEs perform one multiplication and one addition per iteration (one clock cycle). Initially, the upper PEs are loaded with the elements of the first row of the generator matrix  $\mathbf{G}_0$ , as illustrated in Figure 14.19. The lower PEs are loaded with the elements of the second row of the generator matrix  $\mathbf{G}_0$ . The computational process begins with the division PE  $A_1$ , which computes the first reflection coefficient as  $K_1 = -R_{XX}(1)/R_{XX}(0)$ . The value of  $K_1$  is sent simultaneously to all the PEs in the upper and lower branches.

The second step in the computation is to simultaneously update the contents of all processing elements. The contents of the upper and lower PEs are updated as follows.

$$\begin{aligned} \text{PE } A_m: \quad A_m &\leftarrow A_m + K_1 B_m, & m &= 2, 3, \dots, p \\ \text{PE } B_m: \quad B_m &\leftarrow B_m + K_1^* A_m, & m &= 1, 2, \dots, p \end{aligned}$$

The third step involves the shifting of the contents of the upper PEs one place to the left. Thus, we have

$$\text{PE } A_m: \quad A_{m-1} \leftarrow A_m, \quad m = 2, 3, \dots, p$$

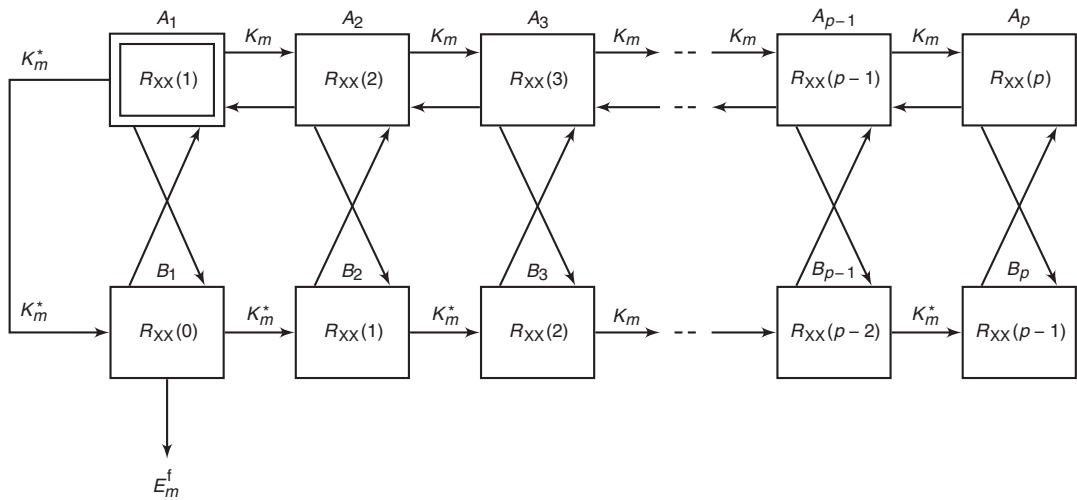


**FIGURE 14.19** Pipelined parallel processor for computing the reflection coefficients

At this point, PE \$A\_1\$ contains \$R\_{XX}(2) + K\_1 R\_{XX}(1)\$ while PE \$B\_1\$ contains \$R\_{XX}(0) + K\_1^\* R\_{XX}(1)\$. Hence the processor \$A\_1\$ is ready to begin the second cycle by computing the second reflection coefficient \$K\_2 = -A\_1/B\_1\$. The three computational steps beginning with the division \$A\_1/B\_1\$ are repeated until all \$p\$ reflection coefficients are computed. Note that PE \$B\_1\$ provides the minimum mean-square error \$E\_m^f\$ for each iteration.

If \$\tau\_d\$ denotes the time for PE \$A\_1\$ to perform a (complex) division and \$\tau\_{ma}\$ is the time required to perform a (complex) multiplication and an addition, the time required to compute all \$p\$ reflection coefficients is \$p(\tau\_d + \tau\_{ma})\$ for the Schur algorithm.

## 14.4 PROPERTIES OF THE LINEAR PREDICTION-ERROR FILTERS

Linear prediction-error filters possess several important properties, which are described in this section. We begin by demonstrating that the forward prediction-error filter is minimum phase.

**Minimum Phase Property of the Forward Prediction-Error Filter** We have already demonstrated that the reflection coefficients \$K\_i\$ are correlation coefficients and, consequently, \$|K\_i| \leq 1\$ for all \$i\$. This condition and the relation \$E\_m^f = (1 - |K\_m|^2)E\_{m-1}^f\$ may be used to show that the zeros of the prediction-error filter are either all inside the unit circle or all on the unit circle.

First, we show that if  $E_p^f > 0$ , then the zeros  $|z_i| < 1$  for every  $i$ . The proof is by induction. Clearly, for  $p = 1$ , the system function for the prediction-error filter is

$$A_1(z) = 1 + K_1 z^{-1} \quad (14.98)$$

Hence  $z_1 = -K_1$  and  $E_1^f = (1 - |K_1|^2)E_0^f > 0$ . Now, suppose that the hypothesis is true for  $p - 1$ . Then, if  $z_i$  is a root of  $A_p(z)$ , we have, from (14.49) and (14.54),

$$\begin{aligned} A_p(z_i) &= A_{p-1}(z_i) + K_p z_i^{-1} B_{p-1}(z_i) \\ &= A_{p-1}(z_i) + K_p z_i^{-p} A_{p-1}^*(\frac{1}{z_i}) = 0 \end{aligned} \quad (14.99)$$

Hence

$$\frac{1}{K_p} = -\frac{z_i^{-p} A_{p-1}^*(\frac{1}{z_i})}{A_{p-1}(z_i)} \equiv Q(z_i) \quad (14.100)$$

We note that the function  $Q(z)$  is allpass. In general, an allpass function of the form

$$P(z) = \prod_{k=1}^N \frac{zz_k^* + 1}{z + z_k}, \quad |z_k| < 1 \quad (14.101)$$

satisfies the property that  $|P(z)| > 1$  for  $|z| < 1$ ,  $|P(z)| = 1$  for  $|z| = 1$ , and  $|P(z)| < 1$  for  $|z| > 1$ . Since  $Q(z) = -P(z)/z$ , it follows that  $|z_i| < 1$  if  $|Q(z_i)| > 1$ . Clearly, this is the case, since  $Q(z_i) = 1/K_p$  and  $E_p^f > 0$ .

On the other hand, suppose that  $E_{p-1}^f > 0$  and  $E_p^f = 0$ . In this case,  $|K_p| = 1$  and  $|Q(z_i)| = 1$ . Since the MMSE is zero, the random process  $X(n)$  is called *predictable* or *deterministic*. Specifically, a purely sinusoidal random process with sample functions of the form

$$x(n) = \sum_{k=1}^M \alpha_k e^{j(n\omega_k + \theta_k)} \quad (14.102)$$

where the phases  $\theta_k$  are statistically independent and uniformly distributed over  $(0, 2\pi)$ , has the autocorrelation

$$R_{XX}(m) = \sum_{k=1}^M \alpha_k^2 e^{jm\omega_k} \quad (14.103)$$

and the power density spectrum

$$S_{XX}(f) = \sum_{k=1}^M \alpha_k^2 \delta(f - f_k), \quad f_k = \frac{\omega_k}{2\pi} \quad (14.104)$$

This process is predictable with a predictor of order  $p \geq M$ .

To demonstrate the validity of this statement, consider passing this process through a prediction-error filter of order  $p > M$ . The MSE at the output of this filter is

$$\begin{aligned}\mathcal{E}_p^f &= \int_{-1/2}^{1/2} S_{XX}(f) |A_p(f)|^2 df \\ &= \int_{-1/2}^{1/2} \left[ \sum_{k=1}^M \alpha_k^2 \delta(f - f_k) \right] |A_p(f)|^2 df \\ &= \sum_{k=1}^M \alpha_k^2 |A_p(f_k)|^2\end{aligned}\quad (14.105)$$

By choosing  $M$  of the  $p$  zeros of the prediction-error filter to coincide with the frequencies  $f_k$ , the MSE  $\mathcal{E}_p^f$  can be forced to zero. The remaining  $p-M$  zeros can be selected arbitrarily to be anywhere inside the unit circle.

Finally, we leave it to the reader to prove that if a random process consists of a mixture of a continuous power spectral density and a discrete spectrum, the prediction-error filter must have all its roots inside the unit circle.

**Maximum Phase Property of the Backward Prediction-Error Filter** The system function for the backward prediction-error filter of order  $p$  is

$$B_p(z) = z^{-p} A_p^*(z^{-1}) \quad (14.106)$$

Consequently, the roots of  $B_p(z)$  are the reciprocals of the roots of the forward prediction-error filter with system function  $A_p(z)$ . Hence, if  $A_p(z)$  is minimum phase, then  $B_p(z)$  is maximum phase. However, if the process  $X(n)$  is predictable, all the roots of  $B_p(z)$  lie on the unit circle.

**Whitening Property** Suppose that the random process  $X(n)$  is an  $AR(p)$  stationary random process that is generated by passing white noise with variance  $\sigma_W^2$  through an all-pole filter with system function

$$H(z) = \frac{1}{1 + \sum_{k=1}^p a_k z^{-1}} \quad (14.107)$$

Then the prediction-error filter of order  $p$  has the system function

$$A_p(z) = 1 + \sum_{k=1}^p a_p(k) z^{-k} \quad (14.108)$$

where the predictor coefficients  $a_p(k) = a_k$ . The response of the prediction-error filter is a white noise process  $W(n)$ . In this case, the prediction-error

filter whitens the input process  $X(n)$  and is called a whitening filter, as previously indicated in Section 14.2.

More generally, even if the input sequence  $X(n)$  is not an AR process, the prediction-error filter attempts to remove the correlation among the signal samples of the input process. As the order of the predictor is increased, the predictor output  $\hat{X}(n)$  becomes a closer approximation to  $X(n)$  and, hence, the difference  $F(n) = \hat{X}(n) - X(n)$  approaches white noise sequence.

- EXAMPLE 14.16** The  $z$ -transform of the autocorrelation  $R_{XX}(m)$ —that is, the complex PSD  $S_{XX}(z)$ —of an ARMA process is given as

$$S_{XX}(z) = \sigma_W^2 H(z) H(z^{-1}) = \frac{4\sigma_W^2}{9} \frac{5 - 2z - 2z^{-1}}{10 - 3z^{-1} - 3z}$$

- (a) Determine the minimum-phase system function  $H(z)$ .
- (b) Determine the system function  $H(z)$  for a mixed-phase stable system.

**Solution**

- (a) The complex PSD can be factored as

$$S_{XX}(z) = \frac{4\sigma_W^2(5 - 2z - 2z^{-1})}{9(10 - 3z - 3z^{-1})} = \frac{4\sigma_W^2(2 - z^{-1})(2 - z)}{9(3 - z^{-1})(3 - z)} = \sigma_W^2 H(z) H(z^{-1})$$

The minimum-phase system  $H(z)$  is obtained by choosing the pole and zero inside the unit circle, or

$$H(z) = \left(\frac{2}{3}\right) \frac{2 - z^{-1}}{3 - z^{-1}} = \left(\frac{4}{9}\right) \frac{1 - \frac{1}{2}z^{-1}}{1 - \frac{1}{3}z^{-1}}$$

- (b) The mixed-phase stable system is obtained by choosing the pole inside and zero outside the unit circle, or

$$H(z) = \left(\frac{4}{3}\right) \frac{\frac{1}{2} - z^{-1}}{3 - z^{-1}} = \left(\frac{2}{9}\right) \frac{1 - 2z^{-1}}{1 - \frac{1}{3}z^{-1}}$$

□

**Orthogonality of the Backward Prediction Errors** The backward prediction error processes  $G_m(k)$  from different stages in the FIR lattice filter are orthogonal. That is,

$$E[G_m(n)G_\ell^*(n)] = \begin{cases} 0, & 0 \leq \ell \leq m-1 \\ E_m^b, & \ell = m \end{cases} \quad (14.109)$$

This property is easily proved by substituting for  $G_m(n)$  and  $G_\ell^*(n)$  in (14.109) and carrying out the expectation. Thus

$$\begin{aligned} E[G_m(n)G_\ell^*(n)] &= \sum_{k=0}^m b_m(k) \sum_{j=0}^\ell b_\ell^*(j) E[X(n-k)X^*(n-j)] \\ &= \sum_{j=0}^\ell b_\ell^*(j) \sum_{k=0}^m b_m(k) R_{XX}(j-k) \end{aligned} \quad (14.110)$$

But the normal equations for the backward linear predictor require that

$$\sum_{k=0}^m b_m(k) R_{XX}(j-k) = \begin{cases} 0, & j = 1, 2, \dots, m-1 \\ E_m^b, & j = m \end{cases} \quad (14.111)$$

Therefore,

$$E[G_m(n)G_\ell^*(n)] = \begin{cases} E_m^b = E_m^f, & m = \ell \\ 0, & 0 \leq \ell \leq m-1 \end{cases} \quad (14.112)$$

## 14.5 AR LATTICE AND ARMA LATTICE-LADDER FILTERS

---

In Section 14.2, we developed the all-zero FIR lattice structure and showed its relationship to linear prediction. The linear predictor with transfer function

$$A_p(z) = 1 + \sum_{k=1}^p a_p(k)z^{-k} \quad (14.113)$$

when excited by an input random process  $X(n)$  produces an output that approaches a white noise sequence as  $p \rightarrow \infty$ . On the other hand, if the input process is an AR( $p$ ), then the output of  $A_p(z)$  is white. Since  $A_p(z)$  generates an MA( $p$ ) when excited by a white noise sequence, the all-zero lattice is sometimes called an *MA lattice*. We develop the lattice structure for the inverse filter  $1/A_p(z)$ , which we call the AR lattice, and the lattice-ladder structure for an ARMA process.

### 14.5.1 AR LATTICE STRUCTURE

Let us consider an all-pole system with system function

$$H(z) = \frac{1}{1 + \sum_{k=1}^p a_p(k)z^{-k}} \quad (14.114)$$

The difference equation for this IIR system is

$$y(n) = - \sum_{k=1}^p a_p(k)y(n-k) + x(n) \quad (14.115)$$

Now, suppose we interchange the roles of the input and output, that is, interchange  $x(n)$  with  $y(n)$ , in (14.115). Thus we obtain the difference equation

$$x(n) = - \sum_{k=1}^p a_p(k)x(n-k) + y(n)$$

or equivalently,

$$y(n) = x(n) + \sum_{k=1}^p a_p(k)x(n-k) \quad (14.116)$$

We observe that (14.116) is a difference equation for an FIR system with system function  $A_p(z)$ . Thus an all-pole IIR system can be converted to an all-zero system by interchanging the roles of the input and output. Based on this observation, we can obtain the structure of an AR( $p$ ) lattice from an MA( $p$ ) lattice by interchanging the input with the output. Since the MA( $p$ ) lattice has  $y(n) = f_p(n)$  as output and  $x(n) = f_0(n)$  as input, we let

$$\begin{aligned} x(n) &= f_p(n) \\ y(n) &= f_0(n) \end{aligned} \quad (14.117)$$

These definitions dictate that the quantities  $f_m(n)$  be computed in descending order. This computation can be accomplished by rearranging the recursive equation for  $f_m(n)$  in (14.34) and solving for  $f_{m-1}(n)$  in terms of  $f_m(n)$ . Thus we obtain

$$f_{m-1}(n) = f_m(n) - K_m g_{m-1}(n-1), \quad m = p, p-1, \dots, 1$$

The equation for  $g_m(n)$  remains unchanged. The result of these changes is the set of equations

$$\begin{aligned} x(n) &= f_p(n) \\ f_{m-1}(n) &= f_m(n) - K_m g_{m-1}(n-1) \\ g_m(n) &= K_m^* f_{m-1}(n) + g_{m-1}(n-1) \\ y(n) &= f_0(n) = g_0(n) \end{aligned} \quad (14.118)$$

The corresponding structure for the AR( $p$ ) lattice is shown in Figure 14.20. Note that the all-pole lattice structure has an all-zero path with input  $g_0(n)$  and output  $g_p(n)$ , which is identical to the all-zero path in the MA( $p$ ) lattice structure. This is not surprising, since the equation for  $g_m(n)$  is identical in the two lattice structures.

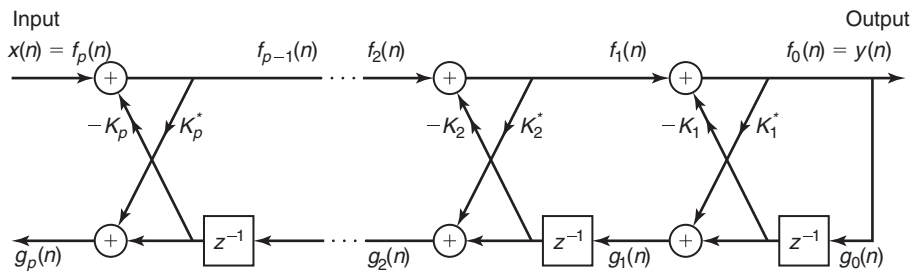


**FIGURE 14.20** Lattice structure for an all-pole AR( $p$ ) system

**MATLAB Implementation** We observe that the AR( $p$ ) and MA( $p$ ) lattice structures are characterized by the same parameters, namely, the reflection coefficients  $K_i$ . Consequently, the equations given in (14.57) and (14.59)—for converting between the system parameters  $a_p(k)$  in the direct form realizations of the all-zero system  $A_p(z)$  and the lattice parameters  $K_i$  of the MA( $p$ ) lattice structure—apply as well to the all-pole structures. Hence the MATLAB functions `fir2latc` and `latc2fir` or `tf2latc` and `latc2tf` discussed in Section 14.2.3 for MA( $p$ ) lattice structures are also applicable to AR( $p$ ) lattice structures. In the case of the `tf2latc` function, the needed invocation is  $K = \text{tf2latc}(1,a)$ . The implementation of the AR( $p$ ) lattice given in (14.118) will be discussed in the next section.

- **EXAMPLE 14.17** Sketch the lattice filter obtained in Example 14.14 for generating  $x(n)$  from a white noise excitation.

**Solution**

The structure is shown in Figure 14.21. □

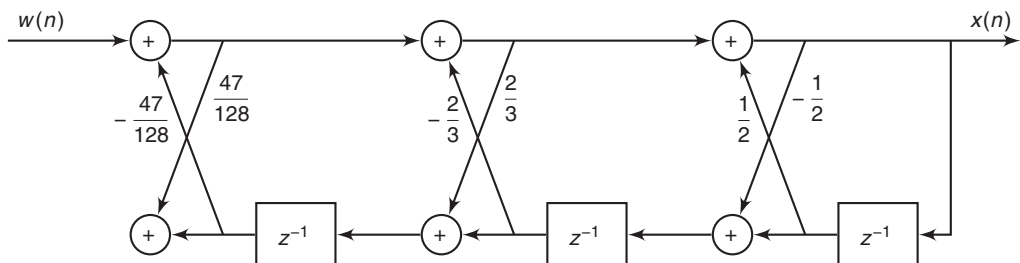


**FIGURE 14.21** The AR(3) lattice filter structure in Example 14.17

#### 14.5.2 ARMA PROCESSES AND LATTICE-LADDER FILTERS

The all-pole lattice provides the basic building block for lattice-type structures that implement IIR systems that contain both poles and zeros. To construct the appropriate structure, let us consider an IIR system with system function

$$H(z) = \frac{\sum_{k=0}^q c_q(k)z^{-k}}{1 + \sum_{k=1}^p a_p(k)z^{-k}} = \frac{C_q(z)}{A_p(z)} \quad (14.119)$$

Without loss of generality, we assume that  $p \geq q$ . This system is described by the difference equations

$$\begin{aligned} v(n) &= -\sum_{k=0}^p a_p(k)v(n-k) + x(n) \\ y(n) &= \sum_{k=0}^q c_q(k)v(n-k) \end{aligned} \quad (14.120)$$

which are obtained by viewing the system as a cascade of an all-pole system followed by an all-zero system. From (14.120), we observe that the output  $y(n)$  is simply a linear combination of delayed outputs from the all-pole system.

Since zeros will result from forming a linear combination of previous outputs, we may carry over this observation to construct a pole-zero system by using the all-pole lattice structure as the basic building block. We have observed that  $g_m(n)$  in the all-pole lattice may be expressed as a linear combination of present and past outputs. In fact, the system

$$H_b(z) \equiv \frac{G_m(z)}{Y(z)} = B_m(z) \quad (14.121)$$

is an all-zero system. Therefore, any linear combination of  $g_m(n)$  is also an all-zero filter.

Let us begin with an all-pole lattice filter with coefficients  $K_m$ ,  $1 \leq m \leq p$ , and add a *ladder* component by taking as the output a weighted linear combination of  $g_m(n)$ . The result is a pole-zero filter that has the lattice-ladder structure shown in Figure 14.22. Its output is

$$y(n) = \sum_{k=0}^q \beta_k g_k(n) \quad (14.122)$$

where  $\beta_k$  are the parameters that determine the zeros of the system. The system function corresponding to (14.122) is

$$H(z) = \frac{Y(z)}{X(z)} = \sum_{k=0}^q \beta_k \frac{G_k(z)}{X(z)} \quad (14.123)$$

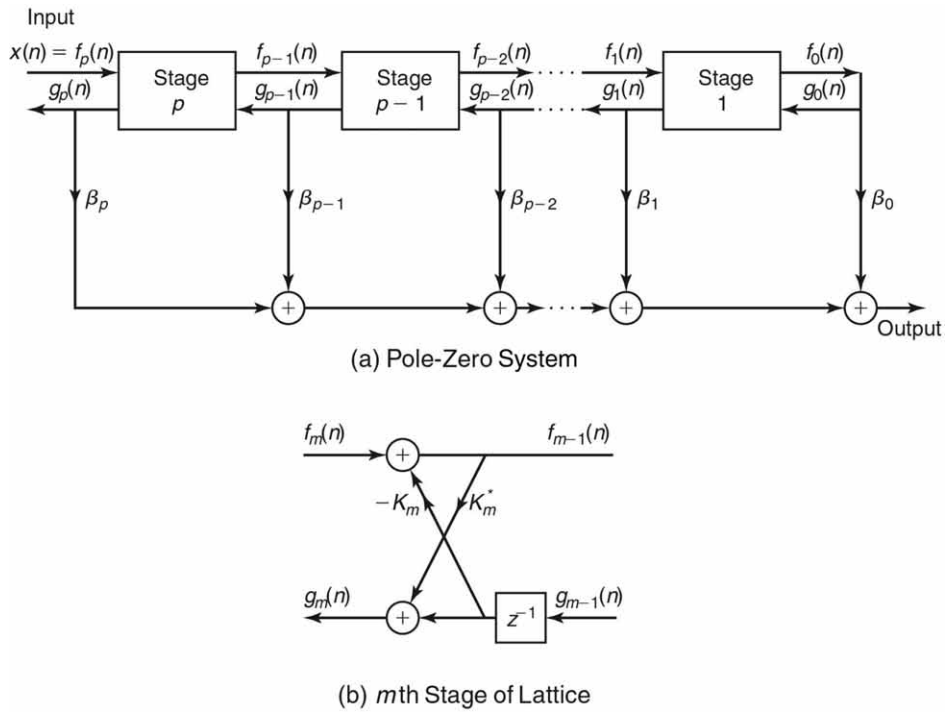


**FIGURE 14.22** Lattice ladder structure for pole-zero system

Since  $X(z) = F_p(z)$  and  $F_0(z) = G_0(z)$ , (14.123) may be expressed as

$$\begin{aligned} H(z) &= \sum_{k=0}^q \beta_k \frac{G_k(z)}{G_0(z)} \frac{F_0(z)}{F_p(z)} \\ &= \frac{1}{A_p(z)} \sum_{k=0}^q \beta_k B_k(z) \end{aligned} \quad (14.124)$$

Therefore,

$$C_q(z) = \sum_{k=0}^q \beta_k B_k(z) \quad (14.125)$$

This is the desired relationship, which can be used to determine the weighting coefficients  $\beta_k$ .

Given the polynomials  $C_q(z)$  and  $A_p(z)$ , where  $p \geq q$ , the reflection coefficients  $K_i$  are determined first from the coefficients  $a_p(k)$ . By means of the step-down recursive relation given by (14.58), we also obtain the

polynomials  $B_k(z)$ ,  $k = 1, 2, \dots, p$ . Then, the ladder parameters can be obtained from (14.125), which can be expressed as

$$\begin{aligned} C_m(z) &= \sum_{k=0}^{m-1} \beta_k B_k(z) + \beta_m B_m(z) \\ &= C_{m-1}(z) + \beta_m B_m(z) \end{aligned} \quad (14.126)$$

or equivalently,

$$C_{m-1}(z) = C_m(z) - \beta_m B_m(z), \quad m = p, p-1, \dots, 1 \quad (14.127)$$

By running this recursive relation backward, we can generate all the lower-degree polynomials,  $C_m(z)$ ,  $m = p-1, \dots, 1$ . Since  $b_m(m) = 1$ , the parameters  $\beta_m$  are determined from (14.127) by setting

$$\beta_m = c_m(m), \quad m = p, p-1, \dots, 1, 0 \quad (14.128)$$

This lattice-ladder filter structure, when excited by a white noise sequence, generates an ARMA( $p, q$ ) process that has a power density spectrum

$$S_{xx}(f) = \sigma_W^2 \frac{|C_q(f)|^2}{|A_p(f)|^2} \quad (14.129)$$

and an autocorrelation function that satisfies (14.18), where  $\sigma_W^2$  is the variance of the input white noise sequence.

**MATLAB Implementation** To obtain a lattice-ladder structure for a general rational IIR system, we can first obtain the lattice coefficients  $\{K_m\}$  from  $A_p(z)$  using the recursion (14.58) and (14.59). Then we can solve (14.127) and (14.128) recursively for the ladder coefficients  $\{\beta_m\}$  to realize the numerator  $C_q(z)$ . This is done in the MATLAB function `iir2ladr`. It can also be used to determine the AR( $p$ ) lattice parameters when the array `b` is set to `b=1`.

```
function [K,beta] = iir2ladr(b,a)
% IIR Direct form to pole-zero Lattice/Ladder form Conversion
%
% [K,beta] = iir2ladr(b,a)
%     K = lattice coefficients (reflection coefficients), [K1,...,KN]
%     beta = ladder coefficients, [C0,...,CN]
%     b = numerator polynomial coefficients (deg <= Num deg)
%     a = denominator polynomial coefficients
%
```

```

a1 = a(1); a = a/a1; b = b/a1;
q = length(b); p = length(a);
if q > p
    error(' *** length of b must be <= length of a ***')
end
b = [b, zeros(1,p-q)]; K = zeros(1,p-1);
A = zeros(p-1,p-1); beta = b;
for m = p-1:-1:1
    A(m,1:m) = -a(2:m+1)*beta(m+1);
    K(m) = a(m+1); J = fliplr(a);
    a = (a-K(m)*J)/(1-K(m)*K(m)); a = a(1:m);
    beta(m) = b(m) + sum(diag(A(m:p-1,1:p-m)));
end

```

It should be noted that to use this function,  $p \geq q$ . If  $q > p$ , the numerator  $A_p(z)$  should be divided into the denominator  $C_q(z)$  using the `deconv` function to obtain a proper rational part and a polynomial part. The proper rational part can be implemented using a lattice-ladder structure, while the polynomial part is implemented using a direct structure.

To convert a lattice-ladder form into a direct form, we first use the recursive procedure in (14.57) on  $\{K_m\}$  coefficients to determine  $\{a_q(k)\}$  and then solve (14.126) recursively to obtain  $\{b_q(k)\}$ . This is done in the following MATLAB function, `ladr2iir`.

```

function [b,a] = ladr2iir(K,beta)
% Lattice/ladder form to IIR direct form conversion
%
% -----
% [b,a] = ladr2iir(K,beta)
%     b = numerator polynomial coefficients
%     a = denominator polynomial coefficients
%     K = lattice coefficients (reflection coefficients)
%     beta = ladder coefficients
%
p = length(K); q = length(beta);
beta = [beta, zeros(1,p-q+1)];
J = 1; a = 1; A = zeros(p,p);
for m=1:1:p
    a = [a,0]+conv([0,K(m)],J);
    A(m,1:m) = -a(2:m+1); J = fliplr(a);
end
b(p+1) = beta(p+1);
for m = p:-1:1
    A(m,1:m) = A(m,1:m)*beta(m+1);
    b(m) = beta(m) - sum(diag(A(m:p,1:p-m+1)));
end

```

The lattice-ladder filter is implemented using (14.34) and (14.122). This is done in the MATLAB function `ladrfilter`. It should be noted that, due to the recursive nature of this implementation along with the feedback loops, this MATLAB function is neither an elegant nor an efficient method of implementation. It is not possible to exploit MATLAB's inherent parallel processing capabilities in implementing this lattice-ladder structure.

```
function [y] = ladrfilter(K,beta,x)
% LATTICE/LADDER form realization of IIR filters
%
% -----
% [y] = ladrfilter(K,beta,x)
%     y = output sequence
%     K = LATTICE (reflection) coefficient array
%     beta = LADDER coefficient array
%     x = input sequence
%
Nx = length(x); y = zeros(1,Nx);
p = length(beta); f = zeros(p,Nx); g = zeros(p,Nx+1);
f(p,:) = x;
for n = 2:1:Nx+1
    for m = p:-1:2
        f(m-1,n-1) = f(m,n-1) - K(m-1)*g(m-1,n-1);
        g(m,n) = K(m-1)*f(m-1,n-1) + g(m-1,n-1);
    end
    g(1,n) = f(1,n-1);
end
y = beta*g(:,2:Nx+1);
```

- EXAMPLE 14.18** Determine the parameters of the lattice-ladder filter structure for the system with system function

$$H(z) = \frac{1 + \frac{1}{4}z^{-1} - \frac{1}{8}z^{-2}}{1 + \frac{3}{8}z^{-1} + \frac{1}{2}z^{-2}}$$

### Solution

From the denominator of  $H(z)$ , we determine that

$$B_2(z) = \frac{1}{2} + \frac{3}{8}z^{-1} + z^{-2}$$

$$B_1(z) = \frac{1}{4} + z^{-1}$$

and that the reflection coefficients are  $K_1 = \frac{1}{4}$  and  $K_2 = \frac{1}{2}$ . Then from the numerator of  $H(z)$ ,

$$C(z) = \beta_0 B_0(z) + \beta_1 B_1(z) + \beta_2 B_2(z)$$

$$= \beta_0 + \beta_1 \left( \frac{1}{4} + z^{-1} \right) + \beta_2 \left( \frac{1}{2} + \frac{3}{8}z^{-1} + z^{-2} \right)$$

$$1 + \frac{3}{8}z^{-1} + \frac{1}{2}z^{-2} = \left( \beta_0 + \frac{1}{4}\beta_1 + \frac{1}{2}\beta_2 \right) + \left( \beta_1 + \frac{3}{8}\beta_2 \right) z^{-1} + \beta_2 z^{-2}$$

Solving, in a step-down recursion, we obtain  $\beta_2 = -\frac{1}{8}$ ,  $\beta_1 = \frac{19}{64}$ , and  $\beta_0 = \frac{253}{256}$ . The MATLAB verification is obtained using

```
>> b = [1, 1/4, -1/8];
>> [K,beta] = iir2ladr(b,a)
K =
    0.2500    0.5000
beta =
    0.9883    0.2969   -0.1250
```

□

□ **EXAMPLE 14.19** Convert the following pole-zero IIR system into a lattice-ladder structure:

$$H(z) = \frac{1 + 2z^{-1} + 2z^{-2} + z^{-3}}{1 + \frac{13}{24}z^{-1} + \frac{5}{8}z^{-2} + \frac{1}{3}z^{-3}}$$

**Solution**

The MATLAB script is

```
>> b = [1, 2, 2, 1] a = [1, 13/24, 5/8, 1/3];
>> [K,beta] = iir2ladr(b,a)
K =
    0.2500    0.5000    0.3333
beta =
    -0.2695   0.8281   1.4583   1.0000
```

Hence

$$K_1 = \frac{1}{4}, K_2 = \frac{1}{5}, K_3 = \frac{1}{3};$$

and

$$\beta_0 = -0.2695, \beta_1 = 0.8281, \beta_2 = 1.4583, \beta_3 = 1$$

The resulting direct form and the lattice-ladder form structures are shown in Figure 14.23. To check that our lattice-ladder structure is correct, let us compute the first eight samples of its impulse response using both forms.

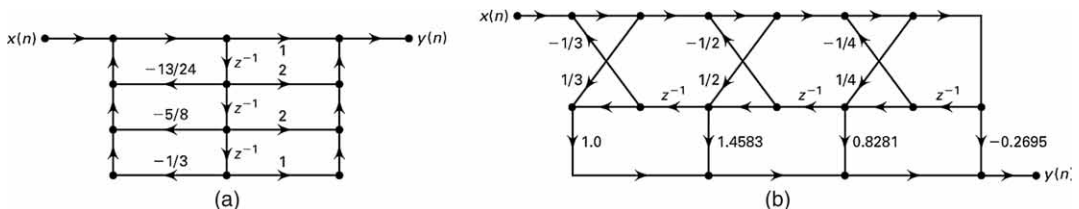


**FIGURE 14.23** IIR system structures in Example 14.19: (a) direct form (b) lattice-ladder form

```

>> [x,n]=impseq(0,0,7)  format long;  hdirect = filter(b,a,x)
hdirect =
    Columns 1 through 4
    1.000000000000000  1.458333333333333  0.585069444444444  -0.56170428240741
    Columns 5 through 8
    -0.54752302758488  0.45261700163162  0.28426911049255  -0.25435705167494
>> hladder = ladrlfilter(K,C,x)
hladder =
    Columns 1 through 4
    1.000000000000000  1.458333333333333  0.585069444444444  -0.56170428240741
    Columns 5 through 8
    -0.54752302758488  0.45261700163162  0.28426911049255  -0.25435705167494

```

□

We note that the SP toolbox functions discussed earlier can also be used to obtain IIR (ARMA) lattice-ladder structures or to implement them. The invocation  $[K, \beta] = \text{tf2latc}(b, a)$  computes the lattice parameters in array  $K$  and the ladder parameters in  $\beta$ , normalized by  $a(1)$ . Note that an error is generated if one or more of the lattice parameters are exactly equal to 1. Similarly, the invocation  $[b, a] = \text{latc2tf}(K, \beta)$  computes the numerator and denominator polynomial coefficients of the system function from  $K$  and  $\beta$ .

Finally, the invocation  $[f, g] = \text{latcfilt}(k, v, x)$  filters input in array  $x$  using the IIR lattice reflection coefficients  $K$  and ladder coefficients  $\beta$ . The forward lattice filter output (or forward prediction error) is in array  $f$ , and the backward lattice filter output (or backward prediction error) is in array  $g$ . If  $|K| \leq 1$ ,  $f$  corresponds to the minimum-phase output and  $g$  corresponds to the maximum-phase output.

## 14.6 WIENER FILTERS FOR FILTERING AND PREDICTION

In many practical applications, we are given an input signal  $x(n)$ , which consists of the sum of a desired signal  $s(n)$  and an undesired noise or interference  $w(n)$ , and we are asked to design a filter that will suppress the undesired interference component. In such a case, the objective is to design a system that filters out the additive interference while preserving the characteristics of the desired signal  $s(n)$ . We assume that these signals are sample sequences of random processes  $X(n)$ ,  $S(n)$ , and  $W(n)$ , respectively.<sup>4</sup>

<sup>4</sup>According to our notation, lowercase variables, such as  $x(n)$ , are sample sequences, while uppercase variables, such as  $X(n)$ , are random processes. In general discussion and in filtering equations, we will use lowercase variables; for expectation purposes, we will use uppercase variables. The distinction between a process and its sample sequence should be clear from the context.

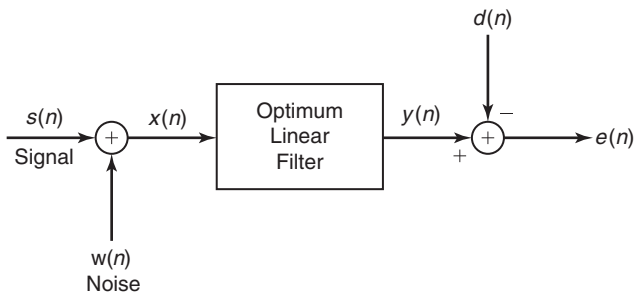


**FIGURE 14.24** Model for linear estimation problem

In this section, we treat the problem of signal estimation in the presence of an additive noise disturbance. The estimator is constrained to be a linear filter with impulse response  $h(n)$ , which is designed so that its output approximates some specified desired signal process  $D(n)$ , with sample sequence  $d(n)$ . Figure 14.24 illustrates the linear estimation problem.

The filter's input sequence is  $x(n) = s(n) + w(n)$  and its output sequence is  $y(n)$ —that is, a sample sequence of the process  $\mathbf{Y}(n)$ . The difference between the desired signal and the filter output is the error sequence  $e(n) \triangleq d(n) - y(n)$ , with the underlying process denoted by  $\mathbf{E}(n)$ . We distinguish three special cases:

- (a) If  $d(n) = s(n)$ , the linear estimation problem is referred to as *filtering*.
- (b) If  $d(n) = s(n + D)$ , where  $D > 0$ , the linear estimation problem is referred to as *signal prediction*. Note that this problem is different than the prediction considered in the previous section, where  $d(n) = x(n + D)$ ,  $D \geq 0$ .
- (c) If  $d(n) = s(n - D)$ , where  $D > 0$ , the linear estimation problem is referred to as *signal smoothing*.

Our treatment will concentrate on filtering and prediction.

The criterion selected for optimizing the filter impulse response  $h(n)$  is the minimization of the mean-square error. This criterion has the advantages of simplicity and mathematical tractability. The basic assumptions are that the processes  $S(n)$ ,  $W(n)$ , and  $D(n)$  are zero mean and wide-sense stationary. The linear filter will be assumed to be either FIR or IIR. If it is IIR, we assume that the input data  $x(n)$  is available over the infinite past. We begin with the design of the optimum FIR filter. The optimum linear filter, in the sense of minimum mean-square error (MMSE), is called a *Wiener filter*.

#### 14.6.1 FIR WIENER FILTER

Suppose that the filter is constrained to be of length  $M$  with coefficients  $h(k)$ ,  $0 \leq k \leq M - 1$ . Hence its output  $y(n)$  depends on the finite data record  $x(n), x(n - 1), \dots, x(n - M + 1)$ ,

$$y(n) = \sum_{k=0}^{M-1} h(k)x(n-k) \quad (14.130)$$

The mean-square value of the error between the desired output  $d(n)$  and the actual output  $y(n)$  is

$$\begin{aligned} \mathcal{E}_M &= E[|E(n)|^2] \\ &= E \left[ \left| D(n) - \sum_{k=0}^{M-1} h(k)X(n-k) \right|^2 \right] \end{aligned} \quad (14.131)$$

Since this is a quadratic function of the filter coefficients, the minimization of  $\mathcal{E}_M$  yields the set of linear equations

$$\sum_{k=0}^{M-1} h(k)R_{XX}(\ell - k) = R_{DX}(\ell), \quad \ell = 0, 1, \dots, M - 1 \quad (14.132)$$

where  $R_{DX}(k) = E[D(n)X^*(n - k)]$  is the cross-correlation between the desired process  $D(n)$  and the input process  $X(n)$ ,  $0 \leq n \leq M - 1$ , and  $R_{XX}(k)$  is the autocorrelation of the input process  $X(n)$ . This set of linear equations that specifies the optimum filter is called the *Wiener–Hopf equation*. (These equations are also called the normal equations, which we encountered earlier in this chapter in the context of linear one-step prediction.)

In general, the equations in (14.132) can be expressed in matrix form as

$$\mathbf{T}_M \mathbf{h}_M = \mathbf{R}_D \quad (14.133)$$

where  $\mathbf{T}_M$  is an  $M \times M$  (Hermitian) Toeplitz matrix with elements  $T_{\ell k} = R_{XX}(\ell - k)$ , and  $\mathbf{R}_D$  is the  $M \times 1$  cross-correlation vector with elements  $R_{DX}(\ell)$ ,  $\ell = 0, 1, \dots, M - 1$ . The solution for the optimum filter coefficients is

$$\mathbf{h}_{\text{opt}} = \mathbf{T}_M^{-1} \mathbf{R}_D \quad (14.134)$$

and the resulting minimum MSE achieved by the Wiener filter is

$$\text{MMSE}_M = \min_{\mathbf{h}_m} \mathcal{E}_M = \sigma_D^2 - \sum_{k=0}^{M-1} \mathbf{h}_{\text{opt}}(k) R_{DX}^*(k) \quad (14.135)$$

or equivalently,

$$\text{MMSE}_M = \sigma_D^2 - \mathbf{R}_D^{*t} \mathbf{T}_M^{-1} \mathbf{R}_D \quad (14.136)$$

where  $\sigma_D^2 = E[|D(n)|^2]$ .

Let us consider some special cases of (14.132). If we are dealing with filtering, then  $D(n) = S(n)$ . Furthermore, if  $S(n)$  and  $D(n)$  are uncorrelated random sequences, as is usually the case in practice, then

$$\begin{aligned} R_{XX}(k) &= R_{SS}(k) + R_{WW}(k) \\ R_{DX}(k) &= R_{SS}(k) \end{aligned} \quad (14.137)$$

and the normal equations in (14.132) become

$$\sum_{k=0}^{M-1} h(k) [R_{SS}(\ell - k) + R_{WW}(\ell - k)] = R_{SS}(\ell), \quad \ell = 0, 1, \dots, M-1 \quad (14.138)$$

If we are dealing with prediction, then  $D(n) = D(n+D)$  where  $D > 0$ . Assuming that  $S(n)$  and  $W(n)$  are uncorrelated random sequences, we have

$$R_{DX}(k) = R_{SS}(k+D) \quad (14.139)$$

Hence the equations for the Wiener prediction filter become

$$\sum_{k=0}^{M-1} h(k) [R_{SS}(\ell - k) + R_{WW}(\ell - k)] = R_{SS}(\ell + D) \quad \ell = 0, 1, \dots, M-1 \quad (14.140)$$

In all these cases, the correlation matrix to be inverted is Toeplitz. Hence the (generalized) Levinson–Durbin algorithm may be used to solve for the optimum filter coefficients.

- EXAMPLE 14.20** Let us consider a signal  $x(n) = s(n) + w(n)$ , where  $s(n)$  is a sample sequence of an AR(1) process  $S(n)$  that satisfies the difference equation

$$s(n) = 0.6s(n-1) + v(n)$$

where  $v(n)$  is a sample sequence of a white noise process  $V(n)$  with variance  $\sigma_V^2 = 0.64$  and  $w(n)$  is a sample sequence of a white noise process  $W(n)$  with variance  $\sigma_W^2 = 1$ .

- a. Design a Wiener FIR filter of length  $M = 2$  to estimate the desired signal  $S(n)$ .
- b. Use MATLAB to design the optimum FIR Wiener filter for lengths  $M = 3, 4$ , and  $5$ , and the corresponding MMSE for these cases. Comment on how the MMSE changes as  $M$  is increased from  $M = 2$  to  $M = 5$ .

### Solution

Since  $S(n)$  is obtained by exciting a single-pole filter by white noise, the power spectral density of  $S(n)$  is

$$\begin{aligned} S_{SS}(f) &= \sigma_V^2 |H(e^{j2\pi f})|^2 = \frac{0.64}{|1 - 0.6e^{-j2\pi f}|^2} \\ &= \frac{0.64}{1.36 - 1.2\cos(2\pi f)} \end{aligned}$$

Using the procedure given in Example 13.14, the corresponding autocorrelation sequence  $R_{SS}(m)$  is

$$R_{SS}(m) = (0.6)^{|m|}$$

a. The equations for the filter coefficients are

$$\begin{aligned} 2h(0) + 0.6h(1) &= 1, \\ 0.6h(0) + 2h(1) &= 0.6 \end{aligned}$$

Solution of these equations yields the result

$$h(0) = 0.451 \quad h(1) = 0.165$$

The corresponding minimum MSE is

$$\begin{aligned} \text{MMSE}_2 &= 1 - h(0)R_{SS}(0) - h(1)R_{SS}(1) \\ &= 1 - 0.451 - (0.165)(0.6) = 0.45 \end{aligned}$$

MATLAB script:

```
>> varW = 1; M = 2; m = 0:M-1;
>> Rss = 0.6.^m; TM = toeplitz(Rss) + varW*eye(M);
>> RD = Rss';
>> hopt2 = TM\RD
hopt2 =
    0.4505
    0.1648
>> MMSE2 = Rss(1) - RD'*hopt2
MMSE2 =
    0.4505
```

b. The filter coefficients and the corresponding MMSE values are obtained using the following MATLAB script.

```
>> M = 3; m = 0:M-1;
>> Rss = 0.6.^m; TM = toeplitz(Rss) + varW*eye(M); RD = Rss';
>> hopt3 = TM\RD; MMSE3 = Rss(1) - RD'*hopt3
MMSE3 =
    0.4451
>> M = 4; m = 0:M-1;
>> Rss = 0.6.^m; TM = toeplitz(Rss) + varW*eye(M); RD = Rss';
>> hopt4 = TM\RD; MMSE4 = Rss(1) - RD'*hopt4
MMSE4 =
    0.4445
>> M = 5; m = 0:M-1;
>> Rss = 0.6.^m; TM = toeplitz(Rss) + varW*eye(M); RD = Rss';
>> hopt5 = TM\RD; MMSE5 = Rss(1) - RD'*hopt5
```

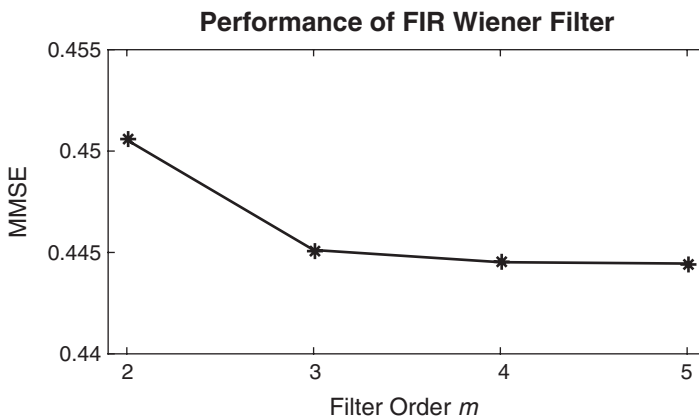


**FIGURE 14.25** Plot of MMSE vs. filter order in Example 14.20

```

MMSE5 =
0.4445
>> MMSE = [MMSE2,MMSE3,MMSE4,MMSE5];
>> % Plotting commands follow

```

The resulting plot of the MMSE vs. filter order is given in Figure 14.25.  $\square$

**EXAMPLE 14.21**

- Repeat Example 14.20 when the variance of  $V(n)$  is  $\sigma_V^2 = 0.64$  and the variance of the additive noise  $W(n)$  is  $\sigma_W^2 = 0.1$ .
- Generate the AR(1) signal sequence  $s(n)$  and the corresponding received sequence

$$x(n) = s(n) + w(n), \quad 0 \leq n \leq 1000$$

Filter the sequence  $x(n)$ ,  $0 \leq n \leq 1000$ , by the Wiener filter with  $M = 2, 3, 4, 5$  and plot the output  $y_2(n)$ ,  $y_3(n)$ ,  $y_4(n)$ , and  $y_5(n)$ , along with the derived signal  $s(n)$ . Comment on the effectiveness of the Wiener filter in estimating the derived signal  $s(n)$ .

**Solution**

From Example 14.20, the PSD and autocorrelation of  $S(n)$ , respectively, are given by

$$S_{SS}(f) = \frac{0.64}{1.36 - 1.2 \cos 2\pi f},$$

$$R_{SS}(m) = (0.6)^{|m|}$$

- Using  $\sigma_W^2 = 0.1$ , we develop and solve new sets of Wiener–Hopf equations to obtain new Wiener filters and their corresponding MMSEs. The details are given in the following MATLAB script.

```

>> varW = 0.1; M = 2; m = 0:M-1;
>> Rss = 0.6.^m; TM = toeplitz(Rss) + varW*eye(M);
>> RD = Rss';
>> hopt2 = TM\RD;
>> MMSE2 = Rss(1) - RD'*hopt2
MMSE2 =
    0.0871
>> M = 3; m = 0:M-1;
>> Rss = 0.6.^m; TM = toeplitz(Rss) + varW*eye(M); RD = Rss';
>> hopt3 = TM\RD; MMSE3 = Rss(1) - RD'*hopt3
MMSE3 =
    0.0870
>> M = 4; m = 0:M-1;
>> Rss = 0.6.^m; TM = toeplitz(Rss) + varW*eye(M); RD = Rss';
>> hopt4 = TM\RD; MMSE4 = Rss(1) - RD'*hopt4
MMSE4 =
    0.0870
>> M = 5; m = 0:M-1;
>> Rss = 0.6.^m; TM = toeplitz(Rss) + varW*eye(M); RD = Rss';
>> hopt5 = TM\RD; MMSE5 = Rss(1) - RD'*hopt5
MMSE5 =
    0.0870
>> % Plotting commands follow

```

Clearly, the MMSE values are very small and quickly settle into a steady-state value of 0.0807. The plot of MMSE vs. filter order is shown in Figure 14.26.

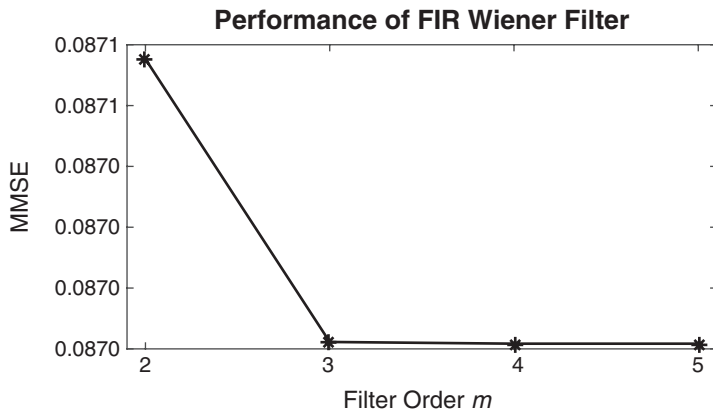


**FIGURE 14.26** Plot of MMSE vs. filter order in Example 14.21(a)

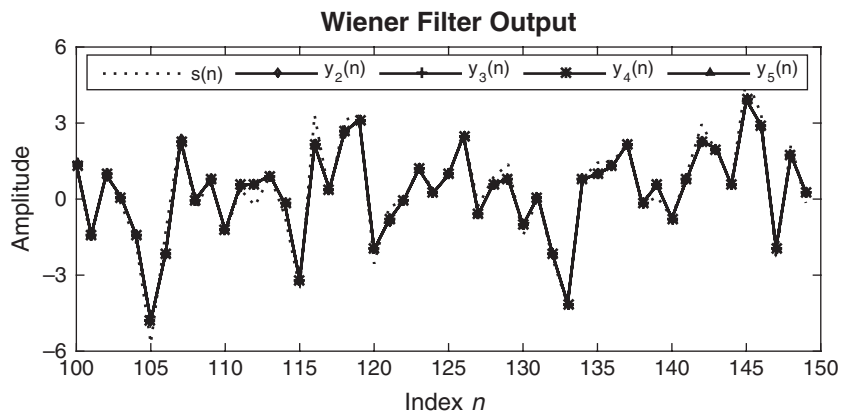


**FIGURE 14.27** Plots of signal  $s(n)$  and Wiener filter estimates  $\{y_k(n)\}_{k=2}^5$  in Example 14.21(b)

- b. Signal generation and Wiener filtering operations are given in the following MATLAB script.

```
>> n = 0:1000; varW = 0.1;
>> varV = 0.64; vn = sqrt(varV)*randn(1,length(n));
>> sn = filter(1,[1-0.6],vn);
>> wn = sqrt(varW)*randn(1,length(n));
>> xn = sn + wn;
>> yn2 = filter(hopt2,1,xn);
>> yn3 = filter(hopt3,1,xn);
>> yn4 = filter(hopt4,1,xn);
>> yn5 = filter(hopt5,1,xn);
```

The plot of signal estimates, containing samples from  $n = 100$  to  $n = 150$ , is shown in Figure 14.27. From it, we conclude that all estimates are very close to each other and that they also follow the signal  $s(n)$  closely.  $\square$

- **EXAMPLE 14.22** Consider the signal  $x(n) = s(n) + w(n)$ , where  $s(n)$  is a sample function of an AR process  $S(n)$  that satisfies the difference equation

$$s(n) = 0.8s(n-1) + v(n)$$

where  $v(n)$  is a sample function of a white Gaussian noise process  $V(n)$  with variance  $\sigma_V^2 = 0.49$  and  $w(n)$  is a sample function of a white Gaussian noise process  $W(n)$  with variance  $\sigma_W^2 = 0.1$ . The processes  $V(n)$  and  $W(n)$  are uncorrelated.

- a. Determine the autocorrelation sequence  $R_{SS}(m)$  and  $R_{XX}(m)$ .  
b. Use MATLAB to design a Wiener filter of length  $M = 2, 3, 4, 5$  and the corresponding MMSE.

- c. Generate the signal sequence  $s(n)$  and the received sequence  $x(n) = s(n) + w(n)$  for  $0 \leq n \leq 1000$ . Filter the sequence  $x(n)$ ,  $0 \leq n \leq 1000$ , by the Wiener filter for  $M = 2, 3, 4, 5$  and plot the output  $y_2(n), y_3(n), y_4(n)$ , and  $y_5(n)$ , along with the derived signal  $s(n)$ . Comment on the effectiveness of the Wiener filter in estimating the derived signal  $s(n)$ .

**Solution**

Since  $S(n)$  is obtained by exciting a single-pole filter by white noise, the power spectral density of  $S(n)$  is

$$\begin{aligned} S_{SS}(f) &= \sigma_V^2 |H(e^{j2\pi f})|^2 = \frac{0.49}{|1 - 0.8e^{-j2\pi f}|^2} \\ &= \frac{0.49}{1.64 - 1.6 \cos(2\pi f)} \end{aligned}$$

- a. Using the procedure given in Example 13.14, the corresponding autocorrelation sequence  $R_{SS}(m)$  is

$$R_{SS}(m) = \left(\frac{7}{6}\right)^2 (0.8)^{|m|} = 1.3611(0.8)^{|m|}$$

The autocorrelation of  $X(n)$  is then given by

$$R_{XX}(m) = R_{SS}(m) + R_{VV}(m) = 1.3611(0.8)^{|m|} + 0.1\delta(m)$$

- b. MATLAB script for Wiener filter design:

```
>> varW = 0.1; M = 2; m = 0:M-1;
>> Rss = 1.3611*0.8.^m; TM = toeplitz(Rss) + varW*eye(M);
>> RD = Rss';
>> hopt2 = TM\RD;
>> MMSE2 = Rss(1) - RD'*hopt2
MMSE2 =
    0.084606379865379
>> M = 3; m = 0:M-1;
>> Rss = 1.3611*0.8.^m; TM = toeplitz(Rss) + varW*eye(M); RD = Rss';
>> hopt3 = TM\RD; MMSE3 = Rss(1) - RD'*hopt3
MMSE3 =
    0.084475619407793
>> M = 4; m = 0:M-1;
>> Rss = 1.3611*0.8.^m; TM = toeplitz(Rss) + varW*eye(M); RD = Rss';
>> hopt4 = TM\RD; MMSE4 = Rss(1) - RD'*hopt4
MMSE4 =
    0.084473602242929
>> M = 5; m = 0:M-1;
>> Rss = 1.3611*0.8.^m; TM = toeplitz(Rss) + varW*eye(M); RD = Rss';
>> hopt5 = TM\RD; MMSE5 = Rss(1) - RD'*hopt5
MMSE5 =
    0.084473571121205
>> % Plotting commands follow
```

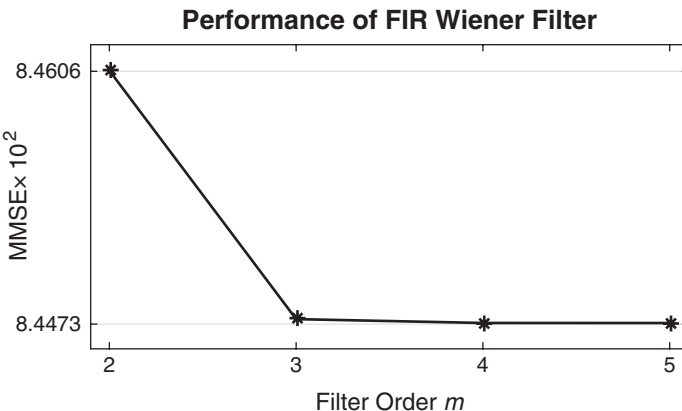


**FIGURE 14.28** Plot of MMSE vs. filter order in Example 14.22(a)

Again, the MMSE values are very small and quickly settle into a steady-state value of 0.0845. The plot of MMSE vs. filter order is shown in Figure 14.28.

- c. Signal generation and FIR Wiener filtering operations are given in the following MATLAB script.

```
>> n = 0:1000; varW = 0.1;
>> varV = 0.49; vn = sqrt(varV)*randn(1,length(n));
>> sn = filter(1,[1-0.8],vn);
>> wn = sqrt(varW)*randn(1,length(n));
>> xn = sn + wn;
>> yn2 = filter(hopt2,1,xn);
>> yn3 = filter(hopt3,1,xn);
>> yn4 = filter(hopt4,1,xn);
>> yn5 = filter(hopt5,1,xn);
```

The plot of signal estimates, containing samples from  $n = 100$  to  $n = 150$ , is shown in Figure 14.29. From it we conclude that all estimates are very close to each other and that they also follow the signal  $s(n)$  closely.  $\square$

#### 14.6.2 ORTHOGONALITY PRINCIPLE IN LINEAR MEAN-SQUARE ESTIMATION

The Wiener–Hopf equation for the optimum filter coefficients given by (14.132) can be obtained directly by applying the orthogonality principle in linear mean-square estimation. Simply stated, the mean-square error  $\mathcal{E}_M$  in (14.131) is a minimum if the filter coefficients  $h(k)$  are

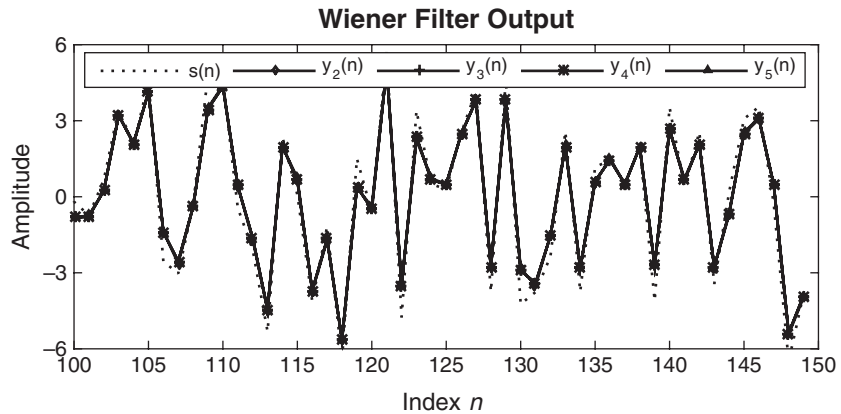


**FIGURE 14.29** Plots of signal  $s(n)$  and Wiener filter estimates  $\{y_k(n)\}_{k=2}^5$  in Example 14.22(b)

selected such that the error is orthogonal to each of the data points in the estimate,

$$\mathbb{E}[\mathbf{E}(n)\mathbf{X}^*(n-\ell)] = 0, \quad \ell = 0, 1, \dots, M-1 \quad (14.141)$$

where

$$e(n) = d(n) - \sum_{k=0}^{M-1} h(k)x(n-k) \quad (14.142)$$

Conversely, if the filter coefficients satisfy (14.141), then the resulting MSE is a minimum.

When viewed geometrically, the output of the filter, which is the estimate

$$\hat{d}(n) = \sum_{k=0}^{M-1} h(k)x(n-k) \quad (14.143)$$

is a vector in the subspace spanned by the data  $x(k)$ ,  $0 \leq k \leq M-1$ . The error  $e(n)$  is a vector from  $d(n)$  to  $\hat{d}(n)$ —that is,  $d(n) = e(n) + \hat{d}(n)$ —as shown in Figure 14.30. The orthogonality principle states that the length  $\mathcal{E}_M = \mathbb{E}[|\mathbf{E}(n)|^2]$  is a minimum when  $e(n)$  is perpendicular to the data subspace—that is,  $e(n)$  is orthogonal to each data point  $x(k)$ ,  $0 \leq k \leq M-1$ .

We note that the solution obtained from the normal equations in (14.132) is unique if the data  $x(n)$  in the estimate  $\hat{d}(n)$  are linearly independent. In that case, the correlation matrix  $\mathbf{T}_M$  is nonsingular. On the other hand, if the data are linearly dependent, then the rank of  $\mathbf{T}_M$  is less than  $M$  and, hence, the solution is not unique. In this case, the

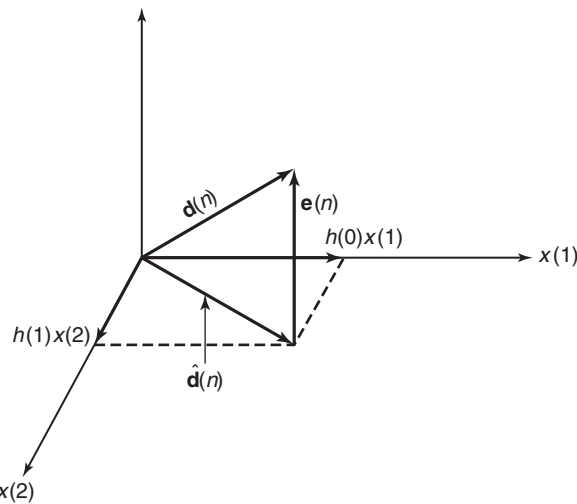


**FIGURE 14.30** Geometric interpretation of linear MSE problem

estimate  $\hat{d}(n)$  can be expressed as a linear combination of a reduced set of *linearly independent* data points equal to the rank of  $\mathbf{T}_M$ .

Since the MSE is minimized by selecting the filter coefficients to satisfy the orthogonality principle, then the residual minimum MSE is simply

$$\text{MMSE}_M = E[\mathbf{E}(n)\mathbf{D}^*(n)] \quad (14.144)$$

which yields the result given in (14.135).

- **EXAMPLE 14.23** Derive the Wiener–Hopf equation in (14.142) and the residual MMSE in equation (14.136) by application of the orthogonality principle.

**Solution**

The derived signal is  $d(n)$  and the estimate of  $d(n)$  is

$$\hat{d}(n) = \sum_{k=0}^{\infty} h(k)x(n-k)$$

where  $x(n)$  is the observed data sequence. The error sequence is defined as

$$\begin{aligned} e(n) &= d(n) - \hat{d}(n) \\ &= d(n) - \sum_{k=0}^{\infty} h(k)x(n-k) \end{aligned}$$

The impulse response  $\{h(k)\}$  of the optimum filter that minimizes the MSE is obtained when the error  $e(n)$  is orthogonal to the data in the estimate. Thus

$$E[\mathbf{E}(n)\mathbf{X}^*(n-\ell)] = 0 \quad \text{for } \ell = 0, 1, \dots$$

Hence

$$\begin{aligned} \mathbb{E} \left[ \left\{ D(n) - \sum_{k=0}^{\infty} h(k)X(n-k) \right\} X^*(n-\ell) \right] &= 0, \quad \ell = 0, 1, \dots \\ \mathbb{E}[D(n)x^*(n-\ell)] &= \sum_{k=0}^{\infty} h(k)\mathbb{E}[X(n-k)X^*(n-\ell)] \\ R_{DX}(\ell) &= \sum_{k=0}^{\infty} h(k)R_{XX}(\ell-k), \quad \ell \geq 0 \end{aligned}$$

The minimum MSE (MMSE) is

$$\begin{aligned} \mathbb{E}[\mathbb{E}(n)D^*(n)] &= \mathbb{E}[|D(n)|^2] - \sum_{k=0}^{\infty} h(k)\mathbb{E}[D^*(n)X(n-k)] \\ &= \sigma_D^2 - \sum_{k=0}^{\infty} h(k)R_{DX}^*(k) \end{aligned}$$

□

#### 14.6.3 IIR WIENER FILTER

In the previous section, we constrained the filter to be FIR and obtained a set of  $M$  linear equations for the optimum filter coefficients. In this section, we shall allow the filter to be infinite in duration (IIR), and the data sequence will also be infinite. Hence the filter output is

$$y(n) = \sum_{k=0}^{\infty} h(k)x(n-k) \quad (14.145)$$

The filter coefficients are selected to minimize the mean-square error between the desired output  $d(n)$  and  $y(n)$ , that is,

$$\begin{aligned} \mathcal{E}_{\infty} &= \mathbb{E}[|\mathbb{E}(n)|^2] \\ &= \mathbb{E} \left[ \left| D(n) - \sum_{k=0}^{\infty} h(k)X(n-k) \right|^2 \right] \end{aligned} \quad (14.146)$$

Application of the orthogonality principle leads to the Wiener-Hopf equation

$$\sum_{k=0}^{\infty} h(k)R_{XX}(\ell-k) = R_{DX}(\ell), \quad \ell \geq 0 \quad (14.147)$$

The residual MMSE is simply obtained by application of the condition given by (14.144). Thus we obtain

$$\text{MMSE}_{\infty} = \min_{\mathbf{h}} \mathcal{E}_{\infty} = \sigma_D^2 - \sum_{k=0}^{\infty} h_{\text{opt}}(k)R_{DX}^*(k) \quad (14.148)$$

The Wiener–Hopf equation given by (14.147) cannot be solved directly with  $z$ -transform techniques, because the equation holds only for  $\ell \geq 0$ . We shall solve for the optimum IIR Wiener filter based on the innovations representation of the stationary random process  $X(n)$ .

Recall that a stationary random process  $X(n)$  with autocorrelation  $R_{XX}(k)$  and power spectral density  $S_{XX}(f)$  may be represented by an equivalent innovations process by passing  $X(n)$  through a noise-whitening filter with system function  $1/G(z)$ , where  $G(z)$  is the minimum-phase component obtained from the spectral factorization of  $S_{XX}(z)$ , that is,

$$S_{XX}(z) = \sigma_I^2 G(z)G(z^{-1}) \quad (14.149)$$

Hence  $G(z)$  is analytic in the region  $|z| > r_1$ , where  $r_1 < 1$ .

Now, the optimum Wiener filter may be viewed as the cascade of the whitening filter  $1/G(z)$  with a second filter—say,  $Q(z)$ —whose output  $y(n)$  is identical to the output of the optimum Wiener filter. Since

$$y(n) = \sum_{k=0}^{\infty} q(k)i(n-k) \quad (14.150)$$

where  $i(n)$  is a sample sequence of the innovations process  $I(n)$ , and  $e(n) = d(n) - y(n)$ , application of the orthogonality principle yields the new Wiener–Hopf equation as

$$\sum_{k=0}^{\infty} q(k)R_{II}(\ell - k) = R_{DI}(\ell), \quad \ell \geq 0 \quad (14.151)$$

But, since  $I(n)$  is white, it follows that  $R_{II}(\ell - k) = 0$ , unless  $\ell = k$ . Thus we obtain the solution as

$$q(\ell) = \frac{R_{DI}(\ell)}{R_{II}(0)} = \frac{R_{DI}(\ell)}{\sigma_I^2}, \quad \ell \geq 0 \quad (14.152)$$

The  $z$ -transform of the sequence  $q(\ell)$  is

$$Q(z) = \sum_{k=0}^{\infty} q(k)z^{-k} = \frac{1}{\sigma_I^2} \sum_{k=0}^{\infty} R_{DI}(k)z^{-k} \quad (14.153)$$

If we denote the  $z$ -transform of the two-sided cross-correlation sequence  $R_{DI}(k)$  by  $S_{DI}(z)$ ,

$$S_{DI}(z) = \sum_{k=-\infty}^{\infty} R_{DI}(k)z^{-k} \quad (14.154)$$

and define  $[S_{DI}(z)]_+$ ,

$$[S_{DI}(z)]_+ = \sum_{k=0}^{\infty} R_{DI}(k)z^{-k} \quad (14.155)$$

then

$$Q(z) = \frac{1}{\sigma_i^2} [S_{DI}(z)]_+ \quad (14.156)$$

To determine  $[S_{DI}(z)]_+$ , we begin with the output of the noise-whitening filter, which may be expressed as

$$i(n) = \sum_{k=0}^{\infty} v(k)x(n-k) \quad (14.157)$$

where  $v(k)$ ,  $k \geq 0$ , is the impulse response of the noise-whitening filter,

$$\frac{1}{G(z)} \equiv V(z) = \sum_{k=0}^{\infty} v(k)z^{-k} \quad (14.158)$$

Then

$$\begin{aligned} R_{DI}(k) &= E[D(n)I^*(n-k)] \\ &= \sum_{m=0}^{\infty} v(m)E[d(n)x^*(n-m-k)] \\ &= \sum_{m=0}^{\infty} v(m)R_{DX}(k+m) \end{aligned} \quad (14.159)$$

The  $z$ -transform of the cross-correlation  $R_{DI}(k)$  is

$$\begin{aligned} S_{DI}(z) &= \sum_{k=-\infty}^{\infty} \left[ \sum_{m=0}^{\infty} v(m)R_{DX}(k+m) \right] z^{-k} \\ &= \sum_{m=0}^{\infty} v(m) \sum_{k=-\infty}^{\infty} R_{DX}(k+m)z^{-k} \\ &= \sum_{m=0}^{\infty} v(m)z^m \sum_{k=-\infty}^{\infty} R_{DX}(k)z^{-k} \\ &= V(z^{-1})S_{DX}(z) = \frac{S_{DX}(z)}{G(z^{-1})} \end{aligned} \quad (14.160)$$

Therefore,

$$Q(z) = \frac{1}{\sigma_i^2} \left[ \frac{S_{DX}(z)}{G(z^{-1})} \right]_+ \quad (14.161)$$

Finally, the optimum IIR Wiener filter has the system function

$$H_{opt}(z) = \frac{Q(z)}{G(z)} = \frac{1}{\sigma_i^2 G(z)} \left[ \frac{S_{DX}(z)}{G(z^{-1})} \right]_+ \quad (14.162)$$

In summary, the solution for the optimum IIR Wiener filter requires that we perform a spectral factorization of  $R_{XX}(z)$  to obtain  $G(z)$ , which is the minimum-phase component, and then we solve for the causal part of  $S_{DX}(z)/G(z^{-1})$ . The following example illustrates the procedure.

- **EXAMPLE 14.24** Let us determine the optimum IIR Wiener filter for the signal given in Example 14.20. For this signal, we have

$$S_{XX}(z) = S_{SS}(z) + 1 = \frac{1.8(1 - \frac{1}{3}z^{-1})(1 - \frac{1}{3}z)}{(1 - 0.6z^{-1})(1 - 0.6z)}$$

where  $\sigma_f^2 = 1.8$  and

$$G(z) = \frac{1 - \frac{1}{3}z^{-1}}{1 - 0.6z^{-1}}$$

The  $z$ -transform of the cross-correlation  $R_{DX}(m)$  is

$$S_{DX}(z) = S_{SS}(z) = \frac{0.64}{(1 - 0.6z^{-1})(1 - 0.6z)}$$

Hence

$$\begin{aligned} \left[ \frac{S_{DX}(z)}{G(z^{-1})} \right]_+ &= \left[ \frac{0.64}{(1 - \frac{1}{3}z)(1 - 0.6z^{-1})} \right]_+ \\ &= \left[ \frac{0.8}{1 - 0.6z^{-1}} + \frac{0.266z}{1 - \frac{1}{3}z} \right]_+ = \frac{0.8}{1 - 0.6z^{-1}} \end{aligned}$$

The optimum IIR filter has the system function

$$H_{\text{opt}}(z) = \frac{1}{1.8} \left( \frac{1 - 0.6z^{-1}}{1 - \frac{1}{3}z^{-1}} \right) \left( \frac{0.8}{1 - 0.6z^{-1}} \right) = \frac{\frac{4}{9}}{1 - \frac{1}{3}z^{-1}}$$

and impulse response

$$\mathbf{h}_{\text{opt}}(n) = \frac{4}{9} \left( \frac{1}{3} \right)^n, \quad n \geq 0$$

□

We conclude this section by expressing the minimum MSE given by (14.148) in terms of the frequency domain characteristics of the filter. First, we note that  $\sigma_D^2 \equiv \{E[|D(n)|^2]\}$  is simply the value of the autocorrelation sequence  $R_{DD}(k)$  evaluated at  $k = 0$ . Since

$$R_{DD}(k) = \frac{1}{2\pi j} \oint_C S_{DD}(z) z^{k-1} dz \quad (14.163)$$

it follows that

$$\sigma_D^2 = R_{DD}(0) = \frac{1}{2\pi j} \oint_C \frac{S_{DD}(z)}{z} dz \quad (14.164)$$

where the contour integral is evaluated along a closed path encircling the origin in the region of convergence of  $S_{DD}(z)$ .

The second term in (14.148) is also easily transformed to the frequency domain by application of Parseval's theorem. Since  $\mathbf{h}_{\text{opt}}(k) = 0$ , for  $k < 0$ , we have

$$\sum_{k=-\infty}^{\infty} \mathbf{h}_{\text{opt}}(k) R_{DX}^*(k) = \frac{1}{2\pi j} \oint_C H_{\text{opt}}(z) S_{DX}(z^{-1}) z^{-1} dz \quad (14.165)$$

where  $C$  is a closed contour encircling the origin that lies within the common region of convergence of  $H_{\text{opt}}(z) S_{DX}(z^{-1})$ . By combining (14.164) with (14.165), we obtain the desired expression for the MMSE, in the form

$$\text{MMSE}_{\infty} = \frac{1}{2\pi j} \oint_C [S_{DD}(z) - H_{\text{opt}}(z) S_{DX}(z^{-1})] z^{-1} dz \quad (14.166)$$

We note that  $S_{DD}(z) = S_{SS}(z)$  and  $S_{DX}(z^{-1}) = S_{SS}(z^{-1})$ .

- EXAMPLE 14.25** For the optimum Wiener filter derived in Example 14.24, the minimum MSE is

$$\text{MMSE}_{\infty} = \frac{1}{2\pi j} \oint_C \left[ \frac{0.3555}{(z - \frac{1}{3})(1 - 0.6z)} \right] dz$$

There is a single pole inside the unit circle at  $z = \frac{1}{3}$ . By evaluating the residue at the pole, we obtain

$$\text{MMSE}_{\infty} = 0.444$$

We observe that this MMSE is only slightly smaller than that for the optimum two-tap Wiener filter in Example 14.20.  $\square$

- EXAMPLE 14.26** Determine the optimum causal IIR Wiener filter for the estimation of the signal

$$s(n) = 0.8s(n-1) + v(n)$$

from the observation

$$x(n) = s(n) + w(n)$$

where  $v(n)$  is a sample sequence of a white noise process  $V(n)$  with  $\sigma_v^2 = 0.49$  and  $w(n)$  is a sample sequence of a white noise process  $W(n)$  with variance  $\sigma_w^2 = 1$ . The process  $V(n)$  and  $W(n)$  are uncorrelated.

### Solution

The complex cross- and auto-PSDs are given by

$$S_{DX}(z) = S_{SS}(z) = \frac{0.49}{(1 - 0.8z^{-1})(1 - 0.8z)} \quad (14.167)$$

from which the auto-PSD of  $X(n)$  is

$$S_{XX}(z) = S_{SS}(z) + 1 = \frac{1.78(1 - 0.45z^{-1})(1 - 0.45z)}{(1 - 0.8z^{-1})(1 - 0.8z)}$$

This gives the whitening filter

$$G(z) = \frac{(1 - 0.45z^{-1})}{(1 - 0.8z^{-1})}$$

The causal part is then given by

$$\begin{aligned} \left[ \begin{matrix} S_{DX}(z) \\ G(z^{-1}) \end{matrix} \right]_+ &= \left[ \begin{matrix} 0.49 \\ \frac{0.49}{(1 - 0.8z^{-1})(1 - 0.45z)} \end{matrix} \right]_+ = \left[ \begin{matrix} 0.766 \\ \frac{0.766}{(1 - 0.8z^{-1})} + \frac{0.345z}{(1 - 0.45z)} \end{matrix} \right]_+ \\ &= \frac{0.766}{(1 - 0.8z^{-1})} \end{aligned}$$

Now the system function of the optimum Wiener filter is

$$H_{\text{opt}}(z) = \frac{1}{1.78} \left( \frac{1 - 0.8z^{-1}}{1 - 0.45z^{-1}} \right) \left( \frac{0.766}{1 - 0.8z^{-1}} \right) = \frac{0.43}{1 - 0.45z^{-1}}$$

and the corresponding impulse response is

$$h_{\text{opt}}(n) = 0.43(0.45)^n u(n)$$

Finally, the MMSE for the causal IIR Wiener filter is given by

$$\begin{aligned} \text{MMSE}_\infty &= \frac{1}{2\pi j} \oint_C [S_{SS}(z) - H_{\text{opt}}(z)S_{SS}(z^{-1})] z^{-1} dz \\ &= \frac{1}{2\pi j} \oint_C \frac{0.28}{(z - 0.45)(1 - 0.8z)} dz = \frac{0.28}{1 - 0.8z} \Big|_{z=0.45} \\ &= 0.438 \end{aligned}$$

□

- **EXAMPLE 14.27** Consider the design of the optimum causal IIR Wiener filter for the signal  $s(n)$  given in Example 14.26, where now the variance of the additive noise  $w(n)$  is  $\sigma_w^2 = 0.1$ .

- a. Determine the system function for the optimum causal IIR filter and the minimum MSE.
- b. Generate the signal sequence  $s(n)$  and the received sequence  $x(n)$  for  $0 \leq n \leq 1000$ , where

$$\begin{aligned} s(n) &= 0.8s(n-1) + v(n) \\ x(n) &= s(n) + w(n) \end{aligned}$$

Filter the sequence  $x(n)$ ,  $0 \leq n \leq 1000$ , by the optimum causal Wiener filter obtained in part (a), and plot the output sequence  $y(n)$  along with the desired sequence  $s(n)$ . Comment on the effectiveness of the causal Wiener filter in estimating the desired signal.

**Solution**

From (14.167), the complex PSD  $S_{ss}(z)$  is

$$S_{ss}(z) = \frac{0.49}{(1 - 0.8z^{-1})(1 - 0.8z)}$$

a. For  $\sigma_w^2 = 0.1$ , the auto-PSD of  $X(n)$  is

$$S_{xx}(z) = S_{ss}(z) + 0.1 = \frac{0.6441(1 - 0.1242z^{-1})(1 - 0.1242z)}{(1 - 0.8z^{-1})(1 - 0.8z)} \quad (14.168)$$

This gives the whitening filter

$$G(z) = \frac{(1 - 0.1242z^{-1})}{(1 - 0.8z^{-1})}$$

The causal part is then given by

$$\begin{aligned} \left[ \begin{array}{c} S_{DX}(z) \\ G(z^{-1}) \end{array} \right]_+ &= \left[ \begin{array}{c} 0.49 \\ \hline (1 - 0.8z^{-1})(1 - 0.1242z) \end{array} \right]_+ \\ &= \left[ \begin{array}{c} 0.5441 \\ \hline (1 - 0.8z^{-1}) + \frac{0.0676z}{(1 - 0.1242z)} \end{array} \right]_+ = \frac{0.5441}{(1 - 0.8z^{-1})} \end{aligned}$$

Now the system function of the optimum Wiener filter is

$$H_{\text{opt}}(z) = \frac{1}{0.6441} \left( \frac{1 - 0.8z^{-1}}{1 - 0.1242z^{-1}} \right) \left( \frac{0.5441}{1 - 0.8z^{-1}} \right) = \frac{0.8447}{1 - 0.1242z^{-1}}$$

and the corresponding impulse response is

$$h_{\text{opt}}(n) = 0.8447(0.1242)^n u(n)$$

Finally, the MMSE for the causal IIR Wiener filter is given by

$$\begin{aligned} \text{MMSE}_\infty &= \frac{1}{2\pi j} \oint_C [S_{ss}(z) - H_{\text{opt}}(z)S_{ss}(z^{-1})] z^{-1} dz \\ &= \frac{1}{2\pi j} \oint_C \frac{0.0761}{(z - 0.1242)(1 - 0.8z)} dz = \frac{0.0761}{1 - 0.8z} \Big|_{z=0.1242} \\ &= 0.08447. \end{aligned}$$

Clearly, this error is lower than the minimum mean-squared errors given in Example 14.22. The above calculations were performed using the following MATLAB script.

```

>> varW = 0.1; varV = 0.49; a = 0.8;
>> Ss_num = varV*[0,-1/a]; Ss_den = conv([1,-a],[1,-1/a]);
>> Sx_num = varW*Ss_den + [Ss_num,0]; Sx_den = Ss_den;
>> Sx_num0 = Sx_num(1);
>> Sx_num_roots = roots(Sx_num/Sx_num0);
>> Sx_den0 = Sx_den(1);
>> Sx_den_roots = roots(Sx_den/Sx_den0);
>> Sx_num_factor = [1,-1/Sx_num_roots(1); 1,- Sx_num_roots(2)];
>> Sx_den_factor = [1,-1/Sx_den_roots(1); 1,- Sx_den_roots(2)];
>> Sx_constant = (Sx_num0*Sx_num_roots(1))/(Sx_den0*Sx_den_roots(1));
>> G_num = Sx_num_factor(2,:); G_den = Sx_den_factor(2,:);
>> [R,p,C] = residuez(varV*[0,-Sx_num_roots(1)],...
    conv([1,-Sx_den_roots(2)],[1,->> Sx_num_roots(1)]));
>> causal_part_num = R(2);
>> anticausal_part_num = R(1)*(-Sx_num_roots(2));
>> Hopt_num = causal_part_num/Sx_constant;
>> Hopt_den = [1,-Sx_num_roots(2)];
>> DHopt_num = Hopt_den-[Hopt_num,0];
>> Int_num = conv(Ss_num,[0,DHopt_num]);
>> MMSEc = Int_num(end)/(1-Sx_den_roots(2)*Sx_num_roots(2));
MMSEc =
0.084473570633519

```

- b. Signal generation and causal IIR Wiener filtering operations are given in the following MATLAB script.

```

>> n = 0:1000; varW = 0.1;
>> varV = 0.49; vn = sqrt(varV)*randn(1,length(n));
>> sn = filter(1,[1-0.8],vn);
>> wn = sqrt(varW)*randn(1,length(n));
>> xn = sn + wn;
>> yn = filter(Hopt_num,Hopt_den,xn);

```

Plot of signal and its estimate, containing samples from  $n = 100$  to  $n = 150$ , is shown in Figure 14.31. From it, we conclude that the estimated signal  $y(n)$  is very close to the signal  $s(n)$ .  $\square$

#### 14.6.4 NONCAUSAL WIENER FILTER

In the previous section, we constrained the optimum Wiener filter to be causal—that is,  $h_{\text{opt}}(n) = 0$  for  $n < 0$ . In this section, we shall drop this condition and allow the filter to include both the infinite past and the infinite future of the sequence  $x(n)$  in forming the output  $y(n)$ ,

$$y(n) = \sum_{k=-\infty}^{\infty} h(k)x(n-k) \quad (14.169)$$

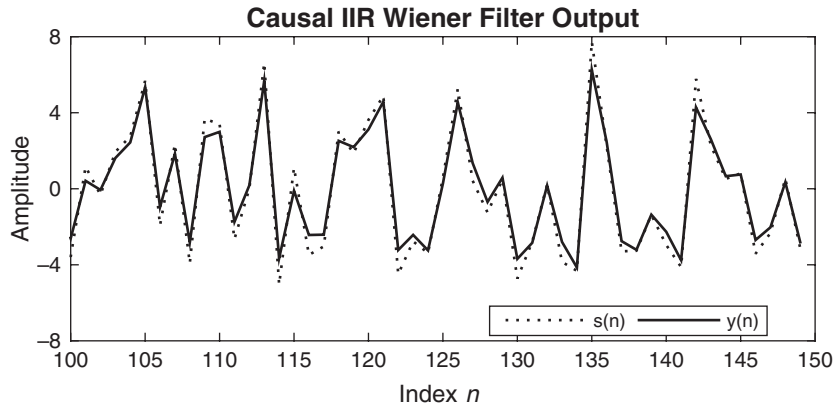


**FIGURE 14.31** Plots of signal  $s(n)$  and causal IIR Wiener filter estimate  $y(n)$  in Example 14.27(b)

The resulting filter is physically unrealizable. It may also be viewed as a smoothing filter in which the infinite future signal values are used to smooth the estimate  $\hat{d}(n) = y(n)$  of the desired signal  $d(n)$ .

Application of the orthogonality principle yields the Wiener-Hopf equation for the noncausal filter in the form

$$\sum_{k=-\infty}^{\infty} h(k)R_{XX}(\ell - k) = R_{DX}(\ell), \quad -\infty < \ell < \infty \quad (14.170)$$

and the resulting MMSE<sub>nc</sub> as

$$\text{MMSE}_{\text{nc}} = \sigma_D^2 - \sum_{k=-\infty}^{\infty} h(k)R_{DX}^*(k) \quad (14.171)$$

Since (14.170) holds for  $-\infty < \ell < \infty$ , this equation can be transformed directly to yield the optimum noncausal Wiener filter as

$$H_{\text{nc}}(z) = \frac{S_{DX}(z)}{S_{XX}(z)} \quad (14.172)$$

The MMSE<sub>nc</sub> can also be simply expressed in the  $z$ -domain as

$$\text{MMSE}_{\text{nc}} = \frac{1}{2\pi j} \oint_C [S_{DD}(z) - H_{\text{nc}}(z)S_{DX}(z^{-1})] z^{-1} dz \quad (14.173)$$

The following example serves to compare the form of the optimal noncausal filter with the optimal causal filter obtained in the previous section.

- **EXAMPLE 14.28** The optimum noncausal Wiener filter for the signal characteristics given in Example 14.20 is given by (14.172), where

$$S_{DX}(z) = S_{SS}(z) = \frac{0.64}{(1 - 0.6z^{-1})(1 - 0.6z)}$$

and

$$S_{XX}(z) = S_{SS}(z) + 1 = \frac{2(1 - 0.3z^{-1} - 0.3z)}{(1 - 0.6z^{-1})(1 - 0.6z)}$$

Then

$$H_{nc}(z) = \frac{0.3556}{(1 - \frac{1}{3}z^{-1})(1 - \frac{1}{3}z)}$$

This filter is clearly noncausal.

The minimum MSE achieved by this filter is determined from evaluating (14.173). The integrand is

$$\frac{1}{z} S_{SS}(z)[1 - H_{nc}(z)] = \frac{0.3555}{(z - \frac{1}{3})(1 - \frac{1}{3}z)}$$

The only pole inside the unit circle is  $z = 1/3$ . Hence the residue is

$$\left. \frac{0.3555}{1 - \frac{1}{3}z} \right|_{z=\frac{1}{3}} = \left. \frac{0.3555}{\frac{8}{9}} \right| = 0.40$$

Hence the minimum achievable MSE obtained with the optimum noncausal Wiener filter is

$$\text{MMSE}_{nc} = 0.40$$

Note that this is lower than the MMSE for the causal filter, as expected. □

- **EXAMPLE 14.29**
- a. Determine the system function for the noncausal IIR Wiener filter for the signal given in Example 14.27, where  $\sigma_v^2 = 0.49$  and  $\sigma_w^2 = 0.1$ .
  - b. Determine the MMSE for this filter and compare this to the MMSE for the optimum IIR causal Wiener filter in Example 14.27.
  - c. Generate the signal sequence  $s(n)$  and the received sequence  $x(n)$  for  $0 \leq n \leq 1000$ . Filter  $x(n)$  by the optimum noncausal Wiener filter obtained in part (a), and plot the output sequence  $y(n)$  along with the desired sequence  $s(n)$ . Comment on the effectiveness of the noncausal Wiener filter in estimating the desired signal.

### Solution

From (14.167), the complex PSD  $S_{SS}(z)$  is

$$S_{SS}(z) = \frac{0.49}{(1 - 0.8z^{-1})(1 - 0.8z)}$$

- a. From (14.168), the complex PSD  $S_{xx}(z)$  is

$$S_{xx}(z) = S_{ss}(z) + 0.1 = \frac{0.6441(1 - 0.1242z^{-1})(1 - 0.1242z)}{(1 - 0.8z^{-1})(1 - 0.8z)}$$

Hence the optimum noncausal IIR wiener filter is

$$H_{nc}(z) = \frac{S_{ss}(z)}{S_{xx}(z)} = \frac{0.7608}{(1 - 0.1242z^{-1})(1 - 0.1242z)} \quad (14.174)$$

with impulse response

$$h_{nc}(n) = 0.7727(0.1242)^{|n|}$$

which is a noncausal filter.

- b. The minimum MSE achieved by this filter is determined from evaluating (14.173). The integrand is

$$\frac{1}{z} S_{ss}(z)[1 - H_{nc}(z)] = \frac{0.07608}{(z - 0.1242)(1 - 0.1242z)}$$

The only pole inside the unit circle is  $z = 0.1242$ . Hence the residue is

$$\left. \frac{0.07608}{1 - 0.1242} \right|_{z=0.1242} = \left. \frac{0.07608}{0.9846} \right| = 0.0773$$

Hence the minimum achievable MSE obtained with the optimum noncausal Wiener filter is

$$\text{MMSE}_{nc} = 0.0773$$

which is lower than the MMSE of 0.08447 for the causal filter, as expected.

- c. Note that the noncausal filter in (14.174) can be expressed as a product of a causal and an anticausal filter—that is,

$$H_{nc}(z) = H_c(z)H_c(z^{-1}) = \left( \frac{\sqrt{0.7608}}{1 - 0.1242z^{-1}} \right) \left( \frac{\sqrt{0.7608}}{1 - 0.1242z} \right) \quad (14.175)$$

Thus the causal filter part is

$$H_c(z) = \frac{0.8722}{1 - 0.1242z^{-1}} \quad (14.176)$$

This filter will be used in the `filtfilt` function to implement the noncausal filter  $H_{nc}(z)$ . This function filters the input data in the forward direction through  $H_c(z)$ , then reverses the resulting output and filters it through  $H_c(z)$  again as a backward pass, and then reverses the resulting output to obtain the output of the noncausal filter. This also amounts to zero-phase filtering, as expected. Signal generation and noncausal IIR Wiener filtering operations are given in the following MATLAB script.

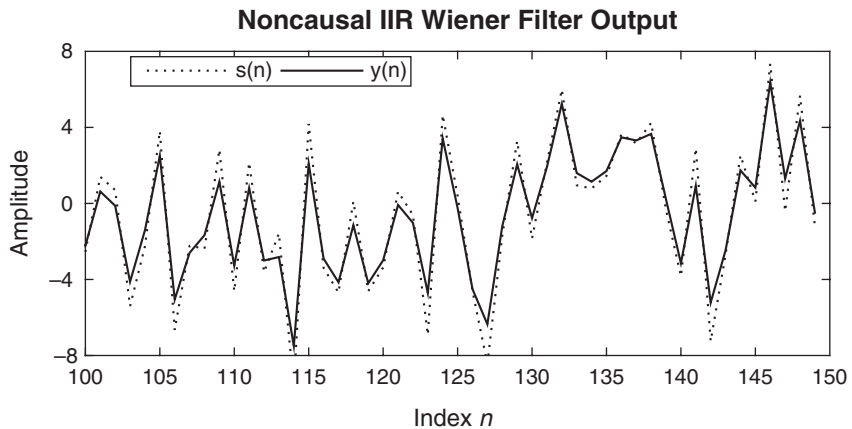


**FIGURE 14.32** Plots of signal  $s(n)$  and noncausal IIR Wiener filter estimate  $y(n)$  in Example 14.29(c)

```

n = 0:1000; varW = 0.1;
varV = 0.49; vn = sqrt(varV)*randn(1,length(n));
sn = filter(1,[1-0.8],vn);
wn = sqrt(varW)*randn(1,length(n));
xn = sn + wn;
Hc_num = sqrt(0.7608); Hc_den = [1,-0.1242];
yn =filtfilt(Hc_num,Hc_den,xn);

```

Plot of signal and its estimate, containing samples from  $n = 100$  to  $n = 150$ , is shown in Figure 14.32. From it we conclude that the estimated signal  $y(n)$  is very close to the signal  $s(n)$ .  $\square$

## 14.7 SUMMARY AND REFERENCES

---

The major focal point in this chapter was the design of optimum linear systems for linear prediction and filtering. The criterion for optimality was the minimization of the mean-square error between a specified desired filter output and the actual filter output.

In the development of linear prediction, we demonstrated that the equations for the forward and backward prediction errors specified a lattice filter whose parameters, the reflection coefficients  $K_m$ , were simply related to the filter coefficients  $a_m(k)$  of the direct form FIR linear predictor and the associated prediction-error filter. The optimum filter coefficients  $K_m$  and  $a_m(k)$  are easily obtained from the solution of the normal equations.

We described two computationally efficient algorithms for solving the normal equations, the Levinson–Durbin and Schur algorithms. Both algorithms are suitable for solving a Toeplitz system of linear equations and have a computational complexity of  $O(p^2)$  when executed on a single processor. However, with full parallel processing, the Schur algorithm solves the normal equations in  $O(p)$  time units, whereas the Levinson–Durbin algorithm requires  $O(p \log p)$ .

In addition to the all-zero lattice filter that resulted from linear prediction, we also derived the AR lattice (all-pole) filter structure and the ARMA lattice-ladder (pole-zero) filter structure. Finally, we described the design of the class of optimum linear filters, called Wiener filters.

Linear estimation theory has had a rich history of development over the past four decades. Kailath [41] presents a historical account of the first three decades. The pioneering work of Wiener [98] on optimum linear filtering for statistically stationary signals is especially significant. The generalization of the Wiener filter theory to dynamical systems with random inputs was developed by Kalman [46] and Kalman and Bucy [47]. Kalman filters are treated in Meditch [66], Brown [3], and Chui and Chen [6]. The monograph by Kailath [42] treats both Wiener and Kalman filters.

There are numerous references on linear prediction and lattice filters. Tutorial treatments on these subjects have been published in the journal papers by Makhoul [57, 58, 59] and Friedlander [17, 18]. Haykin [30], Markel and Gray [63], and Tretter [92] provide comprehensive treatments of these subjects. Applications of linear prediction to spectral analysis are found in Kay [48], Kay and Marple [49], and Marple [64], to geophysics in Robinson and Treitel [86, 87], and to adaptive filtering in Haykin [30].

The Levinson–Durbin algorithm for recursively solving the normal equations was given by Levinson [54] and later modified by Durbin [14]. Variations of this classical algorithm, called *split Levinson algorithms*, have been developed by Delsarte and Genin [12] and Krishna [51]. These algorithms exploit additional symmetries in the Toeplitz correlation matrix and save about a factor of two in the number of multiplications.

The Schur algorithm was originally described by Schur [88] in a paper published in German. An English translation of this paper appears in Gohberg [26]. The Schur algorithm is intimately related to the polynomials  $A_m(z)$ , which may be interpreted as orthogonal polynomials. A treatment of orthogonal polynomials is given in Szegő [91], Grenander and Szegő [28], and Geronimus [22]. The thesis of Vieira [94] and the papers by Kailath, Vieira, and Morf [45], Delsarte, Genin, and Kamp [13], and Youla and Kazanjian [100] provide additional results on orthogonal polynomials. Kailath [43, 44] provides tutorial treatments of the Schur algorithm and its relationship to orthogonal polynomials and the Levinson–Durbin algorithm. The pipelined parallel processing structure for computing the

reflection coefficients based on the Schur algorithm, and the related problem of solving Toeplitz systems of linear equations, is described in the paper by Kung and Hu [52]. Finally, we should mention that some additional computational efficiency can be achieved in the Schur algorithm, by further exploiting symmetry properties of Toeplitz matrices, as described by Krishna [51]. This leads to the so-called split Schur algorithm, which is analogous to the split Levinson algorithm.

# CHAPTER **15**

---

## Adaptive Filters

---

In contrast to filter design techniques described in Chapter 14, which were based on knowledge of the second-order statistics of the signals, there are many digital signal processing applications in which these statistics cannot be specified *a priori*. Examples of such applications include channel equalization and echo cancellation in data communication systems, and system identification and system modeling in control systems. In such applications, the coefficients of the filter to be designed cannot be specified *a priori*, because they depend on the characteristics of the communication channel or the control system. Such filters, with adjustable parameters, are usually called *adaptive filters*, especially when they incorporate algorithms that allow the filter coefficients to adapt to changes in the signal statistics.

Adaptive filters have received considerable attention from researchers over the past 35 years. As a result, many computationally efficient algorithms for adaptive filtering have been developed. In this chapter, we describe two basic algorithms: the least-mean-square (LMS) algorithm, which is based on a gradient optimization for determining the coefficients, and the class of recursive least-squares algorithms. Before we describe the algorithms, we present several practical applications in which adaptive filters have been successfully used in the estimation of signals corrupted by noise and other interference.

### 15.1 APPLICATIONS OF ADAPTIVE FILTERS

---

Adaptive filters have been used widely in communication systems, control systems, and various other systems in which the statistical

characteristics of the signals to be filtered are either unknown a priori or, in some cases, slowly time-variant (nonstationary signals). Numerous applications of adaptive filters have been described in the literature. Some of the more noteworthy applications include (1) adaptive antenna systems, in which adaptive filters are used for beam steering and for providing nulls in the beam pattern to remove undesired interference (Widrow, Mantey, and Griffiths [97]); (2) digital communication receivers, in which adaptive filters are used to provide equalization of intersymbol interference and for channel identification (Lucky [55], Proakis and Miller [80], Gersho [23], George, Bowen, and Storey [21], Proakis [77, 78], Magee and Proakis [56], Picinbono [75], and Nichols, Giordano, and Proakis [70]); (3) adaptive noise canceling techniques, in which adaptive filters are used to estimate and eliminate a noise component in a desired signal (Widrow et al. [96], Hsu and Giordano [34], and Ketchum and Proakis [50]); (4) system modeling, in which adaptive filters are used as models to estimate the characteristics of an unknown system. These are just a few of the best-known examples of the use of adaptive filters.

Although both IIR and FIR filters have been considered for adaptive filtering, the FIR filter is by far the most practical and widely used. The reason for this preference is quite simple: the FIR filter has only adjustable zeros; hence it is free of stability problems associated with adaptive IIR filters, which have adjustable poles as well as zeros. We should not conclude, however, that adaptive FIR filters are always stable. On the contrary, the stability of the filter depends critically on the algorithm for adjusting its coefficients, as will be demonstrated in Sections 15.2 and 15.3.

Of the various FIR filter structures that are possible, the direct form and the lattice form are the ones used in adaptive filtering applications. The direct form FIR filter structure with adjustable coefficients  $h(n)$  is illustrated in Figure 15.1. On the other hand, the adjustable parameters in an FIR lattice structure are the reflection coefficients  $K_n$ . In this chapter, we consider only direct form FIR filter structures.

An important consideration in the use of an adaptive filter is the criterion for optimizing the adjustable filter parameters. The criterion must not only provide a meaningful measure of filter performance, but it must also result in a practically realizable algorithm.

For example, a desirable performance index in a digital communication system is the average probability of error. Consequently, in implementing an adaptive equalizer, we might consider the selection of the equalizer coefficients to minimize the average probability of error as the basis for our optimization criterion. Unfortunately, however, the performance index (average probability of error) for this criterion is a highly nonlinear function of the filter coefficients and the signal statistics. As a consequence, the implementation of an adaptive filter that optimizes such a performance index is complex and impractical.

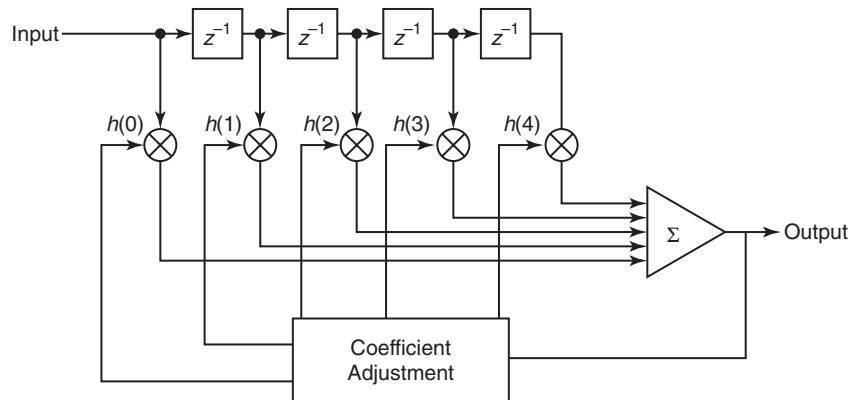


**FIGURE 15.1** Direct form adaptive FIR filter

In some cases, a performance index that is a nonlinear function of the filter parameters possesses many relative minima (or maxima), so that one is not certain whether the adaptive filter has converged to the optimum solution or to one of the relative minima (or maxima). For such reasons, some desirable performance indices, such as the average probability of error in a digital communication system, must be rejected on the grounds that they are impractical to implement.

Two criteria that provide good measures of performance in adaptive filtering applications are the least-squares criterion and its counterpart in a statistical formulation of the problem, namely, the mean-square-error (MSE) criterion. The least-squares (and MSE) criterion results in a quadratic performance index as a function of the filter coefficients and, hence, it possesses a single minimum. The resulting algorithms for adjusting the coefficients of the filter are relatively easy to implement, as we demonstrate in Section 15.2.

In this section, we describe several applications of adaptive filters that serve as a motivation for the mathematical development of algorithms derived in Section 15.2. We find it convenient to use the direct form FIR structure in these examples. Although we will not develop the recursive algorithms for automatically adjusting the filter coefficients in this section, it is instructive to formulate the optimization of the filter coefficients as a least-squares optimization problem. This development will serve to establish a common framework for the algorithms derived in the next two sections.

### 15.1.1 SYSTEM IDENTIFICATION OR SYSTEM MODELING

In system identification or system modeling, we have an unknown system, called a *plant*, that we wish to identify. The system is modeled by an FIR

filter with adjustable coefficients. Both the plant and model are excited by an input sequence  $x(n)$ . If  $y(n)$  denotes the output of the plant and  $\hat{y}(n)$  denotes the output of the model,

$$\hat{y}(n) = \sum_{k=0}^{M-1} h(k)x(n-k) \quad (15.1)$$

we may form the error sequence

$$e(n) = y(n) - \hat{y}(n), \quad n = 0, 1, \dots \quad (15.2)$$

and select the coefficients  $h(k)$  to minimize the sum of squared errors, that is,

$$\mathcal{E}_M = \sum_{n=0}^N \left[ y(n) - \sum_{k=0}^{M-1} h(k)x(n-k) \right]^2 \quad (15.3)$$

where  $N + 1$  is the number of observations. This is the least-squares criterion for determining the filter coefficients, which results in the set of linear equations

$$\sum_{k=0}^{M-1} h(k)r_{xx}(\ell - k) = r_{yx}(\ell), \quad \ell = 0, 1, \dots, M - 1 \quad (15.4)$$

where  $r_{xx}(\ell)$  is the autocorrelation (time average) of the sequence  $x(n)$  and  $r_{yx}(\ell)$  is the cross-correlation (time average) of the system output with the input sequence, defined as<sup>1</sup>

$$r_{xx}(\ell) = \sum_{n=0}^N x(n)x(n-\ell) \quad (15.5a)$$

$$r_{yx}(\ell) = \sum_{n=0}^N y(n)x(n-\ell) \quad (15.5b)$$

By solving (15.4), we obtain the filter coefficients for the model. Since the filter parameters are obtained directly from measurement data at the input and output of the system, without prior knowledge of the plant, we call the FIR filter model an adaptive filter.

If our only objective were to identify the system by use of the FIR model, the solution of (15.4) would suffice. In control systems applications, however, the system being modeled may be time-variant, changing slowly with time, and our purpose for having a model is to ultimately use it for

<sup>1</sup>In this chapter, we use lowercase  $r_{xx}(\ell)$  and  $r_{yx}(\ell)$  to denote the time-average auto-correlations and cross-correlations functions obtained directly from the data sequences.

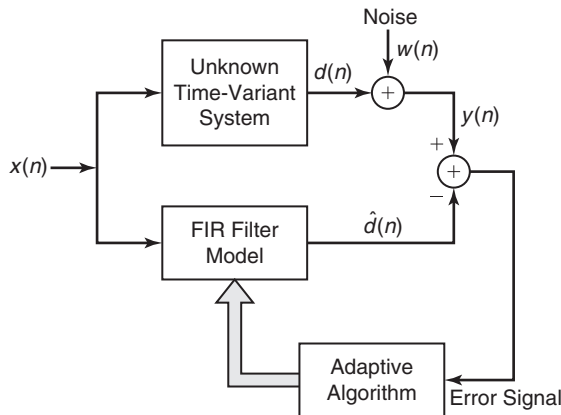


**FIGURE 15.2** Application of adaptive filtering to system identification

designing a controller that controls the plant. Furthermore, measurement noise is usually present at the output of the plant. This noise introduces uncertainty in the measurements and corrupts the estimates of the filter coefficients in the model. Such a scenario is illustrated in Figure 15.2. In this case, the adaptive filter must identify and track the time-variant characteristics of the plant in the presence of measurement noise at the output of the plant. The algorithms to be described in Section 15.2 are applicable to this system identification problem.

#### □ EXAMPLE 15.1 System Identification

Consider the system identification problem as illustrated in Figure 15.2. Suppose the unknown system has two complex-conjugate poles with a system function

$$H(z) = \frac{1}{1 - 2\operatorname{Re}(p)z^{-1} + |p|^2 z^{-2}}$$

where  $p$  is one of the poles. The additive noise sequence  $w(n)$  is a sample sequence of a white, zero-mean Gaussian process  $W(n)$  with variance  $\sigma_W^2 = 0.02$ . The excitation sequence  $x(n)$  is also a sample sequence of a white, zero-mean Gaussian process  $X(n)$  with variance  $\sigma_X^2 = 1$ . The processes  $W(n)$  and  $X(n)$  are uncorrelated. The FIR filter model has impulse response  $h(n)$  for  $0 \leq n \leq M-1$ .

- Generate the output sequence  $y(n)$  for  $0 \leq n \leq 1000$  and the corresponding desired sequence  $d(n)$  for  $0 \leq n \leq 1000$ , when  $p = 0.8e^{j\pi/4}$  and  $M = 15$ .
- Compute the autocorrelation sequence  $r_{xx}(m)$  and the cross-correlation sequence  $r_{yx}(m)$  for  $0 \leq m \leq M-1$ . Then compute the FIR filter coefficients from the least-squares equation in (15.4).
- Plot and compare the impulse response of the unknown system with that of the FIR filter model. Also plot and compare the frequency response of the unknown system with that of the model.

- d. Repeat parts (a), (b), and (c) when the sequence  $x(n)$  is the output of a first-order AR process described by the difference equation

$$x(n) = \frac{1}{2}x(n-1) + v(n)$$

where  $v(n)$  is a sample function of a white Gaussian noise process with variance  $\sigma_v^2 = 1$ .

### Solution

This solution is obtained using MATLAB.

- a. MATLAB script:

```
>> varW = 0.02; % Additive noise variance
>> varX = 1; % Excitation seq Variance
>> N = 1000; n = 0:N; % # of samples and indices
>> p = 0.8*exp(1j*pi/4); % Pole location
>> a = [1,-2*real(p),abs(p)^2]; % Plant denominator coeff
>> M = 15; % FIR filter model order
>> xn = sqrt(varX)*randn(N+1,1); % Input sequence
>> wn = sqrt(varW)*randn(N+1,1); % Noise sequence
>> dn = filter(1,a,xn); % Output of the plant
>> yn = dn+wn; % Noisy plant output
```

- b. MATLAB script:

```
>> [rxx,lags] = xcorr(xn,M-1); % ACRS of x(n)
>> Rxx = toeplitz(rxx(M:end)); % ACRM of x(n)
>> ryx = xcorr(yn,xn,M-1); % CCRS between y(n) and x(n)
>> ryx = ryx(M:end); % CCRV between y(n) and x(n)
>> hm = Rxx\ryx; % Model coeff (or Imp resp)
>> hp = impz(1,a,M+5); % Plant impulse response
```

- c. MATLAB script:

```
>> om = linspace(0,1,1001)*pi;
>> Hm = freqz(hm,1,om);
>> Hm_mag = abs(Hm);
>> Hm_pha = angle(Hm)/pi;
>> Hp = freqz(1,a,om);
>> Hp_mag = abs(Hp);
>> Hp_pha = angle(Hp)/pi;
>> % Plotting commands follow
```

The resulting plots are shown in Figure 15.3. Comparing the impulse response plots, we note that the model FIR impulse response is very close to the plant IIR impulse response for the first  $M = 15$  samples. Similarly, the frequency responses of the two systems are very close to each other. In these plots, a dotted line represents the phase response. A slight ripple in the model frequency response is the result of windowing effect due to FIR model assumption.

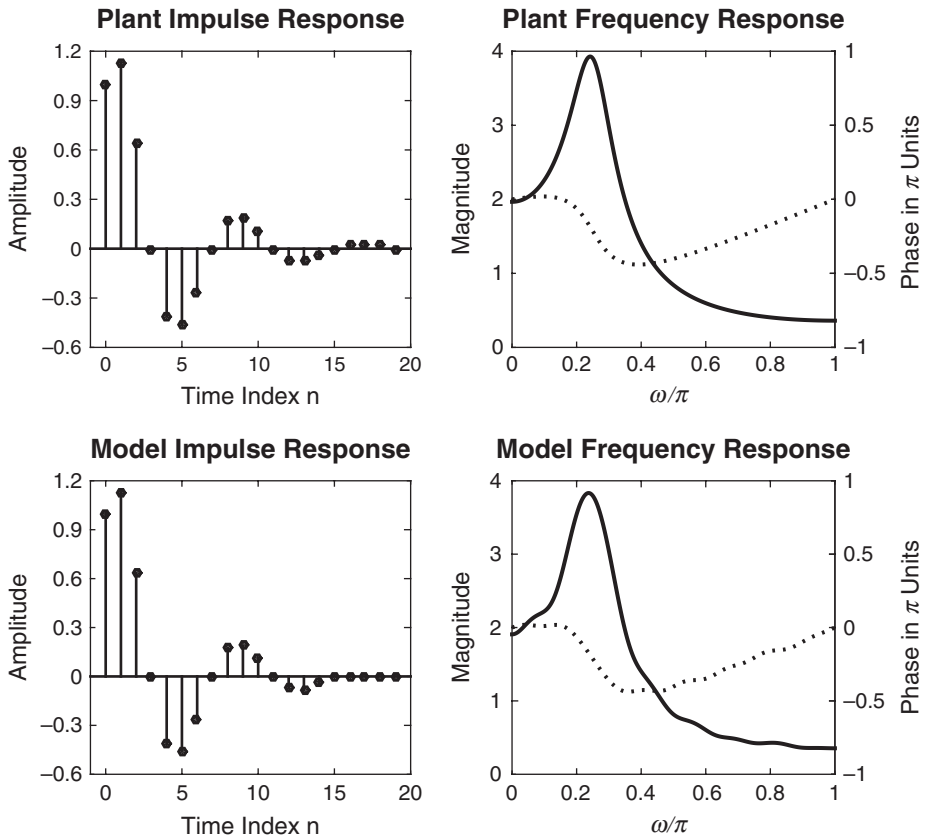


**FIGURE 15.3** Plots of the impulse and frequency responses of the plant and FIR model systems in Example 15.1(c). The dotted lines represent phase responses

- d. The only change in this set up is how the excitation sequence is generated using a first-order AR process.

```

>> varW = 0.02; % Additive noise variance
>> varV = 1; % Excitation seq Variance
>> N = 1000; n = 0:N; % Number of samples and indices
>> p = 0.8*exp(1j*pi/4); % Pole location
>> a = [1,-2*real(p),abs(p)^2]; % Plant denominator coeff
>> M = 15; % FIR filter model order
>> vn = sqrt(varV)*randn(N+1,1); % Gaussian seq for Input x(n)
>> xn = filter(1,[1,-1/2],vn); % Input sequence x(n)
>> wn = sqrt(varW)*randn(N+1,1); % Noise sequence
>> dn = filter(1,a,xn); % Output of the plant
>> yn = dn+wn; % Noisy plant output
>> [rxx,lags] = xcorr(xn,M-1); % ACRS of x(n)

```

```

>> Rxx = toeplitz(rxx(M:end)); % ACRM of x(n)
>> rxy = xcorr(yn,xn,M-1); % CCRS between y(n) and x(n)
>> rxy = rxy(M:end); % CCRV
>> hm = Rxx\rxy; % Model coeff (or Imp resp)
>> hp = impz(1,a,M+5); % Plant impulse response
>> om = linspace(0,1,1001)*pi;
>> Hm = freqz(hm,1,om);
>> Hm_mag = abs(Hm); Hm_pha = angle(Hm)/pi;
>> Hp = freqz(1,a,om);
>> Hp_mag = abs(Hp); Hp_pha = angle(Hp)/pi;

```

The resulting plots are shown in Figure 15.4. Comparisons of the impulse and frequency response plots are similar to those in part (c). Furthermore, the results in part (c) and (d) are almost identical.  $\square$

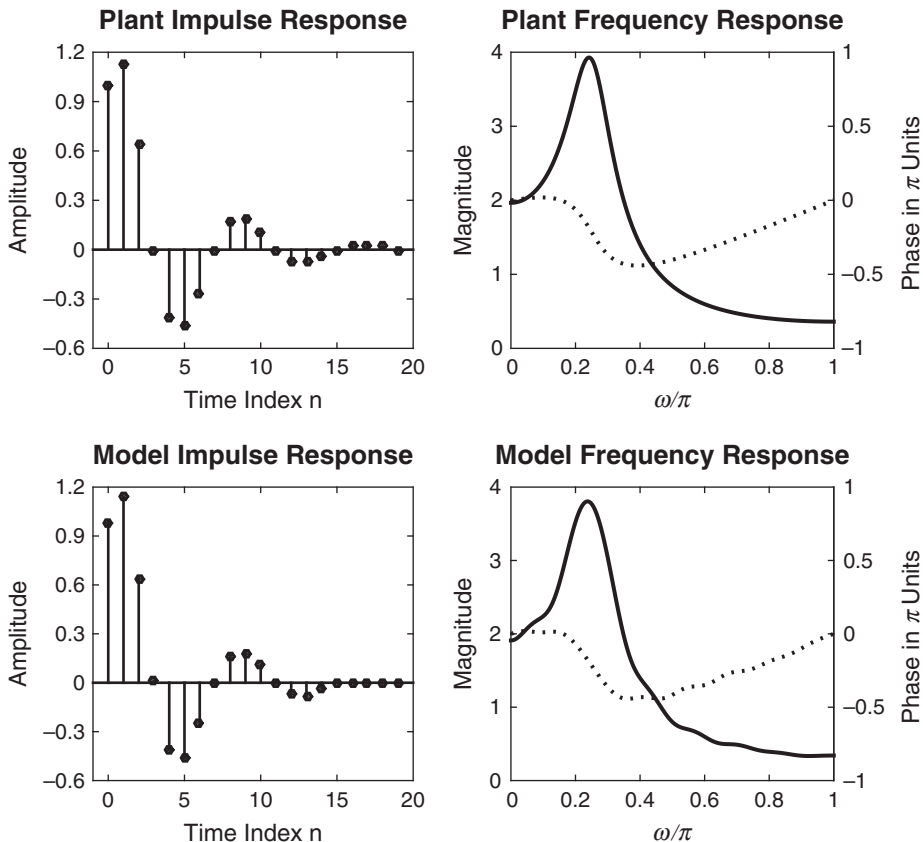


**FIGURE 15.4** Plots of the impulse and frequency responses of the plant and FIR model systems in Example 15.1(d). The dotted lines represent phase responses

### 15.1.2 ADAPTIVE CHANNEL EQUALIZATION

Figure 15.5 shows a block diagram of a digital communication system in which an adaptive equalizer is used to compensate for the distortion caused by the transmission medium (channel). The digital sequence of information symbols  $a(n)$  is fed to the transmitting filter, whose output is

$$s(t) = \sum_{k=0}^{\infty} a(k)p(t - kT_s) \quad (15.6)$$

where  $p(t)$  is the impulse response of the filter at the transmitter and  $T_s$  is the time interval between information symbols—that is,  $1/T_s$  is the symbol rate. For purposes of this discussion, we may assume that  $a(n)$  is a multilevel sequence that takes on values from the set  $\pm 1, \pm 3, \pm 5, \dots, \pm(K - 1)$ , where  $K$  is the number of possible symbol values.

Typically, the pulse  $p(t)$  is designed to have the characteristics illustrated in Figure 15.6. Note that  $p(t)$  has amplitude  $p(0) = 1$  at  $t = 0$  and  $p(nT_s) = 0$  at  $t = nT_s$ ,  $n = \pm 1, \pm 2, \dots$ . As a consequence, successive pulses transmitted sequentially every  $T_s$  seconds do not interfere with one another when sampled at the time instants  $t = nT_s$ . Thus  $a(n) = s(nT_s)$ .

The channel, which is usually well modeled as a linear filter, distorts the pulse and, thus, causes intersymbol interference. For example, in telephone channels, filters are used throughout the system to separate signals in different frequency ranges. These filters cause phase and amplitude distortion. Figure 15.7 illustrates the effect of channel distortion on the pulse  $p(t)$  as it might appear at the output of a telephone channel. Now, we observe that the samples taken every  $T_s$  seconds are corrupted by interference from several adjacent symbols. The distorted signal is also corrupted by additive noise, which is usually wideband.

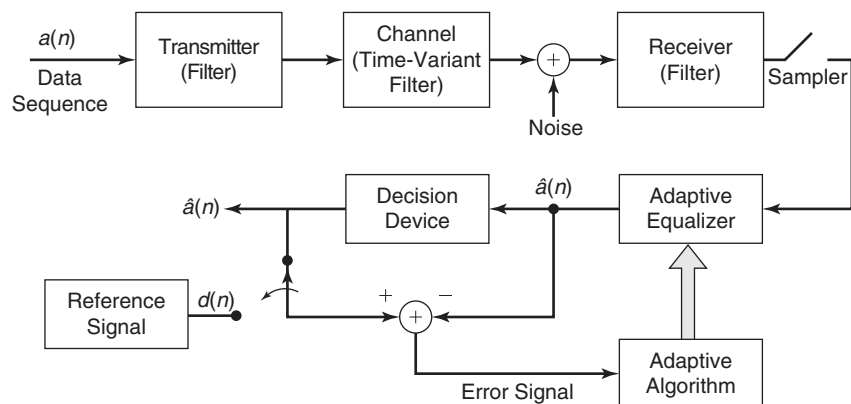


**FIGURE 15.5** Application of adaptive filtering to adaptive channel equalization

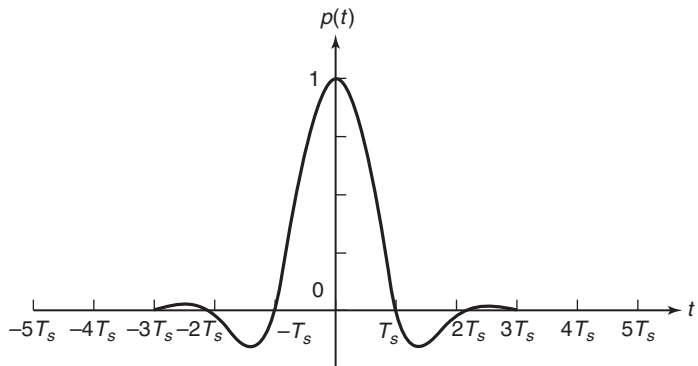


**FIGURE 15.6** Pulse shape for digital transmission of symbols at a rate of  $1/T_s$  symbols per second

At the receiving end of the communication system, the signal is first passed through a filter that is designed primarily to eliminate the noise outside of the frequency band occupied by the signal. We may assume that this filter is a linear-phase FIR filter that limits the bandwidth of the noise but causes negligible additional distortion on the channel-corrupted signal.

Samples of the received signal at the output of this filter reflect the presence of intersymbol interference and additive noise. If we ignore for

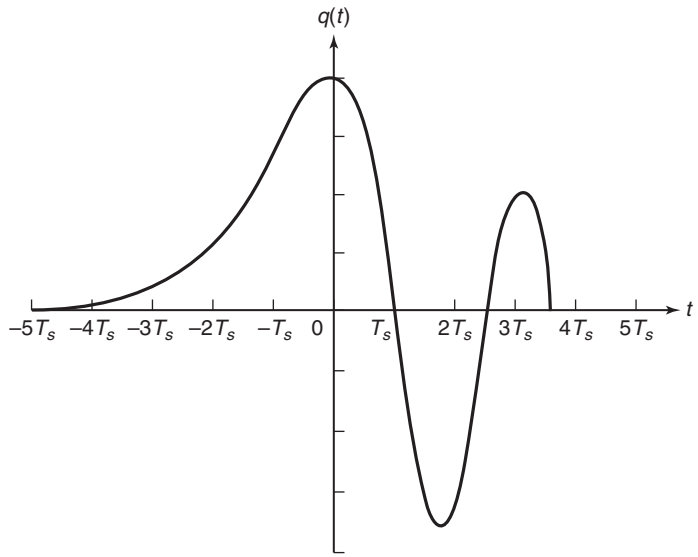


**FIGURE 15.7** Effect of channel distortion on the signal pulse in Figure 15.6

the moment the possible time variations in the channel, we may express the sampled output at the receiver as

$$\begin{aligned} x(nT_s) &= \sum_{k=0}^{\infty} a(k)q(nT_s - kT_s) + w(nT_s) \\ &= a(n)q(0) + \sum_{\substack{k=0 \\ k \neq n}}^{\infty} a(k)q(nT_s - kT_s) + w(nT_s) \end{aligned} \quad (15.7)$$

where  $w(t)$  represents the additive noise and  $q(t)$  represents the distorted pulse at the output of the receiver filter.

To simplify our discussion, we assume that the sample  $q(0)$  is normalized to unity by means of an automatic gain control (AGC) contained in the receiver. Then the sampled signal given in (15.7) may be expressed as

$$x(n) = a(n) + \sum_{\substack{k=0 \\ k \neq n}}^{\infty} a(k)q(n - k) + w(n) \quad (15.8)$$

where  $x(n) \equiv x(nT_s)$ ,  $q(n) \equiv q(nT_s)$ , and  $w(n) \equiv w(nT_s)$ . The term  $a(n)$  in (15.8) is the desired symbol at the  $n$ th sampling instant. The second term,

$$\sum_{\substack{k=0 \\ k \neq n}}^{\infty} a(k)q(n - k)$$

constitutes the intersymbol interference due to the channel distortion, and  $w(n)$  represents the additive noise in the system.

In general, the channel distortion effects embodied through the sampled values  $q(n)$  are unknown at the receiver. Furthermore, the channel may vary slowly with time such that the intersymbol interference effects are time-variant. The purpose of the adaptive equalizer is to compensate the signal for the channel distortion, so that the resulting signal can be detected reliably. Let us assume that the equalizer is an FIR filter with  $M$  adjustable coefficients  $h(n)$ . Its output may be expressed as

$$\hat{a}(n) = \sum_{k=0}^{M-1} h(k)x(n + D - k) \quad (15.9)$$

where  $D$  is some nominal delay in processing the signal through the filter and  $\hat{a}(n)$  represents an estimate of the  $n$ th information symbol. Initially, the equalizer is trained by transmitting a known data sequence  $d(n)$ . Then, the equalizer output,  $\hat{a}(n)$ , is compared with  $d(n)$  and an error is generated that is used to optimize the filter coefficients.

If we again adopt the least-squares error criterion, we select the coefficients  $h(k)$  to minimize the quantity

$$\mathcal{E}_M = \sum_{n=0}^N [d(n) - \hat{a}(n)]^2 = \sum_{n=0}^N \left[ d(n) - \sum_{k=0}^{M-1} h(k)x(n+D-k) \right]^2 \quad (15.10)$$

The result of the optimization is a set of linear equations of the form

$$\sum_{n=0}^{M-1} h(k)r_{xx}(\ell-k) = r_{dx}(\ell-D), \quad \ell = 0, 1, 2, \dots, M-1 \quad (15.11)$$

where  $r_{xx}(\ell)$  is the autocorrelation of the sequence  $x(n)$  and  $r_{dx}(\ell)$  is the cross-correlation between the desired sequence  $d(n)$  and the received sequence  $x(n)$ .

Although the solution of (15.11) is obtained recursively in practice (as demonstrated in the following two sections), in principle we observe that these equations result in values of the coefficients for the initial adjustment of the equalizer. After the short training period, which usually lasts less than 1 second for most channels, the transmitter begins to transmit the information sequence  $a(n)$ . In order to track the possible time variations in the channel, the equalizer coefficients must continue to be adjusted in an adaptive manner while receiving data. As illustrated in Figure 15.5, this is usually accomplished by treating the decisions at the output of the decision device as correct, and using the decisions in place of the reference  $d(n)$  to generate the error signal. This approach works quite well when decision errors occur infrequently (e.g., less than one decision error per hundred symbols). The occasional decision errors cause only small misadjustments in the equalizer coefficients. In Sections 15.2 and 15.3, we describe the adaptive algorithms for recursively adjusting the equalizer coefficients.

#### EXAMPLE 15.2 Channel Equalization

Consider the system configuration illustrated in Figure 15.8, below. The channel filter system function is

$$C(z) = 1 - 2\operatorname{Re}(z_0)z^{-1} + |z_0|^2 z^{-1}$$

and the equalizer system function is

$$H(z) = \sum_{k=0}^{M-1} h(k)z^{-k}$$

The zeros of  $C(z)$  are located at  $z_0 = 0.8e^{j\pi/4}$  and  $z_0^* = 0.8e^{-j\pi/4}$ . The input sequence  $a(n)$  is a pseudo-random sequence of  $\pm 1$ . The additive noise

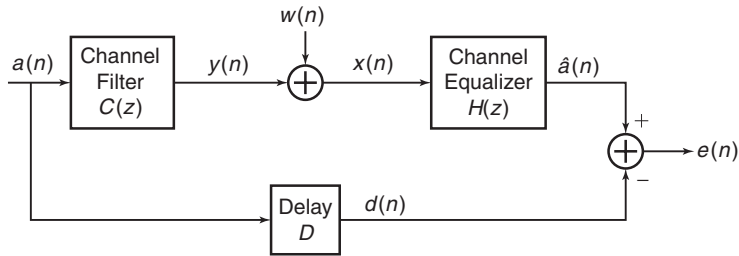


**FIGURE 15.8** Channel equalization for Example 15.2

$w(n)$  is a sample sequence of a white Gaussian noise process with variance  $\sigma_w^2 = 0.1$ .

- Generate the sequence  $a(n)$  and  $x(n)$  for  $0 \leq n \leq 1000$ .
- For  $M = 7$  and  $D = 10$ , compute the equalizer coefficients  $h(k)$ ,  $0 \leq k \leq 6$  based on the least-squares solution

$$\sum_{k=0}^{6} h(k) r_{xx}(\ell - k) = r_{dx}(\ell), \quad \ell = 0, 1, \dots, 6$$

where  $d(n) = a(n)$ ,  $0 \leq n \leq 1000$ .

- Plot the frequency response of the channel filter  $C(z)$ , the equalizer filter  $H(z)$ , and the frequency response of the cascade filter  $C(z)H(z)$ . Comment on the results.

### Solution

This solution is obtained using MATLAB.

- MATLAB script:

```

>> z0 = 0.8*exp(1j*pi/4); % Zero of C(z)
>> Cb = [1, -2*real(z0), abs(z0)^2]; % Numerator of C(z) or imp resp
>> N = 1000; n = 0:N; % Length and timing indices
>> varW = 0.1; % Additive noise variance
>> M = 7; % FIR Equalizer length
>> an = 2*randi([0,1], N+1, 1)-1; % Pseudorandom symbol sequence
>> yn = filter(Cb, 1, an); % Distorted symbol sequence
>> wn = sqrt(varW)*randn(N+1, 1); % Additive noise sequence
>> xn = yn+wn; % Noisy distorted symbols

```

- MATLAB script:

```

>> [rxx, lags] = xcorr(xn, M-1); % ACRS of x(n)
>> Rxx = toeplitz(rxx(M:end)); % ACRM of x(n)
>> rdx = xcorr(an, xn, M-1); % CCRS between d(n) and x(n)
>> rdx = rdx(M:end); % CCRV
>> heq = Rxx\rdx; % Equalizer coeff (or Imp resp)

```

- c. The frequency response plots of the channel, equalizer, and the cascade filter are computed using the following MATLAB script and shown in Figure 15.9.

```
om = linspace(0,1,1001)*pi;
Heq = freqz(heq,1,om);
Heq_mag = abs(Heq); Heq_phd = angle(Heq)/pi;
Cz = freqz(Cb,1,om);
Cz_mag = abs(Cz); Cz_phd = angle(Cz)/pi;
CzHeq = Cz.*Heq;
CzHeq_mag = abs(CzHeq); CzHeq_phd = angle(CzHeq)/pi;
```

The frequency response of the cascade filter is very nearly that of an allpass filter indicating that the equalizer is very close to an inverse filter for the channel.  $\square$

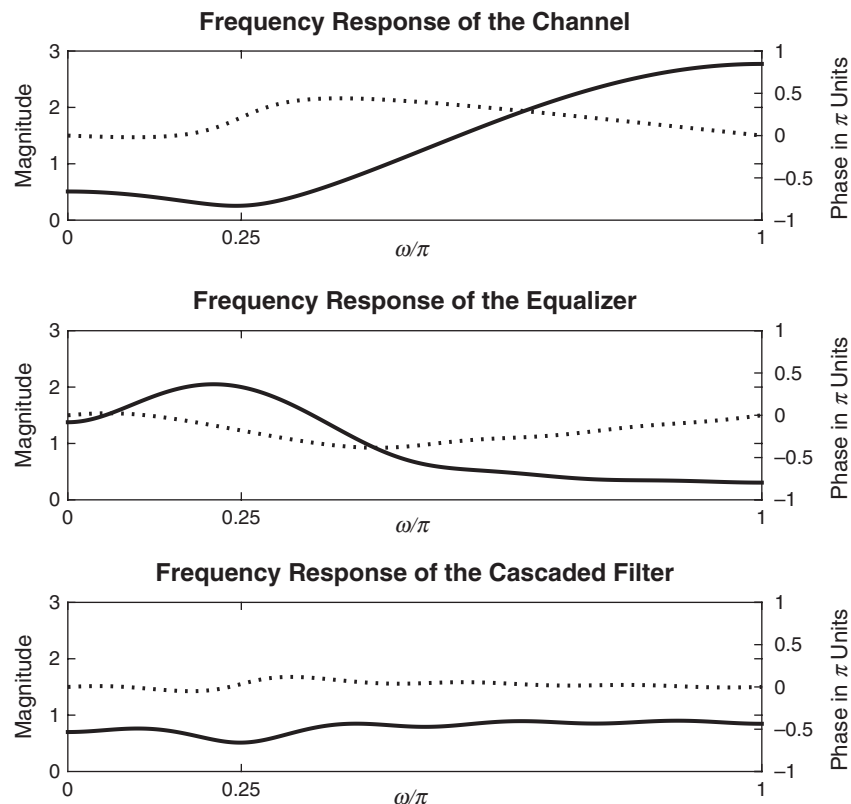


**FIGURE 15.9** Frequency response plots of the channel, equalizer, and the cascade filter in Example 15.2(c). The dotted lines represent phase responses.

### 15.1.3 ECHO CANCELLATION IN DATA TRANSMISSION OVER TELEPHONE CHANNELS

In the transmission of data over telephone channels, modems (modulators/demodulators) are used to provide an interface between the digital data sequence and the analog channel. Shown in Figure 15.10 is a block diagram of a communication system in which two terminals, labeled A and B, transmit data by using modems A and B to interface to a telephone channel. As shown, a digital sequence  $a(n)$  is transmitted from terminal A to terminal B while another digital sequence  $b(n)$  is transmitted from terminal B to A. This simultaneous transmission in both directions is called *full-duplex transmission*.

As described, the two transmitted signals may be represented as

$$s_A(t) = \sum_{k=0}^{\infty} a(k)p(t - kT_s) \quad (15.12)$$

$$s_B(t) = \sum_{k=0}^{\infty} b(k)p(t - kT_s) \quad (15.13)$$

where  $p(t)$  is a pulse as shown in Figure 15.6.

When a subscriber wishes to transmit data over the dial-up switched telephone network, the local communication link between the subscriber and the local central telephone office is a two-wire line, called the *local loop*. At the central office, the subscriber two-wire line is connected to the main four-wire telephone channels that interconnect different central offices, called *trunk lines*, by a device called a *hybrid*. By using transformer coupling, the hybrid is tuned to provide isolation between the transmission and reception channels in full-duplex operation. However, due to impedance mismatch between the hybrid and the telephone channel, the level of isolation is often insufficient, and, consequently, some of the signal on the transmitter side leaks back and corrupts the signal on the receiver

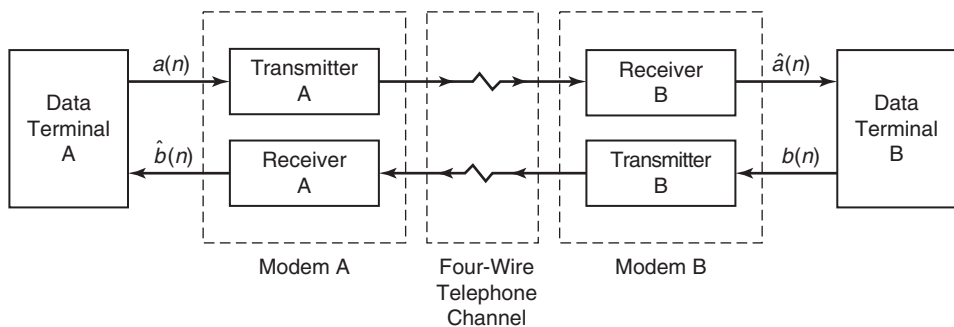


**FIGURE 15.10** Full-duplex data transmission over telephone channels

side, causing an “echo” that is often heard in voice communications over telephone channels.

To mitigate the echoes in voice transmissions, the telephone companies employ a device called an *echo suppressor*. In data transmission, the solution is to use an *echo canceller* within each modem. The echo cancellers are implemented as adaptive filters with automatically adjustable coefficients, just as in the case of transversal (FIR) equalizers.

With the use of hybrids to couple a two-wire to a four-wire channel, and echo cancellers at each modem to estimate and subtract the echoes, the data communication system for the dial-up switched network takes the form shown in Figure 15.11. A hybrid is needed at each modem to isolate the transmitter from the receiver and to couple to the two-wire local loop. Hybrid A is physically located at the central office of subscriber A, while hybrid B is located at the central office to which subscriber B is connected. The two central offices are connected by a four-wire line, one pair used for transmission from A to B and the other pair used for transmission in the reverse direction, from B to A. An echo at terminal A due to the hybrid A is called a *near-end echo*, while an echo at terminal A due to the hybrid B is termed a *far-end echo*. Both types of echoes are usually present in data transmission and must be removed by the echo canceller.

Suppose we neglect the channel distortion for purposes of this discussion and deal with the echoes only. The signal received at modem A may be expressed as

$$s_{RA}(t) = A_1 s_B(t) + A_2 s_A(t - d_1) + A_3 s_A(t - d_2) \quad (15.14)$$

where  $s_B(t)$  is the desired signal to be demodulated at modem A;  $s_A(t - d_1)$  is the near-end echo due to hybrid A,  $s_A(t - d_2)$  is the far-end echo due

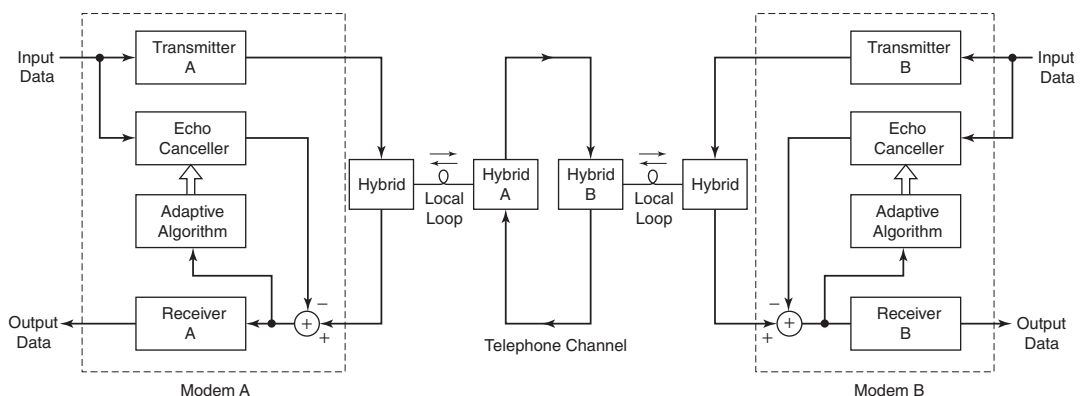


**FIGURE 15.11** Block diagram model of a digital communication system that uses echo cancellers in modems

to hybrid B;  $A_i$ ,  $i = 1, 2, 3$  are the corresponding amplitudes of the three signal components; and  $d_1$  and  $d_2$  are the delays associated with the echo components. A further disturbance that corrupts the received signal is additive noise, so that the received signal at modem A is

$$r_A(t) = s_{RA}(t) + w(t) \quad (15.15)$$

where  $w(t)$  represents the sample function of an additive process.

The adaptive echo canceller attempts to estimate adaptively the two echo components. If its coefficients are  $h(n)$ ,  $n = 0, 1, \dots, M - 1$ , its output is

$$\hat{s}_A(n) = \sum_{k=0}^{M-1} h(k)a(n-k) \quad (15.16)$$

which is an estimate of the echo signal components. This estimate is subtracted from the sampled received signal, and the resulting error signal can be minimized in the least-squares sense to optimally adjust the coefficients of the echo canceller. There are several possible configurations for placement of the echo canceller in the modem, and for forming the corresponding error signal. Figure 15.12 illustrates one configuration, in which the canceller output is subtracted from the sampled output of the receiver filter with input  $r_A(t)$ . Figure 15.13 illustrates a second configuration, in which the echo canceller is generating samples at the Nyquist rate instead of the symbol rate; in this case, the error signal used to adjust the coefficients is simply the difference between  $r_A(n)$ , the sampled received signal, and the canceller output. Finally, Figure 15.14 illustrates the canceller operating in combination with an adaptive equalizer.

Application of the least-squares criterion in any of the configurations shown in Figures 15.12–15.14 leads to a set of linear equations for the

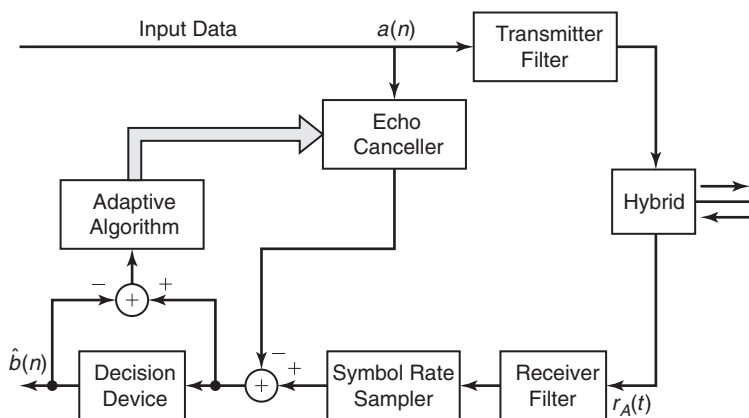


**FIGURE 15.12** Symbol-rate echo canceller

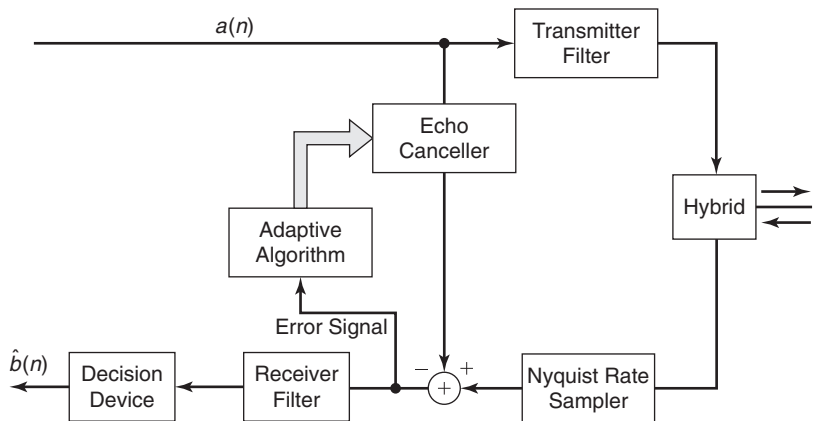


FIGURE 15.13 Nyquist rate echo canceller

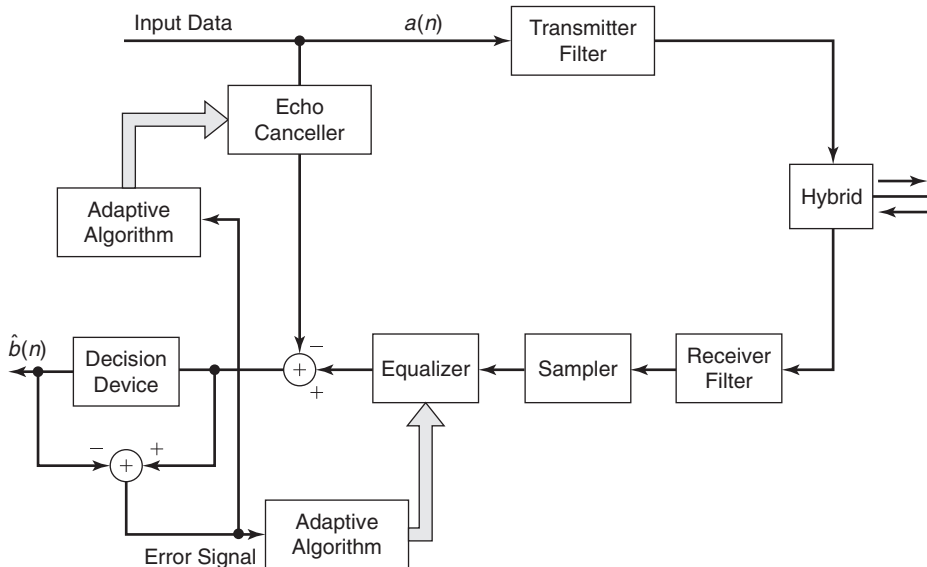


FIGURE 15.14 Modem with adaptive equalizer and echo canceller

coefficients of the echo canceller. The reader is encouraged to derive the equations corresponding to the three configurations.

**EXAMPLE 15.3 Echo Cancellation**

Consider the system configuration shown in Figure 15.15, below, in which an echo canceller is used to suppress the interference in the detection of the desired information sequence  $\{b(n)\}$ . The received sequence  $y(n)$  is expressed as

$$y(n) = b(n) + s_A(n) + w(n)$$

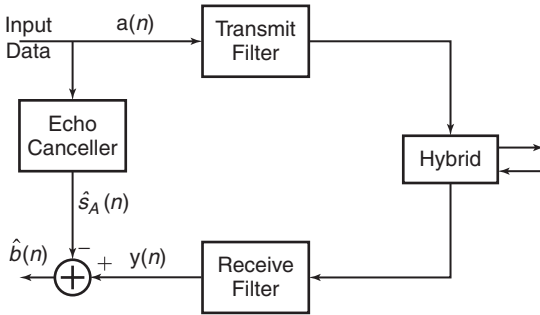


**FIGURE 15.15** Echo cancellation for Example 15.3

where  $b(n)$  represents the desired received information sequence,  $w(n)$  represents the additive noise, and  $s_A(n)$  represents the undesired echo to be suppressed. The desired sequence  $b(n)$  is a pseudo-random sequence of  $\pm 1$ . The additive noise sample sequence  $w(n)$  is white Gaussian with variance  $\sigma_w^2 = 0.1$ . The echo signal sequence is expressed as

$$s_A(n) = \sum_{\ell=0}^4 c(\ell) a(n-\ell)$$

where the echo coefficients are given by the vector

$$\mathbf{c} = [-0.25, -0.5, 0.75, 0.36, 0.25]$$

and the sequence  $a(n)$  is a pseudo-random sequence that takes the values  $\pm 1$ .

The echo canceller is an FIR filter with coefficients  $h(k)$ ,  $0 \leq k \leq M-1$ , whose output is an estimate of the undesired echo, that is,

$$\hat{s}_A(n) = \sum_{k=0}^{M-1} h(k) a(n-k)$$

- a. Generate the sequences  $y(n)$  and  $s_A(n)$ ,  $0 \leq n \leq 1000$ , and use the least-squares criterion to minimize the sum of squares

$$\sum_{n=0}^N [y(n) - s_A(n)]^2 = \sum_{n=0}^N \left[ y(n) - \sum_{k=0}^{M-1} h(k) a(n-k) \right]^2 \quad (15.17)$$

and, thus, solve for the coefficients  $h(k)$ ,  $0 \leq k \leq M-1$ , of the echo canceller. Select  $M = 10$ .

- b. Compare the coefficients of the echo canceller with the echo coefficients  $c(k)$ ,  $0 \leq k \leq 4$ , and comment on the results.

### Solution

The minimization of the sum of squares in (15.17) lead to the following set of equations:

$$\sum_{k=0}^{M-1} h(k) r_{aa}(\ell-k) = r_{ya}(\ell), \quad \ell = 0, 1, \dots, M-1$$

where  $r_{aa}(\ell)$  is the estimated autocorrelation sequence of  $a(n)$  and  $r_{ya}(\ell)$  is the estimated cross-correlation between  $y(n)$  and  $a(n)$ .

- a. The echo canceller coefficients are obtained using the following MATLAB script.

```
>> c = [-0.25,-0.5,0.75,0.36,0.25]; % Echo coefficients
>> N = 1000; n = 0:N; % Length and timing indices
>> varW = 0.1; % Additive noise variance
>> an = 2*randi([0,1],N+1,1)-1; % Pseudorandom symbol seq at Modem-A
>> bn = 2*randi([0,1],N+1,1)-1; % Pseudorandom symbol seq at Modem-B
>> sAn = filter(c,1,an); % Echo signal sequence at modem-A
>> wn = sqrt(varW)*randn(N+1,1); % Additive noise sequence
>> yn = bn + sAn + wn; % Received signal at Modem-A
>> M = 10; % FIR echo canceller order
>> [raa,lags] = xcorr(an,M-1); % ACRS of a(n)
>> Raa = toeplitz(raa(M:end)); % ACRM of a(n)
>> rya = xcorr(yn,an,M-1); % CCRS between y(n) and a(n)
>> rya = rya(M:end); % CCRV
>> hec = Raa\rya; % Echo canceller coeff (or Imp resp)
>> hec'
ans =
    -0.2540    -0.4982     0.7943     0.3285     0.2291
    0.0272     0.0139     0.0017    -0.0446     0.0319
```

- b. The echo coefficients are

$$\mathbf{c} = [-0.25, -0.5, 0.75, 0.36, 0.25]$$

From the echo canceller coefficients  $\{h(k)\}$  from (a), we observe that the first five coefficients are close to the echo coefficients while the remaining coefficients are very small.  $\square$

#### 15.1.4 SUPPRESSION OF NARROWBAND INTERFERENCE IN A WIDEBAND SIGNAL

We now discuss a problem that arises in practice, especially in signal detection and in digital communications. Let us assume that we have a signal sequence  $v(n)$  that consists of a desired wideband signal sequence  $w(n)$  corrupted by an additive narrowband interference sequence  $x(n)$ . The two corresponding processes  $W(n)$  and  $X(n)$ , respectively, are uncorrelated. These sequences result from sampling an analog signal  $v(t)$  at the Nyquist rate (or faster) of the wideband signal  $w(t)$ . Figure 15.16 illustrates the spectral characteristics of  $w(n)$  and  $x(n)$ . Usually, the interference  $|X(e^{j2\pi f})|$  is much larger than  $|W(e^{j2\pi f})|$  within the narrow frequency band that it occupies.

In digital communications and signal detection problems that fit the above model, the desired signal sequence  $w(n)$  is often a *spread-spectrum signal*, while the narrowband interference represents a signal from another

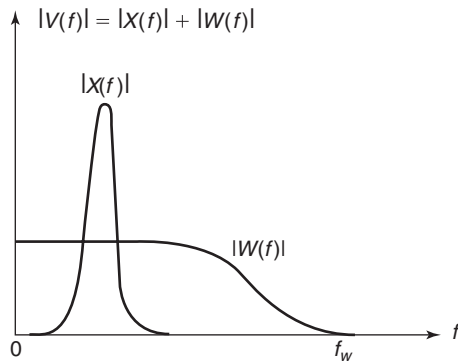


**FIGURE 15.16** Strong narrowband interference  $X(e^{j2\pi f})$  in a wideband signal  $W(e^{j2\pi f})$

user of the frequency band or intentional interference from a jammer who is trying to disrupt the communications or detection system.

Our objective from a filtering viewpoint is to employ a filter that suppresses the narrowband interference. In effect, such a filter will have a notch in the frequency band occupied by  $|X(e^{j2\pi f})|$ , and in practice, the band occupied by  $|X(e^{j2\pi f})|$  is unknown. Moreover, if the interference is nonstationary, its frequency band occupancy may vary with time. Hence an adaptive filter is desired.

From another viewpoint, the narrowband characteristics of the interference allow us to estimate  $x(n)$  from past samples of the sequence  $v(n)$  and to subtract the estimate from  $v(n)$ . Since the bandwidth of  $x(n)$  is narrow compared to the bandwidth of the sequence  $w(n)$ , the samples  $x(n)$  are highly correlated due to the high sampling rate. On the other hand, the samples  $w(n)$  are not highly correlated, since the samples are taken at the Nyquist rate of  $w(n)$ . By exploiting the high correlation between  $x(n)$  and past samples of the sequence  $v(n)$ , it is possible to obtain an estimate of  $x(n)$ , which can be subtracted from  $v(n)$ .

The general configuration is illustrated in Figure 15.17. The signal  $v(n)$  is delayed by  $D$  samples, where  $D$  is selected sufficiently large so that the wideband signal components  $w(n)$  and  $w(n - D)$  contained in  $v(n)$  and  $v(n - D)$ , respectively, are uncorrelated. Usually, a choice of  $D = 1$  or  $2$  is adequate. The delayed signal sequence  $v(n - D)$  is passed through an FIR filter, which is best characterized as a linear predictor of the value  $x(n)$  based on  $M$  samples  $v(n - D - k)$ ,  $k = 0, 1, \dots, M - 1$ . The output of the linear predictor is

$$\hat{x}(n) = \sum_{k=0}^{M-1} h(k)v(n - D - k) \quad (15.18)$$

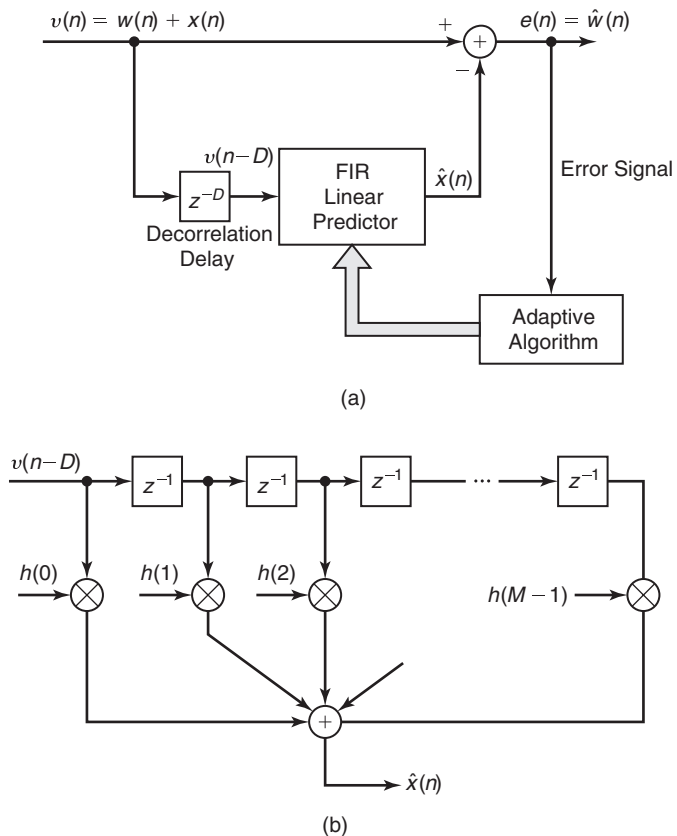


**FIGURE 15.17** Adaptive filter for estimating and suppressing a narrowband interference in a sideband signal

This predicted value of  $x(n)$  is subtracted from  $v(n)$  to yield an estimate of  $w(n)$ , as illustrated in Figure 15.17. Clearly, the quality of the estimate  $x(n)$  determines how well the narrowband interference is suppressed. It is also apparent that the delay  $D$  must be kept as small as possible in order to obtain a good estimate of  $x(n)$ , but must be sufficiently large so that  $w(n)$  and  $w(n - D)$  are uncorrelated.

Let us define the error sequence

$$e(n) = v(n) - \hat{x}(n)$$

$$= v(n) - \sum_{k=0}^{M-1} h(k)v(n - D - k) \quad (15.19)$$

If we apply the least-squares criterion to optimally select the prediction coefficients, we obtain the set of linear equations

$$\sum_{k=0}^{M-1} h(k) r_{vv}(\ell - k) = r_{vv}(\ell + D), \quad \ell = 0, 1, \dots, M-1 \quad (15.20)$$

where  $r_{vv}(\ell)$  is the autocorrelation sequence of  $v(n)$ . Note, however, that the right-hand side of (15.20) may be expressed as

$$\begin{aligned} r_{vv}(\ell + D) &= \sum_{n=0}^N v(n)v(n - \ell - D) \\ &= \sum_{n=0}^N [w(n) + x(n)][w(n - \ell - D) + x(n - \ell - D)] \\ &= r_{ww}(\ell + D) + r_{xx}(\ell + D) + r_{wx}(\ell + D) + r_{xw}(\ell + D) \end{aligned} \quad (15.21)$$

The correlations in (15.21) are time-average correlation sequences. The expected value of  $r_{ww}(\ell + D)$  is

$$E[r_{ww}(\ell + D)] = 0, \quad \ell = 0, 1, \dots, M-1 \quad (15.22)$$

because  $w(n)$  is wideband and  $D$  is large enough that  $w(n)$  and  $w(n - D)$  are uncorrelated. Also,

$$E[r_{xw}(\ell + D)] = E[r_{wx}(\ell + D)] = 0 \quad (15.23)$$

by assumption. Finally,

$$E[r_{xx}(\ell + D)] = R_X(\ell + D) \quad (15.24)$$

Therefore, the expected value of  $r_{vv}(\ell + D)$  is simply the statistical autocorrelation of the narrowband process  $X(n)$ . Furthermore, if the wideband signal is weak relative to the interference, the autocorrelation  $r_{vv}(\ell)$  in the left-hand side of (15.20) is approximately  $r_{xx}(\ell)$ . The major influence of  $w(n)$  is to the diagonal elements of  $r_{vv}(\ell)$ . Consequently, the values of the filter coefficients determined from the linear equations in (15.20) are a function of the statistical characteristics of the interference  $X(n)$ .

The overall filter structure in Figure 15.17 is an adaptive FIR prediction-error filter with coefficients

$$h'(k) = \begin{cases} 1, & k = 0 \\ -h(k - D), & k = D, D + 1, \dots, D + M - 1 \\ 0, & \text{otherwise} \end{cases} \quad (15.25)$$

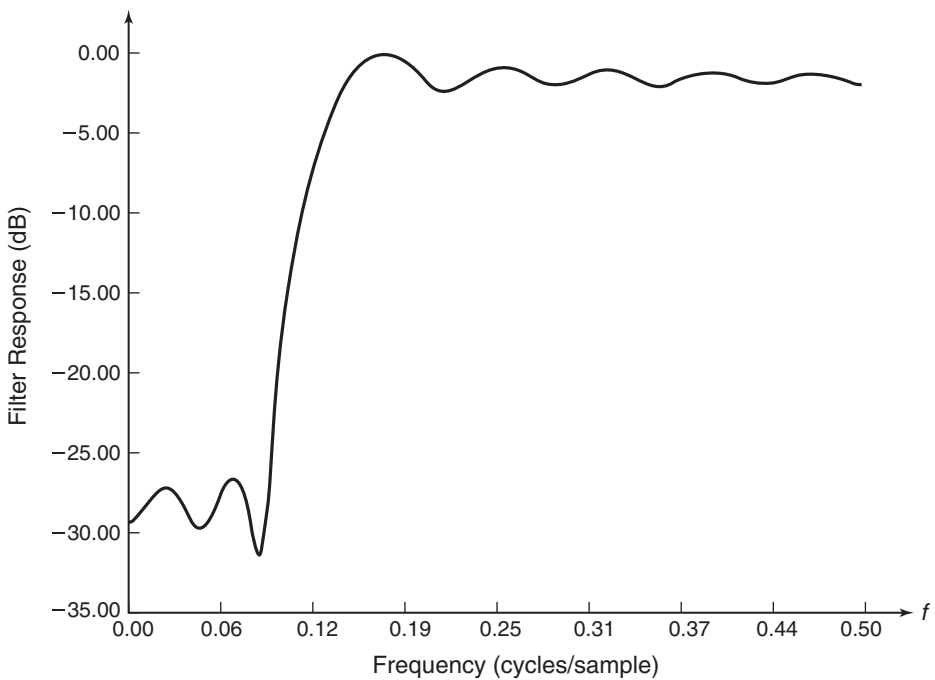


**FIGURE 15.18** Log-magnitude response characteristics of an adaptive notch filter

and a frequency response

$$H(e^{j\omega}) = \sum_{k=0}^{D+M-1} h'(k)e^{-j\omega k} \quad (15.26)$$

This overall filter acts as a notch filter for the interference. For example, Figure 15.18 illustrates the magnitude of the frequency response of an adaptive filter with  $M = 15$  coefficients, which attempts to suppress a narrowband interference that occupies 20% of the frequency band of a desired spread-spectrum signal sequence. The data was generated pseudorandomly by adding a narrowband interference consisting of 100 randomly phased, equal-amplitude sinusoids to a pseudo-noise spread-spectrum signal. The coefficients of the filter were obtained by solving the equations in (15.20), with  $D = 1$ , where the correlation  $r_{vv}(l)$  was obtained from the data. We observe that the overall interference suppression filter has the characteristics of a notch filter. The depth of the notch depends on the power of the interference relative to the wideband signal. The stronger the interference, the deeper the notch.

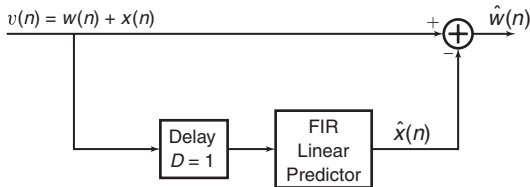


**FIGURE 15.19** System for narrowband interference suppression in Example 15.4

The algorithms presented in Section 15.2 are appropriate for estimating the predictor coefficients continuously, in order to track a nonstationary narrowband interference signal.

#### □ EXAMPLE 15.4 Suppression of Narrowband Interference

Consider the system configuration shown in Figure 15.19. The input sequence  $v(n)$  is the sum of a wideband signal sequence  $w(n)$  and a narrowband interference sequence  $x(n)$ . The sequence  $w(n)$  is a white Gaussian noise sequence with variance  $\sigma_w^2 = 1$ . The narrowband interference sequence consists of a sum of sinusoids and is expressed as

$$x(n) = A \sum_{i=0}^{100} \cos(2\pi f_i n + \theta_i)$$

where  $f_i = 0.1i/100$ ,  $i = 0, 1, \dots, 99$ ,  $\theta_i$  is uniformly distributed on the interval  $(0, 2\pi)$  for each  $i$ , and the scale factor  $A = 1$ . Note that the bandwidth of  $x(n)$  is 0.1 cycles/sample. The estimate of the narrowband interference at the output of the linear predictor is

$$\hat{x}(n) = \sum_{k=0}^{M-1} h(k)v(n-1-k)$$

and the error sequence  $e(n) = v(n) - \hat{x}(n)$  produces an estimate of the wideband signal sequence  $w(n)$ . Application of the least-squares criterion results in the set linear equations given in (15.20) for the predictor coefficients.

- a. Let  $M = 15$ , and generate 2000 samples of the sequence  $v(n)$  and solve (15.20) for the predictor coefficients  $h(k)$ ,  $k = 0, 1, \dots, 14$ .
- b. The FIR prediction-error filter having coefficients  $h'(k)$ ,  $k = 0, 1, \dots, 15$ , is defined by (15.25) and its frequency response is

$$H(e^{j2\pi f}) = \sum_{k=0}^M h'(k)e^{-j2\pi fk}, \quad |f| \leq \frac{1}{2}$$

Compute  $H(e^{j2\pi f})$  and thus illustrate via a plot of  $20 \log[|H(e^{j2\pi f})|]$  that the prediction-error filter is a notch filter that suppresses the narrow band interference contained in the sequence  $v(n)$ .

- c. Repeat parts (a) and (b) when the amplitude of the interference term  $A = 1/10$ .

**Solution**

The narrowband interference signal is obtained using the following MATLAB script.

```
>> i = (0:100)'; fi = 0.1*i/100; thetai = 2*pi*rand(length(i),1);
>> A = 1;
>> N = 2000; n = 0:N;
>> xn = sum(A*cos(2*pi*fi*n+thetai*ones(1,N+1))); xn = xn';
```

- a. The predictor coefficients are obtained using this MATLAB script:

```
>> M = 15; D = 1;
>> varW = 1;
>> wn = sqrt(varW)*randn(N+1,1);
>> vn = xn+wn;
>> [rvv,lags] = xcorr(vn,M-1+D); % ACRS of v(n)
>> Rvv = toeplitz(rvv(M+D:2*M+D-1)); % ACRM of v(n)
>> rv = rvv(M+2*D:end);
>> h = Rvv\rv;
```

- b. Using (15.25), we obtain the predictor error coefficients and its log-magnitude response:

```
>> h1 = zeros(M+D,1);
>> h1(1) = 1;
>> h1(D+1:D+M) = -h;
>> f = linspace(0,1,1001)*0.5;
>> H1 = freqz(h1,1,2*pi*f);
>> H1db = 20*log10(abs(H1)/max(abs(H1)));
>> % Plotting commands follow
```

The plot of the log-magnitude response is shown in Figure 15.20, from which we observe that the prediction error filter creates a notch of about 20 dB down at the bandwidth of the narrowband interfering signal.

- c. The scale factor is now reduced to  $A = 1/10$  and new results are obtained.

```
>> i = (0:100)'; fi = 0.1*i/100; thetai = 2*pi*rand(length(i),1);
>> A = 1/10;
>> N = 2000; n = 0:N;
>> xn = sum(A*cos(2*pi*fi*n+thetai*ones(1,N+1))); xn = xn';
>> M = 15;
>> D = 1;
>> varW = 1;
>> wn = sqrt(varW)*randn(N+1,1);
>> vn = xn+wn;
>> [rvv,lags] = xcorr(vn,M-1+D); % ACRS of v(n)
>> Rvv = toeplitz(rvv(M+D:2*M+D-1)); % ACRM of v(n)
>> rv = rvv(M+2*D:end);
```

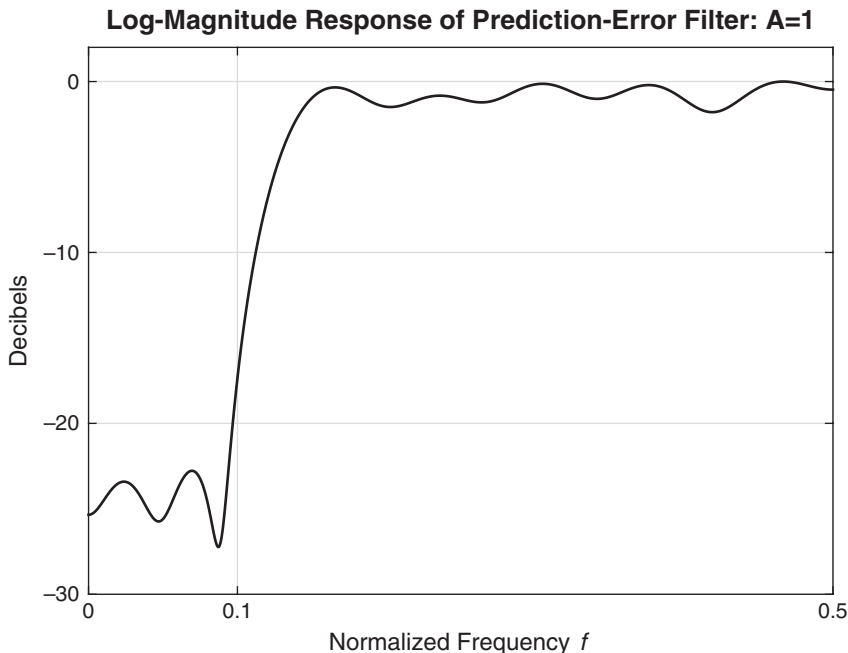


**FIGURE 15.20** Log-magnitude response of the prediction-error filter in Example 15.4(b)

```

>> h = Rvv\rv;
>> h1 = zeros(M+D,1);
>> h1(1) = 1;
>> h1(D+1:D+M) = -h;
>> f = linspace(0,1,1001)*0.5;
>> H1 = freqz(h1,1,2*pi*f);
>> H1db = 20*log10(abs(H1)/max(abs(H1)));
>> % Plotting commands follow

```

The resulting log-magnitude response is shown in Figure 15.21. Now the notch in the frequency response is much shallower at around 5 dB down. □

### 15.1.5 ADAPTIVE LINE ENHANCER

In the preceding example, the adaptive linear predictor was used to estimate the narrowband interference for the purpose of suppressing the interference from the input sequence  $v(n)$ . An adaptive line enhancer (ALE) has the same configuration as the interference suppression filter in Figure 15.17, except that the objective is different.

In the adaptive line enhancer,  $x(n)$  is the desired signal and  $w(n)$  represents a wideband noise component that masks  $x(n)$ . The desired signal

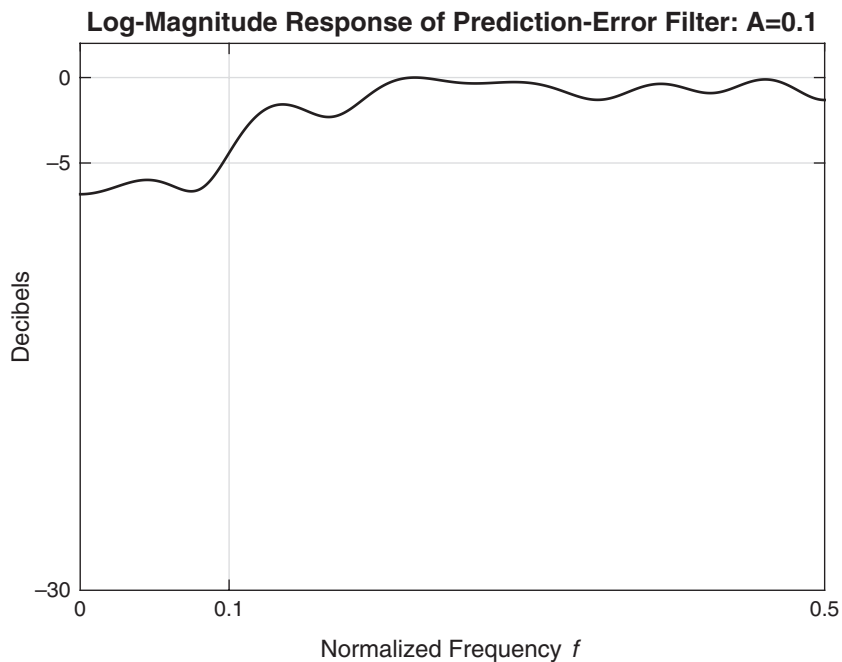


**FIGURE 15.21** Log-magnitude response of the prediction-error filter in Example 15.4(c)

$x(n)$  is either a spectral line or a relatively narrowband signal. The linear predictor shown in Figure 15.17(b) operates in exactly the same fashion as that in Figure 15.17(a) and provides an estimate of the narrowband signal  $x(n)$ . It is apparent that the ALE (i.e., the FIR prediction filter) is a self-tuning filter that has a peak in its frequency response at the frequency of the sinusoid or, equivalently, in the frequency band of the narrowband signal  $x(n)$ . By having a narrow bandwidth, the noise  $w(n)$  outside of the band is suppressed and, thus, the spectral line is enhanced in amplitude relative to the noise power in  $w(n)$ . This explains why the FIR predictor is called an ALE. Its coefficients are determined by the solution of (15.20).

□ **EXAMPLE 15.5 Estimation of Narrowband Signal in Wideband Noise**

Consider the system configuration given in Example 15.4, where now the sequence  $x(n)$  is defined as

$$x(n) = A \cos(2\pi f_0 n + \theta_0)$$

The objective is now to estimate  $x(n)$  in the presence of the wideband noise sequence  $w(n)$ .

- a. Let  $M = 15$ ,  $A = 1$ ,  $f_0 = 0.2$ , and  $\theta_0 = 0$ , and generate 2000 samples of the sequence  $v(n)$ . Solve (15.20) for the predictor coefficients  $h(k)$ ,  $k = 0, 1, \dots, 14$ . Then plot given signal  $x(n)$ , the noisy signal  $v(n)$ , and the estimated signal  $\hat{x}(n)$  for  $50 < n \leq 150$ . Comment on the quality of the estimate.
- b. Compute the frequency response  $H(e^{j2\pi f})$  of the FIR prediction filter and plot  $20 \log[|H(e^{j2\pi f})|]$  for  $|f| \leq \frac{1}{2}$ . Comment on the characteristic of the filter.
- c. Repeat parts (a) and (b) when  $A = \frac{1}{10}$  and when  $A = 10$ .
- d. Repeat parts (a) and (b) when the sequence  $x(n)$  contains two frequency components of the form

$$x(n) = A \cos(2\pi f_1 n + \theta_1) + B \cos(2\pi f_2 n + \theta_2)$$

where  $f_1 = 0.1$ ,  $f_2 = 0.3$ ,  $\theta_1 = 0$ ,  $\theta_2 = \pi$ , and  $A = B = 1$ . Comment on the results of  $\hat{x}(n)$  and  $H(e^{j2\pi f})$ .

### Solution

The sequence  $x(n)$  is obtained using

```
>> N = 2000; n = (0:N-1)';
>> xn = A*cos(2*pi*f0*n+th0);
```

- a. The predictor coefficients and the plots are obtained using the following MATLAB script.

```
>> M = 15; A = 1; f0 = 0.2; th0 = 0; D = 1;
>> varW = 1;
>> wn = sqrt(varW)*randn(N,1);
>> vn = xn + wn;
>> [rvv] = xcorr(vn,M-1+D); % ACRS of v(n)
>> Rvv = toeplitz(rvv(M+D:2*M+D-1)); % ACRM of v(n)
>> rv = rvv(M+2*D:end);
>> h = Rvv\rv;
>> xhatn = filter(h,1,[zeros(D,1);vn]);
>> % Plotting commands follow
```

The plots are shown in Figure 15.22 in which we show samples from  $n = 50$  to  $n = 150$  for clarity. The optimal filter has a remarkable performance given how noisy the signal  $v(n)$  is. The single tone signal  $x(n)$  is clearly enhanced.

- b. MATLAB script:

```
>> f = linspace(-0.5,0.5,1001);
>> Hf = freqz(h,1,2*pi*f);
>> Hfdb = 20*log10(abs(Hf)/max(abs(Hf)));
>> % Plotting commands follow
```

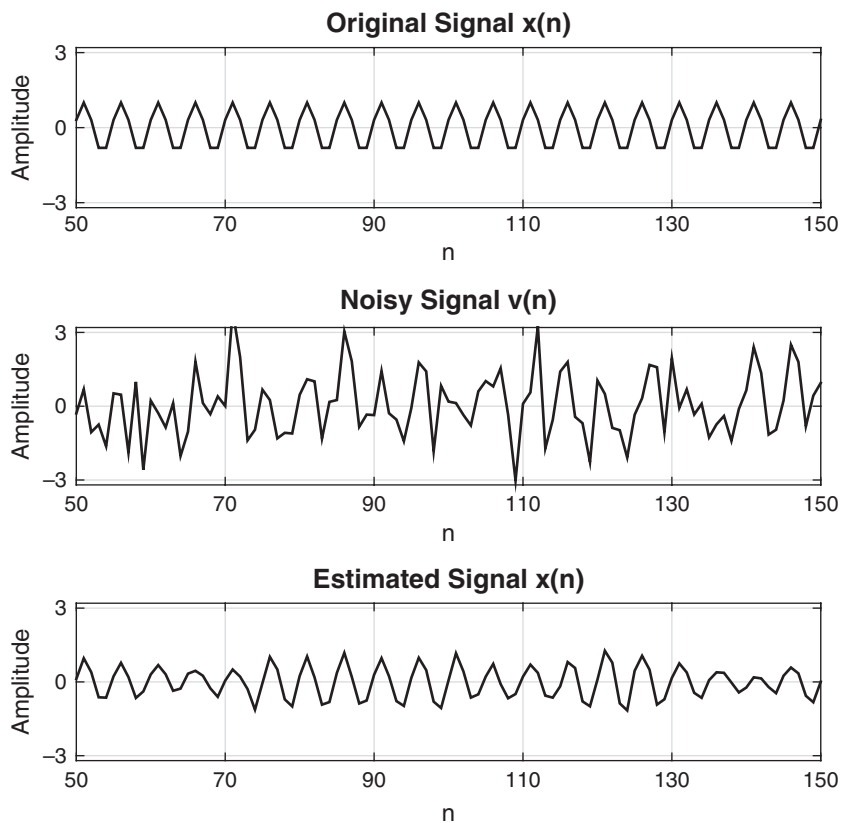


**FIGURE 15.22** Plots of the original signal, noisy signal, and estimated signal in Example 15.5(a)

The log-magnitude plot in decibels is shown in Figure 15.23. Observe that the response has a peak at  $f = \pm 0.2$  and all other peaks are approximately 10 dB below these peaks.

- c. The scripts are almost similar with obvious changes to the scale factor  $A$ .

```
>> % A = 1/10
>> M = 15; A = 1/10; f0 = 0.2; th = 0; D = 1;
>> N = 2000; n = (0:N-1)';
>> xn = A*cos(2*pi*f0*n+th);
>> varW = 1;
>> wn = sqrt(varW)*randn(N,1);
>> vn = xn + wn;
>> [rvv,lags] = xcorr(vn,M-1+D);      % ACRS of v(n)
>> Rvv = toeplitz(rvv(M+D:2*M+D-1)); % ACRM of v(n)
```

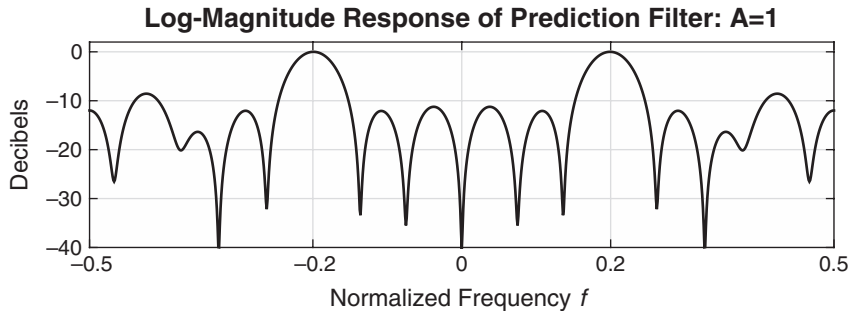


**FIGURE 15.23** Log-magnitude plot in Example 15.5(b)

```

>> rvv = rvv(M+2*D:end);
>> h = Rvv\rvv;
>> xhatn = filter(h,1,[zeros(D,1);vn]);
>> f = linspace(-0.5,0.5,1001);
>> Hf = freqz(h,1,2*pi*f);
>> Hfdb = 20*log10(abs(Hf)/max(abs(Hf)));
>>
>> % A = 10
>> M = 15; A = 10; f0 = 0.2; th = 0; D = 1;
>> N = 2000; n = (0:N-1)';
>> xn = A*cos(2*pi*f0*n+th);
>> varW = 1;
>> wn = sqrt(varW)*randn(N,1);
>> vn = xn + wn;
>> [rvv,lags] = xcorr(vn,M-1+D);      % ACRS of v(n)
>> Rvv = toeplitz(rvv(M+D:2*M+D-1)); % ACRM of v(n)
>> rv = rvv(M+2*D:end);
>> h = Rvv\rv;
>> xhatn = filter(h,1,[zeros(D,1);vn]);
>> f = linspace(-0.5,0.5,1001);
>> Hf = freqz(h,1,2*pi*f);
>> Hfdb = 20*log10(abs(Hf)/max(abs(Hf)));

```

The plots are shown in Figure 15.24. The plots in the left-hand column correspond to  $A = 1/10$ . Clearly, the noise is stronger in this case, and consequently the estimation of  $x(n)$  suffers. Although most of the noise is eliminated, the signal is also distorted. This is also evident from the filter's log-magnitude plot. Although there is a peak at  $f = 0.2$ , there are other significant peaks also present in the response. The plots in the right-hand column correspond to  $A = 10$ . In this case, the signal  $x(n)$  is much stronger

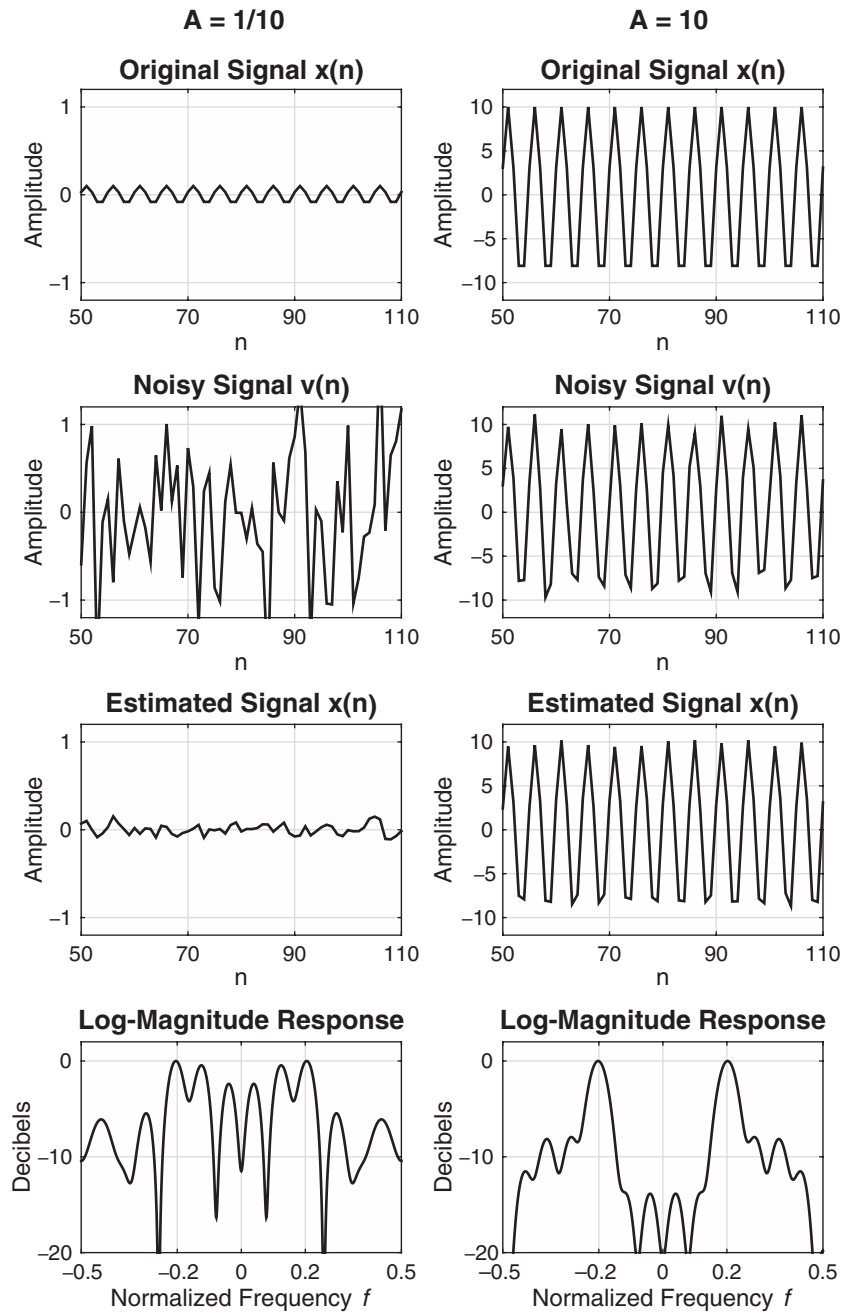


FIGURE 15.24 Signal and log-magnitude plots in Example 15.5(c)

than noise, and consequently the estimation of  $x(n)$  is almost distortion-free. The filter's log-magnitude plot shows a stronger and narrower peak at  $f = 0.2$ , thus eliminating most of the noise.

- d. In this case, we change  $x(n)$  by adding another sinusoid and then execute the previous script.

```
>> M = 15; D = 1;
>> A = 1; f1 = 0.1; th1 = 0;
>> B = 1; f2 = 0.3; th2 = pi;
>> N = 2000; n = (0:N-1)';
>> xn = A*cos(2*pi*f1*n+th1) + B*cos(2*pi*f2*n+th2);
>> varW = 1;
>> wn = sqrt(varW)*randn(N,1);
>> vn = xn + wn;
>> [rvv,lags] = xcorr(vn,M-1+D);      % ACRS of v(n)
>> Rvv = toeplitz(rvv(M+D:2*M+D-1)); % ACRM of v(n)
>> rv = rvv(M+2*D:end);
>> h = Rvv\rv;
>> xhatn = filter(h,1,[zeros(D,1);vn]);
>> f = linspace(-0.5,0.5,1001);
>> Hf = freqz(h,1,2*pi*f);
>> Hfdb = 20*log10(abs(Hf)/max(abs(Hf))');
```

The signal and log-magnitude plots are shown in Figure 15.25. The filter's log-magnitude plot shows that although the response peaks are at the correct locations,  $f_1 = 0.1$  and  $f_2 = 0.3$  cycles/sample, these peaks are broad and let some noise power go through. Consequently, the estimation of two sinusoid is not perfect and the waveform is somewhat distorted. □

### 15.1.6 ADAPTIVE NOISE CANCELLING

Echo cancellation, the suppression of narrowband interference in a wideband signal, and the ALE are related to another form of adaptive filtering called *adaptive noise cancelling*. A model for the adaptive noise canceller is illustrated in Figure 15.26.

The primary input signal consists of a desired signal sequence  $x(n)$  corrupted by an additive noise sequence  $w_1(n)$  and an additive interference (noise)  $w_2(n)$ . The additive interference (noise) is also observable after it has been filtered by some unknown linear system that yields  $v_2(n)$  and is further corrupted by an additive noise sequence  $w_3(n)$ . Thus we have available a secondary signal sequence, which may be expressed as  $v(n) = v_2(n) + w_3(n)$ . The sequences  $w_1(n)$ ,  $w_2(n)$ , and  $w_3(n)$  are assumed to be mutually uncorrelated and zero mean.

As shown in Figure 15.26, an adaptive FIR filter is used to estimate the interference sequence  $w_2(n)$  from the secondary signal  $v(n)$  and

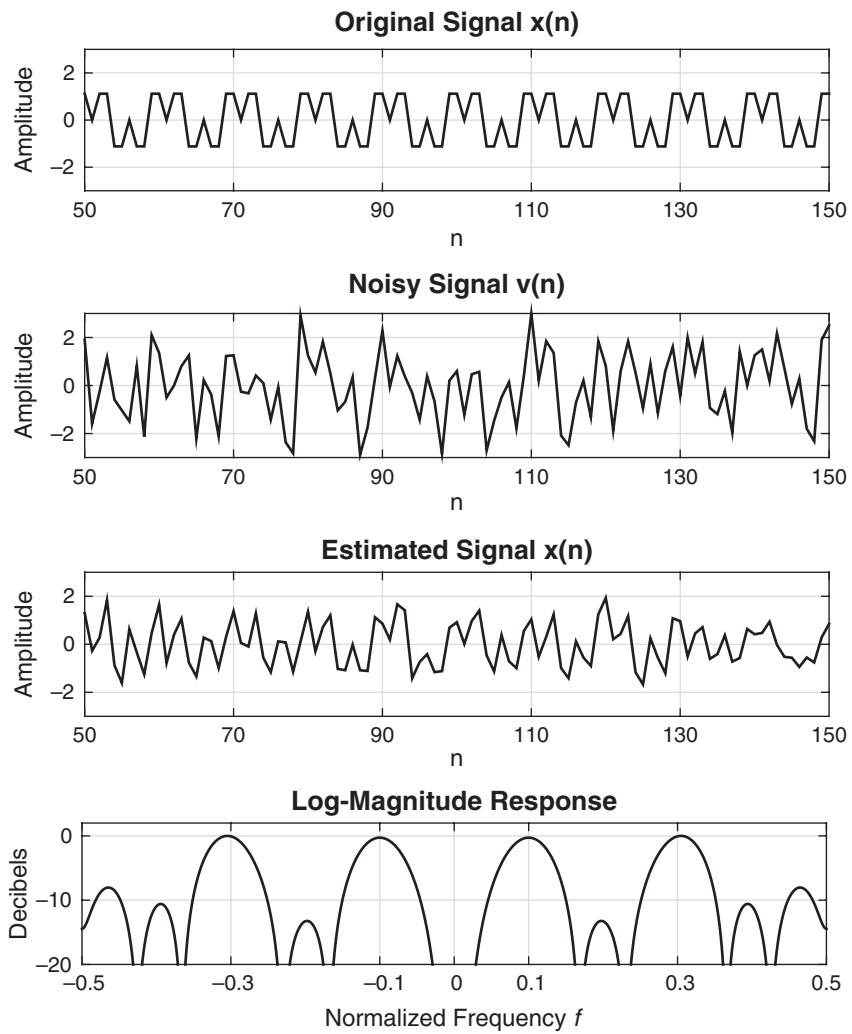


**FIGURE 15.25** Signal and log-magnitude plots in Example 15.5(d)

subtract the estimate  $\hat{w}_2(n)$  from the primary signal. The output sequence, which represents an estimate of the desired signal  $x(n)$ , is the error signal

$$\begin{aligned} e(n) &= y(n) - \hat{w}_2(n) \\ &= y(n) - \sum_{k=0}^{M-1} h(k)v(n-k) \end{aligned} \quad (15.27)$$

This error sequence is used to adaptively adjust the coefficients of the FIR filter.

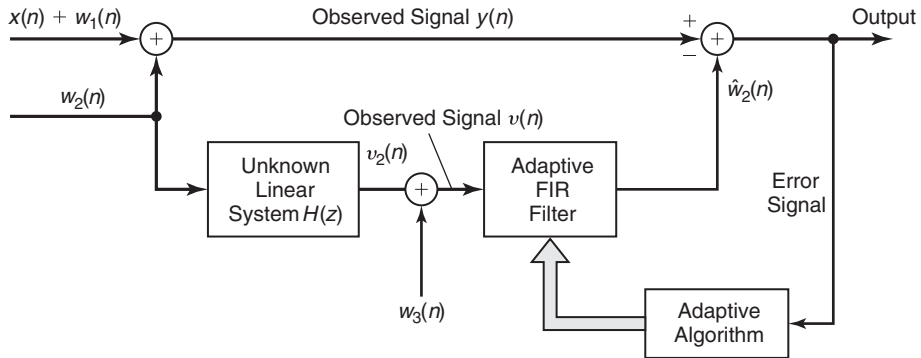


**FIGURE 15.26** Example of an adaptive noise-cancelling system

If the least-squares criterion is used to determine the filter coefficients, the result of the optimization is the set of linear equations

$$\sum_{k=0}^{M-1} h(k)r_{vv}(\ell - k) = r_{yv}(\ell), \quad \ell = 0, 1, \dots, M-1 \quad (15.28)$$

where  $r_{vv}(\ell)$  is the sample (time-average) autocorrelation of the sequence  $v(n)$  and  $r_{yv}(\ell)$  is the sample cross-correlation of the sequences  $y(n)$  and  $v(n)$ . Clearly, the noise cancelling problem is similar to the last three adaptive filtering applications described above.

#### □ EXAMPLE 15.6 Noise Cancellation

Consider the system configuration shown in Figure 15.27. The sequence  $x(n)$  is a sample sequence of a broadband signal that is modeled as a white Gaussian noise process with variance  $\sigma_X^2$ . The sequences  $w_2(n)$  and  $w_3(n)$  are sample sequences of white Gaussian noise processes with equal variance  $\sigma_W^2$ . Sequences  $x(n)$ ,  $w_2(n)$ , and  $w_3(n)$  are mutually uncorrelated. The linear system has a system function

$$H(z) = \frac{1}{1 - \frac{1}{2}z^{-1}}$$

The objective is to design a linear prediction filter that estimates and cancels out the noise component  $w_2(n)$ .

- Consider the following parameters: predictor order  $M = 10$ ,  $\sigma_W^2 = 1$ ,  $\sigma_X^2 = 2$ . Generate 2000 samples of the sequences  $x(n)$ ,  $w_2(n)$ , and  $w_3(n)$ , and the sequences  $y(n)$ ,  $v_2(n)$ , and  $v(n)$ . Then determine the predictor coefficients that are optimal in the least-squares sense.
- Plot  $y(n)$ ,  $x(n)$ , and  $\hat{x}(n)$  on the same graph and comment on the quality of the noise cancellation scheme.
- Repeat parts (a) and (b) when  $\sigma_X^2 = 5$  and when  $\sigma_X^2 = 0.5$ . Comment on the results.

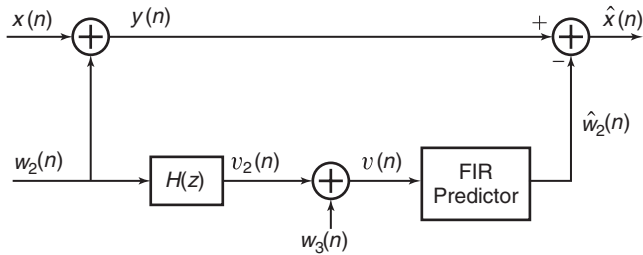


**FIGURE 15.27** Noise cancellation in Example 15.6

### Solution

The unknown linear system is specified using

```
>> HzB = 1; HzA = [1-0.5]; % Unknown LTI system parameters
```

- The specified signal and the predictor coefficients are obtained using the following MATLAB script.

```
>> M = 10; varW = 1; varX = 2;
>> N = 2000; n = 0:N-1;
>> xn = sqrt(varX)*randn(N,1);
>> w2n = sqrt(varW)*randn(N,1);
>> w3n = sqrt(varW)*randn(N,1);
>> v2n = filter(HzB,HzA,w2n);
>> yn = xn+w2n;
>> vn = v2n+w3n;
>> rvv = xcorr(vn,M-1);
>> Rvv = toeplitz(rvv(M:end)); % ACRM of v(n)
>> ryv = xcorr(yn,vn,M-1);      % CCRR between y(n) and v(n)
>> ryv = ryv(M:end);           % CCRV
>> hnc = Rvv\ryv;              % Noise canceller coeff (or Imp resp)
```

- The  $\hat{x}(n)$  is obtained using

```
>> w2hatn = filter(hnc,1,vn);
>> xhatn = yn - w2hatn;
```

The signal plots from  $n = 50$  to  $n = 150$  are shown in Figure 15.28. The wideband signal  $x(n)$  is restored close to its original waveform from its noisy observation, and thus its noise is almost cancelled.

- We now execute the previous MATLAB script with different values for  $\sigma_x$ .

```
>> % (c1) VarX = 5
>> M = 10; varW = 1; varX = 5;
>> N = 2000; n = 0:N-1;
>> xn = sqrt(varX)*randn(N,1);
```

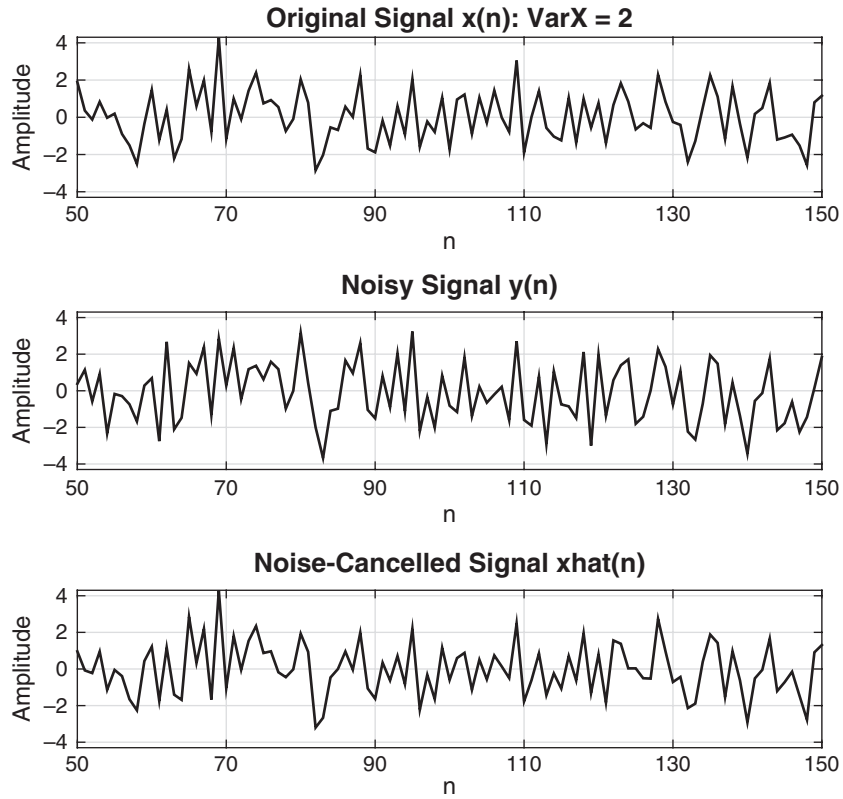


**FIGURE 15.28** Signal plots in Example 15.6(b)

```

>> w2n = sqrt(varW)*randn(N,1);
>> w3n = sqrt(varW)*randn(N,1);
>> v2n = filter(Hzb,Hza,w2n);
>> yn = xn+w2n;
>> vn = v2n+w3n;
>> rvv = xcorr(vn,M-1);
>> Rvv = toeplitz(rvv(M:end)); % ACRM of v(n)
>> ryv = xcorr(yn,vn,M-1);      % CCRS between y(n) and v(n)
>> ryv = ryv(M:end);           % CCRV
>> hnc = Rvv\ryv;              % Noise canceller coeff (or Imp resp)
>> w2hatn = filter(hnc,1,vn);
>> xhatn = yn - w2hatn;
>> % Plotting commands follow

```

The resulting signal plots are shown in Figure 15.29. In this case, the signal is much stronger in power than noise samples. Hence the signal and its estimated waveforms are almost identical.

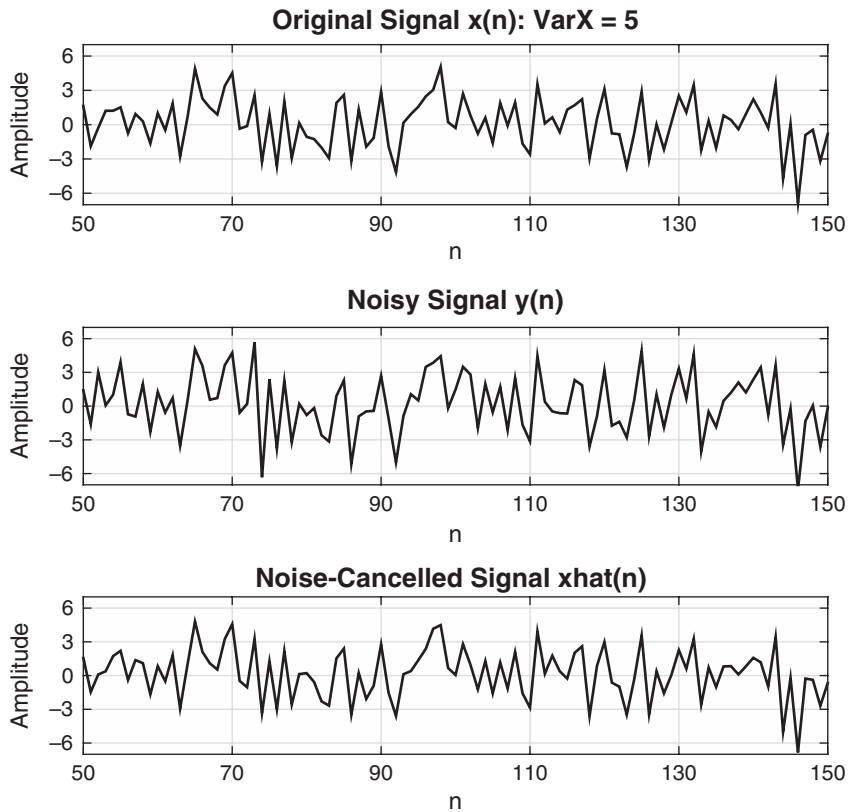


**FIGURE 15.29** Signal plots in Example 15.6(c)1

```

>> % (c2) VarX = 0.5
>> M = 10; varW = 1; varX = 0.5;
>> N = 2000; n = 0:N-1;
>> xn = sqrt(varX)*randn(N,1);
>> w2n = sqrt(varW)*randn(N,1);
>> w3n = sqrt(varW)*randn(N,1);
>> v2n = filter(Hzb,Hza,w2n);
>> yn = xn+w2n;
>> vn = v2n+w3n;
>> rvv = xcorr(vn,M-1);
>> Rvv = toeplitz(rvv(M:end)); % ACRM of v(n)
>> ryv = xcorr(yn,vn,M-1);      % CCRS between y(n) and v(n)
>> ryv = ryv(M:end);          % CCRV
>> hnc = Rvv\ryv;             % Noise canceller coeff (or Imp resp)
>> w2hatn = filter(hnc,1,vn);
>> xhatn = yn - w2hatn;
>> % Plotting commands follow

```

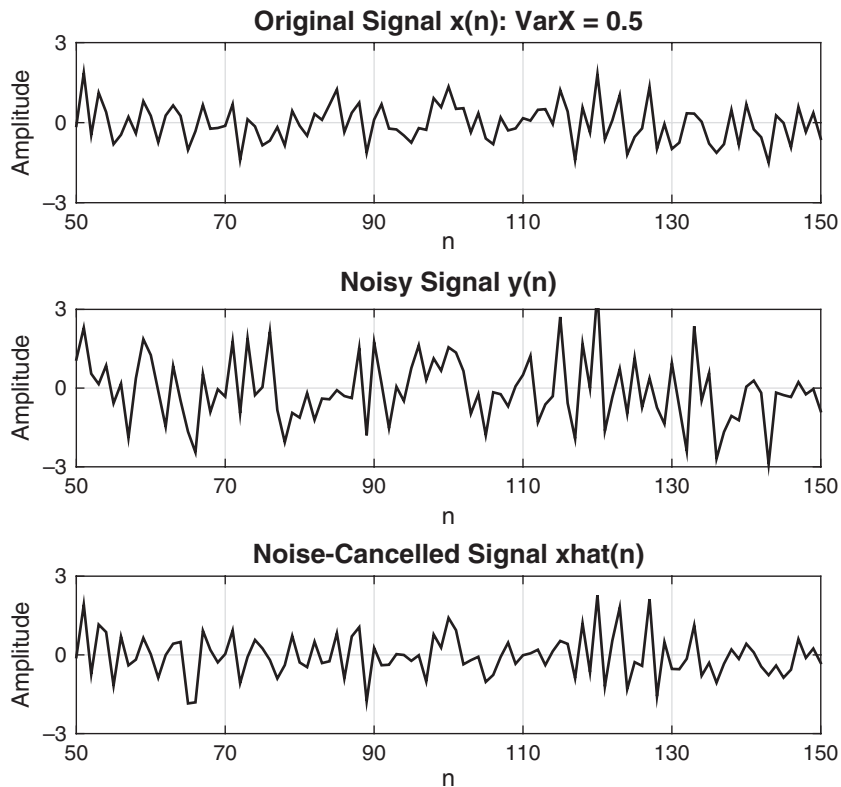


**FIGURE 15.30** Signal plots in Example 15.6(c)2

The resulting signal plots are shown in Figure 15.30. In this case, the signal is much weaker in power than noise samples. Hence the estimated signal waveform is distorted compared to the original signal. □

### 15.1.7 LINEAR PREDICTIVE CODING OF SPEECH SIGNALS

Various methods have been developed over the past four decades for digital encoding of speech signals. In the telephone system, for example, two commonly used methods for speech encoding are pulse code modulation (PCM) and differential PCM (DPCM). These are examples of waveform-coding methods. Other waveform-coding methods have also been developed, such as delta modulation (DM) and adaptive DPCM.

Since the digital speech signal is ultimately transmitted from the source to a destination, a primary objective in devising speech encoders is to minimize the number of bits required to represent the speech signal while maintaining speech intelligibility. This objective has led to the

development of a class of low bit-rate (10,000 bits per second and below) speech-encoding methods that are based on constructing a model of the speech source and transmitting the model parameters. Adaptive filtering finds application in these model-based speech-coding systems. We describe one very effective method called linear predictive coding (LPC).

In LPC, the vocal tract is modeled as a linear all-pole filter having the system function

$$H(z) = \frac{G}{1 - \sum_{k=1}^p a_k z^{-k}} \quad (15.29)$$

where  $p$  is the number of poles,  $G$  is the filter gain, and  $a_k$  are the parameters that determine the poles. There are two mutually exclusive excitation functions, used to model voiced and unvoiced speech sounds. On a short-time basis, voiced speech is periodic with a fundamental frequency  $F_0$ , or a pitch period  $1/F_0$ , which depends on the speaker. Thus voiced speech is generated by exciting the all-pole filter model by a periodic impulse train with a period equal to the desired pitch period. Unvoiced speech sounds are generated by exciting the all-pole filter model by the output of a random-noise generator. This model is shown in Figure 15.31.

Given a short-time segment of a speech signal, the speech encoder at the transmitter must determine the proper excitation function, the pitch period for voiced speech, the gain parameter  $G$ , and the coefficients  $\{a_k\}$ . A block diagram that illustrates the source encoding system is given in Figure 15.32. The parameters of the model are determined adaptively from the data. Then the speech samples are synthesized by using the model, and an error signal sequence is generated (as shown in Figure 15.32) by taking the difference between the actual and the synthesized sequence. The error signal and the model parameters are encoded into a binary sequence and transmitted to the destination. At the receiver, the speech signal is synthesized from the model and the error signal.

The parameters of the all-pole filter model are easily determined from the speech samples by means of linear prediction. To be specific, consider

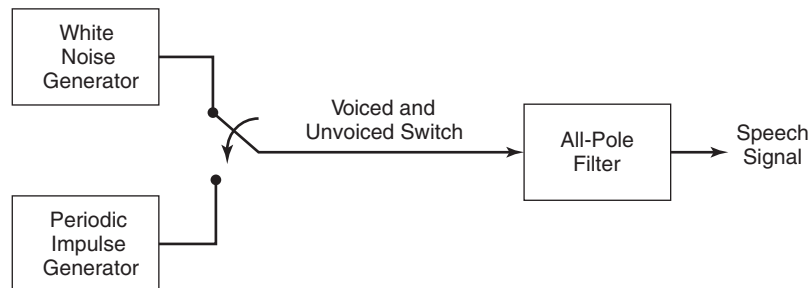


**FIGURE 15.31** Block diagram model for the generation of a speech signal

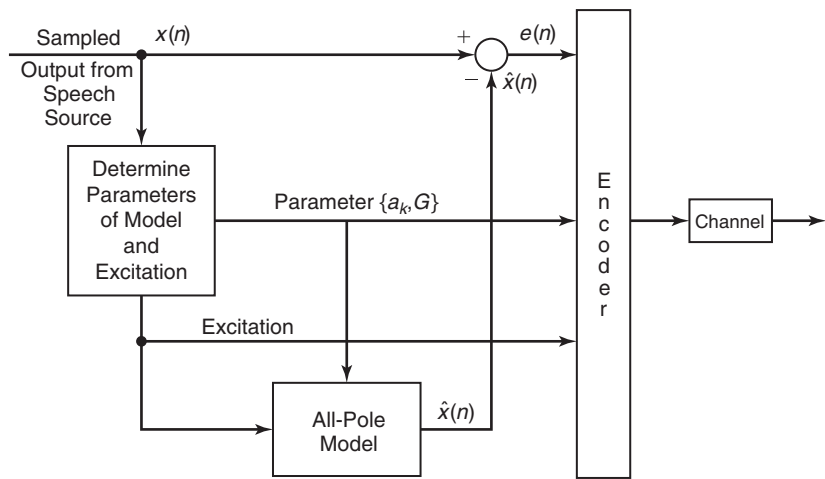


**FIGURE 15.32** Source encoder for a speech signal

the system shown in Figure 15.33 and assume that we have  $N$  signal samples. The output of the FIR filter is

$$\hat{x}(n) = \sum_{k=1}^p a_k x(n-k) \quad (15.30)$$

and the corresponding error between the observed sample  $x(n)$  and the estimate  $\hat{x}(n)$  is

$$e(n) = x(n) - \sum_{k=1}^p a_k x(n-k) \quad (15.31)$$

By applying the least-squares criterion, we can determine the model parameters  $a_k$ . The result of this optimization is a set of linear equations

$$\sum_{k=1}^p a_k r_{xx}(\ell - k) = r_{xx}(\ell), \quad \ell = 1, 2, \dots, p \quad (15.32)$$

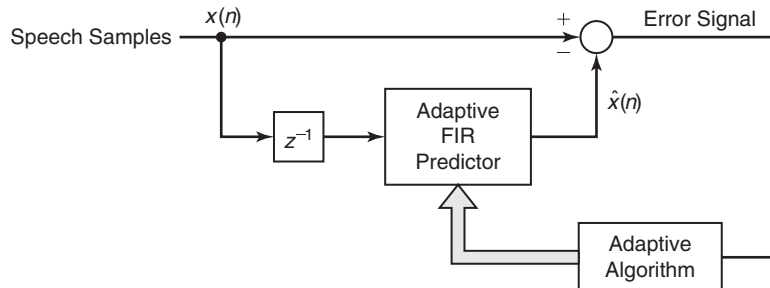


**FIGURE 15.33** Estimation of pole parameters in LPC

where  $r_{xx}(\ell)$  is the time-average autocorrelation of the sequence  $x(n)$ . The gain parameter for the filter can be obtained by noting that its input-output equation is

$$x(n) = \sum_{k=1}^p a_k x(n-k) + Gv(n) \quad (15.33)$$

where  $v(n)$  is the input sequence. Clearly,

$$\begin{aligned} Gv(n) &= x(n) - \sum_{k=1}^p a_k x(n-k) \\ &= e(n) \end{aligned}$$

Then

$$G^2 \sum_{n=0}^{N-1} v^2(n) = \sum_{n=0}^{N-1} e^2(n) \quad (15.34)$$

If the input excitation is normalized to unit energy by design, then

$$\begin{aligned} G^2 &= \sum_{n=0}^{N-1} e^2(n) \\ &= r_{xx}(0) - \sum_{k=1}^p a_k r_{xx}(k) \end{aligned} \quad (15.35)$$

Thus  $G^2$  is set equal to the residual energy resulting from the least-squares optimization.

In this development, we have described the use of linear prediction to adaptively determine the pole parameters and the gain of an all-pole filter model for speech generation. In practice, due to the nonstationary character of speech signals, this model is applied to short-time segments (10 to 20 milliseconds) of a speech signal. Usually, a new set of parameters is determined for each short-time segment. However, it is often advantageous to use the model parameters measured from previous segments to smooth out sharp discontinuities that usually exist in estimates of model parameters obtained from segment to segment. Although our discussion was totally in terms of the FIR filter structure, we should mention that speech synthesis is usually performed by using the FIR lattice structure and the reflection coefficients  $K_i$ . Since the dynamic range of the  $K_i$  is significantly smaller than that of the  $a_k$ , the reflection coefficients require fewer bits to represent them. Hence the  $K_i$  are transmitted over the channel. Consequently, it is natural to synthesize the speech at the destination using the all-pole lattice structure described previously in Section 14.5.1.

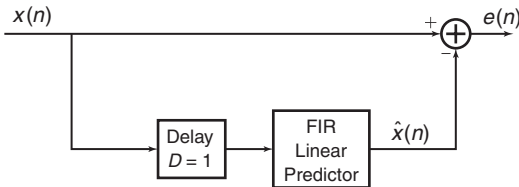


**FIGURE 15.34** Estimation of pole positions in Example 15.7

In our treatment of LPC for speech coding, we have not considered algorithms for the estimation of the excitation and the pitch period. A discussion of appropriate algorithms for these parameters of the model would take us too far afield and, hence, are omitted. The interested reader is referred to Rabiner and Schafer [84] and Deller, Hansen, and Proakis [11] for a detailed treatment of speech analysis and synthesis methods.

□ **EXAMPLE 15.7 Estimation of Poles in an All-Pole System**

Consider an autoregressive process described by the difference equation

$$x(n) = 1.26x(n - 1) - 0.81x(n - 2) + w(n) \quad (15.36)$$

where  $w(n)$  is a sample sequence of a white Gaussian noise process with variance  $\sigma_w^2 = 0.1$ . The system configuration for estimation of the poles is shown in Figure 15.34.

- Generate a sequence  $x(n)$  for  $0 \leq n \leq 1000$ , and use the least-squares criterion to determine the parameters of a second-order predictor.
- Determine the zeros of the prediction-error filter and compare them to the poles of the system that generated  $x(n)$ .
- Repeat parts (a) and (b) when  $\sigma_w^2 = 0.5$  and when  $\sigma_w^2 = 1$ . Comment on the results.

**Solution**

The parameters of the second-order AR model are entered using

```
>> b = 1; a = [1,-1.26,0.81]; % Parameters of the AR model
```

- Sequence generation and the parameters of the second-order predictor are obtained using the following MATLAB script.

```
>> varW = 0.1; M = 2;
>> N = 1000; n = 0:N-1;
>> wn = sqrt(varW)*randn(N,1);
>> xn = filter(b,a,wn);
>> [rxx] = xcorr(xn,M); % ACRS of x(n)
>> Rxx = toeplitz(rxx(M+1:2*M)); % ACRM of x(n)
>> rdx = xcorr(xn,M-1); % CCRS between d(n) and x(n)
```

```

>> rx = rxx(M+2:end);           % CCRV
>> hpr = Rxx\rx;              % Predictor coeff (or Imp resp)
>> hpr'
ans =
    1.2416   -0.8206

```

The predictor coefficients almost agree with the coefficients on the right-hand side of (15.36).

**b.** MATLAB script:

```

>> hpe = [1;-hpr]; % Prediction error imp response
>> hpe_zeros = roots(hpe);
>> fprintf('Zeros and Poles when varW = 0.1\n');
>> fprintf(['    Zeros of the Prediction Error Filter are: ',...
' \n    %6.4f+j%6.4f, %6.4f-j%6.4f\n\n'],...
real(hpe_zeros(1)),imag(hpe_zeros(1)),...
real(hpe_zeros(2)),-imag(hpe_zeros(2)));

>> AR_poles = roots(a);
>> fprintf(['    Poles of the AR Model are: ',...
' \n    %6.4f+j%6.4f, %6.4f-j%6.4f\n\n'],...
real(AR_poles(1)),imag(AR_poles(1)),...
real(AR_poles(2)),-imag(AR_poles(2)));

```

The screen printout is

```

Zeros and Poles when varW = 0.1
Zeros of the Prediction Error Filter are:
0.6208+j0.6597, 0.6208-j0.6597

Poles of the AR Model are:
0.6300+j0.6427, 0.6300-j0.6427

```

Clearly, the poles and zeros are close to each other.

**c.** A similar MATLAB script with different values for  $\sigma_w^2$  gives similar results.

```

Zeros and Poles when varW = 0.5
Zeros of the Prediction Error Filter are:
0.6296+j0.6345, 0.6296-j0.6345

Poles of the AR Model are:
0.6300+j0.6427, 0.6300-j0.6427

```

```

Zeros and Poles when varW = 1.0
    Zeros of the Prediction Error Filter are:
        0.6309+j0.6365, 0.6309-j0.6365

    Poles of the AR Model are:
        0.6300+j0.6427, 0.6300-j0.6427

```

Even though we change the AR model input variance, the estimation of predictor model coefficients are obtained by the ratio of autocorrelation values, which remains unaffected within the statistical variation.  $\square$

### 15.1.8 ADAPTIVE ARRAYS

In the previous examples, we considered adaptive filtering performed on a single data sequence. However, adaptive filtering has also been widely applied to multiple data sequences that result from antenna, hydrophone, and seismometer arrays, where the sensors (antennas, hydrophones, or seismometers) are arranged in some spatial configuration. Each element of the array of sensors provides a signal sequence. By properly combining the signals from the various sensors, it is possible to change the directivity pattern of the array. For example, consider a linear antenna array consisting of five elements, as shown in Figure 15.35(a). If the signals are simply linearly summed, we obtain the sequence

$$x(n) = \sum_{k=1}^5 x_k(n) \quad (15.37)$$

which results in the antenna directivity pattern shown in Figure 15.35(a). Now, suppose that an interference signal is received from a direction corresponding to one of the sidelobes in the array. By properly weighting the sequences  $x_k(n)$  prior to combining, it is possible to alter the side-lobe pattern such that the array contains a null in the direction of the interference, as shown in Figure 15.35(b). Thus we obtain

$$x(n) = \sum_{k=1}^5 h_k x_k(n) \quad (15.38)$$

where the  $h_k$  are the weights.

We may also change or steer the direction of the main antenna lobe by simply introducing delays in the output of the sensor signals prior to combining. Hence from  $K$  sensors, we have a combined signal of the form

$$x(n) = \sum_{k=1}^K h_k x_k(n - n_k) \quad (15.39)$$

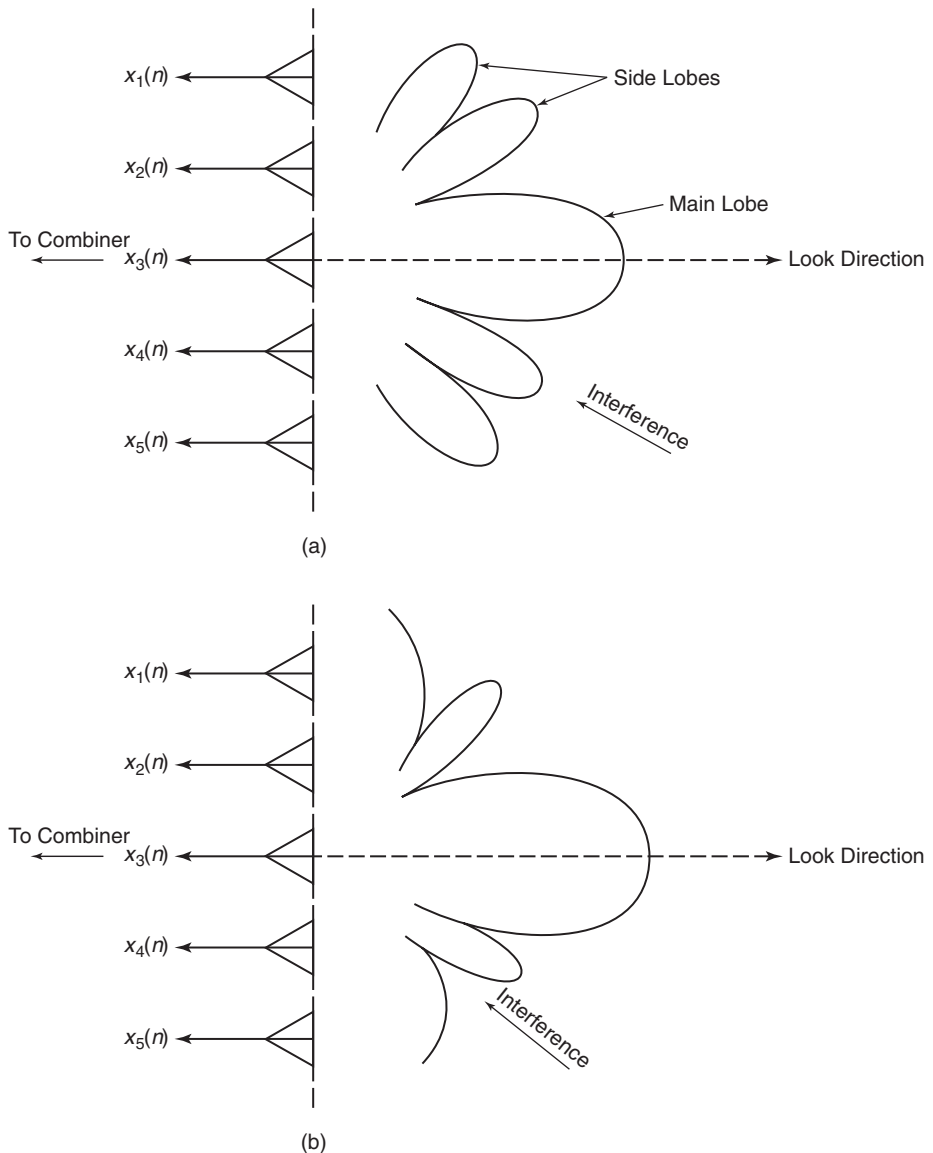


**FIGURE 15.35** Linear antenna array: (a) linear antenna array with antenna pattern; (b) linear antenna array with a null placed in the direction of the interference

where the  $h_k$  are the weights and  $n_k$  corresponds to an  $n_k$ -sample delay in the signal  $x(n)$ . The choice of weights may be used to place nulls in specific directions.

More generally, we may simply filter each sequence prior to combining. In such a case, the output sequence has the general form

$$\begin{aligned} y(n) &= \sum_{k=1}^K y_k(n) \\ &= \sum_{k=1}^K \sum_{\ell=0}^{M-1} h_k(\ell)x_k(n - n_k - \ell) \end{aligned} \quad (15.40)$$

where  $h_k$  is the impulse response of the filter for processing the  $k$ th sensor output and the  $n_k$  are the delays that steer the beam pattern.

The LMS algorithm described in Section 15.2.2 is frequently used in adaptively selecting the weights  $h_k$  or the impulse responses  $h_k(\ell)$ . The more powerful recursive least-squares algorithms described can also be applied to the multisensor (multichannel) data problem.

In the treatment given in this chapter, we deal with single-channel (sensor) signals.

## 15.2 ADAPTIVE DIRECT-FORM FIR FILTERS

---

From the examples of the previous section, we observed that there is a common framework in all the adaptive filtering applications. The least-squares criterion that we have adopted leads to a set of linear equations for the filter coefficients, which may be expressed as

$$\sum_{k=0}^{M-1} h(k)r_{xx}(\ell - k) = r_{dx}(\ell + D), \quad \ell = 0, 1, 2, \dots, M - 1 \quad (15.41)$$

where  $r_{xx}(\ell)$  is the autocorrelation of the sequence  $x(n)$  and  $r_{dx}(\ell)$  is the cross-correlation of the sequences  $d(n)$  and  $x(n)$ . The delay parameter  $D$  is zero in some cases and nonzero in others.

We observe that the autocorrelation  $r_{xx}(\ell)$  and the cross-correlation  $r_{dx}(\ell)$  are obtained from the data and, hence, represent estimates of the true (statistical) autocorrelation and cross-correlation sequences. As a result, the coefficients  $h(k)$  obtained from (15.41) are estimates of the true coefficients. The quality of the estimates depend on the length of the data record that is available for estimating  $r_{xx}(\ell)$  and  $r_{dx}(\ell)$ . This is one problem that must be considered in the implementation of an adaptive filter.

A second problem that must be considered is that the underlying random process  $x(n)$  is usually nonstationary. For example, in channel equalization, the frequency response characteristics of the channel may vary

with time. As a consequence, the statistical autocorrelation and cross-correlation sequences—and, hence, their estimates—vary with time. This implies that the coefficients of the adaptive filter must change with time to incorporate the time-variant statistical characteristics of the signal into the filter. This also implies that the quality of the estimates cannot be made arbitrarily high by simply increasing the number of signal samples used in the estimation of the autocorrelation and cross-correlation sequences.

There are several ways by which the coefficients of the adaptive filter can be varied with time to track the time-variant statistical characteristics of the signal. The most popular method is to adapt the filter recursively on a sample-by-sample basis, as each new signal sample is received. A second approach is to estimate  $r_{xx}(\ell)$  and  $r_{dx}(\ell)$  on a block-by-block basis, with no attempt to maintain continuity in the values of the filter coefficients from one block of data to another. In such a scheme, the block size must be relatively small, encompassing a time interval that is short compared to the time interval over which the statistical characteristics of the data change significantly. In addition to this block-processing method, other block-processing schemes can be devised that incorporate some block-to-block continuity in the filter coefficients.

In our treatment of adaptive filtering algorithms, we consider only time-recursive algorithms that update the filter coefficients on a sample-by-sample basis. In particular, we consider two types of algorithms, the LMS algorithm, which is based on a gradient-type search for tracking the time-variant signal characteristics, and the class of recursive least-squares algorithms, which are significantly more complex than the LMS algorithm, but which provide faster convergence to changes in signal statistics.

### 15.2.1 MINIMUM MEAN-SQUARE-ERROR CRITERION

The LMS algorithm that is described in the following subsection is most easily obtained by formulating the optimization of the FIR filter coefficients as an estimation problem based on the minimization of the mean-square error. Let us assume that we have available the (possibly complex-valued) data sequence  $x(n)$ , which consists of samples from a stationary random process  $X(n)$  with autocorrelation sequence

$$R_{XX}(m) = E[X(n)X^*(n - m)] \quad (15.42)$$

From these samples, we form an estimate of the desired sequence  $D(n)$  by passing the observed data  $x(n)$  through an FIR filter with coefficients  $h(n)$ ,  $0 \leq n \leq M - 1$ . The filter output may be expressed as

$$\hat{d}(n) = \sum_{k=0}^{M-1} h(k)x(n - k) \quad (15.43)$$

where  $\hat{d}(n)$  represents samples of an estimate  $\hat{D}(n)$  of  $D(n)$ . The estimation error process is defined as

$$\begin{aligned} E(n) &= D(n) - \hat{D}(n) \\ &= D(n) - \sum_{k=0}^{M-1} h(k)X(n-k) \end{aligned} \quad (15.44)$$

The mean-square error as a function of the filter coefficients is

$$\begin{aligned} \epsilon_M &= E[|E(n)|^2] \\ &= E\left[\left|D(n) - \sum_{k=0}^{M-1} h(k)X(n-k)\right|^2\right] \\ &= E\left\{|D(n)|^2 - 2\operatorname{Re}\left[\sum_{k=0}^{M-1} h^*(\ell)D(n)X^*(n-\ell)\right]\right. \\ &\quad \left.+ \sum_{k=0}^{M-1} \sum_{\ell=0}^{M-1} h^*(\ell)h(k)X^*(n-\ell)X(n-k)\right\} \\ &= \sigma_D^2 - 2\operatorname{Re}\left[\sum_{\ell=0}^{M-1} h^*(\ell)R_{DX}(\ell)\right] + \sum_{k=0}^{M-1} \sum_{\ell=0}^M h^*(\ell)h(k)R_{XX}(\ell-k) \end{aligned} \quad (15.45)$$

where, by definition,  $\sigma_D^2 = E[|D(n)|^2]$ .

We observe that the MSE is a quadratic function of the filter coefficients. Consequently, the minimization  $\epsilon_M$  with respect to the coefficients leads to the set of  $M$  linear equations,

$$\sum_{k=0}^{M-1} h(k)R_{XX}(\ell-k) = R_{DX}(\ell), \quad \ell = 0, 1, \dots, M-1 \quad (15.46)$$

The filter with coefficients obtained from (15.46), which is the Wiener-Hopf equation previously derived in Section 14.6.1, is called the *Wiener filter*.

If we compare (15.46) with (15.41), it is apparent that these equations are similar in form. In (15.41), we use estimates of the autocorrelation and cross-correlation to determine the filter coefficients, whereas in (15.46) the statistical autocorrelation and cross-correlation are employed. Hence (15.46) yields the optimum (Wiener) filter coefficients in the MSE sense, whereas (15.41) yields estimates of the optimum coefficients.

The equations in (15.46) may be expressed in matrix form as

$$\mathbf{T}_M \mathbf{h}_M = \mathbf{R}_D \quad (15.47)$$

where  $\mathbf{h}_M$  denotes the vector of coefficients,  $\mathbf{T}_M$  is an  $M \times M$  (Hermitian) Toeplitz matrix with elements  $T_{\ell k} = R_{XX}(\ell - k)$ , and  $\mathbf{R}_D$  is an  $M \times 1$  cross-correlation vector with elements  $R_{DX}(\ell)$ ,  $\ell = 0, 1, \dots, M - 1$ . The complex-conjugate of  $\mathbf{h}_M$  is denoted as  $\mathbf{h}_M^*$  and the transpose as  $\mathbf{h}_M^t$ . The solution for the optimum filter coefficients is

$$\mathbf{h}_{\text{opt}} = \mathbf{T}_M^{-1} \mathbf{R}_D \quad (15.48)$$

and the resulting minimum MSE achieved with the optimum coefficients given by (15.48)

$$\begin{aligned} \mathcal{E}_{M\min} &= \sigma_D^2 - \sum_{k=0}^{M-1} h_{\text{opt}}(k) R_{DX}^*(k) \\ &= \sigma_D^2 - \mathbf{R}_D^H \mathbf{T}_M^{-1} \mathbf{R}_D \end{aligned} \quad (15.49)$$

where the exponent H denotes the conjugate transpose.

Recall that the set of linear equations in (15.46) can also be obtained by invoking the orthogonality principle in mean-square estimation (see Section 14.6.2). According to the orthogonality principle, the mean-square estimation error is minimized when the error  $\mathbf{E}(n)$  is orthogonal, in the statistical sense, to the estimate  $\hat{\mathbf{D}}(n)$ , that is,

$$\mathbf{E}[\mathbf{E}(n)\hat{\mathbf{D}}^*(n)] = 0 \quad (15.50)$$

But the condition in (15.50) implies that

$$\mathbf{E}\left[\sum_{k=0}^{M-1} h(k)\mathbf{E}(n)\mathbf{X}^*(n-k)\right] = \sum_{k=0}^{M-1} h(k)\mathbf{E}[\mathbf{E}(n)\mathbf{X}^*(n-k)] = 0$$

or equivalently,

$$\mathbf{E}[\mathbf{E}(n)\mathbf{X}^*(n-\ell)] = 0, \quad \ell = 0, 1, \dots, M - 1 \quad (15.51)$$

If we substitute for  $\mathbf{E}(n)$  in (15.51) using the expression for  $\mathbf{E}(n)$  given in (15.44), and perform the expectation operation, we obtain the equations given in (15.46).

Since  $\hat{\mathbf{D}}(n)$  is orthogonal to  $\mathbf{E}(n)$ , the residual (minimum) mean-square error is

$$\begin{aligned} \mathcal{E}_{M\min} &= \mathbf{E}[\mathbf{E}(n)\mathbf{D}^*(n)] \\ &= \mathbf{E}[|\mathbf{D}(n)|^2] - \sum_{k=0}^{M-1} h_{\text{opt}}(k) R_{DX}^*(k) \end{aligned} \quad (15.52)$$

which is the result given in (15.49).

The optimum filter coefficients given by (15.48) can be solved efficiently by using the Levinson–Durbin algorithm. However, we shall consider the use of a gradient method for solving for  $\mathbf{h}_{\text{opt}}$  iteratively. This development leads to the LMS algorithm for adaptive filtering.

**EXAMPLE 15.8 Parameter Estimation Based on MSE Criterion**

Consider the random process

$$\mathbf{X}(n) = \mathbf{G}v(n) + \mathbf{W}(n), \quad n = 0, 1, \dots, M - 1$$

where  $v(n)$  is a known sequence,  $\mathbf{G}$  is a random variable with  $E[\mathbf{G}] = 0$ , and  $E[\mathbf{G}^2] = \sigma_{\mathbf{G}}^2$ . The sequence  $\mathbf{W}(n)$  is a white noise sequence with variance  $\sigma_{\mathbf{W}}^2$ .

- a. Determine the coefficients of the linear estimator for  $\mathbf{G}$ , given as

$$\widehat{\mathbf{G}} = \sum_{n=0}^{M-1} h(n)\mathbf{X}(n)$$

that minimize the mean-square error

$$\mathcal{E} = E[(\mathbf{G} - \widehat{\mathbf{G}})^2].$$

- b. Determine the values of  $\{h(n)\}$  when  $\{v(n)\} = \{1, 1, 1, -1, -1, -1, 1, -1, -1, 1, -1\}$ , which is the Barker sequence of length  $M = 11$ ,  $\sigma_{\mathbf{G}}^2 = 1$ , and  $\sigma_{\mathbf{W}}^2 = 0.1$ .

**Solution**

- a. The MSE is given by

$$\mathcal{E} = E \left[ \left( \mathbf{G} - \sum_{n=0}^{M-1} h(n)\mathbf{X}(n) \right)^2 \right]$$

The minimum MSE is obtained by performing

$$\frac{\partial \mathcal{E}}{\partial h(k)} = 0 \Rightarrow E \left[ 2 \left( \mathbf{G} - \sum_{n=0}^{M-1} h(n)\mathbf{X}(n) \right) \mathbf{X}(k) \right] = 0, \quad k = 0, 1, \dots, M - 1$$

Thus

$$E[\mathbf{G}\mathbf{X}(k)] = E \left[ \sum_{n=0}^{M-1} h(n)\mathbf{X}(n)\mathbf{X}(k) \right], \quad k = 0, 1, \dots, M - 1 \quad (15.53)$$

Now,

$$E[\mathbf{G}\mathbf{X}(k)] = E[\mathbf{G}\{\mathbf{G}v(k) + \mathbf{W}(k)\}] = \sigma_{\mathbf{G}}^2 v(k), \quad k = 0, 1, \dots, M - 1 \quad (15.54)$$

assuming that  $\mathbf{G}$  and  $\mathbf{W}(k)$  are uncorrelated. Also,

$$E \left[ \sum_{n=0}^{M-1} h(n)\mathbf{X}(n)\mathbf{X}(k) \right] = \sum_{n=0}^{M-1} h(n)E[\mathbf{X}(n)\mathbf{X}(k)] \quad (15.55)$$

It is easily shown that

$$\mathbb{E}[\mathbf{X}(n)\mathbf{X}(k)] = \sigma_G^2 v(k)v(n) + \sigma_W^2 \delta_{nk} \quad (15.56)$$

Therefore, substituting (15.54)–(15.56) into (15.53), we have

$$\sigma_G^2 v(k) = \sigma_G^2 \sum_{n=0}^{M-1} h(n)v(k)v(n) + \sigma_W^2 h(k) \quad (15.57)$$

Hence the filter coefficients are the solution of the linear equations

$$(\sigma_G^2 \mathbf{v} \mathbf{v}^t + \sigma_W^2 \mathbf{I}) \mathbf{h} = \sigma_G^2 \mathbf{v} \quad (15.58)$$

where

$$\begin{aligned} \mathbf{v} &= [v(0), v(1), \dots, v(M-1)]^t, \\ \mathbf{h} &= [h(0), h(1), \dots, h(M-1)]^t \end{aligned}$$

- b. When  $\{v(n)\} = \{1, 1, 1, -1, -1, -1, 1, -1, -1, 1, -1\}$ ,  $\sigma_G^2 = 1$ , and  $\sigma_W^2 = 0.1$ , the solution to the linear equations yields

$$\begin{aligned} \{h(n)\} = &\{0.0901, 0.0901, 0.0901, -0.0901, -0.0901, -0.0901, 0.0901, \\ &-0.0901, -0.0901, 0.0901, -0.0901\} \end{aligned}$$

□

### 15.2.2 THE LMS ALGORITHM

There are various numerical methods that can be used to solve the set of linear equations given by (15.46) or (15.47) for the optimum FIR filter coefficients. In the following, we consider recursive methods that have been devised for finding the minimum of a function of several variables. In our problem, the performance index is the MSE given by (15.45), which is a quadratic function of the filter coefficients. Hence this function has a unique minimum, which we shall determine by an iterative search.

For the moment, let us assume that the autocorrelation matrix  $\mathbf{T}_M$  and the cross-correlation vector  $\mathbf{R}_D$  are known. Hence  $\mathcal{E}_M$  is a known function of the coefficients  $h(n)$ ,  $0 \leq n \leq M-1$ . Algorithms for recursively computing the filter coefficients and, thus, searching for the minimum  $\mathcal{E}_M$  have the form

$$\mathbf{h}_M(n+1) = \mathbf{h}_M(n) + \frac{1}{2} \Delta(n) \mathbf{V}(n), \quad n = 0, 1, \dots \quad (15.59)$$

where  $\mathbf{h}_M(n)$  is the vector of filter coefficients at the  $n$ th iteration,  $\Delta(n)$  is a step size at the  $n$ th iteration, and  $\mathbf{V}(n)$  is a direction vector for the  $n$ th iteration. The initial vector  $\mathbf{h}_M(0)$  is chosen arbitrarily. In this

treatment, we exclude methods that require the computations of  $\mathbf{T}_M^{-1}$ , such as Newton's method, and consider only search methods based on the use of gradient vectors.

The simplest method for finding the minimum of  $\mathcal{E}_M$  recursively is based on a steepest-descent search (see Murray [69]). In the method of steepest descent, the direction vector  $\mathbf{V}(n) = -\mathbf{g}(n)$ , where  $\mathbf{g}(n)$  is the gradient vector at the  $n$ th iteration, defined as

$$\begin{aligned}\mathbf{g}(n) &= \frac{d\mathcal{E}_M(n)}{d\mathbf{h}_M(n)} \\ &= 2[\mathbf{T}_M \mathbf{h}_M(n) - \mathbf{R}_D], \quad n = 0, 1, 2, \dots\end{aligned}\quad (15.60)$$

Hence we compute the gradient vector at each iteration and change the values of  $\mathbf{h}_M(n)$  in a direction opposite the gradient. Thus the recursive algorithm based on the method of steepest descent is

$$\mathbf{h}_M(n+1) = \mathbf{h}_M(n) - \frac{1}{2}\Delta(n)\mathbf{g}(n) \quad (15.61)$$

or equivalently,

$$\mathbf{h}_M(n+1) = [\mathbf{I} - \Delta(n)\mathbf{T}_M]\mathbf{h}_M(n) + \Delta(n)\mathbf{R}_D. \quad (15.62)$$

We state without proof that the algorithm leads to the convergence of  $\mathbf{h}_M(n)$  to  $\mathbf{h}_{\text{opt}}$  in the limit as  $n \rightarrow \infty$ , provided that the sequence of step sizes  $\Delta(n)$  is absolutely summable, with  $\Delta(n) \rightarrow 0$  as  $n \rightarrow \infty$ . It follows that as  $n \rightarrow \infty$ ,  $\mathbf{g}(n) \rightarrow \mathbf{0}$ .

Other candidate algorithms that provide faster convergence are the *conjugate-gradient* algorithm and the Fletcher–Powell algorithm. In the conjugate-gradient algorithm, the direction vectors are given as

$$\mathbf{V}(n) = \beta(n-1)\mathbf{V}(n-1) - \mathbf{g}(n) \quad (15.63)$$

where  $\beta(n)$  is a scalar function of the gradient vectors (see Beckman [1]). In the Fletcher–Powell algorithm, the direction vectors are given as

$$\mathbf{V}(n) = -\mathbf{H}(n)\mathbf{g}(n) \quad (15.64)$$

where  $\mathbf{H}(n)$  is an  $M \times M$  positive definite matrix, computed iteratively, that converges to the inverse of  $\mathbf{T}_M$  (see Fletcher and Powell [16]). Clearly, the three algorithms differ in the manner in which the direction vectors are computed. These three algorithms are appropriate when  $\mathbf{T}_M$  and  $\mathbf{R}_D$  are known. However, this is not the case in adaptive filtering applications, as we have previously indicated. In the absence of knowledge of  $\mathbf{T}_M$  and  $\mathbf{R}_D$ , we may substitute estimates,  $\hat{\mathbf{V}}(n)$ , of the direction vectors in place of the actual vectors,  $\mathbf{V}(n)$ . We consider this approach for the steepest-descent algorithm.

First, we note that the gradient vector given by (15.60) may also be expressed in terms of the orthogonality conditions given by (15.50). In fact, the conditions in (15.50) are equivalent to the expression

$$\mathbb{E}[\mathbf{E}(n)\mathbf{X}_M^*(n)] = \mathbf{R}_D - \mathbf{T}_M \mathbf{h}_M(n) \quad (15.65)$$

where  $\mathbf{X}_M(n)$  is the vector with elements  $X(n-\ell)$ ,  $\ell = 0, 1, \dots, M-1$ . Therefore, the gradient vector is simply

$$\mathbf{g}(n) = -2\mathbb{E}[\mathbf{E}(n)\mathbf{X}_M^*(n)] \quad (15.66)$$

Clearly, the gradient vector  $\mathbf{g}(n) = \mathbf{0}$  when the error is orthogonal to the data in the estimate  $\hat{\mathbf{D}}(n)$ .

An unbiased estimate of the gradient vector at the  $n$ th iteration is simply obtained from (15.66) as

$$\hat{\mathbf{g}}(n) = -2\mathbb{E}(n)\mathbf{X}_M^*(n) \quad (15.67)$$

where  $\mathbb{E}(n) = D(n) - \hat{D}(n)$  and  $\mathbf{X}_M(n)$  is the set of  $M$  signal samples in the filter at the  $n$ th iteration. Thus, with  $\hat{\mathbf{g}}$  substituted for  $\mathbf{g}(n)$ , we have the algorithm

$$\mathbf{h}_M(n+1) = \mathbf{h}_M(n) + \Delta(n)\mathbb{E}(n)\mathbf{X}_M^*(n) \quad (15.68)$$

where  $\mathbf{h}(n)$  is now a vector random process with vector sample sequence given by  $\mathbf{h}(n)$ . This is called a *stochastic-gradient-descent* algorithm. As given by (15.68), it has a variable step size.

It has become common practice in adaptive filtering to use a fixed step-size algorithm for two reasons. The first is that a fixed step-size algorithm is easily implemented in either hardware or software. The second is that a fixed step size is appropriate for tracking time-variant signal statistics, whereas if  $\Delta(n) \rightarrow 0$  as  $n \rightarrow \infty$ , adaptation to signal variations cannot occur. For these reasons, (15.68) is modified to the algorithm

$$\mathbf{h}_M(n+1) = \mathbf{h}_M(n) + \Delta \mathbb{E}(n)\mathbf{X}_M^*(n) \quad (15.69)$$

where  $\Delta$  is now the fixed step size. This algorithm was first proposed by Widrow and Hoff [95] and is now widely known as the LMS (*least-mean-squares*) algorithm. Clearly, it is a stochastic-gradient algorithm.

The LMS algorithm is relatively simple to implement. For this reason, it has been widely used in many adaptive filtering applications. Its properties and limitations have also been thoroughly investigated. In the following section, we provide a brief treatment of its important properties concerning convergence, stability, and the noise resulting from the use of estimates of the gradient vectors. Subsequently, we compare its properties with the more complex recursive least-squares algorithm.

**MATLAB Implementation** The SP Toolbox does not provide any function for implementing the LMS algorithm, although it is available in the Communication Systems Toolbox and DSP Systems Toolbox as an object in an object-oriented programming environment. This discussion is beyond the scope of this book. In Section 11.1, we provided the function `[h,y] = lms(x,d,delta,M)` that computes adaptive filter coefficients  $\{h(n), 0 \leq n \leq M - 1\}$  in array `h` given the input sequence  $\{x(n)\}$ , the desired sequence  $\{d(n)\}$ , step size  $\Delta$ , and the desired adaptive FIR filter length  $M$  in respective arrays `x`, `d`, `delta`, and `M`. In addition, the `lms` function provides the output  $\{y(n)\}$  of the adaptive filter in the array `y`. It is given below again for easy reference.

```

function [h,y] = lms(x,d,delta,M)
% LMS Algorithm for Coefficient Adjustment
%
% [h,y] = lms(x,d,delta,N)
%     h = estimated FIR filter
%     y = output array y(n)
%     x = input array x(n)
%     d = desired array d(n), length must be same as x
% delta = step size
%     M = length of the FIR filter
%
N = length(x); y = zeros(1,N);
h = zeros(1,M);
for n = M:N
    x1 = x(n:-1:n-M+1);
    y = h * x1';
    e = d(n) - y;
    h = h + delta*e*x1;
end

```

Several variations of the basic LMS algorithm have been proposed in the literature and implemented in adaptive filtering applications. One variation is obtained if we average the gradient vectors over several iterations prior to making adjustments of the filter coefficients. For example, the average over  $K$  gradient vectors is

$$\bar{\mathbf{g}}(nK) = -\frac{2}{K} \sum_{k=0}^{K-1} \mathbf{E}(nK+k) \mathbf{X}_M^*(nK+k) \quad (15.70)$$

and the corresponding recursive equation for updating the filter coefficients once every  $K$  iterations is

$$\mathbf{h}_M((n+1)K) = \mathbf{h}_M(nK) - \frac{1}{2} \Delta \bar{\mathbf{g}}(nK) \quad (15.71)$$

In effect, the averaging operation performed in (15.70) reduces the noise in the estimate of the gradient vector, as shown by Gardner [20].

An alternative approach is to filter the gradient vectors by a lowpass filter and use the output of the filter as an estimate of the gradient vector. For example, a simple lowpass filter for the gradients yields as an output

$$\hat{\mathbf{V}}(n) = \beta \hat{\mathbf{V}}(n-1) - \hat{\mathbf{g}}(n), \quad \mathbf{V}(0) = -\hat{\mathbf{g}}(0) \quad (15.72)$$

where the choice of  $0 \leq \beta < 1$  determines the bandwidth of the lowpass filter. When  $\beta$  is close to unity, the filter bandwidth is small and the effective averaging is performed over many gradient vectors. On the other hand, when  $\beta$  is small, the lowpass filter has a large bandwidth and, hence, it provides little averaging of the gradient vectors. With the filtered gradient vectors given by (15.72) in place of  $\hat{\mathbf{g}}(n)$ , we obtain the filtered version of the LMS algorithm, given by

$$\mathbf{h}_M(n+1) = \mathbf{h}_M(n) + \frac{1}{2} \Delta \hat{\mathbf{V}}(n) \quad (15.73)$$

An analysis of the filtered-gradient LMS algorithm is given in Proakis [78].

### 15.2.3 PROPERTIES OF THE LMS ALGORITHM

In this section, we consider the basic properties of the LMS algorithm given by (15.69). In particular, we focus on its convergence properties, its stability, and the excess noise generated as a result of using noisy gradient vectors in place of the actual gradient vectors. The use of noisy estimates of the gradient vectors implies that the filter coefficients will fluctuate randomly, and, hence, an analysis of the characteristics of the algorithm should be performed in statistical terms.

#### *Convergence and Stability*

The convergence and stability of the LMS algorithm may be investigated by determining how the mean value of  $\mathbf{h}_M(n)$  converges to the optimum coefficients  $\mathbf{h}_{\text{opt}}$ . If we take the expected value of (15.69), we obtain

$$\begin{aligned} \bar{\mathbf{h}}_M(n+1) &= \bar{\mathbf{h}}_M(n) + \Delta E[\mathbf{E}(n)\mathbf{X}_M^*(n)] \\ &= \bar{\mathbf{h}}_M(n) + \Delta[\mathbf{R}_D - \mathbf{T}_M \bar{\mathbf{h}}_M(n)] \\ &= (\mathbf{I} - \Delta \mathbf{T}_M) \bar{\mathbf{h}}_M(n) + \Delta \mathbf{R}_D \end{aligned} \quad (15.74)$$

where  $\bar{\mathbf{h}}_M(n) = E[\mathbf{h}_M(n)]$ , and  $\mathbf{I}$  is the identity matrix.

The recursive relation in (15.74) may be represented as a closed-loop control system, as shown in Figure 15.36. The convergence rate and the stability of this closed-loop system are governed by our choice of the step-size parameter  $\Delta$ . To determine the convergence behavior, it is convenient

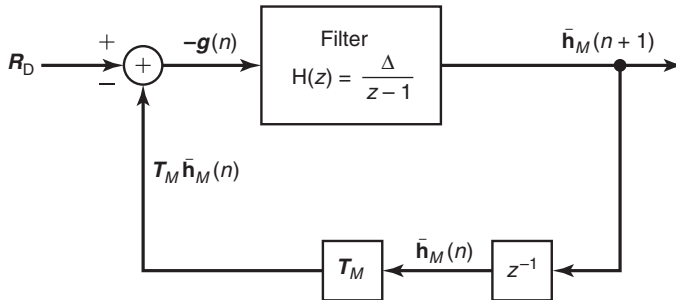


**FIGURE 15.36** Closed-loop control system representation of recursive Equation (15.74)

to decouple the  $M$  simultaneous difference equations given in (15.74), by performing a linear transformation of the mean coefficient vector  $\bar{\mathbf{h}}_M(n)$ . The appropriate transformation is obtained by noting that the autocorrelation matrix  $\mathbf{T}_M$  is Hermitian and, hence, can be represented (see Gantmacher [19]) as

$$\mathbf{T}_M = \mathbf{U} \boldsymbol{\Lambda} \mathbf{U}^H \quad (15.75)$$

where  $\mathbf{U}$  is the normalized modal matrix of  $\mathbf{T}_M$  and  $\boldsymbol{\Lambda}$  is a diagonal matrix with diagonal elements  $\lambda_k$ ,  $0 \leq k \leq M-1$ , equal to the eigenvalues of  $\mathbf{T}_M$ .

When (15.75) is substituted into (15.74), the latter may be expressed as

$$\bar{\mathbf{h}}_M^o(n+1) = (\mathbf{I} - \Delta \boldsymbol{\Lambda}) \bar{\mathbf{h}}_M^o(n) + \Delta \mathbf{R}_D^o \quad (15.76)$$

where the transformed (orthogonalized) vectors are  $\bar{\mathbf{h}}_M^o(n) = \mathbf{U}^H \bar{\mathbf{h}}_M(n)$  and  $\mathbf{R}_D^o = \mathbf{U}^H \mathbf{R}_D$ . The set of  $M$  first-order difference equations in (15.76) are now decoupled. Their convergence and their stability is determined from the homogeneous equation

$$\bar{\mathbf{h}}_M^o(n+1) = (\mathbf{I} - \Delta \boldsymbol{\Lambda}) \bar{\mathbf{h}}_M^o(n) \quad (15.77)$$

If we focus our attention on the solution of the  $k$ th equation in (15.77), we observe that

$$\bar{\mathbf{h}}^o(k, n) = C(1 - \Delta \lambda_k)^n u(n), \quad k = 0, 1, 2, \dots, M-1 \quad (15.78)$$

where  $C$  is an arbitrary constant and  $u(n)$  is the unit step sequence. Clearly,  $\bar{\mathbf{h}}^o(k, n)$  converges to zero exponentially, provided that

$$|1 - \Delta \lambda_k| < 1$$

or equivalently,

$$0 < \Delta < \frac{2}{\lambda_k}, \quad k = 0, 1, \dots, M-1 \quad (15.79)$$

The fastest convergence rate is obtained when  $\Delta = 1/\lambda_k$ .

The condition given by (15.79) for convergence of the homogeneous difference equation for the  $k$ th normalized filter coefficient ( $k$ th mode of the closed-loop system) must be satisfied for all  $k = 0, 1, \dots, M - 1$ . Therefore, the range of values of  $\Delta$  that ensures the convergence of the mean of the coefficient vector in the LMS algorithm is

$$0 < \Delta < \frac{2}{\lambda_{\max}} \quad (15.80)$$

where  $\lambda_{\max}$  is the largest eigenvalue of  $\mathbf{T}_M$ .

Since  $\mathbf{T}_M$  is an autocorrelation matrix, its eigenvalues are nonnegative. Hence an upper bound on  $\lambda_{\max}$  is

$$\lambda_{\max} < \sum_{k=0}^{M-1} \lambda_k = \text{trace } \mathbf{T}_M = M R_{XX}(0) \quad (15.81)$$

where  $R_{XX}(0)$  is the input signal power, which is easily estimated from the received signal. Therefore, an upper-bound on the step size  $\Delta$  is  $2/MR_{XX}(0)$ .

From (15.78), we observe that rapid convergence of the LMS algorithm occurs when  $|1 - \Delta\lambda_k|$  is small, that is, when the poles of the closed-loop system in Figure 15.36 are far from the unit circle. However, we cannot achieve this desirable condition and still satisfy the upper bound in (15.79) when there is a large difference between the largest and smallest eigenvalues of  $\mathbf{T}_M$ . In other words, even if we select  $\Delta$  to be  $1/\lambda_{\max}$ , the convergence rate of the LMS algorithm will be determined by the decay of the mode corresponding to the smallest eigenvalue  $\lambda_{\min}$ . For this mode, with  $\Delta = 1/\lambda_{\max}$  substituted in (15.78), we have

$$\bar{\mathbf{h}}_M^o(k, n) = C \left( 1 - \frac{\lambda_{\min}}{\lambda_{\max}} \right)^n u(n)$$

Consequently, the ratio  $\lambda_{\min}/\lambda_{\max}$  ultimately determines the convergence rate. If  $\lambda_{\min}/\lambda_{\max}$  is small (much smaller than unity), the convergence will be slow. On the other hand, if  $\lambda_{\min}/\lambda_{\max}$  is close to unity, the convergence rate of the algorithm is fast.

#### EXAMPLE 15.9 Choice of Step Size in LMS Algorithm

Let us simulate an adaptive equalizer based on the LMS algorithm. The channel characteristic is given by the following sample values taken at the symbol rate:

$$x = [0.05, -0.063, 0.088, -0.126, -0.25, 0.9047, 0.25, 0, 0.126, 0.038, 0.088]$$

The autocorrelation matrix for this channel has an eigenvalue spread of  $\lambda_{\max}/\lambda_{\min} = 11$ . The number of taps selected for the FIR equalizer is  $M = 11$ . The received signal-plus-noise power is normalized to unity. We wish to illustrate the convergence characteristics of the LMS algorithm for three different values of the step-size,  $\Delta = 0.045, 0.09$ , and  $0.115$ . The upper bound for stability of the algorithm is  $\Delta = 0.18$ .

**Solution**

Figure 15.37 illustrates the convergence characteristics of the LMS algorithm for the three values of  $\Delta$ . These graphs, called *learning curves*, were obtained by averaging the estimated MSE in 200 simulation runs. By selecting  $\Delta = 0.09$  (one-half of the upper bound), we obtain a rapidly decaying convergence rate, as shown in Figure 15.37. If we divide  $\Delta$  by 2 to 0.045, the convergence rate is reduced, but the excess MSE is also reduced, so the algorithm performs better in a time-invariant signal environment; that is, the estimated equalizer coefficients are closer to their optimum values. The MATLAB script for this example is given below.

```

N=500;                                     % length of the information sequence
K=5;
actual_isi=[0.05 -0.063 0.088 -0.126 -0.25 0.9047 0.25 0 0.126 0.038 0.088];
sigma=0.01;
delta=0.115;
Num_of_realizations=1000;
mse_av=zeros(1,N-2*K);
info = zeros(1,N);
noise = zeros(1,N);
mse = zeros(1,N);
for j=1:Num_of_realizations,           % Compute the average over a number of
% realizations.
    % The information sequence
    for i=1:N,
        if (rand<0.5),
            info(i)=-1;
        else
            info(i)=1;
        end
        echo off;
    end;
    % the channel output
    y=filter(actual_isi,1,info);
    for i=1:2:N, [noise(i), noise(i+1)]=gngauss(sigma); end;
    y=y+noise;
    % Now the equalization part follows.
    estimated_c=[0 0 0 0 0 1 0 0 0 0 0];      % Initial estimate of ISI
    for k=1:N-2*K,
        y_k=y(k:k+2*K);
        z_k=estimated_c*y_k.';
        e_k=info(k)-z_k;
        estimated_c=estimated_c+delta*e_k*y_k;
        mse(k)=e_k^2;
        echo off;
    end;
    mse_av=mse_av+mse;
end;
mse_av=mse_av/Num_of_realizations;    % mean-squared error versus iterations
% Plotting commands follow

```



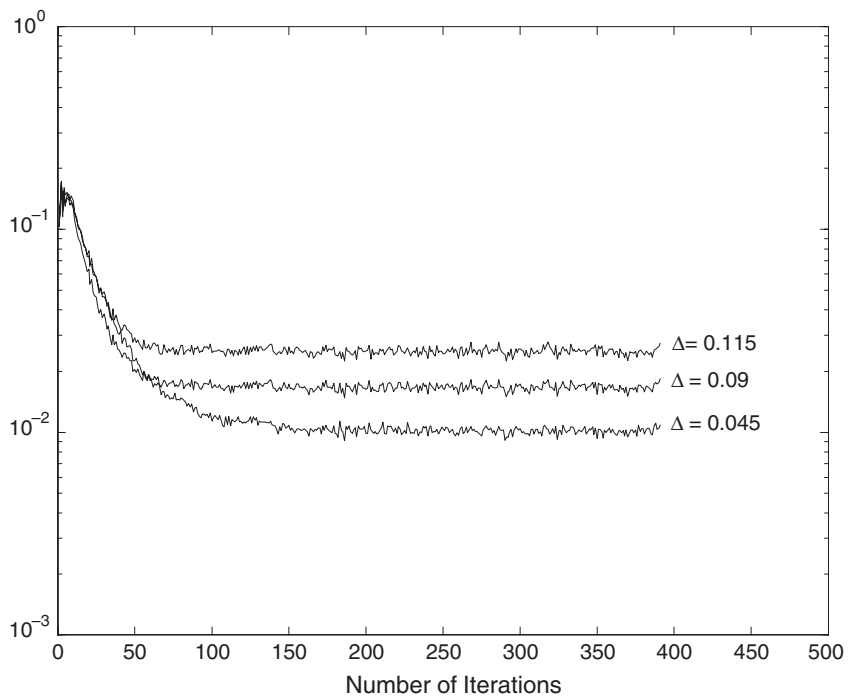


**FIGURE 15.37** Initial convergence characteristics of the LMS algorithm with different step sizes

□ **EXAMPLE 15.10 Choice of the Step Size  $\Delta$  in Steepest-Descent**  
Consider the quadratic performance index

$$J = h^2 - 40h + 28$$

Suppose that we search for the minimum of  $J$  by using the steepest-descent algorithm

$$h(n+1) = h(n) - \frac{1}{2}\Delta g(n), \quad n = 0, 1, \dots$$

where  $g(n)$  is the gradient.

- a. Determine the range of values for  $\Delta$  that provide an overdamped system for the adjustment process.
- b. Plot the expression for  $J$  as a function of  $n$  for a value of  $\Delta$  in this range.

**Solution**

- a. The gradient in the performance index is

$$g(n) = \frac{\partial J}{\partial h(n)} = 2h(n) - 40$$

Therefore, the steepest-descent algorithm is

$$h(n+1) = h(n) - \frac{1}{2}\Delta g(n) = (1 - \Delta)h(n) + 20\Delta$$

For an overdamped system,

$$|1 - \Delta| < 1 \quad \Rightarrow \quad 0 < \Delta < 2$$

- b. Figure 15.38(a) contains a plot of  $J(n)$  vs.  $n$ . The step size  $\Delta$  was set to 0.5 and the initial value of  $h$  was set to 0. In Figure 15.38(b), we have plotted  $J(h(n))$  vs.  $h(n)$ . As it is observed from the figures the minimum value of  $J$  which is  $-372$ , is reached within five iterations of the algorithm.  $\square$

### **Analysis of Excess Noise**

The other important characteristic of the LMS algorithm is the noise resulting from the use of estimates of the gradient vectors. The noise in the gradient-vector estimates causes random fluctuations in the coefficients about their optimal values and, thus, leads to an increase in the MMSE at the output of the adaptive filter. Hence the total MSE is  $\mathcal{E}_{M,\min} + \mathcal{E}_\Delta$ , where  $\mathcal{E}_\Delta$  is called the *excess mean-square error*.

For any given set of filter coefficients  $\mathbf{h}_M(n)$ , the total MSE at the output of the adaptive filter may be expressed as

$$\mathcal{E}_t(n) = \mathcal{E}_{M,\min} + (\mathbf{h}_M(n) - \mathbf{h}_{\text{opt}})^T \mathbf{T}_M (\mathbf{h}_M(n) - \mathbf{h}_{\text{opt}})^* \quad (15.82)$$

where  $\mathbf{h}_{\text{opt}}$  represents the optimum filter coefficients defined by (15.48). A plot  $\mathcal{E}_t(n)$  as a function of the iteration  $n$  is called a *learning curve*. If we substitute (15.75) for  $\mathbf{T}_M$  and perform the linear orthogonal transformation used previously, we obtain

$$\mathcal{E}_t(n) = \mathcal{E}_{M,\min} + \sum_{k=0}^{M-1} \lambda_k |h^o(k, n) - h_{\text{opt}}^o(k)|^2 \quad (15.83)$$

where the term  $(h^o(k, n) - h_{\text{opt}}^o(k))$  represents the error in the  $k$ th filter coefficient (in the orthogonal coordinate system). The excess MSE is defined as the expected value of the second term in (15.83),

$$\mathcal{E}_\Delta = \sum_{k=0}^{M-1} \lambda_k E[|h^o(k, n) - h_{\text{opt}}^o(k)|^2] \quad (15.84)$$

To derive an expression for the excess MSE  $\mathcal{E}_\Delta$ , we assume that the mean values of the filter coefficients  $\mathbf{h}_M(n)$  have converged to their optimum values  $\mathbf{h}_{\text{opt}}$ . Then the term  $\Delta E(n)\mathbf{X}_M^*(n)$  in the LMS algorithm given by (15.69) is a zero-mean noise vector. Its covariance is

$$\text{cov}[\Delta E(n)\mathbf{X}_M^*(n)] = \Delta^2 E[|E(n)|^2] \mathbf{X}_M(n) \mathbf{X}_M^H(n) \quad (15.85)$$

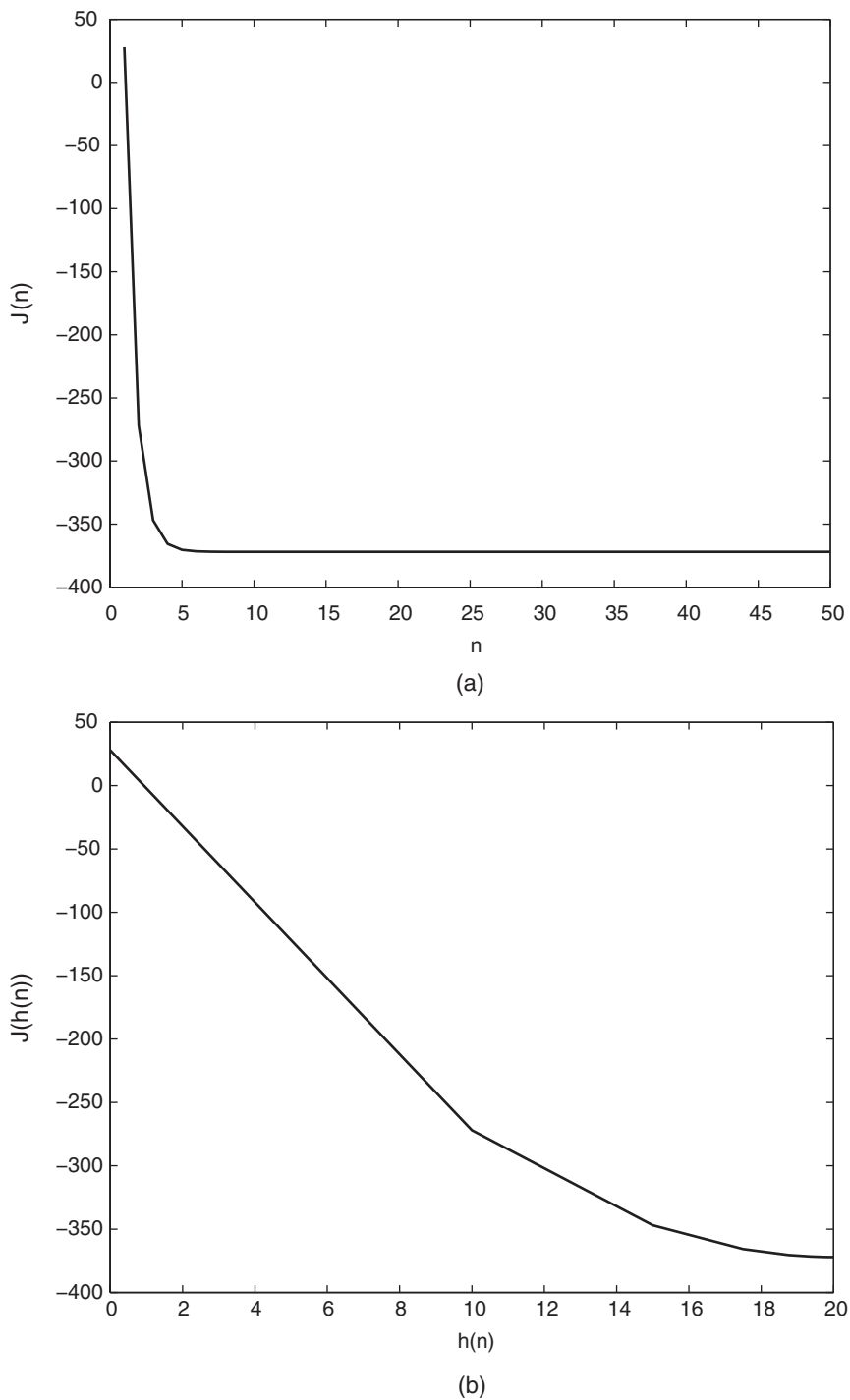


FIGURE 15.38 Convergence characteristics of  $J$  for Example 15.10

To a first approximation, we assume that  $|\mathbf{E}(n)|^2$  is uncorrelated with the signal vector. Although this assumption is not strictly true, it simplifies the derivation and yields useful results. (The reader may refer to Mazo [65], Jones, Cabin, and Reed [40], and Gardner [20] for further discussion on this assumption). Then

$$\begin{aligned}\text{cov}[\Delta \mathbf{E}(n) \mathbf{X}_M^*(n)] &= \Delta^2 \mathbf{E}[|\mathbf{E}(n)|^2] \mathbf{E}[\mathbf{X}_M(n) \mathbf{X}_M^H(n)] \\ &= \Delta^2 \mathcal{E}_{M,\min} \mathbf{T}_M\end{aligned}\quad (15.86)$$

For the orthogonalized coefficient vector  $\mathbf{h}_M^o(n)$  with additive noise, we have the equation

$$\mathbf{h}_M^o(n+1) = (\mathbf{I} - \Delta \mathbf{\Lambda}) \mathbf{h}_M^o(n) + \Delta \mathbf{R}_D^o + \mathbf{W}^o(n) \quad (15.87)$$

where  $\mathbf{W}^o(n)$  is the additive noise vector, which is related to the noise vector  $\Delta \mathbf{E}(n) \mathbf{X}_M^*(n)$  through the transformation

$$\begin{aligned}\mathbf{W}^o(n) &= \mathbf{U}^H [\Delta \mathbf{E}(n) \mathbf{X}_M^*(n)] \\ &= \Delta \mathbf{E}(n) \mathbf{U}^H \mathbf{X}_M^*(n)\end{aligned}\quad (15.88)$$

It is easily seen that the covariance matrix of the noise vector is

$$\begin{aligned}\text{cov}[\mathbf{W}^o(n)] &= \Delta^2 \mathcal{E}_{M,\min} \mathbf{U}^H \mathbf{T}_M \mathbf{U} \\ &= \Delta^2 \mathcal{E}_{M,\min} \mathbf{\Lambda}\end{aligned}\quad (15.89)$$

Therefore, the  $M$  components of  $\mathbf{W}^o(n)$  are uncorrelated and each component has the variance  $\sigma_k^2 = \Delta^2 \mathcal{E}_{M,\min} \lambda_k$ ,  $k = 0, 1, \dots, M-1$ .

Since the noise components of  $\mathbf{W}^o(n)$  are uncorrelated, we may consider the  $M$  uncoupled difference equations in (15.87) separately. Each first-order difference equation represents a filter with impulse response  $(1 - \Delta \lambda_k)^n$ . When such a filter is excited with a noise sequence  $W_k^o(n)$ , the variance of the noise at the output of the filter is

$$\mathbf{E} \left[ |\mathbf{h}^o(k, n) - h_{\text{opt}}^o(k)|^2 \right] = \sum_{n=0}^{\infty} \sum_{m=0}^{\infty} (1 - \Delta \lambda_k)^n (1 - \Delta \lambda_k)^m \mathbf{E} \left[ W_k^o(n) W_k^{o*}(m) \right] \quad (15.90)$$

We make the simplifying assumption that the noise sequence  $W_k^o(n)$  is white. Then (15.90) reduces to

$$\mathbf{E} \left[ |\mathbf{h}^o(k, n) - h_{\text{opt}}^o(k)|^2 \right] = \frac{\sigma_k^2}{1 - (1 - \Delta \lambda_k)^2} = \frac{\Delta^2 \mathcal{E}_{M,\min} \lambda_k}{1 - (1 - \Delta \lambda_k)^2} \quad (15.91)$$

If we substitute the result of (15.91) into (15.84), we obtain the expression for the excess MSE as

$$\mathcal{E}_\Delta = \Delta^2 \mathcal{E}_{M,\min} \sum_{k=0}^{M-1} \frac{\lambda_k^2}{1 - (1 - \Delta \lambda_k)^2} \quad (15.92)$$

This expression can be simplified if we assume that  $\Delta$  is selected such that  $\Delta\lambda_k \ll 1$  for all  $k$ . Then

$$\begin{aligned}\mathcal{E}_\Delta &\approx \Delta^2 \mathcal{E}_{M,\min} \sum_{k=0}^{M-1} \frac{\lambda_k^2}{2\Delta\lambda_k} \\ &\approx \frac{1}{2} \Delta \mathcal{E}_{M,\min} \sum_{k=0}^{M-1} \lambda_k \approx \frac{\Delta M \mathcal{E}_{M,\min} R_{XX}(0)}{2}\end{aligned}\quad (15.93)$$

where  $R_{XX}(0)$  is the power of the input signal.

The expression for  $\mathcal{E}_\Delta$  indicates that the excess MSE is proportional to the step-size parameter  $\Delta$ . Hence our choice of  $\Delta$  must be based on a compromise between fast convergence and a small excess MSE. In practice, it is desirable to have  $\mathcal{E}_\Delta < \mathcal{E}_{M,\min}$ . Hence

$$\frac{\mathcal{E}_\Delta}{\mathcal{E}_{M,\min}} \approx \frac{\Delta M R_{XX}(0)}{2} < 1$$

or equivalently,

$$\Delta < \frac{2}{M R_{XX}(0)} \quad (15.94)$$

But this is just the upper bound that we had obtained previously for  $\lambda_{\max}$ . In steady-state operation,  $\Delta$  should satisfy the upper bound in (15.94), otherwise the excess MSE causes significant degradation in the performance of the adaptive filter.

#### EXAMPLE 15.11

#### Use of LMS Algorithm in System Identification

Use the LMS algorithm to estimate the impulse response of the two-pole system given in Example 15.1. Initially, set  $h(k) = 0$  for  $0 \leq k \leq M - 1$ . The variance of  $W(n)$  is  $\sigma_w^2 = 0.02$  and the variance of  $X(n)$  is  $\sigma_x^2 = 1$ . Select the step size  $\Delta$  in the LMS algorithm to satisfy (15.94). Carry out the simulation for  $0 \leq n \leq 1000$ .

- a. After 1000 iterations, plot and compare the impulse response of the two pole filter with that of the FIR filter model. Also plot and compare the frequency response of the unknown system with that of the model.
- b. Compare the results in part (a) with the results obtained in part (c) of Example 15.1.

#### Solution

The adaptive filter order from Example 15.1 is  $M = 15$ . Since  $\sigma_x^2 = 1$ , the signal power is also  $R_{XX}(0) = 1$ . Hence from (15.94), the upper bound on the step size is  $\Delta = 0.1333$ . We chose the value of  $\Delta = 0.05$ , which gives good convergence and stability.

a. MATLAB script:

```

>> varW = 0.02; varX = 1; % Noise and signal variances
>> N = 1000; n = 0:N; % Number of samples and indices
>> p = 0.8*exp(1j*pi/4); % Pole location
>> a = [1,-2*real(p),abs(p)^2]; % Plant denominator coeff
>> M = 15; % FIR filter model order
>> xn = sqrt(varX)*randn(N+1,1); % Input sequence
>> wn = sqrt(varW)*randn(N+1,1); % Noise sequence
>> dn = filter(1,a,xn); % Output of the plant
>> yn = dn+wn; % Noisy plant output
>> % FIR filter model coefficients using LMS algorithm
>> delta = 0.05; %2/(M*varX)=0.1333;
>> [hm,yhatn] = lms(xn.',yn,delta,M);
>> hp = impz(1,a,M+5); % Plant impulse response
>> % Plots of the impulse and frequency responses
>> om = linspace(0,1,1001)*pi;
>> Hm = freqz(hm,1,om); Hm_mag = abs(Hm); Hm_phd = angle(Hm)/pi;
>> Hp = freqz(1,a,om); Hp_mag = abs(Hp); Hp_phd = angle(Hp)/pi;
>> % Plotting commands follow

```

The resulting plots are shown in Figure 15.39. After 1000 iterations, the model coefficients seem to converge to the plant coefficients with very small residual noise. This is also evident in the frequency response plots. The peak of the model magnitude response is at the correct location but the overall response exhibit the effects of FIR truncation and residual noise.

- b. Here, we compare the model coefficients and its frequency response obtained using the LS method and the LMS algorithm.

```

>> varW = 0.02; varX = 1; % Noise and signal variances
>> N = 1000; n = 0:N; % Number of samples and indices
>> p = 0.8*exp(1j*pi/4); % Pole location
>> a = [1,-2*real(p),abs(p)^2]; % Plant denominator coeff
>> M = 15; % FIR filter model order
>> xn = sqrt(varX)*randn(N+1,1); % Input sequence
>> wn = sqrt(varW)*randn(N+1,1); % Noise sequence
>> dn = filter(1,a,xn); % Output of the plant
>> yn = dn+wn; % Noisy plant output
>> % FIR filter model coefficients using LS method
>> [rxx] = xcorr(xn,M-1); % ACRS of x(n)
>> Rxx = toeplitz(rxx(M:end)); % ACRM of x(n)
>> ryx = xcorr(yn,xn,M-1); % CCRS between y(n) and x(n)
>> ryx = ryx(M:end); % CCRV
>> hls = Rxx\ryx; % Model coeff (or Imp resp)

```

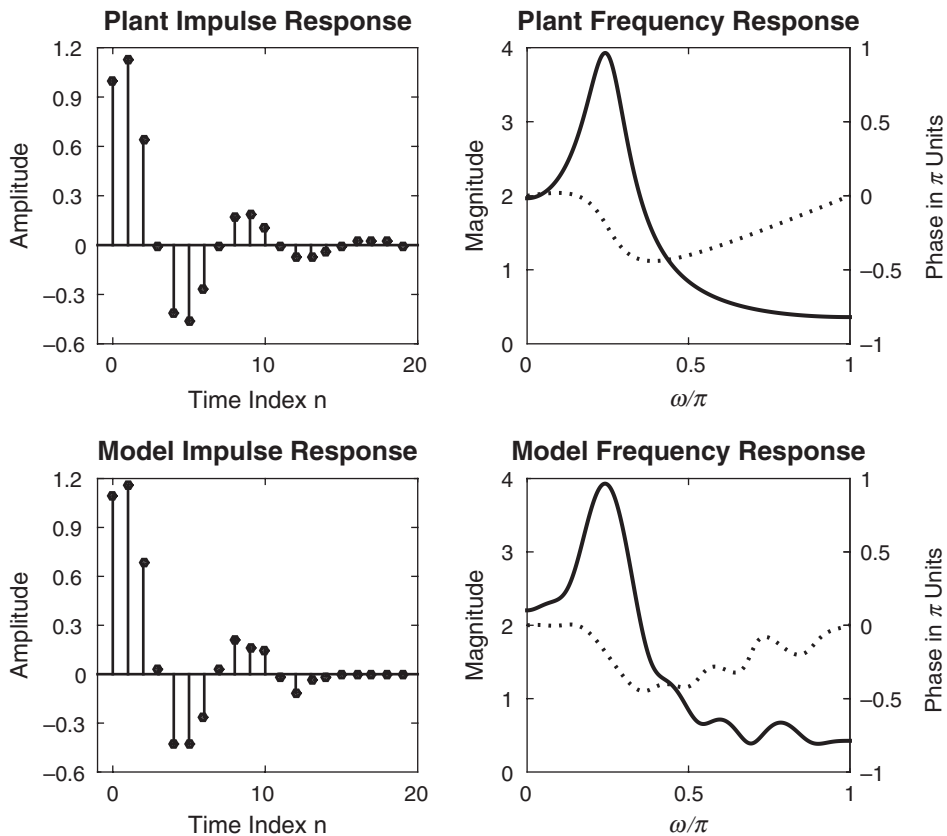


**FIGURE 15.39** Plots of the impulse and frequency responses of the plant and FIR model obtained using the LMS algorithm in Example 15.11(a). The dotted lines represent phase responses

```
>> % Plots of the impulse and frequency responses
>> om = linspace(0,1,1001)*pi;
>> Hls = freqz(hls,1,om); Hls_mag = abs(Hls); Hls_ph = angle(Hls)/pi;
>> % Plotting commands follow
```

The resulting plots are shown in Figure 15.40. Observe that the impulse response coefficients and the frequency responses obtained using LMS algorithm show the effects of excess noise especially at high frequencies. □

#### □ EXAMPLE 15.12 Use of LMS Algorithm in Channel Equalization

Consider the system configuration shown in Example 15.2. For  $M = 7$  and  $D = 10$ , generate the output sequence  $\hat{a}(n)$  and discard the first 10 output samples to compensate for the transient in the system. Thus  $\hat{a}(11)$  corresponds to  $a(1)$ ,  $\hat{a}(12)$  corresponds to  $a(2)$ , and so on. Use the LMS algorithm to adjust

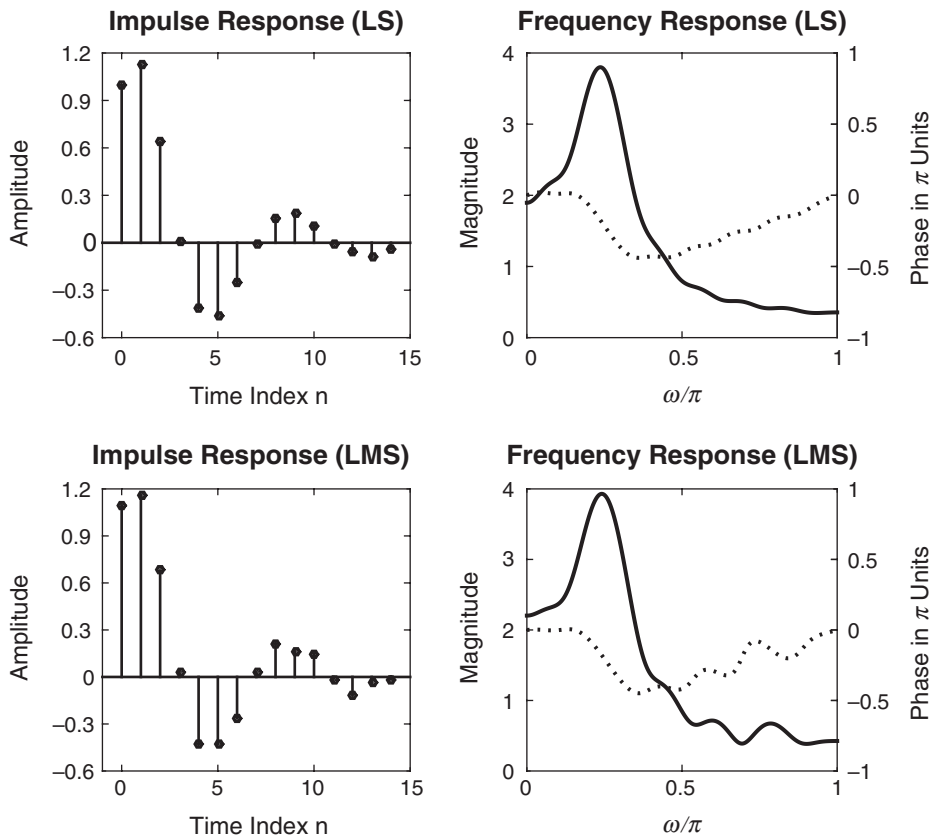


**FIGURE 15.40** Comparison of FIR models obtained using the LS method and the LMS algorithm in Example 15.11(b). The dotted lines represent phase responses

the equalizer filter coefficients  $h(k)$ ,  $0 \leq k \leq 6$ . Carry out the simulation for  $n = 1000$  samples and stop.

- Plot the frequency response of the channel filter  $C(z)$ , the equalizer filter  $H(z)$ , and the frequency response of the cascade filter  $C(z)H(z)$ . Comment on the results.
- Compare the results in part (a) with the results in Example 15.2, part (c), which were obtained from the least-squares criterion.

### Solution

Various signals and the model coefficients using the LMS algorithm are computed using the following MATLAB script.

```
>> z0 = 0.8*exp(1j*pi/4); % Zero of C(z)
>> Cb = [1,-2*real(z0),abs(z0)^2]; % Numerator of C(z) or imp resp
>> N = 1000; n = 0:N-1; % Length and timing indices for sequences
>> varW = 0.1; % Variance of the additive noise
>> % Generation of Sequences a(n), x(n), and d(n)
```

```

>> M = 7; % FIR equalizer length
>> D = 10; % Overall delay in processing
>> an = 2*randi([0,1],N,1)-1; % Pseudorandom symbol sequence
>> yn = filter(Cb,1,an); % Distorted symbol sequence
>> wn = sqrt(varW)*randn(N,1); % Additive noise sequence
>> xn = yn+wn; % Noisy distorted symbols
>> dn = [zeros(D,1);an(1:N)]; % Desired symbols (delayed)
>> % FIR equalizer coefficients using LMS algorithm
>> [rxx,lags] = xcorr(xn,M-1,'unbiased'); % ACRS of x(n)
>> delta = 0.05; %2/(M*rxx(M))=0.1012;
>> [heq,ahatn] = lms(xn.',dn(D+1:end),delta,M);

```

- a. MATLAB script:

```

>> om = linspace(0,1,1001)*pi;
>> Heq = freqz(heq,1,om);
>> Heq_mag = abs(Heq); Heq_phd = angle(Heq)/pi;
>> Cz = freqz(Cb,1,om);
>> Cz_mag = abs(Cz); Cz_phd = angle(Cz)/pi;
>> CzHeq = Cz.*Heq;
>> CzHeq_mag = abs(CzHeq); CzHeq_phd = angle(CzHeq)/pi;

```

The resulting plots are shown in Figure 15.41. The magnitude response of the product filter is close to unity, with a small variation over the entire band due to excess noise characteristics of the LMS algorithm. Overall, the LMS equalizer provides an adequate performance.

- b. Comparison of Figure 15.9 for the LS method and Figure 15.41 shows that the two equalizer performances are similar over the entire band with LS equalizer showing a smoother frequency response. □

#### EXAMPLE 15.13 Use of LMS Algorithm in Echo Cancellation

Consider the echo cancellation system given in Example 15.3. Using the same system parameters as in Example 15.3, use the LMS algorithm to adapt the coefficients of the echo canceller by running the simulation for 1000 samples.

- a. Compare the coefficients of the echo canceller with the echo coefficients  $c(k)$ ,  $0 \leq k \leq 4$ , and comment on the results.
- b. Compare the results obtained with the LMS algorithm with the results obtained by use of the least-squares method used in Example 15.3.

#### Solution

From Example 15.3 the system parameters are.

```

>> c = [-0.25,-0.5,0.75,0.36,0.25]; % Echo coefficients>>
>> N = 1000; n = 0:N; % Length and timing indices
>> varW = 0.1; % Additive noise variance
>> an = 2*randi([0,1],N+1,1)-1; % Pseudorandom symbol sequence at Modem-A
>> bn = 2*randi([0,1],N+1,1)-1; % Pseudorandom symbol sequence at Modem-B

```

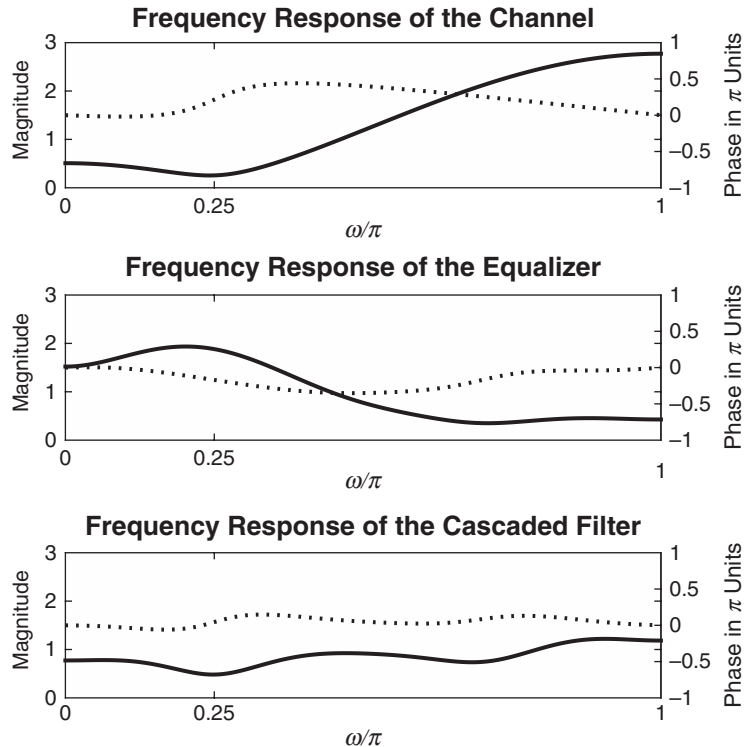


FIGURE 15.41 MATLAB plot in Example 15.12(a)

- a. The upper limit for the step size from (15.94) for this case is 0.2. However, good convergence and stability results for 1000 iterations were obtained using  $\Delta = 0.01$ .

```

>> sAn = filter(c,1,an); % Echo signal sequence at modem-A
>> wn = sqrt(varW)*randn(N+1,1); % Additive noise sequence
>> yn = bn + sAn + wn; % Received signal at Modem-A
>> M = 10; % FIR echo canceller order
>> [raa,lags] = xcorr(an,M-1,'unbiased'); % ACRS of a(n)
>> delta = 0.01; %2/(M*raa(M))=0.2;
>> [hec,Sahatn] = lms(an.',yn,delta,M);
>> hec(1:5)
hec =
-0.2988    -0.5861     0.7469     0.3010     0.2272

```

The resulting echo canceller coefficients are reasonable but noisy after 1000 iterations.

- b. The corresponding echo canceller coefficients using the LS method from Example 15.3 were

```
>> hec'
ans =
-0.2540 -0.4982 0.7943 0.3285 0.2291
```

which were closer to the original echo canceller coefficients. This shows again that the LMS algorithm does produce noisy yet usable results.  $\square$

$\square$  **EXAMPLE 15.14 Use of LMS Algorithm in Suppression of Narrowband Interference**

Consider the system configuration for the suppression of narrowband interference given in Example 15.4. Using the same system parameters as in Example 15.4, use the LMS algorithm to adapt the coefficients of the linear predictor by running the simulation for 1000 iterations.

- As in part (b) of Example 15.4, compute and plot the frequency response of the prediction-error filter and, thus, verify that this filter is a notch filter that suppresses the narrow band interference.
- Compare the results obtained with the LMS algorithm with the results obtained by use of the least-squares method used in Example 15.4.

**Solution**

The signals  $x(n)$  and  $v(n)$  are generated using

```
>> i = (0:100)'; fi = 0.1*i/100; thetai = 2*pi*rand(length(i),1);
>> A = 1; N = 1000; n = 0:N;
>> xn = sum(A*cos(2*pi*fi*n+thetai*ones(1,N+1))); xn = xn';
>> varW = 1; wn = sqrt(varW)*randn(N+1,1);
>> vn = xn+wn;
>> [rvv] = xcorr(vn,M-1+D,'unbiased');
```

The upper limit for the step size from (15.94) for this case using  $r_{vv}(0)$  is 0.0025. However, for the LMS algorithm the value of  $\Delta = 0.001$  was selected and coefficients of the predictor were computed after 1000 iterations.

```
>> M = 15; D = 1;
>> delta = 0.001; %2/(M*rvv(M))=0.0025;
>> [h,xhatn] = lms(vn(1:N-D)',vn(D:N),delta,M);
```

- a. The coefficients of the prediction-error filter and its frequency response were computed using the following MATLAB script.

```
>> h1 = zeros(M+D,1); h1(1) = 1;
>> h1(D+1:D+M) = -h;
>> f = linspace(0,1,1001)*0.5;
>> H1 = freqz(h1,1,2*pi*f);
>> H1db = 20*log10(abs(H1)/max(abs(H1)));
>> % Plotting commands follow
```

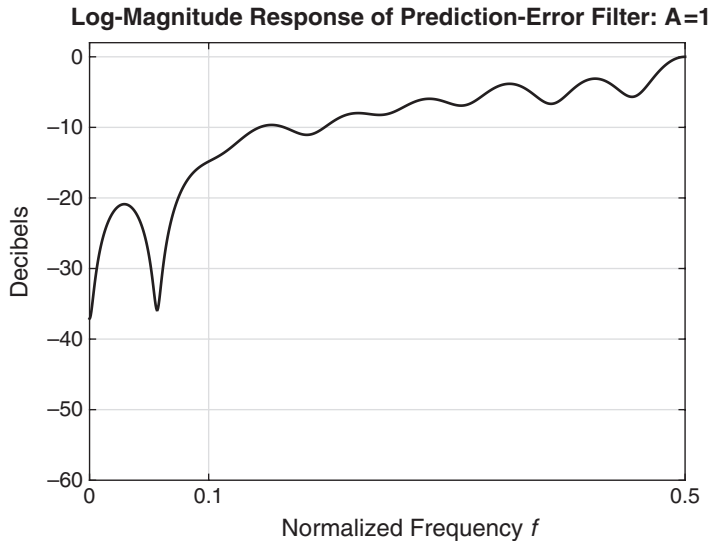


**FIGURE 15.42** Log-magnitude response of the prediction-error filter using the LMS algorithm in Example 15.14(a)

The resulting plot is shown in Figure 15.42. Although the filter creates a notch of more than 15 dB in the band of interfering signal, the passband has undesirable ripple. In this case, LMS algorithm seems to perform barely well.

- b. Comparing Figure 15.20 for the LS method with Figure 15.42 for the LMS algorithm it is clear that the LMS algorithm is effective in suppressing the narrowband interference, but its overall performance is not as good as that of the LS method.  $\square$

### Discussion

The preceding analysis of the excess MSE is based on the assumption that the mean values of the filter coefficients have converged to the optimum solution  $\mathbf{h}_{\text{opt}}$ . Under this condition, the step size  $\Delta$  should satisfy the bound in (15.94). On the other hand, we have determined that convergence of the mean coefficient vector requires that  $\Delta < 2/\lambda_{\max}$ . While a choice of  $\Delta$  near the upper bound  $2/\lambda_{\max}$  may lead to initial convergence of the deterministic (known) gradient algorithm, such a large value of  $\Delta$  will usually result in instability of the stochastic-gradient LMS algorithm.

The initial convergence or transient behavior of the LMS algorithm has been investigated by several researchers. Their results clearly indicate that the step size must be reduced in direct proportion to the length of the adaptive filter, as in (15.94). The upper bound given in (15.94) is necessary to ensure the initial convergence of the stochastic-gradient LMS algorithm. In practice, a choice of  $\Delta < 1/MR_{XX}(0)$  is usually made.

Gitlin and Weinstein [24] and Ungerboeck [93] contain an analysis of the transient behavior and the convergence properties of the LMS algorithm.

In a digital implementation of the LMS algorithm, the choice of the step-size parameter becomes even more critical. In an attempt to reduce the excess MSE, it is possible to reduce the step-size parameter to the point at which the total output MSE actually increases. This condition occurs when the estimated gradient components  $e(n)x^*(n - \ell)$ ,  $\ell = 0, 1, M - 1$ , after multiplication by the small step-size parameter  $\Delta$ , are smaller than one-half of the least significant bit in the fixed-point representation of the filter coefficients. In such a case, adaptation ceases. Consequently, it is important for the step size to be large enough to bring the filter coefficients in the vicinity of  $\mathbf{h}_{\text{opt}}$ . If it is desired to decrease the step size significantly, it is necessary to increase the precision in the filter coefficients. Typically, 16 bits of precision may be used for the filter coefficients, with the 12 most significant bits used for arithmetic operations in the filtering of the data. The 4 least significant bits are required to provide the necessary precision for the adaptation process. Thus the scaled, estimated gradient components  $\Delta e(n)x^*(n - \ell)$  usually affect only the least significant bits. In effect, the added precision also allows for the noise to be averaged out, since several incremental changes in the least significant bits are required before any change occurs in the upper, more significant bits used in arithmetic operations for filtering of the data. For an analysis of round-off errors in a digital implementation of the LMS algorithm, the reader is referred to Gitlin and Weinstein [24], Gitlin et al. [25], and Caraicos and Liu [4].

As a final point, we should indicate that the LMS algorithm is appropriate for tracking slowly time-variant signal statistics. In such a case, the minimum MSE and the optimum coefficient vector will be time-variant. In other words,  $\mathcal{E}_{M,\min}$  is a function of time, and the  $M$ -dimensional error surface is moving with the time index  $n$ . The LMS algorithm attempts to follow the moving minimum  $\mathcal{E}_{M,\min}$  in the  $M$ -dimensional space, but it is always lagging behind due to its use of (estimated) gradient vectors. As a consequence, the LMS algorithm incurs another form of error, called the *lag error*, whose mean-square value decreases with an increase in the step size  $\Delta$ . The total MSE can now be expressed as

$$\mathcal{E}_{\text{total}} = \mathcal{E}_{M,\min} + \mathcal{E}_\Delta + \mathcal{E}_l \quad (15.95)$$

where  $\mathcal{E}_l$  denotes the MSE due to the lag.

In any given nonstationary adaptive filtering problem, if we plot the  $\mathcal{E}_\Delta$  and  $\mathcal{E}_l$  as a function of  $\Delta$ , we expect these errors to behave as illustrated in Figure 15.43. We observe that  $\mathcal{E}_\Delta$  increases with an increase in  $\Delta$ , whereas  $\mathcal{E}_l$  decreases with an increase in  $\Delta$ . The total error will exhibit a minimum, which will determine the optimum choice of the step-size parameter.

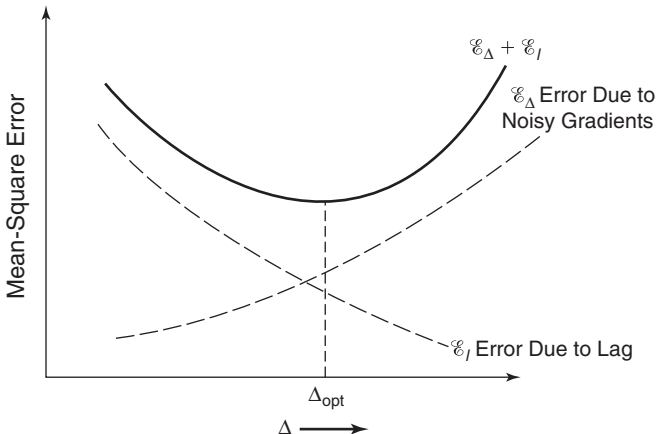


**FIGURE 15.43** Excess mean-square error  $\mathcal{E}_\Delta$  and lag error  $\mathcal{E}_l$  as a function of the step size  $\Delta$

When the statistical time variations of the signals occur rapidly, the lag error will dominate the performance of the adaptive filter. In such a case,  $\mathcal{E}_l \gg \mathcal{E}_{M\min} + \mathcal{E}_\Delta$ , even when the largest possible value of  $\Delta$  is used. When this condition occurs, the LMS algorithm is inappropriate for the application and one must rely on the more complex recursive least-squares algorithms described in Section 15.2.4 to obtain faster convergence and tracking.

#### 15.2.4 RECURSIVE LEAST-SQUARES ALGORITHMS FOR DIRECT-FORM FIR FILTERS

The major advantage of the LMS algorithm lies in its computational simplicity. However, the price paid for this simplicity is slow convergence, especially when the eigenvalues of the autocorrelation matrix  $\mathbf{T}_M$  have a large spread—that is, when  $\lambda_{\max}/\lambda_{\min} \gg 1$ . From another point of view, the LMS algorithm has only a single adjustable parameter for controlling the convergence rate—namely, the step-size parameter  $\Delta$ . Since  $\Delta$  is limited for purposes of stability to be less than the upper-bound in (15.94), the modes corresponding to the smaller eigenvalues converge very slowly.

To obtain faster convergence, it is necessary to devise more complex algorithms, which involve additional parameters. In particular, if the correlation matrix  $\mathbf{T}_M$  has unequal eigenvalues  $\lambda_0, \lambda_1, \dots, \lambda_{M-1}$ , we should use an algorithm that contains  $M$  parameters, one for each of the eigenvalues. In deriving more rapidly converging adaptive filtering algorithms, we adopt the least-squares criterion instead of the statistical approach based on the MSE criterion. Thus we deal directly with the data sequence  $x(n)$  and obtain estimates of correlations from the data.

It is convenient to express the least-squares algorithms in matrix form, in order to simplify the notation. Since the algorithms will be recursive in time, it is also necessary to introduce a time index in the filter-coefficient vector and in the error sequence. Hence we define the filter-coefficient vector at time  $n$  as

$$\mathbf{h}_M(n) = \begin{bmatrix} h(0, n) \\ h(1, n) \\ h(2, n) \\ \vdots \\ h(M-1, n) \end{bmatrix} \quad (15.96)$$

where the subscript  $M$  denotes the length of the filter. Similarly, the input signal vector to the filter at time  $n$  is denoted as

$$\mathbf{X}_M(n) = \begin{bmatrix} x(n) \\ x(n-1) \\ x(n-2) \\ \vdots \\ x(n-M+1) \end{bmatrix} \quad (15.97)$$

We assume that  $x(n) = 0$  for  $n < 0$ . This is usually called *prewindowing* of the input data.

The recursive least-squares problem may now be formulated as follows. Suppose that we have observed the vectors  $\mathbf{X}_M(\ell)$ ,  $\ell = 0, 1, \dots, n$ , and we wish to determine the filter-coefficient vector  $\mathbf{h}_M(n)$  that minimizes the weighted sum of magnitude-squared errors

$$\mathcal{E}_M = \sum_{\ell=0}^n w^{n-\ell} |e_M(\ell, n)|^2 \quad (15.98)$$

where the error is defined as the difference between the desired sequence  $d(\ell)$  and the estimate  $\hat{d}(\ell, n)$ ,

$$\begin{aligned} e_M(\ell, n) &= d(\ell) - \hat{d}(\ell, n) \\ &= d(\ell) - \mathbf{h}_M^t(n) \mathbf{X}_M(\ell) \end{aligned} \quad (15.99)$$

and  $w$  is a weighting factor in the range  $0 < w \leq 1$ .

The purpose of the factor  $w$  is to weight the most recent data points more heavily and, thus, allow the filter coefficients to adapt to time-varying statistical characteristics of the data. This is accomplished by using the exponential weighting factor with the past data. Alternatively, we may use a finite-duration sliding window with uniform weighting over

the window length. We find the exponential weighting factor more convenient, both mathematically and practically. For comparison, an exponentially weighted window sequence has an effective memory of

$$\bar{N} = \frac{\sum_{n=0}^{\infty} nw^n}{\sum_{n=0}^{\infty} w^n} = \frac{w}{1-w} \quad (15.100)$$

and, hence, should be approximately equivalent to a sliding window of length  $\bar{N}$ .

The minimization of  $\mathcal{E}_M$  with respect to the filter-coefficient vector  $\mathbf{h}_M(n)$  yields the set of linear equations

$$\mathbf{R}_M(n)\mathbf{h}_M(n) = \mathbf{D}_M(n) \quad (15.101)$$

where  $\mathbf{R}_M(n)$  is the signal (estimated) correlation matrix defined as

$$\mathbf{R}_M(n) = \sum_{\ell=0}^n w^{n-\ell} \mathbf{X}_M^*(\ell) \mathbf{X}_M^t(\ell) \quad (15.102)$$

and  $\mathbf{D}_M(n)$  is the (estimated) cross-correlation vector

$$\mathbf{D}_M(n) = \sum_{\ell=0}^n w^{n-\ell} \mathbf{X}_M^*(\ell) d(\ell) \quad (15.103)$$

The solution of (15.101) is

$$\mathbf{h}_M(n) = \mathbf{R}_M^{-1}(n) \mathbf{D}_M(n) \quad (15.104)$$

Clearly, the matrix  $\mathbf{R}_M(n)$  is akin to the statistical autocorrelation matrix  $\mathbf{T}_M$ , and the vector  $\mathbf{D}_M(n)$  is akin to the cross-correlation vector  $\mathbf{R}_d$ , defined previously. We emphasize, however, that  $\mathbf{R}_M(n)$  is not a Toeplitz matrix, whereas  $\mathbf{T}_M$  is. We should also mention that for small values of  $n$ ,  $\mathbf{R}_M(n)$  may be ill conditioned, so that its inverse is not computable. In such a case, it is customary to initially add the matrix  $\delta \mathbf{I}_M$  to  $\mathbf{R}_M(n)$ , where  $\mathbf{I}_M$  is an identity matrix and  $\delta$  is a small positive constant. With exponential weighting into the past, the effect of adding  $\delta \mathbf{I}_M$  dissipates with time.

Now, suppose that we have the solution of (15.104) at time  $(n-1)$ —that is, we have  $\mathbf{h}_M(n-1)$  and we wish to compute  $\mathbf{h}_M(n)$ . It is inefficient and, hence, impractical to solve the set of  $M$  linear equations for each new signal component. Instead, we may compute the matrix and vectors recursively. First,  $\mathbf{R}_M(n)$  may be computed recursively as

$$\mathbf{R}_M(n) = w \mathbf{R}_M(n-1) + \mathbf{X}_M^*(n) \mathbf{X}_M^t(n) \quad (15.105)$$

We call (15.105) the *time-update equation* for  $\mathbf{R}_M(n)$ .

Since the inverse of  $\mathbf{R}_M(n)$  is needed, we use the matrix inversion lemma (see Householder [32]),

$$\mathbf{R}_M^{-1}(n) = \frac{1}{w} \left[ \mathbf{R}_M^{-1}(n-1) - \frac{\mathbf{R}_M^{-1}(n-1) \mathbf{X}_M^*(n) \mathbf{X}_M^t(n) \mathbf{R}_M^{-1}(n-1)}{w + \mathbf{X}_M^t(n) \mathbf{R}_M^{-1}(n-1) \mathbf{X}_M^*(n)} \right] \quad (15.106)$$

Thus  $\mathbf{R}_M^{-1}(n)$  may be computed recursively.

For convenience, we define  $\mathbf{P}_M(n) = \mathbf{R}_M^{-1}(n)$ . It is also convenient to define an  $M$ -dimensional vector  $\mathbf{K}_M(n)$ , sometimes called the *Kalman gain vector*, as

$$\mathbf{K}_M(n) = \frac{1}{w + \mu_M(n)} \mathbf{P}_M(n-1) \mathbf{X}_M^*(n) \quad (15.107)$$

where  $\mu_M(n)$  is a scalar defined as

$$\mu_M(n) = \mathbf{X}_M^t(n) \mathbf{P}_M(n-1) \mathbf{X}_M^*(n) \quad (15.108)$$

With these definitions, (15.106) becomes

$$\mathbf{P}_M(n) = \frac{1}{w} \left[ \mathbf{P}_M(n-1) - \mathbf{K}_M(n) \mathbf{X}_M^t(n) \mathbf{P}_M(n-1) \right] \quad (15.109)$$

Let us postmultiply (15.109) by  $\mathbf{X}_M^*(n)$ . Then

$$\begin{aligned} \mathbf{P}_M(n) \mathbf{X}_M^*(n) &= \frac{1}{w} [\mathbf{P}_M(n-1) \mathbf{X}_M^*(n) - \mathbf{K}_M(n) \mathbf{X}_M^t(n) \mathbf{P}_M(n-1) \mathbf{X}_M^*(n)] \\ &= \frac{1}{w} \left\{ [w + \mu_M(n)] \mathbf{K}_M(n) - \mathbf{K}_M(n) \mu_M(n) \right\} = \mathbf{K}_M(n) \end{aligned} \quad (15.110)$$

Therefore, the Kalman gain vector may also be defined as  $\mathbf{P}_M(n) \mathbf{X}_M^*(n)$ .

Now we may use the matrix inversion lemma to derive an equation for computing the filter coefficients recursively. Since

$$\mathbf{h}_M(n) = \mathbf{P}_M(n) \mathbf{D}_M(n) \quad (15.111)$$

and

$$\mathbf{D}_M(n) = w \mathbf{D}_M(n-1) + d(n) \mathbf{X}_M^*(n) \quad (15.112)$$

we have, upon substitution of (15.109) and (15.112) into (15.104),

$$\begin{aligned} \mathbf{h}_M(n) &= \frac{1}{w} [\mathbf{P}_M(n-1) - \mathbf{K}_M(n) \mathbf{X}_M^t(n) \mathbf{P}_M(n-1)] \\ &\quad \times [w \mathbf{D}_M(n-1) + d(n) \mathbf{X}_M^*(n)] \\ &= \mathbf{P}_M(n-1) \mathbf{D}_M(n-1) + \frac{1}{w} d(n) \mathbf{P}_M(n-1) \mathbf{X}_M^*(n) \\ &\quad - \mathbf{K}_M(n) \mathbf{X}_M^t(n) \mathbf{P}_M(n-1) \mathbf{D}_M(n-1) \\ &\quad - \frac{1}{w} d(n) \mathbf{K}_M(n) \mathbf{X}_M^t(n) \mathbf{P}_M(n-1) \mathbf{X}_M^*(n) \\ &= \mathbf{h}_M(n-1) + \mathbf{K}_M(n) [d(n) - \mathbf{X}_M^t(n) \mathbf{h}_M(n-1)] \end{aligned} \quad (15.113)$$

We observe that  $\mathbf{X}_M^t(n)\mathbf{h}_M(n-1)$  is the output of the adaptive filter at time  $n$  based on use of the filter coefficients at time  $n-1$ . Since

$$\mathbf{X}_M^t(n)\mathbf{h}_M(n-1) = \hat{d}(n, n-1) \equiv \hat{d}(n) \quad (15.114)$$

and

$$e_M(n, n-1) = d(n) - \hat{d}(n, n-1) \equiv e_M(n) \quad (15.115)$$

it follows that the time-update equation for  $\mathbf{h}_M(n)$  may be expressed as

$$\mathbf{h}_M(n) = \mathbf{h}_M(n-1) + \mathbf{K}_M(n)e_M(n) \quad (15.116)$$

or equivalently,

$$\mathbf{h}_M(n) = \mathbf{h}_M(n-1) + \mathbf{P}_M(n)\mathbf{X}_M^*(n)e_M(n) \quad (15.117)$$

To summarize, suppose we have the optimum filter coefficients  $\mathbf{h}_M(n-1)$ , the matrix  $\mathbf{P}_M(n-1)$ , and the vector  $\mathbf{X}_M(n-1)$ . When the new signal component  $x(n)$  is obtained, we form the vector  $\mathbf{X}_M(n)$  by dropping the term  $x(n-M)$  from  $\mathbf{X}_M(n-1)$  and adding the term  $x(n)$  as the first element. Then the recursive computation for the filter coefficients proceeds as follows.

1. Compute the filter output:

$$\hat{d}(n) = \mathbf{X}_M^t(n)\mathbf{h}_M(n-1) \quad (15.118)$$

2. Compute the error:

$$e_M(n) = d(n) - \hat{d}(n) \quad (15.119)$$

3. Compute the Kalman gain vector:

$$\mathbf{K}_M(n) = \frac{\mathbf{P}_M(n-1)\mathbf{X}_M^*(n)}{w + \mathbf{X}_M^t(n)\mathbf{P}_M(n-1)\mathbf{X}_M^*(n)} \quad (15.120)$$

4. Update the inverse of the correlation matrix

$$\mathbf{P}_M(n) = \frac{1}{w}[\mathbf{P}_M(n-1) - \mathbf{K}_M(n)\mathbf{X}_M^t(n)\mathbf{P}_M(n-1)] \quad (15.121)$$

5. Update the coefficient vector of the filter

$$\mathbf{h}_M(n) = \mathbf{h}_M(n-1) + \mathbf{K}_M(n)e_M(n) \quad (15.122)$$

The recursive algorithm specified by (15.118) through (15.122) is called the direct form recursive least-squares (RLS) algorithm. It is initialized by setting  $\mathbf{h}_M(-1) = \mathbf{0}$  and  $\mathbf{P}_M(-1) = 1/\delta\mathbf{I}_M$ , where  $\delta$  is a small positive number.

The residual MSE resulting from the preceding optimization is

$$\mathcal{E}_{M,\min}(n) = \sum_{\ell=0}^n w^{n-\ell} |d(\ell)|^2 - \mathbf{h}_M^t(n) \mathbf{D}_M^*(n) \quad (15.123)$$

From (15.122), we observe that the filter coefficients vary with time by an amount equal to the error  $e_M(n)$  multiplied by the Kalman gain vector  $\mathbf{K}_M(n)$ . Since  $\mathbf{K}_M(n)$  is an  $M$ -dimensional vector, each filter coefficient is controlled by one of the elements of  $\mathbf{K}_M(n)$ . Consequently, rapid convergence is obtained. In contrast, the time-update equation for the coefficients of the filter adjusted by use of the LMS algorithm is

$$\mathbf{h}_M(n) = \mathbf{h}_M(n-1) + \Delta \mathbf{X}^*(n) e_M(n) \quad (15.124)$$

which has only the single parameter  $\Delta$  for controlling the adjustment rate of the coefficients.

**EXAMPLE 15.15 Comparison of Convergence Characteristics of LMS Algorithm with RLS Algorithm**

A major advantage of the direct form RLS algorithm over the LMS algorithm is their faster convergence rate. This characteristic behavior is illustrated in Figure 15.44, which shows the convergence rate of the LMS and direct form RLS algorithm for an adaptive FIR channel equalizer of length  $M = 11$ . The statistical autocorrelation matrix  $\mathbf{T}_M$  for the received signal has an eigenvalue ratio  $\lambda_{\max}/\lambda_{\min} = 11$ . All the equalizer coefficients were initially set to zero. The step size for the LMS algorithm was selected as  $\Delta = 0.02$ , which represents a good compromise between convergence rate and excess MSE.

The superiority of the RLS algorithm in achieving faster convergence is clearly evident. The algorithm converges in less than 70 iterations (70 signal samples), while the LMS algorithm has not converged in over 600 iterations.

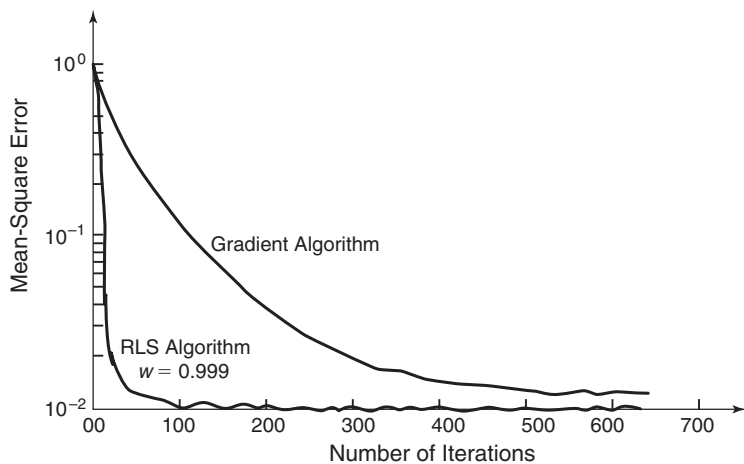


**FIGURE 15.44** Learning curves for RLS and LMS algorithms for adaptive equalizer of length  $M = 11$ . The eigenvalue spread of the channel is  $\lambda_{\max}/\lambda_{\min} = 11$ . The step size for the LMS algorithm is  $\Delta = 0.02$ .

This rapid rate of convergence of the RLS algorithm is extremely important in applications in which the signal statistics vary rapidly with time. For example, the time variations of the characteristics of an ionospheric high frequency (HF) radio channel are too rapid to be adaptively followed by the LMS algorithm. However, the RLS algorithm adapts sufficiently fast to track such rapid variations (Hsu [33]).  $\square$

**The LDU Factorization and Square-Root Algorithms.** The RLS algorithm is very susceptible to round-off noise in an implementation of the algorithm with finite-precision arithmetic. The major problem with round-off errors occurs in the updating of  $\mathbf{P}_M(n)$ . To remedy this problem, we may perform a decomposition of either the correlation matrix  $\mathbf{R}_M(n)$  or its inverse  $\mathbf{P}_M(n)$ . There are several possible decompositions that can be used to reduce the sensitivity to round-off errors. To be specific, let us consider an LDU decomposition of  $\mathbf{P}_M(n)$ . We may write

$$\mathbf{P}_M(n) = \mathbf{L}_M(n)\bar{\mathbf{D}}_M(n)\mathbf{L}_M^H(n) \quad (15.125)$$

where  $\mathbf{L}_M(n)$  is a lower-triangular matrix with elements  $l_{ik}$ ,  $\bar{\mathbf{D}}_M(n)$  is a diagonal matrix with elements  $\delta_k$ , and  $\mathbf{L}_M^H(n)$  is an upper-triangular matrix. The diagonal elements of  $\mathbf{L}_M(n)$  are set to unity (i.e.,  $l_{ii} = 1$ ). Now, instead of computing  $\mathbf{P}_M(n)$  recursively, we can determine a formula for updating the factors  $\mathbf{L}_M(n)$  and  $\bar{\mathbf{D}}_M(n)$  directly, thus avoiding the computation of  $\mathbf{P}_M(n)$ .

The desired update formula is obtained by substituting the factored form of  $\mathbf{P}_M(n)$  into (15.121) and using (15.107). Thus we have

$$\begin{aligned} & \mathbf{L}_M(n)\bar{\mathbf{D}}_M(n)\mathbf{L}_M^H(n) \\ &= \frac{1}{w}\mathbf{L}_M(n-1)\left[\bar{\mathbf{D}}_M(n-1) - \frac{1}{w+\mu_M(n)}\mathbf{V}_M(n-1)\mathbf{V}_M^H(n-1)\right]\mathbf{L}_M^H(n-1) \end{aligned} \quad (15.126)$$

where, by definition,

$$\mathbf{V}_M(n-1) = \bar{\mathbf{D}}_M(n-1)\mathbf{L}_M^H(n-1)\mathbf{X}_M^*(n) \quad (15.127)$$

The term inside the brackets in (15.126) is a Hermitian matrix and may be expressed in an LDU factored form as

$$\begin{aligned} & \hat{\mathbf{L}}_M(n-1)\hat{\mathbf{D}}_M(n-1)\hat{\mathbf{L}}_M^H(n-1) \\ &= \bar{\mathbf{D}}_M(n-1) - \frac{1}{w+\mu_M(n)}\mathbf{V}_M(n-1)\mathbf{V}_M^H(n-1) \end{aligned} \quad (15.128)$$

Then, if we substitute (15.128) into (15.126), we obtain

$$\begin{aligned} & \mathbf{L}_M(n)\bar{\mathbf{D}}_M(n)\hat{\mathbf{L}}_M^H(n) \\ &= \frac{1}{w}[\mathbf{L}_M(n-1)\hat{\mathbf{L}}_M(n-1)\hat{\mathbf{D}}_M(n-1)\hat{\mathbf{L}}_M^H(n-1)\mathbf{L}_M^H(n-1)] \end{aligned} \quad (15.129)$$

Consequently, the desired update relations are

$$\begin{aligned}\mathbf{L}_M(n) &= \mathbf{L}_M(n-1)\hat{\mathbf{L}}_M(n-1) \\ \bar{\mathbf{D}}_M(n) &= \frac{1}{w}\hat{\mathbf{D}}_M(n-1)\end{aligned}\quad (15.130)$$

The resulting algorithm, obtained from the time-update equations in (15.130), depends directly on the data vector  $\mathbf{X}_M(n)$  and not on the “square” of the data vector. Thus the squaring operation of the data vector is avoided, and, consequently, the effect of round-off errors is significantly reduced.

The RLS algorithms obtained from an LDU decomposition of either  $\mathbf{R}_M(n)$  or  $\mathbf{P}_M(n)$  are called *square-root RLS algorithms*. Bierman [2], Carlson and Culmone [5], and Hsu [33] treat these types of algorithms. A square-root RLS algorithm based on the LDU decomposition of  $\mathbf{P}_M(n)$ , as just described, is given in Table 15.1. Its computational complexity is proportional to  $M^2$ .

**TABLE 15.1** LDU form of square-root RLS algorithm

---

```

for  $j = 1, \dots, 2, \dots, M$  do
     $f_j = x_j^*(n)$ 
end loop  $j$ 

for  $j = 1, 2, \dots, M-1$  do
    for  $i = j+1, j+2, \dots, M$  do
         $f_j = f_j + l_{ij}(n-1)f_i$ 
    end loop  $j$ 

for  $j = 1, 2, \dots, M$  do
     $\bar{d}_j(n) = d_j(n-1)/w$ 
     $v_j = \bar{d}_j(n)f_i$ 
end loop  $j$ 

 $\alpha_M = 1 + v_M f_M^*$ 
 $d_M(n) = \bar{d}_M(n)/\alpha_M$ 
 $k_M = v_M$ 

for  $j = M-1, M-2, \dots, 1$  do
     $\bar{k}_j = v_j$ 
     $\alpha_j = \alpha_{j+1} + v_j f_j^*$ 
     $\lambda_j = f_j/\alpha_{j+1}$ 
     $d_j(n) = \bar{d}_j(n)\alpha_{j+1}/\alpha_1$ 
    for  $i = M, M-1, \dots, j+1$  do
         $l_{ij}(n) = l_{ij}(n-1) + \bar{k}_i^* \lambda_j$ 
         $\bar{k}_i = \bar{k}_i + v_j l_{ij}^*(n-1)$  down to  $j=2$ )
    end loop  $i$ 
end loop  $j$ 

 $\bar{\mathbf{K}}_M(n) = [\bar{k}_1, \bar{k}_2, \dots, \bar{k}_M]^t$ 
 $e_M(n) = d(n) - \bar{d}(n)$ 
 $\mathbf{h}_M(n) = \mathbf{h}_M(n-1) + [e_M(n)/\alpha_1]\bar{\mathbf{K}}_M(n)$ 

```

---

## 15.3 SUMMARY AND REFERENCES

---

We have presented adaptive algorithms for direct form FIR filter structures. The algorithms for the direct form FIR filter consisted of the simple LMS algorithm due to Widrow and Hoff [95] and the direct form, time-recursive least-squares algorithms, including the conventional RLS form given by (15.118–15.122), and the square-root RLS forms described by Bierman [2], Carlson and Culmone [5], and Hsu [33].

Of these algorithms, the LMS algorithm is the simplest. It is used in many applications where its slow convergence is adequate. Of the direct form RLS algorithms, the square-root algorithms have been used in applications where fast convergence is required. The algorithms have good numerical properties.

In the direct form RLS algorithms, we used exponential weighting into the past in order to reduce the effective memory in the adaptation process. As an alternative to exponential weighting, we may employ finite-length uniform weighing into the past. This approach leads to the class of finite-memory RLS direct form algorithms described in Cioffi and Kalaith [7] and Manolakis, Ling, and Proakis [62].

## BIBLIOGRAPHY

- [1] F. S. Beckman. "The Solution of Linear Equations by the Conjugate Gradient Method," in *Mathematical Methods for Digital Computers*, A. Ralston and H. S. Wilf, eds., Wiley, New York, 1960.
- [2] G. J. Bierman. *Factorization Methods for Discrete Sequential Estimation*, Academic Press, New York, 1977.
- [3] R. C. Brown. *Introduction to Random Signal Analysis and Kalman Filtering*, Wiley, New York, 1983.
- [4] C. Caraiscos and B. Liu. "A Roundoff Error Analysis of the LMS Adaptive Algorithm," *IEEE Trans. Acoustics, Speech, and Signal Processing*, vol. ASSP-32, pp. 34–41, January 1984.
- [5] N. A. Carlson and A. F. Culmone. "Efficient Algorithms for On-Board Array Processing," *Record 1979 International Conference on Communications*, pp. 58.1.1–58.1.5, Boston, June 10–14, 1979.
- [6] C. K. Chui and G. Chen. *Kalman Filtering*, Springer-Verlag, New York, 1987.
- [7] J. M. Cioffi and T. Kailath. "Windowed Fast Transversal Filters Adaptive Algorithms with Normalization," *IEEE Trans. Acoustics, Speech, and Signal Processing*, vol. ASSP-33, pp. 607–625, June 1985.
- [8] J. W. Cooley and J. W. Tukey. "An Algorithm for the Machine Computation of Complex Fourier Series," *Mathematical Computations*, vol. 19, pp. 297–301, April 1965.
- [9] R. E. Crochiere and L. R. Rabiner. *Multirate Digital Signal Processing*, Prentice Hall, Englewood Cliffs, NJ, 1983.
- [10] C. de Boor. *A Practical Guide to Splines*, Springer-Verlag, New York, 1978.
- [11] J. R. Deller, J. H. L. Hansen, and J. G. Proakis. *Discrete-Time Processing of Speech Signals*, Wiley-IEEE Press, 2000.
- [12] P. Delsarte and Y. Genin. "The Split Levinson Algorithm," *IEEE Trans. Acoustics, Speech, and Signal Processing*, vol. ASSP-34, pp. 470–478, June 1986.
- [13] P. Delsarte, Y. Genin, and Y. Kamp. "Orthogonal Polynomial Matrices on the Unit Circle," *IEEE Trans. Circuits and Systems*, vol. CAS-25, pp. 149–160, January 1978.
- [14] J. Durbin. "Efficient Estimation of Parameters in Moving-Average Models," *Biometrika*, vol. 46, pp. 306–316, 1959.
- [15] J. L. Flanagan et al. "Speech Coding," *IEEE Transactions on Communications*, vol. COM-27, pp. 710–736, April 1979.
- [16] R. Fletcher and M. J. D. Powell. "A Rapidly Convergent Descent Method for Minimization," *Comput. J.*, vol. 6, pp. 163–168, 1963.
- [17] B. Friedlander. "Lattice Filters for Adaptive Processing," *Proc. IEEE*, vol. 70, pp. 829–867, August 1982.
- [18] B. Friedlander. "Lattice Methods for Spectral Estimation," *Proc. IEEE*, vol. 70, pp. 990–1017, September 1982.
- [19] F. R. Gantmacher. *The Theory of Matrices*, vol. I, Chelsea Publishing Company, Chelsea, NY, 1960.
- [20] W. A. Gardner. "Learning Characteristics of Stochastic-Gradient-Descent Algorithms: A General Study, Analysis and Critique," *Signal Processing*, vol. 6, pp. 113–133, April 1984.
- [21] D. A. George, R. R. Bowen, and J. R. Storey. "An Adaptive Decision-Feedback Equalizer," *IEEE Trans. Communication Technology*, vol. COM-19, pp. 281–293, June 1971.
- [22] L. Y. Geromimus. *Orthogonal Polynomials* (in Russian) (English translation by Consultant's Bureau, New York, 1961), 1958.
- [23] A. Gershho. "Adaptive Equalization of Highly Dispersive Channels for Data Transmission," *Bell Syst. Tech. J.*, vol. 48, pp. 55–70, January 1969.

- [24] R. D. Gitlin and S. B. Weinstein. "On the Required Tap-Weight Precision for Digitally Implemented Mean-Squared Equalizers," *Bell Syst. Tech. J.*, vol. 58, pp. 301–321, February 1979.
- [25] R. D. Gitlin, H. C. Meadors, and S. B. Weinstein. "The Tap-Leakage Algorithm: An Algorithm for the Stable Operation of a Digitally Implemented Fractionally Spaced, Adaptive Equalizer," *Bell Syst. Tech. J.*, vol. 61, pp. 1817–1839, October 1982.
- [26] I. Gohberg, ed. *I. Schür Methods in Operator Theory and Signal Processing*, Birkhauser Verlag, Stuttgart, Germany, 1986.
- [27] J. A. Greefies. "A Digitally Companded Delta Modulation Modem for Speech Transmission," In *Proceedings of IEEE International Conference on Communications*, pp. 7.33–7.48, June 1970.
- [28] O. Grenander and G. Szegö. *Toeplitz Forms and Their Applications*, University of California Press, Berkeley, CA, 1958.
- [29] D. Hanselman and B. Littlefield. *Mastering MATLAB 7*, Pearson/Prentice Hall, Englewood Cliffs, NJ, 2005.
- [30] S. Haykin. *Adaptive Filter Theory*, 3rd ed., Prentice-Hall, Englewood Cliffs, NJ, 1996.
- [31] A. S. Householder. "Unitary Triangularization of a Non-Symmetric Matrix," *J. Assoc. Comput. Math.*, vol. 5, pp. 204–243, 1958.
- [32] A. S. Householder. *The Theory of Matrices in Numerical Analysis*, Blaisdell, Waltham, MA, 1964.
- [33] F. M. Hsu. "Square-Root Kalman Filtering for High-Speed Data Received over Fading Dispersive HF Channels." *IEEE Trans. Information Theory*, vol. IT-28, pp. 753–763, September 1982.
- [34] F. M. Hsu and A. A. Giordano. "Digital Whitening Techniques for Improving Spread Spectrum Communications Performance in the Presence of Narrowband Jamming and Interference," *IEEE Trans. Communications*, vol. COM-26, pp. 209–216, February 1978.
- [35] B. R. Hunt, R. L. Lipsman, J. M. Rosenberg, and Kevin R. Coombes. *A Guide to MATLAB: For Beginners and Experienced Users*, Cambridge University Press, New York, NY, 2001.
- [36] V. K. Ingle and J. G. Proakis. *Digital Signal Processing using the ADSP-2101*, Prentice Hall, Englewood Cliffs, NJ, 1991.
- [37] L. B. Jackson. "An Analysis of Limit Cycles Due to Multiplicative Rounding in Recursive Digital Filters," *Proceedings of the 7th Allerton Conference on Circuits and System Theory*, pp. 69–78, 1969.
- [38] N. S. Jayant. "Adaptive Delta Modulation with One-Bit Memory," *Bell System Technical Journal*, pp. 321–342, March 1970.
- [39] N. S. Jayant. "Digital Coding of Speech Waveforms: PCM, DPCM, and DM Quantizers." *Proceedings of the IEEE*, vol. 62, pp. 611–632, May 1974.
- [40] S. K. Jones, R. K. Cavin, and W. M. Reed. "Analysis of Error-Gradient Adaptive Linear Equalizers for a Class of Stationary-Dependent Processes," *IEEE Trans. Information Theory*, vol. IT-28, pp. 318–329, March 1982.
- [41] T. Kailath. "A View of Three Decades of Linear Filter Theory," *IEEE Trans. Information Theory*, vol. IT-20, pp. 146–181, March 1974.
- [42] T. Kailath. *Lectures on Wiener and Kalman Filtering*, Springer-Verlag, New York, 1981.
- [43] T. Kailath. "Linear Estimation for Stationary and Near-Stationary Processes," in *Modern Signal Processing*, T. Kailath, ed., Hemisphere Publishing Corp., Washington, D.C., 1985.
- [44] T. Kailath. "A Theorem of I. Schür and Its Impact on Modern Signal Processing," in [26].
- [45] T. Kailath, A. C. G. Vieira, and M. Morf. "Inverses of Toeplitz Operators, Innovations, and Orthogonal Polynomials," *SIAM Rev.*, vol. 20, pp. 1006–1019, 1978.
- [46] R. E. Kalman. "A New Approach to Linear Filtering and Prediction Problems,"

- Trans. ASME, J. Basic Eng.*, vol. 82D, pp. 35–45, March 1960.
- [47] R. E. Kalman and R. S. Bucy. “New Results in Linear Filtering Theory,” *Trans. ASME, J. Basic Eng.*, vol. 83, pp. 95–108, 1961.
- [48] S. M. Kay. *Modern Spectral Estimation*, Prentice-Hall, Englewood Cliffs, NJ, 1988.
- [49] S. M. Kay and S. L. Marple, Jr. “Spectrum Analysis: A Modern Perspective,” *Proc. IEEE*, vol. 69, pp. 1380–1419, November 1981.
- [50] J. W. Ketchum and J. G. Proakis. “Adaptive Algorithms for Estimating and Suppressing Narrow-Band Interference in PN Spread-Spectrum Systems,” *IEEE Trans. Communications*, vol. COM-30, pp. 913–923, May 1982.
- [51] H. Krishna. “New Split Levinson, Schür, and Lattice Algorithms or Digital Signal Processing,” *Proc. 1988 International Conference on Acoustics, Speech, and Signal Processing*, pp. 1640–1642, New York, April 1988.
- [52] S. Y. Kung and Y. H. Hu. “A Highly Concurrent Algorithm and Pipelined Architecture for Solving Toeplitz Systems,” *IEEE Trans. Acoustics, Speech, and Signal Processing*, vol. ASSP-31, pp. 66–76, January 1983.
- [53] A. Leon-Garcia. *Probability, Statistics, and Random Processes for Electrical Engineering*, Pearson Prentice Hall, Upper Saddle River, NJ, third edition, 2008.
- [54] N. Levinson. “The Wiener RMS Error Criterion in Filter Design and Prediction,” *J. Math. Phys.*, vol. 25, pp. 261–278, 1947.
- [55] R. W. Lucky. “Automatic Equalization for Digital Communications,” *Bell Syst. Tech. J.*, vol. 44, pp. 547–588, April 1965.
- [56] F. R. Magee and J. G. Proakis. “Adaptive Maximum-Likelihood Sequence Estimation for Digital Signaling in the Presence of Intersymbol Interference,” *IEEE Trans. Information Theory*, vol. IT-19, pp. 120–124, January 1973.
- [57] J. Makhoul. “Linear-Prediction: A Tutorial Review,” *Proc. IEEE*, vol. 63, pp. 561–580, April 1975.
- [58] J. Makhoul. “Stable and Efficient Lattice Methods for Linear Prediction,” *IEEE Trans. Acoustics, Speech, and Signal Processing*, vol. ASSP-25, pp. 423–428, 1977.
- [59] J. Makhoul. “A Class of All-Zero Lattice Digital Filters: Properties and Applications.” *IEEE Trans. Acoustics, Speech, and Signal Processing*, vol. ASSP-26, pp. 304–314, August 1978.
- [60] D. G. Manolakis and V. K. Ingle. *Applied Digital Signal Processing*, Cambridge University Press, Cambridge, UK, 2011.
- [61] D. G. Manolakis, V. K. Ingle, and S. M. Kogon. *Statistical and Adaptive Signal Processing*, Artech House, Norwood, MA, 2005.
- [62] D. G. Manolakis, F. Ling, and J. G. Proakis. “Efficient Time-Recursive Least-Squares Algorithms for Finite-Memory Adaptive Filtering,” *IEEE Trans. Circuits and Systems*, vol. CAS-34, pp. 400–408, April 1987.
- [63] J. D. Markel and A. H., Gray, Jr. *Linear Prediction of Speech*, Springer-Verlag, New York, 1976.
- [64] S. L. Marple, Jr. *Digital Spectral Analysis with Applications*, Prentice-Hall, Englewood Cliffs, NJ, 1987.
- [65] J. E. Mazo. “On the Independence Theory of Equalizer Convergence,” *Bell Syst. Tech. J.*, vol. 58, pp. 963–993, May 1979.
- [66] J. E. Meditch. *Stochastic Optimal Linear Estimation and Control*, McGraw-Hill, New York, 1969.
- [67] S. L. Miller and D. G. Childers. *Probability and Random Processes*, Academic Press, Burlington, MA, second edition, 2012.
- [68] S. K. Mitra. *Digital Signal Processing: A Computer-Based Approach*, McGraw-Hill, New York, NY, fourth edition, 2010.
- [69] W. Murray, ed. *Numerical Methods of Unconstrained Minimization*, Academic Press, New York, 1972.
- [70] H. E. Nichols, A. A. Giordano, and J. G. Proakis. “MLD and MSE Algorithms

- for Adaptive Detection of Digital Signals in the Presence of Interchannel Interference,” *IEEE Trans. Information Theory*, vol. IT-23, pp. 563–575, September 1977.
- [71] A. V. Oppenheim and R. W. Schafer. *Discrete-Time Signal Processing*, Prentice Hall, Englewood Cliffs, NJ, third edition, 2010.
- [72] S. J. Orfanidis. *Introduction to Signal Processing*, Prentice Hall, Englewood Cliffs, NJ, 1996, pp. 367–383.
- [73] A. Papoulis and S. U. Pillai. *Probability, Random Variables, and Stochastic Processes*, McGraw-Hill, New York, NY, fourth edition, 2002.
- [74] T. W. Parks and J. H. McClellan. “A Program for the Design of Linear-Phase Finite Impulse Response Digital Filters,” *IEEE Transactions on Audio and Electroacoustics*, vol. AU-20, pp. 195–199, August 1972.
- [75] B. Picinbono. “Adaptive Signal Processing for Detection and Communication,” in *Communication Systems and Random Process Theory*, J. K. Skwirzynski, ed., Sijthoff en Noordhoff, Alphen aan den Rijn, The Netherlands, 1978.
- [76] R. Pratap. *Getting Started with MATLAB7: A Quick Introduction for Scientists and Engineers*, Oxford University Press, USA, 2005.
- [77] J. G. Proakis. “Adaptive Digital Filters for Equalization of Telephone Channels,” *IEEE Trans. Audio and Electroacoustics*, vol. AU-18, pp. 195–200, June 1970.
- [78] J. G. Proakis. “Advances in Equalization for Intersymbol Interference,” in *Advances in Communication Systems*, vol. 4, A. J. Viterbi, ed., Academic Press, New York, 1975.
- [79] J. G. Proakis and D. G. Manolakis. *Digital Signal Processing: Principles, Algorithms and Applications*, Prentice Hall, Upper Saddle River, NJ, third edition, 1996.
- [80] J. G. Proakis and J. H. Miller. “Adaptive Receiver for Digital Signaling through Channels with Intersymbol Interference,” *IEEE Trans. Information Theory*, vol. IT-15, pp. 484–497, July 1969.
- [81] J. G. Proakis and M. Salehi. *Digital Communications*, McGraw-Hill, New York, NY, fifth edition, 2008.
- [82] J. G. Proakis and M. Salehi. *Communication Systems Engineering*, Prentice Hall, Upper Saddle River, NJ, second edition, 2012.
- [83] L. R. Rabiner and B. Gold. *Theory and Applications in Digital Signal Processing*, Prentice Hall, Englewood Cliffs, NJ, 1975.
- [84] L. R. Rabiner and R. W. Schafer. *Digital Processing of Speech Signals*, Prentice Hall, Englewood Cliffs, NJ, 1978.
- [85] L. R. Rabiner, R. W. Schafer, and C. A. McGonegal. “An Approach to the Approximation Problem for Nonrecursive Digital Filters,” *IEEE Transactions on Audio and Electroacoustics*, vol. AU-18, pp. 83–106, June 1970.
- [86] E. A. Robinson and S. Treitel. “Digital Signal Processing in Geophysics,” in *Applications of Digital Signal Processing*, A. V. Oppenheim, ed., Prentice-Hall, Englewood Cliffs, NJ, 1978.
- [87] E. A. Robinson and S. Treitel. *Geophysical Signal Analysis*, Prentice-Hall, Englewood Cliffs, NJ, 1980.
- [88] Schur. “On Power Series Which Are Bounded in the Interior of the Unit Circle,” (in German) *J. Reine Angew. Math.*, vol. 147, pp. 205–232, Berlin, 1917. (For an English translation of this paper, see [26]).
- [89] M. Schetzen and V. K. Ingle. *Discrete Systems Laboratory Using MATLAB*, Brooks/Cole, Pacific Grove, CA, 2000.
- [90] H. Stark and J. W. Woods. *Probability, Random Processes, and Estimation Theory for Engineers*, Prentice Hall, Upper Saddle River, NJ, fourth edition, 2012.
- [91] G. Szegő. *Orthogonal Polynomials*, 3rd ed., Colloquium Publishers, no. 23, American Mathematical Society, Providence, RI, 1967.

- [92] S. A. Tretter. *Introduction to Discrete-Time Signal Processing*, Wiley, New York, 1976.
- [93] G. Ungerboeck. "Theory on the Speed of Convergence in Adaptive Equalizers for Digital Communication," *IBM J. Res. Devel.*, vol. 16, pp. 546–555, November 1972.
- [94] A. C. G. Vieira. "Matrix Orthogonal Polynomials with Applications to Autoregressive Modeling and Ladder Forms," Ph.D. dissertation, Department of Electrical Engineering, Stanford University, Stanford, Calif., December 1977.
- [95] B. Widrow and M. E. Hoff, Jr. "Adaptive Switching Circuits," *IRE WESCON Conv. Rec.*, pt. 4, pp. 96–104, 1960.
- [96] B. Widrow et al. "Adaptive Noise Cancelling Principles and Applications," *Proc. IEEE*, vol. 63, pp. 1692–1716, December 1975.
- [97] B. Widrow, P. Mantey, and L. J. Griffiths. "Adaptive Antenna Systems," *Proc. IEEE*, vol. 55, pp. 2143–2159, December 1967.
- [98] N. Wiener. *Extrapolation, Interpolation and Smoothing of Stationary Time Series with Engineering Applications*, Wiley, New York, 1949.
- [99] R. D. Yates and D. J. Goodman. *Probability and Stochastic Processes*, John Wiley & Sons, Hoboken, NJ, 2005.
- [100] D. Youla and N. Kazanjian. "Bauer-Type Factorization of Positive Matrices and the Theory of Matrices Orthogonal on the Unit Circle," *IEEE Trans. Circuits and Systems*, vol. CAS-25, pp. 57–69, January 1978.

# INDEX

NOTE: Italicized page references are located in the online text.

' operator, 25  
& operator, 26  
(:) construct, 24  
\* operator, 27  
. \* operator, 10, 26  
. ^ operator, 10, 24  
+ operator, 26  
<= operator, 26  
== operator, 26

## A

Absolute specifications, FIR filter design, 292–293  
Adaptive delta modulation (ADM), 599–600, 601  
Adaptive differential PCM (ADPCM), 586  
Adaptive direct-form FIR filters, 815–848  
    least-mean-square (LMS) algorithm, 820–824  
    MATLAB implementation of, 823–824  
    MATLAB scripts, 838  
    minimum mean-square-error criterion, 816–820  
    properties of the LMS algorithm, 824–841  
    recursive least-squares algorithms, 841–848  
Adaptive equalizers, 573  
Adaptive filters, 573–585, 769–849  
    applications of, 769–815  
    arrays, 813–815  
    channel equalization, 582–585, 776–782  
    coefficient adjustment, 575–578  
    echo cancellation, 783–788  
    least-mean-square (LMS) algorithm, 575, 815  
    line enhancement, 582, 795–801  
    MATLAB implementation, 577–578  
    MATLAB scripts, 774, 781–782, 788, 797, 798, 799, 801, 804, 805, 806, 811–813  
    narrowband interference, suppression of, 579–582, 788–795  
    noise canceling, 801–807  
    sinusoidal interference, suppression of, 581–582  
    speech signals, linear predictive coding of, 807–813  
    system identification (modeling), 578–579, 771–776  
    wideband signals, 579–582, 788–795  
Adaptive line enhancer (ALE), 795–801  
Adaptive PCM and DPCM (ADPCM), 593–597  
Adders, 213

Addition, signal operation, 25  
Adjustable coefficients, 573  
A/D quantization noise, 518–530. *See also*  
    Quantization  
        statistics of, 525  
        through digital filters, 527–530  
`afd_butt` function, 392  
`afd_chb1` function, 398  
`afd_elip` function, 405  
Aliasing formula, 81  
Allpass filters, 381–382  
Allpass function, 506  
All-pole systems, estimation of poles in, 811–813  
`alpha` function, 483  
Amplitude response, 298  
`ampl-res` function, 303  
Analog filter design (AFD) tables, 370  
Analog filters  
    Butterworth lowpass, 371, 385–390  
    Chebyshev lowpass, 371, 394–403  
    design equations, 390–391  
    elliptic lowpass, 403–406  
    frequency response, 298–301  
    IIR filter design, 370–457  
    MATLAB implementation, 387–390, 392–394, 396–403, 427–432  
    phase responses, 75–77  
    prototype responses, 385–407  
Analog signals, 3–5, 80–97  
    aliasing formula, 81  
    band-limited, 82  
    cubic spine interpolation, 92  
    digital signal processing (DSP) compared to, 1–2  
    digital-to-analog (D/A) converters, 80–81  
    discrete-time Fourier analysis of, 59–102  
    first-order-hold (FOH) interpolation, 91–92, 94  
    impulse train conversion, 87  
    interpolation, 90–94  
    MATLAB implementation, 84–87, 92–97  
    reconstruction of, 87–92  
    sampling, 81–84  
    signal processing (ASP), 3–5  
    sinusoidal, 75  
    zero-order-hold (ZOH) interpolation, 90–91, 94  
Analog-to-digital conversion (ADC), 80  
    analysis of A/D quantization noise, 518–530

Analog-to-digital transformations, 407–427  
 bilinear transformations, 418–426  
 Butterworth lowpass filters, 371, 385–390  
 Chebyshev lowpass filters, 371, 394–403  
 design procedure, 390–391  
 elliptic lowpass filters, 403–406  
 impulse invariance transformations, 408–418  
 matched- $z$  transformation, 426–427  
**Analysis**  
 error, 182–183  
 of excess noise, 829–832  
**Analyzers**, spectrum, 291  
**angle** function, 63  
**Anticausal sequence**, 106  
**Antisymmetric impulse response**, 230  
**Applications of adaptive filters**, 769–815  
 arrays, 813–815  
 channel equalization, 776–782  
 echo cancellation, 783–788  
 line enhancement, 795–801  
 MATLAB scripts, 774, 781–782, 788, 797, 798, 799, 801, 804, 805, 806, 811–813  
 narrowband interference, suppression of, 788–795  
 noise canceling, 801–807  
 speech signals, linear predictive coding of, 807–813  
 system identification (modeling), 771–776  
 wideband signals, 788–795  
**Approximate transition bandwidth**, 312  
**Approximation error**, 331  
**Approximation theory**, 349  
**Arrays**, adaptive, 813–815  
**Attenuation parameter A**, 372  
**Auto-correlation**, 647  
 power spectral density (PSD), 653–654  
 sequences, relationships, 695–700  
**Automatic gain control (AGC)**, 779  
**Autoregressive (AR) lattice structure**, 734–736  
**Autoregressive moving average (ARMA) filter**, 212  
 lattice-ladder filters, 737–743  
**Autoregressive moving average (ARMA) process**, 692–695  
**Autoregressive (AR) process**, 692  
**Average linear relationships**, 635, 636  
**Average power**, 647  
**Averages**  
 joint statistical, 634–637  
 statistical, 618–619

**B**

Backward prediction-error filter, 732  
**Band-edge frequencies**, 294  
**Band-limited signals**, 82  
 reconstruction of, 89  
 sampling, 83  
**Bandpass filters**, 339, 441  
**Bandpass process**, 679–684  
**Bandstop filters**, 441  
**Bartlett window**, 314–315  
**Bayes rules**, 630  
**beta** function, 330  
**Biased format**, 247–248  
**Bilateral  $z$ -transform**, 103–107  
**bilinear** function, 419, 420  
**Bilinear transformations**, 408, 418–426  
**bin2dec** function, 242  
**Binary digital communications**, 609–610  
**Binary digits (bits)**, 240  
**Binary numbers**, 252–253  
**Binary point**, 248  
**Binary spread-spectrum communications**, 612–613  
**Biquads**, 214  
**bitcmp** function, 243, 245  
**Bivariate Gaussian distribution**, 637–641  
**Blackman window**, 317  
**Block convolutions**, 183–185  
 high-speed, 199  
 overlap-add method, 186  
**Bounded-input bounded-output (BIBO) stability**, 40  
**Butterworth lowpass filters**, 371, 385–390  
 bilinear transformation, 408, 418–426  
 design equations, 390–391  
 frequency-based transformation, 432–435  
 impulse invariance transformation, 408–418  
 MATLAB implementation, 387–390, 392–394  
**buttord** function, 441

**C**

**Cancellation**  
 echo, 783–788, 836–838  
 noise, 801–807  
**cas2dir** function, 219, 230  
**Cascade form**, 214, 216–217, 562–564  
 finite-duration impulse response (FIR) filters, 228, 229–230  
 infinite-duration impulse response (IIR) filters, 214  
**casfiltr** function, 218, 565

- Causal filters, 373  
Causality, 40  
linear time-invariant (LTI) system, 40  
*z*-transform, 125–128  
CCITT standard, 595  
Ceiling function, 197  
Central moments, 619  
Central processing unit (CPU), 240  
Channel equalization, 582–585, 776–782  
least-mean-square (LMS) algorithm, 834–836  
MATLAB scripts, 781–782, 835, 836  
`cheby1` function, 442  
`cheby2` function, 442  
Chebyshev error, 344, 347  
Chebyshev lowpass filters, 371, 394–403  
MATLAB implementation, 396–397, 398–403  
`circevod` function, 169  
`circonvt` function, 177  
Circular conjugate symmetry, 168  
Circular convolution, 174–179  
Circular-even components, 169  
Circular folding, 166  
Circular-odd components, 169  
Circular shift of sequences, 171  
`cirshftt` function, 172, 177  
Closed-loop control systems, 825  
Code division multiple access (CDMA), 611  
Coefficients  
adjustable, 573, 575–578  
correlation, 637  
finite-duration impulse response (FIR) filters, 707–715  
lattice reflection, 707–715  
optimum reflection, 715–716  
prediction, 701  
reflection, 702  
Column vectors, 63, 119  
Comb filters, 379–380  
Commands, MATLAB controls and flow of, 11–13  
Common form, 346  
Communications, 586–613  
adaptive delta modulation (ADM), 599–601  
adaptive PCM and DPCM (ADPCM), 593–597  
binary digital, 609–610  
delta modulation, 597–601  
differential PCM (DPCM), 590–593  
linear predictive coding (LPC) of speech, 601–605  
pulse-code modulation (PCM), 586–590  
spread-spectrum, 611–613  
Comander, 589  
Complex conjugation property, 107  
Complex exponential sequences, 24, 36, 74–75  
Complex power spectral density (PSD), 656  
Complex-valued exponential sequence, 24  
Complex-valued mappings, 270  
Computation  
of cross-correlation, 660  
of cross-spectral density (CSD), 660  
of output mean function, 659–660  
of power spectral density (PSD), 661–664  
Conditional probability functions, 629–630  
Conjugate-summary property, 65  
Conjugation property, 68  
Constant group delay, 297  
Constant phase delay, 296  
Continuous linear function, 298  
Continuously variable slope delta modulation (CVSD), 600  
Continuous random variables, 616  
Continuous-time Fourier transform (CTFT), 81, 86  
Convergence of least-mean-square (LMS) algorithm, 824–828  
`conv` function, 43–44, 108, 435  
`conv_m` function, 108  
Convolution, 40–47  
block, 183–185  
discrete Fourier transform (DFT), 174–179, 180–186  
discrete-time Fourier transform (DTFT), 68  
error analysis, 182–183  
fast, 197–199  
graphical, 42–43  
high-speed, 197  
high-speed block, 199  
linear sum, 39–40  
linear time-invariant (LTI) system, 38–40  
MATLAB implementation of, 43–45, 47  
overlap-add method, 186  
periodic, 69  
sequence correlation, 45–47  
Correlation  
coefficients, 637  
concept of, 636  
cross-correlation functions, 644  
of sequences, 36, 45–47  
`cos` function, 24–25  
Covariance, 636  
cross-covariance functions, 644  
normalized, 637  
`cplxcomp` function, 223  
`cplxpair` function, 218, 223

Cross-correlation, 36, 45–47. *See also* Correlation  
 computation of, 660  
 functions, 644  
 Cross-covariance functions, 644. *See also*  
 Covariance  
 Cross-spectral density (CSD), 654, 660  
 Cubic spine interpolation, 92  
 Cumulative distribution function (CDF), 616  
 Curves, learning, 827  
 Cutoff frequency, 310  
 cutoff function, 473

## D

Dead band, 533  
**dec2bin** function, 242, 243  
**dec3bin** function, 245  
 Decibels (dB), 292  
 Decimal numbers, 251–252  
**decimate** function, 467  
 Decimation  
   design specifications, 494–496  
   downsampling, 461–466  
   by a factor  $D$ , 461–470  
   ideal decimators, 466–470  
   integers, 490–496  
   MATLAB implementation, 462–466, 467–470,  
     491–493  
 Decimation-in-frequency (DIF-FFT), 188, 195  
 Decimation-in-time (DIT-FFT), 188, 193  
 Deconvolution, 109  
 Delay element, 213  
 Delta modulation (DM), 597–601, 807  
 Denominator polynomials, 105  
 Denormalized number, 254  
 Dense spectrum of signals, 159  
 Density, probability, 615  
**dfs** function, 144, 156  
**dft** function, 177  
 Difference equations, 47–53  
   digital filters, 52–53  
   frequency response, 76–80  
   homogeneous solution, 47  
   linear time-invariant (LTI) system, 47–53  
   MATLAB implementation of, 48–51  
   natural frequencies, 48  
   representation, 119  
   zero-state input and responses, 51–52  
 $z$ -transform, 128–134  
 Differential PCM (DPCM), 590–593, 807  
 Differentiators, 341

Digital filters, 52–53, 291, 432  
 A/D quantization noise, 518–530, 525, 527–530  
 MATLAB analysis of, 520–525  
 MATLAB implementation of, 526–527, 528–530  
 round-off effects, 518–522, 530–557  
 truncation operation, 525–527  
 Digital resonators, 374–377  
 Digital signal processing (DSP), 1–21  
   analog signal processing (ASP) compared to, 3–4  
   analysis, 2–4  
   applications of, 18–20  
   echo generation, 18  
   echo removal, 19  
   MATLAB and, 1–2, 18–20  
   method of, 2–5  
   musical sound processing, 18  
   reverberation, 18, 20  
   signal filtering, 5  
 Digital sinusoidal oscillators, 382–384  
 Digital-to-analog conversion (DAC), 80–81  
**dir2cas** function, 217, 223, 228, 230, 268  
**dir2par** function, 221, 223  
 Direct form, 214–215  
   finite-duration impulse response (FIR) filters,  
     228, 229, 501–504  
   infinite-duration impulse response (IIR) filters,  
     214–215  
   MATLAB, 229  
 Direct-form realization, 558  
 Discontinuous function, 298  
 Discrete Fourier series (DFS), 141, 142–147  
   MATLAB implementation of, 143–146  
   matrix, 144  
   relation to the DTFT, 148  
   relation to  $z$ -transform, 146–147  
 Discrete Fourier transform (DFT), 64, 154–165  
   block convolutions, 183–185  
   circular conjugate symmetry, 168  
   circular convolution, 174–179  
   circular-even components, 169  
   circular folding, 166  
   circular-odd components, 169  
   circular shift of sequences, 171  
   decimation-in-frequency (DIF-FFT), 195  
   decimation-in-time (DIT-FFT), 193  
   dense spectrum of signals, 159  
   divide-and-combine approach, 190–193  
   DTFT interpolation formula, 152–153  
   energy spectrum, 180  
   error analysis, 182–183  
   fast convolutions, 197–199  
   fast Fourier transform (FFT), 187–199

- frequency-domain approach, 177  
goal of efficient computation, 187–190  
high-density spectrum, 162  
high-resolution spectrum, 162  
high-speed block convolutions, 199  
linear convolution using, 180–186  
MATLAB implementation of, 143–146, 153,  
    156–165, 185–186, 195–197  
matrix, 156  
merging formula, 193  
 $N$ -point sequence, 154  
Nyquist component, 169  
overlap-add method, 186  
periodic conjugate symmetry, 168  
periodic shift of sequences, 172  
power spectrum, 180  
properties of, 165–180  
radix-2 FFT algorithm, 193–196  
rectangular window, 150  
relation to  $z$ -transform, 146–147  
sampling, 149–152  
time-domain approach, 176  
twiddle factor, 191  
zero-padding operation, 159  
 $z$ -transform reconstruction formula, 152
- Discrete random variables, 616  
Discrete-time filters, 212–290  
    adder, 213  
    basic elements of, 213  
    delay element, 213  
    error characteristics, 255–262  
    filter coefficients, 262–277  
    finite-precision numerical effects, 239–240  
    FIR systems, 228–239  
    IIR systems, 214–228  
    MATLAB implementation of, 216, 217, 221–228,  
        229, 230–233, 234–239, 242, 245, 247  
    multipliers (gain), 213  
    pole-zero locations, 262–269  
    quantization and, 255–277  
    representation of numbers, 240–255
- Discrete-time Fourier transform (DTFT), 59–67  
    analog signals, 80–97  
    arbitrary sequences, 75–76  
    column vectors, 63  
    complex exponential sequences, 74–75  
    conjugate-summary property, 65  
    conjugation property, 68  
    convolution, 68  
    discrete Fourier series (DFS) relation to, 148  
    energy density spectrum, 69  
    energy property, 69
- finite-duration causal sequence, 121  
folding property, 68, 72  
frequency response, 74  
frequency shifting property, 68, 70  
interpolation formula, 152–153  
inverse discrete-time Fourier transform  
    (IDTFT), 60  
linearity property, 67  
linear time-invariant (LTI) systems, 74–80  
MATLAB implementation of, 61–66  
matrix-vector multiplication operation, 62  
multiplication property, 69  
periodicity property, 61  
properties, 60–61, 67–73  
sequences, 66–67  
sinusoidal sequences, 75  
symmetries in real sequences, 68  
symmetry property, 61, 66  
time shifting property, 68
- Discrete-time LTI systems, 664–668  
Discrete-time Markov process, 674–675  
Discrete-time signals, 22–36  
    complex-valued exponential sequence, 24  
    correlation of sequences, 36  
    even and odd synthesis, 34–36  
    exponential sequences, 24, 51  
    finite-duration sequence, 43  
    geometric series, 36, 41  
    infinite-duration sequence, 23  
    MATLAB representations, 23  
    number sequence, 22  
    operations on sequences, 25–32  
    periodic sequence, 25  
    random sequences, 25  
    real-valued exponential sequence, 24  
    sequences, 22–36  
    sinusoidal sequence, 24–25  
    unit sample sequence, 23  
    unit sample synthesis, 34–36  
    unit step sequence, 23–24
- Discrete-time systems, 36–40  
    convolution, 40–47  
    difference equations, 47–53  
    digital filters, 52–53  
    excitation, 36  
    linear, 37–40  
    linear time-invariant (LTI) system, 38, 40, 52  
    MATLAB implementation for, 43–45  
    response, 51–52  
    sequence correlation, 45–47  
    zero-state input and responses, 51–52
- Discrete-time white noise process, 672–674

- Distribution
- Gaussian. *See* Gaussian distribution
  - sinusoidal, 623–625
  - uniform, 620–621
- Divide-and-combine approach, 190–193
- Dot-product, 19
- downsample** function, 462
- dtft** function, 64
- Dual-tone multifrequency (DTMF) signals, 605–609
- E**
- Echo cancellation, 783–788
- least-mean-square (LMS) algorithm, 836–838
  - MATLAB scripts, 788, 836, 837
- Echo cancellers, 784, 785, 787
- modems, 786
  - Nyquist rates, 786
- Echo generation, 18
- Echo suppressors, 784
- edges** function, 617
- ellip** function, 442, 677, 680
- Elliptic filters, 371
- Elliptic lowpass filters, 403–406
- MATLAB implementation, 404–406
- Empirical design functions, 318
- Energy
- density spectrum, 69
  - property, 69
  - signals, 28
  - spectrum, 180
- Equalization, channel, 582–585, 776–782
- Equalizers, adaptive, 573
- Equations
- difference, 47–53
  - normal, 705, 717–730
  - order-recursive, 703
  - Weiner-Hopf, 745
- Equiripple filters, 344–360
- constraint of extrema, 348–350
  - MATLAB implementation, 351–360
  - minimax problem, 344–348
  - Parks-McClellan algorithm, 350–351
  - responses, 394
- Ergodicity, 646–648
- Errors
- analysis, 182–183
  - discrete-time filters, 255–262
  - functions, 621
  - interpolation, 459
- Estimation of the mean, 625–627
- etime** function, 195
- Even and odd synthesis, 34–36
- evenodd** function, 72
- Exact transition bandwidth, 313
- Excess noise, analysis of, 829–832
- Excitation, 36
- Exponential sequences, 24, 51
- complex, 24, 36
  - geometric series, 36
  - real-valued, 24
- Extraripple filters, 350
- Extrema, 344
- constraint of, 348–350
- F**
- Far-end echo, 784
- Fast convolutions, 197–199
- Fast Fourier transform (FFT), 64, 142, 187–199
- ceiling function, 197
  - decimation-in-frequency (DIF-FFT), 188, 195
  - decimation-in-time (DIT-FFT), 188, 193
  - divide-and-combine approach, 190–193
  - dot-product, 19
  - fast convolutions, 197–199
  - goal of efficient computation, 187–190
  - high-speed block convolutions, 199
  - high-speed convolution, 197
  - MATLAB implementation of, 195–197
  - merging formula, 193
  - radix-2 FFT algorithm, 193–196
  - twiddle factor, 191
- fftfilt** function, 199
- Filter coefficients
- discrete-time filters, 262–277
  - finite-duration impulse response (FIR) filters, 274–277
  - infinite-duration impulse response (IIR) filters, 262–274
  - MATLAB implementation, 266–269
- Filtered noise process, 676–684
- bandpass process, 679–684
  - lowpass process, 676–679
  - MATLAB implementation of, 682
- filter** function, 121, 131, 219, 579, 592
- Filters
- adaptive, 769–849
  - adaptive direct-form FIR, 815–848
  - allpass filters, 381–382
  - analog-to-digital filter transformations, 407–427
  - autoregressive moving average (ARMA), 212

- bandpass, 339, 441  
bandstop, 441  
Butterworth lowpass, 371, 385–390  
causal, 373  
Chebyshev, 371  
Chebyshev lowpass, 394–403  
comb filters, 379–380  
design equations, 390–391  
digital, 52–53, 291, 432  
digital resonators, 374–377  
discrete-time, 212–290  
elliptic, 371  
elliptic lowpass, 403–406  
equiripple, 344–360  
extraripple, 350  
finite-duration impulse response (FIR), 52, 212, 228–239  
first-order, 542–545, 555–557  
higher-order, 553–554  
highpass, 339, 441  
ideal, 309  
infinite-duration impulse response (IIR), 53, 212, 214–228  
lattice-ladder, 737–743  
linear prediction, 686  
lowpass, 336  
lowpass filter design using MATLAB, 427–432  
moving average (MA), 52  
noise-whitening, 689  
nonrecursive, 52  
notch filters, 377–379  
optimum linear, 686  
phase responses of, 406–407  
prediction-error, 701  
prototype, 432  
prototype analog, 385–407  
*p*-stage lattice, 704  
second-order, 547–549, 557  
stable, 373  
types of, 374–384  
Wiener, 743–766  
`filtfilt` function, 765  
`filtc` function, 132, 133  
Finite difference approximation, 408  
Finite-duration causal sequence, 121  
Finite-duration impulse response (FIR) filters, 52, 212  
absolute specifications, 292–293  
approximations, 292  
cascade form, 228, 229–230  
coefficients, 575, 707–715  
direct form, 228, 229, 501–504  
discrete-time filters, 228–239  
filter coefficients, 274–277  
fixed-point arithmetic, 557–560  
floating-point arithmetic, 566–569  
frequency-sampling design technique, 330–343  
frequency-sampling form, 228, 233–239  
implementation, 292  
integer decimation, 490–496  
integer interpolation, 482–487  
linear-phase form, 228, 230–233  
MATLAB analysis of, 560–566  
MATLAB implementation, 301–303, 319–320, 351–360  
multiple stopbands, 499–500  
optimal equiripple design technique, 344–360  
polyphase filter structures, 504–507  
properties of linear-phase, 295–309  
rational-factor rate conversion, 497–499  
relative specifications, 293–295  
round-off effects in, 557–569  
sampling rate conversion, 482–510  
specifications, 292  
time-variant filter structures, 507–510  
Wiener filters, 745–752  
windowing, 309–330  
Finite-duration sequence, 23, 43–44, 107, 142  
Finite-precision numerical effects, 239–240  
`fir2` function, 343  
`fir2latc` function, 711, 713, 736  
`firpm` algorithm, 483, 491  
`firpm` function, 275, 351, 353  
`firpmord` function, 353  
First-order filters, 542–545, 555–557  
First-order-hold (FOH) interpolation, 91–92, 94  
Fixed-point arithmetic, 240, 557–560  
one's-complement format, 257–258  
quantization, 256–261  
rounding operation, 260–261  
sign-magnitude format, 256–257  
truncation operation, 256  
two's-complement format, 259–260  
Fixed-point signed integer arithmetic, 241–248  
one's-complement format, 242–244  
sign-magnitude format, 241–242  
ten's-complement format, 246–248  
two's-complement format, 244–245  
`Fletcher-Powell` algorithm, 821  
`fliplr` function, 710, 711  
Floating-point arithmetic, 240, 251–254, 566–569  
binary numbers, 252–253  
decimal numbers, 251–252

Floating-point arithmetic (*continued*)  
     IEEE 754 standard, 254–255  
     quantization, 261–262

Folding property, 68, 72, 107

for...end loop, 143, 177

Forward linear prediction, 701–705

Forward prediction-error filter, 730–732

`freqs_m` function, 392

Frequencies  
     circular shift in, 174  
     natural, 48  
     periodicity in, 33  
     sampling, 141, 150. *See also* Sampling  
     uncountably infinite, 141

Frequency-band  
     MATLAB implementation of, 441–445  
     tolerances, 294  
     transformations, 432–445

Frequency-domain approach, 177  
     downsampling, 462–466  
     resampled signals, 480

Frequency response, 74, 76–80  
     functions, 298–301  
     infinite-duration impulse response (IIR) filters, 269–274

Frequency-sampling form  
     design technique, 330–343  
     finite-duration impulse response (FIR) filters, 228, 233–239  
     MATLAB scripts, 335  
     naive design method, 332–333  
     optimum design method, 333–343

Frequency selective type, 291

Frequency shifting property, 68, 70, 107

`freqz` function, 64, 121, 122, 123, 303, 320

`freqz_m` function, 320, 392

`ftype` function, 330

Full-duplex transmission, 783

**G**

Gain, 75  
     variance, 528

Gaussian distribution  
     bivariate, 637–641  
     random processes, 668–670

General fixed-point arithmetic, 248–251  
     one's-complement format, 249  
     sign-magnitude format, 249  
     two's-complement format, 250–251

Geometric series, 36, 41

Gibbs phenomenon, 313

Goertzel algorithm, 607–609

Granular limit cycles, 532–537

Graphical convolution, 42–43

**H**

Hamming window, 315–316

Hann window, 315

High-density spectrum, 162

Higher-order filters, 553–554

Highpass filters, 339, 441

High-resolution spectrum, 162

High-speed convolution, 197, 199

Histograms  
     as joint pdf approximations, 630  
     as pdf approximations, 616–618

Homogeneous solutions, 47

`hsolpsav` function, 199

`h(X)` function, 624

Hybrid devices, 783

**I**

Ideal filters, 309

`idfs` function, 145, 156

IEEE 754 standard, 254–255, 262

`impinvvar` function, 411

`imp_invr` function, 410, 411, 419

Improper rational function, 109

`impulse` function, 393

Impulse invariance transformation, 408–418

Impulse response, 37, 295–297

`impz` function, 48

Indexing operations, 10–11

Infinite-duration impulse response (IIR) filters, 53, 212  
     allpass filters, 381–382  
     analog-to-digital filter transformations, 407–427  
     bilinear transformation, 408, 418–426  
     Butterworth lowpass filters, 385–390  
     cascade form, 214, 216–217  
     Chebyshev lowpass filters, 394–403  
     comb filters, 379–380  
     design, 370–457  
     design equations, 390–391  
     digital resonators, 374–377  
     digital sinusoidal oscillators, 382–384  
     direct form, 214–215  
     discrete-time filters, 214–228  
     effect on pole-zero locations, 262–269

- effects on frequency response, 269–274  
 elliptic lowpass filters, 403–406  
 filter coefficients, 262–274  
 finite difference approximation, 408  
 first-order filters, 555–557  
 frequency-band transformations, 432–445  
 granular limit cycles, 532–537  
 higher-order filters, 553–554  
 impulse invariance transformation, 408–418  
 limit cycles, 531–532  
 linear fractional transformation, 418  
 lowpass filter design using MATLAB, 427–432  
 matched- $z$  transformation, 426–427  
 MATLAB analysis of, 533–537, 546–547  
 MATLAB implementation, 216, 217, 387–390,  
     392–394, 396–397, 398–403, 404–406, 441–445  
 mirror-image symmetry, 373  
 multiplication quantization error, 539–542  
 notch filters, 374–379  
 overflow limit cycles, 537–539  
 parallel form, 214, 221–228  
 phase responses of, 406–407  
 prototype filters, 385–407, 432  
 relative-linear scale, 371–372  
 round-off effects, 530–557  
 second-order filters, 547–549, 557  
 signal-to-noise ratio (SNR), 545, 550–551  
 statistical noise, 542–545, 554–557  
 transposed structure, 216  
 types of filters, 374–384  
 Wiener filters, 755–762
- Infinite-duration sequence, 23  
 Infinite sums, 141  
 Innovations process, 687–700  
 In-phase components, 681  
 Input  
     poles, 130  
     sequences, 79  
     zero-state responses and, 51–52
- Integers  
     decimation, 490–496  
     design specifications, 487, 494–496  
     interpolation, 482–487  
     MATLAB implementation, 483–487, 491–493
- Interference, 611  
     narrowband, suppression of, 788–795
- Interpolation, 459–461  
     cubic spine, 92  
     design specifications, 487  
     DTFT formula, 152–153  
     by factor  $I$ , 470–475  
     first-order-hold (FOH), 91–92, 94
- integers, 482–487  
 MATLAB implementation, 483–487  
 zero-order-hold (ZOH), 90–91, 94
- Intervals, sampling, 81  
 intfilt function, 483  
 Inverse discrete-time Fourier transform  
     (IDTFT), 60  
 Inversion of  $z$ -transform, 112–118
- J**
- Jamming, 611  
 Joint central moments, 636  
 Joint cumulative distribution function, 628  
 Joint probability functions, 628–634  
     conditional probability functions, 629–630  
     functions, 631–634  
     histograms as joint pdf approximations, 630  
     marginal probability functions, 629  
     scatter-plot as pdf plots, 631  
     statistical independence, 630  
     transformations, 631
- Joint statistical averages, 634–637  
     concepts, 636  
     correlation coefficients, 637  
     orthogonal random variables, 637  
     uncorrelated random variables, 636–637
- K**
- kaiserord function, 329  
 Kaiser window, 317–319  
 Kalman gain vector, 844
- L**
- ladr2iir function, 740  
 ladrfilter function, 741  
 latc2fir function, 710, 714, 736  
 Lattice-ladder filters, 737–743  
     MATLAB implementation of, 739–743  
 Lattice reflection coefficients, 707–715  
 LDU factorization, 847–848  
 Learning curves, 827  
 Least-mean-square (LMS) algorithm, 575–578,  
     815, 816  
     adaptive direct-form FIR filters, 820–824  
     analysis of excess noise, 829–832  
     channel equalization, 834–836  
     convergence of, 824–828

- Least-mean-square (LMS) algorithm (*continued*)  
 echo cancellation, 836–838  
 MATLAB implementation of, 823–824  
 MATLAB scripts, 833, 835, 836, 837, 838  
 narrowband interference, suppression of, 838–839  
 properties of, 824–841  
 recursive least-squares (RLS) algorithms, 846–847  
 stability of, 824–826  
 system identification (modeling), 832–834
- Least-significant bit (LSB), 250
- Least-squares criterion results, 574, 771
- Left-sided sequence, 106
- length function, 473
- Levinson-Durbin algorithm, 718–724, 746
- Limit cycles, 531–532  
 granular, 532–537  
 overflow, 537–539
- Linear convolution  
 block convolutions, 183–185  
 discrete Fourier transform (DFT), 180–186  
 error analysis, 182–183  
 sum, 39–40
- Linear discrete-time systems, 37–40
- Linearity property, 67, 107, 165
- Linear mean-square estimation, 752–755
- Linear operators, 637
- Linear-phase FIR filters, 228, 230–233  
 frequency response functions, 298–301  
 impulse response, 295–297  
 MATLAB implementation, 301–303  
 properties of, 295–309  
 zero locations, 303–309
- Linear prediction  
 filters, 686  
 relationships, 716–717
- Linear prediction-error filters, properties of, 730–734
- Linear predictive coding (LPC) of speech, 601–605, 807–813  
 MATLAB scripts, 811–813
- Linear systems  
 bounded-input bounded-output (BIBO)  
 stability, 40  
 causality, 40  
 discrete-time, 37–40  
 impulse response, 37  
 linear time-invariant (LTI) system, 38–40  
 superposition summation, 37  
 time-varying impulse responses, 37
- Linear time-invariant (LTI) system, 38, 52, 74–80, 658–668  
 bounded-input bounded-output (BIBO)  
 stability, 40  
 causality, 40  
 convolution, 40–47  
 cross-correlation, computation of, 660  
 cross-spectral density (CSD), computation of, 660  
 determination of, 39–40  
 difference equations, 47–53  
 digital filters, 52–53  
 discrete-time, 664–668  
 frequency response, 74, 76–80  
 linear systems, 38–40  
 output auto-correlation, computation of, 661–664  
 output mean function, computation of, 659–660  
 power spectral density (PSD), computation of, 661–664  
 sequence correlation, 45–47  
 zero-state input and responses, 51–52
- Line enhancement, 795–801  
 MATLAB scripts, 797, 798, 799, 801
- `lms` function, 577, 823
- Local loops, 783
- Loops  
`for...end`, 143, 177  
 local, 783
- Lowpass filters, 336  
 design using MATLAB, 427–432  
 process, 676–679
- Low-rate signals, 461

## M

- Magnitude, 75, 77
- Magnitude-only  
 designs, 371  
 specifications, 292
- Mantissa, 251, 262
- Marginal probability functions, 629
- Markov process, 674
- Matched-z transformation, 426–427
- MATLAB, 1–2, 5–17  
 adaptive filtering, 577–578  
 analog signals, 84–87, 92–97  
 autoregressive (AR) lattice structure, 736  
 bivariate Gaussian distribution, 641  
 Butterworth lowpass filters, 387–390, 392–394

- cascade form, 230  
 channel equalization, 835, 836  
 Chebyshev lowpass filters, 396–397, 398–403  
 control and flow of commands, 11–13  
 convolution, 43–45, 47  
 decimation, 467–470  
 difference equations, 48–51  
 digital filters, 520–525  
 digital signal processing (DSP) and, 1–2, 18–20  
 direct form structure, 216, 229  
 discrete Fourier series (DFS), 143–146  
 discrete Fourier transform (DFT), 156–165,  
     185–186, 195–197  
 discrete-time Fourier transform (DTFT), 61–66  
 discrete-time LTI systems, 667  
 discrete-time signals, 23  
 discrete-time systems, 43–45  
 distribution, 621–622  
 downsampling, 462–466  
 echo cancellation, 836, 837  
 elliptic lowpass filters, 404–406  
 equiripple filters, 351–360  
 estimation of the mean, 626–627  
 fast Fourier transform (FFT), 195–197  
 filter coefficients, 266–269  
 filtered noise process, 682  
 finite-duration impulse response (FIR) filters,  
     319–320  
 frequency-band transformations, 441–445  
 frequency-sampling form, 234–239  
 functions, 14  
 histograms as joint pdf approximations, 630  
 indexing operations, 10–11  
 infinite-duration impulse response (IIR) filters,  
     217  
 integer decimation, 491–493  
 integer interpolation, 483–487  
 lattice-ladder filters, 739–743  
 lattice reflection coefficients, 710–711  
 least-mean-square (LMS) algorithm, 823–824,  
     833  
 Levinson-Durbin algorithm, 722–724  
 linear-phase FIR filters, 301–303  
 linear-phase form, 230–233  
 lowpass filter design using, 427–432  
 matrix operations, 8–13  
 narrowband interference, suppression of, 838  
 number representation, 21  
 one's-complement format, 243–244  
 operators, 6, 8  
 parallel form, 221  
 plotting, 14–17  
 power spectral density (PSD), 657–658  
 random processes, 620–621  
 random sequences, 649–650  
 rational factor  $I/D$ , 480–482  
 rational-factor rate conversion, 498–499  
 round-off effects, 526–527, 528–530, 533–537,  
     546–547, 560–566  
 sampling, 153  
 scripts, 13  
 sign-magnitude format, 242  
 sinusoidal distribution, 625  
 sinusoidal sequence, 34  
 system identification, 774  
 ten's-complement format, 247–248  
 two's-complement format, 245  
 upsampling, 471–475  
 use of, 5–17  
 variables, 7–8  
 Wiener filters, 747, 748, 750, 751, 752, 761,  
     762, 766  
 $z$ -transform, 114–118, 120–125, 131–134  
 Matrix operations  
     MATLAB, 8–13  
     matrix-vector multiplication, 92  
 Matrix-vector multiplication operation, 62  
 maxlag index, 649  
 Mean, estimation of the, 625–627  
 mean function, 526  
 Mean-squared values, 619  
 Mean-square-error (MSE), 574, 771  
     parameter estimation based on, 819–820  
 mean(X) function, 626  
 Merging formula, 193  
 Minimax problem, 336, 344–348  
 Minimum mean-square-error criterion, 816–820  
 Minimum MSE (MMSE), 717, 744  
 Minimum stopband attenuation, 313  
 Mirror-image symmetry, 373  
 Mixed-radix FFT algorithm, 193  
 Mixed random variables, 616  
 Models  
     Gaussian distribution, 621–622  
     random variables, 620–625  
     system identification, 578–579, 771–776  
     uniform distribution, 620–621  
 Modems, echo cancellers, 786  
 Modified zero-order Bessel functions, 318  
 Moments, 618, 634–637  
 Monotone function, 348  
 Moving average (MA) filters, 52  
 Moving average (MA) process, 692  
 Moving target indicator (MTI) radars, 379

Multiple-access code, 611  
 Multiple stopbands, 499–500  
 Multiplication-by-a-ramp property, 108, 111  
 Multiplication property, 69, 179  
 Multiplication quantization error, 539–542  
 Multipliers (gain), 213  
 Multirate digital signal processing systems, 458  
 Musical sound processing, 18

## N

Narrowband interference, suppression of, 579–582, 788–795  
 least-mean-square (LMS) algorithm, 838–839  
 MATLAB scripts, 838  
 Narrowband process, 679  
 Narrowband signals in wideband noise, estimation of, 796–801  
 Natural frequencies, 48  
 Near-end echo, 784  
 Noise  
     A/D quantization, 525  
     analysis of excess, 829–832  
     cancellation, 801–807  
     MATLAB scripts, 804, 805, 806  
     pseudo-noise (PN), 612  
     quantization, 519  
     round-off, 558, 564  
     signal-to-noise ratio (SNR), 545, 550–551  
     statistical, 519–520, 539, 542–545, 554–557  
 Noise-whitening filter, 689  
 Noncausal Wiener filters, 762–766  
 Nonrecursive filters, 52  
 Normal equations, 705, 717–730  
     Levinson-Durbin algorithm, 718–724  
     Schur algorithm, 724–730  
 Normalized covariance, 637  
 Normalized form, 251  
 Normalized histograms, 617  
 Not-a-number (NaN), 255  
 Notch filters, 377–379  
 N-point sequence, 154  
 Null space, 104  
 Numbers  
     representation, 21, 240–255  
     sequence, 10  
 Numerator polynomials, 105  
 Numerically computable transforms, 141  
 nx function, 617  
 nxy function, 630  
 Nyquist component, 169

Nyquist rates, 83, 87  
 echo cancellers, 786

## O

oc2sm function, 251  
 One's-complement format, 240, 242–244  
     fixed-point arithmetic, 257–258  
     fixed-point signed integer arithmetic, 242–244  
     general fixed-point arithmetic, 249  
     MATLAB implementation, 243–244  
 onesComplement function, 243  
 One-side  $z$ -transform, 128  
 Operations  
     rounding, 255, 260–261  
     on sequences, 25–32  
     truncation, 255, 256  
 Operators  
     linear, 637  
     MATLAB, 6, 8  
 Optimum linear filters, 686  
 Optimum reflection coefficients, 715–716  
 Order-recursive equations, 703  
 Orthogonality principle, Wiener filters, 752–755  
 Orthogonal random variables, 637  
 Output auto-correlation, computation of, 661–664  
 Output mean function, computation of, 659–660  
 Output sequences, 79  
 Overflow, 531  
     limit cycles, 537–539  
     scaling to avoid, 558  
     scaling to prevent, 564  
 Overlap-add method, block convolutions, 186  
 ovrlpsav function, 185, 186, 199

## P

Pair of random variables, 628–641  
 Pairs,  $z$ -transform, 110–111  
 par2dir function, 224  
 Parallel form, 214, 221–228  
     infinite-duration impulse response (IIR) filters, 214  
 Parameters  
     estimation based on MSE criterion, 819–820  
     signals, 487  
 parfiltr function, 223  
 Parks-McClellan algorithm, 350–351  
 Parseval's relation, 179–180  
 Passband, 292  
 pdf1 function, 617

Pdf approximations, histograms as, 616–618  
 Peak side-lobe magnitude, 312  
 Peaky main-lobe, 311  
 Periodic conjugate symmetry, 168  
 Periodic convolution, 69  
 Periodicity in frequencies, 33  
 Periodicity property, 61  
 Periodic sequence, 25  
 Periodic shift of sequences, 172  
 Phase response, 75, 77  
 Phase responses of prototype filters, 406–407  
 Piecewise linear response, 298  
 Plants, 771, 776  
 Plotting, 14–17  
 Poles, estimation of in all-pole systems, 811–813  
 Pole-zero systems, 738  
     infinite-duration impulse response (IIR) filters, 262–269  
 Poly function, 116  
 Polyphase structures, 500, 504–507  
 Positive-time sequence, 105  
 Power, signal, 28  
 Power spectral density (PSD), 650–658  
     auto-correlation, 653–654  
     computation of, 661–664  
     cross-spectral density (CSD), 654  
     MATLAB implementation of, 657–658  
     properties of, 653–654  
     random sequences, 655–658  
 Power spectrum, 180  
 Prediction  
     backward linear, 706–707  
     forward linear, 701–705  
     linear prediction relationships, 716–717  
     signals, 744  
     Wiener filters, 743–766  
 Prediction-error filter, 701  
 Prewindowing, 842  
 Probability functions, 615–618  
 Processes, random, 614–685  
 Processing elements (PEs), 729  
 prod function, 28  
 Products  
     of biquads, 214  
     sample, 28  
 Properties  
     discrete-time Fourier transform (DTFT), 60–61  
     of discrete-time Fourier transform (DTFT), 67–73  
     Gaussian distribution, 639  
     of least-mean-square (LMS) algorithm, 824–841  
     of linear-phase FIR filters, 295–309

of linear prediction-error filters, 730–734  
 of power spectral density (PSD), 653–654  
 Prototype analog filters, 385–407  
     Butterworth lowpass filters, 385–390  
     Chebyshev lowpass filters, 394–403  
     design equations, 390–391  
     elliptic lowpass filters, 403–406  
     phase responses of, 406–407  
 Prototype filters, 432  
 Pseudo-noise (PN), 612  
 p-stage lattice filter, 704  
 Pulse-code modulation (PCM), 586–590, 807

## Q

qcoeff function, 266  
 qfix function, 546  
 qmode function, 534  
 Quadrature components, 681  
 Quantization  
     A/D quantization noise, 518–530  
     discrete-time filters, 255–262  
     fixed-point arithmetic, 256–261  
     floating-point arithmetic, 261–262  
     multiplication quantization error, 539–542  
     noise, 519

## R

Radix-2 FFT algorithm, 193–196  
 Radix-R FFT algorithm, 193  
 rand function, 25, 578  
 randn function, 675  
 Random processes, 642–650  
     autoregressive moving average (ARMA) process, 692–695  
     autoregressive (AR) process, 692  
     backward linear prediction, 706–707  
     bivariate Gaussian distribution, 637–641  
     cross-correlation, computation of, 660  
     cross-spectral density (CSD), computation of, 660  
     discrete-time LTI systems, 664–668  
     discrete-time Markov process, 674–675  
     discrete-time white noise process, 672–674  
     estimation of the mean, 625–627  
     filtered noise process, 676–684  
     FIR filter coefficients, 707–715  
     forward linear prediction, 701–705  
     Gaussian distribution, 668–670  
     innovations representation of, 687–700

- Random processes (*continued*)
- joint probability functions, 628–634
  - joint statistical averages, 634–637
  - lattice reflection coefficients, 707–715
  - Levinson-Durbin algorithm, 718–724
  - linear and time-invariant systems (LTI), 658–668
  - linear prediction relationships, 716–717
  - Markov process, 674
  - MATLAB implementation of, 620–621
  - models, 620–625
  - moving average (MA) process, 692
  - optimum reflection coefficients, 715–716
  - output auto-correlation, computation of, 661–664
  - output mean function, computation, 659–660
  - pair of random variables, 628–641
  - power spectral density (PSD), 650–658, 661–664
  - rational power spectra, 691–695
  - relationship with autocorrelation sequence, 695–700
  - Schur algorithm, 724–730
  - sinusoidal distribution, 623–625
  - statistical averages, 618–619
  - transformation, 622–623
  - variables, 615–627
  - white noise process, 670–672
- Random sequences, 25, 648–650
- power spectral density (PSD), 655–658
- Random signals. *See* Random processes
- Rational factor  $I/D$ , 477–482
- MATLAB implementation, 480–482
- Rational-factor rate conversion, 497–499
- Rational power spectra, 691–695
- Real-valued exponential sequences, 24
- Reconstruction
- of analog signals, 87–92
  - of band-limited signals, 89
  - signals, 94, 95
- Reconstruction formula ( $z$ -transform), 152
- Rectangular pulse, 35
- Rectangular window, 150, 310, 312–314
- Recursive least-squares (RLS) algorithms, 841–848
- LDU factorization and, 847–848
  - least-mean-square (LMS) algorithm, 846–847
- Reflection coefficient, 702
- Region of convergence (ROC), 104–107
- Relationships
- autocorrelation sequence, 695–700
  - average linear, 635, 636
  - linear prediction, 716–717
  - between representations, 125
- Relative amplitudes, 313
- Relative-linear scale, 371–372
- Relative specifications, 292
- finite-duration impulse response (FIR) filters, 293–295
- rem** function, 154
- Representation
- difference equation, 119
  - relationships between, 125
  - transfer function, 120
  - in  $z$ -transform, 118–128
- Representation of numbers, 240–255
- fixed-point signed integer arithmetic, 241–248
  - floating-point arithmetic, 251–254
  - general fixed-point arithmetic, 248–251
- resample** function, 480, 481, 500
- residue** function, 529
- residuez** function, 114, 115, 224, 410
- Responses
- arbitrary absolutely summable sequences, 75–76
  - discrete-time systems, 51–52
  - frequency, 74, 76–80
  - impulse, 37
  - phase, 75, 77
  - steady-state, 75, 128
  - time-varying impulse, 37
  - transient, 128
  - unbounded, 130
  - zero-state input and, 51–52
- Reverberation
- digital signal processing (DSP), 18, 20
- Reverse polynomials, 707
- Right-sided sequence, 106
- Root-mean-squared (rms), 619
- round** function, 551
- Rounding operation, 255, 520, 525
- fixed-point arithmetic, 260–261
- Round-off effects, 518–572
- A/D quantization noise, 518–530, 525, 527–530
  - finite-duration impulse response (FIR) filters, 557–569
  - first-order filters, 542–545, 555–557
  - fixed-point arithmetic, 557–560
  - floating-point arithmetic, 566–569
  - granular limit cycles, 532–537
  - higher-order filters, 553–554
  - in IIR digital filters, 530–557
  - limit cycles, 531–532, 537–539
  - MATLAB analysis of, 520–525, 533–537, 546–547, 551–553, 560–566
  - MATLAB implementation of, 526–527, 528–530
  - multiplication quantization error, 539–542

- overflow, 531  
rounding operation, 520  
saturation strategies, 531  
second-order filters, 547–549, 557  
signal-to-noise ratio (SNR), 545, 550–551  
statistical noise, 519–520, 539, 542–545, 554–557  
truncation operation, 525–527  
variance gain, 528  
Round-off noise, 558, 564  
Row vectors, 119  
Rules, Bayes, 630  
 $rxy$  function, 649
- S**
- Sample products, 28  
Sample shifting property, 107  
Sampling, 141  
analog signals, 81–84  
discrete Fourier transform (DFT), 149–152  
DTFT interpolation formula, 152–153  
frequencies, 150  
intervals, 81  
MATLAB implementation of, 153  
principles, 83  
 $z$ -transform reconstruction formula, 152  
Sampling rate conversion, 458–517  
decimation by a factor  $D$ , 461–470  
direct form filter structures, 501–504  
downsampling, 461–466  
finite-duration impulse response (FIR) filters, 482–510  
ideal decimators, 466–470  
integer decimation, 490–496  
interpolation by factor  $I$ , 470–475  
interpolation errors, 459–461  
low-rate signals, 461  
MATLAB implementation, 462–466, 467–470, 471–475, 480–482  
multiple stopbands, 499–500  
multirate digital signal processing systems, 458  
polyphase structures, 500, 504–507  
by rational factor  $I/D$ , 477–482  
time-variant filter structures, 507–510  
upsampling, 470–475  
Saturation strategies, 531  
**satur** function, 551  
Scaling, 27  
to avoid overflow, 558  
factor, 249  
to prevent overflow, 564
- Scatter-plot as pdf plots, 631  
Schur algorithm, 724–730  
**sdir2cas** function, 388  
Second-order filters, 547–549, 557  
Sequences, 22–33, 45–47  
absolutely summable, 75  
anticausal, 106  
arbitrary, 75–76  
circular shift of, 171  
complex exponential, 74–75  
complex-valued exponential, 24  
correlation, 36, 45–47  
discrete-time Fourier transform (DTFT), 66–67  
exponential, 24, 51  
finite-duration, 23, 43–44, 107, 142  
infinite-duration, 23  
input, 79  
left-sided, 106  
number, 10, 22  
operations on, 25–32  
output, 79  
periodic, 25  
positive-time, 105  
random, 25, 648–650, 655–658  
real-valued exponential, 24  
right-sided, 106  
sinusoidal, 24–25, 32–33, 75  
symmetry property, 168  
unit sample, 23  
unit step, 23–24  
 $z$ -transform, 110–111  
Series, geometric, 36, 41  
**sigadd** function, 26  
**sig\*** functions, 31  
Signals, 2–20  
addition, 8  
analog, 80–97  
analog processing (ASP), 3–5  
analysis, 2, 4  
band-limited, 82  
cross-correlation functions, 644  
cubic spine interpolation, 92  
dense spectrum of, 159  
digital processing (DSP), 2–20  
discrete-time, 22–36  
dual-tone multifrequency (DTMF), 605–609  
energy, 28  
ergodicity, 646–648  
filtering, 5  
first-order-hold (FOH) interpolation, 91–92, 94  
low-rate, 461  
MATLAB implementation, 84–87, 92–97

- Signals (*continued*)  
 parameters, 487  
 power, 28  
 prediction, 744  
 random, 642–650. *See also* Random processes  
 random sequences, 648–650  
 reconstruction, 94, 95  
 reconstruction of, 87–92  
 sample products, 28  
 sampling, 81–84  
 scaling, 27  
 smoothing, 744  
 speech, linear predictive coding of, 807–813  
 spread-spectrum, 788  
 stationarity, 645–646  
 wideband, 788–795  
 zero-order-hold (ZOH) interpolation, 90–91, 94
- Signal-to-noise ratio (SNR), 545, 550–551
- Significand, 254
- Sign-magnitude format, 240, 241–242  
 fixed-point arithmetic, 256–257  
 fixed-point signed integer arithmetic, 241–242  
 general fixed-point arithmetic, 249  
 MATLAB implementation, 242
- sinc(x)* function, 92
- Sinusoidal distribution, 623–625
- Sinusoidal interference, suppression of, 581–582
- Sinusoidal sequence, 24–25, 32–33  
 correlation of sequences, 36  
 discrete-time, 32–33  
 discrete-time Fourier transform (DTFT), 75  
 even and odd synthesis, 34, 35  
 geometric series, 36  
 MATLAB implementation of, 34  
 unit sample synthesis, 34
- sm2oc** function, 251
- sm2tc** function, 251
- Smoothing signals, 744
- Spectrum analyzers, 291
- Speech signals, linear predictive coding of, 807–813
- spline** function, 95, 97
- Spread-spectrum  
 communications, 611–613  
 signals, 788
- sqrtrm** function, 640
- Square root algorithms, 847–848
- Stability  
 bounded-input bounded-output (BIBO), 40  
 of least-mean-square (LMS) algorithm, 824–828  
 linear systems, 40  
 z-transform, 125–128
- Stable filters, 373
- stairs** function, 94
- Standard deviations, 619
- Stationarity, 645–646  
 strict-sense, 645  
 wide-sense, 645–646
- Stationary random processes  
 autoregressive moving average (ARMA) process, 692–695  
 autoregressive (AR) process, 692  
 backward linear prediction, 706–707  
 FIR filter coefficients, 707–715  
 forward linear prediction, 701–705  
 innovations representation of, 687–700  
 lattice reflection coefficients, 707–715  
 Levinson-Durbin algorithm, 718–724  
 linear and time-invariant systems (LTI), 658–668  
 linear prediction relationships, 716–717  
 moving average (MA) process, 692  
 optimum reflection coefficients, 715–716  
 rational power spectra, 691–695  
 relationship with autocorrelation sequence, 695–700  
 Schur algorithm, 724–730
- Statistical averages, 618–619
- Statistical independence, 630
- Statistical noise, 519–520, 539, 542–545, 554–557
- statModelR** function, 526
- std** function, 526
- Steady-state responses, 75, 128
- stem** function, 48
- Stepband, 293
- Stochastic-gradient-descent algorithm, 822
- Strict-sense stationarity, 645
- Superposition summation, 37
- Symbol-rate echo cancellers, 785
- Symmetric impulse response, 230
- Symmetry property, 66, 168  
 discrete-time Fourier transform (DTFT), 61
- Synthesis, discrete-time signals, 34–36
- System function, 118  
 from the difference equation representation, 119
- System identification (modeling), 578–579, 771–776  
 least-mean-square (LMS) algorithm, 832–834  
 MATLAB scripts, 832–834
- System poles, 130

**T**

- Tables, 370
- tc2sm** function, 251

Telephone  
 channels, data transmission over, 783–788  
 Ten’s-complement format, 246–248  
 fixed-point signed integer arithmetic, 246–248  
 MATLAB implementation, 247–248  
**tensComplement** function, 247  
**tf2sos** function, 218  
 Time  
 periodicity in, 33  
 shifting property, 68  
 Time-domain approach, 176  
 Time-update equation, 843  
 Time-variant filter structures, 507–510  
 Time-varying impulse responses, 37  
 Transfer function, representation, 120  
 Transformation  
 joint probability functions, 631  
 random processes, 622–623  
 Transient response, 128  
 Transition band, 293  
 Transposed structure, 216  
 Truly linear response, 299  
 Truncation operation, 255, 525–527  
 fixed-point arithmetic, 256  
 Trunk lines, 783  
 Twiddle factor, 191  
 Two’s-complement format, 240, 244–245  
 fixed-point arithmetic, 259–260  
 fixed-point signed integer arithmetic, 244–245  
 general fixed-point arithmetic, 250–251  
 MATLAB implementation, 245  
**twosComplement** function, 245  
 Type-1 linear-phase FIR filter, 299  
 Type-2 linear-phase FIR filter, 300  
 Type-3 linear-phase FIR filter, 300  
 Type-4 linear-phase FIR filter, 301  
 Types of filters, 374–384  
 allpass filters, 381–382  
 comb filters, 379–380  
 digital resonators, 374–377  
 digital sinusoidal oscillators, 382–384  
 notch filters, 377–379

**U**

**u\_buttap** function, 392  
**u\_chb1ap** function, 396, 398  
**u\_chb2ap** function, 401  
**u\_elipap** function, 405  
 Unbounded responses, 130

Uncorrelated random variables, 636–637.  
*See also* Variables  
 Uncountably infinite frequencies, 141  
 Uniform distribution, 620–621  
 Unit circle, 104  
 Unit sample sequence, 23  
 Unit sample synthesis, 34–36  
 Unit step sequence, 23–24  
 Unquantized coefficients, 271  
**upfirdn** function, 485, 491, 498, 500  
**upsample** function, 471  
 Upsampling, 470–475  
 MATLAB implementation, 471–475

**V**

**varGain** function, 529

## Variables

bivariate Gaussian distribution, 637–641  
 conditional probability functions, 629–630  
 correlation coefficients, 637  
 discrete random variables, 616  
 estimation of the mean, 625–627  
 histograms as joint pdf approximations, 630  
 histograms as pdf approximations, 616–618  
 joint probability functions, 628–634  
 joint statistical averages, 634–637  
 marginal probability functions, 629  
 MATLAB, 7–8  
 models, 620–625  
 orthogonal random, 637  
 pair of random, 628–641  
 probability functions, 615–618  
 random, 615–627  
 scatter-plot as pdf plots, 631  
 sinusoidal distribution, 623–625  
 statistical averages, 618–619  
 statistical independence, 630  
 transformation, 622–623  
 transformations, 631  
 Variance gain, 528

**W**

Weiner-Hopf equation, 745  
 Whitenning property, 732–733  
 White noise process, 670–672  
 Wideband noise, narrowband signals in, 796–801  
 Wideband signals, 788–795  
 Wide-sense stationarity, 645–646

Wiener filters, 743–766  
 finite-duration  
   impulse response (FIR) filters, 745–752  
 infinite-duration  
   impulse response (IIR) filters, 755–762  
 linear mean-square estimation, 752–755  
 MATLAB  
   scripts, 747, 748, 750, 751, 752, 761, 762, 766  
   noncausal, 762–766  
   orthogonality principle, 752–755  
 Wiener-Khinchin theorem, 653  
 Windowing, 309–330  
   Bartlett window, 314–315  
   basic designs, 311  
   Blackman window, 317  
   cutoff frequency, 310  
   design examples, 320–330  
   Hamming window, 315–316  
   Hann window, 315  
   Kaiser window, 317–319  
   MATLAB implementation of, 319–320  
   peaky main-lobe, 311  
   rectangular window, 310, 312–314  
 Word length, 248  
 World representation, 689

**X**

`xcorr` function, 47, 650  
`xic` function, 131  
`x=rand` function, 620  
`x=randn` function, 622

**Y**

$y = Qfix$  function, 534

**Z**

$z$  array, 388  
 $Z$ -domain stability theorem, 125  
 Zero constellation, 304  
 Zeros  
   interpolation errors, 459  
   linear-phase FIR filters, 303–309  
   pole-zero locations, 262–269  
   pole-zero systems, 738  
 Zero-order-hold (ZOH) interpolation, 90–91, 94  
 Zero-padding operation, 159  
`zerophase` function, 301, 303  
 Zero-state input and responses, 51–52  
`zmapping` function, 435, 437  
`zplane` function, 119, 121, 122  
 $z$ -transform, 103–140  
   bilateral, 103–107  
   causality, 125–128  
   deconvolution, 109  
   difference equation representation, 119  
   discrete Fourier series (DFS) relation to, 146–147  
   finite-duration causal sequence, 121  
   inversion of, 112–118  
   MATLAB  
     implementation of, 114–118, 120–125, 131–134  
   one-side  $z$ -transform, 128  
   pairs, 110–111  
   properties of, 107–111  
   reconstruction formula, 152  
   region of convergence (ROC), 104–107  
   relationships between representations, 125  
   sequences, 110–111  
   solutions of difference equations, 128–134  
   stability, 125–128  
   systematic representation in, 118–128  
   system function, 118  
   transfer function representation, 120  
    $z$ -domain stability theorem, 125